frontiers | Research Topics

Meningioma: From basic research to clinical translational study, volume II

Edited by
Hailiang Tang and Ian Dunn

Published in
Frontiers in Oncology
Frontiers in Neurology

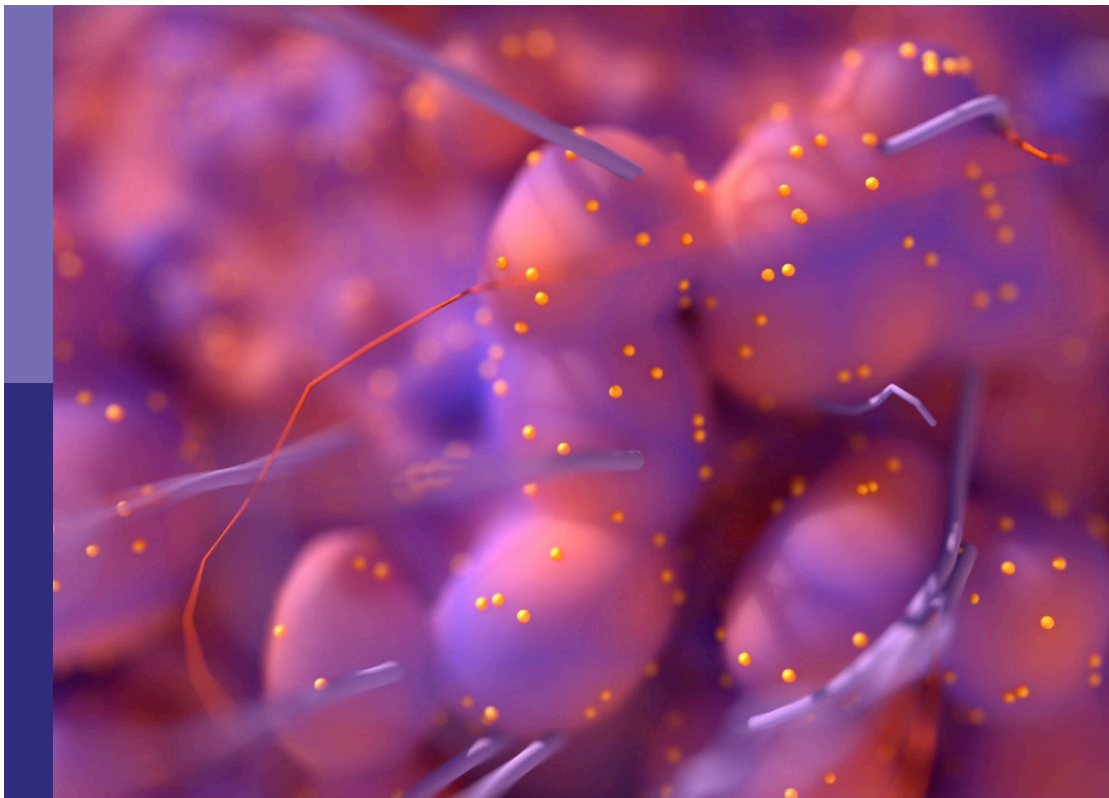

FRONTIERS EBOOK COPYRIGHT STATEMENT

The copyright in the text of individual articles in this ebook is the property of their respective authors or their respective institutions or funders. The copyright in graphics and images within each article may be subject to copyright of other parties. In both cases this is subject to a license granted to Frontiers.

The compilation of articles constituting this ebook is the property of Frontiers.

Each article within this ebook, and the ebook itself, are published under the most recent version of the Creative Commons CC-BY licence. The version current at the date of publication of this ebook is CC-BY 4.0. If the CC-BY licence is updated, the licence granted by Frontiers is automatically updated to the new version.

When exercising any right under the CC-BY licence, Frontiers must be attributed as the original publisher of the article or ebook, as applicable.

Authors have the responsibility of ensuring that any graphics or other materials which are the property of others may be included in the CC-BY licence, but this should be checked before relying on the CC-BY licence to reproduce those materials. Any copyright notices relating to those materials must be complied with.

Copyright and source acknowledgement notices may not be removed and must be displayed in any copy, derivative work or partial copy which includes the elements in question.

All copyright, and all rights therein, are protected by national and international copyright laws. The above represents a summary only. For further information please read Frontiers' Conditions for Website Use and Copyright Statement, and the applicable CC-BY licence.

ISSN 1664-8714
ISBN 978-2-83252-139-7
DOI 10.3389/978-2-83252-139-7

About Frontiers

Frontiers is more than just an open access publisher of scholarly articles: it is a pioneering approach to the world of academia, radically improving the way scholarly research is managed. The grand vision of Frontiers is a world where all people have an equal opportunity to seek, share and generate knowledge. Frontiers provides immediate and permanent online open access to all its publications, but this alone is not enough to realize our grand goals.

Frontiers journal series

The Frontiers journal series is a multi-tier and interdisciplinary set of open-access, online journals, promising a paradigm shift from the current review, selection and dissemination processes in academic publishing. All Frontiers journals are driven by researchers for researchers; therefore, they constitute a service to the scholarly community. At the same time, the *Frontiers journal series* operates on a revolutionary invention, the tiered publishing system, initially addressing specific communities of scholars, and gradually climbing up to broader public understanding, thus serving the interests of the lay society, too.

Dedication to quality

Each Frontiers article is a landmark of the highest quality, thanks to genuinely collaborative interactions between authors and review editors, who include some of the world's best academicians. Research must be certified by peers before entering a stream of knowledge that may eventually reach the public - and shape society; therefore, Frontiers only applies the most rigorous and unbiased reviews. Frontiers revolutionizes research publishing by freely delivering the most outstanding research, evaluated with no bias from both the academic and social point of view. By applying the most advanced information technologies, Frontiers is catapulting scholarly publishing into a new generation.

What are Frontiers Research Topics?

Frontiers Research Topics are very popular trademarks of the *Frontiers journals series*: they are collections of at least ten articles, all centered on a particular subject. With their unique mix of varied contributions from Original Research to Review Articles, Frontiers Research Topics unify the most influential researchers, the latest key findings and historical advances in a hot research area.

Find out more on how to host your own Frontiers Research Topic or contribute to one as an author by contacting the Frontiers editorial office: frontiersin.org/about/contact

Meningioma: From basic research to clinical translational study, volume II

Topic editors

Hailiang Tang — Fudan University, China

Ian Dunn — University of Oklahoma Health Sciences Center, United States

Citation

Tang, H., Dunn, I., eds. (2023). *Meningioma: From basic research to clinical translational study, volume II*. Lausanne: Frontiers Media SA.

doi: 10.3389/978-2-83252-139-7

Table of contents

07 Editorial: Meningioma: From basic research to clinical translational study, volume II
Hailiang Tang, Zhewei Shen, David D. Eisenstat and Ian F. Dunn

11 Establishment and Validation of an Integrated Model to Predict Postoperative Recurrence in Patients With Atypical Meningioma
Xiao-Yong Chen, Jin-Yuan Chen, Yin-Xing Huang, Jia-Heng Xu, Wei-Wei Sun, Yue- Chen, Chen-Yu Ding, Shuo-Bin Wang, Xi-Yue Wu, De-Zhi Kang, Hong-Hai You and Yuan-Xiang Lin

22 A Novel MRI-Based Risk Stratification Algorithm for Predicting Postoperative Recurrence of Meningioma: More Benefits to Patients
Rufei Zhang, Xiaodan Chen, Jialing Cai, Peirong Jiang, Yilin Chen, Bin Sun, Yang Song, Lin Lin and Yunjing Xue

33 A Clinical Semantic and Radiomics Nomogram for Predicting Brain Invasion in WHO Grade II Meningioma Based on Tumor and Tumor-to-Brain Interface Features
Ning Li, Yan Mo, Chencui Huang, Kai Han, Mengna He, Xiaolan Wang, Jiaqi Wen, Siyu Yang, Haoting Wu, Fei Dong, Fenglei Sun, Yiming Li, Yizhou Yu, Minming Zhang, Xiaojun Guan and Xiaojun Xu

48 *TERT* Alterations Predict Tumor Progression in *De Novo* High-Grade Meningiomas Following Adjuvant Radiotherapy
Jiaojiao Deng, Shuchen Sun, Jiawei Chen, Daijun Wang, Haixia Cheng, Hong Chen, Qing Xie, Lingyang Hua and Ye Gong

56 How Much Tumor Volume Is Responsible for Development of Clinical Symptoms in Patients With Convexity, Parasagittal, and Falx Meningiomas?
Shuhei Yamada, Noriyuki Kijima, Tomoyoshi Nakagawa, Ryuichi Hirayama, Manabu Kinoshita, Naoki Kagawa and Haruhiko Kishima

64 Surgical Treatment and Clinical Outcomes of Petroclival Meningiomas: A Single-Center Experience of 107 Patients
Baocheng Gao, Yongfa Zhang, Jiang Tan, Jinsong Ouyang, Bai Tai, Xianbao Cao, Tao Li and Shuang Hu

72 Refined Temporal-to-Frontal Horn Shunt for Treatment of Trapped Temporal Horn After Surgery of Peri- or Intraventricular Tumor: A Case Series Study
Xiaohui Ren, Yong Cui, Chuanwei Yang, Zhongli Jiang, Song Lin and Zhiqin Lin

80 Postoperative Adjuvant Radiotherapy in Atypical Meningioma Patients: A Meta-Analysis Study
Dengpan Song, Dingkang Xu, Hongjie Han, Qiang Gao, Mingchu Zhang, Fang Wang, Guoqing Wang and Fuyou Guo

91 m^{6}A Regulator Expression Segregates Meningiomas Into Biologically Distinct Subtypes
Jiawei Chen, Shuchen Sun, Leihao Ren, Lingyang Hua, Daijun Wang, Qing Xie, Hans-Georg Wirsching, Jiaojiao Deng, Michael Weller and Ye Gong

102 Non-Invasive Preoperative Imaging Differential Diagnosis of Intracranial Hemangiopericytoma and Angiomatous Meningioma: A Novel Developed and Validated Multiparametric MRI-Based Clini-Radiomic Model
Yanghua Fan, Panpan Liu, Yiping Li, Feng Liu, Yu He, Liang Wang, Junting Zhang and Zhen Wu

114 PET/MR Imaging of Somatostatin Receptor Expression and Tumor Vascularity in Meningioma: Implications for Pathophysiology and Tumor Outcomes
Michelle Roytman, Sean Kim, Shannon Glynn, Charlene Thomas, Eaton Lin, Whitney Feltus, Rajiv S. Magge, Benjamin Liechty, Theodore H. Schwartz, Rohan Ramakrishna, Nicolas A. Karakatsanis, Susan C. Pannullo, Joseph R. Osborne, Jonathan P. S. Knisely and Jana Ivanidze

123 Combined Microscopic and Endoscopic Surgery for Pineal Region Meningiomas Using the Occipital-Parietal Transtentorial Approach
Yu Ding, Liang Sun, Yukun Hu, Weiwei Zhai, Liexiang Zhang, Zhengquan Yu, Jiang Wu and Gang Chen

130 The Discrepancy Between Standard Histologic WHO Grading of Meningioma and Molecular Profile: A Single Institution Series
Amanda M. Roehrkasse, Jo Elle G. Peterson, Kar-Ming Fung, Panayiotis E. Pelargos and Ian F. Dunn

139 Deep Learning Model for Intracranial Hemangiopericytoma and Meningioma Classification
Ziyan Chen, Ningrong Ye, Nian Jiang, Qi Yang, Siyi Wanggou and Xuejun Li

149 Clinical Outcomes and Complications of Preoperative Embolization for Intracranial Giant Meningioma Tumorectomy: A Retrospective, Observational, Matched Cohort Study
Yi Yin, Yuhong Li, Zhouyang Jiang, Chao Zhang, Hongfei Ge, Zhi Chen, Rong Hu, Yujie Chen, Xuegang Li, Fei Li and Hua Feng

158 Identification and Management of Aggressive Meningiomas
Bhuvic Patel, Rupen Desai, Sangami Pugazenthi, Omar H. Butt, Jiayi Huang and Albert H. Kim

172 Anatomical Study of Arachnoid Granulation in Superior Sagittal Sinus Correlated to Growth Patterns of Meningiomas
Yuanliang Ye, Wen Gao, Weilin Xu, Jiangu Gong, Minxing Qiu, Lang Long and Jiuyang Ding

180 A Nicotinamide Phosphoribosyltransferase Inhibitor, FK866, Suppresses the Growth of Anaplastic Meningiomas and Inhibits Immune Checkpoint Expression by Regulating STAT1
Yuxuan Deng, Boyi Hu, Yazhou Miao, Jing Wang, Shaodong Zhang, Hong Wan, Zhen Wu, Yifan Lv, Jie Feng, Nan Ji, Deric Park and Shuyu Hao

192 Surgical Management of Falcotentorial Junction Tumors: A Case Series Report
Peixi Liu, Xiaowen Wang, Yingjun Liu, Jiajun Cai, Zixiao Yang, Kai Quan, Wei Zhu and Jianping Song

201 Potential Molecular Mechanisms of Recurrent and Progressive Meningiomas: A Review of the Latest Literature
Wenjie Peng, Pei Wu, Minghao Yuan, Bo Yuan, Lian Zhu, Jiesong Zhou and Qian Li

212 Synthesizing Molecular and Immune Characteristics to Move Beyond WHO Grade in Meningiomas: A Focused Review
Nivedha V. Kannapadi, Pavan P. Shah, Dimitrios Mathios and Christopher M. Jackson

222 Clinicopathologic Characteristics of Grade 2/3 Meningiomas: A Perspective on the Role of Next-Generation Sequencing
Junhyung Kim, Kihwan Hwang, Hyun Jung Kwon, Ji Eun Lee, Kyu Sang Lee, Gheeyoung Choe, Jung Ho Han and Chae-Yong Kim

232 Bone Invasive Meningioma: Recent Advances and Therapeutic Perspectives
Hajime Takase and Tetsuya Yamamoto

245 Meningioma Related Epilepsy- Pathophysiology, Pre/postoperative Seizures Predicators and Treatment
Rasha Elbadry Ahmed, Hailiang Tang, Anthony Asemota, Lei Huang, Warren Boling and Firas Bannout

256 CDK 4/6 inhibitors for the treatment of meningioma
Jacob S. Young, Reilly L. Kidwell, Allison Zheng, Alex F. Haddad, Manish K. Aghi, David R. Raleigh, Jessica D. Schulte and Nicholas A. Butowski

264 Molecular determinants of outcomes in meningiomas
John Lynes, Gabriel Flores-Milan, Sebastian Rubino, John Arrington, Robert Macaulay, James K. C. Liu, Andre Beer-Furlan, Nam D. Tran, Michael A. Vogelbaum and Arnold B. Etame

274 MAC-spinal meningioma score: A proposal for a quick-to-use scoring sheet of the MIB-1 index in sporadic spinal meningiomas
Johannes Wach, Motaz Hamed, Tim Lampmann, Ági Güresir, Frederic Carsten Schmeel, Albert J. Becker, Ulrich Herrlinger, Hartmut Vatter and Erdem Güresir

287 Symptom burden and surgical outcome in non-skull base meningiomas
Tobias Mederer, Sebastian Schachinger, Katharina Rosengarth, Anja Brosig, Karl-Michael Schebesch, Christian Doenitz, Nils-Ole Schmidt and Martin Andreas Proescholdt

299 Application of MRI-Based Radiomics in Preoperative Prediction of *NF2* Alteration in Intracranial Meningiomas
Shuchen Sun, Leihao Ren, Zong Miao, Lingyang Hua, Daijun Wang, Jiaojiao Deng, Jiawei Chen, Ning Liu and Ye Gong

310 Dose-staged Gamma Knife radiosurgery for meningiomas: A retrospective study in a single center
Xiu Gong, Jianbo Ding, Jonathan P. S. Knisely, Enmin Wang, Li Pan, Binjiang Wang, Nan Zhang, Hanfeng Wu, Jiazhong Dai, Tonggang Yu and Xuqun Tang

320 Recent advances in the molecular prognostication of meningiomas
Elaina J. Wang, Alexander F. Haddad, Jacob S. Young, Ramin A. Morshed, Joshua P. H. Wu, Diana M. Salha, Nicholas Butowski and Manish K. Aghi

frontiers | Frontiers in Oncology

TYPE Editorial
PUBLISHED 27 March 2023
DOI 10.3389/fonc.2023.1150514

Check for updates

OPEN ACCESS

EDITED AND REVIEWED BY
Hiroaki Wakimoto,
Massachusetts General Hospital and
Harvard Medical School, United States

*CORRESPONDENCE
Ian F. Dunn
ian-dunn@ouhsc.edu
David D. Eisenstat
david.eisenstat@rch.org.au

†These authors have contributed equally to this work

SPECIALTY SECTION
This article was submitted to Neuro-Oncology and Neurosurgical Oncology, a section of the journal Frontiers in Oncology

RECEIVED 24 January 2023
ACCEPTED 08 March 2023
PUBLISHED 27 March 2023

CITATION
Tang H, Shen Z, Eisenstat DD and Dunn IF (2023) Editorial: Meningioma: From basic research to clinical translational study, volume II.
Front. Oncol. 13:1150514.
doi: 10.3389/fonc.2023.1150514

COPYRIGHT
© 2023 Tang, Shen, Eisenstat and Dunn. This is an open-access article distributed under the terms of the Creative Commons Attribution License (CC BY). The use, distribution or reproduction in other forums is permitted, provided the original author(s) and the copyright owner(s) are credited and that the original publication in this journal is cited, in accordance with accepted academic practice. No use, distribution or reproduction is permitted which does not comply with these terms.

Editorial: Meningioma: From basic research to clinical translational study, volume II

Hailiang Tang[1,2,3,4,5†], Zhewei Shen[1,2,3,4,5†], David D. Eisenstat[6,7*] and Ian F. Dunn[8*]

[1]Department of Neurosurgery, Huashan Hospital, Shanghai Medical College, Fudan University, Shanghai, China, [2]National Center for Neurological Disorders, Shanghai, China, [3]Shanghai Key Laboratory of Brain Function and Restoration and Neural Regeneration, Shanghai, China, [4]Neurosugical Institute of Fudan University, Shanghai, China, [5]Shanghai Clinical Medical Center of Neurosurgery, Shanghai, China, [6]Department of Paediatrics, University of Melbourne, Parkville, VIC, Australia, [7]Murdoch Children's Research Institute, The Royal Children's Hospital Melbourne, Parkville, VIC, Australia, [8]Department of Neurosurgery, University of Oklahoma Health Sciences Center, Oklahoma City, OK, United States

KEYWORDS

meningioma, molecular alteration, genetic mutation, cancer stem cells, targeted therapy

Editorial on the Research Topic
Meningioma: From basic research to clinical translational study, volume II

The last Research Topic "*Meningioma: From Basic Research to Clinical Translational Study*" published in ***Frontiers in Oncology*** (1), featured more than 40 papers on meningiomas discussing aspects of basic research, clinical management, and adjuvant therapies (1). This time, in the 31 manuscripts included in Research Topic II, papers mainly covered advances in molecular genetics of meningiomas and targeted therapies for these tumors.

1 Molecular genetic alterations in meningiomas

Meningiomas are thought to arise from the meninges and many studies are currently focused on meningeal tumorigenesis mechanisms (2, 3). The landmark 2021 World Health Organization (WHO) edition of the classification of central nervous system (CNS) tumors endorsed, for the first time, molecular grading schemes for meningiomas with tumor classification based on genetic/epigenetic alterations (4–6), including methylation patterns, copy number alterations and driver mutations, such as TERT promoter mutation, and homozygous CDKN2A/B deletion in anaplastic meningiomas. Deng et al. found that *TERT* alterations were strongly associated with tumor progression and poor outcome of *de novo* high-grade meningiomas patients after postoperative adjuvant radiotherapy.

In addition, several reviews included in this Research Topic highlighted our current understanding of the molecular and genetic alterations in meningiomas. Peng et al. suggested that thorough understanding of these changes will assist in identifying "high-risk" factors for recurrent and progressive meningiomas with a view towards establishing personalized and precise therapy for patients with meningioma. Wang et al. discussed preclinical and clinical evidence of molecular classification schemes for meningioma

prognostication. Kim et al. explored the clinical significance of next-generation sequencing in characterizing the molecular profiles of high-grade meningiomas.

There is accumulating evidence that the WHO grade alone may not provide an adequate prediction of meningioma behavior (6). In their study, Roehrkasse et al. proposed the integration of routine molecular profiling with histopathologic grading to guide clinical decision-making strategies in patients with meningiomas. Moreover, Chen et al. suggested that the N6-methylation (m6A) regulators segregated meningiomas into two distinct m6A clusters, which correlated with different m6A regulator gene expression and immune cell infiltration.

2 Translational therapies for meningiomas

Molecular data can inform future directions in therapeutic strategies for meningioma. Currently, multiple targetable genetic alterations have been identified in meningiomas, and targeted therapies (including focal adhesion kinase inhibitor GSK2256098 and CDK4/6 inhibitors) are being clinically evaluated in meningioma patients (7, 8). Lynes et al. discussed molecular classification schemes for meningiomas, and reviewed current multi-targeted therapies for meningiomas. Young et al. systematically described the preclinical evidence for CDK4/6 inhibitors as therapies for high-grade meningiomas, and summarized clinical trials with these inhibitors. Patel et al. comprehensively summarized their experience regarding three cases of progressive meningiomas, and discussed targeted drug treatment for aggressive and recurrent meningiomas.

Along with the advances in molecular characterization of meningiomas, there has been recent progress in understanding the immune profile of meningiomas. The meningioma immune microenvironment mostly comprises macrophages, T cells and mast cells. Kannapadi et al. in their excellent review described the immune signatures of meningiomas and discussed the interactions between molecular patterns and immune signatures in meningiomas. Moreover, they detailed several clinical trials using immunotherapy in meningiomas. Programmed death-ligand 1 (PD-L1) is one of the most frequently studied immune checkpoint molecules in meningiomas, and clinical trials on PD-1 blockade have been reported (9, 10). Furthermore, in the cellular and rodent model level, Deng et al. demonstrated that the expression of nicotinamide phosphoribosyltransferase (NAMPT) is upregulated in anaplastic meningiomas, and that the NAMPT inhibitor-FK866 can significantly suppress the growth of anaplastic meningiomas. Moreover, FK866 can inhibit PD-L1 expression in anaplastic meningiomas.

3 Radiomics enabled prediction models for meningiomas

Histopathological grading alone is insufficient to achieve optimal risk stratification. In fact, it is clinically difficult to predict postoperative recurrence and guide individual treatment decisions only by tumor classification. In this Research Topic collection, several papers using radiological techniques for meningioma prediction are included. Zhang et al. in their study generated an MRI-based prediction model of meningioma recurrence after surgery, which was coupled with clinical prognostic factors and histopathological grades. Chen et al. established an integrated model based on clinical, radiological and pathological factors to predict the postoperative recurrence of atypical meningioma. Sun et al. used a combination of radiomics analysis and machine learning, showing clinical utility in the prediction of preoperative NF2 status in meningiomas. Li et al. constructed a model for predicting brain invasion in WHO grade II meningioma by using preoperative MRI. Takase et al. assumed that bone invasion may be a preoperative predictor of the extent of surgical resection for meningiomas.

Interestingly, Roytman et al. used combined PET/MRI to demonstrate a significant correlation between tumor vascularity and somatostatin receptor-2 (SSTR2) expression in WHO II/III, but not in WHO I meningiomas, suggesting biological differences in the relationship between tumor vascularity and SSTR2 expression in higher-grade meningiomas. Chen et al. differentiated intracranial hemangiopericytoma/solitary fibrous tumor (HPC/SFT) and meningioma *via* deep learning approaches based on preoperative MRI. HPC/SFT have similar radiological characteristics as meningioma, but with different clinical management and outcomes. In addition, Fan et al. also used a clinical-radiomic model to preoperatively distinguish HPC and angiomatous meningioma.

4 Clinical management for meningiomas

Meningiomas are very common brain tumors, and diverse in intracranial locations and behavior. In this Research Topic, several papers discussing localization features and clinical therapies for meningiomas were also collected. In the parasagittal meningiomas derived from arachnoidal cap cells distributed in the arachnoid granulations, Ye et al. used anatomical and histological techniques to reveal the different anatomical types of arachnoid granulations. Based on these features, they speculated on the different growth patterns of parasagittal meningioma, which can guide the neurosurgeon to remove the tumor safely. Yamada et al. identified factors predictive of clinical symptoms in patients with convexity, parasagittal and falx meningiomas, which may be useful in improving management of patients. Mederer et al. showed that surgical resection leads to long-term improvement of neurological impairment in the majority of patients with non-skull base meningiomas. However, tumor location, biology and extent of resection are essential factors influencing neurological outcome.

Unlike more superficially based tumors, meningiomas deeply located inside the skull and adjacent to critical neurovascular structures are more challenging to access and more difficult to resect. Gao et al. concluded that the optimal surgical approach for

petroclival meningiomas (PCMs) depends on the size, extension of the tumor and the anatomical relationship between the tumor and the cranial nerves. Ding et al. showed combined microscopic-endoscopic surgery for pineal region meningiomas eliminates microscopic blind spots, thus compensating for the shortcomings of the traditional occipital transtentorial approach. Liu et al. introduced their experiences in the management of falcotentorial junction tumors, and concluded that the surgical approach selection depends on the growth characteristics of the tumor and venous or sinus involvement.

For large meningiomas, adjuvant treatments may also be used. Yin et al. showed that preoperative embolization can significantly lower surgical complications and long-term disabilities for meningioma patients. Gong et al. investigated the efficiency and safety of dose-staged Gamma Knife radiosurgery as an alternative option for large volume meningiomas adjacent to critical structures. Consensus regarding the need for adjuvant radiotherapy in patients with atypical meningiomas has not been reached. Song et al demonstrated that regardless of either gross total resection or subtotal resection of the tumor, postoperative radiotherapy improved progression-free survival and overall survival for patients.

5 Conclusions

Meningioma recurrence is related to multiple factors, including age, extent of surgical excision, and histological grade as the currently accepted surrogate for our understanding of tumor behavior, though this is challenged by our understanding of genomics and epigenomics. Recently, an increasing number of studies have reported that the presence of cancer stem cells (CSCs) within meningioma is closely associated with tumor aggressiveness, recurrence and therapy resistance (11, 12). Furthermore, patient-derived xenograft (PDX) models using patient-derived tumor cells transplanted into immunodeficient mice have also emerged as important tools for translational research in meningiomas (13).

Author contributions

HT wrote the manuscript, ZS collected the references, and DE and ID revised the manuscript. All authors contributed to the article and approved the submitted version.

Funding

DE is supported by an establishment grant from the Royal Children's Hospital Foundation, Parkville VIC Australia (2019-1193).

Acknowledgments

We are very grateful to the journal (***Frontiers in Oncology***) for providing us an additional opportunity to organize the research topic on meningiomas. We thank all the authors who contributed to this research topic, and thank all the potential readers. Also, we express our gratitude to all the reviewers who contributed to the peer review process. Finally, we would like to thank all of the journal editors for assisting us in the processes and completion of this meningioma Research Topic.

Conflict of interest

The authors declare that the research was conducted in the absence of any commercial or financial relationships that could be construed as a potential conflict of interest.

Publisher's note

All claims expressed in this article are solely those of the authors and do not necessarily represent those of their affiliated organizations, or those of the publisher, the editors and the reviewers. Any product that may be evaluated in this article, or claim that may be made by its manufacturer, is not guaranteed or endorsed by the publisher.

References

1. Ho A, Tang H. Editorial: Meningioma: From basic research to clinical translational study. *Front Oncol* (2021) 11:750690. doi: 10.3389/fonc.2021.750690

2. Boetto J, Peyre M, Kalamarides M. Meningiomas from a developmental perspective: exploring the crossroads between meningeal embryology and tumorigenesis. *Acta Neurochir (Wien)* (2021) 163(1):57–66. doi: 10.1007/s00701-020-04650-w

3. Preusser M, Brastianos PK, Mawrin C. Advances in meningioma genetics: Novel therapeutic opportunities. *Nat Rev Neurol* (2018) 14(2):106–15. doi: 10.1038/nrneurol.2017.168

4. Louis DN, Perry A, Wesseling P, Brat DJ, Cree IA, Figarella-Branger D, et al. The 2021 WHO classification of tumors of the central nervous system: A summary. *Neuro Oncol* (2021) 23(8):1231–51. doi: 10.1093/neuonc/noab106

5. Gritsch S, Batchelor TT, Gonzalez Castro LN. Diagnostic, therapeutic, and prognostic implications of the 2021 world health organization classification of tumors of the central nervous system. *Cancer* (2022) 128(1):47–58. doi: 10.1002/cncr.33918

6. Nassiri F, Liu J, Patil V, Mamatjan Y, Wang JZ, Hugh-White R, et al. A clinically applicable integrative molecular classification of meningiomas. *Nature* (2021) 597 (7874):119–25. doi: 10.1038/s41586-021-03850-3

7. Brastianos PK, Twohy EL, Gerstner ER, Kaufmann TJ, Iafrate AJ, Lennerz J, et al. Alliance A071401: Phase II trial of focal adhesion kinase inhibition in meningiomas with somatic NF2 mutations. *J Clin Oncol* (2023) 41(3):618–28. doi: 10.1200/JCO.21.02371

8. Das A, Alshareef M, Martinez Santos JL, Porto GBF, McDonald DG, Infinger LK, et al. Evaluating anti-tumor activity of palbociclib plus radiation in anaplastic and radiation-induced meningiomas: Pre-clinical investigations. *Clin Transl Oncol* (2020) 22(11):2017–25. doi: 10.1007/s12094-020-02341-7

9. Bi WL, Nayak L, Meredith DM, Driver J, Du Z, Hoffman S, et al. Activity of PD-1 blockade with nivolumab among patients with recurrent atypical/anaplastic meningioma: Phase II trial results. *Neuro Oncol* (2022) 24(1):101–13. doi: 10.1093/neuonc/noab118

10. Brastianos PK, Kim AE, Giobbie-Hurder A, Lee EQ, Wang N, Eichler AF, et al. Phase 2 study of pembrolizumab in patients with recurrent and residual high-grade meningiomas. *Nat Commun* (2022) 13(1):1325. doi: 10.1038/s41467-022-29052-7

11. Shivapathasundram G, Wickremesekera AC, Tan ST, Itinteang, T. Tumour stem cells in meningioma: A review. *J Clin Neurosci* (2018) 47:66–71. doi: 10.1016/j.jocn.2017.10.059

12. Tang H, Zhu H, Wang X, Hua L, Li J, Xie Q, et al. KLF4 is a tumor suppressor in anaplastic meningioma stem-like cells and human meningiomas. *J Mol Cell Biol* (2017) 9(4):315–24. doi: 10.1093/jmcb/mjx023

13. Kim E, Kim M, So K, Park YS, Woo CG, Hyun SH, et al. Characterization and comparison of genomic profiles between primary cancer cell lines and parent atypical meningioma tumors. *Cancer Cell Int* (2020) 20:345. doi: 10.1186/s12935-020-01438-x

frontiers in Oncology

ORIGINAL RESEARCH
published: 07 October 2021
doi: 10.3389/fonc.2021.754937

Establishment and Validation of an Integrated Model to Predict Postoperative Recurrence in Patients With Atypical Meningioma

Xiao-Yong Chen[1†], Jin-Yuan Chen[2†], Yin-Xing Huang[3†], Jia-Heng Xu[1], Wei-Wei Sun[1], Yue- Chen[1], Chen-Yu Ding[1,4], Shuo-Bin Wang[1], Xi-Yue Wu[1], De-Zhi Kang[1,4,5], Hong-Hai You[1*] and Yuan-Xiang Lin[1*]*

[1] Department of Neurosurgery, Neurosurgical Research Institute, The First Affiliated Hospital, Fujian Medical University, Fuzhou, China, [2] Department of Ophthalmology, The First Affiliated Hospital, Fujian Medical University, Fuzhou, China, [3] Department of Neurosurgery, Fuzong Clinical Medical College of Fujian Medical University, Fuzhou, China, [4] Fujian Key Laboratory of Precision Medicine for Cancer, The First Affiliated Hospital, Fujian Medical University, Fuzhou, China, [5] Key Laboratory of Radiation Biology of Fujian Higher Education Institutions, The First Affiliated Hospital, Fujian Medical University, Fuzhou, China

OPEN ACCESS

Edited by:
Hailiang Tang,
Fudan University, China

Reviewed by:
Soichi Oya,
Saitama Medical University, Japan
Bharat Guthikonda,
Louisiana State University Health Shreveport, United States

***Correspondence:**
De-Zhi Kang
kdz99999@sina.com
Hong-Hai You
297183067@qq.com
Yuan-Xiang Lin
lyx99070@163.com

[†]These authors have contributed equally to this work and share first authorship

Specialty section:
This article was submitted to Neuro-Oncology and Neurosurgical Oncology, a section of the journal Frontiers in Oncology

Received: 07 August 2021
Accepted: 15 September 2021
Published: 07 October 2021

Citation:
Chen X-Y, Chen J-Y, Huang Y-X, Xu J-H, Sun W-W, Chen Y-, Ding C-Y, Wang S-B, Wu X-Y, Kang D-Z, You H-H and Lin Y-X (2021) Establishment and Validation of an Integrated Model to Predict Postoperative Recurrence in Patients With Atypical Meningioma. Front. Oncol. 11:754937. doi: 10.3389/fonc.2021.754937

Background: This study aims to establish an integrated model based on clinical, laboratory, radiological, and pathological factors to predict the postoperative recurrence of atypical meningioma (AM).

Materials and Methods: A retrospective study of 183 patients with AM was conducted. Patients were randomly divided into a training cohort (n = 128) and an external validation cohort (n = 55). Univariable and multivariable Cox regression analyses, the least absolute shrinkage and selection operator (LASSO) regression analysis, time-dependent receiver operating characteristic (ROC) curve analysis, and evaluation of clinical usage were used to select variables for the final nomogram model.

Results: After multivariable Cox analysis, serum fibrinogen >2.95 g/L (hazard ratio (HR), 2.43; 95% confidence interval (CI), 1.05–5.63; $p = 0.039$), tumor located in skull base (HR, 6.59; 95% CI, 2.46-17.68; $p < 0.001$), Simpson grades III–IV (HR, 2.73; 95% CI, 1.01–7.34; $p = 0.047$), tumor diameter >4.91 cm (HR, 7.10; 95% CI, 2.52–19.95; $p < 0.001$), and mitotic level ≥4/high power field (HR, 2.80; 95% CI, 1.16–6.74; $p = 0.021$) were independently associated with AM recurrence. Mitotic level was excluded after LASSO analysis, and it did not improve the predictive performance and clinical usage of the model. Therefore, the other four factors were integrated into the nomogram model, which showed good discrimination abilities in training cohort (C-index, 0.822; 95% CI, 0.759–0.885) and validation cohort (C-index, 0.817; 95% CI, 0.716–0.918) and good match between the predicted and observed probability of recurrence-free survival.

Conclusion: Our study established an integrated model to predict the postoperative recurrence of AM.

Keywords: atypical meningioma, recurrence, predict, LASSO, nomogram, model

INTRODUCTION

Meningioma is a common primary brain tumor that comprises about 36.4% of all central nervous system (1). According to the 2016 World Health Organization (WHO) grading criterion (2), meningioma has been classified into three grades. WHO grade II meningioma, which is named as atypical meningioma (AM), is rare and more progressive and invasive compared with WHO grade I meningioma, with 5-year recurrence rates ranging from 30% to 60% after surgical resection (3–6). Therefore, identifying predictive factors for recurrence is important to individually manage AM patients. To date, reliable prediction for recurrence of AM patients remains challenging.

At present, pathological diagnosis is the gold standard for the diagnosis of AM. The incidence of this disease is relatively small, and it accounts a relatively small proportion in meningioma. Therefore, prospective studies for AM are difficult to perform. Performing additional retrospective reviews on AM patients could analyze and summarize the characteristics and risk factors for recurrence of those patients, which could provide assistance for preoperative AM diagnosis, postoperative recurrence prediction, and personalized follow-up regimen development. Many factors, including age, extent of resection, tumor location, mitotic index, Ki-67 index, postoperative radiation therapy (PORT), and serum biomarkers have been identified as effective predictive factors of recurrence and prognosis in AM (7–11). However, the current evidence exploring the risk factors for recurrence in AM patients remains equivocal. Considering the limited precision and effectiveness of a single risk factor, an integrated model with multiple factors may be more suitable for recurrence prediction.

Here, we propose an integrated model based on clinical, laboratory, radiological, and pathological factors to predict the recurrence of AM patients after surgical resection, which assists us to predict the therapeutic effects in the heterogeneous patients and make individualized follow-up management.

METHOD

Study Cohort

The medical records of 183 patients diagnosed as AM who received surgical resection at the First Affiliated Hospital of Fujian Medical University and Fuzong Clinical Medical College of Fujian Medical University between January 2011 and June 2019 were retrospectively reviewed. The study was approved by the local ethics committee of the First Affiliated Hospital of Fujian Medical University and Fuzong Clinical Medical College of Fujian Medical University. It was conducted in accordance with the ethical guidelines of the Declaration of Helsinki. Informed consent was waived for this retrospective study. The eligibility criteria for inclusion were as follows: (1) age ≥18 years old; (2) diagnosis of AM was confirmed by pathological examination. Patients operated on before 2016 were examined for pathological results to confirm the diagnosis based on 2016 WHO criterion (2); (3) complete medical records including clinical, laboratory, imaging, and pathological information; (4) no history of surgical treatment and adjuvant therapy before admission; and (5) no other tumor, autoimmune, and inflammatory diseases. There were 29 AM patients which were excluded because of lack of specific information.

Data Collection and Follow-Up

Patient information were retrieved from medical records at the first Affiliated Hospital of Fujian Medical University. For each patient, the following information was obtained: age, sex, comorbid condition, preoperative routine serum test, tumor features (location, size, peritumoral edema) based on computed tomography (CT) or magnetic resonance imaging (MRI), extent of resection (Simpson grades I–II or Simpson grades III–IV), skull invasion, immunohistochemical features (mitotic level and Ki-67 index), and PORT. Tumor features in the MRI were independently assessed by two experienced neurosurgeons who were blind to patient characteristics. Similarly, the pathological diagnoses of all patients were confirmed by two experienced pathologists according to the 2016 WHO CNS tumor grading criterion (2). Based on the preoperative routine serum test, neutrophil-to-lymphocyte ratio (NLR), platelet-to-lymphocyte ratio (PLR), lymphocyte–monocyte ratio (LMR), and systemic inflammatory response index (SIRI) were calculated as follows: NLR = neutrophil/lymphocyte, PLR = platelet/lymphocyte, LMR = lymphocyte/monocyte, and SIRI = monocyte × neutrophil/lymphocyte.

In addition to the first reexamination within 1 month after surgery, patients were regularly screened for recurrence by contrast-enhanced CT or MRI every 3 months in the first year, every 6 months in the second year, and annually thereafter. The primary endpoint was recurrence-free survival (RFS), defined as the time from surgery to initial recurrence (12).

The cutoff values of several serum biomarkers and tumor diameter for predicting tumor recurrence was determined by the receiver operating characteristic (ROC) curve analysis as follows, NLR = 2.59, PLR = 74.9, LMR = 5.46, SIRI = 0.77, serum fibrinogen (FIB) = 2.95 g/L, and tumor diameter = 4.91 cm.

Model Building and Statistics

Considering the sample size of our study, we used training cohort and validation cohort without test cohort during modeling process. Patients were randomly assigned into training cohort ($n = 128$) and validation cohort ($n = 55$) at a common ratio of 7:3 (13) to avoid the potential bias associated with small sample size of validation set. Based on our own experience and previous studies, we hypothesized that a constellation of clinical, laboratory, imaging, and immunohistochemical parameters were related to the recurrence of AM. Continuous factors such as age, mitotic level, and Ki-67 index were turned into dichotomies as suggestions proposed by previous study (14). Univariable Cox regression analysis was initially utilized to identify potential predictive factors for tumor recurrence. Factors with a p-value less than 0.10 in the univariable Cox regression analysis were further analyzed by multivariable analysis. Nonsignificant factors ($p \geq 0.05$) were removed from the model by forward elimination procedure. The factors left after the stepwise procedure of multivariable analysis were further included in the least absolute shrinkage and selection

operator (LASSO) regression analysis in order to avoid overfitting or underfitting of the model. The models were compared before (model A) and after (model B) LASSO regression analysis based on predictive performance and clinical usage. Time-dependent ROC curve was utilized to evaluate the accuracy and effectiveness of the two models at different time points. Decision curve analyses (DCA), integrated discrimination improvements (IDI), and Net Reclassification Index (NRI) were applied to assess and compare the clinical usage of the two models.

After a comprehensive comparison, the final model was applied to establish a nomogram to predict the probability of RFS at 2, 3, and 5 years. In both training and validation cohorts, the discrimination ability of the nomogram was evaluated by Harrell's concordance index (C-index), and the consistency between the actual and predicted RFS rate was confirmed by the calibration curve.

Statistical analysis was performed by SPSS 19.0 statistical software (SPSS, Inc., Chicago, IL, USA) and R statistical software (R version 4.0.3, R Project, www.r-project.org). Continuous variables were presented as mean ± standard deviation (data with normal distribution) for two-sample *t*-test or median (range) (data without normal distribution) for Mann-Whitney *U* test. Categorical variables were presented as frequency (percentage) and compared with Pearson Chi-square test or Fisher exact test. All statistical tests were two sided, and statistical significance was set at $p < 0.05$.

RESULTS

Patient Characteristics

The general characteristics of all patients and comparison of two cohorts were presented in **Table 1**. Of the 183 patients, 63 patients were male and 120 patients were female; the proportion of patients with age ≥60 years was 33.9%. The proportion of recurrence ($p = 0.154$) showed gratifying similarity between the training cohort and the validation cohort. In addition, the other parameters showed the two cohorts were homogeneous and comparable, indicating that the data were reliable with high quality.

The median length of follow-up, RFS, and overall survival of the included patients were 50.00 months (34.00–77.00), 25.50 months (14.00–37.25), and 34.00 months (31.00–48.00), respectively. In the 25 patients with Simpson grades III–IV, the patients with PORT had a longer RFS than those without PORT (54.00 *vs* 17.50 months, $p = 0.034$).

Predictive Factors of Recurrence in the Training Cohort

The ROC curve analysis showed that NLR = 2.59, PLR = 74.90, LMR = 5.46, SIRI = 0.77, FIB = 2.95 g/L, and tumor diameter = 4.91 cm were the optimal cutoff values (**Table 2**). Based on the corresponding cutoff values, the area under curve (AUC) of NLR, PLR, LMR, SIRI, FIB, and tumor diameter were 0.638 (95% confidence interval (CI), 0.549–0.721), 0.503 (95% CI, 0.414–0.593), 0.550 (95% CI, 0.459–0.638), 0.570 (95% CI, 0.479–0.657), 0.679 (95% CI, 0.591–0.759), and 0.702 (95% CI, 0.615–0.780), respectively; the sensitivity of NLR, PLR, LMR, SIRI, FIB, and tumor diameter were 59.26%, 100.00%, 59.26%, 59.26%, 66.67%, and 74.07%, respectively; the specificity of NLR, PLR, LMR, SIRI, FIB, and tumor diameter were 75.25%, 7.92%, 55.45%, 65.35%, 75.25%, and 59.41%, respectively; the *Youden* index of NLR, PLR, LMR, SIRI, FIB, and tumor diameter were 0.345, 0.079, 0.147, 0.246, 0.419, and 0.335, respectively.

The univariable analysis showed that neutrophil count (HR, 1.13; 95% CI, 0.98–1.30; $p = 0.092$), NLR >2.59 (HR, 3.62; 95% CI, 1.67–7.82; $p = 0.001$), SIRI >0.77 (HR, 2.50; 95% CI, 1.14–5.47; $p = 0.022$), FIB >2.95 g/L (HR, 3.56; 95% CI, 1.65–7.69; $p = 0.001$), tumor located in skull base (HR, 2.63; 95% CI, 1.18–5.86; $p = 0.018$), Simpson grades III–IV (HR, 2.53; 95% CI, 1.07–5.98; $p = 0.035$), tumor diameter >4.91 cm (HR, 3.97; 95% CI, 1.68–9.41; $p = 0.002$), mitotic level ≥4/high-power field (HR, 2.21; 95% CI, 1.04–4.70; $p = 0.040$), and PORT (HR, 2.18; 95% CI, 0.95–5.00; $p = 0.065$) were associated with AM recurrence (**Table 3**). In the multivariable analysis, FIB >2.95 g/L (HR, 2.43; 95% CI, 1.05–5.63; $p = 0.039$), tumor located in skull base (HR, 6.59; 95% CI, 2.46–17.68; $p < 0.001$), Simpson grades III–IV (HR, 2.73; 95% CI, 1.01–7.34; $p = 0.047$), tumor diameter >4.91 cm (HR, 7.10; 95% CI, 2.52–19.95; $p < 0.001$), and mitotic level ≥4/high-power field (HR, 2.80; 95% CI, 1.16–6.74; $p = 0.021$) were independently associated with AM recurrence (**Table 3**).

Variable Selection for Final Model Based on LASSO Regression Analysis and Time-Dependent ROC, DCA, IDI, and NRI

The LASSO regression analysis was utilized to identify whether there were overfitting or underfitting in the five independent risk factors for the recurrence (**Figure 1**). The optimal λ (one standard error of the minimum criteria) was selected with a value of 0.08 and four nonzero coefficients. Considering the clinical importance of mitotic level and its exclusion by LASSO regression analysis, we established two models: ModelA, all the five independent risk factors including mitotic level; ModelB, all the independent prognostic factors without mitotic level (**Table 4**).

The time-dependent ROC curves of the two models showed that they both have good predictive performance (AUC >0.7) in the training cohort and validation cohort during the follow-up time (**Figure 2**). Overall, the predictive performance of model B was slightly better than model A in the training cohort but slightly weaker than model A in the first half of the follow-up time in the validation cohort. Comparison of the clinical usage of the two models in the training cohort and validation cohort evaluated by DCA, IDI, and NRI were as follows: the 2-, 3-, and 5-year DCA curves showed that the net benefit of ModelB could be better or worse than model A at different risk thresholds (**Figure 3**); as shown in **Figure 4**, the IDI approach indicated that the clinical utility of model B was similar to model A in both training cohort (2 years after surgery: IDI = −0.01, 95% CI = −0.09–0.04, $p > 0.05$; 3 years after surgery: IDI = −0.01, 95% CI = −0.09–0.04, $p > 0.05$; 5 years after surgery: IDI = −0.02, 95% CI = −0.14–0.04, $p > 0.05$) and validation cohort (2 years after surgery: IDI = 0, 95% CI = −0.07–0.02, $p > 0.05$; 3 years after surgery: IDI = 0, 95% CI = −0.08–0.02, $p > 0.05$; 5 years after

TABLE 1 | Characteristics of patients in the training and validation cohorts.

Characteristic	All (*n* = 183)	Training cohort (*n* = 128)	Validation cohort (*n* = 55)	*p*-Value
Demographics				
Age				
<60 years	121 (66.1%)	80 (62.5%)	41 (74.5%)	0.114
≥60 years	62 (33.9%)	48 (37.5%)	14 (25.5%)	
Sex				
Male	63 (34.4%)	49 (38.3%)	14 (25.5%)	0.094
Female	120 (65.6%)	79 (61.7%)	42 (74.5%)	
Comorbid condition				
Hypertension				
No	151 (82.5%)	104 (81.3%)	47 (85.5%)	0.492
Yes	32 (17.5%)	24 (18.8%)	8 (14.5%)	
Diabetes mellitus				
No	175 (95.6%)	121 (94.5%)	54 (98.2%)	0.476
Yes	8 (4.4%)	7 (5.5%)	1 (1.8%)	
Laboratory data				
RBC count 10^9/L	4.51 (4.17–4.80)	4.56 (4.17–4.87)	4.41 (4.18–4.71)	0.107
WBC count 10^9/L	6.01 (5.10–7.40)	6.03 (5.09–7.46)	5.81 (5.10–7.40)	0.754
NEU count 10^9/L	3.67 (2.92–5.19)	3.52 (2.83–5.11)	4.05 (3.16–5.35)	0.117
MON count 10^9/L	0.35 (0.25–0.45)	0.35 (0.27–0.46)	0.35 (0.23–0.45)	0.535
LYM count 10^9/L	1.82 (1.52–2.19)	1.82 (1.53–2.18)	1.76 (1.48–2.20)	0.757
PLT count 10^9/L	236.00 (190.05–279.00)	234.50 (187.76–276.75)	236.25 (196.00–289.80)	0.431
NLR	2.00 (1.53–3.04)	1.95 (1.52–2.74)	2.61 (1.55–3.31)	0.073
PLR	125.22 (102.12–158.95)	121.22 (99.61–155.24)	131.25 (104.60–171.14)	0.296
LMR	5.58 (4.24–6.90)	5.32 (4.14–6.58)	5.91 (4.48–7.25)	0.209
SIRI	0.66 (0.42–1.10)	0.66 (0.42–1.10)	0.66 (0.42–1.10)	0.944
FIB (g/L)	2.75 (2.43–3.36)	2.69 (2.39–3.26)	2.81 (2.54–3.42)	0.165
HB (g/L)	132.26 ± 14.80	133.33 ± 15.69	129.76 ± 12.27	0.134
Tumor features and surgical factors				
Location				
Nonskull base	141 (77.0%)	101 (78.9%)	40 (72.7%)	0.362
Skull base	42 (23.0%)	27 (21.1%)	15 (27.3%)	
Tumor diameter (cm)	4.93 ± 1.39	4.91 ± 1.49	4.95 ± 1.11	0.859
Peritumoral edema				
≤1 cm	73 (39.9%)	52 (40.6%)	21 (38.2%)	0.757
>1 cm	110 (60.1%)	76 (59.4%)	34 (61.8%)	
Extent of resection				
Simpson grades I–II	158 (86.3%)	112 (87.5%)	46 (83.6%)	0.485
Simpson grades III–IV	25 (13.7%)	16 (12.5%)	9 (16.4%)	
Skull invasion				
No	118 (64.5%)	79 (61.7%)	39 (70.9%)	0.234
Yes	65 (35.5%)	49 (38.3%)	16 (29.1%)	
Immunohistochemical feature				
Mitotic level				
<4/HPF	116 (63.4%)	84 (65.6%)	32 (58.2%)	0.338
≥4/HPF	67 (36.6%)	44 (34.4%)	23 (41.8%)	
Ki-67 index				
<5%	113 (61.7%)	79 (61.7%)	34 (61.8%)	0.990
≥5%	70 (38.3%)	49 (38.3%)	21 (38.2%)	
PORT				
No	151 (82.5%)	109 (85.2%)	42 (76.4%)	0.151
Yes	32 (17.5%)	19 (14.8%)	13 (23.6%)	
Recurrence				
No	139 (76.0%)	101 (78.9%)	38 (69.1%)	0.154
Yes	44 (24.0%)	27 (21.1%)	17 (30.9%)	

Values are reported as number, number (%), median (25%–75%), and mean ± standard deviation.
RBC, red blood cell; HCT, hematocrit; WBC, white blood cell; NEU, neutrophil; MON, monocyte; LYM, lymphocyte; PLT, platelet; NLR, neutrophil-lymphocyte ratio; PLR, platelet-to-lymphocyte ratio; LMR, lymphocyte–monocyte ratio; SIRI, systemic inflammatory response index; FIB, fibrinogen; HB, hemoglobin; HPF, high-power field; PORT, postoperative radiation therapy.

surgery: IDI = 0, 95% CI = −0.10–0.04, $p > 0.05$); the NRI approach shown in **Figure 4** indicated that the clinical utility of model B was also similar to model A in both training cohort (2 years after surgery: NRI = −0.09, 95%CI = −0.46–0.24, $p > 0.05$; 3 years after surgery: NRI = −0.09, 95% CI = −0.39–0.19, $p > 0.05$; 5 years after surgery: NRI = −0.11, 95% CI = −0.49–0.25, $p > 0.05$) and validation cohort (2 years after surgery: NRI = −0.11, 95% CI = −0.56–0.59, $p > 0.05$; 3 years after

TABLE 2 | The cutoff value and area under the curve of the possible predictive factors of recurrence in training cohort.

Parameter	Cutoff value	AUC	Sensitivity (%)	Specificity (%)	Youden index	95% CI of AUC	*p*-Value
NLR	2.59	0.638	59.26	75.25	0.345	0.549–0.721	0.026
PLR	74.90	0.503	100.00	7.92	0.079	0.414–0.593	0.957
LMR	5.46	0.550	59.26	55.45	0.147	0.459–0.638	0.433
SIRI	0.77	0.570	59.26	65.35	0.246	0.479–0.657	0.258
FIB	2.95	0.679	66.67	75.25	0.419	0.591–0.759	0.004
Tumor diameter cm	4.91	0.702	74.07	59.41	0.335	0.615–0.780	<0.001

AUC, area under curve; CI, confidence interval; NLR, neutrophil-to-lymphocyte ratio; PLR, platelet-to-lymphocyte ratio; LMR, lymphocyte–monocyte ratio; SIRI, systemic inflammatory response index; FIB, fibrinogen.

TABLE 3 | Univariable and multivariable cox hazard regression analyses of recurrence in the training cohort.

Parameter	Univariable analysis			Multivariable analysis		
	HR	95% CI	*p*-Value	HR	95% CI	*p*-Value
Age ≥60 years	1.72	0.81–3.65	0.162			
Male	0.60	0.28–1.28	0.184			
Hypertension	1.10	0.42–2.92	0.842			
Diabetes mellitus	0.05	0–92.41	0.427			
RBC	1.21	0.60–2.44	0.592			
WBC	1.11	0.96–1.27	0.167			
NEU	1.13	0.98–1.30	0.092			
MON	0.30	0.03–2.98	0.302			
LYM	0.93	0.45–1.90	0.833			
PLT	1.00	1.00–1.01	0.760			
NLR >2.59	3.62	1.67–7.82	0.001			
PLR >74.90	22.50	0.04–14518.00	0.346			
LMR >5.46	1.79	0.83–3.86	0.138			
SIRI >0.77	2.50	1.14–5.47	0.022			
FIB >.95 g/L	3.56	1.65–7.69	0.001	2.43	1.05–5.63	0.039
HB	1.00	0.98–1.03	0.825			
Tumor located in skull base	2.63	1.18–5.86	0.018	6.59	2.46–17.68	<0.001
Tumor diameter >4.91 cm	3.97	1.68–9.41	0.002	7.10	2.52–19.95	<0.001
Peritumoral edema > 1 cm	0.82	0.38–1.79	0.623			
Simpson grades III–IV	2.53	1.07–5.98	0.035	2.73	1.01–7.34	0.047
Skull invasion	1.47	0.69–3.13	0.321			
Mitotic level ≥4/HPF	2.21	1.04–4.70	0.040	2.80	1.16–6.74	0.021
Ki-67 index ≥5%	1.23	0.57–2.66	0.596			
PORT	2.18	0.95–5.00	0.065			

HR, hazard ratio; CI, confidence interval; RBC, red blood cell; WBC, white blood cell; NEU, neutrophil; MON, monocyte; LYM, lymphocyte; PLT, platelet; NLR, neutrophil-lymphocyte ratio; PLR, platelet-to-lymphocyte ratio; LMR, lymphocyte–monocyte ratio; SIRI, systemic inflammatory response index; FIB, fibrinogen; HB, hemoglobin; HPF, high-power field; PORT, postoperative radiation therapy.

surgery: NRI = 0.06, 95% CI = −0.43–0.27, $p > 0.05$; 5 years after surgery: NRI = −0.06, 95% CI = −0.52–0.34, $p > 0.05$).

The above results showed that mitotic level did not bring significant improvement in predictive ability. Thus, the mitotic level was excluded and the more simplified model (model B) was selected.

Establishment and Verification of Nomogram

FIB, tumor location, extent of resection, and tumor diameter were incorporated into the nomogram for recurrence prediction in the training cohort (**Figure 5**). The nomogram showed good discrimination ability (C-index, 0.822; 95% CI, 0.759–0.885). The calibration curves for the RFS rate at 2, 3, and 5 years showed good consistency between the predicted and observed probability (**Figures 6A–C**). In the validation cohort, the model also showed a good prediction with C-index = 0.817 (95% CI, 0.716–0.918). Good match was observed between the predicted and observed probability in this cohort (**Figures 6D–F**).

DISCUSSION

Currently, the treatment strategy for AM is surgical resection. Even with gross total resection, a considerable fraction of patients may recur years after surgery due to the aggressive progression and invasion (4, 5, 8, 10, 11). Patients who received the same treatment regimen may exhibit heterogeneity in tumor growth and recurrence. Another intrinsic challenge for the nuanced investigation of AM recurrence is its low incidence, resulting in a long-time span of the study to achieve sufficient sample size and follow-up duration. In addition, since the shifting of WHO diagnostic criteria over time, studies focused on AM have become more problematic. Precise and reliable model for recurrence

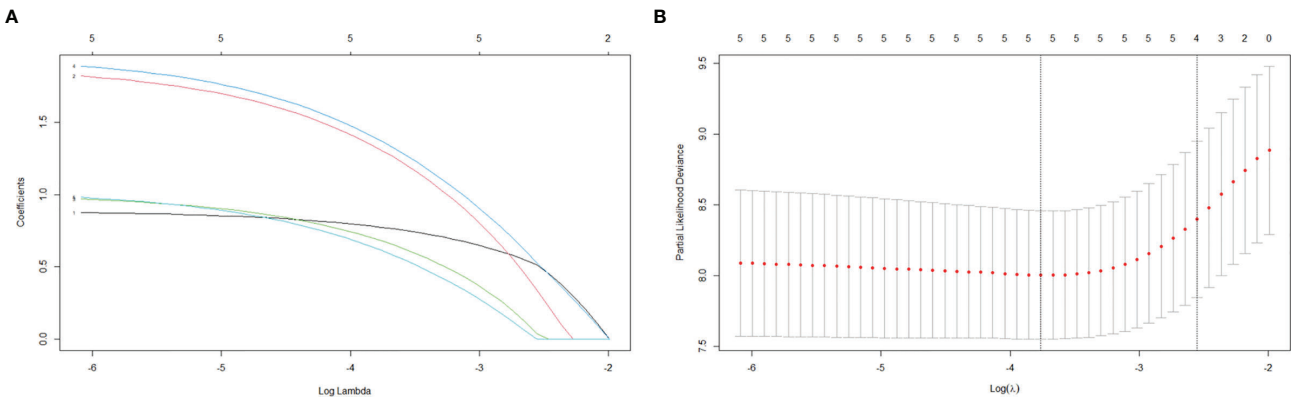

FIGURE 1 | LASSO regression analysis for variable selection. **(A)** LASSO regression coefficients. **(B)** LASSO cross-validation.

TABLE 4 | The composition of two models based on lasso regression analysis.

	Model A			Model B		
	HR	**95% CI**	***p*-Value**	**HR**	**95% CI**	***p*-Value**
FIB >2.95 g/L	2.43	1.05–5.63	0.039	2.73	1.20–6.19	0.016
Tumor located in skull base	6.59	2.46–17.68	<0.001	4.42	1.87–10.45	0.001
Simpson grades III–IV	2.73	1.01–7.34	0.047	2.77	1.06–7.22	0.038
Tumor diameter >4.91 cm	7.10	2.52–19.95	<0.001	4.94	1.99–12.25	0.001
Mitotic level ≥4/HPF	2.80	1.16–6.74	0.021			

HR, hazard ratio; CI, confidence interval; FIB, fibrinogen; HPF, high-power field.

prediction is helpful to guide clinicians in management and follow-up strategy of individual patients. Therefore, predicting recurrence of AM has been an urgent problem and a challenge in clinic.

Considering the interactions of the risk factors and integrating them into a nomogram model may be more practical and reliable for recurrence and prognosis prediction of many malignancies (15, 16). Our study divided the serum biomarkers and tumor diameter as binary variables based on their optimal cutoff value, which may be practical in guiding clinical decision-making. In addition, we divided the patients into a training cohort and a validation cohort based on the ratio of 7:3. The two cohorts were homogeneous and comparable based on the comparison of general characteristics. After multivariable Cox analysis in the training cohort, fibrinogen level, tumor location, extent of resection, tumor diameter, and mitotic level remained independently associated with AM recurrence. Instead of directly applying those factors into a predictive model, we utilized the LASSO regression analysis to avoid over-fitting or under-fitting. This method could analyze all variables at the same time and decrease the estimation variance. After the LASSO regression analysis, mitotic level lost its significance. As part of the diagnostic criteria, mitotic level has been confirmed to be associated with AM recurrence in previous studies (9, 17). To further investigate the impact of mitotic level in recurrence prediction of AM, we established two models according to the independent factors with or without mitotic level. After comparing their predictive performance (time-ROC) and clinical usage (DCA, IDI, NRI), we found that it was hard to determine the improvement of predictive ability brought by mitotic level in both training cohort and validation cohort. Thus, we integrated the other four independent risk factors into the final model and establish a nomogram. The nomogram showed an excellent discriminating ability in both training cohort (C-index: 0.822, 95% CI: 0.759–0.885) and validation cohort (C-index: 0.817, 95% CI: 0.716–0.918). The calibration curves in the both cohorts also showed good consistency between the predicted and observed RFS probability at 2, 3, and 5 years after surgery, which indicated the reliability and repeatability of the nomogram. The results prompted us that early treatment for tumor with small size may reduce the risk of recurrence. Considering those risk factors, surgical strategy may be adjusted to balance the risk of postoperative recurrence and surgical injury in those patients diagnosed as AM *via* intraoperative frozen section analysis. According to our results, we could predict the risk of postoperative recurrence *via* the nomogram based on the obtained risk factors. For those patients with high recurrence risk, shorter follow-up period may be requested to strive for early detection and early treatment.

Fibrinogen is a glycoprotein synthesized in hepatocytes which participates in blood coagulation and is also involved in cancer growth and metastasis (18, 19). Although the mechanism is not clear, the relationship between fibrinogen and tumor progression may be explained as follow: first, deposition of fibrinogen in the extracellular matrix could serve as a scaffold for growth factors and promote cell invasion, adhesion, and migration of tumor (20, 21); second, fibrinogen could induce epithelial-to-mesenchymal transition *via* rapamycin (mTOR)/protein kinase

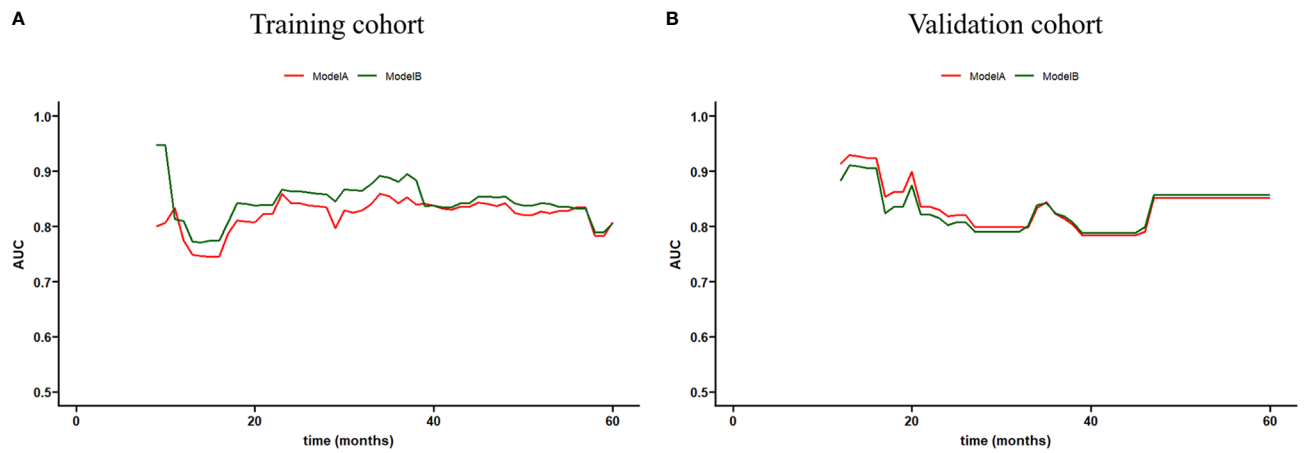

FIGURE 2 | Time-dependent receiver operating characteristic (ROC) curve of models **(A, B)** in the training and validation cohorts.

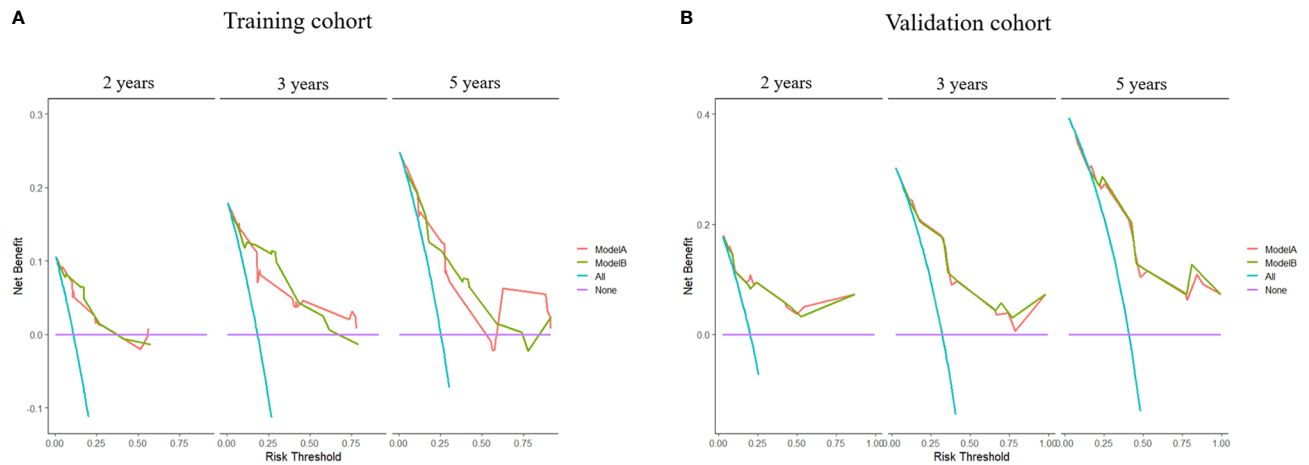

FIGURE 3 | Decision curve analyses (DCA) of models **(A, B)** at 2, 3, and 5 years after surgery in the training cohort and 2, 3, and 5 years after surgery in the validation cohort.

B (AKT) signaling pathway to promote malignant transformation (22); third, the deposition of platelet-fibrin could form physical barrier for tumor cells to prevent the kill contact from NK cell (23) and the platelet-fibrin (OGEN) axis has been confirmed to impede NK cell elimination of tumor cells to promote their metastatic potential (24); fourth, fibrinogen could also be synthesized and released by tumor cells, which in turn promotes tumor cell proliferation *via* the combined effects with growth factors (21, 25, 26). In our study, the preoperative serum fibrinogen level was an independent risk factor of AM recurrence and further included in a predictive model. Serum fibrinogen level in benign meningioma has been confirmed to be significantly lower than that in glioblastomas and metastases (27). Also, in a dog meningioma study, the fibrinogen staining scores in meningioma have been confirmed the gradual increasing trend from WHO grade I to WHO grade III (28). These may provide the basis for the predictive value of fibrinogen in AM recurrence.

Many studies have confirmed the close relationship between extent of resection and AM recurrence (10, 29, 30). In our study, we also found that AM patients with incomplete resection (Simpson grades III–IV) had a higher risk of recurrence. Complete surgical tumor removal is always the goal pursued by surgeons. However, we should acknowledge that tumors located in the skull base are less amenable to be completely resected as they are located adjacent to critical anatomic structures, including cranial nerves, intracranial vessels, and brainstem. Therefore, those patients with tumor located in skull base may inherently have higher risk of tumor residue and recurrence. However, the literature regarding the predictive value of tumor location in AM is rather scarce and controversial. Budohoski et al. reported that parafalcine/parasagittal location was an independent risk factor of

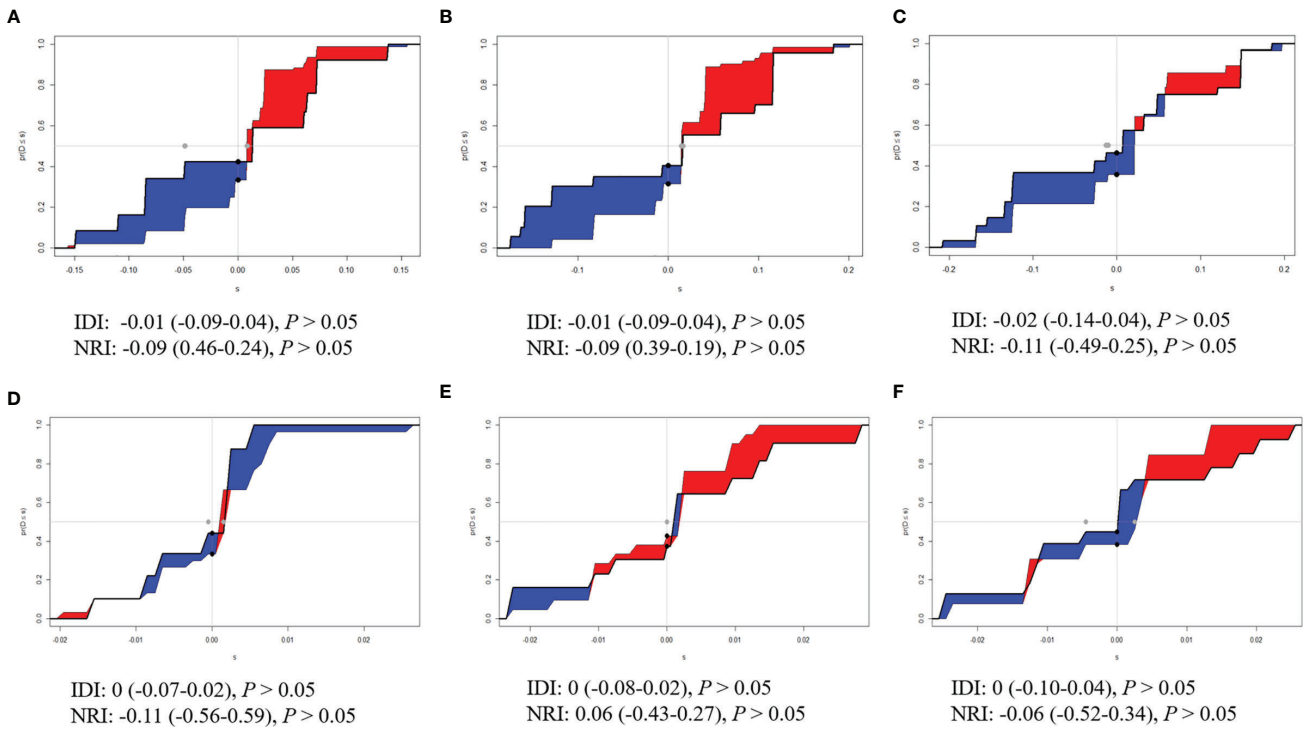

FIGURE 4 | Integrated discrimination improvements (IDI) and Net Reclassification Index (NRI) of model B by comparing with model **(A)**. **(A)** Two years, **(B)** 3 years, and **(C)** 5 years after surgery in the training cohort. **(D)** Two years, **(E)** 3 years, and **(F)** 5 years after surgery in the validation cohort.

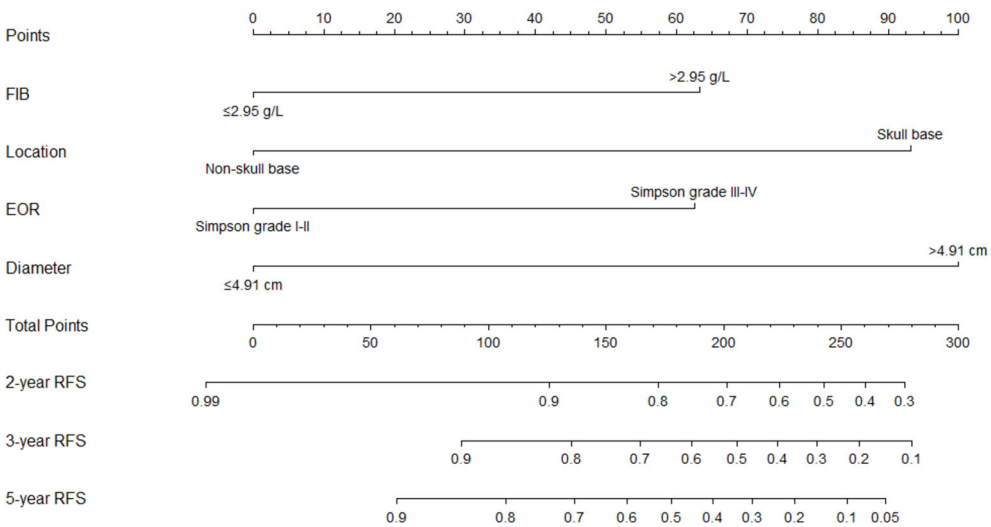

FIGURE 5 | The nomogram for predicting 2-, 3-, and 5-year recurrence-free survival rate of a typical meningioma patients. FIB, fibrinogen; EOR, extent of resection; RFS, recurrence-free survival.

early recurrence in AM (31). Klinger et al. found that tumors located in skull base had a trend towards decreased recurrence in AM (32). However, Da Broi et al. identified a tendency towards more retreatment in AM located in skull base (33). Our study revealed that tumor located in skull base was strongly associated with AM recurrence and excluded from confounding factors in the multivariable Cox analysis. Other than that, tumor size is also an independent risk factor in our study. Although such finding

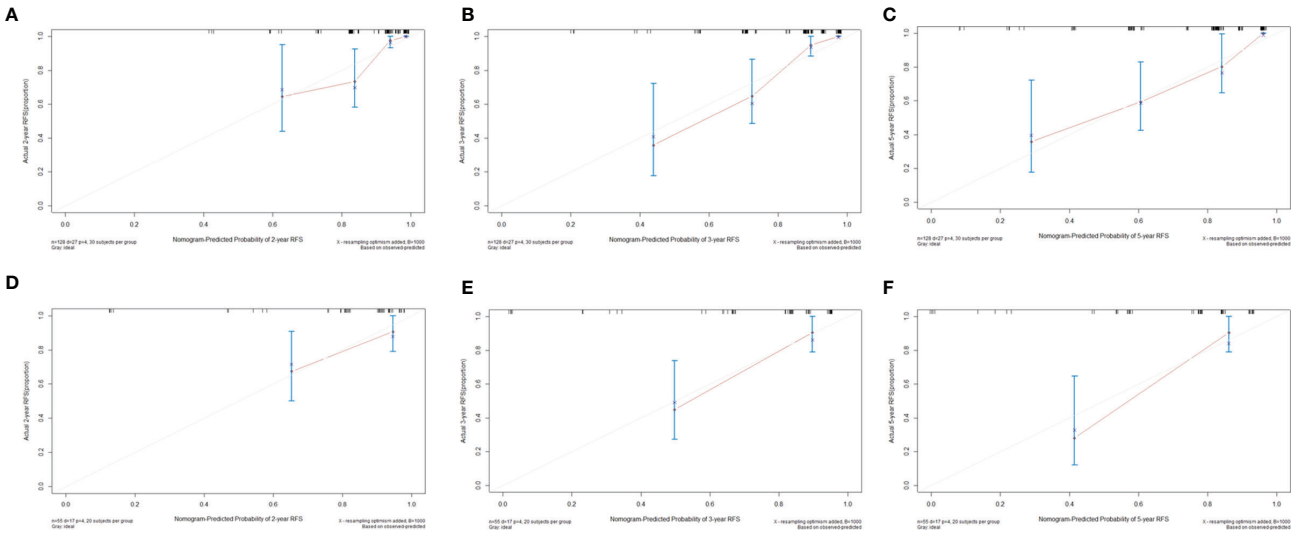

FIGURE 6 | Calibration curves to predict **(A)** 2-year, **(B)** 3-year, and **(C)** 5-year recurrence-free survival rates in the training cohort and **(D)** 2-year, **(E)** 3-year, and **(F)** 5-year recurrence-free survival rates in the validation cohort.

has not been confirmed in other studies, tumor diameter could reflect the growth rate of AM to a certain extent and was confirmed its predictive value in recurrence in other tumors (34, 35). Multiple oncogenic drivers, inhibitors, and regulators could affect tumor growth and survival *via* multiple pathways (36, 37). Therefore, tumor diameter may reflect the combined effects of multiple factors. Our study utilized the ROC analysis to determine the cutoff value of tumor diameter and found that tumor diameter >4.91 cm was independently associated with AM recurrence. The proliferative ability reflected by tumor diameter may explain its relationship with AM recurrence.

Although many studies affirmed the efficacy of PORT in AM recurrence patients (11, 38), there was also contradictory report exist in whether PORT could decrease the risk of AM recurrence (39). For example, Masalha et al. claimed no significant correlation between PORT and AM recurrence (39). There is no consensus guideline on recommendations for AM patients (https://www.nccn.org/professionals/physician_gls/f_guidelines.asp#site). Considering the potential toxicities of PORT, its execution should be considered with caution based on many risk factors of complications, such as age, tumor location and so on. In addition, execution of PORT may also be affected by patients' wishes and their financial capability. In our study, we failed to determine the association between PORT and recurrence risk of AM patients. In the multivariable Cox hazard regression analysis, PORT lost its significance after being adjusted by other factors. Therefore, it was excluded from our final analysis. The European Association of Neuro Oncology guidelines recommend that PORT should be considered in patients with incomplete resection (40). In the 25 patients with Simpson grades III–IV of our study, the patients with PORT had a longer RFS than those without PORT (54.00 *vs.* 17.50 months, $p = 0.034$), revealing the potential therapeutic benefits of PORT in AM patients with incomplete resection. Also, the curative effect of PORT in AM patients should be investigated and validated in further research with a larger sample.

Our study was not free from limitations. First, the retrospective design of the study may suffer the interference and selection bias. Second, some laboratory or immunohistochemical factors were not included in our study due to the lack of examination in the early cases. Also, some molecular profiling and genotyping which have a high impact on predicting the recurrence were not available in our study. Third, the low incidence of the disease limits the collection of large amounts of sample in a short period. Therefore, the patients included in our study were operated both before and after the occurrence of 2016 WHO criterion. With the updated definition of WHO criteria for AM, the proportion of AM was increased. In addition, our study incorporated patients treated as recently as 2019, resulting in a dilution of aggressiveness and recurrence rate in this study cohort due to the combined effects of updated definition of criteria and advancements of medical technology. Fourth, our study did not use objective scale for edema evaluation. Accurate evaluation for edema *via* neuronavigation and objective scale are requested to reduce measurement errors in the further study. Fifth, the mechanism of the relationship between fibrinogen and AM recurrence was not investigated in our study. Further work is needed to address this point.

CONCLUSION

Our study established a comprehensive model for the recurrence prediction in AM patients based on multiple factors, including fibrinogen level, tumor location, extent of resection, and tumor diameter. The nomogram could assist clinicians to predict the treatment effects and make individualized follow-up management in the heterogeneous patients. Further

multicenter and prospective studies with lager sample size are required to verify the accurate application of nomogram.

DATA AVAILABILITY STATEMENT

The raw data supporting the conclusions of this article will be made available by the authors, without undue reservation.

ETHICS STATEMENT

The studies involving human participants were reviewed and approved by the local ethics committee of the First Affiliated Hospital of Fujian Medical University and Fuzong Clinical Medical College of Fujian Medical University. The ethics committee waived the requirement of written informed consent for participation.

AUTHOR CONTRIBUTIONS

Y-XL, H-HY, and D-ZK performed and designed the study and wrote the manuscript. X-YC, J-YC, Y-XH, J-HX, W-WS, Y-C, C-YD, S-BW, and X-YW collected, interpreted, and analyzed the data. All authors contributed to the article and approved the submitted version

FUNDING

This study was supported by grants from the National Natural Science Foundation of China (No. 81901395), Startup Fund for Scientific Research of Fujian Medical University (No. 2018QH1049), the project of improving the diagnosis and treatment ability of complicated diseases (No. PT-YNBZW2018), and Professor Academic Development Fund of Fujian Medical University (No. JS15014).

REFERENCES

1. Ostrom QT, Gittleman H, Fulop J, Liu M, Blanda R, Kromer C, et al. CBTRUS Statistical Report: Primary Brain and Central Nervous System Tumors Diagnosed in the United States in 2008-2012. *Neuro Oncol* (2015) 17 Suppl 4(1523-5866(1523-5866 (Electronic):iv1–iv62. doi: 10.1093/neuonc/nov189
2. Louis DN, Perry A, Reifenberger G, von Deimling A, Figarella-Branger D, Cavenee WK, et al. The 2016 World Health Organization Classification of Tumors of the Central Nervous System: A Summary. *Acta Neuropathol* (2016) 131(6):803–20. doi: 10.1007/s00401-016-1545-1
3. Pasquier D, Bijmolt S, Veninga T, Rezvoy N, Villa S, Krengli M, et al. Atypical and Malignant Meningioma: Outcome and Prognostic Factors in 119 Irradiated Patients. A Multicenter, Retrospective Study of the Rare Cancer Network. *Int J Radiat Oncol Biol Phys* (2008) 71(5):1388–93. doi: 10.1016/j.ijrobp.2007.12.020
4. Cao X, Hao S, Wu Z, Wang L, Jia G, Zhang L, et al. Treatment Response and Prognosis After Recurrence of Atypical Meningiomas. *World Neurosurg* (2015) 84(4):1014–9. doi: 10.1016/j.wneu.2015.05.032
5. Nowak A, Dziedzic T, Krych P, Czernicki T, Kunert P, Marchel A. Benign Versus Atypical Meningiomas: Risk Factors Predicting Recurrence. *Neurol Neurochir Pol* (2015) 49(1):1–10. doi: 10.1016/j.pjnns.2014.11.003
6. Pisćević I, Villa A, Milićević M, Ilić R, Nikitović M, Cavallo LM, et al. The Influence of Adjuvant Radiotherapy in Atypical and Anaplastic Meningiomas: A Series of 88 Patients in a Single Institution. *World Neurosurg* (2015) 83(6):987–95. doi: 10.1016/j.wneu.2015.02.021
7. Sofela AA, McGavin L, Whitfield PC, Hanemann CO. Biomarkers for Differentiating Grade II Meningiomas From Grade I: A Systematic Review. *Br J Neurosurg* (2021) 1360-046X(Electronic):1–7. doi: 10.1080/02688697.2021.1940853
8. Wang D, Sun S, Hua L, Deng J, Luan S, Cheng H, et al. Prognostic Model That Predicts Benefits of Adjuvant Radiotherapy in Patients With High Grade Meningioma. *Front Oncol* (2020) 10(2234-943X:568079(2234-943X (Print). doi: 10.3389/fonc.2020.568079
9. Domingo RA, Tripathi S, Vivas-Buitrago T, Lu VM, Chaichana KL, Quinones-Hinojosa A. Mitotic Index and Progression-Free Survival in Atypical Meningiomas. *World Neurosurg* (2020) 142(1878-8769(1878-8769 (Electronic):191–6. doi: 10.1016/j.wneu.2020.06.189
10. Keric N, Kalasauskas D, Freyschlag CF, Gempt J, Misch M, Poplawski A, et al. Impact of Postoperative Radiotherapy on Recurrence of Primary Intracranial Atypical Meningiomas. *J Neurooncol* (2020) 146(2):347–55. doi: 10.1007/s11060-019-03382-x
11. Phonwijit L, Khawprapa C, Sitthinamsuwan B. Progression-Free Survival and Factors Associated With Postoperative Recurrence in 126 Patients With Atypical Intracranial Meningioma. *World Neurosurg* (2017) 107(1878-8769 (1878-8769 (Electronic):698–705. doi: 10.1016/j.wneu.2017.08.057
12. Liu L, Zheng Z, Li J, Li Y, Ni J. Supraclavicular Recurrence in Completely Resected (Y)Pn2 Non-Small Cell Lung Cancer: Implications for Postoperative Radiotherapy. *Front Oncol* (2020) 10(2234-943X:1414(2234-943X (Print). doi: 10.3389/fonc.2020.01414
13. Shi X, Xu L, Ma B, Wang S. Development and Validation of a Nomogram to Predict the Prognosis of Patients With Gastric Cardia Cancer. *Sci Rep* (2020) 10(1):14143. doi: 10.1038/s41598-020-71146-z
14. Royston P, Moons KG, Altman DG, Vergouwe Y. Prognosis and Prognostic Research: Developing a Prognostic Model. *BMJ* (2009) 338(1756-1833(1756-1833 (Electronic):b604. doi: 10.1136/bmj.b604
15. Han DS, Suh YS, Kong SH, Lee HJ, Choi Y, Aikou S, et al. Nomogram Predicting Long-Term Survival After D2 Gastrectomy for Gastric Cancer. *J Clin Oncol* (2012) 30(31):3834–40. doi: 10.1200/JCO.2012.41.8343
16. Liang W, Zhang L, Jiang G, Wang Q, Liu L, Liu D, et al. Development and Validation of a Nomogram for Predicting Survival in Patients With Resected Non-Small-Cell Lung Cancer. *J Clin Oncol* (2015) 33(8):861–9. doi: 10.1200/JCO.2014.56.6661
17. Barresi VA-O, Lionti S, Caliri S, Caffo M. Histopathological Features to Define Atypical Meningioma: What Does Really Matter for Prognosis? *Brain Tumor Pathol* (2018) 35(3):168–80. doi: 10.1007/s10014-018-0318-z
18. Takeuchi H, Ikeuchi S, Kitagawa Y, Shimada A, Oishi T, Isobe Y, et al. Pretreatment Plasma Fibrinogen Level Correlates With Tumor Progression and Metastasis in Patients With Squamous Cell Carcinoma of the Esophagus. *J Gastroenterol Hepatol* (2007) 22(12):2222–7. doi: 10.1111/j.1440-1746.2006.04736.x
19. Wu Y, Song Z, Sun K, Rong S, Gao P, Wang F, et al. A Novel Scoring System Based on Peripheral Blood Test in Predicting Grade and Prognosis of Patients With Glioma. *Onco Targets Ther* (2019) 12(1178-6930(1178-6930 (Print):11413–23. doi: 10.2147/OTT.S236598
20. Simpson-Haidaris PJ, Rybarczyk B. Tumors and Fibrinogen. The Role of Fibrinogen as an Extracellular Matrix Protein. *Ann N Y Acad Sci* (2001) 936 (0077-8923(0077-8923 (Print):406–25.
21. Sahni A, Simpson-Haidaris PJ, Sahni SK, Vaday GG, Francis CW. Fibrinogen Synthesized by Cancer Cells Augments the Proliferative Effect of Fibroblast Growth Factor-2 (FGF-2). *J Thromb Haemost* (2008) 6(1):176–83. doi: 10.1111/j.1538-7836.2007.02808.x
22. Zhang F, Wang Y, Sun P, Wang ZQ, Wang DS, Zhang DS, et al. Fibrinogen Promotes Malignant Biological Tumor Behavior Involving Epithelial-

Mesenchymal Transition via the P-AKT/p-mTOR Pathway in Esophageal Squamous Cell Carcinoma. *J Cancer Res Clin Oncol* (2017) 143(12):2413–24. doi: 10.1007/s00432-017-2493-4
23. Nieswandt B, Hafner M, Echtenacher B, Männel DN. Lysis of Tumor Cells by Natural Killer Cells in Mice Is Impeded by Platelets. *Cancer Res* (1999) 59 (6):1295–300.
24. Palumbo JS, Talmage KE, Massari JV, La Jeunesse CM, Flick MJ, Kombrinck KW, et al. Platelets and Fibrin(Ogen) Increase Metastatic Potential by Impeding Natural Killer Cell-Mediated Elimination of Tumor Cells. *Blood* (2005) 105(1):178–85. doi: 10.1182/blood-2004-06-2272
25. Yamaguchi T, Yamamoto Y, Yokota S, Nakagawa M, Ito M, Ogura T. Involvement of Interleukin-6 in the Elevation of Plasma Fibrinogen Levels in Lung Cancer Patients. *Jpn J Clin Oncol* (1998) 28(12):740–4. doi: 10.1093/jjco/28.12.740
26. Sahni A, Francis CW. Vascular Endothelial Growth Factor Binds to Fibrinogen and Fibrin and Stimulates Endothelial Cell Proliferation. *Blood* (2000) 96(12):3772–8.
27. Stover JF, Hopf NJ, Perneczky A, Kempski OS. Unspecific Metabolic Blood Parameters as Used in Clinical Routine may Differentiate Malignant From Benign Cerebral Tumors. *Cancer Lett* (1995) 95(1-2):147–52. doi: 10.1016/0304-3835(95)03880-6
28. Font C, de la Fuente C, Pumarola M, Blasco E, Fernandez F, Viu J, et al. Canine Intracranial Meningiomas: Immunohistochemical Evaluation of Tissue Factor, Fibrin/Fibrinogen and D-Dimers. *Vet J* (2015) 206(3):426–8. doi: 10.1016/j.tvjl.2015.07.008
29. Dobran M, Marini A, Splavski B, Rotim K, Liverotti V, Nasi D, et al. Surgical Treatment and Predictive Factors for Atypical Meningiomas: A Multicentric Experience. *World Neurosurg* (2020) 144(1878-8769(1878-8769 (Electronic): e1–8. doi: 10.1016/j.wneu.2020.03.201
30. Soni P, Davison MA, Shao J, Momin A, Lopez D, Angelov L, et al. Extent of Resection and Survival Outcomes in World Health Organization Grade II Meningiomas. *J Neurooncol* (2021) 151(2):173–9. doi: 10.1007/s11060-020-03632-3
31. Budohoski KP, Clerkin J, Millward CP, O'Halloran PJ, Waqar M, Looby S, et al. Predictors of Early Progression of Surgically Treated Atypical Meningiomas. *Acta Neurochir (Wien)* (2018) 160(9):1813–22. doi: 10.1007/s00701-018-3593-x
32. Klinger DR, Flores BC, Lewis JJ, Hatanpaa K, Choe K, Mickey B, et al. Atypical Meningiomas: Recurrence, Reoperation, and Radiotherapy. *World Neurosurg* (2015) 84(3):839–45. doi: 10.1016/j.wneu.2015.04.033
33. Da Broi M, Borrelli PA-OX, Meling TA-O. Predictors of Survival in Atypical Meningiomas. *Cancers (Basel)* (2021) 13(8):1970. doi: 10.3390/cancers13081970
34. Ma E, Li J, Xing H, Li R, Shen C, Zhang Q, et al. Development of a Predictive Nomogram for Early Recurrence of Hepatocellular Carcinoma in Patients Undergoing Liver Transplantation. *Ann Transl Med* (2021) 9(6):468. doi: 10.21037/atm-21-334
35. Zhang H, Ma Y, Wang H, Xu L, Yu Y. MMP-2 Expression and Correlation With Pathology and MRI of Glioma. *Oncol Lett* (2019) 17(2):1826–32. doi: 10.3892/ol.2018.9806
36. He JH, Han ZP, Luo JG, Jiang JW, Zhou JB, Chen WM, et al. Hsa_Circ_0007843 Acts as a mIR-518c-5p Sponge to Regulate the Migration and Invasion of Colon Cancer SW480 Cells. *Front Genet* (2020) 11(1664-8021:9(1664-8021 (Print). doi: 10.3389/fgene.2020.00009
37. Parikh AA-O, Shin J, Faquin W, Lin DT, Tirosh I, Sunwoo JB, et al. Malignant Cell-Specific CXCL14 Promotes Tumor Lymphocyte Infiltration in Oral Cavity Squamous Cell Carcinoma. LID - 10.1136/Jitc-2020-001048 [Doi] LID - E001048. *J Immunother Cancer* (2020) 8(2):e001048. doi: 10.1136/jitc-2020-001048
38. Hemmati SM, Ghadjar P, Grun A, Badakhshi H, Zschaeck S, Senger C, et al. Adjuvant Radiotherapy Improves Progression-Free Survival in Intracranial Atypical Meningioma. *Radiat Oncol* (2019) 14(1):160. doi: 10.1186/s13014-019-1368-z
39. Masalha WA-O, Heiland DH, Franco P, Delev D, Haaker JG, Schnell O, et al. Atypical Meningioma: Progression-Free Survival in 161 Cases Treated at Our Institution With Surgery Versus Surgery and Radiotherapy. *J Neurooncol* (2018) 136(1):147–54. doi: 10.1007/s11060-017-2634-2
40. Goldbrunner R, Minniti G, Preusser M, Jenkinson MD, Sallabanda K, Houdart E, et al. EANO Guidelines for the Diagnosis and Treatment of Meningiomas. *Lancet Oncol* (2016) 17(9):e383–91. doi: 10.1016/S1470-2045(16)30321-7

Conflict of Interest: The authors declare that the research was conducted in the absence of any commercial or financial relationships that could be construed as a potential conflict of interest.

Publisher's Note: All claims expressed in this article are solely those of the authors and do not necessarily represent those of their affiliated organizations, or those of the publisher, the editors and the reviewers. Any product that may be evaluated in this article, or claim that may be made by its manufacturer, is not guaranteed or endorsed by the publisher.

Copyright © 2021 Chen, Chen, Huang, Xu, Sun, Chen, Ding, Wang, Wu, Kang, You and Lin. This is an open-access article distributed under the terms of the Creative Commons Attribution License (CC BY). The use, distribution or reproduction in other forums is permitted, provided the original author(s) and the copyright owner(s) are credited and that the original publication in this journal is cited, in accordance with accepted academic practice. No use, distribution or reproduction is permitted which does not comply with these terms.

frontiers in Oncology

ORIGINAL RESEARCH
published: 19 October 2021
doi: 10.3389/fonc.2021.737520

A Novel MRI-Based Risk Stratification Algorithm for Predicting Postoperative Recurrence of Meningioma: More Benefits to Patients

Rufei Zhang[1†], *Xiaodan Chen*[1,2†], *Jialing Cai*[1], *Peirong Jiang*[1,3], *Yilin Chen*[1,3], *Bin Sun*[1,3], *Yang Song*[4], *Lin Lin*[1,3*] *and Yunjing Xue*[1,3*]

[1] Department of Radiology, Fujian Medical University Union Hospital, Fuzhou, China, [2] Department of Radiology, Fujian Medical University Cancer Hospital, Fuzhou, China, [3] School of Medical Technology and Engineering, Fujian Medical University, Fuzhou, China, [4] MR Scientific Marketing, Siemens, Healthineers Ltd, Shanghai, China

Pathological grading of meningioma is insufficient to predict recurrence after resection and to guide individualized treatment strategies. One hundred and thirty-three patients with meningiomas who underwent total resection were enrolled in this retrospective study. Univariate analyses were conducted to evaluate the association between factors and recurrence. Least absolute shrinkage and selection operator (Lasso) was used to further select variables to build a logistic model. The predictive efficiency of the model and WHO grade was compared by using receiver operating characteristic curve (ROC), decision curve analysis (DCA), and net reclassification improvement (NRI). Patients were given a new risk layer based on a nomogram. The recurrence of meningioma in different groups was observed through the Kaplan-Meier curve. Univariate analysis demonstrated that 11 risk factors were associated with prognosis ($P < 0.05$). The result of ROC proved that the quantified risk-scoring system (AUC = 0.853) had a higher benefit than pathological grade (AUC = 0.689, P = 0.011). The incidence of recurrence of the high risk cohort (69%) was significantly higher than that of the low risk cohort (9%) by Kaplan-Meier analysis ($P < 0.001$). And all patients who did not relapse in the high risk group received adjuvant radiotherapy. The novel risk stratification algorithm has a significant value for the recurrence of meningioma and can help in optimizing the individualized design of clinical therapy.

Keywords: meningioma, recurrence, prediction model, relative apparent diffusion coefficient, heterogeneous tumor enhancement, pathological grade

OPEN ACCESS

Edited by:
Hailiang Tang,
Fudan University, China

Reviewed by:
Ruiping Wang,
Tongji University, China
Zhiyuan Xu,
University of Virginia, United States

***Correspondence:**
Lin Lin
linlin@fjmu.edu.cn
Yunjing Xue
xueyunjing@126.com

[†]*These authors have contributed equally to this work and share first authorship*

Specialty section:
This article was submitted to Neuro-Oncology and Neurosurgical Oncology, a section of the journal Frontiers in Oncology

Received: *07 July 2021*
Accepted: *04 October 2021*
Published: *19 October 2021*

Citation:
Zhang R, Chen X, Cai J, Jiang P, Chen Y, Sun B, Song Y, Lin L and Xue Y (2021) A Novel MRI-Based Risk Stratification Algorithm for Predicting Postoperative Recurrence of Meningioma: More Benefits to Patients. Front. Oncol. 11:737520. doi: 10.3389/fonc.2021.737520

INTRODUCTION

Meningiomas are the most common primary intracranial tumors, accounting for 38.3% of all tumors of the central nervous system, and are continuing to increase in incidence with the aged tendency of the population (1). They result in severe neurological morbidity by having a space occupying effect on adjacent brain regions. Complete surgical resection of the meningioma is the first choice of treatment (2).

Up to now, the most reliable clinical factor for recurrence of meningioma after radical surgical resection is the World Health Organization (WHO) grade of the tumor (2–4). The WHO grade is currently used to guide the development of strategies for postoperative radiotherapy and follow-up (2, 4). However, despite radical surgical resection, some benign meningiomas (WHO grade I) have early recurrence after surgery and exhibit aggressive biological behavior, resulting in chronic courses of diseases and treatment-related complications (3). In contrast, some high grade tumors (WHO grade II, III) have indolent tumor behaviors, which suggests that histopathological grading alone is not enough to achieve optimal risk stratification. Therefore, it is clinically difficult to predict postoperative recurrence and guide individual decisions only by tumor classification and it is particularly important to clarify the risk changes within the inter-layer variability (5–8). Although numerous studies have identified the histological, clinical, and radiological parameters regarding aggressive meningioma behavior, the accurate prediction of postoperative recurrence of meningioma remains challenging and requires further research (4–6, 8, 9).

The purpose of our study was to generate and validate an MRI-based prediction model of meningioma recurrence after surgery that could be coupled with potential clinical prognostic factors and histopathological grade. We hypothesis that the new prognostic stratification constructed by this new model might individualize decisions regarding the need for postoperative therapeutic interventions and support the optimization of treatment strategies for patients.

MATERIALS AND METHODS

Patient Characteristics

Patients with meningioma who underwent surgical resection at the department of neurosurgery of the Fujian Medical University Union Hospital between June 2010 and December 2020 were enrolled in this retrospective study. This study was approved by the local ethics committee of the hospital, and the requirement of written informed consent was waived. The inclusion criteria for this study were patients who underwent preoperative and postoperative craniocerebral MRI examination and were pathologically confirmed as meningioma in our hospital. We excluded patients with prior craniocerebral radiation therapy, neurofibromatosis type 2 (NF2), preoperative imaging outside our hospital, poor image quality, or less than 2 years of clinical and radiological follow-up in our hospital.

Imaging Acquisition

MR images were performed on 1.5T (Siemens, MAGNETOM Amira, n = 67) or a 3.0T (GE Healthcare, Discovery MR750, n = 57, or Siemens, MAGNETOM Trio, n = 9) MR scanners according to a standard institutional protocol in our hospital. MRI examinations included axial T1-weighted spin-echo, T2-weighted, T2 fluid attenuated inversion recovery (FLAIR), T2-weighted gradient-recalled echo, diffusion weighted images (DWI), and apparent diffusion coefficient (ADC), T1-weighted images after contrast administration. Detailed MRI acquisitions were provided in **Supplementary Appendix E1**.

Pathological Examination

The detailed histopathology reports and the histopathologic slides of surgical specimens were re-evaluated by a neuropathologist (with more than 10 years' experience), and the pathologic diagnoses and tumor grading were based on the 2016 WHO Classification of Tumors of the Central Nervous System (10). According to 2016 WHO criteria, meningiomas can be classified into three grades based on histological and cytological characteristics: WHO grade I with < 4 mitoses/10 high power field (HPF), WHO grade II with 4–19 mitoses/10 HPF and/or brain invasion, and WHO grade III with ≥ 20 mitoses/10 HPF (**Supplementary Table**). For every case, the representative hematoxylin-eosin (HE) staining slide which was most representative of the mitotic count or other grading standards was determined and calculated for the pathological grade by the experienced neuropathologist. Subsequently, WHO grade I meningiomas was defined as low grade meningiomas, and WHO grade II and III meningioma were defined as high grade meningiomas based on previous literature (3, 6, 11, 12).

Recorded Variables

All clinical data and imaging features were evaluated by two neuroradiologists (with more than 10 years' experience) who were not informed of the prognosis. Patients' gender, age at the time of surgery, pre-operative Karnofsky Performance Scale (KPS) scores, Ki-67 index, and administration of adjuvant radiation were determined from clinical records. The grade of resection was determined by reviewing surgical records, MRI, and best clinical judgment in the absence of explicit instructions.

T2 hyperintensity was determined by comparison with the gray matter signal. Tumor sites were divided into "skull base" and "non–skull base" lesions (including convexity and falcine/parasagittal meningiomas and tumors arising from other intracranial non–skull base locations). The maximum diameters were measured in 3 directions (axial, coronal, and sagittal) on MRI, and the tumor and edema volume were calculated according to the elliptical sphere volume formula. The edema index was defined as the ratio of the volume of edema to the sum of the tumor plus edema, EI = $(V_{Edema}+V_{Tumor})/V_{Tumor}$). Regular tumor shapes included round or oval shapes, other shapes were irregular. Tumor calcification was diagnosed by reference to preoperative CT images. Heterogeneous tumor enhancement did not include heterogeneity due to cystic change or calcifications. The presence of the arachnoid layer was

examined with T2 predominant MR screenings. Observations of dural tail sign and cystic change were made using T1-weighted contrast images. Venous sinus invasion and bone change were determined by combining radiological data and surgical records.

For ADC measurement, the region of interest (ROI) was placed at the largest level of the tumor while avoiding calcification and cystic change and varying with the tumor size (20 – 600 mm^2). To normalize individual variance, the ADC value of the tumor was divided by the corresponding value of contralateral semioval center normal appearing white matter (NAWM) to calculate the relative ADC (rADC) (13).

As the current gold standard, biopsy is used to determine tumor recurrence, but it might lead to more stress and pain for the patient. Fortunately, the recurrence can also be determined by other non-invasive methods, such as follow-up enhanced MRI scans. Follow-up MR images showing new enhanced lesions appeared in the surgical area can be considered as evidence of tumor recurrence (**Supplementary Figure**). In previous studies, follow-up enhanced MR has been used as one of the diagnostic criteria for determining tumor recurrence (3, 11–13). Accordingly, tumor recurrence was determined by at least one of the following conditions in this study: (I) follow-up enhanced MRI scans indicated tumor recurrence; (II) tumor recurrence was pathologically confirmed by reoperation or biopsy.

Statistical Analyses

All statistical analyses, model generation, and model validation were carried out using statistical software SPSS (version 23.0) and R (version 4.0.3). The interobserver reliability of categorical data was determined by the Cohen kappa (κ) coefficient, whereas the consistency of consecutive data was determined by the intra-group correlation coefficient (Cohen κ values ranged from 0.757 to 0.931 and ICC from 0.831 to 0.983).

The distribution uniformity of the continuous parameters was evaluated by the Kolmogorov-Smirnov test. The mean ± standard deviation was used to represent the normally distributed data, and the median and interquartile range (IQR) was used to express non-normally distributed data. Chi-square test (or Fisher exact test) and Mann–Whitney U test (or Student's t-test) were performed for categorical and continuous data respectively. The overfitting problem caused by multicollinearity was solved by the regularization method. Based on univariate analysis, Lasso regression cross-validation was further used to screen out meaningful variables and the logistic regression equation was finally calculated. Then, based on the proposed Lasso-logistic regression model, a nomogram was generated. The collinearity diagnosis was performed by calculating the variance inflation factor (VIF) of the variables in the nomogram. Variables with VIFs > 10 indicated severe multicollinearities. Area under curve was used to measure the discriminability of the nomograms. Calibration curve was plotted through bootstrap (1,000 resamplings) to determine the conformity between the predicted probability and the actual probability. In addition, the nomogram was conducted internally validated by the Bootstrap validation with 1000 resamplings. The clinical utility of the model was measured by decision curve analysis. Delong test was used to measure the differences in ROC curves between the prediction model and the pathological grade. Subsequently, the patients were grouped according to NRI. The relationship between benefits and risks brought by the model was evaluated by DCA. Finally, the recurrence of meningiomas in different groups was observed by Kaplan-Meier analysis. Unless otherwise specified, P value < 0.05 was considered statistically significant.

RESULTS

Patient Characteristics

In total, 198 patients with meningiomas were diagnosed pathologically in our hospital. Forty and five cases were excluded due to the follow-up time of less than 2 years. Thirteen cases were excluded due to postoperative residual (Simpson IV-V), and 7 cases were excluded because the image quality did not meet the research requirements (2 patients with poor DWI/ADC imaging quality (air-bone interface or motion artifacts) and 5 patients with incomplete MRI) (**Figure 1**).

Finally, 133 patients with a median age of 52 years (range 13–78 years), including 94 females (71%) and 39 males (29%), were enrolled in this study. The median follow-up duration of non-recurrence patients was 40 months (IQR = 31–59 months). Of the 133 patients included in the analysis, the most predominant lesion of 3 patients with multiple lesions was selected for the analysis. The pathological classification included 96 low grade (WHO grade I, n = 96, 72%), 37 high grade (WHO grade II,

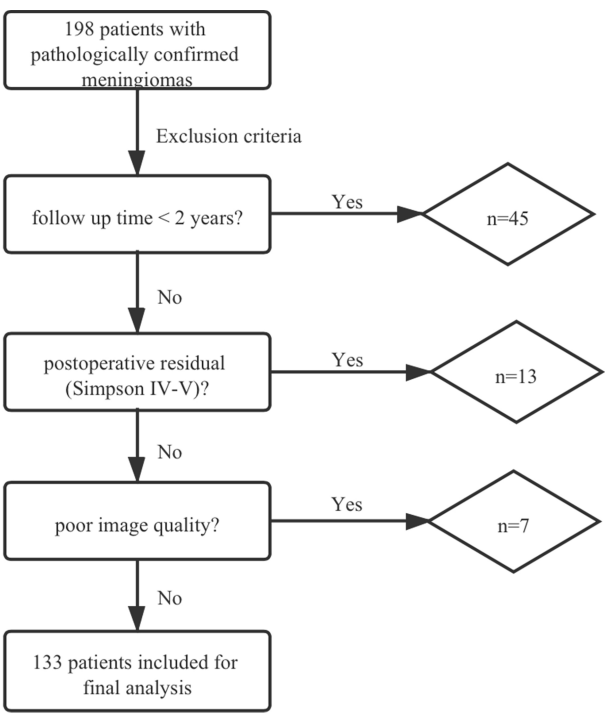

FIGURE 1 | Flowchart of the patient selection process.

n = 33, 24%; WHO grade III, n = 4, 3%) meningiomas. Eight (8%) low grade patients and thirteen (35%) high grade patients received adjuvant radiotherapy. Twenty cases (15%) experienced recurrence after radical surgery. **Table 1** summarizes the baseline clinical, radiological, and histopathological data of patients with meningioma.

Univariate Analysis

On univariate analysis, pathological grade (I *vs*. II-III, P < 0.001), tumor shape (regular *vs*. irregular, P = 0.017), peritumoral edema volume (P = 0.004), peritumoral edema index (P = 0.016), tumor volume (P = 0.005), heterogeneous tumor enhancement (P < 0.001), cystic change (P = 0.038), venous sinus invasion (P = 0.023), arachnoid layer (P = 0.009), age (P = 0.014), and rADC (P < 0.001) were significantly associated with postoperative recurrence (**Table 1**). There were no significant associations between recurrence and sex, preoperative SKP, bone change, dural tail sign, tumor location, T2 hyperintensity, tumor calcification or adjuvant radiotherapy.

Feature Selection and Lasso-Logistic Model Construction

Among the 11 candidate features, potential predictive variables were obtained by dimensionality reduction through Lasso

TABLE 1 | Patient characteristics and univariate analysis of the risk of recurrence.

Factor	Recurrence	Non-Recurrence	P
Sex			0.095
Female	11	83	
Male	9	30	
Preoperative SKP			0.280
≥ 70	8	60	
< 70	12	53	
Pathological grade			< 0.001***
I	8	88	
II-III	12	25	
Tumor shape			0.017**
Regular	3	49	
Irregular	17	64	
Cystic change			0.038*
Yes	8	19	
No	12	94	
Heterogeneous tumor enhancement			0.001**
Yes	9	14	
No	11	99	
Bone change			0.386
Yes	7	29	
No	13	84	
Dural tail sign			0.405
Yes	14	68	
No	6	45	
Tumor location			0.160
skull base	10	38	
non-skull base	10	75	
Venous sinus invasion			0.023*
Yes	9	24	
No	11	89	
T2 hyperintensity			0.953
Yes	8	46	
No	12	67	
Arachnoid layer			0.009**
Yes	10	88	
No	10	25	
Calcification			0.499
Yes	1	15	
No	19	98	
Adjuvant radiotherapy			0.119
Yes	6	15	
No	14	98	
Age (years)	59.50 (48.5-67.50)	51 (45.5-58)	0.014*
Tumor volume (cm^3)	87.35 (24.74-133.59)	28.83 (12.83-72.89)	0.005**
Peritumoral edema volume (cm^3)	46.59 (23.70-99.48)	2.55 (0-62.44)	0.004**
Peritumoral edema index	1.79 (1.30-2.40)	1.07 (1.00-2.17)	0.016*
Relative apparent diffusion coefficient	0.99 ± 0.20	1.19 ± 0.18	< 0.001***

**P < 0.05, ***P < 0.01, ***P < 0.001.*

regression cross validation. Variables were selected based on a model with excellent performance and the least number of independent variables given by Least Squares Error (**Figures 2A, B**), and then the Lasso-logistic model was established. The formula for Lasso was provided in **Supplementary Appendix E2**. Pathological grade, heterogeneous tumor enhancement, and rADC were significantly correlated with the actual postoperative status, and these three variables showed significant differences between patients with and without recurrence ($P < 0.001$). By using the collinearity diagnosis, the VIFs for pathological grade, heterogeneous tumor enhancement, and rADC were less than 10 (WHO grade: 1.0370; Tumor enhancement: 1.0360; rADC: 1.0726), indicating no severe collinearity existing in these factors. These independent predictors were used to construct a nomogram for the prediction of tumor recurrence (**Figure 3**). The formula for the nomogram was computed by:

$$\begin{aligned} &\textit{Nomogram score} \\ &= 13.33824 \times \textit{WHO Grade level} + 24.67939 \\ &\quad \times \textit{Tumor Enhancement type} - 90.909090909 \times \textit{rADC value} \\ &\quad + 163.636363636 \end{aligned}$$

In the given nomogram score formula, the value of low level (WHO I grade) was 0 and that of high level (WHO II, III grade) was 1. For tumor enhancement type, the value of homogeneous enhancement was 0 and that of heterogeneous enhancement was 1.

Evaluation and Validation of Lasso-Logistic Model

The unadjusted AUC value based on the prediction model was 0.853 (95%CI: 0.764-0.942). The internal validation of the model

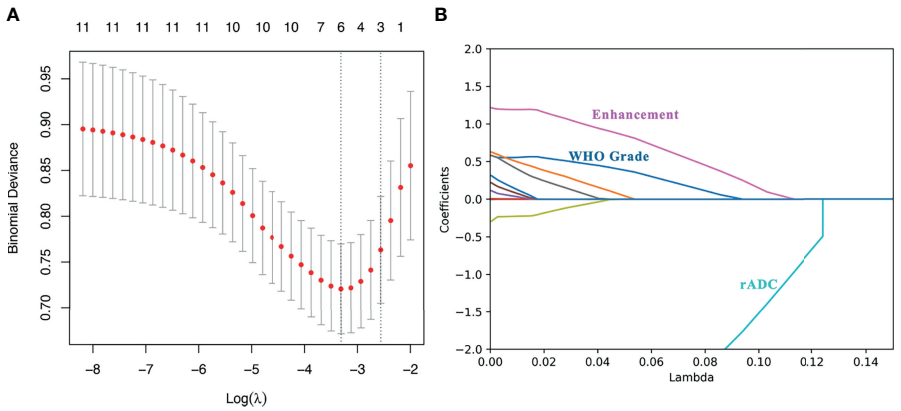

FIGURE 2 | Lasso regression for predicting postoperative recurrence of meningioma. **(A)** The number of independent variables of the model with good performance was 3; **(B)** The three variables were WHO grade, heterogeneous tumor enhancement and rADC value, respectively.

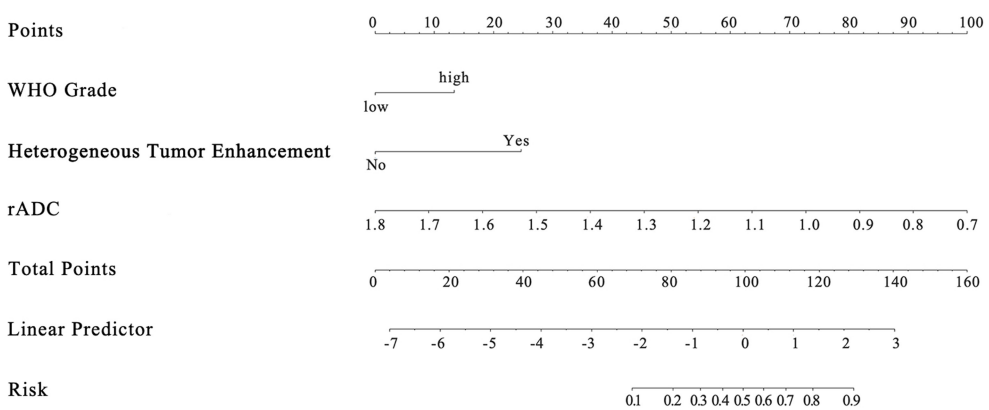

FIGURE 3 | The novel algorithm nomogram for predicting postoperative recurrence of meningioma.

was executed by the bootstrap resampling method. The corrected AUC value (AUC = 0.824) was calculated by using the 1000 times bootstrap. Besides, the calibration curve showed that the probability of recurrence predicted by the nomogram was in good agreement with the actual probability (**Figure 4B**). The insignificant statistics (P = 0.439) of H-L test revealed that there was no significant deviation from an ideal fitting. Further, Delong's test showed that the nomogram had significantly better predictive power than pathological grade alone (P = 0.011). The ROC curve of the model and pathological grade were shown in **Figure 4A**. NRI quantified the extent to which the addition of risk factors (two radiological features) led to an improved classification of risks. The decision curve for the nomogram and the pathological grade alone were used to assess the clinical utilities. **Figure 5** showed that the area under the decision curve of the nomogram (yellow) was higher than that of the pathological grade alone (green).

Novel Risk Stratification for Recurrence

The optimal threshold value for the nomogram score determined by the NRI is 105. Subsequently, the patients were divided into two subgroups. Based on this cutoff value, 120 patients with a score less than or equal to 105 were classified as low risk recurrence group, while the remaining patients with a score greater than 105 were classified as high risk recurrence group (n = 13). According to pathological grading, the recurrence rates were 8% for low grade (n = 96) and 32% for high grade (n = 37), respectively. Based on the novel risk stratification system, the recurrence rate in the patients with scores of 0–105 (n = 120), 116–160 (n = 13) were 9% and 69%, respectively (**Table 2**). The predicted probabilities of recurrence-free survival were plotted as a Kaplan-Meier curve. Kaplan-Meier curve also consistently showed significant differences in postoperative recurrence between the two groups (P < 0.001) (**Figure 6**). The incidence of recurrence of the high risk cohort was significantly higher than that of the low risk cohort (P < 0.001).

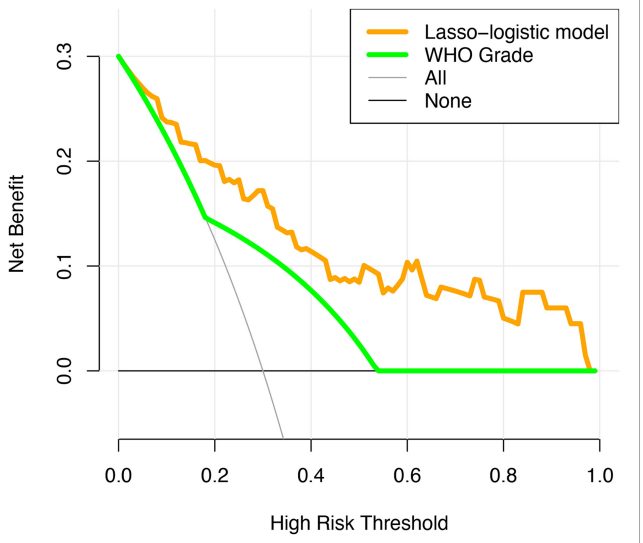

FIGURE 5 | The decision curve analysis for the novel algorithm and WHO grade. The yellow and green dotted lines represent the decision curve of the novel algorithm and WHO grade, respectively.

DISCUSSION

We developed and validated a nomogram by using the Lasso-logistic model for postoperative recurrence prediction of meningioma in this study. To our knowledge, this is the first time that this novel algorithm is used to predict postoperative recurrence of meningioma. In this study, we also first discovered that the nomogram to predict the risk of meningioma recurrence based on pathological grade, conventional MR (enhanced tumor heterogeneity), and functional MR (rADC) was superior to WHO histopathological grade alone. The AUC value and the calibration curve also demonstrated that our nomogram had a good predictive performance. This result was further supported by the DCA and

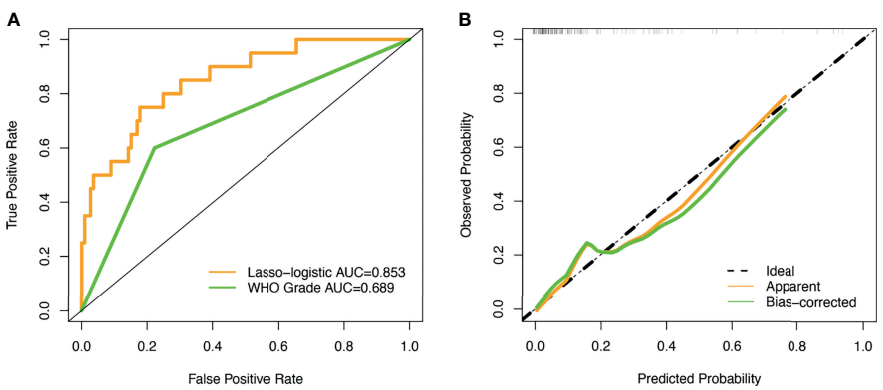

FIGURE 4 | ROC curve and calibration curve. **(A)** The AUC values of the novel algorithm and WHO grade was 0.853 (yellow) and 0.689 (green), respectively; **(B)** The calibration curve demonstrated that consistency between the predicted risk of recurrence probability and the actual probability by the nomogram.

TABLE 2 | Postoperative recurrence in each group of the novel algorithm and WHO grade.

Prediction method	Group	Score	Postoperative recurrence rate (%)
Novel algorithm	Low risk	0-115	9
WHO grade	Low grade	—	8
Novel algorithm	High risk	116-160	69
WHO grade	High grade	—	32

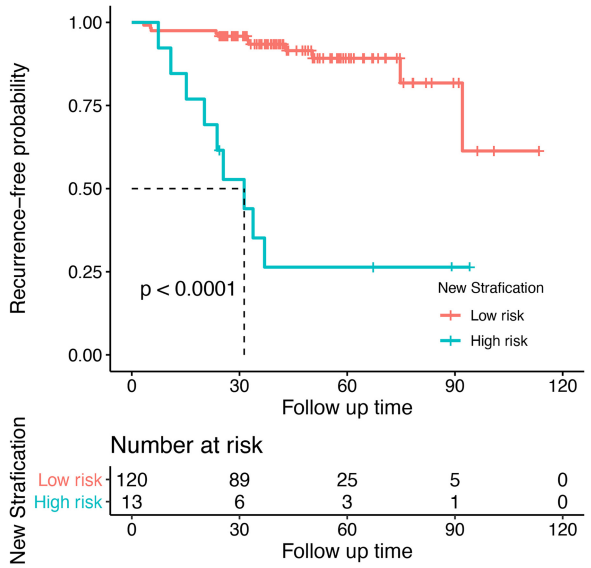

FIGURE 6 | Recurrent risk stratification for patients with meningioma after surgery. Kaplan-Meier curve showed significant differences in postoperative recurrence between the two groups (P < 0.001).

NRI. As a complement to pathological grade, non-invasive image-based techniques will help to better determine the risk of tumor recurrence and develop individualized treatment strategies (3, 6).

In univariate analysis, we found that pathological grade, tumor shape, peritumoral edema volume, peritumoral edema index, tumor volume, heterogeneous tumor enhancement, cystic change or necrosis, venous sinus invasion, arachnoid layer, age, and rADC were significantly associated with prognosis. Previous studies have investigated the relationship between potential factors and recurrence risk. Cohen-Inbar et al. have shown that older patients undergoing resection of meningiomas have higher recurrence rates compared with younger patients (14). Likewise, this study suggested that age proved to inversely correlate with prognosis. The observed association between cystic degeneration and high risk group was consistent with prior studies (8). Cyst formation in meningiomas may be associated with the rapid growth or aggressivity of tumor cells, including cystic variation, ischemic necrosis, direct liquid secretion by tumor cells, and absorption of intratumoral haemorrhage (4, 8, 12, 15). Our results indicated significant differences in tumor shape and volume between the recurrent and non-recurrent groups. Similarly, several researchers found that irregular tumor shape and larger tumor volumes were associated with greater proliferative potential, and active proliferation leads to increased recurrence after resection (4, 6, 15–17). In addition, we demonstrated that peritumoral brain edema (PTBE), including peritumoral edema volume and peritumoral edema index, was strongly associated with prognosis. PTBE was considered to predict brain invasion in most series (18, 19). Leehi et al. revealed that radiomics combined with peritumoral edema and interface showed high performance for the prediction of brain invasion based on a large cohort (n = 641) in both training (AUC: 0.97, 95% CI: 0.95–0.98) and independent validation sets (AUC: 0.91, 95% CI: 0.84–0.98) (19). However, further study is needed to reveal the relation between PTBE and aggressive biological behaviour because there are several in-consistent reports (4, 13). We also observed that disruption of the arachnoid layer was in relation to increased risk of recurrence, which closely agreed with previous studies (11, 15). The presence of the arachnoid layer indicates a slow and suppressing growth manner of the tumor (15). However, the loss of integrity of the arachnoid layer is not characteristic of brain invasion on microscopic analyses (20). Thus, the correlations between arachnoid layer and prognosis remain controversial. In the attainable data, venous sinus invasion was difficult to include because it is difficult to clearly distinguish the intravenous sinus tumor by contrast-enhanced MRI alone. Hence, we assessed venous sinus invasion by combining radiological data and surgical record judgment. We noted that venous sinus invasion was remarkably related to a higher recurrence rate, highlighting the importance of evaluating venous sinus involvement by adjacent lesions. Kei et al. reported that it was difficult to completely remove the entire tumor in a patient with an extensive venous sinus infiltrating tumor (21). Nevertheless, several studies recently reported that the recurrence rate in patients with venous sinus infiltration was rather variable, and there was no significant difference in incidence between patients with and without complete sinus resection (22–24). These findings suggest that postoperative recurrence of venous sinus invasion cannot simply be attributed to the residual tumor. Notably, there was a significant association between high grade tumors and venous sinus invasion by chi-square tests (P = 0.043) in this study, which suggested that tumor involving venous sinuses tended to be more aggressive.

Heterogeneous tumor enhancement is thought to be due to the uneven distribution of dividing cells and tumor necrosis, which may indicate the presence of local necrosis and a higher degree of malignancy in meningiomas (6, 11, 15, 20, 25). Some studies have shown that small focal necrosis in meningioma is related to a higher recurrence rate (11, 26, 27). Necrosis is presumed to result from hypoxia due to cellular undernutrition and hypermetabolism, suggesting that it may be associated with more aggressive progression (27). Hypoxic tumor cells in necrotic areas may dedifferentiate and develop into malignant cells (27). Inflammatory cells tend to cluster in necrotic areas, while degraded tumor cells release proinflammatory cytokines which may stimulate angiogenesis and tumor progression (28). Most studies have suggested that heterogeneous enhancement is an independent predictor of high grade meningiomas and postoperative recurrence (4, 6, 11, 12, 14, 15, 20, 25). Durand

et al. showed the presence of heterogeneous contrast seemed to predict aggressive behavior in high grade meningiomas (25). Our study is consistent with previous studies confirming that heterogeneous tumor enhancement was an independent predictor of meningioma recurrence.

Diffusion weighted imaging and associated ADC maps are widely used in oncology to differentiate between malignant and non-malignant lesions. ADC is generally lower in malignant lesions than in benign lesions and surrounding normal tissues. The non-invasive observation of the distribution of displacements driven by water diffusion provides unique clues to the fine structural characteristics and geometrical structure of tissues and how these characteristics change with physiological or pathological states (6, 13, 29–31). William et al. have shown that meningiomas with non-Simpson grade I resection and low ADC have a significantly increased risk of progression/recurrence (P/R) (6). Ching-Chung et al. have demonstrated that lower ADC values (< 0.83×10^{-3} mm^2/s)/ratios (<1.09) were significantly associated with P/R. Moreover, ROC analysis indicated that ADC ratio (AUC = 0.91; Sensitivity = 0.79; Specificity = 0.94) had a better performance for differentiating skull base meningiomas with and without P/R than ADC value (AUC = 0.86; Sensitivity = 0.73; Specificity = 0.88) (13). Regrettably, the above study did not further include rADC in the multivariate analysis. As far as we know, this is the first study to comprehensively discuss the relationship between rADC and prognosis in meningiomas. Our study was the first to confirm that rADC was a strong predictor of postoperative recurrence of meningioma. Yuan et al. observed that the ADC showed a moderate negative correlation with the Ki67 proliferation index in murine models of rhabdomyosarcoma (r = – 0.543, P = 0.003), which was generally consistent with what we observed in 66 meningioma patients (r = -0.305, P = 0.023) (31). Moreover, Manabu et al. found a stronger correlation between rADC and cell density than ADC (30). This may be because rADC to some extent eliminated the differences between the individuals and the scanning instruments. Therefore, rADC can more accurately reflect the proliferative activity and microstructure of the tumor.

At present, several studies still suggested that the histological grade remains the most important indicator of postoperative recurrence of meningioma (2, 11, 32). In this study, we also demonstrated a significant correlation between pathological grade and postoperative recurrence in patients who underwent total resection (P < 0.001). Although grade II/III meningiomas have more aggressive biological behavior and might exhibit faster recurrence, there are also some high grade meningiomas that biologically behave more like benign lesions by our observation (**Figure 7**). Likewise, many studies showed that it was inadequate to predict postoperative recurrence and develop individualized treatment strategies based solely on WHO classification (3, 6, 8, 9, 11–13, 17). Consequently, in this study, we established a prediction model integrating clinical data, imaging, and pathology for tumor prognosis, and explored and developed personalized treatment strategies base on this model.

On the other hand, sex, preoperative SKP, T2 relative high signal, dural tail sign, bone change, calcification, tumor location, and postoperative adjuvant radiotherapy were not independent risk factors in our study. There were controversial reports about the influence of sex on meningioma recurrence. Some studies revealed that male patients had a high risk of recurrence (11, 12, 33), while others did not (6, 9, 13, 17, 25). Although we observed a trend towards an association between preoperative SKP and

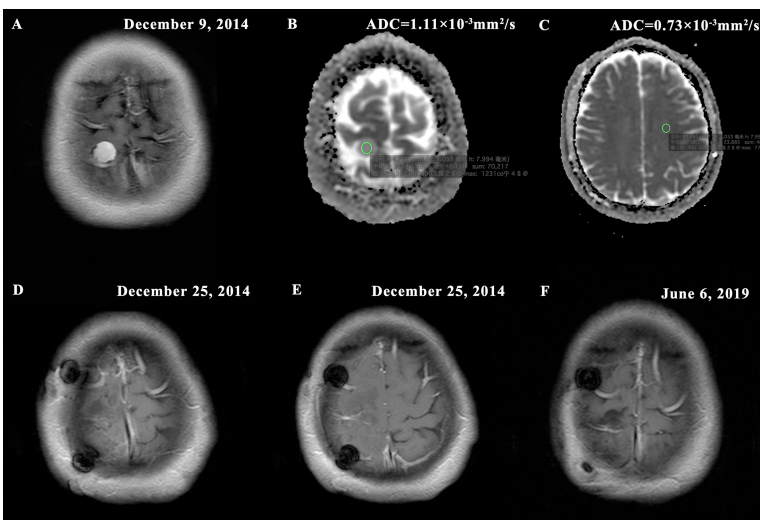

FIGURE 7 | Typical MR images of a WHO II grade meningioma with non-invasive biological behavior demonstrating **(A)** homogeneous enhancement (presurgical T1-postcontrast); **(B)** high tumor apparent diffusion coefficient (ADC) = 1.11×10-3mm2/s (ADC map); **(C)** contralateral normal appearing white matter (NAWM) ADC = 0.73×10-3mm2/s and rADC = 1.52; **(D–E)** Simpson grade I resection (postsurgical T1-postcontrast); **(F)** no imaging manifestation of tumor recurrence (postoperative T1-postcontrast). The new risk stratification puts the patient in the low risk group for recurrence (nomogram score = 50). The patient was followed up for 55 months without tumor recurrence.

recurrence, it did not reach significance. We agreed with previous studies that the T2 relative high signal was generally not correlated with prognosis (4, 6, 12, 13, 15). The presence of linear enhancement of the dural caudate or adjacent dura may distinguish the meningioma from other intracranial masses following the use of contrast agents (34). Although the dural tail sign is helpful in the diagnosis of meningioma, it has little prognostic significance (4, 6, 11, 13). Anthofer et al. found that bone invasion was an important risk factor in meningiomas adjacent to major venous sinuses. In contrast, there was no statistical difference between bone invasion and recurrence in our study. The presence of tumor calcification may have lower proliferative potential than noncalcified tumor, but not an increased risk of recurrence (4, 6). McGovern et al. have suggested that advances in surgical techniques have improved the grade of resection of skull base tumors in the modern case series (35). Skull base meningiomas were no longer a risk factor for postoperative recurrence. Clinically, adjuvant radiotherapy (RT) is a standard procedure in many institutions after subtotal resection (STR) of high grade meningiomas, but the role of RT as adjuvant therapy after gross total resection (GTR) is still unclear (2, 6, 36). In fact, we found no apparent effect of radiotherapy on the recurrence of high-grade meningiomas (with radiotherapy *vs.* without radiotherapy: 31% *vs.* 33%), which may indicate that WHO classification is not an ideal indicator of radiotherapy. On the contrary, in the high-risk population screened by our model, the recurrence rate of patients with and without radiotherapy was 43% and 100%, respectively. Notably, all 4 high-risk patients without recurrence received radiotherapy. Although further studies are needed to evaluate this finding, it indicates that our model may be a potential method to screen patients for postoperative radiotherapy.

In a previous study, William et al. reviewed 144 patients with a pathologically confirmed meningioma and selected Simpson grade and ADC value to constructed multivariate Cox proportional hazards models according to maximizing predictive ability and minimizing model complexity (HC, 0.73; AIC, 244; BIC, 250). On univariate Cox proportional hazards methods, there was only a marginal correlation between histopathological grade and prognosis (HR, 2.01; 95% CI, 0.929-0.4.33; P = 0.076). Thus, William et al. suggested that the combination of preoperative ADC and extent of surgical resection was superior to histopathological grading in predicting the hazard of tumor recurrence (6). This is undoubtedly an exciting finding, but we cannot take this conclusion with complete confidence because it is not convincing that pathological grade does not make a statistically significant difference in predicting postoperative recurrence of meningioma. Therefore, we tried to use conventional MRI, functional MRI (fMRI), and clinical data as a complement to the pathological grade and developed a predictor based on a novel algorithm. The result of the ROC curve proved that the model by integrating pathological grade, heterogeneous tumor enhancement and rADC (AUC = 0.853, 95%CI: 0.764-0.942) had a higher prognostic value than the pathological grade alone (AUC = 0.689, 95%CI: 0.573-0.806), which was further proved by DCA and NRI. Zhu et al. used multiple logistic regression analysis to establish a scoring system that accurately predicted recurrence in combination with conventional MRI and pathological grading, and divided patients into the following 4 subgroups. The incidences of recurrence in each subgroup were as follows: subgroup 1 (1.2%); subgroup 2 (5.7%); subgroup 3 (26.1%); subgroup 4 (66.7%) (P < 0.001) (11). However, consistency between predicted probability and actual probability was not assessed by using calibration curves in their study. Besides, the repeatability and reproducibility of the model were not tested by performing validation of the prediction model. In contrast, our study made up for the above deficiencies. While conventional MRI has limited ability to predict recurrence of meningiomas after radical resection. ADC map renders microstructure regard to cellular density and tumor matrix (29). Therefore, in addition to conventional MRI, our work also included fMRI to improve the predictive potential of meningiomas after treatment. Recently, Farshad et al. generated and validate predictors of postoperative meningioma recurrence and a nomogram based on the Cox model that incorporated methylation, pathological grade, and Simpson grade recurrence in a multicenter retrospective study (3). The discrimination of the meningioma recurrence was up to 82% in combined validation cohorts (AUC = 0.82, 95% CI: 0.76–0.87) (3). In this work, we used Lasso to select variables, which not only improved the accuracy of prediction, but also ensured the interpretability and stability of the model, and reduced the complexity of the model (37). In brief, this method can well overcome the shortcomings of traditional methods. Although the Lasso-logistic model, which combines pathological grading and imaging features, performed similarly to the methylated group-based model, non-invasive imaging is more convenient, economical, reproducible, and has greater potential for continuous monitoring.

Although our work can improve the accuracy of prediction of postoperative meningioma recurrence, this study still has some limitations. First of all, our study is a retrospective study at a single institution. Therefore, it lacks external validation to test the generalization ability of the model. Furthermore, the sample size was not large enough, which may lead to statistical bias. Also, follow-up time might be still not long enough for benign tumors. In the future, prospective studies based on large-scale multiple centres are needed to verify the reliability and generalization of our model. Finally, the expensive examination fee of MRI may also limit our research objectively.

In this study, we spotted the independent prognostic factor for post-treatment recurrence of meningioma, and combined conventional magnetic resonance with functional magnetic resonance using the Lasso-logistic algorithm to establish a simple and reliable meningioma prediction model. We found that non-invasive imaging techniques were used to supplement the pathological grade, which had a higher prognostic value than the pathologic grade alone and helped to distinguish between patients at different risks of recurrence. Moreover, the proposed model can help in optimizing the individualized design of clinical therapy.

DATA AVAILABILITY STATEMENT

The raw data supporting the conclusions of this article will be made available by the authors, without undue reservation.

ETHICS STATEMENT

The studies involving human participants were reviewed and approved by the Institutional Review Board (Fujian Medical University Union Hospital). Written informed consent from the participants' legal guardian/next of kin was not required to participate in this study in accordance with the national legislation and the institutional requirements. Written informed consent was not obtained from the individual(s), nor the minor(s)' legal guardian/next of kin, for the publication of any potentially identifiable images or data included in this article.

AUTHOR CONTRIBUTIONS

Conceptualization, YX, LL, and RZ. Data processing: RZ, LL, and YS. Data collection: RZ and XC. Methodology: YX, LL, RZ, and XC. Statistical analysis: RZ and XC. Software: RZ and JC. Manuscript drafting: RZ and XC. Manuscript proofreading: JC and PJ. Critical revision: YX and LL. Manuscript approval: all authors. All authors contributed to the article and approved the submitted version.

FUNDING

Sponsored by Joint Funds for the Innovation of Science and Technology, Fujian province (Grant number: 2018Y9044); Fujian Provincial Health Technology Project (Grant number: 2020GGA039); Startup Fund for Scientific Research, Fujian Medical University (Grant number: 2019QH1062); Innovation and Entrepreneurship Training Program of Fujian Medical University (Grant number: S202110392011).

ACKNOWLEDGMENTS

RZ and XC have contributed equally to this work. The authors would like to thank Zhangli Xin for their valuable contributions in collecting data for this manuscript.

SUPPLEMENTARY MATERIAL

The Supplementary Material for this article can be found online at: https://www.frontiersin.org/articles/10.3389/fonc.2021.737520/full#supplementary-material

REFERENCES

1. Ostrom Q, Patil N, Cioffi G, Waite K, Kruchko C, Barnholtz-Sloan J. CBTRUS Statistical Report: Primary Brain and Other Central Nervous System Tumors Diagnosed in the United States in 2013-2017. *Neuro Oncol* (2020) 22:iv1–iv96. doi: 10.1093/neuonc/noaa200.s
2. Goldbrunner R, Minniti G, Preusser M, Jenkinson M, Sallabanda K, Houdart E, et al. EANO Guidelines for the Diagnosis and Treatment of Meningiomas. *Lancet Oncol* (2016) 17(9):e383–91. doi: 10.1016/s1470-2045(16)30321-7
3. Nassiri F, Mamatjan Y, Suppiah S, Badhiwala J, Mansouri S, Karimi S, et al. DNA Methylation Profiling to Predict Recurrence Risk in Meningioma: Development and Validation of a Nomogram to Optimize Clinical Management. *Neuro Oncol* (2019) 21(7):901–10. doi: 10.1093/neuonc/noz061
4. Spille D, Sporns P, Heß K, Stummer W, Brokinkel B. Prediction of High-Grade Histology and Recurrence in Meningiomas Using Routine Preoperative Magnetic Resonance Imaging: A Systematic Review. *World Neurosurg* (2019) 128:174–81. doi: 10.1016/j.wneu.2019.05.017
5. Ildan F, Erman T, Göçer A, Tuna M, Bağdatoğlu H, Cetinalp E, et al. Predicting the Probability of Meningioma Recurrence in the Preoperative and Early Postoperative Period: A Multivariate Analysis in the Midterm Follow-Up. *Skull Base* (2007) 17(3):157–71. doi: 10.1055/s-2007-970554
6. Hwang W, Marciscano A, Niemierko A, Kim D, Stemmer-Rachamimov A, Curry W, et al. Imaging and Extent of Surgical Resection Predict Risk of Meningioma Recurrence Better Than WHO Histopathological Grade. *Neuro Oncol* (2016) 18(6):863–72. doi: 10.1093/neuonc/nov285
7. Weber D, Ares C, Villa S, Peerdeman S, Renard L, Baumert B, et al. Adjuvant Postoperative High-Dose Radiotherapy for Atypical and Malignant Meningioma: A Phase-II Parallel non-Randomized and Observation Study (EORTC 22042-26042). *Radiother Oncol* (2018) 128(2):260–5. doi: 10.1016/j.radonc.2018.06.018
8. Kalasauskas D, Kronfeld A, Renovanz M, Kurz E, Leukel P, Krenzlin H, et al. Identification of High-Risk Atypical Meningiomas According to Semantic and Radiomic Features. *Cancers* (2020) 12(10):2942. doi: 10.3390/cancers12102942
9. Liu Y, Chotai S, Chen M, Jin S, Qi S, Pan J. Preoperative Radiologic Classification of Convexity Meningioma to Predict the Survival and Aggressive Meningioma Behavior. *PloS One* (2015) 10(3):e0118908. doi: 10.1371/journal.pone.0118908
10. Louis D, Perry A, Reifenberger G, von Deimling A, Figarella-Branger D, Cavenee W, et al. The 2016 World Health Organization Classification of Tumors of the Central Nervous System: A Summary. *Acta Neuropathol* (2016) 131(6):803–20. doi: 10.1007/s00401-016-1545-1
11. Zhu Z, Wang C, Xu J, Wang C, Xia L, Li Q, et al. A Quantified Risk-Scoring System for the Recurrence of Meningiomas: Results From a Retrospective Study of 392 Patients. *Front Oncol* (2020) 10:585313. doi: 10.3389/fonc.2020.585313
12. Spille D, Adeli A, Sporns P, Heß K, Streckert E, Brokinkel C, et al. Predicting the Risk of Postoperative Recurrence and High-Grade Histology in Patients With Intracranial Meningiomas Using Routine Preoperative MRI. *Neurosurg Rev* (2021) 44(2):1109–17. doi: 10.1007/s10143-020-01301-7
13. Ko C, Lim S, Chen T, Chen J, Li C, Shiue Y. Prediction of Progression in Skull Base Meningiomas: Additional Benefits of Apparent Diffusion Coefficient Value. *J Neurooncol* (2018) 138(1):63–71. doi: 10.1007/s11060-018-2769-9
14. Cohen-Inbar O, Soustiel JF, Zaaroor M. Meningiomas in the Elderly, the Surgical Benefit and a New Scoring System. *Acta Neurochir* (2010) 152(1):87–97. doi: 10.1007/s00701-009-0552-6
15. Li H, Zhao M, Jiao Y, Ge P, Li Z, Ma J, et al. Prediction of High-Grade Pediatric Meningiomas: Magnetic Resonance Imaging Features Based on T1-Weighted, T2-Weighted, and Contrast-Enhanced T1-Weighted Images. *World Neurosurg* (2016) 91:89–95. doi: 10.1016/j.wneu.2016.03.079
16. Ho D, Hsu C, Ting L, Chiang H. Histopathology and MIB-1 Labeling Index Predicted Recurrence of Meningiomas: A Proposal of Diagnostic Criteria for Patients With Atypical Meningioma. *Cancer* (2002) 94(5):1538–47. doi: 10.1002/cncr.10351
17. Fujimoto T, Ishida Y, Uchiyama Y, Nakase H, Sakaki T, Nakamura M, et al. Radiological Predictive Factors for Regrowth of Residual Benign Meningiomas. *Neurol Med Chir* (2011) 51(6):415–22. doi: 10.2176/nmc.51.415
18. Hess K, Spille D, Adeli A, Sporns P, Brokinkel C, Grauer O, et al. Brain Invasion and the Risk of Seizures in Patients With Meningioma. *J Neurosurg* (2018) 130(3):789–96. doi: 10.3171/2017.11.Jns172265
19. Joo L, Park J, Park S, Nam S, Kim Y, Kim J, et al. Extensive Peritumoral Edema and Brain-to-Tumor Interface MRI Features Enable Prediction of Brain Invasion in Meningioma: Development and Validation. *Neuro Oncol* (2021) 23(2):324–33. doi: 10.1093/neuonc/noaa190
20. Adeli A, Hess K, Mawrin C, Streckert E, Stummer W, Paulus W, et al. Prediction of Brain Invasion in Patients With Meningiomas Using

Preoperative Magnetic Resonance Imaging. *Oncotarget* (2018) 9(89):35974–82. doi: 10.18632/oncotarget.26313
21. Yamashiro K, Hasegawa M, Higashiguchi S, Kato H, Hirose Y. Intravenous Sinus Meningioma With Intraluminal Extension to the Internal Jugular Vein: Case Report and Review of the Literature. *Br J Neurosurg* (2020), 1–6. doi: 10.1080/02688697.2020.1777258
22. Sughrue M, Rutkowski M, Shangari G, Parsa A, Berger M, McDermott M. Results With Judicious Modern Neurosurgical Management of Parasagittal and Falcine Meningiomas. Clinical article. *J Neurosurg* (2011) 114(3):731–7. doi: 10.3171/2010.9.Jns10646
23. Anthofer J, Seidel-Schulz R, Proescholdt M, Brawanski A, Schebesch K. Meningiomas Adjacent to Major Venous Sinuses-Clinical Outcome and Recurrence. *World Neurosurg* (2017) 104:560–6. doi: 10.1016/j.wneu.2017.05.025
24. Maiuri F, Donzelli R, Pagano S, Mariniello G. The Management of the Venous Sinuses During Surgery for Posterior Fossa Meningiomas. *World Neurosurg* (2019) 125:357–63. doi: 10.1016/j.wneu.2019.02.032
25. Durand A, Labrousse F, Jouvet A, Bauchet L, Kalamaridès M, Menei P, et al. WHO Grade II and III Meningiomas: A Study of Prognostic Factors. *J Neurooncol* (2009) 95(3):367–75. doi: 10.1007/s11060-009-9934-0
26. McLean C, Jolley D, Cukier E, Giles G, Gonzales M. Atypical and Malignant Meningiomas: Importance of Micronecrosis as a Prognostic Indicator. *Histopathology* (1993) 23(4):349–53. doi: 10.1111/j.1365-2559.1993.tb01218.x
27. Góes P, Santos B, Suzuki F, Salles D, Stávale J, Cavalheiro S, et al. Necrosis Is a Consistent Factor to Recurrence of Meningiomas: Should It be a Stand-Alone Grading Criterion for Grade II Meningioma? *J Neurooncol* (2018) 137(2):331–6. doi: 10.1007/s11060-017-2721-4
28. Vakkila J, Lotze MT. Inflammation and Necrosis Promote Tumour Growth. *Natrevimmunol* (2004) 4(8):641–8. doi: 10.1038/nri1415
29. Le Bihan D. Apparent Diffusion Coefficient and Beyond: What Diffusion MR Imaging can Tell Us About Tissue Structure. *Radiology* (2013) 268(2):318–22. doi: 10.1148/radiol.13130420
30. Kinoshita M, Arita H, Okita Y, Kagawa N, Kishima H, Hashimoto N, et al. Comparison of Diffusion Tensor Imaging and C-Methionine Positron Emission Tomography for Reliable Prediction of Tumor Cell Density in Gliomas. *J Neurosurg* (2016) 125(5):1136–42. doi: 10.3171/2015.11.Jns151848
31. Yuan Y, Zeng D, Liu Y, Tao J, Zhang Y, Yang J, et al. DWI and IVIM Are Predictors of Ki67 Proliferation Index: Direct Comparison of MRI Images and Pathological Slices in a Murine Model of Rhabdomyosarcoma. *Eur Radiol* (2020) 30(3):1334–41. doi: 10.1007/s00330-019-06509-w
32. Marciscano A, Stemmer-Rachamimov A, Niemierko A, Larvie M, Curry W, Barker F, et al. Benign Meningiomas (WHO Grade I) With Atypical Histological Features: Correlation of Histopathological Features With Clinical Outcomes. *J Neurosurg* (2016) 124(1):106–14. doi: 10.3171/2015.1.Jns142228
33. Escribano Mesa J, Alonso Morillejo E, Parrón Carreño T, Huete Allut A, Narro Donate J, Méndez Román P, et al. Risk of Recurrence in Operated Parasagittal Meningiomas: A Logistic Binary Regression Model. *World Neurosurg* (2018) 110:e112–8. doi: 10.1016/j.wneu.2017.10.087
34. Alorainy I. Dural Tail Sign in Spinal Meningiomas. *Eur J Radiol* (2006) 60 (3):387–91. doi: 10.1016/j.ejrad.2006.06.012
35. McGovern S, Aldape K, Munsell M, Mahajan A, DeMonte F, Woo S. A Comparison of World Health Organization Tumor Grades at Recurrence in Patients With non-Skull Base and Skull Base Meningiomas. *J Neurosurg* (2010) 112(5):925–33. doi: 10.3171/2009.9.Jns09617
36. Delgado-López P, Corrales-García E. Role of Adjuvant Radiotherapy in Atypical (WHO Grade II) and Anaplastic (WHO Grade III) Meningiomas: A Systematic Review. *Clin Transl Oncol* (2021) 23(2):205–21. doi: 10.1007/s12094-020-02434-3
37. Tibshirani RJ. Regression Shrinkage and Selection *via* the LASSO. *J R Stat Soc Ser B Methodol* (1996) 73(1):273–82. doi: 10.1111/j.2517-6161.1996.tb02080.x

Conflict of Interest: Author YS was employed by Siemens, Healthineers Ltd.

The remaining authors declare that the research was conducted in the absence of any commercial or financial relationships that could be construed as a potential conflict of interest.

Publisher's Note: All claims expressed in this article are solely those of the authors and do not necessarily represent those of their affiliated organizations, or those of the publisher, the editors and the reviewers. Any product that may be evaluated in this article, or claim that may be made by its manufacturer, is not guaranteed or endorsed by the publisher.

Copyright © 2021 Zhang, Chen, Cai, Jiang, Chen, Sun, Song, Lin and Xue. This is an open-access article distributed under the terms of the Creative Commons Attribution License (CC BY). The use, distribution or reproduction in other forums is permitted, provided the original author(s) and the copyright owner(s) are credited and that the original publication in this journal is cited, in accordance with accepted academic practice. No use, distribution or reproduction is permitted which does not comply with these terms.

frontiers in Oncology

ORIGINAL RESEARCH
published: 22 October 2021
doi: 10.3389/fonc.2021.752158

A Clinical Semantic and Radiomics Nomogram for Predicting Brain Invasion in WHO Grade II Meningioma Based on Tumor and Tumor-to-Brain Interface Features

Ning Li[1,2†], Yan Mo[3†], Chencui Huang[3], Kai Han[3], Mengna He[1], Xiaolan Wang[1], Jiaqi Wen[1], Siyu Yang[1], Haoting Wu[1], Fei Dong[1], Fenglei Sun[3], Yiming Li[3], Yizhou Yu[3], Minming Zhang[1], Xiaojun Guan[1] and Xiaojun Xu[1*]*

[1] Department of Radiology, the Second Affiliated Hospital, Zhejiang University School of Medicine, Hangzhou, China, [2] Department of Radiology, Fuyang District First People's Hospital, Hangzhou, China, [3] Deepwise AI Lab, Beijing Deepwise & League of PHD Technology Co., Ltd., Beijing, China

OPEN ACCESS

Edited by:
Hailiang Tang,
Fudan University, China

Reviewed by:
Xiaohua Qian,
Shanghai Jiao Tong University, China
Meimei Chen,
Jilin University, China

***Correspondence:**
Xiaojun Xu
xxjmailbox@zju.edu.cn
Xiaojun Guan
xiaojunguan1102@zju.edu.cn

†These authors have contributed equally to this work

Specialty section:
This article was submitted to Neuro-Oncology and Neurosurgical Oncology, a section of the journal Frontiers in Oncology

Received: 02 August 2021
Accepted: 04 October 2021
Published: 22 October 2021

Citation:
Li N, Mo Y, Huang C, Han K, He M, Wang X, Wen J, Yang S, Wu H, Dong F, Sun F, Li Y, Yu Y, Zhang M, Guan X and Xu X (2021) A Clinical Semantic and Radiomics Nomogram for Predicting Brain Invasion in WHO Grade II Meningioma Based on Tumor and Tumor-to-Brain Interface Features. Front. Oncol. 11:752158. doi: 10.3389/fonc.2021.752158

Background: Brain invasion in meningioma has independent associations with increased risks of tumor progression, lesion recurrence, and poor prognosis. Therefore, this study aimed to construct a model for predicting brain invasion in WHO grade II meningioma by using preoperative MRI.

Methods: One hundred seventy-three patients with brain invasion and 111 patients without brain invasion were included. Three mainstream features, namely, traditional semantic features and radiomics features from tumor and tumor-to-brain interface regions, were acquired. Predictive models correspondingly constructed on each feature set or joint feature set were constructed.

Results: Traditional semantic findings, e.g., peritumoral edema and other four features, had comparable performance in predicting brain invasion with each radiomics feature set. By taking advantage of semantic features and radiomics features from tumoral and tumor-to-brain interface regions, an integrated nomogram that quantifies the risk factor of each selected feature was constructed and had the best performance in predicting brain invasion (area under the curve values were 0.905 in the training set and 0.895 in the test set).

Conclusions: This study provided a clinically available and promising approach to predict brain invasion in WHO grade II meningiomas by using preoperative MRI.

Keywords: atypical meningioma, brain invasion, magnetic resonance imaging, radiomics, semantic

1 INTRODUCTION

Brain invasion becomes a stand-alone criterion for atypical grade II meningioma in the updated 2016 World Health Organization (WHO) Classification of Tumors of the CNS (1), because of its independent associations with increased risks of tumor progression, lesion recurrence, and poor prognosis (2–5). Therefore, the existence of brain invasion can significantly impact preoperative

evaluation and decision-making. Regarding this rising clinical significance, the recognition of brain invasion for brain meningioma especially before clinical intervention is very important, but few biomarkers are routinely used in clinical practice.

As the only golden standard for the diagnosis of brain invasion in meningioma, histopathological examination is greatly dependent on the acquisition of peritumoral brain tissue, leading to a heterogeneous assessments of brain invasion (6). Alternatively, in the preoperative diagnosis/assessment, magnetic resonance imaging (MRI) is the most important technique for brain meningioma by taking advantage of its ultra-high tissue resolution and spatial resolution. Previous existing documents suggested that traditional MRI findings, like peri-tumoral edema, heterogeneous contrast enhancement, and irregular tumor shape, have values in predicting brain invasion (6, 7). However, the outcomes of these imaging signs are not widely supportive (8), which may be resulting from the limited and insufficient information they provided.

Radiomics can convert medical images into mineable high-dimensional quantitative data that may reflect underlying pathophysiology of the tumor (9). By employing radiomics, a number of studies reported the relevant values in grading and classifying brain meningiomas (10–13), while only several documents related it to predict brain invasion in meningioma. Zhang et al. demonstrated that some radiomics features within tumor and sex jointly reached the best performance in predicting brain invasion (14). Joo et al. constructively suggested that the radiomics features from the tumor-to-brain interface region could help predict brain invasion in meningioma (15). Therefore, this couple of studies leads an important role in introducing radiomics to assess the risk of brain invasion in meningioma. However, it is worth noting that 1) both studies merely arbitrarily extracted radiomics features from the tumor region or tumor-to-brain interface region and (2) WHO grade I meningiomas occupied the majority of the training dataset, which might bring pathological bias in model construction (14, 15). Therefore, since grade I meningioma with brain invasion has been assigned to WHO grade II (1), it deserves to predict brain invasion in high grade meningioma (WHO grade II) by integrating the value of radiomics features in tumor and tumor-to-brain interface regions, as well as the traditional radiological findings (semantic features).

In the present study, three mainstream features, namely, radiomics features from the tumor region, radiomics features from the tumor-to-brain interface region, and semantic features, were subsequently extracted from each meningioma. Feature selection and model construction were conducted step by step, and the value of each selected feature was estimated. Finally, an integrated nomogram constructed on the selected features was built to comprehensively estimate the risk points as a composite predictor for brain invasion in meningioma.

2 MATERIALS AND METHODS

This retrospective study was approved by the Medical Ethics Committee of the Second Affiliated Hospital of Zhejiang University School of Medicine. The written informed consent from the patients was waived. All the methods were carried out in accordance with relevant guidelines and regulations.

2.1 Subjects

Initially, 2,878 meningioma patients with pathological confirmation from January 2011 to August 2020 were screened. In the 2016 WHO Classification of Tumors of the CNS, a significant revision for meningioma was that the presence of brain invasion in a WHO grade I meningioma is assigned to WHO grade II (1). Thus, in consideration of this update, a total of 339 patients were included according to the following inclusion criteria: 1) since 2016, WHO grade II meningioma with (N = 117) and without (N = 135) brain invasion should have histopathological evidence; and 2) before 2016, because histopathological assessment of brain invasion was not a regular guideline for grading meningioma, only meningioma with brain invasion (N = 87) was histopathologically confirmed and included. Then, 55 patients were further excluded according to the exclusion criteria shown in **Figure 1**. Finally, 173 meningiomas with brain invasion and 111 meningiomas without brain invasion were recruited.

2.2 Image Acquisition

All the MRI examinations were completed 1 week before the operation in the Second Affiliated Hospital of Zhejiang University School of Medicine. All the images (T1-weighted, T2-weighted, and enhanced T1-weighted imaging) were acquired using clinical scanning protocols in eight MRI scanners (3.0 T scanners, e.g., GE Discovery MR 750, GE Discovery MR 750W, GE Signal HDxt, and United Imaging MRI 790; 1.5 T scanners, e.g., Siemens

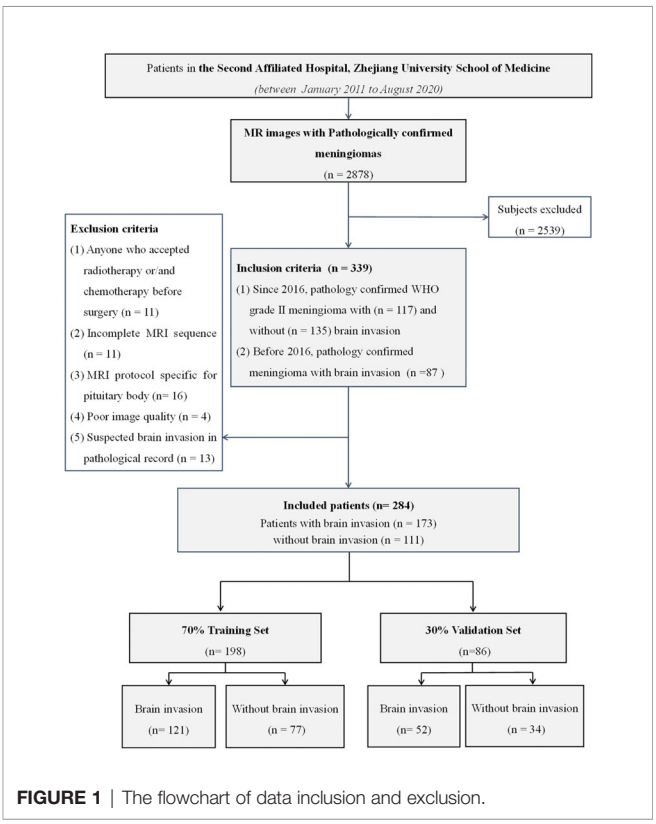

FIGURE 1 | The flowchart of data inclusion and exclusion.

Magnetom Aera, Siemens Magnetom Avento, Siemens Magnetom Sonata, and GE Signal HDxt).

2.3 Clinical Semantic Assessment

Two neuroradiologists with 5 years of experience who were blinded to the clinical and pathological information of the patients evaluated the clinical semantic features for each meningioma. When an inconsistency occurred, the result will be rechecked by a senior neuroradiologist with 30 years of experience. Semantic features including radiological findings and demographic information were recorded (10, 11): 1) tumor location: anterior/middle/posterior cranial fossa, sphenoid crest, saddle tubercle, lateral/midline convexity, tentorium cerebelli, ventricle, other; 2) number of tumors: single or multiple; 3) the largest diameter of the tumor; 4) short diameter perpendicular to the maximum length diameter; 5) T1 signal intensity; 6) T2 signal intensity; 7) degree of contrast enhancement on gadolinium-enhanced T1 imaging; 8) intratumoral heterogeneity after enhancement; 9) tumor margin; 10) peritumoral edema; 11) cystic or necrosis; 12) bone invasion; 13) hyperostosis; 14) dural tail; 15) venous sinus invasion; 16) CSF cleft sign; 17) arterial narrowing; 18) sunburst; 19) age; and 20) sex.

2.4 Radiomics Modeling

2.4.1 Semi-Automatic Region of Interest Segmentation

For every meningioma lesion, manual segmentation was conducted to extract the tumor region, while a semi-automatic segmentation was used to acquire the tumor-to-brain interface region (**Figure 2**). The details were shown below:

1) Manual segmentation of the tumor region [region of interest (ROI)]. Two radiologists with about 5 years of clinical experience manually segmented the tumor ROI along the sharp tumor margin in the axial enhanced T1-weighted images in a slice-by-slice way. Before manual segmentation, these two radiologists were trained by a neuroradiologist with 30 years of experience, and then both of them blinded to the patient information manually segmented 40 randomly selected tumors. DICE similarity coefficient was calculated to test the interoperator agreement (16, 17). As a result, the DICE similarity coefficient was 0.914 ± 0.035, indicating an excellent agreement.

2) Automatic segmentation of tumor-to-brain interface ROI. Based on the outer edge of the tumor region segmented in the first step, the 5 mm in the spatial scale was firstly converted to the

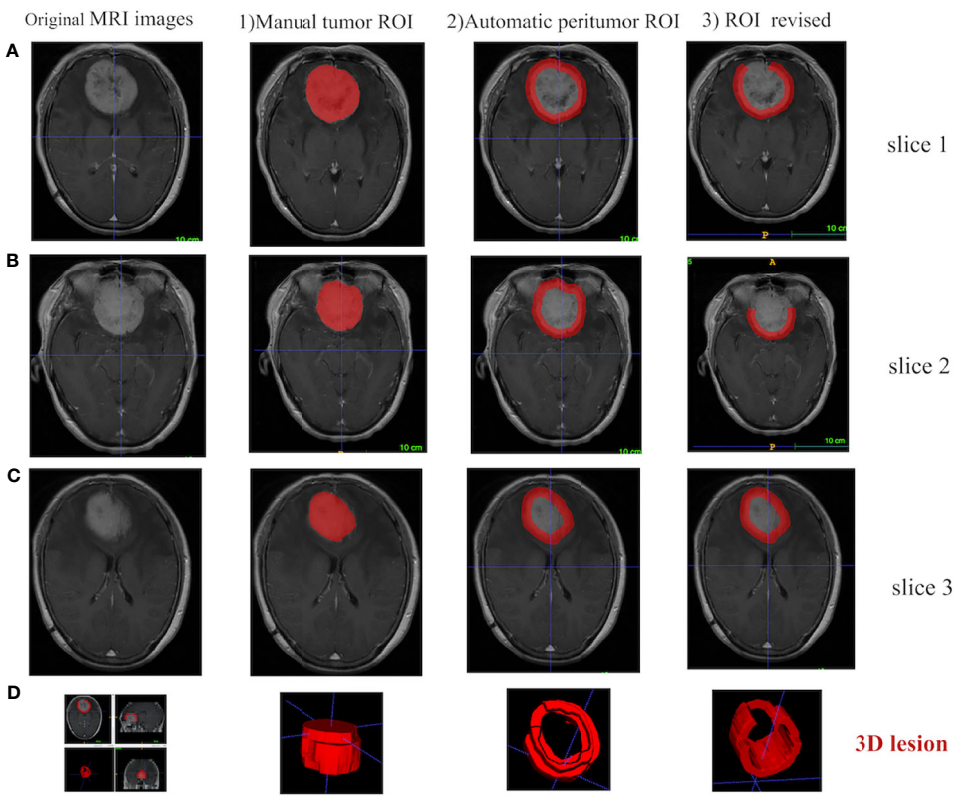

FIGURE 2 | Different ROI segmentation conditions are displayed in 2D and 3D in ITK-SNAP software, including the original image, the manually segmented tumoral ROI, and the semi-automatically segmented tumor-to-brain interface ROI. **(A)** Tumor located in anterior cranial fossa with overlap of non-brain tissues (i.e., bone) after 5 mm expansion, which is manually revised to only keep tumor-to-brain interface. **(B)** The same tumor with overlap of non-brain tissues (i.e., postorbital tissues) after 5 mm expansion, which is manually revised to only keep tumor-to-brain interface. **(C)** The same tumor without any overlap of non-brain tissues after 5 mm expansion. **(D)** 3D visualization. ROI, region of interest.

pixel scale in the image, and then the morphology operations of image expansion and corrosion (Python, Skimage.Morphology) (18) were carried out to automatically segment the tumor-to-brain interface ROI. The initial region was formed by the annular region with the outer boundary of the tumor and the amplification boundary as the inner and outer boundary.

3) Final review and revision for the tumor-to-brain interface region. The initial tumor-to-brain interface region was reviewed layer by layer by the neuroradiologist. If the expansion boundary included non-interested brain/non-brain regions, manual correction was carried out; if no correction was needed, automatic segmentation was retained.

2.4.2 Image Preprocessing and Radiomics Feature Extraction

The original MRI images and the corresponding annotation files were upload to the Deepwise multimodal research platform (https://keyan.deepwise.com, V1.6.2) for radiomics feature quantification, feature engineering on the volume map of the semi-automatically labeled two-dimensional ROI. The complete process of this study is shown in **Figure 3**, which is mainly composed of six steps: ROI segmentation, image preprocessing, feature extraction, feature selection, model building, and model evaluation.

Firstly, in the image preprocessing, *Z*-score normalization was used to process the images with a normalize scale of 100 (19), and the B-spline interpolation sampling method was used to resample MRI images with different resolutions to the same resolution [1,1,1] (20). Then, eight different image transforms (https://pyradiomics.readthedocs.io/en/latest/radiomics.html#module-radiomics.imageoperations), such as high-pass wavelet filter, low-pass wavelet filter, Laplace, gradient, and Gaussian transform, were used to obtain more pixel-level high-throughput image features. Secondly, based on the original and transformed images, we extracted and quantified the radiomics features of tumor and peritumor ROIs, respectively, which included three categories: first-order, shapes, and texture features (21). The three described global information such as gray mean value and variance, local information such as shape and edge of ROI, and mutual information between pixels inside ROI and neighborhood, respectively. Texture features mainly include the GLCM (gray level co-occurrence matrix), GLRLM (gray level run length matrix), GLSZM (gray level size zone matrix), GLDM (gray level dependence matrix), and NGLD (neighboring gray level dependence matrix) (https://pyradiomics.readthedocs.io/en/latest/features.html). See **Supplement Material 1** for specific features.

Finally, a total of 1,763 radiomics features were extracted and normalized for each ROI in our study. *Z*-score normalization was used to eliminate the influence of feature dimensions and speed up the solution of the gradient descent algorithm, $Z = (X - \text{mean})/\text{SD}$.

2.4.3 Features Selection of Radiomics and Semantic Features

2.4.3.1 Selection of Radiomics Features

It consisted of two stages: first, interobserver interclass coefficient (ICC) analysis and correlation analysis were used (22, 23). ICC analysis was used to exclude features with interobserver instability (ICC coefficient < 0.9), and correlation analysis between features was used to exclude features with high correlation (Pearson correlation coefficient > 0.7) and retain low correlation (Pearson correlation coefficient < 0.7). Secondly, the *F*-hypothesis test (ANOVA, *F*-test of homogeneity of variance) (https://statisticsbyjim.com/anova/f-tests-anova/) was used for further feature selection. The *F*-test looked for the linear relationship between the two data groups and returned two statistics of *F*-value and *P*-value. We retain the features that were significantly correlated with the true label (*P*-value < 0.01) and delete those without significantly linear correlation (*P*-value > 0.01) (https://scikit-learn.org/stable/modules/feature_selection.html).

2.4.3.2 Selection of Semantic Features

Statistical tests, univariate and multivariate analyses, and stepping-regression methods were used to select semantic features which were associated with brain invasion of meningioma.

2.4.4 CSRN Construction

The significant semantic and radiomics features were selected as the independent variables, while the meningioma invasion was taken as the dependent variable. The logistic regression (LR) was used to establish a multivariate regression model for predicting brain invasion for meningioma.

We developed five models, namely, 1) tumoral radiomics model (TRM), 2) tumor-to-brain interface radiomics model (TbRM), 3) clinical semantic model (CSM), 4) tumor combined tumor-to-brain interface radiomics model

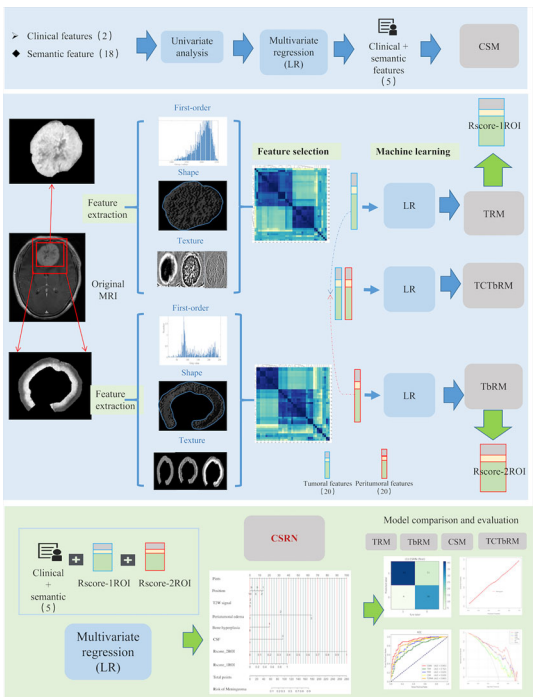

FIGURE 3 | Workflow of this study, which mainly composed of six steps: ROI segmentation, image preprocessing, feature extraction, feature selection, model building, and model comparative evaluation. ROI, region of interest.

(TCTbRM), and 5) clinical semantic and radiomics nomogram (CSRN).

LR is a traditional machine learning binary classifier, which is often used to analyze the risk factors of a certain disease and is suitable for predicting categorical variable (such as meningioma invasion and non-invasion events in this study) (24). This method could output a quantized non-linear model and probabilistic values (continuous variable).

The CSRN was established and evaluated as follows:

1) Model training. All patients were divided into training set and test set in a ratio of 7:3, and it was iterated for 2,000 times to get a stable result. Considering the AUC performance of the training set and test set comprehensively, and following the fact that the number of modeling features accounted for 10%–20% of the total sample size to simplify the prediction model (25), we selected radiomics features, respectively, and examined their statistical differences between meningioma with and without brain invasion.

2) Calculation of radiomics scores. TRM and TbRM based on LR were constructed by selecting 20 significant tumor and 20 tumor-to-brain interface radiomics features, respectively, and the output probability scores of the combination of modeling features and weights were converted into radiomics score, Rad_score (Rscore_1ROI, Rscore_2ROI) (26).

$$\text{Rad_score} = \frac{1}{1 + \exp\left(\Sigma \quad \beta_i * f_i\right)}$$

f_i represents radiomics feature i, while ß$_i$ represents the coefficient corresponding to this feature.

3) Quantitative representation of CSRN. With the inclusion of significant semantic features, Rscore_1ROI and Rscore_2ROI, a CSRN for predicting the meningioma invasion probability was established using multivariate LR (24). Thus, each factor and the predicted probability of brain invasion were described and calculated numerically.

4) Establishment of different models. Similarly, we extracted the features of single category and multiple categories, respectively, and established the remaining four models, namely, TRM, TbRM, CSM, and TCTbRM. See **Supplement Material 2** for details.

5) Comparison and evaluation among the models. The semantic features, tumoral radiomics features, and tumor-to-brain interface radiomics features involved in the modeling were discussed in detail for their application value in clinical scenarios, and the contribution and clinical significance of this study to predict the invasion of WHO grade II meningiomas were also discussed.

The ROC curve, the area under the ROC curve (AUC), accuracy, sensitivity, specificity, negative predictive value (NPV), and positive predictive value (PPV) indexes comprehensively described the performance of the five classifiers. Calibration curves were used to describe the predictive accuracy of CSRN, and decision curve analysis (DCA) was used to describe the clinical efficacy between the models. Feature heat maps were used to describe the correlations between radiomics features, and Python's image processing package was used to visualize these features.

2.5 Statistical Analysis

SPSS 22.0 (released 2013; IBM SPSS Statistics for Windows, Version 22.0), R (https://www.rstudio.com), Python 4.0 (https://www.python.org/), and Deepwise DXAI Platform (https://dxonline.deepwise.com/) were used for statistical validation, analysis, and visualization. Mean and standard deviation (SD) were used to describe numerical variables. Two-independent sample *t*-test was used for the variables with normal distribution, while Wilcoxon test was used for skewed distribution. Frequency was used to describe categorical variables, chi-square test or corrected chi-square test was used for disordered variables, and Kruskal–Wallis *H* test was used for ordered variables. DeLong test was used to compare the ROC curves among the five models, and *Z*-test was used to compare the differences between AUC, accuracy, sensitivity, specificity, NPV, PPV, and other indicators. This study was a bilateral significance test, and a two-tailed $P < 0.05$ was considered statistically significant.

3 RESULTS

3.1 Demographic Information

A total of 284 patients with WHO grade II meningioma were enrolled, consisting of 173 patients with brain invasion and 111 patients without brain invasion. **Table 1** specifies the overall distribution of demographic information and semantic features.

No significant difference in age, the largest diameter of the tumor, and the short diameter perpendicular to the maximum length diameter was observed between meningiomas with and without brain invasion ($P > 0.05$), while significant differences in tumor location, hyperostosis, CSF cleft sign, T2-weighted signal, and peritumoral edema were observed between two groups ($P < 0.05$), suggesting that meningiomas with brain invasion had higher frequency in the location of anterior cranial fossa but lower frequency in midline convexity; higher frequencies of hyperostosis, hypointense T2-weighted signal, and peritumoral edema; and lower frequency of CSF cleft sign in comparison with meningioma without brain invasion (**Table 2**).

3.2 Radiomics Features Selection and Significance Analysis

A total of 1,740 tumoral and 1,740 tumor-to-brain interface radiomics features were extracted. After ICC analysis and correlation analysis, 20 tumoral and 20 tumor-to-brain interface features were selected using *F*-test and LR methods. The Pearson correlation heat maps of the original features and the selected features were respectively shown in **Figure 4**, and it could be clearly seen that the selected 20 features had low correlation in pairs, which reduced the feature redundancy. The radiomics feature distribution of randomly selected meningioma cases with and without brain invasion for each is shown in **Figure 5**. All the selected radiomics features are summarized in **Table 3** and ranked according to their classification contributions (absolute value of weights). Among 40 radiomics features, texture features *vs.* first-order features *vs.*

TABLE 1 | Demographic information of the 284 patients.

Index	Patients (*n* = 284)		
	Non-invasion group (*n* = 111)	Invasion group (*n* = 173)	*p*-value
Age	57.1 ± 12.3	56.6 ± 11.5	0.745[a]
The largest diameter of the tumor	42.8 ± 16.8	44.6 ± 14.5	0.358[a]
Short diameter perpendicular to the maximum length diameter	31 (24–39.5)	34 (25–41)	0.226[b]
Sex			0.843[c]
Female	68 (61.3%)	108 (62.4%)	
Male	43 (38.7%)	65 (37.6%)	
Tumor location			0.000**[c]
Anterior cranial fossa	7 (6.3%)	38 (22.0%)	
Middle cranial fossa	5 (4.5%)	3 (1.7%)	
Posterior cranial fossa	11 (9.9%)	3 (1.7%)	
Sphenoid crest	10 (9.0%)	14 (8.1%)	
Saddle tubercle	0 (0.0%)	4 (2.3%)	
Lateral convexity	44 (39.6%)	78 (45.1%)	
Midline convexity	24 (21.6%)	20 (11.6%)	
Tentorium cerebelli	7 (6.3%)	9 (5.2%)	
Ventricle	1 (0.9%)	4 (2.3%)	
Other	2 (1.8%)	0 (0.0%)	
Number of tumors			0.073[c]
Single	109 (98.2%)	162 (93.6%)	
Multiple	2 (1.8%)	11 (6.4%)	
Cystic or necrosis	59 (53.2%)	105 (60.7%)	0.209[c]
Bone invasion	47 (42.3%)	67 (38.7%)	0.544[c]
Hyperostosis	43 (38.7%)	96 (55.5%)	0.006**[c]
Venous sinus invasion	18 (16.2%)	30 (17.3%)	0.805[c]
Dural tail	100 (90.1%)	148 (85.5%)	0.262[c]
CSF cleft sign	97 (87.4%)	126 (72.8%)	0.004**[c]
Arterial narrowing	4 (3.6%)	6 (3.5%)	1.000[c]
Sunburst	1 (0.9%)	3 (1.7%)	0.948[c]
T1			0.200[d]
Hyperintense	6 (5.4%)	2 (1.2%)	
Isointense	73 (65.8%)	113 (65.3%)	
Hypointense	32 (28.8%)	58 (33.5%)	
T2			0.029[d]*
Hyperintense	49 (44.1%)	68 (39.3%)	
Isointense	61 (55.0%)	91 (52.6%)	
Isointense	1 (0.9%)	14 (8.1%)	
T1+C (degree of CE)			0.325[d]
Mild	15 (13.5%)	31 (17.9%)	
Marked	96 (86.5%)	142 (82.1%)	
Intratumoral heterogeneity			0.689[d]
Uniformly	41 (36.9%)	68 (39.3%)	
Uneven	70 (63.1%)	105 (60.7%)	
Tumor margins			0.572[d]
Clear	24 (21.6%)	32 (18.5%)	
Unclear	55 (49.5%)	88 (50.9%)	
Indistinct	32 (28.8%)	53 (30.6%)	
Peritumoral edema			0.000**[d]
None	38 (34.2%)	10 (5.8%)	
Mild	55 (49.5%)	101 (58.4%)	
Marked	18 (16.2%)	62 (35.8%)	

[a]*Two sample t-test.*
[b]*Wilcoxon test.*
[c]*Chi-square test.*
[d]*Kruskal–Wallis H test.*
*$p < 0.05$, **$p < 0.01$.

shape features = 1.8162 *vs* 0.2743 *vs.* 0.0643 (about 28:4:1, the ratio of absolute value to the sum).

Based on the above features, the LR algorithm was applied to construct the TRM and TbRM by training on each tumoral and tumor-to-brain interface radiomics feature set, respectively, which subsequently converted the output probability scores into radiomics scores (Rscore_1ROI, Rscore_2ROI) by the formula in **Supplement Material 3**.

TABLE 2 | Demographic information of meningioma patients in the training set and test set.

Index	Training set (*n* = 198)			Test set (*n* = 86)			*p*-value
	Non-invasion group (*n* = 77)	Invasion group (*n* = 121)	*p*-value	Non-invasion group (*n* = 34)	Invasion group (*n* = 52)	*p*-value	
Age	57.1 ± 11.7			56.2 ± 12.2			0.564[a]
The largest diameter of the tumor	42.2 ± 16.4	45.6 ± 14.3	0.132[a]	44.3 ± 17.7	42.3 ± 14.8	0.571[a]	0.542[a]
Short diameter perpendicular to the maximum length diameter	31 (24–39)	34.8 (26–41)	0.092[b]	34.5 (24.3–41.3)	34 (23.5–40.1)	0.477[b]	0.899[b]
Sex			0.934			0.803[c]	0.324[c]
Female	46 (59.7%)	73 (60.3%)		22 (64.7%)	35 (67.3%)		
Male	31 (40.3%)	48 (39.7%)		12 (35.3%)	17 (32.7%)		
Tumor location			0.010**			0.053[c]	0.769[c]
Anterior cranial fossa	5 (6.5%)	27 (22.3%)		2 (5.9%)	11 (21.2%)		
Middle cranial fossa	4 (5.2%)	3 (2.5%)		1 (2.9%)	0 (0.0%)		
Posterior cranial fossa	7 (9.1%)	2 (1.7%)		4 (11.8%)	1 (1.9%)		
Sphenoid crest	8 (10.4%)	11 (9.1%)		2 (5.9%)	3 (5.8%)		
Saddle tubercle	0 (0.0%)	2 (1.7%)		0 (0.0%)	2 (3.8%)		
Lateral convexity	32 (41.6%)	52 (43.0%)		12 (35.3%)	26 (50.0%)		
Midline convexity	15 (19.5%)	16 (13.2%)		9 (26.5%)	4 (7.7%)		
Tentorium cerebelli	4 (5.2%)	5 (4.1%)		3 (8.8%)	4 (7.7%)		
Ventricle	0 (0.0%)	3 (2.5%)		1 (2.9%)	1 (1.9%)		
Other	2 (2.6%)	0 (0.0%)		0 (0.0%)	0 (0.0%)		
Number of tumors			0.162			0.932[c]	1.000[c]
Single	76 (98.7%)	113 (93.4%)		33 (97.1%)	49 (94.2%)		
Multiple	1 (1.3%)	8 (6.6%)		1 (2.9%)	3 (5.8%)		
Cystic or necrosis	42 (54.5%)	74 (61.2%)	0.357	17 (50.0%)	31 (59.6%)	0.380[c]	0.664[c]
Bone invasion	31 (40.3%)	47 (38.8%)	0.842	16 (47.1%)	20 (38.5%)	0.429[c]	0.697[c]
Hyperostosis	30 (39.0%)	68 (56.2%)	0.018*	13 (38.2%)	28 (53.8%)	0.156[c]	0.778[c]
Venous sinus invasion	10 (13.0%)	22 (18.2%)	0.333	8 (23.5%)	8 (15.4%)	0.343[c]	0.614[c]
Dural tail	68 (88.3%)	106 (87.6%)	0.882	32 (94.1%)	42 (80.8%)	0.153[c]	0.670[c]
CSF cleft sign	66 (85.7%)	93 (76.9%)	0.127	31 (91.2%)	33 (63.5%)	0.004**[c]	0.267[c]
Arterial narrowing	2 (2.6%)	6 (5.0%)	0.651	2 (5.9%)	0 (0.0%)	0.299[c]	0.711[c]
Sunburst	0 (0.0%)	1 (0.8%)	1.000	1 (2.9%)	2 (3.8%)	1.000[c]	0.158[c]
T1			0.671			0.089[d]	0.223[d]
Hyperintense	4 (5.2%)	1 (0.8%)		2 (5.9%)	1 (1.9%)		
Isointense	47 (61.0%)	79 (65.3%)		26 (76.5%)	34 (65.4%)		
Hypointense	26 (33.8%)	41 (33.9%)		6 (17.6%)	17 (32.7%)		
T2			0.069			0.897[d]	0.749[d]
Hyperintense	37 (48.1%)	45 (37.2%)		12 (35.3%)	23 (44.2%)		
Isointense	39 (50.6%)	68 (56.2%)		22 (64.7%)	23 (44.2%)		
Hypointense	1 (1.3%)	8 (6.6%)		0 (0.0%)	6 (11.5%)		
T1+C (degree of CE)			0.257			1.000[d]	0.168[d]
Mild	11 (14.3%)	25 (20.7%)		4 (11.8%)	6 (11.5%)		
Marked	66 (85.7%)	96 (79.3%)		30 (88.2%)	46 (88.5%)		
Intratumoral heterogeneity			0.987			0.451[d]	0.789[d]
Uniform	30 (39.0%)	47 (38.8%)		11 (32.4%)	21 (40.4%)		
Uneven	47 (61.0%)	74 (61.2%)		23 (67.6%)	31 (59.6%)		
Tumor margins			0.514			0.961[d]	0.830[d]
Clear	19 (24.7%)	21 (17.4%)		5 (14.7%)	11 (21.2%)		
Unclear	35 (45.5%)	64 (52.9%)		20 (58.8%)	24 (46.2%)		
Indistinct	23 (29.9%)	36 (29.8%)		9 (26.5%)	17 (32.7%)		
Peritumoral edema			0.000**			0.000**[d]	0.587[d]
None	27 (35.1%)	6 (5.0%)		11 (32.4%)	4 (7.7%)		
Mild	35 (45.5%)	72 (59.5%)		20 (58.8%)	29 (55.8%)		
Marked	15 (19.5%)	43 (35.5%)		3 (8.8%)	19 (36.5%)		

[a]*Two-sample t-test.*
[b]*Wilcoxon test.*
[c]*Chi-square analysis.*
[d]*Kruskal–Wallis H test.*
*$p < 0.05$, **$p < 0.01$.

3.3 Multivariate Analysis of LR: Semantic Features and Rscore

Then, all the semantic features and Rscore, including peritumoral edema, tumor location, hyperostosis, T2W signal, and CSF cleft sign, and Rscore_1ROI and Rscore_2ROI, were combined to construct an integrated model, CSRN, by using multivariate analysis of LR. The variance inflation factor (VIF) test was performed. **Table 4** lists all these included features and their

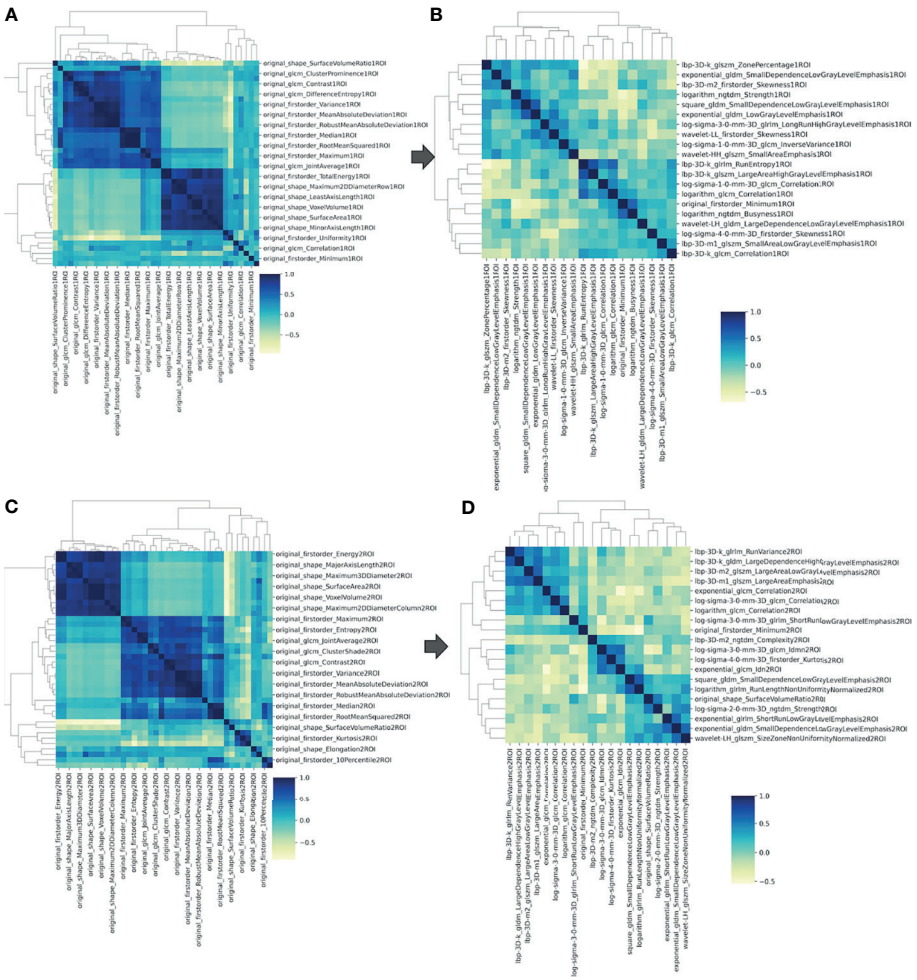

FIGURE 4 | The Pearson correlation heat maps of radiomics features. **(A)** Sixty of the original 1,740 radiomics features of tumoral ROI; **(B)** 20 selected radiomics features of tumoral ROI; **(C)** 60 of the original 1,740 radiomics features of tumor-to-brain interface ROI; **(D)** 20 selected radiomics features of tumor-to-brain interface ROI. ROI, region of interest.

statistical data and ranked them according to *P*-values. As a result, the importance order of brain invasion predictors was as follows: peritumoral edema > Rscore_2ROI (tumor-to-brain interface radiomics features) > Rscore_1ROI (tumoral radiomics features) > tumor location > CSF cleft sign > T2-weighted signal > osteogenesis.

3.4 The Performance of CSRN, TRM, TbRM, CSM, and TCTbRM

CSRN combined seven factors and the LR algorithm to calculate the risk probability of brain invasion for meningioma patients. In **Figure 6A**, the input and output of CSRN had be quantified in the nomogram. According to the value of each patient in each factor, each quantized point ("Point") would be obtained and the total points were summed ("Total points"), and then the risk of brain invasion was calculated ("Risk of invasion"). The detailed explanation of each factor is shown in **Supplement Material 4**. The higher the total score, the greater the risk of brain invasion of the patient is. We drew nomogram correction curves (**Figures 6B, C**) on the training set and the test set, respectively. It can be seen that the prediction curve is close to the reference line (slope = 1), indicating its prediction ability is excellent.

Furthermore, the performances of CSRN and the other four models (TRM, TbRM, CSM, TCTbRM) are shown in **Figure 7**, respectively, by confusion matrix, and it can be seen that the number of false-positive and false-negative samples of CSRN was lower than that of the other models in both training and test sets. The ROC curves and AUCs of the five models in the training set and the test set are, respectively, shown in **Figures 8A, B**, indicating that the AUC of CSRN was the largest.

Youden coefficient was used to find the cutoff point of the ROC curve and to calculate the accuracy, sensitivity, specificity, NPV, and PPV for each model, and all indexes are shown in **Table 5**. In **Supplement Material 5**, we demonstrated the

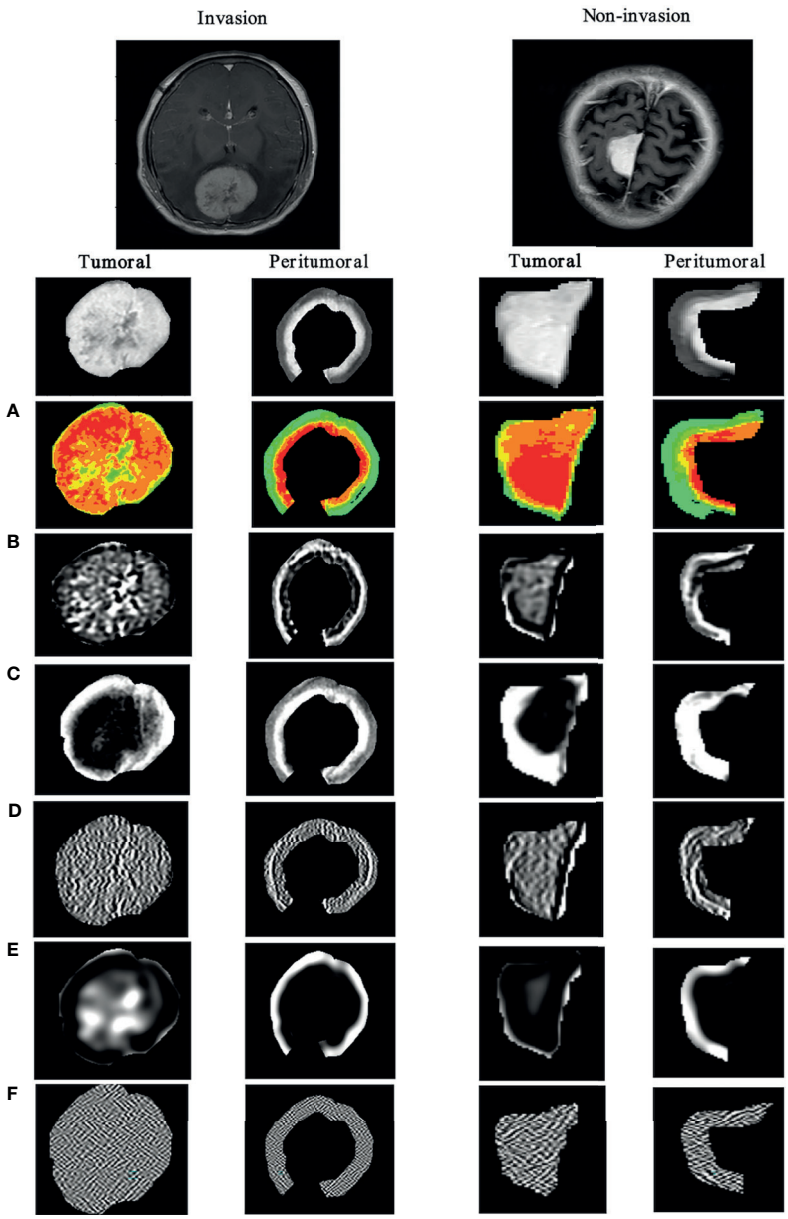

FIGURE 5 | Visualization of tumoral and tumor-to-brain interface significant radiomics features of brain invasion and non-invasion in patients with meningioma. The results show the differences between two ROIs in the high-throughput radiomics features. In meningioma with brain invasion, the signal in the tumor is more dense, and the texture signal intensity around the 5-mm tumor is higher, that is, the information complexity is higher. **(A)** Original_firstorder (pseudo-color image); **(B)** wavelet-LLH_gldm; **(C)** log-sigma-1-0-mm-_glcm; **(D)** lbp-m2_ngtdm; **(E)** log-sigma-3-0-mm-_glrlm; **(F)** wavelet-HHL_glszm. ROI, region of interest.

process of using Youden to find the cutoff point on the training set of the CSRN.

The results in **Table 5** show the following: in the training set, CSRN had the highest AUC of 0.905 (95% CI 0.863–0.9472), which was significantly higher than those of the TRM (0.762, 95% CI 0.695–0.829), TbRM (0.829, 95% CI 0.771–0.888), CSM (0.828, 95% CI 0.769–0.887), and TCTbRM (0.860, 95% CI 0.807–0.913), and the AUC of the TCTbRM was better than that of the CSM, while the AUC of the TbRM was close to that of the CSM. Specifically, in the test set, the AUC of CSRN was 0.895 (95% CI 0.828–0.962), which was significantly higher than that of the TRM (0.701, 95% CI 0.588–0.814) and significantly higher than those of the TbRM (0.769, 95% CI 0.67–0.867), CSM (0.761, 95% CI 0.658–0.863), and TCTbRM (0.817, 95% CI 0.723–0.91) (DeLong test, $P < 0.05$).

The accuracy, sensitivity, specificity, NPV, and PPV of CSRN on the test set were 0.826, 0.788, 0.882, 0.732, and 0.911, respectively, among which accuracy, specificity, and NPV were

TABLE 3 | Statistics of all the selected radiomics features.

Features	Weights	Mean	Standard deviation	*p*-value	Test	Feature source	Sort	Image
LoG-sigma-3-0-mm-3D_glrlm_ShortRunLowGrayLevelEmphasis2ROI	0.1468	0.0069	0.0058	0.001*	W	Tumor-to-brain interface ROI	Texture	LoG
LBP-3D-m2_ngtdm_Complexity2ROI	–0.1455	3.8204	1.2285	0.004*	W	Tumor-to-brain interface ROI	Texture	LBP
exponential_gldm_SmallDependenceLowGrayLevelEmphasis2ROI	–0.1226	0.0199	0.0024	0.000*	*t*	Tumor-to-brain interface ROI	Texture	Exponential
square_gldm_SmallDependenceLowGrayLevelEmphasis2ROI	–0.1015	0.0228	0.0057	0.000*	W	Tumor-to-brain interface ROI	Texture	Square
logarithm_ngtdm_Busyness1ROI	0.0942	0.0975	0.1218	0.000*	W	Tumor ROI	Texture	LoG
LoG-sigma-4-0-mm-3D_firstorder_Kurtosis2ROI	–0.0935	2.9566	0.8304	0.000*	W	Tumor-to-brain interface ROI	First-order	LoG
LoG-sigma-3-0-mm-3D_glcm_Correlation2ROI	0.0923	0.9341	0.0101	0.000*	W	Tumor-to-brain interface ROI	Texture	LoG
LoG-sigma-3-0-mm-3D_glcm_Idmn2ROI	–0.0921	0.996	0.0016	0.007*	*t*	Tumor-to-brain interface ROI	Texture	LoG
logarithm_ngtdm_Strength1ROI	–0.0882	26.2279	32.0014	0.000*	W	Tumor ROI	Texture	LoG
LoG-sigma-1-0-mm-3D_glcm_InverseVariance1ROI	0.0828	0.4085	0.0516	0.000*	W	Tumor ROI	Texture	LoG
LoG-sigma-3-0-mm-3D_glrlm_LongRunHighGrayLevelEmphasis1ROI	–0.0695	971.5188	765.1715	0.000*	W	Tumor ROI	Texture	LoG
LoG-sigma-1-0-mm-3D_glcm_Correlation1ROI	0.0694	0.5867	0.0538	0.002	*t*	Tumor ROI	Texture	LoG
LBP-3D-k_glrlm_RunVariance2ROI	0.0655	18.9969	6.2895	0.007*	W	Tumor-to-brain interface ROI	Texture	LBP
original_shape_SurfaceVolumeRatio2ROI	–0.0643	0.3724	0.0438	0.006*	*t*	Tumor-to-brain interface ROI	Shape	Original image
logarithm_glcm_Correlation2ROI	0.0636	0.7629	0.0834	0.000*	*t*	Tumor-to-brain interface ROI	Texture	LoG
LBP-3D-m2_glszm_LargeAreaLowGrayLevelEmphasis2ROI	0.0614	86.305	63.3261	0.001*	W	Tumor-to-brain interface ROI	Texture	LBP
exponential_glcm_Correlation2ROI	0.0581	0.7174	0.1598	0.000*	W	Tumor-to-brain interface ROI	Texture	Exponential
LoG-sigma-2-0-mm-3D_ngtdm_Strength2ROI	–0.0533	5.7185	6.7859	0.009*	W	Tumor-to-brain interface ROI	Texture	LoG
original_firstorder_Minimum1ROI	0.0501	–5.0574	41.7556	0.000*	*t*	Tumor ROI	First-order	Original image
wavelet-HH_glszm_SmallAreaEmphasis1ROI	–0.0495	0.7119	0.0341	0.000*	*t*	Tumor ROI	Texture	Wavelet
exponential_gldm_SmallDependenceLowGrayLevelEmphasis1ROI	–0.0473	0.0231	0.0067	0.000*	W	Tumor ROI	Texture	Exponential
exponential_gldm_LowGrayLevelEmphasis1ROI	–0.0462	0.4158	0.2573	0.000*	W	Tumor ROI	Texture	Exponential
LBP-3D-m2_firstorder_Skewness1ROI	–0.046	–0.595	0.2577	0.000*	W	Tumor ROI	First-order	LBP
wavelet-LL_firstorder_Skewness1ROI	0.0374	–0.3226	0.5985	0.006*	*t*	Tumor ROI	First-order	Wavelet
LBP-3D-k_gldm_LargeDependenceHighGrayLevelEmphasis2ROI	0.0365	61.6663	2.7931	0.000*	*t*	Tumor-to-brain interface ROI	Texture	LBP
original_firstorder_Minimum2ROI	0.0357	–46.631	32.7178	0.000*	*t*	Tumor-to-brain interface ROI	First-order	Original image
LBP-3D-m1_glszm_SmallAreaLowGrayLevelEmphasis1ROI	0.0353	0.1478	0.026	0.008*	*t*	Tumor ROI	Texture	LBP
LBP-3D-k_glcm_Correlation1ROI	0.03	0.2733	0.092	0.004*	*t*	Tumor ROI	Texture	LBP
LBP-3D-m1_glszm_LargeAreaEmphasis2ROI	0.0298	497.883	349.1798	0.000*	W	Tumor-to-brain interface ROI	Texture	LBP
LBP-3D-k_glrlm_RunEntropy1ROI	–0.0266	4.1129	0.2879	0.031*	*t*	Tumor ROI	Texture	LBP
wavelet-LH_gldm_LargeDependenceLowGrayLevelEmphasis1ROI	0.0245	0.016	0.0189	0.000*	W	Tumor ROI	Texture	Wavelet
wavelet-LH_glszm_SizeZoneNonUniformityNormalized2ROI	–0.0196	0.5121	0.0603	0.000*	*t*	Tumor-to-brain interface ROI	Texture	Wavelet
exponential_glrlm_ShortRunLowGrayLevelEmphasis2ROI	–0.0176	0.1056	0.0286	0.005*	W	Tumor-to-brain interface ROI	Texture	Exponential
LBP-3D-k_glszm_LargeAreaHighGrayLevelEmphasis1ROI	–0.016	36,713.5462	24,915.5914	0.021*	*t*	Tumor ROI	Texture	LBP
LoG-sigma-4-0-mm-3D_firstorder_Skewness1ROI	–0.0116	0.0814	0.4851	0.033*	*t*	Tumor ROI	First-order	LoG
logarithm_glrlm_RunLengthNonUniformityNormalized2ROI	–0.0098	0.8039	0.0714	0.000*	*t*	Tumor-to-brain interface ROI	Texture	LoG
logarithm_glcm_Correlation1ROI	0.0094	0.7269	0.1057	0.000*	W	Tumor ROI	Texture	LoG

(Continued)

TABLE 3 | Continued

Features	Weights	Mean	Standard deviation	*p*-value	Test	Feature source	Sort	Image
LBP-3D-k_glszm_ZonePercentage1ROI	0.0064	0.0224	0.0075	0.001*	*t*	Tumor ROI	Texture	LBP
exponential_glcm_Idn2ROI	−0.0031	0.9767	0.011	0.007*	*t*	Tumor-to-brain interface ROI	Texture	Exponential
square_gldm_SmallDependenceLowGrayLevelEmphasis1ROI	−0.0018	0.0124	0.0084	0.000*	W	Tumor ROI	Texture	Square

ROI, region of interest; W, Wilcoxon test; t, t-test.
**p < 0.05.*

TABLE 4 | The result of multiple logistic regression.

Features	Coef	t/χ^2	*p*-value
Peritumoral edema	1.3079	42.592	<0.0001
Tumor location	−0.0633	33.021	0.0046**
Hyperostosis	0.8289	7.594	0.0309*
T2-weighted signal	−0.0210	7.075	0.0095**
CSF cleft sign	−1.3991	8.493	0.0063**
Rscore_1ROI	1.5849	−10.338	0.0013**
Rscore_2ROI	4.1189	−7.516	<0.0001

**p < 0.05, **p < 0.01.*

significantly higher than those of all the other models (*Z*-test, $P < 0.05$); the specificity and NPV of TCTbRM were higher than those of CSRN (0.885 *vs.* 0.788, 0.786 *vs.* 0.732) (*Z*-test, $P < 0.05$), while accuracy, specificity, and PPV were lower than those of the CSRN.

In order to explore the auxiliary value of different types of features in making clinical decision, we performed clinical decision analysis (DCA) on different models, and these are shown in **Figures 8C, D** of the training set and test set. The results showed that the clinical net benefit (NB) of CSRN was higher than that of all the other models in the training set. If the prediction probability of 35%–90% was selected as the diagnostic model, the clinical NB of CSRN in the test set is higher than that of all the other models, while when the prediction probability was 20%–35%, the NB of all the models were close.

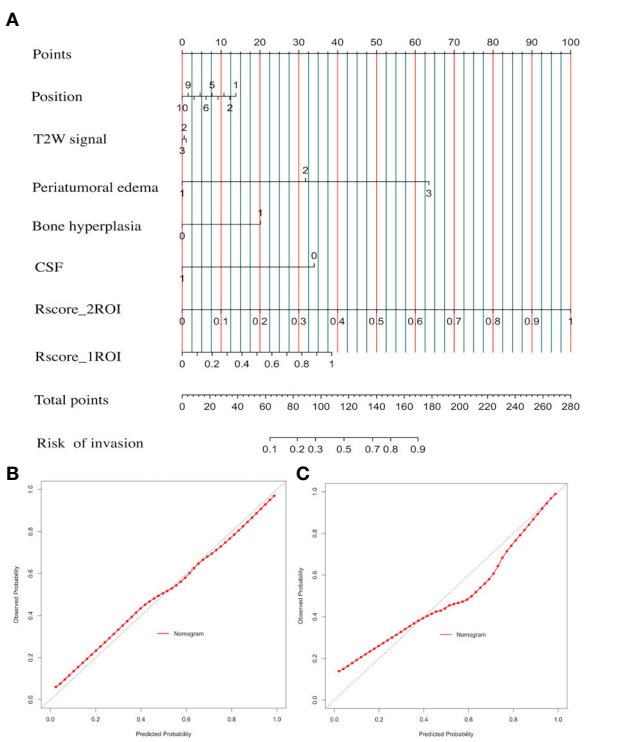

FIGURE 6 | Clinical semantic and radiomics nomogram (CSRN) and its calibration curves. **(A)** Nomogram; **(B)** correction curve of the training set; **(C)** calibration curves of the test set.

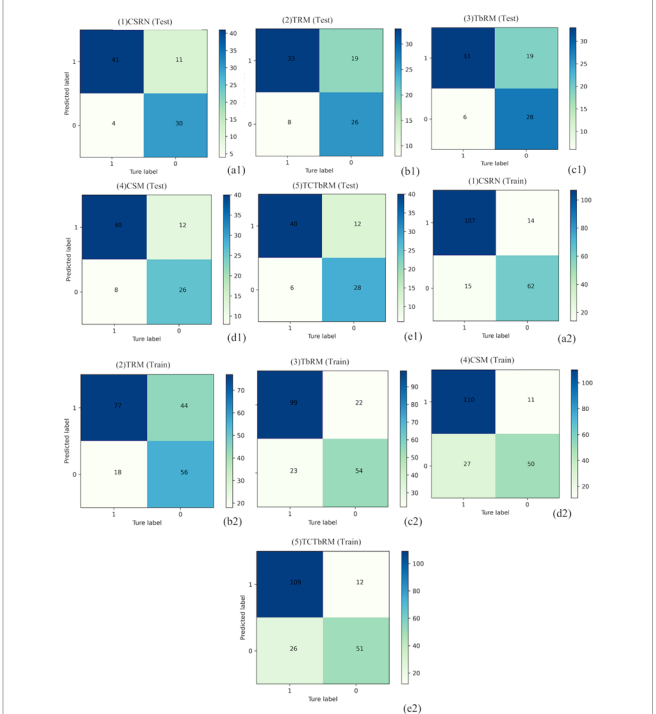

FIGURE 7 | Confusion matrixes of the five models. Test set: CSRN **(A1)**, TRM **(B1)**, TbRM **(C1)**, CSM **(D1)**, and TCTbRM **(E1)**; training set: CSRN **(A2)**, TRM **(B2)**, TbRM **(C2)**, CSM **(D2)**, and TCTbRM **(E2)**. CSRN, clinical semantic and radiomics model/nomogram; TRM, tumoral radiomics model; TbRM, tumor-to-brain interface radiomics model; CSM, clinical semantic model; TCTbRM, tumor combined tumor-to-brain interface radiomics model.

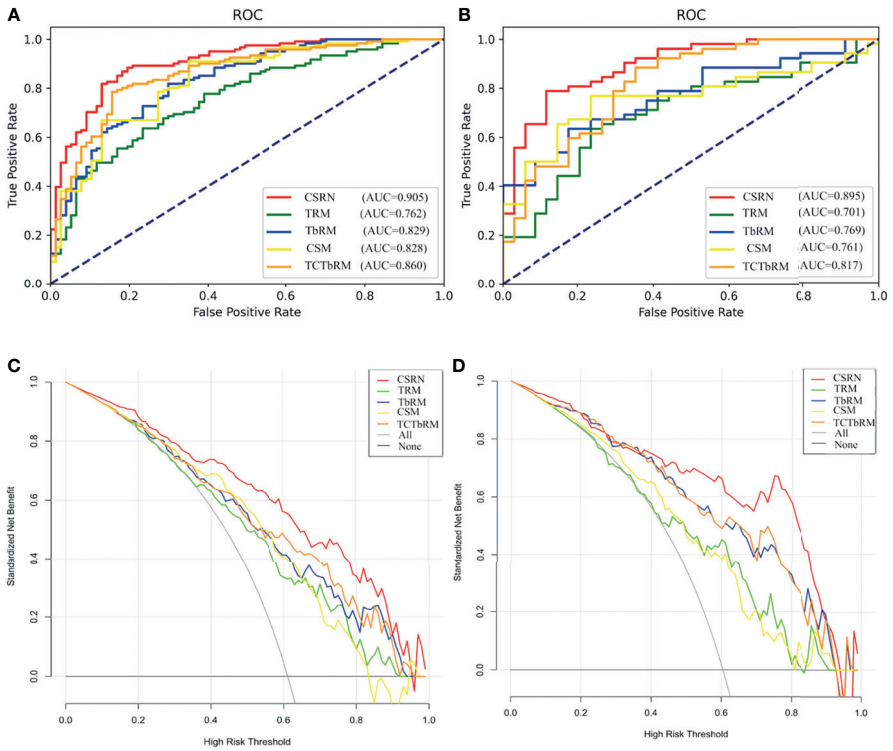

FIGURE 8 | Performance of the five models. **(A)** ROC curve of the training set; **(B)** ROC curve of the test set; **(C)** DCA curve of the training set; **(D)** DCA curve of the test set. ROI, region of interest; DCA, decision curve analysis.

TABLE 5 | Comparison of the performance of the models.

Model	Training set (*n* = 198)							Test set (*n* = 86)						
	AUC (95% CI)	*p*-value (*vs.* CSRN)	ACC	SEN	SPE	NPV	PPV	AUC (95% CI)	*p*-value *vs.* CSRN	ACC	SEN	SPE	NPV	PPV
CSRN	0.905 (0.863–0.9472)	–	0.854	0.884 (0.813–0.935)	0.81 (0.699–0.887)	0.816 (0.717–0.893)	0.877 (0.800–0.931)	0.895 (0.828–0.962)	–	0.826	0.788 (0.653–0.889)	0.882 (0.725–0.967)	0.732 (0.579–0.914)	0.911 (0.783–0.957)
TRM	0.762 (0.695–0.829)	0.0004**	0.689	0.636 (0.544–0.722)	0.77 (0.656–0.855)	0.573 (0.478–0.707)	0.811 (0.713–0.864)	0.701 (0.588–0.814)	0.004**	0.686	0.635 (0.490–0.764)	0.765 (0.588–0.893)	0.578 (0.430–0.778)	0.805 (0.645–0.885)
TbRM	0.829 (0.771–0.888)	0.039*	0.773	0.818 (0.738–0.882)	0.701 (0.586–0.800)	0.711 (0.605–0.807)	0.812 (0.722–0.878)	0.769 (0.671–0.867)	0.039*	0.709	0.635 (0.490–0.764)	0.84 (0.655–0.932)	0.596 (0.449–0.813)	0.846 (0.691–0.911)
CSM	0.828 (0.769–0.887)	0.037*	0.808	0.909 (0.843–0.954)	0.649 (0.53–0.755)	0.820 (0.710–0.883)	0.803 (0.714–0.894)	0.761 (0.658–0.863)	0.033*	0.767	0.769 (0.632–0.875)	0.765 (0.588–0.893)	0.684 (0.527–0.847)	0.833 (0.687–0.913)
TCTbRM	0.860 (0.807–0.913)	0.072	0.808	0.785 (0.701–0.855)	0.844 (0.744–0.917)	0.714 (0.616–0.836)	0.888 (0.809–0.927)	0.817 (0.723–0.910)	0.046*	0.791	0.885 (0.766–0.956)	0.647 (0.46–0.803)	0.786 (0.610–0.890)	0.793 (0.645–0.917)

ACC, accuracy; SEN, sensitivity; SPE, specificity; NPV, negative predictive value; PPV, positive predictive value.
**Indicates significant difference after the DeLong test.*
**p< 0.05, **p < 0.01.*

4 DISCUSSION

This study comprehensively extracted high-throughput radiomics features from tumoral and tumor-to-brain interface regions as well as traditional semantic features and also explored the performance in predicting brain invasion in meningioma among different predictive models that were constructed on corresponding radiomics and semantic features. We had two

main findings: 1) all the CSM, TRM, and TbRM had significant but similar contributions to predicting brain invasion in meningioma; and 2) an individually available nomogram that was composed of semantic feature set, radiomics feature set of tumor, and tumor-to-brain interface regions was constructed, which had the best prediction of brain invasion in both training and test sets.

In the building of CSM, traditional radiological findings, like peritumoral edema, CSF cleft sign, hyperostosis, T2-weigthed signal, and tumor location, were finally included, suggesting that meningiomas with severe peritumoral edema, loss of CSF cleft sign, obvious hyperostosis, low T2-weighted signal, and anterior fossa base location would have a higher risk of brain invasion. Peritumoral edema is the most important semantic feature in predicting brain invasion of meningioma, which was consistently reported by previous studies (6, 15, 27). As demonstrated in the present study, meningioma with one or several of these findings may be indirectly indicating aggressive biological behavior, e.g., regional infiltration to the brain and bone tissues (the occurrence of peritumoral edema, loss of CSF cleft sign, and hyperostosis) (28), high tumor cell density (low T2-weighted signal), and various tumor microenvironments and histopathological origins in different anatomical locations (29). When estimating this CSM, we observed a moderate performance (AUC = 0.761) in predicting brain invasion in the test dataset. Therefore, it remains active to further improve the performance and facilitate the clinical translation of preoperative MRI.

Radiomics measurements from tumor and related regions have been well established as a promising approach to quantify tumor shapes, intensity distributions, spatial relationships, and texture heterogeneity that are difficult to find on routine imaging and imperceptible to the human eyes (9). Therefore, the current study extracted radiomics features to assist in predicting brain invasion for meningioma by two steps. First, we extracted radiomics features within the tumor region, built TRM, and calculated Rscore to represent its performance in predicting brain invasion individually. The AUCs in training set and test set were 0.762 and 0.701, respectively, which were relatively consistent with a recent study (AUC = 0.682 in the training set and 0.735 in the validation set) by employing enhanced T1-weighted imaging (14). Moreover, several studies hypothesized that the tumor-to-brain interface radiomics features may reflect tumor-associated alterations, e.g., direct tumor involvement and indirect immunoreaction (15, 30). By singly learning tumor-to-brain interface radiomics features, the AUCs of TbRM reached 0.829 and 0.769 in the training set and test set, respectively. However, the prediction performances of TRM, TbRM, and CSM remained moderate, and no intermodel difference was observed among them, which suggested that current protocols were still hard to be potentially translated in clinical practice. Alternatively, it should be worth noting that those three kinds of imaging features were enriched with very different but complementary biological information, i.e., TRM indicated intrinsic tumor property [e.g., spatial heterogeneity of tumor tissue (9)], TbRM specified tumor-related infiltration (15, 30), and CSM provided both tumor and tumor-to-brain interface information in a macroscopic way. Therefore, to advance the study, we improved our protocol by training model from different sets of features that may increase understanding of tumor biology.

Herein, a TCTbRM was constructed and its performance was estimated with AUCs of 0.860 and 0.817 in the training set and test set. This radiomics model comprehensively explained tumor behavior in a voxel-to-voxel way. Although the model performance was not significantly better than that mentioned above, a trend of increased prediction efficacy was indicated with TCTbRM > TbRM ≈ CSM > TRM in the test set. However, to the best of our knowledge, such radiomics model was not included following information, but CSM provided the following: 1) the relationship with neighboring tissues (e.g., bone) cannot be considered, 2) the distal and severe edema related to tumor was ignored since only 5 mm from the tumor margin was estimated, and 3) the tumor tissue origin may be different from intracranial sites. Therefore, a prediction model (CSRN) that combined all three kinds of tumor features was constructed, and a significant improvement in performance was observed (AUCs were 0.905 in the training set and 0.895 in the test dataset). A nomogram was then built that quantified the risk point of each semantic feature and Rscore from tumoral and tumor-to-brain interface radiomics. Furthermore, DCA demonstrated that, with the assistance of CSRN, radiologists would obtain higher clinical benefits in clinical decision-making.

This study had several limitations. First, the pathological diagnosis of brain invasion may be subject to sampling error, especially when diagnosing meningioma without brain invasion. In our study, all patients with brain invasion were confirmed by pathological evidence; however, the diagnosis of negative cases may be to some extent associated with insufficient tissue blocks during operation. Therefore, future radiologic–pathologic association analysis would be helpful to confirm the present findings. Second, even though this study included all meningioma patients with brain invasion from 2011 to 2020 with pathological confirmation, the sample size was relatively small and only single-center data were available. Therefore, it is promising to make CSRN go through multicenter dataset with a larger sample size in the future. Third, the enlargement of features in the model construction may cause overfitting; here, we reduce the overfitting risk by randomly splitting the dataset into training set and independent test set. In the future, more external validations are warranted. Fourth, although we performed image preprocessing to minimize the variability, including *Z*-score normalization and B-spline interpolation sampling method, the MRI data used in the present study were acquired using different scanners, which may bring some biases. In reverse, as there was no correction by scanner type, this illustrates the translational potential of our results and it is a strong argument in favor of a multicentric application of radiomics.

In conclusion, this study firstly disclosed that traditional semantic findings had comparable performance in predicting brain invasion of meningioma with radiomics information. By taking advantage of semantic features and radiomics features from tumoral and tumor-to-brain interface regions, an integrated nomogram model was constructed that had

excellent efficacy in predicting brain invasion, which currently was available for further clinical validation.

DATA AVAILABILITY STATEMENT

The raw data supporting the conclusions of this article will be made available by the authors, without undue reservation.

ETHICS STATEMENT

The studies involving human participants were reviewed and approved by the Second Affiliated Hospital of Zhejiang University School of Medicine. Written informed consent for participation was not required for this study in accordance with the national legislation and the institutional requirements.

AUTHOR CONTRIBUTIONS

XX and XG conceived the project. XX, XG, and NL designed the experiments. XX, XG, NL, MH, XW, JW, SY, HW, FD, and MZ acquired the MRI data. XX, XG, NL, YM, CH, KH, MH, XW, JW, SY, HW, FD, FS, YL, and YY performed the experiments. XX, XG, NL, and YM wrote the manuscript. All authors contributed to the article and approved the submitted version.

FUNDING

This study was supported by the National Key Research and Development Program of China (Grant No. 2017YFC0113400), Natural Science Foundation of Zhejiang Province (Grant No. LQ21H180008) and the China Postdoctoral Science Foundation (Grant No. 2021T140599 and 2019M662082).

ACKNOWLEDGMENTS

The authors sincerely thank the intelligence contributions from the members in Deepwise AI Lab who were not listed as co-authors.

SUPPLEMENTARY MATERIAL

The Supplementary Material for this article can be found online at: https://www.frontiersin.org/articles/10.3389/fonc.2021.752158/full#supplementary-material

REFERENCES

1. Louis DN, Perry A, Reifenberger G, von Deimling A, Figarella-Branger D, Cavenee WK, et al. The 2016 World Health Organization Classification of Tumors of the Central Nervous System: A Summary. *Acta Neuropathol* (2016) 131:803–20. doi: 10.1007/s00401-016-1545-1
2. Nowosielski M, Galldiks N, Iglseder S, Kickingereder P, von Deimling A, Bendszus M, et al. Diagnostic Challenges in Meningioma. *Neuro Oncol* (2017) 19:1588–98. doi: 10.1093/neuonc/nox101
3. Brokinkel B, Hess K, Mawrin C. Brain Invasion in Meningiomas-Clinical Considerations and Impact of Neuropathological Evaluation: A Systematic Review. *Neuro Oncol* (2017) 19:1298–307. doi: 10.1093/neuonc/nox071
4. Sun SQ, Kim AH, Cai C, Murphy RK, DeWees T, Sylvester P, et al. Management of Atypical Cranial Meningiomas, Part 1: Predictors of Recurrence and The Role of Adjuvant Radiation After Gross Total Resection. *Neurosurgery* (2014) 75:347–354. doi: 10.1227/neu.0000000000000461
5. Ho DM, Hsu CY, Ting LT, Chiang H. Histopathology and MIB-1 Labeling Index Predicted Recurrence of Meningiomas: A Proposal of Diagnostic Criteria for Patients With Atypical Meningioma. *CANCER-AM Cancer Soc* (2002) 94:1538–47. doi: 10.1002/cncr.10351
6. Adeli A, Hess K, Mawrin C, Streckert E, Stummer W, Paulus W, et al. Prediction of Brain Invasion in Patients With Meningiomas Using Preoperative Magnetic Resonance Imaging. *Oncotarget* (2018) 9:35974–82. doi: 10.18632/oncotarget.26313
7. Ong T, Bharatha A, Alsufayan R, Das S, Lin AW. MRI Predictors for Brain Invasion in Meningiomas. *Neuroradiol J* (2021) 34:3–7. doi: 10.1177/1971400920953417
8. Huang RY, Bi WL, Griffith B, Kaufmann TJ, la Fougere C, Schmidt NO, et al. Imaging and Diagnostic Advances for Intracranial Meningiomas. *Neuro Oncol* (2019) 21:i44–61. doi: 10.1093/neuonc/noy143
9. Lambin P, Rios-Velazquez E, Leijenaar R, Carvalho S, van Stiphout RG, Granton P, et al. Radiomics: Extracting More Information From Medical Images Using Advanced Feature Analysis. *Eur J Cancer* (2012) 48:441–6. doi: 10.1016/j.ejca.2011.11.036
10. Chen C, Guo X, Wang J, Guo W, Ma X, Xu J. The Diagnostic Value of Radiomics-Based Machine Learning in Predicting the Grade of Meningiomas Using Conventional Magnetic Resonance Imaging: A Preliminary Study. *Front Oncol* (2019) 9:1338. doi: 10.3389/fonc.2019.01338
11. Coroller TP, Bi WL, Huynh E, Abedalthagafi M, Aizer AA, Greenwald NF, et al. Radiographic Prediction of Meningioma Grade by Semantic and Radiomic Features. *PloS One* (2017) 12:e187908. doi: 10.1371/journal.pone.0187908
12. Wei J, Li L, Han Y, Gu D, Chen Q, Wang J, et al. Accurate Preoperative Distinction of Intracranial Hemangiopericytoma From Meningioma Using a Multihabitat and Multisequence-Based Radiomics Diagnostic Technique. *Front Oncol* (2020) 10:534. doi: 10.3389/fonc.2020.00534
13. Morin O, Chen WC, Nassiri F, Susko M, Magill ST, Vasudevan HN, et al. Integrated Models Incorporating Radiologic and Radiomic Features Predict Meningioma Grade, Local Failure, and Overall Survival. *Neurooncol Adv* (2019) 1:z11. doi: 10.1093/noajnl/vdz011
14. Zhang J, Yao K, Liu P, Liu Z, Han T, Zhao Z, et al. A Radiomics Model for Preoperative Prediction of Brain Invasion in Meningioma Non-Invasively Based on MRI: A Multicentre Study. *EBiomedicine* (2020) 58:102933. doi: 10.1016/j.ebiom.2020.102933
15. Joo L, Park JE, Park SY, Nam SJ, Kim YH, Kim JH, et al. Extensive Peritumoral Edema and Brain-to-Tumor Interface MRI Features Enable Prediction of Brain Invasion in Meningioma: Development and Validation. *Neuro Oncol* (2021) 23:324–33. doi: 10.1093/neuonc/noaa190
16. Zijdenbos AP, Dawant BM, Margolin RA, Palmer AC. Morphometric Analysis of White Matter Lesions in MR Images: Method and Validation. *IEEE Trans Med Imaging* (1994) 13:716–24. doi: 10.1109/42.363096
17. Bartko JJ. Measurement and Reliability: Statistical Thinking Considerations. *Schizophr Bull* (1991) 17:483–9. doi: 10.1093/schbul/17.3.483
18. Stokking R, Vincken KL, Viergever MA. Automatic Morphology-Based Brain Segmentation (MBRASE) From MRI-T1 Data. *Neuroimage* (2000) 12:726–38. doi: 10.1006/nimg.2000.0661
19. Friston KJ, Ashburner J, Frith CD, Poline JB, Heather JD, Frackowiak RSJ. Spatial Registration and Normalization of Images. *Hum Brain MAPP* (1995) 3:165–89. doi: 10.1002/hbm.460030303

20. van Valenberg W, Klein S, Vos FM, Koolstra K, van Vliet LJ, Poot D. An Efficient Method for Multi-Parameter Mapping in Quantitative MRI Using B-Spline Interpolation. *IEEE Trans Med Imaging* (2020) 39:1681–9. doi: 10.1109/TMI.2019.2954751
21. Zwanenburg A, Vallieres M, Abdalah MA, Aerts HJWL, Andrearczyk V, Apte A, et al. The Image Biomarker Standardization Initiative: Standardized Quantitative Radiomics for High-Throughput Image-Based Phenotyping. *Radiology* (2020) 295:328–38. doi: 10.1148/radiol.2020191145
22. Romeo V, Cavaliere C, Imbriaco M, Verde F, Petretta M, Franzese M, et al. Tumor Segmentation Analysis at Different Post-Contrast Time Points: A Possible Source of Variability of Quantitative DCE-MRI Parameters in Locally Advanced Breast Cancer. *Eur J Radiol* (2020) 126:108907. doi: 10.1016/j.ejrad.2020.108907
23. Pablo Holgado-Tello F, Chacon-Moscoso S, Barbero-Garcia I, Vila-Abad E. Polychoric *Versus* Pearson Correlations in Exploratory and Confirmatory Factor Analysis of Ordinal Variables. *Qual Quant* (2010) 44:153–66. doi: 10.1007/s11135-008-9190-y
24. Huang YQ, Liang CH, He L, Tian J, Liang CS, Chen X, et al. Development and Validation of a Radiomics Nomogram for Preoperative Prediction of Lymph Node Metastasis in Colorectal Cancer. *J Clin Oncol* (2016) 34:2157–64. doi: 10.1200/JCO.2015.65.9128
25. Hatt M, Le Rest CC, Tixier F, Badic B, Schick U, Visvikis D. Radiomics: Data Are Also Images. *J Nucl Med* (2019) 60:38S–44S. doi: 10.2967/jnumed.118.220582
26. Hand DJ. Machine Learning: An Algorithmic Perspective by Stephen Marsland. *Int Stat Rev* (2010) 78:325. doi: 10.1111/j.1751-5823.2010.00118_11.x
27. Hess K, Spille DC, Adeli A, Sporns PB, Brokinkel C, Grauer O, et al. Brain Invasion and the Risk of Seizures in Patients With Meningioma. *J Neurosurg* (2018) 130:789–96. doi: 10.3171/2017.11.JNS172265
28. Tamiya T, Ono Y, Matsumoto K, Ohmoto T. Peritumoral Brain Edema in Intracranial Meningiomas: Effects of Radiological and Histological Factors. *Neurosurgery* (2001) 49:1046–1051, 1051-1052. doi: 10.1097/00006123-200111000-00003
29. Cornelius JF, Slotty PJ, Steiger HJ, Hanggi D, Polivka M, George B. Malignant Potential of Skull Base *Versus* Non-Skull Base Meningiomas: Clinical Series of 1,663 Cases. *Acta Neurochir (Wien)* (2013) 155:407–13. doi: 10.1007/s00701-012-1611-y
30. Beig N, Khorrami M, Alilou M, Prasanna P, Braman N, Orooji M, et al. Perinodular and Intranodular Radiomic Features on Lung CT Images Distinguish Adenocarcinomas From Granulomas. *Radiology* (2019) 290:783–92. doi: 10.1148/radiol.2018180910

Conflict of Interest: The authors YM, CH, KH, FS, YL, and YY were employed by Beijing Deepwise & League of PHD Technology Co., Ltd.

The remaining authors declare that the research was conducted in the absence of any commercial or financial relationships that could be construed as a potential conflict of interest.

Publisher's Note: All claims expressed in this article are solely those of the authors and do not necessarily represent those of their affiliated organizations, or those of the publisher, the editors and the reviewers. Any product that may be evaluated in this article, or claim that may be made by its manufacturer, is not guaranteed or endorsed by the publisher.

Copyright © 2021 Li, Mo, Huang, Han, He, Wang, Wen, Yang, Wu, Dong, Sun, Li, Yu, Zhang, Guan and Xu. This is an open-access article distributed under the terms of the Creative Commons Attribution License (CC BY). The use, distribution or reproduction in other forums is permitted, provided the original author(s) and the copyright owner(s) are credited and that the original publication in this journal is cited, in accordance with accepted academic practice. No use, distribution or reproduction is permitted which does not comply with these terms.

frontiers in Oncology

ORIGINAL RESEARCH
published: 29 October 2021
doi: 10.3389/fonc.2021.747592

TERT Alterations Predict Tumor Progression in *De Novo* High-Grade Meningiomas Following Adjuvant Radiotherapy

Jiaojiao Deng[1,2,3†], *Shuchen Sun*[1,2,3†], *Jiawei Chen*[1,2,3†], *Daijun Wang*[1,2,3], *Haixia Cheng*[4], *Hong Chen*[4], *Qing Xie*[1,2,3], *Lingyang Hua*[1,2,3*] and *Ye Gong*[1,2,3,5*]

[1] Department of Neurosurgery, Huashan Hospital, Fudan University, Shanghai, China, [2] Institute of Neurosurgery, Fudan University, Shanghai, China, [3] Shanghai Key Laboratory of Brain Function Restoration and Neural Regeneration, Fudan University, Shanghai, China, [4] Department of Neuropathology, Huashan Hospital, Fudan University, Shanghai, China, [5] Department of Critical Care Medicine, Huashan Hospital, Fudan University, Shanghai, China

Background: Adjuvant radiotherapy (RT) is one of the most commonly used treatments for *de novo* high-grade meningiomas (HGMs) after surgery, but genetic determinants of clinical benefit are poorly characterized.

Objective: We describe efforts to integrate clinical genomics to discover predictive biomarkers that would inform adjuvant treatment decisions in *de novo* HGMs.

Methods: We undertook a retrospective analysis of 37 patients with *de novo* HGMs following RT. Clinical hybrid capture-based sequencing assay covering 184 genes was performed in all cases. Associations between tumor clinical/genomic characteristics and RT response were assessed. Overall survival (OS) and progression-free survival (PFS) curves were plotted using the Kaplan–Meier method.

Results: Among the 172 HGMs from a single institution, 42 cases (37 WHO grade 2 meningiomas and five WHO grade 3 meningiomas) were identified as *de novo* HGMs following RT. Only *TERT* mutations [62.5% C228T; 25% C250T; 12.5% copy number amplification (CN amp.)] were significantly associated with tumor progression after postoperative RT (adjusted $p = 0.003$). Potential different somatic interactions between *TERT* and other tested genes were not identified. Furthermore, *TERT* alterations (*TERT*-alt) were the predictor of tumor progression (Fisher's exact tests, $p = 0.003$) and were associated with decreased PFS (log-rank test, $p = 0.0114$) in *de novo* HGMs after RT.

Conclusion: Our findings suggest that *TERT*-alt is associated with tumor progression and poor outcome of newly diagnosed HGM patients after postoperative RT.

Keywords: high-grade meningiomas, adjuvant radiotherapy, *de novo*, *TERT* alterations, prognosis

OPEN ACCESS

Edited by:
Ian Dunn,
University of Oklahoma Health Sciences Center, United States

Reviewed by:
Tim J. Kruser,
University of Wisconsin System, United States
Jiang Wu,
Soochow University, China

***Correspondence:**
Ye Gong
gong_ye@fudan.edu.cn
Lingyang Hua
hua.ling.yang@163.com

†These authors have contributed equally to this work

Specialty section:
This article was submitted to Neuro-Oncology and Neurosurgical Oncology, a section of the journal Frontiers in Oncology

Received: *26 July 2021*
Accepted: *30 September 2021*
Published: *29 October 2021*

Citation:
Deng J, Sun S, Chen J, Wang D, Cheng H, Chen H, Xie Q, Hua L and Gong Y (2021) TERT Alterations Predict Tumor Progression in De Novo High-Grade Meningiomas Following Adjuvant Radiotherapy. Front. Oncol. 11:747592. doi: 10.3389/fonc.2021.747592

INTRODUCTION

Meningiomas are the most frequent tumors of the central nervous system and are generally benign (1, 2). The World Health Organization (WHO) defines three grades predictive of the risk of recurrence (3). High-grade meningiomas (HGMs) (WHO grades 2–3) are rare but aggressive tumors with considerably poorer prognosis than WHO grade 1 meningiomas (4, 5). The 5-year progression-free survival (PFS-5) and overall survival (OS) rate for HGM patients are 8%–68% and 35%–91%, respectively (4–8).

Patients with WHO grade 1 meningiomas are traditionally managed in follow-up with surveillance imaging (9). However, a standardized treatment approach to HGMs after resection has not been established (4). The benefit to survival outcomes of HGMs with adjuvant radiotherapy (RT) post-surgical resection remains unclear. Retrospective series on adjuvant RT after gross total resection led to differing results (4, 10, 11).

Meningiomas have a diverse genetic background that varies with biologic behavior (12). Alterations in the tumor suppressor gene *NF2* were the first discovered genetic etiology of meningiomas (13, 14). In *NF2* wild-type meningiomas, mutations in *TRAF7*, *KLF4*, *AKT1*, and *SMO* were noted (15–17). In addition, several mutations have been described with potential prognostic implications in HGMs (12, 14, 18). Data published recently have also shown that activating *TERT* promoter mutations, frequent inactivation of *BAP1*, deletions of *CDKN2A/B*, and mutations in *DMD* are frequent in meningiomas with malignant histological progression (18–21). These data suggest that convergent gene-expression programs may underlie HGMs, which could be leveraged to develop prognostic biomarkers.

Our previous work found that patients with *de novo* anaplastic meningiomas benefit from adjuvant RT after surgery (5, 22). However, the molecular factors associated with RT efficacy in *de novo* HGMs are largely unknown. In the present study, we describe efforts to integrate clinical genomics of 37 cases from 173 HGMs to address this issue.

METHODS

Patient Selection

Patients were identified for study through a review of the clinical records of the Department of Neurosurgery, Huashan Hospital of Fudan University, Shanghai, China. A total of 172 HGMs (**Supplementary Table S1**) were included following study approval by the Human Subjects Institutional Review Board at Huashan Hospital, Fudan University (KY-2017-09). Clinical characteristics including age, gender, tumor location, extent of surgical resection, and outcome data were collected. In general, adjuvant radiation was recommended to both atypical and anaplastic meningioma patients, regardless of gross total resection (GTR; Simpson grades I–III) or subtotal resection (STR; Simpson grades IV–V). And the final decision was made based on the negotiation with the relatives of patients. The details of postoperative RT were described in our previous work (5). Tumor pathological subtypes were reconfirmed by at least two experienced neuropathologists. Follow-up was conducted routinely according to the guidelines of Huashan Neurosurgical Center. Written informed consent was obtained from all patients involved in our study.

A total of 172 patients with a confirmed diagnosis of HGM who met inclusion criteria (141 WHO grade 2 meningiomas and 31 WHO grade 3 meningiomas; **Supplementary Table S1**). Out of 172 cases, 87 cases received RT after surgery. Among the 87 patients, 42 (48.3%) were *de novo* meningiomas, while the remaining 45 patients presented with recurrent meningioma following prior surgical resection. And finally, 37 *de novo* meningioma samples with adequate quality of DNA concentration were included for further next-generation sequencing.

Next-Generation Sequencing

Tumor genotyping was performed on formalin-fixed paraffin-embedded (FFPE) tumor tissue by next-generation sequencing (NGS) covering 184 genes, including common pathological relevant genes of meningiomas (**Supplementary Table S2**) (13–21, 23). Five DNA samples were excluded for sequencing due to inadequate quality of concentration. High-throughput sequencing was performed on Illumina miniseq platform by KuoRan Biomedical Technology as previously described (**Supplementary Material**) (24).

Sanger Sequencing

The *TERT* promoter mutations were evaluated using Sanger sequencing. Genomic DNA was obtained from FFPE using the HiPure FFPE DNA Kit (Magen, D3126-03) following polymerase chain reaction-based amplification of the target region (forward primer: GGATTCGCGGGC ACAGAC; reverse primer: CAGCGCTGCCTGAAA CTC; details on PCR conditions are available upon request).

Statistical Tests

The specific details of statistical tests are included in the figure legends. A two-tailed Fisher's exact test was used to calculate statistical significance between different groups using a χ^2 2×2 table. Categorical variables were compared with the Fisher's exact tests, and continuous variables with the independent-samples Student's *t*-test (data with normal distribution) or Mann–Whitney U-test (data with skewed distribution). Continuous data were expressed as the mean ± standard deviation (SD). Overall survival (OS) and progression-free survival (PFS) curves were plotted using the Kaplan–Meier method. Statistical analysis was performed using Statistical Package for Social Sciences (SPSS, Version 20.0, Chicago, IL, USA). Data were considered to be significant when $p < 0.05$.

RESULTS

Prevalence of Somatic Alterations in 37 *De Novo* High-Grade Meningiomas

We identified 172 patients with a confirmed diagnosis of HGM who met inclusion criteria (141 WHO grade 2 meningiomas and

31 WHO grade 3 meningiomas; **Supplementary Table S1**). Out of 172 cases, 87 cases received RT after surgery, including external beam radiation therapy (EBRT), stereotactic radiosurgery (SRS), and cyber knife (CK). Among the 87 patients, 42 (48.3%) were *de novo* meningiomas while the remaining 45 patients presented with recurrent meningioma following prior surgical resection. Five of the 42 (11.9%) meningiomas were excluded for sequencing due to inadequate quality of DNA concentration. Thus, tumor genotyping covering 184 genes was performed on the 37 *de novo* meningioma cases (**Supplementary Tables S2, S3**). In total of the 37 cases, 23 males (62%) and 14 females (38%) with a median age of 45 years (range: 34–73) harboring 31 atypical (83.8%), five anaplastic (13.5%), and one atypical/chordoid coexisting (2.7%) meningiomas were included. Tumors were located at the convexity (n = 17, 45.9%), the falx/parasagittal (n = 13, 35.1%), the skull base (n = 5, 13.5%), or in other locations (n = 2, 5.5%). Among these patients, 28 (75.7%) were treated with EBRT, six (16.2%) were treated with SRS, and three cases were treated with CK (8.1%) (**Figure 1**).

In order to identify tumor mutations associated with efficacy of postoperative RT, we determined the association between recurrent mutations and tumor progression in the cohort of 37 patients (**Figure 1**). Of the 37 *de novo* HGMs following RT, 19 cases (51.4%) had tumor progression. Progression individuals was defined as tumor regrowth within the radiation field based on the criterion of Response Assessment in Neuro-Oncology Working Group (RANO) radiologic criteria for meningiomas (25). Part of the genomic mutational landscape of 37 patients with *de novo* meningioma is displayed in **Figure 2**. Nine mutations met our predetermined recurrence frequency threshold of >20% (**Figure 2** and **Supplementary Table S2**). Consistent with previous studies, high mutational rates of *NF2* (n = 22; 59%) were discovered in this cohort. Additional common pathological relevant genes of meningiomas, including *AKT1* (n = 3; 8%), *CDKN2A* (n = 2; 5%), *SMO* (n = 0; 0%), *SUFU* (n = 0; 0%), *POLR2A* (n = 6; 16%), *TRAF7* (n = 1; 3%), and *SMARCB1* (n = 2; 5%), were observed as well (**Supplementary Table S2**). Besides, the most frequently altered genes including *ATRX* (n = 13; 35%), *ARID1A* (n = 11; 30%), *ATM* (n = 11; 30%), *NF1* (n = 11; 30%), *ROS1* (n = 10; 27%), *KDM6A* (n = 9; 24%), *FAT1* (n = 8; 22%), and *TERT* (n = 8; 22%) were observed (**Figure 2**).

TERT Mutations Predict Tumor Progression of *De Novo* High-Grade Meningiomas Following Radiotherapy

Strikingly, only *TERT* mutations were significantly associated with tumor progression (n = 8, adjusted $p = 0.031$), and all these mutations were present in tumors that progressed after RT (**Figure 3A**). Of the *TERT* mutant cases, 87.5% (7/8) presented with *TERT* promoter mutations (62.5% C228T variant and 25% C250T variant; **Supplementary Figure S1**), and 12.5% (1/8) harbored copy number amplification (CN amp.). As many tumor driver genes are co-occurring or show strong exclusiveness in their mutation pattern, we next explored the potential different somatic interactions in the cohort. None of the gene mutations

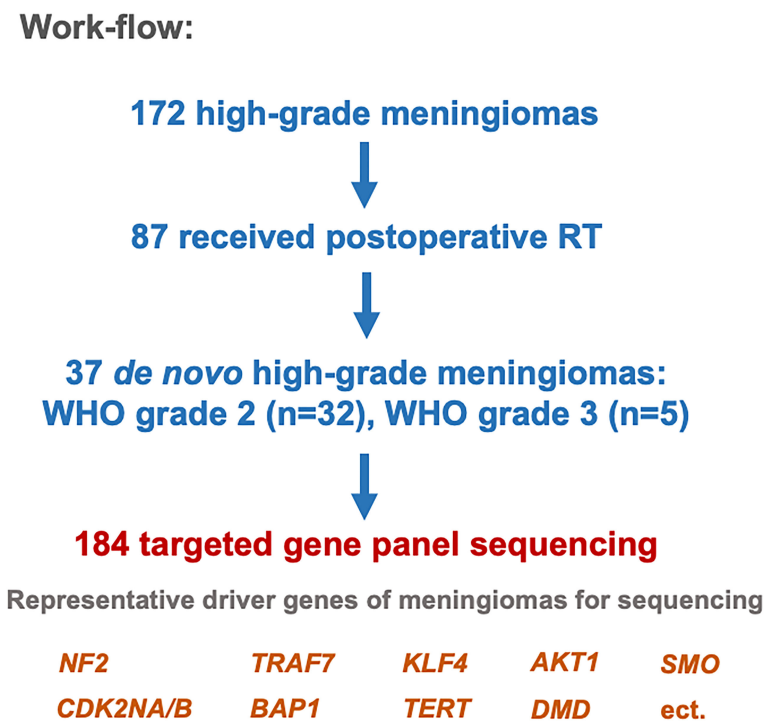

FIGURE 1 | Study design.

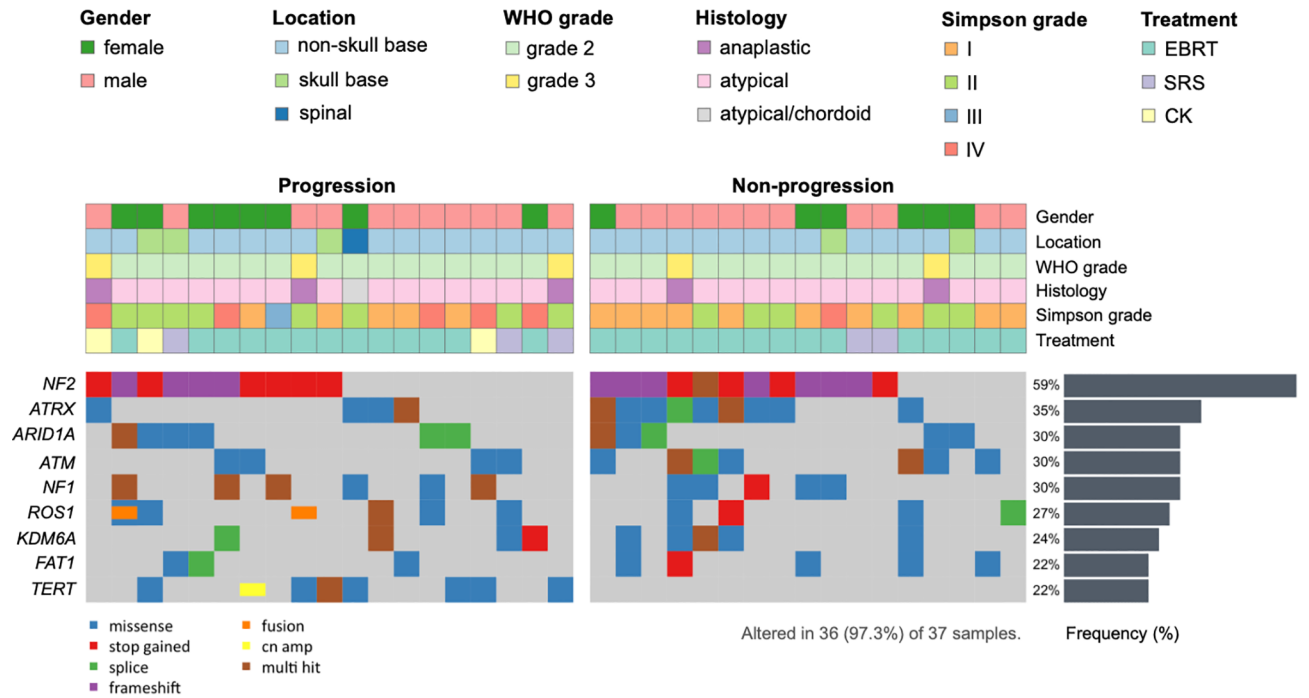

FIGURE 2 | Recurrent mutations in *de novo* high-grade meningioma (HGM) patients with and without progression after adjuvant radiotherapy (RT). Top 9 genes with most frequent mutations are depicted. Each column corresponds to a single patient. The colors of bars are indicative of the type of mutation, with gray indicating wild type. Barplot at the top of the figure represents the status a patient has. The vertical plot on the right of the figure represents the frequency of mutations in each gene in a decreasing manner.

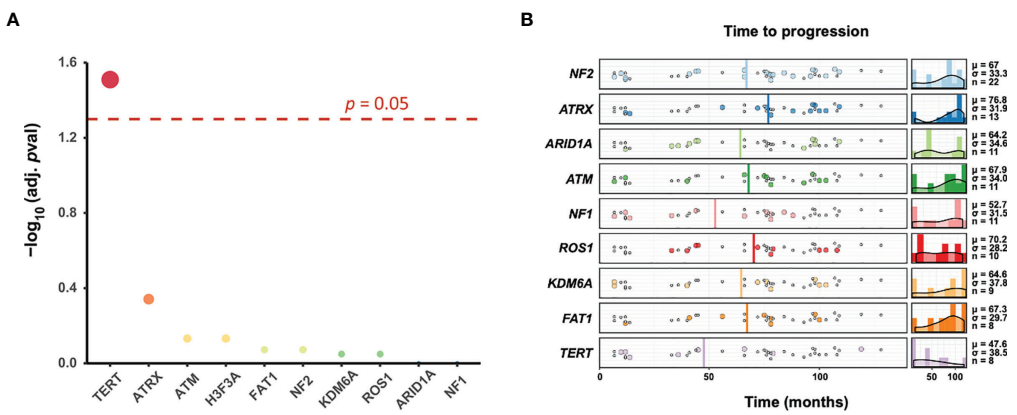

FIGURE 3 | *TERT* mutations predict tumor progression of *de novo* high-grade meningiomas (HGMs) following radiotherapy (RT). **(A)** Association of recurrent mutations with tumor progression. Fisher's test was utilized to detect differentially mutated genes on top 9 most frequent mutation genes between two cohorts (progression *vs.* non-progression). The point size in dotplot corresponds to the -log10(adj. *p*-val) value, together with the red color indicates the higher -log10(adj. *p*-val) value, and blue indicates the lower value. Horizontal dash line marked the *p*-value 0.05. **(B)** Timing of tumor progression. Shown is the time to progression (colored dots) or last progression-free scan (gray dots) for top 9 most frequent mutation genes in months. The average progression time was depicted in vertical line. The average time to recurrence of *TERT* mutant meningiomas was less than other tumors (Wilcoxon rank sum test with continuity correction, W = 491, $p = 0.0864$). Density plot of each subgroup's progression is shown on the right, along with the mean (μ), standard deviation (σ), and number of progression (n).

presents co-occurring or mutually exclusive in HGM cases (**Supplementary Figure S2**). Thus, *TERT* mutations appear to be the dominant cause of tumor progression among mutations in this cohort. Furthermore, we found that *TERT* mutation status ($p = 0.003$), as well as extent of resection (EOR) ($p < 0.001$), was significantly associated with tumor progression by Fisher's exact tests (**Table 1**). Neither tumor location ($p = 1.00$) nor WHO grade ($p = 1.00$) predicted tumor progression after postoperative

TABLE 1 | Analysis of progression factors in *de novo* HGM patients after RT.

Feature		Progression	Non-progression	*p*-value
Patients, n (%)		19 (51.35)	18 (48.65)	
Age, n (%)				
	<65	13 (68.42)	14 (77.78)	0.71
	≥65	6 (31.58)	4 (22.22)	
Gender, n (%)				
	Male	11 (57.89)	12 (66.67)	0.74
	Female	8 (42.11)	6 (33.33)	
Location, n (%)				
	Skull base	3 (15.79)	2 (11.11)	1.00
	Non-skull base	16 (84.21)	16 (88.89)	
WHO grade, n (%)				
	2	16 (84.21)	16 (88.89)	1.00
	3	3 (15.79)	2 (11.11)	
EOR, n (%)				
	GTR	14 (73.68)	1 (5.56)	<0.001**
	STR	5 (26.32)	17 (94.44)	
***TERT* status, n (%)**				
	TERT (+)	8 (42.11)	0 (0)	0.003*
	TERT (-)	11 (57.89)	18 (100)	

GTR, gross total resection; HGM, high-grade meningioma; RT, radiotherapy; STR, subtotal resection; EOR, extent of resection.
**p < 0.05 and **p < 0.001 considered statistically significant.*

RT. After adjustment for multiple comparisons, these associations were not significant. Importantly, *TERT* mutation cases were more likely to have unfavorable time to recurrence (TTR) over the entire cohort, with a mean observation time of 47.6 months (**Figure 3B**). However, no significant differences in the average time to recurrence between *TERT* mutant and wild-type cases were observed (Wilcoxon rank sum test with continuity correction W = 491, $p = 0.0864$).

Meningioma with *TERT* alterations, regardless of WHO grades or pathological subtypes, had a highly significant risk of recurrence (26). To exclude the disruption to RT efficacy might be caused by *TERT*-related malignant biological behavior, we thus performed analysis on newly diagnosed HGMs depending on *TERT* alterations only in progression group. Of the 19 cases in the progression group, mitotic index (ki-67%) depending on *TERT* alterations did not show any significantly difference (unpaired t-test, $p = 0.051$; **Supplementary Figure S3A**). Additionally, *TERT* alterations of *de novo* HGMs had no predictive effect on tumor recurrence in progression group following postoperative RT ($p = 0.074$ with log-rank test; **Supplementary Figure S3B**).

TERT Mutations Were Associated With Decreased Progression-Free Survival and Overall Survival in *De Novo* High-Grade Meningiomas After Radiotherapy

With these findings, we next analyzed the effect of *TERT* mutation status on PFS in patients with *de novo* HGMs after RT. The primary endpoint of PFS, defined as time from surgery to date of progression, was assessed on the basis of progression of meningioma after initial surgery on imaging follow-up. The median PFS of 75 months (range: 7–109 months) was observed for the entire cohort. Subgroup analysis revealed a median PFS of 25 months (range: 10–79 months) in *TERT* mutant group and 77 months (range: 7–109 months) in *TERT* wild-type group. *TERT* mutants were significantly associated with decreased PFS in *de novo* HGM cases that underwent postoperative RT ($p = 0.0114$ with log-rank test; **Figure 4A**).

The relationship between *TERT* mutations and OS was analyzed using the log-rank test (**Figure 4B**). The median OS of 84 months (range: 13–123 months) was observed for the entire cohort. Subgroup analysis revealed a median OS of 66 months (range: 13–123 months) in *TERT* mutant group and 85 months (range: 24–109 months) in *TERT* wild-type group. Patients with *de novo* HGMs after RT harboring *TERT* mutations had worse OS ($p = 0.0562$; **Figure 4B**).

DISCUSSION

In this retrospective study, we investigated genetic predictors that might inform the potential progressive risk in *de novo* HGMs after postoperative RT. We found *TERT*-alt in HGMs to be a significant predictor of tumor progression compared to *TERT* wild-type cases. Although a merely descriptive finding, our

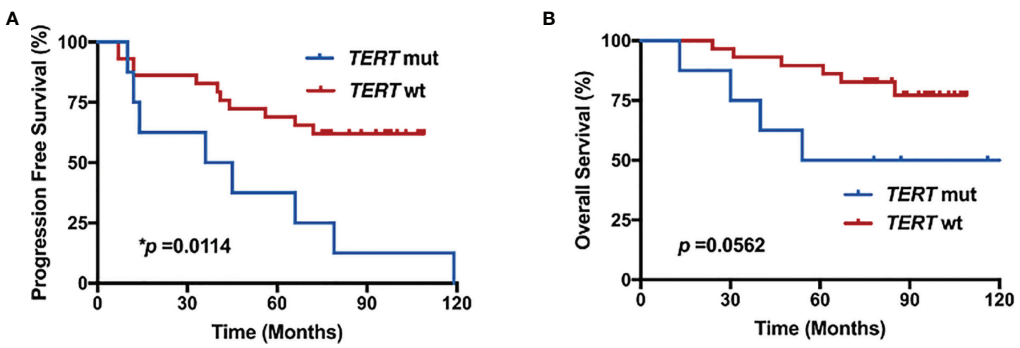

FIGURE 4 | *TERT* mutations were associated with decreased progression-free survival (PFS) and overall survival (OS) in *de novo* high-grade meningiomas (HGMs) after radiotherapy (RT). Kaplan–Meier curves for **(A)** PFS and **(B)** OS in *de novo* HGMs with or without *TERT* mutation following RT.

data have potential implications for the clinical management of patients with *TERT*-alt *de novo* HGMs.

HGMs are rare but aggressive tumors with considerably poorer prognosis than lower-grade meningiomas. Adjuvant RT is the only nonsurgical standard of care treatment option for these tumors (9). However, radiotherapeutic options for meningioma are diverse, and there are no randomized trials to identify individuals who are more likely to benefit from adjuvant RT. Indeed, until recently, the evidence supporting postoperative RT for meningioma, especially HGMs, was largely limited. Moreover, no molecular prognostic markers have yet been established for new diagnosed HGMs following RT. To our knowledge, this study is the first to investigate predictive biomarkers that would inform tumor progression in *de novo* HGMs after postoperative RT.

Leveraging the next-generation sequencing techniques led to advances in description of the mutational landscape of meningiomas (15–17). In line with the previous findings, *NF2*-mutant meningiomas represent the largest percentage (59%) of cases in our study (14, 15). In large-scale genomic studies of meningioma, HGMs were in some studies exclusively related to pathogenic variants in *NF2*, associated with mutations in the *TERT* promoter (27). In our study, high mutational rates of *ATRX*, *ARID1A*, *ATM*, *NF1*, *ROS1*, *KDM6A*, *FAT1*, and *TERT* were observed, indicating that these frequently altered genes might play a role in HGMs. Of note, other common pathological relevant genes of meningiomas, including *AKT1* (n = 3; 8%), *CDKN2A* (n = 2; 5%), *SMO* (n = 0; 0%), *SUFU* (n = 0; 0%), *POLR2A* (n = 6; 16%), *TRAF7* (n = 1; 3%), and *SMARCB1* (n = 2; 5%), were detected as well. However, we did not observe previously described mutational rates of some of these genes due to limited cases.

Among the 184 sequenced genes, only *TERT* alterations were significantly associated with tumor progression (n = 8, adjusted $p = 0.031$), and all these mutations were present in tumors that progressed after RT. *TERT*-alt comprise, but are not limited to, promoter mutations, gene translocations, and DNA amplifications (28). We found 87.5% (7/8) of the *TERT* mutant cases presented with *TERT* promoter mutations (62.5% C228T variant and 25% C250T variant). As reported, the most common alterations occur in specific "hotspots" of the promoter (*TERT*p) region known as C228T and C250T (29). These C>T transition mutations lead to maintenance of the telomere length, as binding of E-twenty six (ETS)-transcription factors is involved in the upregulation of TERT expression (28, 30).

TERT alterations, specifically *TERT* promoter mutations, have been identified in a subset of HGMs with progression from low-grade meningioma (31–34). In the present study, we found that *TERT*-alt was associated with decreased PFS and OS in *de novo* HGMs after RT. Besides, our data have shown decreased time to progression among *TERT*-alt *de novo* HGMs as well. *TERT* gene is transcriptionally inactive in most non-neoplastic cells (28). *TERT* gene alterations (*TERT*-alt) may enforce cell immortalization by counteracting telomere shortening, thus promoting growth (28). Several studies have provided evidence that *TERT*-alt mutations are associated with rapid recurrence and malignant progression in meningioma (26, 31, 35). In addition, *TERT*p meningiomas have been found to have a worse PFS and OS, though not many cases have been reported (18). Activating *TERT* gene mutations in the upstream promoter allows overexpression of this enzyme and is responsible for immortalization of tumor cells in many cancers (12). Thus, we have excluded that the disruption to RT efficacy might be caused by *TERT*-related malignant biological behavior in this study. As results, the *TERT*-alt status and progressive variables did not show any relevance in progression group.

The Simpson grade of EOR has long been used to guide clinical expectations after resection of meningiomas (9); our results support the relevance of EOR in recurrence of HGMs as well ($p < 0.001$). The literature widely recognizes the role that EOR plays in determining HGM prognosis (36, 37). However, Cox regression analysis failed to identify any factor with significant association with the progression of *de novo* HGMs following RT. Thus, a larger cohort or multicenter clinical trial is needed to investigate the effect of RT in this subgroup.

In summary, our data identified *TERT* alterations, especially *TERT*p mutation, are associated with tumor progression and poor outcome of newly diagnosed HGM patients after postoperative RT. Several limitations of this study warrant consideration. Firstly, our findings on a discovery series were not substantiated by any independent validation series due to the limited available samples. Prospective studies are clearly needed to validate *TERT*-alt status of radiation response in *de novo* HGMs. Another important limitation in this study is its observational nature, which could have led to selection bias. It would be useful to repeat these analyses in cohorts from other institutions in the future.

CONCLUSION

In summary, examining a cohort of *de novo* HGMs following adjuvant RT, we find *TERT* alteration to be strongly associated with tumor progression and poor outcome of HGM patients included in this study.

DATA AVAILABILITY STATEMENT

The datasets presented in this study can be found in online repositories. The names of the repository/repositories and accession number(s) can be found below: NCBI [accession: PRJNA753598].

ETHICS STATEMENT

The studies involving human participants were reviewed and approved by the Human Subjects Institutional Review Board at Huashan Hospital, Fudan University. The patients/participants provided their written informed consent to participate in this study. Written informed consent was obtained from the individuals for the publication of any potentially identifiable images or data included in this article.

AUTHOR CONTRIBUTIONS

JD, LH, and YG, study design. JD, SS, JC, DW, and QX, clinical data. JD, article preparation. HaC and HoC, tumor pathological subtypes reconfirmed and Sanger sequencing. All authors contributed to the article and approved the submitted version.

FUNDING

This study was supported by grants from the National Key R&D Program of China (2018YFC1312600 and 2018YFC1312604 to YG) and the National Natural Science Foundation of China (82072788 and 81772674 to YG).

SUPPLEMENTARY MATERIAL

The Supplementary Material for this article can be found online at: https://www.frontiersin.org/articles/10.3389/fonc.2021.747592/full#supplementary-material

Supplementary Figure S1 | Pie chart fraction of *TERT* alterative subtypes occurring in *TERT*-alt HGMs.

Supplementary Figure S2 | Heatmap of mutually exclusive or co-occurring set of genes in the mutation pattern of *de novo* HGMs following RT. Pairwise Fisher's exact tests were performed to detect significant pairs of genes, mutually exclusive or co-occurring set of genes which colored by brown or green can be detected using the *somaticInteractions* function in R/Bioconductor package 'maftools'.

Supplementary Figure S3 | The *TERT*-alt status and progressive variables did not show any relevancy in progression group.

REFERENCES

1. Kshettry VR, Ostrom QT, Kruchko C, Ossama A-M, Barnett GH, Barnholtz-Sloan JS, et al. Descriptive Epidemiology of World Health Organization Grades II and III Intracranial Meningiomas in the United States. *Neuro Oncol* (2015) 17:1166–73. doi: 10.1093/neuonc/nov069
2. Ostrom QT, Gittleman H, Liao P, Rouse C, Chen Y, Dowling J, et al. CBTRUS Statistical Report: Primary Brain and Central Nervous System Tumors Diagnosed in the United States in 2007-2011. *Neuro Oncol* (2014) null:iv1–63. doi: 10.1093/neuonc/nou223
3. Louis DN, Perry A, Wesseling P, Brat DJ, Cree IA, Figarella-Branger D, et al. The 2016 World Health Organization Classification of Tumors of the Central Nervous System: A Summary. *Acta Neuropathol* (2016) 131:803–20. doi: 10.1007/s00401-016-1545-1
4. Unterberger A, Nguyen T, Duong C, Kondajji A, Kulinich D, Yang I, et al. Meta-Analysis of Adjuvant Radiotherapy for Intracranial Atypical and Malignant Meningiomas. *J Neurooncol* (2021) 152:205–16. doi: 10.1007/s11060-020-03674-7
5. Wang D, Sun S, Hua L, Deng J, Luan S, Cheng H, et al. Prognostic Model That Predicts Benefits of Adjuvant Radiotherapy in Patients With High Grade Meningioma. *Front Oncol* (2020) 10:568079. doi: 10.3389/fonc.2020.568079
6. Yang S-Y, Park C-K, Park S-H, Kim DG, Chung YS, Jung H-W, et al. Atypical and Anaplastic Meningiomas: Prognostic Implications of Clinicopathological Features. *J Neurol Neurosurg Psychiatry* (2008) 79:574–80. doi: 10.1136/jnnp.2007.121582
7. Dziuk TW, Woo S, Butler EB, Thornby J, Grossman R, Dennis WS, et al. Malignant Meningioma: An Indication for Initial Aggressive Surgery and Adjuvant Radiotherapy. *J Neurooncol* (1998) 37:177–88. doi: 10.1023/A:1005853720926
8. Choi Y, Lim DoH, Jo K, Nam D-H, Seol HJ, Lee J-I, et al. Efficacy of Postoperative Radiotherapy for High Grade Meningiomas. *J Neurooncol* (2014) 119:405–12. doi: 10.1007/s11060-014-1507-1
9. Goldbrunner R, Minniti G, Preusser M, Jenkinson MD, Sallabanda K, Houdart E, et al. EANO Guidelines for the Diagnosis and Treatment of Meningiomas. *Lancet Oncol* (2016) 17:e383–91. doi: 10.1016/S1470-2045(16)30321-7
10. Mair R, Morris K, Scott I, Carroll TA. Radiotherapy for Atypical Meningiomas. *J Neurosurg* (2011) 115:811–9. doi: 10.3171/2011.5.JNS11112
11. Rogers CL, Won M, Vogelbaum MA, Perry A, Ashby LS, Modi JM, et al. High-Risk Meningioma: Initial Outcomes From NRG Oncology/RTOG 0539. *Int J Radiat Oncol Biol Phys* (2020) 106:790–9. doi: 10.1016/j.ijrobp.2019.11.028
12. Bunevicius A, Laws ER, Saudargiene A, Tamasauskas A, Iervasi G, Deltuva V, et al. Common Genetic Variations of Deiodinase Genes and Prognosis of Brain Tumor Patients. *Endocrine* (2019) 66:563–72. doi: 10.1007/s12020-019-02016-6
13. Yuzawa S, Nishihara H, Tanaka S. Genetic Landscape of Meningioma. *Brain Tumor Pathol* (2016) 33:237–47. doi: 10.1007/s10014-016-0271-7
14. Birzu C, Peyre M, Sahm F. Molecular Alterations in Meningioma: Prognostic and Therapeutic Perspectives. *Curr Opin Oncol* (2020) 32:613–22. doi: 10.1097/CCO.0000000000000687
15. Clark VE, Erson-Omay EZ, Serin A, Yin J, Cotney J. Genomic Analysis of non-NF2 Meningiomas Reveals Mutations in TRAF7, KLF4, AKT1, and SMO. *Science* (2013) 339:1077–80. doi: 10.1126/science.1233009
16. Clark VE, Harmancı AS, Bai H, Youngblood MW, Lee TI, Baranoski JF, et al. Recurrent Somatic Mutations in POLR2A Define a Distinct Subset of Meningiomas. *Nat Genet* (2016) 48:1253–9. doi: 10.1038/ng.3651
17. Delgado-López PD, Cubo-Delgado E, González-Bernal JJ, Martín-Alonso J. A Practical Overview on the Molecular Biology of Meningioma. *Curr Neurol Neurosci Rep* (2020) 20:62. doi: 10.1007/s11910-020-01084-w
18. Biczok A, Kraus T, Suchorska B, Terpolilli NA, Thorsteinsdottir J, Giese A. TERT Promoter Mutation Is Associated With Worse Prognosis in WHO Grade II and III Meningiomas. *J Neurooncol* (2018) 139:671–8. doi: 10.1007/s11060-018-2912-7
19. Shankar GM, Santagata S. BAP1 Mutations in High-Grade Meningioma: Implications for Patient Care. *Neuro Oncol* (2017) 19:1447–56. doi: 10.1093/neuonc/nox094
20. Sievers P, Hielscher T, Schrimpf D, Stichel D, Reuss DE, Berghoff AS, et al. CDKN2A/B Homozygous Deletion Is Associated With Early Recurrence in Meningiomas. *Acta Neuropathol* (2020) 140:409–13. doi: 10.1007/s00401-020-02188-w
21. Juratli Tareq A, McCabe D, Nayyar N, Williams EA, Silverman IM, Tummala SS, et al. DMD Genomic Deletions Characterize a Subset of Progressive/Higher-Grade Meningiomas With Poor Outcome. *Acta Neuropathol* (2018) 136:779–92. doi: 10.1007/s00401-018-1899-7
22. Zhu H, Bi WL, Aizer A, Hua L, Tian M, Den J, et al. Efficacy of Adjuvant Radiotherapy for Atypical and Anaplastic Meningioma. *Cancer Med* (2019) 8:13–20. doi: 10.1002/cam4.1531
23. Toland A, Huntoon K, Dahiya SM. Meningioma: A Pathology Perspective. *Neurosurgery* (2021) 89:11–21. doi: 10.1093/neuros/nyab001
24. Jin L, Shi F, Chun Q, Chen H, Ma Y, Wu S, et al. Artificial Intelligence Neuropathologist for Glioma Classification Using Deep Learning on Hematoxylin and Eosin Stained Slide Images and Molecular Markers. *Neuro Oncol* (2021) 23:44–52. doi: 10.1093/neuonc/noaa163
25. Huang Raymond Y, Bi WL, Weller M, Kaley T, Blakeley, Dunn I, et al. Proposed Response Assessment and Endpoints for Meningioma Clinical Trials: Report From the Response Assessment in Neuro-Oncology Working Group. *Neuro Oncol* (2019) 21:26–36. doi: 10.1093/neuonc/noy137
26. Mirian C, Duun-Henriksen AK, Juratli T, Sahm F, Spiegl-Kreinecker S, Peyre M, et al. Poor Prognosis Associated With TERT Gene Alterations in Meningioma Is Independent of the WHO Classification: An Individual Patient Data Meta-Analysis. *J Neurol Neurosurg Psychiatry* (2020) 91:378–87. doi: 10.1136/jnnp-2019-322257
27. Sahm F, Schrimpf D, Stichel D, Jones David TW, Hielscher T, Schefzyk S, et al. DNA Methylation-Based Classification and Grading System for Meningioma: A Multicentre, Retrospective Analysis. *Lancet Oncol* (2017) 18:682–94. doi: 10.1016/S1470-2045(17)30155-9
28. Barthel Floris P, Wei W, Tang M, Martinez-Ledesma E, Hu X, Amin Samirkumar B, et al. Systematic Analysis of Telomere Length and Somatic

Alterations in 31 Cancer Types. *Nat Genet* (2017) 49:349–57. doi: 10.1038/ng.3781
29. Yuan X, Larsson C, Xu D. Mechanisms Underlying the Activation of TERT Transcription and Telomerase Activity in Human Cancer: Old Actors and New Players. *Oncogene* (2019) 38:6172–83. doi: 10.1038/s41388-019-0872-9
30. Horn S, Figl A, Rachakonda PS, Fischer C, Sucker A, Gast A, et al. TERT Promoter Mutations in Familial and Sporadic Melanoma. *Science* (2013) 339:959–61. doi: 10.1126/science.1230062
31. Sahm F, Schrimpf D, Olar A, Koelsche C, Reuss D, Bissel J, et al. TERT Promoter Mutations and Risk of Recurrence in Meningioma. *J Natl Cancer Inst* (2016) 108(5). doi: 10.1093/jnci/djv377
32. Koelsche C, Sahm F, Capper D, Reuss D, Sturm D, Jones TW, et al. Distribution of TERT Promoter Mutations in Pediatric and Adult Tumors of the Nervous System. *Acta Neuropathol* (2013) 126:907–15. doi: 10.1007/s00401-013-1195-5
33. Goutagny Stéphane, Nault JC, Mallet M, Henin D, Rossi JZ, Kalamarides M, et al. High Incidence of Activating TERT Promoter Mutations in Meningiomas Undergoing Malignant Progression. *Brain Pathol* (2014) 24:184–9. doi: 10.1111/bpa.12110
34. Peyre M, Gauchotte G, Giry M, Froehlich S, Pallud J, Graillon T, et al. *De Novo* and Secondary Anaplastic Meningiomas: A Study of Clinical and Histomolecular Prognostic Factors. *Neuro Oncol* (2018) 20:1113–21. doi: 10.1093/neuonc/nox231
35. Spiegl-Kreinecker S, Lötsch D, Neumayer K, Kastler L, Gojo J, Kumar C, et al. TERT Promoter Mutations Are Associated With Poor Prognosis and Cell Immortalization in Meningioma. *Neuro Oncol* (2018) 20:1584–93. doi: 10.1093/neuonc/noy104
36. Nanda A, Bir SC, Konar S, Maiti T, Kalakoti P, Jacobsohn JA, et al. Outcome of Resection of WHO Grade II Meningioma and Correlation of Pathological and Radiological Predictive Factors for Recurrence. *J Clin Neurosci* (2016) 31:112–21. doi: 10.1016/j.jocn.2016.02.021
37. Sun Sam Q, Hawasli AH, Huang J, Chicoine MR, Kim AH. An Evidence-Based Treatment Algorithm for the Management of WHO Grade II and III Meningiomas. *Neurosurg Focus* (2015) 38:E3. doi: 10.3171/2015.1.FOCUS14757

Conflict of Interest: The authors declare that the research was conducted in the absence of any commercial or financial relationships that could be construed as a potential conflict of interest.

Publisher's Note: All claims expressed in this article are solely those of the authors and do not necessarily represent those of their affiliated organizations, or those of the publisher, the editors and the reviewers. Any product that may be evaluated in this article, or claim that may be made by its manufacturer, is not guaranteed or endorsed by the publisher.

Copyright © 2021 Deng, Sun, Chen, Wang, Cheng, Chen, Xie, Hua and Gong. This is an open-access article distributed under the terms of the Creative Commons Attribution License (CC BY). The use, distribution or reproduction in other forums is permitted, provided the original author(s) and the copyright owner(s) are credited and that the original publication in this journal is cited, in accordance with accepted academic practice. No use, distribution or reproduction is permitted which does not comply with these terms.

frontiers in Neurology

ORIGINAL RESEARCH
published: 17 November 2021
doi: 10.3389/fneur.2021.769656

How Much Tumor Volume Is Responsible for Development of Clinical Symptoms in Patients With Convexity, Parasagittal, and Falx Meningiomas?

Shuhei Yamada, Noriyuki Kijima, Tomoyoshi Nakagawa, Ryuichi Hirayama, Manabu Kinoshita, Naoki Kagawa and Haruhiko Kishima*

Department of Neurosurgery, Osaka University Graduate School of Medicine, Suita, Japan

OPEN ACCESS

Edited by:
Hailiang Tang,
Fudan University, China

Reviewed by:
Rintaro Hashizume,
Northwestern University, United States
Ryota Tamura,
Keio University, Japan
Nora F. Dengler,
Charité—Universitätsmedizin Berlin, Germany

***Correspondence:**
Noriyuki Kijima
n-kijima@nsurg.med.osaka-u.ac.jp

Specialty section:
This article was submitted to Neuro-Oncology and Neurosurgical Oncology, a section of the journal Frontiers in Neurology

Received: *02 September 2021*
Accepted: *25 October 2021*
Published: *17 November 2021*

Citation:
Yamada S, Kijima N, Nakagawa T, Hirayama R, Kinoshita M, Kagawa N and Kishima H (2021) How Much Tumor Volume Is Responsible for Development of Clinical Symptoms in Patients With Convexity, Parasagittal, and Falx Meningiomas? Front. Neurol. 12:769656. doi: 10.3389/fneur.2021.769656

Purpose: Meningiomas are the most common primary intracranial neoplasms and clinical symptom appearance depends on their volume and location. This study aimed to identify factors that influence clinical symptoms and to determine a specific threshold tumor volume for the prediction of symptomatic progression in patients with convexity, parasagittal, and falx meningiomas.

Materials and Methods: We retrospectively studied patients with radiologically suspected convexity, parasagittal, or falx meningiomas at our institution.

Results: The data of three hundred thirty-three patients were analyzed. We further divided patients into two groups based on clinical symptoms: an asymptomatic group (250 cases) and a symptomatic group (83 cases). Univariate analysis revealed significant differences between the groups in terms of sex ($p = 0.002$), age at the time of volumetric analysis ($p < 0.001$), hyperintense lesions on T2-weighted images ($p = 0.029$), peritumoral edema ($p < 0.001$), maximum tumor diameter ($p < 0.001$), and tumor volume ($p < 0.001$). Further multivariate analysis revealed significant differences between the groups in terms of age at the time of volumetric analysis ($p = 0.002$), peritumoral edema ($p < 0.001$), and tumor volume ($p < 0.001$). The receiver operating characteristic curve revealed a threshold tumor volume of 21.1 ml for predicting whether a patient would develop symptoms (sensitivity 0.843, specificity 0.880, an area under the curve 0.919 [95% confidence interval: 0.887–0.951]).

Conclusion: We identified factors predictive of clinical symptoms in patients with convexity, parasagittal, and falx meningiomas and determined the first-ever threshold tumor volume for predicting symptomatic progression in such patients.

Keywords: convexity meningioma, falx meningioma, parasagittal meningioma, symptomatic progression, tumor volume

INTRODUCTION

Meningiomas are the most common primary intracranial tumors, accounting for ∼25–38% of all such lesions (1, 2). The number of incidentally discovered meningiomas has increased with the widespread use of neuroimaging modalities such as computed tomography and magnetic resonance imaging (MRI) (3). In fact, radiological studies have revealed that neuroimaging could incidentally reveal suspected meningioma lesions with an incidence ranging from 0.9 to 2.5% in individuals aged in their middle years and older (4, 5). On the other hand, meningiomas are often discovered because of a variety of symptoms, including motor and sensory deficits, cognitive decline, and epilepsy (6–8). However, the factors that determine whether a lesion is symptomatic remain unclear.

Meningiomas are benign neoplasms that can exhibit a variety of growth patterns (9, 10) and, eventually, 67–75% of them enlarge (7, 10, 11). In one study in which the median tumor volume was 35.7 ml (range 1.1–133.1 ml) and 90% (52 patients) were symptomatic, tumor volume was statistically significantly related to the appearance of clinical symptoms (6). In recent meta-analyses, 4.7–8.1% of patients with incidentally discovered intracranial meningiomas developed related symptoms at follow-up visits (11, 12). However, the specific locations of the tumors were not examined in either report. The location of such a tumor is important as it is related to the symptoms a patient will experience (8), as well as the clinical and biological behavior of the tumor (6, 13, 14).

Convexity, parasagittal, and falx meningiomas account for almost 50% of all meningiomas (15). In the report in which the association between tumor volume and clinical symptoms was observed in intracranial meningiomas, nearly half of the cases were skull-base meningiomas (6). Convexity, parasagittal, and falx meningiomas differ from skull-base meningiomas in that they are located in the supratentorial space and do not involve cranial nerves. Thus, the tumor volume that causes clinical symptoms differs between supratentorial and skull-base meningiomas, and it is important to analyze the tumor volume that causes clinical symptoms exclusively for convexity, parasagittal, and falx meningiomas.

The purpose of this retrospective study was to identify factors that influence clinical symptoms and to determine a specific threshold tumor volume for the prediction of symptomatic progression in patients with convexity, parasagittal, and falx meningiomas.

MATERIALS AND METHODS

Study Design and Patient Selection

We conducted a retrospective case-control study of patients with primary radiologically suspected convexity, parasagittal, or falx meningiomas. We collected data from patients whose first visit was from 1990 to 2020 at our institution. We excluded patients diagnosed with neurofibromatosis, those for whom MRI Digital Imaging and Communications in Medicine (DICOM) data were not available, and those whose symptoms were unknown due to insufficient medical records of their first visit. When patients had more than one convexity, parasagittal, or falx meningioma, we selected the largest one for analysis. The Osaka University Clinical Research Review Committee approved the study (approval number 14231) and waived the need for written informed consent, as all data were retrospective.

Definition of Symptoms

We determined from their medical records whether patients had clinical findings, which we defined as clinical symptoms. When patients exhibited more than one symptom, we selected the one that mainly interfered with their daily life. We further defined neurological symptoms as excluding epilepsy or non-specific symptoms such as headache.

Volumetric Analysis

We measured the volume of each lesion using the latest MRI DICOM data for asymptomatic patients or the MRI DICOM data at the time of symptom onset for symptomatic patients. We used Horos for macOS to perform the measurements (Horos is a free and open-source code software program that is distributed free of charge under the LGPL license at Horosproject.org and sponsored by Nimble Co LLC d/b/a Purview in Annapolis, MD USA). Using T2-weighed images (T2WIs) or contrast-enhanced T1 weighted images (T1WIs) of ∼5 mm slice thickness, we measured the tumor area in each slice by manually tracing the tumor boundary. Thereafter, we multiplied the sum of all the areas by the thickness between slices, including the gaps.

Tumor Diameter

We used the same MRI DICOM data as for volumetric analysis to measure tumor diameter. The maximum tumor diameter was determined using either axial, coronal, or sagittal images.

Tumor Location, Side, and Area

The lead author (SY) carefully determined the locations of the lesions via MRI, which was independently confirmed by the senior author (NKi). We divided tumor location in three ways: convexity, parasagittal angle, and falx cerebri; right, and left; frontal, middle, and occipital area. We used "frontal area" for the anterior one-third, "occipital area" for the posterior one-third, and "middle area" for the rest.

Interpretation of T2-Weighted Images

We classified lesions according to the radiologic characteristics on T2WIs. They were classified as either "T2-hyperintense" or "other" according to the brightness of the lesion. Lesions that were too heterogenous to classify were assigned to the "other" group. One case with a maximum diameter of only 1 mm was excluded from analysis because the lesion was too small to evaluate.

Abbreviations: ROC, receiver operating characteristic; OR, odds ratio; CI, confidence interval; AUC, area under the curve; WHO, World Health Organization.

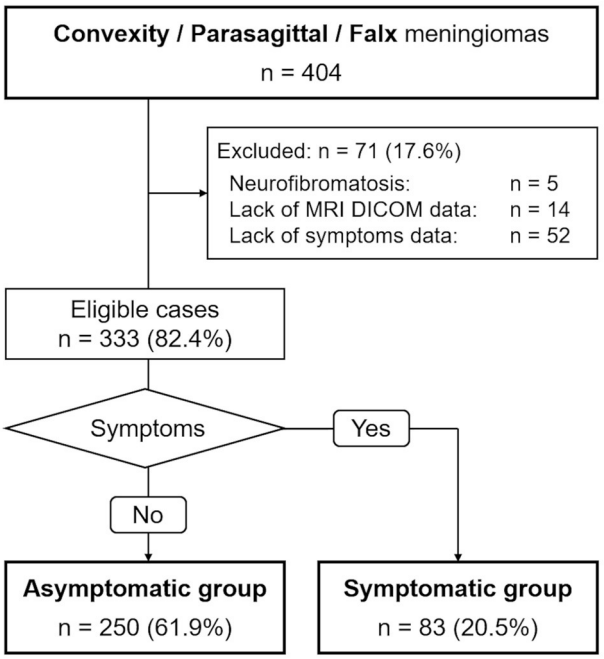

FIGURE 1 | Flow of patient selection and classification.

Statistical Analysis

All statistical analyses were performed using R 3.6.3 for Windows (www.R-project.org; R Foundation for Statistical Computing, Vienna, Austria). Statistical differences for categorical variables were examined using a two-tailed Fisher's exact test. Continuous variables were assessed using the Mann-Whitney U test or the Kruskal-Wallis test adjusted by Bonferroni correction. Multivariate logistic regression analysis was performed with variables that were significant in those univariate analyses. The thresholds were calculated by receiver operating characteristic (ROC) analysis using the distance from the upper left-hand corner (16). Probability values <0.05 were considered significant.

RESULTS

Overall Patient Cohort

Figure 1 illustrates the flow of patient selection. The data of 333 patients (84 male and 249 female) were analyzed. The median age at volumetric analysis was 70 years (range 23–90 years). The median tumor volume and the median maximum tumor diameter were 8.2 ml (range 0.1–188.9 ml) and 30 mm (range 5–100 mm), respectively. We further divided patients into two groups based on clinical symptoms: an asymptomatic group (250 cases) and a symptomatic group (83 cases).

Comparison Between the Asymptomatic and Symptomatic Groups

Table 1 summarizes the characteristics of each group. Univariate analysis revealed significant differences between the groups in terms of sex ($p = 0.002$), age at the time of volumetric analysis ($p < 0.001$), hyperintense lesions on T2WIs ($p = 0.029$), peritumoral edema ($p < 0.001$), maximum tumor diameter ($p < 0.001$), and tumor volume ($p < 0.001$, **Figure 2A**). For multivariate analysis, the maximum tumor diameter was excluded as it is a similar metric to tumor volume (17). Multivariate analysis revealed significant differences between the groups in terms of age at the time of volumetric analysis ($p = 0.002$), peritumoral edema ($p < 0.001$), and tumor volume ($p < 0.001$). The odds ratio (OR) for peritumoral edema was 5.94 (95% confidence interval [CI]: 2.74–12.86).

Thresholds for Predicting Development of Clinical Symptoms

Patients in the symptomatic group experienced motor deficits (37 cases), epilepsy (18 cases), gait disorder (seven cases), visual impairment (seven cases), cognitive decline (six cases), aphasia (four cases), headaches (two cases), sensory deficits (one case), and a subcutaneous mass (one case). The ROC curve revealed a threshold tumor volume of 21.1 ml for predicting whether a patient would develop symptoms, with a sensitivity of 0.843, a specificity of 0.880, and an area under the curve (AUC) of 0.919 (**Figure 2B**, 95% CI: 0.887–0.951). In addition, a threshold maximum tumor diameter of 40 mm may also be a reliable marker for predicting which patients will become symptomatic, with a sensitivity of 0.819, a specificity of 0.840, and an AUC of 0.893 (95% CI: 0.856–0.930). For 13 patients in the symptomatic group, we obtained MRI DICOM data when they had been asymptomatic at their first visit. Of these, the 21.1-ml and 40-mm threshold correctly predicted the development of symptoms in seven cases (54%).

Threshold for Predicting Development of Neurological Symptoms

When focusing only on neurological symptoms (62 cases), the threshold for tumor volume was also 21.1 ml (sensitivity 0.871, specificity 0.880, AUC 0.937 [95% CI: 0.910–0.965]). The threshold for maximum tumor diameter for prediction of neurological symptoms was almost the same as that for all symptoms: 41 mm (sensitivity 0.839, specificity 0.856, AUC 0.914 [95% CI: 0.880–0.948]).

Comparison by Age at the Time of Volumetric Analysis

When divided into three age groups; <65, 65–74, 75≤, the rates of symptomatic patients were 40.7, 24.6, and 9.9%, and the ORs for presenting clinical symptoms were 1 (Reference), 0.47 (95% CI: 0.27–0.84), and 0.16 (95% CI: 0.08–0.33), respectively. In all age groups, the tumor volume was significantly larger in the symptomatic than in the asymptomatic group ($p < 0.001$, **Table 2**). The threshold for predicting patients in which symptoms would develop was similar: 21.9 ml for patients <65 years, 19.0 ml for patients 64–74 years, and 21.1 ml for patients ≥75 years.

Comparison by Tumor Location

Tumor volume of the asymptomatic and symptomatic group based on tumor location is shown in **Table 3**. For all locations,

TABLE 1 | Characteristics of 333 patients and tumors.

Variable	Asymptomatic group ($n = 250$)	Symptomatic group ($n = 83$)	*p*-value		OR (95% CI)
			Univariate	Multivariate	
Sex (Male/Female)	52/198	32/51	0.002	0.140	1.79 (0.83–3.86)
Age at volumetric analysis (yrs)*	72 (23–90)	63 (31–89)	<0.001	0.002	–
Tumor location (Convexity/Parasagittal/Falx)	138/58/54	35/25/23	0.115	–	–
Tumor side (Right/Left)	124/126	41/42	1	–	–
Tumor area (Frontal/Middle/Occipital)	80/125/45	20/49/14	0.324	–	–
MRI T2WI (Hyper/Others)†	162/87	65/18	0.029	0.154	1.82 (0.80–4.16)
Multiple lesions (Yes/No)	22/228	4/79	0.345	–	–
Peritumoral edema (Yes/No)	60/190	69/14	<0.001	<0.001	5.94 (2.74–12.86)
Maximum tumor diameter (mm)*	24 (5–78)	52 (18–100)	<0.001	–	–
Tumor volume (ml)*	5.0 (0.1–148.0)	45.7 (2.8–188.9)	<0.001	<0.001	–

CI, confidence interval.
**Median (range).*
†Too small to evaluate: n = 1.

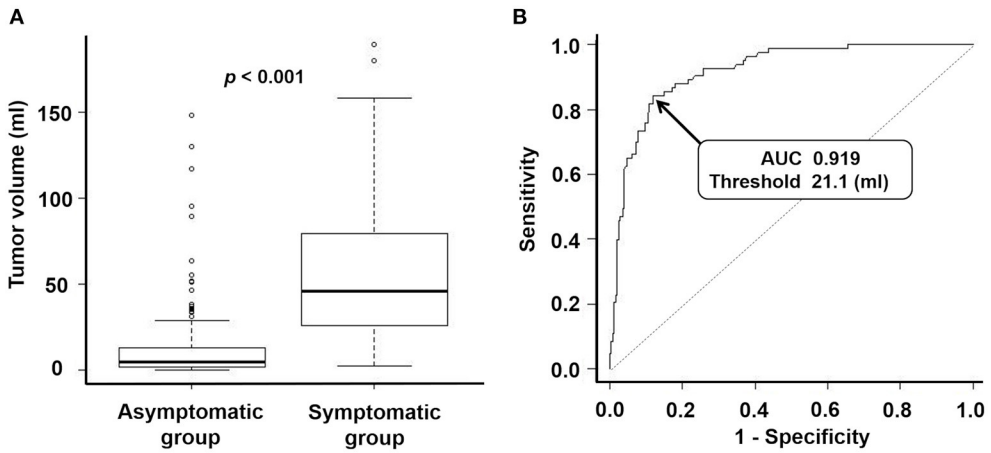

FIGURE 2 | (A) Box-and-whisker plots representing tumor volume of an asymptomatic group and symptomatic group. The median tumor volume of the asymptomatic group and the symptomatic group were 5.0 ml and 45.7 ml, respectively. *P*-value for the Mann-Whitney U test: <0.001. **(B)** Receiver operating characteristic curve for predicting which patients will become symptomatic via tumor volume. Area under the curve: 0.919 (95% confidence interval: 0.887–0.951). Threshold for tumor volume: 21.1 ml. Sensitivity: 0.843. Specificity: 0.880.

TABLE 2 | Comparison by age at the time of volumetric analysis.

Age at volumetry (yrs)	Tumor volume (ml)*		*p*-value	AUC (95% CI)	Threshold (ml)
	Asymptomatic group ($n = 250$)	Symptomatic group ($n = 83$)			
<65 ($n = 108$)	7.8 (0.3–148.0)	52.8 (2.8–180.0)	<0.001	0.875 (0.806–0.944)	21.9
65–74 ($n = 114$)	4.2 (0.2–117.1)	45.2 (7.9–188.9)	<0.001	0.921 (0.872–0.970)	19.0
75≤ ($n = 111$)	4.3 (0.1–63.6)	40.6 (21.1–103.3)	<0.001	0.971 (0.942–0.999)	21.1

**Median (range).*
AUC, Area under the curve; CI, confidence interval.

tumor volume was significantly larger in the symptomatic than in the asymptomatic group ($p < 0.001$). Falx meningiomas had a slightly lower threshold for symptomatic progression than other locations.

TABLE 3 | Comparison by tumor location.

Tumor location	Tumor volume (ml)*		*p*-value	AUC (95% CI)	Threshold (ml)
	Asymptomatic group ($n = 250$)	Symptomatic group ($n = 83$)			
Convexity ($n = 173$)	4.5 (0.1–117.1)	61.2 (2.8–151.6)	<0.001	0.941 (0.897–0.984)	20.5
Parasagittal angle ($n = 83$)	7.0 (0.5–148.0)	29.4 (6.0–180.0)	<0.001	0.868 (0.787–0.950)	18.9
Falx cerebri ($n = 77$)	4.7 (0.3–129.7)	45.7 (7.9–188.9)	<0.001	0.931 (0.876–0.986)	14.0

**Median (range).*
AUC, Area under the curve; CI, confidence interval.

Correlation Between Tumor Volume and Tumor Side/Area

Table 4 displays the difference in tumor volume between the asymptomatic and symptomatic groups, depending on the side or area of the tumor. For all areas, the symptomatic group had significantly larger tumor volume than the asymptomatic group ($p < 0.001$). The threshold for predicting patients to develop clinical symptoms was also around 21.1 ml for all areas except the occipital area of the left hemisphere.

Comparison by WHO Grade

Thirty-three patients in the asymptomatic and 77 in the symptomatic group received surgical treatment. Of the 110 patients, the meningiomas of 90 (81.8%) were World Health Organization (WHO) grade I, 10 (9.1%) were WHO grade II, 3 (2.7%) were WHO grade III, and 7 (6.4%) were not mentioned in WHO grade. There were no significant differences between patients with WHO grade I and those with WHO grade II/III meningiomas, except in the maximum tumor diameter, which was larger in the latter than in the former (**Table 5**).

DISCUSSION

In the present study, we identified factors that are related to clinical symptoms of patients with convexity, parasagittal, and falx meningiomas, and, to our knowledge, we determined the first-ever threshold of tumor volume for predicting symptomatic progression in such patients. This may allow clinicians to predict when a growing, asymptomatic meningioma will become symptomatic. Currently, observation is the first choice for management of patients with asymptomatic meningiomas (18); these results may be useful to determine the necessity of treatment and its appropriate timing.

In this study, we also determined a threshold maximum tumor diameter of 40 mm for the prediction of symptomatic progression of patients (sensitivity 0.819, specificity 0.840, AUC 0.893). However, a tumor volume of 21.1 ml was a more accurate threshold (sensitivity 0.843, specificity 0.880, AUC 0.919). Maximum tumor diameter and tumor volume are highly correlated (17). However, tumors do not always grow in the direction of their maximum diameter, which may be why we discovered tumor volume to be the more accurate predictive factor. Maximum tumor diameter is one of the most convenient clinical metrics; however, our results indicate that the development and widespread use of a simple method to measure tumor volume is needed.

Meningiomas manifest in a variety of symptoms (8), including non-specific symptoms such as headaches and dizziness (7). Such non-specific symptoms make clinicians wonder if interventions such as surgery or radiotherapy are required for the existing meningioma. In this study, we also calculated thresholds for tumor volume and maximum tumor diameter to predict the development of neurological symptoms. However, the thresholds were similar to those for all clinical symptoms. Therefore, it may be less important for clinicians to examine whether non-specific symptoms are caused by a given meningioma.

The hemisphere in which glioblastomas and strokes occur affects the symptoms that the patient experiences (19, 20); however, in this study of meningiomas, we detected no differences between hemispheres. This may be because few patients presented with cognitive decline (7%) or aphasia (5%). The low threshold of the tumor volume only in the occipital area of the left hemisphere may be due to the small number of symptomatic patients itself. Falx meningiomas also had a lower threshold for symptomatic progression than other locations, but as in previous studies (21–23), the number of cases may not have been sufficient. Therefore, further large-scale studies are needed to validate our location-specific findings.

In multiple meta-analyses (11, 24), a T2-hyperintense sign was correlated with radiological progression, and peritumoral edema was the only imaging metric that correlated with symptomatic progression, which was confirmed in this study. Since T2WIs may be appropriate for follow-up of untreated meningiomas (25), symptom-related radiological indicators that do not require contrast-enhanced T1WIs are needed.

We should note that this study has several limitations. The first is the fact that this was a single-center, retrospective study conducted in Japan. As Japan has the largest number of MRIs per unit population in the world (26), a larger proportion of small, asymptomatic meningiomas may be detected than in other countries. This would have lowered the thresholds of tumor volume and maximum tumor diameter for

TABLE 4 | Correlation between tumor side/area and tumor volume (ml).

Tumor side	Right hemisphere $n = 165$					Left hemisphere $n = 168$					Total $n = 333$				
Tumor area	Tumor volume (ml)*		*p*-value	AUC	Threshold (ml)	Tumor volume (ml)*		*p*-value	AUC	Threshold (ml)	Tumor volume (ml)*		*p*-value	AUC	Threshold (ml)
	Asymptomatic group $n = 124$	Symptomatic group $n = 41$				Asymptomatic group $n = 126$	Symptomatic group $n = 42$				Asymptomatic group $n = 250$	Symptomatic group $n = 83$			
Frontal $n = 100$	4.3 (0.2–148)	82.9 (8.7–131.1)	0.002	0.901 (0.797–1)	17.6	5.0 (0.2–129.7)	53.5 (13.4–114.8)	<0.001	0.918 (0.846–0.990)	22.7	4.8 (0.2–148)	53.5 (8.7–131.1)	<0.001	0.907 (0.847–0.966)	17.6
Middle $n = 174$	4.9 (0.1–89.6)	47.9 (6.0–188.9)	<0.001	0.947 (0.900–0.993)	21.9	6.7 (0.3–37.0)	49.2 (2.8–151.6)	<0.001	0.898 (0.815–0.981)	23.4	5.6 (0.1–89.6)	47.9 (2.8–188.9)	<0.001	0.930 (0.887–0.973)	21.9
Occipital $n = 59$	4.1 (0.7–63.6)	55.0 (7.9–180.0)	<0.001	0.940 (0.848–1)	21.1	3.6 (0.6–35.3)	22.7 (7.7–158.1)	<0.001	0.917 (0.815–1)	12.6	3.9 (0.6–63.6)	36.0 (7.7–180.0)	<0.001	0.925 (0.858–0.993)	12.6
Total $n = 333$	4.6 (0.1–148.0)	47.9 (6.0–188.9)	<0.001	0.928 (0.887–0.968)	21.1	5.5 (0.2–129.7)	45.2 (2.8–158.1)	<0.001	0.907 (0.857–0.957)	22.7	5.0 (0.1–148.0)	45.7 (2.8–188.9)	<0.001	0.919 (0.887–0.951)	21.1
p-value	0.969	0.859	–	–	–	0.489	0.504	–	–	–	0.775	0.976	–	–	–

*Median (range).
AUC, Area under the curve; CI, confidence interval.

TABLE 5 | Comparison of WHO grade I and grade II/III meningioma.

Variable	WHO grade		*p*-value
	I ($n = 90$)	II/III ($n = 13$)	
Sex (Male/Female)	35/55	5/8	1
Age at volumetry (yrs)*	63 (23–83)	67 (41–77)	0.471
Tumor location (Convexity/Parasagittal/Falx)	42/19/29	7/5/1	0.113
Tumor side (Right/Left)	41/49	7/6	0.767
Tumor area (Frontal/Middle/Occipital)	24/50/16	2/8/3	0.778
MRI T2WI (Hyper/Others)	75/15	8/5	0.125
Multiple lesions (Yes/No)	8/82	0/13	0.592
Peritumoral edema (Yes/No)	65/25	12/1	0.176
Maximum tumor diameter (mm)*	48 (18–82)	63 (22–100)	0.044
Tumor volume (ml)*	37.6 (2.8–188.9)	71.2 (5.0–123.9)	0.111

*Median (range).
WHO, World Health Organization.

predicting symptomatic progression of patients in this study. The second limitation is the possibility of errors in volumetric measurements. Volumetric measurement may be inaccurate especially for small tumors (27), and manual segmentation may be inconsistent (28). Finally, this study was conducted on radiologically presumed meningiomas; therefore, 2.9–3.4% of our study population may actually have had other tumors (10, 29).

CONCLUSION

In the present study, we identified factors predictive of clinical symptoms in patients with convexity, parasagittal, and falx meningiomas and, to our knowledge, determined the first-ever threshold tumor volume for predicting symptomatic progression in such patients. These results may be useful in allowing clinicians to estimate when a growing, asymptomatic meningioma will develop clinical symptoms, thereby improving management of patients with the disease.

DATA AVAILABILITY STATEMENT

The original contributions presented in the study are included in the article/supplementary material, further inquiries can be directed to the corresponding author.

ETHICS STATEMENT

The studies involving human participants were reviewed and approved by Osaka University Clinical Research Review Committee. Written informed consent for participation was not required for this study in accordance with the national legislation and the institutional requirements.

AUTHOR CONTRIBUTIONS

SY and NKi contributed to the concept, drafting, and writing the manuscript. TN contributed to the acquisition of data. RH and NKa contributed to the manuscript editing. MK contributed to the provision of insightful thought and design. HK contributed to the study supervision. All authors contributed to the article and approved the submitted version.

ACKNOWLEDGMENTS

We would like to thank Editage (www.editage.com) for English language editing.

REFERENCES

1. Claus EB, Bondy ML, Schildkraut JM, Wiemels JL, Wrensch M, Black PM. Epidemiology of intracranial meningioma. *Neurosurgery.* (2005) 57:1088–94. doi: 10.1227/01.NEU.0000188281.91351.B9
2. Ostrom QT, Patil N, Cioffi G, Waite K, Kruchko C, Barnholtz-Sloan JS, et al. Statistical report: primary brain and other central nervous system tumors diagnosed in the United States in 2013–2017. *Neuro Oncol.* (2020) 22:iv1–iv96. doi: 10.1093/neuonc/noaa200
3. Islim AI, Kolamunnage-Dona R, Mohan M, Moon RDC, Crofton A, Haylock BJ, et al. prognostic model to personalize monitoring regimes for patients with incidental asymptomatic meningiomas. *Neuro Oncol.* (2020) 22:278–89. doi: 10.1093/neuonc/noz160
4. Vernooij MW, Ikram MA, Tanghe HL, Vincent AJPE, Hofman A, Krestin GP, et al. Incidental findings on brain MRI in the general population. *N Engl J Med.* (2007) 357:1821–8. doi: 10.1056/NEJMoa070972
5. Bos D, Adams HHH, Zonneveld HI, Verlinden VJA, Verbruggen JGJ. Course of incidental findings on brain MR images: the population. *Radiology.* (2016) 281:507–15. doi: 10.1148/radiol.2016160218
6. Kauke M, Safi AF, Stavrinou P, Krischek B, Goldbrunner R, Timmer M. Does meningioma volume correlate with clinical disease manifestation irrespective of histopathologic tumor grade? *J Craniofac Surg.* (2019) 30:e799–802. doi: 10.1097/SCS.0000000000005845
7. Kim KH, Kang SJ, Choi J-W, Kong D-S, Seol HJ, Nam D-H, et al. Clinical and radiological outcomes of proactive Gamma Knife surgery for asymptomatic meningiomas compared with the natural course without intervention. *J Neurosurg.* (2019) 130:1740–9. doi: 10.3171/2017.12.JNS171943
8. Fathi AR, Roelcke U. Meningioma. *Curr Neurol Neurosci Rep.* (2013) 13:337. doi: 10.1007/s11910-013-0337-4
9. Hashiba T, Moto NH, Izumoto S, Suzuki T, Kagawa N, Maruno M, et al. Serial volumetric assessment of the natural history and growth pattern of incidentally discovered meningiomas: clinical article. *J Neurosurg.* (2009) 110:675–84. doi: 10.3171/2008.8.JNS08481
10. Behbahani M, Skeie GO Eide GE, Hausken A, Lund-Johansen M. Skeie BS. A prospective study of the natural history of incidental meningioma-Hold your horses! *Neuro Oncol Pract.* (2019) 6:438–50. doi: 10.1093/nop/npz011
11. Nakasu S, Nakasu Y. Natural history of meningiomas: review with meta-analyses. *Neurol Med Chir (Tokyo).* (2020) 60:109–20. doi: 10.2176/nmc.ra.2019-0213
12. Islim AI, Mohan M, Moon RDC, Srikandarajah N, Mills SJ, Brodbelt AR, et al. Incidental intracranial meningiomas: a systematic review and meta-analysis of prognostic factors and outcomes. *J Neurooncol.* (2019) 142:211–21. doi: 10.1007/s11060-019-03104-3
13. Maiuri F, Mariniello G, Guadagno E, Barbato M, Corvino S, Del Basso De Caro M, et al. grade, proliferation index, and progesterone receptor expression are different according to the location of meningioma. *Acta Neurochir (Wien).* (2019) 161:2553–61. doi: 10.1007/s00701-019-04084-z
14. Hashimoto N, Rabo CS, Okita Y, Kinoshita M, Kagawa N, Fujimoto Y, et al. Slower growth of skull base meningiomas compared with non–skull base meningiomas based on volumetric and biological studies. *J Neurosurg.* (2012) 116:574–80. doi: 10.3171/2011.11.JNS11999
15. Sun C, Dou Z, Wu J, Jiang B, Iranmanesh Y, Yu X, et al. The preferred locations of meningioma according to different biological characteristics based on voxel-wise analysis. *Front Oncol.* (2020) 10:1412. doi: 10.3389/fonc.2020.01412
16. Akobeng AK. Understanding diagnostic tests 3: receiver operating characteristic curves. *Acta Paediatr Int J Paediatr.* (2007) 96:644–7. doi: 10.1111/j.1651-2227.2006.00178.x
17. Ishi Y, Terasaka S, Yamaguchi S, Yoshida M, Endo S, Kobayashi H, et al. Reliability of the size evaluation method for meningiomas: maximum diameter, ABC/2 formula, and planimetry method. *World Neurosurg.* (2016) 94:80–8. doi: 10.1016/j.wneu.2016.06.108
18. Goldbrunner R, Minniti G, Preusser M, Jenkinson MD, Sallabanda K, Houdart E, et al. EANO guidelines for the diagnosis and treatment of meningiomas. *Lancet Oncol.* (2016) 17:e383–91. doi: 10.1016/S1470-2045(16)30321-7
19. Baumann C, Tichy J, Schaefer JH, Steinbach JP, Mittelbronn M, Wagner M, et al. Delay in diagnosing patients with right-sided glioblastoma induced by hemispheric-specific clinical presentation. *J Neurooncol.* (2020) 146:63–9. doi: 10.1007/s11060-019-03335-4
20. Foerch C, Misselwitz B, Sitzer M, Berger K, Steinmetz H, Neumann-Haefelin T. Difference in recognition of right and left hemispheric stroke. *Lancet.* (2005) 366:392–3. doi: 10.1016/S0140-6736(05)67024-9
21. Das KK, Gosal JS, Sharma P, Mehrotra A, Bhaisora K, Sardhara J, et al. Falcine meningiomas: analysis of the impact of radiologic tumor extensions and proposal of a modified preoperative radiologic classification scheme. *World Neurosurg.* (2017) 104:248–58. doi: 10.1016/j.wneu.2017.04.159
22. Zuo FX, Wan JH Li XJ, Qian HP, Meng XL, A. proposed scheme for the classification and surgical planning of falcine meningioma treatment. *J Clin Neurosci.* (2012) 19:1679–83. doi: 10.1016/j.jocn.2012.01.034
23. Chung S-B, Kim C-Y, Park C-K, Kim DG, Jung H-W. Falx meningiomas: surgical results and lessons learned from 68 cases. *J Korean Neurosurg Soc.* (2007) 42:276. doi: 10.3340/jkns.2007.42.4.276
24. Sughrue ME, Rutkowski MJ, Aranda D, Barani IJ, McDermott MW, Parsa AT. Treatment decision making based on the published natural history and growth rate of small meningiomas. *J Neurosurg.* (2010) 113:1036–42. doi: 10.3171/2010.3.JNS091966
25. Boto J, Guatta R, Fitsiori A, Hofmeister J, Meling TR, Vargas MI. Is contrast medium really needed for follow-up MRI of untreated intracranial meningiomas? *Am J Neuroradiol.* (2021) 42:1421–8. doi: 10.3174/ajnr.A7170
26. Matsumoto M, Koike S, Kashima S, Awai K. Geographic distribution of CT, MRI and PET devices in Japan: a longitudinal analysis based on national census data. *PLoS ONE.* (2015) 10:e0126036. doi: 10.1371/journal.pone.0126036
27. Pan HC, Cheng FC, Sun MH, Chen CCC, Sheehan J. Prediction of volumetric data errors in patients treated with Gamma Knife radiosurgery. *Stereotact Funct Neurosurg.* (2007) 85:184–91. doi: 10.1159/000101297
28. Mazzara GP, Velthuizen RP, Pearlman JL, Greenberg HM, Wagner H. Brain tumor target volume determination for radiation treatment planning through automated MRI segmentation. *Int J Radiat Oncol Biol Phys.* (2004) 59:300–12. doi: 10.1016/j.ijrobp.2004.01.026

29. Jadid KD, Feychting M, Höijer J, Hylin S, Kihlström L, Mathiesen T. Long-term follow-up of incidentally discovered meningiomas. *Acta Neurochir (Wien)*. (2015) 157:225–30. doi: 10.1007/s00701-014-2306-3

Conflict of Interest: The authors declare that the research was conducted in the absence of any commercial or financial relationships that could be construed as a potential conflict of interest.

Publisher's Note: All claims expressed in this article are solely those of the authors and do not necessarily represent those of their affiliated organizations, or those of the publisher, the editors and the reviewers. Any product that may be evaluated in this article, or claim that may be made by its manufacturer, is not guaranteed or endorsed by the publisher.

Copyright © 2021 Yamada, Kijima, Nakagawa, Hirayama, Kinoshita, Kagawa and Kishima. This is an open-access article distributed under the terms of the Creative Commons Attribution License (CC BY). The use, distribution or reproduction in other forums is permitted, provided the original author(s) and the copyright owner(s) are credited and that the original publication in this journal is cited, in accordance with accepted academic practice. No use, distribution or reproduction is permitted which does not comply with these terms.

frontiers in Oncology

ORIGINAL RESEARCH
published: 22 November 2021
doi: 10.3389/fonc.2021.761284

Surgical Treatment and Clinical Outcomes of Petroclival Meningiomas: A Single-Center Experience of 107 Patients

Baocheng Gao[1], Yongfa Zhang[1], Jiang Tan[1], Jinsong Ouyang[1], Bai Tai[1], Xianbao Cao[2], Tao Li[1] and Shuang Hu[2]**

[1] Department of Neurosurgery, The First People's Hospital of Yunnan Province, The Affiliated Hospital of Kunming University of Science and Technology, Kunming, China, [2] Department of Ear, Nose and Throat (ENT) and Head and Neck (HN) Surgery, The First People's Hospital of Yunnan Province, The Affiliated Hospital of Kunming University of Science and Technology, Kunming, China

OPEN ACCESS

Edited by:
Hailiang Tang,
Fudan University, China

Reviewed by:
Bharat Guthikonda,
Louisiana State University Health Shreveport, United States
Gustavo Isolan,
Centro Avançado de Neurologia e Neurocirurgia (CEANNE), Brazil

***Correspondence:**
Tao Li
taoli_kh@163.com
Shuang Hu
hushuangkh@163.com

Specialty section:
This article was submitted to Neuro-Oncology and Neurosurgical Oncology, a section of the journal Frontiers in Oncology

Received: *19 August 2021*
Accepted: *04 November 2021*
Published: *22 November 2021*

Citation:
Gao B, Zhang Y, Tan J, Ouyang J, Tai B, Cao X, Li T and Hu S (2021) Surgical Treatment and Clinical Outcomes of Petroclival Meningiomas: A Single-Center Experience of 107 Patients. Front. Oncol. 11:761284. doi: 10.3389/fonc.2021.761284

Objective: This study aimed to establish optimal surgical strategies *via* reviewing the clinical outcomes of various surgical approaches for the pertroclival meningiomas (PCMs).

Methods: This retrospective study enrolled 107 patients with PCMs at the authors' institution from year 2010 to 2020. Patient demographics, the clinical characteristics, various operative approaches, major morbidity, post-operative cranial nerve deficits and tumor progression or recurrence were analyzed.

Results: The subtemporal transtentorial approach (STA), the Kawase approach (KA), the retrosigmoid approach (RSA) and the anterior sigmoid approach (ASA), namely the posterior petrosal approach (PPA) were adopted for 17 cases, 22 cases, 31 cases and 34 cases respectively. Total or subtotal resection was achieved in 96 cases (89.7%). The incidence of new-onset and aggravated cranial nerve dysfunction were 13.1% (14/107) and 10.4% (15/144), respectively. Furthermore, 14 cases suffered from intracranial infection, 9 cases had cerebrospinal fluid leakage, and 3 cases sustained intracranial hematoma (1 case underwent second operation). The mean preoperative and postoperative Karnofsky Performance Status (KPS) score was 80 (range 60-100) and 78.6 (range 0-100), but this was not statistically significant (P>0.05). After a mean follow-up of 5.1 years (range 0.3- 10.6 years), tumor progression or recurrence was confirmed in 23 cases. Two cases died from postoperative complications.

Conclusions: For the treatment of PCMs, it is still a challenge to achieve total resection. With elaborate surgical plans and advanced microsurgical skills, most patients with PCMs can be rendered tumor resection with satisfactory extent and functional preservation, despite transient neurological deterioration during early postoperative periods.

Keywords: petroclival, meningioma, surgical approach, skull base, neuronal function

INTRODUCTION

Petroclival meningiomas (PCMs) refer to meningiomas that occur on the upper two-thirds of the clivus and medially to the internal auditory canal (IAC), adjacent to the major neurovascular structures, including brainstem, basilar artery, perforating arteries, and III-VII cranial nerves (CN) (1). Since most PCMs are World Health Organization (WHO) grade I tumors, the treatment goal should be curative total resection (TR) during the first operation when the arachnoid membranes are intact. In terms of the surgical approaches, the subtemporal transtentorial approach (STA) and the Kawase approach (KA) have the characteristics of short operative distance, convenient tumor base resection and less intraoperative bleeding but with the limitation for large posterior petrosal PCMS; the retrosigmoid approach (RSA) has the feature of fewer approach-related complications while the restriction to the petroclival region; the anterior sigmoid approach (ASA), also named the posterior petrosal approach (PPA), can facilitate the exposure of tumors, reduce the traction of the brainstem but perplexes the neurosurgeons for harder maneuver. Although there are many surgical approaches for PCMs and the relevant studies have repeatedly reported, the optimal choice for the operation is of extreme difficulty (2–5) and no uniform standard establishing the superiority of one approach over another is acknowledged currently (6, 7), due to the anatomical complexity, the multiformity of tumor invasion and the intricacy of a balance between neurofunctional preservation and tumor recurrence.

Despite remarkable advances in microsurgical techniques during the past decades, many recent reports (1) still reveal a low TR rate and suggest that aggressive extirpation is often associated with severe morbidity. For this reason, some authors proposed subtotal resection (STR) followed by radiotherapy in order to preserve the neurological functions. However, others insist that aggressive resection using various skull base surgical techniques should guarantee more favorable outcomes and the control of high-grade tumors. The surgical treatment of PCMs has always been a challenge for skull base neurosurgeons due to the deep location, complex adjacent structures and their scarcity (less than 0.15% of all intracranial meningiomas) (1). This study aimed to establish optimal surgical strategies *via* reviewing the clinical outcomes of various surgical approaches for PCMs based on our 107 cases.

MATERIALS AND METHODS

Patients

The present study was approved by the Ethics Committee of the First People's Hospital of Yunnan Province. All procedures performed in studies that involved human participants were in accordance with the ethics standards of the Institutional and National Research Committee, and the 1964 Helsinki Declaration and its later amendments or comparable ethics standards. Written consent was obtained from the patients.

This retrospective study enrolled 107 patients from the Department of Neurosurgery, the First People's Hospital of Yunnan Province, from January 2010 and December 2020. All patients were diagnosed with PCMs based on radiological and histopathological results. The exclusion criteria were as follows: (1) patients with a magnetic resonance imaging (MRI) revealing that the main body of the tumor is located on the inferior clivus or lateral wall of the IAC; (2) patients with multiple (≥2) intracranial meningiomas; (3) patients with no successful follow-up.

Clinical and Radiological Evaluation

The demographic and clinical profiles were collected, and the operative logs were reviewed. The neurological functions were evaluated preoperatively and 2 weeks after operation using the Karnofsky Performance Status (KPS) scale, and all patients underwent perioperative MRI scans. The extent of the resection was determined based on the intraoperative finding and enhanced MRI within 72 hours postoperatively. Total resection was defined as Simpson grade I and II, subtotal resection was defined as Simpson grade III and IV, and partial resection was defined as Simpson grade V. According to the classification system proposed by Kawase et al. (8) in 1996 and Ichimura et al. (9) in 2008, the PCMs were divided into four groups: upper clival type, cavernous type, tentorium type, and petrous apex type. According to the size-based classification criteria proposed by Sekhar et al. (10), measured on the maximum diameter, tumors were small (<10 mm), medium (10-24 mm), large (25-44 mm), and giant (≥45 mm).

Surgical Treatment

The surgical resection was performed with the assistance of electrophysiological monitoring, and the selection of surgical approaches was shown in **Table 1**. For petrous apex type PCMs,

TABLE 1 | Selection of surgical approaches based on imaging classification.

Imaging classification	Cases (*n*)	Approach (*n*)					TR (*n*)	SR (*n*)	PR (*n*)
		STA	KA	RSA	ASA	CA			
PAT	16	11	5	0	0	0	16	0	0
TT	38	6	0	19	13	0	15	23	0
CT	19	0	13	5	0	1[a]	0	10	9
UCT	34	0	4	7	21	2[b]	26	6	2
SUM	107	17	22	31	34	3	57	39	11

PAT, petrous apex type; TT, tentorium type; CT, Cavernous type; UCT, upper clivus type; SUM, summation; STA, subtemporal transtentorium approach; KA, Kawase approach; RSA, retrosigmoid approach; ASA, anterior sigmoid approach; CA, combined posterior and anterior petrosal approach; TR, total resection; SR, subtotal resection; PR, partial resection.

[a]*The Fisch's type A approach was used, because the tumor invaded the infratemporal fossa.*

[b]*The combined posterior and anterior petrosal approach was used, because the tumors extensively invaded the cavernous sinus and crossed the midline of the clivus.*

the subtemporal transtentorium approach (STA) was preferred. However, when the tumor was large, the Kawase approach (KA) was used. For cavernous type PCMs, KA was the first choice. However, when the tumor was located in the posterior fossa and barely invaded the middle fossa, the retrosigmoid approach (RSA) was used. For upper clivus type PCMs, the anterior sigmoid sinus approach (ASA) was adopted. However, when the tumor did not cross the midline of the clivus, the KA or RSA were selected. For tentorium type PCMs, the STA was used when the tumor size was small or medium, while the tumor was large or giant the RSA or ASA should be used depending on whether the tumor crossed the midline of the clivus.

Follow-Up and Statistical Analysis

The follow-up was implemented on an outpatient basis. Clinical and radiological examinations were performed. The SPSS 20.0 software (IBM Corp., Armonk, NY, USA) was used for the statistical analysis. The KPS scores was compared using *t*-test, and the progression or recurrence rate was evaluated using a chi-square test (or a Fisher exact test when necessary). And the probability (*P*) values <0.05 were considered statistically significant.

RESULTS

Demographic Characteristics

There were 28 males (26.2%) and 79 females (73.8%), with an average age of 42.8 years old (range 19-72 years). The clinical symptoms were as follows: headache in 33 cases (30.8%); CN III, IV, and/or VI dysfunction (diplopia) in 25 cases (23.4%); CN V dysfunction (trigeminal neuralgia and/or facial numbness) in 61 cases (57.0%); CN VIII dysfunction (hearing impairment) in 28 cases (26.2%), CN VII dysfunction (facial paralysis) in 11 cases (10.3%); posterior group cranial nerves dysfunction in 19 cases (17.8%); ataxia in 24 cases (22.4%), and progressive hemiparesis in 10 cases (9.3%). In addition, 13 patients (12.1%) were asymptomatic, who requested surgical operation due to psychological stress and other factors. The median duration between onset and surgical treatment were 29 months (range 4-156 months). The mean tumor size was 39.1 mm (range 6.2-75.9 mm), in which 59 patients (55.1%) had large tumors, 40 cases (37.4%) with giant tumors, 6 cases (5.6%) had medium tumors, and only 2 patients (1.9%) had small tumors. The mean follow-up period was 5.1 years (range 0.3-10.6 years). The patient characteristics and detailed clinical information are shown in **Table 2**.

TABLE 2 | Demographic data for 107 patients with petroclival meningiomas.

Demographic data	Value
Mean age (range, yrs)	42.8 (19-72)
Male/female ratio	28:79
Mean preoperative KPS score (range)	80 (60-100)
Mean clinical follow-up (range, yrs)	5.1 (0.3-10.6)
Symptoms & signs at onset (no., %)	
Headache	33 (30.8%)
Diplopia	25 (23.4%)
Trigeminal neuralgia and/or facial numbness	61 (57.0%)
Acoustic-facial bundle dysfunction	39 (36.4%)
Posterior cranial nerve dysfunction	19 (17.8%)
Ataxia	24 (22.4%)
Progressive hemiparesis	10 (9.3%)
Asymptomatic and others	13 (12.1%)
Mean tumor size (range, mm)	39.1 (6.2-75.9)
Small (<10 mm)	2 (1.9%)
Medium (10mm≤diameter<25mm)	6 (5.6%)
Large (25mm≤diameter<45mm)	59 (55.1%)
Giant (≥45mm)	40 (37.4%)

Surgical Approaches and the Extent of Surgical Resection

STA was used in 17 cases, KA was selected in 22 cases, ASA was adopted in 34 cases, and RSA was employed in 31 cases. The combined posterior and anterior petrosal approach was used in two cases and the Fisch's type A approach was used in one case. A total of 57 patients underwent Simpson grade I or II resection (total resection, **Figure 1**). Total or subtotal resection was achieved in 96 patients (89.7%), whereas subtotal and partial resection were achieved in 39 patients and 11 patients respectively. Details of the surgical approaches and the extent of removal were shown in **Table 1**.

Postoperative Histopathology of the Tumors

Pathology was reported as WHO grade I in 95 cases (88.8%), 9 tumors were reported as WHO grade II (atypical type) and 3 as WHO grade III (anaplastic type). Among the 95 cases of grade I meningiomas, the meningothelial subtype (66 cases, 69.5%) was most common, followed by transitional subtype (17 patients, 17.9%), secretory subtypes (6 cases, 6.3%) and other subtypes (6 cases, 6.3%). There was no statistical significance between the WHO grade and degree of tumor resection (P>0.05, **Figure 2**).

Postoperative Complications and Functional Outcome

The incidence of new-onset and aggravated cranial nerve dysfunction were 13.1% (14/107) and 10.4% (15/144), respectively. The CN IV to VIII dysfunction was common, and most of them had improved at recent follow-up. Detailed cranial nerve dysfunctions were shown in **Table 3**. Other major postoperative morbidities were intracranial infection (14 cases, 13.1%), cerebrospinal fluid leakage (9 patients, 8.4%), postoperative hematoma (3 patients, 2.8%), in which 1 case needed second operation (**Figure 3**). Two patients with postoperative hematoma died of pneumonia and multiple organ failure, respectively. The mean preoperative and postoperative KPS scores were 80 (range 60-100) and 78.6 (range 0-100), respectively. This was not statistically significant (t=-0.102, P=0.922). Furthermore, at their most recent follow-up, 57 cases (53.3%) were stable with no worsened KPS, and 36 cases (33.6%) had improved, only 14 patients (13.1%) had aggravated KPS score.

Tumor Progression or Recurrence

During the follow-up, overall progression or recurrence was confirmed in 23 cases (21.5%). According to the extent of

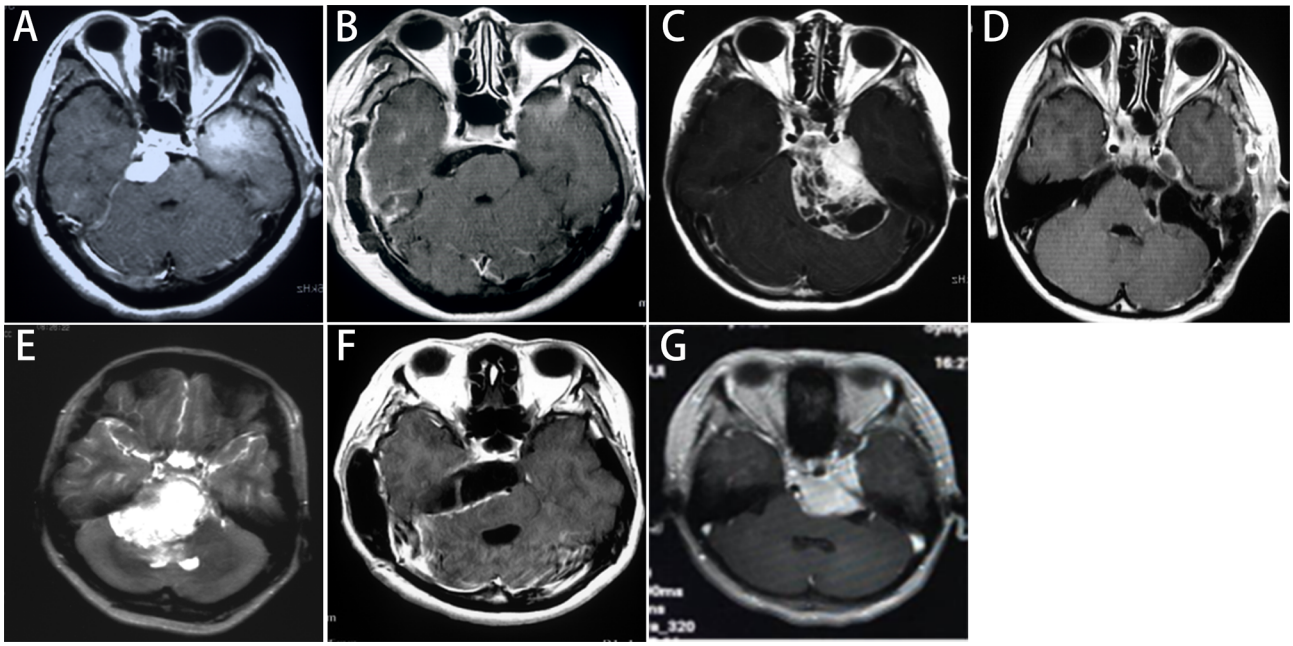

FIGURE 1 | Imaging classification and selection of surgical approaches for PCMs. Petrous apex type: **(A)** The preoperative enhanced MRI shows that the subtemporal transtentorial approach was used; **(B)** The MRI within postoperative 72 hours shows a Simpson grade I resection. Tentorium type: **(C)** The preoperative enhanced MRI shows that the retrosigmoid approach was used; **(D)** The MRI within postoperative 72 hours shows that the tumor invading the posterior wall of the cavernous sinus was removed, yielding a Simpson grade II resection. Upper clivus type: **(E)** The preoperative enhanced MRI shows that the anterior sigmoid approach was used; **(F)** The MRI within postoperative 72 hours shows a Simpson grade II resection. Cavernous type: **(G)** The preoperative enhanced MRI shows that the Kawase approach was used, and a Simpson grade III resection was achieved.

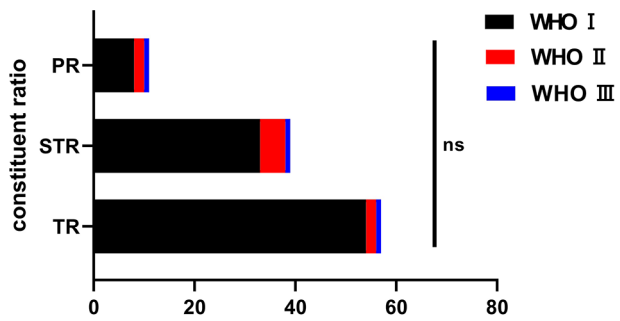

FIGURE 2 | The pathological classification among the groups and the resection degree. ns, no significance.

tumor resection, the progression or recurrence rate was 72.7% (8 of 11 patients) in the partial resection group, 28.2% (11 of 39 cases) in the subtotal resection group, and 7% (4 of 57 patients) in the total resection group. This was statistically significant among groups ($P<0.05$, **Figure 4**). According to the pathological subtypes, the progression or recurrence rate was 15.8% (15/95 cases), 55.6% (5/9 patients) and 100% in the WHO grade I, II and III group, respectively. This was statistically significant when WHO grade I compared with WHO grade II and III ($P<0.05$, **Figure 5**).

DISCUSSION

PCMs usually adjoin the brainstem and cranial nerves. Although the surgical techniques have been greatly improved in recent years, the total resection rate of PCMs remains low (approximately 30-70%), and the incidence of postoperative complications is approximately 20-30% (11). Hence surgical management is still one of the most challenging problems for skull base neurosurgeons (12–15), and the selection of surgical approaches for PCMs has become a hot topic (3, 16, 17). According to the experience of the investigators, petrous apex type PCMs are often located above the trigeminal nerve, which is often displaced by the tumor. Therefore, STA gives priority to surgeons to cut off the tumor base and effectively reduces bleeding. In the study, a total of 17 patients (11 cases of petrous apex type and 6 cases of tentorial type) underwent surgical resection *via* the STA. It was found that this approach could facilitate the exposure and complete removal of small-to-medium petrous apex type and tentorial type PCMs. Cavernous type PCMs often invade the middle and posterior fossa in a dumbbell-like fashion. The KA can help anteriorly reach the anterior clinoid process (18) and posteriorly reach the plane of the IAC, completely expose the lateral wall of the cavernous sinus, which facilitates the gross total resection. In the present study, a total of 22 cases (13 cases of cavernous type, 5 cases of petrous apex type, and 4 cases of upper clivus type) were treated

TABLE 3 | Dysfunctions of the cranial nerves.

Cranial nerve	Preoperation	2 weeks after operation				Follow-up
		Unchanged	Aggravated	New-onset	Improved	
III	9	4	1	1	4	5
IV	4	1	2	3	1	3
V	61	17	2	2	42	11
VI	12	6	1	1	5	5
VII	11	3	5	4	3	6
VIII	28	13	3	2	12	15
IX-XII	19	7	1	1	11	2
Sum	144	51	15	14	78	47

Sum, summation.

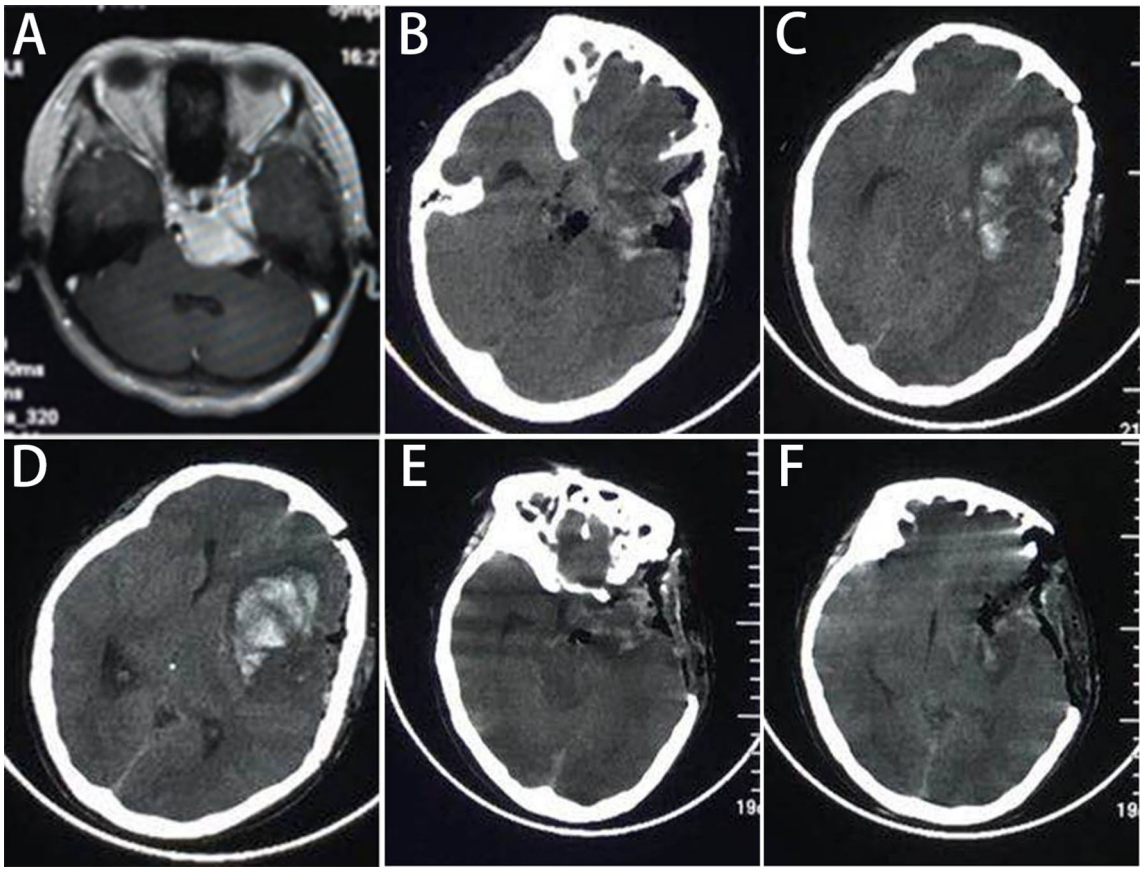

FIGURE 3 | The one patient who had postoperative hematoma and needed second operation. **(A)** The MR scan shows the cavernous type PCMs, and **(B–D)** the CT at 6h postoperatively show a hematoma in the frontal lobe with midline displacement. **(E, F)** The postoperative CT shows that the hematoma was evacuated.

with the KA. The investigators consider the KA to be suitable for the majority of PCMs, especially the cavernous type tumors that straddle the middle and posterior fossa. Upper clivus type PCMs often invade across the midline of the clivus, and the ASA can reduce the traction of the brainstem (19). In this study, a total of 34 patients (21 patients with upper clivus type PCM and 13 patients with tentorium type PCM) were treated with the ASA. The ASA is preferred for large tumors, especially those involving the lateral part of the IAC and midline of the clivus (20). For tentorium type PCMs, the tumor base is located at the tentorium, and the tumor often grows into the posterior cranial fossa. When the tumor was large to giant, surgical exposure *via* the STA is limited, whereas the RSA can serve the tumor exposure. In addition, through the RSA, the separation of the tumor from the trigeminal nerve and acoustic and facial nerve was under direct vision, which can effectively reduce the incidence of postoperative complications. Moreover, the tentorium can be incised and the tumor that invades the posterior wall of the cavernous sinus can

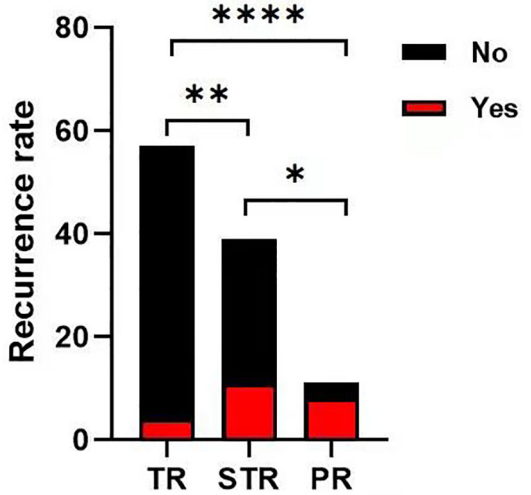

FIGURE 4 | The progression or recurrence rate among the groups. The progression or recurrence rate was 72.7% (8 of 11 cases) in PR group, 28.2% (11 of 39 cases) in STR group, 7% (4 of 57 cases) in TR group, respectively. The differences were statistically significant between each two groups (Chi-square test, *p < 0.05 **p < 0.01, ****p < 0.0001).

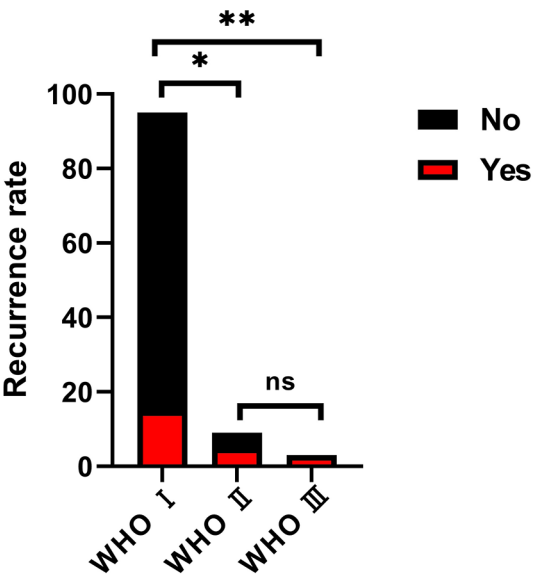

FIGURE 5 | The progression or recurrence rate among groups on the basis of the pathological classification. the progression or recurrence rate was 15.8% (15/95 cases), 55.6% (5/9 patients) and 100% in the WHO grade I, II and III group, respectively. This was statistically significant when WHO grade I compared with WHO grade II (Chi-square test, *p < 0.05) and III (Chi-square test, **p < 0.05), but no significance between grade II and grade III. (Chi-square test, ns, no significance).

also be well-exposed. A total of 31 cases (19 cases of tentorium type, 7 cases of upper clivus type, and 5 cases of cavernous type) were treated using the RSA.

In addition, the selection of a specific surgical approach should be based on the location of the tumor base, tumor size, degree of invasion, and surgeon's familiarity with the approach. If the tumor extensively involved the cavernous sinus and midline of the clivus, the combined posterior and anterior petrosal approach should be applied. In our study, two patients were treated with this combined approach. Additionally, one patient underwent the Fisch A-type approach due to the tumor invasion into the infratemporal fossa. Moreover, preoperative assessment of the venous anatomy for surgical planning is also essential (21, 22). We recommend that all patients with PCMs should have MRV or CTV imaging, or/and DSA when it is necessary, before surgery. For example, if the preoperative results show that the Labbé vein flows into the superior petrosal sinus or the patient have a high jugular bulb, the lateral skull base approach (such as ASA) should be avoided prudently. If the tumor invades the middle and posterior fossa, the modified ASA approach is used to protect the superior petrosal sinus (23, 24). Likewise, if the Labbé vein drains into the transverse sinus at the anterior part of the temporal lobe, the STA or KA approach is restricted. If the tumor is small and slightly invades the cavernous sinus, we can also use STA or KA. In order to avoid damage to the Labbé vein, we often use mannitol or implant the lumbar cistern drainage to lower intracranial pressure. In the meantime, according to the situation of the Labbé vein during the operation, sharp separation or the removal of part of temporal lobe can be adopted to increase its mobility.

In this study, total or subtotal resection was achieved in 96 cases (89.7%). For petrous apex type PCMs, 16 cases (100%) had total resection. For upper clivus type PCMs, total resection was achieved in 26 cases (76.5%). For tentorium type PCMs, 15 cases achieved total resection, and 23 cases (60.5%) subtotal resection. Cavernous type PCMs was characterized as the tight adhesion between the tumor and adjacent nerves and vessels in the cavernous sinus. Ten cases (52.6%) were achieved subtotal resection and 9 cases (47.4%) merely partial resection.

Another difficulty in the surgical management of PCMs is the intraoperative protection of cranial nerves (25, 26). A most frequent complication for any skull base approach is the ever-present risk of the injury to the CNs. According to the literature, the incidence of cranial nerve dysfunction after surgery is 20-100% (27–29). In this study, preoperative cranial nerve dysfunction mainly involved the III-IX cranial nerves. The incidence of new-onset and aggravated cranial nerve dysfunction were 13.1% (14/107) and 10.4% (15/144), respectively. Most neurological disorders were improved during the follow-up. For intraoperative neurological protection, the experience of the investigators was as follows: (1) The trigeminal nerve is located below the superior petrosal sinus, thus the cauterization of superior petrosal sinus should be given with more attention. The trochlear nerve is often located in the medial of the tumor, and the facial nerve and vestibular nerve are located on the lower lateral side of the tumor, the separation of them from the tumor should along the arachnoid membrane interface hence. (2) If the cranial nerves were tightly enclosed, such as III-VI nerves in cavernous type PCMs, the cranial nerve dysfunction is usually aggravated postoperatively. Therefore, the goal of surgery has

been transferred from the total resection to maximum preservation, since preserving neurological functions is pivotal to improve postoperative quality of life. Thus, we recommend incomplete resection followed by adjuvant radiotherapy for this type PCMs (3). Serviceable hearing preservation is also very important. The hearing protection during tumor resection is mainly the protection of the auditory nerve. The same as for vestibular schwannomas, the translabyrinthine approach (labyrinthectomy) sacrifices hearing to achieve greater exposure and total resection, whereas the middle fossa approach (such as STA and KA) and retrosigmoid approach offer the possibility of hearing preservation (30). This highly influences the choice of surgical approaches: if PCM patients have practical hearing before surgery, the trans-middle cranial fossa approaches and retrosigmoid sinus approach can be used; if the patient does not have practical hearing before surgery, the translabyrinthine approach may be considered based on the tumor location. However, for PCMs, patients often suffer from cranial nerve dysfunction in CN V and posterior group cranial nerves; the vestibulocochlear nerve complex often located caudally, making it a crucial maneuver to keep an intact arachnoid plane between the tumor and the surrounding structures. Under the protection of electrophysiological testing, the in-capsule tumor decompression should be implemented, and then the sharp separation between the residual envelope from the surrounding structures upon the arachnoid interface. The complete arachnoid interface must be ensured, so that the maximum tumor resection and hearing preservation can be achieved. In this study, most patients with preoperative hearing impairment had an improvement significantly at follow-up. Therefore, we claim that meticulous techniques and the knowledge of microsurgical anatomy shall lead to feasible hearing preservation with maximum tumor removal under contemporary circumstances.

With respect to the other postoperative complications, there were 14 cases suffering intracranial infection, 9 cases had cerebrospinal fluid leakage, and 3 cases with postoperative hematoma (1 case needed second operation). And there were two deaths because of pneumonia and multiple organ failure after postoperative hematoma. It is clear that modern cranial base techniques and resection skills can significantly reduce the complications. Despite transient neurological deterioration that may occurred during early postoperative periods after total resection. In this group, the incidence of new-onset and aggravated cranial nerve dysfunction were 13.1% (14/107) and 10.4% (15/144), respectively. Though the mean preoperative and postoperative KPS scores were 80 (range 60-100 points) and 78.6 (range 0-100 points) respectively, this was not statistically significant (t=-0.102, P=0.922). Furthermore, at their most recent follow-up, 57 cases (53.3%) were stable with no worsened KPS, 36 cases (33.6%) had improved, only 14 patients (13.1%) had aggravated KPS score. In addition, the progression or recurrence rate was statistically significant among TR, STR and PR groups (P<0.05) and there was no statistically significance between the WHO grade and degree of tumor resection (P<0.05). Thus, we suggest total resection appears to be advantageous for various skull base approaches on PCMs. This is consistent with Almefty et al. (1) who concluded that multiple skull base approaches to PCMs not only facilitate an improved chance of total resection, but also decrease the risk of morbidity. In our study, there was a statistically significance of the progression or recurrence rate when WHO grade I compared with WHO grade II and III, but it was insignificant between WHO grade II and III, which might be due to the invasive nature of grade II and III tumors, or simply the bias caused by the small amount of the two groups and the shortness of follow-up time.

CONCLUSIONS

In conclusion, resection of PCMs remains a challenge. The optimal surgical approach depends on the size, extension of the tumor and the anatomical relationship between the tumor and the cranial nerves. RSA and petrosal approaches were the most commonly used. With elaborate surgical plans and advanced microsurgical skills, most patients with PCMs can be rendered tumor resection with satisfactory extent and functional preservation, despite transient neurological deterioration during early postoperative periods.

DATA AVAILABILITY STATEMENT

The original contributions presented in the study are included in the article/supplementary material. Further inquiries can be directed to the corresponding authors.

ETHICS STATEMENT

The studies involving human participants were reviewed and approved by the Ethics Committee of the First People's Hospital of Yunnan Province. The patients/participants provided their written informed consent to participate in this study.

AUTHOR CONTRIBUTIONS

BG initiated the study and wrote the manuscript. YZ and JT collected the data. JO, BT, and XC analyzed the data. TL and SH coordinated the study and revised the article. All authors contributed to the article and approved the submitted version.

FUNDING

This work was supported by National Natural Science Foundation of China (Grant NO. 82001278), The Fund for Young Doctors with the First People's Hospital of Yunnan Province (Grant NO. KHBS-2020-014), Yunnan Fundamental Research Projects (Grant NO. 202101AU070106), and Joint Projects of Yunnan Provincial Science and Technology Department and Kunming Medical University for Applied Basic Research (Grant NO. 202101AY070001-252).

REFERENCES

1. Almefty R, Dunn IF, Pravdenkova S, Abolfotoh M, Al-Mefty O. True Petroclival Meningiomas: Results of Surgical Management. *J Neurosurg* (2014) 120(1):40–51. doi: 10.3171/2013.8.JNS13535
2. Bhattacharya RN. Large-To-Giant Petroclival Meningiomas: The Additional Features in Management. *Neurol India* (2018) 66(5):1314–5. doi: 10.4103/0028-3886.241381
3. Kim JW, Jung HW, Kim YH, Park CK, Chung HT, Paek SH, et al. Petroclival Meningiomas: Long-Term Outcomes of Multimodal Treatments and Management Strategies Based on 30 Years of Experience at a Single Institution. *J Neurosurg* (2019) 132(6):1675–82. doi: 10.3171/2019.2.JNS182604
4. Shibao S, Borghei-Razavi H, Orii M, Yoshida K. Anterior Transpetrosal Approach Combined With Partial Posterior Petrosectomy for Petroclival Meningiomas With Posterior Extension. *World Neurosurg* (2015) 84(2):574–9. doi: 10.1016/j.wneu.2015.03.055
5. Steiger HJ. Surgical Management of Medium and Large Petroclival Meningiomas: Benchmark and Limits. *Acta Neurochir (Wien)* (2016) 158 (3):407–8. doi: 10.1007/s00701-015-2686-z
6. Lin Y, Gao Q, Jin H, Wang N, Xu D, Wang F, et al. Analysis of Approaches in the Microsurgical Treatment of 102 Cases of Petroclival Meningioma in a Single Center. *Front Neurol* (2021) 12:627736. doi: 10.3389/fneur.2021.627736
7. Kawase T. Advantages and Disadvantages of Surgical Approaches to Petroclival Lesions. *World Neurosurg* (2011) 75(3-4):421. doi: 10.1016/j.wneu.2010.12.045
8. Kawase T, Shiobara R, Ohira T, Toya S. Developmental Patterns and Characteristic Symptoms of Petroclival Meningiomas. *Neurol Med Chir (Tokyo)* (1996) 36(1):1–6. doi: 10.2176/nmc.36.1
9. Ichimura S, Kawase T, Onozuka S, Yoshida K, Ohira T. Four Subtypes of Petroclival Meningiomas: Differences in Symptoms and Operative Findings Using the Anterior Transpetrosal Approach. *Acta Neurochir (Wien)* (2008) 150(7):637–45. doi: 10.1007/s00701-008-1586-x
10. Sekhar LN, Schramm VLJr, Jones NF. Subtemporal-Preauricular Infratemporal Fossa Approach to Large Lateral and Posterior Cranial Base Neoplasms. *J Neurosurg* (1987) 67(4):488–99. doi: 10.3171/jns.1987.67.4.0488
11. Natarajan SK, Sekhar LN, Schessel D, Morita A. Petroclival Meningiomas: Multimodality Treatment and Outcomes at Long-Term Follow-Up. *Neurosurgery* (2007) 60(6):965–79; discussion 979-81. doi: 10.1227/01.NEU.0000255472.52882.D6
12. Li D, Hao SY, Wang L, Tang J, Xiao XR, Jia GJ, et al. Recurrent Petroclival Meningiomas: Clinical Characteristics, Management, and Outcomes. *Neurosurg Rev* (2015) 38(1):71–86; discussion 86-7. doi: 10.1007/s10143-014-0575-1
13. Li D, Hao SY, Wang L, Tang J, Xiao XR, Zhou H, et al. Surgical Management and Outcomes of Petroclival Meningiomas: A Single-Center Case Series of 259 Patients. *Acta Neurochir (Wien)* (2013) 155(8):1367–83. doi: 10.1007/s00701-013-1795-9
14. Li D, Tang J, Ren C, Wu Z, Zhang LW, Zhang JT. Surgical Management of Medium and Large Petroclival Meningiomas: A Single Institution's Experience of 199 Cases With Long-Term Follow-Up. *Acta Neurochir (Wien)* (2016) 158 (3):409–25; discussion 425. doi: 10.1007/s00701-015-2671-6
15. Li P, Yang Z, Wang Z, Zhou Q, Li S, Wang X, et al. Clinical Features of Clear Cell Meningioma: A Retrospective Study of 36 Cases Among 10,529 Patients in a Single Institution. *Acta Neurochir (Wien)* (2016) 158(1):67–76. doi: 10.1007/s00701-015-2635-x
16. Bambakidis NC, Kakarla UK, Kim LJ, Nakaji P, Porter RW, Daspit CP, et al. Evolution of Surgical Approaches in the Treatment of Petroclival Meningiomas: A Retrospective Review. *Neurosurgery* (2008) 62(6 Suppl 3):1182–91. doi: 10.1227/01.NEU.0000333784.04435.65
17. Borghei-Razavi H, Tomio R, Fereshtehnejad SM, Shibao S, Schick U, Toda M, et al. Anterior Petrosal Approach: The Safety of Kawase Triangle as an Anatomical Landmark for Anterior Petrosectomy in Petroclival Meningiomas. *Clin Neurol Neurosurg* (2015) 139:282–7. doi: 10.1016/j.clineuro.2015.10.032
18. Altieri R, Sameshima T, Pacca P, Crobeddu E, Garbossa D, Ducati A, et al. Detailed Anatomy Knowledge: First Step to Approach Petroclival Meningiomas Through the Petrous Apex. *Anat Lab Experience Surg series Neurosurg Rev* (2017) 40(2):231–9. doi: 10.1007/s10143-016-0754-3
19. Calbucci F. Treatment Strategy for Sphenopetroclival Meningiomas. *World Neurosurg* (2011) 75(3-4):419–20. doi: 10.1016/j.wneu.2010.12.033
20. Morisako H, Goto T, Ohata K. Petroclival Meningiomas Resected *via* a Combined Transpetrosal Approach: Surgical Outcomes in 60 Cases and a New Scoring System for Clinical Evaluation. *J Neurosurg* (2015) 122(2):373–80. doi: 10.3171/2014.8.JNS132406
21. Wayhs SY, Lepski GA, Frighetto L, Isolan GR. Petroclival Meningiomas: Remaining Controversies in Light of Minimally Invasive Approaches. *Clin Neurol Neurosurg* (2017) 152:68–75. doi: 10.1016/j.clineuro.2016.11.021
22. Isolan GR, Wayhs SY, Lepski GA, Dini LI, Lavinsky J. Petroclival Meningiomas: Factors Determining the Choice of Approach. *J Neurol Surg B Skull Base* (2018) 79:367–78. doi: 10.1055/s-0037-1608654
23. Almefty KK, Al-Mefty O. Petrosal Approach With Preservation of the Superior Petrosal Sinus (the Graceful Petrosal) for Resection of Giant Trigeminal Schwannoma: 2-Dimensional Operative Video. *Oper Neurosurg (Hagerstown)* (2021) 20:E342–342E343. doi: 10.1093/ons/opaa427
24. Hafez A, Nader R, Al-Mefty O. Preservation of the Superior Petrosal Sinus During the Petrosal Approach. *J Neurosurg* (2011) 114:1294–8. doi: 10.3171/2010.6.JNS091461
25. Maurer AJ, Safavi-Abbasi S, Cheema AA, Glenn CA, Sughrue ME. Management of Petroclival Meningiomas: A Review of the Development of Current Therapy. *J Neurol Surg B Skull Base* (2014) 75(5):358–67. doi: 10.1055/s-0034-1373657
26. Beniwal M, Bhat DI, Rao N, Bhagavatula ID, Somanna S. Surgical Management of Petroclival Meningiomas: Factors Affecting Early Post-Operative Outcome. *Br J Neurosurg* (2015) 29(4):559–64. doi: 10.3109/02688697.2015.1019422
27. Couldwell WT, Fukushima T, Giannotta SL, Weiss MH. Petroclival Meningiomas: Surgical Experience in 109 Cases. *J Neurosurg* (1996) 84 (1):20–8. doi: 10.3171/jns.1996.84.1.0020
28. Little KM, Friedman AH, Sampson JH, Wanibuchi M, Fukushima T. Surgical Management of Petroclival Meningiomas: Defining Resection Goals Based on Risk of Neurological Morbidity and Tumor Recurrence Rates in 137 Patients. *Neurosurgery* (2005) 56(3):546–59. doi: 10.1227/01.NEU.0000153906.12640.62
29. Seifert V. Clinical Management of Petroclival Meningiomas and the Eternal Quest for Preservation of Quality of Life: Personal Experiences Over a Period of 20 Years. *Acta Neurochir (Wien)* (2010) 152(7):1099–116. doi: 10.1007/s00701-010-0633-6
30. Raheja A, Bowers CA, MacDonald JD, Shelton C, Gurgel RK, Brimley C, et al. Middle Fossa Approach for Vestibular Schwannoma: Good Hearing and Facial Nerve Outcomes With Low Morbidity. *World Neurosurg* (2016) 92:37–46. doi: 10.1016/j.wneu.2016.04.085

Conflict of Interest: The authors declare that the research was conducted in the absence of any commercial or financial relationships that could be construed as a potential conflict of interest.

Publisher's Note: All claims expressed in this article are solely those of the authors and do not necessarily represent those of their affiliated organizations, or those of the publisher, the editors and the reviewers. Any product that may be evaluated in this article, or claim that may be made by its manufacturer, is not guaranteed or endorsed by the publisher.

Copyright © 2021 Gao, Zhang, Tan, Ouyang, Tai, Cao, Li and Hu. This is an open-access article distributed under the terms of the Creative Commons Attribution License (CC BY). The use, distribution or reproduction in other forums is permitted, provided the original author(s) and the copyright owner(s) are credited and that the original publication in this journal is cited, in accordance with accepted academic practice. No use, distribution or reproduction is permitted which does not comply with these terms.

frontiers in Oncology

ORIGINAL RESEARCH
published: 25 November 2021
doi: 10.3389/fonc.2021.781396

Refined Temporal-to-Frontal Horn Shunt for Treatment of Trapped Temporal Horn After Surgery of Peri- or Intraventricular Tumor: A Case Series Study

Xiaohui Ren[1,2], *Yong Cui*[1], *Chuanwei Yang*[1], *Zhongli Jiang*[1], *Song Lin*[1,2*†] *and Zhiqin Lin*[1,3*†]

[1] Department of Neurosurgery, Beijing Tiantan Hospital, Capital Medical University, Beijing, China, [2] Beijing Neurosurgical Institute, Capital Medical University, Beijing, China, [3] Department of Neurosurgery, Longyan First Affiliated Hospital of Fujian Medical University, Fujian, China

OPEN ACCESS

Edited by:
Hailiang Tang,
Fudan University, China

Reviewed by:
Seifollah Gholampour,
University of Chicago, United States
Rahsan Kemerdere,
Cerrahpasa Medical Faculty, Turkey

***Correspondence:**
Zhiqin Lin
linzhiqin007@163.com
Song Lin
linsong2005@126.com

†*These authors have contributed equally to this work and share senior authorship*

Specialty section:
This article was submitted to Neuro-Oncology and Neurosurgical Oncology, a section of the journal Frontiers in Oncology

Received: *22 September 2021*
Accepted: *08 November 2021*
Published: *25 November 2021*

Citation:
Ren X, Cui Y, Yang C, Jiang Z, Lin S and Lin Z (2021) Refined Temporal-to-Frontal Horn Shunt for Treatment of Trapped Temporal Horn After Surgery of Peri- or Intraventricular Tumor: A Case Series Study. Front. Oncol. 11:781396. doi: 10.3389/fonc.2021.781396

Background: Trapped temporal horn (TTH) is a localized hydrocephalus that can be treated with cerebrospinal fluid diversion. Refined temporal-to-frontal horn shunt (RTFHS) through the parieto-occipital approach is rarely reported in the literature and its effectiveness remains unclear. The aim of the present study is to investigate the efficacy and outcome of RTFHS for treatment of TTH.

Materials and Methods: We consecutively enrolled 10 patients who underwent RTFHS for TTH after surgical resection of peri- or intraventricular tumors from February 2018 to March 2021. Clinical, radiological, and follow-up data were collected and analyzed. The most common underlying pathology was meningioma (n=4), followed by central neurocytoma (n=3), thalamic glioblastoma (n=2), and anaplastic ependymoma (n=1).

Results: The mean Karnofsky performance scale (KPS) score and TTH volume at onset were 54.0 ± 15.1 (range 40-80) and 71.3 ± 33.2cm^3 (range 31.7-118.6cm^3), respectively. All patients (10/10, 100.0%) presented with periventricular brain edema (PVBE), while midline shift was observed in 9 patients (9/10, 90.0%). RTFHSs were implanted using valveless shunting catheters. No patients developed acute intracranial hemorrhage or new neurological deficit postoperatively. During the follow-up of 17.2 ± 13.7 months (range 3-39 months), all patients showed clinical and radiological improvement. The mean KPS score at the last follow-up was significantly increased to 88.0 ± 10.3 (range 70-100, p<0.0001). RTFHS resulted in significant complete remission in PVBE and midline shift in 8 (80.0%, p=0.0007) and 9 (100.0%, p=0.0001) patients, respectively. As the postoperative follow-up duration prolonged, the mean TTH volume decreased in a consistent, linear trend (p<0.0001). At last follow-up, the mean TTH volume was significantly reduced to 15.4 ± 11.5 cm^3 (range 5.6-44.1 cm^3, p=0.0003), resulting in a mean relative reduction of 77.2 ± 13.1% compared with the volume of TTH at onset. Over drainage was not

observed during the follow-up. No patient suffered from proximal or distal shunt obstruction or shunt related infection, and the revision rate was 0%.

Conclusion: RTFHS seems to be safe and effective for the treatment of TTH with favorable outcomes. Advantages of this technique could be technically less complex and invasive, cost-effective, avoidance of various intraperitoneal complications, and maintaining a near-physiological CSF pathway.

Keywords: hydrocephalus, trapped temporal horn, surgical treatment, temporal to-frontal horn shunt, outcome, intraventricular tumor

INTRODUCTION

Trapped temporal horn (TTH) can be a complication after surgery of lesion within or adjacent to the lateral ventricular trigone (1–3). The obstruction of trigone outlet with continuous CSF production in a relatively closed fluid space lead to dilatation of the temporal horn (4).

As a localized hydrocephalus, TTH can be managed with CSF shunting to extracranial compartments, most commonly the peritoneal cavity (5). However, the conventional ventriculo-peritoneal shunt (VPS) is not ideal with high revision rates on long-term follow-up (6–12). Temporal-to-frontal horn shunt (TFHS) was firstly reported by Hervey-Jumper et al. in 2010 as a feasible strategy for TTH (2). Shunting the CSF from the temporal horn to the frontal horn could mimic the physiological conditions with the added advantages of avoiding intraperitoneal complications and spread of malignant tumor cells. Nevertheless, the described entry point into the temporal horn through the squamous temporal bone carries the risk of injuring the sylvian veins and the middle cerebral artery and its branches (2, 13). Frazier's point, located 6 cm superior to the inion and 3 cm lateral from the midline, is a safe and established anatomic landmark for placing a frontal catheter through parieto-occipital approach in a VPS. Therefore, penetrating the temporal horn through the Frazier's point could theoretically afford a safer trajectory than through the squamous temporal bone. However, few reports involving this technique are available in the literature and its effectiveness remains unclear.

The freehand technique for frontal catheter insertion is based on fixed anatomical landmarks and does not take individual variation, such as midline shift and distorted ventricle, into consideration. Neuro-navigation has been applied and improved the accuracy of catheter insertion. However, this technique requires more time and resources (14). A patient-tailored approach based on the use of augmented-reality techniques can address this shortcoming. The Sina neurosurgical assist (Sina), a precise and simple Android application in smartphone, has been reported and utilized for intraoperative neurosurgical planning aid (15).

The aim of the present study is to describe the technique of refined temporal-to-frontal horn shunt (RTFHS) through the parieto-occipital approach with assistance of Sina application and report the preliminary experiences on the efficacy and outcome of RTFHS for the treatment of TTH.

Abbreviations: TTH, trapped temporal horn; TFHS, temporal-to-frontal horn shunt; RTFHS, refined temporal-to-frontal horn shunt; VPS, ventriculo-peritoneal shunt; PVBE, periventricular brain edema; KPS, Karnofsky performance scale; CSF, cerebrospinal fluid.

METHODS

Patient Population and Data Collection

We retrospectively analyzed the clinical records of 10 consecutive patients who underwent RTFHS for TTH after surgery of peri- or intraventricular tumors between February 2018 and March 2021 at our institution. Medical records and radiological findings were reviewed. The underlying pathology included meningioma in 4 cases, central neurocytoma in 3 cases, thalamic glioblastoma in 2 cases, and anaplastic ependymoma in 1 case. The neurological status was evaluated with Karnofsky performance scale (KPS). CT and/or MRI were employed for diagnosis of TTH preoperatively and to monitor TTH evolution in the following days. The TTH volume index was calculated according to the formula for the volume of a spheroid: $4/3 \times \pi \times (\text{length}/2) \times (\text{width}/2) \times (\text{height}/2)$. Reduction of the TTH volume, and periventricular brain edema (PVBE) were defined and calculated as reported in the previous study (5). This study was approved by the Research Ethics Board of Beijing Tiantan Hospital, Capital Medical University. Written informed consent was obtained from all patients.

Surgical Procedure

Schematic diagram of RTFHS technique is illustrated in **Figure 1**. The patient position, skin incision, and catheter localization are shown in **Figure 2**. The patient is placed in the supine position with head turned opposite the side of the affected temporal horn. The head should be rotated 60° to 70°, as is illustrated in **Figure 2A** (superior view), 2B (rostral view), and 2C (left view). The key anatomic landmarks for placing a frontal and temporal catheter include the medial canthus, the tragus, and the zygomatic process. Two burr holes are created. The proximal catheter (Medtronic, Inc., Minneapolis, Minnesota) is placed in the temporal horn from a parieto-occipital approach (Frazier's point, located 3 cm lateral from the midline and 6 cm superior to the inion) and the target point is the zygomatic process of the ipsilateral face (white arrow in **Figure 2A**). Then, the catheter passes the planned trajectory with a depth of approximately 10.5 cm as measured from the level of the dura. The catheter tip rests near the front wall of temporal horn, away from the rich choroid plexus of trigone. The distal catheter is

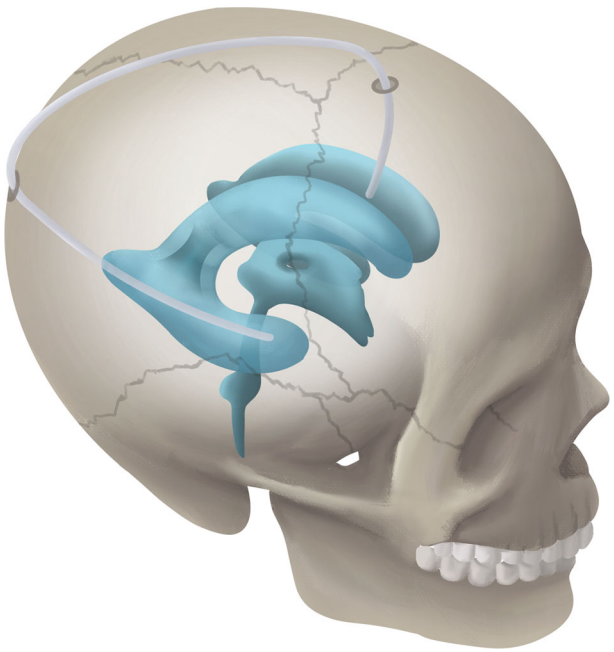

FIGURE 1 | Schematic diagram showing the RTFHS technique, shunting CSF from temporal horn to frontal horn.

inserted into the frontal horn through an usual frontal approach (Kocher's point, located 2.5 cm anterior to the coronal suture and 2.5 cm lateral from the midline). The trajectory is toward the medial canthus of the ipsilateral eye on the coronal plane and a point 1 cm anterior to the tragus on the sagittal plane. The catheter advances for a depth of 5 cm and lies in front of the foramen of Monro. A middle skin incision (white arrow in **Figure 2B**) was made for subcutaneous connection of the proximal and distal catheters by a straight connector without a programmable anti-siphon valve. The ideal catheter tip localization in the frontal and temporal horn were showed in **Figures 2F, G**, respectively. The orientation of catheter in the temporal horn was shown in **Figure 2H**.

In some cases, the TTH may presents as giant mass (**Figure 2D**), leading to severe PVBE and midline shift (**Figure 2E**). The displaced, distorted, and small frontal horn makes it difficult to place a frontal catheter through a freehand technique. Then, the Sina neurosurgical assist (Sina) application was introduced to provide guidance and continuous monitoring during insertion of the frontal catheter. The Sina application was used according to the method described by Eftekhar B (15). Briefly, the appropriate axial and coronary CT or MRI slices are selected at the level of the foramen of Monro. Photographs of these images are taken in portrait mode. With the application assist, the orientation of the puncture was marked with electrode stickers (**Figure 2A**). The unscrubbed assistant overlaps the

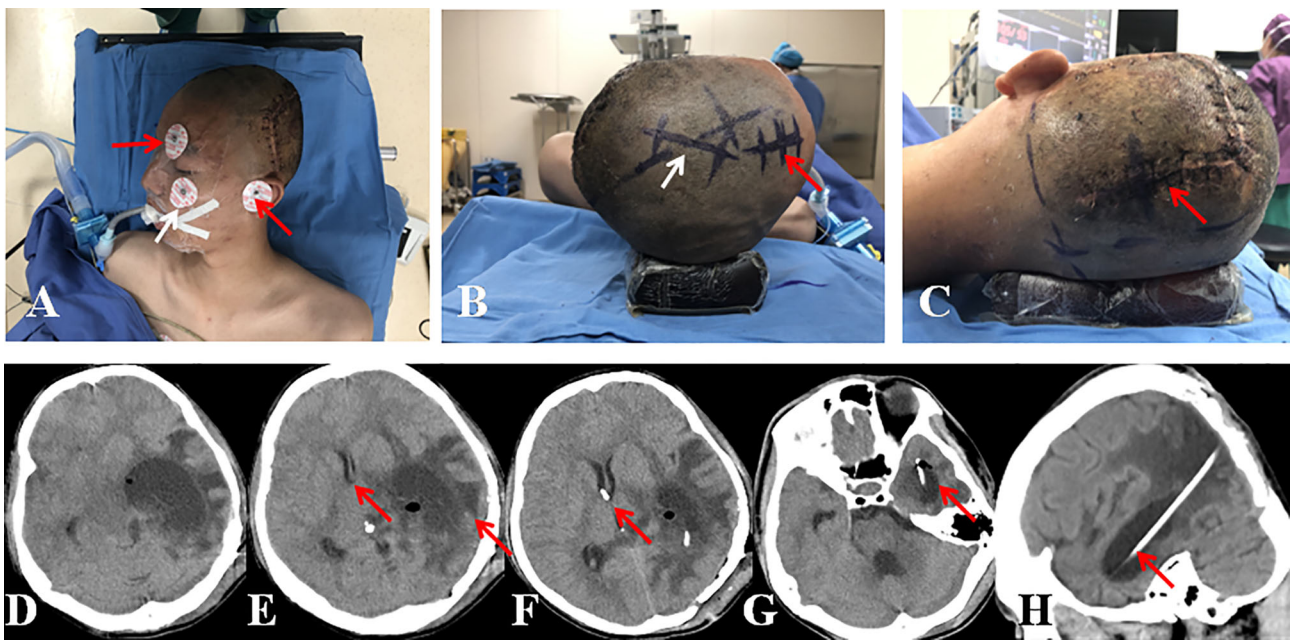

FIGURE 2 | **(A)** Patient position in superior view (red arrow, landmarks of medial canthus and tragus; white arrow, landmark of zygomatic process). **(B)** Patient position in rostral view (red arrow, skin incision for frontal burr hole; white arrow, skin incision for subcutaneous connection of the temporal and frontal catheters). **(C)** Patient position in left view (red arrow, skin incision for occipito-parietal burr hole). **(D)** CT scan showed severe dilation of the left temporal horn with compression of the brainstem. **(E)** CT scan showed prominent midline shift, PVBE, and displaced frontal horn (red arrows). **(F, G)** CT scan showed the suggested localization of catheter tips in the frontal and temporal horns (red arrows). **(H)**: CT scan showed the trajectory of temporal catheter (red arrow).

coronal radiological image onto the real-time view of the patient's head. The device is held by an assistant who aligns the images and provides information about the relative position of the target and frontal catheter to the surgeon.

Statistical Analysis

The demographics and clinical characteristics were described in terms of means (± SD) and frequencies. Fisher's exact test and Wilcoxon matched-pairs signed ranks test was used to assess the differences of clinical and radiological data between TTH at onset and at last follow-up. The statistical software SPSS 13.0 (SPSS for Windows, version 13.0 [SPSS Inc., Chicago, Illinois]) was used. Probability values were reported as 2 sided, with statistical significance defined as $P<0.05$.

RESULTS

Baseline Characteristics

There were 4 male and 6 female with a mean age of 40.0 ± 22.1 years. The mean time interval from tumor resection to TTH onset was 5.2 ± 6.6 months (range 8 days-19 months). Symptoms of intracranial hypertension was the most common presentation (60.0%). The mean KPS score at onset was 54.0 ± 15.1 (range 40-80). Eight TTHs (80.0%) were located in the left hemisphere and 2 (20.0%) in the right. Moderate and severe PVBE were presented in 3 (30.0%) and 7 (70.0%) patients, respectively. Midline shift was observed in 9 cases (90.0%), and the mean distance of midline shift was 6.2 ± 4.1 mm (range 0-11mm). The mean TTH volume at onset was 71.3 ± 33.2cm^3 (range 31.7-118.6cm^3). The clinical data are summarized in **Table 1**.

Surgical Complications and Outcomes

No patients developed acute intracranial hemorrhage or new neurological deficit postoperatively. During the follow-up of 17.2 ± 13.7 months (range 3-39 months), all patients showed clinical and radiological improvement. The mean KPS score at the last follow-up was 88.0 ± 10.3 (range 70-100). All patients demonstrated immediate and further radiographic resolution after RTFHS (**Figure 3A**). The mean TTH volume at 2 weeks, 3 months, and the last follow-up was 34.5 ± 22.4 cm^3 (range 3.3-73.2 cm^3), 19.8 ± 14.8cm^3 (range 5.6-53.0 cm^3), and 15.4 ± 11.5 cm^3 (range 5.6-44.1 cm^3), respectively (**Figure 3B**). The mean volume reduction at 2 weeks, 3 months, and the last follow-up was 51.4 ± 26.9% (range 18.0-91.9%), 69.6 ± 19.6% (range 40.6-91.4%), and 77.2 ± 13.1% (range 50.6-91.3%), respectively (**Figure 3C**). PVBE complete resolution and return of the midline to a normal position were observed in 8 cases (80.0%, 8/10) and 9 cases (100.0%, 9/9), respectively. Over drainage was not observed during the follow-up. The revision rate was 0%; in no case was a proximal or distal shunt obstruction or shunt related infection encountered.

Differences Between the Preoperative and Postoperative Data

The mean KPS score was significantly increased after RTFHS (54.0 ± 15.1 at onset *vs* 88.0 ± 10.3 at the last follow-up, p=0.0057). Radiologically, RTFHS resulted in a significant complete remission in PVBE (p=0.0007) and midline shift (p=0.0001). In addition, the

TABLE 1 | Baseline characteristics of patients with trapped temporal horn who were treated with refined temporal-to-frontal horn shunt[a].

Case No.	Sex/ age (years)	Underlying pathology	Presentation	PVBE	FU (months)	Midline shift (mm)	TTH volume at onset (cm^3)	Mean volume reduction at 2 weeks (%)	TTH volume at last FU (cm^3)	Mean volume reduction at last FU (%)	KPS before shunt/at last FU
1	M/30	Central neurocytoma	ICH, seizure	severe	39	6	114.6	60.4	14.2	87.6	50/90
2	M/17	Central neurocytoma	Blurred vision	moderate	38	3	68.6	18	9.6	86	70/100
3	F/25	Central neurocytoma	Memory disturbance, right limb weakness	severe	24	8	91.2	72.2	14.5	84.1	60/100
4	F/64	Thalamic glioblastoma	ICH, herniation, aphasia	severe	20	10	84.8	35.2	25	70.5	50/70
5	F/38	Meningioma	Vertigo, memory disturbance	moderate	22	0	34	22.2	9.8	71	70/90
6	M/17	Anaplastic ependymoma	ICH	severe	11	10	118.6	73	10.3	91.4	40/90
7	M/71	Thalamic glioblastoma	ICH, herniation	severe	5	10	40.4	91.9	5.6	86.2	40/70
8	F/16	Meningioma	Memory disturbance	moderate	7	2	89.2	18	44.1	50.6	80/90
9	F/57	Meningioma	ICH, herniation, aphasia, right limb weakness	severe	3	11	31.7	74.8	5.7	82	40/90
10	F/65	Meningioma	ICH, memory disturbance; mental symptoms	severe	3	2	39.9	48	15	62.4	40/90

[a]*TTH, trapped temporal horn; PVBE, periventricular brain edema; FU, follow-up; ICH, intracranial hypertension; KPS, Karnofsky Performance Scale.*

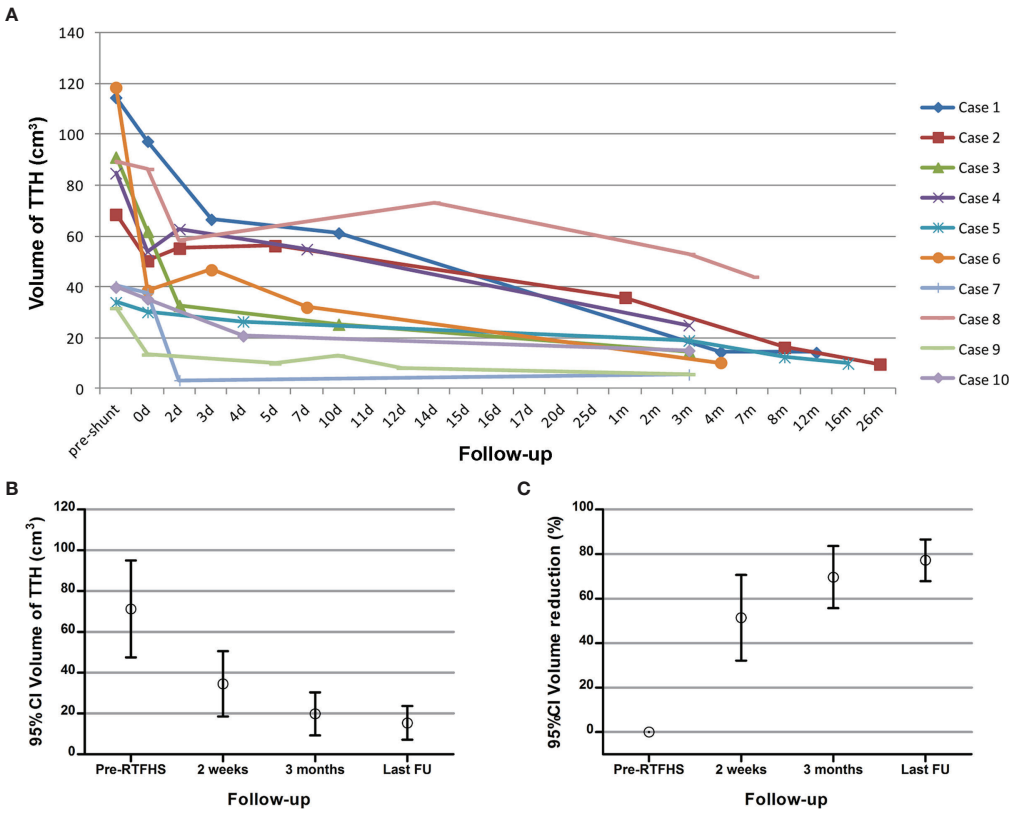

FIGURE 3 | **(A)** The volume curve of the TTH from each patient during the follow-up. **(B, C)** The mean TTH volume and the mean reduction of TTH volume before shunt, at 2 weeks, at 3 months, and at last follow-up.

mean TTH volume at last follow-up was significantly reduced (71.3 ± 33.2cm^3 at onset *vs* 15.4 ± 11.5 cm^3 at last follow-up, p=0.002). As the postoperative follow-up duration prolonged, the mean TTH volume decreased in a consistent, linear trend (**Figure 3B**, p<0.0001).

Illustrative Cases

Case 6

This 17-year-old male underwent craniotomy for resection of anaplastic ependymoma in the left lateral ventricular trigone. Eight days following surgery, he developed symptoms of intracranial hypertension. A CT scan revealed a giant TTH with prominent PVBE and midline shift (**Figures 4A, B**). RTFHS was performed. Postoperatively, the patient's symptoms resolved. A series of CT scan showed gradual resolution of PVBE and immediate and further reduction of TTH volume at the level of midbrain (upper panel) and Foremen of Monro (lower panel) (**Figures 4C–J**). The volume reduction at Days 3, Day 7, and 4 months were 60.8%, 73.0%, and 91.3%, respectively.

DISCUSSION

The Current Difficulties in Treating the TTH

TTH is a rare entity and only a few studies with a limited number of patients have studied the surgical intervention for it. Surgical treatment options are diversely described in the literature, ranging from microsurgery *via* craniotomy to CSF diversion to neuroendoscopic techniques (2, 4, 16–20). To date, the optimal surgical modality is yet to be definitively determined. Some patients might even require multiple operations until the situation is well controlled. Microsurgical fenestration through craniotomy enables to open the scarred trigone and remove the ventricular septation (4, 5). Furthermore, simultaneous choroid plexectomy reduced the production of CSF from the temporal horn. Nevertheless, this technique is traumatic and carry the risk of injury to the surrounding critical structures. Endoscopic fenestration of the choroidal fissure has been described; however, it may sometimes limited by technically challenging, surgeon experience, and unknown long-term patency of the stoma (18, 19). Besides, this technique should takes the individual anatomical variation into account (19). Although VPS remains to be the mainstay of CSF diversion for treatment of TTH, there are risks specific to VPS, including intraperitoneal complications, malfunction, infection, and dependence in the long-term follow-up (1, 21).

The Novelty, Safety, and Feasibility of RTFHS

The efficacy of TFHS have been firstly illustrated by Hervey-Jumper et al. in 2010 as a report of 3 cases (2). They advocated

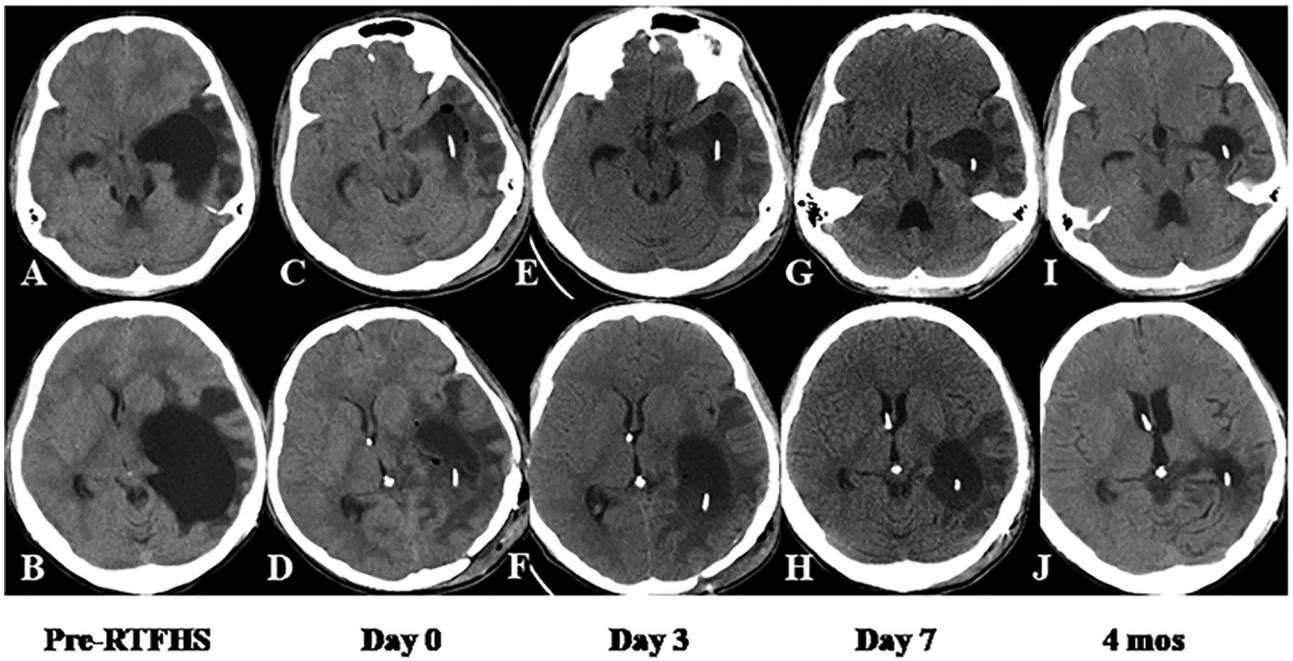

FIGURE 4 | Case 6. CT scan showed immediate and further reduction of TTH volume at the level of midbrain (upper panel) and Foremen of Monro (lower panel). The volume and morphometric changes of TTH were shown before RTFHS **(A, B)**, at Day 0 **(C, D)**, Day 3 **(E, F)**, Day 7 **(G, H)**, and 4 months **(I, J)**.

that this technique could be considered in patients with neurological symptoms resulting from TTH secondary to peri- or intraventricular malignant tumors in which seeding of distant sites by CSF diversion is a concern. With regard to the entry point into the enlarged temporal horn, a bur hole on the squamous temporal bone was suggested in this study (2). However, the described perpendicular or lateral approach harbored the risk of damaging the sylvian veins and the middle cerebral artery and its branches (2). Therefore, the safety and feasibility of TFHS for a greater number of patients are still unclear. In addition, the overshooting catheter might result in injury to the midbrain and even some critical structures in the surrounding cisternal system, such as basilar artery, oculomotor nerve, posterior communicating artery, and anterior choroidal artery (13). Furthermore, it cannot ensure the catheter permanently long enough within the temporal horn, especially for a decompressed TTH following shunt. Frazier's point has been established as a common and safe anatomic landmark for placing a frontal catheter through parieto-occipital approach in VPS. Then, we proposed the RTFHS by penetrating the temporal horn through the Frazier's point. The occipito-parietal approach paved a safe trajectory and enabled the catheter away from the sylvian vessels, midbrain, and some other critical structures. Moreover, a longer shunt path in the temporal horn and keeping the catheter tip away from the rich trigonal choroid plexus prevented catheter displacement and obstruction. No patients experienced acute intracranial hemorrhage or new neurological deficit associated with RTFHS in this case series. These results support the safety of RTFHS.

Another critical stage of RTFHS procedure is the insertion of the distal catheter. In our series, the mean TTH volume at onset was 71.3 ± 33.2cm^3 and more than half of the cases presented with severe PVBE. The giant TTH with brain edema inevitably led to midline shift and displaced ventricle. As such, placing a frontal catheter through a freehand technique can be challenging. Although stereotactic navigation and image guidance ensure a more accurate placement of the ventricular catheter, they impose a longer duration of plan and surgery, require more operating room resources utilization, and increase the patients' health care costs. Then, Sina application, a precise and available software in smartphone, was used as a simple intraoperative neurosurgical planning aid in placement of catheter. We did not experience difficulty in placing a frontal catheter in cases with severe midline shift or distorted ventricle. Sina application-assisted Kocher's point puncture is used to perfectly locate the catheter, taking the place of neuro-navigation. This application not only offers a simple, realistic, and available manner in the placement of shunt, but also demonstrates high degrees of achieved accuracy. In our series, midline shift was observed in 9 cases (90.0%), 4 of which demonstrated a severe degree. Nevertheless, successful penetration of the frontal horn was achieved in all cases and the postoperative imaging confirmed the distal end in position.

The present study included a much larger number of cases treated with TFHS than prior studies. Clinical improvement was achieved immediately after shunt insertion. TTH volume, PVBE, and midline shift were substantially improved at the last follow-up. No patients suffered from proximal or distal shunt obstruction or shunt related infection during the follow-up.

Our experience demonstrates that the refined and modified technique can be a safe, effective, and durable CSF diversionary procedure. Further prospective multicenter study with more cases and extended follow-up will be necessary to validate this technical approach.

Advantages of RTFHS Compared With Conventional VPS

The RTFHS has several advantages over the conventional VPS. First, the shunt system in RTFHS is shorter in length and confined to the skull, which makes the operation technically less complex and invasive and minimizes the risk of mechanical failure and infection. Second, siphoning phenomenon and overdrainage always occur in patients with VPS and have not been eliminated despite with the use of antisiphoning devices (6–9). RTFHS decreases the pressure gradient, avoids shunt siphoning, and prevents overdrainage, maintaining a natural and near-physiological CSF pathway. At the last follow-up, no cases presented with overdrainage in our series. Moreover, without having to use antisiphoning device and programmable valve, RTFHS can also significantly decreases the cost of implant. Third, the peritoneum is the cause for VPS revision in many cases on the long-term follow-up. RTFHS obviates distal catheter occlusion and various intraperitoneal complications. In addition, there are high risks for adhesions and surgical bowel perforation in patients with multiple previous abdominal surgeries or with a previous abdominal shunt infection. RTFHS can be an effective alternative in treating these patients. Finally, in cases of TTH caused by primary peri- or intraventricular malignant tumors, RTFHS prevents spreading malignant tumor cells to distant sites.

El-Shafei et al. (22) pioneered the technique of retrograde ventriculosinus shunt for treatment of hydrocephalus by shunting the CSF to the superior sagittal sinus against the direction of blood flow. A system review by Toma et al. (23) with a total of 265 patients treated with ventriculosinus shunt demonstrated that this technique is safe and feasible, and do not increase the risk of sinus thrombosis, air embolism, uncontrollable intraoperative bleeding, or shunt-associated nephritis. There are several similarities and advantages between the RTFHS and retrograde ventriculosinus shunt since both of them divert CSF back to the intracranial compartment. In our opinion, the temporal horn to sagittal sinus shunt, which is developed and evolved from these two techniques, might be a feasible alternative for treatment of TTH sometimes when a RTFHS is not available. To date, the temporal horn to sagittal sinus shunt has not been reported in the literature. This procedure would be a choice and attempt in selected patients in our future practice.

Limitations

This was a retrospective review of a rare series of TTH cases that was treated by RTFHS. Although the morphometric changes including TTH volume, PVBE, and midline shift were evaluated, there were some important CSF hydrodynamic parameters that were not investigated due to the retrospective nature of the study. These hydrodynamic parameters can help to gain more insight into the pathophysiology of non-communicating hydrocephalus patients. In recent studies, 3D fluid-structure interaction modeling was utilized to examine the correlation between CSF hydrodynamic changes and non-communicating hydrocephalus patients' clinical symptoms before and after shunting (24, 25). The ventricular system volume and maximum CSF pressure were found to be more effective and accurate than the other parameters in evaluating the patients' conditions. Future prospective investigation assessing the hydrodynamic parameters changes of the CSF flow during the treatment process of TTH is warranted. In addition, this series included a small and uncontrolled patient group, which provided limited statistical analysis and comparison between different treatment options. A thorough understanding of the RTFHS technique requires a prospective multicenter study with great number of patients in the future.

CONCLUSION

RTFHS seems to be safe and effective for the treatment of TTH with favorable outcomes. RTFHS might be a potential alternative to traditional VPS for patient with TTH. Advantages of this technique could be technically less complex and invasive, cost-effective, avoidance of various intraperitoneal complications, and maintaining a natural and near-physiological CSF pathway. Multicenter prospective study with a great number of patients is necessary to validate the potential benefits of this technique so that it can be widely recommended.

DATA AVAILABILITY STATEMENT

The original contributions presented in the study are included in the article/supplementary material. Further inquiries can be directed to the corresponding authors.

ETHICS STATEMENT

The studies involving human participants were reviewed and approved by Ethics Committee of Beijing Tiantan Hospital. Written informed consent to participate in this study was provided by the participants' legal guardian/next of kin. Written informed consent was obtained from the individual(s), and minor(s)' legal guardian/next of kin, for the publication of any potentially identifiable images or data included in this article.

AUTHOR CONTRIBUTIONS

XR, SL, and ZL contributed to conception and design of the study. XR organized the database. XR and ZL performed the statistical analysis. XR and ZL drafted the manuscript. XR and ZL wrote sections of the manuscript. All authors contributed to manuscript revision, read, and approved the submitted version.

ACKNOWLEDGMENTS

We would like to give special thanks to Dr Dongxia Liao (Longyan First Hospital, Fujian Medical University) for her assistance in **Figure 1** drawing and manuscript editing.

REFERENCES

1. Lin Z, Zhang X, Shen S, Gao Z, Guan C, Liu T, et al. Postoperative Delayed Trapped Temporal Horn in Patients With Lateral Ventricular Trigone Meningioma: Risk Factors, Surgical Management, and Literature Review. *Eur J Surg Oncol* (2020) 46(12):2324–30. doi: 10.1016/j.ejso.2020.04.033
2. Hervey-Jumper SL, Ziewacz JE, Heth JA, Sullivan SE. Frontal-To-Temporal Horn Shunt as Treatment for Temporal Horn Entrapment. *J Neurosurg* (2010) 112(2):410–3. doi: 10.3171/2009.3.JNS081423
3. Pagani-Estevez GL, Couillard P, Lanzino G, Wijdicks EF, Rabinstein AA. Acutely Trapped Ventricle: Clinical Significance and Benefit From Surgical Decompression. *Neurocrit Care* (2016) 24(1):110–7. doi: 10.1007/s12028-015-0145-6
4. Maurice-Williams RS, Choksey M. Entrapment of the Temporal Horn: A Form of Focal Obstructive Hydrocephalus. *J Neurol Neurosurg Psychiatry* (1986) 49(3):238–42. doi: 10.1136/jnnp.49.3.238
5. Lin Z, Wang C, Gao Z, Li X, Lan F, Liu T, et al. Clinical Characteristics of and Treatment Protocol for Trapped Temporal Horn Following Resection of Lateral Ventricular Trigone Meningioma: A Single-Center Experience. *J Neurosurg* (2019) 132(2):481–90. doi: 10.3171/2018.11.JNS182710
6. Browd SR, Ragel BT, Gottfried ON, Kestle JR. Failure of Cerebrospinal Fluid Shunts: Part I: Obstruction and Mechanical Failure. *Pediatr Neurol* (2006) 34 (2):83–92. doi: 10.1016/j.pediatrneurol.2005.05.020
7. Lo P, Drake JM. Shunt Malfunctions. *Neurosurg Clin N Am* (2001) 12(4):695–701, viii. doi: 10.1016/S1042-3680(18)30026-3
8. Browd SR, Gottfried ON, Ragel BT, Kestle JR. Failure of Cerebrospinal Fluid Shunts: Part II: Overdrainage, Loculation, and Abdominal Complications. *Pediatr Neurol* (2006) 34(3):171–6. doi: 10.1016/j.pediatrneurol.2005.05.021
9. Gupta N, Park J, Solomon C, Kranz DA, Wrensch M, Wu YW. Long-Term Outcomes in Patients With Treated Childhood Hydrocephalus. *J Neurosurg* (2007) 106(5 Suppl):334–9. doi: 10.3171/ped.2007.106.5.334
10. Feletti A, d'Avella D, Wikkelso C, Klinge P, Hellstrom P, Tans J, et al. Ventriculoperitoneal Shunt Complications in the European Idiopathic Normal Pressure Hydrocephalus Multicenter Study. *Oper Neurosurg (Hagerstown)* (2019) 17(1):97–102. doi: 10.1093/ons/opy232
11. Rinaldo L, Bhargav AG, Nesvick CL, Lanzino G, Elder BD. Effect of Fixed-Setting Versus Programmable Valve on Incidence of Shunt Revision After Ventricular Shunting for Idiopathic Normal Pressure Hydrocephalus. *J Neurosurg* (2020) 133(2):564–72. doi: 10.3171/2019.3.JNS183077
12. Anderson IA, Saukila LF, Robins JMW, Akhunbay-Fudge CY, Goodden JR, Tyagi AK, et al. Factors Associated With 30-Day Ventriculoperitoneal Shunt Failure in Pediatric and Adult Patients. *J Neurosurg* (2018) 130(1):145–53. doi: 10.3171/2017.8.JNS17399
13. Bohl MA, Almefty KK, Nakaji P. Defining a Standardized Approach for the Bedside Insertion of Temporal Horn External Ventricular Drains: Procedure Development and Case Series. *Neurosurgery* (2016) 79(2):296–304. doi: 10.1227/NEU.0000000000001164
14. Srinivasan VM, O'Neill BR, Jho D, Whiting DM, Oh MY. The History of External Ventricular Drainage. *J Neurosurg* (2014) 120(1):228–36. doi: 10.3171/2013.6.JNS121577
15. Eftekhar B. App-Assisted External Ventricular Drain Insertion. *J Neurosurg* (2016) 125(3):754–8. doi: 10.3171/2015.6.JNS1588
16. Chen CC, Kasper EM, Zinn PO, Warnke PC. Management of Entrapped Temporal Horn by Temporal Horn to Prepontine Cistern Shunting. *World Neurosurg* (2013) 79(2):404 e7–10. doi: 10.1016/j.wneu.2011.02.025
17. Hana T, Tanaka S, Shin M, Mukasa A, Kugasawa K, Saito N. Neuroendoscopic Ventriculocisternostomy With Stent Placement for Trapped Temporal Horn After the Resection of Glioblastoma. *World Neurosurg* (2015) 84(6):2078.e5–8. doi: 10.1016/j.wneu.2015.08.019
18. Krahenbuhl AK, Baldauf J, Gaab MR, Schroeder HW. Endoscopic Temporal Ventriculocisternostomy: An Option for the Treatment of Trapped Temporal Horns. *J Neurosurg Pediatr* (2013) 11(5):568–74. doi: 10.3171/2013.2.PEDS12417
19. Paredes I, Orduna J, Fustero D, Salgado JA, de Diego JM, de Mesa FG. Endoscopic Temporal Ventriculocisternostomy for the Management of Temporal Horn Entrapment: Report of 4 Cases. *J Neurosurg* (2017) 126 (1):298–303. doi: 10.3171/2016.1.JNS152248
20. Parrent AG. Endoscopically Guided Fenestration of the Choroidal Fissure for Treatment of Trapped Temporal Horn. *J Neurosurg* (2000) 93(5):891–4. doi: 10.3171/jns.2000.93.5.0891
21. Gliemroth J, Kasbeck E, Kehler U. Ventriculocisternostomy Versus Ventriculoperitoneal Shunt in the Treatment of Hydrocephalus: A Retrospective, Long-Term Observational Study. *Clin Neurol Neurosurg* (2014) 122:92–6. doi: 10.1016/j.clineuro.2014.03.022
22. El-Shafei IL, El-Shafei HI. The Retrograde Ventriculosinus Shunt: Concept and Technique for Treatment of Hydrocephalus by Shunting the Cerebrospinal Fluid to the Superior Sagittal Sinus Against the Direction of Blood Flow. Preliminary Report. *Childs Nerv Syst* (2001) 17(8):457–65; discussion 66. doi: 10.1007/s003810100456
23. Toma AK, Tarnaris A, Kitchen ND, Watkins LD. Ventriculosinus Shunt. *Neurosurg Rev* (2010) 33(2):147–52; discussion 53. doi: 10.1007/s10143-010-0242-0
24. Gholampour S. FSI Simulation of CSF Hydrodynamic Changes in a Large Population of Non-Communicating Hydrocephalus Patients During Treatment Process With Regard to Their Clinical Symptoms. *PLoS One* (2018) 13(4):e0196216. doi: 10.1371/journal.pone.0196216
25. Gholampour S, Fatouraee N. Boundary Conditions Investigation to Improve Computer Simulation of Cerebrospinal Fluid Dynamics in Hydrocephalus Patients. *Commun Biol* (2021) 4(1):394. doi: 10.1038/s42003-021-01920-w

Conflict of Interest: The authors declare that the research was conducted in the absence of any commercial or financial relationships that could be construed as a potential conflict of interest.

Publisher's Note: All claims expressed in this article are solely those of the authors and do not necessarily represent those of their affiliated organizations, or those of the publisher, the editors and the reviewers. Any product that may be evaluated in this article, or claim that may be made by its manufacturer, is not guaranteed or endorsed by the publisher.

Copyright © 2021 Ren, Cui, Yang, Jiang, Lin and Lin. This is an open-access article distributed under the terms of the Creative Commons Attribution License (CC BY). The use, distribution or reproduction in other forums is permitted, provided the original author(s) and the copyright owner(s) are credited and that the original publication in this journal is cited, in accordance with accepted academic practice. No use, distribution or reproduction is permitted which does not comply with these terms.

frontiers in Oncology

SYSTEMATIC REVIEW
published: 02 December 2021
doi: 10.3389/fonc.2021.787962

Postoperative Adjuvant Radiotherapy in Atypical Meningioma Patients: A Meta-Analysis Study

Dengpan Song[1†], Dingkang Xu[1†], Hongjie Han[2], Qiang Gao[1], Mingchu Zhang[1], Fang Wang[1], Guoqing Wang[1] and Fuyou Guo[1]*

[1] Department of Neurosurgery, The First Affiliated Hospital of Zhengzhou University, Zhengzhou, China, [2] Department of Neurosurgery, Pingdingshan Second People's Hospital, Pingdingshan, China

Background and Purpose: Consensus regarding the need for adjuvant radiotherapy (RT) in patients with atypical meningiomas (AMs) is lacking. We compared the effects of adjuvant RT after surgery, gross total resection (GTR), and subtotal resection (STR) on progression-free survival (PFS) and overall survival (OS) in patients with AMs, respectively.

Methods: We performed a systematic review and meta-analysis of the literature published in PubMed, Embase, and the Cochrane Library from inception to February 1, 2021, to identify articles comparing the PFS and OS of patients receiving postoperative RT after surgery, GTR and STR.

Results: We identified 2307 unique studies; 24 articles including 3078 patients met the inclusion criteria. The sensitivity analysis results showed that for patients undergoing undifferentiated surgical resection, adjuvant RT reduced tumor recurrence (HR=0.70, p<0.0001) with no significant effect on survival (HR=0.89, p=0.49). Postoperative RT significantly increased PFS (HR=0.69, p=0.01) and OS (HR=0.55, p=0.007) in patients undergoing GTR. The same improvement was observed in patients undergoing STR plus RT (PFS: HR=0.41, p<0.00001; OS: HR=0.47, p=0.01). A subgroup analysis of RT in patients undergoing GTR showed no change in PFS in patients undergoing Simpson grade I and II resection (HR=1.82, p=0.22) but significant improvement in patients undergoing Simpson grade III resection (HR=0.64, p=0.02).

Conclusion: Regardless of whether GTR or STR was performed, postoperative RT improved PFS and OS to varying degrees. Especially for patients undergoing Simpson grade III or IV resection, postoperative RT confers the benefits for recurrence and survival.

Keywords: atypical meningioma, adjuvant radiotherapy, meta-analysis, gross total resection, subtotal resection, progression-free survival, overall survival

OPEN ACCESS

Edited by:
Hailiang Tang,
Fudan University, China

Reviewed by:
Marco Vincenzo Corniola,
Geneva University Hospitals (HUG), Switzerland
Mueez Waqar,
Salford Royal NHS Foundation Trust, United Kingdom
Maria Caffo,
University of Messina, Italy

****Correspondence:***
Fuyou Guo
chyou666@hotmail.com

[†]These authors have contributed equally to this work

Specialty section:
This article was submitted to Neuro-Oncology and Neurosurgical Oncology, a section of the journal Frontiers in Oncology

Received: *01 October 2021*
Accepted: *16 November 2021*
Published: *02 December 2021*

Citation:
Song D, Xu D, Han H, Gao Q, Zhang M, Wang F, Wang G and Guo F (2021) Postoperative Adjuvant Radiotherapy in Atypical Meningioma Patients: A Meta-Analysis Study. Front. Oncol. 11:787962. doi: 10.3389/fonc.2021.787962

INTRODUCTION

Meningiomas are the most common primary tumors of the brain, representing more than one-third of all intracranial tumors (1). According to the most recent WHO definition, meningioma should be classified according to 3 histological grades, with benign meningioma (BM) classified as grade I, atypical meningioma (AM) as grade II, and malignant meningioma (MM) as grade III (2). Atypical

meningiomas (AMs) accounts for about 15-20% of all meningiomas, and associated with a higher risk of recurrence and a worse prognosis than benign meningiomas (3, 4). Maximal safe surgical resection is currently the preferred treatment for atypical meningiomas, but there is no clear consensus on the use of adjuvant radiotherapy (RT) in these patients (5). There are two points to consider, namely, whether adjuvant radiation therapy can significantly improve the patient's prognosis and whether the side effects of adjuvant radiation therapy can offset the benefits (2, 6).

Although the effect of postoperative RT on AMs has been analyzed in many reports, the results were inconsistent. Therefore, it is necessary to perform a meta-analysis to evaluate the efficacy of surgical resection with RT on survival outcomes, including overall survival (OS) and progression-free survival (PFS), in patients suffering from AMs.

METHODS

Search Strategy

We comprehensively searched eligible studies using several electronic databases, including the PubMed, Embase, and Cochrane databases and followed PRISMA guidelines. Search terms included a strategic combination of 'atypical' AND 'meningioma', or 'atypical meningioma' or 'grade II meningioma'. All papers published until February 1, 2021 were included. The titles and abstracts of each article searched were reviewed to exclude any apparently unrelated research. The full texts of the remaining articles were read to determine whether they contained information on the subject under review.

Study Selection

Two investigators independently reviewed each eligible study, with a consensus being reached by the third investigator when there was a disagreement between the two investigators. Articles that satisfied the following criteria were included: (1) cohort studies or randomized controlled trials, (2) patients with atypical meningioma verified by pathology, (3) studies that investigated different treatment modalities, including GTR and STR plus RT, and (4) OS and/or PFS data that were provided or allowed for the calculation of hazard ratios (HRs) with corresponding 95% confidence intervals (CIs). Studies were excluded based on any of the following criteria: (1) reviews, letters, case reports, and database-based studies; (2) studies with a sample size of less than 20; (3) non-English studies, studies with duplicate data; and (4) studies that lacked key information for calculation. The definitions of GTR and STR were based on the description in the original article. In general, GTR was defined as a Simpson Grade I or II tumor resection, or Simpson Grade I, II or III tumor resection, and STR was defined as a Simpson Grade IV tumor resection. In addition, to further clarify the potential impact of GTR plus RT on AM under real-world conditions, a subgroup analysis of the GTR group was performed according to Simpson's classification. Radiotherapy was considered to include both conventional radiotherapy and stereotactic radiosurgery (SRS).

Quality Assessment

Two investigators independently assessed the quality of each eligible study using the Newcastle-Ottawa Scale (7). Three aspects were generally assessed: population selection, study comparability, and reporting of the outcome, with a score ranging from 0 to 9. Studies with a score greater than six were considered to be of high quality.

Statistical Analysis

All the comparisons were based on data from cohort studies. The endpoints of interest in the analyses were OS and PFS. A hazard ratio (HR) with a 95% CI was used to evaluate the association of postoperative radiotherapy. The lnHRs were considered to obey a normal distribution. We extracted the HRs and corresponding 95% CIs of the multivariate analysis explicitly given in these articles; otherwise, the HRs and 95% CIs of the univariate analysis were utilized. If the above value was not provided in the paper, the Kaplan-Meier survival curve in the paper was used to transform the Figure into a data sheet and used the log rank test to obtain the lnHR, 95% CI and SE (8). The I^2 statistic and Cochrane Q test were used to analyze between-study heterogeneity (9). Data analyses were performed using Review Manager software version 5.3 (The Cochrane Collaboration Oxford, United Kingdom). When $I^2 < 50\%$ or a P value > 0.10 was identified, indicating homogeneity among studies, we used the fixed-effects model; otherwise, a random-effects model was adopted. Publication bias was determined using the funnel graph. We performed a sensitivity analysis by omitting each study in turn. A P value of <0.05 indicated a statistically significant difference.

RESULTS

Literature Selection, Quality Evaluation, and Demographics

The process of literature screening based on the inclusion and exclusion criteria is depicted in **Figure 1**. The initial search yielded 2307 results. Of these, 775 studies were excluded because they were duplicates. After scanning the titles and abstracts, 85 studies were retained for further analysis. Finally, after a full-text screening, a total of 24 were eligible for inclusion in the meta-analysis. The quality of 24 comparative studies with a total of 3078 patients is summarized in **Supplementary Table 1**, and the results of our systematic analysis of patients with AMs undergoing postoperative RT are detailed in **Table 1**. The mean age was 57.17 years, and the male to female ratio was 1:1.26. The mean RT dose was 56.42 Gy and mean follow-up was 55.7 months.

Results of the Meta-Analysis

Meta-Analysis of PFS and OS Between Surgery+RT and Surgery

In the analysis of PFS and OS in atypical meningioma patients treated with surgery and RT or surgery alone, 19 and 7 studies were included, respectively, and the results are shown in

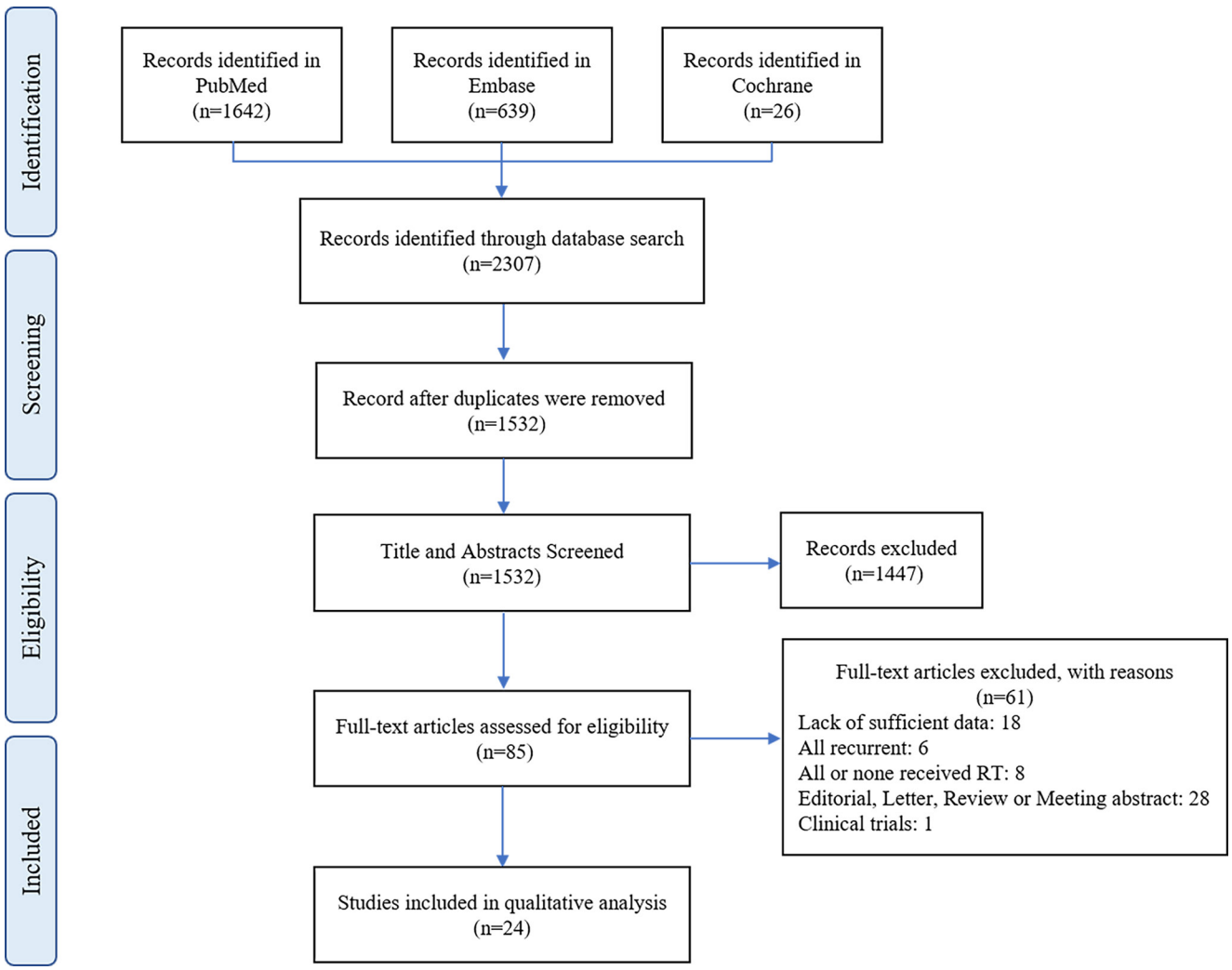

FIGURE 1 | The flow diagram of the selection process as per PRISMA.

Figure 2. For PFS, the P value of the Q statistic and the Higgins I^2 statistic for heterogeneity were 0.00001 and 87%, respectively. Similarly, for OS, the P value and I^2 were 0.004 and 68%, respectively. This result indicated that both studies were heterogeneous, so we applied a random-effects model. Benefits of RT were found in both the PFS and OS analyses (PFS: HR = 0.71, 95% CI: 0.47-1.08, P = 0.11, and OS: HR = 0.52, 95% CI: 0.27-1.00, P = 0.05). The publication bias of the PFS and OS analyses is shown as a funnel graph in **Figure 3**. The results show that both of them have significant publication bias. A significant improvement in publication bias was observed after 6 and 2 articles were removed by the sensitivity analysis (**Figure 4**). The Higgins I^2 statistics for heterogeneity were 18% (p = 0.26) and 0% (p = 0.53), respectively, which indicates that the remaining studies are homogeneous. Thus, the fixed-effect model is used to present the results in **Figure 5**. The improve of adjuvant RT on prognosis remained (PFS: HR = 0.70, 95% CI: 0.59-0.82, P < 0.0001, and OS: HR = 0.89,95% CI: 0.64-1.24, P = 0.49).

Meta-Analysis of PFS and OS Between GTR With RT and GTR

In the analyses of PFS and OS in AM patients treated with GTR+RT and GTR, 16 and 8 studies were included, respectively, which are shown in **Figure 2**. In the PFS analysis, the P value of the Q statistic and the Higgins I^2 statistic for heterogeneity were 0.00001 and 83%, respectively. In the OS analysis, the P value and I^2 were 0.47 and 0%, respectively. This result indicated that the former was heterogeneous and the latter was homoplasmic, so we applied a random-effects model and fixed-effects model, respectively. Benefits of RT were found in both the PFS and OS analyses (PFS: HR = 0.73, 95% CI: 0.39-1.34, P = 0.31, and OS: HR = 0.55, 95% CI: 0.36-0.85, P = 0.007). As shown in the funnel diagram in **Figure 3**, significant publication bias was observed in the PFS results. After the removal of 5 studies, the bias was improved (I^2 = 38%, P = 0.01), and a fixed-effects model was used to present the results (**Figures 4**, **5**). The results of the sensitivity analysis indicated that adjuvant RT also significantly

TABLE 1 | Demographics.

Author & year	Study duration (standard)	Design	Country	Sample size	Male: Female	Median age	Median follow-up (months)	Median dose (Gy)	HR					
									Surgery+RT *vs* Surgery		GTR+RT *vs* GTR		STR+RT *vs* STR	
									PFS	OS	PFS	OS	PFS	OS
Jo (10)	1997-2008 (2000)	Retrospective	Korea	35	18:17	40	56	NR	0.626	NR	NR	NR	0.204	NR
Mair (11)	2001-2010 (2000)	Retrospective	UK	114	55:59	57	NR	51.8	0.831	NR	NR	NR	NR	NR
Komotar (12)	1992-2011 (2000)	Retrospective	US	45	20:25	56.1	44.1	59.4	NR	NR	0.236	NR	NR	NR
Hammouche (13)	1996-2009 (2007)	Retrospective	UK	79	43:36	58	50	56.2	0.960	NR	NR	NR	NR	NR
Aizer (14)	1997-2011 (NR)	Retrospective	US	91	41:50	57	58.8	60	0.240	0.210	0.250	0.247	NR	NR
Wang (15)	2001-2009 (2007)	Retrospective	China	28	13:15	56.8	57.4	57	NR	NR	0.029	0.354	NR	NR
Zhao (16)	2001-2011 (2000)	Retrospective	China	89	42:47	53.3	25	NR	0.722	1.111	NR	NR	NR	NR
Champeaux (17)	2007-2015 (2007)	Retrospective	UK	194	93:101	54.2	52.8	NR	3.820	1.050	NR	NR	NR	NR
Jenkinson (18)	2001-2010 (2007)	Retrospective	UK, Italy, Ireland,	133	68:65	62	57.4	60	NR	NR	0.842	0.926	NR	NR
Endo (19)	2000-2013 (2007)	Retrospective	Japan	45	25:20	58.7	81	50	1.200	NR	NR	NR	NR	NR
Bagshaw (20)	1991-2014 (2007)	Retrospective	US	63	29:33	53	42	54	0.388	NR	0.026	NR	NR	NR
Graffeo (21)	1988-2011 (2016)	Retrospective	US	69	25:44	60	95	54	NR	NR	1.781	0.492	NR	NR
Phonwijit (22)	2004-2014 (2007)	Retrospective	Thailand	126	42:84	55	52	NR	0.402	NR	NR	NR	NR	NR
Dohm (23)	1993-2014 (2007)	Retrospective	US	83	32:51	63.6	36.9	55.7	0.430	0.523	0.657	NR	0.193	NR
Masalha (24)	2001-2015 (2016)	Retrospective	Germany	161	76:85	70	62.4	NR	0.860	NR	NR	NR	NR	NR
Shakir (25)	1992-2013 (2007)	Retrospective	Canada	70	32:38	62	67	54	0.046	NR	0.017	NR	0.081	NR
Chen (26)	1993-2014 (2000/2007)	Retrospective	US	182	71:111	57	52.8	59.4	0.150	NR	0.010	0.494	0.180	0.642
Li (27)	2008-2015 (2007)	Retrospective	China	302	136:166	51	41.6	NR	0.662	0.096	0.811	0.036	0.470	0.401
Zhu (28)	2005-2008 (2000)	Retrospective	China	99	48:51	NR	76.5	NR	NR	NR	0.695	0.646	0.238	0.223
Streckert (4)	1991-2018 (2016)	Retrospective	Germany	138	74:64	62	62	59.4	3.409	NR	4.340	NR	1.670	NR
Wang (29)	2009-2018 (2007/2016)	Retrospective	China	263	99:164	52	41	56	0.629	0.026	0.966	0.026	0.246	NR
Keric (30)	2007-2017 (2007)	Retrospective	Germany	258	117:141	60	31	NR	0.788	NR	2.776	NR	0.724	NR
Lee (5)	2000-2015 (2000/2007)	Retrospective	US	230	93:137	56.6	82.8	59.4	0.210	0.987	0.451	NR	0.471	NR
Garcia-Segura (31)	1995-2015 (2007)	Retrospective	US	181	72:109	59.6	NR	NR	4.352	NR	6.328	NR	1.793	NR

NR, no reported.

reduced the recurrence rate in patients with GTR (PFS: HR = 0.69, 95% CI: 0.52-0.92, P = 0.01).

Meta-Analysis of PFS and OS Between STR With RT and STR Alone

In the analyses of PFS and OS in AM patients treated with STR +RT and STR alone, 11 and 3 studies were included, respectively, and the results are shown in **Figure 2**. In the PFS analysis, the P value of the Q statistic and the Higgins I^2 statistic for heterogeneity were 0.001 and 66%, respectively. This implies the existence of heterogeneity, so we applied a random-effects model. In contrast, the fixed-effect model was chosen for the OS analysis because of homogeneity (I^2 = 0% and p=0.37). Benefits of RT were found in both the PFS and OS analyses (PFS: HR =

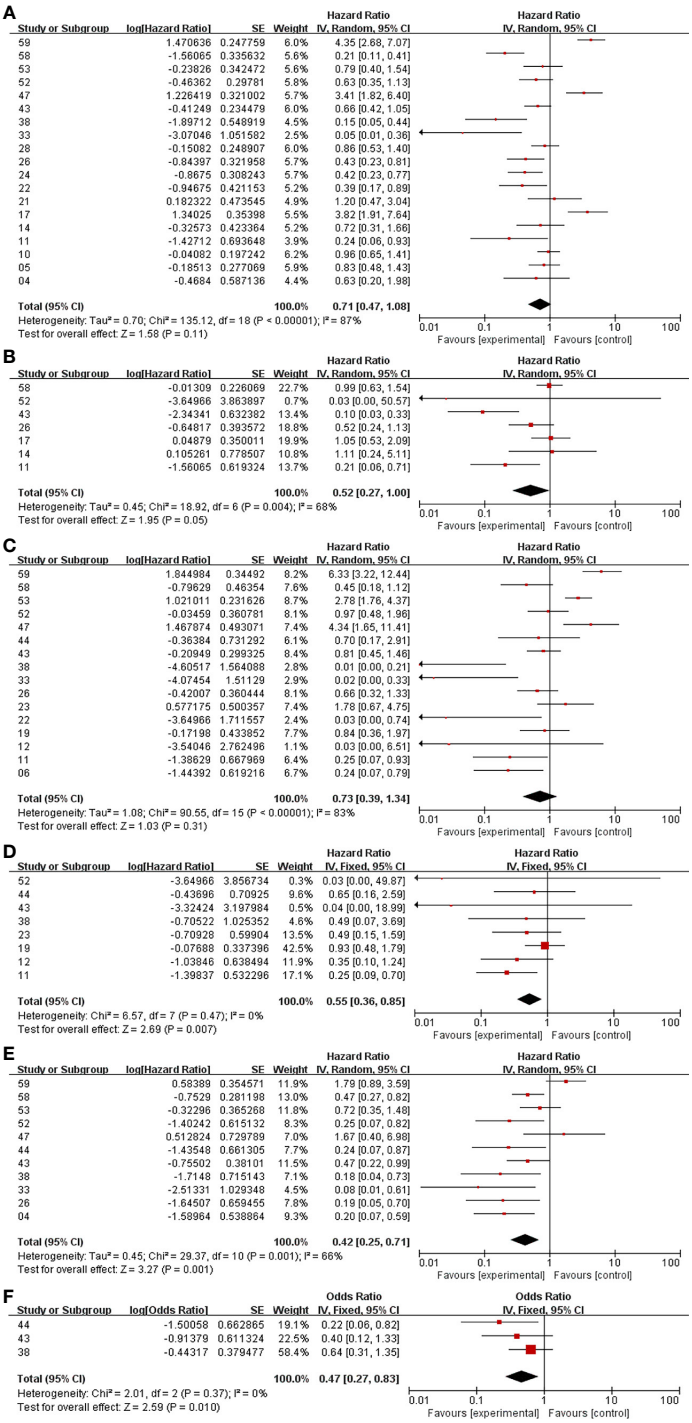

FIGURE 2 | Meta-analysis. Surgery+RT *vs* Surgery, PFS **(A)**. Surgery+RT *vs* Surgery, OS **(B)**. GTR+RT *vs* GTR, PFS **(C)**. GTR+RT *vs* GTR, OS **(D)**. STR+RT *vs* STR, PFS **(E)**. STR+RT *vs* STR, OS **(F)**.

0.42, 95% CI: 0.25-0.71, P = 0.001, and OS: R = 0.47, 95% CI: 0.27-0.83, P = 0.01). A funnel plot (**Figure 3**) confirmed the existence of publication bias in the PFS results, which was significantly improved after Garcia-Segura's study (31) were removed by the sensitivity analysis (I^2 = 39%, p=0.1), so a fixed-effects model was used to present the results (**Figures 4**, **5**). The PFS was still significantly improved after the sensitivity analysis (PFS: HR = 0.41, 95% CI: 0.30-0.55, P < 0.00001).

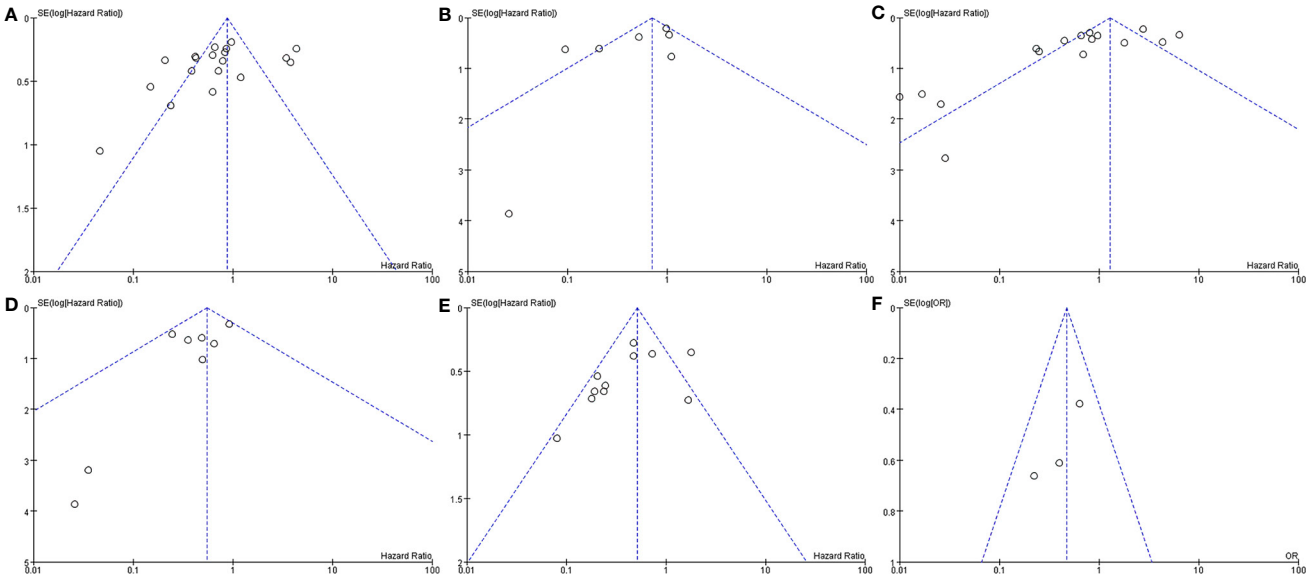

FIGURE 3 | Funnel plot. Surgery+RT vs Surgery, PFS **(A)**. Surgery+RT vs Surgery, OS **(B)**. GTR+RT vs GTR, PFS **(C)**. GTR+RT vs GTR, OS **(D)**. STR+RT vs STR, PFS **(E)**. STR+RT vs STR, OS **(F)**.

DISCUSSION

According to the latest EANO guidelines, maximum surgical resection with guaranteed safety is currently recognized as the preferred treatment for atypical meningioma (32). However, to date, there are no clear conclusions regarding whether postoperative radiotherapy is needed in patients with AMs (32). We performed the largest systematic review to date and extracted Hazard Ratio (HR) data with higher evidence level to compare the impact of STR and GTR on OS and/or PFS in AM patients with a rigorous assessment of the quality of the existing evidence. At the same time, we are the first to perform a subgroup analysis of different Simpson excision grade methods for GTR. Therefore, our results and conclusions have higher reference value.

Surgery With RT and Surgery Alone

Much of the literature does not provide detailed data on GTR and STR but rather combines them into a single analysis. We are the first study to perform a meta-analysis with these data. Because of the large amount of related literature and a large sample size, this part of the analysis also has some value. Of the 19 articles including PFS, 15 reported HR < 1 for RT, of which 7 showed significant statistical significance, while only 4 reported the opposite results. Similarly, 5 of 7 studies examined the positive effects of RT on OS. After the sensitivity analysis, postoperative RT was associated with a 30% reduction in recurrence ($p<0.0001$) and an 11% reduction in mortality ($p=0.49$) compared with surgery alone, especially for the former, indicating that postoperative RT was associated with a significant improvement in PFS. Therefore, it is considered reasonable to consider postoperative RT for patients when the extent of surgical resection cannot be determined.

GTR With RT and GTR Alone

The debate over whether postoperative RT should be routinely performed in patients with GTR is most intense. Some people suggest that because of the thoroughness of resection, patients with GTR have fewer tumor recurrence events and longer survival times than patients with STR, so no postoperative RT is required (11, 29). A meta-analysis by Hasan et al. (33) focused specifically on the potential benefits of adjuvant RT after the complete removal of atypical meningiomas, with no clear benefits reported in terms of local control or 5-year survival. Even in Garcia-Segura's cohort, adjuvant RT was associated with worse PFS and OS (31). However, in a prospective phase II study involving 15 centers in seven countries (34), as the highest level of inclusion in the literature, the data showed that the 3-year PFS for AM patients undergoing complete resection was greater than 70% when treated with high-dose (60 Gy) RT. In our analysis, postoperative RT was negatively correlated with recurrence and mortality across all the literature. For OS, the HR after GTR + RT in all studies was < 1, but for PFS, the heterogeneity among the articles was greater. The heterogeneity may be due to differences in the definitions of GTR and STR and differences in treatment protocols or techniques in different studies. After the deletion of 5 articles in the sensitivity analysis, there was less residual heterogeneity. Studies have shown that RT after GTR could significantly reduce the rate of recurrence. As one of the highlights, we are the first to perform a subgroup analysis of GTR. Five of these studies defined GTR as Simpson grade I or II tumor resection (**Figure 6**), while six studies included grade III

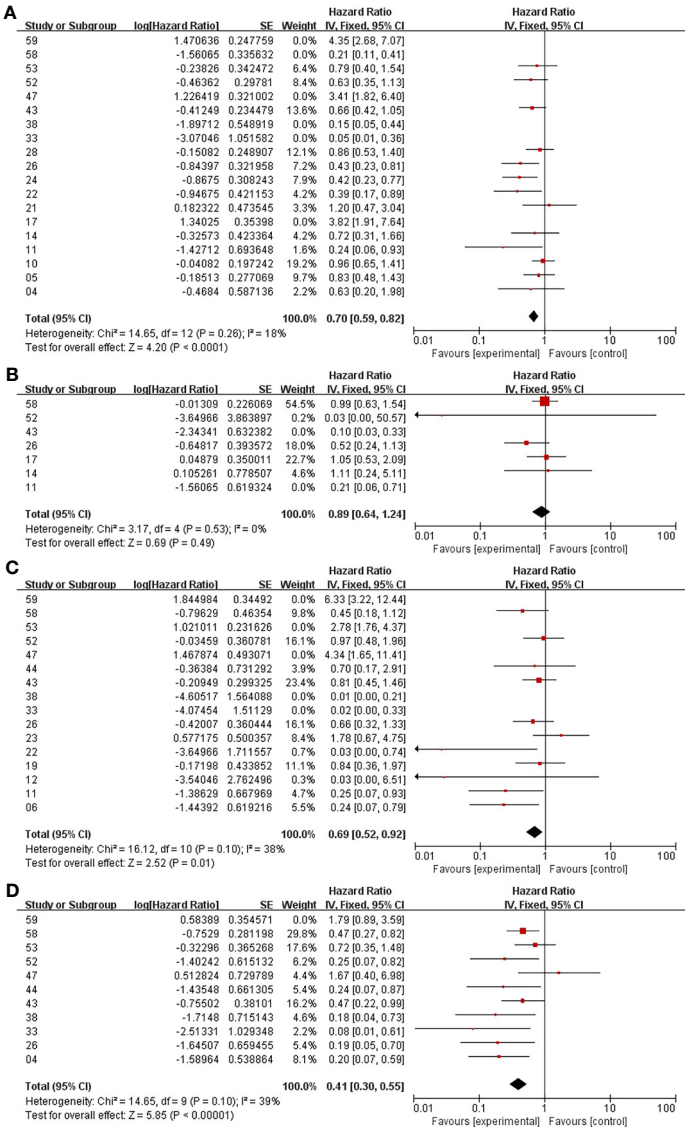

FIGURE 4 | Meta-analysis after sensitivity analysis. Surgery+RT vs Surgery, PFS **(A)**. Surgery+RT vs Surgery, OS **(B)**. GTR+RT vs GTR, PFS **(C)**. STR+RT vs STR, PFS **(D)**.

resection. There was no significant effect on the recurrence rate in patients with RT after GTR defined as Simpson grade I or II tumor resection (HR=1.82, p=0.22), while PFS may be significantly prolonged with postoperative adjuvant RT in GTR, including grade III resection (HR=0.64, p=0.02). However, the findings related to the former should be interpreted with caution because of the small sample size, high heterogeneity (I^2 = 89%) and lack of statistical significance (p=0.22). We suggest that grade III resection should not be attributed to GTR but should be treated as STR based on a combination of surgical records and postoperative MRI examination. According to our clinical experience, tumors in sites such as the cavernous sinus, the paraclinoid process, and the petroclival region may adhere to important structures such as the internal carotid artery, the basilar artery, and the brain stem. Although postoperative MRI and other imaging studies have failed to detect residual tumors, the presence of residual parenchyma is noted in the surgical record, and postoperative RT is recommended, especially in view of OS improvement. In summary, we believe that for patients with GTR, postoperative RT should be given appropriately, but tumor recurrence should be closely monitored, especially in Simpson grade I or II resection patients. In addition, the ROAM/EORTC 1308 trial (ISRCTN71502099), a multicenter, phase III, randomized controlled trial, has been developed to better answer whether early adjuvant radiotherapy for patients who have undergone GTR of AMs reduces recurrences compared with monitoring (35).

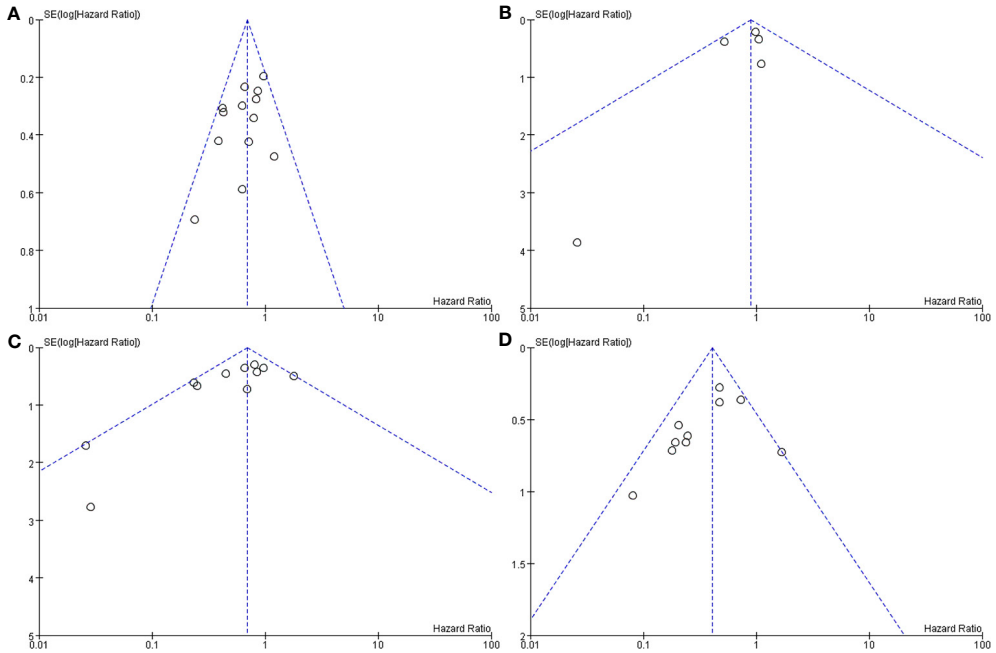

FIGURE 5 | Funnel plot after sensitivity analysis. Surgery+RT vs Surgery, PFS **(A)**. Surgery+RT vs Surgery, OS **(B)**. GTR+RT vs GTR, PFS **(C)**. STR+RT vs STR, PFS **(D)**.

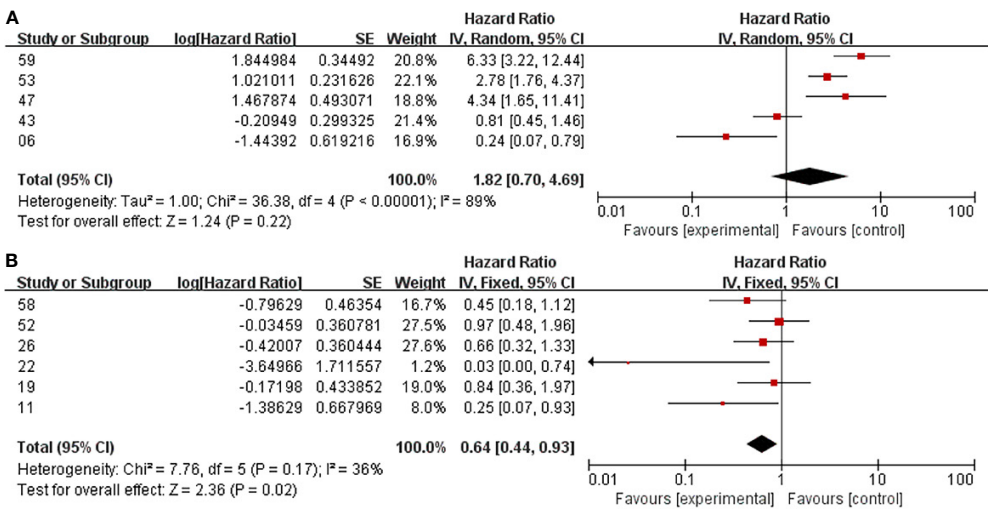

FIGURE 6 | Subgroup analysis. GTR+RT vs GTR, PFS, GTR= Simpson Grade I or II tumor resection **(A)**. GTR+RT vs GTR, PFS, GTR= Simpson Grade I, II or III tumor resection **(B)**.

STR With RT and STR Alone

It is generally accepted that patients with STR should be treated with postoperative radiation due to residual tumors after surgery (26), especially for PFS benefits (36). In Pant's study cohort, 97% of patients who received radiation immediately after the initial resection had a recurrence rate, compared with 15% of patients who did not receive radiation (36). However, in Streckert's study, none of the analyzed radiological features were correlated with survival (4). Garcia-Segura et al. even found that STR with RT significantly predicted tumor recurrence (31). Our results after sensitivity analysis confirmed that STR with postoperative RT reduced recurrence by 59% and mortality by 53%, both of which were statistically significant. To this end, we recommend that all STR patients undergo postoperative RT under appropriate conditions to extend PFS and OS.

TABLE 2 | Toxicity of postoperative adjuvant RT.

Study	RT Toxicity (%)	Description
Bagshaw et al. (20)	14	Grade 2 or 3 toxicities
Graffeo et al. (21)	12.5	
Dohm et al. (23)	15	Grade 3 or 4 toxicities (radiation necrosis, cognitive disturbances, peripheral neuropathy, seizures, aphasia, optic nerve disorders)
Shakri et al. (25)	20	Grade 1 or 2 toxicities (headache, dizziness, aparesthesia)
Chen et al. (26)	14	Grade 2+ toxicities (radiation necrosis, lower-extremity paresis, short-term visual blurring, transient radiation-induced encephalopathy) Intracranial hemorrhage

Radiotherapy Toxicity

There may be some side effects from radiotherapy, which must be considered for postoperative RT (37). The Common Terminology Criteria for Adverse Effects grading scale (version 4) has been used to observe and describe toxicity from RT and is usually classified into 4 levels. Levels 1 and 2 are more common, while level 4 is extremely rare. The relevant statistics are shown in **Table 2**. In Shakir's study, grade 1 or 2 toxicities were noted in 8 patients (radiotherapy-attributed toxicity rate was 20%) and included headache (4 patients), dizziness (3 patients) and paresthesia (1 patient). These toxicities were self-limiting and managed with short-course corticotherapy (25). In Chen's and Dohma's study cohorts, there were 5 (12%) and 8 (15%) cases with grade 2+ adverse effects of RT, respectively, and 1 case with grade 4 toxicity. The former suffered from cerebral hemorrhage and died, while the latter developed medically intractable epileptic seizures and had to be hospitalized (23, 26). According to our analysis, we suggest that although the possible side effects are not negligible, there are overall benefits to postoperative RT relative to significant improvements in recurrence and survival. Close observation, follow-up and evaluation of adverse reactions to real-time adjustment of regimens, and active symptomatic treatment should be performed in conjunction with postoperative RT.

Assessment of Heterogeneity

There is significant clinical and methodological heterogeneity in our systematic review, which can be evidenced by the wide range of patient numbers, ages, follow-up times, radiation doses, modes of radiotherapy and definitions of GTR and STR classifications. The only known prognostic factor for AM is the extent of resection; however, age (38), tumor volume, and Mib-1 (29) have been associated with PFS and OS in a number of single institution studies. With regard to some of the more heterogeneous results we have obtained, we suspect that the possible reasons are the different definitions of GTR and STR in different studies, and the application time and methods of radiation therapy after surgery were inconsistent. In summary, we used a random-effects model for heterogeneity > 50 and carried out sensitivity analyses and subsection analyses.

Limitations

The WHO classification definition of AMs changed in 2000, 2007 and 2016. All the studies included were retrospective cohort studies. Therefore, more prospective and long-term follow-up studies are needed to better verify the impact of RT on prognosis. The large sample size also brings some heterogeneity. Finally, the exclusion of non-English literature may leading to potential language bias.

CONCLUSION

Maximum surgical resection with guaranteed safety is currently recognized as the preferred treatment for AM, but whether to perform postoperative RT remains a controversial issue. To the best of our knowledge, the present study is the largest meta-analysis on this topic using high-evidence-level HR data and reveals the benefits of postoperative RT assistance in patients with AMs, especially for OS. Regardless of whether GTR or STR is performed, postoperative RT was found to effectively increase PFS and OS to varying degrees. Especially for patients undergoing Simpson grade III or IV resection, postoperative RT confers the benefits for recurrence and survival. Moreover, long-term surveillance should be tailored based on the Simpson grade of AMs. Clinical trials such as ROAM will investigate further.

DATA AVAILABILITY STATEMENT

The original contributions presented in the study are included in the article/**Supplementary Material**. Further inquiries can be directed to the corresponding author.

AUTHOR CONTRIBUTIONS

DS and DX have contributed equally. DS: data processing and manuscript writing, DX: conception and data collection. HH and GW: critical review. QG, MZ, and FW: data collection and evaluation. FG: conception and critical review. All authors contributed to the article and approved the submitted version.

ACKNOWLEDGMENTS

The authors thank the members of their research group for useful discussions.

SUPPLEMENTARY MATERIAL

The Supplementary Material for this article can be found online at: https://www.frontiersin.org/articles/10.3389/fonc.2021.787962/full#supplementary-material

REFERENCES

1. Ostrom QT, Gittleman H, Truitt G, Boscia A, Kruchko C, Barnholtz-Sloan JS. Cbtrus Statistical Report: Primary Brain and Other Central Nervous System Tumors Diagnosed in the United States in 2011-2015. *Neuro Oncol* (2018) 20: v1–86. doi: 10.1093/neuonc/noy131
2. Wang C, Kaprealian TB, Suh JH, Kubicky CD, Ciporen JN, Chen Y, et al. Overall Survival Benefit Associated With Adjuvant Radiotherapy in Who Grade Ii Meningioma. *Neuro Oncol* (2017) 19:1263–70. doi: 10.1093/neuonc/nox007
3. Fathi AR, Roelcke U. Meningioma. *Curr Neurol Neurosci Rep* (2013) 13:337. doi: 10.1007/s11910-013-0337-4
4. Streckert E, Hess K, Sporns PB, Adeli A, Brokinkel C, Kriz J, et al. Clinical, Radiological, and Histopathological Predictors for Long-Term Prognosis After Surgery for Atypical Meningiomas. *Acta Neurochir (Wien)* (2019) 161:1647–56. doi: 10.1007/s00701-019-03956-8
5. Lee G, Lamba N, Niemierko A, Kim DW, Chapman PH, Loeffler JS, et al. Adjuvant Radiation Therapy Versus Surveillance After Surgical Resection of Atypical Meningiomas. *Int J Radiat Oncol Biol Phys* (2021) 109:252–66. doi: 10.1016/j.ijrobp.2020.08.015
6. Whittle IR, Smith C, Navoo P, Collie D. Meningiomas. *Lancet* (2004) 363:1535–43. doi: 10.1016/S0140-6736(04)16153-9
7. Stang A. Critical Evaluation of the Newcastle-Ottawa Scale for the Assessment of the Quality of Nonrandomized Studies in Meta-Analyses. *Eur J Epidemiol* (2010) 25:603–5. doi: 10.1007/s10654-010-9491-z
8. Tierney JF, Stewart LA, Ghersi D, Burdett S, Sydes MR. Practical Methods for Incorporating Summary Time-to-Event Data Into Meta-Analysis. *Trials* (2007) 8:16. doi: 10.1186/1745-6215-8-16
9. Mittlbock M, Heinzl H. A Simulation Study Comparing Properties of Heterogeneity Measures in Meta-Analyses. *Stat Med* (2006) 25:4321–33. doi: 10.1002/sim.2692
10. Jo K, Park HJ, Nam DH, Lee JI, Kong DS, Park K, et al. Treatment of Atypical Meningioma. *J Clin Neurosci* (2010) 17:1362–6. doi: 10.1016/j.jocn.2010.03.036
11. Mair R, Morris K, Scott I, Carroll TA. Radiotherapy for Atypical Meningiomas. *J Neurosurg* (2011) 115:811–9. doi: 10.3171/2011.5.JNS11112
12. Komotar RJ, Iorgulescu JB, Raper DM, Holland EC, Beal K, Bilsky MH, et al. The Role of Radiotherapy Following Gross-Total Resection of Atypical Meningiomas. *J Neurosurg* (2012) 117:679–86. doi: 10.3171/2012.7.JNS112113
13. Hammouche S, Clark S, Wong AH, Eldridge P, Farah JO. Long-Term Survival Analysis of Atypical Meningiomas: Survival Rates, Prognostic Factors, Operative and Radiotherapy Treatment. *Acta Neurochir (Wien)* (2014) 156:1475–81. doi: 10.1007/s00701-014-2156-z
14. Aizer AA, Arvold ND, Catalano P, Claus EB, Golby AJ, Johnson MD, et al. Adjuvant Radiation Therapy, Local Recurrence, and the Need for Salvage Therapy in Atypical Meningioma. *Neuro Oncol* (2014) 16:1547–53. doi: 10.1093/neuonc/nou098
15. Wang YC, Chuang CC, Wei KC, Hsu YH, Hsu PW, Lee ST, et al. Skull Base Atypical Meningioma: Long Term Surgical Outcome and Prognostic Factors. *Clin Neurol Neurosurg* (2015) 128:112–6. doi: 10.1016/j.clineuro.2014.11.009
16. Zhao P, Hu M, Zhao M, Ren X, Jiang Z. Prognostic Factors for Patients With Atypical or Malignant Meningiomas Treated at a Single Center. *Neurosurg Rev* (2015) 38:101–7. doi: 10.1007/s10143-014-0558-2
17. Champeaux C, Wilson E, Shieff C, Khan AA, Thorne L. Who Grade Ii Meningioma: A Retrospective Study for Outcome and Prognostic Factor Assessment. *J Neurooncol* (2016) 129:337–45. doi: 10.1007/s11060-016-2181-2
18. Jenkinson MD, Waqar M, Farah JO, Farrell M, Barbagallo GM, McManus R, et al. Early Adjuvant Radiotherapy in the Treatment of Atypical Meningioma. *J Clin Neurosci* (2016) 28:87–92. doi: 10.1016/j.jocn.2015.09.021
19. Endo T, Narisawa A, Ali HS, Murakami K, Watanabe T, Watanabe M, et al. A Study of Prognostic Factors in 45 Cases of Atypical Meningioma. *Acta Neurochir (Wien)* (2016) 158:1661–7. doi: 10.1007/s00701-016-2900-7
20. Bagshaw HP, Burt LM, Jensen RL, Suneja G, Palmer CA, Couldwell WT, et al. Adjuvant Radiotherapy for Atypical Meningiomas. *J Neurosurg* (2017) 126:1822–8. doi: 10.3171/2016.5.JNS152809
21. Graffeo CS, Leeper HE, Perry A, Uhm JH, Lachance DJ, Brown PD, et al. Revisiting Adjuvant Radiotherapy After Gross Total Resection of World Health Organization Grade Ii Meningioma. *World Neurosurg* (2017) 103:655–63. doi: 10.1016/j.wneu.2017.04.095
22. Phonwijit L, Khawprapa C, Sitthinamsuwan B. Progression-Free Survival and Factors Associated With Postoperative Recurrence in 126 Patients With Atypical Intracranial Meningioma. *World Neurosurg* (2017) 107:698–705. doi: 10.1016/j.wneu.2017.08.057
23. Dohm A, McTyre ER, Chan MD, Fan C, Isom S, Bourland JD, et al. Early or Late Radiotherapy Following Gross or Subtotal Resection for Atypical Meningiomas: Clinical Outcomes and Local Control. *J Clin Neurosci* (2017) 46:90–8. doi: 10.1016/j.jocn.2017.08.023
24. Masalha W, Heiland DH, Franco P, Delev D, Haaker JG, Schnell O, et al. Atypical Meningioma: Progression-Free Survival in 161 Cases Treated at Our Institution With Surgery Versus Surgery and Radiotherapy. *J Neurooncol* (2018) 136:147–54. doi: 10.1007/s11060-017-2634-2
25. Shakir SI, Souhami L, Petrecca K, Mansure JJ, Singh K, Panet-Raymond V, et al. Prognostic Factors for Progression in Atypical Meningioma. *J Neurosurg* (2018) 129:1240–8. doi: 10.3171/2017.6.JNS17120
26. Chen WC, Magill ST, Wu A, Vasudevan HN, Morin O, Aghi MK, et al. Histopathological Features Predictive of Local Control of Atypical Meningioma After Surgery and Adjuvant Radiotherapy. *J Neurosurg* (2018) 130:443–50. doi: 10.3171/2017.9.JNS171609
27. Li H, Zhang YS, Zhang GB, Zhang GJ, Wang B, Li D, et al. Treatment Protocol, Long-Term Follow-Up, and Predictors of Mortality in 302 Cases of Atypical Meningioma. *World Neurosurg* (2019) 122:e1275–84. doi: 10.1016/j.wneu.2018.11.032
28. Zhu H, Bi WL, Aizer A, Hua L, Tian M, Den J, et al. Efficacy of Adjuvant Radiotherapy for Atypical and Anaplastic Meningioma. *Cancer Med* (2019) 8:13–20. doi: 10.1002/cam4.1531
29. Wang F, Xu D, Liu Y, Lin Y, Wei Q, Gao Q, et al. Risk Factors Associated With Postoperative Recurrence in Atypical Intracranial Meningioma: Analysis of 263 Cases at a Single Neurosurgical Centre. *Acta Neurochir (Wien)* (2019) 161:2563–70. doi: 10.1007/s00701-019-04073-2
30. Keric N, Kalasauskas D, Freyschlag CF, Gempt J, Misch M, Poplawski A, et al. Impact of Postoperative Radiotherapy on Recurrence of Primary Intracranial Atypical Meningiomas. *J Neurooncol* (2020) 146:347–55. doi: 10.1007/s11060-019-03382-x
31. Garcia-Segura ME, Erickson AW, Jairath R, Munoz DG, Das S. Necrosis and Brain Invasion Predict Radio-Resistance and Tumor Recurrence in Atypical Meningioma: A Retrospective Cohort Study. *Neurosurgery* (2020) 88:E42–8. doi: 10.1093/neuros/nyaa348
32. Goldbrunner R, Stavrinou P, Jenkinson MD, Sahm F, Mawrin C, Weber DC, et al. Eano Guideline on the Diagnosis and Management of Meningiomas. *Neuro Oncol* (2021) 23(11):1821–34. doi: 10.1093/neuonc/noab150
33. Hasan S, Young M, Albert T, Shah AH, Okoye C, Bregy A, et al. The Role of Adjuvant Radiotherapy After Gross Total Resection of Atypical Meningiomas. *World Neurosurg* (2015) 83:808–15. doi: 10.1016/j.wneu.2014.12.037
34. Weber DC, Ares C, Villa S, Peerdeman SM, Renard L, Baumert BG, et al. Adjuvant Postoperative High-Dose Radiotherapy for Atypical and Malignant Meningioma: A Phase-Ii Parallel Non-Randomized and Observation Study (Eortc 22042-26042). *Radiother Oncol* (2018) 128:260–5. doi: 10.1016/j.radonc.2018.06.018
35. Jenkinson MD, Javadpour M, Haylock BJ, Young B, Gillard H, Vinten J, et al. The Roam/Eortc-1308 Trial: Radiation Versus Observation Following Surgical Resection of Atypical Meningioma: Study Protocol for a Randomised Controlled Trial. *Trials* (2015) 16:519. doi: 10.1186/s13063-015-1040-3
36. Pant S, Tonse R, Kannan S, Moiyadi A, Shetty P, Epari S, et al. Impact of Timing of Radiation Therapy on Outcomes in Atypical Meningioma: A Clinical Audit. *Pract Radiat Oncol* (2018) 8:e275–84. doi: 10.1016/j.prro.2018.01.010
37. Detti B, Scoccianti S, Di Cataldo V, Monteleone E, Cipressi S, Bordi L, et al. Atypical and Malignant Meningioma: Outcome and Prognostic Factors in 68 Irradiated Patients. *J Neurooncol* (2013) 115:421–7. doi: 10.1007/s11060-013-1239-7
38. Zaher A, Abdelbari MM, Zayed DH, Ellatif RA, Ashamallah SA. Atypical Meningioma: A Study of Prognostic Factors. *World Neurosurg* (2013) 80:549–53. doi: 10.1016/j.wneu.2013.07.001

Conflict of Interest: The authors declare that the research was conducted in the absence of any commercial or financial relationships that could be construed as a potential conflict of interest.

Publisher's Note: All claims expressed in this article are solely those of the authors and do not necessarily represent those of their affiliated organizations, or those of the publisher, the editors and the reviewers. Any product that may be evaluated in

this article, or claim that may be made by its manufacturer, is not guaranteed or endorsed by the publisher.

Copyright © 2021 Song, Xu, Han, Gao, Zhang, Wang, Wang and Guo. This is an open-access article distributed under the terms of the Creative Commons Attribution License (CC BY). The use, distribution or reproduction in other forums is permitted, provided the original author(s) and the copyright owner(s) are credited and that the original publication in this journal is cited, in accordance with accepted academic practice. No use, distribution or reproduction is permitted which does not comply with these terms.

frontiers in Oncology

ORIGINAL RESEARCH
published: 22 December 2021
doi: 10.3389/fonc.2021.760892

m^{6}A Regulator Expression Segregates Meningiomas Into Biologically Distinct Subtypes

Jiawei Chen[1,2,3†], *Shuchen Sun*[1,2,3†], *Leihao Ren*[1,2,3†], *Lingyang Hua*[1,2,3], *Daijun Wang*[1,2,3], *Qing Xie*[1,2,3], *Hans-Georg Wirsching*[4], *Jiaojiao Deng*[1,2,3*], *Michael Weller*[4*] *and Ye Gong*[1,2,3,5*]

[1] Department of Neurosurgery, Huashan Hospital, Fudan University, Shanghai, China, [2] Institute of Neurosurgery, Fudan University, Shanghai, China, [3] Shanghai Key Laboratory of Brain Function Restoration and Neural Regeneration, Fudan University, Shanghai, China, [4] Department of Neurology, University Hospital and University of Zurich, Zurich, Switzerland, [5] Department of Critical Care Medicine, Huashan Hospital, Fudan University, Shanghai, China

OPEN ACCESS

Edited by:
Ian Dunn,
University of Oklahoma Health Sciences Center, United States

Reviewed by:
Lingyun Wu,
Nanjing University, China
Rohadi Muhammad Rosyidi,
University of Mataram, Indonesia

***Correspondence:**
Ye Gong
gong_ye@fudan.edu.cn
Jiaojiao Deng
djjewel@163.com
Michael Weller
Michael.Weller@usz.ch

†These authors have contributed equally to this work

Specialty section:
This article was submitted to Neuro-Oncology and Neurosurgical Oncology, a section of the journal Frontiers in Oncology

Received: 19 August 2021
Accepted: 29 November 2021
Published: 22 December 2021

Citation:
Chen J, Sun S, Ren L, Hua L, Wang D, Xie Q, Wirsching H-G, Deng J, Weller M and Gong Y (2021) m^{6}A Regulator Expression Segregates Meningiomas Into Biologically Distinct Subtypes. Front. Oncol. 11:760892. doi: 10.3389/fonc.2021.760892

Background: Meningiomas are the most common primary intracranial tumors in adults. According to the 2021 World Health Organization (WHO) classification of central nervous system tumors, approximately 80% of meningiomas are WHO grade 1, that is, histopathologically benign, whereas about 20% are WHO grade 2 or grade 3, showing signs of atypia or malignancy. The dysregulation of N6-methylation (m^{6}A) regulators is associated with disorders of diverse critical biological processes in human cancer. This study aimed to explore whether m^{6}A regulator expression was associated with meningioma molecular subtypes and immune infiltration.

Methods: We evaluated the m^{6}A modification patterns of 160 meningioma samples based on 19 m^{6}A regulators and correlated them with immune infiltration characteristics. Novel molecular subtypes were defined based on prognostic hub gene expression.

Results: Two meningioma clusters were identified based on the expression of 19 m^{6}A regulators. In cluster 1, 607 differentially expressed genes (DEGs) were upregulated and 519 were downregulated. A total of 1,126 DEGs comprised three gene expression modules characterized by turquoise, blue, and gray. Functional annotation suggested that the turquoise module was involved in Wnt-related and other important cancer-related pathways. We identified 32 hub genes in this module by constructing a protein–protein interaction network. The meningioma samples were divided into two molecular subtypes. *EPN1*, *EXOSC4*, *H2AX*, and *MZT2B* not only showed significant differences between meningioma molecular subtypes but also had the potential to be the marker genes of specific meningioma subtypes.

Conclusion: m^{6}A regulator gene expression may be a novel prognostic marker in meningioma.

Keywords: meningioma, immune infiltration, m^{6}A, WGCNA, molecular subtype

INTRODUCTION

Meningiomas arise from arachnoid cap cells attached to the inner layer of the dura, which covers the spinal cord and brain. They represent about 37.6% of primary central nervous system tumors, making them the most common histological types of intracranial tumor, with an incidence of 8.83 per 100,000 (1). They primarily occur in elderly individuals, with increased incidence in individuals older than 65 years (1). The incidence of meningiomas has also increased among adolescents and young adults; these tumors now represent about 16% of all intracranial tumors in people aged 15–39 years (2). Meningiomas preferentially affect women, with a female-to-male ratio between 2:1 and 3.5:1 (3–5). According to the 2021 World Health Organization (WHO) classification of central nervous system tumors, approximately 80% of cases are WHO grade 1 meningiomas with benign histology, whereas about 20% of cases are WHO grade 2 and 3 meningiomas showing signs of increased malignancy at histology (6).

RNA methylation, including 5-methylcytosine (m^{5}C), N6-methyladenosine (m^{6}A), and N1-methyladenosine (m^{1}A), has become a common phenomenon and a critical regulating factor for transcript expression in different types of cancer (7, 8). N6-methylation (m^{6}A), methylated at the N6 position of adenosine, has been regarded as the most pervasive, abundant, and conserved internal transcriptional modification within eukaryotic messenger RNAs (mRNAs), microRNAs (miRNAs), and long non-coding RNAs (lncRNAs) (9, 10). The deposition of m^{6}A is encoded by a methyltransferase complex involving three homologous factors: methyltransferases (termed as "writers"), demethylases (termed as "erasers"), and recognition from m^{6}A-binding proteins (termed as "readers") (11). The m^{6}A dysregulation, caused by dysregulated expression and genetic changes in m^{6}A regulators, is related to the disorders of multiple critical biological processes in human cancer (12, 13). Qi et al. reported that the self-renewal and tumorigenesis of glioma stem cells (GSCs) were regulated by m^{6}A RNA methylation, and an m^{6}A mRNA demethylase FTO inhibitor could suppress the progression of GSC-initiated tumor (14). Yang et al. demonstrated that FTO played an important role in promoting melanoma tumorigenesis and anti-PD-1 resistance, and the combination of FTO inhibitors with anti-PD-1 blockers could reduce the resistance to immunotherapy in melanoma (15). Miao et al. revealed that m^{6}A methyltransferase METTL3 promoted osteosarcoma cell progression by regulating the m^{6}A level of LEF1 and activating the Wnt/β-catenin signaling pathway (16). Besides, Vengoechea J. et al. observed that IGF2BP1, one of the m^{6}A regulators, could increase the malignant potential of meningiomas by enhancing cell adhesion (17). Hwang M. et al. identified significantly higher expression of HNRNPA2B1 in benign meningioma compared to normal brain tissue (18).

Numerous studies revealed that the tumor microenvironment (TME) was fundamental for tumor survival, growth, and progression. The immune part of TME contained tumor-associated macrophages, tumor-associated neutrophils, dendritic cells, myeloid-derived suppressor cells (MDSCs), and Tie2-expressing monocytes comprising tumor-associated myeloid cells (19). Patients with meningiomas exhibit signs of peripheral immunosuppression, including increased PD-L1 on myeloid cells and elevated MDSC abundance proportional to tumor grade (20). The accumulation of mast cells in meningiomas could contribute to the aggressiveness of tumors (21). Chen et al. revealed that the proportions of tumor-infiltrating immune cells were associated with the prognosis for patients with meningioma (22). Overall, tumor cells elicited multiple biological behavioral changes through direct and indirect interactions with immune cells, such as inducing proliferation and angiogenesis, inhibiting apoptosis, avoiding hypoxia, and inducing immune tolerance (23–26). Therefore, a deeper understanding of the immune infiltration of meningiomas could help parse the TME landscape and finding promising biomarkers for immunotherapy. However, whether immune infiltration in meningiomas is regulated through the modification of m^{6}A patterns is still unknown. To address this question, we established a meningioma classification based on m^{6}A regulator gene expression and evaluated the associations of m^{6}A-deduced subtypes with immune infiltration in meningioma.

MATERIALS AND METHODS

Meningioma Dataset Resource and Processing

The Gene Expression Omnibus (GEO) database, restoring high-throughput gene expression data and hybridization arrays, chips, and microarrays, allows an easy access to gene expression data of human cancer. Public gene expression data and related clinical annotation data were obtained from the GEO database. GSE136661 and GSE43290 were gathered in the present study for further analysis (**Table 1**) (27, 28). The expression dataset GSE136661 with 160 meningioma samples from the Illumina HiSeq 4000 platform and GSE43290 with 47 meningioma samples and 4 normal meningeal samples from the Affymetrix Human Genome U133A Array platform were downloaded from the GEO database. Multiple probes corresponding to a gene were retained and shown as the median of the gene expression level, while probes corresponding to multiple genes were eliminated. The clinical information was also extracted from GEO raw data.

m^{6}A Regulator Data Retrieval From GEO Datasets

According to Zhang et al., 21 m^{6}A regulators were extracted from 5 integrated GEO datasets, including 8 writers (METTL3, METTL14, RBM15, RBM15B, WTAP, KIAA1429, CBLL1, and ZC3H13), 2 erasers (ALKBH5 and FTO), and 11 readers (YTHDC1, YTHDC2, YTHDF1, YTHDF2, YTHDF3, IGF2BP1, HNRNPA2B1, HNRNPC, FMR1, LRPPRC, and ELAVL1) (29). After intersecting with the GSE136661 dataset,

TABLE 1 | Meningioma gene expression data from GEO database.

Dataset ID	Platform	Samples
GSE136661	GPL20301	160
GSE43290	GPL96	51

19 m^{6}A regulators were included for further analysis, except for RBM15B and KIAA1429.

Differentially Expressed Genes Screening

Data analysis was performed using the limma package and *t* test. Fold change > 2.0 or <0.5 and P <0.05 were defined as cutoffs to screen for differentially expressed genes (DEGs) between different m^{6}A clusters.

Immune Cell Infiltration Analysis

CIBERSORT (https://cibersort.stanford.edu/index.php) was employed to characterize cell composition based on the gene expression profiles of complex tissues (30). A white blood cell gene matrix (LM22) consisting of 547 genes was used to identify 22 immune cell types, including myeloid subsets, natural killer cells, plasma cells, naive and memory B cells, and T cells. CIBERSORT was combined with the LM22 eigenmatrix to estimate the proportions of 22 immune cell phenotypes in different m^{6}A cluster 1 and m^{6}A cluster 2.

Weighted Gene Co-Expression Network Construction and Hub Gene Screening

The expression profile of the aforementioned DEGs was obtained to establish a gene co-expression network by the weighted gene co-expression network analysis (WGCNA) package in R (Version 4.1.0). The threshold power of β was used for constructing co-expression modules based on size independence and average connectivity of modules. We built a scale-free topology by underlining the strong correlations and attenuating the weak correlations with the soft threshold power of $\beta = 3$ (scale-free $R^2 = 0.85$). Then, the topological overlap matrix was calculated based on adjacency matrices. We applied the dynamic tree cut algorithm to classify genes according to their expression patterns and merged gene modules (at least 30 genes were included). The module eigengene (ME) was calculated as a summary profile for all genes in a module. These modules were merged into three major modules (blue, gray, and turquoise) by clustering analysis. We calculated the Pearson correlation coefficient of these three modules and m^{6}A cluster characteristics and selected the most correlated module for further analysis. Gene significance (GS) was employed as the correlation coefficient between transcriptome expression and module traits. Module significance was defined as the correlation coefficient between the module and the traits. Module membership (MM) was defined by the correlation coefficient of the ME and transcriptome data. Genes with a GS >0.60 and MM >0.80 were selected as each module's candidate hub genes. STRING is a database of known and predicted protein–protein interactions. The interactions include direct (physical) and indirect (functional) associations; they stem from computational prediction, from knowledge transfer between organisms, and from interactions aggregated from other (primary) databases. (30476243) A protein–protein interaction (PPI) network contained all candidate hub genes obtained from the STRING database. Nodes with 10 or more edges in the PPI network were selected to intersect with the module's candidate hub genes, and the key hub genes were finally identified.

Functional Enrichment Analysis

The functional enrichment analysis of DEGs was performed to identify Gene Ontology categories by their biological processes, molecular functions (MF), and cellular components and Kyoto Encyclopedia of Genes and Genomes (KEGG) enrichment analyses using the DAVID tool (https://david.ncifcrf.gov/tools.jsp) (31).

Unsupervised Clustering for Meningioma m^{6}A Clusters and Molecular Subtypes

Meningioma m^{6}A clusters and molecular subtypes were determined according to the expression profile of m^{6}A regulators and hub genes, respectively. The best K value (number of categories) was determined by finding the optimal sum of the squared error (SSE). The meningioma samples were divided into different subtypes by unsupervised clustering K-means and *t*-Distributed Stochastic Neighbor Embedding (t-SNE) descending dimension method. Significant DEGs, which might potentially become the marker genes of meningioma, were identified between different molecular subtypes using the Kruskal–Wallis test ($P < 0.05$).

Statistics Analysis

The expression levels of DEGs higher and lower than the median value were considered high and low expression levels, respectively. The Kruskal–Wallis test was used to conduct different comparisons of three or more groups. All statistical P values were two-sided, with P <0.05 indicating statistically significance. All data processing was done in R software (Version 4.1.0).

RESULTS

A total of 19 m^{6}A regulators were identified in the present study, including 6 writers, 2 erasers, and 11 readers. The genes of these regulators were distributed widely on multiple human chromosomes (**Figure 1A**). Several m^{6}A regulators were co-expressed, including (a) HNRNPA2B1 and YTHDC2, (b) LRPPRC, CBLL1, and FMR1, (c) FTO, YTHDC1, RMB15, ELAVL1, HNRNPC, and ALKBH5, and (d) YTHDF2 and WTAP (**Figure 1C**). K-means unsupervised clustering based on the expression of the 19 m^{6}A regulators segregated meningioma samples into 2 clusters (**Figure 1B** and **Supplementary Figures 1A, B**). PCA showed that these two different m^{6}A clusters could be well separated (**Supplementary Figure 1C**). Eight m^{6}A regulators were differentially expressed between both clusters, including WTAP, ALKBH5, ELAVL1, FTO, YTHDC1, YTHDC2, HNRNPA2B1, and METTL3 ($P <$ 0.05, **Figure 1D**). Employing CIBERSORT to estimate immune infiltration in both clusters suggested different numbers of plasma B cells, resting mast cells, and neutrophils in the two m^{6}A clusters ($P < 0.05$, **Figure 1E**). As for some major inflammatory reaction–related genes, we found that the expression of IL-15 and IL-18 was also significantly different between the two distinct m^{6}A clusters ($P < 0.05$, **Figure 1F**).

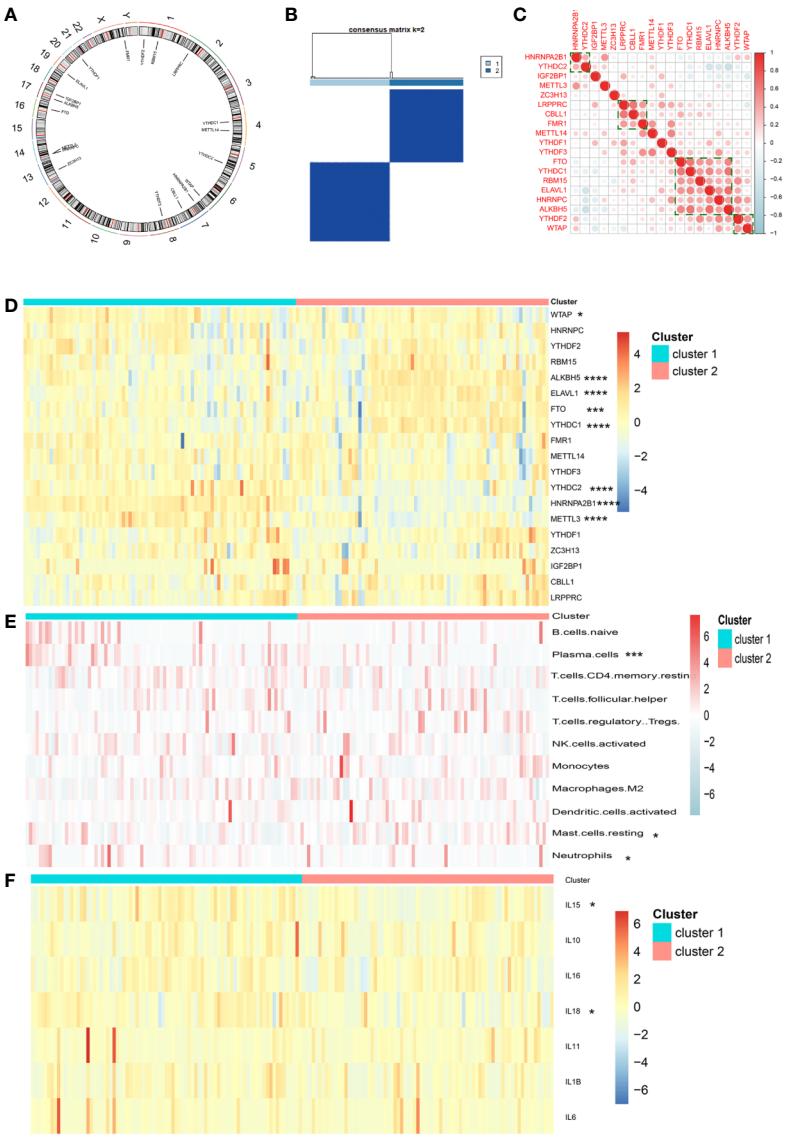

FIGURE 1 | **(A)** Location of 19 m^{6}A regulators on 23 chromosomes using GSE136661 cohort. **(B)** Clustering of meningioma samples. **(C)** Correlations between among 19 m^{6}A regulators in the GSE136661 cohort using Spearman analysis. Negative correlation was marked with blue and positive correlation with red. **(D)** Heatmap of the expression of 19 m^{6}A regulators in two distinct m^{6}A clusters. **(E)** Heatmap of immune cell infiltration in two distinct m^{6}A clusters. **(F)** Heatmap of the expression of inflammatory reaction-related genes in two distinct m^{6}A clusters (*$P < 0.05$; ***$P < 0.005$; ****$P < 0.001$).

Next, we performed weighted gene co-expression network analyses to better characterize the biological traits of both clusters. A total of 1,126 DEGs were used for the construction of weighted gene co-expression networks. A soft threshold power of $\beta = 3$ was used to construct co-expression modules (**Supplementary Figures 2A, B**). Three modules were identified and designated as the blue, gray, and turquoise modules, comprising 137, 179, and 810 genes, respectively (**Supplementary Figure 2C**). WGCNA was then applied to explore the module-trait relationships of different modules and m^{6}A clusters, and the turquoise module was identified as a hub gene set for explaining the difference between both clusters (**Supplementary Figure 2D**). Gene set enrichment analysis of the 810 genes in the turquoise module identified Notch and Wnt signaling as the key differentially expressed oncogenic pathways in either cluster (**Figures 2A–D**).

We chose a combined approach by (i) employing the STRING tool for functional interaction analyses to identify key network nodes (**Supplementary Figure 3A**) and (ii) calculating the Pearson correlation coefficient of the turquoise module and m^{6}A cluster characteristics to define hub genes and further characterize each m^{6}A cluster (**Supplementary Figure 3B**).

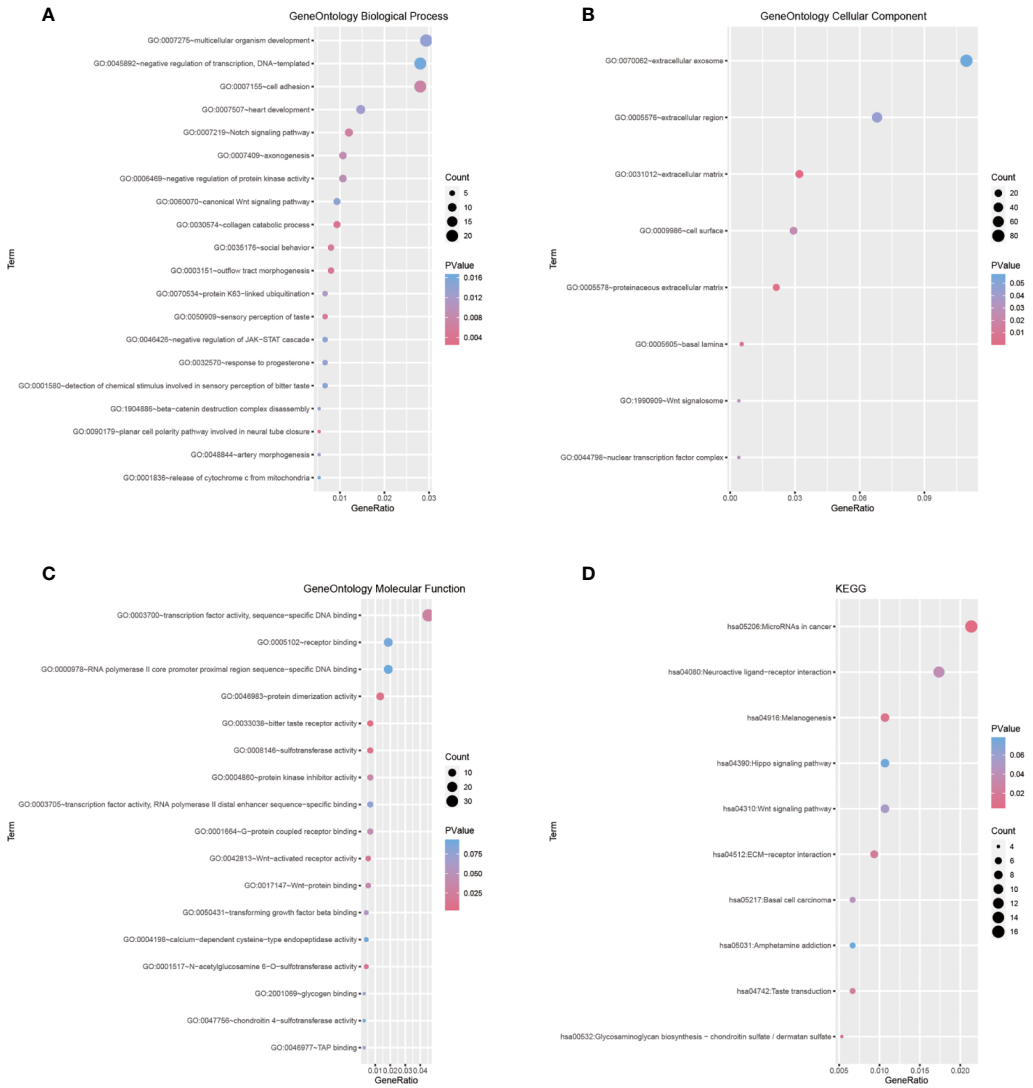

FIGURE 2 | **(A–C)** Gene Ontology terms in the biological process, cellular component, and molecular function categories. **(D)** Enrichment plot conducted *via* KEGG analysis.

After intersecting these two results, 32 key hub genes were identified (**Supplementary Figure 3C**). These key hub genes comprised *ACOT2*, *ALDH16A1*, *ALKBH7*, *BAD*, *C1orf122*, *C6orf226*, *CTSD*, *DNPH1*, *EPN1*, *EXOSC4*, *FAAP20*, *FAM207A*, *FZD2*, *H2AX*, *LINC00863*, *LTBP3*, *MAP1S*, *MEMO1*, *MFSD3*, *MZT2B*, *NME3*, *NT5C*, *PGLS*, *RPL13*, *RPL21P28*, *RPS15*, *SCAND1*, *STUB1*, *TIGD5*, *UBE2S*, *WDR18*, and *ZNF358*. All of these 32 hub genes had lower expression in cluster 1 and higher expression in cluster 2 ($P < 0.05$, **Figure 3A**). Moreover, 8 hub genes were associated with WHO grade (**Figure 3B**) and 20 were associated with age (**Figure 3C**), but no gene was related to the sex of patients with meningioma.

Besides, we also analyzed the association of key hub genes with normal meningeal tissues and meningiomas. Further, 18 out of 32 key hub genes were included in the GSE43290 dataset, and 11 key hub genes (*CTSD*, *DNPH1*, *EPN1*, *EXOSC4*, *FZD2*, *H2AX*, *MAP1S*, *MZT2B*, *RPS15*, *STUB1*, and *WDR18*) showed significantly different expression between normal meningeal tissues and meningiomas ($P < 0.05$, **Figure 4A**).

Based on the expression profile of these 32 key genes, we divided the meningioma samples into two clusters by K-means unsupervised clustering (**Supplementary Figures 4A, B**). Based on the heatmap drawn by R language, the combination of these 32 key hub genes could help distinguish the meningioma dataset into two subtypes, indicating that these 32 key hub genes were critical for meningioma molecular subtypes (**Figure 4B**). Furthermore, we analyzed the expression of these 32 key hub genes and discovered that all these 32 key hub genes had significantly different expression levels between two different molecular

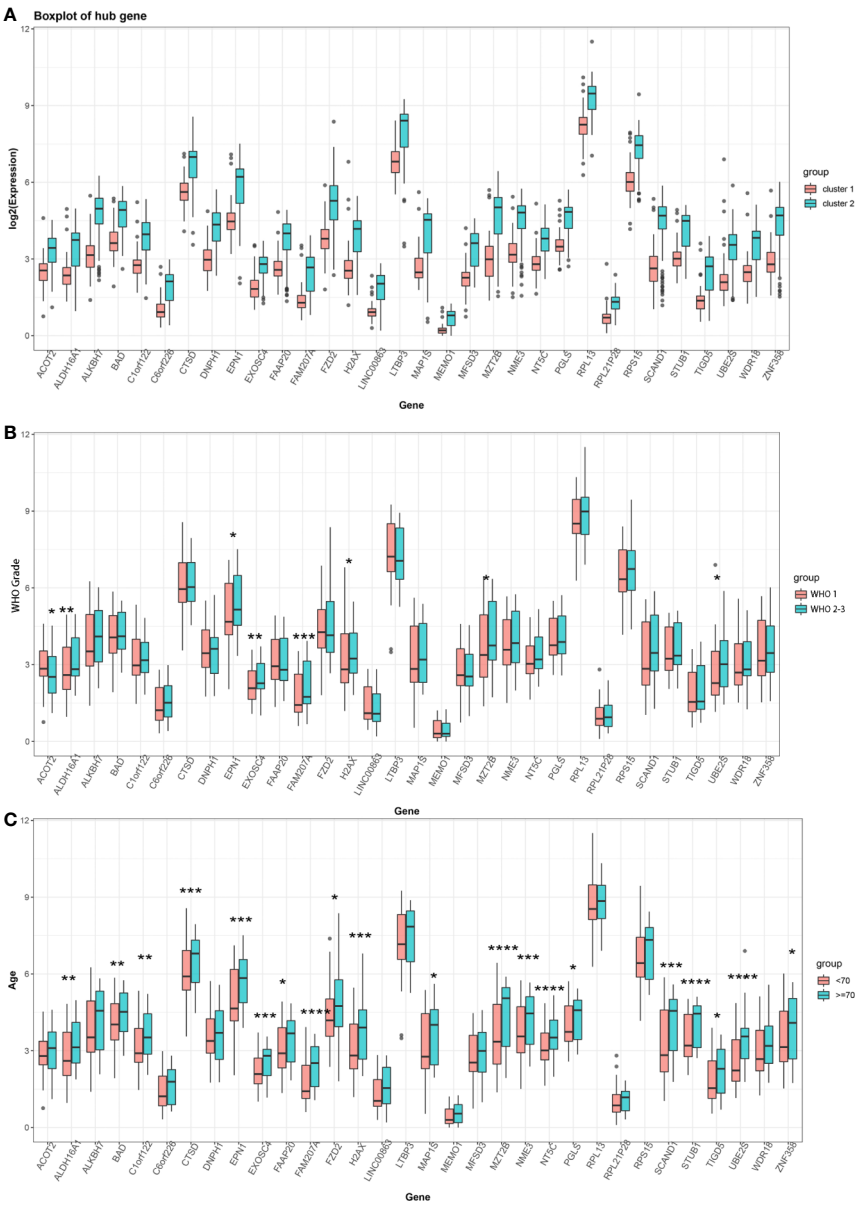

FIGURE 3 | **(A)** Expression of 32 key hub genes in two distinct m^{6}A clusters. **(B)** Expression of 32 key hub genes in different meningioma WHO grades (Grade 1 *vs* Grade 2–3). **(C)** Expression of 32 key hub genes at different ages of patients with meningioma (<70 years old *vs* ≥70 years old). (*$P < 0.05$; **$P < 0.01$; ***$P < 0.005$; ****$P < 0.001$).

subtypes. Also, all of them had lower expression in subtype 1 and higher expression in subtype 2, which uncovered that these key hub genes might function as the marker genes of different meningioma molecular subtypes (**Figure 4C**).

For a better understanding of the association of m^{6}A clusters and molecular subtypes with the sex, age, and WHO grade of patients with meningioma, we conducted a correlation analysis and found that every WHO grade was composed of two m^{6}A clusters and two molecular subtypes, and the age of patients was most likely between 30 and 70 years (**Figure 5**).

DISCUSSION

Increasing evidence revealed that m^{6}A modification played an important role in regulating tumor immunity and shaping TME through interaction with various m^{6}A regulators. However, most research focused on a single m^{6}A regulator, and the integrated roles of multiple m^{6}A regulators were not comprehensively understood, especially for meningioma.

The present study investigated the association of meningioma with multiple m^{6}A regulators, established meningioma

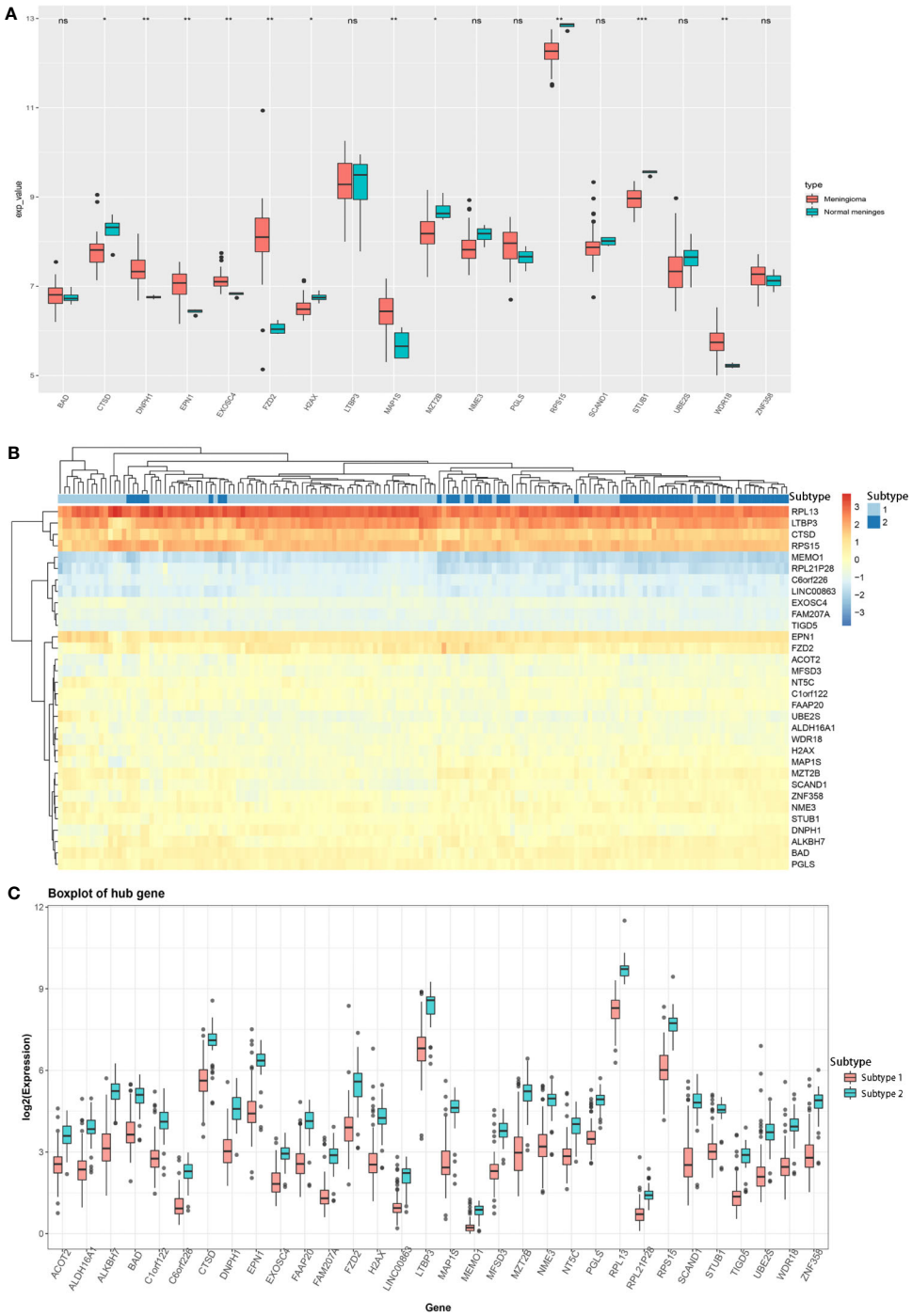

FIGURE 4 | **(A)** Expression of 18 key hub genes between normal meningeal tissues and meningioma tissues. **(B)** Heatmap of the expression of 32 key hub genes between two different meningioma molecular subtypes. **(C)** Expression of 32 key hub genes in two different meningioma molecular subtypes. (*P < 0.05; **P < 0.01; ***P < 0.005; ns, Non-significant.

classification based on m^{6}A regulator gene expression, and evaluated its merit with immune infiltration in meningioma. Based on 19 m^{6}A regulators, we constructed and segregated meningiomas into two clusters. We found that the genes of 19 m^{6}A regulators distributed widely on multiple human chromosomes and different m^{6}A regulators [e.g., (a) HNRNPA2B1 and YTHDC2; (b) LRPPRC, CBLL1, and FMR1; (c) FTO, YTHDC1, RMB15, ELAVL1, HNRNPC, and ALKBH5; and (d) YTHDF2 and WTAP] might have common effects. As for the difference between two distinct m^{6}A clusters, we revealed

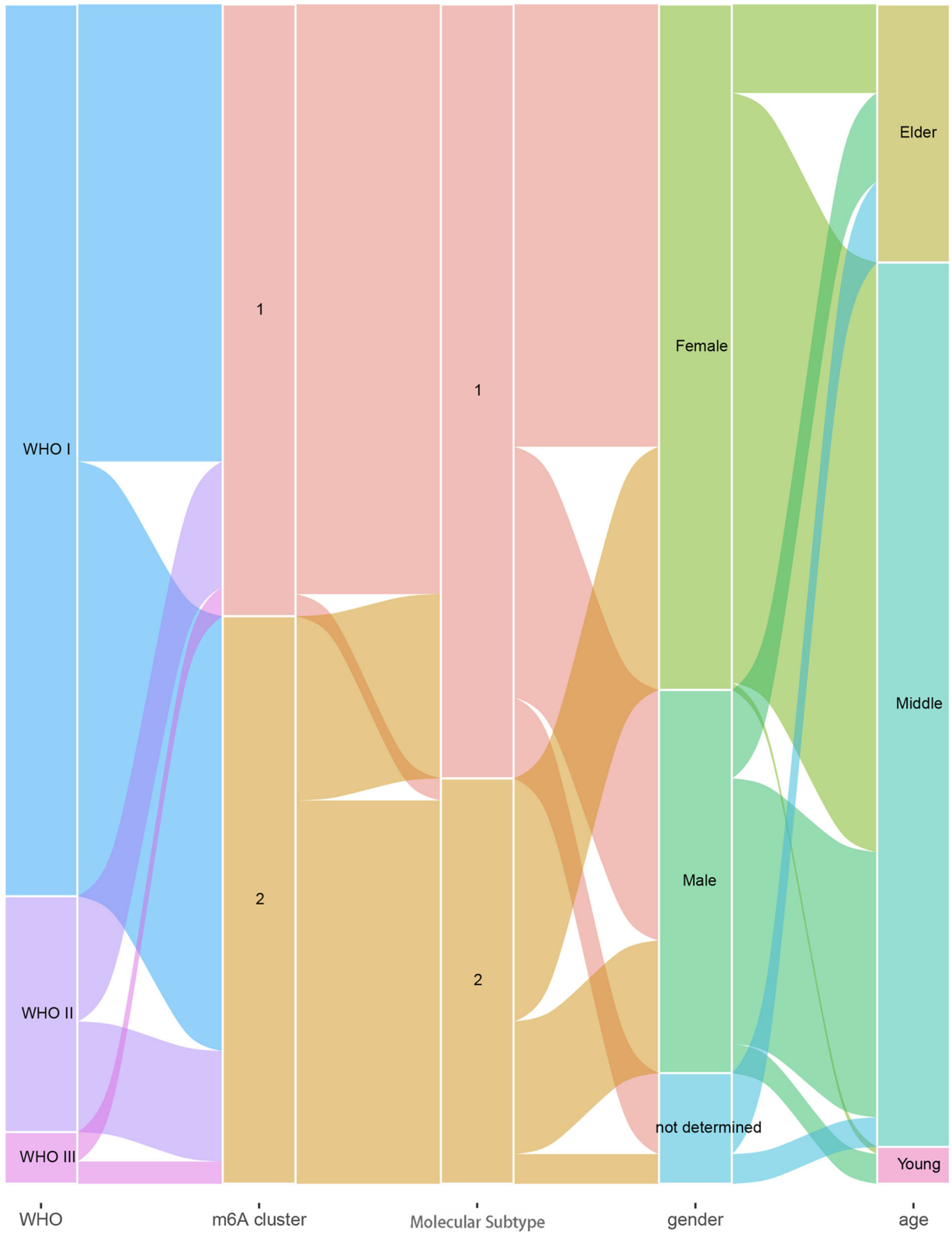

FIGURE 5 | Relation diagram of meningioma WHO grades, m^{6}A clusters, molecular subtypes, sex, and age.

that the gene expression of WTAP, ALKBH5, ELAVL1, FTO, YTHDC1, YTHDC2, HNRNPA2B1, and METTL3; the infiltration of some immune cells (plasma cells, resting mast cells, and neutrophils); and the expression of IL15 and IL18 were significantly different. A total of 1,126 DEGs were included in their different modules between the two different m^{6}A clusters, and the turquoise module containing 810 DEGs was the key module. Besides, these 810 DEGs played regulatory roles in organ and tissue generation and development and multiple important signaling pathways involved in tumor development. *ACOT2*, *ALDH16A1*, *ALKBH7*, *BAD*, *C1orf122*, *C6orf226*, *CTSD*, *DNPH1*, *EPN1*, *EXOSC4*, *FAAP20*, *FAM207A*, *FZD2*, *H2AX*, *LINC00863*, *LTBP3*, *MAP1S*, *MEMO1*, *MFSD3*, *MZT2B*, *NME3*, *NT5C*, *PGLS*, *RPL13*, *RPL21P28*, *RPS15*, *SCAND1*, *STUB1*, *TIGD5*, *UBE2S*, *WDR18*, and *ZNF358* were identified as key hub genes, and all these genes could be the marker genes to distinguish different m^{6}A clusters for their different expression. Among these DEGs, the expression of *FAM207A*, *EXOSC4*, *ALDH16A1*, *MZT2B*, *UBE2S*, *ACOT2*, *EPN1*, and *H2AX* was significantly related to WHO grades, while the expression of *UBE2S*, *FAM207A*, *NT5C*, *STUB1*, *MZT2B*, *SCAND1*, *EPN1*, *CTSD*, *EXOSC4*, *H2AX*, *NME3*, *ALDH16A1*, *C1orf122*, *BAD*, *TIGD5*, *MAP1S*, *FAAP20*, *FZD2*, *PGLS*, and *ZNF358* was significantly related to the age of patients with meningioma. Additionally, *CTSD*, *DNPH1*, *EPN1*, *EXOSC4*, *FZD2*, *H2AX*, *MAP1S*, *MZT2B*, *RPS15*, *STUB1*, and *WDR18* showed significantly different expression levels between normal meningeal tissues and meningiomas. Furthermore, the combination of these 32 DEGs could be marker genes to help in segregating meningiomas into 2 subtypes based on their gene expression. The expression of *EPN1*, *EXOSC4*, *H2AX*, and *MZT2B* was related to both WHO grades and age of patients and was significantly different between normal meningeal tissues and meningiomas.

Several studies revealed the importance of the m^{6}A modification pattern, regulated by m^{6}A regulators, for the development and progression of a tumor. Liu et al. revealed reduced m^{6}A mRNA methylation as an oncogenic mechanism in endometrial cancer and identified m^{6}A methylation as a regulator of Akt signaling (32). However, Li et al. found enhanced m^{6}A mRNA methylation as an oncogenic mechanism in hepatoblastoma because METTL3 was significantly upregulated and promoted hepatoblastoma development (33). Du et al. suggested two distinct m^{6}A modification patterns (an immune-activated differentiation pattern and an immune-desert dedifferentiation pattern) in lower-grade glioma, which were associated with different clinical outcomes, burden of neoepitope, immune infiltration, and stemness (34). The emerging functions of m^{6}A regulators in GSCs and immune infiltration have been confirmed, including roles in radio-chemotherapy resistance, tumorigenesis, promotion of the self-renewal of cancer stem cells, programmed proliferation of cancer cells, induction of apoptosis, and reduction of migration (8, 35, 36). Xu et al.'s work demonstrated the carcinogenic activity of FTO in promoting the invasion and migration of breast cancer cells *via* the FTO/miR-181b-3p/ARL5B signaling pathway, which highlighted the important role of FTO in tumor pathogenesis (37). Chang et al. uncovered an essential role of YTHDF3 in regulating the interaction between breast cancer cells and brain microenvironment by upregulating key brain metastatic proteins, thereby facilitating brain metastasis (38). Wang et al.'s research suggested that the upregulation of METTL14 could lead to the decrease of PERP mRNA levels *via* m^{6}A modification, promoting the growth, invasion, and metastasis of pancreatic cancer cells (39). Our results were consistent with the former findings. The m^{6}A regulators played an important role in meningiomas and segregated them into two distinct m^{6}A clusters, which were correlated with different m^{6}A regulator gene expression, interleukin gene expression, and immune cell infiltration. Besides, Mathoux et al. elaborated that m^{6}A was enriched in the brain and emerged as a key regulator of neuronal activity and function in processes including neurodevelopment, learning and memory, synaptic plasticity, and stress response (40). Li et al. revealed that YTHDF2, an m^{6}A regulator, functioned as a contributor to lung adenocarcinoma development through the upregulation of the AXIN1/Wnt/β-catenin signaling pathway (41). Another study revealed that m^{6}A mRNA methylation contributed significantly to regulate the Wnt/β-catenin pathway (33). Similar to the research listed earlier, our present study also found that m^{6}A modification patterns were related to several important signaling pathways in meningioma, such as Wnt signaling pathway, and development of organs and tissues in the nervous system.

With the rapid development of multi-omics and big data analysis, more research focuses on meningioma molecular subtypes. DNA methylation-based classification and grading system for meningioma had a higher power for tumor recurrence and progression prediction compared with the WHO classification (42). Another study demonstrated a highly distinct epigenetic signature of clear cell meningiomas, which was associated with frequent mutations within the SMARCE1 gene and/or loss of SMARCE1 protein expression (43). Zador et al. found that WHO grade II meningiomas could be further segregated into two distinct subgroups (a benign "grade I-like" and a malignant "grade III-like") with different tumor recurrence rates (0 and 75%, respectively) (44). Williams et al. found that the patterns of genomic alterations in high-grade/progressive meningiomas were commonly grouped into three different categories. The NF2-associated canonical group frequently harbored CDKN2A/B alterations, which was potentially amenable to targeted therapies. An NF2-agnostic group harbored frequent TERTp and TP53 mutations. An NF2-exclusive group was partly characterized by BAP1/PBRM1 alterations (rhabdoid/papillary histology) or skull-base disease (45). Also, it was of great importance to identify some marker genes to help distinguish the molecular subtypes of meningioma. EPN1 was identified as one of the hub genes in pediatric medulloblastoma by multiple-microarray analysis (46). EXOSC4 functioned as a potential oncogene in the development and progression of colorectal cancer and was identified as a potential diagnostic molecular biomarker (47).

To the best of our knowledge, *EPN1*, *EXOSC4*, *H2AX*, and *MZT2B* have not been identified as the marker genes of specific meningioma subtype.

This study had several limitations. First, the dataset we analyzed lacked survival information, and our results might have been affected by the small sample size. Therefore, improving the sample size, sequencing data, and clinical information of patients with meningioma is of great necessity in further studies. In addition, our results and conclusions are based on the bioinformatics analysis of datasets, which require further verification by basic biological experiments and clinical research.

CONCLUSIONS

In conclusion, this study suggested that the m^{6}A regulators played an important role in meningiomas and segregated them into two distinct m^{6}A clusters, which were correlated with different m^{6}A regulator gene expression, interleukin gene expression, and immune cell infiltration. Also, m^{6}A modification patterns were related to several important signaling pathways in meningioma and the development of organs and tissues in the nervous system. Among 32 key hub genes screened, *EPN1*, *EXOSC4*, *H2AX*, and *MZT2B* not only showed significant differences between meningioma molecular subtypes but also had the potential to be the marker genes of specific meningioma subtype.

DATA AVAILABILITY STATEMENT

Publicly available datasets were analyzed in this study. This data can be found here: https://www.ncbi.nlm.nih.gov/geo/query/acc.cgi?acc=GSE136661 https://www.ncbi.nlm.nih.gov/geo/query/acc.cgi?acc=GSE43290.

AUTHOR CONTRIBUTIONS

JC and YG designed the study. SS, LR, DW, and QX obtained and processed the data from GEO database. JC, SS, LH, and JD performed the data analysis. JC, HW, and MW prepared this manuscript. JD managed the research work in the subsequent revision. All authors contributed to the article and approved the submitted version.

FUNDING

This study was supported by grants from the National Key R&D Program of China (2018YFC1312600 and 2018YFC1312604 to YG), National Natural Science Foundation of China (82072788 and 81772674 to YG), Shanghai Sailing Program (20YF1403900 to LH).

SUPPLEMENTARY MATERIAL

The Supplementary Material for this article can be found online at: https://www.frontiersin.org/articles/10.3389/fonc.2021.760892/full#supplementary-material

Supplementary Figure 1 | (A, B) Best inflection point identified by the sum of squares for the error method. **(C)** Principal component analysis of two m^{6}A clusters of the GSE136661 cohort.

Supplementary Figure 2 | (A, B) Analysis of network topology for various soft-thresholding powers. **(C)** Gene dendrogram and module colors. **(D)** Module–trait relationships of different modules and m^{6}A clusters.

Supplementary Figure 3 | (A) PPI network of the turquoise module obtained from the STRING database. **(B)** Correlation analysis of the turquoise module and m^{6}A cluster characteristics. **(C)** Venn diagram of central nodes in PPI network and candidate genes in the turquoise module.

Supplementary Figure 4 | (A) Best inflection point identified by the SSE method. **(B)** Dimensionality reduction and clustering of meningioma samples conducted by the t-SNE algorithm.

REFERENCES

1. Ostrom QT, Cioffi G, Gittleman H, Patil N, Waite K, Kruchko C, et al. CBTRUS Statistical Report: Primary Brain and Other Central Nervous System Tumors Diagnosed in the United States in 2012-2016. *Neuro Oncol* (2019) 21: v1–v100. doi: 10.1093/neuonc/noz150
2. Ostrom QT, Gittleman H, de Blank PM, Finlay JL, Gurney JG, McKean-Cowdin R, et al. American Brain Tumor Ass Ociation Adolescent and Young Adult Primary Brain and Central Nervous System Tumors Diagnosed in the United States in 2008-2012. *Neuro Oncol* (2016) 18 Suppl 1:i1–i50. doi: 10.1093/neuonc/nov297
3. Grunberg SM, Weiss MH, Spitz IM, Ahmadi J, Sadun A, Russell CA, et al. Treatment of Unresectable Meningiomas With the Antiprogesterone Agent Mifepristone. *J Neurosurg* (1991) 74:861–6. doi: 10.3171/jns.1991.74.6.0861
4. Rohringer M, Sutherland GR, Louw DF, Sima AA. Incidence and Clinicopathological Features of Meningioma. *J Neurosurg* (1989) 71:665–72. doi: 10.3171/jns.1989.71.5.0665
5. Klaeboe L, Lonn S, Scheie D, Auvinen A, Christensen HC, Feychting M, et al. Incidence of Intracranial Meningiomas in Denmark, Finland, Norway and Sweden, 1968-1997. *Int J Cancer* (2005) 117:996–1001. doi: 10.1002/ijc.21255
6. Louis DN, Perry A, Wesseling P, Brat DJ, Cree IA, Figarella-Branger D, et al. The 2021 WHO Classification of Tumors of the Central Nervous System: A Summary. *Neuro Oncol* (2021) 23(8):1231–51. doi: 10.1093/neuonc/noab106
7. Roundtree IA, Evans ME, Pan T, He C. Dynamic RNA Modifications in Gene Expression Regulation. *Cell* (2017) 169:1187–200. doi: 10.1016/j.cell.2017.05.045
8. Lan Q, Liu PY, Haase J, Bell JL, Huttelmaier S, Liu T. The Critical Role of RNA M(6)A Methylation in Cancer. *Cancer Res* (2019) 79:1285–92. doi: 10.1158/0008-5472.CAN-18-2965
9. Sample A, He YY. Mechanisms and Prevention of UV-Induced Melanoma. *Photodermatol Photoimmunol Photomed* (2018) 34:13–24. doi: 10.1111/phpp.12329
10. Chen XY, Zhang J, Zhu JS. The Role of M(6)A RNA Methylation in Human Cancer. *Mol Cancer* (2019) 18:103. doi: 10.1186/s12943-019-1033-z
11. Lin Y, Wang S, Liu S, Lv S, Wang H, Li F. Identification and Verification of Molecular Subtypes With Enhanced Immune Infiltration Based on M6a Regulators in Cutaneous Melanoma. *BioMed Res Int* (2021) 2021:2769689. doi: 10.1155/2021/2769689
12. Tong J, Cao G, Zhang T, Sefik E, Amezcua Vesely MC, Broughton JP, et al. M(6)A mRNA Methylation Sustains Treg Suppressive Functions. *Cell Res* (2018) 28:253–6. doi: 10.1038/cr.2018.7

13. Pinello N, Sun S, Wong JJ. Aberrant Expression of Enzymes Regulating M(6)A mRNA Methylation: Implication in Cancer. *Cancer Biol Med* (2018) 15:323–34. doi: 10.20892/j.issn.2095-3941.2018.0365
14. Cui Q, Shi H, Ye P, Li L, Qu Q, Sun G, et al. M(6)A RNA Methylation Regulates the Self-Renewal and Tumorigenesis of Glioblastoma Stem Cells. *Cell Rep* (2017) 18:2622–34. doi: 10.1016/j.celrep.2017.02.059
15. Yang S, Wei J, Cui YH, Park G, Shah D, Deng Y, et al. M(6)A mRNA Demethylase FTO Regulates Melanoma Tumorigenicity and Response to Anti-PD-1 Blockade. *Nat Commun* (2019) 10:2782. doi: 10.1038/s41467-019-10669-0
16. Miao W, Chen J, Jia L, Ma J, Song D. The M6a Methyltransferase METTL3 Promotes Osteosarcoma Progression by Regulating the M6a Level of LEF1. *Biochem Biophys Res Commun* (2019) 516:719–25. doi: 10.1016/j.bbrc.2019.06.128
17. Vengoechea J, Sloan AE, Chen Y, Guan X, Ostrom QT, Kerstetter A, et al. Methylation Markers of Malignant Potential in Meningiomas. *J Neurosurg* (2013) 119:899–906. doi: 10.3171/2013.7.JNS13311
18. Hwang M, Han MH, Park HH, Choi H, Lee KY, Lee YJ, et al. LGR5 and Downstream Intracellular Signaling Proteins Play Critical Roles in the Cell Proliferation of Neuroblastoma, Meningioma and Pituitary Adenoma. *Exp Neurobiol* (2019) 28:628–41. doi: 10.5607/en.2019.28.5.628
19. Pitt JM, Marabelle A, Eggermont A, Soria JC, Kroemer G, Zitvogel L. Targeting the Tumor Microenvironment: Removing Obstruction to Anticancer Immune Responses and Immunotherapy. *Ann Oncol* (2016) 27:1482–92. doi: 10.1093/annonc/mdw168
20. Li YD, Veliceasa D, Lamano JB, Lamano JB, Kaur G, Biyashev D, et al. Systemic and Local Immunosuppression in Patients With High-Grade Meningiomas. *Cancer Immunol Immunother* (2019) 68:999–1009. doi: 10.1007/s00262-019-02342-8
21. Polyzoidis S, Koletsa T, Panagiotidou S, Ashkan K, Theoharides TC. Mast Cells in Meningiomas and Brain Inflammation. *J Neuroinflamm* (2015) 12:170. doi: 10.1186/s12974-015-0388-3
22. Chen X, Tian F, Lun P, Feng Y. Profiles of Immune Infiltration and Its Relevance to Survival Outcome in Meningiomas. *Biosci Rep* (2020) 40(5): BSR20200538. doi: 10.1042/BSR20200538
23. Lu B, Finn OJ. T-Cell Death and Cancer Immune Tolerance. *Cell Death Differ* (2008) 15:70–9. doi: 10.1038/sj.cdd.4402274
24. Liu Y, Cao X. Characteristics and Significance of the Pre-Metastatic Niche. *Cancer Cell* (2016) 30:668–81. doi: 10.1016/j.ccell.2016.09.011
25. Corbet C, Feron O. Tumour Acidosis: From the Passenger to the Driver's Seat. *Nat Rev Cancer* (2017) 17:577–93. doi: 10.1038/nrc.2017.77
26. Li L, Yu R, Cai T, Chen Z, Lan M, Zou T, et al. Effects of Immune Cells and Cytokines on Inflammation and Immunosuppression in the Tumor Microenvironment. *Int Immunopharmacol* (2020) 88:106939. doi: 10.1016/j.intimp.2020.106939
27. Tabernero MD, Maillo A, Gil-Bellosta CJ, Castrillo A, Sousa P, Merino M, et al. Gene Expression Profiles of Meningiomas are Associated With Tumor Cytogenetics and Patient Outcome. *Brain Pathol* (2009) 19:409–20. doi: 10.1111/j.1750-3639.2008.00191.x
28. Patel AJ, Wan YW, Al-Ouran R, Revelli JP, Cardenas MF, Oneissi M, et al. Molecular Profiling Predicts Meningioma Recurrence and Reveals Loss of DREAM Complex Repression in Aggressive Tumors. *Proc Natl Acad Sci USA* (2019) 116:21715–26. doi: 10.1073/pnas.1912858116
29. Zhang B, Wu Q, Li B, Wang D, Wang L, Zhou YL. M(6)A Regulator-Mediated Methylation Modification Patterns and Tumor Microenvironment Infiltration Characterization in Gastric Cancer. *Mol Cancer* (2020) 19:53. doi: 10.1186/s12943-020-01170-0
30. Steen CB, Liu CL, Alizadeh AA, Newman AM. Profiling Cell Type Abundance and Expression in Bulk Tissues With CIBERSORTx. *Methods Mol Biol* (2020) 2117:135–57. doi: 10.1007/978-1-0716-0301-7_7
31. Jiao X, Sherman BT, Huang da W, Stephens R, Baseler MW, Lane HC, et al. DAVID-WS: A Stateful Web Service to Facilitate Gene/Protein List Analysis. *Bioinformatics* (2012) 28:1805–6. doi: 10.1093/bioinformatics/bts251
32. Liu J, Eckert MA, Harada BT, Liu SM, Lu Z, Yu K, et al. M(6)A mRNA Methylation Regulates AKT Activity to Promote the Proliferation and Tumorigenicity of Endometrial Cancer. *Nat Cell Biol* (2018) 20:1074–83. doi: 10.1038/s41556-018-0174-4
33. Liu L, Wang J, Sun G, Wu Q, Ma J, Zhang X, et al. M(6)A mRNA Methylation Regulates CTNNB1 to Promote the Proliferation of Hepatoblastoma. *Mol Cancer* (2019) 18:188. doi: 10.1186/s12943-019-1119-7
34. Du J, Ji H, Ma S, Jin J, Mi S, Hou K, et al. M6a Regulator-Mediated Methylation Modification Patterns and Characteristics of Immunity and Stemness in Low-Grade Glioma. *Brief Bioinform* (2021) 22(5):bbab013. doi: 10.1093/bib/bbab013
35. Huang H, Weng H, Chen J. M(6)A Modification in Coding and Non-Coding RNAs: Roles and Therapeutic Implications in Cancer. *Cancer Cell* (2020) 37:270–88. doi: 10.1016/j.ccell.2020.02.004
36. Dong Z, Cui H. The Emerging Roles of RNA Modifications in Glioblastoma. *Cancers (Basel)* (2020) 12(3):L736. doi: 10.3390/cancers12030736
37. Xu Y, Ye S, Zhang N, Zheng S, Liu H, Zhou K, et al. The FTO/miR-181b-3p/ARL5B Signaling Pathway Regulates Cell Migration and Invasion in Breast Cancer. *Cancer Commun (Lond)* (2020) 40:484–500. doi: 10.1002/cac2.12075
38. Chang G, Shi L, Ye Y, Shi H, Zeng L, Tiwary S, et al. YTHDF3 Induces the Translation of M(6)A-Enriched Gene Transcripts to Promote Breast Cancer Brain Metastasis. *Cancer Cell* (2020) 38:857–71.e857. doi: 10.1016/j.ccell.2020.10.004
39. Wang M, Liu J, Zhao Y, He R, Xu X, Guo X, et al. Upregulation of METTL14 Mediates the Elevation of PERP mRNA N(6) Adenosine Methylation Promoting the Growth and Metastasis of Pancreatic Cancer. *Mol Cancer* (2020) 19:130. doi: 10.1186/s12943-020-01249-8
40. Mathoux J, Henshall DC, Brennan GP. Regulatory Mechanisms of the RNA Modification M(6)A and Significance in Brain Function in Health and Disease. *Front Cell Neurosci* (2021) 15:671932. doi: 10.3389/fncel.2021.671932
41. Li Y, Sheng H, Ma F, Wu Q, Huang J, Chen Q, et al. RNA M(6)A Reader YTHDF2 Facilitates Lung Adenocarcinoma Cell Proliferation and Metastasis by Targeting the AXIN1/Wnt/beta-Catenin Signaling. *Cell Death Dis* (2021) 12:479. doi: 10.1038/s41419-021-03763-z
42. Sahm F, Schrimpf D, Stichel D, Jones DTW, Hielscher T, Schefzyk S, et al. DNA Methylation-Based Classification and Grading System for Meningioma: A Multicentre, Retrospective Analysis. *Lancet Oncol* (2017) 18:682–94. doi: 10.1016/S1470-2045(17)30155-9
43. Sievers P, Sill M, Blume C, Tauziede-Espariat A, Schrimpf D, Stichel D, et al. Clear Cell Meningiomas Are Defined by a Highly Distinct DNA Methylation Profile and Mutations in SMARCE1. *Acta Neuropathol* (2021) 141:281–90. doi: 10.1007/s00401-020-02247-2
44. Zador Z, Landry AP, Saha A, Cusimano MD. Gene Expression Signatures Identify Biologically Homogenous Subgroups of Grade 2 Meningiomas. *Front Oncol* (2020) 10:541928. doi: 10.3389/fonc.2020.541928
45. Williams EA, Santagata S, Wakimoto H, Shankar GM, Barker FG 2nd, Sharaf R, et al. Distinct Genomic Subclasses of High-Grade/Progressive Meningiomas: NF2-Associated, NF2-Exclusive, and NF2-Agnostic. *Acta Neuropathol Commun* (2020) 8:171. doi: 10.1186/s40478-020-01040-2
46. Huang P, Guo YD, Zhang HW. Identification of Hub Genes in Pediatric Medulloblastoma by Multiple-Microarray Analysis. *J Mol Neurosci* (2020) 70:522–31. doi: 10.1007/s12031-019-01451-4
47. Pan Y, Tong JHM, Kang W, Lung RWM, Chak WP, Chung LY, et al. EXOSC4 Functions as a Potential Oncogene in Development and Progression of Colorectal Cancer. *Mol Carcinog* (2018) 57:1780–91. doi: 10.1002/mc.22896

Conflict of Interest: The authors declare that the research was conducted in the absence of any commercial or financial relationships that could be construed as a potential conflict of interest.

Publisher's Note: All claims expressed in this article are solely those of the authors and do not necessarily represent those of their affiliated organizations, or those of the publisher, the editors and the reviewers. Any product that may be evaluated in this article, or claim that may be made by its manufacturer, is not guaranteed or endorsed by the publisher.

Copyright © 2021 Chen, Sun, Ren, Hua, Wang, Xie, Wirsching, Deng, Weller and Gong. This is an open-access article distributed under the terms of the Creative Commons Attribution License (CC BY). The use, distribution or reproduction in other forums is permitted, provided the original author(s) and the copyright owner(s) are credited and that the original publication in this journal is cited, in accordance with accepted academic practice. No use, distribution or reproduction is permitted which does not comply with these terms.

frontiers in Oncology

ORIGINAL RESEARCH
published: 04 January 2022
doi: 10.3389/fonc.2021.792521

Non-Invasive Preoperative Imaging Differential Diagnosis of Intracranial Hemangiopericytoma and Angiomatous Meningioma: A Novel Developed and Validated Multiparametric MRI-Based Clini-Radiomic Model

Yanghua Fan[1,2†], Panpan Liu[1,3†], Yiping Li[4], Feng Liu[5], Yu He[6], Liang Wang[1], Junting Zhang[1*] and Zhen Wu[1*]*

[1] Department of Neurosurgery, Beijing Tiantan Hospital, Capital Medical University, Beijing, China, [2] Department of Neurosurgery, Beijing Neurosurgical Institute, Beijing, China, [3] Department of Neurosurgery, Weihai Municipal Hospital, Cheeloo College of Medicine, Shandong University, Weihai, China, [4] Department of Gastroenterology, Weihai Municipal Hospital, Cheeloo College of Medicine, Shandong University, Weihai, China, [5] Department of Neurosurgery, Jiangxi Provincial Children's Hospital, The Affiliated Children's Hospital of Nanchang University, Nanchang, China, [6] Department of Craniomaxillofacial Surgery, Plastic Surgery Hospital, Chinese Academy of Medical Sciences & Peking Union Medical College, Beijing, China

OPEN ACCESS

Edited by:
Hailiang Tang,
Fudan University, China

Reviewed by:
Tingfan Wu,
GE Healthcare, China
Xiaohua Qian,
Shanghai Jiao Tong University, China

***Correspondence:**
Zhen Wu
wz_ttyy@163.com
Junting Zhang
zhangjunting2003@aliyun.com
Liang Wang
ttyywangliang@163.com

†These authors have contributed equally to this work

Specialty section:
This article was submitted to Neuro-Oncology and Neurosurgical Oncology, a section of the journal Frontiers in Oncology

Received: *10 October 2021*
Accepted: *29 November 2021*
Published: *04 January 2022*

Citation:
Fan Y, Liu P, Li Y, Liu F, He Y, Wang L, Zhang J and Wu Z (2022) Non-Invasive Preoperative Imaging Differential Diagnosis of Intracranial Hemangiopericytoma and Angiomatous Meningioma: A Novel Developed and Validated Multiparametric MRI-Based Clini-Radiomic Model. Front. Oncol. 11:792521. doi: 10.3389/fonc.2021.792521

Background: Accurate preoperative differentiation of intracranial hemangiopericytoma and angiomatous meningioma can greatly assist operation plan making and prognosis prediction. In this study, a clini-radiomic model combining radiomic and clinical features was used to distinguish intracranial hemangiopericytoma and hemangioma meningioma preoperatively.

Methods: A total of 147 patients with intracranial hemangiopericytoma and 73 patients with angiomatous meningioma from the Tiantan Hospital were retrospectively reviewed and randomly assigned to training and validation sets. Radiomic features were extracted from MR images, the elastic net and recursive feature elimination algorithms were applied to select radiomic features for constructing a fusion radiomic model. Subsequently, multivariable logistic regression analysis was used to construct a clinical model, then a clini-radiomic model incorporating the fusion radiomic model and clinical features was constructed for individual predictions. The calibration, discriminating capacity, and clinical usefulness were also evaluated.

Results: Six significant radiomic features were selected to construct a fusion radiomic model that achieved an area under the curve (AUC) value of 0.900 and 0.900 in the training and validation sets, respectively. A clini-radiomic model that incorporated the radiomic model and clinical features was constructed and showed good discrimination and calibration, with an AUC of 0.920 in the training set and 0.910 in the validation set. The

analysis of the decision curve showed that the fusion radiomic model and clini-radiomic model were clinically useful.

Conclusions: Our clini-radiomic model showed great performance and high sensitivity in the differential diagnosis of intracranial hemangiopericytoma and angiomatous meningioma, and could contribute to non-invasive development of individualized diagnosis and treatment for these patients.

Keywords: intracranial hemangiopericytoma, angiomatous meningioma, radiomics, algorithm, diagnosis

INTRODUCTION

Intracranial hemangiopericytoma is a rare mesenchymal tumor with strong aggressiveness and high degree of vascularization (1). Many features of intracranial hemangiopericytoma are similar to meningioma; intracranial hemangiopericytoma and meningioma both originate from the meninges and have similar imaging features. In particular, angiomatous meningioma with invasive image but benign behavior is difficult to distinguish from intracranial hemangiopericytoma before operation. However, angiomatous meningioma and intracranial hemangiopericytoma have different histological characteristics and biological behaviors (2). Angiomatous meningioma is a rare benign variant tumor classified as WHO grade 1 meningioma. Compared with angiomatous meningiomas, intracranial hemangiopericytoma is classified as a malignant tumor (WHO grades II–III) with the tendency of recurrence and metastasis (3). Intracranial hemangiopericytoma is more aggressive, highly vascularized and prone to intraoperative hemorrhage, has a higher postoperative recurrence rate and a worse prognosis (1).

More preoperative preparation is needed to ensure the maximum surgical resection and safety for intracranial hemangiopericytoma, such as more detailed surgical strategy, preoperative tumor feeding artery embolization, the use of intraoperative navigation equipment, and more adequate spare blood (4, 5). Therefore, their preoperative preparation and treatment principles are largely different thus the preoperative differential diagnosis is crucial. The high overlap of the radiological characteristics of intracranial hemangiopericytoma and angiomatous meningioma poses a great challenge to the preoperative imaging identification (2). Although intracranial hemangiopericytoma is usually male and the age of onset is relatively early, it is difficult to diagnose based on this (6). Previous studies have shown that radiomic features may help distinguish intracranial hemangiopericytoma from meningioma (7), but more attention should be paid to the identification of angiomatous meningioma and intracranial hemangiopericytoma, which are more likely to be confused in the clinic.

Radiomics emerges as a potent approach for the non-invasive high-throughput mining of tumor characteristics (8, 9). Neuro-oncologic radiomic studies can potentially mine the hidden data that cannot be obtained through single-parameter and conventional imaging approach; meanwhile, they can also enhance the accuracy and effectiveness in the differential diagnosis for intracranial tumor (10–12). Due to a relatively low incidence, previous studies (13) on the identification of angiomatous meningioma and intracranial hemangiopericytoma have many shortcomings such as the small number of patients included and no verification set. Consequently, based on a relatively large number of patients, the purpose of this study is to establish a clini-radiomic combined model that combines radiomic and clinical features to distinguish intracranial hemangiopericytoma and angiomatous meningioma before surgery, and to assist in preoperative planning for the management and treatment of the two types of tumors.

MATERIALS AND METHODS

Patients

A total of 220 patients (Angiomatous meningioma: n = 73; Hemangiopericytoma: n = 147) were included from the Beijing Tiantan Hospital, Capital Medical University. The inclusion criteria of enrolled patients in this study were as follows: 1) intracranial hemangiopericytoma or atypical meningioma patients who underwent initial tumor resection surgery from 2010 to 2019 at the Beijing Tiantan Hospital; 2) available postoperative pathological diagnosis results information; 3) patient underwent preoperative head T2-weighted imaging (T2WI) and contrast-enhanced T1-weighted imaging (CE-T1WI) MRI examination; and 4) complete clinical information at initial diagnosis. All included patients were randomized to the training set (used for model building, n = 147) and validation set (used for model validation, n = 73) at a ratio of 2:1.

Clinical Characteristics

Seven preoperative clinical characteristics from all included patients were collected: age, gender, location 1 (supratentorial or infratentorial), location 2 (skull base or non-skull base), location 3 (paravenous sinus or non-paravenous sinus), dural tail (negative or positive), and peritumoral serious edema (negative or positive). Moreover, the patient's postoperative pathological results determine whether it is angiomatous

Abbreviations: HPC, hemangiopericytoma; T2WI, T2-weighted imaging; CE-T1WI, contrast-enhanced T1-weighted imaging; ROI, regions of interest; GLCM, gray level co-occurrence matrix; GLRLM, gray level run-length matrix; LASSO, least absolute shrinkage and selection operator; RFE, recursive feature elimination; ROC, receiver operating characteristic; AIC, Akaike information criterion; AUC, area under curve; DCA, Decision curve analysis; ACC, accuracy; PPV, positive predictive value; NPV, negative predictive value.

meningioma or hemangiopericytoma that needs to be collected. According to the WHO pathology guidelines (3), angiomatous meningioma is defined as meningioma with >50% vascular components (14).

Regions of Interest (ROI) Delineating and Radiomic Feature Extraction

The flowchart and scheme of this study are similarly described in detail in our previous researches (15, 16). All patients underwent preoperative brain T2WI and CE-T1WI MR imaging. CE-T1WI was carried out the T1WI sequence parameters after rapid injection of a gadolinium-DTPA contrast agent. A neuroradiologist with 8 years of experience used ITK-SNAP software to map the three-dimensional ROIs of the tumor on T2WI and CE-T1WI MR imaging. Then, another neurosurgeon with 13 years of experience reviewed, modified, and confirmed the above segmentation results. Any disagreements between the two neuroradiologists are resolved through mutual consultation.

Then, the PyRadiomics algorithm (Version 2.1.2; https://github.com/Radiomics/pyradiomics) was used to extract quantitative four types of 1,562 radiomic features from the above segmented ROI, all features are standardized to a value of 0 to 1 (12, 17). The four types of features were described as follows (15, 18): 1) shape and size features (n = 14) were independent of the gray-scale intensity distribution of the tumor; 2) the first-order statistics (n = 180) described the distribution of voxel intensity in the image through basic metrics; 3) Texture features (n = 680) are calculated from the gray-level co-occurrence matrix (GLCM) and gray-level run-length matrix (GLRLM), respectively, to describe the pattern or the spatial distribution of voxel intensity; and 4) Wavelet features (n = 688) transform effectively decouples textural information by decomposing the original image at low and high frequencies in a manner similar to Fourier analysis.

Radiomic Features Selection and Fusion Radiomic Model Construction

After radiomic feature extraction, a selection process is adopted to reduce overfitting (19). First, the Mann–Whitney U test was used to determine the significantly different radiomic features of patients with intracranial hemangiopericytoma and atypical meningioma. Then, the elastic net algorithm (20), a method that combines the minimum absolute shrinkage and selection operator (LASSO) and ridge regression, was used to select the most informative features. LASSO is a commonly used high-dimensional data analysis method, which can improve the prediction accuracy and interpretation ability (21). Finally, recursive feature elimination (RFE) is used to determine the final radiomic features through a five-time cross-validation algorithm.

Through the support vector machine (SVM) method of training set, a T1 radiomic model, a T2 radiomic model, and a fusion radiomic model were constructed from the meaningful features selected from the separate CE-T1WI radiomic feature, separate T2WI radiomic features, and mixed CE-T1WI and T2WI radiomic features, respectively.

Construction and Validation of Clinical and Clini-Radiomic Model

Multivariable logistic regression analysis was applied to construct a clinical model based on all included clinical features. Then, to establish a more accurate and comprehensive model for discriminating the hemangiopericytoma and angiomatous meningioma, a clini-radiomic model was constructed by combining the above clinical model with the fusion radiomic model. The structure and parameters of the clini-radiomic model was presented as a nomogram.

Calibration Curve Analysis and Decision Curve Analysis

Calibration curves and the Hosmer–Lemeshow test were used to assess the similarity between the observed pathological results and predicted diagnosis results of fusion radiomic model and clini-radiomic model (22). Decision curve analysis (DCA) was performed to evaluate the clinical application of the fusion radiomic model and clini-radiomic model by quantifying the net benefits at different threshold probabilities (23).

Statistical Analysis

A two-sided *P*-value of <0.05 was deemed to be statistically significant. Categorical variables were presented as the number (percentage). Continuous variables consistent with a normal distribution were presented as mean ± standard deviation, otherwise the median and quartile are used. Chi-Square test was used to compare the differences in categorical variables. The independent sample t-test was used to compare the differences in continuous variables that conform to the normal distribution, otherwise the nonparametric test was used to compare the differences in continuous variables with non-normal distribution.

The statistical software R (version 3.4.1, R Foundation for Statistical Computing, Vienna, Austria) was used to perform the statistical analysis. The violin plot algorithm was used to show the differences in the signature distribution of fusion radiomic model between intracranial hemangiopericytoma and atypical meningiomas in the training set and validation set. The receiver operating characteristic (ROC) curve was used to show the predicted value of the above constructed models (24). The calibration plot was analyzed with the 'hdnom' packages. The decision curve analysis is performed by the "dca.R: function written by us in the software R. The DeLong's test was used to compare the prediction performance differences of the constructed models.

RESULTS

Clinical Characteristics

According to the inclusion and exclusion criteria, 220 patients with intracranial hemangiopericytoma or angiomatous meningioma were identified and included in this study. The mean age at diagnosis was 49.0 (37.0–55.0) years, with a female-to-male ratio of 1.157:1 (118/102). Of the 220 patients, 80

(36.4%) patients had peritumoral edema, and 29 (13.2%) patients had dural tail in CET1 images. A total of 147 (66.8%) patients were pathologically diagnosed as intracranial hemangiopericytoma and 73 (33.2%) patients were diagnosed as angiomatous meningioma. All included clinical characteristics are summarized in **Table 1**.

All patients were randomly divided into a training set (n = 147) and a validation set (n = 73). There was no significant interclass difference in terms of age (P = 0.900), gender (P = 0.965), locations 1, 2, and 3 (P = 0.140, 0.656, and 0.233), dural tail (P = 0.153), peritumoral edema (P = 0.465), and diagnosis (P = 0.946) between the training set and the validation set (**Table 1**). The results justify the use of the two datasets for training and testing.

Univariate Analysis of Clinical Characteristics and Postoperative Pathological Diagnosis

As shown in **Table 2**, age, location 1, location 2, location 3, dural tail, and peritumoral edema showed significant relationships with postoperative pathological diagnosis (all P <0.05). The results demonstrated that elder patients who had infratentorial, non-skull base, paravenous sinus, dural tail or peritumoral serious edema tumor were more likely to have angiomatous meningioma. Conversely, we found no significant differences in gender (P = 0.965) between the intracranial hemangiopericytoma and angiomatous meningioma patients.

As shown in **Table 3**, univariate analysis was used to determine the independent clinical risk features for postoperative pathological diagnosis in the training and the validation sets, respectively. Similar to the previous results, in the training set, we found a significant association between pathological diagnosis and age (P = 0.007), location 1 (P = 0.001), location 2 (P = 0.030), location 3 (P = 0.010), dural tail (P = 0.009), and peritumoral edema (P <0.0001). In the validation set, age (P = 0.003), location 1 (P = 0.467), dural tail (P <0.0001), and peritumoral edema (P = 0.001) tended to be associated with pathological diagnosis.

Radiomic Feature Selection and Radiomic Model Construction

Based on the extracted 1,562 CE-T1WI radiomic features, 262 radiomic features were selected by Mann–Whitney U test. Then, we use 'elastic net' algorithm to determine 21 informative features. Through the screening by RFE algorithm with 5-fold cross validation, 2 CE-T1WI radiomic features were selected as the final features for subsequent use. The selected two CE-T1WI radiomic features were entered into an SVM to build a T1 radiomic model, which showed discrimination in predicting the postoperative pathological diagnosis with AUC values of 0.840 (95% confidence interval [CI], 0.814–0.863) and 0.750 (95% CI, 0.718–0.788) in the training and validation sets, respectively (**Figure 1A**). Similar to the previous, 9 T2WI radiomic features were selected and then entered into an SVM to build a T2 radiomic model, with AUC value of 0.850 (95% CI, 0.829–0.879) in the training set and 0.850 (95% CI, 0.828-0.873) in the validation set (**Figure 1B**). The DeLong's test showed that there was no significant difference between the T1 and T2 radiomic models (P = 0.275).

Finally, among the 3,124 mixed CE-T1WI and T2WI radiomic features, 399 radiomic features were selected by Mann–Whitney U test. 'Elastic net' algorithm was used to determine 37 informative features. Finally, through the screening by RFE algorithm with 5-fold cross validation, 6 radiomic features (2 first order feature and 4 texture features) that gave the best performance were selected as the final features for subsequent use. Only 1 feature was selected from the CE-T1WI images, and

TABLE 1 | Patients' characteristics of training and validation sets.

Characteristics	All sets (n = 220)	Training set (n = 147)	Validation set (n = 73)	P-value
Age (year)	49.0 (37.0–55.0)	49.0 (35.0–56.0)	49.0 (40.0–54.0)	0.900
Gender				
Female	118 (53.6%)	79 (53.7%)	39 (51.5%)	0.965
Male	102 (46.4%)	68 (46.3%)	34 (48.5%)	
Location 1				
Supratentorial	181 (82.3%)	117 (79.6%)	64 (87.7%)	0.140
Infratentorial	39 (17.7%)	30 (20.4%)	9 (12.3%)	
Location 2				
Non skull base	152 (69.1%)	103 (70.1%)	49 (67.1%)	0.656
Skull base	68 (30.9%)	44 (29.9%)	24 (32.9%)	
Location 3				
Non paravenous sinus	111 (50.5%)	70 (47.6%)	41 (56.2%)	0.233
Paravenous sinus	109 (49.5%)	77 (52.4%)	32 (43.8%)	
Dural tail				
Negative	191 (86.8%)	131 (89.1%)	60 (82.2%)	0.153
Positive	29 (13.2%)	16 (10.9%)	13 (17.8%)	
Peritumoral edema				
Negative	140 (63.6%)	96 (65.3%)	44 (60.3%)	0.465
Positive	80 (36.4%)	51 (34.7%)	29 (39.7%)	
Diagnosis				
Angiomatous meningioma	73 (33.2%)	49 (33.3%)	24 (32.9%)	0.946
Hemangiopericytoma	147 (66.8%)	98 (66.7%)	49 (67.1%)	

TABLE 2 | Clinical characteristics of patients with intracranial hemangiopericytoma and angiomatous meningioma.

Characteristics	All patients (n = 220)	Angiomatous meningioma (n = 73)	Hemangiopericytoma (n = 147)	P-value
Age (year)	49.0 (37.0–55.0)	53.0 (44.5–59.0)	46.0 (35.0–53.0)	0.000
Gender				
Female	118 (53.6%)	39 (53.4%)	79 (53.7%)	0.965
Male	102 (46.4%)	34 (46.6%)	68 (46.3%)	
Location 1				
Supratentorial	181 (82.3%)	69 (94.5%)	112 (76.2%)	0.001
Infratentorial	39 (17.7%)	4 (5.5%)	35 (23.8%)	
Location 2				
Non skull base	152 (69.1%)	57 (78.1%)	95 (64.6%)	0.042
Skull base	68 (30.9%)	16 (21.9%)	52 (35.4%)	
Location 3				
Non paravenous sinus	111 (50.5%)	29 (39.7%)	82 (55.8%)	0.025
Paravenous sinus	109 (49.5%)	44 (60.3%)	65 (44.2%)	
Dural tail				
Negative	191 (86.8%)	51 (69.9%)	140 (95.2%)	0.000
Positive	29 (13.2%)	22 (30.1%)	7 (4.8%)	
Peritumoral edema				
Negative	140 (63.6%)	27 (37.0%)	113 (76.9%)	0.000
Positive	80 (36.4%)	46 (63.0%)	34 (46.3%)	

5 features from the T2WI images. All 6 selected radiomic features had significant differences between patients with intracranial hemangiopericytoma and angiomatous meningioma (All P <0.0001, **Table 4** and **Figure 2**). All 6 selected features were used to build a fusion radiomic model. The violin plot showed significant differences in the signature distribution of fusion radiomic model between intracranial hemangiopericytoma and angiomatous meningioma in both training and validation sets (all P <0.01; **Figure 3**). The fusion radiomic model showed favorable discrimination in predicting the postoperative pathological diagnosis with AUC values of 0.900 (95% CI, 0.879–0.916) and 0.900 (95% CI, 0.879–0.919) in the training and validation sets, respectively (**Figure 1C**). The results of DeLong's test showed that the fusion radiomic model performed significantly better than the T1 radiomic model (P = 0.013), but there was no significant difference between the fusion radiomic model and T2 radiomic model (P = 0.189).

Moreover, the calibration curve analysis and Hosmer–Lemeshow test for fusion radiomic model demonstrated good agreement between observations and predictions in the training set (P = 0.211; **Figure 4A**) and the validation set (P = 0.407; **Figure 4B**). The DCA of the fusion radiomic model is presented in **Figures 4C, D**. The fusion radiomic model clearly provided a net benefit over the two schemes, with a threshold probability

TABLE 3 | Univariate analysis of clinical characteristics of intracranial hemangiopericytoma and angiomatous meningioma patients in the training set and validation set.

Characteristics	Training set (n = 147)		P-value	Validation set (n = 73)		P-value
	Angiomatous meningioma (n = 49)	Hemangiopericytoma (n = 98)		Angiomatous meningioma (n = 24)	Hemangiopericytoma (n = 49)	
Age (year)	54.0 (43.0–58.5)	46.5 (32.75–54.25)	0.007	51.0 (47.5–60.75)	46.0(37.0-51.0)	0.003
Gender						
Female	25 (51.0%)	54 (55.1%)	0.640	14 (58.3%)	25 (51.0%)	0.556
Male	24 (49.0%)	44 (44.9%)		10 (41.7%)	24 (49.0%)	
Location 1						
Supratentorial	47 (95.9%)	70 (71.4%)	0.001	22 (91.7%)	42 (85.7%)	0.467
Infratentorial	2 (4.1%)	28 (28.6%)		2 (8.3%)	7 (14.3%)	
Location 2						
Non skull base	40 (81.6%)	63 (64.3%)	0.030	17 (70.8%)	32 (65.3%)	0.637
Skull base	9 (18.4%)	35 (35.7%)		7 (29.2%)	17 (34.7%)	
Location 3						
Non paravenous sinus	16 (32.7%)	54 (55.1%)	0.010	13 (54.2%)	28 (57.1%)	0.810
Paravenous sinus	33 (67.3%)	44 (44.9%)		11 (45.8%)	21 (42.9%)	
Dural tail						
Negative	39 (79.6%)	92 (93.9%)	0.009	12 (50.0%)	48 (98.0%)	0.000
Positive	10 (20.4%)	6 (6.1%)		12 (50.0%)	1 (2.0%)	
Peritumoral edema						
Negative	19 (38.8%)	77 (78.6%)	0.000	8 (33.3%)	36 (73.5%)	0.001
Positive	30 (61.2%)	21 (21.4%)		16 (66.7%)	13 (26.5%)	

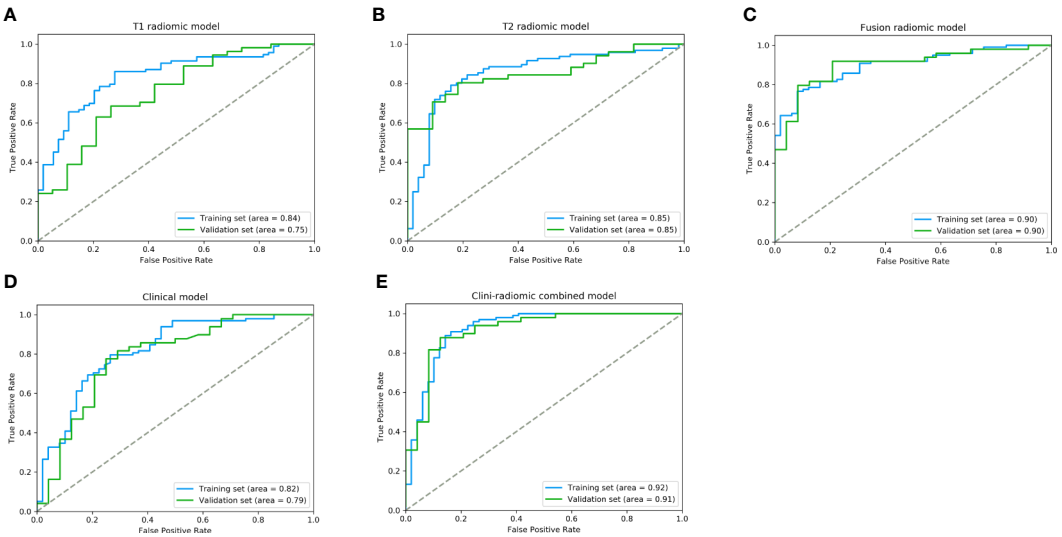

FIGURE 1 | The performance of ROC curves for the predictive models the training and validation sets. **(A)** T1 radiomic model; **(B)** T2 radiomic model; **(C)** fusion radiomic model; **(D)** Clinical model; and **(E)** Clini-radiomic combined model.

of >5 and >20% for the training and validation sets, respectively, suggesting the clinical usefulness of the fusion radiomic model.

Performance of Clinical and Clini-Radiomic Combined Model

The seven available clinical features in the training set were used to build a clinical model based on multivariable logistic regression analysis. We then verified the performance of these models in the validation set. As shown in **Figure 1D**, the AUCs were 0.820 (95% CI, 0.790–0.847) and 0.790 (95% CI, 0.753–0.818) in the training and validation sets, respectively.

In addition, the above clinical model and signature of fusion radiomic model were determined to establish the clini-radiomic combined model, yielded an AUC of 0.920 (95% CI, 0.902–0.942) in the training set and 0.910 (95% CI, 0.894–0.935) in the validation set (**Figure 1E**). The clini-radiomic combined model's

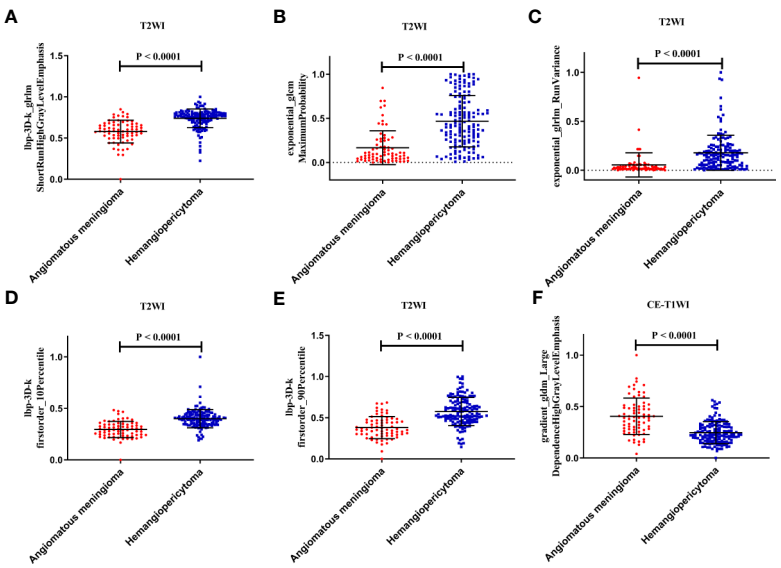

FIGURE 2 | The six selected radiomic features had significant differences between patients with intracranial hemangiopericytoma and angiomatous meningiomas. **(A)** lbp-3D-k_glrlmShortRunHighGrayLevelEmphasis; **(B)** exponential_glcm MaximumProbability; **(C)** exponential_glrlm_RunVariance; **(D)** lbp-3D-k firstorder_10Percentile; **(E)** lbp-3D-k firstorder_90Percentile; and **(F)** gradient_gldm_Large DependenceHighGrayLevelEmphasis.

TABLE 4 | Detail information of six selected key radiomic features.

Sequence	Feature name	Feature type	Angiomatous meningioma (n = 73)	Hemangiopericytoma (n = 147)	P-value
T2WI	lbp-3D-k_glrlm ShortRunHighGrayLevelEmphasis	Texture	0.5791 ± 0.0163	0.7400 ± 0.0093	0.0001
	exponential_glcm MaximumProbability	Texture	0.1670 ± 0.0224	0.4673 ± 0.0240	0.0001
	exponential_glrlm_RunVariance	Texture	0.0546 ± 0.0144	0.1784 ± 0.0148	0.0001
	lbp-3D-k firstorder_10Percentile	Firstorder	0.2953 ± 0.0092	0.4000 ± 0.0072	0.0001
	lbp-3D-k firstorder_90Percentile	Firstorder	0.3802 ± 0.0157	0.5754 ± 0.0141	0.0001
CET1	gradient_gldm_Large DependenceHighGrayLevelEmphasis	Texture	0.4053 ± 0.0207	0.2464 ± 0.0088	0.0001

T2WI, T2-weighted imaging; CE-T1WI, contrast-enhanced T1-weighted imaging.

predictive accuracy of tumor diagnosis was 0.884 (0.865–0.905) in the training set and 0.863 (0.842–0.883) in the validation set. The detailed predictive indicators of the aforementioned models are shown in **Table 5**. Bar plots showed the accuracy of clini-radiomic model in the diagnosis of intracranial hemangiopericytoma or angiomatous meningioma (**Figure 5**). As shown in **Figure 6**, the clini-radiomic combined model is presented as a nomogram. The DeLong's test showed that the clini-radiomic combined model and fusion radiomic model performed significantly better than the clinical model (P <0.01), but there was no significant difference between the clini-radiomic combined model and fusion radiomic model (P = 0.510).

The calibration curve analysis, Hosmer–Lemeshow test, and DCA for clini-radiomic combined model are shown in **Figure 7**. The results showed demonstrated good agreement between observations and predictions in both the training (P = 0.240; **Figure 7A**) and validation sets (P = 0.457; **Figure 7B**) for clini-radiomic combined model. The clini-radiomic combined model performed a higher net benefit than both schemes, with a threshold probability of >0% for training set (**Figure 7C**) and >0% for validation set (**Figure 7D**). The results indicating that the clini-radiomic combined model were clinically useful. The decision curve attained better performance for the constructed clini-radiomic model with regard to clinical application.

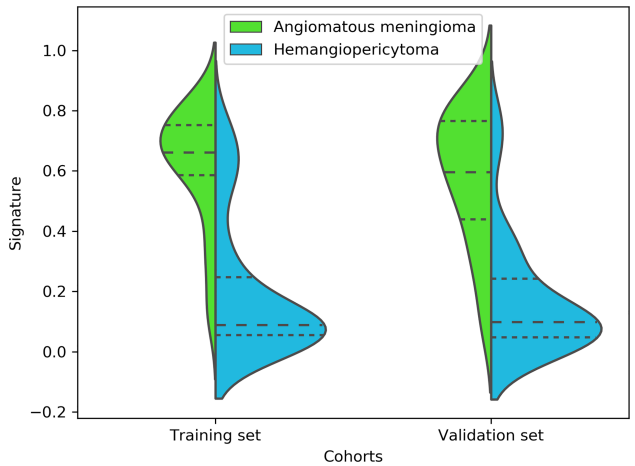

FIGURE 3 | A violin plot showing the signature distribution of the fusion radiomic model between intracranial hemangiopericytoma and angiomatous meningioma patients.

DISCUSSION

In this study, we conducted a retrospective analysis of high-quality data from a 10-year cohort of patients with histopathologically confirmed intracranial hemangiopericytoma and angiomatous meningioma, and we used the T2WI and CE-T1WI MRI based radiomic approach to effectively identify intracranial hemangiopericytoma and angiomatous meningioma before operation.

Hemangiopericytoma that originates from the central nervous system is very rare (25). Intracranial hemangiopericytoma was originally classified as hemangioblastic meningioma, and it was later confirmed to be derived from the epithelial cells of meningeal mesenchymal capillaries, rather than meningeal epithelial cells (1). Intracranial hemangiopericytoma is usually isolated and mainly connected to the dura mater, which is attached to the falx or sagittal sinus of the brain, or occurs in the epidural area (26). Intracranial hemangiopericytoma is classified as a malignant tumor (WHO grades II–III) with the tendency of recurrence and metastasis (3). Intracranial hemangiopericytoma exhibits more aggressive behaviors like bone erosions or necrosis, low ADC values and heterogeneous enhancement (27, 28), however, these visual based features are not always effective and reliable. Angiomatous meningioma is a rare WHO grade I meningioma type with a total incidence rate of 2.1–2.59% of all meningiomas (29). The blood supply of angiomatous meningioma is very rich (30), and according to Hasselblatt et al., meningiomas with >50% vascular components can be diagnosed as angiomatous meningioma (14).

In the preoperative radiological examination, compared with other meningiomas, angiomatous meningioma showed more obvious enhancement and vascular signs, and fewer meningeal tail signs, which made it difficult to distinguish angiomatous meningioma from hemangiopericytoma on conventional imaging (30). The imaging characteristics of intracranial hemangiopericytoma and angiomatous meningiomas are similar, but their treatment and prognosis are very different.

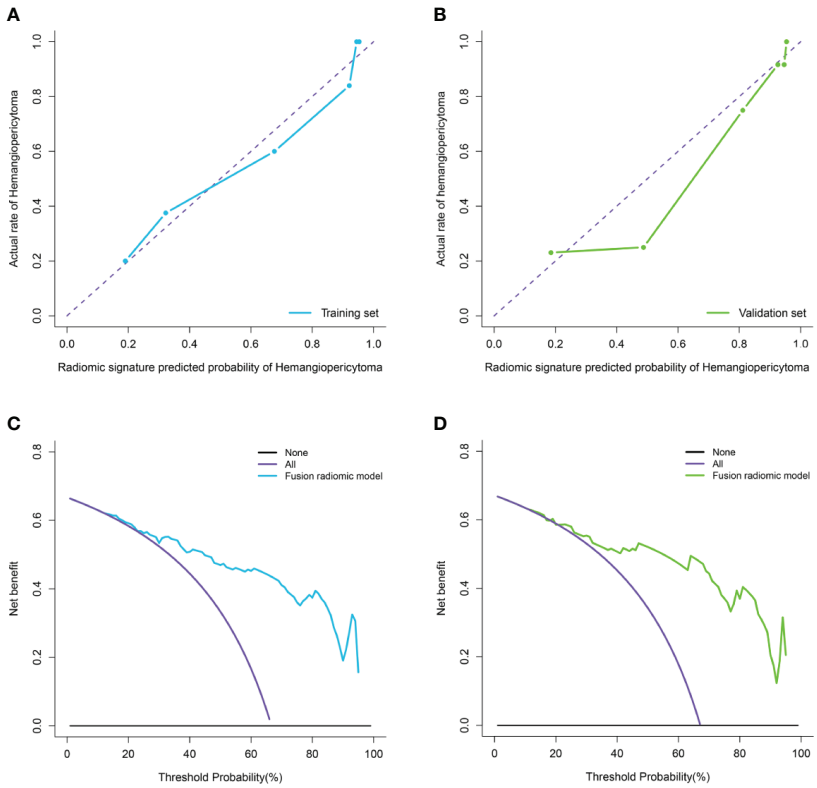

FIGURE 4 | Calibration curve analysis and decision Curve Analysis for the fusion radiomic model. **(A, B)**. Calibration curves of the fusion radiomic model in the training set **(A)** and validation set **(B)**. Calibration curves depict the calibration of model in terms of the agreement between the actual observations and predictions of tumor diagnosis. The Y axis represents the actual rate. The X axis represents the predicted probability. The diagonal purple line represents perfect prediction by an ideal model. The blue **(A)** and green **(B)** lines represent the performance of the model, of which a closer fit to the diagonal purple line represents a better prediction. **(C, D)**. Decision curve analysis for the fusion radiomic model in the training set **(C)** and validation set **(D)**. The Y axis measures the net benefit. The blue **(C)** and green **(D)** line represents the fusion radiomic model. The purple line represents the assumption that all patients were diagnosed as intracranial hemangiopericytoma. The black line represents the assumption that all patients diagnosed as angiomatous meningioma.

TABLE 5 | Details diagnostic ability of all constructed models.

Model	Performance	AUC	ACC	SE	SP	PPV	NPV
T1 radiomic model	Training set	0.840 (0.814–0.863)	0.775 (0.750–0.802)	0.763 (0.731–0.797)	0.796 (0.757–0.837)	0.866 (0.839–0.894)	0.662 (0.617–0.707)
	Validation set	0.750 (0.718–0.788)	0.699 (0.670–0.728)	0.685 (0.651–0.719)	0.737 (0.682–0.792)	0.881 (0.855–0.907)	0.452 (0.403–0.499)
T2 radiomic model	Training set	0.850 (0.829–0.879)	0.701 (0.673–0.729)	0.958 (0.943–0.974)	0.216 (0.173–0.259)	0.697 (0.667–0.727)	0.733 (0.645–0.820)
	Validation set	0.850 (0.828–0.873)	0.726 (0.699–0.754)	0.980 (0.970–0.991)	0.136 (0.098–0.175)	0.725 (0.697–0.753)	0.750 (0.636–0.865)
Clinical model	Training set	0.820 (0.790–0.847)	0.762 (0.735–0.788)	0.857 (0.830–0.884)	0.571 (0.517–0.624)	0.800 (0.770–0.829)	0.667 (0.612–0.722)
	Validation set	0.790 (0.753–0.818)	0.767 (0.741–0.793)	0.796 (0.765–0.826)	0.708 (0.659–0.757)	0.848 (0.820–0.876)	0.630 (0.579–0.678)
Fusion radiomic model	Training set	0.900 (0.879–0.916)	0.810 (0.785–0.834)	0.765 (0.733–0.797)	0.898 (0.866–0.931)	0.938 (0.917–0.959)	0.657 (0.612–0.700)
	Validation set	0.900 (0.879–0.919)	0.822 (0.798–0.846)	0.796 (0.765–0.827)	0.875 (0.840–0.910)	0.929 (0.907–0.950)	0.677 (0.633–0.722)
Clini-radiomic model	Training set	0.920 (0.902–0.942)	0.884 (0.865–0.905)	0.939 (0.921–0.957)	0.776 (0.732–0.821)	0.893 (0.871–0.916)	0.864 (0.825–0.904)
	Validation set	0.910 (0.894–0.935)	0.863 (0.842–0.883)	0.939 (0.921–0.956)	0.708 (0.658–0.757)	0.868 (0.843–0.892)	0.850 (0.809–0.891)

ACC, accuracy; AUC, area under curve; PPV, positive predict value; NPV, negative predictive value.

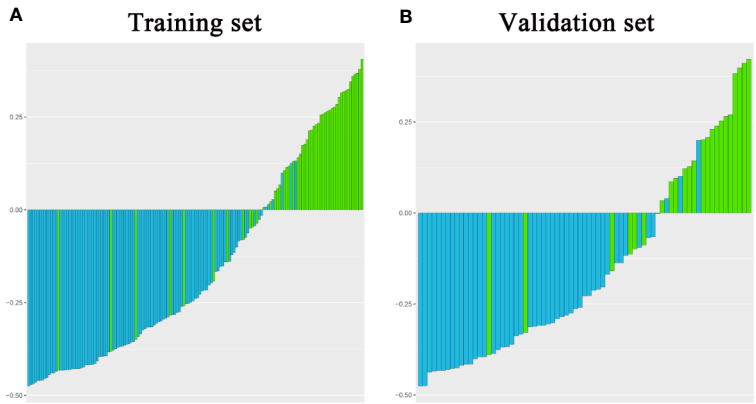

FIGURE 5 | Bar plots for the clini-radiomic combined model in the training **(A)** and validation sets **(B)**. The blue histogram above the horizontal axis and the green histogram below the horizontal axis indicate the patients with correct diagnosis of the clini-radiomic combined model.

Intracranial hemangiopericytoma is more aggressive, highly vascularized and prone to intraoperative hemorrhage, has a higher postoperative recurrence rate and a worse prognosis (1). However, angiomatous meningioma is benign and its clinical presentation, surgical management, and prognosis are almost similar to the classical meningioma (2). The surgical resection of angiomatous meningioma is more difficult than other types of meningioma, with more intraoperative bleeding and more serious complications such as neurological impairment (30). Therefore, accurate preoperative diagnosis of intracranial hemangiopericytoma and angiomatous meningioma is of great clinical significance for the planning of operation and the evaluation of prognosis.

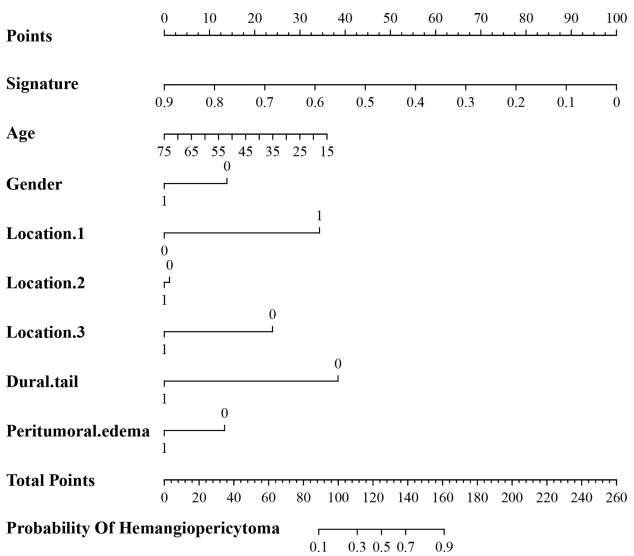

FIGURE 6 | A nomogram derived from the clini-radiomic combined model. This nomogram is used based on the value of signature of radiomic model and clinical characteristics, namely, age, location 1 (supratentorial or infratentorial), location 2 (skull base or non-skull base), location 3 (paravenous sinus or non-paravenous sinus), dural tail, and peritumoral edema. Draw a vertical line from the corresponding axis of each factor until it reaches the first "Points" line. Next, summarize the points of all risk factors, and then draw a vertical line that falls vertically from the "Total Points" axis until it reaches the last axis to the diagnostic probability of intracranial hemangiopericytoma.

Due to the lack of effective molecular markers, the researchers tried to use preoperative images to identify intracranial hemangiopericytoma and angiomatous meningioma. Intracranial hemangiopericytoma have various manifestations in MRI, most of which are irregular or lobulated, with mixed signals and uneven enhancement due to cystic degeneration and necrosis (25). Benign meningiomas have smooth edges, uniform signals, few lobes, and may have signs of calcification and dural tail. However, different from benign meningiomas, MRI features of angiomatous meningiomas are similar to those of intracranial hemangiopericytoma, such as uneven signal, cystic necrosis, irregular lobulation, irregular meningeal tail, etc. Thus, in clinical practice, angiomatous meningiomas and intracranial hemangiopericytoma are difficult to distinguish accurately only by conventional imaging (7). Therefore, an effective, accurate and widely used tool for preoperative identification of angiomatous meningioma and intracranial hemangiopericytoma is in urgent need of development.

As an emerging study field, radiomics can possibly depict the intratumoral heterogeneity based on the quantitative and the classified high-throughput data (31). Typically, novel image-based computational models have played increasingly important roles in the accurate diagnosis and also treatment guidance in neuro-oncology, thanks to the development of clinical imaging data (32). Radiomics has many applications in the central nervous system, such as differential diagnosis (10, 33–35) and classification (12, 15), prediction of molecular characteristics (11, 36), therapeutic response and progress of central nervous system diseases (32, 37). Radiomics mainly uses the following 4 steps to convert image images into mineable data, namely, image acquisition and reconstruction, tumor ROI segmentation, radiomic feature extraction and screening, model construction and verification (38). There is currently a study using radiomics to

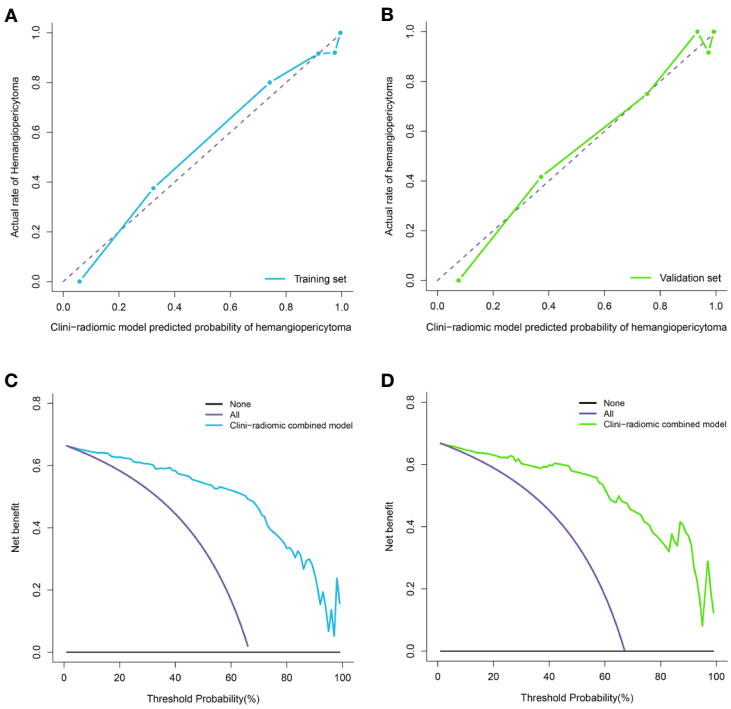

FIGURE 7 | Calibration curve analysis and decision Curve Analysis for the clini-radiomic model. **(A, B)**. Calibration curves of the clini-radiomic model in the training set **(A)** and validation set **(B)**. Calibration curves depict the calibration of model in terms of the agreement between the actual observations and predictions of tumor diagnosis. The Y axis represents the actual rate. The X axis represents the predicted probability. The diagonal purple line represents perfect prediction by an ideal model. The blue **(A)** and green **(B)** lines represent the performance of the model, of which a closer fit to the diagonal purple line represents a better prediction. **(C, D)**. Decision curve analysis for the clini-radiomic model in the training set **(C)** and validation set **(D)**. The Y axis measures the net benefit. The blue **(C)** and green **(D)** line represents the clini-radiomic model. The purple line represents the assumption that all patients were diagnosed as intracranial hemangiopericytoma. The black line represents the assumption that all patients diagnosed as angiomatous meningioma.

distinguish intracranial hemangiopericytoma and meningioma before surgery (7), but there are many types of meningiomas, and more attention should be paid to the identification of hemangiopericytoma that is easily confused with intracranial hemangiopericytoma. Meanwhile, previous studies have shown that Li et al. (13) intend to use the radiomic approach of texture analysis to identify intracranial hemangiopericytoma and angiomatous meningioma, but it has many shortcomings. First of all, the number of patients included in the study is small, with only 24 cases intracranial hemangiopericytoma and 43 cases angiomatous meningioma. A smaller number of patients make it more difficult to draw more accurate conclusions. Secondly, the study does not have a corresponding validation set, which limits the clinical applicability of the conclusions. Finally, the study only extracts the texture features of the tumor, and lacks high-latitude radiomic features and more complete model construction methods. Therefore, in the present study, we used the radiomic method to differentiate intracranial hemangiopericytoma from angiomatous meningioma preoperatively.

In the current study, Mann–Whitney U test, elastic net, and RFE algorithm were sequentially utilized to reduce redundant features and select the most appropriate features for the construction of a fusion radiomic model. It is crucial to exclude irrelevant features, because these features may obscure important information and affect the performance of the prediction model (39). First, after the Mann–Whitney U test, we conducted a preliminary screening and obtained 399 radiomic features. Then, 37 radiomic features were further obtained through the elastic net algorithm, and a feasible number that balances insufficient fitting and over fitting is obtained. Finally, 6 features were determined by the RFE algorithm, and the constructed fusion radiomic model achieved balanced performance in both the training [0.900 (95% CI, 0.879–0.916)] and validation [0.900 (95% CI, 0.879–0.919)] sets. Next, the clini-radiomic combined model was constructed in this study, which had incorporated both the fusion radiomic model and the clinical model, with the AUC of 0.920 (95% CI, 0.902–0.942) and 0.910 (95% CI, 0.894–0.935) in training set and validation set, respectively. Both fusion radiomic model and clini-radiomic combined model had displayed good calibration and discrimination. Thirdly, this clini-radiomic combined model was convenient in use, which could accurately differentiate angiomatous meningioma and intracranial hemangiopericytoma before surgery.

Research in intracranial hemangiopericytoma and angiomatous meningioma has been historically limited due to a relatively low

incidence, we collected the imaging, clinical and pathological data of 147 cases of intracranial hemangiopericytoma and 73 cases of angiomatous meningioma from a single center for this radiomic research. It is very precious, and the large sample size enrolled in this study will lead to more reliable results than previous scattered case studies. This study also has some limitations. First, this was a single center study, more patients from multiple centers could be used to validate the robustness and repeatability of our clini-radiomic model. Second, prospective studies are necessary to verify the effectiveness and robustness of this clin-radiomics combined model. Thirdly, the research methods of radiomics are various, and different researchers adopt different analyses and preprocessing steps, namely, feature extraction, selection and model construction, so the results may be further optimized.

CONCLUSION

Preoperative identification of angiomatous meningioma and intracranial hemangiopericytoma can greatly assist surgery plans making and improve patient prognosis. The clini-radiomic model incorporating the fusion radiomic model and clinical characteristics showed great performance and high sensitivity in the differential diagnoses of angiomatous meningioma and intracranial hemangiopericytoma, and to assist in the development of individualized treatment of patients with angiomatous meningioma and intracranial hemangiopericytoma.

DATA AVAILABILITY STATEMENT

The raw data supporting the conclusions of this article will be made available by the authors, without undue reservation.

ETHICS STATEMENT

The studies involving human participants were reviewed and approved by the Beijing Tiantan Hospital. Written informed consent for participation was not required for this study in accordance with the national legislation and the institutional requirements.

AUTHOR CONTRIBUTIONS

YF and PL revised the manuscript for important intellectual content. JZ, ZW, and LW take final responsibility for this article. All authors analyzed and interpreted the data. All authors contributed to the article and approved the submitted version.

FUNDING

This work was supported by the Natural Science Foundation of China (Grant No: 82102144, 81472370 and 81672506) and the Natural Science Foundation of Beijing (Grant No. 7192056 and J180005).

REFERENCES

1. Cohen-Inbar O. Nervous System Hemangiopericytoma. *Can J Neurol Sci* (2020) 47(1):18–29. doi: 10.1017/cjn.2019.311
2. Verma PK, Nangarwal B, Verma J, Dwivedi V, Mehrotra A, Das KK, et al. A Clinico-Pathological and Neuro-Radiological Study of Angiomatous Meningioma: Aggressive Look With Benign Behaviour. *J Clin Neurosci* (2021) 83:43–8. doi: 10.1016/j.jocn.2020.11.032
3. Louis DN, Perry A, Reifenberger G, von Deimling A, Figarella-Branger D, Cavenee WK, et al. The 2016 World Health Organization Classification of Tumors of the Central Nervous System: A Summary. *Acta Neuropathol* (2016) 131(6):803–20. doi: 10.1007/s00401-016-1545-1
4. Stout AP, Murray MR. Hemangiopericytoma: A Vascular Tumor Featuring Zimmermann's Pericytes. *Ann Surg* (1942) 116(1):26–33. doi: 10.1097/00000658-194207000-00004
5. Schiariti M, Goetz P, El-Maghraby H, Tailor J, Kitchen N. Hemangiopericytoma: Long-Term Outcome Revisited. *Clin Article J Neurosurg* (2011) 114(3):747–55. doi: 10.3171/2010.6.JNS091660
6. Wu W, Shi JX, Cheng HL, Wang HD, Hang CH, Shi QL, et al. Hemangiopericytomas in the Central Nervous System. *J Clin Neurosci* (2009) 16(4):519–23. doi: 10.1016/j.jocn.2008.06.011
7. Wei J, Li L, Han Y, Gu D, Chen Q, Wang J, et al. Accurate Preoperative Distinction of Intracranial Hemangiopericytoma From Meningioma Using a Multihabitat and Multisequence-Based Radiomics Diagnostic Technique. *Front Oncol* (2020) 10:534. doi: 10.3389/fonc.2020.00534
8. Gillies RJ, Kinahan PE, Hricak H. Radiomics: Images Are More Than Pictures. *They Are Data Radiol* (2016) 278(2):563–77. doi: 10.1148/radiol.2015151169
9. Lambin P, Leijenaar RTH, Deist TM, Peerlings J, de Jong EEC, van Timmeren J, et al. Radiomics: The Bridge Between Medical Imaging and Personalized Medicine. *Nat Rev Clin Oncol* (2017) 14(12):749–62. doi: 10.1038/nrclinonc.2017.141
10. Kang D, Park JE, Kim YH, Kim JH, Oh JY, Kim J, et al. Diffusion Radiomics as a Diagnostic Model for Atypical Manifestation of Primary Central Nervous System Lymphoma: Development and Multicenter External Validation. *Neuro Oncol* (2018) 20(9):1251–61. doi: 10.1093/neuonc/noy021
11. Zhou H, Vallieres M, Bai HX, Su C, Tang H, Oldridge D, et al. MRI Features Predict Survival and Molecular Markers in Diffuse Lower-Grade Gliomas. *Neuro Oncol* (2017) 19(6):862–70. doi: 10.1093/neuonc/now256
12. Fan Y, Hua M, Mou A, Wu M, Liu X, Bao X, et al. Preoperative Noninvasive Radiomics Approach Predicts Tumor Consistency in Patients With Acromegaly: Development and Multicenter Prospective Validation. *Front Endocrinol (Lausanne)* (2019) 10:403. doi: 10.3389/fendo.2019.00403
13. Li X, Lu Y, Xiong J, Wang D, She D, Kuai X, et al. Presurgical Differentiation Between Malignant Haemangiopericytoma and Angiomatous Meningioma by a Radiomics Approach Based on Texture Analysis. *J Neuroradiol* (2019) 46(5):281–7. doi: 10.1016/j.neurad.2019.05.013
14. Hasselblatt M, Nolte KW, Paulus W. Angiomatous Meningioma: A Clinicopathologic Study of 38 Cases. *Am J Surg Pathol* (2004) 28(3):390–3. doi: 10.1097/00000478-200403000-00013
15. Fan Y, Chai Y, Li K, Fang H, Mou A, Feng S, et al. Non-Invasive and Real-Time Proliferative Activity Estimation Based on a Quantitative Radiomics Approach for Patients With Acromegaly: A Multicenter Study. *J Endocrinol Invest* (2020) 43(6):755–65. doi: 10.1007/s40618-019-01159-7
16. Xiao B, Fan Y, Zhang Z, Tan Z, Yang H, Tu W, et al. Three-Dimensional Radiomics Features From Multi-Parameter MRI Combined With Clinical Characteristics Predict Postoperative Cerebral Edema Exacerbation in Patients With Meningioma. *Front Oncol* (2021) 11:625220. doi: 10.3389/fonc.2021.625220
17. van Griethuysen JJM, Fedorov A, Parmar C, Hosny A, Aucoin N, Narayan V, et al. Computational Radiomics System to Decode the Radiographic Phenotype. *Cancer Res* (2017) 77(21):e104–7. doi: 10.1158/0008-5472.CAN-17-0339
18. Aerts HJ, Velazquez ER, Leijenaar RT, Parmar C, Grossmann P, Carvalho S, et al. Decoding Tumour Phenotype by Noninvasive Imaging Using a

Quantitative Radiomics Approach. *Nat Commun* (2014) 5:4006. doi: 10.1038/ncomms5644
19. Wang Q, Li Q, Mi R, Ye H, Zhang H, Chen B, et al. Radiomics Nomogram Building From Multiparametric MRI to Predict Grade in Patients With Glioma: A Cohort Study. *J Magn Reson Imaging* (2019) 49(3):825–33. doi: 10.1002/jmri.26265
20. Qu J, Shen C, Qin J, Wang Z, Liu Z, Guo J, et al. The MR Radiomic Signature can Predict Preoperative Lymph Node Metastasis in Patients With Esophageal Cancer. *Eur Radiol* (2019) 29(2):906–14. doi: 10.1007/s00330-018-5583-z
21. Zinn PO, Singh SK, Kotrotsou A, Hassan I, Thomas G, Luedi MM, et al. A Coclinical Radiogenomic Validation Study: Conserved Magnetic Resonance Radiomic Appearance of Periostin-Expressing Glioblastoma in Patients and Xenograft Models. *Clin Cancer Res* (2018) 24(24):6288–99. doi: 10.1158/1078-0432.CCR-17-3420
22. Kramer AA, Zimmerman JE. Assessing the Calibration of Mortality Benchmarks in Critical Care: The Hosmer-Lemeshow Test Revisited. *Crit Care Med* (2007) 35(9):2052–6. doi: 10.1097/01.CCM.0000275267.64078.B0
23. Vickers AJ, Cronin AM, Elkin EB, Gonen M. Extensions to Decision Curve Analysis, a Novel Method for Evaluating Diagnostic Tests, Prediction Models and Molecular Markers. *BMC Med Inform Decis Mak* (2008) 8:53. doi: 10.1186/1472-6947-8-53
24. Obuchowski NA. Receiver Operating Characteristic Curves and Their Use in Radiology. *Radiology* (2003) 229(1):3–8. 10.1148/radiol.2291010898
25. Liu F, Cai B, Du Y, Huang Y. Diagnosis and Treatment of Hemangiopericytoma in the Central Nervous System. *J Cancer Res Ther* (2018) 14(7):1578–82. doi: 10.4103/jcrt.JCRT_210_18
26. Melone AG, D'Elia A, Santoro F, Salvati M, Delfini R, Cantore G, et al. Intracranial Hemangiopericytoma–Our Experience in 30 Years: A Series of 43 Cases and Review of the Literature. *World Neurosurg* (2014) 81(3-4):556–62. doi: 10.1016/j.wneu.2013.11.009
27. Meng Y, Chaohu W, Yi L, Jun P, Songtao Q. Preoperative Radiologic Characters to Predict Hemangiopericytoma From Angiomatous Meningioma. *Clin Neurol Neurosurg* (2015) 138:78–82. doi: 10.1016/j.clineuro.2015.08.005
28. Liu L, Yin B, Geng DY, Li Y, Zhang BY, Peng WJ. Comparison of ADC Values of Intracranial Hemangiopericytomas and Angiomatous and Anaplastic Meningiomas. *J Neuroradiol* (2014) 41(3):188–94. doi: 10.1016/j.neurad.2013.07.002
29. Hua L, Luan S, Li H, Zhu H, Tang H, Liu H, et al. Angiomatous Meningiomas Have a Very Benign Outcome Despite Frequent Peritumoral Edema at Onset. *World Neurosurg* (2017) 108:465–73. doi: 10.1016/j.wneu.2017.08.096
30. Yang L, Ren G, Tang J. Intracranial Angiomatous Meningioma: A Clinicopathological Study of 23 Cases. *Int J Gen Med* (2020) 13:1653–9. doi: 10.2147/IJGM.S292202
31. Park JE, Kim HS. Radiomics as a Quantitative Imaging Biomarker: Practical Considerations and the Current Standpoint in Neuro-Oncologic Studies. *Nucl Med Mol Imaging* (2018) 52(2):99–108. doi: 10.1007/s13139-017-0512-7
32. Zhou M, Scott J, Chaudhury B, Hall L, Goldgof D, Yeom KW, et al. Radiomics in Brain Tumor: Image Assessment, Quantitative Feature Descriptors, and Machine-Learning Approaches. *AJNR Am J Neuroradiol* (2018) 39(2):208–16. doi: 10.3174/ajnr.A5391
33. Artzi M, Bressler I, Ben Bashat D. Differentiation Between Glioblastoma, Brain Metastasis and Subtypes Using Radiomics Analysis. *J Magn Reson Imaging* (2019) 50(2):519–28. doi: 10.1002/jmri.26643
34. Qian Z, Li Y, Wang Y, Li L, Li R, Wang K, et al. Differentiation of Glioblastoma From Solitary Brain Metastases Using Radiomic Machine-Learning Classifiers. *Cancer Lett* (2019) 451:128–35. doi: 10.1016/j.canlet.2019.02.054
35. Kim JY, Park JE, Jo Y, Shim WH, Nam SJ, Kim JH, et al. Incorporating Diffusion- and Perfusion-Weighted MRI Into a Radiomics Model Improves Diagnostic Performance for Pseudoprogression in Glioblastoma Patients. *Neuro Oncol* (2019) 21(3):404–14. doi: 10.1093/neuonc/noy133
36. Xi YB, Guo F, Xu ZL, Li C, Wei W, Tian P, et al. Radiomics Signature: A Potential Biomarker for the Prediction of MGMT Promoter Methylation in Glioblastoma. *J Magn Reson Imaging* (2018) 47(5):1380–7. doi: 10.1002/jmri.25860
37. Fan Y, Jiang S, Hua M, Feng S, Feng M, Wang R. Machine Learning-Based Radiomics Predicts Radiotherapeutic Response in Patients With Acromegaly. *Front Endocrinol (Lausanne)* (2019) 10:588. doi: 10.3389/fendo.2019.00588
38. Fan Y, Feng M, Wang R. Application of Radiomics in Central Nervous System Diseases: A Systematic Literature Review. *Clin Neurol Neurosurg* (2019) 187:105565. doi: 10.1016/j.clineuro.2019.105565
39. Niu J, Zhang S, Ma S, Diao J, Zhou W, Tian J, et al. Preoperative Prediction of Cavernous Sinus Invasion by Pituitary Adenomas Using a Radiomics Method Based on Magnetic Resonance Images. *Eur Radiol* (2019) 29(3):1625–34. doi: 10.1007/s00330-018-5725-3

Conflict of Interest: The authors declare that the research was conducted in the absence of any commercial or financial relationships that could be construed as a potential conflict of interest.

Publisher's Note: All claims expressed in this article are solely those of the authors and do not necessarily represent those of their affiliated organizations, or those of the publisher, the editors and the reviewers. Any product that may be evaluated in this article, or claim that may be made by its manufacturer, is not guaranteed or endorsed by the publisher.

Copyright © 2022 Fan, Liu, Li, Liu, He, Wang, Zhang and Wu. This is an open-access article distributed under the terms of the Creative Commons Attribution License (CC BY). The use, distribution or reproduction in other forums is permitted, provided the original author(s) and the copyright owner(s) are credited and that the original publication in this journal is cited, in accordance with accepted academic practice. No use, distribution or reproduction is permitted which does not comply with these terms.

frontiers in Oncology

ORIGINAL RESEARCH
published: 28 January 2022
doi: 10.3389/fonc.2021.820287

PET/MR Imaging of Somatostatin Receptor Expression and Tumor Vascularity in Meningioma: Implications for Pathophysiology and Tumor Outcomes

*Michelle Roytman[1], Sean Kim[2], Shannon Glynn[2], Charlene Thomas[2], Eaton Lin[1], Whitney Feltus[3], Rajiv S. Magge[4], Benjamin Liechty[5], Theodore H. Schwartz[6], Rohan Ramakrishna[6], Nicolas A. Karakatsanis[1], Susan C. Pannullo[6], Joseph R. Osborne[1], Jonathan P. S. Knisely[7] and Jana Ivanidze[1]**

[1] Departments of Radiology, Weill Cornell Medicine/NewYork-Presbyterian Hospital, New York, NY, United States, [2] Weill Cornell Medical College, Weill Cornell Medicine/NewYork-Presbyterian Hospital, New York, NY, United States, [3] Departments of Radiology, New York-Presbyterian Hospital/Columbia University Medical Center, New York, NY, United States, [4] Department of Neurology, Weill Cornell Medicine/NewYork-Presbyterian Hospital, New York, NY, United States, [5] Department of Pathology and Laboratory Medicine, Weill Cornell Medicine/NewYork-Presbyterian Hospital, New York, NY, United States, [6] Department of Neurological Surgery, Weill Cornell Medicine/NewYork-Presbyterian Hospital, New York, NY, United States, [7] Department of Radiation Oncology, Weill Cornell Medicine/NewYork-Presbyterian Hospital, New York, NY, United States

OPEN ACCESS

Edited by:
Hailiang Tang, Fudan University, China

Reviewed by:
Franziska Vettermann, Ludwig Maximilian University of Munich, Germany
Anne Barlier, Aix Marseille Université, France

***Correspondence:**
Jana Ivanidze
jai9018@med.cornell.edu

Specialty section:
This article was submitted to Neuro-Oncology and Neurosurgical Oncology, a section of the journal Frontiers in Oncology

Received: *22 November 2021*
Accepted: *21 December 2021*
Published: *28 January 2022*

Citation:
Roytman M, Kim S, Glynn S, Thomas C, Lin E, Feltus W, Magge RS, Liechty B, Schwartz TH, Ramakrishna R, Karakatsanis NA, Pannullo SC, Osborne JR, Knisely JPS and Ivanidze J (2022) PET/MR Imaging of Somatostatin Receptor Expression and Tumor Vascularity in Meningioma: Implications for Pathophysiology and Tumor Outcomes. Front. Oncol. 11:820287. doi: 10.3389/fonc.2021.820287

Background and Purpose: Meningiomas, the most common primary intracranial tumor, are vascular neoplasms that express somatostatin receptor-2 (SSTR2). The purpose of this investigation was to evaluate if a relationship exists between tumor vascularity and SSTR2 expression, which may play a role in meningioma prognostication and clinical management.

Materials and Methods: Gallium-68-DOTATATE PET/MRI with dynamic contrast-enhanced (DCE) perfusion was prospectively performed. Clinical and demographic patient characteristics were recorded. Tumor volumes were segmented and superimposed onto parametric DCE maps including flux rate constant (*Kep*), transfer constant (*Ktrans*), extravascular volume fraction (*Ve*), and plasma volume fraction (*Vp*). Meningioma PET standardized uptake value (SUV) and SUV ratio to superior sagittal sinus ($SUVR_{SSS}$) were recorded. Pearson correlation analyses were performed. In a random subset, analysis was repeated by a second investigator, and intraclass correlation coefficients (ICCs) were determined.

Results: Thirty-six patients with 60 meningiomas (20 WHO-1, 27 WHO-2, and 13 WHO-3) were included. Mean *Kep* demonstrated a strong significant positive correlation with SUV ($r = 0.84$, $p < 0.0001$) and $SUVR_{SSS}$ ($r = 0.81$, $p < 0.0001$). When stratifying by WHO grade, this correlation persisted in WHO-2 ($r = 0.91$, $p < 0.0001$) and WHO-3 ($r = 0.92$, $p = 0.0029$) but not WHO-1 ($r = 0.26$, $p = 0.4$, $SUVR_{SSS}$). ICC was excellent (0.97–0.99).

Conclusion: DOTATATE PET/MRI demonstrated a strong significant correlation between tumor vascularity and SSTR2 expression in WHO-2 and WHO-3, but not WHO-1 meningiomas, suggesting biological differences in the relationship between tumor vascularity and SSTR2 expression in higher-grade meningiomas, the predictive value of which will be tested in future work.

Keywords: meningioma, somatostatin receptor, DOTATATE, PET/MRI, DCE = dynamic contrast enhanced, DCE Perfusion MRI

INTRODUCTION

Meningiomas, highly vascular neoplasms arising from the arachnoid cap cells, are the most common primary intracranial tumor, accounting for approximately 40% of all primary brain tumors (1). Various histopathological classification systems have been utilized for their characterization, with the current 2021 World Health Organization (WHO) classification of central nervous system (CNS) tumors recognizing 15 distinct histological subtypes, subdivided into three grades—Grade 1 (benign), Grade 2 (atypical), and Grade 3 (malignant)—relying largely on mitotic rate, histological, and cytomorphological criteria (2, 3). Higher grade meningiomas have been reported to exhibit increased vascularity, likely related to higher levels of vascular endothelial growth factor (VEGF) and microvessel density, which are surrogate markers for angiogenesis (4). However, meningioma vascularity remains a complex topic. While approximately 80% of meningiomas are considered benign and managed with observation or curative surgical resection, a subset of meningiomas demonstrate aggressive features and may recur or progress despite intervention (5). Importantly, histopathological WHO criteria has been found to be a poor predictor of clinical course, as a subset of patients with grade 2 meningiomas demonstrate a benign course while up to 20% of patients with grade 1 meningiomas experience recurrence (2, 6). Upon failing surgical and/or radiotherapeutic treatments, prognosis is often poor with no available effective medical treatment options, despite numerous clinical trials investigating the use of medications such as temozolomide, hydroxyurea, irinotecan, imatinib, erlotinib, gefitinib, bevacizumab, sunitinib, everolimus, and trabectidin (2).

Surgical resection is the mainstay of treatment for most meningiomas, with postresection Simpson grade serving as a strong predictor of outcome (2). Patients with WHO Grade 1 meningiomas typically undergo imaging and clinical observation, while patients with WHO Grade 3 meningiomas often undergo postsurgical radiation (RT). However, the use of RT post-initial resection in WHO Grade 2 meningiomas is controversial and varies in clinical practice across institutions, with an overall consensus that RT improves outcomes. Advanced adjunct imaging modalities are emerging as potential tools for the management of WHO Grade 2 meningiomas, most notably the use of [^{68}Ga]-DOTATATE, a positron emission tomography (PET) radiotracer targeting somatostatin receptor 2 (SSTR2), which has been immunohistochemically proven to be present on the cell surface of 79%–100% of meningiomas (7, 8), and other Gallium-68-labeled somatostatin analogs (9, 10). [^{68}Ga]-DOTATATE binds to SSTR2 on the cell surface of meningiomas, with high specificity, serving as an imaging biomarker for the detection of meningiomas. While vascularity may aid in transporting the radiotracer to its destination, vascularity in itself would not explain the sustained binding identified in meningiomas. Additionally, while higher grade meningiomas have been reported to exhibit increased vascularity, such a correlation does not exist between WHO grade and degree of [^{68}Ga]-DOTATATE avidity. [^{68}Ga]-DOTATATE PET has demonstrated promise in the assessment of resected/irradiated meningiomas and in the assessment of treatment-naive meningiomas by allowing for improved diagnosis and evaluation of extent of disease (11). In addition to serving as a potential predictive imaging biomarker, SSTR2 may serve as a potential therapeutic target utilizing peptide receptor radionuclide therapy (PPRT) *via* ^{177}Lutetium[^{177}Lu]-DOTATATE. [^{177}Lu]-DOTATATE is currently being investigated in two prospective clinical studies (NCT03971461 and NCT04082520) for patients with progressive intracranial meningiomas, serving as a potential novel therapeutic option in the arena of precision medicine (2, 11).

Dynamic contrast-enhanced MRI (DCE-MRI) is an advanced imaging modality allowing for *in vivo* evaluation of tissue perfusion and blood–brain barrier (BBB) disruption (12, 13). Perfusion imaging, which may be performed as DCE-MRI or as dynamic susceptibility contrast (DSC-MRI), is increasingly utilized in clinical practice for both primary and secondary brain neoplasms. In the context of meningiomas, perfusion MRI has been shown to successfully distinguish between lower and higher grades, guide in the differentiation between meningiomas and dural-based metastases, provide information regarding RT response, and provide useful information regarding peritumoral edema surrounding meningiomas, indicative of BBB disruption (13–17).

While meningiomas have distinct and often pathognomonic conventional imaging features (e.g., dural-based, extra-axial, homogeneous enhancement, dural tail, associated hyperostosis), conventional gadolinium-enhanced MRI has its limitations, including the inability to reliably distinguish between meningioma subtypes/grades and challenges discerning posttreatment change from residual or recurrent disease. In this study, we sought to investigate whether advanced imaging modalities may play a role in predicting the biological nature of meningiomas and/or serving as a predictive imaging biomarker to guide and optimize clinical management. To that end, we

explored the relationship between DCE-perfusion parameters and [^{68}Ga]-DOTATATE PET/MRI standardized uptake value (*SUV*) to determine whether a relationship may exist between vascularity, as represented by DCE perfusion parameters, and SSTR2 expression, as represented by [^{68}Ga]-DOTATATE *SUV*.

MATERIALS AND METHODS

Study Design

In this institutional review board-approved prospective study, patients with clinically suspected or histologically proven meningioma were enrolled as part of our active clinical trial and underwent [^{68}Ga]-DOTATATE PET/MRI with DCE perfusion between August 2018 and April 2021. Patient exclusion criteria included contraindications to gadolinium-based contrast agents, a history of an allergic reaction to [^{68}Ga]-DOTATATE, and pregnancy. Patients with histologically proven and/or with one histologically proven and additional suspected meningioma(s) on the basis of conventional MRI and measuring ≥1 cm in size in at least one dimension were included. In patients with multiple meningiomas, WHO grade of the histologically proven meningioma was assumed for all meningiomas present (18). [^{68}Ga]-DOTATATE has been widely used in the diagnosis, staging, and treatment management of neuroendocrine tumors with a favorable safety profile (19), including lack of significant toxicity, lower radiation exposure, and improved accuracy compared to indium-111-pentetreotide (19).

Imaging

All patients underwent gadolinium-enhanced MR imaging of the brain on a 3-Tesla clinical scanner (Biograph mMR, Siemens Healthcare, Erlangen, Germany), which included 3-dimensional T1 SPACE (TR/TE, 600–700 ms/11–19 ms, 120°C flip, 1 mm slice thickness), and 3-dimensional T2 FLAIR (TR/TE, 6,300–8,500 ms/394–446 ms, 120°C flip, 1 mm slice thickness). T1-weighted DCE perfusion MRI was performed and available for all patients (TR = 4 ms; TE = 1–2 ms; flip angle, 13°C; slice thickness, 3 mm; 44 slices to cover the entire lesion volume; 24 phases with 4 phases before and 20 phases after intravenous bolus administration of 0.1 ml/kg gadobutrol).

PET acquisition was performed in dynamic 3D list mode for a total of 60 min starting simultaneously with [^{68}Ga]-DOTATATE injection and concurrent with the above-described MR sequences. Absolute maximum SUV was extracted for each lesion, and SUV of the superior sagittal sinus (SSS), serving as background blood pool for normalization purposes based on previously published methodology (11).

DCE Perfusion Analysis

DCE perfusion analysis was performed using Olea Sphere Medical 3.0-SP22 software (Olea Medical, La Ciotat, France). For each imaging study, a single investigator (MR) created a volume of interest (VOI) encompassing the meningioma utilizing the postcontrast T1-weighted sequence with intermittent guidance of the fused MRI/PET scan (e.g., in cases where conventional MRI was difficult to discern residual meningioma from adjacent dura), as shown as in **Figure 1**. The following Extended Tofts model DCE perfusion parameters were derived and analyzed from each VOI: flux rate constant (*Kep*), transfer constant (*Ktrans*), volume fraction of the extravascular extracellular space (*Ve*) in the tissue, and volume fraction of plasma in the tissue (*Vp*) (**Figure 2**). Briefly, these parameters are based upon a two-compartment model and the principle that intravenously injected contrast agent leaks from the intravascular space (IVS; compartment 1) into the EVS (compartment 2), and whether or not the tracer is freely diffusible. The rate of contrast exchange between these two compartments are described using transfer rate constants, including *Ktrans* (forward volume transfer constant), *Kep* (flux rate constant between EES and IVS), *Ve* (extracellular extravascular volume fraction whereby Ve = Ktrans/Kep), and *Vp* (plasma per unit volume of tissue).

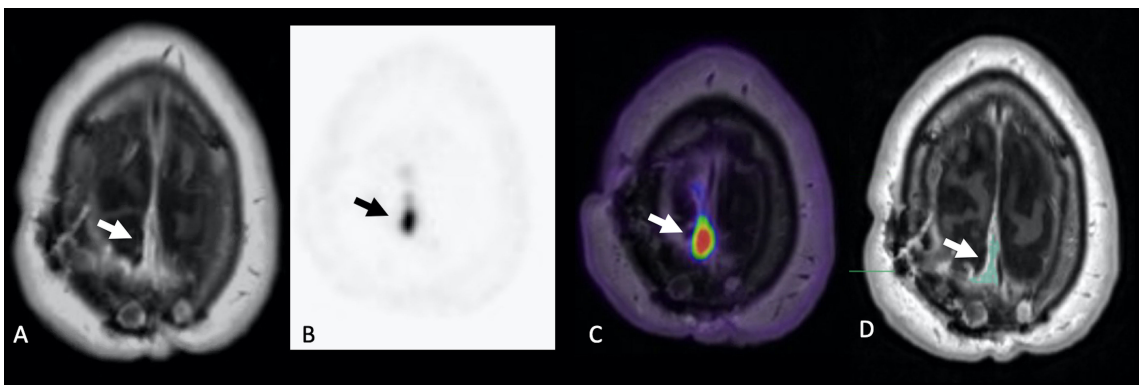

FIGURE 1 | Example of VOI segmentation for DCE analysis in a 56-year-old man with WHO-2 right parietal meningioma post prior surgical resection and RT. Gadolinium-enhanced axial T1-weighted MRI **(A)**, static 68-Gallium-DOTATATE PET image **(B)**, and fused axial PET/MR **(C)** demonstrate extra-axial homogeneously enhancing soft tissue with corresponding 68-Gallium-DOTATATE avidity (arrows), compatible with residual/recurrent meningioma. Gadolinium-enhanced axial T1-weighted MRI with volume of interest **(D)** is shown, corresponding to region of suspected residual/recurrent meningioma.

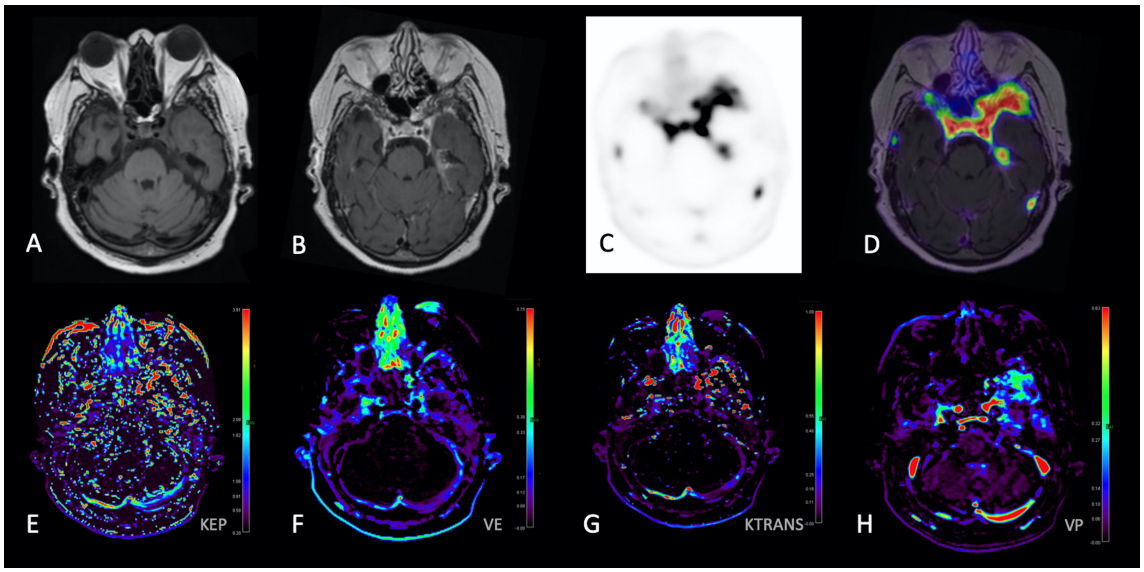

FIGURE 2 | 68-Gallium-DOTATATE PET and DCE Perfusion MRI images in a 68-year-old woman with WHO-1 left anterior temporal convexity meningioma post prior surgical resection and RT. Axial T1-weighted **(A)**, gadolinium-enhanced axial T1-weighted **(B)**, static 68-Gallium-DOTATATE PET image **(C)**, axial PET/MR fusion image **(D)**, Kep parametric map **(E)**, Ve parametric map **(F)**, Ktrans parametric map **(G)**, and Vp parametric map demonstrates extra-axial homogeneously enhancing soft tissue with corresponding 68-Gallium-DOTATATE avidity [**(D)**, with SUV measured along the left anterior temporal convexity] and abnormal perfusion parametric maps **(E–H)**, corresponding to region of suspected residual/recurrent meningioma.

In a randomly selected sample of eight meningiomas, volumetric segmentation and DCE perfusion analysis was repeated by a second investigator (SG).

Statistical Analysis

Statistical analysis was performed using R version 4.0.5 (R Foundation for Statistical Computing, Vienna, Austria). Pearson correlation coefficient was calculated to identify whether a statistically significant correlation existed between DCE permeability parameters and [^{68}Ga]-DOTATATE SUV. Intraclass correlation coefficient (ICC) was determined to assess interrater reliability between the two investigators.

RESULTS

Study cohort demographics are described in **Table 1**. This prospective study included 36 patients, with mean age of 53.6 years (range, 21–83; standard deviation, 14.8 years), of whom 61% (22 of 36) were female. A total of 60 meningiomas (20 WHO-1, 27 WHO-2, and 13 WHO-3) with average tumor volume of 2.3 cc (range, 0.04–26.11 cc; standard deviation, 4.25 cc) were included in this analysis. Of the 60 meningiomas included in our study, 30% (18/60) were located in the skull base. Of the 60 lesions in the cohort, 43 lesions were considered pathology-proven (72%).

Kep demonstrated a strong significant positive correlation with [^{68}Ga]-DOTATATE SUV ($r = 0.84$, $p < 0.0001$), which remained robust when normalized to background blood pool SSS SUV ($SUVR_{SSS}$) ($r = 0.81$, $p < 0.0001$). When stratifying by WHO Grade, this strong significant positive correlation only existed in WHO-2 ($r = 0.91$, $p < 0.0001$; $SUVR_{SSS}$, $r = 0.91$, $p < 0.0001$) and WHO-3 ($r = 0.92$, $p = 0.0029$; $SUVR_{SSS}$, $r = 0.82$, $p = 0.023$) but did not exist with WHO-1 ($r = 0.26$, $p = 0.4$; $SUVR_{SSS}$, $r = 0.22$, $p = 0.46$).

Ktrans demonstrated a moderate significant positive correlation with [^{68}Ga]-DOTATATE SUV ($r = 0.39$, $p = 0.019$), which did not remain statistically significant with $SUVR_{SSS}$ ($r = 0.28$, $p = 0.11$), and did not remain statistically significant when stratifying by WHO Grade.

When analyzing separately only lesions located in the skull base [30% (18/60)], there remained a strong positive significant correlation between *Kep* and SUV ($r = 0.91$, $p < 0.0001$) and a moderate positive significant correlation between Ktrans and SUV ($r = 0.50$, $p = 0.04$).

When analyzing separately only the pathology proven lesions [72% (43/60)], there remained a strong positive significant correlation between *Kep* and SUV ($r = 0.72$, $p < 0.0001$) and a moderate positive significant correlation between Ktrans and SUV ($r = 0.49$, $p = 0.0009$).

No other statistically significant correlation existed between [^{68}Ga]-DOTATATE SUV and *Vp*, *Ve*, and *Ktrans*. All correlations are reported in **Tables 2**, **3** and **Figure 3**.

The intraclass correlation coefficients (ICCs) for perfusion parameters *Kep*, *Vp*, and *Ve* were excellent: 0.998, 0.990 and 0.992, respectively. The ICC for *Ktrans* was unable to be calculated, and, upon directed review, an error was detected in the sampling of one meningioma resulting in an outlier data point for that measurement by one of the two readers. Upon

TABLE 1 | Clinical characteristics of the patient population.

N Patients	36
Age	53.6 (21–83; STD: 14.8)
Sex	61% F (22/36)
N meningiomas identified on PET	60
Tumor volume	2.3 (.04–26.11; STD: 4.25)
N meningiomas per patient	1 meningioma: 63.9% (24/36)
	33% (8/24) WHO Grade 1
	42% (10/24) WHO Grade 2
	25% (6/24) WHO Grade 3
	2-3 meningiomas: 25% (9/36)
	56% (5/9) WHO Grade 1
	33% (3/9) WHO Grade 2
	11% (1/9) WHO Grade 3
	≥4 meningiomas: 11.1% (3/36)
	0% (0/3) WHO Grade 1
	67% (2/3) WHO Grade 2
	33% (1/3) WHO Grade 3
	Median:1 meningioma per patient
WHO grade	0% (0/36) WHO grade unknown
	36% (13/36) WHO grade 1
	42% (15/36) WHO grade 2
	22% (8/36) WHO grade 3
Surgical history	94% (34/36)
Time from surgery to PET	26.5 months (1.4–118 months)
Prior radiation history	50% (18/36)
Prior radiation type	56% (10/18) SRS
	17% (3/18) gamma knife
	22% (4/18) proton
	6% (1/18) IMRT
Time from prior radiation to PET	31.6 months (0.26–205 months)
Radiation dose	41.5 Gy (5–123)

exclusion of that data point, the ICC for *Ktrans* was also found to be excellent: 0.967. There was only a moderate reliability of assessed tumor volume, 0.742.

DISCUSSION

Dynamic contrast-enhanced MRI utilizes the acquisition of multiple serial images before, during, and after a bolus of low-molecular weight gadolinium contrast media, which allows for the determination of measurements of enhancement as a function of time (12, 20). Intravenously injected contrast material passes from the arteries to the tissue microvasculature and extravasates within seconds to the extravascular extracellular space (EES), or leakage space, resulting in shortening of the local relaxation time. DCE-MRI subsequently uses this T1 shortening (i.e., high signal or enhancement on T1-weighted sequence) to detect areas of BBB disruption. The ability to assess contrast agent extravasation, or vessel leakiness, is complex and relies on several factors, most notably blood flow. Therefore, the signal measured with DCE-MRI, particularly when using a sufficiently long acquisition time, reflects both perfusion and permeability and DCE-MRI can be impacted by alterations in vascular permeability, blood flow, and EES. Perfusion imaging may alternatively be performed with DSC-MRI, relying on T2*-weighted gradient-echo echo-planar imaging, which has several theoretical differences and a number of advantages, including faster acquisition, higher temporal resolution, and the ability to determine relative cerebral blood volume (rCBV), a widely used variable to assess tumor vascularity and grade (21).

A number of complex pharmacokinetic models have been proposed including Tofts et al. (22), Brix et al. (23), and Larsson et al. (24), many of which rely on a two-compartment model and the principle that intravenously injected contrast agent leaks from the intravascular space (IVS; compartment 1) into the EVS (compartment 2), and whether or not the tracer is freely diffusible. Most pharmacokinetic models determine the rate of contrast exchange between these two compartments using transfer rate constants, including *Ktrans* (forward volume transfer constant), *Kep* (flux rate constant between EES and IVS), *Ve* (extracellular extravascular volume fraction whereby Ve = Ktrans/Kep), and *Vp* (plasma per unit volume of tissue).

An initial model of BBB permeability was developed by Tofts et al., ignoring the contribution of plasma to total tissue concentration and consequently only applicable in normal brain

TABLE 2 | SUV and DCE parameters.

SUV Lesion	25.06 (4.2–111.8; STD: 21.39)
SUV SSS	1.47 (0.6–2.5; STD: 0.5)
$SUVR_{SSS}$ (SUV lesion/SSS)	18.55 (1.2–136.1; STD: 21.9)
Kep	3.18 (0.40–16.33; STD: 3.16)
Ktrans	1.68 (0.21–7.85; STD: 1.60)
Vp	0.10 (.0009–0.47; STD: 0.11)
Ve	0.56 (.091–0.99; STD: 0.21)

TABLE 3 | SUV Correlations.

DCE Parameter to SUV		R	p-value
Kep	WHO Grade 1	0.26	0.4
	WHO Grade 2	0.91	< 0.001
	WHO Grade 3	0.92	< 0.01
Ktrans	WHO Grade 1	0.43	0.14
	WHO Grade 2	0.40	0.14
	WHO Grade 3	0.62	0.13
Vp	WHO Grade 1	-0.15	0.61
	WHO Grade 2	0.2	0.47
	WHO Grade 3	0.48	0.28
Ve	WHO Grade 1	0.21	0.49
	WHO Grade 2	0.13	0.64
	WHO Grade 3	-0.47	0.28
DCE Parameters to $SUVR_{SSS}$			
Kep	WHO Grade 1	0.22	0.46
	WHO Grade 2	0.91	< 0.001
	WHO Grade 3	0.82	0.02
Ktrans	WHO Grade 1	0.23	0.45
	WHO Grade 2	0.4	0.14
	WHO Grade 3	0.46	0.3
Vp	WHO Grade 1	.0012	1
	WHO Grade 2	0.21	0.44
	WHO Grade 3	0.55	0.2
Ve	WHO Grade 1	-0.028	0.93
	WHO Grade 2	0.17	0.55
	WHO Grade 3	-0.32	0.48

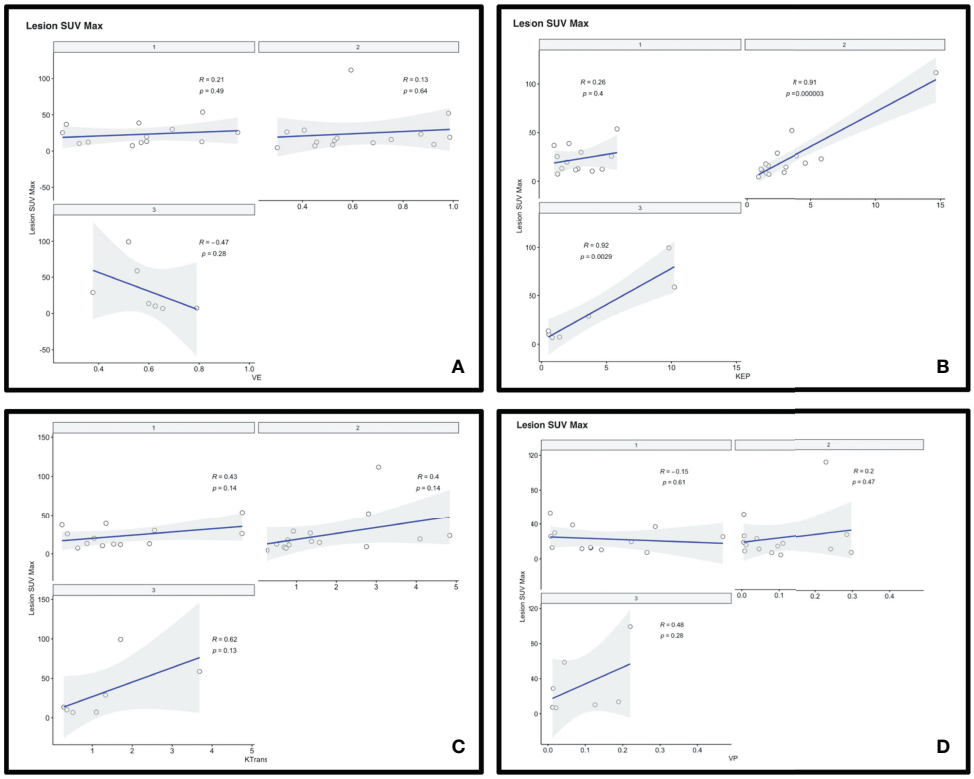

FIGURE 3 | Scatterplots depicting the correlation between 68-Gallium-DOTATATE PET SUV and DCE perfusion parameters *Ve* **(A)**, *Kep* **(B)**, *Ktrans* **(C)**, and *Vp* **(D)**.

tissue with an intact BBB. A subsequent model, the Extended Tofts model, incorporates the vascular contribution to signal intensity and is more commonly used in tumor applications, including in this analysis (25). While quantitative DCE-MRI measurements and parametric maps are increasingly used for diagnostic purposes, it is critical to understand the complexity of these measurements and the numerous variables that affect their results, including the arterial input function (AIF; i.e., measured concentration in an artery) and physiological factors (e.g., changes in cardiac output), for which determination of consistent and accurate data, both in the clinical and research settings, may be a challenge. Of note, the data presented in this analysis demonstrated an excellent ICC across the assessed parameters. The assessed tumor volume demonstrated only moderate reliability, suggesting robust DCE analysis results even with varying sampled volume. Therefore, the consistency of data obtained by two independent observers supports the accuracy of the results presented.

Prior immunohistochemical analyses investigating the relationship of vascularity in meningiomas identified a significant upregulation of VEGF-A in WHO Grade III as compared to WHO Grade II tumors (26). In this radiological analysis, the only perfusion parameter to demonstrate statistical significance with [^{68}Ga]-DOTATATE SUV was *Kep*, a parameter infrequently used in clinical practice but often described in the literature. Awasthi et al. investigated whether an association may exist in glioblastoma (GBM) between DCE-MRI parameters and tissue matrix metalloproteinase 9 (MMP-9) expression, with MMPs known to be responsible for targeting the extracellular matrix and contributing to BBB permeability and angiogenesis/neovascularization of glial tumors. In their study, they determined that MMP-9 expression was best estimated by *Kep*, of all perfusion parameters, and demonstrated an association with survival, suggesting *Kep* as a potential imaging biomarker of GBM progression and its prognostication (27).

It is important to note, however, that GBM are intra-axial in location while meningiomas are extra-axial in location, raising the question as to whether tumor origin impacts the interpretation of DCE-MRI findings. Physiological extreme vessel leakiness is observed with both tumor types—in GBM due to BBB destruction of preexisting vessels and faulty BBB in angiogenic tumoral vessels, while in meningiomas due to their highly vascular nature and inherent absence of a BBB given their extra-axial location (21). Cha et al. compared DCE-MRI and DSC-MRI microvascular permeability measurement *Ktrans* in gliomas and meningiomas, observing that *Ktrans* could distinguish between higher- and lower-grade gliomas, although correlated poorly in meningiomas (21). However, Chidambaram et al. investigated DCE-MRI in meningiomas treated with resection and adjuvant radiosurgery, revealing a moderately positive correlation with *Ktrans* and time to progression, approaching but not reaching statistical significance, which supports a role of DCE-MRI as a biomarker in meningioma diagnosis, treatment planning, and predicting clinical outcomes (13).

A study evaluating DSC-MRI characteristics of meningiomas compared to dural-based metastases by Lui et al. identified relative wash-in time, a metric describing the wash-in phase of perfusion, to be lower in metastases as compared to meningiomas. This study also investigated the use of rCBV, a metric that is frequently used to assess tumor vascularity and grade, in the distinction of meningioma from dural-based metastases. However, in distinction to other reports describing the utility of rCBV for extra-axial lesions, the use of rCBV was found to be limited within this patient cohort (28). While many of the aforementioned studies utilized DSC-MRI and did not specifically investigate the perfusion parameter *Kep*, the overarching theme among these studies is in support of the potential role and added value of perfusion imaging for the assessment of meningiomas.

The significance of *Kep* with respect to other tumor types has been previously described in the literature. For example, *Kep* has been shown to negatively correlate with histological vessel maturity in breast cancer osseous metastases (29), positively correlate with Ki67 and p53- and triple negative status in breast cancers (30), positively correlate with invasive ductal carcinoma tumor size (31), and positively correlate with microvessel density (32) and PTEN expression in prostate cancer (33). *Kep* has also been shown to effectively differentiate between benign and malignant soft tissue tumors (34) and demonstrate a significant positive correlation with serum angiogenesis-related biomarkers and advanced tumor stage in patients with non-small cell lung cancer (35). The relationship between *Kep* and SSTR2A expression in higher grade meningiomas may be of significance in the treatment planning and response assessment of meningiomas. To this end, bevacizumab, a monoclonal antibody targeting vascular endothelial growth factor (VEGF), has been used in meningioma off label with reports of improved overall PFS (36). The mechanism of action may be related to decrease in vascularity and associated decrease in SSTR2A expression, which may serve as a clinical response biomarker. The identified correlation between DCE-MRI perfusion parameter *Kep* and [^{68}Ga]-DOTATATE *SUV* in higher grade meningiomas suggests underlying biological differences in the relationship between tumor vascularity and SSTR2 expression, perhaps related to biomarkers of angiogenesis, such as VEGF and microvessel density. This may be of importance given ongoing efforts to apply peptide receptor radionuclide therapy (PPRT) with ^{177}Lutetium[^{177}Lu]-DOTATATE in meningioma, which has been reported to have modest effects in small pilot cohorts and individual cases (2, 37, 38). To that end, PRRT with [^{177}Lu]-DOTATATE in gastrointestinal neuroendocrine tumors metastatic to the liver was recently shown to have improved dosimetry with intra-arterial interventional radiology-guided administration compared to systemic intravenous administration (39). Conceivably, the correlation between perfusion metrics and [68Ga]-DOTATATE PET SUV may thus play a role when determining patients for clinical trials incorporating PRRT who are most likely to benefit. The relationship between *Kep* and SUV may also be clinically relevant to other therapeutic options that specifically address tumor vascularity.

A limitation of this study is the relatively small sample size, with 36 patients with 60 meningiomas. Additionally, in patients with multiple meningiomas and WHO grade documented for one meningioma, the assumption was made for the additional unresected lesions to have the same WHO grade, as previously published (18). While this approach has previously been validated, there remains the theoretical possibility for heterogeneity of WHO grades in patients with multiple meningiomas. While this study only included meningiomas measuring ≥1 cm in at least one dimension, some of the sampled tumor volumes were relatively low, which raises the possibility of partial volume averaging effects in these smaller sampled volumes. Furthermore, 50% (18/36) of meningiomas within this cohort had received prior RT, potentially serving as a confounder for our data correlating vascularity with [^{68}Ga]-DOTATATE avidity. Future work assessing this correlation in treatment-naive meningiomas is warranted. Additionally, future immunohistochemical investigation utilizing SSTR2 stains and those investigating vascularity on resected tumor samples can assist in supporting the results of this study. Finally, future work evaluating the cost effectiveness of utilizing [^{68}Ga]-DOTATATE PET in meningioma management will be important, as this approach may ultimately reduce costs related to decreased complications from RT and has the potential to improve progression-free survival by improving targeted radiation dose delivery in patients with small volume residual disease (7).

CONCLUSIONS

In this study, we found a strong, significant correlation between the DCE-MRI perfusion parameter *Kep* and [^{68}Ga]-DOTATATE *SUV* in WHO Grade 2/3 meningiomas, which suggests biological differences in the relationship between tumor vascularity and SSTR2 expression in higher-grade meningiomas. Our findings may have pathophysiological implications for clinical management of patients with meningiomas. Future work to understand the potential prognostic role of combined DOTATATE PET and DCE MRI in meningioma treatment planning and response assessment is warranted.

DATA AVAILABILITY STATEMENT

The original contributions presented in the study are included in the article/supplementary material. Further inquiries can be directed to the corresponding author.

ETHICS STATEMENT

The studies involving human participants were reviewed and approved by New York-Presbyterian Hospital, Weill Cornell Medicine. The patients/participants provided their written informed consent to participate in this study. Written informed consent was obtained from the individual(s) for the publication of any potentially identifiable images or data included in this article.

AUTHOR CONTRIBUTIONS

All authors provided contributions to study conception and design, acquisition of data or analysis and interpretation of data, drafting the article or revising it critically for important intellectual content, and final approval for publication. Most important contributions of each author are as follows: conceptualization, JI and MR; data curation, MR, SK, SG, CT, EL, WF, RM, TS, RR, NK, SP, and JK; formal analysis, MR, SK, SG, CT, and JI; resources, RM, TS, RR, SP, JO, JK, and JI; writing—original draft, MR and JI; writing—review and editing, MR, EL, RM, BL, TS, RR, NK, SP, JO, JK, and JI.

FUNDING

This study was designed, conducted, analyzed, and reported entirely by the authors. This paper presents independent research funded by the 2019-2020 RSNA Radiology Resident Research Grant (#RR1962 PI: MR), the 2021-2022 RSNA Medical Student Research Grant (PI: SK), Weill Cornell Medical College (PI: JI) and Novartis Pharmaceuticals (Investigator-Initiated Trial, PI: JI). Novartis Pharmaceuticals was not involved in the study design, collection, analysis, interpretation of data, the writing of this article or the decision to submit it for publication.

REFERENCES

1. Lum MA, Martin AJ, Alexander MD, McCoy DB, Cooke DL, Lillaney P, et al. Intra-Arterial MR Perfusion Imaging of Meningiomas: Comparison to Digital Subtraction Angiography and Intravenous Mr Perfusion Imaging. *PloS One* (2016) 11:1–13. doi: 10.1371/journal.pone.0163554
2. Cordova C, Kurz SC. Advances in Molecular Classification and Therapeutic Opportunities in Meningiomas. *Curr Oncol Rep* (2020) 22:1–10. doi: 10.1007/s11912-020-00937-4
3. Louis DN, Perry A, Wesseling P, Brat DJ, Cree IA, Figarella-Branger D, et al. The 2021 WHO Classification of Tumors of the Central Nervous System: A Summary. *Neuro Oncol* (2021) 23:1231–51. doi: 10.1093/neuonc/noab106
4. Ansari SF, Shah KJ, Hassaneen W, Cohen-Gadol AA. Vascularity of Meningiomas. *Handb Clin Neurol* (2020) 169:153–65. doi: 10.1016/B978-0-12-804280-9.00010-X
5. Rogers L, Barani I, Chamberlain M, Kaley TJ, McDermott M, Raizer J, et al. Meningiomas: Knowledge Base, Treatment Outcomes, and Uncertainties. A RANO Review. *J Neurosurg* (2015) 122:4–23. doi: 10.3171/2014.7.JNS131644
6. Gallagher MJ, Jenkinson MD, Brodbelt AR, Mills SJ, Chavredakis E. WHO Grade 1 Meningioma Recurrence: Are Location and Simpson Grade Still Relevant? *Clin Neurol Neurosurg* (2016) 141:117–21. doi: 10.1016/j.clineuro.2016.01.006
7. Mahase SS, Roth O'Brien DAR, No D, Roytman M, Skafida ME, Lin E, et al. [68ga]-DOTATATE PET/MRI as an Adjunct Imaging Modality for Radiation Treatment Planning of Meningiomas. *Neuro-Oncol Adv* (2021) 3:1–9. doi: 10.1093/noajnl/vdab012
8. Roytman M, Pisapia DJ, Liechty B, Lin E, Skafida M, Magge RS, et al. Somatostatin Receptor-2 Negative Meningioma: Pathologic Correlation and Imaging Implications. *Clin Imaging* (2020) 66:18–22. doi: 10.1016/j.clinimag.2020.04.026
9. Ivanidze J, Roytman M, Sasson A, Skafida M, Fahey TJ III, Osborne JR, et al. Molecular Imaging and Therapy of Somatostatin Receptor Positive Tumors. *Clin Imaging* (2019) 56:146–54. doi: 10.1016/j.clinimag.2019.04.006
10. Hofman MS, Eddie Lau WF, Hicks RJ. Somatostatin Receptor Imaging With 68 Ga DOTATATE PET/CT: Clini- Cal Utility, Normal Patterns, Pearls, and Pitfalls in Interpretation. *Radioraphics* (2016) 35:500–16. doi: 10.1148/rg.352140164
11. Ivanidze J, Roytman M, Lin E, Magge RS, Pisapia DJ, Liechty B, et al. Gallium-68 DOTATATE PET in the Evaluation of Intracranial Meningiomas. *J Neuroimaging* (2019) 0:1–7. doi: 10.1111/jon.12632
12. Heye AK, Culling RD, Valdés Hernández MC, Thrippleton MJ, Wardlaw JM. Assessment of Blood-Brain Barrier Disruption Using Dynamic Contrast-Enhanced MRI. A Systematic Review. *NeuroImage Clin* (2014) 6:262–74. doi: 10.1016/j.nicl.2014.09.002
13. Chidambaram S, Pannullo SC, Roytman M, Pisapia DJ, Liechty B, Magge RS, et al. Dynamic Contrast-Enhanced Magnetic Resonance Imaging Perfusion Characteristics in Meningiomas Treated With Resection and Adjuvant Radiosurgery. *Neurosurg Focus* (2019) 46:1–6. doi: 10.3171/2019.3.FOCUS1954
14. Tamrazi B, Shiroishi MS, Liu CSJ. Advanced Imaging of Intracranial Meningiomas. *Neurosurg Clin N Am* (2016) 27:137–43. doi: 10.1016/j.nec.2015.11.004
15. Zhang H, Rödiger LA, Shen T, Miao J, Oudkerk M. Preoperative Subtyping of Meningiomas by Perfusion MR Imaging. *Neuroradiology* (2008) 50:835–40. doi: 10.1007/s00234-008-0417-3
16. Yang S, Law M, Zagzag D, Wu HH, Cha S, Golfinos JG, et al. Dynamic Contrast-Enhanced Perfusion MR Imaging Measurements of Endothelial Permeability: Differentiation Between Atypical and Typical Meningiomas. *Am J Neuroradiol* (2003) 24:1554–9.
17. Sacco S, Ballati F, Gaetani C, Lomoro P, Farina LM, Bacila A, et al. Multi-Parametric Qualitative and Quantitative MRI Assessment as Predictor of Histological Grading in Previously Treated Meningiomas. *Neuroradiology* (2020) 62:1441–9. doi: 10.1007/s00234-020-02476-y
18. Sommerauer M, Burkhardt J, Frontzek K, Rushing E, Buck A, Krayenbuehl N, et al. 68Gallium-DOTATATE PET in Meningioma: A Reliable Predictor of Tumor Growth Rate? *Neuro Oncol* (2016) 18:1021–7. doi: 10.1093/neuonc/now001
19. Deppen SA, Liu E, Blume JD, Clanton J, Shi C, Jones-Jackson LB, et al. Safety and Efficacy of 68Ga-DOTATATE PET/CT for Diagnosis, Staging, and Treatment Management of Neuroendocrine Tumors. *J Nucl Med* (2016) 57:708–14. doi: 10.2967/jnumed.115.163865
20. Verma S, Turkbey B, Muradyan N, Rajesh A, Cornud F, Haider MA, et al. Overview of Dynamic Contrast-Enhanced MRI in Prostate Cancer Diagnosis and Management. *Am J Roentgenol* (2012) 198:1277–88. doi: 10.2214/AJR.12.8510
21. Cha S, Yang L, Johnson G, Lai A, Chen M-H, Tihan T, et al. Comparison of Microvascular Permeability Measurements, Ktrans, Determined With Conventional Steady-State T1-Weighted and First-Pass T2*-Weighted MR Imaging Methods in Gliomas and Meningiomas. *Am J Neuroradiol* (2006) 27:409–17.
22. Tofts PS, Brix G, Buckley DL, Evelhoch JL, Henderson E, Knopp MV, et al. Estimating Kinetic Parameters From Dynamic Contrast-Enhanced T1-Weighted MRI of a Diffusable Tracer. *J Magn Reson Imaging* (1999) 10:223–32. doi: 10.1002/(SICI)1522-2586(199909)10:3<223::AID-JMRI2>3.0.CO;2-S
23. Brix G, Semmler P, Rudiger S, Lothar R, Layer G, Lorenz WJ. Pharmacokinetic Parameters in Cns Gd-Dtpa Enhanced Mr Imaging. *J Comput Assist Tomogr* (1991) 15:621–8. doi: 10.1097/00004728-199107000-00018
24. Larsson HBW, Stubgaard M, Frederiksen JL, Jensen M, Henriksen O, Paulson OB. Quantitation of Blood-Brain Barrier Defect by Magnetic Resonance Imaging and Gadolinium-DTPA in Patients With Multiple Sclerosis and Brain Tumors. *Magn Reson Med* (1990) 16:117–31. doi: 10.1002/mrm.1910160111
25. Sourbron SP, Buckley DL. On the Scope and Interpretation of the Tofts Models for DCE-MRI. *Magn Reson Med* (2011) 66:735–45. doi: 10.1002/mrm.22861
26. Bernatz S, Monden D, Gessler F, Radic T, Hattingen E, Senft C, et al. Influence of VEGF-A, VEGFR-1-3, and Neuropilin 1-2 on Progression-Free: And Overall Survival in WHO Grade II and III Meningioma Patients. *J Mol Histol* (2021) 52:233–43. doi: 10.1007/s10735-020-09940-2
27. Awasthi R, Pandey CM, Sahoo P, Behari S, Kumar V, Kumar S, et al. Dynamic Contrast-Enhanced Magnetic Resonance Imaging-Derived K Ep as a Potential

Biomarker of Matrix Metalloproteinase 9 Expression in Patients With Glioblastoma Multiforme: A Pilot Study. *J Comput Assist Tomogr* (2012) 36:125–30. doi: 10.1097/RCT.0b013e31823f6c59
28. Lui YW, Malhotra A, Farinhas JM, Dasari SB, Weidenheim K, Freeman K, et al. Dynamic Perfusion MRI Characteristics of Dural Metastases and Meningiomas: A Pilot Study Characterizing the First-Pass Wash-in Phase Beyond Relative Cerebral Blood Volume. *Am J Roentgenol* (2011) 196:886–90. doi: 10.2214/AJR.10.5309
29. Merz M, Seyler L, Bretschi M, Semmler W, Bauerle T. Diffusion-Weighted Imaging and Dynamic Contrast-Enhanced MRI of Experimental Breast Cancer Bone Metastases - A Correlation Study With Histology. *Eur J Radiol* (2015) 84:623–30. doi: 10.1016/j.ejrad.2015.01.002
30. Kang SR, Kim HW, Kim HS. Evaluating the Relationship Between Dynamic Contrast-Enhanced MRI (DCE-MRI) Parameters and Pathological Characteristics in Breast Cancer. *J Magn Reson Imaging* (2020) 52:1360–73. doi: 10.1002/jmri.27241
31. Liu F, Wang M, Li H. Role of Perfusion Parameters on DCE-MRI and ADC Values on DWMRI for Invasive Ductal Carcinoma at 3.0 Tesla. *World J Surg Oncol* (2018) 16:1–12. doi: 10.1186/s12957-018-1538-8
32. Schlemmer H-P, Merkle J, Grobholz R, Jaeger T, Michel MS, Werner A, et al. Can Pre-Operative Contrast-Enhanced Dynamic MR Imaging for Prostate Cancer Predict Microvessel Density in Prostatectomy Specimens? *Eur Radiol* (2004) 14:309–17. doi: 10.1007/s00330-003-2025-2
33. McCann SM, Jiang Y, Fan X, Wang J, Antic T, Prior F, et al. Quantitative Multiparametric MRI Features and PTEN Expression of Peripheral Zone Prostate Cancer: A Pilot Study. *Am J Roentgenol* (2016) 206:559–65. doi: 10.2214/AJR.15.14967
34. Choi YJ, Lee IS, Song YS, Kim JI, Choi K, Song JW. Diagnostic Performance of Diffusion-Weighted (DWI) and Dynamic Contrast-Enhanced (DCE) MRI for the Differentiation of Benign From Malignant Soft-Tissue Tumors. *J Magn Reson Imaging* (2019) 50:798–809. doi: 10.1002/jmri.26607
35. Huang YS, Chen JLY, Chen HM, Yeh LH, Shih JY, Yen RF, et al. Assessing Tumor Angiogenesis Using Dynamic Contrast-Enhanced Integrated Magnetic Resonance-Positron Emission Tomography in Patients With non-Small-Cell Lung Cancer. *BMC Cancer* (2021) 21:1–13. doi: 10.1186/s12885-021-08064-4
36. Scerrati A, Mongardi L, Visani J, Lofrese G, Cavallo MA, Fiorentino A, et al. The Controversial Role of Bevacizumab in the Treatment of Patients With Intracranial Meningioma: A Comprehensive Literature Review. *Expert Rev Anticancer Ther* (2020) 20:197–203. doi: 10.1080/14737140.2020.1736567
37. Seystahl K, Stoecklein V, Schüller U, Rushing E, Nicolas G, Schafer N, et al. Somatostatin Receptor-Targeted Radionuclide Therapy for Progressive Meningioma: Benefit Linked to 68Ga-DOTATATE/-TOC Uptake. *Neuro Oncol* (2016) 18:1538–47. doi: 10.1093/neuonc/now060
38. Makis W, McCann K, McEwan AJB. Rhabdoid Papillary Meningioma Treated With 177Lu DOTATATE PRRT. *Clin Nucl Med* (2015) 40:237–40. doi: 10.1097/RLU.0000000000000669
39. Thakral P, Sen I, Das SS, Manda D, CB V, Malik D. Dosimetric Analyses of Intra-Arterial Versus Standard Intravenous Administration of 177Lu-DOTATATE in Patients of Well Differentiated Neuroendocrine Tumor With Liver-Dominant Metastatic Disease. *Br J Radiol* (2021) 94:1–11. doi: 10.1259/bjr.20210403

Conflict of Interest: The authors declare that the research was conducted in the absence of any commercial or financial relationships that could be construed as a potential conflict of interest.

Publisher's Note: All claims expressed in this article are solely those of the authors and do not necessarily represent those of their affiliated organizations, or those of the publisher, the editors and the reviewers. Any product that may be evaluated in this article, or claim that may be made by its manufacturer, is not guaranteed or endorsed by the publisher.

Copyright © 2022 Roytman, Kim, Glynn, Thomas, Lin, Feltus, Magge, Liechty, Schwartz, Ramakrishna, Karakatsanis, Pannullo, Osborne, Knisely and Ivanidze. This is an open-access article distributed under the terms of the Creative Commons Attribution License (CC BY). The use, distribution or reproduction in other forums is permitted, provided the original author(s) and the copyright owner(s) are credited and that the original publication in this journal is cited, in accordance with accepted academic practice. No use, distribution or reproduction is permitted which does not comply with these terms.

frontiers in Oncology

ORIGINAL RESEARCH
published: 04 February 2022
doi: 10.3389/fonc.2022.828361

Combined Microscopic and Endoscopic Surgery for Pineal Region Meningiomas Using the Occipital-Parietal Transtentorial Approach

Yu Ding[1,2†], Liang Sun[1†], Yukun Hu[1], Weiwei Zhai[1], Liexiang Zhang[2], Zhengquan Yu[1], Jiang Wu[1*] and Gang Chen[1]*

[1] Department of Neurosurgery, The First Affiliated Hospital of Soochow University, Suzhou, China, [2] Department of Neurosurgery, The Affiliated Suqian Hospital of Xuzhou Medical University, Suqian, China

OPEN ACCESS

Edited by:
Hailiang Tang,
Fudan University, China

Reviewed by:
Awadhesh Jaiswal,
Sanjay Gandhi Post Graduate Institute of Medical Sciences (SGPGI), India
Tomasz Dziedzic,
Medical University of Warsaw, Poland

***Correspondence:**
Zhengquan Yu
zqyu_2000@163.com
Jiang Wu
szjiangwu@163.com

†These authors have contributed equally to this work

Specialty section:
This article was submitted to Neuro-Oncology and Neurosurgical Oncology, a section of the journal Frontiers in Oncology

Received: *03 December 2021*
Accepted: *17 January 2022*
Published: *04 February 2022*

Citation:
Ding Y, Sun L, Hu Y, Zhai W, Zhang L, Yu Z, Wu J and Chen G (2022) Combined Microscopic and Endoscopic Surgery for Pineal Region Meningiomas Using the Occipital-Parietal Transtentorial Approach. Front. Oncol. 12:828361. doi: 10.3389/fonc.2022.828361

Objective: Pineal region meningiomas are deeply located and adjacent to critical neurovascular structures, making them one of the most challenging areas to access. The authors presented a combined microscopic and endoscopic surgery and investigated its value in resecting pineal region meningiomas.

Methods: Twelve patients with pineal region meningiomas from February 2017 to December 2020 were retrospectively reviewed. All patients underwent combined microscopic and endoscopic surgery using the occipital-parietal transtentorial approach. Perioperative clinical, surgical, and radiographic data were collected.

Results: The endoscope provided a wider view and increased visualization of residual tumors. All tumors were completely resected, and none of the patients died. Total resection was believed to have been achieved in four patients, but the residual tumor was detected after endoscopic exploration and was completely resected with an endoscope. Only one patient had transient visual field deficits. No recurrence was observed during follow-up.

Conclusions: Combined microscopic-endoscopic surgery for pineal region meningiomas eliminates microscopic blind spots, thus compensating for the shortcomings of the traditional occipital transtentorial approach. It is a promising technique for minimally invasive maximal resection of pineal region meningiomas.

Keywords: meningiomas, pineal, endoscope, trans-bitentorial approach, falcotentorial junction

INTRODUCTION

Meningiomas of the pineal region are rare, accounting for approximately 8% of tumors in this region (1, 2). According to the tumor origin, pineal region meningiomas are classified into two main subtypes: falcotentorial and velum interpositum meningiomas. Falcotentorial meningiomas originate from the junction of the dural folds between the falx cerebri and tentorium. In contrast, velum interpositum meningiomas arise from the double-layered pia of the velum interpositum

and have no direct dural attachment (3–6).Most pineal region meningiomas grow slowly, occupying the pineal region and compressing surrounding structures, such as the pineal gland, midbrain, deep venous system, and the third ventricle. Due to the deep location and close relationship with critical neurovascular structures, radical resection of meningiomas in the pineal region remains a significant challenge.

Numerous surgical approaches have been advocated for the resection of meningiomas in the pineal region. The most commonly used approaches are occipital transtentorial and supracerebellar infratentorial approaches. However, both approaches have disadvantages. Visualization of the surgical field without blind spots is changing using these approaches because the tumor is obscured by the dural structures and deep venous system (7–9). Previous studies have reported various modifications to overcome these disadvantages, including the occipital bitranstentorial/falcine approach, bilateral occipital craniotomy, and simultaneous combined supratentorial/infratentorial approaches (10–12). These approaches provide a wider exposure but are associated with significant risks, such as venous infarction and cortical blindness.

The concept of using endoscopy to resect pineal lesions is not novel. However, most endoscopic approaches reported previously were through the infratentorial supracerebellar corridor to access the pineal region (13, 14). This study presents a combined microscopic and endoscopic surgery using the occipital-parietal transtentorial approach for the radical resection of pineal region meningiomas.

METHODS

Patients

During this retrospective study, 12 patients at the First Affiliated Hospital of Soochow University underwent surgery to resect pineal region meningiomas from February 2017 to December 2020. All patients underwent combined microscopic and endoscopic surgery using the occipital-parietal transtentorial approach. Perioperative clinical, surgical, and radiographic data were collected.

There were four female and eight male patients, ranging in age from 39 to 71 (mean age, 54.3) years. The patients' clinical course varied from 2 weeks to 4 months (median, 2.1 months). This study was approved by the local ethics committee (S2018087), and informed consent was obtained from the patients. Patient profiles are summarized in **Table 1**.

Combined Microscopic and Endoscopic Video Monitor System

We used an endoscope (Karl Storz, Germany) and a microscope (Pentero; Carl Zeiss, Germany) in our integrated operating room. Both endoscopic and microscopic views were simultaneously displayed on a high-definition screen (picture-in-picture, **Figure 1A**) visible to the entire surgical team, including the surgeon, assistant surgeon, and assisting nurses.

Neuroimaging

All patients underwent preoperative computed tomography and magnetic resonance imaging (MRI). Tumor size, peri-tumor edema, tumor shape, and hydrocephalus were assessed. In addition, magnetic resonance venography was performed before surgical intervention for multimodal fusion to evaluate the patency of the deep veins and to understand the location of the tumor in relation to the deep veins. The extent of resection (EOR) represents the percentage of the preoperative tumor volume resected (preoperative volume – postoperative volume)/preoperative volume. Tumor volume was measured on T1-weighted gadolinium-enhanced magnetic resonance images using iPlan Cranial software (BrainLab, Germany). Gross total resection (GTR) was defined as the tumor that was confirmed to be completely resected by the surgeon with no residual tumor detected on postoperative contrast MRI (EOR = 100%). Gross total resection included Simpson grades I-III. Near-total resection

TABLE 1 | Clinical characteristics of 12 patients undergoing the combined microscopic and endoscopic surgery for resection of pineal region meningiomas.

Case no.	Age (yrs), sex	Tumor size (mm)	Presenting symptoms	Hydrocephalus	EOR	Surgical complications	Dural attachment	Histological subtype	Post-op mRS score
1	42, M	25	Incidental	N/A	GTR	None	Tentorium	Fibrous	0
2	71, M	57	HA, vomiting, blurred vision	Yes, transient EVD post-op, resolved afterwards	GTR	Transient VFD	Tentorium/falx	Meningothelial	2
3	67, F	52	HA, blurred vision	Yes, transient EVD post-op, resolved afterwards	GTR	None	Tentorium/falx	Meningothelial	1
4	39, F	38	HA, vomiting	N/A	GTR	None	Falx	Transitional	0
5	49, F	37	HA, dizziness	N/A	GTR	None	Tentorium	Fibrous	0
6	39, M	41	HA	N/A	GTR	None	Tentorium/falx	Fibrous	1
7	57, M	43	HA, memory issues, imbalance	Yes, transient EVD post-op, resolved afterwards	GTR	None	Tentorium/falx	Psammomatous	1
8	52, F	26	Incidental	N/A	GTR	None	Velum interpositum	Meningothelial	0
9	45, M	29	Dizziness, fatigue	N/A	GTR	None	Tentorium	Meningothelial	0
10	65, M	34	Dizziness, memory issues	Yes, relieved after surgery	GTR	None	Tentorium	Transitional	0
11	58, M	31	Incidental	N/A	GTR	None	Tentorium/falx	Angioblastic	0
12	67, M	38	HA, dizziness	Yes, relieved after surgery	GTR	None	Tentorium/falx	Meningothelial	1

EVD, external ventricular drainage; HA, headache; N/A, no hydrocephalus; GTR, gross total resection; VFD, visual field defect.

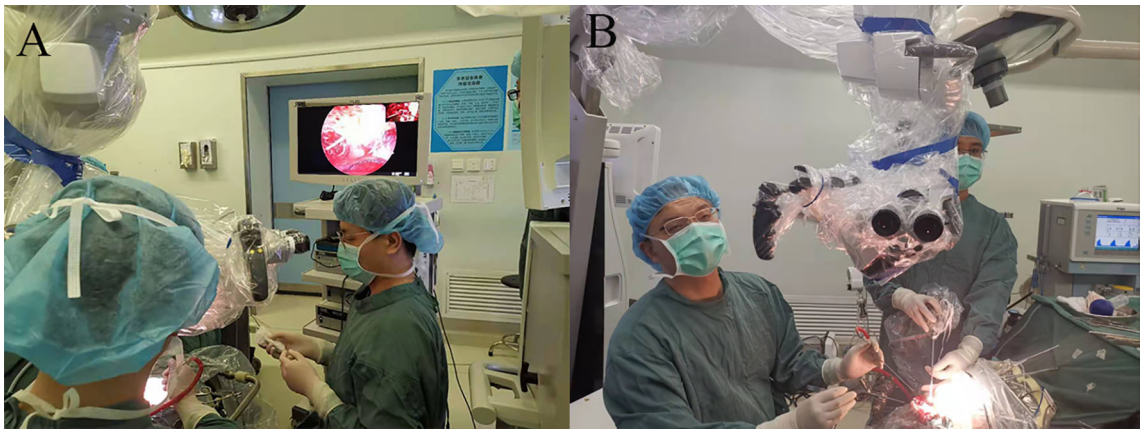

FIGURE 1 | **(A)** Setup of the microscope, endoscope, and image-merged screen in the operating room. The introduction and movement of the endoscope are well supervised under microscopic view. The endoscopic view is displayed in full screen, and the microscopic view is shown in the upper right corner. **(B)** The position of the main surgeon and the assistant. The assistant holds the endoscope while the main surgeon performs bimanual dissection.

was defined as the resection of more than 90% of the neoplasm (90 ≤ EOR <100%), and subtotal resection was defined as the resection of less than 90% of the neoplasm (EOR < 90%).

Follow–Up and Outcome Evaluation

Follow-up imaging was performed immediately (<3 days), 3 months, 6 months, and then each year after the operation. All patients visited our clinic at 3 months, 6 months, and then each year after the operation, and the symptoms, histopathology, and modified Rankin Scale score at the last follow-up were assessed.

Surgical Technique

The patient was placed in a 3/4 prone position with the head slightly rotated toward the contralateral side. This position allowed the occipital lobe to be retracted by gravity. A U-shaped skin incision was created, followed by an occipital craniotomy with a small bone window of approximately 3×5 cm. The bone window exposed the transverse and superior sagittal sinus margins. The dura mater was opened with a semicircular incision, based on the superior sagittal sinus. After gradual drainage of cerebrospinal fluid, the falx cerebri, straight sinus, and tentorium cerebelli were identified in turn under the microscope. A linear incision parallel to the straight sinus was made in the tentorium. Because most pineal region meningiomas originated near the falcotentorial junction receiving blood supply from the meningeal arteries along the tentorium and falx, we could eliminate the tumor blood supply early in most cases. However, the location of the tumor in relation to the deep veins could not be determined with the microscope at this time. We then inserted the endoscope under microscopic surveillance. After dissecting the arachnoid membrane, identified the vein of Galen and tributaries. The adhesion between the tumor and the deep veins was clearly exposed, which allowed the surgeon to separate the tumor from the veins under direct vision. At this stage, the endoscope could cross the falx, extend the contralateral operative field, and directly observe the rear of the third ventricle. In addition, once the suitable position was located, we fixed the endoscope with an endoscope holder, which allowed us to separate and dissect the tumor with both hands. In the final stage of surgery, the angled endoscope could look around the corner to detect any residual tumors. If the residual tumor was detected, it was resected with dedicated angled instruments under 30° visualization. Intraoperative photographs (**Figure 2A–C**) and MRI images (**Figure 2D–F**) of a patient with a pineal meningioma are shown in **Figure 2**.

RESULTS

Table 1 summarizes the clinical characteristics of the 12 patients with meningiomas in the pineal region. In this study, the mean follow-up period was 2.09 years (range, 8 months and 3.5 years). None of the patients died during the study period. Postoperative complications were observed in only one patient who presented with visual field defects, which resolved completely at 3 months after surgery. Five patients had preoperative hydrocephalus, and three of them received transient extraventricular drainage (< 10 days) after surgery; all patients were relieved of hydrocephalus. None of the patients required further ventriculoperitoneal (VP) shunts during follow-up. All deep veins were well protected, and no venous injury was observed during the operation. GTR was achieved in all patients. Total resection was believed to have been achieved in four patients, but the residual tumor was detected after endoscopic exploration and was completely resected using an endoscope. The residual tumor was often located at the ventral aspect of the deep veins or the roof of the third ventricle hidden by the corpus callosum (**Figure 2C**; **Figure 3**). Tumor recurrence was not detected during the follow-up period.

DISCUSSION

The pineal region is one of the most intricate anatomical regions in the human body. Resection of pineal region tumors is

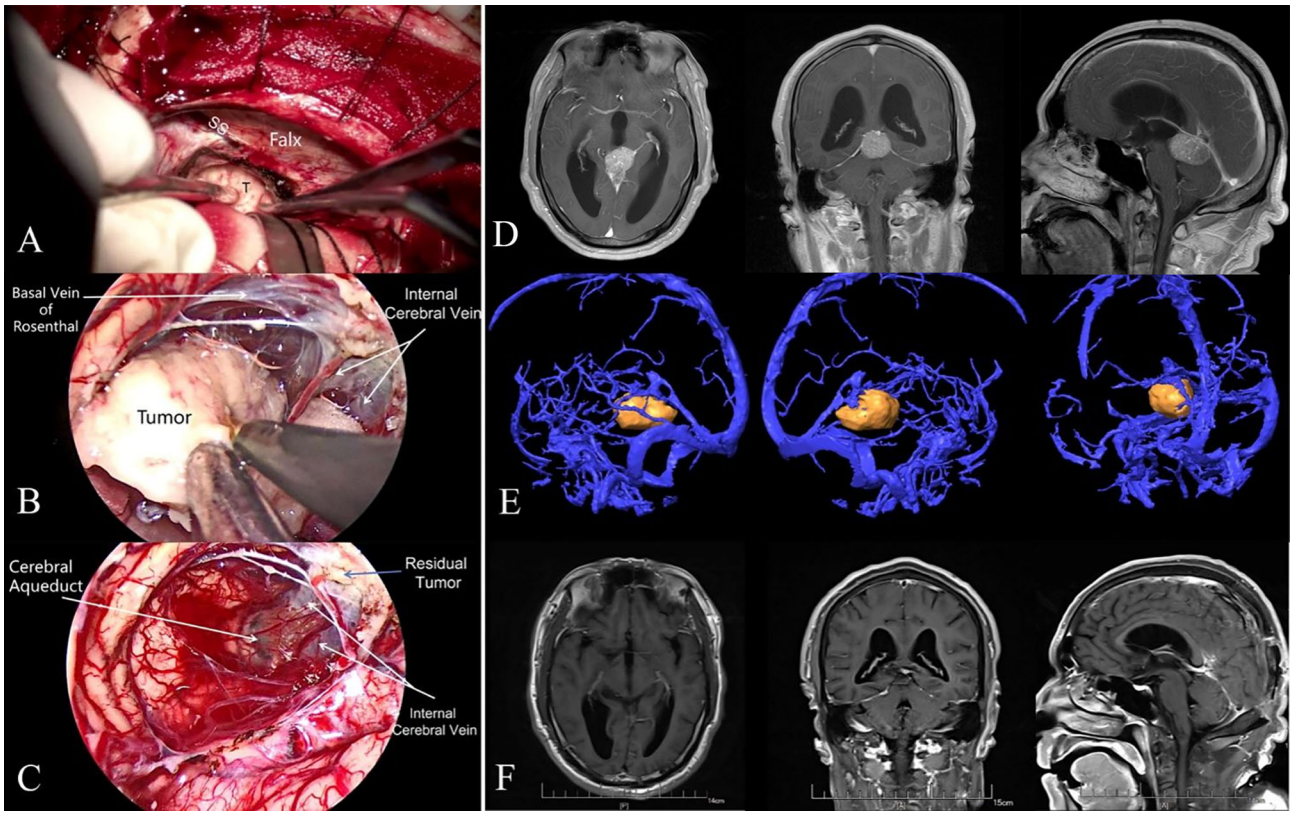

FIGURE 2 | **(A)** Intraoperative microscopic view. Due to the occlusion of the falx cerebri, the microscopic view had a poor exposure of the internal cerebral vein and great cerebral vein. **(B)** Intraoperative endoscopic view. The endoscope increased the visualization of the deep venous system and allowed separating the tumor from the deep vein under direct vision. **(C)** Intraoperative endoscopic view. A small residual tumor was found adhering to the internal cerebral vein. **(D)** Preoperative contrast-enhanced T1-weighted MRI showed a pineal region meningioma in a 65-year-old man. **(E)** Multimodal fusion showed the meningioma lay underneath the deep venous complex. **(F)** Postoperative MRI confirmed a gross total resection at 3 months after surgery. *SS*, straight sinus; *T*, tumor.

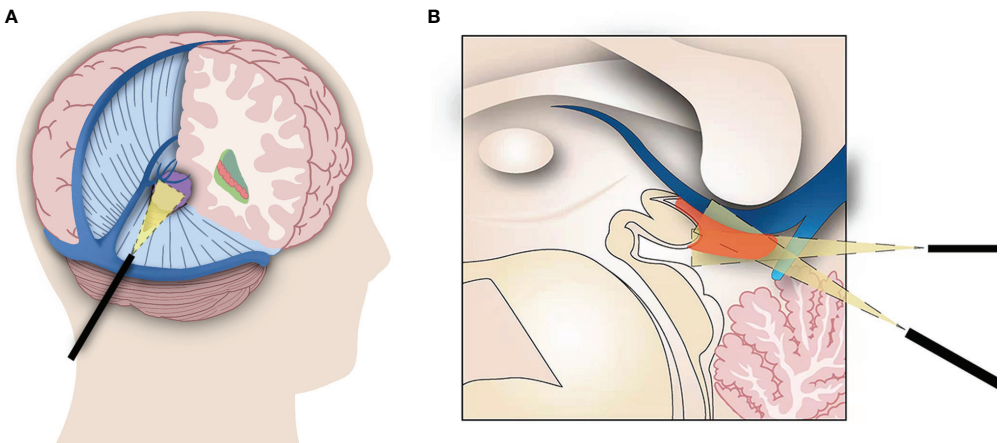

FIGURE 3 | **(A)** Surgical approach of the combined microscopic and endoscopic surgery for pineal region meningiomas. The endoscope accesses the pineal region through the incision in the tentorium. **(B)** The endoscope improves visualization of the ventral aspect of the deep veins and the roof of the third ventricle, where tumors often remain. This combined technique also allows the tumor to be isolated from the veins under direct vision, reducing the risk of deep vein injury.

challenging, even for experienced neurosurgeons. Different from many pineal region malignant tumors, pineal region meningioma is a slow-growing benign tumor for which complete resection is the best treatment strategy. Therefore, despite surgical challenges, radical resection remains the primary treatment goal (15). In the present study, we treated 12 consecutive patients with meningiomas in the pineal region. All tumors were completely resected using the occipital-parietal transtentorial approach. We also found that the combined microscopic and endoscopic surgery is a promising technique.

The occipital transtentorial and supracerebellar infratentorial approaches are the most common approaches when accessing the pineal region. The supracerebellar infratentorial approach provides a posterior midline approach to the pineal region. The main advantage of this approach is that it utilizes the natural corridor between the superior cerebellar surface and tentorium without brain retraction. In addition, the pineal region is located underneath the major deep veins, which reduces the risk of damage to critical neurovascular structures (16, 17). However, this approach requires the sacrifice of midline bridging veins, leading to venous infarction and cerebellar edema. Furthermore, the supracerebellar infratentorial approach has poor visualization of supratentorial structures, and it is difficult to reach the lesions in the posterior floor of the third ventricle (8).

In contrast, the occipital transtentorial approach (OTA) provides the most extensive exposure of both the supratentorial and infratentorial compartments. It provides direct visualization of the deep venous structure and ipsilateral dorsal and lateral extension of the midbrain (15, 18). In this study, an OTA was used in all 12 patients, as we found that this approach has particular advantages for meningiomas in the pineal region. First, since most pineal region meningiomas derive their blood supply from the tentorium and falx, OTA allows for early devascularization of the feeding arteries along the tentorium and falx (18, 19). Second, meningiomas in the pineal region are slow growing, and there is a long duration between the onset of symptoms and diagnosis. Therefore, the tumor is usually relatively large at the time of detection and mostly grows in both the supratentorial and infratentorial compartments with lateral extension. The mean diameter of the tumors reported in this study was 3.8 cm, and the largest tumor diameter was 5.7 cm. Compared to the restricted visualization at the supratentorial structures in the supracerebellar infratentorial approach, OTA allows extensive exposure of both the supratentorial and infratentorial spaces and provides superior views of brainstem attachments. A previous study (12) suggested that the surgical approach should be selected according to the position of the tumor and the deep venous complex. The supracerebellar infratentorial approach is recommended for pineal region meningiomas displacing the deep venous complex superiorly. However, we believe that this positional relationship is not the sole determinant. When the meningioma lies underneath the deep venous complex, the OTA allows the surgeon to use either the interhemispheric or suboccipital supratentorial space; thus, the operator does not have to operate continuously among the deep veins.

However, the OTA also has the inherent limitations of restricted views around the neurovascular structures. This approach allows poor visualization of the ventral aspect of the vein of Galen, contralateral basal vein, and contralateral quadrigeminal region (**Figure 2A**). A transfalcine approach has been reported to improve exposure of the contralateral operative field through additional incisions above the sagittal sinus in the falx, but it is associated with significant risks (20). Meningiomas in the pineal region often compress the vital deep venous systems and develop collateral venous channels in the falx and tentorium. Additional incision of the falx could injure the collateral venous channels, resulting in venous infarction (19). In addition, the OTA is sometimes unable to expose the roof of the third ventricle, which is hidden by a prominent splenium (**Figure 3**), and sacrifice of the splenium may cause a disconnection syndrome.

In this study, we present a combined microscopic and endoscopic surgery for the resection of meningiomas in the pineal region using the OTA. This technique compensates for the shortcomings of the conventional microscopic OTA. First, the endoscope contributes to expanding the surgical field. The endoscope can cross the falx, extend the contralateral operative field, and increase the visualization of the contralateral internal cerebral vein and basal vein of Rosenthal. This allows the tumor to be isolated from the vein under direct vision, reducing the risk of deep vein injury (**Figure 2B**). In addition, through the tentorial incisura, the endoscope allows an extension of the microsurgical approach from the supratentorial region to the infratentorial region. Second, this combined microscopic and endoscopic surgery increases visualization of residual tumors. In the OTA, the ventral aspect of the vein of Galen and the roof of the third ventricle may not be adequately exposed using a microscope. The endoscope was invaluable in resolving the issue of hidden tumor remnants by allowing angled views around the deep venous structures and into the anterior third ventricle (21) (**Figure 2C**; **Figure 3**). In our series, total resection was believed to have been achieved in four patients, but the residual tumor was detected after endoscopic exploration and was completely resected using an endoscope.

However, insertion and movement of the endoscope may damage bridging veins and deep cerebral veins due to the lack of a posterior and lateral view. Some studies have indicated the importance of performing all endoscopic movements under microscopic surveillance (22, 23). However, when the microscope and endoscope are combined in the same setting, the surgeon has to switch between the microscope ocular view and the endoscope monitor view. This nonintegrated visual information can disrupt the flow of the operative procedure. Few studies have attempted to integrate endoscopes and microscopes. Here, we applied a picture-in-picture mode (**Figure 1**) in which microscopic and endoscopic images were merged on the same screen. With simultaneous microscope monitoring, the surgeon can safely place and move the endoscope and easily transition between the two modalities.

The pineal region is surrounded by critical neurovascular structures, such as the deep venous system, third ventricle, and midbrain. Despite the advancements in preoperative multimodal neuroimaging, intraoperative navigation, and microsurgical techniques, surgery for pineal region meningiomas remains a great challenge. The combined microscopic and endoscopic surgery using the OTA presented in this study provides an attractive treatment option for pineal region meningiomas. There

were almost no blind spots in this approach. In our study, GTR was achieved in all 12 patients, and no recurrence occurred during the follow-up period. This ergonomic integration of the endoscope and microscope also reduced the risk of damage to critical neurovascular structures. No venous injury was observed during the operation, and there were no signs of brainstem injury after surgery. Five patients had preoperative hydrocephalus, which were relieved after surgery, and none of the patients required further VP shunts during the follow-up period. This study has some potential limitations. Because of the low incidence of pineal region meningiomas, this is a relatively small series of patients who underwent combined microscopic and endoscopic surgery, and we limited our analysis to a retrospective study. In the future, additional case–control studies should be conducted to validate our findings.

CONCLUSION

The combined microscopic and endoscopic surgery for pineal region meningiomas eliminates microscope blind spots, thus compensating for the shortcomings of the traditional OTA. It is a promising technique for minimally invasive maximal resection of pineal region meningiomas.

DATA AVAILABILITY STATEMENT

The original contributions presented in the study are included in the article/supplementary material. Further inquiries can be directed to the corresponding authors.

ETHICS STATEMENT

The studies involving human participants were reviewed and approved by Ethics committee, The First Affiliated Hospital of Soochow University. The patients/participants provided their written informed consent to participate in this study.

AUTHOR CONTRIBUTIONS

YD: Conceptualization, Methodology, Writing- Original draft preparation, Investigation. LS: Methodology, Writing- Original draft preparation, Investigation. YH: Formal analysis, Visualization. WZ: Investigation, Data Curation. LZ: Formal analysis, Investigation. ZY: Conceptualization, Methodology, Resources, Supervision, Project administration. JW: Conceptualization, Methodology, Resources, Writing - Review & Editing, Project administration. GC: Resources. All authors contributed to the article and approved the submitted version.

FUNDING

This work was supported by Jiangsu Provincial Medical Key Talent grant (ZDRCA2016040) and grant (SYS2019045) from Suzhou Government, the grant from the National Natural Science Foundation of China (number 82171294), the National Natural Science Foundation for Youth of China (No. 81801137), and the Joint Funds of Jiangsu Province (yl2020lh05).

REFERENCES

1. Okami N, Kawamata T, Hori T, Takakura K. Surgical Treatment of Falcotentorial Meningioma. *J Clin Neurosci* (2001) 8(Suppl 1):15–8. doi: 10.1054/jocn.2001.0870
2. Raco A, Agrillo A, Ruggeri A, Gagliardi FM, Cantore G. Surgical Options in the Management of Falcotentorial Meningiomas: Report of 13 Cases. *Surg Neurol* (2004) 61(2):157–164; discussion 164. doi: 10.1016/S0090-3019(03)00573-1
3. Konovalov AN, Spallone A, Pitzkhelauri DI. Meningioma of the Pineal Region: A Surgical Series of 10 Cases. *J Neurosurg* (1996) 85(4):586–90. doi: 10.3171/jns.1996.85.4.0586
4. Nowak A, Dziedzic T, Czernicki T, Kunert P, Marchel A. Falcotentorial and Velum Interpositum Meningiomas: Two Distinct Entities of the Pineal Region. *Neurologia i Neurochirurgia Polska* (2014) 48(6):397–402. doi: 10.1016/j.pjnns.2014.09.009
5. Yu L, Orazmyradov B, Qi S, Song Y, Fang L. Reinvestigation of the Origins of Pineal Meningiomas Based on its Related Veins and Arachnoid Membranes. *BMC Neurol* (2020) 20(1):200. doi: 10.1186/s12883-020-01783-4
6. Behari S, Das KK, Kumar A, Mehrotra A, Srivastava AK, Sahu RN, et al. Large/Giant Meningiomas of Posterior Third Ventricular Region: Falcotentorial or Velum Interpositum? *Neurol India* (2014) 62(3):290–5. doi: 10.4103/0028-3886.136934
7. Bassiouni H, Asgari S, Konig HJ, Stolke D. Meningiomas of the Falcotentorial Junction: Selection of the Surgical Approach According to the Tumor Type. *Surg Neurol* (2008) 69(4):339–349; discussion 349. doi: 10.1016/j.surneu.2007.02.029
8. Yamamoto I. Pineal Region Tumor: Surgical Anatomy and Approach. *J Neurooncol* (2001) 54(3):263–75. doi: 10.1023/A:1012790213818
9. Lozier AP, Bruce JN. Meningiomas of the Velum Interpositum: Surgical Considerations. *Neurosurg Focus* (2003) 15(1):E11. doi: 10.3171/foc.2003.15.1.11
10. Quinones-Hinojosa A, Chang EF, Chaichana KL, McDermott MW. Surgical Considerations in the Management of Falcotentorial Meningiomas: Advantages of the Bilateral Occipital Transtentorial/Transfalcine Craniotomy for Large Tumors. *Neurosurgery* (2009) 64(5 Suppl 2):260–268; discussion 268. doi: 10.1227/01.NEU.0000344642.98597.A7
11. Sekhar LN, Goel A. Combined Supratentorial and Infratentorial Approach to Large Pineal-Region Meningioma. *Surg Neurol* (1992) 37(3):197–201. doi: 10.1016/0090-3019(92)90230-K
12. Goto T, Ohata K, Morino M, Takami T, Tsuyuguchi N, Nishio A, et al. Falcotentorial Meningioma: Surgical Outcome in 14 Patients. *J Neurosurg* (2006) 104(1):47–53. doi: 10.3171/jns.2006.104.1.47
13. Shahrestani S, Ravi V, Strickland B, Rutkowski M, Zada G. Pure Endoscopic Supracerebellar Infratentorial Approach to the Pineal Region: A Case Series. *World Neurosurg* (2020) 137:e603–9. doi: 10.1016/j.wneu.2020.02.074
14. Gore PA, Gonzalez LF, Rekate HL, Nakaji P. Endoscopic Supracerebellar Infratentorial Approach for Pineal Cyst Resection: Technical Case Report. *Neurosurgery* (2008) 62(3 Suppl 1):108–109; discussion 109. doi: 10.1227/01.neu.0000317380.60938.79
15. Zhao X, Belykh E, Przybylowski CJ, Moreira LB, Gandhi S, Meybodi AT, et al. Surgical Treatment of Falcotentorial Meningiomas: A Retrospective Review of a Single-Institution Experience. *J Neurosurg* (2019) 1–12. doi: 10.3171/2019.4.JNS19208
16. Mottolese C, Szathmari A, Ricci-Franchi AC, Gallo P, Beuriat PA, Capone G. Supracerebellar Infratentorial Approach for Pineal Region Tumors: Our Surgical and Technical Considerations. *Neurochirurgie* (2015) 61(2-3):176–83. doi: 10.1016/j.neuchi.2014.02.004
17. Zaidi HA, Elhadi AM, Lei T, Preul MC, Little AS, Nakaji P. Minimally Invasive Endoscopic Supracerebellar-Infratentorial Surgery of the Pineal Region: Anatomical Comparison of Four Variant Approaches. *World Neurosurg* (2015) 84(2):257–66. doi: 10.1016/j.wneu.2015.03.009

18. Qiu B, Wang Y, Ou S, Guo Z, Wang Y. The Unilateral Occipital Transtentorial Approach for Pineal Region Meningiomas: A Report of 15 Cases. *Int J Neurosci* (2014) 124(10):741–7. doi: 10.3109/00207454.2013.878341
19. Otani N, Mori K, Wada K, Tomiyama A, Toyooka T, Takeuchi S. Multistaged, Multidirectional Strategy for Safe Removal of Large Meningiomas in the Pineal Region. *Neurosurg Focus* (2018) 44(4):E13. doi: 10.3171/2017.12.FOCUS17602
20. Okada T, Miyahara K, Tanino S, Suzuki K, Watanabe N, Tanaka Y, et al. Parieto-Occipital Interhemispheric Transfalcine, Trans-Bitentorial Approach for Radical Resection of Falcotentorial Meningiomas. *J Neurol Surg A Cent Eur Neurosurg* (2020) 81(4):355–61. doi: 10.1055/s-0039-1685181
21. Broggi M, Darbar A, Teo C. The Value of Endoscopy in the Total Resection of Pineocytomas. *Neurosurgery* (2010) 67(3 Suppl Operative):ons159–65. doi: 10.1227/01.NEU.0000383136.40033.2D
22. Little AS, Almefty KK, Spetzler RF, Almefty KA, Boskovitz A, Dunn LF. Endoscopic Surgery of the Posterior Fossa: Strengths and Limitations. *World Neurosurg* (2014) 82(3-4):322–4. doi: 10.1016/j.wneu.2013.08.044
23. Abolfotoh M, Bi WL, Hong CK, et al. The Combined Microscopic-Endoscopic Technique for Radical Resection of Cerebellopontine Angle Tumors. *J Neurosurg* (2015) 123(5):1301–11. doi: 10.3171/2014.10.JNS141465

Conflict of Interest: The authors declare that the research was conducted in the absence of any commercial or financial relationships that could be construed as a potential conflict of interest.

Publisher's Note: All claims expressed in this article are solely those of the authors and do not necessarily represent those of their affiliated organizations, or those of the publisher, the editors and the reviewers. Any product that may be evaluated in this article, or claim that may be made by its manufacturer, is not guaranteed or endorsed by the publisher.

Copyright © 2022 Ding, Sun, Hu, Zhai, Zhang, Yu, Wu and Chen. This is an open-access article distributed under the terms of the Creative Commons Attribution License (CC BY). The use, distribution or reproduction in other forums is permitted, provided the original author(s) and the copyright owner(s) are credited and that the original publication in this journal is cited, in accordance with accepted academic practice. No use, distribution or reproduction is permitted which does not comply with these terms.

frontiers in Oncology

ORIGINAL RESEARCH
published: 01 March 2022
doi: 10.3389/fonc.2022.846232

The Discrepancy Between Standard Histologic WHO Grading of Meningioma and Molecular Profile: A Single Institution Series

*Amanda M. Roehrkasse[1], Jo Elle G. Peterson[2], Kar-Ming Fung[2,3], Panayiotis E. Pelargos[1] and Ian F. Dunn[1]**

[1] Dunn Laboratory, Department of Neurosurgery, University of Oklahoma Health Sciences Center, Oklahoma City, OK, United States, [2] Department of Pathology, University of Oklahoma Health Sciences Center, Oklahoma City, OK, United States, [3] Stephenson Cancer Center, University of Oklahoma Health Sciences Center, Oklahoma City, OK, United States

OPEN ACCESS

Edited by:
Alireza Mansouri, The Pennsylvania State University (PSU), United States

Reviewed by:
Varun R. Kshettry, Cleveland Clinic, United States
Kristin Huntoon, University of Texas MD Anderson Cancer Center, United States

***Correspondence:**
Ian F. Dunn
ian-dunn@ouhsc.edu

Specialty section:
This article was submitted to Neuro-Oncology and Neurosurgical Oncology, a section of the journal Frontiers in Oncology

Received: *30 December 2021*
Accepted: *09 February 2022*
Published: *01 March 2022*

Citation:
Roehrkasse AM, Peterson JG, Fung KM, Pelargos PE and Dunn IF (2022) The Discrepancy Between Standard Histologic WHO Grading of Meningioma and Molecular Profile: A Single Institution Series. Front. Oncol. 12:846232. doi: 10.3389/fonc.2022.846232

Introduction: Meningiomas are the most common primary central nervous system (CNS) tumor. They are most often benign, but a subset of these can behave aggressively. Current World Health Organization (WHO) guidelines classify meningiomas into three grades based on the histologic findings and presence or absence of brain invasion. These grades are intended to guide treatment, but meningiomas can behave inconsistently with regard to their assigned histopathological grade, influencing patient expectations and management. Advanced molecular profiling of meningiomas has led to the proposal of alternative molecular grading schemes that have shown superior predictive power. These include methylation patterns, copy number alterations, and mutually exclusive driver mutations affecting oncogenes, including *BAP1, CDKN2A/B*, and the *TERT* promoter, which are associated with particularly aggressive tumor biology. Despite the evident clinical value, advanced molecular profiling methods are not widely incorporated in routine clinical practice for meningiomas.

Objective: To assess the degree of concordance between the molecular profile of meningiomas and the histopathologic WHO classification, the current method of predicting meningioma behavior.

Methods: In a two-year single-institution experience, we used commercially available resources to determine molecular profiles of all resected meningiomas. Copy number aberrations and oncogenic driver mutations were identified and compared with the histopathologic grade.

Results: One hundred fifty-one total meningioma cases were included for analysis (85.4% WHO grade 1, 13.3% WHO grade 2, and 1.3% grade 3). Chromosomal analysis of 124 of these samples showed that 29% of WHO grade 1 tumor featured copy number profiles consistent with higher grade meningioma, and 25% of WHO grade 2 meningiomas had copy number profiles consistent with less aggressive tumors. Furthermore, 8% harbored mutations in *TERT, CDKN2A/B*, or *BAP1* of which 6% occurred in grade 1 meningiomas.

Conclusions: Routine advanced molecular profiling of all resected meningiomas using commercially available resources allowed for identification of a significant number of meningiomas whose molecular profiles were inconsistent with WHO grade. Our work shows the clinical value of integrating routine molecular profiling with histopathologic grading to guide clinical decision making.

Keywords: meningioma, *TERT*, *BAP1*, *CDKN2A/B*, microarray, genetic profiling, copy number alteration, CNS tumors

INTRODUCTION

Meningiomas, named for their cell of origin, are the most common intracranial central nervous system (CNS) tumors in adults representing approximately one-third of all primary adult CNS tumors (1–3). The World Health Organization (WHO) Classification of Tumours of the CNS subdivides meningiomas into three grades (i.e., 1, 2, or 3) that are intended to correlate with prognosis and guide management (4, 5). The majority of meningiomas fall into 9 histologic subtypes comprising grade 1 meningiomas (see **Supplementary Table 1**), which have a reported progression-free survival (PFS) of 75%-90%. Grade 2 meningiomas are defined by either pathognomonic histology (i.e., clear cell or chordoid), or a grade 1 histologic subtype with a mitotic rate of 4-19 mitoses per 10 microscopic high-powered fields (HPF), brain invasion, and/or the presence of three of five atypical features as defined by the WHO. Grade 2 meningiomas have higher rates of recurrence and morbidity with a PFS of 23-78%. Grade 3 meningiomas are considered malignant with a PFS of 0% and are defined as a grade 1 histologic subtype with a mitotic index of ≥20 per 10 HPF, or the presence of rhabdoid or papillary histologic subtypes (4–6).

In current practice, WHO grade and extent of resection are the most widely used metrics to predict tumor behavior and guide management of meningiomas (6, 7). Most management paradigms involve adjuvant radiation after total or subtotal resection of grade 3 meningiomas. The use of radiation therapy as an adjunct treatment for recurrent grade 1 as well as grade 2 meningiomas following gross-total or sub-total resection is variable but commonly deployed, largely based on institutional retrospective series (7–9). An emerging observation is that meningiomas can behave inconsistently with the assigned WHO grade: grade 1 tumors can recur or behave aggressively despite successful gross total resection, while tumors with more advanced grades may have favorable natural histories (10, 11).

A developing understanding of the molecular landscape of meningioma suggests that WHO grade alone may not provide an adequate prediction of tumor behavior, for surveillance or adjuvant treatment planning considerations. Several recent publications have proposed alternative grading systems that incorporate genomic and/or epigenomic data in order to better predict meningioma behavior, particularly targeting those that do not behave in concordance with their assigned WHO grade (10–14). These grading systems incorporate molecular data including sequence alterations, methylation data and copy number alterations, among other modalities, and have shown a compelling ability to predict meningioma recurrence and progression-free survival when compared with the WHO histologic-based schema alone.

While methylation data are highly predictive, their availability is limited compared to genomic methods that are currently available to most centers. In particular, emerging data on mutational profiling and copy number variation have identified specific molecular features that, when present, are correlated with higher recurrence risks and poorer prognoses. The evolving molecular profiling of meningiomas seeks to minimize interobserver variability inherent to applying subjective phenotypic grading criteria and creates smaller, more homogenous subclassifications (15, 16). Several recurring oncogenic mutations have been identified that are relatively rare but associated with particularly aggressive behavior, even when encountered in histologically low-grade meningiomas. These include alterations in the *BAP1*, *CDKN2A/B*, and mutations within the promotor region of the *TERT* genes (17–20). Copy number alterations have also been shown to have strong predictive potential, with their ease of acquisition at most centers (either in-house or *via* vendor) enhancing their appeal (10, 13). These studies have highlighted that, regardless of histology, a greater degree of chromosomal disruption is more reliable in the forecasting of recurrence and outcome than WHO grading alone.

The rapid advances in molecular profiling of meningiomas and evident clinical benefit of acquiring genetic data for clinical management has led to incorporation of molecular designations in the most recent update to the WHO classification (21). In light of the putative superiority of molecular profiling in predicting meningioma behavior, we sought to determine how routine incorporation of readily obtainable advanced molecular profiling (copy number and mutational data) would compare with assigned WHO histopathologic grade in a prospective series of meningiomas.

MATERIALS AND METHODS

Human Subjects

All methods were approved by the institutional review board (IRB) of the University of Oklahoma Health Sciences Center (OUHSC) (IRB protocol number 10195). All patients who underwent their index surgery with a histopathologic diagnosis of meningioma following CNS tumor resection from May 2019-April 2021 were included in the study. Patient data including demographics, tumor location, and history of prior resection were collected by retrospective chart review.

Histopathologic Grading

Following routine pathology processing, resected meningiomas were assigned a histopathologic grade by board-certified neuropathologists within the Department of Pathology at OU Health according to the guidelines set forth in the revised 4th edition of the WHO Classification of Tumours of the CNS published in 2016 (4, 5). Immunohistochemical stains, such as glial fibrillary acid protein (GFAP) and epithelial membrane antigen (EMA), were performed on a case-by-case basis as deemed necessary for diagnostic evaluation. Ki-67 immunostaining was performed on at least one block in all cases. All samples were analyzed, graded, and independently confirmed by two neuropathologists (JGP and KMF).

Molecular Profiling by Next-Generation Sequencing and Chromosomal Microarray

Beginning in November 2019, chromosomal profiling and mutational data were prospectively acquired on all meningiomas in collaboration with the Mayo Clinic Laboratories, where chromosomal profiling and sequencing of 118 CNS tumor-associated genes was performed. Based on prior studies that investigated clinical progression of genetic subgroups of meningiomas, grade 1 meningiomas that harbored mutations in *BAP1*, *CDKN2A* or *B*, or the *TERT* promoter were considered to have molecular profiles that were higher risk and inconsistent with histopathologic grading (17, 19, 20, 22). Copy number data consistent with a higher grade (2/3) meningioma was defined as any loss of chromosome 1p, 3p, 4p/q, 6p/q, 10p/q, 14q, 18p/q, and/or 19p/q. Normal copy number and minor copy number alterations not involving the chromosomes listed, monosomy of chromosome 22, and cases with multiple polysomies consistent with angiomatous meningioma were considered to be consistent with grade 1 meningiomas. (6, 10, 11, 23).

Tumor Location

To assign tumor location, all available imaging was reviewed. Meningiomas were classified based on their location into anterior skull base, middle skull base – medial, middle skull base – lateral, anteromedial posterior cranial fossa, posterolateral posterior cranial fossa, spinal, anterior convexity (anterior to central sulcus), posterior convexity (posterior to central sulcus), falcine/parasagittal, tentorial, tentorial sinus, peritorcular, intraventricular, or multifocal. Meningiomas were further classified based on their sublocation (i.e., anterior clinoid process, posterior clinoid process, clival, etc.) (**Supplementary Figure 1**).

Data Analysis

Descriptive statistics, scatter plots, and figures were generated using GraphPad Prism (GraphPad Software, San Diego, CA). Summary statistics are reported as counts or proportions for categorical variables. For continuous variables (e.g., Ki-67) mean and standard deviation are shown in figures. Statistical analysis of copy number alterations and Ki-67 between meningiomas with high-grade and low-grade copy number variations were done by one-way analysis of variance (ANOVA) with Tukey's *post-hoc* test for multiple comparisons. Significance was defined as a p-value of less than 0.05.

RESULTS

A Two-Year Cohort of Resected Meningiomas Used to Assess the Clinical Value of Routine Advanced Molecular Profiling

We obtained advanced molecular profiling to supplement our histopathologic analysis of a prospective series of meningiomas with molecular data from May 2019 to April 2021. A total of 156 cases of meningioma were resected at OU Health during this two-year period and a minimal number of cases were excluded from this cohort (**Figure 1A**). Of the five cases that were excluded from analysis, two lacked molecular data due to insufficient DNA, one was located outside of the CNS, and two were duplicate cases that recurred within the two-year period of this study. The remaining 151 cases that were included in analysis comprised mostly WHO grade 1 cases (85%), but ~15% were WHO grade 2/3 (**Figure 1B** and **Supplementary Table 1**). Alterations in the *NF2* gene, the most common genetic disturbance associated with meningiomas, were evenly distributed across grades and comprised approximately 40% of the total meningioma cohort. The common histopathologic subtypes were all represented in our cohort with meningothelial and transitional comprising the majority of grade 1 tumors (**Figure 1C**) (1, 3). Demographics of our cohort also aligned with national data with grade 1 meningiomas occurring more frequently in females, while this discrepancy diminishes in WHO grades 2 and 3 (**Figure 1D** and **Supplementary Table 1**) (3, 6). Molecular data obtained from Mayo Clinic Laboratories included the Neuro-Oncology Expanded Gene Panel which reports sequence alterations in 118 genes and copy number alterations determined by chromosomal microarray. Sequence alterations were probed by the Neuro-Oncology Expanded Gene Panel for 99% of cases. Copy number alterations were determined by chromosomal microarray for 82% of cases. 81% of cases had data from both the Neuro-Oncology Expanded Gene Panel and chromosomal microarray (**Figure 1E** and **Supplementary Table 1**). The cohort included mostly intracranial meningiomas with only 2.6% of cases located in the spine and 6% of cases with multiple meningiomas. Meningiomas arising from the meninges overlying the anterior and posterior convexities, the falx, and tentorium were included in the cohort, and more than half of cases (52%) were classified as skull base meningiomas (**Figure 1F**).

Copy Number and Sequence Alterations Consistent With High Grade Seen in a Significant Number of WHO Grade I Meningiomas

Copy number data have been shown to predict tumor behavior, and several groups have proposed molecular grading systems based on copy number data due to the accessibility of this data in a non-research clinical setting (6, 10, 12, 23, 24). We determined whether meningiomas in our cohort had copy number profiles

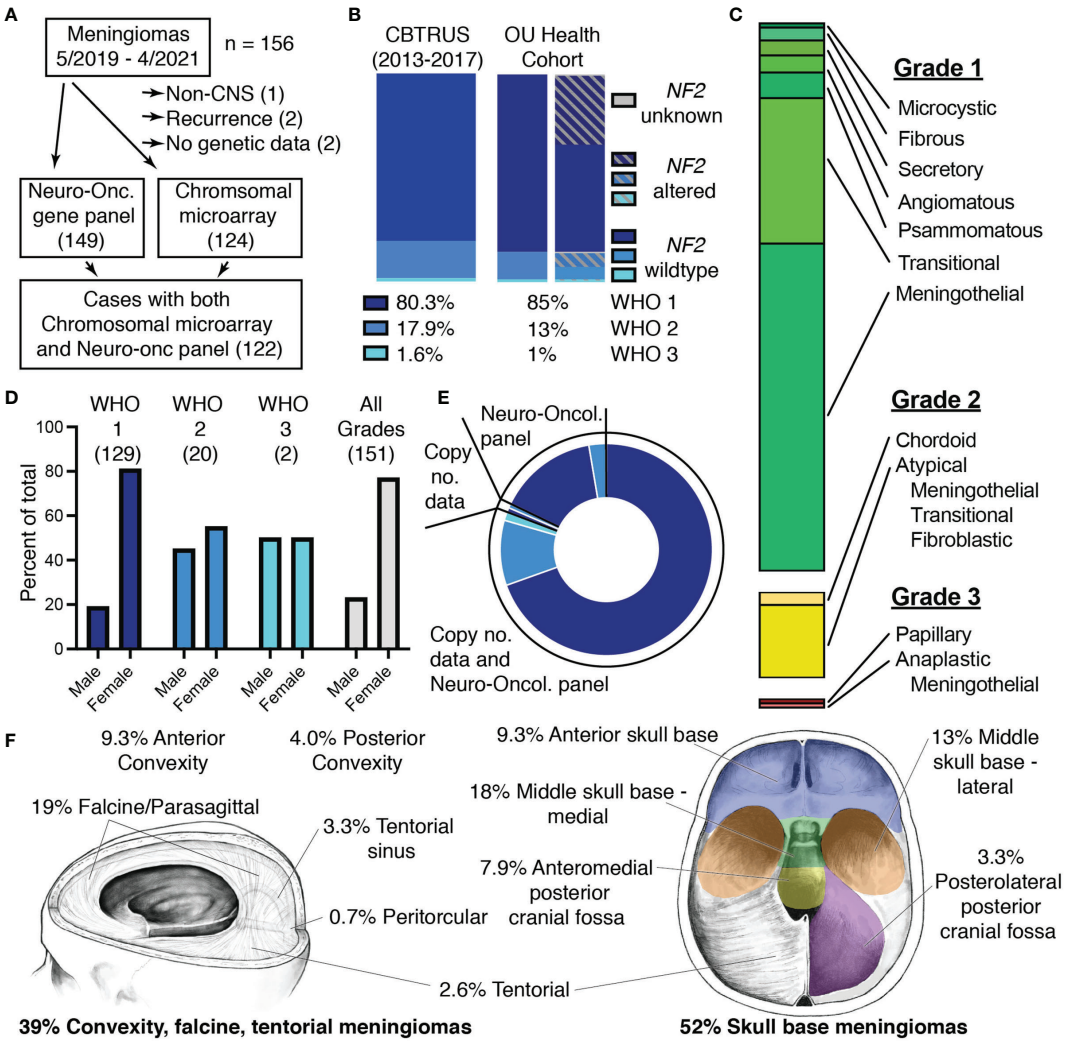

FIGURE 1 | Characteristics of the two-year OU Health meningioma cohort. **(A)** Flowchart depicting selection of meningiomas for the OU Health cohort and molecular data collected with the number of cases shown in parentheses. **(B)** Percentages and *NF2*-status of meningiomas assigned to each WHO grade in the meningioma cohort with national data from the 2020 CBTRUS statistical report shown for reference (2). **(C)** Histologic architecture seen in the meningioma cohort. Proportions of Grade I (green), Grade II (yellow), and Grade III (red) meningiomas are shown. **(D)** Proportion of male and female patients for each WHO Grade and the total cohort. The number of patients in each category is shown in parentheses. **(E)** Plot depicting the proportion of cases with data from either the Neuro-Oncology Panel, copy number data (chromosomal microarray), or cases with Neuro-Oncology Panel as well as copy number data. Shades of blue correspond to WHO Grade I-III as in panel **(B)**. **(F)** Location of meningiomas included in the cohort. Meningiomas classified as spinal (2.6%), optic nerve (0.7%), and cases with multiple meningiomas (6%) are not shown.

consistent with low-grade or high-grade meningiomas – thereby classified as "low" or "high" risk profiles – based on prior literature. These profiles were then compared to the assigned histopathologic WHO grade (**Figure 2A**). Copy number events were frequently loss events and increased significantly with increasing WHO grade ($p < 0.0001$) (**Figure 2B**). Grade 1 meningiomas generally have more balanced copy number profiles or isolated monosomy 22. WHO grade 1 meningiomas with higher grade copy number profiles have been shown to progress to a higher WHO grade over time (6, 25). Aside from chromosome 22, loss of 1p was the most common chromosomal abnormality in WHO grade 1 as well as WHO grade 2/3 in our series, consistent with prior reports. Losses involving 6q and 14q also occurred frequently. (**Supplementary Table 2**). Low grade copy number profiles were seen in 71% of WHO grade 1 meningiomas of which 44% had no significant copy alterations. Surprisingly, the remaining 29% of WHO grade 1 meningiomas had copy number profiles suggestive of a higher-grade tumor and were therefore referred to as "higher risk" profiles. For WHO grade 2/3 meningiomas, 78% of cases had copy number profiles consistent with high grade, but 22% exhibited copy number profiles usually found in grade 1 meningiomas (**Figure 2A**). The difference in copy number loss events for meningiomas with low grade copy number profiles was not statistically different between WHO Grade 1 when compared to WHO Grade 2/3 meningiomas ($p > 0.999$).

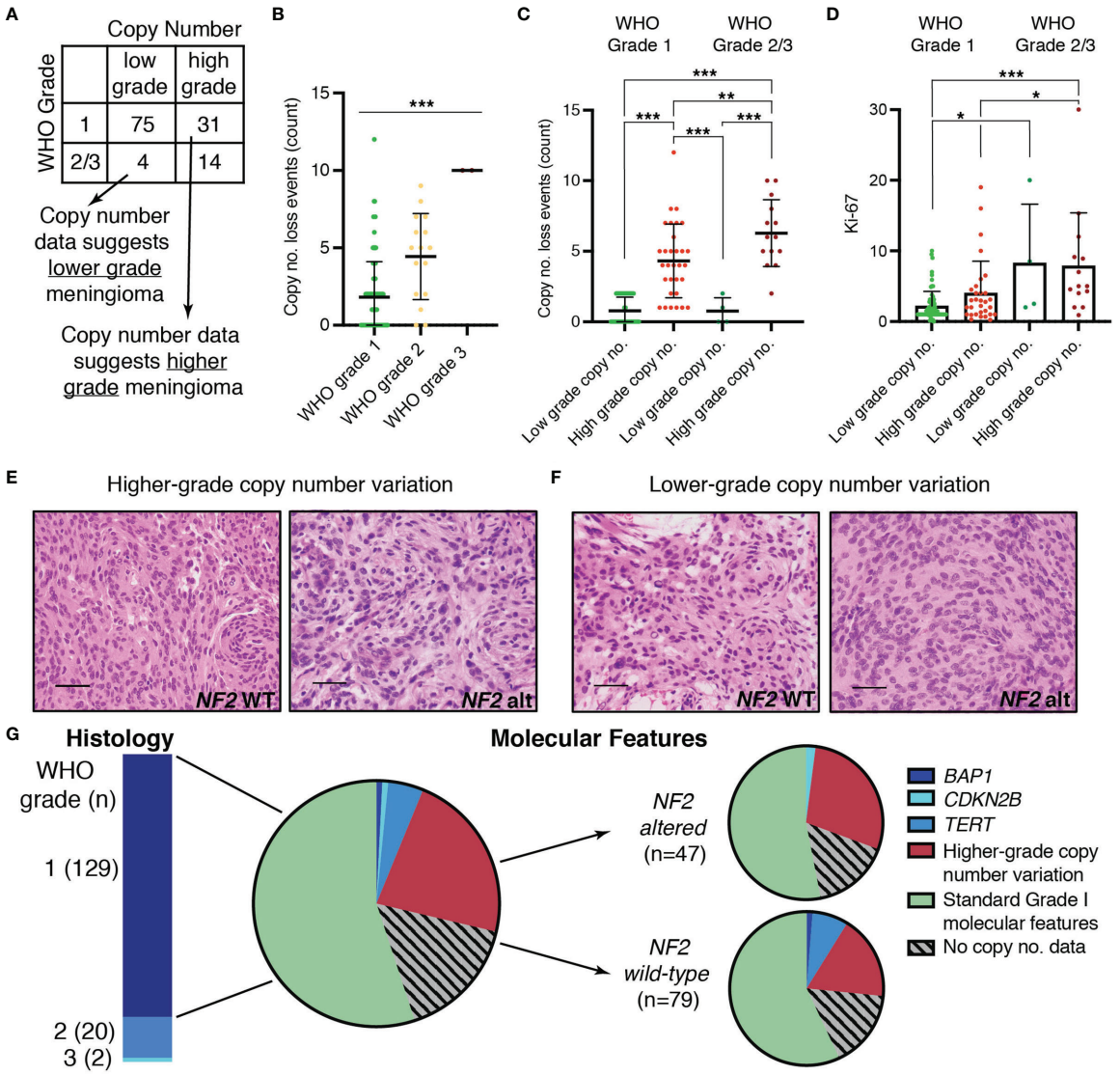

FIGURE 2 | Cases with inconsistencies between molecular data and histopathologic WHO grading. **(A)** Comparison of "molecular grade" suggested by copy number data with histopathologic WHO grade. **(B)** Absolute count of chromosome arms with copy number loss events in any of: 1p, 3p, 4p/q, 6p/q, 10 p/q, 14q, 18p/q, 19p/q, 22 p/q in each WHO grade. **(C)** Absolute count of copy number loss events for cases with low-grade or high-grade copy number profiles in WHO grade 1 and WHO grade 2/3 meningiomas. **(D)** Scatter plot showing maximum Ki-67 for WHO grade 1 and WHO grade 2/3 meningiomas with low-grade or high-grade copy number profiles. **(E, F)** Representative images showing hematoxylin and eosin (H&E)-stained slides at 40X demonstrating the histomorphology of *NF2* wild-type (left) and *NF2* altered (right) meningiomas with **(E)** higher-grade or **(F)** lower-grade copy number profiles. **(G)** Pie chart depicting the proportion of WHO grade 1 cases with higher-grade copy number profiles or with sequence alterations in *BAP1, CDKN2B*, or *TERT* in the total cohort (middle) and in *NF2* wild-type versus *NF2* altered meningiomas (right). Mutations in the *TERT* promoter were seen 17% (1/6) of the *TERT* alterations. For panels **(B–D)**, mean and standard deviation is shown and statistical significance is indicated by asterisks (*$p < 0.05$, **$p < 0.01$, ***$p < 0.001$).

Copy number loss events were significantly higher for cases with higher-grade copy number profiles when compared to those with lower grade copy number profiles regardless of WHO grade ($p < 0.001$) (**Figure 2C**). The mitotic index (Ki-67) was higher for WHO grade 1 meningiomas with high grade copy number profiles when compared to WHO grade 1 meningiomas with low grade copy number profiles (4.0 ± 4.5 vs. 2.2 ± 2.08). However, there was considerable variability, and this difference did not reach statistical significance ($p = 0.14$) (**Figure 2D**). Similarly, the mitotic index was not statistically different between WHO grade 2/3 meningiomas with low risk compared to high-risk copy number profiles ($p = 0.998$). WHO grade 1 meningiomas with high risk molecular profiles were not distinguishable from those with low risk molecular profiles based on histologic architecture alone (**Figures 2E, F**). In addition to copy number alterations, sequence alterations in *BAP1*, *CDKN2A/B*, and *TERT* are associated with a more aggressive clinical course. In our cohort, 8% of meningiomas harbored mutations in one of these genes with most of these cases

(8 out of 12) occurring in WHO grade 1 meningiomas (**Figure 2G**). These discrepancies occurred in both *NF2* wild-type as well as *NF2*-altered meningiomas, although higher grade copy number alterations were more common in *NF2*-altered meningiomas. *TERT* mutations occurred more frequently in *NF2* wild-type meningiomas. Mutations in the *TERT* promoter accounted for 29% of *TERT* mutations. Interestingly, most cases with sequence alterations in *BAP1*, *CDKN2A/B*, and *TERT* occurred in meningiomas with a low-grade cytogenetic background. Taken together, higher-risk copy number profiles or adverse mutational profiles were present in 29% of WHO grade 1 cases, and these were not distinguished by mitotic index nor histologic architecture.

Genomic Landscape of the Cohort Identifies Molecular Subpopulations of Meningiomas

Efforts to better understand the biology of meningiomas have identified mutually exclusive subpopulations of WHO grade 1 meningiomas with unique driver mutations. These include meningiomas with mutations in *AKT1*, *PIK3CA*, *POLR2A*, *SMO*, *KLF4*, and POLR2A, *TRAF7*. Mutations in these genes have been shown to correlate with tumor location and, in some cases, determine histologic subtype of meningioma or inform tumor behavior (6, 16, 26, 27). A focused mutational profile of our cohort is shown in **Figure 3A**. Mutational profiles subdivided meningiomas into genetically distinct subgroups most of which had either a single oncogenic driver mutation or previously described co-mutations such as *KLF4* K409Q (K443Q) with an altered *TRAF7* or *AKT1* E17K with an altered *TRAF7* (**Figure 3A** and **Supplementary Table 3**). With few exceptions, mutations occurred in a bland cytogenetic background, which is consistent with these mutations being associated with a more benign clinical course when compared to meningiomas with high-grade copy number alterations (6, 24, 25). Since most meningioma cases in our cohort were WHO grade 1, the genomic data for our WHO grade 2/3 meningiomas is more limited (**Figure 3B**). Nevertheless, our analysis of WHO grade 2/3 meningiomas is consistent with previous reports of the genomic landscape seen in higher WHO grade meningiomas (25). While *NF2* alterations are frequently encountered in WHO grade 2/3 meningiomas, the abovementioned driver mutations encountered in *NF2* wildtype meningiomas occur less frequently in grade 2/3 meningiomas. One exception to this was a recurring co-mutation *AKT1* and *TRAF7* that occurred in higher grade meningiomas with a low-grade cytogenetic background.

Correlation in Demographics and Tumor Location Are Seen in Meningiomas With Similar Molecular Profiles

Molecular profiling allowed us to further subdivide meningiomas into several molecular sub-groups that are predicted to behave similarly based on previous studies (**Figure 4A**). Of note, sub-groups with low-grade copy number and sequence alterations exhibited similar ratios of M:F (~25:75) regardless of WHO grade (**Figure 4B**). Furthermore, meningiomas with low grade features tended to occur more frequently in skull base locations with *NF2* wild-type meningiomas occurring more frequently in the anterior and middle fossae, whereas *NF2*-altered meningiomas were more commonly located in the posterior and middle fossae and along the falx (**Figure 4C**). In contrast, meningiomas with higher grade copy number alterations had more balanced M:F ratios which is often seen in higher grade meningiomas (**Figure 4B**). Furthermore, these tended to occur more frequently in paravenous locations (i.e., parasagittal, falcine) and rarely occurred in the anterior skull base where grade 1 meningiomas more frequently occurred (**Figure 4C**) (25).

DISCUSSION

Molecular data have been incorporated in the WHO grading criteria for other CNS tumors since 2016, while grading of

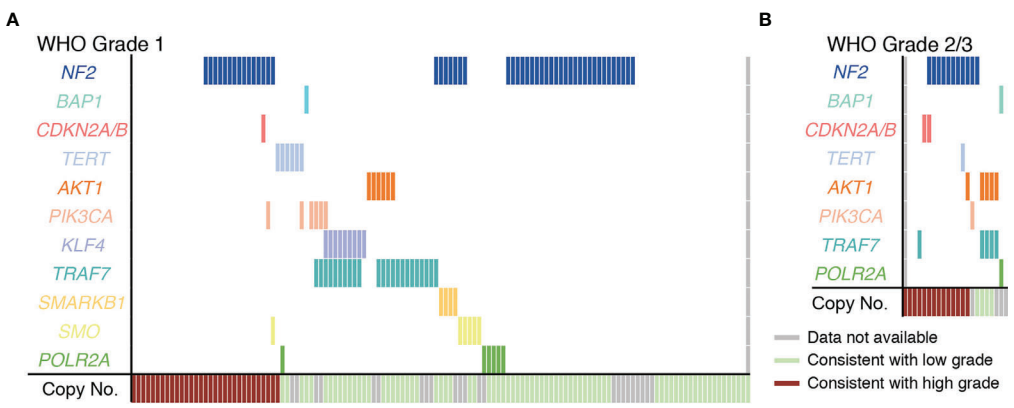

FIGURE 3 | Genomic landscape of meningiomas included in the cohort. **(A)** Depiction of all Grade 1 meningioma cases harboring high grade (red) or low grade (green) copy number profiles and sequence alterations as determined by advanced molecular profiling. **(B)** Plot showing copy number alterations and sequence alteration for all WHO grade 2 and 3 cases included in the study. For both **(A, B)** each vertical column represents one case. *TERT* mutations were in the promoter in 17% (1 case) of WHO Grade 1 meningiomas **(A)** and in all of the WHO grade 2 *TERT* mutated meningiomas (1 case) **(B)**.

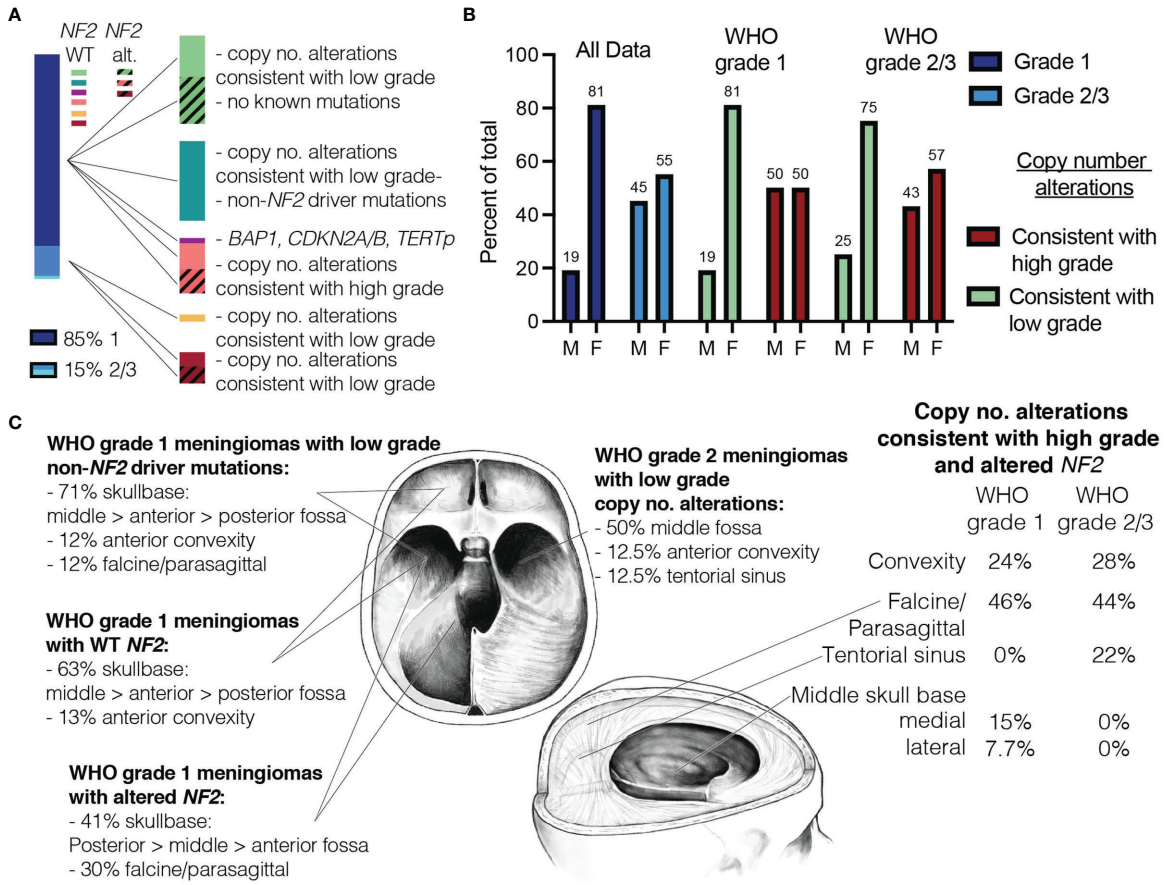

FIGURE 4 | Similarities in demographics and tumor location are seen in meningiomas with similar copy number data. **(A)** Proportion of grade 1 vs. grade 2/3 meningiomas based on histopathologic grading shown on left. Meningiomas divided by molecular data (right). **(B)** Male-to-female ratio plotted side by side for all WHO grade 1 and grade 2/3 meningiomas (blue), meningiomas with copy number alterations consistent with low grade (green) and those consistent with high grade (red). **(C)** Meningiomas with low grade copy number alterations predominately occur in skull base locations (WHO grade 1 meningiomas shown on left). WHO grade 2 meningiomas with low grade copy no. alterations and meningiomas with high grade copy no. alterations are shown on right.

meningiomas has been largely based on histopathologic data (5). This year, molecular alterations, including *CDKN2A/B* and *TERTp*, were added to the WHO classification for meningiomas (21). While alterations in these genes are recognized as negative prognostic markers, they occur in a small number of meningiomas and do not aid in identification of intermediate risk meningiomas (7). In recent years, there has also been a rapidly growing body of literature supporting the use of advanced molecular profiling in classifying meningiomas. Classification schemes based on methylation, sequence alterations, and copy number data have been introduced and have been shown to be superior to WHO grading in predicting tumour behaviour (10, 12–14). Nevertheless, such molecular methods are not widely incorporated in clinical practice where histopathologic WHO grade remains the standard that guides management of patients with meningioma.

A major hurdle to incorporation of advanced molecular profiling in the routine care of patients with meningiomas is that access to advanced molecular profiling methods, including DNA and RNA sequencing as well as methylome studies, is limited to major academic and research institutions (28, 29). To address this, we used resources that are commercially available for routine determination of tumour genetics through the Mayo Clinic Laboratories and assessed the clinical value of incorporating advanced molecular profiling of all resected meningiomas into routine clinical management. The advanced molecular profiling methods employed in this study are ones that could therefore feasibly be accessed widely by treatment groups in the management of meningiomas. While this additional testing adds upfront cost to the evaluation of meningiomas, the potential benefits of accurately predicting clinical behaviour and improving clinical management are invaluable, potentially avoiding unnecessary treatment in patients with WHO grade 2/3 tumors expected to be low-risk and possibly improving outcomes for WHO grade 1 meningiomas with high-risk genetic profiles.

An important consideration in the management of meningiomas is the use of adjunct radiation for treatment of tumors that are difficult to control with surgical resection alone. Recent trials have evaluated the benefits of radiation in

meningiomas with an intermediate risk of recurrence, including recurrent grade 1 meningiomas and grade 2 meningiomas following gross-total resection (8, 9), while randomized trials are ongoing. While the proper use of radiation in this subset of meningiomas remains an area of debate, proper and consistent classification of meningiomas into low-, intermediate-, and high-risk categories is crucial in order to accurately evaluate the appropriateness of radiation therapy in management (7, 30). Systemic therapies targeting oncogenic driver mutations have had limited success in the treatment of meningiomas and are not widely incorporated in clinical practice (31, 32). However, molecular targets continue to be an area of research for meningiomas with ongoing clinical trials (33). If systemic therapies become a viable option for treatment of meningioma, molecular data will be crucial for clinical decision making.

We found a significant percentage of meningiomas within our cohort that were predicted to behave inconsistent with their assigned WHO grade based on the molecular profiles (nearly 30%). This is consistent with a recent report that applied advanced genomics to create a molecular grade with improved prediction of meningioma behaviour, with up to 32% of cases reclassified when molecular data were applied (10). There are limitations inherent to our study design that are important to consider. While our sample generally mirrors national data, we include a slightly higher proportion of grade 1 cases (85% vs. the reported 80% (2). With a sample size of 151 patients, we have a cohort with relatively small numbers of grade 2 cases and only two grade 3 cases. Our cohort is also fairly heterogenous, including cranial and spinal cases as well as eleven recurrent cases, and with a larger fraction of skull base tumors. While such heterogeneity can introduce variables that confound interpretation, we felt that for the purpose of this study it was important to minimize the exclusion of cases to accurately represent a two-year meningioma cohort. The data we have included are from recently resected meningiomas; therefore, we do not include prospective data providing patient follow-up and critical metrics, such as rates of recurrence of meningiomas and overall survival. The goal of this study was to quantify the rate of discrepancy between molecular profiles and histopathologic grading; however, patient follow-up to determine the predictive power of the molecular profile when compared to histopathologic grade will be a critical next step in reconciling molecular data with histopathologic grade.

In recent years, the clinical impact of molecular data in the treatment and management of meningiomas has become evident. Numerous classifications that incorporate molecular data have been shown to improve the prediction of tumour behaviour for meningiomas. With the rapid advances in molecular understanding of meningiomas over the recent years, it will be important to determine how this information can be integrated in routine clinical settings and standardized nationally, in particular for institutions with limited resources, and to correlate this information with clinical outcomes.

DATA AVAILABILITY STATEMENT

The original contributions presented in the study are included in the article/**Supplementary Material**. Further inquiries can be directed to the corresponding author.

ETHICS STATEMENT

The studies involving human participants were reviewed and approved by Institutional Review Board University of Oklahoma Health Sciences Center. Written informed consent for participation was not required for this study in accordance with the national legislation and the institutional requirements.

AUTHOR CONTRIBUTIONS

Study design and data analysis: AR, PP, and ID. Histopathologic grading, processing, and shipment of meningioma samples for advanced molecular profiling: JP and K-MF. Drafting of manuscript: AR and PP. Proofreading, finalizing, and approval of manuscript: all authors.

ACKNOWLEDGMENTS

The authors thank Jennifer Hooper and the molecular and neuropathologists at the Mayo Clinic Laboratories for providing advanced molecular profiling. The authors thank Tressie Stephens for her help with the IRB protocol, Huy Vuong for assisting with statistical analysis, and Adam Brazle for the skull illustrations used in **Figures 1**, **4** and **Supplementary Figure 1.**

SUPPLEMENTARY MATERIAL

The Supplementary Material for this article can be found online at: https://www.frontiersin.org/articles/10.3389/fonc.2022.846232/full#supplementary-material

REFERENCES

1. Kalamarides M, Stemmer-Rachamimov AO, Niwa-Kawakita M, Chareyre F, Taranchon E, Han ZY, et al. Identification of a Progenitor Cell of Origin Capable of Generating Diverse Meningioma Histological Subtypes. *Oncogene* (2011) 30:2333–44. doi: 10.1038/onc.2010.609
2. Ostrom QT, Patil N, Cioffi G, Waite K, Kruchko C, Barnholtz-Sloan JS. CBTRUS Statistical Report: Primary Brain and Other Central Nervous System Tumors Diagnosed in the United States in 2013-2017. *Neuro Oncol* (2020) 22: iv1–iv96. doi: 10.1093/neuonc/noaa200
3. Whittle IR, Smith C, Navoo P, Collie D. Meningiomas. *Lancet* (2004) 363:1535–43. doi: 10.1016/S0140-6736(04)16153-9
4. Louis DN, Ohgaki H, Wiestler OD, Cavenee WK, Burger PC, Jouvet A, et al. The 2007 WHO Classification of Tumours of the Central Nervous System. *Acta Neuropathol* (2007) 114:97–109. doi: 10.1007/s00401-007-0243-4

5. Louis DN, Perry A, Reifenberger G, von Deimling A, Figarella-Branger D, Cavenee WK, et al. The 2016 World Health Organization Classification of Tumors of the Central Nervous System: A Summary. *Acta Neuropathol* (2016) 131:803–20. doi: 10.1007/s00401-016-1545-1
6. Bi WL, Abedalthagafi M, Horowitz P, Agarwalla PK, Mei Y, Aizer AA, et al. Genomic Landscape of Intracranial Meningiomas. *J Neurosurg* (2016) 125:525–35. doi: 10.3171/2015.6.JNS15591
7. Rogers L, Barani I, Chamberlain M, Kaley TJ, McDermott M, Raizer J, et al. Meningiomas: Knowledge Base, Treatment Outcomes, and Uncertainties. A RANO Review. *J Neurosurg* (2015) 122:4–23. doi: 10.3171/2014.7.JNS131644
8. Rogers L, Zhang P, Vogelbaum MA, Perry A, Ashby LS, Modi JM, et al. Intermediate-Risk Meningioma: Initial Outcomes From NRG Oncology RTOG 0539. *J Neurosurg* (2018) 129:35–47. doi: 10.3171/2016.11.JNS161170
9. Weber DC, Ares C, Villa S, Peerdeman SM, Renard L, Baumert BG, et al. Adjuvant Postoperative High-Dose Radiotherapy for Atypical and Malignant Meningioma: A Phase-II Parallel Non-Randomized and Observation Study (EORTC 22042-26042). *Radiother Oncol* (2018) 128:260–5. doi: 10.1016/j.radonc.2018.06.018
10. Driver J, Hoffman SE, Tavakol S, Woodward E, Maury EA, Bhave V, et al. A Molecularly Integrated Grade for Meningioma. *Neuro Oncol* (2021), 1–13. doi: 10.1093/neuonc/noab213
11. Nassiri F, Mamatjan Y, Suppiah S, Badhiwala JH, Mansouri S, Karimi S, et al. DNA Methylation Profiling to Predict Recurrence Risk in Meningioma: Development and Validation of a Nomogram to Optimize Clinical Management. *Neuro Oncol* (2019) 21:901–10. doi: 10.1093/neuonc/noz061
12. Maas SLN, Stichel D, Hielscher T, Sievers P, Berghoff AS, Schrimpf D, et al. Integrated Molecular-Morphologic Meningioma Classification: A Multicenter Retrospective Analysis, Retrospectively and Prospectively Validated. *J Clin Oncol* (2021) 39(34):JCO2100784. doi: 10.1200/JCO.21.00784
13. Nassiri F, Liu J, Patil V, Mamatjan Y, Wang JZ, Hugh-White R, et al. A Clinically Applicable Integrative Molecular Classification of Meningiomas. *Nature* (2021) 597:119–25. doi: 10.1038/s41586-021-03850-3
14. Sahm F, Schrimpf D, Stichel D, Jones DTW, Hielscher T, Schefzyk S, et al. DNA Methylation-Based Classification and Grading System for Meningioma: A Multicentre, Retrospective Analysis. *Lancet Oncol* (2017) 18:682–94. doi: 10.1016/S1470-2045(17)30155-9
15. Rogers CL, Perry A, Pugh S, Vogelbaum MA, Brachman D, McMillan W, et al. Pathology Concordance Levels for Meningioma Classification and Grading in NRG Oncology RTOG Trial 0539. *Neuro Oncol* (2016) 18:565–74. doi: 10.1093/neuonc/nov247
16. Youngblood MW, Duran D, Montejo JD, Li C, Omay SB, Ozduman K, et al. Correlations Between Genomic Subgroup and Clinical Features in a Cohort of More Than 3000 Meningiomas. *J Neurosurg* (2019) 133(5):1–10. doi: 10.3171/2019.8.JNS191266
17. Bostrom J, Meyer-Puttlitz B, Wolter M, Blaschke B, Weber RG, Lichter P, et al. Alterations of the Tumor Suppressor Genes CDKN2A (P16(INK4a)), P14 (ARF), CDKN2B (P15(INK4b)), and CDKN2C (P18(INK4c)) in Atypical and Anaplastic Meningiomas. *Am J Pathol* (2001) 159:661–9. doi: 10.1016/S0002-9440(10)61737-3
18. Juratli TA, Thiede C, Koerner MVA, Tummala SS, Daubner D, Shankar GM, et al. Intratumoral Heterogeneity and TERT Promoter Mutations in Progressive/Higher-Grade Meningiomas. *Oncotarget* (2017) 8:109228–37. doi: 10.18632/oncotarget.22650
19. Mirian C, Duun-Henriksen AK, Juratli T, Sahm F, Spiegl-Kreinecker S, Peyre M, et al. Poor Prognosis Associated With TERT Gene Alterations in Meningioma is Independent of the WHO Classification: An Individual Patient Data Meta-Analysis. *J Neurol Neurosurg Psychiatry* (2020) 91:378–87. doi: 10.1136/jnnp-2019-322257
20. Shankar GM, Abedalthagafi M, Vaubel RA, Merrill PH, Nayyar N, Gill CM, et al. Germline and Somatic BAP1 Mutations in High-Grade Rhabdoid Meningiomas. *Neuro Oncol* (2017) 19:535–45. doi: 10.1093/neuonc/now235
21. Louis DN, Perry A, Wesseling P, Brat DJ, Cree IA, Figarella-Branger D, et al. The 2021 WHO Classification of Tumors of the Central Nervous System: A Summary. *Neuro Oncol* (2021) 23:1231–51. doi: 10.1093/neuonc/noab106
22. Sievers P, Hielscher T, Schrimpf D, Stichel D, Reuss DE, Berghoff AS, et al. CDKN2A/B Homozygous Deletion Is Associated With Early Recurrence in Meningiomas. *Acta Neuropathol* (2020) 140:409–13. doi: 10.1007/s00401-020-02188-w
23. Aizer AA, Abedalthagafi M, Bi WL, Horvath MC, Arvold ND, Al-Mefty O, et al. A Prognostic Cytogenetic Scoring System to Guide the Adjuvant Management of Patients With Atypical Meningioma. *Neuro Oncol* (2016) 18:269–74. doi: 10.1093/neuonc/nov177
24. Bi WL, Prabhu VC, Dunn IF. High-Grade Meningiomas: Biology and Implications. *Neurosurg Focus* (2018) 44:E2. doi: 10.3171/2017.12.FOCUS17756
25. Bi WL, Greenwald NF, Abedalthagafi M, Wala J, Gibson WJ, Agarwalla PK, et al. Genomic Landscape of High-Grade Meningiomas. *NPJ Genom Med* (2017) 2. doi: 10.1038/s41525-017-0014-7
26. Boetto J, Bielle F, Sanson M, Peyre M, Kalamarides M. SMO Mutation Status Defines a Distinct and Frequent Molecular Subgroup in Olfactory Groove Meningiomas. *Neuro Oncol* (2017) 19:345–51. doi: 10.1093/neuonc/now276
27. Youngblood MW, Miyagishima DF, Jin L, Gupte T, Li C, Duran D, et al. Associations of Meningioma Molecular Subgroup and Tumor Recurrence. *Neuro Oncol* (2021) 23:783–94. doi: 10.1093/neuonc/noaa226
28. Curry WTJr., Barker FG2nd. Racial, Ethnic and Socioeconomic Disparities in the Treatment of Brain Tumors. *J Neurooncol* (2009) 93:25–39. doi: 10.1007/s11060-009-9840-5
29. Zhu P, Du XL, Zhu JJ, Esquenazi Y. Improved Survival of Glioblastoma Patients Treated at Academic and High-Volume Facilities: A Hospital-Based Study From the National Cancer Database. *J Neurosurg* (2019) 132:491–502. doi: 10.3171/2018.10.JNS182247
30. Day SE, Halasz LM. Radiation Therapy for WHO Grade I Meningioma. *Chin Clin Oncol* (2017) 6:S4. doi: 10.21037/cco.2017.06.01
31. Kaley T, Barani I, Chamberlain M, McDermott M, Panageas K, Raizer J, et al. Historical Benchmarks for Medical Therapy Trials in Surgery- and Radiation-Refractory Meningioma: A RANO Review. *Neuro Oncol* (2014) 16:829–40. doi: 10.1093/neuonc/not330
32. Wen PY, Quant E, Drappatz J, Beroukhim R, Norden AD. Medical Therapies for Meningiomas. *J Neurooncol* (2010) 99:365–78. doi: 10.1007/s11060-010-0349-8
33. Karsy M, Azab MA, Abou-Al-Shaar H, Guan J, Eli I, Jensen RL, et al. Clinical Potential of Meningioma Genomic Insights: A Practical Review for Neurosurgeons. *Neurosurg Focus* (2018) 44:E10. doi: 10.3171/2018.2.FOCUS1849

Conflict of Interest: The authors declare that the research was conducted in the absence of any commercial or financial relationships that could be construed as a potential conflict of interest.

Publisher's Note: All claims expressed in this article are solely those of the authors and do not necessarily represent those of their affiliated organizations, or those of the publisher, the editors and the reviewers. Any product that may be evaluated in this article, or claim that may be made by its manufacturer, is not guaranteed or endorsed by the publisher.

Copyright © 2022 Roehrkasse, Peterson, Fung, Pelargos and Dunn. This is an open-access article distributed under the terms of the Creative Commons Attribution License (CC BY). The use, distribution or reproduction in other forums is permitted, provided the original author(s) and the copyright owner(s) are credited and that the original publication in this journal is cited, in accordance with accepted academic practice. No use, distribution or reproduction is permitted which does not comply with these terms.

frontiers in Oncology

ORIGINAL RESEARCH
published: 03 March 2022
doi: 10.3389/fonc.2022.839567

Deep Learning Model for Intracranial Hemangiopericytoma and Meningioma Classification

Ziyan Chen[1,2], *Ningrong Ye*[1,2*], *Nian Jiang*[1,2], *Qi Yang*[1,2], *Siyi Wanggou*[1,2] *and Xuejun Li*[1,2*]

[1] Department of Neurosurgery, Xiangya Hospital, Central South University, Changsha, China, [2] Hunan International Scientific and Technological Cooperation Base of Brain Tumor Research, Xiangya Hospital, Central South University, Changsha, China

Background: Intracranial hemangiopericytoma/solitary fibrous tumor (SFT/HPC) is a rare type of neoplasm containing malignancies of infiltration, peritumoral edema, bleeding, or bone destruction. However, SFT/HPC has similar radiological characteristics as meningioma, which had different clinical managements and outcomes. This study aims to discriminate SFT/HPC and meningioma *via* deep learning approaches based on routine preoperative MRI.

Methods: We enrolled 236 patients with histopathological diagnosis of SFT/HPC (n = 144) and meningioma (n = 122) from 2010 to 2020 in Xiangya Hospital. Radiological features were extracted manually, and a radiological diagnostic model was applied for classification. And a deep learning pretrained model ResNet-50 was adapted to train T1-contrast images for predicting tumor class. Deep learning model attention mechanism was visualized by class activation maps.

Results: Our study reports that SFT/HPC was found to have more invasion to venous sinus (p = 0.001), more cystic components (p < 0.001), and more heterogeneous enhancement patterns (p < 0.001). Deep learning model achieved a high classification accuracy of 0.889 with receiver-operating characteristic curve area under the curve (AUC) of 0.91 in the validation set. Feature maps showed distinct clustering of SFT/HPC and meningioma in the training and test cohorts, respectively. And the attention of the deep learning model mainly focused on the tumor bulks that represented the solid texture features of both tumors for discrimination.

Keywords: hemangiopericytoma, meningioma, magnetic resonance imaging, deep learning, classification

OPEN ACCESS

Edited by:
Hailiang Tang,
Fudan University, China

Reviewed by:
Muhammad Usman Tariq,
Abu Dhabi School of Management, United Arab Emirates
Sri Andreani Utomo,
Airlangga University, Indonesia

***Correspondence:**
Xuejun Li
lxjneuro@csu.edu.cn
Ningrong Ye
yeningrong0@163.com

Specialty section:
This article was submitted to Neuro-Oncology and Neurosurgical Oncology, a section of the journal Frontiers in Oncology

Received: *20 December 2021*
Accepted: *31 January 2022*
Published: *03 March 2022*

Citation:
Chen Z, Ye N, Jiang N, Yang Q, Wanggou S and Li X (2022) Deep Learning Model for Intracranial Hemangiopericytoma and Meningioma Classification. Front. Oncol. 12:839567. doi: 10.3389/fonc.2022.839567

INTRODUCTION

Intracranial hemangiopericytoma (HPC) is a rare type of neoplasm developing from meningeal mesenchyme around vessels. Considering the overlapping molecular characteristics (1–3), the 2016 World Health Organization (WHO) classification of tumors of the central nervous system (CNS) combined HPC and solitary fibrous tumor (SFT) into one term SFT/HPC and assigned three grades within the entity (4). As such, this low proportion of intracranial tumors has a high risk of

recurrence and systemic metastasis (5–7). Once diagnosed, SFT/HPC must be treated aggressively with a more detailed surgical treatment followed by radiotherapy and chemotherapy due to its malignancy of infiltration, peritumoral edema, bleeding, and bone destruction (8–11). However, it might be difficult to discriminate SFT/HPC from meningioma because of the different incidences but similar characteristics on clinical and radiological manifestations (**Supplementary Figure S1**) (12). On the contrary, not all meningiomas need to be treated aggressively. Therefore, precise distinction between SFT/HPCs and meningiomas are essential before surgery or therapy.

Previous studies have revealed that MRI-based imaging may contribute to the diagnosis of SFT/HPC (13–15). Radiologically, SFT/HPCs exhibit more aggressive behaviors like necrosis and bone erosions and heterogenous enhancement (16). And preoperative multimodal MRI images could supply sufficient information on tumor location, size, and peritumoral tissues for surgical planning. Previous quantitative analysis provides effective markers such as apparent diffusion coefficient (ADC) values in diffusion-weighted imaging (DWI) and the degree of intratumoral susceptibility signal intensity (ITSS) in susceptibility weight imaging (SWI) (14, 15, 17). However, SFT/HPC has a very low incidence, so that physicians might neglect the prescription of multimodal imaging. And these multimodal images are not always obtainable due to the machine-hour shortage and patients' economic condition in many developing countries. Preoperative classification by routine MRI images is urgently needed.

Artificial intelligence approaches for routine MRI images have been proven to be efficient ways to achieve semantic segmentation of lesions and extraction of multidimensional information (18–20). State-of-the-art deep learning architectures such as convolutional neural network (CNN) have powerful performance in brain tumor classification, objection, and segmentation (21–23). And another advantage is to implement transfer learning that uses large pretrained model weights and fine-tunes the classification layers to obtain higher accuracy with few data.

In this study, we retrospectively collected data from patients from Xiangya Hospital with histopathologically confirmed SFT/HPCs and meningiomas. The aim was to adopt a pretrained deep learning neural network model ResNet-50 (24). By implementing the deep learning algorithms through single-modal conventional MRI images, our model achieved a high accuracy of preoperative diagnosis of SFT/HPCs and meningiomas. Hence, it can assist in surgical planning and treatment after the operation.

MATERIALS AND METHODS

Clinical Cohort and Data Acquisition

In our retrospectively study, a total of 236 patients with MRI data were enrolled in Xiangya Hospital from 2010 to 2020, with their clinical and pathological data collected from the Electronic Medical Record System. Considering that meningioma is way more common in our center, we selected similar numbers of patients to prevent model overfitting. Among them, 114 cases were pathologically diagnosed with SFT/HPC and 122 cases were pathologically diagnosed with meningioma. Exclusion criteria included previous relevant treatment history or recurring cases; patients without MRI images in our hospital or poor image qualities (**Figure 1**). Brain MRI was performed as part of routine clinical care on scanners from various manufacturers with different magnetic field strengths (**Table 1**) and acquisition parameters. This study was approved by the institutional review board of our hospital.

Imaging Preprocessing

For each patient, presegmentation image registration was performed with T1, T2, T1-weighted contrast-enhanced (T1C), and T2-weighted fluid-attenuated inversion recovery (FLAIR) images. Affine images were coregistered into the same geometric space using the Elastic toolbox (25). Voxels of different sets of images were resliced into an average size of 0.52 mm × 0.52 mm × 4.74 mm. All the sequences of images were used for the segmentation of tumors, peritumoral edemas, and cysts. ITK-SNAP, an open-source 3D image analysis software (26), was implemented for delineating tumor boundaries in a semiautomated fashion on a slice-by-slice basis. All regions of interest (ROIs) containing the main disease components were manually delineated on each MRI image by two neuroradiologists (NY and NJ) who had 5 and 10 years of combined experience in neurosurgery and brain tumor imaging, respectively. They were blinded to the patients' medical information.

We evaluated the interobserver (reader 1 vs. reader 2) and intraobserver (reader 1 twice) reproducibility of lesion labeling by calculating the interclass and intraclass correlation coefficients (ICCs). For interobserver reproducibility, reader 1 and reader 2 segmented the lesions independently and they were blinded to each other's segmentations. In addition, and for intraobserver reproducibility, reader 1 repeated the segmentation procedure within 1 week of the first analysis. Generally, ICC >0.80 indicated a good agreement for segmentation.

Simultaneously, we extracted the radiological factors including tumor boundary, bone erosion, dural sign, T1C enhancement patterns, venous sinus invasion, cystic components, and peritumoral edema. And we adapted a logistic regression to train a radiological diagnostic model for classification.

Deep Learning Training and Validation

ResNet-50 pretrained model was adapted to train the classification model, and we selected the center slice for each lesion to build our datasets. To fit the pretrained initial weights of 3 color channels, we applied the Jet colormap to convert the gray-level images into RGB images, then data augmentation was performed to prevent overfitting and extend the datasets. Concretely, 5 data augmentation approaches were used by *TorchIO* (27) including random flip random noise, random motion, random blur, and random ghosting. Finally, all images were normalized and recropped to 3 × 224 × 224 initial input size as expected by the model and divided into batches by batch size 16 for more efficient training (**Figure 2**). In this study, we compared different sequences including T1, T1C, and T2 and found superior model performance with a single T1C. Thus, we

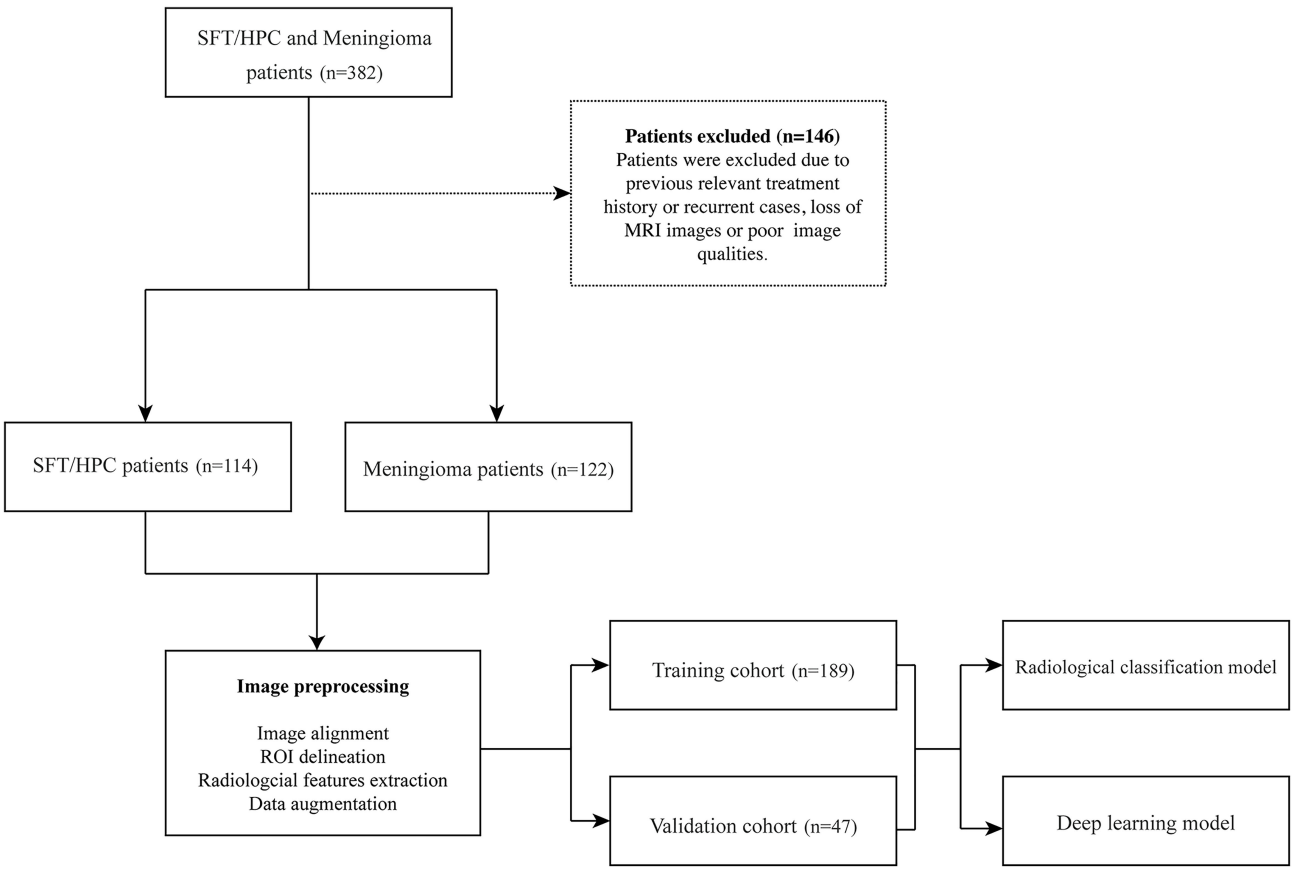

FIGURE 1 | Flowchart of the whole study.

only used T1C and chose the center image of ROI in axial slice as input data. Given that T1C-based MRIs are commonplace among clinical protocols for patients with SFT/HPC or meningioma, our model would be broadly applicable.

We trained our model on an Ubuntu 18.04 computer with 1 Intel Core i9-7940 CPU using an NVIDIA GTX 1080Ti 11GB GPU, with 256 GB available system RAM. Training in all categories was run for 300 epochs by an SGD optimizer with momentum 0.9 and weight decay 4e-5 and cross entropy loss function. To fine-tune the pretrained model, we froze the convolutional layers and retrained the final fully connected classification layer. Learning rate was initially set as 2e-5 in the frozen layers and 1e-5 in the classification layer and utilized a decay rate of 0.9 for each of the 4 steps until the model reached convergence. In this study, we split our data into training set and validation set according to a 4:1 ratio (training cohort = 189, validation cohort = 47).

TABLE 1 | Clinical scanners used in the study.

	SFT/HPC (n = 114)	Meningioma (n = 122)	*p*-value
All manufacturers			0.451
Total at 1.5T	81	68	
Total at 3T	33	36	
3.0T Scanners			0.847
SIEMENS	5	5	
GE Medical Systems	28	31	
1.5T Scanners			0.925
SIEMENS	53	58	
TOSHIBA	18	19	
Alltech Medical Systems	10	9	

HPC, hemangiopericytoma; SFT, solitary fibrous tumor.

Feature Analysis

We applied classification activation maps (CAMs) to visualize network attention. Internal mechanisms of deep learning algorithms have often been referred to as a "black box." Implementation of CAMs could improve transparency and understand the operations and attentions of the model. We applied Smooth Grad-CAM++ (28) that uses the gradients of the target concepts to produce a coarse localization heatmap highlighting the important regions in images for predicting the concept for model visualization. Specifically, in any class c, Grad-CAM firstly computed the gradient of the score y^c before softmax with respect to feature maps A^k, then random samples in a neighborhood of inputs are taken to smooth the feature maps,

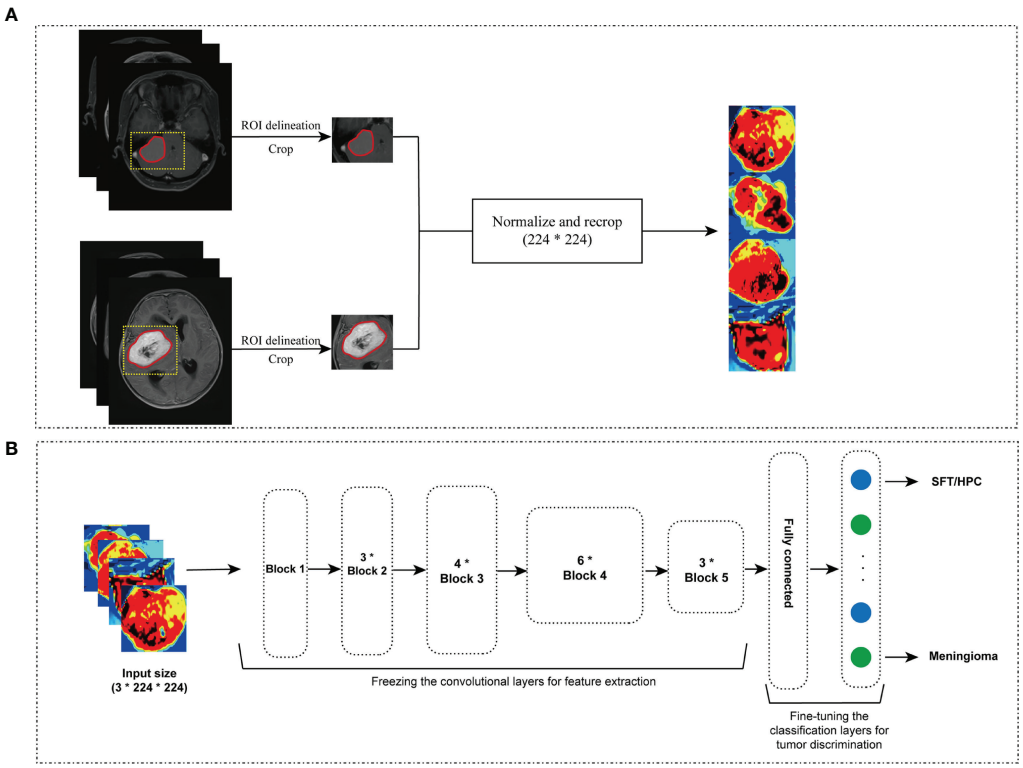

FIGURE 2 | Image preprocessing and model training. Regions of interest (ROIs) were extracted from the aligned images, and the jet colormap was applied to grayscale MRI images, followed by the use of 5 image augmentation techniques **(A)**. After preprocessing, input image size was reshaped to 3 × 224 × 224. ResNet-50 convolutional layers were frozen, and the last classification layers were retrained for solitary fibrous tumor/hemangiopericytoma (SFT/HPC) and meningioma discrimination **(B)**.

and gradients flow back to obtain the importance weights from A^k. To produce Smooth Grad-CAM++, we calculated the gradient of the ground truth with respect to the last layer before classification and used the *pytorch-grad-cam* github repository (https://github.com/jacobgil/pytorch-grad-cam). And we calculated the distance from the activation center to the center or edge of the tumor to compare the difference of the tumor recognition patterns.

We also extracted feature maps of the last layer before classification in the ResNet model and analyzed them by an unsupervised algorithm t-distributed stochastic neighbor embedding (t-SNE). This showed similarity between data points to joint probabilities and reduce the number of dimensions of image features depending on the non-linear function. And t-SNE was also applied to visualize high-dimensional radiological factors.

Statistical Analysis

We used Student t and χ^2 tests to evaluate differences in patient demographics between data split. Deep learning model performance was also assessed using positive predictive value (PPV), negative predictive value (NPV), sensitivity, specificity, f1-score, receiver-operating characteristic curve area under the curve (AUC), and average precision (AP) score. And $p < 0.05$ was considered statistically significant. All statistical analysis and visualization were performed using *scikit-learn*, *numpy*, *pandas*, *matplotlib*, *scipy*, *statsmodels*, and *seaborn* libraries in Python 3.8.0.

RESULTS

Demographics and Radiological Characteristics

A total of 236 cases were enrolled in this study (**Table 2**), of which 114 cases were pathologically diagnosed as SFT/HPCs and 122 cases were pathologically diagnosed as meningiomas. There were no significant differences between the two groups in terms of gender (p = 0.770) and age (p = 0.163). Almost half the cases of both tumors occurred in the convexity, including cerebrum and cerebellum. Yet, 50 cases of meningiomas were located at the skull base compared to 32 cases of HPCs. For radiological factors, most cases showed clear tumor boundary without bone erosion. Meningiomas displayed more dural tail sign, while only 9.3% of SFT/HPCs displayed the dural tail sign. However, SFT/HPC lesions showed more invasion to venous sinus (p = 0.001) and more cystic components (p < 0.001). A heterogeneous enhancement pattern was observed in 79.6% of all SFT/HPCs and in 64.7% of all meningiomas with significant differences (p <

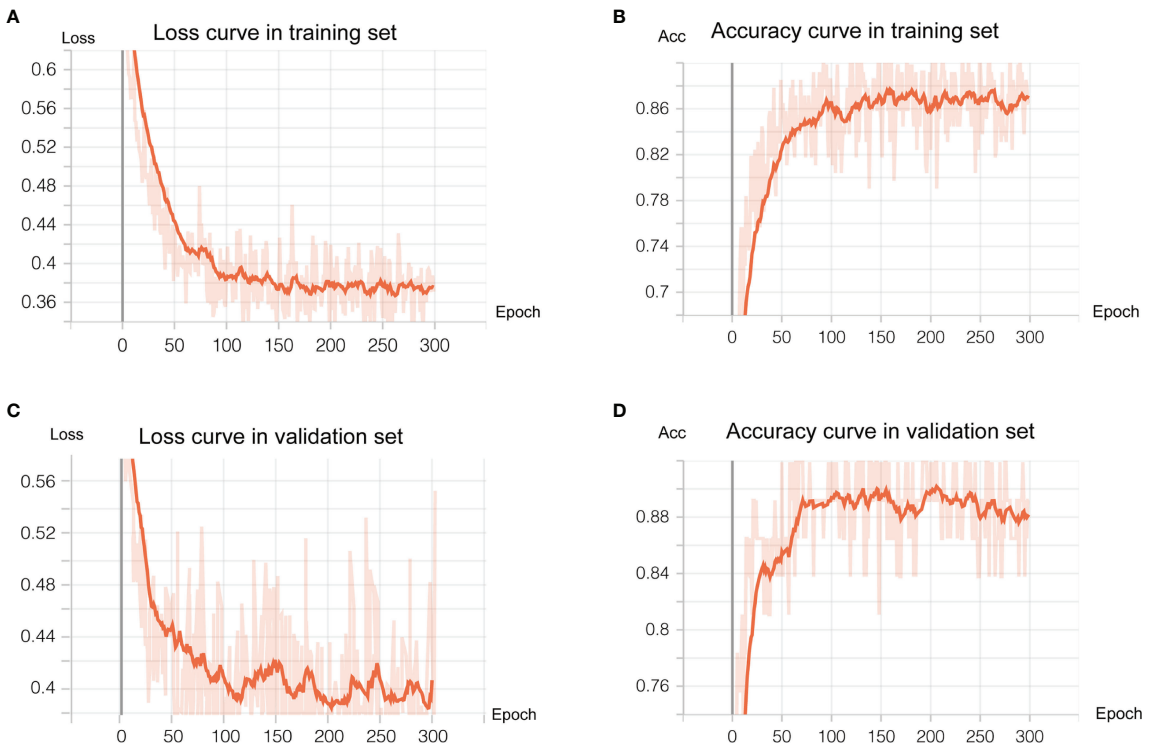

FIGURE 3 | Deep learning training and validation. We trained 300 epochs and training and validation loss reached convergence at around 100 epochs. **(A, B)** showed loss curve of the transfer model in the training set and validation set, respectively. **(C, D)** showed the accuracy curve of the transfer model in the training set and validation set, respectively.

0.001). No significant differences in bone erosion (p = 0.39) and peritumoral edema (p = 0.361) were present.

Diagnostic Performance of Radiological Features and Deep Learning Model

As shown in **Figure 3**, the transfer learning model reached a stable convergence at around 100 steps of training. After a model convergence, we got an average loss of 0.400 ± 0.040 [mean ± standard deviation (SD)] and an accuracy of 0.889 ± 0.024 in the validation set. The deep learning model reached satisfactory AUCs (**Figures 4A, C**) of 0.92 and 0.91 in the training and validation cohorts, respectively. In comparison, applying these radiological features (tumor boundary, bone erosion, dural sign, T1C enhancement patterns, venous sinus invasion, cystic

TABLE 2 | Demographic table.

	SFT/HPC (n = 114)	Meningioma (n = 122)	Total (n = 236)	*p*-value
Age (years)	42.72 ± 14.87	45.13 ± 11.64	43.97 ± 13.32	0.167
Female (n, %)	52 (45.6%)	59 (48.3%)	111 (47.0%)	0.77
Location				0.024
Convexity	74	58	132	
Skull base	40	50	90	
Falx	5	11	16	
Intraventricular	5	3	8	
Boundary Clear (n, %)	89 (78.1%)	108 (88.5%)	197 (83.5%)	0.05
Bone Erosion (n, %)	12 (10.5%)	8 (6.6%)	20 (8.5%)	0.39
Dural Tail (n, %)	10 (8.8%)	41 (33.6%)	51 (21.6%)	<0.001
Enhancement	n = 109	n = 119		0.011
homogeneous	21	42	63	
heterogeneous	88	77	165	
Venous sinus invasion (n, %)	49 (43.0%)	28 (23.0%)	77 (32.6%)	0.001
Peritumoral edema (n, %)	41 (36.0%)	52 (42.6%)	93 (39.4%)	0.361
Cystic component (n, %)	26 (22.8%)	6 (4.9%)	35 (14.8%)	<0.001

HPC, hemangiopericytoma; SFT, solitary fibrous tumor.

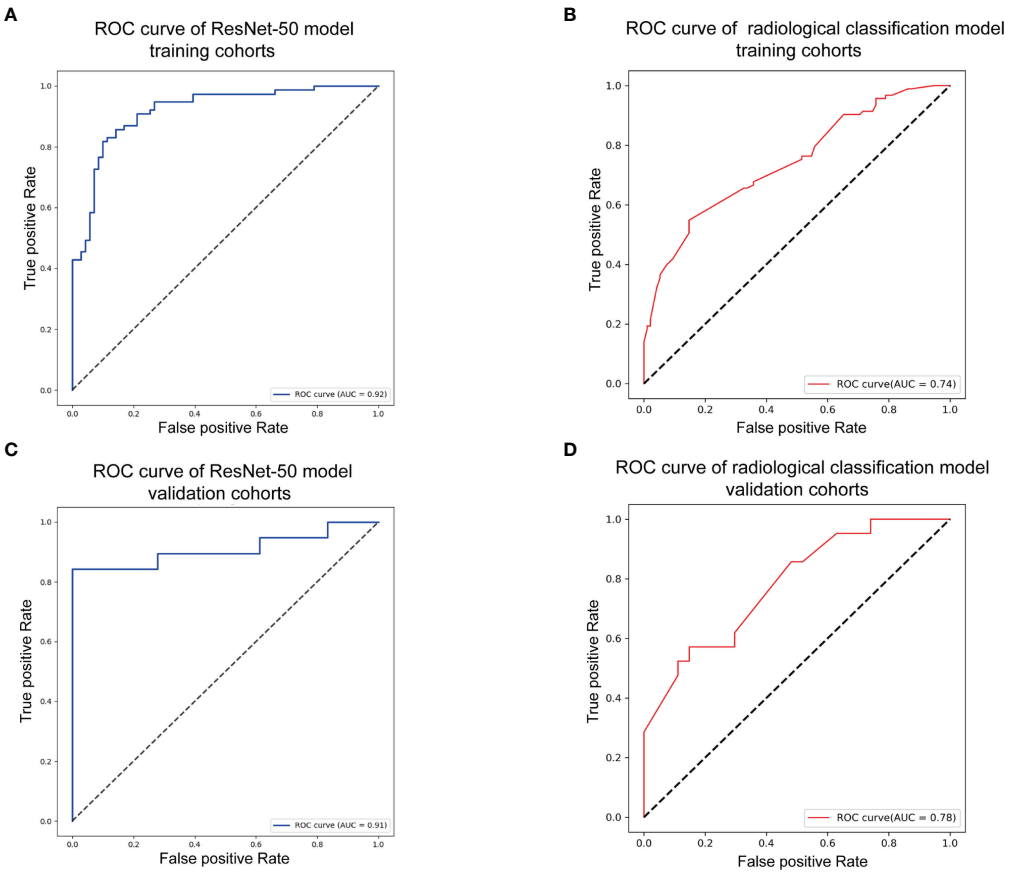

FIGURE 4 | Model evaluation. **(A)** Receiver-operating characteristic (ROC) curve of the transfer model in the training set with receiver-operating characteristic curve area under the curve (AUC) of 0.92. **(B)** ROC curve of the radiological feature classification model in the training set with AUC of 0.74. **(C)** ROC curve of the transfer model in the validation set with AUC of 0.91. **(D)** ROC curve of the radiological feature classification model in the validation set with AUC of 0.78.

components, and peritumoral edema) for differentiating SFT/HPC from meningiomas in our study only reached AUCs (**Figures 4B, D**) of 0.74 and 0.78 in the training and validation cohorts, respectively. And for the validation set, quantitative metrics were calculated and shown in **Table 3**. The model achieved higher NPV (100% for SFT/HPC and 86.00% for meningioma) and sensitivity (100% for SFT/HPC and 84.21% for meningioma) for SFT/HPC compared to meningioma. And the model achieved higher PPV (85.71% for SFT/HPC and 100% for meningioma) and specificity (84.21% for SFT/HPC and 100% for meningioma) for meningioma compared to SFT/HPC. The f1-score for both tumors was similar (0.92 for SFT/HPC and 0.91 for meningioma). The AP value for SFT/HPC was 0.92 and for meningioma was 0.86.

Analysis of Feature Maps in Convolutional Layers

The feature maps we extracted represent the average pooling layer before the classification layer. Furthermore, results from the t-SNE show a distinct clustering of SFT/HPC and meningioma in the training and test cohorts (**Figures 5A, C**). However, t-SNE of patients based on radiological features did not show an obvious cluster tendency of the two kinds of tumor (**Figures 5B, D**). By implementing Smooth Grad-CAM ++, we identified the regions within the image that mostly contributed to the prediction model (**Figure 6C**). The warm tones in the heatmap in the vicinity of the tumor show attention regions of the model. We found that for truly predicted groups, network attention overlapped with the tumor areas for SFT/HPC and meningioma. For incorrectly predicted groups, the attention regions of the model were deviated from the tumor bulks. And we calculated the distance from the attention focal point to the tumor bulk and found no significant differences between the SFT/HPC and meningioma for the ground truth group (p = 0.124) (**Figure 6A**, left) and the true predicted group (p = 0.125) (**Figure 6A**, right). Also, no significant differences in the distance were found from the focal points (when outside of the tumor) to the outer edge of the tumor for the truly predicted group (p = 0.432) (**Figure 6B**, right). But for the ground truth group, SFT/HPC showed a little bit higher distance from the focal points to the outer edge of the tumor (p = 0.03) (**Figure 6B**, left). The results suggested tumor bulks of both tumors are the attention areas for the model.

TABLE 3 | Quantitative results for the validation set.

	PPV	NPV	Sensitivity	Specificity	F1-score	AUC	AP
SFT/HPC	85.71%	100%	100%	84.21%	0.92	0.91	0.92
Meningioma	100%	86%	84.21%	100%	0.91	0.91	0.86

HPC, hemangiopericytoma; SFT, solitary fibrous tumor; PPV, positive predictive value; NPV, negative predictive value; AUC, receiver-operating characteristic curve area under the curve; AP score, average precision score.

DISCUSSION

In our study, we established a neural network classification model to distinguish SFT/HPC from meningioma. State-of-the-art deep learning architecture based on pretrained ResNet-50 was adapted on single T1C sequence images, and it achieved a high prediction accuracy of 0.899 with AUCs of 0.92 and 0.91 in the training and validation sets. Extracting the feature maps and applying unsupervised learning also showed good performance of image feature training. Our results suggest a promising approach for automated discriminating these two types of tumors.

Intracranial SFT/HPC is a rare tumor with a diagnostic age of 35–50 years and a similar male-to-female ratio (5, 29, 30). Consistent with previous studies, our study reports that SFT/HPC and meningioma occur on similar average age and gender ratios, and we also reported a similar location distribution in convexity and skull base. Using demographic features to diagnose SFT/HPC was difficult, so physicians relied on the preoperative radiological factors to make decisions. Specifically, firstly, the "dural tail" sign, described as the thickness of the dura adjacent and traditionally considered as a specific sign (31), was significantly different in SFT/HPC and meningioma. Thus, its appearance points toward diagnosing meningioma. Secondly, intracranial SFT/HPC has a rich blood supply, leading to marked heterogeneous enhancement detected in most cases, which may be explained by pathological characteristics (13, 32, 33). Thirdly, HPC is more aggressive and tends to have more sinus invasions,

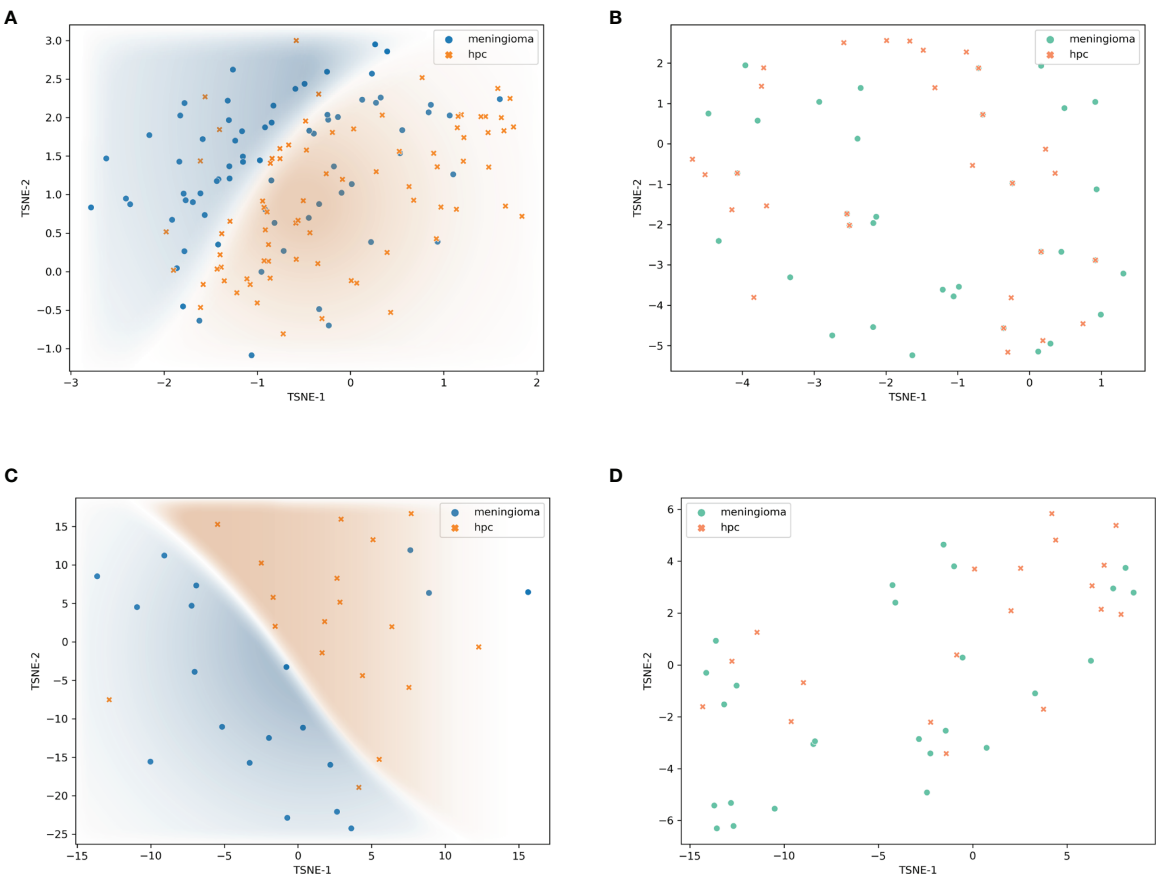

FIGURE 5 | Visualization of feature maps. Features extracted by transfer model and visualized by t-distributed stochastic neighbor embedding (t-SNE) showed distinct clustering in the training set **(A)** and validation set **(C)**, respectively. Features extracted by radiological feature classification model and visualized by t-SNE showed non-distinct clustering in the training set **(B)** and validation set **(D)**, respectively.

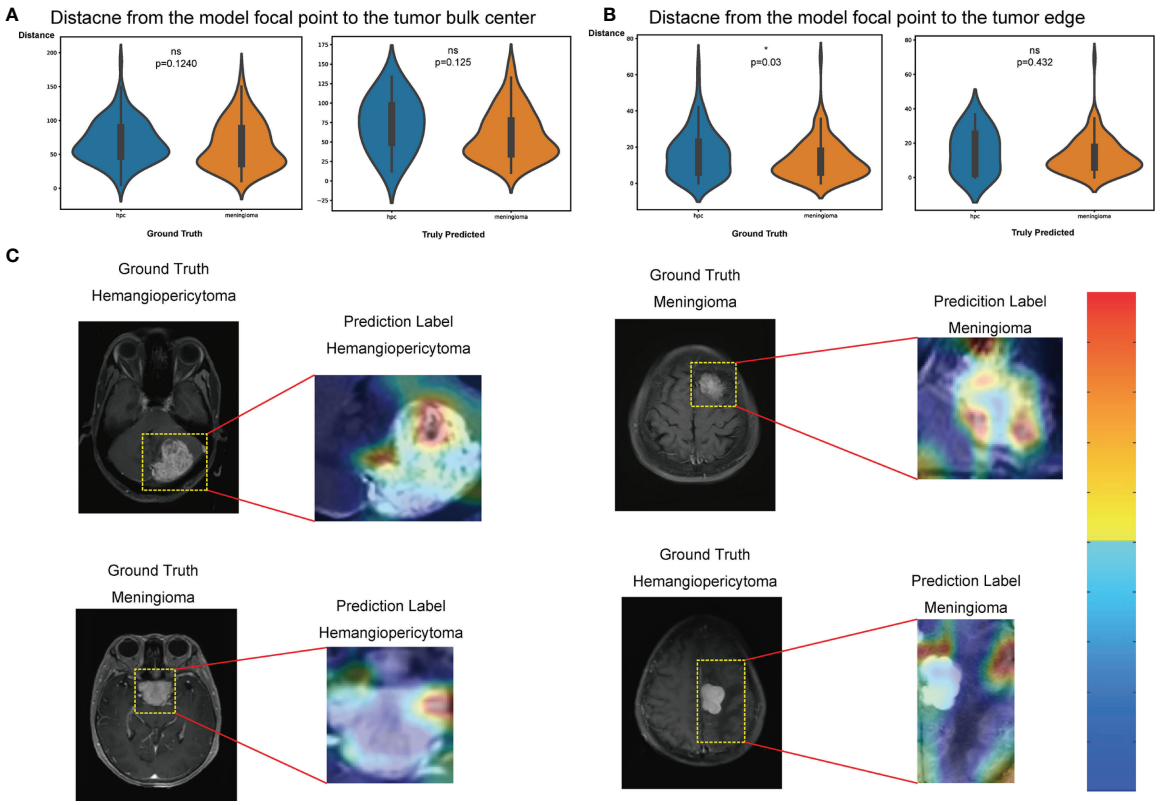

FIGURE 6 | Classification activation maps. **(A)** Distance from the model's focal point to the tumor bulk in the ground truth group (left) and truly predicted (right) group, respectively. Wilcoxon rank test, $^*p < 0.05$. **(B)** Distance from the model's focal point (outside the tumor) to the tumor edge in the ground truth group (left) and truly predicted (right) group, respectively. Wilcoxon rank test, $^*p < 0.05$. **(C)** Coarse attention maps generated using Smooth Grad-CAM++ for correctly (upper row) and incorrectly (lower row) solitary fibrous tumor/hemangiopericytoma (SFT/HPC) and meningioma classification. For each pair, the postcontrast T1-weighted scan and the Smooth Grad-CAM++ attention maps (overlaid on scan) have been shown in the cropped images. In activation maps, warmer and colder colors represent high and low contribution of pixels toward a correct prediction, respectively. ns, no significance.

cysts components, and peritumoral edema (13, 34). Yet, our study reported no significant difference in edema. On the other hand, edema and cystic properties of the tumor indicate a high malignancy and the necessity of surgical resection. We also evaluated the classification performance by using radiological features. The results of the radiological diagnostic model in our study are not good; however, these features are quite important for a preliminary clinical impression to discriminate the tumors. Lastly, other studies (14, 15; 35, 36) examined DWI and SWI characteristics of these two tumors. These studies reported higher ADC values in SFT/HPC due to its redundant vascular spaces and increased perfusion. And mean ADC values in peritumoral edema in SFT/HPC were lower. It may be speculated that the rapid growth and infiltration into adjacent normal tissue caused the edema and lower ADC values (36).

Recent advances in deep learning-assisted approaches have been explored, extracting more quantitative information from limited data. In 2019, Li etal. (36) investigated the classification of the two tumors by a radiomics approach on texture analysis. They reported an accuracy of 77.3% and 87.5% based on DWI and T1 images. However, the small sample size and lack of validation set limited the confidence of their results. Wei et al. (20) developed a clinic-radiomics diagnostic approach called Intracranial hemangiopericytoma (IHPC) and Meningioma Diagnostic Tool (HMDT). It achieved an AUC performance of 0.941 in classification of intracranial HPC and meningioma. And Dong et al. (37) also proposed similar radiomics classification methods. Compared to our model, radiomics semantic feature extraction and machine learning classification were independent and might be biased by different feature extraction and model classification approaches and researchers. And it mainly relied on feature fusion of multimodal MRI images, which limited the application in practice. Thus, our study proposed a transfer model that could combine feature extraction and prediction based on only single-modal images with a strong performance and it could accomplish an end-to-end deployment. In our training strategies, we also compared the T1 and T2 sequences with T1C, but they did not reach quite good performance. SFT/HPC and meningioma often showed enhancement in T1C, which could appear different with normal brain tissue in signal intensity. This may help the neural network to recognize the tumor patterns. T2 sequences may provide more information about peritumoral edema. However, edema surrounding tumors showed similar signals with tumors that made the boundary hard

to identify. On the other hand, we lack some T2 or FLAIR scanning images because those patients could have scanned in other hospitals or only have poor image qualities, and approximative edema pattern of SFT/HPC and meningioma also increased the difficulty of classification. Thus, our single-modal model has wider implications in clinical work especially in primary hospitals, and it is easy to integrate the imaging systems.

By implementing CAMs, the attention area of the model suggested that the tumor bulk regions are quite essential for recognition. In other words, the tumor enhancement patterns play a critical role in model classification. And pseudo color reflection in our preprocessing steps also was useful for training by modifying the image contrasts. The results suggested that we should specifically focus on the enhancement regions and compare the characteristics of contrast differences. Texture features caused by abundant blood supply and necrosis in the tumor bulks made the heterogeneous enhancement patterns. Visualizing the model activation areas could assist us to pay more attention to these regions when suspecting a tumor of SFT/HPC. In addition, postcontrast images that we used are more trustworthy for clinical explanation and model understanding in clinical practice.

Our study illustrates a classification model with an improved performance. Yet, there are several limitations in our study. First of all, only patients in one particular hospital were enrolled in the study. Hence, to better extend the robustness of the model, external validation datasets need to be applied to test the model reliability. Second, DWI and SWI and even functional MRI are reliable to predict tumor types that we need to explore and excavate in future studies. Third, both kinds of tumors have distinct subgroups that require different management strategies and prognoses. Our model only reached a generalized classification. More data such as age, gender, and laboratory tests need to be combined for a more precise prediction. Lastly, considering that tumor bulk is very important for both tumor recognition, further biological and molecular characteristics would be investigated in the future.

CONCLUSIONS

We proposed a deep learning model to classify preoperative MRI of SFT/HPC and meningioma based on single T1C modal MRI images. Our model shows high performance to distinguish the two tumor types with an average accuracy of 0.899 and AUC of 0.91 in the validation set. The tumor bulks that represent the solid texture features of both tumors are essential for model discrimination. Hence, our study paves the way toward an improved clinical diagnosis and management of these tumor diseases.

DATA AVAILABILITY STATEMENT

The data analyzed in this study are subject to the following licenses/restrictions: The data were collected from our hospital that contain the privacy of patients. Requests to access these datasets should be directed to lxjneuro@csu.edu.cn.

ETHICS STATEMENT

The studies involving human participants were reviewed and approved by the Ethics Committee of the Xiangya Hospital, Central South University. Written informed consent to participate in this study was provided by the participants' legal guardian/next of kin.

AUTHOR CONTRIBUTIONS

XL and NY designed this study, NY, ZC, QY performed the analysis, ZC wrote the manuscript, NY, NJ, SW finished the segmentation of all MRI images, ZC, NY, QY contributed in acquisition of the data used in this study. All authors read and approved the final manuscript.

FUNDING

This work was supported by the National Natural Science Foundation of China (for XL, Grant No. 81770781 and No. 81472594) and the Natural Science Foundation of Hunan Province of China (for SW, Grant No. 2019JJ50978).

SUPPLEMENTARY MATERIAL

The Supplementary Material for this article can be found online at: https://www.frontiersin.org/articles/10.3389/fonc.2022.839567/full#supplementary-material

REFERENCES

1. Schweizer L, Koelsche C, Sahm F, Piro RM, Capper D, Reuss DE, et al. Meningeal Hemangiopericytoma and Solitary Fibrous Tumors Carry the NAB2-STAT6 Fusion and can be Diagnosed by Nuclear Expression of STAT6 Protein. *Acta Neuropathol* (2013) 125(5):651–8 doi: 10.1007/s00401-013-1117-6
2. Barthelmess S, Geddert H, Boltze C, Moskalev EA, Bieg M, Sirbu H, et al. Solitary Fibrous Tumors/Hemangiopericytomas With Different Variants of the NAB2-STAT6 Gene Fusion are Characterized by Specific Histomorphology and Distinct Clinicopathological Features. *Am J Pathol* (2014) 184(4):1209–18. doi: 10.1016/j.ajpath.2013.12.016
3. Fritchie K, Jensch K, Moskalev EA, Caron A, Jenkins S, Link M, et al. The Impact of Histopathology and NAB2-STAT6 Fusion Subtype in Classification and Grading of Meningeal Solitary Fibrous Tumor/Hemangiopericytoma. *Acta Neuropathol* (2019) 137(2):307–19. doi: 10.1007/s00401-018-1952-6
4. Louis DN, Perry A, Reifenberger G, von Deimling A, Figarella-Branger D, Cavenee WK, et al. The 2016 World Health Organization Classification of Tumors of the Central Nervous System: A Summary. *Acta Neuropathol* (2016) 131(6):803–20. doi: 10.1007/s00401-016-1545-1

5. Giordan E, Marton E, Wennberg AM, Guerriero A, Canova G. A Review of Solitary Fibrous Tumor/Hemangiopericytoma Tumor and a Comparison of Risk Factors for Recurrence, Metastases, and Death Among Patients With Spinal and Intracranial Tumors. *Neurosurg Rev* (2021) 44(3):1299–312. doi: 10.1007/s10143-020-01335-x
6. Kinslow CJ, Bruce SS, Rae AI, Sheth SA, McKhann GM, Sisti MB, et al. Solitary-Fibrous Tumor/Hemangiopericytoma of the Central Nervous System: A Population-Based Study. *J Neurooncol* (2018) 138(1):173–82. doi: 10.1007/s11060-018-2787-7
7. Rutkowski MJ, Jian BJ, Bloch O, Chen C, Sughrue ME, Tihan T, et al. Intracranial Hemangiopericytoma: Clinical Experience and Treatment Considerations in a Modern Series of 40 Adult Patients. *Cancer* (2012) 118 (6):1628–36. doi: 10.1002/cncr.26411
8. Melone AG, D'Elia A, Santoro F, Salvati M, Delfini R, Cantore G, et al. Intracranial Hemangiopericytoma-Our Experience in 30 Years: A Series of 43 Cases and Review of the Literature. *World Neurosurg* (2014) 81(3-4):556–62. doi: 10.1016/j.wneu.2013.11.009
9. Kim BS, Kim Y, Kong DS, Nam DH, Lee JI, Suh YL, et al. Clinical Outcomes of Intracranial Solitary Fibrous Tumor and Hemangiopericytoma: Analysis According to the 2016 WHO Classification of Central Nervous System Tumors. *J Neurosurg* (2018) 129(6):1384–96. doi: 10.3171/2017.7.JNS171226
10. Wang K, Mei F, Wu S, Tan Z. Hemangiopericytoma: Incidence, Treatment, and Prognosis Analysis Based on SEER Database. *BioMed Res Int* (2020) 2020:2468320. doi: 10.1155/2020/2468320
11. Shin DW, Kim JH, Chong S, Song SW, Kim YH, Cho YH, et al. Intracranial Solitary Fibrous Tumor/Hemangiopericytoma: Tumor Reclassification and Assessment of Treatment Outcome via the 2016 WHO Classification. *J Neurooncol* (2021) 154:171–8. doi: 10.1007/s11060-021-03733-7
12. Meng Y, Chaohu W, Yi L, Jun P, Songtao Q. Preoperative Radiologic Characters to Predict Hemangiopericytoma From Angiomatous Meningioma. *Clin Neurol Neurosurg* (2015) 138:78–82. doi: 10.1016/j.clineuro.2015.08.005
13. Zhou JL, Liu JL, Zhang J, Zhang M. Thirty-Nine Cases of Intracranial Hemangiopericytoma and Anaplastic Hemangiopericytoma: A Retrospective Review of MRI Features and Pathological Findings. *Eur J Radiol* (2012) 81(11):3504–10. doi: 10.1016/j.ejrad.2012.04.034
14. Shankar JJS, Hodgson L, Sinha N. Diffusion Weighted Imaging may Help Differentiate Intracranial Hemangiopericytoma From Meningioma. *J Neuroradiol* (2019) 46(4):263–7. doi: 10.1016/j.neurad.2018.11.002
15. Chen T, Jiang B, Zheng Y, She D, Zhang H, Xing Z, et al. Differentiating Intracranial Solitary Fibrous Tumor/Hemangiopericytoma From Meningioma Using Diffusion-Weighted Imaging and Susceptibility-Weighted Imaging. *Neuroradiology* (2020) 62(2):175–84. doi: 10.1007/s00234-019-02307-9
16. Liu L, Yin B, Geng DY, Li Y, Zhang BY, Peng WJ. Comparison of ADC Values of Intracranial Hemangiopericytomas and Angiomatous and Anaplastic Meningiomas. *J Neuroradiol* (2014) 41(3):188–94. doi: 10.1016/j.neurad.2013.07.002
17. He WL, Xiao X, Li XD, Guo YH, Guo LJ, Liu XM, et al. Whole-Tumor Histogram Analysis of Apparent Diffusion Coefficient in Differentiating Intracranial Solitary Fibrous Tumor/Hemangiopericytoma From Angiomatous Meningioma. *Eur J Radiol* (2019) 112:186–91. doi: 10.1016/j.ejrad.2019.01.023
18. Hosny A, Parmar C, Quackenbush J, Schwartz LH. And Hjwl Aerts. 2018. Artificial Intelligence in Radiology. *Nat Rev Cancer* (2018) 18(8):500–5105. doi: 10.1038/s41568-018-0016-5
19. Mazurowski MA, Buda M, Saha A, Bashir MR. Deep Learning in Radiology: An Overview of the Concepts and a Survey of the State of the Art With Focus on MRI. *J Magn Reson Imaging* (2019) 49(4):939–54. doi: 10.1002/jmri.26534
20. Wei J, Li L, Han Y, Gu D, Chen Q, Wang J, et al. Accurate Preoperative Distinction of Intracranial Hemangiopericytoma From Meningioma Using a Multihabitat and Multisequence-Based Radiomics Diagnostic Technique. *Front Oncol* (2020) 10:534. doi: 10.3389/fonc.2020.00534
21. Quon JL, Bala W, Chen LC, Wright J, Kim LH, Han M, et al. Deep Learning for Pediatric Posterior Fossa Tumor Detection and Classification: A Multi-Institutional Study. *AJNR Am J Neuroradiol* (2020) 41(9):1718–25. doi: 10.3174/ajnr.A6704
22. Muhammad K, Khan S, Ser JD, Albuquerque VHC. Deep Learning for Multigrade Brain Tumor Classification in Smart Healthcare Systems: A Prospective Survey. *IEEE Trans Neural Netw Learn Syst* (2021) 32(2):507–22. doi: 10.1109/TNNLS.2020.2995800
23. Gauriau R, Bizzo BC, Kitamura FC, Landi Junior O, Ferraciolli SF, Macruz FBC, et al. A Deep Learning-Based Model for Detecting Abnormalities on Brain MR Images for Triaging: Preliminary Results From a Multisite Experience. *Radiol Artif Intell* (2021) 3(4):e200184. doi: 10.1148/ryai.2021200184
24. He KM, Zhang XY, Ren SQ, Sun J. Deep Residual Learning for Image Recognition. *2016 IEEE Conf Comput Vision Pattern Recognit (Cvpr)* (2016), 770–8. doi: 10.1109/Cvpr.2016.90
25. Chappelow J, Bloch BN, Rofsky N, Genega E, Lenkinski R, DeWolf W, et al. Elastic Registration of Multimodal Prostate MRI and Histology *via* Multiattribute Combined Mutual Information. *Med Phys* (2011) 38 (4):2005–18. doi: 10.1118/1.3560879
26. Yushkevich PA, Pashchinskiy A, Oguz I, Mohan S, Schmitt JE, Stein JM, et al. User-Guided Segmentation of Multi-Modality Medical Imaging Datasets With ITK-SNAP. *Neuroinformatics* (2019) 17(1):83–102. doi: 10.1007/s12021-018-9385-x
27. Pérez-García F, Sparks R, Ourselin S. TorchIO: A Python Library for Efficient Loading, Preprocessing, Augmentation and Patch-Based Sampling of Medical Images in Deep Learning. *Comput Methods Programs Biomed* (2021) 208:106236. doi: 10.1016/j.cmpb.2021.106236
28. Omeiza D, Speakman S, Cintas C, Weldermariam K. Smooth Grad-Cam++: An Enhanced Inference Level Visualization Technique for Deep Convolutional Neural Network Models. (2019). arXiv preprint arXiv:1908.01224.
29. Tian R, Hao S, Hou Z, Bian L, Zhang Y, Wu W, et al. Clinical Characteristics and Prognostic Analysis of Recurrent Hemangiopericytoma in the Central Nervous System: A Review of 46 Cases. *J Neurooncol* (2013) 115(1):53–9. doi: 10.1007/s11060-013-1193-4
30. Guthrie BL, Ebersold MJ, Scheithauer BW, Shaw EG. Meningeal Hemangiopericytoma: Histopathological Features, Treatment, and Long-Term Follow-Up of 44 Cases. *Neurosurgery* (1989) 25(4):514–22. doi: 10.1227/00006123-198910000-00003
31. Rokni-Yazdi H, Azmoudeh Ardalan F, Asadzandi Z, Sotoudeh H, Shakiba M, Adibi A, et al. Pathologic Significance of the Dural Tail Sign. *Eur J Radiol* (2009) 70(1):10–6. doi: 10.1016/j.ejrad.2008.01.010
32. Ma C, Xu F, Xiao YD, Paudel R, Sun Y, Xiao EH. Magnetic Resonance Imaging of Intracranial Hemangiopericytoma and Correlation With Pathological Findings. *Oncol Lett* (2014) 8(5):2140–4. doi: 10.3892/ol.2014.2503
33. Park BJ, Kim YI, Hong YK, Jeun SS, Lee KS, Lee YS. Clinical Analysis of Intracranial Hemangiopericytoma. *J Korean Neurosurg Soc* (2013) 54(4):309–16. doi: 10.3340/jkns.2013.54.4.309
34. Mama N, Ben Abdallah A, Hasni I, Kadri K, Arifa N, Ladib M, et al. MR Imaging of Intracranial Hemangiopericytomas. *J Neuroradiol* (2014) 41 (5):296–306. doi: 10.1016/j.neurad.2013.10.007
35. Liu G, Chen ZY, Ma L, Lou X, Li SJ, Wang YL. Intracranial Hemangiopericytoma: MR Imaging Findings and Diagnostic Usefulness of Minimum ADC Values. *J Magn Reson Imaging* (2013) 38(5):1146–51. doi: 10.1002/jmri.24075
36. Li XX, Lu YP, Xiong J, Wang DD, She DJ, Kuai XP, et al. Presurgical Differentiation Between Malignant Haemangiopericytoma and Angiomatous Meningioma by a Radiomics Approach Based on Texture Analysis. *J Neuroradiol* (2019) 46(5):281–7. doi: 10.1016/j.neurad.2019.05.013
37. Dong JY, Yu MM, Miao YW, Shen HC, Sui Y, Liu YYQ, et al. Differential Diagnosis of Solitary Fibrous Tumor/Hemangiopericytoma and Angiomatous Meningioma Using Three-Dimensional Magnetic Resonance Imaging Texture Feature Model. *BioMed Res Int* (2020) 2020:5042356. doi: 10.1155/2020/5042356

Conflict of Interest: The authors declare that the research was conducted in the absence of any commercial or financial relationships that could be construed as a potential conflict of interest.

Publisher's Note: All claims expressed in this article are solely those of the authors and do not necessarily represent those of their affiliated organizations, or those of the publisher, the editors and the reviewers. Any product that may be evaluated in this article, or claim that may be made by its manufacturer, is not guaranteed or endorsed by the publisher.

Copyright © 2022 Chen, Ye, Jiang, Yang, Wanggou and Li. This is an open-access article distributed under the terms of the Creative Commons Attribution License (CC BY). The use, distribution or reproduction in other forums is permitted, provided the original author(s) and the copyright owner(s) are credited and that the original publication in this journal is cited, in accordance with accepted academic practice. No use, distribution or reproduction is permitted which does not comply with these terms.

frontiers in Oncology

ORIGINAL RESEARCH
published: 08 March 2022
doi: 10.3389/fonc.2022.852327

Clinical Outcomes and Complications of Preoperative Embolization for Intracranial Giant Meningioma Tumorectomy: A Retrospective, Observational, Matched Cohort Study

Yi Yin[1,2,3‡], Yuhong Li[1,2,3‡], Zhouyang Jiang[1,2,3‡], Chao Zhang[1,2,3], Hongfei Ge[1,2,3], Zhi Chen[1,2,3], Rong Hu[1,2,3], Yujie Chen[1,2,3†], Xuegang Li[1,2,3*], Fei Li[1,2,3*] and Hua Feng[1,2,3]*

[1] Department of Neurosurgery, Southwest Hospital, Third Military Medical University (Army Medical University), Chongqing, China, [2] Chongqing Clinical Research Center for Neurosurgery, Southwest Hospital, Third Military Medical University (Army Medical University), Chongqing, China, [3] Chongqing Key Laboratory of Precision Neuromedicine and Neuroregenaration, Southwest Hospital, Third Military Medical University (Army Medical University), Chongqing, China

Objective: The potential benefits of preoperative embolization for intracranial meningiomas are still under debate. We aimed to investigate whether preoperative embolization can improve surgical and functional outcomes, based on controlling patient- and tumor-related confounding factors.

Methods: We reviewed all meningioma cases in our department from January 2016 to May 2021. Cases in the nonembolization cohort were matched to the embolization cohort by 1:1 ratio propensity score matching, through controlling patient- and tumor-related confounds. Surgical outcomes, complications, and functional outcomes were retrospectively compared between these two groups.

Results: Sixty-six cases in each group were included in our study after being matched. We did not find any significant differences of estimated blood loss (600.00 (400) vs. 500.00 (500.00) ml, $p = 0.31$), decrease of HGB level (30.81 ± 15.82 vs. 26.59 ± 12.90 g/L, $p = 0.09$), gross total resection rate (74.24% vs. 77.27%, $p = 0.68$), surgical time (302.50 (136) vs. 300.00 (72) min, $p = 0.48$), blood transfusion rates (53.03% vs. 42.42%, $p = 0.35$), blood transfusion volume [650.00 (657.50) vs. 535.00 (875.00) ml, $p = 0.63$] between the embolization group and nonembolization group. The number of patients who experience postsurgery complications were significantly higher in the nonembolization group (39.39% vs. 21.21%, $p = 0.02$). Patients in the nonembolization group were more likely to have a higher rate of mRS decline postsurgery (31.82% vs. 15.15%, $p = 0.04$).

Conclusion: Our study showed significant lower rates of surgical complications and long-term disabilities of meningioma patients treated with preoperative embolization. There were no significant differences in estimated blood loss, surgical time, and blood transfusion volume between embolization and nonembolization groups.

Keywords: meningioma, embolization, outcome, complication, preoperative

OPEN ACCESS

Edited by:
Hailiang Tang,
Fudan University, China

Reviewed by:
Bharat Guthikonda,
Louisiana State University Health Shreveport, United States
Lin Song,
Capital Medical University, China

****Correspondence:***
Yujie Chen
yujiechen6886@foxmail.com;
chenyj@tmmu.edu.cn
Xuegang Li
67433433@qq.com
Fei Li
feifly7887@126.com

†ORCID:
Yujie Chen
orcid.org/0000-0002-9905-9138

‡These authors have contributed equally to this work and share first authorship

Specialty section:
This article was submitted to Neuro-Oncology and Neurosurgical Oncology, a section of the journal Frontiers in Oncology

Received: *11 January 2022*
Accepted: *09 February 2022*
Published: *08 March 2022*

Citation:
Yin Y, Li Y, Jiang Z, Zhang C, Ge H, Chen Z, Hu R, Chen Y, Li X, Li F and Feng H (2022) Clinical Outcomes and Complications of Preoperative Embolization for Intracranial Giant Meningioma Tumorectomy: A Retrospective, Observational, Matched Cohort Study. Front. Oncol. 12:852327. doi: 10.3389/fonc.2022.852327

INTRODUCTION

Meningiomas are the most common type of primary brain tumors, accounting for one-third of all central nervous system (CNS) tumors (1). Meningiomas always tend to be rich in vascularity, which complicates surgical resection due to substantial intraoperative blood loss. Devascularization of meningioma by preoperative endovascular embolization of feeding vessels was firstly introduced by Manelfe et al. (2). The intentions of such adjunctive therapy are to reduce surgical blood loss, soften tumor, and shorten the surgical time (3–6). However, discrepancies are found between results reported by different groups (7–9). Recent updated meta-analysis study indicates no clear benefit is observed in operative and postoperative outcomes of embolization (10), which is inconsistent with findings in an earlier meta-analysis (11).

Currently, no consensus or guidelines have elucidated the issue whether preoperative embolization benefits patients with meningiomas. Surgeons tend to embolize large and highly vascularized meningiomas, which may contribute to intergroup selection bias of baseline characteristics. Thus, moderate to high heterogeneity is observed in meta-analysis (10). An investigation performed by Przybylowski et al. has found that the surgical outcomes exhibit no obvious improvements using cohort matching method to control patient- and tumor-related confounds. As only WHO grade I meningiomas, which are generally less aggressive and complicated than WHO grades II and III meningiomas, are enrolled in this study, that limits generalizability of interpretation. Furthermore, their results demonstrate that embolization is found to lead to a greater chance of clinical improvement (12).

Therefore, this cohort-matching study retrospectively was performed with reviewing data of patients with meningioma who underwent with/without preoperative embolization at the Department of Neurosurgery of the Southwest Hospital Affiliated to Army Medical University from January 2016 to May 2021. Cases in the nonembolization cohort were matched to the embolization cohort by a 1:1 ratio propensity score matching through controlling patient- and tumor-related confounds. Surgical outcomes, complications, and functional outcomes were retrospectively compared between these two cohorts. The aim of the study is to validate the effect of preoperative embolization on surgical outcomes, complications, and functional outcomes in patients with meningioma.

MATERIALS AND METHODS

Patients

Patients diagnosed with meningioma were enrolled in the present study at the Department of Neurosurgery of the Southwest Hospital Affiliated to Army Medical University from January 2016 to May 2021. All eligible patients with or without preoperative superselective tumor embolization were recruited in this study. The inclusion criteria included supratentorial WHO grades I, II, and III meningioma histopathology, age ≥18 years, and follow-up duration >6 months. Exclusion criteria included meningiomatosis, maximum diameter <2.0 cm, simultaneously discovered intracranial aneurysms, vascular malformations, intracranial hemorrhage, recent oral anticoagulant medications, and loss of follow-up.

A total of 333 cases were included, among which 66 patients underwent preoperative embolization. The decision of whether performing preoperative tumor embolization usually depends on presence of flowing void effects on magnetic resonance imaging (MRI) or rich vasculature on CTA. However, these were not the strict protocols, and the choices were usually made depending on surgeons' experiences. All procedures were performed under the approval of the ethics committee of the Southwest Hospital Affiliated to Army Medical University (Ethics Approval No. KY2021150). Written consents were acquired for all surgical procedures. Informed patient consent for the data collection and analysis was waived by the ethical committee due to the retrospective nature of the study.

Cohort Matching

Before cohort matching, categories of patient- and tumor-related variables for controlling covariates between two groups were collected *via* medical records or PAC system. Patient-related variables included sex and age at diagnosis. Tumor-related variables included the tumor location indicated as convexity, falcine, anterior skull base, and medial skull base; tumor encasement of large cerebral arteries encompassing the internal carotid artery (ICA) and the middle cerebral artery (MCA) assessed from computed tomography angiography (CTA); major sinus invasion by tumor verified both from magnetic resonance venography (MRV) and surgery records; and maximum diameter assessed by preoperative MRI or CT.

Patients were divided into embolization and nonembolization cohorts, depending on whether preoperative tumor embolization was performed. To perform 1:1 ratio cohort matching, we implemented the propensity score matching algorithm with MatchIt Package (Version 4.3.2) (13) in R (Version 4.1.2). Parameters were set as follows: tumor location, tumor encasement of ICA/MCA, and sinus invasion by tumor were exactly matched between cohorts; tumor maximum diameter, patients' age and sex were matched using *nearest-neighbor matching* method by default; and distance measurements were set to *glm* by default for propensity score matching. Quality of matches was assessed by *p*-value, eCDF statistics, jitter plots, eQQ plots, and Love plots.

Clinical and Neuroimaging Assessment

Detailed neuroimaging, neuropathological, surgical, complication, and functional outcome data were acquired after successful cohort matching. Neuroimaging data were independently reviewed by two experienced doctors. Gross total resection (GTR) was verified as complete resection of the enhancing tumor mass on contrast-enhanced T1 MRI.

Surgical data included gross total resection data, surgery duration, estimated blood loss (EBL), volume of autologous blood transfusion and allogeneic blood transfusion, and preoperative and postoperative hemoglobin (HGB). Patients with postoperative brain herniation due to large hematoma,

severe brain edema, or large hemispheric infarction, underwent secondary surgery to reduce the intracranial pressure by means of decompressive craniectomy and/or hematoma evacuation. Other surgery-related complications included death, hemiparesis, cranial nerve palsy, visual defect, decreased hearing, aphasia, mental disorder, intracranial infection, seizure, cerebrospinal fluid leakage, and respiratory failure.

Functional assessments were carried out with Modified Rankin Scale (mRS) both before and during follow-up. mRS decline was defined as follow-up mRS score increase by at least 1 grade when compared with preoperative mRS.

Statistical Analysis

Continuous variables conforming to normal distribution were presented as *mean* ± *standard deviation* (*SD*), while continuous variables, that were not conforming to normal distribution, were presented as *median* (*interquartile spacing*). Student's t-test was used for intergroup comparison when normal distribution and equal variance examination were met. In the contrary, Wilcoxon's rank sum test was used for the comparison. Categorical data are presented as *frequency* (*percentage*). For comparison of categorical data between groups, Wilcoxon's rank sum test or Chi-square test or Fisher's exact test were performed. A $p < 0.05$ was considered to be statistically significant, and two-sided statistical tests were performed. All statistical analysis was performed in R (Version 4.1.2).

RESULTS

Cohort Matching

By retrieving the electronic medical record system, a total of 452 patients underwent meningioma resection surgery at our institution, of which 333 patients meet our selection and exclusion criteria and included in the cohort-matching process. Preoperative embolization was performed only in 66 (19.82%) patients but not in the other 267 (80.18%). To reduce the confound effects of covariates, we performed 1:1 ratio propensity score matching. Sixty-six patients from the nonembolization group ($n = 267$) were matched to the preoperative embolization patient's cohort and enrolled in the nonembolization group, with algorithm parameters described in the **Materials and Methods** section.

Between the embolization and nonembolization groups, the exact matching criteria about tumor location yielded successful matching ($p = 1.00$) compared with $p = 0.50$ before matching. Other exact controlling variables such as ICA/MCA encasement ($p = 1.00$ vs. $p = 0.11$) and sinus invasion ($p = 1.00$ vs. $p = 0.44$) also achieved successful matching. Categorical variable, sex, also achieved perfect matching, with $p = 1.00$ after matching compared with $p = 0.33$ without matching. For continuous variable max tumor diameter, propensity score matching increased the *p*-value of the comparison between two cohorts from $p < 0.0001$ to $p = 0.69$. Another continuous variable age at diagnosis, the matching method increased the *p*-value of the comparison between two cohorts from $p = 0.77$ to $p = 0.90$. *p*-value, eCDF statistics, jitter plot, eQQ plot, and Love plot also indicate satisfying matches between two cohorts (**Supplementary Table S1** and **Supplementary Figures S1**–**S3**).

Patient Characteristics

The average ages at diagnosis of the embolization and nonembolization group were 56.64 ± 11.39 and 56.39 ± 11.16 years, respectively ($p = 0.90$). There were both 44 (66.67%) female cases in two cohorts ($p = 1.00$). The distribution of pathological grade in the embolization cohort was 51 (77.27%), 13 (19.70%), and 2 (3.03%) for WHO grades I, II, and III, while in the nonembolization group, the distribution was 58 (87.88%), 8 (12.12%), and 0 (0), respectively ($p = 0.16$). The maximum diameter of the tumor was 54.59 ± 15.84 mm in the embolization cohort versus 53.50 ± 15.07 mm in the nonembolization group ($p = 0.69$). The distribution of tumor laterality (left/right/midline) in the embolization cohort was 36 (54.55%), 28 (42.42%), and 2 (3.03%) and 34 (51.52%), 26 (39.39%), and 6 (9.09%) in the nonembolization cohort ($p = 0.45$). Tumors located along the convexity, falcine, anterior skull base, and middle skull base were 18 (27.27%), 24 (36.36%), 20 (30.30%), and 4 (6.06%) in both cohorts ($p = 1.00$). Approximately 10 (15.15%) cases were found to have ICA/MCA encasement in both groups. Sinus invasion occurred in 4 (10.60%) in both the embolization group and the nonembolization group (**Table 1**).

Surgery-Related Outcomes

Operative time in the embolization group was 302.50 (136) min and 300.00 (72) min in the nonembolization group ($p = 0.48$). There was no significant difference in gross total resection rate between the two groups ($p = 0.68$). The estimated blood loss was 600.00 (400.00) ml in the embolization group versus 500.00 (500.00) ml in the nonembolization group ($p = 0.31$). There was also no significant difference in the decrease of perioperative HGB level between the two groups, which is calculated as the preoperative HGB level minus the postoperative HGB level ($p = 0.68$). Thirty-five patients (53.03%) received blood transfusion during surgery in the embolization group compared with 28 (42.42%) patients in the nonembolization group ($p = 0.35$). There was no significant difference in the volume of blood transfusion in the two groups ($p = 0.63$) (**Table 2**).

Postoperative Complications

Postoperative complications were retrieved from both inpatient and postoperative outpatient follow-up medical records. Patients with postoperative brain herniation due to large hematoma, severe brain edema, and large hemispheric infarction underwent secondary emergency surgery to remove the blood clot and/or decompressive craniectomy. Two (3.03%) patients in the embolization group and 3 (4.54%) in the nonembolization group developed large intracranial hematoma postsurgery ($p = 0.63$). Two (3.03%) patients in the embolization group and 4 (6.06%) in the nonembolization group experienced postoperative large hemispheric infarction, brain edema, and chronic hemiplegia ($p = 0.68$). These patients were treated with decompressive craniectomy. One patient in the non-embolization group suffered from brain herniation due to postoperative hematoma and severe brain edema.

TABLE 1 | Baseline clinical characteristics.

Characteristics	Embolization group (*n* = 66)	Nonembolization group (*n* = 66)	*p*
Age at diagnosis (years; mean ± SD)	56.64 ± 11.39	56.39 ± 11.16	0.90
Sex (female; %)	44 (66.67)	44 (66.67)	1.00
WHO grade			
I (%)	51 (77.27)	58 (87.88)	0.16
II (%)	13 (19.70)	8 (12.12)	
III (%)	2 (3.03)	0 (0)	
Maximal diameter (mm; mean ± SD)	54.59 ± 15.84	53.50 ± 15.07	0.69
Laterality			
Left (%)	36 (54.55)	34 (51.52)	0.45
Right (%)	28 (42.42)	26 (39.39)	
Midline (%)	2 (3.03)	6 (9.09)	
Location			
Falcine (%)	24 (36.36)	24 (36.36)	1.00
Anterior skull base (%)	20 (30.30)	20 (30.30)	
Convexity (%)	18 (27.27)	18 (27.27)	
Middle skull base (%)	4 (6.06)	4 (6.06)	
ICA/MCA encasement (%)	10 (15.15)	10 (15.15)	1.00
Sinus invasion (%)	4 (10.60)	4 (10.60)	1.00

TABLE 2 | Comparisons of surgical outcomes between the embolization and nonembolization group.

Surgical outcomes	Embolization group (*n* = 66)	Nonembolization group (*n* = 66)	*p*
Surgical time [minutes; median (IQR)]	302.50 (136.00)	300.00 (72)	0.48
GTR (%)	49 (74.24)	51 (77.27)	0.68
EBL (ml; mean ± SD)	600.00 (400.00)	500.00 (500.00)	0.31
Decreasement of HGB (g/L; mean ± SD)	30.81 ± 15.82	26.59 ± 12.90	0.09
Blood transfusion (%)	35 (53.03)	28 (42.42)	0.35
Blood transfusion volume [ml; median (IQR)]	650.00 (657.50) (*n* = 35)	535.00 (875.00) (*n* = 28)	0.63

Though emergency decompressive craniectomy and hematoma evacuation were performed, the patient unfortunately passed away.

Neurological deficits include hemiplegia, hemiparesis, CN VII palsy, visual defect, decreased hearing, aphasia, mental disorder, infection, and seizure (**Table 3**). Hemiparesis is the major postoperative neurological deficits in our observation, which occurred in 7 (10.61%) patients in the embolization group and 12 (18.18%) in the nonembolization group ($p = 0.22$).

We observed a statistically significant lower rate of patients with at least one postoperative complication in the embolization group (21.21% vs. 39.39%, $p = 0.02$). *Post-hoc* analysis showed significantly higher level of estimated blood loss in the group of patients suffering from surgical complications (600.00 (525.00) vs. 500.00 (500.00) ml, $p = 0.037$).

Functional Outcomes

The follow-up duration in our study ranged from 6.2 to 37.5 months. The last postoperative follow-up mRS score showed no significant difference between these two groups ($p = 0.167$). Because higher complication rate occurred in the nonembolization group, we wondered whether relevant complications would affect patients' daily living independence. To compare preoperative mRS scores, we utilized decline of mRS score to assess worsening of patients' functional independence after surgery. We observed a significantly higher rate of patients with mRS decline in the nonembolization group (31.81%) compared with the embolization group (15.15%) ($p = 0.04$) (**Table 4**).

DISCUSSION

We presented a matched cohort study to compare the postoperative complications and long-tern functional outcomes in patients who underwent with/without preoperative embolization. Based on matching potential confounds between groups, such as patients' age, sex, tumor location, tumor maximum diameter, sinus invasion, and MCA/ICA encasement, our results showed significant lower rates of postoperative complications and reduced mRS decline of patients with preoperative embolization. We did not find any significant differences between groups with respect to surgical outcomes, such as estimated blood loss, operation duration, and blood transfusion.

Surgical resection of large and highly vascularized meningioma is challenging due to life-threatening blood loss and related surgical risks. Preoperative endovascular devascularization sounds reasonable to reduce subsequent intraoperative blood loss. Though increasing clinical studies are being conducted since this technique was established almost four decades ago (2), discrepancies exist on whether patients would benefit from the manipulation (14, 15). Some groups reported reduced intraoperative blood loss (6, 8),

TABLE 3 | Comparisons of postoperative complications between the embolization and nonembolization group.

Complications	Embolization group (*n* = 66)	Nonembolization group (*n* = 66)	*p*
Brain herniation			
Postop hematoma (%)	2 (3.03)	3 (4.54)	1.00
Postop infarction (%)	2 (3.03)	4 (6.06)	0.68
Postop edema (%)	2 (3.03)	4 (6.06)	0.68
Hemiplegia (%)	2 (3.03)	4 (6.06)	0.68
Hemiparesis (%)	7 (10.61)	12 (18.18)	0.22
CN VII palsy (%)	1 (1.52)	1 (1.52)	1.00
Visual defect (%)	0 (0)	3 (4.54)	0.24
Decreased hearing (%)	0 (0)	1 (1.52)	1.00
Aphasia (%)	0 (0)	4 (6.06)	0.11
Mental disorder (%)	1 (1.52)	1 (1.52)	1.00
Infection (%)	0 (0)	1 (1.52)	1.00
Seizure (%)	2 (3.03)	1 (1.52)	1.00
CSF leakage (%)	0 (0)	1 (1.52)	1.00
Respiratory failure (%)	1 (1.52)	4 (6.06)	0.37
Mortality (%)	0 (0)	1 (1.52)	1.00
Patients with postoperative complications (%)	14 (21.21)	26 (39.39)	0.02

softening of the tumor mass to facilitate the operation (5), and shortening of the operation duration (6, 9). However, other data suggest embolization associated with higher rates of neurological adverse events after surgery (16) and added risk for morbidity and mortality (14). Recent meta-analysis also reported controversial conclusion on whether preoperative embolization would be beneficial in terms of reducing the estimated blood loss and surgical time (10, 11).

It is noteworthy that most previous studies were conducted in a manner to enroll consecutive meningioma patients in their institute, without controlling possible patient- and tumor-related confounds (10, 12). It may result in heterogeneity between groups and limits the interpretation of their results. From our own experiences and previous literatures, factors such as large tumor size, unfavorable location, artery encasement, and sinus invasion may complicate the operation and produce potential risks (9, 17–19). Raper et al. analyze a total cohort of 470 meningioma patients and did not find any significant differences on surgery time and complications between embolization and nonembolization groups (7). Blood loss is significantly lower in the nonembolization group due to variances in baseline patient and tumor characteristics. As shown in their baseline characteristics, tumor location and maximum tumor diameter differ significantly between groups.

Przybylowski et al. firstly introduced retrospective cohort matching to control critical confounds between embolization and nonembolization groups to yield more convincing interpretation of comparisons (12). Their results indicated that preoperative embolization did not alter the surgical outcomes of patients but could lead to a greater chance of improving functional outcomes. However, their study only included WHO grade I intracranial meningiomas. In our study, WHO grades II and III meningiomas account for 17.4% of the total number of cases we investigated whereas other groups reported 10%–15% of all meningiomas (9, 20). More importantly, advanced WHO grades II and III meningiomas are associated with more aggressive behavior (21) which may complicate the surgical operation and produce potential risks. Thus, it is reasonable to include the more aggressive and advanced grade meningiomas in the current study.

Preoperative embolization was carried out in a minority of patients at our institution. With the large total consecutive meningioma surgery cases, we were able to perform a successful 1:1 ratio matching between the embolization and

TABLE 4 | Comparisons of postoperative mRS score between the embolization and nonembolization group.

Last follow-up mRS score	Embolization group (*n* = 66)	Nonembolization group (*n* = 66)	*p*
0 (%)	43 (65.15)	36 (54.55)	0.167
1 (%)	11 (16.67)	9 (13.63)	
2 (%)	6 (9.09)	13 (19.70)	
3 (%)	2 (3.03)	4 (6.06)	
4 (%)	1 (1.52)	3 (4.55)	
5 (%)	1 (1.52)	1 (1.52)	
6 (%)	1 (1.52)	0	
mRS change			
Without mRS decline (%)	56 (84.85)	45 (68.18)	0.04
mRS decline (%)	10 (15.15)	21 (31.82)	

nonembolization groups, which met the matching criteria and minimized the influence of patient- and tumor-related confounds. Specifically, the maximum tumor diameter, which differs significantly between groups in the original unmatched dataset ($p < 0.0001$), reached a statistical intergroup balance after matching ($p = 0.69$). Such bias also exists in other studies (7, 12), which may indicate surgeons' preferences to embolize potential risky meningiomas.

The rationales of preoperative embolization include the reduction of intraoperative blood loss and softening of the tumor mass to ease surgical operation and reduce surgery duration. Intriguingly, we did not find a significant improvement on the surgical outcomes of embolization, including estimated blood loss, surgical time, and volume of blood transfusion. The results are distinct from earlier studies (6, 9) but in line with Przybylowski's findings (12). As discussed above, surgeons prefer embolization in patients with meningiomas that are highly vascularized and large, which may increase the chance to find differences on surgical outcomes. Another important issue is the time interval between endovascular embolization and cranial surgery. The greatest tumor softening may occur 7–9 days after embolization (5). At our institution, meningioma resection surgery is arranged within 24 h after embolization. This schedule takes into consideration tumor ischemia, necrosis (22), and edema which could contribute to elevated intracranial pressure postembolization. Within such short period, tumors may not reach the ideal softening point and thus limits the improvement of surgical outcomes, especially blood loss and surgical time.

Our data showed that preoperative embolization could significantly reduce the rate of surgical complication and the possibilities of mRS decline, which were distinct from others (7, 12). Sensory and motor function deficits were the majority of postsurgical complications and contribute to degrees of daily life disabilities, as shown in **Tables 3** and **4**. However, we did not find statistically significant differences between groups regarding surgical outcomes as discussed above. We speculate several factors may contribute to these findings. To establish a clear surgical view, surgeons may use aggressive surgical maneuvers such as retraction and electrocauterization to deal with complex tumor feeding vasculatures when dissecting vascularity-rich meningiomas. It may increase the difficulty to protect the adjacent critical structures (9) and raise potential risks to damage the proximity eloquent cortex, cranial nerves, and deep feeding vessels, thus contributing to higher postoperative complications. Immune attacks were shown to play a critical role in surgical-induced brain injury (SBI), through inducing cell death and brain edema (23). Recent murine studies revealed the meninges host a rich reservoir of myeloid immune cells (24). The cells may traffic to the brain parenchyma under CNS injury and autoimmune conditions. Preoperative embolization may potentially block the infiltration of immune cells and reduce the surgery-induced immune injuries. The potential roles of meningeal immune cell repertoire in meningioma need to be further investigated in future studies. *Post-hoc* analysis showed that in cases who suffered from postsurgical complications, the estimated blood loss was significantly higher. As the two cases of sphenoid wing meningioma presented in **Figure 1**, the nonembolized one suffered from greater blood loss and postsurgical hemiparesis and long-term limb weakness. These data indicated that preoperative embolization reduces postoperative complications and long-term disability, possibly through improved operative feasibility and safety.

Though the results of the presented study indicate that preoperative embolization could reduce unfavorable outcomes of meningioma patients, requirements in identifying which population would benefit from embolization still exist. In our study, the decision largely depends on the surgeons' personal experiences in consideration with the tumor characteristics obtained from preoperative MRI and/or CTA. To our current knowledge, there are no consensus or guidelines about which patient population are suitable for preoperative embolization. Iacobucci et al. and Raper et al. suggested that it is reasonable to consider extensive devascularization for large meningiomas, tumors located deep in the surgeon's line of sight, tumors in proximity to eloquent cortical areas, and tumors without extensive calcification. Beyond these structural characteristics, functional MRI imaging might provide objective and quantitative assessments of vascularity of certain meningiomas and necessity of preoperative embolization. Adachi et al. utilized normalized cerebral blood flow values (nCBF) and CBF images obtained from dynamic susceptibility contrast perfusion-weighted imaging (DSC-PWI) to predict the necessity of preoperative embolization (25). Mayercik et al. provided a noninvasive approach using arterial spin labeling MRI (ASL-MRI) to identify hypervascular meningiomas (26). We believe these objective functional imaging modalities may provide a more precise risk stratification of meningioma surgery.

We recognized that our study has several limitations to be considered. Though we matched possible confounds, the retrospective nature limits the robustness of the results. The conclusions need to be validated in large multicenter controlled trials. Bias could also arise from the surgeons' individual preferences and surgical skills. The time interval between embolization and resection in our study is much shorter than that was reported in literatures, which may reduce the possibility of understanding the benefits associated with good surgical outcomes. We did not perform subgroup analysis on the relationships between the extent of devascularization and the outcomes of patients. As assessment of the angiographic myocardial blush grade is sometimes subjective, we were unable to carry out advanced neuroimaging modalities such as DSC-PWI and ASL-MRI to predict the necessity of preoperative embolization.

CONCLUSION

The single-center matched cohort retrospective study showed significant lower rates of surgical complications and long-term disabilities of meningioma patients with preoperative embolization. There was no significant difference in estimated

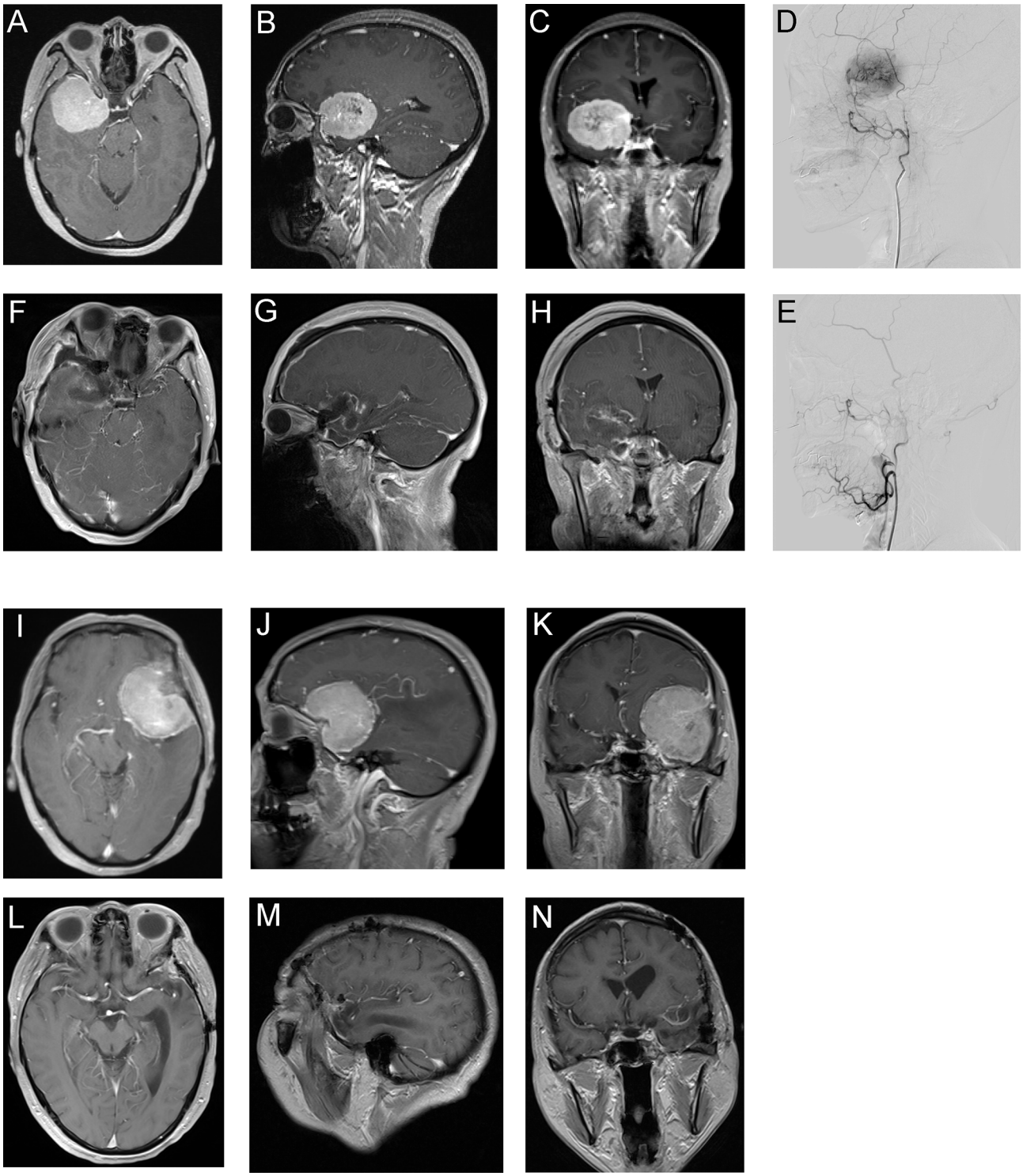

FIGURE 1 | Two representative meningioma cases underwent preoperative embolization **(A–H)** or direct surgery **(I–N)**. Patient 1, 53-year-old woman. **(A–C)** Preoperative Gd-enhanced MRI showed sphenoid wing meningioma. **(D)** Lateral view of pre-embolization angiography showed hypervascular tumor feeding by branches originated from the middle meningeal artery. **(E)** Lateral view of postembolization angiography showed occlusion of the feeding vessel. The estimated blood loss of patient 1 was 500 ml and did not receive blood transfusion. **(F–H)** Postoperative Gd-enhanced MRI of patient 1. Patient 1 discharged routinely without surgical complication and last follow-up showed mRS improved by 1 grade. **(I–K)** Preoperative Gd-enhanced MRI of patient 2, a 55-year-old woman with sphenoid wing meningioma. The estimated blood loss of patient 2 was 1,800 ml and total volume of blood transfusion was 1,680 ml. **(L–N)** Postoperative Gd-enhanced MRI of patient 2. The patient discharged with right-side hemiparesis and last follow-up mRS declined by 2 grades.

blood loss, operation duration, and blood transfusion volume between the embolization and nonembolization groups. Future studies are needed to investigate which subset of meningioma patients would benefit from preoperative embolization by incorporating objective and quantitative imaging approaches.

DATA AVAILABILITY STATEMENT

The original contributions presented in the study are included in the article/**Supplementary Material**. Further inquiries can be directed to the corresponding authors.

ETHICS STATEMENT

The studies involving human participants were reviewed and approved by the ethics committee of the Southwest Hospital Affiliated to Army Medical University (Ethics Approval No. KY2021150). Written informed consent for participation was not required for this study in accordance with the national legislation and the institutional requirements.

AUTHOR CONTRIBUTIONS

FL, XL, YY, and YC designed the experiments. YY, YL, XL, and ZJ collected the data. CZ and HG reviewed the radiological imaging. ZC, RH, and YC evaluated the dataset. YY and CZ performed the cohort matching. YL, YY, and ZJ performed statistical analyses. YY, YL, ZJ, XL, FL, and HF drafted the manuscript. All authors contributed to the article and approved the submitted version.

FUNDING

This work was supported by grant from the National Natural Science Foundation of China (Grant number: 81802509).

SUPPLEMENTARY MATERIAL

The Supplementary Material for this article can be found online at: https://www.frontiersin.org/articles/10.3389/fonc.2022.852327/full#supplementary-material

Supplementary Figure 1 | Jitter plots were shown to visualize the distribution of propensity scores of matched and unmatched cases from embolization and non-embolization group.

Supplementary Figure 2 | eQQ plots were shown to visualize the balance on the covariates before and after cohort matching.

Supplementary Figure 3 | Love plots were shown to visualize the balance via absolute standardized mean difference between groups before and after cohort matching, as distance were estimated using generalized linear model.

REFERENCES

1. Ostrom QT, Cioffi G, Waite K, Kruchko C, Barnholtz-Sloan JS. CBTRUS Statistical Report: Primary Brain and Other Central Nervous System Tumors Diagnosed in the United States in 2014-2018. *Neuro Oncol* (2021) 23:iii1–iii105. doi: 10.1093/neuonc/noab200
2. Manelfe C, Guiraud B, David J, Eymeri JC, Tremoulet M, Espagno J, et al. Embolization by Catheterization of Intracranial Meningiomas. *Rev Neurol (Paris)* (1973) 128:339–51.
3. Dean BL, Flom RA, Wallace RC, Khayata MH, Obuchowski NA, Hodak JA, et al. Efficacy of Endovascular Treatment of Meningiomas: Evaluation With Matched Samples. *AJNR Am J Neuroradiol* (1994) 15:1675–80.
4. Chun JY, Mcdermott MW, Lamborn KR, Wilson CB, Higashida R. And Berger, MS. Delayed Surgical Resection Reduces Intraoperative Blood Loss for Embolized Meningiomas. *Neurosurgery* (2002) 50:1231–1235; discussion 1235-1237. doi: 10.1097/00006123-200206000-00010
5. Kai Y, Hamada J, Morioka M, Yano S, Todaka T, Ushio Y. Appropriate Interval Between Embolization and Surgery in Patients With Meningioma. *AJNR Am J Neuroradiol* (2002) 23:139–42.
6. Fang QR, He XY, Li XF, Zhang X, Chen M, Li H, et al. Comparative Efficacy of Glubran and Polyvinyl-Alcohol Particles in the Embolization of Meningiomas. *Int J Neurosci* (2016) 126:1112–9. doi: 10.3109/00207454.2015.1134525
7. Raper DM, Starke RM, Henderson FJr., Ding D, Simon S, Evans AJ, et al. Preoperative Embolization of Intracranial Meningiomas: Efficacy, Technical Considerations, and Complications. *AJNR Am J Neuroradiol* (2014) 35:1798–804. doi: 10.3174/ajnr.A3919
8. Ishihara H, Ishihara S, Niimi J, Neki H, Kakehi Y, Uemiya N, et al. The Safety and Efficacy of Preoperative Embolization of Meningioma With N-Butyl Cyanoacrylate. *Interv Neuroradiol* (2015) 21:624–30. doi: 10.1177/1591019915590537
9. Iacobucci M, Danieli L, Visconti E, Maresca M, Anile C, Colosimo C, et al. Preoperative Embolization of Meningiomas With Polyvinyl Alcohol Particles: The Benefits are Not Outweighed by Risks. *Diagn Interv Imaging* (2017) 98:307–14. doi: 10.1016/j.diii.2016.08.006
10. Jumah F, Aburmilah A, Raju B, Jaber S, Adeeb N, Narayan V, et al. Does Preoperative Embolization Improve Outcomes of Meningioma Resection? A Systematic Review and Meta-Analysis. *Neurosurg Rev* (2021) 44:3151–63. doi: 10.1007/s10143-021-01519-z
11. Chen L, Li DH, Lu YH, Hao B, Cao YQ. Preoperative Embolization Versus Direct Surgery of Meningiomas: A Meta-Analysis. *World Neurosurg* (2019) 128:62–8. doi: 10.1016/j.wneu.2019.02.223
12. Przybylowski CJ, Zhao X, Baranoski JF, Borba Moreira L, Gandhi S, Chapple KM, et al. Preoperative Embolization Versus No Embolization for WHO Grade I Intracranial Meningioma: A Retrospective Matched Cohort Study. *J Neurosurg* (2020) 134:693–700. doi: 10.3171/2020.1.JNS19788
13. Ho D, Imai K, King G, Stuart EA. MatchIt: Nonparametric Preprocessing for Parametric Causal Inference. *J Stat Softw* (2011) 42:28. doi: 10.18637/jss.v042.i08
14. Shah AH, Patel N, Raper DM, Bregy A, Ashour R, Elhammady MS, et al. The Role of Preoperative Embolization for Intracranial Meningiomas. *J Neurosurg* (2013) 119:364–72. doi: 10.3171/2013.3.JNS121328
15. Singla A, Deshaies EM, Melnyk V, Toshkezi G, Swarnkar A, Choi H, et al. Controversies in the Role of Preoperative Embolization in Meningioma Management. *Neurosurg Focus* (2013) 35:E17. doi: 10.3171/2013.9.FOCUS13351
16. Wirsching HG, Richter JK, Sahm F, Morel C, Krayenbuehl N, Rushing EJ, et al. Post-Operative Cardiovascular Complications and Time to Recurrence in Meningioma Patients Treated With Versus Without Pre-Operative Embolization: A Retrospective Cohort Study of 741 Patients. *J Neurooncol* (2018) 140:659–67. doi: 10.1007/s11060-018-2996-0
17. Champagne PO, Lemoine E, Bojanowski MW. Surgical Management of Giant Sphenoid Wing Meningiomas Encasing Major Cerebral Arteries. *Neurosurg Focus* (2018) 44:E12. doi: 10.3171/2018.1.FOCUS17718
18. Ilyas A, Przybylowski C, Chen CJ, Ding D, Foreman PM, Buell TJ, et al. Preoperative Embolization of Skull Base Meningiomas: A Systematic Review. *J Clin Neurosci* (2019) 59:259–64. doi: 10.1016/j.jocn.2018.06.022

19. Meling TR, Da Broi M, Scheie D, Helseth E. Meningiomas: Skull Base Versus Non-Skull Base. *Neurosurg Rev* (2019) 42:163–73. doi: 10.1007/s10143-018-0976-7
20. Shah A, Choudhri O, Jung H, Li G. Preoperative Endovascular Embolization of Meningiomas: Update on Therapeutic Options. *Neurosurg Focus* (2015) 38: E7. doi: 10.3171/2014.12.FOCUS14728
21. Perry A, Louis D, Budka H, von Deimling A, Sahm F, Rushing E, et al. Meningioma. In: D Louis, O Hiroko, O Wiestler, W Cavenee, editors. *WHO Classification of Tumours of the Central Nervous System*, *4th*. Lyon: IARC (2016). p. 232–45.
22. Nania A, Granata F, Vinci S, Pitrone A, Barresi V, Morabito R, et al. Necrosis Score, Surgical Time, and Transfused Blood Volume in Patients Treated With Preoperative Embolization of Intracranial Meningiomas. Analysis of a Single-Centre Experience and a Review of Literature. *Clin Neuroradiol* (2014) 24:29–36. doi: 10.1007/s00062-013-0215-0
23. Travis ZD, Sherchan P, Hayes WK, Zhang JH. Surgically-Induced Brain Injury: Where Are We Now? *Chin Neurosurg J* (2019) 5:29. doi: 10.1186/s41016-019-0181-8
24. Cugurra A, Mamuladze T, Rustenhoven J, Dykstra T, Beroshvili G, Greenberg ZJ, et al. Skull and Vertebral Bone Marrow are Myeloid Cell Reservoirs for the Meninges and CNS Parenchyma. *Science* (2021) 373:eabf7844. doi: 10.1126/science.abf7844
25. Adachi K, Murayama K, Hayakawa M, Hasegawa M, Muto J, Nishiyama Y, et al. Objective and Quantitative Evaluation of Angiographic Vascularity in Meningioma: Parameters of Dynamic Susceptibility Contrast-Perfusion-Weighted Imaging as Clinical Indicators of Preoperative Embolization. *Neurosurg Rev* (2021) 44:2629–38. doi: 10.1007/s10143-020-01431-y
26. Mayercik V, Ma M, Holdsworth S, Heit J, Iv M. Arterial Spin-Labeling MRI Identifies Hypervascular Meningiomas. *AJR Am J Roentgenol* (2019) 213:1124–8. doi: 10.2214/AJR.18.21026

Conflict of Interest: The authors declare that the research was conducted in the absence of any commercial or financial relationships that could be construed as a potential conflict of interest.

Publisher's Note: All claims expressed in this article are solely those of the authors and do not necessarily represent those of their affiliated organizations, or those of the publisher, the editors and the reviewers. Any product that may be evaluated in this article, or claim that may be made by its manufacturer, is not guaranteed or endorsed by the publisher.

Copyright © 2022 Yin, Li, Jiang, Zhang, Ge, Chen, Hu, Chen, Li, Li and Feng. This is an open-access article distributed under the terms of the Creative Commons Attribution License (CC BY). The use, distribution or reproduction in other forums is permitted, provided the original author(s) and the copyright owner(s) are credited and that the original publication in this journal is cited, in accordance with accepted academic practice. No use, distribution or reproduction is permitted which does not comply with these terms.

frontiers in Oncology

REVIEW
published: 23 March 2022
doi: 10.3389/fonc.2022.851758

Identification and Management of Aggressive Meningiomas

Bhuvic Patel[1], *Rupen Desai*[1], *Sangami Pugazenthi*[1], *Omar H. Butt*[2,3], *Jiayi Huang*[3,4] *and Albert H. Kim*[1,3*]

[1] Department of Neurological Surgery, Washington University School of Medicine, St. Louis, MO, United States, [2] Department of Medicine, Division of Medical Oncology, Washington University School of Medicine, St. Louis, MO, United States, [3] The Brain Tumor Center, Siteman Cancer Center, Washington University School of Medicine, St. Louis, MO, United States, [4] Department of Radiation Oncology, Washington University School of Medicine, St. Louis, MO, United States

Meningiomas are common primary central nervous system tumors derived from the meninges, with management most frequently entailing serial monitoring or a combination of surgery and/or radiation therapy. Although often considered benign lesions, meningiomas can not only be surgically inaccessible but also exhibit aggressive growth and recurrence. In such cases, adjuvant radiation and systemic therapy may be required for tumor control. In this review, we briefly describe the current WHO grading scale for meningioma and provide demonstrative cases of treatment-resistant meningiomas. We also summarize frequently observed molecular abnormalities and their correlation with intracranial location and recurrence rate. We then describe how genetic and epigenetic features might supplement or even replace histopathologic features for improved identification of aggressive lesions. Finally, we describe the role of surgery, radiotherapy, and ongoing systemic therapy as well as precision medicine clinical trials for the treatment of recurrent meningioma.

Keywords: meningioma, CNS tumors, chemotherapy, radiation therapy, immunotherapy, skull base surgery

OPEN ACCESS

Edited by:
Hailiang Tang,
Fudan University, China

Reviewed by:
Teresa Somma,
Federico II University Hospital, Italy
Vincenzo Di Nunno,
AUSL Bologna, Italy

***Correspondence:**
Albert H. Kim
alberthkim@wustl.edu

Specialty section:
This article was submitted to Neuro-Oncology and Neurosurgical Oncology, a section of the journal Frontiers in Oncology

Received: *10 January 2022*
Accepted: *23 February 2022*
Published: *23 March 2022*

Citation:
Patel B, Desai R, Pugazenthi S, Butt OH, Huang J and Kim AH (2022) Identification and Management of Aggressive Meningiomas. Front. Oncol. 12:851758. doi: 10.3389/fonc.2022.851758

INTRODUCTION

Meningiomas are the most common primary central nervous system (CNS) tumor, constituting more than 35% of adult brain tumors (1). At present, these tumors are classified by the World Health Organization (WHO) into three grades: WHO grade 1 (benign, representing the majority of all meningiomas), WHO grade 2 (atypical), and WHO grade 3 (malignant) (2). Although lower grade tumors are considered benign, these lesions can clinically behave aggressively. In a subset of individuals, low WHO grade meningiomas will recur despite multimodal management including surgical resection, radiation therapy, and systemic therapy (3). Studies with long follow-up have demonstrated recurrence rates as high as 47% after 25 years, but the role of WHO grade in recurrence is unclear, making it challenging to select patients who would benefit from adjuvant therapies (4). Indeed, emerging data suggest that many factors not previously included in the WHO grading schema can alter the prognosis of even benign WHO grade 1 lesions (5–10). As we will discuss, the recently released WHO 2021 classification marks a pivotal alteration in meningioma grading by incorporating for the first time key genomic alterations into the grading scheme (2, 11).

In this review, we highlight the incongruence between histologic grading and the clinical course of meningiomas, particularly aggressively behaving lesions. First, we describe illustrative case examples of

meningiomas with different presenting WHO grade but uniformly aggressive clinical course. We then summarize more recently discovered histopathological and genomic features that may better predict meningioma aggressiveness. Finally, we describe the current surgical, radiotherapy, and targeted drug options available for treatment of aggressive, recurrent meningioma.

CASE EXAMPLES

While most meningiomas exhibit a benign clinical course and favorable response to treatment with surgery or radiotherapy, challenging cases are not uncommon. Few evidence-based treatment algorithms have been developed to address treatment-resistant meningiomas, in part due to the paucity of alternatives to the traditional treatments of surgical resection and radiotherapy (12). In this section we describe the clinical course and treatments used to treat three meningiomas that exemplify challenging lesions recalcitrant to treatment and that deviate from their expected clinical course based on the 2016 WHO classification scheme.

WHO Grade 1 to WHO Grade 2

A 40-year-old woman presented with blurry vision in her left eye and was discovered to have a left frontal mass centered above the sphenoid wing that underwent Simpson Grade II resection and was diagnosed as a WHO grade 1 meningioma with low Ki-67 index and no brain invasion. Within a year, the patient's meningioma recurred, with growth demonstrated on magnetic resonance imaging (MRI). During her second surgical resection, involved bone of the skull base near the orbital apex and roof was removed (Simpson Grade I). Despite the aggressive course, histopathological analysis once again demonstrated WHO grade 1 meningioma, with invasion of bone, and the patient underwent adjuvant fractionated radiotherapy to the resection bed.

The patient remained symptom-free for 14 years before experiencing worsening visual acuity, double vision with transient left eye deviation, and pain in her left orbit. MRI demonstrated a 2.5 cm diameter recurrence of her tumor, invading the left orbital apex and encasing the optic nerve. She experienced little improvement with a two-week course of prednisone and her symptoms progressed to left eye visual loss and proptosis over the course of a month before she underwent Gamma Knife stereotactic radiosurgery (SRS) as salvage therapy (15 Gy to the 50% isodose line).

The tumor initially decreased in size on serial MRI, but two years later the patient presented with epistaxis and sinonasal congestion, with tumor invasion of the sphenoid sinus, pterygopalatine fossa, and masticator space. She underwent tumor embolization followed by subtotal resection *via* expanded endoscopic endonasal approach, with histopathological analysis now consistent with WHO grade 2 meningioma with rhabdoid features and *NF2* mutation (genomic sequencing was not available at the time of prior resections). Within 3 months post-operatively, the size of the residual tumor increased, and by 6 months post-operatively the tumor filled the orbit and had increased from 1.8 cm to 4.5 cm in maximal diameter. Despite radical resection including a frontotemporal craniotomy, orbital exenteration and radial forearm free flap, the patient had multifocal tumor recurrence and over the course of 6 months underwent SRS twice and additional surgery for debulking and symptom relief. She was initiated on octreotide, pembrolizumab, and everolimus but was unable to tolerate the treatments due to skin rashes, thrush, and constipation. Ultimately, the patient elected to proceed with hospice care for her treatment-refractory meningioma and passed away soon thereafter.

WHO Grade 2

A 54-year-old man presented with deteriorating right eye vision over the course of several years and trigeminal nerve distribution pain, and was found to have a large cavernous sinus, middle fossa, and infratemporal fossa mass. The patient underwent tumor embolization followed by craniotomy and subtotal resection, with a pathological diagnosis of WHO grade 2 meningioma with bony invasion, low MIB-1 index, no intratumoral necrosis, and no brain invasion. The residual tumor encasing the carotid artery was treated with fractionated radiotherapy (54 Gy in 30 fractions).

The patient was lost to follow up but presented 4 years later with progressive right-sided hearing loss, and his tumor was found to have invaded the right external auditory canal, middle cranial fossa, cavernous sinus, sphenoid sinus, and sella. The patient underwent a craniotomy for tumor resection with mastoidectomy and temporal bone resection, with residual tumor encasing the petrous carotid artery deemed too high-risk to resect. One year later, the residual tumor was found to have grown to involve the sphenoid sinus and left medial orbital wall. He underwent embolization and tumor debulking *via* a combined endonasal and transfacial approach. Eight months later, the patient presented with persistent epistaxis requiring embolization and was found to have extensive recurrence of his tumor for which he underwent endoscopic endonasal debulking once again. The pathological diagnosis after all his resections remained WHO grade 2 meningioma, with sequencing after his second surgery revealing only a *NF2* mutation.

During subsequent observation, the patient developed right eye blindness and left eye decline in visual acuity. He was deemed not to be a candidate for surgical or radiation therapies and therefore received therapy with compassionate use temsirolimus. Unfortunately, the tumor did not respond, and the patient developed side effects of severe hyperglycemia and eczematous dermatitis. Two years after his last surgery, the patient developed significant sinonasal disease and difficulty eating. A gastrostomy tube was placed for feeding and the patient underwent palliative debulking of tumor in his sinonasal cavity before transitioning to hospice care and expiring 3 months later.

WHO Grade 2 to WHO Grade 3

A 49-year-old female was diagnosed with a left spheno-orbital meningioma after presenting with left eye proptosis and underwent tumor embolization followed by craniotomy with gross total resection (Simpson Grade I) and adjuvant fractionated radiotherapy with a dose of 54 Gy. Her

histopathological diagnosis at that time was WHO grade 2 meningioma with increased mitotic activity of 8 mitoses per 10 high powered fields and bony invasion. After 10 years of follow-up with serial MRI, she was found to have a thin area of recurrent tumor, which was treated with SRS (20 Gy to the 50% isodose line).

Three years later, the patient's tumor was found to have slightly increased in size on annual MRI scan. This was initially managed with continued close serial observation, but one year later the patient presented with proptosis, inferior displacement of the left globe and diminished left eyelid function with increase in tumor size. Subtotal surgical resection was performed, and histopathological diagnosis remained WHO grade 2 meningioma, this time with Ki-67 index of 24.8%, and *SMO* mutation detected on genomic sequencing. Her tumor increased in size two years later, and she was initiated on octreotide and everolimus. She tolerated octreotide well but developed mucositis, elevated liver enzymes, anemia, and hyperlipidemia necessitating decreased dosing of everolimus.

This therapy was continued for 2 years, until serial MRI showed tumor progression and the patient's left eye visual acuity began to decline. She was enrolled in an institutional clinical trial of proton beam therapy [20 Gy relative biological equivalents (GyRBE) in 5 fractions], neoadjuvant avelumab (6 doses), and surgical resection, including complete orbital exenteration, near total tumor resection, and left thigh free flap for skull base reconstruction. Histopathological examination of the tissue was now consistent with WHO grade 3 meningioma with foci of rhabdoid and papillary arrangements, necrosis, brain invasion, and 23 mitoses per high powered field. The patient has been followed with serial MRI showing stable residual disease one year postoperatively.

HISTOPATHOLOGY & GENETICS

Although most meningiomas are easily diagnosed with computed tomography or magnetic resonance imaging, histopathological analysis of tumor tissue remains the cornerstone of tumor subtyping and grading. In recognition of the value of molecular features in brain tumor subtyping, the 2016 World Health Organization Classification of Tumors of the Central Nervous System for the first time integrated molecular parameters in addition to histological features for classification of many CNS tumors (13). Unfortunately, no molecular features were included for an integrated diagnosis of meningiomas, and, aside from including brain invasion as a histological criterion for WHO grade 2 meningiomas, no changes were made to meningioma grading (13). However, certain histopathological features, such as necrosis, have been found to predict more aggressive treatment-resistant behavior, and there is a growing body of evidence that specific molecular features may more clearly delineate meningioma subtypes that better correlate with clinical course (5–7, 14–16). The 2021 World Health Organization Classification of Tumors of the Central Nervous System integrated these newer data in its recent revision of meningioma taxonomy, with the addition of molecular markers denoting a higher grade even in the absence of traditional anaplastic features on histology (2, 11).

Histopathology

The first internationally agreed upon subtypes of meningioma were characterized by Bailey and Cushing based on histopathological features (17). Histopathological analysis continues to be the basis for characterization of meningiomas, with the current WHO grading system still retaining 15 meningioma subtypes. While previous WHO revisions further subclassified 9 subtypes as WHO grade 1, 3 as WHO grade 2, and 3 as WHO grade 3, tumor grade is no longer coupled to subtype in the 2021 revision (2, 11).

Each update to the WHO classification has resulted in dramatic shifts in the proportion of meningiomas of each grade and have improved upon the correlation between WHO grade and clinical course. For example, the 2000 and 2007 updates to the WHO classification resulted in the number of meningiomas graded as WHO grade 2 increasing from 5% to 20% (18). With the addition of brain invasion as a criterion for WHO grade 2 meningiomas in the 2016 update, this proportion is approximately 35%, and has increased further with the WHO 2021 classification upgrading chordoid and clear cell meningioma from grade 1 to grade 2 (1, 2).

More recent studies focusing on WHO grade 2 meningiomas have uncovered histopathological features that identify a more aggressive clinical subtype within this group of tumors, further complicating treatment decision making for patients diagnosed with grade 2 tumors. In 2014, Sun et al. reported that tumor necrosis predicted radiation resistance in WHO grade 2 meningiomas that were sub-totally resected (15). Additionally, the co-occurrence of brain invasion and high mitotic index and the co-occurrence of brain invasion and necrosis have both been reported to increase the risk of radiotherapy resistance and recurrence in WHO grade 2 meningiomas (16, 19). Ultimately, despite these improvements in correlating histopathological features with clinical outcomes, such features remain subject to high interobserver and sampling bias, increasing the need for more reliable molecular markers that predict tumor behavior and therapy resistance.

Genomic Analysis

The meningioma genomic landscape has been an area of significant investigation as early as 1994 when Ruttledge et al. first highlighted the prevalence of mutations in the *NF2* gene, located on chromosome 22q (20). At the time, it was well known that loss of heterozygosity (LOH) on chromosome 22 was present in up to 80% of meningiomas. Sequencing of the *NF2* tumor suppressor gene in tumors with chromosome 22 LOH revealed that a significant number of tumors harbor inactivating mutations of *NF2* (20). Mutations in *NF2* in the absence of chromosome 22 LOH are rarely observed in meningiomas, corroborating the two-hit hypothesis for the function of the *NF2* gene as a tumor suppressor in spontaneous meningiomas.

Notably, higher grade tumors more often harbor *NF2* mutations in addition to large-scale chromosomal

abnormalities and overall higher mutational burden (14, 21, 22). Further investigation of *NF2* mutations in meningiomas has also revealed that these mutations are generally associated with convexity meningiomas rather than meningiomas of the anterior skull base (**Figure 1**) (14, 23). Merlin, the protein encoded by *NF2*, is as an intracellular scaffolding protein that indirectly links F-actin, transmembrane receptors and intracellular effectors. It has been shown to function as a tumor suppressor by inhibiting cell growth through contact inhibition and resultant activation of the Rac1 pathway in the setting of high cell density. Loss of merlin function therefore results in loss of contact inhibition of growth. *NF2* mutation also results in activation of the Hippo, Notch, phosphoinositide 3-kinase (PI3K)/AKT, mammalian target of rapamycin (mTOR), and Ras/mitogen-activated protein kinase (MAPK) pathways with resultant increase in cell proliferation (25–29). As described later, these insights into the molecular biology of meningiomas have identified targets for pharmacological agents such as tyrosine kinase inhibitors that subsequently also decrease activation of the PI3K, mTOR, and ERK pathways.

Given that 40% of meningiomas do not have mutations in *NF2*, more recent investigation has focused on identifying other drivers of meningioma tumorigenesis using next-generation sequencing techniques that facilitate genome-wide sequencing in large cohorts of patients. In 2013, two seminal studies evaluating key genetic characteristics of meningioma were published (14, 30). Clark et al. identified mutations in *TRAF7* (*tumor necrosis factor [TNF] receptor–associated factor 7*), *KLF4* (*Kruppel-like factor 4*), *AKT1* (*v-akt murine thymoma viral oncogene homolog 1*), and *SMO* (*smoothened*) after sequencing a cohort of 300 WHO grade 1 and 2 meningiomas (14). Interestingly, these additional mutations identified three non-overlapping groups of tumors with distinct locations: those with chromosome 22 LOH and *NF2* mutations occurring along the convexities and posterior skull base, those with mutations in *SMO* occurring in the midline anterior skull base, and those with mutations in *TRAF7*, *AKT1*, and/or *KLF4* occurring in the sphenoid wing and floor of the middle fossa (**Figure 1**) (14). Identification of these non-*NF2* driver mutations revealed that the meningioma genomic landscape was more diverse than previously assumed, leading to the identification of additional meningioma driver mutations including *POLR2A*, *SMARCB1 germline variants (including SMARCE1)*, *AKT3*, *PIK3CA*, *PIK3R1*, *PRKAR1A*, *SUFU*, and *BAP1* (21, 24, 30–33). At the same time, Brastianos et al. performed genomic sequencing of 17 meningiomas with further targeted sequencing on an additional 48 meningiomas, finding WHO grade 1 meningiomas have significantly lower rates of genomic disruptions than either systemic tumors or WHO grade 2 or 3 meningiomas (30). In the discovery set, some Grade 1 meningiomas were found to have copy number loss on chromosomes 1p, 7p, 14p, and 19 with copy

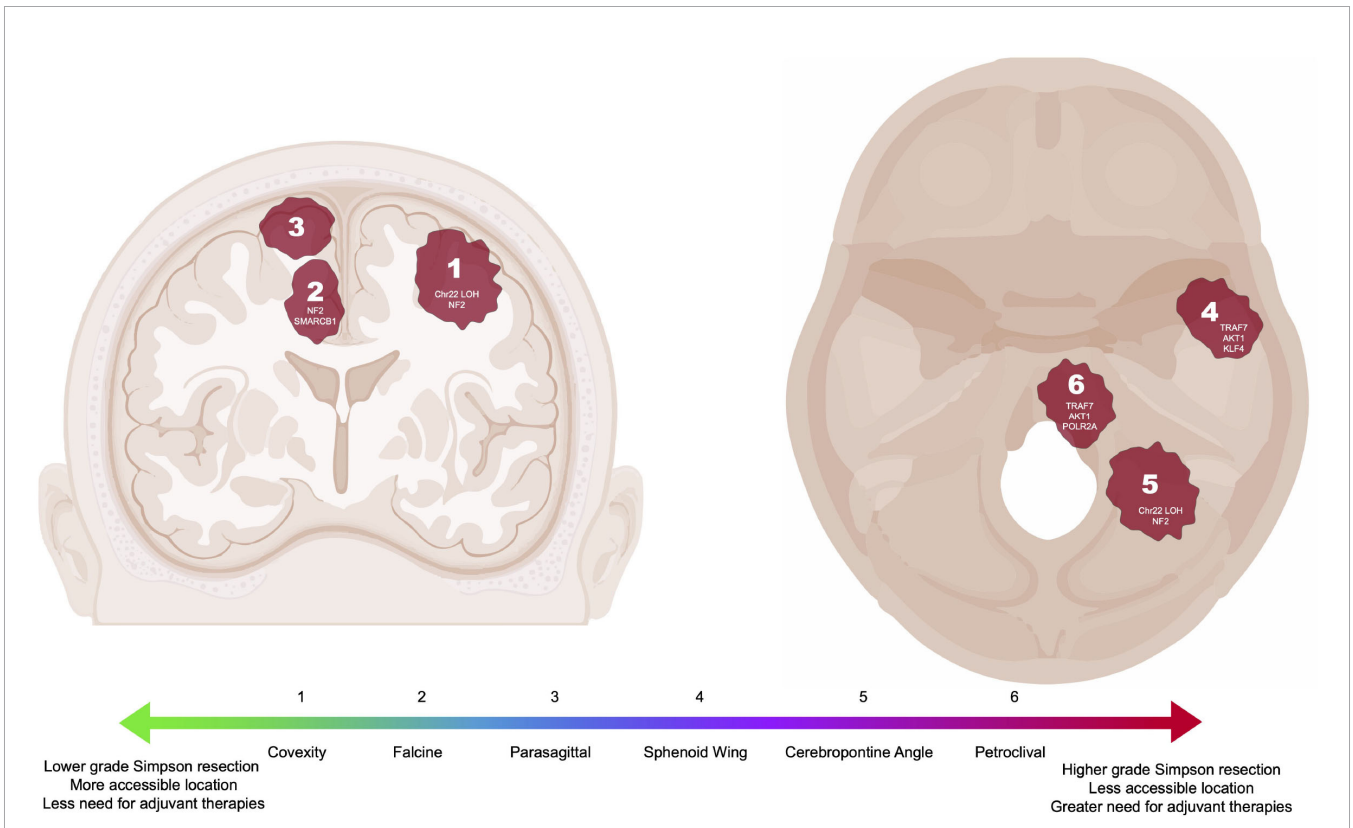

FIGURE 1 | Common intracranial locations of meningiomas highlighted in this review with associated DNA driver mutations or chromosomal loss (6, 14, 23, 24). Locations correlated to a generalized scale ranging from less (green) to more (red) complicated to resect and manage. Meningioma locations not pictured include clinoid, foramen magnum, cavernous sinus, suprasellar, and tentorial.

number gains on chromosomes 5 and 10, while higher grade tumors were associated with copy number loss of chromosomes 10q and 14q. Targeted gene analysis identified non-synonymous mutations in *NF2* (the most common alteration), *KDM5C, SMO, AKT1, RGPD3*, and *CD300C*. The specific *SMO* mutations were previously known oncogenic mutations in basal cell carcinoma and desmoplastic medulloblastoma and were only found in meningiomas without *NF2* alterations. Similarly, the *AKT1* mutations were oncogenic mutations previously described in breast, colorectal, and lung cancer and were mutually exclusive with *NF2* or *SMO* mutations in meningioma. In validation cohorts, the *AKT1* and *SMO* mutations were observed in skull base and higher grade meningiomas. Together, the findings from Clark et al. and Brastianos et al. laid the foundation for the inclusion of genomic alterations in the 2021 WHO classification.

The genomic landscape specifically of WHO grade 3 meningiomas has historically been less well characterized. To address this question, Bi et al. analyzed 134 high-grade meningiomas. In their cohort of high grade meningiomas, most tumors were characterized by *NF2* mutations, with very few tumors having mutations in *TRAF7, KLF4*, *AKT1* and *SMO*, suggesting that high grade meningiomas have few targetable genetic mutations. Associations were also reported between *AKTI/PIK3CA* mutations and meningothelial subtype, *NF2* mutations and fibroblastic subtype, and *TRAF7/KLF4* mutations and secretory subtype. Bi et al. also found that high grade lesions were characterized by increased copy number alterations, and, interestingly, low grade lesions that progressed to high grade meningiomas exhibited patterns of genomic disruption similar to high grade meningiomas and have been associated with activating *TERT* promoter mutations (21, 34). Presence of a *TERT* promoter mutation is further associated with progression and poor survival (35, 36). This observation combined with other groups demonstrating a strong association between homozygous deletion of *CDKN2A/B* or *BAP1* mutations and aggressive clinical outcome led to a significant revision in the 2021 WHO criteria (2, 37–39).

While the 2021 classification recommends considering sequencing, it is not required for diagnosis (2). Nonetheless, the current criteria now integrates driver mutations such as *NF2*, *AKT1*, *SMO*, and *PIK3CA* for conventional, *TRAF7* and *KLF4* for secretory, *SMARCE1* for clear cell, and *BAP1* for rhabdoid subtypes (2, 11). Furthermore, a meningioma harboring either a *TERT* promotor mutation or homozygous deletion of *CDKN2A/B* is classified as a grade 3 anaplastic tumor, regardless of histologic grade (11).

Expression Profile and Epigenomic Analysis

Given that WHO grade and DNA mutations do not optimally predict the clinical behavior of meningiomas, recent studies have used several molecular analysis techniques to create classification schemes more aligned with meningioma clinical course (**Table 1**). Many groups have hypothesized that chromatin structure and gene expression profiles, governed largely by DNA methylation, might be more useful in this regard (40–42). For example, the loss of H3K27 trimethyl (H3K27me3) identified by immunohistochemistry has been corroborated as a marker of poor survival and shorter time to recurrence, specifically in Grade 2 meningioma (43, 44).

In 2017 Sahm et al. performed genome-wide methylation analysis of 497 meningiomas across all WHO grades and 309 extra-axial tumors that mimic meningiomas histologically (5). Unsupervised clustering not only segregated meningiomas from the other tumors but also identified six clinically relevant methylation classes of meningiomas. Three classes clustered together and were defined as methylation class benign 1 to 3 (MC ben-1 to MC ben-3) based on having a more benign clinical course. Two classes, defined as methylation class intermediate A and B (MC int-A and MC int-B) had an intermediate progression-free survival, and the final class, methylation class malignant (MC mal), had a markedly poor progression-free survival. Notably, while WHO grade 1 meningiomas were enriched in the benign methylation classes and WHO grade 3 meningiomas in the malignant methylation class, WHO grade 2 lesions, which often have a heterogenous clinical course, were scattered across all but one of the methylation classes. Furthermore, *NF2* mutations were found in at least 30% of all methylation classes except for MC ben-2. Consistent with findings from genomic sequencing studies, non-*NF2* and *NF2*

TABLE 1 | A comparative representation of studies describing molecular reclassification of meningiomas.

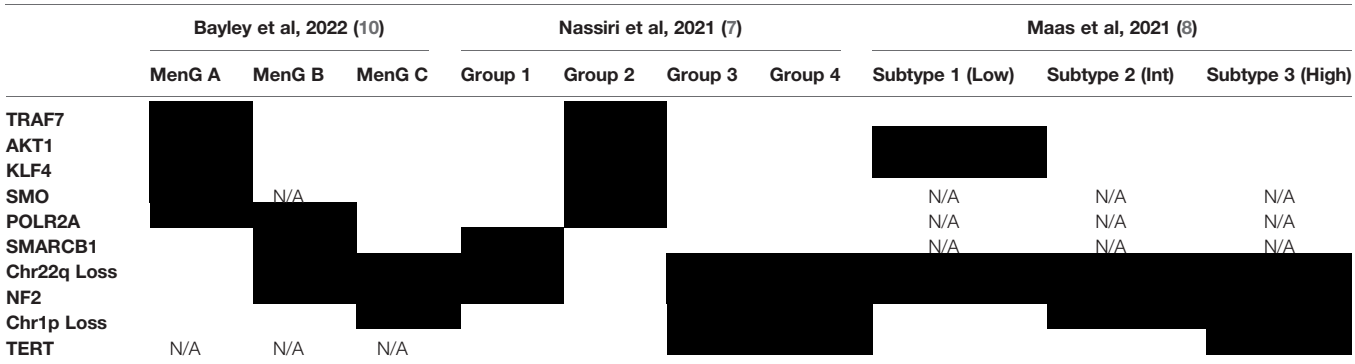

Within each classification scheme, meningioma subgroups are ordered from left to right based on increasingly worse progression free survival. Genetic mutations and chromosomal losses were compared across each subgroup with black shading indicating predominant mutation/loss in that group, empty cell indicating that the mutation/loss was tested for but was not present or significantly less predominant in that group, and N/A indicating that the mutation/loss was not tested for or not reported in that study.

mutations occurred almost mutually exclusively, with non-*NF2* mutations being enriched in MC ben-2, while *NF2* mutations were rare in this group (5). Taken together, these findings suggest that methylation classes are superior to WHO grade for predicting clinical behavior, especially in the case of WHO grade 2 tumors, and that although *NF2* mutational status may not be an entirely specific predictor for clinical behavior, non-*NF2* driver mutations may be useful in identifying meningiomas with a more benign clinical course.

In 2019 Patel et al. reported their classification scheme based on combined bulk RNA sequencing and whole exome sequencing analysis of 160 meningiomas (6). They too reported 3 molecular subgroups, named type A, B, and C that predicted recurrence more reliably than the WHO grading schema. Interestingly, they found that more than half of the tumors in their most aggressive subgroup (type C) were predicted to be benign by WHO grading criteria. Like prior studies, the least aggressive tumors (type A) were found to have no notable copy number alterations while the most aggressive tumors (type C) were found to have the greatest rates of chromosome 22q and 1p losses. Importantly, gene set enrichment analysis of type B and type C tumors revealed loss of PRC2 complex function in type B and loss of DREAM complex function in type C tumors, insights which might guide targeted treatment strategies in the future (6).

More recently, Nassiri et al. performed an integrative analysis of 121 meningiomas with methylation array, bulk RNA sequencing, and whole exome sequencing analysis to develop an integrated classification system to better predict outcome than the WHO grading system (7). They identified 4 molecular subgroups of meningioma, MG1-4, and designated each subgroup based on pathway analysis of enriched genes: immunogenic (MG1), benign *NF2* wild-type (MG2), hypermetabolic (MG3), and proliferative (MG4). Interestingly, mapping drugs to target-enriched genes identified possible drug candidates for specific meningioma subtypes. For example, the histone deacetylase inhibitor vorinostat, which mapped to the MG4 subtype, was found to specifically decrease the viability of the MG4 meningioma cell line *in vitro* and decrease the size of MG4 xenografts *in vivo*, highlighting the value of molecular analysis of meningiomas both in classification and in development of novel therapies (7).

Maas et al. and Bayley et al. have similarly created meningioma classification systems that integrate a combination of methylation array data, copy number alterations, DNA mutations, and histopathological findings to better stratify patients (**Table 2**) (8, 10). Importantly, Maas et al. demonstrated that copy number alteration data can readily be inferred from methylation arrays, thus streamlining the molecular diagnostic workup of meningiomas, although they also provide alternative assays (targeted gene analysis or FISH) for stratification depending on resource availability (8). Bayley et al. combined DNA methylation, RNA-seq, and cytogenic profiling on WHO grade 1 and 2 meningiomas yielding three subgroups of meningiomas, two malignant and one benign. Notably chromosome 1p loss was strongly correlated with malignant tumors (10). These integrated models yielded a greater accuracy for prognosis compared to RNA-sequencing and cytogenic profiling or DNA methylation alone.

Meanwhile, Driver at al. incorporated 15 targeted, high-risk molecular alterations (13 chromosomal alterations and loss of *CDKN2A/B*) with histologic (presence of frequent mitoses) and clinical (extent of resection, tumor volume, and recurrence status) factors to stratify meningioma. This classification system highlights the importance of incorporating *CDKN2A* mutations, with their classification system resulting in reclassification of 32% of tumors into either a higher or lower risk integrated grade compared to their WHO grade (9). Taken together, these recent studies suggest that a combination of molecular and histopathological properties need to be considered for accurate stratification of meningiomas. Indeed,

TABLE 2 | Comparison of contemporary aggressive meningioma prognostication.

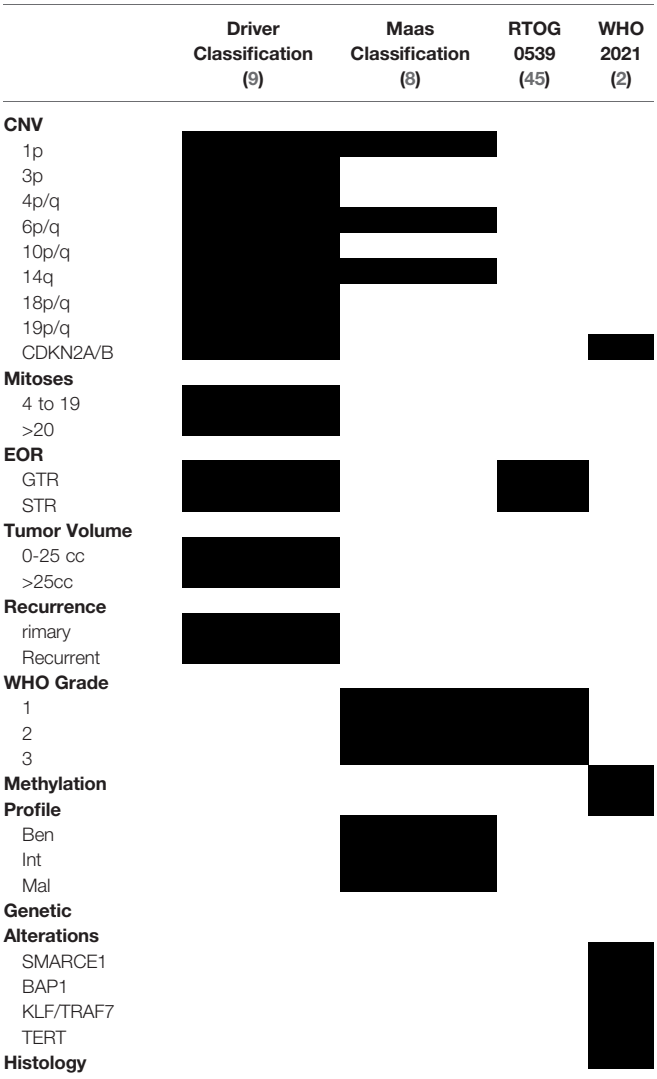

Key factors of four contemporary meningioma grading schemata, including genetic and epigenetic alterations, histologic characteristics, and clinical characteristics, are compared. Within each classification scheme, black shading indicates use of the factor in the prognostication score.

use of machine learning techniques may allow for inclusion of even more information, such as MRI characteristics of tumors, into intergrated grading schema that more accurately stratify meningiomas (46).

CLINICAL MANAGEMENT

Active meningioma management includes surgical resection, radiation therapy, and pharmacological options (47, 48). Observation is another option, generally reserved for small, asymptomatic, or incidental lesions and for patients that are deemed poor candidates for other therapeutic options (49). These patients are typically monitored with serial MRI scans. Tumor growth or symptom progression can indicate that observation has failed, and additional treatment may be necessary. In a retrospective study of 244 patients, Oya et al. demonstrated tumor diameter at diagnosis greater than 25 mm, MRI T2 signal hyperintensity, absence of calcification, and edema predicted tumor growth (50). Additional retrospective studies validated these findings and demonstrated tumors > 40 mm at diagnosis and with initial volumetric growth rates of 20% per year are highly likely to progress (51–53). Presence of focal or diffuse calcification is perhaps one of the strongest preoperative radiographic predictors that a meningioma is unlikely to recur, demonstrating 0% recurrence rate in one retrospective study of 101 patients, compared to nearly 21% recurrence rates in meningiomas without calcification observed (54). While many patients with meningioma under observation are asymptomatic, temporarily mitigating mild symptoms is possible with low-dose steroids to alleviate edema and antiepileptic medications for patients that present with seizure.

Surgery

With symptomatic lesions, tumor progression, or mitigating factors such as patient preference, an active management strategy is often required. For patients without significant medical comorbidities, surgical resection is considered first-line treatment and can often be curative. Selecting a surgical approach is a nuanced decision based on the specific meningioma location that must balance surgical risk with a need to achieve complete resection as described by the Simpson Grading Scale, defined by removal of the tumor with tumor-infiltrated dura, bone, and venous sinuses (47, 55, 56). Fundamentals of meningioma surgery are based on the general principle that they are extra-axial lesions, and bone must be removed to permit sufficient exposure of the lesion and minimize injury to surrounding neurovascular structures. The meningioma is first devascularized at its base to minimize bleeding, the core is debulked, and the now malleable capsule dissected from neurovascular structures. In select cases, preoperative embolization may aid devascularization. Tumor removal can be significantly more complicated for meningiomas with close involvement of cranial nerves or a venous sinus. Gross total resection of a meningioma is highly dependent on the consistency of the tumor, its involvement with surrounding structures, and tumor shape (57–59).

The location of a meningioma greatly affects a surgeon's ability to achieve complete resection, with increasing complexity, for example, for convexity, parasagittal, sphenoid wing, cerebellopontine, and petroclival meningiomas (**Figure 1**). Convexity meningiomas typically present to the surface of the brain, placing fewer neurovascular structures at risk during dissection. Thus, given a generally low surgical risk, complete resection represents the standard of care for both initial surgical resection and for recurrence of aggressive convexity meningiomas. Similarly, falcine meningiomas that by definition arise from the falx but do not involve the superior sagittal sinus can generally be completely resected, frequently by an interhemispheric approach (60). In contrast, parasagittal meningiomas can abut or even invade the superior sagittal sinus, limiting a surgeon's ability to achieve a gross total resection without incurring the risks associated with sinus thrombosis and venous infarction. Such cases require close monitoring of residual tumor for progression, with consideration for adjuvant therapy for clinically aggressive lesions (61, 62).

Clinoidal, sphenoid wing, and spheno-orbital meningiomas can also be more technically challenging, particularly with increasing meningioma size and more medial location along the sphenoid wing, given proximity to the optic nerve, internal carotid artery and its branches, and the cavernous sinus (47, 63). Such tumors may be amenable to frontotemporal craniotomy, an eyebrow approach, or in some cases a TONES (TransOrbital NeuroEndoscopic Surgery) approach to remove the lesion. Additional bony removal to improve resection of larger, more invasive lesions might include anterior clinoidectomy, optic nerve decompression, orbitozygomatic osteotomy, and removal of hyperostotic, tumor-infiltrated bone. Complete resection of aggressive, recurrent lesions may be limited by encasement of critical structures such as the internal carotid artery or infiltration into the cavernous sinus. Fortunately, adjuvant treatment of such lesions can yield control rates as high as 70%, although more aggressive approaches such as carotid bypass or cavernous sinus entry to remove additional tumor should be considered in certain cases (64).

Meningiomas localized within the cerebellopontine angle are associated with further operative risk due to proximity to the brainstem, cranial nerves, and high-flow vasculature. The operative corridor to the cerebellopontine angle depends on size of the meningioma and relationship to the cranial nerves. Possible approaches include the retrosigmoid craniotomy and posterior petrosal approach, among others. A case study of 34 patients with cerebellopontine angle meningiomas demonstrated a 35.3% rate of cranial nerve deficits postoperatively, particularly when tumor is greater than 3 cm or extends into the jugular foramen (65). Given the critical structures surrounding the cerebellopontine angle, complete resection might not be possible, particularly with significant extension into the jugular foramen or with brainstem invasion. Tentorial meningiomas, which represent 3-6% of intracranial meningiomas, represent a

similarly technically complex subset of meningiomas. Depending on the location, surgical approaches include the subtemporal, suboccipital, or supracerebellar infratentorial approaches (66).

Petroclival meningiomas, originating at the upper clival dura medial to the trigeminal nerve, represent one of the most technically challenging meningiomas to treat surgically, given their ventral location in relation to the brainstem and involvement of multiple cranial nerves, with high rates of surgical morbidity (67). Variants such as the sphenopetroclival meningiomas can further extend into the middle fossa and invade the cavernous sinus. Complete resection of these tumors is often not possible and a combination of approaches, such as retrosigmoid, presigmoid, subtemporal transtentorial transpetrosal, and pretemporal transcavernous approaches, may be needed. Recent advances in endoscopy have opened a new avenue for resection, with the endonasal corridor providing direct access to the ventrally located meningioma *via* the clivus, reducing retraction on the brainstem or cranial nerves and greatly improving extent of resection (68–71).

Similarly, meningiomas of the anterior midline skull base (e.g. parasellar or olfactory groove) may be accessed by either expanded endoscopic approach or open craniotomy, often through frontotemporal or subfrontal approaches (72, 73). The expanded endoscopic approach is an increasingly viable option providing early visibility of the anterior fossa with minimal brain retraction and provides an opportunity for early decompression of the optic canal to reduce the risk of optic nerve injury. While such approaches are associated with increased risk of anosmia and cerebrospinal fluid (CSF) leak, advent of the vascularized nasoseptal flap has vastly reduced the rate of CSF leak.

Other locations of intracranial meningiomas are described in the literature but are less commonly observed and are therefore not comprehensively discussed in this review. For example, intraventricular meningiomas, which represent less than 3% of intracranial meningiomas, account for up to 15% of adult intraventricular neoplasms and can present with either mass effect or obstructive hydrocephalus; the most common left trigonal location is often approached through a superior parietal lobule or occipital avenues (74). Surgical approach for each subset of intracranial meningioma not discussed must be tailored to maximize resection while minimizing risk of injury to vasculature, cranial nerves, and brain parenchyma.

Radiation Therapy

In elderly or medically ill patients, for surgically inaccessible tumors, or as an adjunct to open surgery, stereotactic radiosurgery is a treatment option that is particularly effective for smaller lesions, with 5 year progression-free survival rates ranging from 86-100% (18). Although surgery is widely considered first-line treatment for symptomatic or progressive meningiomas in a healthy patient population, complex tumors that are closely involved with critical neurovascular structures may not permit complete resection. Particularly for aggressive meningiomas, residual tumor, such as that left within the superior sagittal sinus, cavernous sinus, or encasing cranial nerves, is associated with a 5-year recurrence rate greater than 60% (75). Therefore, adjuvant therapy must be considered for these lesions and is considered standard of care even after complete resection for aggressive or grade 3 lesions (76).

Small (< 3 cm) WHO grade 1 meningioma may be treated with single- or multi-session radiosurgery, though this is not commonly used in higher-grade meningiomas except in cases of repeat irradiation (77–79). For larger meningiomas of high grade or with aggressive features, fractionated radiotherapy alone or in addition to surgery is often recommended, typically 54 Gy for grade 1 and 59.4 – 60 Gy for grade 2-3 lesions. Fractionated radiosurgery following subtotal resection in patients with WHO grade 1 meningiomas demonstrated 5-year progression free survival (PFS) of 91%, compared to 52% of patients that had subtotal resection alone (80). Similar comparisons in WHO grade 2 and 3 patients demonstrated significant increase in median PFS from 37 months to 64 months with addition of adjuvant fractionated radiotherapy, although this benefit is likely reduced in aggressive and recurrent meningiomas, which may be identified based on the presence of intratumoral necrosis or brain invasion, as previously described (81–83).

The efficacy of radiation therapy is highly relevant for surgically complex tumors where gross total resection is not possible. Large retrospective analyses of symptomatic patients with petroclival, cavernous sinus, and cerebellopontine meningiomas reveal tumor control by radiation therapy in greater than 90% of cases with significant improvement in cranial nerve function (46.5%), particularly in petroclival and cavernous sinus meningiomas (84, 85). These findings were replicated in a series of retrospective analyses meta-analyses specifically looking at patients with cavernous sinus meningiomas treated with fractionated radiotherapy, demonstrating a local control rate of approximately 90% at 10 years with cranial nerve deficit improvement in 26-45% of patients and a 10% rate of new cranial nerve dysfunction (86–90). Clinical trials further investigating the application of fractionated radiotherapy in the treatment of meningioma are ongoing with encouraging results. For example, preliminary results from RTOG 0539, a phase II clinical trial in which patients were assigned radiation treatment protocols based on grouping into low, intermediate and high-risk groups by extent of resection, WHO grade, and recurrence status indicate a PFS of 94% for intermediate- and 59% for high-risk meningiomas treated with adjuvant fractionated radiotherapy (45, 91). A lingering question is the need for adjuvant radiation therapy following gross total resection of an intermediate grade meningioma, and may be answered by an ongoing phase 3 clinical trial (NCT03180268). Of note, inclusion in this trial requires pathologic diagnosis of WHO grade 2 meningioma according to the 2016 criteria, and therefore may not entirely assess the genetic and epigenetic subclassifications described in recent years and incorporated into the WHO 2021 classification.

Systemic Therapy

Medical management for meningioma is typically reserved as salvage therapy in aggressive, recurrent cases without surgical or radiotherapeutic options. Unfortunately, there is a lack of large-scale positive controlled trials on which to base recommendations, highlighting the importance of ongoing clinical trials. Instead, recommendations are based on small-scale studies evaluating a

wide variety of drug classes. These include recombinant antibodies (such as the anti-angiogenesis drug class), small peptides (e.g. somatostatin analogues), and a range of small molecule targeted therapies (48, 92–94). Traditional cytotoxic agents have had limited success (95, 96).

The NCCN guidelines (version 2.2021) for the treatment of recurrent meningioma has four category 2 recommended treatments: bevacizumab (2A), sunitinib (2B), a combination of bevacizumab with everolimus (2B), and somatostatin analogue (2B, "useful in certain circumstances"). Here we first review the NCCN recommendations for different salvage therapies before discussing additional treatment options.

Therapies targeting angiogenesis predominately affect the Vascular Endothelial Growth Factor (VEGF) pathway. A ten-fold elevation of VEGF levels have been reported in high grade as compared to low grade meningiomas (97). Vasogenic edema associated with meningiomas likewise is correlated with tumor VEGF expression levels, suggesting promise for therapies targeting angiogenesis in certain meningiomas (98). Drugs directly and indirectly targeting this pathway include bevacizumab (targeted inhibition of VEGF-A), vatalanib (VEGF/PDGF receptor inhibition), and sunitinib (non-specific tyrosine kinase inhibitor) (48, 95). Of these agents, bevacizumab is the best studied, with reported median PFS ranging from 6 to 15 months across several retrospective and prospective phase 2 studies (94, 99–101). As summarized by Graillon et al. in their recent review, the majority of these studies are small, enrolling between 8 and 38 patients with grade 2 or 3 meningiomas (94, 100). This combined with heterogeneity of study populations between studies warrants caution when interpreting consensus guidelines. When compared to a range of systemic agents as part of a retrospective study, Furtner et al. also noted those receiving bevacizumab demonstrated an 80% reduction in tumor diameter and 107% reduction in peritumoral edema (95). While promising, a prospective study by Furuse et al. suggests this may be due to bevacizumab treating post-radiation intraparenchymal radiation necrosis rather than targeting viable tumor (100). Bevacizumab is the only NCCN 2A recommended systemic treatment for recurrent meningioma. Likewise, the European Association of Neuro-Oncology (EANO) recommends bevacizumab in cases without alternative local treatment options, with a European evidence level of III (48, 102).

One prospective phase 2 and one retrospective study have examined sunitinib in recurrent meningiomas, enrolling 36 and 11 patients respectively (103, 104). Kaley et al. reported expression of VEGF-R2 in high grade meningiomas was associated with a median PFS of 1.4 months compared to 6.4 in patients who lacked its expression. Unfortunately, hemorrhages were observed in 4 of 36 patients on the study (two grade 3, one grade 4, and one grade 5), with additional thrombotic microangiopathy noted in 2 patients (103). More recently, Cardona et al. reported a median PFS of 9.1 months in eleven patients treated with sunitinib, notably without reports of CNS hemorrhage or angiopathy their smaller retrospective cohort (104). Sunitinib carries a NCCN 2B recommendation and a recommendation level C from EANO, though caution is warranted given potential bleeding risk (48, 102).

Meningiomas demonstrate the highest incidence of somatostatin receptor expression of all human tumors, garnering interest in leveraging somatostatin analogues for treatment of refractory lesions (105). The somatostatin receptor subtype overexpressed in 70% of meningiomas, SST_{2A}, strongly binds the widely available analog, octreotide (106). *In vitro*, octreotide inhibits meningioma cell proliferation, but does not induce cell death, particularly in cells expressing high levels of the SST_{2A} receptor (107). A prospective pilot study that treated 16 patients with recurrent meningioma with octreotide yielded a radiographic response in 31% of patients, with an additional one-third of patients exhibiting stable disease at 6 months, with minimal associated drug toxicity (108). While this benefit was not observed in a prospective, phase II study of 8 patients with recurrent, treatment-resistant meningioma or hemangiopericytoma, a large retrospective analysis of 43 (only 11 of whom were grade 2 or 3) patients with refractory meningioma treated with octreotide demonstrated improved progression-free survival particularly in skull base lesions (109, 110). Given the possible clinical benefit of octreotide with minimal toxicity, the CNS NCCN guideline classifies it as a level 2B drug for patients with recurrent meningioma.

Disruptions in the mTOR pathway are well documented in high grade meningiomas, with mTOR inhibition associated with decreased proliferation *in vitro* (107, 111). This has resulted in several studies examining combination therapy of everolimus, a small molecule mTOR kinase inhibitor, to other systemic treatments for recurrent meningiomas, including octreotide and bevacizumab (104, 112, 113). The phase II CEVOREM trial of 20 patients reported a median PFS of 6.6 months of the combination of octreotide and everolimus, while a median PFS of 12.1 months was reported by Cardona and colleagues for their retrospective study of 14 patients treated with everolimus, octreotide, and sunitinib (104). Finally, the combination of everolimus and bevacizumab has also been promising, with a median PFS of 22 months in grade 2 and 3 meningiomas (112). Though it remains unclear if there was additional benefit from combinatorial therapy, the combination of everolimus and bevacizumab carries a level 2B recommendation from the NCCN, with multiple mTOR pathway-targeting drugs being actively investigated.

Immunotherapeutic agents have demonstrated mixed efficacy to date in meningioma. Recombinant interferon-α is one such agent that demonstrated *in vitro* inhibition of meningioma cells (114). A prospective study of 35 patients with treatment-refractory WHO grade 1 meningiomas treated with interferon-α had promising results, yielding a median progression-free survival of 7 months. Although no radiographic response was noted in these patients, the study did demonstrate a modest control rate compared to historical controls. Unfortunately, interferon-α had limited efficacy for aggressive, high-grade tumors; a retrospective study of 35 patients receiving interferon-α demonstrated just 17% PFS at 6 months and no evident radiographic response (115). Similarly, immune

checkpoint inhibition by the programmed death-1 ligand (PD-L1) pathway (known to be upregulated in high-grade meningiomas) has failed to demonstrate significant response to date, with a recent phase 2 study of nivolumab monotherapy in 25 patients failing to demonstrate improved progression free survival (116). Despite initial setbacks, several immunotherapies remain under active evaluation including nivolumab, pembrolizumab, and avelumab.

Also under investigation for the treatment of meningioma are tyrosine kinase inhibitors. Interest in this category arose from the finding of activated PI3K and MAPK signaling pathways in aggressive meningiomas (117–119). Two such tyrosine kinase inhibitors with proven tolerability and efficacy in other tumors, sorafenib and regorafenib, were shown to impair cell viability and increase apoptosis *in vitro* with meningioma cells and to improve survival in an *in vivo* murine xenograft (120). A 2014 phase II clinical study treated 25 patients with aggressive meningioma with an oral tyrosine kinase inhibitor of VEGFR, vatalanib, with 6 month PFS of 54% (121). There are multiple additional tyrosine kinase inhibitors under investigation, targeting various receptor tyrosine kinase such as EGFR, PDGF, and FGFR with results pending (122–125).

As described above, molecular analysis of meningiomas has identified numerous driver mutations in genes that can be targeted with small molecular inhibitors or other therapeutic strategies. A promising phase 2 clinical trial, NCT02523014, led by Brastianos et al. is currently ongoing with 4 arms (2 closed, 2 ongoing) designed to tailor therapy to the specific molecular alterations identified in patients' meningiomas (126). Meningiomas with *SMO* or *PTCH1* mutations were treated with vismodegib, an FDA-approved Hedgehog signaling pathway inhibitor. Those with *NF2* mutations received a FAK inhibitor, thought to act as a synthetic lethal with *NF2* loss-of-function, with results from this arm reported as showing improved PFS at 6 months (33%) compared to historical controls with minimal adverse effects (127). Tumors with *AKT1*, *PIK3CA* or *PTEN* mutations are treated with capivasertib, an AKT kinase inhibitor, and those with *CDK4*, *CDK6*, *CDKN2A*, *CCND1*, *CCND2*, *CCND3*, and *CCNE1* treated with abemaciclib, a CDK inhibitor. As additional molecular drivers of meningioma pathophysiology are identified, additional targeted therapies will undoubtedly be revealed for recurrent lesions.

CONCLUSIONS

Although often considered a benign entity, many intracranial meningiomas are anything but, requiring potentially morbid surgical resections and radiation treatments with few viable systemic therapy alternatives. WHO grading predicts aggressiveness of meningiomas relatively well, but as demonstrated in the descriptive case examples, is not perfect, particularly in the broad classes of grade 2 lesions. Recent progress in characterization of the genetic and epigenetic landscape of these lesions may significantly improve our ability to better delineate aggressive tumors. Such tumors may be well-served with immediate postoperative adjuvant therapy or closer monitoring. Finally, improved molecular understanding has permitted targeted therapies including antiangiogenic agents, tyrosine kinase inhibitors, somatostatin inhibitors, and genetically targeted small molecular inhibitors with highly anticipated results from ongoing clinical trials.

AUTHOR CONTRIBUTIONS

BP, RD, SP, OB, JH, and AK prepared the manuscript and figures. AK oversaw the project. All authors contributed to the article and approved the submitted version.

REFERENCES

1. Ostrom QT, Patil N, Cioffi G, Waite K, Kruchko C, Barnholtz-Sloan JS. CBTRUS Statistical Report: Primary Brain and Other Central Nervous System Tumors Diagnosed in the United States in 2013-2017. *Neuro Oncol* (2020) 22:iv1–iv96. doi: 10.1093/neuonc/noaa200
2. Louis DN, Perry A, Wesseling P, Brat DJ, Cree IA, Figarella-Branger D, et al. The 2021 WHO Classification of Tumors of the Central Nervous System: A Summary. *Neuro Oncol* (2021) 23:1231–51. doi: 10.1093/neuonc/noab106
3. Saraf S, McCarthy BJ, Villano JL. Update on Meningiomas. *Oncologist* (2011) 16:1604–13. doi: 10.1634/theoncologist.2011-0193
4. Pettersson-Segerlind J, Orrego A, Lonn S, Mathiesen T. Long-Term 25-Year Follow-Up of Surgically Treated Parasagittal Meningiomas. *World Neurosurg* (2011) 76:564–71. doi: 10.1016/j.wneu.2011.05.015
5. Sahm F, Schrimpf D, Stichel D, Jones DTW, Hielscher T, Schefzyk S, et al. DNA Methylation-Based Classification and Grading System for Meningioma: A Multicentre, Retrospective Analysis. *Lancet Oncol* (2017) 18:682–94. doi: 10.1016/S1470-2045(17)30155-9
6. Patel AJ, Wan YW, Al-Ouran R, Revelli JP, Cardenas MF, Oneissi M, et al. Molecular Profiling Predicts Meningioma Recurrence and Reveals Loss of DREAM Complex Repression in Aggressive Tumors. *Proc Natl Acad Sci USA* (2019) 116:21715–26. doi: 10.1073/pnas.1912858116
7. Nassiri F, Liu J, Patil V, Mamatjan Y, Wang JZ, Hugh-White R, et al. A Clinically Applicable Integrative Molecular Classification of Meningiomas. *Nature* (2021) 597:119–25. doi: 10.1038/s41586-021-03850-3
8. Maas SLN, Stichel D, Hielscher T, Sievers P, Berghoff AS, Schrimpf D, et al. Integrated Molecular-Morphologic Meningioma Classification: A Multicenter Retrospective Analysis, Retrospectively and Prospectively Validated. *J Clin Oncol* (2021) 39:3839–52. doi: 10.1200/JCO.21.00784
9. Driver J, Hoffman SE, Tavakol S, Woodward E, Maury EA, Bhave V, et al. A Molecularly Integrated Grade for Meningioma. *Neuro Oncol* (2021). doi: 10.1093/neuonc/noab213
10. Bayley JC, Hadley CC, Harmanci AO, Harmanci AS, Klisch TJ, Patel AJ, et al. Multiple Approaches Converge on Three Biological Subtypes of Meningioma and Extract New Insights From Published Studies. *Sci Adv* (2022) 8:eabm6247. doi: 10.1126/sciadv.abm6247
11. Gritsch S, Batchelor TT, Gonzalez Castro LN. Diagnostic, Therapeutic, and Prognostic Implications of the 2021 World Health Organization Classification of Tumors of the Central Nervous System. *Cancer* (2022) 128:47–58. doi: 10.1002/cncr.33918
12. Sun SQ, Hawasli AH, Huang J, Chicoine MR, Kim AH. An Evidence-Based Treatment Algorithm for the Management of WHO Grade II and III Meningiomas. *Neurosurg Focus* (2015) 38:E3. doi: 10.3171/2015.1.FOCUS14757

13. Louis DN, Perry A, Reifenberger G, von Deimling A, Figarella-Branger D, Cavenee WK, et al. The 2016 World Health Organization Classification of Tumors of the Central Nervous System: A Summary. *Acta Neuropathol* (2016) 131:803–20. doi: 10.1007/s00401-016-1545-1
14. Clark VE, Erson-Omay EZ, Serin A, Yin J, Cotney J, Özduman K, et al. Genomic Analysis of non-NF2 Meningiomas Reveals Mutations in TRAF7, KLF4, AKT1, and SMO. *Science* (2013) 339:1077–80. doi: 10.1126/science.1233009
15. Sun SQ, Cai C, Murphy RKJ, DeWees T, Dacey RG, Grubb RL, et al. Management of Atypical Cranial Meningiomas, Part 2: Predictors of Progression and the Role of Adjuvant Radiation After Subtotal Resection. *Neurosurgery* (2014) 75:356–63. doi: 10.1227/NEU.0000000000000462
16. Garcia-Segura ME, Erickson AW, Jairath R, Munoz DG, Das S. Necrosis and Brain Invasion Predict Radio-Resistance and Tumor Recurrence in Atypical Meningioma: A Retrospective Cohort Study. *Neurosurgery* (2020) 88(1): E42–8. doi: 10.1093/neuros/nyaa348
17. Bailey P, Cushing H, Eisenhardt L. Angioblastic Meningiomas. *Arch Pathol* (1928) 6:953–90.
18. Rogers L, Barani I, Chamberlain M, Kaley TJ, McDermott M, Raizer J, et al. Meningiomas: Knowledge Base, Treatment Outcomes, and Uncertainties. A RANO Review. *J Neurosurg* (2015) 122:4–23. doi: 10.3171/2014.7.JNS131644
19. Barresi V, Lionti S, Caliri S, Caffo M. Histopathological Features to Define Atypical Meningioma: What Does Really Matter for Prognosis? *Brain Tumor Pathol* (2018) 35:168–80. doi: 10.1007/s10014-018-0318-z
20. Ruttledge MH, Sarrazin J, Rangaratnam S, Phelan CM, Twist E, Merel P, et al. Evidence for the Complete Inactivation of the NF2 Gene in the Majority of Sporadic Meningiomas. *Nat Genet* (1994) 6:180–4. doi: 10.1038/ng0294-180
21. Bi WL, Greenwald NF, Abedalthagafi M, Wala J, Gibson WJ, Agarwalla PK, et al. Genomic Landscape of High-Grade Meningiomas. *NPJ Genomic Med* (2017) 2:1. doi: 10.1038/s41525-017-0014-7
22. Williams EA, Santagata S, Wakimoto H, Shankar GM, Barker FG 2nd, Sharaf R, et al. Distinct Genomic Subclasses of High-Grade/Progressive Meningiomas: NF2-Associated, NF2-Exclusive, and NF2-Agnostic. *Acta Neuropathol Commun* (2020) 8:171. doi: 10.1186/s40478-020-01040-2
23. Kros J, de Greve K, van Tilborg A, Hop W, Pieterman H, Avezaat C, et al. NF2 Status of Meningiomas is Associated With Tumour Localization and Histology. *J Pathol* (2001) 194:367–72. doi: 10.1002/path.909
24. Clark VE, Harmanci AS, Bai H, Youngblood MW, Lee TI, Baranoski JF, et al. Recurrent Somatic Mutations in POLR2A Define a Distinct Subset of Meningiomas. *Nat Genet* (2016) 48:1253–9. doi: 10.1038/ng.3651
25. Hamaratoglu F, Willecke M, Kango-Singh M, Nolo R, Hyun E, Tao C, et al. The Tumour-Suppressor Genes NF2/Merlin and Expanded Act Through Hippo Signalling to Regulate Cell Proliferation and Apoptosis. *Nat Cell Biol* (2006) 8:27–36. doi: 10.1038/ncb1339
26. Morrison H, Sperka T, Manent J, Giovannini M, Ponta H, Herrlich P. Merlin/neurofibromatosis Type 2 Suppresses Growth by Inhibiting the Activation of Ras and Rac. *Cancer Res* (2007) 67:520–7. doi: 10.1158/0008-5472.CAN-06-1608
27. James MF, Han S, Polizzano C, Plotkin SR, Manning BD, Stemmer-Rachamimov AO, et al. NF2/merlin Is a Novel Negative Regulator of mTOR Complex 1, and Activation of Mtorc1 Is Associated With Meningioma and Schwannoma Growth. *Mol Cell Biol* (2009) 29:4250–61. doi: 10.1128/MCB.01581-08
28. Petrilli AM, Fernandez-Valle C. Role of Merlin/NF2 Inactivation in Tumor Biology. *Oncogene* (2016) 35:537–48. doi: 10.1038/onc.2015.125
29. Mei Y, Du Z, Hu C, Greenwald NF, Abedalthagafi M, Agar NYR, et al. Osteoglycin Promotes Meningioma Development Through Downregulation of NF2 and Activation of mTOR Signaling. *Cell Commun Signal* (2017) 15:34. doi: 10.1186/s12964-017-0189-7
30. Brastianos PK, Horowitz PM, Santagata S, Jones RT, McKenna A, Getz G, et al. Genomic Sequencing of Meningiomas Identifies Oncogenic SMO and AKT1 Mutations. *Nat Genet* (2013) 45:285–9. doi: 10.1038/ng.2526
31. Abedalthagafi M, Bi WL, Aizer AA, Merrill PH, Brewster R, Agarwalla PK, et al. Oncogenic PI3K Mutations are as Common as AKT1 and SMO Mutations in Meningioma. *Neuro Oncol* (2016) 18:649–55. doi: 10.1093/neuonc/nov316
32. Shankar GM, Santagata S. BAP1 Mutations in High-Grade Meningioma: Implications for Patient Care. *Neuro Oncol* (2017) 19:1447–56. doi: 10.1093/neuonc/nox094
33. Holsten T, Bens S, Oyen F, Nemes K, Hasselblatt M, Kordes U, et al. Germline Variants in SMARCB1 and Other Members of the BAF Chromatin-Remodeling Complex Across Human Disease Entities: A Meta-Analysis. *Eur J Hum Genet* (2018) 26:1083–93. doi: 10.1038/s41431-018-0143-1
34. Goutagny S, Nault JC, Mallet M, Henin D, Rossi JZ, Kalamarides M. High Incidence of Activating TERT Promoter Mutations in Meningiomas Undergoing Malignant Progression. *Brain Pathol* (2014) 24:184–9. doi: 10.1111/bpa.12110
35. Sahm F, Schrimpf D, Olar A, Koelsche C, Reuss D, Bissel J, et al. TERT Promoter Mutations and Risk of Recurrence in Meningioma. *J Natl Cancer Inst* (2016) 108:377. doi: 10.1093/jnci/djv377
36. Juratli TA, Thiede C, Koerner MVA, Tummala SS, Daubner D, Shankar GM, et al. Intratumoral Heterogeneity and TERT Promoter Mutations in Progressive/Higher-Grade Meningiomas. *Oncotarget* (2017) 8:109228–37. doi: 10.18632/oncotarget.22650
37. Perry A, Banerjee R, Lohse CM, Kleinschmidt-DeMasters BK, Scheithauer BW. A Role for Chromosome 9p21 Deletions in the Malignant Progression of Meningiomas and the Prognosis of Anaplastic Meningiomas. *Brain Pathol* (2002) 12:183–90. doi: 10.1111/j.1750-3639.2002.tb00433.x
38. Shankar GM, Abedalthagafi M, Vaubel RA, Merrill PH, Nayyar N, Gill CM, et al. Germline and Somatic BAP1 Mutations in High-Grade Rhabdoid Meningiomas. *Neuro Oncol* (2017) 19:535–45. doi: 10.1093/neuonc/now235
39. Sievers P, Hielscher T, Schrimpf D, Stichel D, Reuss DE, Berghoff AS, et al. CDKN2A/B Homozygous Deletion Is Associated With Early Recurrence in Meningiomas. *Acta Neuropathol* (2020) 140:409–13. doi: 10.1007/s00401-020-02188-w
40. Kishida Y, Natsume A, Kondo Y, Takeuchi I, An B, Okamoto Y, et al. Epigenetic Subclassification of Meningiomas Based on Genome-Wide DNA Methylation Analyses. *Carcinogenesis* (2012) 33:436–41. doi: 10.1093/carcin/bgr260
41. Gao F, Shi L, Russin J, Zeng L, Chang X, He S, et al. DNA Methylation in the Malignant Transformation of Meningiomas. *PloS One* (2013) 8:e54114. doi: 10.1371/journal.pone.0054114
42. Bi WL, Mei Y, Agarwalla PK, Beroukhim R, Dunn IF. Genomic and Epigenomic Landscape in Meningioma. *Neurosurg Clin N Am* (2016) 27:167–79. doi: 10.1016/j.nec.2015.11.009
43. Nassiri F, Wang JZ, Singh O, Karimi S, Dalcourt T, Ijad N, et al. Loss of H3K27me3 in Meningiomas. *Neuro Oncol* (2021) 23:1282–91. doi: 10.1093/neuonc/noab036
44. Jung M, Kim SI, Lim KY, Bae J, Park CK, Choi SH, et al. The Substantial Loss of H3K27me3 can Stratify Risk in Grade 2, But Not in Grade 3 Meningioma. *Hum Pathol* (2021) 115:96–103. doi: 10.1016/j.humpath.2021.06.005
45. Rogers L, Zhang P, Vogelbaum MA, Perry A, Ashby LS, Modi JM, et al. Intermediate-Risk Meningioma: Initial Outcomes From NRG Oncology RTOG 0539. *J Neurosurg* (2018) 129:35–47. doi: 10.3171/2016.11.JNS161170
46. Zhang H, Mo J, Jiang H, Li Z, Hu W, Zhang C, et al. Deep Learning Model for the Automated Detection and Histopathological Prediction of Meningioma. *Neuroinformatics* (2021) 19:393–402. doi: 10.1007/s12021-020-09492-6
47. Zhao L, Zhao W, Hou Y, Wen C, Wang J, Wu P, et al. An Overview of Managements in Meningiomas. *Front Oncol* (2020) 10:1523. doi: 10.3389/fonc.2020.01523
48. Goldbrunner R, Stavrinou P, Jenkinson MD, Sahm F, Mawrin C, Weber DC, et al. EANO Guideline on the Diagnosis and Management of Meningiomas. *Neuro Oncol* (2021) 23:1821–34. doi: 10.1093/neuonc/noab150
49. Vernooij MW, Ikram MA, Tanghe HL, Vincent AJ, Hofman A, Krestin GP, et al. Incidental Findings on Brain MRI in the General Population. *N Engl J Med* (2007) 357:1821–8. doi: 10.1056/NEJMoa070972
50. Oya S, Kim SH, Sade B, Lee JH. The Natural History of Intracranial Meningiomas. *J Neurosurg* (2011) 114:1250–6. doi: 10.3171/2010.12.JNS101623
51. Lee EJ, Park JH, Park ES, Kim JH. "Wait-And-See" Strategies for Newly Diagnosed Intracranial Meningiomas Based on the Risk of Future Observation Failure. *World Neurosurg* (2017) 107:604–11. doi: 10.1016/j.wneu.2017.08.060

52. Lee EJ, Kim JH, Park ES, Kim YH, Lee JK, Hong SH, et al. A Novel Weighted Scoring System for Estimating the Risk of Rapid Growth in Untreated Intracranial Meningiomas. *J Neurosurg* (2017) 127:971–80. doi: 10.3171/2016.9.JNS161669
53. Islim AI, Mohan M, Moon RDC, Srikandarajah N, Mills SJ, Brodbelt AR, et al. Incidental Intracranial Meningiomas: A Systematic Review and Meta-Analysis of Prognostic Factors and Outcomes. *J Neuro-oncol* (2019) 142:211–21. doi: 10.1007/s11060-019-03104-3
54. Nakasu S, Nakasu Y, Nakajima M, Matsuda M, Handa J. Preoperative Identification of Meningiomas That are Highly Likely to Recur. *J Neurosurg* (1999) 90:455–62. doi: 10.3171/jns.1999.90.3.0455
55. Simpson D. The Recurrence of Intracranial Meningiomas After Surgical Treatment. *J Neurol Neurosurg Psychiatry* (1957) 20:22–39. doi: 10.1136/jnnp.20.1.22
56. Bi WL, Dunn IF. Current and Emerging Principles in Surgery for Meningioma. *Chin Clin Oncol* (2017) 6:S7. doi: 10.21037/cco.2017.06.10
57. Itamura K, Chang KE, Lucas J, Donoho DA, Giannotta S, Zada G. Prospective Clinical Validation of a Meningioma Consistency Grading Scheme: Association With Surgical Outcomes and Extent of Tumor Resection. *J Neurosurg* (2018) 131(5):1356–60. doi: 10.3171/2018.7.JNS1838
58. Maiuri F, Mariniello G, Peca C, Guadagno E, Corvino S, d'Avanzo F, et al. Multicentric and Diffuse Recurrences of Meningiomas. *Br J Neurosurg* (2020) 34:439–46. doi: 10.1080/02688697.2020.1754335
59. Al Abdulsalam HK, Aldahish AK, Albakr A, Hussain S, Alroqi A, Alromaih S, et al. Endoscopic Transnasal Resection of Midline Skull Base Meningiomas: Tumor Consistency and Surgical Outcomes. *J Neurol Surg B Skull Base* (2021) 82:500–5. doi: 10.1055/s-0040-1714111
60. Murrone D, De Paulis D, di Norcia V, Di Vitantonio H, Galzio RJ. Surgical Management of Falcine Meningiomas: Experience of 95 Patients. *J Clin Neurosci* (2017) 37:25–30. doi: 10.1016/j.jocn.2016.11.002
61. Han MS, Kim YJ, Moon KS, Lee KH, Yang JI, Kang WD, et al. Lessons From Surgical Outcome for Intracranial Meningioma Involving Major Venous Sinus. *Med (Baltimore)* (2016) 95:e4705. doi: 10.1097/MD.0000000000004705
62. Anthofer J, Seidel-Schulz R, Proescholdt M, Brawanski A, Schebesch KM. Meningiomas Adjacent to Major Venous Sinuses-Clinical Outcome and Recurrence. *World Neurosurg* (2017) 104:560–6. doi: 10.1016/j.wneu.2017.05.025
63. Sankhla S. Medial Sphenoid Wing Meningioma. *Neurol India* (2016) 64:476–7. doi: 10.4103/0028-3886.181566
64. Nakamura M, Roser F, Jacobs C, Vorkapic P, Samii M. Medial Sphenoid Wing Meningiomas: Clinical Outcome and Recurrence Rate. *Neurosurgery* (2006) 58:626–639, discussion 626-639. doi: 10.1227/01.NEU.0000197104.78684.5D
65. Agarwal V, Babu R, Grier J, Adogwa O, Back A, Friedman AH, et al. Cerebellopontine Angle Meningiomas: Postoperative Outcomes in a Modern Cohort. *Neurosurg Focus* (2013) 35:E10. doi: 10.3171/2013.10.FOCUS13367
66. Bassiouni H, Hunold A, Asgari S, Stolke D. Tentorial Meningiomas: Clinical Results in 81 Patients Treated Microsurgically. *Neurosurgery* (2004) 55:108–116; discussion 116-108. doi: 10.1227/01.neu.0000126886.48372.49
67. Zhao Z, Yuan X, Yuan J, Cai L, Jiang W, Xie Y, et al. Treatment Strategy for Petroclival Meningiomas Based on a Proposed Classification in a Study of 168 Cases. *Sci Rep* (2020) 10:4655. doi: 10.1038/s41598-020-61497-y
68. Gardner PA, Kassam AB, Thomas A, Snyderman CH, Carrau RL, Mintz AH, et al. Endoscopic Endonasal Resection of Anterior Cranial Base Meningiomas. *Neurosurgery* (2008) 63:36–52; discussion 52-34. doi: 10.1227/01.NEU.0000335069.30319.1E
69. Jean WC, Felbaum DR, Anaizi A, DeKlotz TR. Endoscopic Endonasal Approach for Transclival Resection of a Petroclival Meningioma: A Technical Note. *Cureus* (2016) 8:e641. doi: 10.7759/cureus.641
70. Gunaldi O, Kina H, Tanriverdi O, Erdogan U, Postalci LS. Endoscopic Endonasal Transclival Resection of the Upper Clival Meningioma. *Turk Neurosurg* (2018) 28:505–9. doi: 10.5137/1019-5149.JTN.17010-16.4
71. Bossi Todeschini A, Montaser AS, Hardesty DA, Carrau RL, Prevedello DM. The Limits of the Endoscopic Endonasal Transclival Approach for Posterior Fossa Tumors. *J Neurosurg Sci* (2018) 62:322–31. doi: 10.23736/S0390-5616.18.04411-9
72. de Divitiis E, Esposito F, Cappabianca P, Cavallo LM, de Divitiis O, Esposito I. Endoscopic Transnasal Resection of Anterior Cranial Fossa Meningiomas. *Neurosurg Focus* (2008) 25:E8. doi: 10.3171/FOC.2008.25.12.E8
73. Algattas HN, Wang EW, Zenonos GA, Snyderman CH, Gardner PA. Endoscopic Endonasal Surgery for Anterior Cranial Fossa Meningiomas. *J Neurosurg Sci* (2021) 65:118–32. doi: 10.23736/S0390-5616.20.05085-7
74. Pereira BJA, de Almeida AN, Paiva WS, de Aguiar PHP, Teixeira MJ, Marie SKN. Natural History of Intraventricular Meningiomas: Systematic Review. *Neurosurg Rev* (2020) 43:513–23. doi: 10.1007/s10143-018-1019-0
75. Jaaskelainen J. Seemingly Complete Removal of Histologically Benign Intracranial Meningioma: Late Recurrence Rate and Factors Predicting Recurrence in 657 Patients. A Multivariate Analysis. *Surg Neurol* (1986) 26:461–9. doi: 10.1016/0090-3019(86)90259-4
76. Goldbrunner R, Minniti G, Preusser M, Jenkinson MD, Sallabanda K, Houdart E, et al. EANO Guidelines for the Diagnosis and Treatment of Meningiomas. *Lancet Oncol* (2016) 17:e383–391. doi: 10.1016/S1470-2045(16)30321-7
77. Lin AJ, Hui C, Dahiya S, Lu HC, Kim AH, Campian JL, et al. Radiologic Response and Disease Control of Recurrent Intracranial Meningiomas Treated With Reirradiation. *Int J Radiat Oncol Biol Phys* (2018) 102:194–203. doi: 10.1016/j.ijrobp.2018.05.011
78. Huang SH, Wang CC, Wei KC, Chang CN, Chuang CC, Chen HC, et al. Treatment of Intracranial Meningioma With Single-Session and Fractionated Radiosurgery: A Propensity Score Matching Study. *Sci Rep* (2020) 10:18500. doi: 10.1038/s41598-020-75559-8
79. Momin AA, Shao J, Soni P, Almeida JP, Suh JH, Murphy ES, et al. Outcomes of Salvage Radiation for Recurrent World Health Organization Grade II Meningiomas: A Retrospective Cohort Study. *J Neuro-Oncol* (2021) 152:373–82. doi: 10.1007/s11060-021-03711-z
80. Soyuer S, Chang EL, Selek U, Shi W, Maor MH, DeMonte F. Radiotherapy After Surgery for Benign Cerebral Meningioma. *Radiother Oncol* (2004) 71:85–90. doi: 10.1016/j.radonc.2004.01.006
81. Chohan MO, Ryan CT, Singh R, Lanning RM, Reiner AS, Rosenblum MK, et al. Predictors of Treatment Response and Survival Outcomes in Meningioma Recurrence With Atypical or Anaplastic Histology. *Neurosurgery* (2018) 82:824–32. doi: 10.1093/neuros/nyx312
82. Hemmati SM, Ghadjar P, Grun A, Badakhshi H, Zschaeck S, Senger C, et al. Adjuvant Radiotherapy Improves Progression-Free Survival in Intracranial Atypical Meningioma. *Radiat Oncol* (2019) 14:160. doi: 10.1186/s13014-019-1368-z
83. Zhu H, Bi WL, Aizer A, Hua L, Tian M, Den J, et al. Efficacy of Adjuvant Radiotherapy for Atypical and Anaplastic Meningioma. *Cancer Med* (2019) 8:13–20. doi: 10.1002/cam4.1531
84. Faramand A, Kano H, Niranjan A, Johnson SA, Hassib M, Park KJ, et al. Cranial Nerve Outcomes After Primary Stereotactic Radiosurgery for Symptomatic Skull Base Meningiomas. *J Neuro-Oncol* (2018) 139:341–8. doi: 10.1007/s11060-018-2866-9
85. Faramand A, Kano H, Niranjan A, Park KJ, Flickinger JC, Lunsford LD. Tumor Control and Cranial Nerve Outcomes After Adjuvant Radiosurgery for Low-Grade Skull Base Meningiomas. *World Neurosurg* (2019) 127:E221–9. doi: 10.1016/j.wneu.2019.03.052
86. Dufour H, Muracciole X, Metellus P, Regis J, Chinot O, Grisoli F. Long-Term Tumor Control and Functional Outcome in Patients With Cavernous Sinus Meningiomas Treated by Radiotherapy With or Without Previous Surgery: Is There an Alternative to Aggressive Tumor Removal? *Neurosurgery* (2001) 48:285–294; discussion 294-286. doi: 10.1097/00006123-200102000-00006
87. Park KJ, Kano H, Iyer A, Liu X, Tonetti DA, Lehocky C, et al. Gamma Knife Stereotactic Radiosurgery for Cavernous Sinus Meningioma: Long-Term Follow-Up in 200 Patients. *J Neurosurg* (2018) 130(6):1799–808. doi: 10.3171/2018.2.JNS172361
88. Leroy HA, Tuleasca C, Reyns N, Levivier M. Radiosurgery and Fractionated Radiotherapy for Cavernous Sinus Meningioma: A Systematic Review and Meta-Analysis. *Acta Neurochir (Wien)* (2018) 160:2367–78. doi: 10.1007/s00701-018-3711-9
89. Ruesß D, Fritsche F, Grau S, Treuer H, Hoevels M, Kocher M, et al. Stereotactic Radiosurgery of Cavernous Sinus Meningiomas. *J Neurol Surg B Skull Base* (2020) 81:158–64. doi: 10.1055/s-0039-1683430
90. Martinez-Perez R, Florez-Perdomo W, Freeman L, Ung TH, Youssef AS. Long-Term Disease Control and Treatment Outcomes of Stereotactic Radiosurgery in Cavernous Sinus Meningiomas. *J Neuro-Oncol* (2021) 152:439–49. doi: 10.1007/s11060-021-03732-8

91. Rogers CL, Won M, Vogelbaum MA, Perry A, Ashby LS, Modi JM, et al. High-Risk Meningioma: Initial Outcomes From NRG Oncology/RTOG 0539. *Int J Radiat Oncol Biol Phys* (2020) 106:790–9. doi: 10.1016/j.ijrobp.2019.11.028
92. Chamberlain MC, Barnholtz-Sloan JS. Medical Treatment of Recurrent Meningiomas. *Expert Rev Neurother* (2011) 11:1425–32. doi: 10.1586/ern.11.38
93. Kaley T, Barani I, Chamberlain M, McDermott M, Panageas K, Raizer J, et al. Historical Benchmarks for Medical Therapy Trials in Surgery- and Radiation-Refractory Meningioma: A RANO Review. *Neuro Oncol* (2014) 16:829–40. doi: 10.1093/neuonc/not330
94. Graillon T, Tabouret E, Chinot O. Chemotherapy and Targeted Therapies for Meningiomas: What is the Evidence? *Curr Opin Neurol* (2021) 34:857–67. doi: 10.1097/WCO.0000000000001002
95. Furtner J, Schopf V, Seystahl K, Le Rhun E, Ruda R, Roelcke U, et al. Kinetics of Tumor Size and Peritumoral Brain Edema Before, During, and After Systemic Therapy in Recurrent WHO Grade II or III Meningioma. *Neuro Oncol* (2016) 18:401–7. doi: 10.1093/neuonc/nov183
96. Preusser M, Silvani A, Le Rhun E, Soffietti R, Lombardi G, Sepulveda JM, et al. Trabectedin for Recurrent WHO Grade II or III Meningioma: A Randomized Phase II Study of the EORTC Brain Tumor Group (EORTC-1320-BTG). *J Clin Oncol* (2019) 37. doi: 10.1200/JCO.2019.37.15_suppl.2007
97. Lamszus K, Lengler U, Schmidt NO, Stavrou D, Ergun S, Westphal M. Vascular Endothelial Growth Factor, Hepatocyte Growth Factor/Scatter Factor, Basic Fibroblast Growth Factor, and Placenta Growth Factor in Human Meningiomas and Their Relation to Angiogenesis and Malignancy. *Neurosurgery* (2000) 46:938–947; discussion 947-938. doi: 10.1097/00006123-200004000-00033
98. Goldman CK, Bharara S, Palmer CA, Vitek J, Tsai JC, Weiss HL, et al. Brain Edema in Meningiomas is Associated With Increased Vascular Endothelial Growth Factor Expression. *Neurosurgery* (1997) 40:1269–77. doi: 10.1097/00006123-199706000-00029
99. Nayak L, Iwamoto FM, Rudnick JD, Norden AD, Lee EQ, Drappatz J, et al. Atypical and Anaplastic Meningiomas Treated With Bevacizumab. *J Neuro-oncol* (2012) 109:187–93. doi: 10.1007/s11060-012-0886-4
100. Furuse M, Nonoguchi N, Kawabata S, Miyata T, Toho T, Kuroiwa T, et al. Intratumoral and Peritumoral Post-Irradiation Changes, But Not Viable Tumor Tissue, may Respond to Bevacizumab in Previously Irradiated Meningiomas. *Radiat Oncol* (2015) 10:156. doi: 10.1186/s13014-015-0446-0
101. Le Van T, Graillon T, Jacob J, Vauleon E, Feuvret L, Boch AL, et al. Multimodal Management of Surgery- and Radiation-Refractory Meningiomas: An Analysis of the French National Tumor Board Meeting on Meningiomas Cohort. *J Neuro-oncol* (2021) 153:55–64. doi: 10.1007/s11060-021-03741-7
102. Brainin M, Barnes M, Baron JC, Gilhus NE, Hughes R, Selmaj K, et al. Guidance for the Preparation of Neurological Management Guidelines by EFNS Scientific Task Forces–Revised Recommendations 2004. *Eur J Neurol* (2004) 11:577–81. doi: 10.1111/j.1468-1331.2004.00867.x
103. Kaley TJ, Wen P, Schiff D, Ligon K, Haidar S, Karimi S, et al. Phase II Trial of Sunitinib for Recurrent and Progressive Atypical and Anaplastic Meningioma. *Neuro Oncol* (2015) 17:116–21. doi: 10.1093/neuonc/nou148
104. Cardona AF, Ruiz-Patino A, Zatarain-Barrón ZL, Hakim F, Jimenez E, Mejia JA, et al. Systemic Management of Malignant Meningiomas: A Comparative Survival and Molecular Marker Analysis Between Octreotide in Combination With Everolimus and Sunitinib. *PloS One* (2019) 14:e0217340. doi: 10.1371/journal.pone.0217340
105. Lamberts SW, Krenning EP, Reubi JC. The Role of Somatostatin and its Analogs in the Diagnosis and Treatment of Tumors. *Endocr Rev* (1991) 12:450–82. doi: 10.1210/edrv-12-4-450
106. Schulz S, Pauli SU, Schulz S, Handel M, Dietzmann K, Firsching R, et al. Immunohistochemical Determination of Five Somatostatin Receptors in Meningioma Reveals Frequent Overexpression of Somatostatin Receptor Subtype Sst2a. *Clin Cancer Res* (2000) 6:1865–74.
107. Graillon T, Romano D, Defilles C, Saveanu A, Mohamed A, Figarella-Branger D, et al. Octreotide Therapy in Meningiomas: *In Vitro* Study, Clinical Correlation, and Literature Review. *J Neurosurg* (2017) 127:660–9. doi: 10.3171/2016.8.JNS16995
108. Chamberlain MC, Glantz MJ, Fadul CE. Recurrent Meningioma: Salvage Therapy With Long-Acting Somatostatin Analogue. *Neurology* (2007) 69:969–73. doi: 10.1212/01.wnl.0000271382.62776.b7
109. Johnson DR, Kimmel DW, Burch PA, Cascino TL, Giannini C, Wu W, et al. Phase II Study of Subcutaneous Octreotide in Adults With Recurrent or Progressive Meningioma and Meningeal Hemangiopericytoma. *Neuro Oncol* (2011) 13:530–5. doi: 10.1093/neuonc/nor044
110. Hrachova M, Nguyen ENT, Fu BD, Dandekar MJ, Kong XT, Cadena G, et al. A Retrospective Interventional Cohort Study to Assess the Safety and Efficacy of Sandostatin LAR for Treatment of Recurrent and/or Refractory Meningiomas. *Front Neurol* (2020) 11:373. doi: 10.3389/fneur.2020.00373
111. Graillon T, Defilles C, Mohamed A, Lisbonis C, Germanetti AL, Chinot O, et al. Combined Treatment by Octreotide and Everolimus: Octreotide Enhances Inhibitory Effect of Everolimus in Aggressive Meningiomas. *J Neuro-oncol* (2015) 124:33–43. doi: 10.1007/s11060-015-1812-3
112. Shih KC, Chowdhary S, Rosenblatt P, Weir AB 3rd, Shepard GC, Williams JT, et al. A Phase II Trial of Bevacizumab and Everolimus as Treatment for Patients With Refractory, Progressive Intracranial Meningioma. *J Neuro-Oncol* (2016) 129:281–8. doi: 10.1007/s11060-016-2172-3
113. Graillon T, Sanson M, Campello C, Idbaih A, Peyre M, Peyriere H, et al. Everolimus and Octreotide for Patients With Recurrent Meningioma: Results From the Phase II CEVOREM Trial. *Clin Cancer Res* (2020) 26:552–7. doi: 10.1158/1078-0432.CCR-19-2109
114. Koper JW, Zwarthoff EC, Hagemeijer A, Braakman R, Avezaat CJJ, Bergstrom M, et al. Inhibition of the Growth of Cultured Human Meningioma Cells by Recombinant Interferon-Alpha. *Eur J Cancer* (1991) 27:416–9. doi: 10.1016/0277-5379(91)90375-n
115. Chamberlain MC. IFN-Alpha for Recurrent Surgery- and Radiation-Refractory High-Grade Meningioma: A Retrospective Case Series. *CNS Oncol* (2013) 2:227–35. doi: 10.2217/cns.13.17
116. Bi WL, Nayak L, Meredith DM, Driver J, Du Z, Hoffman S, et al. Activity of PD-1 Blockade With Nivolumab Among Patients With Recurrent Atypical/Anaplastic Meningioma: Phase II Trial Results. *Neuro Oncol* (2021) 24 (1):101–13. doi: 10.1093/neuonc/noab118
117. Johnson M, Toms S. Mitogenic Signal Transduction Pathways in Meningiomas: Novel Targets for Meningioma Chemotherapy? *J Neuropathol Exp Neurol* (2005) 64:1029–36. doi: 10.1097/01.jnen.0000189834.63951.81
118. Mawrin C, Sasse T, Kirches E, Kropf S, Schneider T, Grimm C, et al. Different Activation of Mitogen-Activated Protein Kinase and Akt Signaling is Associated With Aggressive Phenotype of Human Meningiomas. *Clin Cancer Res* (2005) 11:4074–82. doi: 10.1158/1078-0432.CCR-04-2550
119. Johnson MD, Reeder JE, O'Connell M. MKP-3 Regulates PDGF-BB Effects and MAPK Activation in Meningioma Cells. *J Clin Neurosci* (2015) 22:752–7. doi: 10.1016/j.jocn.2014.10.030
120. Tuchen M, Wilisch-Neumann A, Daniel EA, Baldauf L, Pachow D, Scholz J, et al. Receptor Tyrosine Kinase Inhibition by Regorafenib/Sorafenib Inhibits Growth and Invasion of Meningioma Cells. *Eur J Cancer* (2017) 73:9–21. doi: 10.1016/j.ejca.2016.12.004
121. Raizer JJ, Grimm SA, Rademaker A, Chandler JP, Muro K, Helenowski I, et al. A Phase II Trial of PTK787/ZK 222584 in Recurrent or Progressive Radiation and Surgery Refractory Meningiomas. *J Neuro-Oncol* (2014) 117:93–101. doi: 10.1007/s11060-014-1358-9
122. Norden AD, Raizer JJ, Abrey LE, Lamborn KR, Lassman AB, Chang SM, et al. Phase II Trials of Erlotinib or Gefitinib in Patients With Recurrent Meningioma. *J Neuro-oncol* (2010) 96:211–7. doi: 10.1007/s11060-009-9948-7
123. Ragel BT, Jensen RL. Aberrant Signaling Pathways in Meningiomas. *J Neuro-oncol* (2010) 99:315–24. doi: 10.1007/s11060-010-0381-8
124. Johnson MD, O'Connell MJ, Pilcher W, Reeder JE. Fibroblast Growth Factor Receptor-3 Expression in Meningiomas With Stimulation of Proliferation by the Phosphoinositide 3 Kinase-Akt Pathway. *J Neurosurg* (2010) 112:934–9. doi: 10.3171/2009.7.JNS09726
125. Choy W, Kim W, Nagasawa D, Stramotas S, Yew A, Gopen Q, et al. The Molecular Genetics and Tumor Pathogenesis of Meningiomas and the Future Directions of Meningioma Treatments. *Neurosurg Focus* (2011) 30: E6. doi: 10.3171/2011.2.FOCUS1116
126. Ippen FM, Colman H, van den Bent MJ, Brastianos PK. Precision Medicine for Primary Central Nervous System Tumors: Are We There Yet? *Am Soc Clin Oncol Educ Book* (2018) 38:158–67. doi: 10.1200/EDBK_199247
127. Brastianos PK, Twohy E, Gerstner ER, Kaufmann TJ, Iafrate AJ, Jeyapalan SA, et al. Alliance A071401: Phase II Trial of FAK Inhibition in Meningiomas With Somatic NF2 Mutations. *J Clin Oncol* (2020) 38:2502–2. doi: 10.1200/JCO.2020.38.15_suppl.2502

Conflict of Interest: AK is a consultant for Monteris Medical and has received research grants from Monteris Medical for a mouse laser therapy study as well as from Stryker and Collagen Matrix for clinical outcomes studies about a dural substitute, which have no direct relation to this study.

The remaining authors declare that the research was conducted in the absence of any commercial or financial relationships that could be construed as a potential conflict of interest.

Publisher's Note: All claims expressed in this article are solely those of the authors and do not necessarily represent those of their affiliated organizations, or those of the publisher, the editors and the reviewers. Any product that may be evaluated in this article, or claim that may be made by its manufacturer, is not guaranteed or endorsed by the publisher.

Copyright © 2022 Patel, Desai, Pugazenthi, Butt, Huang and Kim. This is an open-access article distributed under the terms of the Creative Commons Attribution License (CC BY). The use, distribution or reproduction in other forums is permitted, provided the original author(s) and the copyright owner(s) are credited and that the original publication in this journal is cited, in accordance with accepted academic practice. No use, distribution or reproduction is permitted which does not comply with these terms.

frontiers in Oncology

ORIGINAL RESEARCH
published: 30 March 2022
doi: 10.3389/fonc.2022.848851

Anatomical Study of Arachnoid Granulation in Superior Sagittal Sinus Correlated to Growth Patterns of Meningiomas

Yuanliang Ye[1†], Wen Gao[2†], Weilin Xu[3], Jiangu Gong[4], Minxing Qiu[5], Lang Long[1] and Jiuyang Ding[6*]*

[1] Department of Neurosurgery, Liuzhou People's Hospital, Liuzhou, China, [2] Department of Neurology, Liuzhou People's Hospital, Liuzhou, China, [3] Department of Neurosurgery, Second Affiliated Hospital, School of Medicine, Zhejiang University, Hangzhou, China, [4] Department of Anatomy, Guangxi Medical University, Nanning, China, [5] Department of Pathology, Southern Medical University, Guangzhou, China, [6] School of Forensic Medicine, Guizhou Medical University, Guiyang, China

OPEN ACCESS

Edited by:
Hailiang Tang,
Fudan University, China

Reviewed by:
Subhas K. Konar,
National Institute of Mental Health and Neurosciences (NIMHANS), India
Bharat Guthikonda,
Louisiana State University Health Shreveport, United States

***Correspondence:**
Yuanliang Ye
yeyuanlliangy@163.com
Jiuyang Ding
djy09099@163.com

[†]These authors have contributed equally to this work

Specialty section:
This article was submitted to Neuro-Oncology and Neurosurgical Oncology, a section of the journal Frontiers in Oncology

Received: 05 January 2022
Accepted: 02 March 2022
Published: 30 March 2022

Citation:
Ye Y, Gao W, Xu W, Gong J, Qiu M, Long L and Ding J (2022) Anatomical Study of Arachnoid Granulation in Superior Sagittal Sinus Correlated to Growth Patterns of Meningiomas. Front. Oncol. 12:848851. doi: 10.3389/fonc.2022.848851

Meningiomas in the parasagittal region were formed by arachnoidal cells disseminated among arachnoid granulations. The purpose of this study was to characterize the morphology of chordae willisii, and AGs found in the superior sagittal sinus. This study used 20 anatomical specimens. Rigid endoscopes were introduced *via* torcula herophili into the sinus lumen. The morphological features of arachnoid granulation and chordae willisii were analyzed, and then arachnoid granulations and chordae willisii were assessed by elastic fiber stains, Masson's stains, and imaging analysis. Three types of arachnoid granulations were present in the examined sinuses. There were 365 counts of arachnoid granulations in examined sinuses by imaging analysis, averaging 1.36 ± 2.58 per sinus. Types I, II, and III made up 20.27, 45.20, and 34.52% of 268 patients, respectively. Microscopy of chordae willisii transverse sections indicated the existence of a single layer and a multiple-layered dura sinus wall. The dural sinus wall was the thickest one in the superior sagittal sinus. The thickness of longitudinal lamellae was significantly greater than trabeculae. This study reveals the anatomical differences between arachnoid granulations in the superior sagittal sinus. The arachnoid granulations classification enables surgeons to predict preoperatively growth patterns, followed by safely achieving the optimal range of parasagittal meningioma resection.

Keywords: parasagittal meningioma, arachnoid granulations, endoscopy, chordae willisii, superior sagittal sinus

INTRODUCTION

The parasagittal meningioma (PSM) subgroup comprises 19.5 to 45% of all intracranial meningiomas (1–3). Patients with symptoms are generally treated surgically as there are no effective medical therapies (4, 5). The tendency for these tumors to invade or even encase the superior sagittal sinus (SSS) requires a multimodal treatment approach to reduce the rate of surgical complications (5–7).

Abbreviations: PSM, parasagittal meningioma; SSS, superior sagittal sinus; AG, arachnoid granulation; CW, chordae willisii.

The PSM was derived from arachnoidal cap cells distributed in the arachnoid granulations (AGs) (8). The AG essentially consisted of four components: a central core, cap cell cluster, arachnoid cell layer, and fibrous capsule (9, 10). The AG included a network of arachnoid cells and connective tissue fibers. (11, 12). AG occurs in the subarachnoid space along the arachnoid membrane, extending into the dural venous sinuses (13, 14) and results in different growth patterns of parasagittal meningioma. However, the relationship between AGs and development of parasagittal meningioma has not been established.

Based on the degree of sinus invasion by imaging analysis, PSM has been classified as various types, aiming to choose the best surgical strategy (15, 16). The membranous structure has been recognized as an effective barrier limiting the extension of the tumors (16, 17). The internal membranous structures in the SSS, especially for chordae willisii (CW), including the different types (bands, bridges, chords, lamellar, trabecular, and valve-like lamellae), were visualized and described as they behaved physiologically with the aid of an endoscope (18, 19). Nevertheless, CWs around AGs, which could affect the sinus extension in meningioma, had not been fully characterized.

We used an advanced rigid endoscope in this study to physiologically describe the distribution of AGs and paid attention to CWs in the SSS. Furthermore, we investigated for arachnoid cell and membranous structure in AG by H&E staining, Masson's staining, and elastic fiber staining, aiming to illuminate possible growth patterns of parasagittal meningioma.

MATERIALS AND METHODS

Subjects

At the Guangxi Medical University's Department of Anatomy, 20 anatomical specimens taken during the fresh autopsy were maintained in 10% formalin solution for at least two weeks. Each specimen was over the age of 18 years. This study was approved by the ethics committee of Guangxi Medical University (ID No. KY-2021-007). The following exclusion criteria were used: 1) craniocerebral trauma, 2) neurological illness, and 3) sinus disease. The members of the families signed individual consent permitting the use of resected samples for research.

Endoscope Assessment

There were 12 male and 8 female specimens with the mean age at death of 62 ± 10.33 years (range: 45–80 years). To describe the intraluminal structure in the SSS, the latex was not injected into vein vessels and sinus. The scalps were removed, and by using a surgical power device (Xishan, China), the cranial vault above the axial plane across the nasion and inion was removed. A 4.5-gauge needle was inserted into the SSS, flushing with tap water to remove blood clots. With the cadavers in supine, fixed in Mayfield head holder, an advanced rigid endoscope (Karl Storz, Germany) with a diameter of 4.0 mm and optics of 0 and 30° was inserted into the sinus lumen from the forehead to the coronal. The endoscopes were connected to a digital camera and a video system, enabling photographic recording of the relevant structures. The morphology of the arachnoid granulation and chordae willisii received special attention. Afterward, the SSS samples were carefully removed en bloc using a surgical microscope (OPMI6, Zeiss), and the SSS samples were cut into 1 cm sections from the torcula herophili. AG and its surrounding structures were placed in the observatory area of interest.

Light Microscopy Assessment

Following sectioning, the arachnoid granules and their surrounding structures were prepared for microscopic assessment. To assess those morphological characteristics, H&E staining was used in addition to the particular staining method for detecting collagen fibers (Masson's trichrome) and elastic fibers (Victoria blue). A Zeiss Axioskop plus microscope (Carl Zeiss Microscopy) was used to analyze and document the histological sections at ×50, ×100, and ×400 magnification. Axio Vision software was used to capture and save the images.

MRI-T_2WI Analysis

The research involved 268 patients: 167 men and 191 women. At diagnosis, the mean age was 51.63 ± 12.23 years (range: 34–78 years). In addition to conventional cerebral MR sequences, all of these patients acquired 3D high-resolution volumetric MR images [3D T2-SPACE sequence]. Our institutional review board granted approval for this study. This retrospective examination of medical data and imaging studies did not need written informed permission. Consensual analysis of all MR images was performed by two neuroradiologists. Arachnoid granulation was hyperintense on T2WI, and CWs were isointense. Each case was carefully evaluated to determine the numbers and location. Exclusion criteria included the following: (1) cerebral vascular diseases involved with SSS; (2) intracranial tumor involved with SSS; and (3) image data were incomplete or of poor image quality. As previously described, MRI images were captured (14, 20).

Statistical Analysis

SPSS 22.0 for Windows was used to perform all statistical analyses (SPSS Inc., Chicago, Illinois). Descriptive statistics was used to summarize the categorical data, such as arachnoid granulations and percentages. Means, standard deviations, minimums, and maximums were used to express numerical data. Pearson's chi-square tests were used to determine any statistical difference about proportions. Continuous variables were compared using independent t-test.

RESULTS

Arachnoid Granulation

Endoscopic Observations

Various sizes of AG were presented either single or in a cluster. The endoscopic study showed AGs with different distributions

physiologically that we classified in three types based on their location (**Figure 1**). The first type (type I): the arachnoid granulations were fixed on the lateral wall of the sagittal sinus and faced to the lumen directly (**Figure 1a1**). The second type (type II): AGs were located in the chambers formed by CW and sinus walls; the surface of these AGs was covered with a transparent membrane (**Figure 1a2**). The third type (type III): AGs were demonstrated in the junction between the side and upper walls and protruded into subarachnoid space around the sagittal sinus, attached to an arachnoid tightly (**Figure 1a3**).

Morphological Observations

The arachnoid cell layer encompassing the central core was covered by a fibrous capsule with an endothelial investment. A large number of vacuole-like tissues were present in the neck. The number of arachnoid cells was more in the apical portion compared with that in the central core (**Table 1** and **Figure 2**). The collagen fibers in the junction between AG and the side wall were arranged irregularly. Type I AG has the largest diameter and type II AG has the smallest diameter (**Table 2**).

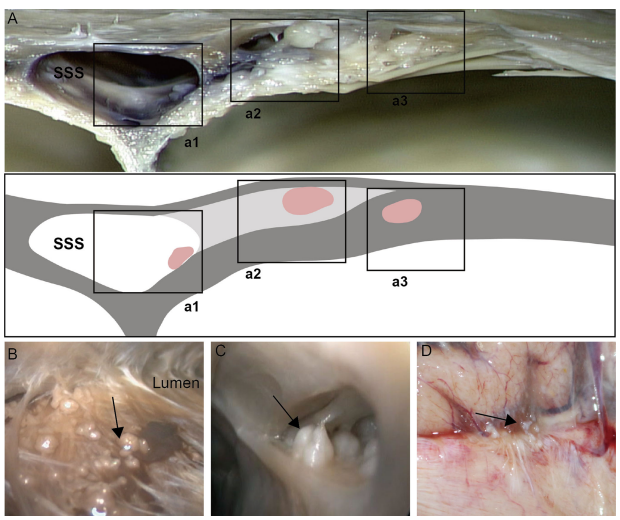

FIGURE 1 | Distribution of arachnoid granulation (black arrow) in cerebral venous sinus. Arachnoid granulation in the lumen **(a1, B)**, lateral sinus **(a2, C)** and subarachnoid space **(a3, D)**.

TABLE 1 | Characteristics of AG, CW and dural wall in the superior sagittal sinus.

Arachnoid cell number in AG subregion	Mean ± SD
Apical portion	87.6 ± 6.58
Central core	11.6 ± 2.41
Neck	8.80 ± 1.92
Bottom	37.80 ± 4.66
CW thickness around AG	mm (Mean ± SD)
trabeculae	0.26 ± 0.19
Valve-like lamellae	0.42 ± 0.36
Longitudinal lamellae	0.73 ± 0.51
Dural wall thickness	mm (Mean ± SD)
Side wall	0.82 ± 0.48
Upper wall	0.92 ± 0.39

Imaging Analysis

With the thin layer MRI scanning, three types of AG in SSS were delineated from normal cerebral tissues with hyper-intensity on T_2WI (**Figures 3A–C**). Longitudinal lamellae and trabeculae were also observed in SSS (**Figures 3D–E**). There were 365 counts of AGs in examined sinuses, averaging 1.36 + 2.58 per SSS. The percent of Types I, II and III was 20.27%, 45.20%, and 34.52% respectively in 268 patients (**Figure 3F** and **Table 1**). There was no difference in the types of AG between female patients and male patients (p=0.352)

Chordae Willisii Around the Arachnoid Granulation

Endoscopic Observations

Various sized chambers were formed by valve-like lamellae, lateral walls, and upper wall in the SSS. Door-like structures were developed by valve-like lamellae, and AGs were located in chambers (**Figure 4A**). The trabeculae could be found either in or outside the chambers and appeared either solitary or in clusters (**Figures 4B–D**). Laminar chordae were also observed around the arachnoid granules, and arachnoid granules were fixed to the sinus wall (**Figures 4E, F**).

Morphological Observations

Chordae willisii around AGs were arranged irregularly. The presence of one layer was revealed with microscopic studies of CW transverse sections and dura sinus wall with multiple layers (**Figures 5A–C**). The thickness of longitudinal lamellae around the AG was the same as the side walls of the SSS and greater than trabeculae or Valve-like lamellae (**Table 1** and **Figure 5D**).

DISCUSSION

This study demonstrated that arachnoid granulations (AGs) were located on the surface of the sinus wall, in the lateral sinus cavity, or the subarachnoid space. Collagen fibers around AGs were disorderly arranged, and CWs around AGs revealed the presence of multiple layers. The anatomical and histological characteristics of AGs could result in different parasagittal meningioma growth patterns.

Structure of AGs

AGs were pseudopodia anatomic structures that protrude into the venous sinuses lumen. AGs were detected by an anatomy and MRI scan. Some studies stated the presence of intrasinus structure in the SSS with the aid of a rigid endoscopy. They found arachnoid granulation protruded from the venous lacuna into the lumen of the SSS. With age, the percentage of patients with AGs in SSS increases significantly and there are no AGs in the dura sinuses regarding numerous individuals of various ages (14). The AGs in the cranial bones were discovered for the first time around the SSS at the age of 10, and their number

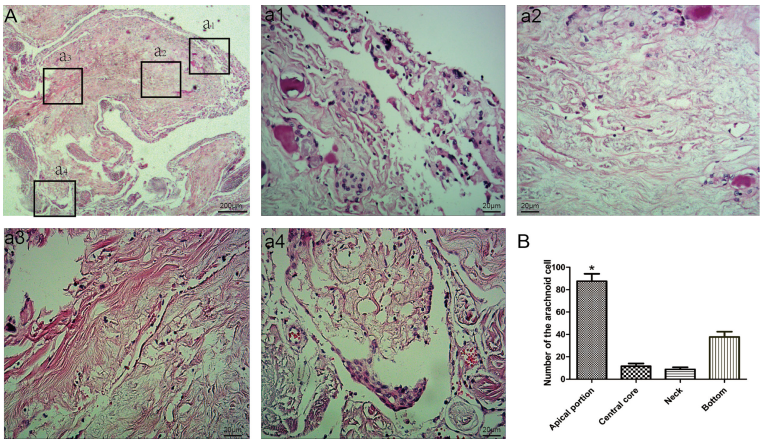

FIGURE 2 | Morphological characteristics of arachnoid granulations. Endothelial cells and arachnoid cells present in the cap cell section (**a1**; HE staining, ×200); Loose connective tissue can be seen in the central core, with a net-like structure (**a2**; HE staining, ×200); Dense connective tissue at the base (**a3**; HE staining, ×200); A large number of vacuole-like tissues present in the neck (**a4**; HE stain, ×200); Comparison of the number of arachnoid cells in different parts; *: means compared with central core, neck and bottom, ($P < 0.05$) **(B)**.

TABLE 2 | Type of AG in cadaveric specimens and 268 patients.

AG Type	AGs by endoscopy No. (%)	AGs by imaging No. (%)	AGs by morphological (mean ± SD, mm)
Type I	33 (16.58)	74 (20.27)	0.75 ± 0.36
Type II	91 (45.73)	165 (45.20)	0.31 ± 0.28
Type III	75 (37.68)	126 (34.52)	0.52 ± 0.26

grows dramatically with time. AGs were more prevalent in the cranial bones than in dura sinuses after the age of 60. Three-dimensional high-resolution magnetic resonance imaging sequences such as T2-weighted sampling perfection with application optimized contrasts using different flip-angle evolution and post-contrast T1-weighted magnetization prepared rapid gradient echo was used to diagnose AGs in our study (21). AGs could be clearly observed by an endoscopy

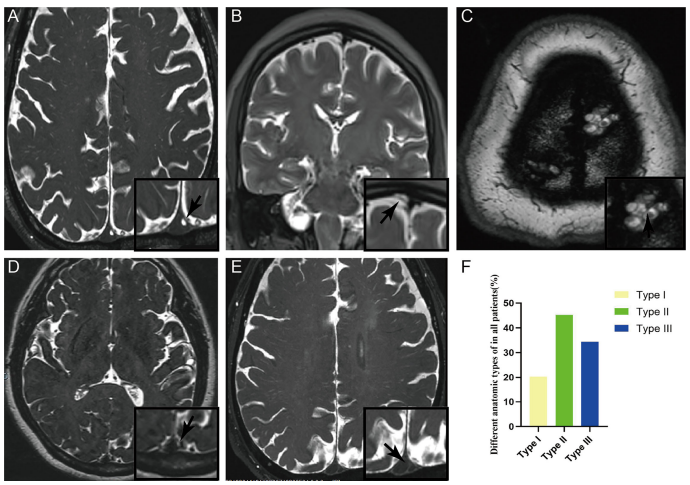

FIGURE 3 | Three types of arachnoid granulation in the superior sagittal sinus were delineated from normal cerebral tissues with hyper-intensity on T2WI. CWs were also present in the lumen of superior sagittal sinus. Arachnoid granulation in the lumen **(A)**, lateral sinus **(B)**, and subarachnoid space **(C)**. Both longitudinal lamellae **(D)** and trabeculae **(E)** in the lumen of superior sagittal sinus. Graphs showing comparisons of the number of type I, type II and type III in the superior sagittal sinus **(F)**.

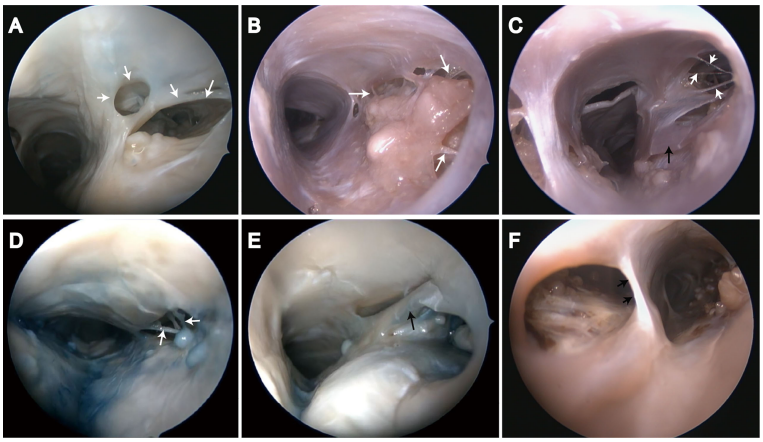

FIGURE 4 | Endoscopic view of chordae willisii around arachnoid granulation in the superior sagittal sinus. **(A)** Valvelike chordae (white arrow); **(B–D)** Trabecular chordae (white arrow); **(E, F)** Longitudinal lamellae (black arrow).

and are divided into three types based on their anatomical position. The three types of AGs were also confirmed on the MRI of normal population.

Many studies focused on the histological characteristics of AGs. AGs were made of four distinct components: a central core, a cap cell cluster, an arachnoid cell layer, and a fibrous capsule (22). The arachnoid cell layer that encircled the central core was mostly covered by a thin fibrous capsule with an endothelial investment. The arachnoid cell layer was thickened in places, forming cap cell clusters (23). The central core is contained by arachnoid cells network mixed with connective tissue fibers. Vimentin was found to be localized to intermediate filaments as determined by ultrastructural immunohistochemistry. Depending on their location, the arachnoid cells showed a marked variety in both the cell forms and the number of intermediate filaments or desmosomes. The ultrastructure of arachnoid cell membranes was also investigated by a conventional transmission electron microscope in human AGs. Arachnoid cells exhibited extensive membrane in granulations, namely, desmosomes, gap junctions, tight junctions, and intermediate junctions (9). The arachnoid cells in AGs are not only densely adherent to form a firm structure for CSF transit, but the arachnoid cells also lining the CSF channel exhibit intensive cell–cell contact (24, 25). Similar to previous studies, AGs refer to a narrow neck, broad body, and wide bottom in the dura. The bottom portion protruding into the dura mater formed

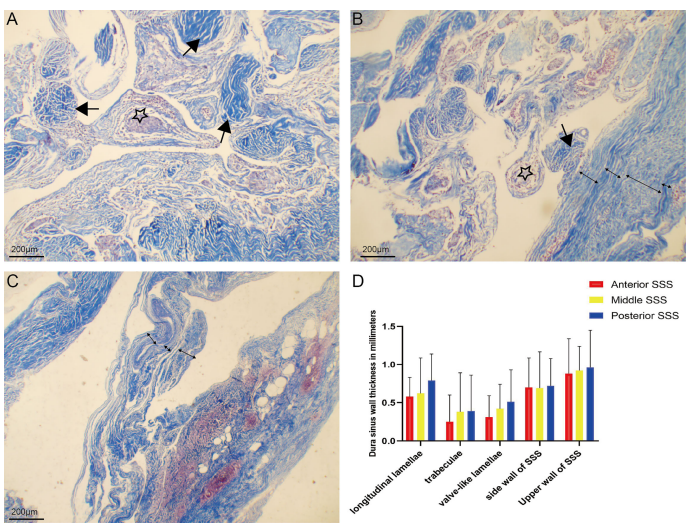

FIGURE 5 | Chordae willisiis around arachnoid granulation were arranged irregularly **(A)**. Chordae willisiis revealed the presence of one layer **(B)**, and dura sinus wall with multiple layers **(C)**. Comparison of thickness of trabecular chordae, longitudinal lamellae, valve-like lamellae and dural sinus wall in the superior sagittal sinus **(D)**.

a single or finger-like dural sheath. We found that type I AGs were larger than type II AGs and the arrangement of collagen fibers in the bottom of type I was more disordered than that of type III. Furthermore, the arachnoid cells were evenly distributed in the body, bottom, and neck.

Chordae Willisii Around the Arachnoid Granulation

The morphological characteristics of CW in the SSS resulted in the classification of CW into three distinct forms: lamellae resembling valves, longitudinal lamellae, and trabeculae. The most prevalent form was valve-like lamellae, whereas the longitudinal lamellae were the least common form (26). CMs were visualized and described with the aid of a rigid endoscopy. They also identified three types of CW in all examined specimens (27, 28). Similar to previous research, they also confirmed that CW was the most common in the parietooccipital region of the SSS and its most common type was the valve-like. The relationship between CW and dura sinus walls was demonstrated, and CW divided the lumen of the dura sinus into two separate parts. The thickness of CWs was variable in different parts of dural sinuses (29). In our study, we paid more attention to CW around AGs. We found that valve-like lamellae were presented in type II AG, trabeculae in type I AG, and longitudinal lamellae in type III AG. The collagen fibers on the sinus wall were loosely arranged in type I AG.

Clinical Significance

Parasagittal meningioma grew inside the dural sinus and may displace or conform to the CW with lumen occlusion without expanding through it (30). The chordae may thus provide a barrier to its spreading into adjacent dura sinus. If the tumor enlarges and extends through CW well behind, the chordae may complicate the process by acting as a barrier to getting behind it and entirely removing the tumor. The dura sinus wall incision, which is often limited to the area where the tumor infiltrates the wall, does not have to provide appropriate exposure, making it necessary for extension behind CW (29). Based on anatomical and histological characteristics of AGs and CWs, we summarize the different growth patterns of PMS (**Figure 6**). The tumors originating from type I AGs grew inside or outside the SSS lateral wall, and tumors outside the sinus wall could completely achieve tumor resection. To ensure venous blood flow in the SSS, tumor protruding into sinus was partially removed. Residual tumor was treated with radiotherapy three months after operation and observed by imaging. The tumor originating from type II AGs grew into the lateral sinus and subdural space. For CWs blocked tumor growth into the sinus lumen, resectioning the tumor on the outside of CW could safely and completely achieve maximum tumor resection. The tumors originating from type III AGs grew into subdural space. The dura mater, which was invaded by the tumor, could also be resected completely.

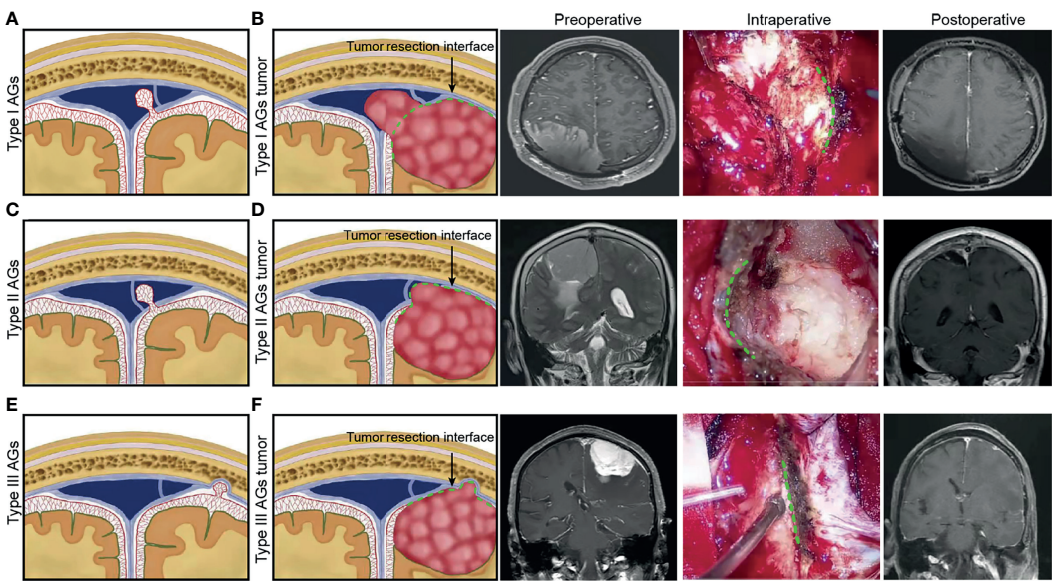

FIGURE 6 | For different anatomical type of arachnoid granulation, schematic diagram illustrating the hypothesized different growth patterns of parasagittal meningioma was presented. Preoperative, intraoperative and postoperative pictures of different types of meningioma were used to illustrate the type of tumor origin and the interface for maximum safe resection of tumors during operation. **(A)** Type I AGs. **(B)** tumor growth patterns of Type I AGs and tumor resection interface (green dotted line) during surgery. **(C)** Type II AGs. **(D)** tumor growth patterns of Type II AGs and tumor resection interface (green dotted line). **(E)** Type III AGs. **(F)** tumor growth patterns of Type III AGs and tumor resection interface (green dotted line).

Limitations

We recognize that our study has a number of limitations. First, cadaveric heads vascular replica did not perfectly reflect the flexibility of intracranial vessels. Second, it makes no recommendations for avoiding intraoperative damage to CWs during tumor removal. Third, it does not identify which part of the tumor invaded the dura mater.

Conclusion

This study uses anatomical and histological techniques to reveal the different anatomical types of AGs. Meanwhile, the morphological structure of CWs around AGs was described. Based on the anatomic characteristics of AG, we speculate the different growth patterns of PMS, which guided the surgeon to remove the tumor safely.

DATA AVAILABILITY STATEMENT

The original contributions presented in the study are included in the article/supplementary material. Further inquiries can be directed to the corresponding authors.

ETHICS STATEMENT

The studies involving human participants were reviewed and approved by the Ethics Committee of Guangxi Medical University. The patients/participants provided their written informed consent to participate in this study.

AUTHOR CONTRIBUTIONS

Conception and design: YY and WG. Acquisition of data: YY. Analysis and interpretation of data: YY, JG, and MQ. Drafting the article: YY, JD, and LL. Statistical analysis: WX. Study supervision: JD. All authors listed have made a substantial, direct, and intellectual contribution to the work and approved it for publication.

FUNDING

This work was supported by the Clinical Research of Liuzhou [grant no. 2021CBB0103], the Clinical Research of Guangxi Autonomous Region (grant no. Z20210107), the Clinical Research of Guangxi Autonomous Region (grant no. Z20200158), the Clinical Research of Liuzhou General Hospital [grant no. LRYGCC202120], the Liuzhou Clinical Research Support Project [2018AF10502] (to YY), the Research Foundation for Advanced Talents of Guizhou Medical University (grant no. University Contract of Doctors J [2021] 014), and the Natural Science Foundation of Guizhou Medical University Incubation Program (grant no. 20NSP084) to JD.

REFERENCES

1. Mathiesen T, Pettersson-Segerlind J, Kihlström L, Ulfarsson E. Meningiomas Engaging Major Venous Sinuses. *World Neurosurg* (2014) 81:116–24. doi: 10.1016/j.wneu.2013.01.095
2. Anthofer J, Seidel-Schulz R, Proescholdt M, Brawanski A, Schebesch KM. Meningiomas Adjacent to Major Venous Sinuses-Clinical Outcome and Recurrence. *World Neurosurg* (2017) 104:560–6. doi: 10.1016/j.wneu.2017.05.025
3. Buerki RA, Horbinski CM, Kruser T, Horowitz PM, James CD, Lukas RV. An Overview of Meningiomas. *Future Oncol* (2018) 14:2161–77. doi: 10.2217/fon-2018-0006
4. Paramasivam N, Hübschmann D, Toprak UH, Ishaque N, Neidert M, Schrimpf D, et al. Mutational Patterns and Regulatory Networks in Epigenetic Subgroups of Meningioma. *Acta Neuropathol* (2019) 138:295–308. doi: 10.1007/s00401-019-02008-w
5. Nassiri F, Liu J, Patil V, Mamatjan Y, Wang JZ, Hugh-White R, et al. A Clinically Applicable Integrative Molecular Classification of Meningiomas. *Nature* (2021) 597:119–25. doi: 10.1038/s41586-021-03850-3
6. Gatterbauer B, Gevsek S, Höftberger R, Lütgendorf-Caucig C, Ertl A, Mallouhi A, et al. Multimodal Treatment of Parasagittal Meningiomas: A Single-Center Experience. *J Neurosurg* (2017) 127:1249–56. doi: 10.3171/2016.9.JNS161859
7. Apra C, Peyre M, Kalamarides M. Current Treatment Options for Meningioma. *Expert Rev Neurother* (2018) 18:241–9. doi: 10.1080/14737175.2018.1429920
8. Mei Y, Bi WL, Greenwald NF, Agar NY, Beroukhim R, Dunn GP, et al. Genomic Profile of Human Meningioma Cell Lines. *PloS One* (2017) 12: e0178322. doi: 10.1371/journal.pone.0178322
9. D'avella D, Cicciarello R, Albiero F, Andrioli G. Scanning Electron Microscope Study of Human Arachnoid Villi. *J Neurosurg* (1983) 59:620–6. doi: 10.3171/jns.1983.59.4.0620
10. Ohnishi Y, Iwatsuki K, Morii E, Kobayashi M, Hori Y, Moriwaki T, et al. Histopathological Study of Spinal Meningioma Originating From the Arachnoid Villi. *Brain Tumor Pathol* (2011) 28:77–81. doi: 10.1007/s10014-010-0003-3
11. Hasegawa M, Yamashima T, Kida S, Yamashita J. Membranous Ultrastructure of Human Arachnoid Cells. *J Neuropathol Exp Neurol* (1997) 56:1217–27. doi: 10.1097/00005072-199711000-00006
12. Kutomi O, Takeda S. Identification of Lymphatic Endothelium in Cranial Arachnoid Granulation-Like Dural Gap. *Microscopy (Oxf)* (2020) 69:391–400. doi: 10.1093/jmicro/dfaa038
13. Umeh R, Loukas M, Oskouian RJ, Tubbs RS. Ectopic Arachnoid Granulation Involving a Rare Intracranial Venous Sinus Variant. *Folia Morphol (Warsz)* (2017) 76:319–21. doi: 10.5603/FM.a2016.0062
14. Radoš M, Živko M, Periša A, Orešković D, Klarica M. No Arachnoid Granulations-No Problems: Number, Size, and Distribution of Arachnoid Granulations From Birth to 80 Years of Age. *Front Aging Neurosci* (2021) 13:698865. doi: 10.3389/fnagi.2021.698865
15. Sindou M. Meningiomas Invading the Sagittal or Transverse Sinuses, Resection With Venous Reconstruction. *J Clin Neurosci* (2001) 8(Suppl 1):8–11. doi: 10.1054/jocn.2001.0868
16. Zeeshan Q, Patel A, Cheng CY, Zhao NH, Barber J, Ghodke BV, et al. Resection of Meningiomas Involving Major Dural Venous Sinuses: Classification, Technique, and Long-Term Results. *World Neurosurg* (2019) 125:e521–36. doi: 10.1016/j.wneu.2019.01.128
17. Song-Tao Q, Xi-An Z, Hao L, Jun F, Jun P, Yun-Tao L. The Arachnoid Sleeve Enveloping the Pituitary Stalk: Anatomical and Histologic Study. *Neurosurgery* (2010) 66:585–9. doi: 10.1227/01.NEU.0000365371.50165.06
18. Ye Y, Ding J, Huang S, Wang Q. Related Structures in the Straight Sinus: An Endoscopic Anatomy and Histological Study. *Front Neuroanat* (2020) 14:573217. doi: 10.3389/fnana.2020.573217

19. Ye Y, Ding J, Liu S, Huang S, Li Z, Yang J, et al. Impacts on Thrombus and Chordae Willisii During Mechanical Thrombectomy in the Superior Sagittal Sinus. *Front Neurol* (2021) 12:639018. doi: 10.3389/fneur.2021.639018
20. Ogul H, Guven F, Izgi E, Kantarci M. Evaluation of Giant Arachnoid Granulations With High-Resolution 3D-Volumetric MR Sequences at 3T. *Eur J Radiol* (2019) 121:108722. doi: 10.1016/j.ejrad.2019.108722
21. Gozgec E, Ogul H, Izgi E, Kantarci M. Tissue Damage in Herniated Brain Parenchyma Into Giant Arachnoid Granulations: Demonstration With High Resolution MRI. *Acta Radiol* (2021) 62:799–806. doi: 10.1177/0284185120941829
22. Takahashi Y, Shigemori M, Inokuchi T, Miyajima S, Maehara T, Wakimoto M, et al. Scanning Electron Microscopic Observations of the Arachnoid Granulations in Monkeys With Cerebrospinal Fluid Hypotension. *Kurume Med J* (1993) 40:201–11. doi: 10.2739/kurumemedj.40.201
23. Adeeb N, Deep A, Griessenauer CJ, Mortazavi MM, Watanabe K, Loukas M, et al. The Intracranial Arachnoid Mater : A Comprehensive Review of its History, Anatomy, Imaging, and Pathology. *Childs Nerv Syst* (2013) 29:17–33. doi: 10.1007/s00381-012-1910-x
24. Vinje V, Eklund A, Mardal KA, Rognes ME, Støverud KH. Intracranial Pressure Elevation Alters CSF Clearance Pathways. *Fluids Barriers CNS* (2020) 17:29. doi: 10.1186/s12987-020-00189-1
25. Proulx ST. Cerebrospinal Fluid Outflow: A Review of the Historical and Contemporary Evidence for Arachnoid Villi, Perineural Routes, and Dural Lymphatics. *Cell Mol Life Sci* (2021) 78:2429–57. doi: 10.1007/s00018-020-03706-5
26. Schmutz HK. The Chordae Willisii in the Superior Sagittal Sinus: Morphology and Classification. *Acta Anat (Basel)* (1980) 108:94–7. doi: 10.1159/000145286
27. Sharifi M, Kunicki J, Krajewski P, Ciszek B. Endoscopic Anatomy of the Chordae Willisii in the Superior Sagittal Sinus. *J Neurosurg* (2004) 101:832–5. doi: 10.3171/jns.2004.101.5.0832
28. Shao Y, Sun JL, Yang Y, Cui QK, Zhang QL. Endoscopic and Microscopic Anatomy of the Superior Sagittal Sinus and Torcular Herophili. *J Clin Neurosci* (2009) 16:421–4. doi: 10.1016/j.jocn.2008.02.024
29. Balik V, Uberall I, Sulla I, Ehrmann J, Kato Y, Sulla IJ, et al. Variability in Wall Thickness and Related Structures of Major Dural Sinuses in Posterior Cranial Fossa: A Microscopic Anatomical Study and Clinical Implications. *Oper Neurosurg (Hagerstown)* (2019) 17:88–96. doi: 10.1093/ons/opy287
30. Mantovani A, Di Maio S, Ferreira MJ, Sekhar LN. Management of Meningiomas Invading the Major Dural Venous Sinuses: Operative Technique, Results, and Potential Benefit for Higher Grade Tumors. *World Neurosurg* (2014) 82:455–67. doi: 10.1016/j.wneu.2013.06.024

Conflict of Interest: The authors declare that the research was conducted in the absence of any commercial or financial relationships that could be construed as a potential conflict of interest.

Publisher's Note: All claims expressed in this article are solely those of the authors and do not necessarily represent those of their affiliated organizations, or those of the publisher, the editors and the reviewers. Any product that may be evaluated in this article, or claim that may be made by its manufacturer, is not guaranteed or endorsed by the publisher.

Copyright © 2022 Ye, Gao, Xu, Gong, Qiu, Long and Ding. This is an open-access article distributed under the terms of the Creative Commons Attribution License (CC BY). The use, distribution or reproduction in other forums is permitted, provided the original author(s) and the copyright owner(s) are credited and that the original publication in this journal is cited, in accordance with accepted academic practice. No use, distribution or reproduction is permitted which does not comply with these terms.

frontiers | Frontiers in Oncology

ORIGINAL RESEARCH
published: 20 April 2022
doi: 10.3389/fonc.2022.836257

A Nicotinamide Phosphoribosyltransferase Inhibitor, FK866, Suppresses the Growth of Anaplastic Meningiomas and Inhibits Immune Checkpoint Expression by Regulating STAT1

*Yuxuan Deng[1], Boyi Hu[2], Yazhou Miao[1], Jing Wang[2], Shaodong Zhang[2], Hong Wan[2], Zhen Wu[1], Yifan Lv[1], Jie Feng[2], Nan Ji[1], Deric Park[3] and Shuyu Hao[1]**

[1] Department of Neurosurgery, Beijing Tiantan Hospital, Capital Medical University, Beijing, China, [2] Beijing Neurosurgical Institute, Capital Medical University, Beijing, China, [3] Department of Neurology, University of Chicago Medical Center, Chicago, IL, United States

Anaplastic meningioma is classified as a World Health Organization (WHO) grade III tumor and shows a strong tendency to recur. Although the incidence of anaplastic meningioma is low, the high rate of recurrence and death still makes treatment a challenge. A proteomics analysis was performed to investigate the differentially expressed proteins between anaplastic meningiomas and fibrous meningiomas by micro-LC-MS/MS. The key metabolic enzyme nicotinamide phosphoribosyltransferase (NAMPT) showed upregulated expression in anaplastic meningiomas. However, targeting NAMPT to treat anaplastic meningiomas has not been reported. *In vitro*, NAMPT inhibitor -FK866 reduced the viability of anaplastic meningiomas by inducing cell cycle arrest at the G2/M phase. Intriguingly, the NAMPT inhibitor -FK866 decreased the protein expression of immune checkpoints PD-L1 and B7-H3 by down-regulating the STAT1 and p-STAT1 expression *in vitro*. Furthermore, FK866 suppressed the growth of anaplastic meningiomas in an *in vivo* xenograft model. The expression of Ki-67 and immune checkpoint proteins (PD-L1 and B7-H3) showed significant differences between the group treated with FK866 and the control group treated with DMSO. In conclusion, the expression of NAMPT, which plays a crucial role in energy metabolism, was upregulated in anaplastic meningiomas. The NAMPT inhibitor -FK866 significantly suppressed the growth of anaplastic meningiomas *in vitro* and *in vivo*. More strikingly, FK866 potently inhibited immune checkpoint protein (PD-L1 and B7-H3) expression by regulating STAT1 *in vitro* and *in vivo*. Our results demonstrated that NAMPT inhibitors could potentially be an effective treatment method for patients suffering from anaplastic meningiomas.

Keywords: anaplastic meningioma, NAMPT, NAMPT inhibitor, immune checkpoint, cell cycle, proteomics

OPEN ACCESS

Edited by:
Hailiang Tang,
Fudan University, China

Reviewed by:
Daniel Paul Heruth,
Children's Mercy Hospital,
United States
Rodney Shackelford,
Ochsner LSU Health, United States
Shu-Na Wang,
Second Military Medical University,
China

***Correspondence:**
Shuyu Hao
shuyuhao@hotmail.com

Specialty section:
This article was submitted to Neuro-Oncology and Neurosurgical Oncology, a section of the journal Frontiers in Oncology

Received: *15 December 2021*
Accepted: *22 March 2022*
Published: *20 April 2022*

Citation:
Deng Y, Hu B, Miao Y, Wang J, Zhang S, Wan H, Wu Z, Lv Y, Feng J, Ji N, Park D and Hao S (2022) A Nicotinamide Phosphoribosyltransferase Inhibitor, FK866, Suppresses the Growth of Anaplastic Meningiomas and Inhibits Immune Checkpoint Expression by Regulating STAT1. Front. Oncol. 12:836257. doi: 10.3389/fonc.2022.836257

INTRODUCTION

Anaplastic meningioma is classified as a World Health Organization (WHO) grade III tumor. The incidence of anaplastic meningioma is low, but the high rate of recurrence and related deaths make treatment a challenge. The 5-year overall survival rate for patients with anaplastic meningioma is 35%–61% (1–3). The treatment strategy is complete tumor resection (4). Radiotherapy approaches are also used for the treatment of anaplastic meningiomas when surgery alone is insufficient (5). However, there is no known effective medical therapy for anaplastic meningiomas (6). Therefore, it is necessary to find a novel therapy for patients with anaplastic meningiomas.

Nicotinamide phosphoribosyltransferase (NAMPT) is an enzyme involved in nicotinamide adenine dinucleotide (NAD) biosynthesis (7). NAD is an important coenzyme for redox reactions, making it central to energy metabolism. Moreover, NAD is a cofactor or substrate for hundreds of enzymes, and it can directly and indirectly influence many key cellular functions, including metabolic pathways, DNA repair, chromatin remodeling, cellular senescence and immune function. Because of the Warburg effect (8), cancer cells need to maintain a redox state and synthesize building blocks to support tumor proliferation and progression, which means they need high levels of NAD. Previous studies have shown that NAD is synthesized from tryptophan, nicotinic acid (NA) and nicotinamide (NM) through three major pathways: the *de novo*, Preiss-Handler, and salvage pathways (9–11) (**Figure 3**). NAMPT is the key rate-limiting enzyme in the salvage pathway.

High levels of NAMPT expression have been observed in many studies (12–15). NAMPT can facilitate tumor initiation and progression and it can induce cancer stem cell-like properties in colon cancer and glioma (15, 16). In breast cancer, NAMPT can facilitate tumor cell proliferation and invasiveness (17). It is also important for prostate cell growth and survival (18). Recent studies have also shown that NAMPT serves as a promoter of an immunosuppressive environment. Travelli et al. found that NAMPT can facilitate the mobilization of immature myeloid-derived suppressor cells (MDSCs), and this mobilization can be suppressed by NAMPT inhibitors (19). Audrito V, et al. found that NAMPT plays an important role in macrophage differentiation to the M2 phenotype and polarization in tumorigenesis-associated macrophages in leukemia (20). In general, NAMPT can promote the progression of tumors and regulate the tumor immune microenvironment.

Given the high turnover of NAD in cancer cells and the fact that NAMPT is the rate-limiting enzyme in the salvage pathway, inhibitors of NAMPT were first reported as possible anticancer agents by Hasmann et al. in 2003 (21). As a kind of small-molecule NAMPT inhibitor, FK866 has shown anticancer activity in several tumor models by depleting NAD levels (21–23). Other studies have shown that FK866 can inhibit the growth of tumors and induce the apoptosis of cancer cells (24, 25). However, the specific anticancer mechanism of FK866 is still unknown in anaplastic meningiomas.

Previous studies have shown that the inhibition of NAMPT expression can dramatically reduce the activation of STAT1 (26). STAT1 performs various important biological functions in normal cells, such as promoting cell death, inhibiting cell growth, stimulating the immune system, and regulating cell differentiation. In tumors, STAT1 is often considered to be a promotor of antitumor activity, but STAT1 induction has also been implicated in cancer progression. For example, STAT1 plays a critical role in mediating IFN-induced PD-L1 transcription in cancer cells (27), blocking T cell activation and causing tumor immune escape.

In this study, we assessed whether NAMPT plays a critical role during the tumorigenesis of anaplastic meningiomas and investigated the potential mechanism by which FK866 suppresses the growth of tumors. We also aimed to determine whether NAMPT regulates the immune checkpoint in anaplastic meningiomas by regulating STAT1.

METHODS

Patients and Specimens

Six patients were diagnosed with fibrous meningiomas and four patients were diagnosed with anaplastic meningiomas. The diagnosis was based on pathological examination. All patients underwent surgery at Beijing Tiantan Hospital, Capital Medical University. Fresh tumor tissue samples from these patients were frozen at − 80°C in isopentane and stored in liquid nitrogen. All tumor tissue samples were used for proteomic analysis. All nine of tumor tissues were used for Western blot analysis and immunohistochemical staining. This study was approved by the Ethics Committees of Beijing Tiantan Hospital (KY2021-158-01). Informed consent was obtained from all enrolled subjects, and the study was performed in full compliance with all principles of the Declaration of Helsinki.

Protein Preparation and Nano-Liquid Chromatography With Tandem Mass Spectroscopy (Micro-LC-MS/MS) Analysis

The workflow of protein preparation and proteomics analysis is shown in **Figure 1**. The protein from tissue samples was extracted with lysis buffer (4% SDS and 100 mM HEPES, pH 7.6). The homogenate was sonicated for 10 min on ice. After centrifugation at 25,000 g for 30 min at 4°C, the supernatant was collected and stored at − 80°C. The total protein concentration was measured with a bicinchoninic acid (BCA) kit (23227, Pierce, Rockford, IL, USA).

Equal protein samples from each of six fibrous meningiomas or four anaplastic meningioma tissues were combined into a single pool, as shown in **Figure 1**. A mass of 200 mg of each pooled sample was reduced using reducing reagent at 60°C for 1h and alkylated with cysteine blocking reagent at room temperature for 10 min as described in the iTRAQ protocol (Applied Biosystems). Trypsin was added to the sample at a mass ratio of 1:50 (enzyme:protein) and incubated at 37°C overnight. The digested samples were labeled with 113 and 116 iTRAQ tags,

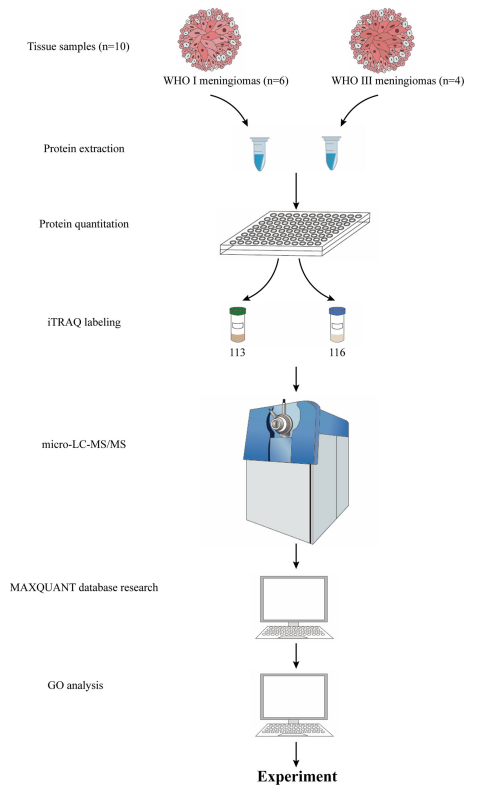

FIGURE 1 | The workflow of proteomic strategy.

respectively, as shown in **Figure 1**, according to the manufacturer's protocol (AB Sciex). The tagged peptides were dried *via* vacuum centrifugation and combined in one tube. The pooled sample was separated on apoly-LC SCX column (4.6 × 250 mm, 5 μm, 100 Å) using an Nexera XR instrument (LC-20ADXR, Shimadzu), and the labeled peptides were detected by ultraviolet radiation using SPD-20A (Shimadzu, Japan). In this study, a total of 55 fractions were collected, dried by speed vacuum centrifugation, and combined into 12 fractions according to the SCX chromatogram. Each fraction was injected onto a desalting column (10 × 0.3 mm, 5 μm-C18, 120 Å) and separated on an analytical column (0.3 × 150 mm, 3μmC18, 120 Å) using an Eksigent microLC instrument (Eksigent, Dublin, CA, USA). The samples separated *via* capillary high-performance liquid chromatography were subsequently analyzed using a Triple TOF 5600+ system (AbSciex, USA).

Protein identification and proteome annotation were performed using the ProteinPilot™ software package 5.0 (Applied Biosystems) and searched against the SwissProt database (March 2020). The following search parameters were utilized to analyze the MS/MS data: trypsin as the digestion enzyme with a maximum of two missed cleavages allowed; fixed modifications of carbamidomethyl (C) and iTRAQPlex (K and N-terminus); variable modifications of oxidation (M); peptide mass tolerance of ±20 ppm; fragment mass tolerance of ±0.1 Da; and peptide FDR ≤ 0.01.

The mass spectrometry proteomics data have been deposited to the ProteomeXchange Consortium (http://proteomecentral.proteomexchange.org) *via* the iProX partner repository (28) with the dataset identifier PXD032342.

Bioinformatics Analysis

The differentially expressed proteins were analyzed *via* enrichment analyses using Gene Ontology (GO) (available at www.geneontology.org) for the identification of associated biological processes and molecular functions.

Cell Culture and Viability Measurement

The anaplastic meningioma cell line (CRL-3370) was obtained from the American Type Culture Collection. The cell culture medium consisted of DMEM supplemented with 10% fetal bovine serum (FBS) (Gibco, USA). The cell line was maintained at 37 °C in a humidified incubator with 5% CO_2.

Cell viability was determined using Cell Counting Kit-8 (CCK-8) (Biosharp, China, BS350B). Briefly, 5mg FK866 (Selleck, USA, S2799) was dissolved in 1.2771 ml dimethyl sulfoxide (DMSO) (Sigma, USA, D2650), then 10 mM FK866 was obtained. Then 10 mM FK866 was diluted with DMSO to obtain 10 μM FK866. After incubation with DMSO or different concentration of FK866 (25μM, 12.5μM, 2.5μM, 0.01μM, 0.005μM) for 24h, 48h or 72 h, 10 μl of CCK-8 reagent was added to each well, and the plates were further incubated in an incubator for 2h. Subsequently, the absorbance was measured at 450 nm by a microplate reader (Biotex, Synergy H1, USA). The cell viability (%) was calculated as follows: (average OD of treated groups at 24, 48 or 72 h/average OD of untreated groups at the same time point) x 100%.

Colony Formation Assay

The indicated cells were digested and resuspended and counted under a microscope. The cells were cultured in 6-cm plates at a density of 500 cells per well. The cells were cultured under normal culture conditions with DMSO or FK866 for 7 days. The supernatant was removed, the cells were fixed with paraformaldehyde, and the cells were dyed with purple crystal. Then, the plates were washed with PBS twice. The whole field of view was photographed and counted. ImageJ (V1.48, NIH, Bethesda, MD, USA) was used for counting and measurement of colony mean size as described earlier (29). In brief, after converting the image to 8-bit format, the threshold was adjusted to exclude the dazzle. Then, colonies were counted and measured using the "Analyze Particles" function.

Western Blot Analysis

Tumor cells were lysed using RIPA buffer with a protease inhibitor cocktail (Millipore Sigma). Lysates were separated by SDS-PAGE (Bio-Rad) and transferred to PVDF membranes. The membranes were probed for NAMPT (Abcam, ab236874), STAT1 (CST, 14994), phosphorylated(p)-STAT1 (CST, 9167), PD-L1 (CST, 13684), B7-H3 (CST, 14058) and β-actin (Abcam, ab20272).

Immunohistochemical Staining

Immunohistochemical staining was performed on consecutive sections from xenograft tumors removed from nude mice treated with vehicle controls and FK866 (5 mg/kg by intraperitoneal (i.p.) injection once per day). The tumor samples were fixed in 10% buffered formalin and embedded in paraffin. The sections cut from paraffin embedded blocks were deparaffinized with xylene and ethanol, and then immersed for 40 min in 10 mM citric acid buffer (pH 6.0) or EDTA antigen retrieval solution (pH 9.0). The activity of endogenous peroxides was quenched for 20 min in 3% H_2O_2 in methanol. After rinsing in PBS, the sections were incubated at 4°C with anti-Ki-67 (Abcam, ab16667), anti-PD-L1 (CST, 13684) and anti-B7-H3 (CST, 14058) antibodies overnight. Then, a brown immunostain was developed using 3,3-diaminobenzidine tetrahydrochloride and hydrogen peroxidase, and counterstained with hematoxylin. The sections were then dehydrated, cleared with xylene and scanned with a digital slice scanning system (Leica, AT2, USA).

Reverse Transcription-Quantitative Polymerase Chain Reaction (RT-qPCR)

Total RNA was isolated from IOMM cell line using QIAzol Lysis Reagent (Qiagen Sciences, Maryland, USA). cDNA was synthesized using a High Capacity cDNA Reverse Transcription Kit (Applied Biosystems, CA, USA). The cDNA was subsequently analyzed using QuantStudio 5 (Applied Biosystems, CA, USA). The amplification program was as follows: initial denaturation step at 95°C for 30 s, followed by 40 cycles at 95°C for 15 s and 60°C for 60 s. The expression of each specific gene was calculated relative to the expression of the internal reference gene GAPDH using the 2–ΔΔCt method. The primer sequences are shown in **Supplementary Table 1**. All assays were performed in triplicate.

Staining With 5-ethynyl-2′-deoxyuridine (Edu)

An EdU (RiboBio, China, C10310-1) assay was used to determine the cell proliferation rate. Cells were seeded in 96-well plates (1×10^3 cells/well) and cultured with DMEM (10% FBS) for 48 h. Then, 100 μl of EdU solution (50 μM) was added to each well and incubated for 2 h at 37°C. Then, the cells were fixed with 4% formaldehyde for 30 min and permeabilized with 0.5% Triton X-100 for 10 min at room temperature. Next the cells were washed with PBS for 5 min and 1X ApolloR reaction cocktail was added to each well (100 μl/well). Thirty minutes later, the cells were incubated with 100 μl Hoechst 33342 for 30 min. Finally, the cells were observed with an inverted microscope (Zeiss, Axio Observer. ZI, USA).

Cell Cycle Assay

The Cell Cycle and Apoptosis Analysis Kit (Biosharp, China, BL114A) was used to detect cell cycle of IOMM cells treated with FK866 or DMSO. The cells were washed with cold PBS, fixed in 70% ethanol, and stored at 4°C for subsequent cell cycle analysis. The fixed cells were washed with PBS once and then re-suspended in 1 mL of PI staining reagent (50 mg/ml propidium iodide and 1 mg/ml RNAse in 1 ml of sodium citrate buffer, pH 7.4). The samples were incubated in the dark for 30 min before cell cycle analysis. The distribution of cells in the cell cycle was measured by an Amnis imaging flow cytometer (ImageStreamX MarkII), and quantitation of cell cycle distribution was performed using FlowJo 10.6.2 Software. The percentages of cells in the G1, S and G2 phases were calculated.

Xenograft Experiments

To construct the subcutaneous tumor xenograft mouse model, 2×10^6 IOMM cells were suspended in 100 μL of solution (PBS) and injected subcutaneously into the right dorsal flank of 6–8-week-old female nude mice. Tumors were allowed to establish until the tumor size was measurable, and then the mice were randomly assigned to be treated for two weeks with vehicle controls or FK866 (5 mg/kg i.p. once per day). The dose of the compound was determined based on previous studies (30–32). FK866 was suspended in 45% propylene glycol + 5% Tween 80 + double distilled H_2O (ddH_2O). Tumor size was measured twice per week by two investigators as follows: tumor size (mm^3) = $[d^2 \text{ x } D]/2$, where d is the shortest diameter and D is the largest diameter. After two weeks of treatments, tumor samples were surgically removed and the tumor weights were measured as a surrogate for tumor burden.

Statistical Analysis

The data obtained from the above experiments were statistically analyzed with SPSS 22.0 software. The measurement data are expressed by as the mean ± standard deviation (SD). T tests were performed to compare the differences between two groups. One-way ANOVA was performed to compare the differences between the three groups. Each experiment was repeated at least 3 times. $P < 0.05$ was considered to be statistically significant.

RESULTS

NAMPT Was Upregulated in Human Anaplastic Meningioma Tissues

In the present study, we explored differentially expressed proteins between fibrous meningioma and anaplastic meningioma tissues by performing a proteomic analysis. In total, 429 differentially expressed proteins were identified. Of these proteins, 352 proteins were upregulated and 77 proteins were downregulated in anaplastic meningioma tissues (with both a P value and false discovery rate (FDR) both < 0.05, with fold change > 1.5 or < 0.67) (**Supplementary Material 2**).

Based on the protein class of Protein Analysis Through Evolutionary Relationships (PANTHER) Classification System in the Gene Oncology (GO) database (www.geneontology.org) (33), all of these differential proteins were classified (**Figure 2**). A large portion of the differentially expressed proteins was involved with metabolite interconversion enzymes (PC00262). A third of the metabolite interconversion enzymes were transferases (PC00220). Of these transferases, 14 proteins were upregulated and 8 proteins were downregulated in anaplastic meningiomas.

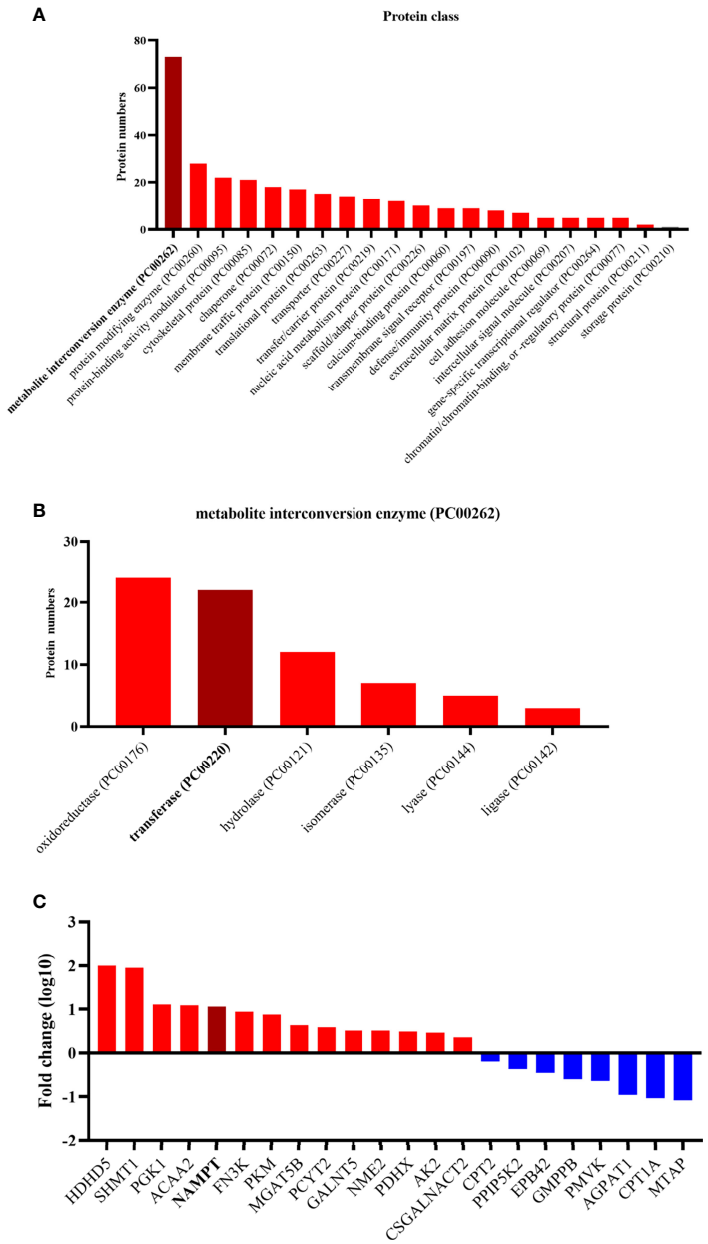

FIGURE 2 | **(A)** The twenty enriched biological processes according to GO analysis. Most of differentially expressed proteins are metabolite interconversion enzymes (PC00262). **(B)** The different functions of the metabolite interconversion enzymes (PC00262). Oxidoreductase (PC00176) and transferase (PC00220) enzymes accounts for more than half of the metabolic interconversion enzymes. **(C)** Diagram listing the transferases related to the differentially expressed proteins. The y-axis represents the fold change, and the x-axis lists the names of transferases. Red represents a high expression level in anaplastic meningiomas, while blue represents a low expression level.

The expression of NAMPT was obviously different between fibrous meningiomas and anaplastic meningiomas.

To validate the differential expression of NAMPT between fibrous meningiomas and anaplastic meningiomas, we detected the protein level of NAMPT in fibrous meningioma samples (n=6) and anaplastic meningiomas samples (n=3) by Western blot analysis. There was a significant difference in NAMPT expression between fibrous meningiomas and anaplastic meningiomas (P=0.0229) (**Figures 3B, C**). The expression of NAMPT was significantly higher in the anaplastic meningioma tissues than in the fibrous meningioma tissues. We also detected the expression of NAMPT in tissues by immunohistochemical staining. There was a significant difference of NAMPT expression between fibrous meningioma tissues and anaplastic

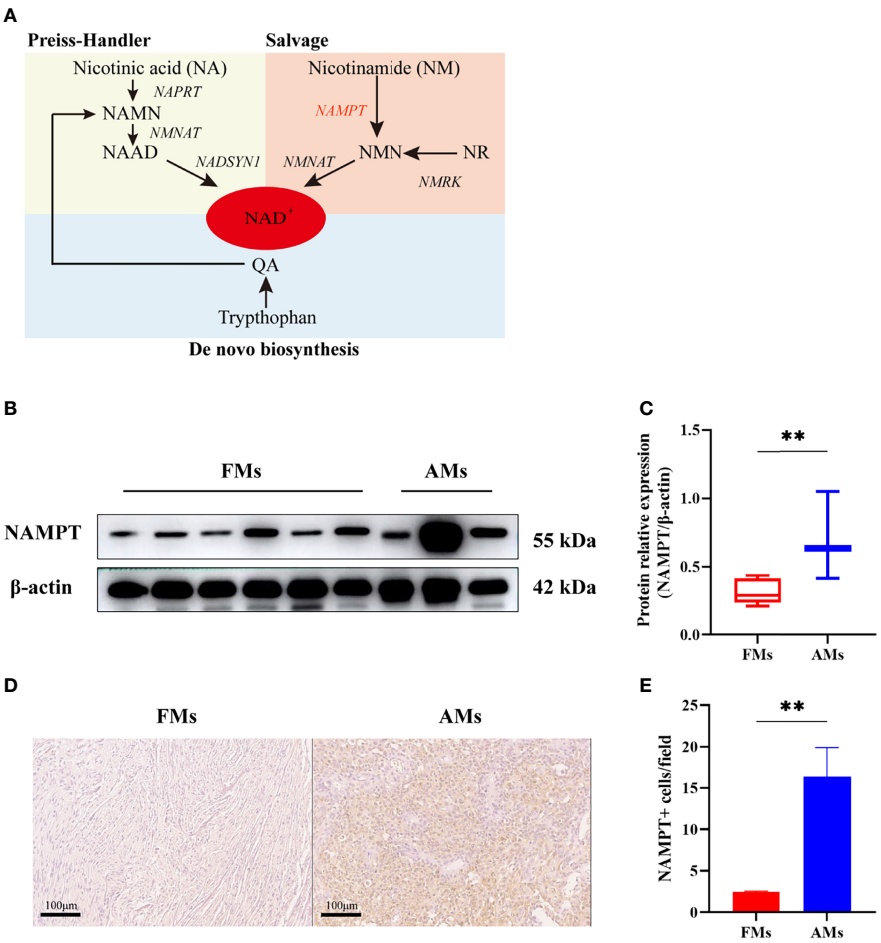

FIGURE 3 | **(A)** NAD is synthesized from tryptophan, nicotinic acid (NA) and nicotinamide (NM) through *de novo*, Preiss-Handler, and salvage pathways. **(B, C)** The relative expression of NAMPT (NAMPT/β-actin) in fibrous meningioma samples (n=6) and anaplastic meningiomas samples (n=3) was detected by Western blotting. **(D, E)** The expression of NAMPT in fibrous meningioma samples and anaplastic meningiomas samples was detected by immunohistochemical staining. FMs: fibrous meningiomas AMs: anaplastic meningiomas. **p < 0.01.

meningioma tissues (P=0.0024) (**Figures 3D, E**). The expression of NAMPT was significantly higher in anaplastic meningiomas than in fibrous meningioma tissues.

The Inhibition of NAMPT by FK866 Suppressed the Proliferation of IOMM Cells *In Vitro*

In this study, the inhibitory effect of FK866 on the viability of IOMM cells was investigated at different concentrations (0-25 μM) (**Figure 4A**). The viability of the IOMM cells was detected at different times (24, 48 and 72 h). A dose-dependent inhibition of cell growth was observed with increasing FK866 concentration at 24, 48 and 72 h. We also thought that a high concentration of FK866 induces toxicity in normal cells. We therefore chose the dose of 2.5 μM in subsequent *in vitro* studies to examine the effect of FK866 on IOMM cells. A significant difference was observed between the DMSO group and the FK866-treated groups at 2.5 μM after 48 h of incubation (p=0.0022) (**Figure 4B**). The effect of FK866 on IOMM proliferation was also detected by colony formation and EdU assays. The colony formation assays revealed that FK866 inhibited colony formation of IOMM cells (**Figure 4C**). Colony numbers were significantly different between the FK866-treated group and DMSO-treated group (p=0.0032) (**Figure 4D**). The results of the EdU assay are shown in **Figures 4E, F**. The number of cells in the proliferative phase was significantly between the FK866-treated group and the DMSO-treated group (p=0.0025). There were fewer cells in the proliferative phase in the FK866-treated group than in the DMSO-treated group. In summary, FK866 inhibited the proliferation of IOMM cells.

The Inhibition of NAMPT Was Effective Against Cell Cycle Progression

To understand how FK866 influenced the proliferation of the IOMM cell line, flow cytometry was used to analyze the effect of FK866 on the cell cycle. The percentage of cells in the G2/M

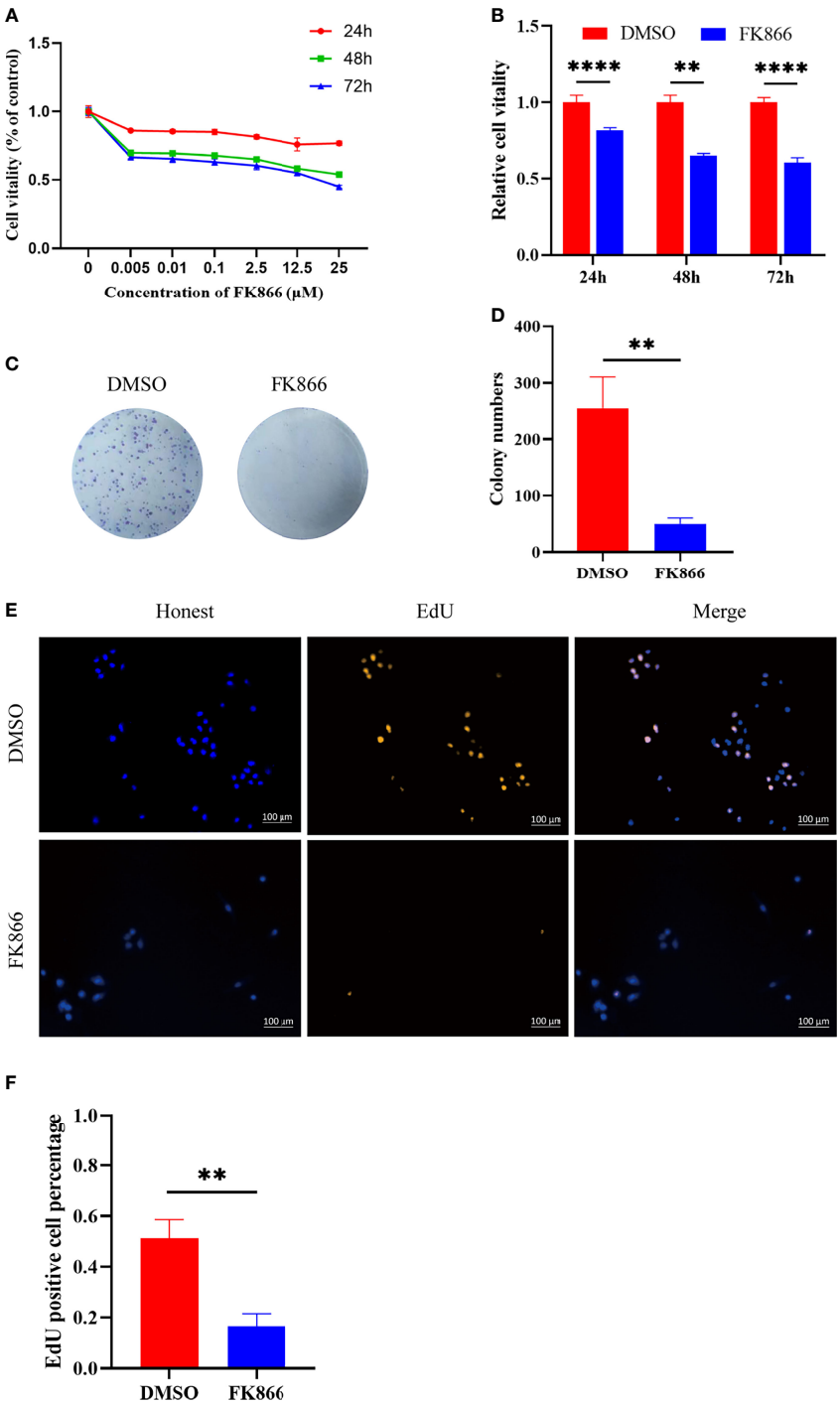

FIGURE 4 | **(A, B)** Inhibitory effects of FK866 on IOMM cells as demonstrated using the CCK-8 assay. The cells were treated with various concentrations of FK866 (0–25 μM) for 24, 48 and 72 h. **(C, D)** The proliferation of IOMM cells treated with FK866 or DMSO was detected by colony formation assay. **(E, F)** Percentage of EdU positive cells among IOMM cells. $^{**}p < 0.01$, $^{****}p < 0.0001$.

phase was significantly different between the FK866-treated group and the DMSO-treated group (p= 0.0025) (**Figures 5A, B**). The proportion of cells in the G2/M phase among FK866-treated IOMM cells had increased. In addition, a significant difference in the number of cells in the S phase was also observed between the FK866-treated group and the DMSO-treated group (p=0.0041) (**Figures 5A, B**). FK866 reduced the number of cells in the S phase.

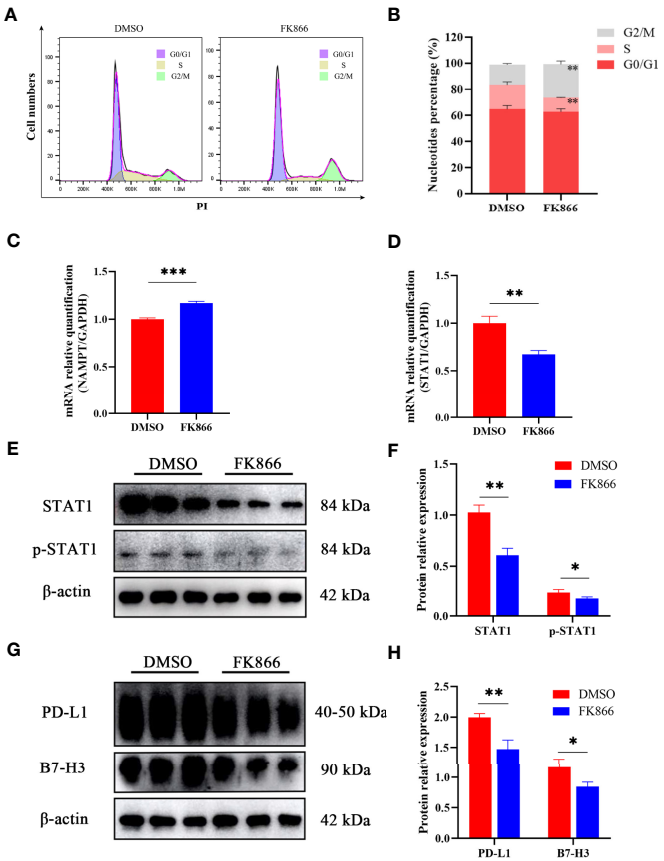

FIGURE 5 | **(A, B)** Distribution of the cell cycle in IOMM cells treated with FK866 or DMSO. **(C, D)** Changes in NAMPT (NAMPT/GAPDH) and STAT1 (STAT1/GAPDH) mRNA relative expression in IOMM cells treated with FK866 or DMSO. **(E, F)** Changes in STAT1 (STAT1/β-actin) and p-STAT1 (p-STAT1/β-actin) protein relative expression in IOMM cells treated with FK866 or DMSO. **(G, H)** Changes in PD-L1 (PD-L1/β-actin) and B7-H3 (B7-H3/β-actin) protein relative expression in IOMM cells treated with FK866 or DMSO. *p < 0.05, **p < 0.01, ***p < 0.001.

The NAMPT Inhibitor-FK866-Suppressed Immune Checkpoint Expression and Proliferation of IOMM Cells by Downregulating the Expression of STAT1

Reverse transcription-quantitative polymerase chain reaction (RT-qPCR) was preformed to detect the mRNA relative expression of NAMPT and STAT1. The results showed that FK866 can elevate the mRNA expression of NAMPT (**Figure 5C**) and reduce the mRNA expression of STAT1 (**Figure 5D**). And the mRNA relative expression of NAMPT and STAT1 showed significant differences between the DMSO group and the FK866 group (p=0.0003 and p=0.0022). Western blotting was preformed to detect the expression of STAT1 and p-STAT1. A significant difference was observed between the DMSO group and the FK866 group (p=0.0019 and p=0.0353) (**Figure 5F**). The results showed that FK866 reduced the expression of STAT1 and p-STAT1 (**Figure 5E**). Intriguingly, STAT1 can promote the expression of the immune checkpoint (PD-L1) (27, 34–36), which can lead to immune escape (26). Therefore, we performed Western blotting to detect the expression of immune checkpoint proteins. The expression of PD-L1 and B7-H3, indeed, showed significant differences between the DMSO group and the FK866 group (p=0.0053 and p=0.0250) (**Figure 5H**). FK866 may decrease the expression of PD-L1 and B7-H3 by downregulating STAT1 and p-STAT1 (**Figure 5G**).

The Small-Molecular Inhibitor of NAMPT, FK866, Inhibited the Growth of Anaplastic Meningiomas and Immune Checkpoint Expression *In Vivo*

To confirm the effect of FK866 on anaplastic meningiomas *in vivo*, we injected IOMM cells to generate an in vivo xenograft model (**Figure 6A**). Mice bearing IOMM subcutaneous xenograft tumors were randomized into two groups: (i) the Control and (ii) FK866 (5 mg/kg) groups (**Figure 6B**). Our results showed that tumor volumes were significantly lower in animals treated with FK866 than in animals treated with DMSO (p<0.0001) (**Figure 6C**). The tumor weight was significantly different between the FK866 group and the Control group

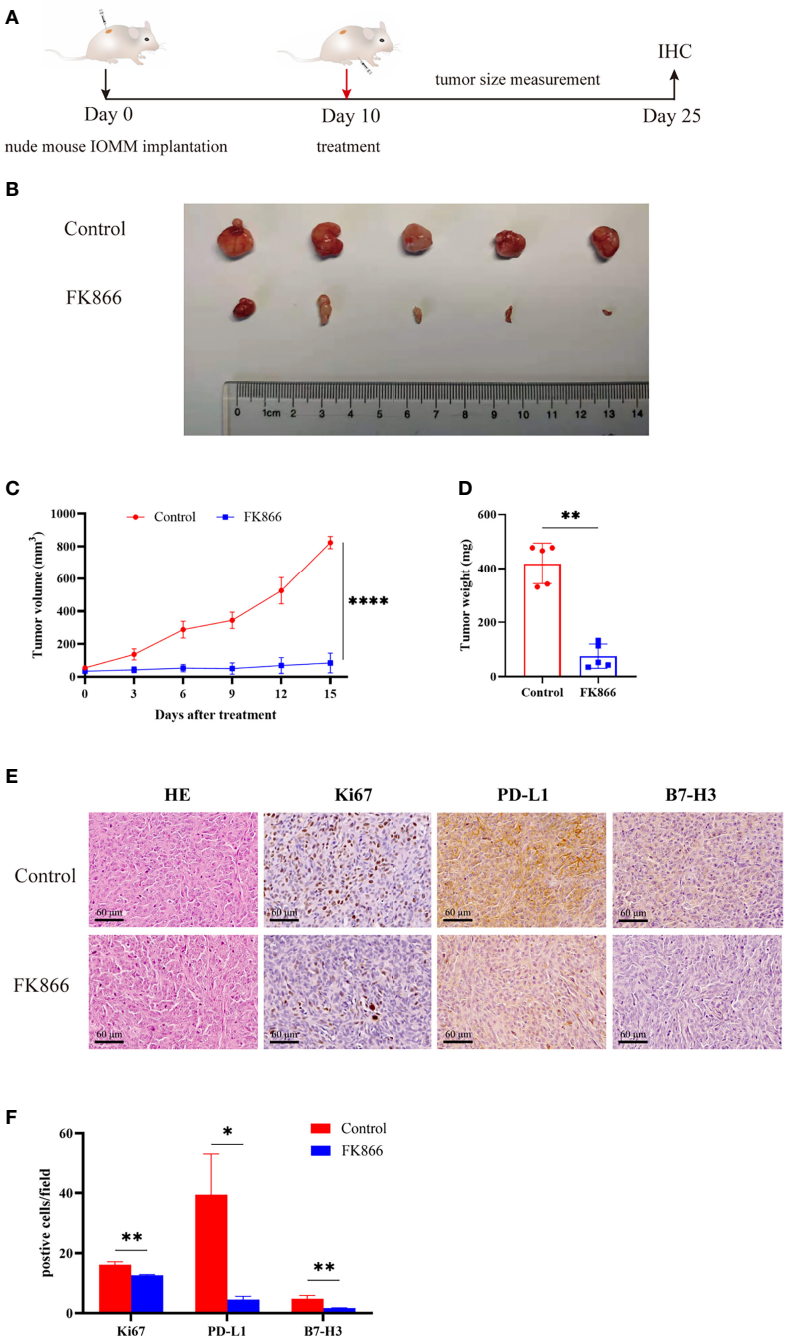

FIGURE 6 | **(A, B)** Mice bearing IOMM meningiomas were treated with intraperitoneal injections of FK866 or DMSO on day 10, and the tumors were collected on day 25 (N=5/group).**(C)** The tumor volume at 3, 6, 9, 12 and 15 days after treatment. Tumor size (mm3) = [d2 x D]/2, d is the shortest diameter and D is the largest diameter. **(D)** The results of tumor weight analysis. **(E, F)** Immunohistochemical staining for Ki-67, PD-L1, B7-H3 in IOMM cell-derived meningiomas treated with DMSO and FK866. *p < 0.05, **p < 0.01, ****p < 0.0001.

(p=0.0079) (**Figure 6D**). Taken together, these results suggested that FK866 can be an effective curative therapy in anaplastic meningiomas. Moreover, changes of Ki-67, PD-L1 and B7-H3 expression *in vivo* were detected by immunohistochemical staining. The expression of Ki-67, PD-L1 and B7-H3 showed significant differences (p=0.0030, p=0.0113 and p=0.0077) (**Figure 6F**). The IOMM meningioma models treated with FK866 had low levels of Ki-67, PD-L1 and B7-H3 expression (**Figure 6E**). This suggested that FK866 can inhibit the growth of tumors and prohibit immune escape.

DISCUSSION

In this study, we used proteomic analysis to identify the differentially expressed proteins between fibrous meningiomas and anaplastic meningiomas. Then, NAMPT was identified as the critical protein during the tumorigenesis of anaplastic meningiomas. As the key rate-limiting enzyme in the salvage pathway of NAD synthesis, NAMPT has recently been shown to be a promoter of cancer (12–14). Sun M. Hong et al. reported that NAMPT can promote the proliferation of colorectal cancer cells (37). Zahra Hesari et al. reported that NAMPT promotes tumor progression and invasion of breast cancer cells (38). NAMPT can also facilitate pancreatic ductal adenocarcinoma cell growth (30). An increasing number of studies have proven that targeting NAMPT can be a feasible strategy for inhibiting tumor progression. However, targeting NAMPT to treat anaplastic meningiomas has not been reported. The NAMPT inhibitor, FK866, has shown anticancer activity in several tumor models (21–23) and has been tested in clinical trials (39). Li-Yuan Zhang et al. reported that FK866 can inhibit cell proliferation and induce G2/M cell-cycle arrest in glioblastoma cells (40), which corresponded to our results. We first validated that NAMPT plays a critical role in the tumorigenesis of anaplastic meningioma and can be a therapeutic target. Therefore, we posited that FK866 can suppress the progression of malignant meningiomas and experiments were performed to validate this assumption. In general, FK866 has a potential therapeutic effect on anaplastic meningiomas.

Previous studies have shown that the inhibition of NAMPT can dramatically reduce the activation of STAT1 (26). We wondered whether a NAMPT inhibitor suppresses the proliferation of IOMM cells by reducing STAT1. The results showed that inhibiting NAMPT by FK866 can reduce the expression of STAT1. The role of STAT1 in cancer is disputed. Most studies have suggested that STAT1 is a tumor suppresser (41). However, STAT1 can promote the progression of tumors in pleural mesothelioma (42), breast cancer (43) and head and neck cancer (44). Hongwei Lv et al. validated results showing that the NAMPT protein can facilitate the expression of STAT1. p-STAT1 expression was reduced in NAMPT-deficient cells or FK866-treated cells (26). In our study, the results showed that FK866 can reduce the expression of STAT1 and inhibit its activation. Intriguingly, a novel study revealed that STAT1 occupies a conserved element within the first intron of NAMPT. By binding this site, STAT1 can promote NAMPT expression in tumor-associated macrophages (45). It seems that there is a positive feedback mechanism involving STAT1 and NAMPT. Further study is needed to determine the relationship between these factors.

Recent studies have shown that NAMPT is a promoter of an immunosuppressive environment. Travelli et al. found that NAMPT can facilitate the mobilization of immature myeloid-derived suppressor cells (MDSCs), which can be suppressed by NAMPT inhibitors (19). Audrito V et al. found that NAMPT plays an important role into macrophage differentiation to the M2 phenotype and polarization into tumorigenesis-associated macrophages in leukemia (20). A number of previous studies have shown that NAMPT affects immune cells in tumors. However, the mechanism by which NAMPT regulates immune molecules in cancer cells needs to be determined. The relationship between NAMPT and immune checkpoints is still confusing. In glioblastoma, NAMPT inhibitors can upregulate PD-L1 in tumor cells, which makes combination therapy with NAMPT inhibitor and blockade of the PD-L1/PD-1 axis more efficient (46). However, Hongwei Lv et al. reported that inhibition of NAMPT reduced PD-L1 expression and that NAMPT deficiency impaired the therapeutic effect of PD-L1 checkpoint blockade on liver cancer in mice, which was further validated in melanoma samples obtained from patients (26). In our study, NAMPT inhibitors were used to suppress the growth of anaplastic meningiomas; at the same time, the expression of PD-L1 and B7-H3 was reduced, which means that FK866 can improve the tumor microenvironment and inhibit immune escape. Further work needs to be performed to determine the mechanism by which FK866 regulates the expression of immune checkpoints. This line of inquiry is important since the results may enable us to improve the efficacy of immune therapy for patients.

There are two major limitations in this study that could be addressed in future research. First, the study focused on the therapeutic effect of NAMPT inhibitor FK866 on anaplastic meningiomas and immune checkpoints expression. However, NAMPT knockdown experiments could be performed to investigate the mechanism about how NAMPT reduced STAT1 and immune checkpoints expression. Second, Although NAMPT was found at proteomic profiling and validated by western-blot and IHC, sample sizes could be increased for proteomic analysis to identify the more differentially expressed proteins at NAD metabolism.

In conclusion, we showed that anaplastic meningiomas have a high level of NAMPT expression, and we inhibited the growth of tumors *in vivo* and *in vitro* by applying an NAMPT inhibitor FK866. Notably, NAMPT inhibitors can reduce PD-L1 and B7-H3 expression in tumor cells, indicating their potential as targeted therapeutics for immune therapy.

DATA AVAILABILITY STATEMENT

The original contributions presented in the study are publicly available. This data can be found here: http://proteomecentral.proteomexchange.org; PXD032342.

ETHICS STATEMENT

The studies involving human participants were reviewed and approved by the Ethics Committees of Beijing Tiantan Hospital (KY2021-158-01). The patients/participants provided their written informed consent to participate in this study. The animal study was reviewed and approved by Animals Welfare Ethics Committees of Beijing Neurosurgical Institute.

AUTHOR CONTRIBUTIONS

Study concept and design: YD and JF. Acquisition of data: YD, BH, YM, and JW. Analysis and interpretation of data: YD and YL. Drafting of the manuscript: YD and JF. Critical revision of the manuscript for important intellectual content: JF, NJ, ZW, and SH. Statistical analysis: YD and BH. Administrative, technical, and material support: YM, JW, SZ, DP, and HW. Study supervision: JF and SH. All authors contributed to the article and approved the submitted version.

FUNDING

This work was supported by grants from the National Natural Science Foundation of China (81872052).

SUPPLEMENTARY MATERIAL

The Supplementary Material for this article can be found online at: https://www.frontiersin.org/articles/10.3389/fonc.2022.836257/full#supplementary-material

REFERENCES

1. Cao X, Hao S, Wu Z, Wang L, Jia G, Zhang L, et al. Survival Rates, Prognostic Factors and Treatment of Anaplastic Meningiomas. *J Clin Neurosci* (2015) 22 (5):828–33. doi: 10.1016/j.jocn.2014.11.022
2. Yang SY, Park CK, Park SH, Kim DG, Chung YS, Jung HW. Atypical and Anaplastic Meningiomas: Prognostic Implications of Clinicopathological Features. *J Neurol Neurosurg Psychiatry* (2008) 79(5):574–80. doi: 10.1136/jnnp.2007.121582
3. Sughrue ME, Sanai N, Shangari G, Parsa AT, Berger MS, McDermott MW. Outcome and Survival Following Primary and Repeat Surgery for World Health Organization Grade III Meningiomas. *J Neurosurg* (2010) 113(2):202–9. doi: 10.3171/2010.1.JNS091114
4. Palma L, Celli P, Franco C, Cervoni L, Cantore G. Long-Term Prognosis for Atypical and Malignant Meningiomas: A Study of 71 Surgical Cases. *J Neurosurg* (1997) 86(5):793–800. doi: 10.3171/jns.1997.86.5.0793
5. Goldbrunner R, Minniti G, Preusser M, Jenkinson MD, Sallabanda K, Houdart E, et al. EANO Guidelines for the Diagnosis and Treatment of Meningiomas. *Lancet Oncol* (2016) 17(9):e383–91. doi: 10.1016/S1470-2045(16)30321-7
6. Giles AJ, Hao S, Padget M, Song H, Zhang W, Lynes J, et al. Efficient ADCC Killing of Meningioma by Avelumab and a High-Affinity Natural Killer Cell Line, Hank. *JCI Insight* (2019) 4(20):1–12. doi: 10.1172/jci.insight.130688
7. Rongvaux A, Shea RJ, Mulks MH, Gigot D, Urbain J, Leo O, et al. Pre-B-Cell Colony-Enhancing Factor, Whose Expression is Up-Regulated in Activated Lymphocytes, is a Nicotinamide Phosphoribosyltransferase, a Cytosolic Enzyme Involved in NAD Biosynthesis. *Eur J Immunol* (2002) 32 (11):3225–34. doi: 10.1002/1521-4141(200211)32:11<3225::AID-IMMU3225>3.0.CO;2-L
8. Vander Heiden MG, Cantley LC, Thompson CB. Understanding the Warburg Effect: The Metabolic Requirements of Cell Proliferation. *Sci (New York N.Y.)* (2009) 324(5930):1029–33. doi: 10.1126/science.1160809
9. Chiarugi A, Dolle C, Felici R, Ziegler M. The NAD Metabolome–a Key Determinant of Cancer Cell Biology. *Nat Rev Cancer* (2012) 12(11):741–52. doi: 10.1038/nrc3340
10. Revollo JR, Grimm AA, Imai S. The NAD Biosynthesis Pathway Mediated by Nicotinamide Phosphoribosyltransferase Regulates Sir2 Activity in Mammalian Cells. *J Biol Chem* (2004) 279(49):50754–63. doi: 10.1074/jbc.M408388200
11. Badawy AA. Kynurenine Pathway of Tryptophan Metabolism: Regulatory and Functional Aspects. *Int J Tryptophan Res* (2017) 10:1178646917691938. doi: 10.1177/1178646917691938
12. Gujar AD, Le S, Mao DD, Dadey DY, Turski A, Sasaki Y, et al. An NAD+-Dependent Transcriptional Program Governs Self-Renewal and Radiation Resistance in Glioblastoma. *Proc Natl Acad Sci USA* (2016) 113(51):E8247–56. doi: 10.1073/pnas.1610921114
13. Ohanna M, Cerezo M, Nottet N, Bille K, Didier R, Beranger G, et al. Pivotal Role of NAMPT in the Switch of Melanoma Cells Toward an Invasive and Drug-Resistant Phenotype. *Genes Dev* (2018) 32(5-6):448–61. doi: 10.1101/gad.305854.117
14. Nacarelli T, Lau L, Fukumoto T, Zundell J, Fatkhutdinov N, Wu S, et al. NAD(+) Metabolism Governs the Proinflammatory Senescence-Associated Secretome. *Nat Cell Biol* (2019) 21(3):397–407. doi: 10.1038/s41556-019-0287-4
15. Lucena-Cacace A, Otero-Albiol D, Jiménez-García MP, Peinado-Serrano J, Carnero A, et al. NAMPT Overexpression Induces Cancer Stemness and Defines a Novel Tumor Signature for Glioma Prognosis. *Oncotarget* (2017) 8 (59):99514–30. doi: 10.18632/oncotarget.20577
16. Lucena-Cacace A, Otero-Albiol D, Jimenez-Garcia MP, Munoz-Galvan S, Carnero A. NAMPT is a Potent Oncogene in Colon Cancer Progression That Modulates Cancer Stem Cell Properties and Resistance to Therapy Through Sirt1 and PARP. *Clin Cancer Res* (2018) 24(5):1202–15. doi: 10.1158/1078-0432.CCR-17-2575
17. Zhang H, Zhang N, Liu Y, Su P, Liang Y, Li Y, et al. Epigenetic Regulation of by Drives Metastatic Progression in Triple-Negative Breast Cancer. *Cancer Res* (2019) 79(13):3347–59. doi: 10.1158/0008-5472.CAN-18-3418
18. Wang B, Hasan MK, Alvarado E, Yuan H, Wu H, Chen WY. NAMPT Overexpression in Prostate Cancer and its Contribution to Tumor Cell Survival and Stress Response. *Oncogene* (2011) 30(8):907–21. doi: 10.1038/onc.2010.468
19. Travelli C, Consonni FM, Sangaletti S, Storto M, Morlacchi S, Grolla AA, et al. Nicotinamide Phosphoribosyltransferase Acts as a Metabolic Gate for Mobilization of Myeloid-Derived Suppressor Cells. *Cancer Res* (2019) 79 (8):1938–51. doi: 10.1158/0008-5472.CAN-18-1544
20. Audrito V, Managò A, Gaudino F, Sorci L, Messana VG, Raffaelli N, et al. NAD-Biosynthetic and Consuming Enzymes as Central Players of Metabolic Regulation of Innate and Adaptive Immune Responses in Cancer. *Front Immunol* (2019) 10:1720–0. doi: 10.3389/fimmu.2019.01720
21. Hasmann M, Schemainda I. FK866, a Highly Specific Noncompetitive Inhibitor of Nicotinamide Phosphoribosyltransferase, Represents a Novel Mechanism for Induction of Tumor Cell Apoptosis. *Cancer Res* (2003) 63 (21):7436–42.
22. Lee J, Kim H, Lee JE, Shin SJ, Oh S, Kwon G, et al. Selective Cytotoxicity of the NAMPT Inhibitor FK866 Toward Gastric Cancer Cells With Markers of the Epithelial-Mesenchymal Transition, Due to Loss of NAPRT. *Gastroenterology* (2018) 155(3):799–+. doi: 10.1053/j.gastro.2018.05.024
23. Ogino Y, Sato A, Uchiumi F, Tanuma S-I. Genomic and Tumor Biological Aspects of the Anticancer Nicotinamide Phosphoribosyltransferase Inhibitor FK866 in Resistant Human Colorectal Cancer Cells. *Genomics* (2019) 111 (6):1889–95. doi: 10.1016/j.ygeno.2018.12.012
24. Kozako T, Aikawa A, Ohsugi T, Uchida YI, Kato N, Sato K, et al. High Expression of NAMPT in Adult T-Cell Leukemia/Lymphoma and Anti-Tumor Activity of a NAMPT Inhibitor. *Eur J Pharmacol* (2019) 865:172738. doi: 10.1016/j.ejphar.2019.172738
25. Schuster S, Penke M, Gorski T, Gebhardt R, Weiss TS, Kiess W, et al. FK866-Induced NAMPT Inhibition Activates AMPK and Downregulates Mtor Signaling in Hepatocarcinoma Cells. *Biochem Biophys Res Commun* (2015) 458(2):334–40. doi: 10.1016/j.bbrc.2015.01.111
26. Lv H, Lv G, Chen C, Zong Q, Jiang G, Ye D, et al. NAD(+) Metabolism Maintains Inducible PD-L1 Expression to Drive Tumor Immune Evasion. *Cell Metab* (2021) 33(1):110–127 e5. doi: 10.1016/j.cmet.2020.10.021
27. Garcia-Diaz A, Shin DS, Moreno BH, Saco J, Escuin-Ordinas H, Rodriguez GA, et al. Interferon Receptor Signaling Pathways Regulating PD-L1 and PD-L2 Expression. *Cell Rep* (2017) 19(6):1189–201. doi: 10.1016/j.celrep.2017.04.031
28. Ma J, Chen T, Wu S, Yang C, Bai M, Shu K, et al. Iprox: An Integrated Proteome Resource. *Nucleic Acids Res* (2019) 47(D1):D1211–7. doi: 10.1093/nar/gky869

29. Rajendran V, Jain MV. *In Vitro* Tumorigenic Assay: Colony Forming Assay for Cancer Stem Cells. *Methods Mol Biol (Clifton N.J.)* (2018) 1692:89–95.
30. Ju H-Q, Zhuang Z-N, Li H, Tian T, Lu Y-X, Fan X-Q, et al. Regulation of the Nampt-Mediated NAD Salvage Pathway and its Therapeutic Implications in Pancreatic Cancer. *Cancer Lett* (2016) 379(1):1–11. doi: 10.1016/j.canlet.2016.05.024
31. Bajrami I, Kigozi A, Van Weverwijk A, Brough R, Frankum J, Lord CJ, et al. Synthetic Lethality of PARP and NAMPT Inhibition in Triple-Negative Breast Cancer Cells. *EMBO Mol Med* (2012) 4(10):1087–96. doi: 10.1002/emmm.201201250
32. Daniels VW, Zoeller JJ, van Gastel N, McQueeney KE, Parvin S, Potter DS, et al. Metabolic Perturbations Sensitize Triple-Negative Breast Cancers to Apoptosis Induced by BH3 Mimetics. *Sci Signaling* (2021) 14(686):1–30. doi: 10.1126/scisignal.abc7405
33. Gene Ontology C. The Gene Ontology Resource: Enriching a Gold Mine. *Nucleic Acids Res* (2021) 49(D1):D325–34.
34. Loke P.n., Allison JP. PD-L1 and PD-L2 are Differentially Regulated by Th1 and Th2 Cells. *Proc Natl Acad Sci USA* (2003) 100(9):5336–41. doi: 10.1073/pnas.0931259100
35. Chen S, Crabill GA, Pritchard TS, McMiller TL, Wei P, Pardoll DM, et al. Mechanisms Regulating PD-L1 Expression on Tumor and Immune Cells. *J Immunother Cancer* (2019) 7(1):305–5. doi: 10.1186/s40425-019-0770-2
36. Sasidharan Nair V, Toor SM, Ali BR, Elkord E. Dual Inhibition of STAT1 and STAT3 Activation Downregulates Expression of PD-L1 in Human Breast Cancer Cells. *Expert Opin Ther Targets* (2018) 22(6):547–57. doi: 10.1080/14728222.2018.1471137
37. Hong SM, Hwang SW, Wang T, Park CW, Ryu Y-M, Jung J-H, et al. Increased Nicotinamide Adenine Dinucleotide Pool Promotes Colon Cancer Progression by Suppressing Reactive Oxygen Species Level. *Cancer Sci* (2019) 110(2):629–38. doi: 10.1111/cas.13886
38. Hesari Z, Nourbakhsh M, Hosseinkhani S, Abdolvahabi Z, Alipour M, Tavakoli-Yaraki M, et al. Down-Regulation of NAMPT Expression by Mir-206 Reduces Cell Survival of Breast Cancer Cells. *Gene* (2018) 673:149–58. doi: 10.1016/j.gene.2018.06.021
39. Yaku K, Okabe K, Hikosaka K, Nakagawa T. NAD Metabolism in Cancer Therapeutics. *Front Oncol* (2018) 8:622. doi: 10.3389/fonc.2018.00622
40. Zhang LY, Liu LY, Qie LL, Ling KN, Xu LH, Wang F, et al. Anti-Proliferation Effect of APO866 on C6 Glioblastoma Cells by Inhibiting Nicotinamide Phosphoribosyltransferase. *Eur J Pharmacol* (2012) 674(2-3):163–70. doi: 10.1016/j.ejphar.2011.11.017
41. Kovacic B, Stoiber D, Moriggl R, Weisz E, Ott RG, Kreibich R, et al. STAT1 Acts as a Tumor Promoter for Leukemia Development. *Cancer Cell* (2006) 10(1):77–87. doi: 10.1016/j.ccr.2006.05.025
42. Arzt L, Kothmaier H, Halbwedl I, Quehenberger F, Popper HH. Signal Transducer and Activator of Transcription 1 (STAT1) Acts Like an Oncogene in Malignant Pleural Mesothelioma. *Virchows Arch* (2014) 465(1):79–88. doi: 10.1007/s00428-014-1584-8
43. Greenwood C, Metodieva G, Al-Janabi K, Lausen B, Alldridge L, Leng L, et al. Stat1 and CD74 Overexpression is Co-Dependent and Linked to Increased Invasion and Lymph Node Metastasis in Triple-Negative Breast Cancer. *J Proteomics* (2012) 75(10):3031–40. doi: 10.1016/j.jprot.2011.11.033
44. Khodarev NN, Beckett M, Labay E, Darga T, Roizman B, Weichselbaum RR. STAT1 is Overexpressed in Tumors Selected for Radioresistance and Confers Protection From Radiation in Transduced Sensitive Cells. *Proc Natl Acad Sci USA* (2004) 101(6):1714–9. doi: 10.1073/pnas.0308102100
45. Huffaker TB, Ekiz HA, Barba C, Lee SH, Runtsch MC, Nelson MC, et al. A Stat1 Bound Enhancer Promotes Nampt Expression and Function Within Tumor Associated Macrophages. *Nat Commun* (2021) 12(1):1–19. doi: 10.1038/s41467-021-22923-5
46. Li M, Kirtane AR, Kiyokawa J, Nagashima H, Lopes A, Tirmizi ZA, et al. Local Targeting of NAD(+) Salvage Pathway Alters the Immune Tumor Microenvironment and Enhances Checkpoint Immunotherapy in Glioblastoma. *Cancer Res* (2021) 81(7):1922. doi: 10.1158/0008-5472.CAN-21-0525

Conflict of Interest: The authors declare that the research was conducted in the absence of any commercial or financial relationships that could be construed as a potential conflict of interest.

Publisher's Note: All claims expressed in this article are solely those of the authors and do not necessarily represent those of their affiliated organizations, or those of the publisher, the editors and the reviewers. Any product that may be evaluated in this article, or claim that may be made by its manufacturer, is not guaranteed or endorsed by the publisher.

Copyright © 2022 Deng, Hu, Miao, Wang, Zhang, Wan, Wu, Lv, Feng, Ji, Park and Hao. This is an open-access article distributed under the terms of the Creative Commons Attribution License (CC BY). The use, distribution or reproduction in other forums is permitted, provided the original author(s) and the copyright owner(s) are credited and that the original publication in this journal is cited, in accordance with accepted academic practice. No use, distribution or reproduction is permitted which does not comply with these terms.

frontiers | Frontiers in Oncology

ORIGINAL RESEARCH
published: 10 May 2022
doi: 10.3389/fonc.2022.866225

Surgical Management of Falcotentorial Junction Tumors: A Case Series Report

Peixi Liu[1,2,3,4,5†], *Xiaowen Wang*[1,2,3,4,5†], *Yingjun Liu*[1,2,3,4,5†], *Jiajun Cai*[1,2,3,4,5], *Zixiao Yang*[1,2,3,4,5], *Kai Quan*[1,2,3,4,5], *Wei Zhu*[1,2,3,4,5] *and Jianping Song*[1,2,3,4,5*]

[1] Department of Neurosurgery, Huashan Hospital, Shanghai Medical College, Fudan University, Shanghai, China, [2] National Center for Neurological Disorders, Fudan University, Shanghai, China, [3] Shanghai Key Laboratory of Brain Function and Restoration and Neural Regeneration, Fudan University, Shanghai, China, [4] Neurosurgical Institute, Fudan University, Shanghai, China, [5] Shanghai Clinical Medical Center of Neurosurgery, Fudan University, Shanghai, China

OPEN ACCESS

Edited by:
Hailiang Tang,
Fudan University, China

Reviewed by:
Joao Paulo Almeida,
Mayo Clinic Florida, United States
Xiaochun Zhao,
University of Oklahoma Health Sciences Center, United States

***Correspondence:**
Jianping Song
neurosurgerysong@foxmail.com

†These authors have contributed equally to this work and share first authorship

Specialty section:
This article was submitted to Neuro-Oncology and Neurosurgical Oncology, a section of the journal Frontiers in Oncology

Received: *31 January 2022*
Accepted: *22 March 2022*
Published: *10 May 2022*

Citation:
Liu P, Wang X, Liu Y, Cai J, Yang Z, Quan K, Zhu W and Song J (2022) Surgical Management of Falcotentorial Junction Tumors: A Case Series Report. Front. Oncol. 12:866225. doi: 10.3389/fonc.2022.866225

Objective: The surgical strategy for falcotentorial junction tumors remains complex. Different approaches are selected according to the location and growth pattern of the tumor and the operator's experience. This report reviews our single-institution experience in the surgical management of falcotentorial junction tumors.

Methods: We retrospectively reviewed the clinical and imaging data, surgical strategy, and follow-up outcomes of 49 patients treated from 2007 to 2020.

Result: All 49 patients (12 male, 37 female, mean age: 56.3 ± 11.3 years) underwent safe tumor resection. The most common complaints were headache (43%), dizziness (39%), and unstable gait (16%). Thirty percent of the tumors showed calcification, and the computed tomography scans revealed hydrocephalus in 36% of the patients. On magnetic resonance imaging, 43% of the tumors were unilateral. According to the Asari classification, the tumors were divided into inferior (16%), superior (29%), anterior (22%), and posterior (33%) types. The occipital interhemispheric approach (88%) and supracerebellar–infratentorial approach (10%) were primarily used to reach the tumors. The pathology examination results revealed that 85.7% of the tumors were meningioma and 14.3% were hemangiopericytoma. Of the 49 patients, 15 achieved a Simpson grade I resection, and 29 achieved a Simpson grade II resection. The follow-up rate was 77.6% (38/45); 94.7% of patients (36/38) achieved a favorable outcome, and 9 experienced tumor recurrences.

Conclusion: Surgical approach selection depends on the growth characteristics of the tumor and the degree of venous or sinus involvement. The occipital interhemispheric

approach is the most commonly used and safest approach for falcotentorial junction tumors with multiple brain pressure control assistance techniques.

Keywords: falcotentorial, hemangiopericytoma, meningioma, surgery, hybrid operation

INTRODUCTION

Falcotentorial junction tumors are located at the anterior portion of the junction between the falx and the tentorium (1–3). Rare falcotentorial junction tumors, such as meningiomas or hemangiopericytoma, are substantial surgical challenges due to their deep location and the presence of adjacent critical neurovascular structures. Different approaches can be selected according to the location and growth pattern of the tumor and operator preference (3–10). This study reviews our center's experience in the surgical management of falcotentorial junction tumors.

METHODS

Patient Cohort

The authors retrospectively reviewed the medical charts from our hospital's main campus from June 2007 to April 2020 and roughly identified a total of 131 clinical cases of potential falcotentorial junction tumors. By carefully reviewing the clinical data and radiological images and excluding "peritorcular" tumors with torcular involvement or velum interpositum meningiomas (1–3, 11, 12), 49 patients with comprehensive medical data were enrolled in this study. The institutional review board of the authors' hospital approved this study. The STROBE guidelines for observational cohort studies were followed. Due to the retrospective nature of the study, informed consent was waived.

The age, sex, clinical presentation, radiological findings, tumor location, surgical details, pathology, postoperative complications, surgical outcome, and follow-up data of the patients were collected and analyzed. The classic Asari classification, including inferior, superior, anterior, and posterior typing, was used to define the tumor location (13). There were four types. The anterior type means the tumor extension between the inferior sagittal sinus and the great vein of Galen). The inferior type means the tumor extension between the great vein of Galen and the straight sinus. The posterior type means the tumor extension along the straight sinus, and the superior type means the tumor extension above the cerebellar tentorium.

The Simpson grade was used to assess the extent of the resection. CT scanning was completed at 1 month after surgery. The MRI contrast was completed at 6 months after surgery. After that, if there was nothing special, a follow-up MRI contrast was required annually. Patient follow-up was conducted at the outpatient clinic or by telephone interview, and the recurrence rate and outcome were assessed. The modified Rankin Scale (mRS) score was used to quantify the outcome, in which a favorable outcome was defined as mRS ≤2.

Literature Review

The authors performed a literature search on PubMed for articles on falcotentorial junction tumors published in English in the last 10 years. The search strategy was as follows: "(falcotentorial meningioma) OR (pineal region meningioma) [Allfield]". A total of 68 results were retrieved; after reading their full texts, seven articles describing case series reports (more than 5 cases) were included for the literature review.

Statistical Analysis

Statistical analysis was performed using SPSS 22.0 (IBM, USA). Numerical variables are presented as the mean ± standard deviation (range). A p-value <0.05 was set as the threshold of significance.

RESULTS

Clinical Characteristics

The clinical characteristics of all 49 patients with falcotentorial junction tumors are summarized in **Table 1** (more detailed information can be found in the **Supplementary Table**). There were 12 males (24.5%) and 37 females (75.5%) in our series, aged 33 to 81 years (mean, 56.3 ± 11.3 years). The chief complaints were nonspecific symptoms such as headache (n = 21, 42.9%) and dizziness (n = 19, 38.8%), followed by unstable gait (n = 8, 16.3%), blurred vision (n = 5, 10.2%), limb weakness (n = 4, 8.2%), facial numbness (n = 2, 4.1%), and seizures (n = 1, 2.0%). Some lesions were found accidentally (n = 6, 12.2%).

All patients were preliminarily diagnosed with meningioma preoperatively. The computerized tomography (CT) results showed 15 patients (30.6%) with calcification inside the tumor and 18 (36.7%) with hydrocephalus. On magnetic resonance imaging (MRI), the tumor was unilateral in 21 patients (42.9%) and bilateral in 28 (57.1%). According to the Asari classification, 8 tumors (16.3%) were of the inferior type, 14 (28.6%) were of the superior type, 11 (22.5%) were of the anterior type, and 16 (32.7%) were of the posterior type. The magnetic resonance venography (MRV) revealed a straight sinus occlusion rate of 79.6%.

Surgical Strategy

In terms of surgical approach selection, the occipital interhemispheric approach (OIA, n = 43 87.8%) and supracerebellar–infratentorial approach (SCITA, n = 5, 10.2%) were mainly used. Only 1 tumor was resected by the subtemporal approach (2.0%, **Figure 1**). Three patients (12.2%; cases 6, 46, and 47) underwent preoperative external ventricular drainage, and 1 patient (2.0%, case 48; **Figure 3**) underwent preoperative tumor embolization.

TABLE 1 | Clinical characteristics of patients with falcotentorial junction tumors.

Clinical characteristics	Value
Age (mean)	56.3 ± 11.3 years
Sex	
Male	12 (24.5%)
Female	37 (75.5%)
Clinical presentation	
Headache	21 (42.9%)
Dizziness	19 (38.8%)
Unstable gait	8 (16.3%)
Accidentally found	6 (12.2%)
Blurred vision	5 (10.2%)
Limb weakness	4 (8.2%)
Others	3 (6.1%)
Laterality	
Unilateral	21 (42.9%)
Bilateral	28 (57.1%)
Asari types	
Anterior	11 (22.5%)
Inferior	8 (16.3%)
Posterior	16 (32.7%)
Superior	14 (28.6%)
Straight sinus occlusion	
Yes	39 (79.6%)
No	10 (20.4%)
Preoperative GOS ≥4	49 (100%)
Surgical approach	
Occipital interhemispheric approach	43 (87.8%)
Supracerebellar–infratentorial approach	5 (10.2%)
Subtemporal approach	1 (2.0%)
Surgical results (Simpson grade)	
Simpson I	15 (30.6%)
Simpson II	29 (59.2%)
Simpson III	1 (2.0%)
Simpson IV	4 (8.2%)
Major postoperative complications	
Hydrocephalus	2 (4.1%)
Brain contusion	2 (4.1%)
Pathology	
Meningioma	42 (85.7%)
Fibrous type, WHO grade I	28 (57.1%)
Epithelial type, WHO grade I	12 (24.5%)
Angiomatous type, WHO grade I	1 (2.0%)
Transitional type, WHO grade I	1 (2.0%)
Hemangiopericytoma	7 (14.3%)
WHO grade I	1 (2.0%)
WHO grade II	3 (6.1%)
WHO grade III	3 (6.1%)
Follow-up	38 (77.6%)
Recurrence	9 (23.7%)
mRS ≤2	36 (94.7%)
mRS >2	2 (5.3%)[a]

mRS, modified Rankin Scale; WHO, World Health Organization.
[a]*Including case 18 who passed away naturally in year 2015.*

Surgical Outcome and Follow-Up

Gross total resection (Simpson grades I and II resection) was achieved in 44 (89.8%) surgeries; Simpson grades III and IV resections were achieved in 1 (2.0%) and 4 (8.2%) surgeries, respectively. For those patients with a diagnosis of hemangiopericyma, preoperative embolization may be helpful to reduce the blood supply in these cases. We have adopted such a strategy in recent clinical practice. All the patients with WHO II or beyond accepted radiotherapy after operation. The major postoperative complications were hydrocephalus treated by a V–P shunt (n = 2, 4.1%) and visual field impairment caused by contusion (n = 2, 4.1%). The pathology examination results confirmed a diagnosis of meningioma for 42 patients (85.7%) and hemangiopericytoma for 7 patients (14.3%). The mean follow-up time was 82.1 ± 39.9 months (15 to 169 months). The follow-up rate was 77.6% (38/49). Nine patients (23.7%) were found to have tumor recurrence in these followed-up patients. The pathology for 2 patients was hemangiopericytoma (WHO II), and the other 7 patients had meningioma (WHO I). No case reached Simpson I resection during the operation. Five cases reached Simpson II resection, and 1 case reached Simpson III resection. The other 3 cases were Simpson IV during operation. In total, 94.7% cases (36/38) achieved a favorable outcome.

Literature Review

In the retrieved literature, the OIA or its modifications (occipital transtentorial approach, parieto-occipital, occipito-suboccipital) were the preferred approach for falcotentorial junction tumors (85.7%). Visual field impairment and hydrocephalus requiring shunting were the major surgical complications. The pathology examination results typically led to a diagnosis of meningioma, and most of the patients achieved a favorable outcome.

Case Illustration

Case 1

A 52-year-old man complained of blurred vision and unsteady gait for 2 months. The physical examination showed left hemianopsia, and both left and right vision were 0.1. The MRI results revealed a falcotentorial meningioma, which had an isointense signal on T1-/T2-weighted imaging and homogeneous enhancement on contrast-enhanced MRI. The MRV showed that the straight sinus was occluded (**Figure 2A**). We implanted an Ommaya reservoir at 1 week before tumor resection and maintained drainage at 200 ml per day. The patient then underwent tumor resection using the OIA. During the operation, the majority of the tumor base was located at the falx end and the tentorium. The tumor was removed in a piecemeal fashion. Finally, the tumor and the base were totally removed (Simpson grade I resection). The postoperative CT showed no hemorrhage or infarction (**Figure 2B**). The pathology examination result revealed that the tumor was a hemangiopericytoma, WHO grade I. The 26-month follow-up showed no tumor recurrence.

Case 2

A 33-year-old man complained of headache for 2 months. The CT results revealed a mixed-density, right occipital lesion. The MRI revealed a right occipital, mixed-signal lesion and flow voids on T1- and T2-weighted imaging. The lesion showed obvious enhancement on contrast-enhanced MRI. The MRV showed an obstructed sagittal sinus (**Figure 3A**). We performed the operation in a hybrid operating room. The cerebral digital subtraction angiography (DSA) results revealed abundant tumor blood supply. The feeding arteries were the right posterior cerebral artery (PCA), right external carotid artery (ECA), right meningiohypophyseal trunk, and left ECA

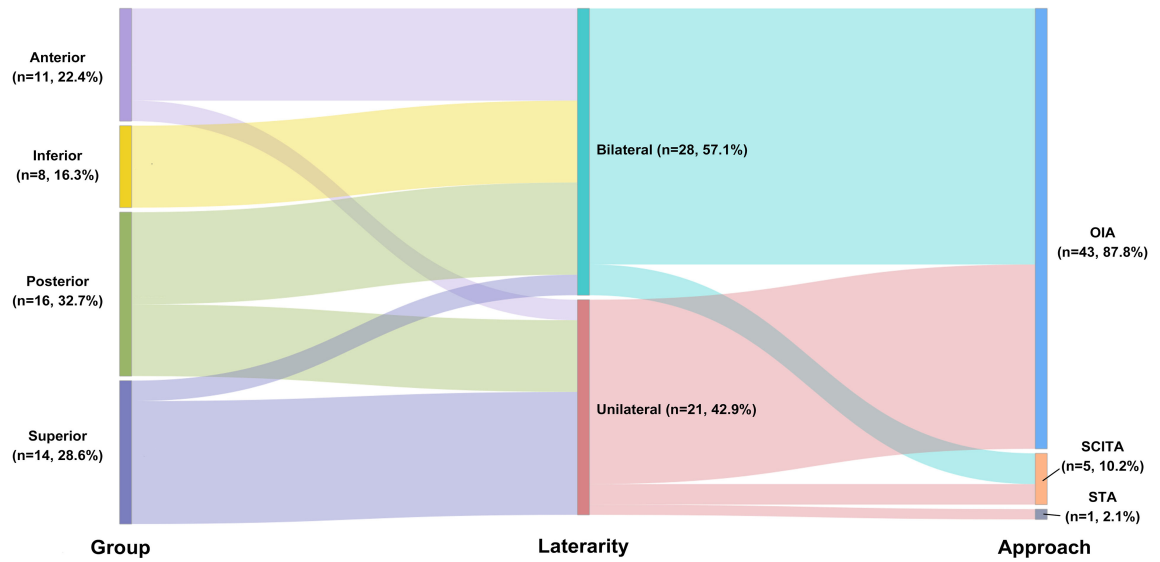

FIGURE 1 | Sankey diagram showing the relationship among location, Asari type, and surgical approach selection.

(**Figure 3B**). Onyx-18 was used for feeding artery embolization for the right PCA, right occipital artery, and left occipital artery. The DSA reexamination showed that 90% of the blood supply was embolized (**Figure 3C**). Craniotomy was then performed. The occipital interhemispheric transtentorial approach was used to reach the tumor under navigation. The tumor was tenacious, with partial calcification. Piecemeal removal was performed, and we achieved a Simpson grade II resection. The postoperative CT results showed no hemorrhage or infarction (**Figure 3D**). The pathology examination results revealed that the tumor was a hemangiopericytoma, and the 10-month follow-up showed no tumor recurrence.

DISCUSSION

Relationship Between the Tumor Growth Pattern and Approach Selection

MRI and angiography can provide abundant information on the location of the lesion and adjacent vascular structures, and the Asari classification can be used to define the tumor extension into four tiers according to the MRI findings (13). The choice of surgical approach depends on the relationship between the tumor, the deep venous system, and the tentorium (1, 13). The Asari classification gives us an imaging classification according to tumor extension. In most studies, OIA or one of its modifications was selected as the primary approach for falcotentorial junction tumors (**Figure 1** and **Tables 1**, **2**) (6, 12, 14, 15). Routine OIA was quite suitable for tumors that originated from the falx (similar to the superior Asari type) immediately above the junction of the vein of Galen with a straight sinus, especially if the tumor displaced the galenic venous system inferiorly. Parietal extension of the OIA (parietooccipital approach) can be performed for the posterior group, and transtentorial maneuver can be added for the anterior, inferior, and posterior groups.

We believe that the key point regarding the selection of surgical approach is whether the straight sinus is occluded. Theoretically, if an occluded straight sinus is observed on MRV, the OIA can be applied for all four Asari groups, supplemented by transtentorial maneuver (8, 16). Ergonomics may be the reason that neurosurgeons preferred the OIA. However, an unobstructed straight sinus should not be occluded under any circumstances. Although the SCITA was also suggested and might lower the chance of severe deep neurovascular compromise, the need for a semi-seated patient position might increase the risk of air embolism and surgeon fatigue. The author preferred to apply the SCITA only if the tumor was classified into the anterior or the inferior group, without a straight sinus occlusion, and/or the Galenic venous system was elevated. Bleeding from an injured straight sinus might be an issue for hemostasis with SCITA. Currently, the authors use a "head-up" park bench position for the SCITA to lower the risk of air embolism and improve the surgeons' ergonomics and bleeding control (17). Regardless of the choice of surgical approach, the galenic venous system and collateral circulation should be preserved during surgery, both of which are more important than achieving gross-total removal. Based on these strategies, the authors achieved a favorable outcome rate of 94.7%.

Postoperative Complications

The two major postoperative complications were hydrocephalus and visual field impairment, both in the authors' practice and in the literature (**Figure 1** and **Tables 1**, **2**). The rate of preoperative hydrocephalus was considerable, and the condition usually presented with radiographic evidence (3, 5, 6, 12, 14, 15). Some

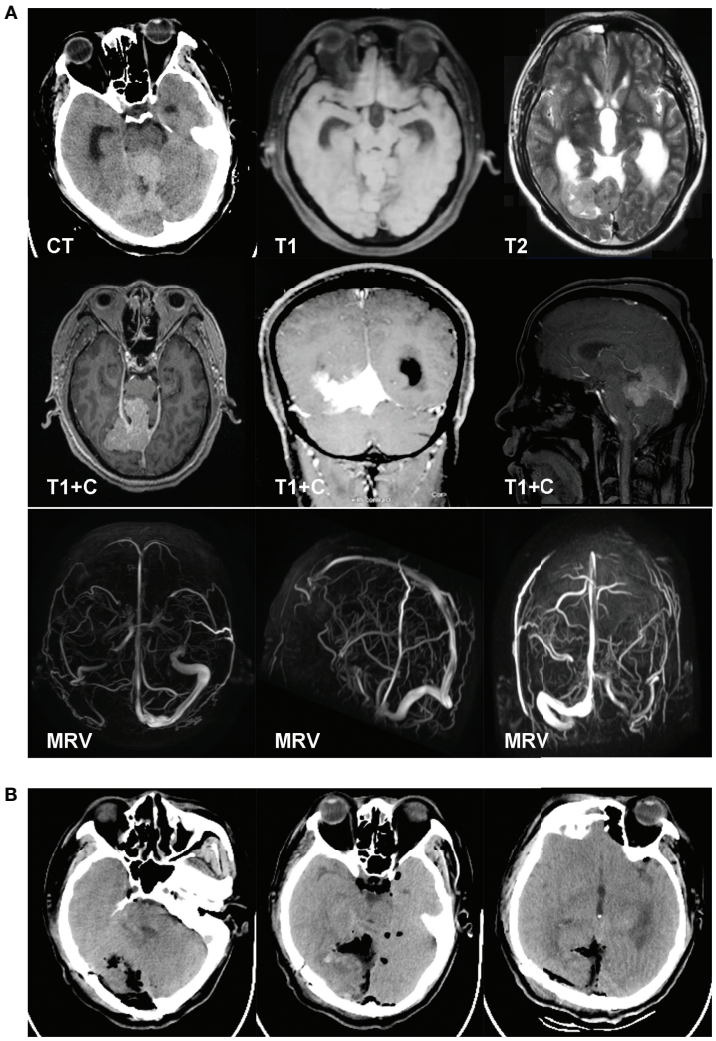

FIGURE 2 | A 52-year-old man complained of blurred vision and unsteady gait for 2 months. The physical examination results showed left hemianopsia, and both VOS and VOD were 0.1. The MRI results revealed a falcotentorial meningioma, which had an isointense signal on T1-/T2-weighted imaging and homogeneous enhancement on contrast-enhanced MRI. The magnetic resonance venography results showed that the straight sinus was occluded **(A)**. We implanted an Ommaya reservoir at 1 week before tumor resection and maintained the drainage at 200 ml per day. The patient then underwent tumor resection using the occipital interhemispheric approach. During the operation, the majority of the tumor base was located at the falx end and the tentorium. The tumor was removed in a piecemeal fashion. Finally, the tumor and the base were totally removed (Simpson grade I resection). The postoperative CT showed no hemorrhage or infarction **(B)**. The pathology examination results revealed that the tumor was a hemangiopericytoma, WHO grade I.

patients had to receive an external ventricular drain or endoscopic third ventriculostomy before the surgery, and in most cases, the condition was relieved after tumor removal. The remaining cases required further V–P shunts to cure the hydrocephalus. In our cases, Ommaya implantation was performed for those pre-operation hydrocephalus conditions. It could be used not only for pre-operative hydrocephalus relief but also for post-operation hydrocephalus temporary therapy.

Regarding visual field impairment, it appeared that fewer cases were reported in our research than in previous studies. Given the advances in anesthesia and related techniques, we can achieve appropriate intracranial pressure control. In addition, we prefer to control intracranial pressure *via* gravity assistance, cerebrospinal fluid release by lumbar puncture, or extraventricular drainage. If necessary, a brain spatula is used to prod the falx to gain more operating space instead of pulling on the occipital lobe.

The hybrid concept, in combination with microsurgery and interventional therapy, is incorporated into the neurosurgical procedure to help lower intraoperative bleeding for complex lesions and reduce iatrogenic damage to the brain parenchyma (case 48). Given the progress in modern anesthesia, the combination of endoscopic and hybrid interventional embolization may be helpful for promoting minimally invasive incision and reducing complications (18).

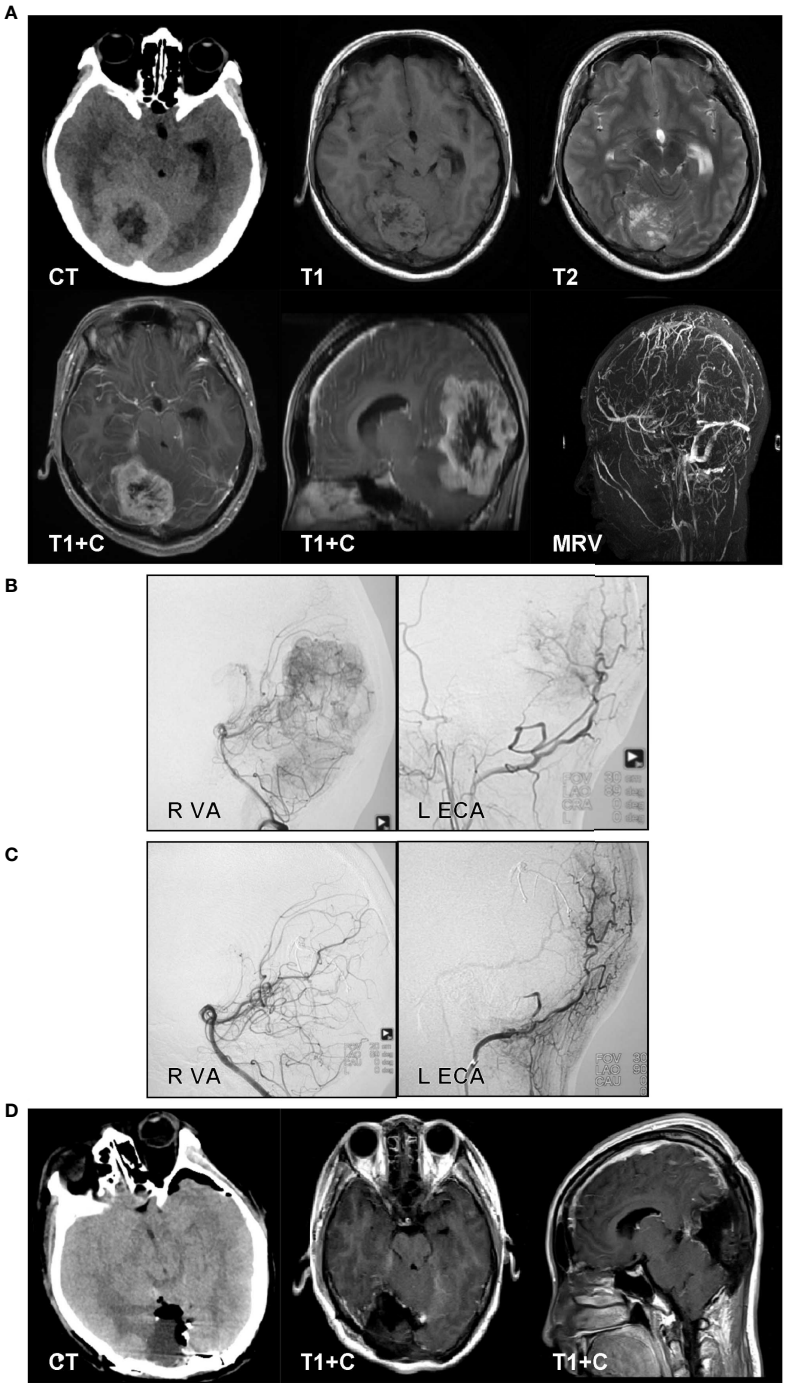

FIGURE 3 | A 33-year-old man complained of headache for 2 months. The CT results revealed a mixed-density, right occipital lesion. The MRI results revealed a right occipital, mixed-signal lesion and flow voids on T1- and T2-weighted imaging. The lesion showed obvious enhancement on contrast-enhanced MRI. The magnetic resonance venography results showed an obstructed sagittal sinus **(A)**. We performed the operation in a hybrid operating room. The cerebral digital subtraction angiography (DSA) results revealed abundant tumor blood. The feeding arteries were the right posterior cerebral artery (PCA), right external carotid artery (ECA), right meningiohypophyseal trunk, and left ECA **(B)**. Onyx-18 was used for feeding artery embolization for the right PCA, right occipital artery, and left occipital artery. The DSA reexamination results showed that 90% of the blood supply was embolized **(C)**. Craniotomy was then performed. The occipital interhemispheric transtentorial approach was used to reach the tumor under navigation. The tumor was tenacious, with partial calcification. Piecemeal removal was performed, and we achieved a Simpson grade II resection. The postoperative CT results showed no hemorrhage or infarction **(D)**. The pathology examination results revealed that the tumor was a hemangiopericytoma.

TABLE 2 | Literature review and summary of previously published studies on pineal meningioma.

Authors and year	Number of operations	Age (years)	Sex (M/F)	Tumor type (number)	Surgical approach (number)	Extent of resection	Pathology	Surgical-related complication	Hydrocephalus	Follow-up (month)	Recurrence	Outcome
Li, et al., 2011 (14)	10	53.3	4/6	Infratentorial > supratentorial (3) Supratentorial > infratentorial (2) Supratentorial = infratentorial (3) Infratentorial (2)	Poppen (10)	GTR (6)	Meningioma WHO I, (8); atypical WHO II(2)	Intracranial infection (1) Intraventricular hemorrhage and pneumocephalus (1)	9/10 Relieved 1/10 VP shunt	14 (6–24)	No	KPS >70 (10)
Nowak et al., 2014 (12)	6	52	1/5	Superior (5) Inferior (1)	Poppen (6)	GTR (2) (Simpson I: 1, II: 1) NTR (4) (Simpson III: 4)	Meningiomas	Temporary homonymous hemianopsia (5) Postoperative intraventricular hemorrhage (1) Transient hemiparesis (1) Upward-gaze palsy (1)	Pre-op: 1/3VP shunt, 1/3 ETV Post-op: 1/3 VP shunt	102 (24–160)	No	KPS >70 (6)
Qiu et al., 2014 (15)	15	51.3	5/10	Bassiouni's classification Type I (7) Type II (4) Type III (4)	Poppen (15)	GTR (Ⅱ) NTR (3) STR (Ⅰ)	Meningiomas Endotheliomatous (4) Fibrous (3) Transitional (3) Angioblastic (2) Psammomatous (1)	Homonymous visual deficit (2)	6/7 Relieved 1/7 VP shunt	28.3 (12–50)	No	NR
Chang et al., 2016 (6)	11	52.9	5/6	Asari classification Anterior (4), superior (2) Inferior (4), posterior (1) Bassiouni's classification Type I (4), type II (4) Type III (2), type IV (1)	Poppen (8) Parieto-occipital (2) Occipital (1)	GTR (10) (Simpson I: 10) STR (1) (Simpson IV: 1)	Meningiomas Meningothelial (4) Fibrous (1) Transitional (4) Atypical (2)	Homonymous hemianopsia (2) Diplopia (1) Occipito-cerebellar hemorrhage (1) PCA infarction (1)	2/11 Relieved 1/11 VP shunt	35 (3–150)	No	Last follow-up KPS >70 (10) KPS <70 (1)
Tal acc hi et al., 2018 (5)	28	59.8	10/18	Supertentorial (12) Infratentorial (11) Supra-infratentorial (5)	Median suboccipital (11) Parieto-occipital and occipital (12) Suboccipital (5)	GTR (13) (Simpson I: 5, II: 8) STR (15) (Simpson III: 7, IV: 8)	Meningiomas (28)	Died of intractable cerebral edema (1) Tetraparesis (1), IV Cranial nerve deficit (1) Tumor bed hematoma requiring evacuation (2) Cerebrospinal fluid fistulae (2), Surgical wound infection (1)	Pre-op 9/28 Relieved Post-op 1/28 VP shunt	57.6	2/28 atypical	12 months follow-up KPS >70 (18) KPS<70 (4) Lost (6)
Joham Choque-Velasquez et al., 2019 (4)	10 (10/76)	NR	NR	NR	SCIT (N.A.) Occipital interhemispheric (N.A.)	GTR (9), PR (1)	Meningiomas (9) Anaplastic meningioma (1)	Thalamic infarction and died 1 month after surgery (1)	NR	94.5 (1–205)	No	Last follow-up 50% overall survival rate mRS
Zhao et al., 2019 (3)	17 (14 patients)	59.8	1/13	Asari classification Anterior (2), superior (4) Inferior (9), posterior (1)	Poppen (4) SCIT (4) AIH (3) Torcular (2)	Simpson I (4) Simpson II (1)	Meningioma	Visual field defects (2 permanent, 4 transient) Hemiparesis (2)	Pre-op: 3/17 EVD, 1/17 ETV	29 (2–72)	3/17 (same patient)	Improved (4) Unchanged (9)

(Continued)

TABLE 2 | Continued

Authors and year	Number of operations	Age (years)	Sex (M/F)	Tumor type (number)	Surgical approach (number)	Extent of resection	Pathology	Surgical-related complication	Hydrocephalus	Follow-up (month)	Recurrence	Outcome
				Bassiouni's classification type I (1), type II (9), type III (4), type IV (2)	Transventricular (1) Staged Poppen + SCIT (3)	Simpson III (3) Simpson IV (9)	WHO I (9), WHO II (5)	Hemidysesthesia (1) Cerebellar hematoma (1) Hydrocephalus (1)	Post-op: 4/17 Resolved 1/17 VP shunt			Worsened (4)

NR, not reported; SCIT, supracerebellar infratentorial approach; AIH, anterior interhemispheric transsplenial approach; GTR, gross total resection; NTR, near-total resection; STR, subtotal resection; PR, partial resection., N.A., not applicable.

Recurrence

Among the nine patients who experienced recurrence in our study, none achieved a Simpson grade I resection. The corresponding pathology showed two cases of angiopericytoma (WHO II) and seven cases of meningioma (WHO I). Six tumor locations were of the superior type, and four of the tumors were calcified. Similar to the literature, recurrences are mainly observed in patients after nonradical resection and/or with atypical or anaplastic meningiomas or hemangiopericytoma (3, 5). Usually, MR contrast images were obtained after operation to make sure the tumor residual, during the follow-up period, and following therapy. Recurrence is the outcome event in this study. For the primary recurrent tumor, craniotomy tumor resection is optimal. The appropriate stopping point comes when it is difficult to remove the tumor totally.

Limitation

The retrospective nature of this study may have led to a selection bias. A total of 22.4% of patients were lost to follow-up, which may be a confounder that led to the high recurrence rate. Small samples may also induce complication loss, such as seizure attack or sinus injury in our study.

CONCLUSION

The OIA is the most commonly used and safest approach for resecting falcotentorial junction tumors with multiple brain pressure control assistance techniques, followed by the SCITA. The selection of surgical approach must be based on imaging features, such as laterality, Asari types, and the presence of a straight sinus occlusion.

DATA AVAILABILITY STATEMENT

The raw data supporting the conclusions of this article will be made available by the authors, without undue reservation.

ETHICS STATEMENT

The studies involving human participants were reviewed and approved by Huashan Hospital Institutional Review Board. The patients/participants provided their written informed consent to participate in this study.

AUTHOR CONTRIBUTIONS

Study conception and design were contributed by WZ and JS. Acquisition of data and follow up was contributed by PL.

Surgical participation was rendered by JS, PL, XW, KQ, YL, and WZ. Pathological confirmation was performed by ZY. Drafting of manuscript was done by PL. Critical revision was carried out by all authors. All authors contributed to the article and approved the submitted version.

FUNDING

This study was supported by the Shanghai Rising-Star Program (18QA1400900).

ACKNOWLEDGMENTS

The authors thank Jianbin Shi for brain imaging processing and Geng Xu for intraoperative electrophysiological monitoring support and clinical database management.

SUPPLEMENTARY MATERIAL

The Supplementary Material for this article can be found online at: https://www.frontiersin.org/articles/10.3389/fonc.2022.866225/full#supplementary-material

REFERENCES

1. Bassiouni H, Asgari S, Konig HJ, Stolke D. Meningiomas of the Falcotentorial Junction: Selection of the Surgical Approach According to the Tumor Type. *Surg Neurol* (2008) 69(1):339–49; discussion 349. doi: 10.1016/j.surneu.2007.02.029
2. Bassiouni H, Hunold A, Asgari S, Stolke D. Tentorial Meningiomas: Clinical Results in 81 Patients Treated Microsurgically. *Neurosurgery* (2004) 55:108–16; discussion 116-8. doi: 10.1227/01.NEU.0000126886.48372.49
3. Zhao X, Belykh E, Przybylowski CJ, Borba ML, Gandhi S, Tayebi MA, et al. Surgical Treatment of Falcotentorial Meningiomas: A Retrospective Review of a Single-Institution Experience. *J Neurosurg* (2019) 133(3):630–41. doi: 10.3171/2019.4.JNS19208
4. Blasco GDAG, Delgado-Fernandez J, Penanes CJ, Gil-Simoes R, Frade-Porto N, Sanchez MP. Meningiomas Originated at the Falcotentorial Region: Analysis of Topographic and Diagnostic Features Guiding an Optimal Surgical Planning. *World Neurosurg* (2019) 123:e723–33. doi: 10.1016/j.wneu.2018.12.013
5. Talacchi A, Biroli A, Hasanbelliu A, Locatelli F. Surgical Management of Medial Tentorial Meningioma: Falcotentorial and Torcular. *World Neurosurg* (2018) 115:e437–47. doi: 10.1016/j.wneu.2018.04.066
6. Hong CK, Hong JB, Park H, Moon JH, Chang JH, Lee KS, et al. Surgical Treatment for Falcotentorial Meningiomas. *Yonsei Med J* (2016) 57:1022–8. doi: 10.3349/ymj.2016.57.4.1022
7. Lensing FD, Abele TA, Sivakumar W, Taussky P, Shah LM, Salzman KL. Pineal Region Masses–Imaging Findings and Surgical Approaches. *Curr Probl Diagn Radiol* (2015) 44:76–87. doi: 10.1067/j.cpradiol.2014.05.007
8. Rey-Dios R, Cohen-Gadol AA. A Surgical Technique to Expand the Operative Corridor for Supracerebellar Infratentorial Approaches: Technical Note. *Acta Neurochir (Wien)* (2013) 155:1895–900. doi: 10.1007/s00701-013-1844-4
9. Odake G. Meningioma of the Falcotentorial Region: Report of Two Cases and Literature Review of Occlusion of the Galenic System. *Neurosurgery* (1992) 30:788–93; discussion 793-4. doi: 10.1227/00006123-199205000-00027
10. Yamazaki T, Takahashi S, Ishii K, Matsumoto K, Ishibashi T, Sakamoto K, et al. Meningioma in the Pineal Region: Preoperative Diagnosis With CT, MRI, and Angiography. *Radiat Med* (1991) 9:22–5.
11. Behari S, Das KK, Kumar A, Mehrotra A, Srivastava AK, Sahu RN, et al. Large/Giant Meningiomas of Posterior Third Ventricular Region: Falcotentorial or Velum Interpositum? *Neurol India* (2014) 62:290–5. doi: 10.4103/0028-3886.136934
12. Nowak A, Dziedzic T, Czernicki T, Kunert P, Marchel A. Falcotentorial and Velum Interpositum Meningiomas: Two Distinct Entities of the Pineal Region. *Neurol i Neurochirurgia Polska* (2014) 48:397–402. doi: 10.1016/j.pjnns.2014.09.009
13. Asari S, Maeshiro T, Tomita S, Kawauchi M, Yabuno N, Kinugasa K, et al. Meningiomas Arising From the Falcotentorial Junction. *Clin Features Neuroimaging Studies Surg Treat J Neurosurg* (1995) 82:726–38. doi: 10.3171/jns.1995.82.5.0726
14. Li Y, Zhao G, Wang H, Zhu W, Qu L, Li Y, et al. Use of 3D-Computed Tomography Angiography for Planning the Surgical Removal of Pineal Region Meningiomas Using Poppen's Approach: A Report of Ten Cases and a Literature Review. *World J Surg Oncol* (2011) 9:64. doi: 10.1186/1477-7819-9-64
15. Qiu B, Wang Y, Ou S, Guo Z, Wang Y. The Unilateral Occipital Transtentorial Approach for Pineal Region Meningiomas: A Report of 15 Cases. *Int J Neurosci* (2014) 124:741–7. doi: 10.3109/00207454.2013.878341
16. Bonney PA, Boettcher LB, Cheema AA, Maurer AJ, Sughrue ME. Operative Results of Keyhole Supracerebellar-Infratentorial Approach to the Pineal Region. *J Clin Neurosci* (2015) 22:1105–10. doi: 10.1016/j.jocn.2014.12.029
17. Song J, Hua W, Pan Z, Zhu W. Fully Endoscopic Supracerebellar Infratentorial Approach for Resection of Third Ventricle Germ Cell Tumor: 2-Dimensional Operative Video. *Oper Neurosurg (Hagerstown)* (2019) 16:389–90. doi: 10.1093/ons/opy150
18. Liu JK, Cohen MA. Endoscopic-Assisted Posterior Interhemispheric Retrocallosal Transfalcine Approach for Microsurgical Resection of a Pineal Region Falcotentorial Meningioma: Operative Video and Technical Nuances. *Neurosurg Focus* (2016) 40(videosuppl1):1. doi: 10.3171/2016.1.FocusVid.15453

Conflict of Interest: The authors declare that the research was conducted in the absence of any commercial or financial relationships that could be construed as a potential conflict of interest.

Publisher's Note: All claims expressed in this article are solely those of the authors and do not necessarily represent those of their affiliated organizations, or those of the publisher, the editors and the reviewers. Any product that may be evaluated in this article, or claim that may be made by its manufacturer, is not guaranteed or endorsed by the publisher.

Copyright © 2022 Liu, Wang, Liu, Cai, Yang, Quan, Zhu and Song. This is an open-access article distributed under the terms of the Creative Commons Attribution License (CC BY). The use, distribution or reproduction in other forums is permitted, provided the original author(s) and the copyright owner(s) are credited and that the original publication in this journal is cited, in accordance with accepted academic practice. No use, distribution or reproduction is permitted which does not comply with these terms.

frontiers | Frontiers in Oncology

REVIEW
published: 30 May 2022
doi: 10.3389/fonc.2022.850463

Potential Molecular Mechanisms of Recurrent and Progressive Meningiomas: A Review of the Latest Literature

Wenjie Peng[1], *Pei Wu*[2], *Minghao Yuan*[3], *Bo Yuan*[4], *Lian Zhu*[1], *Jiesong Zhou*[5*] and *Qian Li*[1*]

[1] Department of Pediatrics, Army Medical Center, Army Medical University, Chongqing, China, [2] Department of Neurosurgery, The First Affiliated Hospital of Harbin Medical University, Harbin, China, [3] Department of Neurology, Chongqing Medical University, Chongqing, China, [4] Department of Nephrology, The Dazu District People's Hospital, Chongqing, China, [5] Department of Plastic Surgery, Changhai Hospital Affiliated to Naval Medical University, Shanghai, China

OPEN ACCESS

Edited by:
Hailiang Tang,
Fudan University, China

Reviewed by:
Tao Xu,
Shanghai Changzheng Hospital, China
Fukai Ma,
Shanghai Jiao Tong University, China

***Correspondence:**
Qian Li
liqian12210@sina.com
Jiesong Zhou
jiesong_zhou@126.com

Specialty section:
This article was submitted to Neuro-Oncology and Neurosurgical Oncology, a section of the journal Frontiers in Oncology

Received: *07 January 2022*
Accepted: *28 April 2022*
Published: *30 May 2022*

Citation:
Peng W, Wu P, Yuan M, Yuan B, Zhu L, Zhou J and Li Q (2022) Potential Molecular Mechanisms of Recurrent and Progressive Meningiomas: A Review of the Latest Literature. Front. Oncol. 12:850463. doi: 10.3389/fonc.2022.850463

Meningiomas, the most frequent primary intracranial tumors of the central nervous system in adults, originate from the meninges and meningeal spaces. Surgical resection and adjuvant radiation are considered the preferred treatment options. Although most meningiomas are benign and slow-growing, some patients suffer from tumor recurrence and disease progression, eventually resulting in poorer clinical outcomes, including malignant transformation and death. It is thus crucial to identify these "high-risk" tumors early; this requires an in-depth understanding of the molecular and genetic alterations, thereby providing a theoretical foundation for establishing personalized and precise treatment in the future. Here, we review the most up-to-date knowledge of the cellular biological alterations involved in the progression of meningiomas, including cell proliferation, neo-angiogenesis, inhibition of apoptosis, and immunogenicity. Focused genetic alterations, including chromosomal abnormalities and DNA methylation patterns, are summarized and discussed in detail. We also present latest therapeutic targets and clinical trials for meningiomas' treatment. A further understanding of cellular biological and genetic alterations will provide new prospects for the accurate screening and treatment of recurrent and progressive meningiomas.

Keywords: meningioma, mechanisms, cell proliferation, neo-angiogenesis, apoptosis, immunogenicity, genetic alterations

INTRODUCTION

Meningiomas generally originate from the meninges and meningeal spaces. They are the most frequently occurring primary intracranial tumors of the central nervous system in adults, with an incidence of 7.86 cases per 100,000 people every year (1). According to the 2021 World Health Organization (WHO) tumor classification, meningiomas are classified as benign (>80%), atypical (15%–20%), and anaplastic (1.0%–3.0%), depending on the mitotic rate, brain invasion, or specific histological features (2–4). Although the majority (~80%) of meningiomas are benign and could be cured or become stable through surgical resection, some present with high-risk behaviors and poor prognosis, including early or high-rate recurrence and rapidly progressive course even after radiotherapy (5). More interestingly, among meningiomas with benign pathological features, 7–25% histologically tend to relapse or become malignant after surgical resection (6). Atypical and anaplastic meningiomas are naturally substantially more aggressive, and their recurrence rates in 5 years reach up to 30–50% and 90%, respectively (7, 8). Radiotherapy is recommended for partially resected Grade II and all Grade III meningiomas. Nevertheless, a subset of patients with Grade II meningiomas may live through a benign clinical course with no need for radiotherapy (9). The histological grade does not fully reflect the biological behavior of meningiomas to currently guide treatment. Hence, there is a need to explore useful predictors of the clinical behavior or overall prognosis of meningiomas.

Previous studies have shown that the risk factors of meningiomas are complex, including age, sex, radiation, trauma, diabetes mellitus, and arterial hypertension (1, 7), and the progression of recurrent meningiomas involves numerous factors, including Simpson grade IV/V resection, a larger tumor size, tumor location, high vascular endothelial growth factor receptor (VEGFR) expression, WHO Grade II/III, high Ki-67 expression, and lack of progesterone receptor expression (10). Recurrent meningiomas may be accompanied with malignant transformation and multiple treatments or limited optional drugs, making management much more challenging (7, 11). Therefore, a further understanding of the molecular mechanisms underlying the recurrence or progression will help predict the clinical behavior, which is beneficial for early recognition of high-risk meningiomas and timely adjustment of treatment protocols.

Abbreviations: WHO, World Health Organization; FOXM1, Forkhead box protein M1; VEGFR, Vascular endothelial growth factor receptor; MDM2, Murine double minute 2 protein; FAK, Focal adhesion kinase; CDKN2A/B, Cyclin-dependent kinase inhibitor 2A/B; DMD, Dystrophin-encoding and muscular dystrophy-associated; AKT1, v-Akt murine thymoma viral oncogene; HIF-1α, Hypoxia-inducible factor 1α; PI3K, Phosphatidylinositol 3-kinase; mTOR, mammalian Target of rapamycin; CDK, Cyclin-dependent kinase; BAP1, Breast cancer 1-associated protein-1; TERTp, promoter of Telomerase reverse transcriptase; p-CREB, phosphorylated Cyclic-AMP responsive element-binding protein; RAS, Rat sarcoma; PFS, Progression-free survival; KLF4, Krüppel-like factor 4; VEGF, Vascular endothelial growth factor; MC, Methylation classification; PD-1, Programmed death 1; PD-L1, Programmed death-ligand 1.

In addition to the traditional WHO grading, the latest studies on meningiomas have provided insights into the genomic alterations, including DNA somatic copy number, DNA point mutation, DNA methylation, and transcriptomic and proteomic data (12). Advances in molecular classification through DNA methylation have gradually been approved by researchers (1, 6, 9, 12, 13). Similar to other central nervous system neoplasms, such as glioma, Nassiri reported that meningiomas could be classified into different molecular groups with distinct and prototypical biological features after a comprehensive analysis combining copy number, DNA methylation, and mRNA sequencing data (12), complementing existing WHO grades. Here, based on the most up-to-date biomedical research knowledge, we review the potential cellular biological mechanisms and molecules involved in the recurrence or progression of meningiomas from several perspectives, including the excessive proliferation of tumor cells, neo-angiogenesis, inhibition of apoptosis, immunogenicity, and genetic alterations involving chromosomes and genes related to meningiomas (3, 13). Further, we summarize existing therapeutic targets and clinical trials for meningiomas' treatment. We expect this information to allow for an exploration of more accurate prognostic markers and potential targeted therapies for meningiomas.

CELL PROLIFERATION

Recurrent or progressive meningiomas usually begin with excessive cell growth and proliferation. Evidence suggests that tumor cell growth and proliferation are tightly linked to cell-cycle dysregulation (4). Disordered cell-cycle proteins, the uncontrolled regulation of transcription factors, and mutations in cell-cycle-related genes can promote cell proliferation and differentiation in meningioma (14–17). The cell-cycle-related proteins topoisomerase IIα and mitosin, which play important roles in regulating mitotic chromosome condensation and separation (18), are positively associated with a high risk of meningioma recurrence (15). Forkhead box protein M1 (FOXM1), a master transcription factor for cell growth and proliferation, is closely associated with hepatocellular carcinoma (19), prostate cancer (20), glioma (21), and basal cell carcinoma (22). FOXM1 is thought to accelerate G1/S and G2/M transition to promote mitotic progression (14). A recent comprehensive molecular profiling study indicated that the expression of FOXM1 is relevant to increased proliferation and poor clinical prognosis (23). Similarly, the results obtained in a newly established model of meningioma showed that FOXM1 overexpression increases proliferation in benign meningioma, whereas its depletion decreases proliferation in malignant meningioma (24). As such, thiostrepton, a FOXM1 inhibitor, combined with radiation therapy, was found to noticeably prevent the proliferation of malignant meningioma cells **(Figure 1)** (24).

Gene mutations in v-Akt murine thymoma viral oncogene (*AKT1*), homolog 1 smoothened, frizzled class receptor (*SMO*), focal adhesion kinase (*FAK*), cyclin-dependent kinase inhibitor 2A/B (*CDKN2A/B*), and dystrophin-encoding and muscular

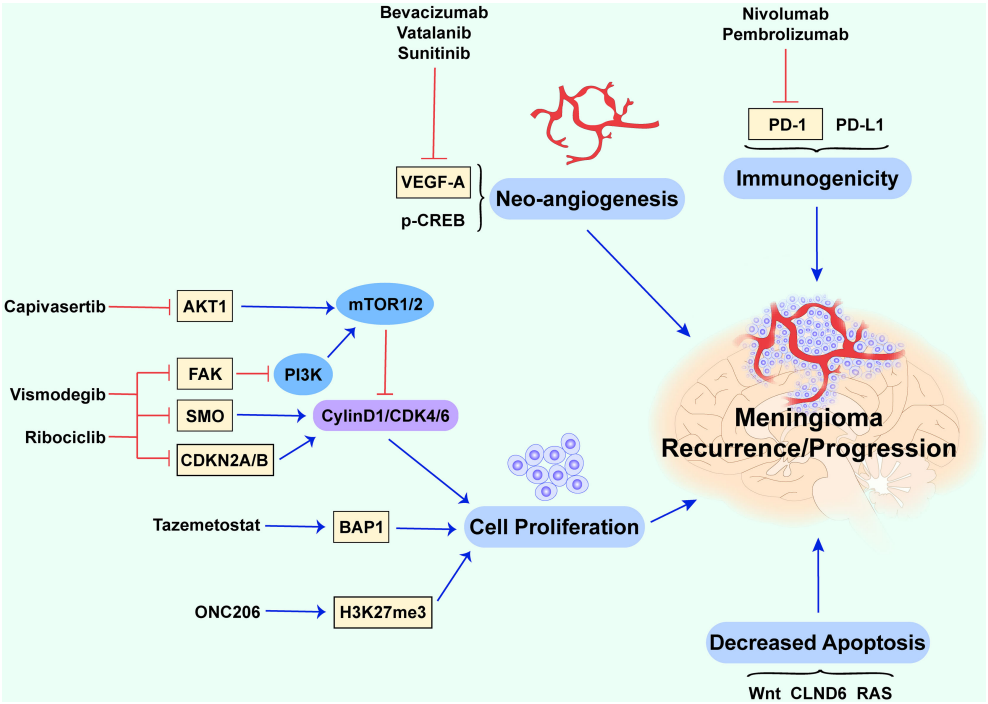

FIGURE 1 | Potential biological mechanisms of recurrent and progressive meningiomas. This figure briefly summarizes several cellular biological mechanisms and molecules contributing to recurrent and progressive meningiomas. The abnormal proliferation of tumor cells, downregulation of apoptotic processes, neo-angiogenesis, and immunogenicity together promote recurrence and progression (the red lines show an inhibitory effect and the blue arrows show a promoting effect).

dystrophy-associated (*DMD*) are also considered to be associated with cell proliferation in meningioma (17). *AKT1* encodes the AKT1 kinase (a serine/threonine-protein kinase), and the overactivation of AKT1 can lead to uncontrolled cell growth and proliferation *via* the phosphatidylinositol 3-kinase (PI3K)/AKT/mammalian target of rapamycin (mTOR) signaling pathway **(Figure 1)** (25, 26). mTOR, mainly regulated by the PI3K/AKT pathway, is highly expressed in various tumors and is closely associated with cell growth and proliferation (17). Studies have indicated that the overactivation of mTOR results in a high mitotic index (27) and contributes to the recurrence of meningioma (28) and poorer outcomes (27).

SMO mutations lead to cell-specific proliferation and mediate the development of meningioma through uncontrolled activation of the sonic hedgehog signaling pathway (25, 29, 30). *FAK*, which encodes a cytoplasmic protein tyrosine kinase that mediates cell growth, proliferation, and survival, is overexpressed in some meningiomas (31). Ribociclib, a cyclin-dependent kinase (CDK) inhibitor, was evaluated for its effect on other highly mutated genes (other than the common *NF2*), such as *AKT1* and *SMO* (NCT02933736) (**Table 1**) (38). Moreover, a national Alliance-sponsored cooperative group phase II clinical trial evaluated the efficacy of SMO, AKT1, and FAK inhibitors for recurrent or progressive meningiomas with targetable alterations in SMO, AKT1, and NF2, respectively (NCT02523014/A071401) (5). Vismodegib, included in an ongoing Alliance clinical trial, is a hedgehog pathway-targeting agent tested for SMO/PTCH1-mutated progressive/recurrent meningiomas (NCT02523014) (32).

CDKN2A encodes p16INK4A and p14ARF, and *CDKN2B* encodes p15INK4B. p15INK4B and p16INK4A prevent S-phase entry by inhibiting the CDK4/cyclin D complex and are generally mutated in Grade II and III meningiomas. p14ARF prevents cell proliferation in the G1 phase and decelerates p53 degradation through downregulation of the proto-oncogene murine double minute 2 protein (*MDM2*) (41). The mutation or deletion of *CDKN2A* and *CDKN2B* has been linked to a poorer prognosis in meningioma (42). A CDK inhibitor combined with ribociclib could be a potential treatment approach for meningiomas with mutations in the tumor-suppressor genes *CDKN2A* and *CDKN2B* (NCT02933736) (32). Moreover, mutations in the tumor-suppressor gene *p53* also affect the occurrence and development of meningioma (43). When mutations occur, p53 changes from a tumor suppressor to a tumor promoter owing to structural changes that suppress its roles in inhibiting cell growth and apoptosis, leading to cancer (44). The p53 mutation rate is higher in atypical and malignant meningiomas, and most importantly, it is higher in recurrent than in non-recurrent diseases (45). Some researchers also found that the combination of p53 and Ki67 could be a promising predictor of recurrence in meningiomas (45). *DMD* encodes dystrophin, which regulates cytoskeleton remodeling and cell proliferation in response to extracellular signal stimulation (46, 47). The deletion of *DMD* contributes to progressive meningioma and a

TABLE 1 | Summarization of key molecules and potential targeted therapy in recurrent and progressive meningiomas.

	Targets	Inhibitors	Ongoing Clinical Trial	Reference
Cell proliferation	AKT1	Capivasertib	NCT02523014	(5, 32)
		Ribociclib	NCT02933736	
	SMO	Vismodegib	NCT02523014	(5, 32)
		Ribociclib	NCT02933736	
	FAK	Vismodegib	NCT02523014	(5)
	CDKN2A/B	Ribociclib	NCT02933736	(32)
	BAP1	Tazemetostat	NCT02860286	(33)
	H3K27me3	ONC206	NCT04541082	(34)
Neo-angiogenesis	VEGF-A	Bevacizumab Vatalanib Sunitinib Apatinib mesylate	NCT01125046	(35, 36)
		Erlotinib hydrochloride	NCT00348790 NCT00589784 NCT04501705 NCT00045110	
Immunogenicity	PD-1	Nivolumab Pembrolizumab	NCT02648997 NCT04659811 NCT03279692	(37)
Chromosomal abnormalities	NF2 and/or SMARCB1	Everolimus Vistusertib Dasatinib Selumetinib	NCT00972335 NCT03095248 NCT00788125 NCT03095248	(5, 35, 38–40)

shorter overall survival (16), partly due to the defective inhibition of cell proliferation leading to disease progression (48). Breast cancer 1-associated protein-1 (BAP1), a deubiquitylating enzyme, is a tumor suppressor. Familial and sporadic BAP1-deficient meningiomas tend to be rare, and aggressive malignant tumors (grade III) are associated with increased aggressiveness and poorer prognosis (49). Tazemetostat, a BAP1 inhibitor, increases the level of the PCR2 complex protein EZH2, activated by BAP1, and might be a potential drug for rhabdoid meningioma caused by BAP1 loss (NCT02860286) (50).

In addition to the genes mentioned previously herein, a 2018 study showed that mutations in the promoter of telomerase reverse transcriptase (*TERTp*) enhance the degree of malignancy of meningiomas and lead to poor prognosis (51). Other studies have corroborated that *TERTp* mutations predict poor survival in progressive/high-grade meningiomas (33, 52, 53). Telomere maintenance is a marker of tumor formation, and most tumors express telomerase to prevent telomere shortening (52). Telomerase activation caused by *TERTp* mutations enforces cell immortalization and promotes the growth of tumors (51), which could be observed in recurrent and malignant tumors (54). Furthermore, a 2021 study revealed that *TERT* alterations are a biomarker of meningioma progression and reduce progression-free survival after adjuvant radiotherapy (55). Hence, we suggest that *TERTp* mutations can significantly predict poor prognosis in meningiomas, but no effective targeted drugs have been found to date.

In recent years, it has been reported that the loss of H3K27 trimethylation (H3K27me3) plays a prominent role in the recurrence of meningioma (56). Further research found that the loss of H3K27me3 predicts early recurrence and death for grade 2, but not for grade 3, meningioma (57). H3K27me3 affects DNA damage repair and contributes to several biological processes, including cell differentiation, proliferation, and stem-cell plasticity (58). The latest study found that ONC206, a DRD2 antagonist and ClpP agonist, is orally bioavailable, penetrates the blood-brain barrier, and exhibits anti-cancer efficacy without toxicity, and it is currently the subject of an ongoing trial (NCT04541082) for H3K27M-mutant, malignant meningiomas and other central nervous system tumors (34). However, its therapeutic effect on tumorigenesis or cancer recurrence with respect to H3K27me3 requires further clinical trials.

NEO-ANGIOGENESIS

Neo-angiogenesis is one of the most important features of higher-grade meningiomas. On the one hand, it makes the tumor grow rapidly, and on the other hand, it makes surgical resection more difficult based on the rich blood supply. Tumor vessel density is a key feature during oncogenesis and is tightly correlated with the upregulation of vascular endothelial growth factor (VEGF), placental growth factor, and insulin-like growth factor-binding protein-3 (59). A recent follow-up study investigated VEGF and its three receptors in meningiomas and demonstrated a significant increase in VEGF-A levels in WHO grade III meningiomas (60). VEGF-A, an endothelial cell-specific mitogen, contributes to new blood vessel growth (35, 61). Upon overexpression, VEGF-A contributes to the rapid growth of tumors (35) and regulates maturation and stabilization during the late stages of tumors (62). VEGF-A is a powerful mitogenic and angiogenic disulfide-linked homodimer, which is secreted from tumors and increased under conditions of ischemia for the rapid expansion of tumor vessels (63). VEGF-A is tightly associated with refractory or higher-grade meningiomas (35), becoming a potential therapeutic target with the foundation of anti-angiogenic agents blocking the VEGF pathway (64). Antiangiogenic drugs, such as bevacizumab, vatalanib, and sunitinib, were reported to reduce the recurrence rate of meningiomas significantly (1). Two prospective phase II trials involving patients with refractory meningiomas have evaluated the efficacy and safety of bevacizumab (36). One study of 40 patients treated with bevacizumab indicated that the progression-free survival (PFS) at 6 months is 87% for grade I meningiomas, 77% for grade II meningiomas, and 46% for grade III meningiomas (NCT01125046). Another clinical trial in 2016 combining bevacizumab with everolimus found a median PFS of 22 months for those with recurrent and progressive meningiomas

after surgery and/or radiation therapy (95% CI 4.5–26.8). This combination could block disease progression in 88% of patients (NCT00972335) (35, 36). Both vatalanib (NCT00348790) and sunitinib (NCT00589784) are tyrosine kinase inhibitors targeting VEGFR and were shown to act partly on recurrent meningiomas. Furthermore, other trials like those for apatinib mesylate (NCT04501705) and erlotinib hydrochloride (NCT00045110) found on ClinicalTrials.gov have demonstrated that VEGFR is an emerging therapeutic target.

In addition to VEGF-A, phosphorylated cyclic-AMP responsive element-binding protein (p-CREB) is a novel high-risk molecule abundantly expressed in the endothelia of tumor vessels in all meningiomas, and high p-CREB levels are closely associated with the recurrence of meningiomas (65). p-CREB was found in various tumors, including glioma, because of its physical properties, including binding to upstream signaling kinases and downstream genes (66). It is a transcription factor that participates in numerous cellular processes and induces VEGF expression, leading to neo-angiogenesis in meningiomas (65). Barresi et al. reported that p-CREB expression can be identified in tumor vessels but disappears in the vessels of the normal adult and neonatal leptomeninges, implying that p-CREB is related to neo-angiogenesis (65). The relationship between p-CREB and VEGF has not been fully elucidated and requires further study.

The levels of inflammation in perivascular areas of the tumor, induced by ischemia or other proteins, can also affect the neo-angiogenesis of meningiomas. VEGF-A is a downstream target of hypoxia-inducible factor 1α (HIF-1α), a molecular marker of hypoxia (67). A large cohort study of 263 patients with meningiomas found that upregulated levels of HIF-1α and VEGF-A could significantly predict the recurrence of meningiomas (68). Moreover, HIF-1α and VEGF-A are correlated with peritumoral edema (69), which was demonstrated to be associated with poor prognosis in meningiomas.

RESISTANCE TO APOPTOSIS

Apoptosis, a well-known form of cell death that occurs in response to external stimuli or internal stresses, is generally inhibited in tumor cells, resulting in uncontrolled proliferation (70). Numerous studies have indicated that the Wnt signaling pathway has an important role in resistance to apoptosis in neurological disorders, such as stroke (71, 72), spinal cord injury (73, 74), neuroblastoma (75), and glioma (76). The Wnt signaling pathway was recently reported to be associated with the apoptosis of meningioma cells *via* three pathways, the classical Wnt/β-catenin signaling, the planar cell polarity pathway, and the Wnt-Ca^{2+} pathway (77–80). Inhibition of the Wnt/β-catenin pathway by plant medicines leads to apoptosis in human meningioma cells (81). The long non-coding (lnc) RNA SNHG1 was found to inhibit apoptosis in BEN-1-1 and IOMM-Lee cells, and SNHG1 deficiency restrains cell growth and accelerates apoptosis in meningioma cell lines *via* the Wnt pathway (79). Moreover, downregulation of the lncRNA LINC00702 reportedly inhibits Wnt activity and induces apoptosis in malignant meningioma (78). Thus, the Wnt pathway seems to play a negative regulatory role in the apoptosis of meningioma cells; however, the precise underlying mechanism remains unclear.

Recent studies have reported several potential mechanisms of resistance to apoptosis in meningioma. CD163 is a type I membrane protein, the overexpression of which leads to reduced apoptosis in human meningioma cells (82). CLND6, also called claudin6, is a component of tight junctions that contributes to maintaining cell–cell junctions in epithelial cells (83). The downregulation of CLND6 has been associated with tumor occurrence, and its overexpression accelerates apoptosis in cancer cells (84–87). Additionally, CLND6 has been found to regulate migration and invasion capacities in malignant meningioma cell models (88). Rat sarcoma (RAS) is a member of the small GTPase family that participates in the regulation of embryonic development, differentiation, cell-cycle progression, and cell survival (89). The downregulation of RAS activity leads to significantly reduced ERK and AKT phosphorylation, suppresses proliferation, and induces the apoptosis of human meningioma cells (88). Furthermore, let-7d, a member of the let-7 family, has been regarded as a tumor suppressor in various cancers (90–92). Let-7d promotes apoptosis and suppresses the proliferation of meningioma by targeting AEG-1 (93). Based on a genomics analysis of 300 meningiomas, Clark et al. reported that mutations in TNF receptor-associated factor 7 (TRAF7) are also common, and they identified the accumulation of mutations in Krüppel-like factor 4 (KLF4), AKT1, and SMO (29). TRAF7, a pro-apoptotic protein containing an N-terminal RING finger domain, an adjacent TRAF-type zinc finger domain, a coiled-coil domain, and seven C-terminal WD40 repeats, affects several signaling pathways, including the NF-κB pathway, and the ubiquitination of proteins, such as c-FLIP (29, 94). TRAF7 is usually mutated together with KLF4, AKT1, or the phosphatidylinositol-4, 5-diphosphate 3-kinase catalytic subunit α protein (PIK3CA) (95, 96). KLF4 is a transcription factor. AKT1 activates the PI3K/mTOR pathway (96). In 2016, mutations in PIK3CA were found to be frequent drivers of certain meningiomas (97). Mutations in TRAF7, KLF4, AKT1, or PIK3CA are commonly associated with grade 1 meningioma, whereas combined mutations might be associated with a high recurrence rate (98). Therefore, therapies targeting the pro-apoptotic roles in recurrence and malignancy *via* different approaches might contribute to improved prognosis.

IMMUNOGENICITY

Subsets of patients still experience a progressive clinical course even after surgery and radiation, because tumors can evade the immune system *via* certain mechanisms, leading to the formation of an immunosuppressive tumor microenvironment, including the upregulation of programmed death-1 (PD-L1), suppressive cells, such as regulatory T cells, or other unknown

proteins (99). Nassiri found that meningiomas are immunogenic, characterized by massive immune infiltration and pertinent pathways including immune regulation and signaling (12). The proteins associated with immune regulation include IL-1, TNF, ING-α, and PD-1. Depending on these data, immunotherapy could be another treatment for these malignant meningiomas (99, 100). NF2 mutations and the loss of chromosome 22 are frequently observed in these meningiomas (12). Therefore, Yeung et al. explored the immunological landscape of meningiomas in an NF2-mutant murine meningioma model and found that these tumors were heavily infiltrated by anti-inflammatory M2 macrophages. Intervention with an anti-CSF1/CSF1R antibody was found to normalize the tumor microenvironment, indicating that targeting the CSF1/CSF1R axis might be a potential treatment for malignant meningiomas (99). PD-1 and PD-L1 are closely associated with higher-grade meningiomas. PD-1 inhibitors, such as nivolumab (NCT02648997) and pembrolizumab (NCT04659811), have a significant effect on preventing the recurrence of meningiomas. A phase II study in 2022 showed that pembrolizumab exerts promising efficacy on a subset of recurrent and progressive grade 2 and 3 meningiomas (NCT03279692). This study reported a lower PFS-6 rate of 0.48 and median PFS of 7.6 months for higher-grade meningiomas compared to those in previous studies (37). Masaki summarized several clinical trials investigating whether PD-1 might affect recurrent meningiomas (100). In addition, the effect of IFN-α was demonstrated in several highly vascularized tumors, such as gliomas and meningiomas (32). A clinical trial of IFN-α-2B found that it could improve the prognosis of grade I recurrent meningiomas and induce disease stability (101).

CHROMOSOMAL ABNORMALITIES

Epigenomics studies have revealed that transcriptional and epigenomic regulatory mechanisms occupy an important part in recurrent and progressive meningiomas. Except for gene mutations and some special molecules, chromosomal abnormalities have been the hot topics these years. It was reported that higher rates of copy-number alterations and karyotypic abnormalities are linked to higher-grade meningiomas (9). Chromosome 22 is the most commonly reported abnormal chromosome in meningiomas. It shows alterations in more than half of meningiomas, especially in benign tumors, with a large proportion of deletions of chromosome 22 occurring in the neurofibromatosis type 2 gene (*NF2*) region, which contributes to the development of meningiomas (4, 102). NF2 promotes contact inhibition and tumor suppression by inhibiting mitotic signaling in the cell cortex (90). However, another study suggested that NF2 might not be involved in meningioma progression (103). A study including 775 samples revealed that the loss of *NF2* or co-occurrence with recurrent *SMARCB1* mutations frequently occurs in atypical meningiomas. *SMARCB1*, located on chromosome 22, might induce the progression of meningiomas. In addition, *NF2* alterations combined with abnormalities in AKT1 and mTOR are associated with the overgrowth of various tissues, which could be responsible for the recurrence of meningiomas (104).

Strong expression of SSTR2A receptors, inhibition of the osteoglycin/mTOR pathway, and activation of NF2 signaling promote apoptosis in malignant meningioma cells (39, 105). A recent phase II CEVOREM trial showed that the combination of everolimus, an mTOR inhibitor, and octreotide, a somatostatin agonist, has an antiproliferative effect on meningiomas (NCT00972335) (39). Atypical *NF2* mutants demonstrate chromosomal instability, which might be related to tumor invasiveness (106). Brigatinib, an inhibitor of multiple tyrosine kinases, was capable of stopping the growth of NF2-deficient xenograft meningiomas for the inhibition of multiple tyrosine kinases, including EphA2, Fer, and focal adhesion kinase 1 (FAK1) (107). A FAK inhibitor (GSK2256098) was identified to significantly improve the survival rates of patients with recurrent or progressive NF2-mutated meningiomas (NCT02933736) (108). Further, a phase II trial revealed another MEK1/2 inhibitor, selumetinib, to have an effect on NF2-related meningiomas (NCT03095248) (5, 38). These advances on NF2-related meningiomas represent a major step forward in therapeutics.

Except for chromosome 22, loss of chromosome 1p was related to recurrent meningiomas, despite total resection and was involved in the activation of the cell cycle (23, 109). Further, the loss of chromosome 14q and complex karyotypes (multiple chromosome mutations) have also been reported as independent recurrence-specific prognostic indicators of meningiomas or malignancy development (103, 106, 110–112). The genes located on chromosome 1p include TP73, CDKN2C, RAD54, EPB41, GADD45A, and ALPL, while the genes inactivated on chromosome 14q are NDRG family member 2 and maternally expressed gene 3 (113). Moreover, the loss of chromosomes 9p, 6q, 10, and 18q or the abnormal gain of 1q, 9q, 12q, 15q, 17q, and 20q has been recently reported (17, 96, 114).

DNA METHYLATION PATTERNS

In addition to those on the aforementioned mutations, studies have been conducted in recent years to understand genetic and epigenetic alterations in meningiomas. Researchers have attempted to compare meningioma grading with DNA methylation classification (MC) (6). Sahm et al. distinguished six methylation classes among 479 patients and found that these classes might predict more current clinical courses than histology (115). DNA MC could finally prove superior to traditional light microscopy in distinguishing recurrent or progressive meningiomas. The DNA MC was divided into two major epigenetic groups, including six subclasses, MC benign 1–3, MC intermediate A and B, and MC malignant, which did not correspond exactly to the WHO grade. Interestingly, most *NF2* mutations were observed in MC benign-1 meningiomas, and other *NF2* mutations were

scattered in the different groups. Mutations in four main genes, *AKT1*, *SMO*, *KLF4*, and *TRAF7*, were identified in MC benign-2 tumors. The frequency of CDKN2A and TERT mutations was higher in MC intermediate-B and MC malignant groups. MC benign-1 was related to the loss of chromosome 22q, MC benign-3 was related to frequent mutations in chromosome 5, and MC intermediates A/B and MC malignant were related to the loss of chromosome 1p. The loss of chromosome 22q was related to MC intermediate-B and MC malignant (116) **(Table 2)**. All of these mutations were found to be tightly associated with the recurrent or progressive meningiomas described previously herein, proving that DNA methylation patterns are helpful for the risk stratification of meningiomas. The authors also showed that DNA methylation patterns provide a more precise prediction of progression-free survival outcomes at 10 years of follow-up than does WHO grading. The predictive power of single or combined DNA MCs was determined to be stronger than that of WHO grades, especially for meningiomas with a WHO grade I histology and patients at a lower risk of recurrence among WHO grade II meningiomas ($p = 0.0096$) from the Brier prediction test (115). For those genes presenting with mutations associated with any clinical courses, such as *NF2*, DNA methylation guides further risk stratification compared to that with whole-genome sequencing only. Nassiri et al. also found that DNA methylation, combined with clinical factors, leads to a reliable individualized estimation of the 5-year recurrence risk of meningiomas (40). Moreover, DNA methylation patterns could distinguish intracranial meningiomas from metastatic meningiomas. A case report in 2020 showed that DNA methylation clusters distinguished liver metastasis samples from intracranial meningioma samples, indicating that DNA methylation is also a robust method for diagnosing metastatic lesions (117).

A 2022 study classified meningiomas into three methylation groups, similar to the study by Sahm and co-workers (102), and showed that DNA methylation is more accurate than histopathology in identifying high-risk tumors and is closely correlated with gene expression in meningiomas (118). This study further compared the predictive accuracy of DNA methylation with that of RNA-sequencing and cytogenetics and found a strong concordance between these groups. The authors also demonstrated that both DNA promoter methylation and copy-number variability correlated with differential gene expression (118). Further, a recent study analyzed four types of alterations together, namely DNA somatic copy-number aberrations, DNA somatic point mutations, DNA methylation, and messenger RNA abundance, and found that these could be classified into four groups (M1–4) owing to distinct biology as follows: immunogenic (M1), benign NF2 wild-type (M2), hypermetabolic (M3), and proliferative (M4) (12) **(Table 2)**. **Table 2** describes the different classifications of meningiomas. From the authors' perspective, the M2 group might be associated with angiogenesis and vasculature development. Hypermetabolic (MG3) meningiomas are enriched in protein pathways involved in nucleotide and lipid metabolism and could be related to degradation of the extracellular matrix and endothelial proliferation. Moreover, proliferative (MG4) meningiomas are enriched in proteins and genes regulating the cell cycle and proliferation. Distorted DNA methylation processes can be associated with the most aggressive molecular groups (M3–4). Those patients with MG3 and MG4 meningiomas have significantly shorter times to recurrence (log-rank test, $P = 5 \times 10^{-15}$) (12). No other studies have discussed the direct association between DNA methylation and biological mechanisms. These data show that DNA methylation has a powerful predictive value. The combination of DNA methylation and other features might be a new direction for identifying high-risk recurrent or progressive meningiomas. In the future, classifications based on more molecular features might be more accurate to predict the prognosis and guide the treatment of meningiomas.

TABLE 2 | Overview of different classifications of meningiomas in latest studies.

DNA Methylation Classification (MC)	WHO Grade	Possible Biological Group
MC Benign 1 (Mc ben-1)	Grade I/II	immunogenic
MC Benign 2 (Mc ben-2)	Grade I	benign NF2 wild-type
MC Benign 3 (Mc ben-3)	Grade I/II	hypermetabolic
MC intermediate A (Mc int-A)	Grade I/II	proliferative
MC intermediate B (Mc int-B)	Grade II/III	
MC malignant (Mc mal)	Grade II/III	
(115)		(12)

CONCLUSIONS AND PERSPECTIVES

Here, we reviewed the potential mechanisms underlying recurrent and progressive meningiomas from focused perspectives, specifically the excessive proliferation of tumor cells, neo-angiogenesis, the inhibition of apoptosis, and genetic alterations. We also describe some potential therapeutic targets and prognostic biomarkers for meningiomas from these perspectives. Although we discussed these pathological processes separately, studies have shown that they do not occur in isolation. The histological classification of tumors has shown that those high-risk meningiomas often have the following characteristics: abundant blood vessels, increased nuclear mitosis, increased cell density, loss of tumor inherent structure, blurred basement membrane, and cerebral invasion or metastasis. In the final subsection, we also summarized the chromosomal abnormalities associated with these recurrent or progressive meningiomas, but research on the key biological pathways and their characteristics is still limited. We briefly compared the latest classification of meningiomas based on DNA methylation with the WHO grade and showed that the DNA methylation classification provides a more current prognosis, which requires further confirmation. Because of the complex and subtle changes caused by genetic abnormalities or other undetected factors, the precise mechanism underlying the pathology of meningiomas remains an enigma. Therefore, an

in-depth understanding of the development of recurrent and progressive meningiomas is further required to block the disease process and improve the prognosis of the disease.

AUTHOR CONTRIBUTIONS

All authors listed have made a substantial, direct, and intellectual contribution to the work, and approved it for publication. WP, JZ and QL were responsible for the conception of the idea, and manuscript preparation; MY and LZ primarily created the figure and tables; PW and JZ prepared and revised the manuscript.

FUNDING

This work was supported by grants from the National Natural Science Foundation (81901527) and Natural Science Foundation of Chongqing (cstc2021jcyj-msxmX0862).

REFERENCES

1. Preusser M, Brastianos P, Mawrin C. Advances in Meningioma Genetics: Novel Therapeutic Opportunities. *Nat Rev Neurol* (2018) 14:106–15. doi: 10.1038/nrneurol.2017.168
2. Goldbrunner R, Stavrinou P, Jenkinson M, Sahm F, Mawrin C, Weber D, et al. EANO Guideline on the Diagnosis and Management of Meningiomas. *Neuro-Oncology* (2021) 23(11):1821–34. doi: 10.1093/neuonc/noab150
3. Qin C, Huang M, Pan Y, Li Y, Long W, Liu Q. Brain-Invasive Meningiomas: Molecular Mechanisms and Potential Therapeutic Options. *Brain Tumor Pathol* (2021) 38:156–72. doi: 10.1007/s10014-021-00399-x
4. Shao Z, Liu L, Zheng Y, Tu S, Pan Y, Yan S, et al. Molecular Mechanism and Approach in Progression of Meningioma. *Front Oncol* (2020) 10:538845. doi: 10.3389/fonc.2020.538845
5. Brastianos P, Galanis E, Butowski N, Chan J, Dunn I, Goldbrunner R, et al. Advances in Multidisciplinary Therapy for Meningiomas. *Neuro-oncology* (2019) 21:i18–31. doi: 10.1093/neuonc/noy136
6. Delgado-López P, Cubo-Delgado E, González-Bernal J, Martín-Alonso J. A Practical Overview on the Molecular Biology of Meningioma. *Curr Neurol Neurosci Rep* (2020) 20:62. doi: 10.1007/s11910-020-01084-w
7. Buerki R, Horbinski C, Kruser T, Horowitz P, James C, Lukas R. An Overview of Meningiomas. *Future Oncol (London England)* (2018) 14:2161–77. doi: 10.2217/fon-2018-0006
8. Kshettry V, Ostrom Q, Kruchko C, Al-Mefty O, Barnett G, Barnholtz-Sloan J. Descriptive Epidemiology of World Health Organization Grades II and III Intracranial Meningiomas in the United States. *Neuro-Oncology* (2015) 17:1166–73. doi: 10.1093/neuonc/nov069
9. Cordova C, Kurz S. Advances in Molecular Classification and Therapeutic Opportunities in Meningiomas. *Curr Oncol Rep* (2020) 22:84. doi: 10.1007/s11912-020-00937-4
10. Quddusi A, Virani Q, Shamim M. Factors Affecting Post-Operative Recurrence or Growth of Meningiomas, Other Than Histological Grade and Extent of Resection. *JPMA J Pakistan Med Assoc* (2019) 69:1570–1.
11. Wilson T, Huang L, Ramanathan D, Lopez-Gonzalez M, Pillai P, De Los Reyes K, et al. Review of Atypical and Anaplastic Meningiomas: Classification, Molecular Biology, and Management. *Front Oncol* (2020) 10:565582. doi: 10.3389/fonc.2020.565582
12. Nassiri F, Liu J, Patil V, Mamatjan Y, Wang J, Hugh-White R, et al. A Clinically Applicable Integrative Molecular Classification of Meningiomas. *Nature* (2021) 597:119–25. doi: 10.1038/s41586-021-03850-3
13. Driver J, Hoffman S, Tavakol S, Woodward E, Maury E, Bhave V, et al. A Molecularly Integrated Grade for Meningioma. *Neuro-Oncology* (2021) 24(5):796–808. doi: 10.1093/neuonc/noab213
14. Alvarez-Fernández M, Medema R. Novel Functions of FoxM1: From Molecular Mechanisms to Cancer Therapy. *Front Oncol* (2013) 3:30. doi: 10.3389/fonc.2013.00030
15. Winther T, Torp S. DNA Topoisomerase Iiα and Mitosin Expression Predict Meningioma Recurrence Better Than Histopathological Grade and MIB-1 After Initial Surgery. *PloS One* (2017) 12:e0172316. doi: 10.1371/journal.pone.0172316
16. Juratli T, McCabe D, Nayyar N, Williams E, Silverman I, Tummala S, et al. DMD Genomic Deletions Characterize a Subset of Progressive/Higher-Grade Meningiomas With Poor Outcome. *Acta Neuropathologica* (2018) 136:779–92. doi: 10.1007/s00401-018-1899-7
17. Lee Y, Lee Y. Molecular Characteristics of Meningiomas. *J Pathol Trans Med* (2020) 54:45–63. doi: 10.4132/jptm.2019.11.05
18. Ohta S, Taniguchi T, Sato N, Hamada M, Taniguchi H, Rappsilber J. Quantitative Proteomics of the Mitotic Chromosome Scaffold Reveals the Association of BAZ1B With Chromosomal Axes. *Mol Cell Proteomics MCP* (2019) 18:169–81. doi: 10.1074/mcp.RA118.000923
19. Kalinichenko V, Major M, Wang X, Petrovic V, Kuechle J, Yoder H, et al. Foxm1b Transcription Factor is Essential for Development of Hepatocellular Carcinomas and is Negatively Regulated by the P19arf Tumor Suppressor. *Genes Dev* (2004) 18:830–50. doi: 10.1101/gad.1200704
20. Kalin T, Wang I, Ackerson T, Major M, Detrisac C, Kalinichenko V, et al. Increased Levels of the FoxM1 Transcription Factor Accelerate Development and Progression of Prostate Carcinomas in Both TRAMP and LADY Transgenic Mice. *Cancer Res* (2006) 66:1712–20. doi: 10.1158/0008-5472.Can-05-3138
21. Liu M, Dai B, Kang S, Ban K, Huang F, Lang F, et al. FoxM1B Is Overexpressed in Human Glioblastomas and Critically Regulates the Tumorigenicity of Glioma Cells. *Cancer Res* (2006) 66:3593–602. doi: 10.1158/0008-5472.Can-05-2912
22. Teh M, Wong S, Neill G, Ghali L, Philpott M, Quinn A. FOXM1 Is a Downstream Target of Gli1 in Basal Cell Carcinomas. *Cancer Res* (2002) 62:4773–80.
23. Vasudevan H, Braunstein S, Phillips J, Pekmezci M, Tomlin B, Wu A, et al. Comprehensive Molecular Profiling Identifies FOXM1 as a Key Transcription Factor for Meningioma Proliferation. *Cell Rep* (2018) 22:3672–83. doi: 10.1016/j.celrep.2018.03.013
24. Yamazaki S, Ohka F, Hirano M, Shiraki Y, Motomura K, Tanahashi K, et al. Newly Established Patient-Derived Organoid Model of Intracranial Meningioma. *Neuro-Oncology* (2021) 23(11):1936–48. doi: 10.1093/neuonc/noab155
25. Brastianos P, Horowitz P, Santagata S, Jones R, McKenna A, Getz G, et al. Genomic Sequencing of Meningiomas Identifies Oncogenic SMO and AKT1 Mutations. *Nat Genet* (2013) 45:285–9. doi: 10.1038/ng.2526
26. Carpten J, Faber A, Horn C, Donoho G, Briggs S, Robbins C, et al. A Transforming Mutation in the Pleckstrin Homology Domain of AKT1 in Cancer. *Nature* (2007) 448:439–44. doi: 10.1038/nature05933
27. Barresi V, Lionti S, La Rocca L, Caliri S, Caffo M. High p-mTOR Expression is Associated With Recurrence and Shorter Disease-Free Survival in Atypical Meningiomas. *Neuropathology* (2019) 39:22–9. doi: 10.1111/neup.12524
28. Yesilöz Ü, Kirches E, Hartmann C, Scholz J, Kropf S, Sahm F, et al. Frequent AKT1E17K Mutations in Skull Base Meningiomas Are Associated With mTOR and ERK1/2 Activation and Reduced Time to Tumor Recurrence. *Neuro-oncology* (2017) 19:1088–96. doi: 10.1093/neuonc/nox018
29. Clark V, Erson-Omay E, Serin A, Yin J, Cotney J, Ozduman K, et al. Genomic Analysis of Non-NF2 Meningiomas Reveals Mutations in TRAF7, KLF4, AKT1, and SMO. *Sci (New York N.Y.)* (2013) 339:1077–80. doi: 10.1126/science.1233009
30. Ng J, Curran T. The Hedgehog's Tale: Developing Strategies for Targeting Cancer. *Nat Rev Cancer* (2011) 11:493–501. doi: 10.1038/nrc3079
31. Wang X, Gong Y, Wang D, Xie Q, Zheng M, Zhou Y, et al. Analysis of Gene Expression Profiling in Meningioma: Deregulated Signaling Pathways

Associated With Meningioma and EGFL6 Overexpression in Benign Meningioma Tissue and Serum. *PloS One* (2012) 7:e52707. doi: 10.1371/journal.pone.0052707
32. Kim L. A Narrative Review of Targeted Therapies in Meningioma. *Chin Clin Oncol* (2020) 9:76. doi: 10.21037/cco-2020-mbt-01
33. Maier A, Stenman A, Svahn F, Mirian C, Bartek J, Juhler M, et al. TERT Promoter Mutations in Primary and Secondary WHO Grade III Meningioma. *Brain Pathol (Zurich Switzerland)* (2021) 31:61–9. doi: 10.1111/bpa.12892
34. Wei Y, Xia W, Zhang Z, Liu J, Wang H, Adsay N, et al. Loss of Trimethylation at Lysine 27 of Histone H3 Is a Predictor of Poor Outcome in Breast, Ovarian, and Pancreatic Cancers. *Mol Carcinog* (2008) 47:701–6. doi: 10.1002/mc.20413
35. Dasanu C, Alvarez-Argote J, Limonadi F, Codreanu I. Bevacizumab in Refractory Higher-Grade and Atypical Meningioma: The Current State of Affairs. *Expert Opin Biol Ther* (2019) 19:99–104. doi: 10.1080/14712598.2019.1559292
36. Franke A, Skelton W, Woody L, Bregy A, Shah A, Vakharia K, et al. Role of Bevacizumab for Treatment-Refractory Meningiomas: A Systematic Analysis and Literature Review. *Surg Neurol Int* (2018) 9:133. doi: 10.4103/sni.sni_264_17
37. Brastianos P, Kim A, Giobbie-Hurder A, Lee E, Wang N, Eichler A, et al. Phase 2 Study of Pembrolizumab in Patients With Recurrent and Residual High-Grade Meningiomas. *Nat Commun* (2022) 13:1325. doi: 10.1038/s41467-022-29052-7
38. Moussalem C, Massaad E, Minassian G, Ftouni L, Bsat S, Houshiemy M, et al. Meningioma Genomics: A Therapeutic Challenge for Clinicians. *J Integr Neurosci* (2021) 20:463–9. doi: 10.31083/j.jin2002049
39. Graillon T, Sanson M, Campello C, Idbaih A, Peyre M, Peyrière H, et al. Everolimus and Octreotide for Patients With Recurrent Meningioma: Results From the Phase II CEVOREM Trial. *Clin Cancer Res* (2020) 26:552–7. doi: 10.1158/1078-0432.Ccr-19-2109
40. Nassiri F, Mamatjan Y, Suppiah S, Badhiwala J, Mansouri S, Karimi S, et al. DNA Methylation Profiling to Predict Recurrence Risk in Meningioma: Development and Validation of a Nomogram to Optimize Clinical Management. *Neuro-oncology* (2019) 21:901–10. doi: 10.1093/neuonc/noz061
41. Boström J, Meyer-Puttlitz B, Wolter M, Blaschke B, Weber R, Lichter P, et al. Alterations of the Tumor Suppressor Genes CDKN2A (P16(INK4a)), P14 (ARF), CDKN2B (P15(INK4b)), and CDKN2C (P18(INK4c)) in Atypical and Anaplastic Meningiomas. *Am J Pathol* (2001) 159:661–9. doi: 10.1016/s0002-9440(10)61737-3
42. Perry A, Banerjee R, Lohse C, Kleinschmidt-DeMasters B, Scheithauer B. A Role for Chromosome 9p21 Deletions in the Malignant Progression of Meningiomas and the Prognosis of Anaplastic Meningiomas. *Brain Pathol (Zurich Switzerland)* (2002) 12:183–90. doi: 10.1111/j.1750-3639.2002.tb00433.x
43. Trott G, Pereira-Lima J, Leães C, Ferreira N, Barbosa-Coutinho L, Oliveira M. Abundant Immunohistochemical Expression of Dopamine D2 Receptor and P53 Protein in Meningiomas: Follow-Up, Relation to Gender, Age, Tumor Grade, and Recurrence. *Braz J Med Biol Res = Rev Bras Pesquisas Medicas e Biologicas* (2015) 48:415–9. doi: 10.1590/1414-431x20144163
44. Hansen S, Hart M, Busi S, Parker T, Goerndt A, Jones K, et al. Fischer-344 Tp53-Knockout Rats Exhibit a High Rate of Bone and Brain Neoplasia With Frequent Metastasis. *Dis Models Mech* (2016) 9:1139–46. doi: 10.1242/dmm.025767
45. Pavelin S, Becic K, Forempoher G, Mrklic I, Pogorelic Z, Titlic M, et al. Expression of Ki-67 and P53 in Meningiomas. *Neoplasma* (2013) 60:480–5. doi: 10.4149/neo_2013_062
46. Ervasti J. Dystrophin, its Interactions With Other Proteins, and Implications for Muscular Dystrophy. *Biochim Biophys Acta* (2007) 1772:108–17. doi: 10.1016/j.bbadis.2006.05.010
47. Prins K, Humston J, Mehta A, Tate V, Ralston E, Ervasti J. Dystrophin Is a Microtubule-Associated Protein. *J Cell Biol* (2009) 186:363–9. doi: 10.1083/jcb.200905048
48. Reuss D, Piro R, Jones D, Simon M, Ketter R, Kool M, et al. Secretory Meningiomas Are Defined by Combined KLF4 K409Q and TRAF7 Mutations. *Acta Neuropathologica* (2013) 125:351–8. doi: 10.1007/s00401-013-1093-x
49. Shankar G, Abedalthagafi M, Vaubel R, Merrill P, Nayyar N, Gill C, et al. Germline and Somatic BAP1 Mutations in High-Grade Rhabdoid Meningiomas. *Neuro-oncology* (2017) 19:535–45. doi: 10.1093/neuonc/now235
50. Collord G, Tarpey P, Kurbatova N, Martincorena I, Moran S, Castro M, et al. An Integrated Genomic Analysis of Anaplastic Meningioma Identifies Prognostic Molecular Signatures. *Sci Rep* (2018) 8:13537. doi: 10.1038/s41598-018-31659-0
51. Spiegl-Kreinecker S, Lötsch D, Neumayer K, Kastler L, Gojo J, Pirker C, et al. TERT Promoter Mutations Are Associated With Poor Prognosis and Cell Immortalization in Meningioma. *Neuro-oncology* (2018) 20:1584–93. doi: 10.1093/neuonc/noy104
52. Juratli T, Thiede C, Koerner M, Tummala S, Daubner D, Shankar G, et al. TERTIntratumoral Heterogeneity and Promoter Mutations in Progressive/Higher-Grade Meningiomas. *Oncotarget* (2017) 8:109228–37. doi: 10.18632/oncotarget.22650
53. Mellai M, Porrini Prandini O, Mustaccia A, Fogazzi V, Allesina M, Krengli M, et al. Human TERT Promoter Mutations in Atypical and Anaplastic Meningiomas. *Diagnostics (Basel Switzerland)* (2021) 11:1624. doi: 10.3390/diagnostics11091624
54. Goutagny S, Nault J, Mallet M, Henin D, Rossi J, Kalamarides M. High Incidence of Activating TERT Promoter Mutations in Meningiomas Undergoing Malignant Progression. *Brain Pathol (Zurich Switzerland)* (2014) 24:184–9. doi: 10.1111/bpa.12110
55. Deng J, Sun S, Chen J, Wang D, Cheng H, Chen H, et al. TERT Alterations Predict Tumor Progression in High-Grade Meningiomas Following Adjuvant Radiotherapy. *Front Oncol* (2021) 11:747592. doi: 10.3389/fonc.2021.747592
56. Katz L, Hielscher T, Liechty B, Silverman J, Zagzag D, Sen R, et al. Loss of Histone H3K27me3 Identifies a Subset of Meningiomas With Increased Risk of Recurrence. *Acta Neuropathologica* (2018) 135:955–63. doi: 10.1007/s00401-018-1844-9
57. Jung M, Kim S, Lim K, Bae J, Park C, Choi S, et al. The Substantial Loss of H3K27me3 can Stratify Risk in Grade 2, But Not in Grade 3 Meningioma. *Hum Pathol* (2021) 115:96–103. doi: 10.1016/j.humpath.2021.06.005
58. Nassiri F, Wang J, Singh O, Karimi S, Dalcourt T, Ijad N, et al. Loss of H3K27me3 in Meningiomas. *Neuro-oncology* (2021) 23:1282–91. doi: 10.1093/neuonc/noab036
59. Hess K, Spille D, Adeli A, Sporns P, Zitta K, Hummitzsch L, et al. Occurrence of Fibrotic Tumor Vessels in Grade I Meningiomas Is Strongly Associated With Vessel Density, Expression of VEGF, PlGF, IGFBP-3 and Tumor Recurrence. *Cancers* (2020) 12:3075. doi: 10.3390/cancers12103075
60. Bernatz S, Monden D, Gessler F, Radic T, Hattingen E, Senft C, et al. Influence of VEGF-A, VEGFR-1-3, and Neuropilin 1-2 on Progression-Free: And Overall Survival in WHO Grade II and III Meningioma Patients. *J Mol Histol* (2021) 52:233–43. doi: 10.1007/s10735-020-09940-2
61. Nassehi D, Dyrbye H, Andresen M, Thomsen C, Juhler M, Laursen H, et al. Vascular Endothelial Growth Factor A Protein Level and Gene Expression in Intracranial Meningiomas With Brain Edema. *APMIS* (2011) 119:831–43. doi: 10.1111/j.1600-0463.2011.02764.x
62. Xiao Z, Chen X, Pan Q, Yang Q, Li K. Expression of Nestin, CD133 and Sox2 in Meningiomas. *Turkish Neurosurg* (2018) 28:910–4. doi: 10.5137/1019-5149.Jtn.21234-17.2
63. Nassehi D. Intracranial Meningiomas, the VEGF-A Pathway, and Peritumoral Brain Oedema. *Danish Med J* (2013) 60:B4626.
64. Dasanu C, Samara Y, Codreanu I, Limonadi F, Hamid O, Alvarez-Argote J. Systemic Therapy for Relapsed/Refractory Meningioma: Is There Potential for Antiangiogenic Agents? *J Oncol Pharm Pract* (2019) 25:638–47. doi: 10.1177/1078155218799850
65. Barresi V, Branca G, Caffo M, Tuccari G. P-CREB Expression in Human Meningiomas: Correlation With Angiogenesis and Recurrence Risk. *J Neuro-Oncol* (2015) 122:87–95. doi: 10.1007/s11060-014-1706-9
66. Barresi V, Mondello S, Branca G, Rajan T, Vitarelli E, Tuccari G. P-CREB Expression in Human Gliomas: Potential Use in the Differential Diagnosis

Between Astrocytoma and Oligodendroglioma. *Hum Pathol* (2015) 46:231–8. doi: 10.1016/j.humpath.2014.10.011
67. Khan I, Baeesa S, Bangash M, Schulten H, Alghamdi F, Qashqari H, et al. Pleomorphism and Drug Resistant Cancer Stem Cells Are Characteristic of Aggressive Primary Meningioma Cell Lines. *Cancer Cell Int* (2017) 17:72. doi: 10.1186/s12935-017-0441-7
68. Ager E, Neo J, Christophi C. The Renin-Angiotensin System and Malignancy. *Carcinogenesis* (2008) 29:1675–84. doi: 10.1093/carcin/bgn171
69. Tirakotai W, Mennel H, Celik I, Hellwig D, Bertalanffy H, Riegel T. Secretory Meningioma: Immunohistochemical Findings and Evaluation of Mast Cell Infiltration. *Neurosurgical Rev* (2006) 29:41–8. doi: 10.1007/s10143-005-0402-9
70. Mohammad R, Muqbil I, Lowe L, Yedjou C, Hsu H, Lin L, et al. Broad Targeting of Resistance to Apoptosis in Cancer. *Semin Cancer Biol* (2015) 35: S78–103. doi: 10.1016/j.semcancer.2015.03.001
71. Che Q, Huang T, Zhang Y, Qian X. Effect of miR-124 on Neuronal Apoptosis in Rats With Cerebral Infarction Through Wnt/β-Catenin Signaling Pathway. *Eur Rev Med Pharmacol Sci* (2019) 23:6657–64. doi: 10.26355/eurrev_201908_18556
72. Ruan W, Hu J, Zhou H, Li Y, Xu C, Luo Y, et al. Intranasal Wnt-3a Alleviates Neuronal Apoptosis in Early Brain Injury Post Subarachnoid Hemorrhage *via* the Regulation of Wnt Target PPAN Mediated by the Moonlighting Role of Aldolase C. *Neurochem Int* (2020) 134:104656. doi: 10.1016/j.neuint.2019.104656
73. Gao K, Shen Z, Yuan Y, Han D, Song C, Guo Y, et al. Simvastatin Inhibits Neural Cell Apoptosis and Promotes Locomotor Recovery *via* Activation of Wnt/β-Catenin Signaling Pathway After Spinal Cord Injury. *J Neurochem* (2016) 138:139–49. doi: 10.1111/jnc.13382
74. Li C, Jiao G, Wu W, Wang H, Ren S, Zhang L, et al. Exosomes From Bone Marrow Mesenchymal Stem Cells Inhibit Neuronal Apoptosis and Promote Motor Function Recovery *via* the Wnt/β-Catenin Signaling Pathway. *Cell Transplant* (2019) 28:1373–83. doi: 10.1177/0963689719870999
75. Tian X, Hou W, Fang Y, Fan J, Tong H, Bai S, et al. XAV939, a Tankyrase 1 Inhibitior, Promotes Cell Apoptosis in Neuroblastoma Cell Lines by Inhibiting Wnt/β-Catenin Signaling Pathway. *J Exp Clin Cancer Res CR* (2013) 32:100. doi: 10.1186/1756-9966-32-100
76. Li Q, Shen K, Zhao Y, Ma C, Liu J, Ma J. MiR-92b Inhibitor Promoted Glioma Cell Apoptosis *via* Targeting DKK3 and Blocking the Wnt/beta-Catenin Signaling Pathway. *J Trans Med* (2013) 11:302. doi: 10.1186/1479-5876-11-302
77. Pećina-Šlaus N, Kafka A, Lechpammer M. Molecular Genetics of Intracranial Meningiomas With Emphasis on Canonical Wnt Signalling. *Cancers* (2016) 8. doi: 10.3390/cancers8070067
78. Shi Z, Fan Z, Chen Y, Xie X, Jiang W, Wang W, et al. Ferroptosis in Carcinoma: Regulatory Mechanisms and New Method for Cancer Therapy. *OncoTargets Ther* (2019) 12:11291–304. doi: 10.2147/ott.S232852
79. Zhang Y, Yu R, Li Q, Li Y, Xuan T, Cao S, et al. SNHG1/miR-556-5p/TCF12 Feedback Loop Enhances the Tumorigenesis of Meningioma Through Wnt Signaling Pathway. *J Cell Biochem* (2020) 121:1880–9. doi: 10.1002/jcb.29423
80. Sharma S, Ray S, Mukherjee S, Moiyadi A, Sridhar E, Srivastava S. Multipronged Quantitative Proteomic Analyses Indicate Modulation of Various Signal Transduction Pathways in Human Meningiomas. *Proteomics* (2015) 15:394–407. doi: 10.1002/pmic.201400328
81. Das A, Miller R, Lee P, Holden C, Lindhorst S, Jaboin J, et al. A Novel Component From Citrus, Ginger, and Mushroom Family Exhibits Antitumor Activity on Human Meningioma Cells Through Suppressing the Wnt/β-Catenin Signaling Pathway. *Tumour Biol J Int Soc Oncodevelopmental Biol Med* (2015) 36:7027–34. doi: 10.1007/s13277-015-3388-0
82. Kanno H, Nishihara H, Wang L, Yuzawa S, Kobayashi H, Tsuda M, et al. Expression of CD163 Prevents Apoptosis Through the Production of Granulocyte Colony-Stimulating Factor in Meningioma. *Neuro-Oncology* (2013) 15:853–64. doi: 10.1093/neuonc/not028
83. Tsukita S, Furuse M. Claudin-Based Barrier in Simple and Stratified Cellular Sheets. *Curr Opin Cell Biol* (2002) 14:531–6. doi: 10.1016/s0955-0674(02)00362-9
84. Liu Y, Jin X, Li Y, Ruan Y, Lu Y, Yang M, et al. DNA Methylation of Claudin-6 Promotes Breast Cancer Cell Migration and Invasion by Recruiting MeCP2 and Deacetylating H3Ac and H4Ac. *J Exp Clin Cancer Res CR* (2016) 35:120. doi: 10.1186/s13046-016-0396-x
85. Guo Y, Lin D, Zhang M, Zhang X, Li Y, Yang R, et al. CLDN6-Induced Apoptosis *via* Regulating ASK1-P38/JNK Signaling in Breast Cancer MCF-7 Cells. *Int J Oncol* (2016) 48:2435–44. doi: 10.3892/ijo.2016.3469
86. Torres-Martínez A, Gallardo-Vera J, Lara-Holguin A, Montaño L, Rendón-Huerta E. Claudin-6 Enhances Cell Invasiveness Through Claudin-1 in AGS Human Adenocarcinoma Gastric Cancer Cells. *Exp Cell Res* (2017) 350:226–35. doi: 10.1016/j.yexcr.2016.11.025
87. Wang Q, Zhang Y, Zhang T, Han Z, Shan L. Low Claudin-6 Expression Correlates With Poor Prognosis in Patients With Non-Small Cell Lung Cancer. *OncoTargets Ther* (2015) 8:1971–7. doi: 10.2147/ott.S85478
88. Yang A, Yang X, Wang J, Wang X, Wu H, Fan L, et al. Effects of the Tight Junction Protein CLDN6 on Cell Migration and Invasion in High-Grade Meningioma. *World Neurosurg* (2021) 151:e208-e216. doi: 10.1016/j.wneu.2021.04.005
89. Takashima A, Faller D. Targeting the RAS Oncogene. *Expert Opin Ther Targets* (2013) 17:507–31. doi: 10.1517/14728222.2013.764990
90. Garzon R, Pichiorri F, Palumbo T, Visentini M, Aqeilan R, Cimmino A, et al. MicroRNA Gene Expression During Retinoic Acid-Induced Differentiation of Human Acute Promyelocytic Leukemia. *Oncogene* (2007) 26:4148–57. doi: 10.1038/sj.onc.1210186
91. Ramberg H, Alshbib A, Berge V, Svindland A, Taskén K. Regulation of PBX3 Expression by Androgen and Let-7d in Prostate Cancer. *Mol Cancer* (2011) 10:50. doi: 10.1186/1476-4598-10-50
92. Masood F, Khan W, Uddin R. Computational-Based Identification and Analysis of Globally Expressed Differential Genes in High-Grade Serous Ovarian Carcinoma Cell Lines. *Comput Biol Chem* (2020) 88:107333. doi: 10.1016/j.compbiolchem.2020.107333
93. Li H, Zhao J. Let-7d Suppresses Proliferation and Invasion and Promotes Apoptosis of Meningioma by Targeting AEG-1. *OncoTargets Ther* (2017) 10:4895–904. doi: 10.2147/ott.S141008
94. Castilla-Vallmanya L, Selmer K, Dimartino C, Rabionet R, Blanco-Sánchez B, Yang S, et al. Phenotypic Spectrum and Transcriptomic Profile Associated With Germline Variants in TRAF7. *Genet Med* (2020) 22:1215–26. doi: 10.1038/s41436-020-0792-7
95. Birzu C, Peyre M, Sahm F. Molecular Alterations in Meningioma: Prognostic and Therapeutic Perspectives. *Curr Opin Oncol* (2020) 32:613–22. doi: 10.1097/cco.0000000000000687
96. Venur V, Santagata S, Galanis E, Brastianos P. New Molecular Targets in Meningiomas: The Present and the Future. *Curr Opin Neurol* (2018) 31:740–6. doi: 10.1097/wco.0000000000000615
97. Bi W, Prabhu V, Dunn I. High-Grade Meningiomas: Biology and Implications. *Neurosurgical Focus* (2018) 44:E2. doi: 10.3171/2017.12.Focus17756
98. Abedalthagafi M, Bi W, Aizer A, Merrill P, Brewster R, Agarwalla P, et al. Oncogenic PI3K Mutations Are as Common as AKT1 and SMO Mutations in Meningioma. *Neuro-Oncology* (2016) 18:649–55. doi: 10.1093/neuonc/nov316
99. Yeung J, Yaghoobi V, Miyagishima D, Vesely M, Zhang T, Badri T, et al. Targeting the CSF1/CSF1R Axis Is a Potential Treatment Strategy for Malignant Meningiomas. *Neuro-Oncology* (2021) 23:1922–35. doi: 10.1093/neuonc/noab075
100. Terabe M, Wu J. Rethinking Immunotherapy in Meningiomas. *Neuro-Oncology* (2021) 23:1812–13. doi: 10.1093/neuonc/noab168
101. Chamberlain M, Glantz M. Interferon-Alpha for Recurrent World Health Organization Grade 1 Intracranial Meningiomas. *Cancer* (2008) 113:2146–51. doi: 10.1002/cncr.23803
102. Parada C, Osbun J, Kaur S, Yakkioui Y, Shi M, Pan C, et al. Kinome and Phosphoproteome of High-Grade Meningiomas Reveal AKAP12 as a Central Regulator of Aggressiveness and its Possible Role in Progression. *Sci Rep* (2018) 8:2098. doi: 10.1038/s41598-018-19308-y
103. Riemenschneider M, Perry A, Reifenberger G. Histological Classification and Molecular Genetics of Meningiomas. *Lancet Neurol* (2006) 5:1045–54. doi: 10.1016/s1474-4422(06)70625-1
104. Keppler-Noreuil K, Baker E, Sapp J, Lindhurst M, Biesecker L. Somatic AKT1 Mutations Cause Meningiomas Colocalizing With a Characteristic Pattern of Cranial Hyperostosis. *Am J Med Genet Part A* (2016) 170:2605–10. doi: 10.1002/ajmg.a.37737

105. Wang J, Lv P. Chrysophanol Inhibits the Osteoglycin/mTOR and Activats NF2 Signaling Pathways to Reduce Viability and Proliferation of Malignant Meningioma Cells. *Bioengineered* (2021) 12:755–62. doi: 10.1080/21655979.2021.1885864
106. Harmancı A, Youngblood M, Clark V, Coşkun S, Henegariu O, Duran D, et al. Integrated Genomic Analyses of *De Novo* Pathways Underlying Atypical Meningiomas. *Nat Commun* (2017) 8:14433. doi: 10.1038/ncomms14433
107. Chang L, Oblinger J, Smith A, Ferrer M, Angus S, Hawley E, et al. Brigatinib Causes Tumor Shrinkage in Both NF2-Deficient Meningioma and Schwannoma Through Inhibition of Multiple Tyrosine Kinases But Not ALK. *PloS One* (2021) 16:e0252048. doi: 10.1371/journal.pone.0252048
108. Brastianos PK, Twohy E, Gerstner ER, Kaufmann TJ, Iafrate AJ, Jeyapalan SA, et al. Alliance A071401: Phase II Trial of FAK Inhibition in Meningiomas With Somatic NF2 Mutations. *J Clin Oncol* (2020) 38:2502–2. doi: 10.1200/JCO.2020.38.15_suppl.2502
109. Patel A, Wan Y, Al-Ouran R, Revelli J, Cardenas M, Oneissi M, et al. Molecular Profiling Predicts Meningioma Recurrence and Reveals Loss of DREAM Complex Repression in Aggressive Tumors. *Proc Natl Acad Sci USA* (2019) 116:21715–26. doi: 10.1073/pnas.1912858116
110. Lamszus K. Meningioma Pathology, Genetics, and Biology. *J Neuropathol Exp Neurol* (2004) 63:275–86. doi: 10.1093/jnen/63.4.275
111. Och W, Szmuda T, Kulbacki K, Witek K, Sikorska B, Zakrzewska M, et al. The Correlation of Clinical and Chromosomal Alterations of Benign Meningiomas and Their Recurrences. *Neurologia i Neurochirurgia Polska* (2016) 50:395–402. doi: 10.1016/j.pjnns.2016.07.001
112. Och W, Szmuda T, Sikorska B, Springer J, Jaskólski D, Zakrzewska M, et al. Recurrence-Associated Chromosomal Anomalies in Meningiomas: Single-Institution Study and a Systematic Review With Meta-Analysis. *Neurologia i Neurochirurgia Polska* (2016) 50:439–48. doi: 10.1016/j.pjnns.2016.08.003
113. Ogasawara C, Philbrick B, Adamson D. Meningioma: A Review of Epidemiology, Pathology, Diagnosis, Treatment, and Future Directions. *Biomedicines* (2021) 9:319. doi: 10.3390/biomedicines9030319
114. Aizer A, Abedalthagafi M, Bi W, Horvath M, Arvold N, Al-Mefty O, et al. A Prognostic Cytogenetic Scoring System to Guide the Adjuvant Management of Patients With Atypical Meningioma. *Neuro-Oncology* (2016) 18:269–74. doi: 10.1093/neuonc/nov177
115. Sahm F, Schrimpf D, Stichel D, Jones D, Hielscher T, Schefzyk S, et al. DNA Methylation-Based Classification and Grading System for Meningioma: A Multicentre, Retrospective Analysis. *Lancet Oncol* (2017) 18:682–94. doi: 10.1016/s1470-2045(17)30155-9
116. Youngblood M, Miyagishima D, Jin L, Gupte T, Li C, Duran D, et al. Associations of Meningioma Molecular Subgroup and Tumor Recurrence. *Neuro-oncology* (2021) 23:783–94. doi: 10.1093/neuonc/noaa226
117. Vasudevan H, Castro M, Lee J, Villanueva-Meyer J, Bush N, McDermott M, et al. DNA Methylation Profiling Demonstrates Superior Diagnostic Classification to RNA-Sequencing in a Case of Metastatic Meningioma. *Acta Neuropathologica Commun* (2020) 8:82. doi: 10.1186/s40478-020-00952-3
118. Bayley J, Hadley C, Harmanci A, Harmanci A, Klisch T, Patel A. Multiple Approaches Converge on Three Biological Subtypes of Meningioma and Extract New Insights From Published Studies. *Sci Adv* (2022) 8:eabm6247. doi: 10.1126/sciadv.abm6247

Conflict of Interest: The authors declare that the research was conducted in the absence of any commercial or financial relationships that could be construed as a potential conflict of interest.

Publisher's Note: All claims expressed in this article are solely those of the authors and do not necessarily represent those of their affiliated organizations, or those of the publisher, the editors and the reviewers. Any product that may be evaluated in this article, or claim that may be made by its manufacturer, is not guaranteed or endorsed by the publisher.

Copyright © 2022 Peng, Wu, Yuan, Yuan, Zhu, Zhou and Li. This is an open-access article distributed under the terms of the Creative Commons Attribution License (CC BY). The use, distribution or reproduction in other forums is permitted, provided the original author(s) and the copyright owner(s) are credited and that the original publication in this journal is cited, in accordance with accepted academic practice. No use, distribution or reproduction is permitted which does not comply with these terms.

frontiers | Frontiers in Oncology

REVIEW
published: 31 May 2022
doi: 10.3389/fonc.2022.892004

Synthesizing Molecular and Immune Characteristics to Move Beyond WHO Grade in Meningiomas: A Focused Review

Nivedha V. Kannapadi[†], *Pavan P. Shah*[†], *Dimitrios Mathios and Christopher M. Jackson*[*]

Department of Neurosurgery, Johns Hopkins University School of Medicine, Baltimore, MD, United States

OPEN ACCESS

Edited by:
Hailiang Tang,
Fudan University, China

Reviewed by:
Subhas K. Konar,
National Institute of Mental Health and Neurosciences (NIMHANS), India
Hiroaki Wakimoto,
Massachusetts General Hospital and Harvard Medical School, United States
Raj Shrivastava,
Mount Sinai Hospital, United States

***Correspondence:**
Christopher M. Jackson
Cjacks53@jhmi.edu

[†]*These authors have contributed equally to this work and share first authorship*

Specialty section:
This article was submitted to Neuro-Oncology and Neurosurgical Oncology, a section of the journal Frontiers in Oncology

Received: *08 March 2022*
Accepted: *02 May 2022*
Published: *31 May 2022*

Citation:
Kannapadi NV, Shah PP, Mathios D and Jackson CM (2022) Synthesizing Molecular and Immune Characteristics to Move Beyond WHO Grade in Meningiomas: A Focused Review. Front. Oncol. 12:892004. doi: 10.3389/fonc.2022.892004

No portion of this manuscript has previously been presented. Meningiomas, the most common primary intracranial tumors, are histologically categorized by the World Health Organization (WHO) grading system. While higher WHO grade is generally associated with poor clinical outcomes, a significant subset of grade I tumors recur or progress, indicating a need for more reliable models of meningioma behavior. Several groups have developed risk scores based on molecular or immunologic characteristics. These classification schemes show promise, with several models preliminarily demonstrating similar or superior accuracy to WHO grading. Improved understanding of immune system recognition and targeting of meningioma subtypes is necessary to advance the predictive power, as well as develop new therapies. Here, we characterize meningioma molecular drivers, predictive of recurrence and progression, and describe specific aspects of the immune response to meningiomas while highlighting critical questions and ongoing research. Relevant manuscripts of interest were identified using a systematic approach and synthesized into this focused review. Finally, we summarize the ongoing and completed clinical trials for immunotherapy in meningiomas and offer perspective on future directions.

Keywords: meningioma, immunotherapy, immune microenvironment, prognostic model, risk score, meningioma WHO grade I

INTRODUCTION

Meningiomas are the most common primary intracranial neoplasm, comprising approximately 40% of all primary central nervous system tumors (1). Treatment for symptomatic or enlarging tumors consists of maximum safe surgical resection with radiation therapy applied to residual, recurrent, or high-risk lesions (2). There are no effective chemotherapy regimens for meningiomas and clinical trials for targeted therapies are ongoing (3). Meningiomas are classified according to World Health Organization (WHO) grade, with the majority (69-78%) classified as grade I, followed by grades II and III (20.4-30% and 1-1.6%, respectively) (4, 5). Grades II and III tumors recur more frequently, with rates varying between 28-52% and 40-84%, respectively (6–9). The degree of surgical resection correlates with the risk of tumor recurrence or progression and is classified by the Simpson grading

scale (10). However, many tumors recur despite aggressive resection. Simpson grade 1 involves gross total resection of the tumor with removal of affected dura and bone and has a 5-year recurrence rate ranging from 0 to 21% (11). Grade 2, which involves gross total resection with cautery of dural margin, and grade 3, gross total resection, are associated with 5-year recurrence rates of 5-33% and 0-40%, respectively (11). Subtotal resection, classified as grade 4, is associated with a 5- and 10-year recurrence rate of 49-52% and 83%, respectively (12, 13). While higher WHO grades are associated with worse clinical outcomes, a grade I designation does not reliably predict tumor behavior, as 10-47% of grade I meningiomas recur or progress (14, 15).

WHO grade-matched meningiomas exhibit considerable heterogeneity, particularly in genetic alterations and immune cell infiltration. This diversity implies that a molecular and inflammatory classification framework might ultimately prove superior to the WHO grading system for predicting meningioma behavior. Predictive risk scores based on these factors have shown promise in identifying both high-risk grade I tumors and low-risk grade III tumors. One such molecular classification system defined four unique consensus molecular phenotypes and found that an "immunogenic" phenotype was associated with improved clinical outcomes (16). These findings indicate that a detailed understanding of how the immune system recognizes and attacks specific meningioma subtypes could more reliably predict progression.

In this focused review, we consider meningioma tumor characteristics, such as mutations, chromosomal aberrations, and hypermethylation, that may carry prognostic value independent of WHO grade. We also discuss specific aspects of the immune response to meningiomas, including tumor-intrinsic factors such as mutational burden as well as the mechanics of immune recognition and tumor cell elimination. Finally, we synthesize the available data and highlight some of the necessary steps to develop a molecular and immunologic classification scheme for meningiomas.

METHODS

We systematically reviewed the relevant literature on molecular and immune environments of meningiomas, published on Pubmed from database inception to April 2022. We identified 750 studies, using the search string "(Meningioma AND immunology) OR (Meningioma AND chemokine) OR (Meningioma AND molecular AND classification)". Included studies must (1) describe meningiomas and (2) include characterization of immunologic or molecular disease features. Exclusion criteria include (1) non-English primary language (2) abstract only with no full-text manuscript (3) studies of other brain tumors with no data on meningiomas and (4) no discussion of clinical implications of molecular/immune markers. 66 manuscripts were included after abstract screening, and 40 manuscripts were included after full text review. Remaining studies of interest were accessed based on the reference lists of these manuscripts.

MOLECULAR DRIVERS OF MENINGIOMA RECURRENCE AND PROGRESSION

Meningiomas have several key molecular alterations that have been extensively described (17, 18). The 2021 WHO classification criteria incorporates 10 genes that are frequently altered in meningiomas, including *NF2, AKT1, TRAF7, SMO, PIK3CA* (19). Additionally, *TERT* promoter mutations have been significantly associated with progressive recurrence in grade I meningiomas (20). Since 40-60% of sporadic meningiomas have a loss of *NF2* expression, meningiomas can be molecularly categorized into *NF2* mutants and non-*NF2* mutants, with the latter predominantly comprised of *TRAF7*, *KLF4*, *AKT1*, *SMO*, and *P13K* mutations (17, 18). Some of these molecular biomarkers have been independently associated with meningioma progression and recurrence (21, 22). In low grade meningiomas, Youngblood et al. established a link between mutations in the *HH* and *TRAF7* genes and increased recurrence rates (23). Recently, a number of studies have demonstrated the prognostic implications of PI3K/AKT/mTOR pathway mutations (24–26). One study of over 80 samples found that an activating *AKT1* mutation, upstream of mTOR, was associated with recurrence and present in 32% of grade I tumors (27). Mutations in the *SMO* gene have also been associated with poor prognosis in grade I meningiomas (28). In a study of over 500 patients, Sievers et al. found that meningiomas with *CDKN2A/B* homozygous deletions had a significantly shorter time to progression or recurrence (29)

Several studies have also revealed that chromosomal aberrations, such as 1p/14q codeletion, correlate with recurrence (30–33). In one study of mostly grade I orbital meningiomas, progressive tumors were more likely to have loss of chromosome 1p and 6q (34). Specific metabolite concentrations within tumor tissue have also been associated with clinical outcome. Pfisterer et al. used magnetic resonance spectroscopy to demonstrate that higher glycine to glutamine/glutamate ratio, glutamine to glutamate ratio, and creatine concentration is associated with rapidly recurring meningiomas (35). Another study characterized a highly metabolically active subgroup of benign meningiomas, linked to mutations in genes regulating transcription and metabolism, and found this subgroup to be associated with increased recurrence rates (36).

Radiation also has an important effect on the molecular background and immune environment. Agnihotri et al. compared the mutational and methylation profiles of radiation-induced meningiomas, as a result of childhood radiotherapy to the brain, with those of sporadic meningiomas. Radiation-induced meningiomas were associated with structural rearrangements of the *NF2* gene, loss of chromosomes 1p and 22q, and decreased focal gene mutations that are characteristic of non-*NF2* tumors (37). Using whole genome sequencing, RNA sequencing, and ChIP sequencing for histone H3K27ac, Paramasivam et al. identified important differences between sporadic meningiomas and those arising after radiation (38). This study showed that although both sporadic and radiation-induced meningiomas have features of homologous

recombination repair (HRR) failure, the underlying cause varies, with the former exhibiting greater genomic instability resulting in deficiency of HRR genes and the later having exhausted HRR at sites of radiation-induced DNA damage.

Characterizing the embryological origins of the meninges has elucidated location-specific meningioma biomarkers that show promise as prognostic indicators (39). Kalamarides et al. characterize prostaglandin D synthase-positive meningioma precursor cells and the embryonic window when mutations in these cells cause meningioma development with distinct genetic signatures (40). Using over 250 meningioma cases, Okano et al. found that tumors originating from the paraxial mesoderm were associated with mutations in *AKT*, *KLF4*, *SMO*, and *POLR2A*, whereas neural crest-derived meningiomas were associated with *NF2* mutations (41). Additionally, this group identified *POLR2A* mutations as a risk factor for recurrence.

The field of radiomics, which typically uses machine learning to correlate quantitative imaging characteristics with tumor features, has emerged as a promising, noninvasive method of studying the molecular characteristics of tumors. While several studies use imaging to accurately predict clinical outcome in meningiomas (42, 43), researchers have only recently examined the associations between imaging and the molecular landscape of meningiomas. One study of 314 meningioma samples identified specific radiologic features that predicted recurrence and overall survival and found that tumors with certain features were more likely to have higher somatic mutational burden, DNA methylation, and expression of the pro-mitotic transcription factor *FOXM1* (44). In a prediction model using over 60 grade II meningiomas, Shin et al. found that lower apparent diffusion coefficient 10^{th} percentile was an independent predictor of *TERT* promoter mutation (45). Although the current understanding of meningioma radiomics is in its nascency, the field shows great promise for diagnostic and therapeutic application.

Recent efforts have made strides towards synthesizing molecular risk factors into predictive models. Schmidt et al. conducted a transcriptomic analysis that identified 8 differentially expressed genes, including *PTTG1* and *LEPR* which were associated with poor prognosis (46). Another group used microarray transcriptomics to cluster meningiomas into three prognostic groups, showing that *CKS2*, *UBE2C*, and *TFPI2* were associated with recurrence (47). Patel et al. generated a transcriptomics-based grading system which was superior WHO grade in predicting recurrence. This study found that the group associated with the highest recurrence rate typically showed loss of the DREAM complex, which regulates the cell cycle (48). Chen et al. identified a 36-gene signature characteristic of clinically aggressive meningiomas and developed a risk score that reliably predicted recurrence and survival (49). This risk score was significantly associated with overall survival, whereas WHO grade was not, suggesting increased prediction accuracy. Dai et al. identified over 1600 differentially expressed genes, enriched in PI3K-Akt signaling pathways, extracellular matrix organization, and cytokine-chemokine receptor interactions, among others (50). While this group did not develop a prediction model for recurrence based on these enriched pathways, further characterization of these genes in aggressive meningiomas shows promise for improved classification schemes.

Epigenetic factors correlate with meningioma recurrence and progression. Loss of trimethylated histone H3K27 has been associated with recurrence of grades I and II tumors (51) (52) (53). One study described a 49-gene expression signature associated with high-risk tumors and found that hypermethylation of genes associated with cell-cycle regulation and the WNT signaling pathway, such as UCHL1 and SFRP1, predicted aggressive behavior (54). Using 140 meningioma samples, Olar et al. established a 64-CpG loci methylation predictor to categorize tumors into two prognostic groups, which were independently associated with recurrence (55). Both Sahm et al.'s classification into 6 prognostic groups based on methylation of 40 genes and Nassiri et al.'s methylome-based model more accurately predict 5-year recurrence-free survival than clinical factors and WHO grade (56, 57). Recently, Maas et al. developed a molecular-morphologic score, based on histology, copy-number variation, and methylation class, that significantly outperformed WHO grading in predicting recurrence (58). Berghoff et al. defined three prognostic methylation clusters, based on 126 meningioma samples, that are significantly better at predicting PFS than WHO grade is (22). Synthesizing DNA methylation, RNA sequencing, and cytogenetic data, Baylev et al. classified meningiomas into three biological groups with unique signatures and distinct prognoses (59). These efforts demonstrate the potential superiority of molecular classification schemes over histologic classification in predicting meningioma outcomes.

IMMUNE SIGNATURES OF MENINGIOMAS

Alongside advances in molecular characterization, there has been recent progress in understanding the immune composition of meningiomas (**Figure 1**). The meningioma immune microenvironment is mostly comprised of macrophages, T cells, and mast cells. Macrophages are the predominant immune cell in meningiomas (60–62). Proctor et al. found that tumor-associated macrophages account for almost 20% of all cells in meningioma tissues, and that M2 polarization is associated with recurrence (63, 64). An increase in peripheral myeloid-derived suppressor cells (MDSCs) and programmed death ligand 1 (PD-L1)+ monocytes is seen in patients with high-grade meningiomas (65). Interestingly, a study of patients with grade I and II meningiomas described expansion of peripheral "MDSC-like" monocytes, with MDSC markers but no T cell suppressive activity, and increased functional MDSCs in tumor samples, suggesting the importance of MDSC induction at the tumor site (66). A study of 40 brain-invasive meningiomas found that 25% had macrophages or microglia at the tumor-brain interface (67). These findings suggest a central role for macrophages in driving meningioma-immune cell interactions.

Cytotoxicity of tumor-infiltrating lymphocytes is essential to immune responses against tumor cells. Regulatory T cells, programmed cell death protein 1 (PD-1)+ CD8+ cells, and

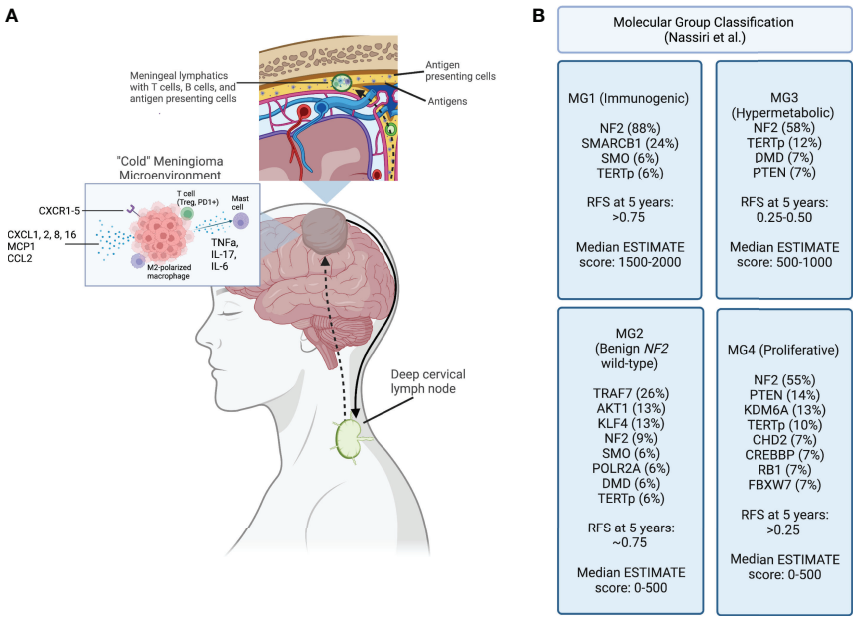

FIGURE 1 | **(A)** Meningioma tumor antigens are taken up by antigen presenting cells and carried to the meningeal lymphatic system, which drain to the deep cervical lymph node. After antigen presentation and immune activation occurs in the lymph node, immune cells are trafficked to the tumor site. A "cold" meningioma microenvironment consists of immunoregulatory cytokines, and immunosuppressive cell populations such as M2 polarized macrophages and regulatory T cells. **(B)** Molecular classification schema developed using a multimodal characterization approach by Nassiri et al., including the most frequently point-mutated genes within each category. Recurrence-free survival (RFS) at 5 years and the ESTIMATE score, quantifying immune infiltration based on expression of genes, are reported for each group. Created with BioRender.com.

PD-1+ CD4+ cells are associated with high-grade and aggressive tumors (65, 68, 69). High density of regulatory T cells are also a prognostic marker for recurrence (68, 70). In a study of over 200 high-grade meningiomas, Rapp et al. report that increased cytotoxic tumor-infiltrating lymphocytes are associated with prolonged PFS (71). Tumor location may further play a role in T cell infiltration. Comparing skull base to convexity meningiomas, Zador et al. found increased activity of oncolytic gamma-delta T cells in grade I skull base tumors (72). On the other hand, cavernous sinus meningiomas exhibit decreased immune cell infiltration, including cytotoxic lymphocytes, regulatory T cells, and tumor-associated macrophages (TAMs), as compared to convexity meningiomas (73). While this study does not independently correlate these immune findings to outcomes, further characterization of site-specific immune microenvironments may better predict the role for immunotherapy based on location and elucidate fundamental mechanisms of immune cell egress into specific intracranial compartments.

In a systemic review of studies evaluating the meningioma immune environment, mast cells were found to be present in up to 90% of meningiomas classified as grades 2 and 3 and were primarily located in perivascular areas (74). Peritumoral edema was also correlated with mast cell infiltration. Another study of secretory meningiomas, comprising 1.1% of meningiomas at this institution, showed increased mast cell infiltration and edema when compared to non-secretory tumors (75). Although this subtype is rare and it is not clear whether mast cell presence is causative, the presence of mast cells may be leveraged as a prognostic tool. In a study of grade I meningiomas, convexity tumors were more associated with the presence of activated mast cells compared with skull base tumors, and cytokine-cell networks showed mast cells were most strongly correlated with IL-6 (72).

Other important cells present in the tumor microenvironment include dendritic cells. Interestingly, when Chen et al. used CIBERSORT technology in 68 meningioma samples to characterize the immune environment, increased dendritic cells were found to be significantly associated with poor prognosis. Samples were categorized as "high" or "low" dendritic cell count based on the median content of cells, and differentially expressed genes were identified in each group. The B cell receptor signaling pathway was found to be activated in the "low" group, indicating increased presence of B cells in these groups. The authors hypothesized that increased dendritic cells may directly or indirectly reduce B cell infiltration in meningiomas, leading to worse outcome (76).

Alterations in antigen presentation appear to play an important role in meningioma biology. Tumor mutations lead to generation of neoantigens that can be processed by antigen presenting cells (APCs) and loaded onto major histocompatibility complex (MHC) molecules. Both soluble neo-antigens as well as APCs can travel *via* the meningeal lymph vessels to the deep cervical lymph nodes (77). Because meningiomas are extra-axial and have varying degrees of brain invasion, the relative

contributions of brain-specific vs head and neck lymphatics in driving antigen availability is unclear. Particularly, it is important to determine the contribution of the glymphatic system, which is characterized by the exchange of cerebrospinal fluid and parenchymal interstitial fluid with eventual drainage into the deep cervical lymph nodes *via* narrow periarterial channels (78). Of potential importance, lymphatic vessels located in the meninges are much wider than these periarterial channels. Accordingly, the APCs presenting antigens could more readily drain through the meninges vs. periarterial channels, which may be limited to soluble antigens (79). Additionally, T cells, B cells, and dendritic cells are present in meningeal lymphatics and participate in immune surveillance (80). Lastly, studies describing the effects of meningiomas on the cerebral vasculature have shown increased permeability to proteins (81). As such, it is possible that meningiomas are not protected by the full complement of immunoregulatory mechanisms in the CNS and, therefore, may be more susceptible to immune clearance compared with other brain tumors once an adequate immune response has been initiated.

The link between the glymphatic and meningeal lymphatic systems is poorly understood. To-date there are no studies examining the implications of these systems on antigen presentation in meningiomas. As data emerge on this topic, it may be of particular interest to characterize how proximity of the tumor to lymphatic vessels, degree of immune surveillance, and vascular permeability affect prognosis. Although T cell migration from peripheral lymph nodes to meningioma tissue has yet to be explored directly, extrapolating data from other brain tumors and CNS inflammatory conditions it is likely that antigen-educated lymphocytes travel *via* the afferent meningeal lymphatic vessels. Immune cells then home to brain tumors by chemokine stimulation (82). It remains to be shown which pathways mediate meningioma antigen-specific responses. However, meningiomas have been found to express several cytokines and chemokines, indicating that they are immunologically active (83, 84). Barbieri et al. found that at least one of the CXC receptors 1-5 was constitutively expressed in over 75% of meningiomas (85). Expression of CX3CL1, a chemokine that mediates migration of T cells, dendritic cells, and natural killer (NK) cells, positively correlates with tumor grade, whereas CXCL16, a T cell and monocyte chemoattractant, has increased expression in grade I samples (86). In a study characterizing differentially expressed genes between meninges and atypical meningiomas, Cao et al. found that CXCL2 and CXCL8 levels were not only upregulated in tumor tissue, but also independently associated with overall survival and recurrence (87). Another group investigated the role of monocyte chemoattractant protein-1 (MCP-1) in meningiomas and found high expression and a positive correlation between MCP-1 expression and macrophage infiltration (88). Similarly, CCL2, a monocyte chemoattractant, was found to be highly expressed in meningioma tissue (89). Cytokine-cytokine receptor interaction networks have already been developed to inform prognostic scoring of meningioma samples (72, 90). A consistent finding of these studies is that the cytokine milieu is extraordinarily heterogenous between tumors, and some have posited that ligand/receptor imbalance may impact tumor progression (86). Taken together, these data suggest that a predictive model accounting for the interactions between immune cells and meningiomas could have a prognostic potential.

INTERACTIONS BETWEEN MOLECULAR PATTERNS AND IMMUNE SIGNATURES

Tumor mutational patterns influence the composition of the immune microenvironment. Broadly, increased mutational burden has been reported in progressive and high-grade meningiomas and may correlate with inflammation (91). Gill et al. described more peritumoral edema in patients with increased single nucleotide variants (92) and higher tumor mutational burden is associated with increased immune cell infiltration (33). Rutland et al. evaluated 145 meningioma samples and found that a scattered distribution of lymphocytes was associated with increased point mutations (93). In a phase II clinical trial of 25 patients receiving nivolumab for grade II/III meningiomas, patients with higher mutational burden were more likely to respond to immunotherapy (94). The patient with the longest recurrence-free survival was also deficient in *MSH2*, a DNA mismatch repair gene (95). These studies provide evidence that, as in many other neoplasms, availability of high-quality antigens is a driver of immune responses against meningiomas.

While overall mutational burden may influence immune infiltration, several specific mutational patterns have related to unique immune signatures. Williams et al. described three molecular patterns of high-grade and progressive grade I meningiomas, and the majority of these 850 aggressive tumors were classified as NF2-mutant (96). NF2-mutated grade I tumors have a higher density of M2 macrophage infiltration than that of tumors with AKT1 activating mutations, suggesting that this genetic subset of grade I meningiomas may drive immunosuppression. Alternatively, AKT1 activation may also cause M1 polarization (97). M1 macrophages, along with NK cells and recently activated lymphocytes, are also enriched in tumors with chromosome 22 monosomy, indicating that genes on chromosome 22 may be closely linked to immunosuppression (98). Genetic alterations in meningiomas have been linked to activity of immune checkpoint pathways. Among non-NF2-mutated tumors, TRAF7 and AKT1 mutations are associated with expression of PD-L1, IDO, and TDO2 (99). Tumors with SMO and PIK3CA mutations have been linked to cytotoxic T-lymphocyte-associated protein 4 (CTLA-4)+ lymphocyte infiltration (100). One study found a significant association between DNA polymerase epsilon mutations and CD8+ infiltration as well as improved PFS (101). Mast cell infiltration has also been correlated with specific molecular drivers: Xie et al. developed a risk score by analyzing differentially expressed genes related to resting mast cells, immune cell abundance, miRNA-mRNA co-expression network, and drug-gene interaction prediction. Importantly, the 9 key genes identified were

important in the signaling of TNF-alpha, IL-17, and other cytokines, supporting the importance of further elucidating the interplay between molecular and immunologic signatures (90).

Several groups have used data processing tools to further characterize how the molecular tumor signature impacts the immune environment. Nassiri et al. recently performed a molecular analysis of 124 meningiomas of various locations and histological subtypes that included DNA sequencing, DNA methylation, RNA expression and single cell RNA sequencing. They reported 4 distinct molecular subgroups based on an integrative analysis of multi-platform genomic and epigenomic data. One of the subgroups (MG1) was characterized by expression of several immune pathways. This group of patients had recurrent NF2 mutations and loss of chromosomal arm 22q that resulted in biallelic inactivation of the *NF2* gene. Interestingly, this group was significantly enriched in T cell and macrophage genes and demonstrated the highest levels of cytokine and immune checkpoint molecule expression among the subgroups. This group of patients also exhibited the longest recurrence free survival. In contrast, subgroup MG4 was characterized by expression programs that allow for higher proliferation of tumor cells and contained the fewest macrophage-associated genes. This group had the highest recurrence rate compared to the other groups as well as the highest tumor mutational burden. While the latter finding contrasts with some previous reports, this data indicates that proliferation of tumor cells may outpace immunologic clearance. If this is the case, this subgroup may have a higher response rate to immune checkpoint inhibitors (16). Chen et al. created two clusters based on high versus low expression of RNA methylation regulators (m^6A regulators) and correlated the groups to immune infiltration. There were significant differences between infiltration of plasma B cells, resting mast cells, and neutrophils, as well as expression of IL-15 and IL-18 (102). These findings suggest that incorporating the presence of specific mutations into a predictive model may have value and guide implementation of immunotherapy.

PD-L1 is one of the most frequently studied checkpoint molecules in meningioma. Several studies have shown that PD-L1 expression is independently correlated with worse clinical outcome (103, 104). Additionally, Karimi et al. found that co-expression of PD-L1 with hypoxia-induced genes, such as NFKB2 and CA9, correlates with tumor progression (105). While these studies have established an association between PD-L1 expression and tumor progression, the use of PD-L1 alone as a biomarker may be limited by generally infrequent expression. Johnson et al. reported PD-L1 positivity values of 3%, 6%, and 18% for grades I, II, and III, respectively (106). The Tumor Immunity in the MicroEnvironment (TIME) scale, which categorizes tumors according to PD-L1 and tumor-infiltrating lymphocyte (TIL) positivity, has been implemented to predict responses to immunotherapy in several types of tumors (107). Yeung et al. used multiplex quantitative immunofluorescence to classify 73 meningiomas according to the TIME scale and found that most fell into the poor responder groups of $PD\text{-}L1^{low}TIL^{low}$ and $PD\text{-}L1^{low}TIL^{high}$. Notably, PD-L1 was more highly expressed on CD68+ macrophages than tumor cells, and PD-L2 was more strongly associated with T cell proliferation and cytotoxicity than PD-L1 (108). Both PD-L2 and B7-H3 expression have been associated with mutations of the mTOR pathway, including PI3K, AKT1, and mTOR (100). Interestingly, this study found PD-L2 to be most enriched in grade I meningiomas. Taken together, these findings indicate that PD-L2 and B7-H3 may play a more central role in meningiomas and, accordingly, PD-1 blockade may have activity in PD-L1 negative tumors. Based on the emerging relationship between tumor genomics and the immune microenvironment, further exploration of genomic alterations and immune-based risk predictors is warranted.

CLINICAL STUDIES

Clinical implementation of immunotherapy for meningiomas is still in its nascency. Early studies investigating the use of interferon alpha for recurrent meningiomas produced negative results (109). One retrospective case series of patients with recurrent grade II or III meningiomas treated with interferon alpha noted no radiographic responses at first evaluation and progression free survival was 17% at 6 months (110). A phase 2 study investigating interferon alpha for recurrent grade I intracranial meningiomas also reported no neuroradiographic responses, and PFS at 6 months was 54% (111).

Immune checkpoint inhibition has shown anecdotal promise and is currently being evaluated in clinical trials. Two case reports have been published describing the use of nivolumab for recurrent meningiomas. A case report of a patient on nivolumab for advanced lung cancer who also had recurrent right sphenoid wing meningioma reported significant reduction in both tumor size and brain edema following initiation of therapy (112). Another report described a response to checkpoint blockade in a MSH2-deficient tumor. After therapy the patient had a marked increase in CD8+ T cell infiltration of the tumor. The patient continued to receive nivolumab bi-weekly for over 2 years and experienced a marked response (95).

Based on these early reports, there are now several ongoing clinical trials aimed at evaluating checkpoint blockade for meningiomas (**Table 1**). While three of the trials are recruiting patients for anti-PD1 monotherapy, most studies include at least one treatment arm investigating combination therapy regimens. Given Han et al.'s findings that patients who received radiation have higher expression of PD-L1, four trials are investigating the synergy between immunotherapies targeting the PD-1/PD-L1 axis and various types of radiation therapy (103). In a phase II study of the anti-PD1 agent pembrolizumab, patients have improved PFS rates at 6 months, compared to historical controls, and a non-significant association between increased PD-L1 expression and reduced tumor growth (113). Additionally, two trials include treatments targeting the CD28-CTLA-4 pathway. While nivolumab with or without ipilimumab therapy in recurrent atypical meningiomas does not show improvement in 6 month PFS, a subset of tumors with increased mutational burden may have higher response rates (94, 95). Successful completion of these

TABLE 1 | Active clinical trials assessing immunotherapy for meningiomas registered on ClinicalTrials.gov.

Identifier	Status	Intervention	Study design	Estimated Enrollment	Patient cohort	Summary of published data
NCT03173950	Recruiting	Nivolumab	Phase 2; Non-Randomized, Parallel Assignment	180	Grade II or III; recurrent	Not applicable
NCT02648997	Recruiting	Nivolumab ± ipilimumab and external beam radiation therapy	Phase 2; Non-Randomized, Sequential Assignment	50	Grade II or III; recurrent	Well tolerated but no improvement in progression-free survival (94) Responder to therapy shows high tumor mutational burden (95)
NCT03604978	Recruiting	Nivolumab and radiosurgery ± ipilimumab	Phase 1/2; Randomized, Parallel Assignment	15	Grade II or III; recurrent	Not applicable
NCT03016091	Recruiting	Pembrolizumab	Phase 2; Single Group Assignment	25	Grade II or III; recurrent	Not applicable
NCT04659811	Recruiting	Pembrolizumab and radiosurgery	Phase 2; Non-Randomized, Parallel Assignment	90	Grade I, II, or III; recurrent	Not applicable
NCT03267836	Recruiting	Avelumab and proton beam radiotherapy	Phase 1; Single Group Assignment	12	Grade I, II, or III; recurrent	Not applicable
NCT03279692	Active, not recruiting	Pembrolizumab	Phase 2; Single Group Assignment	26	Grade II or III; recurrent or residual	Improved progression-free survival at 6 monthsTrend between increased PD-L1 expression and decreased tumor growth (113)

trials will provide valuable insights into the clinical utility of immune checkpoint blockade for meningiomas.

CONCLUSION

Ongoing work focused on tumor-immune interactions has the potential to afford valuable insights into the drivers of meningioma behavior. The link between tumor cell alterations and the immune landscape is particularly intriguing intersection. Although immune-based characterization of meningiomas has only recently garnered interest, ongoing efforts in this area will drive more robust prediction models and new therapeutic strategies for patients with recurrent and progressive tumors.

AUTHOR CONTRIBUTIONS

NK, PS, DM, and CJ contributed to conception and design of the review. NK and PS wrote the first draft of the manuscript. DM and CJ wrote sections of the manuscript. All authors contributed to manuscript revision, read, and approved the submitted version.

FUNDING

Meningioma research in CJ's laboratory is supported by the Goldhirsh-Yellin Foundation, Grant number (138405).

REFERENCES

1. Ostrom QT, Cioffi G, Waite K, Kruchko C, Barnholtz-Sloan JS. CBTRUS Statistical Report: Primary Brain and Other Central Nervous System Tumors Diagnosed in the United States in 2014-2018. *Neuro-Oncol* (2021) 23:iii1–105. doi: 10.1093/neuonc/noab200
2. Proctor DT, Ramachandran S, Lama S, Sutherland GR. Towards Molecular Classification of Meningioma: Evolving Treatment and Diagnostic Paradigms. *World Neurosurg* (2018) 119:366–73. doi: 10.1016/j.wneu.2018.08.019
3. Goldbrunner R, Stavrinou P, Jenkinson MD, Sahm F, Mawrin C, Weber DC, et al. EANO Guideline on the Diagnosis and Management of Meningiomas. *Neuro-Oncol* (2021) 23:1821–34. doi: 10.1093/neuonc/noab150
4. Willis J, Smith C, Ironside JW, Erridge S, Whittle IR, Everington D. The Accuracy of Meningioma Grading: A 10-Year Retrospective Audit. *Neuropathol Appl Neurobiol* (2005) 31:141–9. doi: 10.1111/j.1365-2990.2004.00621.x
5. Backer-Grøndahl T, Moen BH, Torp SH. The Histopathological Spectrum of Human Meningiomas. *Int J Clin Exp Pathol* (2012) 5:231–42.
6. Aghi MK, Carter BS, Cosgrove GR, Ojemann RG, Amin-Hanjani S, Martuza RL, et al. Long-Term Recurrence Rates of Atypical Meningiomas After Gross Total Resection With or Without Postoperative Adjuvant Radiation. *Neurosurgery* (2009) 64:56–60. doi: 10.1227/01.NEU.0000330399.55586.63
7. Palma L, Celli P, Franco C, Cervoni L, Cantore G. Long-Term Prognosis for Atypical and Malignant Meningiomas: A Study of 71 Surgical Cases. *J Neurosurg* (1997) 86:793–800. doi: 10.3171/jns.1997.86.5.0793
8. Perry A, Scheithauer BW, Stafford SL, Lohse CM, Wollan PC. "Malignancy" in Meningiomas. *Cancer* (1999) 85:2046–56. doi: 10.1002/(SICI)1097-0142(19990501)85:9<2046::AID-CNCR23>3.0.CO;2-M
9. Chen R, Aghi MK. Chapter 23 - Atypical Meningiomas. In: McDermott MW, editor. *Handbook of Clinical Neurology. Meningiomas, Part II*. Amsterdam: Elsevier (2020). p. 233–44. doi: 10.1016/B978-0-12-822198-3.00043-4
10. Schwartz TH, McDermott MW. The Simpson Grade: Abandon the Scale But Preserve the Message. *J Neurosurg* (2020) 1:1–8. doi: 10.3171/2020.6.JNS201904
11. Lam Shin Cheung V, Kim A, Sahgal A, Das S. Meningioma Recurrence Rates Following Treatment: A Systematic Analysis. *J Neurooncol* (2018) 136:351–61. doi: 10.1007/s11060-017-2659-6
12. Adegbite AB, Khan MI, Paine KWE, Tan LK. The Recurrence of Intracranial Meningiomas After Surgical Treatment. *J Neurosurg* (1983) 58:51–6. doi: 10.3171/jns.1983.58.1.0051

13. Goyal LK, Suh JH, Mohan DS, Prayson RA, Lee J, Barnett GH. Local Control and Overall Survival in Atypical Meningioma: A Retrospective Study. *Int J Radiat Oncol* (2000) 46:57–61. doi: 10.1016/S0360-3016(99)00349-1
14. Haddad AF, Young JS, Kanungo I, Sudhir S, Chen J-S, Raleigh DR, et al. WHO Grade I Meningioma Recurrence: Identifying High Risk Patients Using Histopathological Features and the MIB-1 Index. *Front Oncol* (2020) 10:1522. doi: 10.3389/fonc.2020.01522
15. Pettersson-Segerlind J, Orrego A, Lönn S, Mathiesen T. Long-Term 25-Year Follow-Up of Surgically Treated Parasagittal Meningiomas. *World Neurosurg* (2011) 76:564–71. doi: 10.1016/j.wneu.2011.05.015
16. Nassiri F, Liu J, Patil V, Mamatjan Y, Wang JZ, Hugh-White R, et al. A Clinically Applicable Integrative Molecular Classification of Meningiomas. *Nature* (2021) 597:119–25. doi: 10.1038/s41586-021-03850-3
17. Pemov A, Dewan R, Hansen NF, Chandrasekharappa SC, Ray-Chaudhury A, Jones K, et al. Comparative Clinical and Genomic Analysis of Neurofibromatosis Type 2-Associated Cranial and Spinal Meningiomas. *Sci Rep* (2020) 10:12563. doi: 10.1038/s41598-020-69074-z
18. Abedalthagafi M, Bi WL, Aizer AA, Merrill PH, Brewster R, Agarwalla PK, et al. Oncogenic PI3K Mutations are as Common as AKT1 and SMO Mutations in Meningioma. *Neuro-Oncol* (2016) 18:649–55. doi: 10.1093/neuonc/nov316
19. Louis DN, Perry A, Wesseling P, Brat DJ, Cree IA, Figarella-Branger D, et al. The 2021 WHO Classification of Tumors of the Central Nervous System: A Summary. *Neuro-Oncol* (2021) 23:1231–51. doi: 10.1093/neuonc/noab106
20. Sahm F, Schrimpf D, Olar A, Koelsche C, Reuss D, Bissel J, et al. TERT Promoter Mutations and Risk of Recurrence in Meningioma. *JNCI J Natl Cancer Inst* (2016) 108:djv377. doi: 10.1093/jnci/djv377
21. Comtesse N, Heckel D, Rácz A, Brass N, Glass B, Meese E. Five Novel Immunogenic Antigens in Meningioma: Cloning, Expression Analysis, and Chromosomal Mapping. *Clin Cancer Res Off J Am Assoc Cancer Res* (1999) 5:3560–8.
22. Berghoff AS, Hielscher T, Ricken G, Furtner J, Schrimpf D, Widhalm G, et al. Prognostic Impact of Genetic Alterations and Methylation Classes in Meningioma. *Brain Pathol* (2022) 32:e12970. doi: 10.1111/bpa.12970
23. Youngblood MW, Miyagishima DF, Jin L, Gupte T, Li C, Duran D, et al. Associations of Meningioma Molecular Subgroup and Tumor Recurrence. *Neuro-Oncol* (2021) 23:783–94. doi: 10.1093/neuonc/noaa226
24. Graillon T, Sanson M, Campello C, Idbaih A, Peyre M, Peyrière H, et al. Everolimus and Octreotide for Patients With Recurrent Meningioma: Results From the Phase II CEVOREM Trial. *Clin Cancer Res Off J Am Assoc Cancer Res* (2020) 26:552–7. doi: 10.1158/1078-0432.CCR-19-2109
25. Johnson MD, Okedli E, Woodard A, Toms SA, Allen GS. Evidence for Phosphatidylinositol 3-Kinase-Akt-P7s6k Pathway Activation and Transduction of Mitogenic Signals by Platelet-Derived Growth Factor in Meningioma Cells. *J Neurosurg* (2002) 97:668–75. doi: 10.3171/jns.2002.97.3.0668
26. Johnson MD, O'Connell MJ, Pilcher W, Reeder JE. Fibroblast Growth Factor Receptor-3 Expression in Meningiomas With Stimulation of Proliferation by the Phosphoinositide 3 Kinase-Akt Pathway. *J Neurosurg* (2010) 112:934–9. doi: 10.3171/2009.7.JNS09726
27. Yesilöz Ü, Kirches E, Hartmann C, Scholz J, Kropf S, Sahm F, et al. Frequent AKT1E17K Mutations in Skull Base Meningiomas are Associated With mTOR and ERK1/2 Activation and Reduced Time to Tumor Recurrence. *Neuro-Oncol* (2017) 19:1088–96. doi: 10.1093/neuonc/nox018
28. Boetto J, Bielle F, Sanson M, Peyre M, Kalamarides M. SMO Mutation Status Defines a Distinct and Frequent Molecular Subgroup in Olfactory Groove Meningiomas. *Neuro-Oncol* (2017) 19:345–51. doi: 10.1093/neuonc/now276
29. Sievers P, Hielscher T, Schrimpf D, Stichel D, Reuss DE, Berghoff AS, et al. CDKN2A/B Homozygous Deletion is Associated With Early Recurrence in Meningiomas. *Acta Neuropathol (Berl)* (2020) 140:409–13. doi: 10.1007/s00401-020-02188-w
30. Barbera S, San Miguel T, Gil-Benso R, Muñoz-Hidalgo L, Roldan P, Gonzalez-Darder J, et al. Genetic Changes With Prognostic Value in Histologically Benign Meningiomas. *Clin Neuropathol* (2013) 32:311–7. doi: 10.5414/NP300580
31. Maillo A, Orfao A, Espinosa AB, Sayagués JM, Merino M, Sousa P, et al. Early Recurrences in Histologically Benign/Grade I Meningiomas are Associated With Large Tumors and Coexistence of Monosomy 14 and Del (1p36) in the Ancestral Tumor Cell Clone. *Neuro-Oncol* (2007) 9:438–46. doi: 10.1215/15228517-2007-026
32. Pérez-Magán E, Rodríguez de Lope Á, Ribalta T, Ruano Y, Campos-Martín Y, Pérez-Bautista G, et al. Differential Expression Profiling Analyses Identifies Downregulation of 1p, 6q, and 14q Genes and Overexpression of 6p Histone Cluster 1 Genes as Markers of Recurrence in Meningiomas. *Neuro-Oncol* (2010) 12:1278–90. doi: 10.1093/neuonc/noq081
33. Ruiz J, Martínez A, Hernández S, Zimman H, Ferrer M, Fernández C, et al. Clinicopathological Variables, Immunophenotype, Chromosome 1p36 Loss and Tumour Recurrence of 247 Meningiomas Grade I and II. *Histol Histopathol* (2010) 25:341–9. doi: 10.14670/HH-25.341
34. Ho C-Y, Mosier S, Safneck J, Salomao DR, Miller NR, Eberhart CG, et al. Genetic Profiling by Single-Nucleotide Polymorphism-Based Array Analysis Defines Three Distinct Subtypes of Orbital Meningioma. *Brain Pathol* (2015) 25:193–201. doi: 10.1111/bpa.12150
35. Pfisterer WK, Hendricks WP, Scheck AC, Nieman RA, Birkner TH, Krampla WW, et al. Fluorescent *in Situ* Hybridization and Ex Vivo 1H Magnetic Resonance Spectroscopic Examinations of Meningioma Tumor Tissue: Is it Possible to Identify a Clinically-Aggressive Subset of Benign Meningiomas? *Neurosurgery* (2007) 61:1048–61. doi: 10.1227/01.neu.0000303201.62123.5c
36. Serna E, Morales JM, Mata M, Gonzalez-Darder J, Miguel TS, Gil-Benso R, et al. Gene Expression Profiles of Metabolic Aggressiveness and Tumor Recurrence in Benign Meningioma. *PloS One* (2013) 8:e67291. doi: 10.1371/journal.pone.0067291
37. Agnihotri S, Suppiah S, Tonge PD, Jalali S, Danesh A, Bruce JP, et al. Therapeutic Radiation for Childhood Cancer Drives Structural Aberrations of NF2 in Meningiomas. *Nat Commun* (2017) 8:186. doi: 10.1038/s41467-017-00174-7
38. Paramasivam N, Hübschmann D, Toprak UH, Ishaque N, Neidert M, Schrimpf D, et al. Mutational Patterns and Regulatory Networks in Epigenetic Subgroups of Meningioma. *Acta Neuropathol (Berl)* (2019) 138:295–308. doi: 10.1007/s00401-019-02008-w
39. Fountain DM, Smith MJ, O'Leary C, Pathmanaban ON, Roncaroli F, Bobola N, et al. The Spatial Phenotype of Genotypically Distinct Meningiomas Demonstrate Potential Implications of the Embryology of the Meninges. *Oncogene* (2021) 40:875–84. doi: 10.1038/s41388-020-01568-6
40. Kalamarides M, Stemmer-Rachamimov AO, Niwa-Kawakita M, Chareyre F, Taranchon E, Han Z-Y, et al. Identification of a Progenitor Cell of Origin Capable of Generating Diverse Meningioma Histological Subtypes. *Oncogene* (2011) 30:2333–44. doi: 10.1038/onc.2010.609
41. Okano A, Miyawaki S, Hongo H, Dofuku S, Teranishi Y, Mitsui J, et al. Associations of Pathological Diagnosis and Genetic Abnormalities in Meningiomas With the Embryological Origins of the Meninges. *Sci Rep* (2021) 11:6987. doi: 10.1038/s41598-021-86298-9
42. Ko C-C, Zhang Y, Chen J-H, Chang K-T, Chen T-Y, Lim S-W, et al. Pre-Operative MRI Radiomics for the Prediction of Progression and Recurrence in Meningiomas. *Front Neurol* (2021) 12:636235. doi: 10.3389/fneur.2021.636235
43. Zhang Y, Chen J-H, Chen T-Y, Lim S-W, Wu T-C, Kuo Y-T, et al. Radiomics Approach for Prediction of Recurrence in Skull Base Meningiomas. *Neuroradiology* (2019) 61:1355–64. doi: 10.1007/s00234-019-02259-0
44. Morin O, Chen WC, Nassiri F, Susko M, Magill ST, Vasudevan HN, et al. Integrated Models Incorporating Radiologic and Radiomic Features Predict Meningioma Grade, Local Failure, and Overall Survival. *Neuro-Oncol Adv* (2019) 1:vdz011. doi: 10.1093/noajnl/vdz011
45. Shin I, Park YW, Ahn SS, Kang S-G, Chang JH, Kim SH, et al. Clinical and Diffusion Parameters May Noninvasively Predict TERT Promoter Mutation Status in Grade II Meningiomas. *J Neuroradiol J Neuroradiol* (2022) 49:59–65. doi: 10.1016/j.neurad.2021.02.007
46. Schmidt M, Mock A, Jungk C, Sahm F, Ull AT, Warta R, et al. Transcriptomic Analysis of Aggressive Meningiomas Identifies PTTG1 and LEPR as Prognostic Biomarkers Independent of WHO Grade. *Oncotarget* (2016) 7:14551–68. doi: 10.18632/oncotarget.7396
47. Fèvre-Montange M, Champier J, Durand A, Wierinckx A, Honnorat J, Guyotat J, et al. Microarray Gene Expression Profiling in Meningiomas: Differential Expression According to Grade or Histopathological Subtype. *Int J Oncol* (2009) 35:1395–407. doi: 10.3892/ijo_00000457
48. Patel AJ, Wan Y-W, Al-Ouran R, Revelli J-P, Cardenas MF, Oneissi M, et al. Molecular Profiling Predicts Meningioma Recurrence and Reveals Loss of

DREAM Complex Repression in Aggressive Tumors. *Proc Natl Acad Sci* (2019) 116:21715–26. doi: 10.1073/pnas.1912858116
49. Chen WC, Vasudevan HN, Choudhury A, Pekmezci M, Lucas C-HG, Phillips J, et al. A Prognostic Gene-Expression Signature and Risk Score for Meningioma Recurrence After Resection. *Neurosurgery* (2020) 88:202–10. doi: 10.1093/neuros/nyaa355
50. Dai J, Ma Y, Chu S, Le N, Cao J, Wang Y. Identification of Key Genes and Pathways in Meningioma by Bioinformatics Analysis. *Oncol Lett* (2018) 15:8245–52. doi: 10.3892/ol.2018.8376
51. Katz LM, Hielscher T, Liechty B, Silverman J, Zagzag D, Sen R, et al. Loss of Histone H3K27me3 Identifies a Subset of Meningiomas With Increased Risk of Recurrence. *Acta Neuropathol (Berl)* (2018) 135:955–63. doi: 10.1007/s00401-018-1844-9
52. Nassiri F, Wang JZ, Singh O, Karimi S, Dalcourt T, Ijad N, et al. Loss of H3K27me3 in Meningiomas. *Neuro-Oncol* (2021) 23:1282–91. doi: 10.1093/neuonc/noab036
53. Behling F, Fodi C, Gepfner-Tuma I, Kaltenbach K, Renovanz M, Paulsen F, et al. H3K27me3 Loss Indicates an Increased Risk of Recurrence in the Tübingen Meningioma Cohort. *Neuro-Oncol* (2021) 23:1273–81. doi: 10.1093/neuonc/noaa303
54. Pèrez-Magán E, Campos-Martín Y, Mur P, Fiaño C, Ribalta T, García JF, et al. Genetic Alterations Associated With Progression and Recurrence in Meningiomas. *J Neuropathol Exp Neurol* (2012) 71:882–93. doi: 10.1097/NEN.0b013e31826bf704
55. Olar A, Wani KM, Wilson CD, Zadeh G, DeMonte F, Jones DTW, et al. Global Epigenetic Profiling Identifies Methylation Subgroups Associated With Recurrence-Free Survival in Meningioma. *Acta Neuropathol (Berl)* (2017) 133:431–44. doi: 10.1007/s00401-017-1678-x
56. Sahm F, Schrimpf D, Stichel D, Jones DTW, Hielscher T, Schefzyk S, et al. DNA Methylation-Based Classification and Grading System for Meningioma: A Multicentre, Retrospective Analysis. *Lancet Oncol* (2017) 18:682–94. doi: 10.1016/S1470-2045(17)30155-9
57. Nassiri F, Mamatjan Y, Suppiah S, Badhiwala JH, Mansouri S, Karimi S, et al. DNA Methylation Profiling to Predict Recurrence Risk in Meningioma: Development and Validation of a Nomogram to Optimize Clinical Management. *Neuro-Oncol* (2019) 21:901–10. doi: 10.1093/neuonc/noz061
58. Maas SLN, Stichel D, Hielscher T, Sievers P, Berghoff AS, Schrimpf D, et al. Integrated Molecular-Morphologic Meningioma Classification: A Multicenter Retrospective Analysis, Retrospectively and Prospectively Validated. *J Clin Oncol* (2021) 34:3839–52. doi: 10.1200/JCO.21.00784
59. Bayley JC, Hadley CC, Harmanci AO, Harmanci AS, Klisch TJ, Patel AJ. Multiple Approaches Converge on Three Biological Subtypes of Meningioma and Extract New Insights From Published Studies. *Sci Adv* (2022) 8:eabm6247. doi: 10.1126/sciadv.abm6247
60. Domingues PH, Teodósio C, Ortiz J, Sousa P, Otero Á, Maillo A, et al. Immunophenotypic Identification and Characterization of Tumor Cells and Infiltrating Cell Populations in Meningiomas. *Am J Pathol* (2012) 181:1749–61. doi: 10.1016/j.ajpath.2012.07.033
61. Borch J de S, Haslund-Vinding J, Vilhardt F, Maier AD, Mathiesen T. Meningioma–Brain Crosstalk: A Scoping Review. *Cancers* (2021) 13:4267. doi: 10.3390/cancers13174267
62. Yeung J, Yaghoobi V, Miyagishima D, Vesely MD, Zhang T, Badri T, et al. Targeting the CSF1/CSF1R Axis Is a Potential Treatment Strategy for Malignant Meningiomas. *Neuro-Oncol* (2021) 23:1922–35. doi: 10.1093/neuonc/noab075
63. Proctor DT, Huang J, Lama S, Albakr A, Van Marle G, Sutherland GR. Tumor-Associated Macrophage Infiltration in Meningioma. *Neuro-Oncol Adv* (2019) 1:vdz018. doi: 10.1093/noajnl/vdz018
64. Presta I, Guadagno E, Di Vito A, Malara N, Mignogna C, Maisano D, et al. Innate Immunity may Play a Role in Growth and Relapse of Chordoid Meningioma. *Int J Immunopathol Pharmacol* (2017) 30:429–33. doi: 10.1177/0394632017730241
65. Li YD, Veliceasa D, Lamano JB, Lamano JB, Kaur G, Biyashev D, et al. Systemic and Local Immunosuppression in Patients With High-Grade Meningiomas. *Cancer Immunol Immunother CII* (2019) 68:999–1009. doi: 10.1007/s00262-019-02342-8
66. Pinton L, Solito S, Masetto E, Vettore M, Canè S, Della Puppa A, et al. Immunosuppressive Activity of Tumor-Infiltrating Myeloid Cells in Patients With Meningioma. *OncoImmunology* (2018) 7:e1440931. doi: 10.1080/2162402X.2018.1440931
67. Grund S, Schittenhelm J, Roser F, Tatagiba M, Mawrin C, Kim YJ, et al. The Microglial/Macrophagic Response at the Tumour-Brain Border of Invasive Meningiomas. *Neuropathol Appl Neurobiol* (2009) 35:82–8. doi: 10.1111/j.1365-2990.2008.00960.x
68. Fang L, Lowther DE, Meizlish ML, Anderson RCE, Bruce JN, Devine L, et al. The Immune Cell Infiltrate Populating Meningiomas is Composed of Mature, Antigen-Experienced T and B Cells. *Neuro-Oncol* (2013) 15:1479–90. doi: 10.1093/neuonc/not110
69. Everson RG, Hashimoto Y, Freeman JL, Hodges TR, Huse J, Zhou S, et al. Multiplatform Profiling of Meningioma Provides Molecular Insight and Prioritization of Drug Targets for Rational Clinical Trial Design. *J Neurooncol* (2018) 139:469–78. doi: 10.1007/s11060-018-2891-8
70. Herold-Mende C, Ull T, Rapp C, Dettling S, Jungk C, Sahm F, et al. IMPS-14Prognostic Role of Regulatory T-Cells in Primary and Recurrent Meningioma. *Neuro-Oncol* (2015) 17:v116. doi: 10.1093/neuonc/nov217.14
71. Rapp C, Dettling S, Liu F, Ull AT, Warta R, Jungk C, et al. Cytotoxic T Cells and Their Activation Status are Independent Prognostic Markers in Meningiomas. *Clin Cancer Res* (2019) 25:5260–70. doi: 10.1158/1078-0432.CCR-19-0389
72. Zador Z, Landry AP, Balas M, Cusimano MD. Landscape of Immune Cell Gene Expression Is Unique in Predominantly WHO Grade 1 Skull Base Meningiomas When Compared to Convexity. *Sci Rep* (2020) 10:9065. doi: 10.1038/s41598-020-65365-7
73. Kosugi K, Tamura R, Ohara K, Morimoto Y, Kuranari Y, Oishi Y, et al. Immunological and Vascular Characteristics in Cavernous Sinus Meningioma. *J Clin Neurosci* (2019) 67:198–203. doi: 10.1016/j.jocn.2019.06.003
74. Polyzoidis S, Koletsa T, Panagiotidou S, Ashkan K, Theoharides TC. Mast Cells in Meningiomas and Brain Inflammation. *J Neuroinflamm* (2015) 12:170. doi: 10.1186/s12974-015-0388-3
75. Tirakotai W, Mennel H-D, Celik I, Hellwig D, Bertalanffy H, Riegel T. Secretory Meningioma: Immunohistochemical Findings and Evaluation of Mast Cell Infiltration. *Neurosurg Rev* (2006) 29:41–8. doi: 10.1007/s10143-005-0402-9
76. Chen X, Tian F, Lun P, Feng Y. Profiles of Immune Infiltration and its Relevance to Survival Outcome in Meningiomas. *Biosci Rep* (2020) 40: BSR20200538. doi: 10.1042/BSR20200538
77. Yankova G, Bogomyakova O, Tulupov A. The Glymphatic System and Meningeal Lymphatics of the Brain: New Understanding of Brain Clearance. *Rev Neurosci* (2021) 32:693–705. doi: 10.1515/revneuro-2020-0106
78. Eide PK, Vatnehol SAS, Emblem KE, Ringstad G. Magnetic Resonance Imaging Provides Evidence of Glymphatic Drainage From Human Brain to Cervical Lymph Nodes. *Sci Rep* (2018) 8:7194. doi: 10.1038/s41598-018-25666-4
79. Carare RO, Bernardes-Silva M, Newman TA, Page AM, Nicoll JAR, Perry VH, et al. Solutes, But Not Cells, Drain From the Brain Parenchyma Along Basement Membranes of Capillaries and Arteries: Significance for Cerebral Amyloid Angiopathy and Neuroimmunology. *Neuropathol Appl Neurobiol* (2008) 34:131–44. doi: 10.1111/j.1365-2990.2007.00926.x
80. Louveau A, Smirnov I, Keyes TJ, Eccles JD, Rouhani SJ, Peske JD, et al. Structural and Functional Features of Central Nervous System Lymphatic Vessels. *Nature* (2015) 523:337–41. doi: 10.1038/nature14432
81. Long DM. Vascular Ultrastructure in Human Meningiomas and Schwannomas. *J Neurosurg* (1973) 38:409–19. doi: 10.3171/jns.1973.38.4.0409
82. Ousman SS, Kubes P. Immune Surveillance in the Central Nervous System. *Nat Neurosci* (2012) 15:1096–101. doi: 10.1038/nn.3161
83. Würth R, Barbieri F, Bajetto A, Pattarozzi A, Gatti M, Porcile C, et al. Expression of CXCR7 Chemokine Receptor in Human Meningioma Cells and in Intratumoral Microvasculature. *J Neuroimmunol* (2011) 234:115–23. doi: 10.1016/j.jneuroim.2011.01.006
84. Tang T, Xia Q-J, Chen J-B, Xi M-R, Lei D. Expression of the CXCL12/SDF-1 Chemokine Receptor CXCR7 in Human Brain Tumours. *Asian Pac J Cancer Prev APJCP* (2012) 13:5281–6. doi: 10.7314/apjcp.2012.13.10.5281
85. Barbieri F, Bajetto A, Porcile C, Pattarozzi A, Massa A, Lunardi G, et al. CXC Receptor and Chemokine Expression in Human Meningioma. *Ann NY Acad Sci* (2006) 1090:332–43. doi: 10.1196/annals.1378.037

86. Li G, Hattermann K, Mentlein R, Mehdorn HM, Held-Feindt J. The Transmembrane Chemokines CXCL16 and CX3CL1 and Their Receptors are Expressed in Human Meningiomas. *Oncol Rep* (2013) 29:563–70. doi: 10.3892/or.2012.2164
87. Cao M, Wang Y. Bioinformatic Analyses Determine the Importance of CXCL2 and CXCL8 in Atypical Meningioma Development and Reoccurrence. *Turk Neurosurg* (2021). doi: 10.5137/1019-5149.JTN.34984-21.2
88. Sato K, Kuratsu J, Takeshima H, Yoshimura T, Ushio Y. Expression of Monocyte Chemoattractant Protein-1 in Meningioma. *J Neurosurg* (1995) 82:874–8. doi: 10.3171/jns.1995.82.5.0874
89. Mehdipour P, Javan F, Jouibari MF, Khaleghi M, Mehrazin M. Evolutionary Model of Brain Tumor Circulating Cells: Cellular Galaxy. *World J Clin Oncol* (2021) 12:13–30. doi: 10.5306/wjco.v12.i1.13
90. Xie H, Yuan C, Ding X, Li J, Li Z, Lu W. Identification of Key Genes and Pathways Associated With Resting Mast Cells in Meningioma. *BMC Cancer* (2021) 21:1–12. doi: 10.1186/s12885-021-08931-0
91. Bi WL, Greenwald NF, Abedalthagafi M, Wala J, Gibson WJ, Agarwalla PK, et al. Genomic Landscape of High-Grade Meningiomas. *NPJ Genomic Med* (2017) 2:15. doi: 10.1038/s41525-017-0014-7
92. Gill CM, Loewenstern J, Rutland JW, Arib H, Pain M, Umphlett M, et al. Peritumoral Edema Correlates With Mutational Burden in Meningiomas. *Neuroradiology* (2021) 63:73–80. doi: 10.1007/s00234-020-02515-8
93. Rutland JW, Gill CM, Loewenstern J, Arib H, Pain M, Umphlett M, et al. NF2 Mutation Status and Tumor Mutational Burden Correlate With Immune Cell Infiltration in Meningiomas. *Cancer Immunol Immunother CII* (2021) 70:169–76. doi: 10.1007/s00262-020-02671-z
94. Bi WL, Nayak L, Meredith DM, Driver J, Du Z, Hoffman S, et al. Activity of PD-1 Blockade With Nivolumab Among Patients With Recurrent Atypical/Anaplastic Meningioma: Phase II Trial Results. *Neuro-Oncol* (2022) 24:101–13. doi: 10.1093/neuonc/noab118
95. Dunn IF, Du Z, Touat M, Sisti MB, Wen PY, Umeton R, et al. Mismatch Repair Deficiency in High-Grade Meningioma: A Rare But Recurrent Event Associated With Dramatic Immune Activation and Clinical Response to PD-1 Blockade. *JCO Precis Oncol* (2018) 2:PO.18.00190. doi: 10.1200/PO.18.00190
96. Williams EA, Santagata S, Wakimoto H, Shankar GM, Barker FG, Sharaf R, et al. Distinct Genomic Subclasses of High-Grade/Progressive Meningiomas: NF2-Associated, NF2-Exclusive, and NF2-Agnostic. *Acta Neuropathol Commun* (2020) 8:171. doi: 10.1186/s40478-020-01040-2
97. Adams CL, Ercolano E, Ferluga S, Sofela A, Dave F, Negroni C, et al. A Rapid Robust Method for Subgrouping Non-NF2 Meningiomas According to Genotype and Detection of Lower Levels of M2 Macrophages in AKT1 E17K Mutated Tumours. *Int J Mol Sci* (2020) 21:1273. doi: 10.3390/ijms21041273
98. Domingues PH, Teodósio C, Otero Á, Sousa P, Ortiz J, Macias M del CG, et al. Association Between Inflammatory Infiltrates and Isolated Monosomy 22/Del(22q) in Meningiomas. *PloS One* (2013) 8:e74798. doi: 10.1371/journal.pone.0074798
99. Hao S, Huang G, Feng J, Li D, Wang K, Wang L, et al. Non-NF2 Mutations Have a Key Effect on Inhibitory Immune Checkpoints and Tumor Pathogenesis in Skull Base Meningiomas. *J Neurooncol* (2019) 144:11–20. doi: 10.1007/s11060-019-03198-9
100. Proctor DT, Patel Z, Lama S, Resch L, van Marle G, Sutherland GR. Identification of PD-L2, B7-H3 and CTLA-4 Immune Checkpoint Proteins in Genetic Subtypes of Meningioma. *Oncoimmunology* (2019) 8:e1512943. doi: 10.1080/2162402X.2018.1512943
101. Rutland JW, Dullea JT, Gill CM, Chaluts D, Ranti D, Ellis E, et al. Association of Mutations in DNA Polymerase Epsilon With Increased CD8+ Cell Infiltration and Prolonged Progression-Free Survival in Patients With Meningiomas. *Neurosurg Focus* (2022) 52:E7. doi: 10.3171/2021.11.FOCUS21592
102. Chen J, Sun S, Ren L, Hua L, Wang D, Xie Q, et al. M6a Regulator Expression Segregates Meningiomas Into Biologically Distinct Subtypes. *Front Oncol* (2021) 11:760892. doi: 10.3389/fonc.2021.760892
103. Han SJ, Reis G, Kohanbash G, Shrivastav S, Magill ST, Molinaro AM, et al. Expression and Prognostic Impact of Immune Modulatory Molecule PD-L1 in Meningioma. *J Neurooncol* (2016) 130:543–52. doi: 10.1007/s11060-016-2256-0
104. Du Z, Abedalthagafi M, Aizer AA, McHenry AR, Sun HH, Bray M-A, et al. Increased Expression of the Immune Modulatory Molecule PD-L1 (CD274) in Anaplastic Meningioma. *Oncotarget* (2015) 6:4704–16. doi: 10.18632/oncotarget.3082
105. Karimi S, Mansouri S, Mamatjan Y, Liu J, Nassiri F, Suppiah S, et al. Programmed Death Ligand-1 (PD-L1) Expression in Meningioma; Prognostic Significance and its Association With Hypoxia and NFKB2 Expression. *Sci Rep* (2020) 10:14115. doi: 10.1038/s41598-020-70514-z
106. Johnson MD. PD-L1 Expression in Meningiomas. *J Clin Neurosci Off J Neurosurg Soc Australas* (2018) 57:149–51. doi: 10.1016/j.jocn.2018.08.023
107. Zhang Y, Chen L. Classification of Advanced Human Cancers Based on Tumor Immunity in the MicroEnvironment (TIME) for Cancer Immunotherapy. *JAMA Oncol* (2016) 2:1403–4. doi: 10.1001/jamaoncol.2016.2450
108. Yeung J, Yaghoobi V, Aung TN, Vesely MD, Zhang T, Gaule P, et al. Spatially Resolved and Quantitative Analysis of the Immunological Landscape in Human Meningiomas. *J Neuropathol Exp Neurol* (2021) 80:150–9. doi: 10.1093/jnen/nlaa152
109. Muhr C, Gudjonsson O, Lilja A, Hartman M, Zhang ZJ, Långström B. Meningioma Treated With Interferon-Alpha, Evaluated With [(11)C]-L-Methionine Positron Emission Tomography. *Clin Cancer Res Off J Am Assoc Cancer Res* (2001) 7:2269–76.
110. Chamberlain MC. IFN-α for Recurrent Surgery- and Radiation-Refractory High-Grade Meningioma: A Retrospective Case Series. *CNS Oncol* (2013) 2:227–35. doi: 10.2217/cns.13.17
111. Chamberlain MC, Glantz MJ. Interferon-Alpha for Recurrent World Health Organization Grade 1 Intracranial Meningiomas. *Cancer* (2008) 113:2146–51. doi: 10.1002/cncr.23803
112. Gelerstein E, Berger A, Jonas-Kimchi T, Strauss I, Kanner AA, Blumenthal DT, et al. Regression of Intracranial Meningioma Following Treatment With Nivolumab: Case Report and Review of the Literature. *J Clin Neurosci* (2017) 37:51–3. doi: 10.1016/j.jocn.2016.11.011
113. Brastianos PK, Kim AE, Giobbie-Hurder A, Lee EQ, Wang N, Eichler AF, et al. Phase 2 Study of Pembrolizumab in Patients With Recurrent and Residual High-Grade Meningiomas. *Nat Commun* (2022) 13:1325. doi: 10.1038/s41467-022-29052-7

Conflict of Interest: CJ is the co-founder and owns equity interest in Egret Therapeutics. This arrangement has been reviewed and approved by the Johns Hopkins University in accordance with its conflict of interest policies.

The remaining authors declare that the research was conducted in the absence of any commercial or financial relationships that could be construed as a potential conflict of interest.

Publisher's Note: All claims expressed in this article are solely those of the authors and do not necessarily represent those of their affiliated organizations, or those of the publisher, the editors and the reviewers. Any product that may be evaluated in this article, or claim that may be made by its manufacturer, is not guaranteed or endorsed by the publisher.

Copyright © 2022 Kannapadi, Shah, Mathios and Jackson. This is an open-access article distributed under the terms of the Creative Commons Attribution License (CC BY). The use, distribution or reproduction in other forums is permitted, provided the original author(s) and the copyright owner(s) are credited and that the original publication in this journal is cited, in accordance with accepted academic practice. No use, distribution or reproduction is permitted which does not comply with these terms.

frontiers | Frontiers in Oncology

ORIGINAL RESEARCH
published: 13 June 2022
doi: 10.3389/fonc.2022.885155

Clinicopathologic Characteristics of Grade 2/3 Meningiomas: A Perspective on the Role of Next-Generation Sequencing

Junhyung Kim[1†], Kihwan Hwang[1†], Hyun Jung Kwon[2], Ji Eun Lee[2], Kyu Sang Lee[2], Gheeyoung Choe[2], Jung Ho Han[1] and Chae-Yong Kim[1*]*

[1] Department of Neurosurgery, Seoul National University Bundang Hospital, Seoul National University College of Medicine, Seongnam, South Korea, [2] Department of Pathology, Seoul National University Bundang Hospital, Seoul National University College of Medicine, Seongnam, South Korea

OPEN ACCESS

Edited by:
Hailiang Tang,
Fudan University, China

Reviewed by:
Christopher Hong,
Yale Medicine, United States
Anne Barlier,
Aix Marseille Université, France

***Correspondence:**
Chae-Yong Kim
chaeyong@snu.ac.kr
Kyu Sang Lee
tigerkyu@gmail.com

[†]These authors share first authorship

Specialty section:
This article was submitted to Neuro-Oncology and Neurosurgical Oncology, a section of the journal Frontiers in Oncology

Received: 27 February 2022
Accepted: 04 May 2022
Published: 13 June 2022

Citation:
Kim J, Hwang K, Kwon HJ, Lee JE, Lee KS, Choe G, Han JH and Kim C-Y (2022) Clinicopathologic Characteristics of Grade 2/3 Meningiomas: A Perspective on the Role of Next-Generation Sequencing. Front. Oncol. 12:885155. doi: 10.3389/fonc.2022.885155

Background: Grade 2/3 meningiomas have locally aggressive behaviors often requiring additional treatment plans after surgical resection. Herein, we explored the clinical significance of next-generation sequencing (NGS) in characterizing the molecular profiles of high-grade meningiomas.

Methods: Patients with intracranial meningioma who underwent surgical resection in a single institution were retrospectively reviewed. Clinicopathologic relevance was evaluated using recurrence-free survival (RFS) as an outcome measure. NGS for the targeted gene regions was performed in 40 participants.

Results: Among the 713 individuals in the study population, 143 cases (20.1%) were identified as having grade 2 or 3 meningiomas with a significantly lower female predominance. While the difference in RFS between grade 2 and 3 meningiomas was insignificant, a few conventional grade 2 cases, but with *TERT* promoter hotspot mutation, were highly progressive and refractory to the treatment. From the NGS study, recurrent mutations in *TRAF* and *AKT1* were identified with a higher prevalence (17.5% and 12.5%, respectively) compared with grade 2/3 meningiomas reported in previous literature. However, their relations to other histopathologic properties or clinical factors were rarely observed.

Conclusions: Grade 2/3 meningiomas show a broad spectrum of molecular profiles, as they have heterogeneous histologic characteristics.

Keywords: meningioma, atypical meningioma, anaplastic meningioma, next-generation sequencing, *TERT* promoter mutation

INTRODUCTION

Meningioma is a single pathologic entity of benign extra-axial tumors in the central nervous system (CNS) with a broad morphological spectrum reflected in various histopathologic subtypes (1). Although exhibiting a mostly benign nature, up to 25% of cases have shown to have aggressive behaviors, as classified as grade 2 or 3 (2, 3). The primary mode of treatment is surgery; however, due to anatomical obstacles or some other circumstances, complete tumor resection is often unachievable. The tumor characteristics, together with the surgical outcome, have been considered an important prognostic factor associated with local recurrence, and additional treatment plans are always considered for grade 2/3 meningiomas.

Recently, numerous studies have suggested molecular signatures representing aggressive tumor characteristics and several specific biomarkers, i.e., *TERT* promoter mutation and *CDKN2A/B* homozygous deletion, which have been added to the updated diagnostic criteria for anaplastic meningiomas (1, 4). This, in an addition to the rapid adoption of next-generation sequencing (NGS) beside clinical practice, has increased the interests in genomic characterization of specific meningioma subtypes (3). Thus, we explored the clinical significance of molecular diagnostic studies in grade 2/3 meningiomas. We also validated previously published recurrent mutations and their clinicopathologic relevance in our cohort with the NGS study.

MATERIALS AND METHODS

Study Population

This study was intended for patients with intracranial meningioma. The study population was retrospectively selected from the institutional tumor registry. Patients who had agreed with biobanking and genetic testing of tumor tissue for a scientific purpose have enrolled under the approval of the institutional review board. Patients were not compensated for their participation, and each participant provided written informed consent. All experiments were performed following the relevant guidelines and regulations.

Tissue Acquisition and Histopathologic Diagnosis

Formalin-fixed paraffin-embedded (FFPE) tissue specimens were obtained after surgical resection. Two senior pathologists (K.S.L. and G.C.) independently reviewed the hematoxylin and eosin (H&E)-stained slides and confirmed the diagnosis according to the fourth edition of the World Health Organization classification of tumors of the CNS (WHO CNS) to identify the histological subtypes of meningiomas.

Immunostaining was performed for a single representative sample block showing specific histomorphologic characteristics from each case. Sections were transferred to poly-L-lysine coated adhesive slides, dried, deparaffinized, and rehydrated. The slides were subsequently subjected to heat-induced antigen retrieval. The following antibodies were used according to the manufacturer's instruction: c-MET (prediluted, rabbit monoclonal antibody, Ventana, Tucson, AZ, USA), EGFR (1:150, mouse monoclonal antibody, Dako, Camarillo, CA, USA), p16 (prediluted, mouse monoclonal antibody, Ventana, Tucson, AZ, USA), and Ki-67 (1:50, mouse monoclonal antibody, Dako, Carpinteria, CA, USA). The sections were incubated with appropriate reagents from the Dako REAL EnVision Detection System (Dako, Glostrup, Denmark) and were counterstained with Mayer's hematoxylin. Each case was categorized as either positive — when it showed moderate-to-strong cytoplasmic and/or membranous positivity in tumor cells — or negative, as controls without antibodies. For p16 staining, loss of expression was recorded if the tumor cells showed complete negative, while partial expression was considered positive.

TERT Promoter Mutation Analysis by Pyrosequencing

A sample FFPE block with the most representative morphologic characteristics was selected from each case, and tumor areas were manually microdissected from the unstained slides. DNA was extracted using the Maxwell 16 FFPE Purification Kit (Promega, Madison, WI, USA) according to the manufacturer's instructions. The *TERT* promoter region covering the hotspot mutations C228T (g.1,295,228C>T in GRCh37) and C250T (g.1,295,250C>T) were amplified by polymerase chain reaction (PCR) using the HotStarTaq Plus Master Mix Kit (Qiagen, Valencia, CA, USA) and primers forward 5'-GTCCTGCCCCTTCACCTT-3' and reverse 5'-CAGCGCTGCCTGAAACTC-3', which was run on Verti 96-well Thermal Cycler (Applied Biosystems, Waltham, MA, USA) with the following conditions: 96°C for 5 min; 44 cycles with 96°C for 30 s, 64°C for 30 s and 72°C for 1 min; 72°C for 10 min and 4°C for hold. The quality of PCR products was confirmed by gel electrophoresis on 2% agarose gel. Pyrosequencing of the *TERT* promoter mutations C228T and C250T was carried out on the PyroMark Q24-MDX system (Qiagen, Valencia, CA, USA) with a sequencing primer 5'-ACCCCGCCCCGTCCCGACCCC-3', based on the manufacturer's instructions. TERT promoter mutation was considered positive if T allele frequency at the mutation sites was ≥10%.

Genomic Characterization by Next-Generation Sequencing

DNA was extracted from the FFPE tissue sample using the QIAamp DNA FFPE Tissue Kit (Qiagen, Valencia, CA, USA) according to the manufacturer's instructions. The extracted DNA was quantitated using a Quantus fluorometer (Promega, Madison, WI, USA) and Agilent 4200 TapeStation system (Agilent Technologies, Santa Clara, CA, USA). DNA was sheared into fragments with a mean peak size of approximately 180 bp to 200 bp, using Adaptive Focused Acoustics (Covaris, Woburn, MA, USA). The paired-end libraries were prepared with a SureSelectXT HS Target Enrichment System kit (Agilent Technologies, Santa Clara, CA, USA), based on the

manufacturer's instruction, using commercially available targeted panels that cover *NF2*, *AKT1*, *TRAF7*, *KLF4*, *SMO*, *PIK3CA*, *SMARCB1*, and other cancer-related genes (**Supplementary Table 1**). The quality of the DNA library was evaluated using a Bioanalyzer 2100 (Agilent Technologies, San Francisco, CA, USA) and quantified using a Qubit dsDNA HS Assay kit and a Qubit 2.0 fluorometer (Life Technologies, Carlsbad, CA, USA). The libraries were paired-end sequenced (2 × 150 bp) using a NextSeq 550Dx (Illumina, San Diego, CA, USA) or a HiSeq 2500 (Illumina, San Diego, CA, USA).

Sequencing data quality assessment and trimming were performed using FastQC v0.11.8 (RRID : SCR_014583). The sequence reads were aligned to the reference genome GRCh37 (hg19) using BWA v0.7.15 (RRID : SCR_010910), Picard v2.16.0 (RRID : SCR_006525), and Samtools v1.3.1 (RRID : SCR_002105). Single nucleotide variants (SNVs) and indels were identified using GATK v4.1.4.0 (RRID : SCR_001876), where a threshold of at least 10 reads and an allelic frequency of ≥10% were used for variant calling. The sequencing variants were annotated using SnpEff & SnpSift v5.1 (RRID : SCR_005191/SCR_015624). The variants found in the population databases, the Exome Aggregation Consortium (RRID : SCR_004068), and the Genome Aggregation Database (RRID : SCR_014964), were filtered out to demonstrate somatic mutations minimizing germline contamination. All variants were interpreted based on the Association for Molecular Pathology (AMP) standards and guidelines (5).

Clinical Evaluation

All patients received regular follow-up after initial treatment. Magnetic resonance images (MRIs) were performed within 48 hours after surgery, and the extent of resection was evaluated by neurosurgeons. For patients with visible residual tumors, adjuvant stereotactic radiosurgery or radiotherapy was usually performed within three to six months from surgery. Patients with grade 2 or 3 meningiomas were referred to the institution's multidisciplinary neuro-oncology outpatient clinic, where a team of neurosurgeon, neuroradiologist, pathologist, medical oncologist, and radiation oncologist participated in a discussion to select the most optimal therapeutic plan for each patient.

Patients were usually followed up every six months for the first two years and then annually thereafter. The recurrence-free survival (RFS) was calculated from the date of surgical resection to the first recurrence of meningioma requiring further therapeutic plans. Evidence of local tumor recurrence was provided by MRI showing meningioma in a location contiguous with the previous operation site.

Statistical Consideration

For descriptive statistics, the frequency with percentages was provided for categorical data and median with interquartile ranges for continuous data. Differences between grades 1 and 2/3 meningiomas were compared using the Chi-square test for categorical variables and the t-test for continuous variables. The statistical correlations between genomic features and clinicopathological parameters were evaluated using the Fisher's exact test. Differences in RFS between distinct subgroups were assessed by the log-rank test. The prevalence of known recurrent variants in this study was compared to the pooled data from external cohorts using the Chi-squared test. Each result from statistical tests was considered statistically significant if a two-tailed p-value was less than 0.05. All statistical analyses were performed using R v3.6.3 (RRID : SCR_001905).

RESULTS

Baseline Characteristics

A total of 713 cases with intracranial meningiomas who received surgical treatment between 2003 and 2020 were reviewed (**Figure 1**). The median age of the study population was 56 (47-65) years, and females made up 71.6% of the population. Grade 2/3 meningiomas were identified in 143 (20.1%) cases. Patients with grade 2/3 meningiomas tended to have a lower female predominance compared with those with grade 1 tumors (**Table 1**): male, 44.8% vs. 24.3% ($p < 0.001$). There was no significant association between grades and the location of tumors.

A sample of 40 patients with grade 2/3 meningiomas participated in the targeted NGS panel study, whose tissue specimens were acquired between 2012 and 2019. The baseline characteristics of the sample and the study population were evenly distributed. Most candidates provided the tissue specimens from the initial surgery, except three patients with recurrent meningiomas who had a history of prior surgery and/or stereotactic radiosurgery. The candidates had no past medical

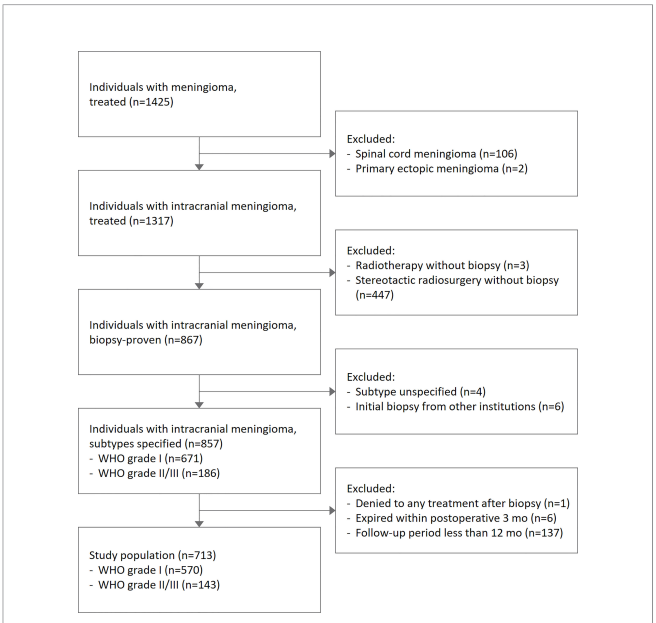

FIGURE 1 | Selection of study population.

TABLE 1 | Baseline characteristics of the study population.

	Study cohort (n=713)		Sample (n=40)
	Grade 1 (n=570)	Grade 2/3 (n=143)	
Age (yr)	56 [47, 64]	57 [47, 67]	55 [48, 66]
≥65	136 (24)	45 (31)	11 (28)
Sex			
Male	138 (24)	64 (45)	16 (40)
Location			
Convexity	164 (30)	46 (32)	22 (55)
Parasagittal/falx	95 (17)	43 (30)	12 (30)
Skull-based†	244 (43)	45 (31)	4 (10)
Intraventricular	11 (2)	8 (6)	2 (5)
Miscellaneous	51 (9)	1 (1)	.
Etiology			
Sporadic	568 (100)	139 (97)	40 (100)
NF2	2 (0)	3 (2)	.
Radiation	.	1 (1)	.
Prior treatment			
Untreated	561 (99)	128 (90)	37 (92)
Treated	9 (1)	15 (10)	3 (8)
Treatment type			
Resection only	491 (86)	68 (48)	13 (33)
Resection + SRS	76 (13)	22 (15)	8 (20)
Resection + RT	3 (1)	53 (37)	19 (48)
Pathology			
Meningothelial	232 (41)	.	.
Fibrous	95 (17)	.	.
Transitional	152 (27)	.	.
Psammomatous	16 (3)	.	.
Angiomatous	44 (8)	.	.
Microcystic	19 (3)	.	.
Secretory	3 (1)	.	.
LPR	1 (0)	.	.
Metaplastic	8 (1)	.	.
Atypical	.	123 (86)	35 (88)
Chordoid	.	5 (3)	.
Clear cell	.	.	.
Anaplastic	.	8 (6)	2 (5)
Papillary	.	4 (3)	1 (3)
Rhabdoid	.	3 (2)	2 (5)

Values are median [IQR] or number (percent). †Skull-based includes olfactory groove, planum sphenoidale, tuberculum sellae, sphenoid wing, cavernous sinus, petroclival, petrosal, and foramen magnum lesions. NF2, neurofibromatosis type 2; LPR, lymphoplasmocyte-rich; SRS, stereotactic radiosurgery; RT, radiotherapy.

history of underlying malignancies at the time of tissue acquisition, except one patient who had extracranial metastasis and received systemic chemotherapy with hydroxyurea before tumor sampling.

Clinical Outcome and Molecular Diagnosis

The study population was followed up for 59.1 (30.0-98.0) months. During the follow-up period, 59 cases of grade 1 meningiomas and 40 cases of grade 2/3 meningiomas had an event of recurrence, showing distinct outcomes ($p < 0.001$) (**Figure 2A**). Five-year recurrence-free survival (RFS) estimates were 86.0 [95% CI, 82.7-89.5%] and 66.8% [95% CI, 58.5-76.2%] for grade 1 and 2/3 meningiomas, respectively.

For grade 2/3 meningiomas, Simpson grade I resection was achieved in 33 (23.1%) cases, followed by 44 (30.8%) cases for grade II, 19 (13.3%) cases for grade III, 43 (30.1%) cases for grade IV, and 4 (2.8%) cases for grade V resection. While the survival difference between grades 2 and 3 was insignificant, the achievement of Simpson grade I resection significantly influenced the clinical outcome in grade 2 meningiomas ($p = 0.005$) (**Figure 2B**). Other treatment factors regarding adjuvant stereotactic radiosurgery or radiotherapy did not significantly change the outcome.

In the sample population, local recurrence has been developed in 10 patients during the follow-up period of 68.5 (55.8-97.3) months. Simpson grade I resection was achieved in 10 (25.0%) cases. Those patients with recurrence received additional treatment with stereotactic radiosurgery, and two of them underwent reoperation for surgical resection of the recurred tumor. The five-year RFS was 65.4% for a subset of participants whose long-term follow-up data were available, representing the grade 2/3 meningiomas in the study cohort.

To evaluate the clinicopathologic relevance regarding the molecular diagnostic criteria in WHO CNS 5, we assessed the *TERT* promoter and *CDKN2A/B* status of meningioma. The *TERT* promoter hotspot mutation PCR was available for 52 cases (40 samples and additional 12 cases) with grade 2/3 meningiomas. Positive results were identified in three cases; these were conventionally diagnosed as atypical meningiomas with high mitotic activity, and all recurred during the follow-up period and highly refractory to the selected treatments (**Figures 3**–**5**). Interestingly, two of them had distant metastasis with rapid progression. Those formerly diagnosed as grade 3 meningiomas (7 cases) did not present a positive *TERT* promoter mutation. The molecularly integrated classifying group with conventional grade 3 and positive *TERT* promoter mutation showed a poorer outcome than the others (**Figure 2C**).

We also assessed the immunohistochemistry of CDKN2A (p16) that homozygotic deletion of the corresponding gene would be represented by loss of expression. Among 40 sample participants, 17 patients with grade 2 meningiomas were reclassified into a higher grade, as they presented negative p16 staining. However, the immunohistochemical status of CDKN2A did not show a significant difference in RFS (**Figure 2D**).

Mutational Profiling of Grade 2/3 Meningiomas

All 40 samples achieved the institutional quality standard of the NGS study. The tumor purity of FFPE samples ranged from 50 to 90%. The sequencing achieved the 100× coverage of 98.0% (96.2-98.5%) for the target regions with a mean depth of 750 (517-901) (**Supplementary Table 2**). A total of 160 somatic variants from 66 different genes were identified (**Supplementary Table 3**). The mutational profiles were highly heterogeneous, and no statistical association between genomic alterations and clinicopathologic features was observed (**Figure 6**).

SNVs and indels were the most frequent in *NF2* (42.5%), which consists of eight frameshift, three stop-gain and five splice site variants. Other mutations in previously documented genes associated with meningiomas, including *AKT1* (one missense

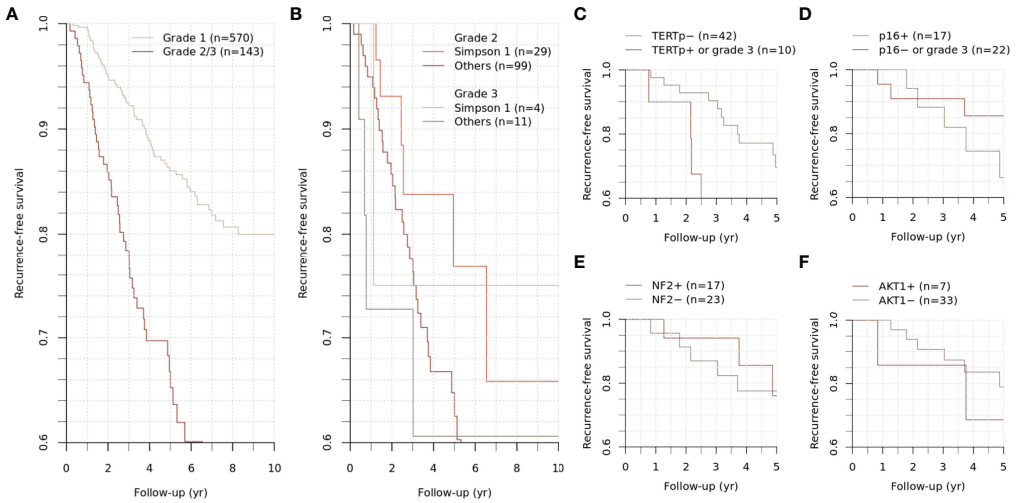

FIGURE 2 | Recurrence-free survival of grade 2/3 meningiomas. Differential recurrence-free survival was observed between grade 1 and grade 2/3 meningiomas **(A)**. The survival difference between grades 2 and 3 was insignificant **(B)**. The subgroups of grade 2/3 meningiomas were stratified according to the mutational status of specific genes **(C–F)**.

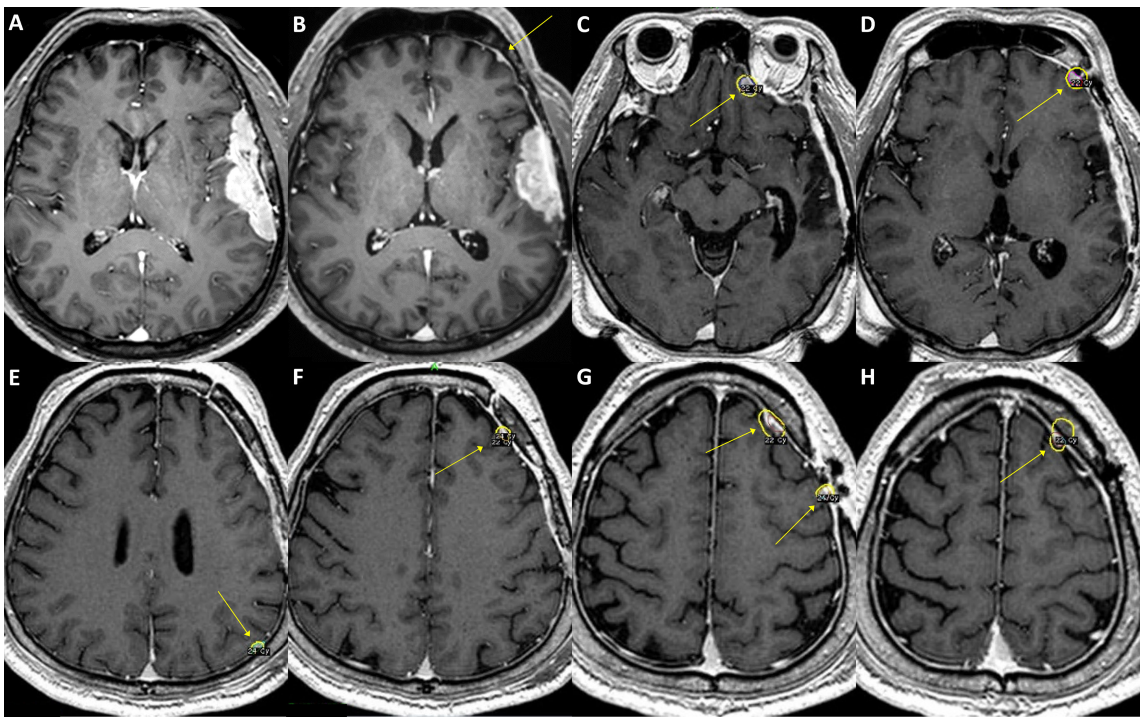

FIGURE 3 | A case of convexity meningioma with *TERT* promoter mutation. A 52-year-old male presented with an en plaque meningioma in the left temporal convexity **(A)**. The tumor was partially resected during the initial surgery, and the residual superior temporal mass, severely adhered to the brain parenchyma and the vascular structures in the Sylvian fissure, was further treated by adjuvant stereotactic radiosurgery. However, the tumor regrew **(B)**, and another operation was performed after two years from the initial treatment. The specimens from the first and second operations both presented C250T *TERT* promoter mutation. Although the primary lesion was successfully removed, a new, tiny lesion at the left frontal convexity (**B**, arrow) had been rapidly grown at six-month follow-up, in addition to other multiple distant lesions (**C–H**, arrows). The patient underwent stereotactic radiosurgery six times over the next five years, one more reoperation at the primary location, and then another two times of stereotactic radiosurgery for the refractory tumors. In 9 years from the initial treatment, the leptomeningeal spread of the tumor cells was confirmed by cerebrospinal fluid examination, and the patient received a ventriculoperitoneal shunt operation for hydrocephalus.

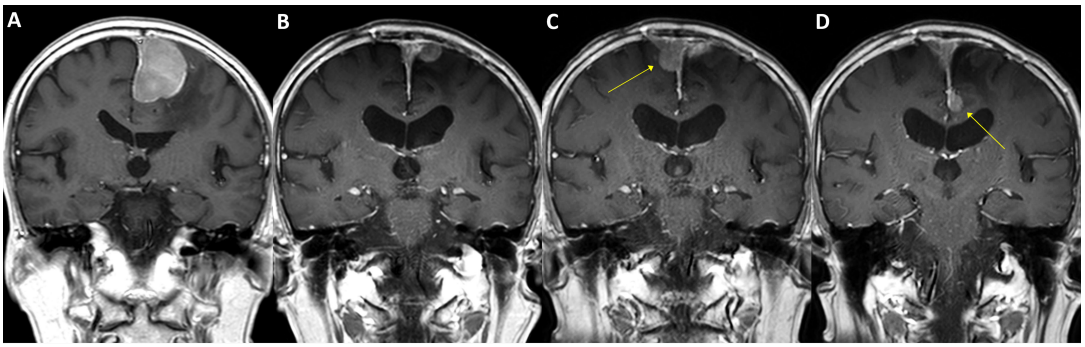

FIGURE 4 | A case of parasagittal meningioma with *TERT* promoter mutation. A 78-year-old male with a 4.5 cm-sized left parasagittal meningioma **(A)** underwent surgery achieving subtotal resection, followed by adjuvant radiotherapy. In two years, the tumor recurred at the primary location **(B)** and was treated by secondary radiosurgery. In the following year, two new lesions as well as the progressed primary lesion were detected (**C, D**, arrows) and retreated by radiosurgery. The patient had suffered from impaired gait function and expired due to pneumonia after having a femur neck fracture on the sixth year from the initial treatment. The specimen acquired from the initial surgery has presented C228T *TERT* promoter mutation.

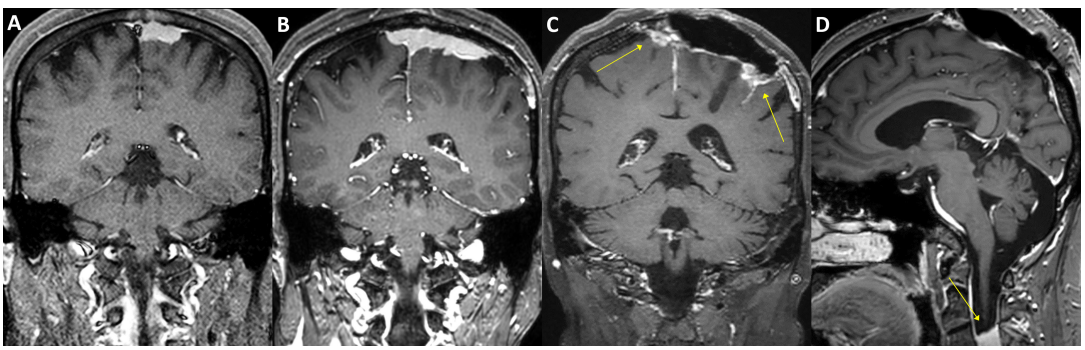

FIGURE 5 | A case of parasagittal meningioma with *TERT* promoter mutation. A 47-year-old female with a 2.5 cm-sized left parasagittal meningioma **(A)** underwent stereotactic radiosurgery. In seven years, the tumor, however, progressed **(B)** and was treated by partial resection and adjuvant radiotherapy. The tumor was refractory to the treatments and required another operation and three-stage radiosurgery after two years. The tumor still progressed in the following year (**C**, arrows) and was further treated with radiosurgery three times. One year after, a total of 11 years from the initial treatment, a new rapidly growing lesion was found in the second cervical spine level (**D**, arrow). Multiple pulmonary metastases were also found in the positron-emission tomography scan. The patient received laminectomy and tumor removal for the distant lesion, and the specimen presented C228T *TERT* promoter mutation.

and one splice site variants) and *TRAF* (five missense and one splice site variants), were also found. In particular, *AKT1* c.49G>A (p.E17K) mutation was recurrent in five cases, most of which concurrently harbored a missense variant in *TRAF7*. However, there was no clinical relevance in exploratory survival analyses (**Figures 2E, F**).

The prevalence of recurrent variants in meningioma was investigated by comparing the results between pooled data from previous literature and this study (**Table 2**). Interestingly, the prevalence of mutations in *AKT1* and *TRAF7* were significantly higher than that in grade 2/3 cases previously reported in external cohorts [*AKT1* p.E17K mutation in samples vs. external cohorts (#1-6), $p < 0.001$; *TRAF7* mutations, $p = 0.017$]. Other known recurrent mutations, such as *KLF4* c.1225A>C (p.K409Q) or *SMO* c.1234C>T (p.L412F), were not detected. A few individual cases presented possible pathogenic variants, *PIK3CA* c.1633G>A (p.E545K) or *SMARCB1* (also known as *BAF47*, *INI1*, or *SNF5L1*) c.1130G>A (p.R377H), while others were tiered as benign or had uncertain significance.

DISCUSSION

This study demonstrated the clinical, histopathologic, and genomic characteristics of grade 2/3 meningiomas. In our cohort, there was a significantly larger proportion of males with grade 2/3 meningiomas than with grade 1 meningiomas.

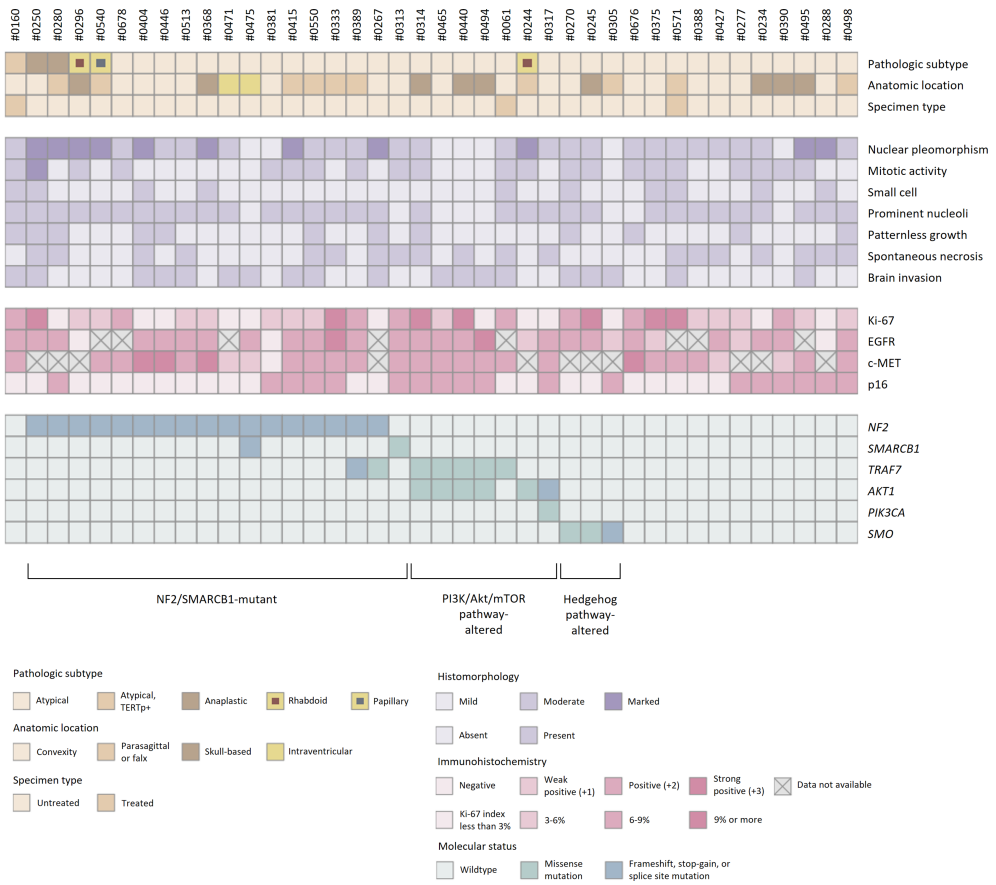

FIGURE 6 | Histopathologic features and molecular status of grade 2/3 meningiomas. Grade 2/3 meningiomas exhibited heterogeneous clinical, histopathologic, and genomic features.

This finding was consistent with those observed in a nationwide cohort study and relevant literature (14). Considering a high female predominance in benign meningiomas and the effect of hormones in meningioma pathogenesis (15), it is interesting that sex distribution is more even in higher grades meningiomas. Perhaps, the invasiveness of meningioma might be affected by the different biological factors rather than hormones or other sex-related conditions, which could be discovered from genomic aberrations.

Among the variable morphologic subtypes of meningiomas, our sample population did not show novel findings of recurrent somatic variations. Nevertheless, there were a few interesting points in our results. First, the prevalence of *NF2* mutations in grade 2/3 meningiomas was not as frequent as reported in some previous literature (2, 16). Another known pathogenic gene *SMARCB1*, which has been suggested to be associated with a high Ki-67 index (17), was identified in a single case; however, the histopathologic feature was not specific. Also, we observed that the common recurrent mutations *AKT1* p.E17K and *TRAF7* mutations were as frequent as previously reported in grade 1 meningiomas. Those *AKT1*-mutant and *TRAF7*-mutant cases did not show a significantly different prognosis from the others, which was inconsistent with previous reports (18). Conversely, a recurrent mutation *KLF4* p.K409Q has not been detected in our grade 2/3 samples, which supports that this variant might be predominantly harbored in low-grade tumors and possibly associated with a favorable prognosis without tumor recurrence (17, 19).

The recent article with the updated CNS WHO classification also demonstrated several variants associated with specific subtypes (1). *TERT* promoter mutation, now adopted to molecular diagnosis of grade 3 meningioma, represented highly progressive tumors in our cases. Regarding the emerging issues on molecular diagnosis of meningioma, some experts suggest considering NGS for all grade 2 meningiomas (4): however, there is a lack of consensus on the standardization of diagnostic method regarding the source of specimens, sequencing protocol, or analysis pipeline. Besides, *TERT* promoter mutation was not adequately detectable by targeted NGS study using the common commercial panels, and additional PCR tests have been needed for diagnosis in most institutions. Since the expense of the study is considerably high, the cost-effectiveness

TABLE 2 | Prevalence of recurrent variants in meningiomas according to the histopathologic grade.

	External cohort #1	External cohort #2	External cohort #3	External cohort #4	External cohort #5	External cohort #6	Current study	Overall
***NF2* (any variants)**								
Grade 1	28.8% (164 of 570)	36.4% (28 of 77)	22.9% (33 of 144)	23.2% (22 of 99)	36.8% (81 of 220)	38.7% (94 of 243)	.	31.3% (423 of 1353)
Grade 2/3	44.6% (100 of 224)	47.8% (32 of 67)	33.1% (51 of 154)	64.3% (18 of 28)	61.9% (382 of 617)	46.2% (12 of 26)	42.5% (17 of 40)	52.9% (612 of 1156)
***SMARCB1* p.R374Q or p.R377H[†]**								
Grade 1	3.9% (18 of 463)	1.3% (1 of 77)	.	3.0% (3 of 99)	0.9% (2 of 220)	.	.	2.8% (24 of 859)
Grade 2/3	2.1% (4 of 194)	0.0% (0 of 67)	.	3.6% (1 of 28)	0.5% (3 of 617)	.	2.5% (1 of 40)	1.0% (9 of 946)
***TRAF7* (any variants)**								
Grade 1	28.6% (163 of 570)	3.2% (1 of 31)	28.5% (41 of 144)	23.2% (23 of 99)	.	.	.	27.0% (228 of 844)
Grade 2/3	11.2% (25 of 224)	5.3% (3 of 57)	1.3% (2 of 154)	0.0% (0 of 28)	.	.	17.5% (7 of 40)	7.4% (37 of 503)
***AKT1* p.E17K**								
Grade 1	12.6% (72 of 570)	7.8% (6 of 77)	16.0% (23 of 144)	11.1% (11 of 99)	8.6% (19 of 220)	11.1% (27 of 243)	.	11.7% (158 of 1353)
Grade 2/3	6.7% (15 of 224)	4.5% (3 of 67)	0.6% (1 of 154)	0.0% (0 of 28)	2.1% (13 of 617)	3.8% (1 of 26)	12.5% (5 of 40)	3.3% (38 of 1156)
***PIK3CA* p.E542K, p.E545K/A, or p.H1047R/L/Q**								
Grade 1	4.2% (16 of 385)	0.0% (0 of 31)	0.7% (1 of 144)	2.0% (2 of 99)	3.2% (7 of 220)	.	.	3.0% (26 of 879)
Grade 2/3	2.4% (4 of 164)	0.0% (0 of 57)	1.9% (3 of 154)	0.0% (0 of 28)	0.6% (4 of 617)	.	2.5% (1 of 40)	1.1% (12 of 1060)
***KLF4* p.K409Q**								
Grade 1	10.0% (57 of 570)	0.0% (0 of 31)	11.1% (16 of 144)	8.1% (8 of 99)	.	6.6% (16 of 243)	.	8.9% (97 of 1087)
Grade 2/3	2.7% (6 of 224)	0.0% (0 of 57)	0.0% (0 of 154)	0.0% (0 of 28)	.	0.0% (0 of 26)	0.0% (0 of 40)	1.1% (6 of 529)
***SMO* p.L412F or p.W535L**								
Grade 1	4.6% (26 of 570)	3.9% (3 of 77)	3.5% (5 of 144)	4.0% (4 of 99)	2.7% (6 of 220)	0.4% (1 of 243)	.	3.3% (45 of 1353)
Grade 2/3	0.4% (1 of 224)	0.0% (0 of 67)	0.0% (0 of 154)	0.0% (0 of 28)	0.2% (1 of 617)	0.0% (0 of 26)	0.0% (0 of 40)	0.2% (2 of 1156)

Values are percentage (number of cases/total number of screened cases). Data are curated from the following references: External cohort #1 (6, 7); External cohort #2 (8–10); External cohort #3 (11); External cohort #4 (12); External cohort #5 (2); External cohort #6 (13). Variants were screened by either whole genome or exome sequencing, targeted sequencing, Sanger sequencing, or PCR. [†]Corresponding to R383Q and R386H in GRCh38, respectively.

of molecular diagnostic studies should be carefully discussed, with full consideration of the patient's best interest.

Several studies suggested a histopathologic and genomic relevance, but the mutational profiles of meningiomas are highly heterogeneous and inconsistent among previous reports (20). We utilized p16 immunohistochemistry to represent *CDKN2A* deletion; however, it seemed unfeasible to detect the gene-level copy number aberration from protein expression (21). Although some studies also showed certain mutational patterns according to the anatomical location of tumors (18, 22, 23), mutations in *AKT1* or *SMO* that have been frequently reported in skull-based lesions were not specific in our samples. Intraventricular meningiomas, on the other hand, certainly harbored *NF2* mutations without the other common variants, as reported elsewhere (24). Since the clinical significance of most genomic alterations has not been fully understood, further studies are needed to validate the clinicopathologic relevance. Perhaps, different genomic approaches, such as epigenetic studies that were utilized in several studies to identify specific methylation status (11, 25, 26),?A3B2 show [#,32] ?> might provide better understanding of the tumor characteristics.

This study is limited due to the lack of available prognostic measures for patients with meningioma; and as such, the clinical significance of NGS in characterizing the molecular profiles of high-grade meningiomas remains inconclusive. The RFS, the outcome measure utilized in this study, was relatively low compared with other studies (11, 12, 25, 27, 28). Most grade 2/3 meningiomas in this study cohort were successfully controlled by adjunctive treatments, including stereotactic radiosurgery and radiotherapy from conventional decision making without the molecular diagnosis. Future investigations should focus more on specific populations of patients with highly malignant or metastatic lesions that are refractory to the current treatment modalities. In this perspective, molecular targets from NGS can lead to a possible therapeutic implication (15, 29, 30). Nevertheless, for a majority of meningioma cases, surgical outcome and other clinical factors appears to be more critical than tumor properties characterized by NGS at this time.

CONCLUSION

Grade 2/3 meningiomas show a broad spectrum of molecular profiles, as they have heterogeneous histologic characteristics. Further studies are needed to validate the clinical significance of the NGS study.

DATA AVAILABILITY STATEMENT

The datasets presented in this study can be found in online repositories. The names of the repository/repositories and accession number(s) can be found below: ENA, PRJEB51397.

ETHICS STATEMENT

The studies involving human participants were reviewed and approved by the Institutional Review Board in Seoul National University Bundang Hospital. The patients/participants provided their written informed consent to participate in this study. Written informed consent was obtained from the individual(s) for the publication of any potentially identifiable images or data included in this article.

AUTHOR CONTRIBUTIONS

All authors contributed to the conception and design of the study. JK performed data analysis and wrote the first draft of the manuscript. KH and KL contributed to material preparation. All authors read and approved the final manuscript.

FUNDING

This study was supported by grants from Seoul National University Bundang Hospital (13-2019-0009 & 06-2021-0483).

SUPPLEMENTARY MATERIAL

The Supplementary Material for this article can be found online at: https://www.frontiersin.org/articles/10.3389/fonc.2022.885155/full#supplementary-material

REFERENCES

1. Louis DN, Perry A, Wesseling P, Brat DJ, Cree IA, Figarella-Branger D, et al. The 2021 WHO Classification of Tumors of the Central Nervous System: A Summary. *Neuro Oncol* (2021) 23(8):1231–51. doi: 10.1093/neuonc/noab106
2. Williams EA, Santagata S, Wakimoto H, Shankar GM, Barker FG2nd, Sharaf R, et al. Distinct Genomic Subclasses of High-Grade/Progressive Meningiomas: NF2-Associated, NF2-Exclusive, and NF2-Agnostic. *Acta Neuropathol Commun* (2020) 8(1):171. doi: 10.1186/s40478-020-01040-2
3. Wilson TA, Huang L, Ramanathan D, Lopez-Gonzalez M, Pillai P, De Los Reyes K, et al. Review of Atypical and Anaplastic Meningiomas: Classification, Molecular Biology, and Management. *Front Oncol* (2020) 10:565582. doi: 10.3389/fonc.2020.565582
4. Gritsch S, Batchelor TT, Gonzalez Castro LN. Diagnostic, Therapeutic, and Prognostic Implications of the 2021 World Health Organization Classification of Tumors of the Central Nervous System. *Cancer* (2022) 128 (1):47–58. doi: 10.1002/cncr.33918
5. Li MM, Datto M, Duncavage EJ, Kulkarni S, Lindeman NI, Roy S, et al. Standards and Guidelines for the Interpretation and Reporting of Sequence Variants in Cancer: A Joint Consensus Recommendation of the Association for Molecular Pathology, American Society of Clinical Oncology, and College of American Pathologists. *J Mol Diagn* (2017) 19(1):4–23. doi: 10.1016/j.jmoldx.2016.10.002
6. Clark VE, Erson-Omay EZ, Serin A, Yin J, Cotney J, Ozduman K, et al. Genomic Analysis of non-NF2 Meningiomas Reveals Mutations in TRAF7, KLF4, AKT1, and SMO. *Science* (2013) 339(6123):1077–80. doi: 10.1126/science.1233009
7. Clark VE, Harmanci AS, Bai H, Youngblood MW, Lee TI, Baranoski JF, et al. Recurrent Somatic Mutations in POLR2A Define a Distinct Subset of Meningiomas. *Nat Genet* (2016) 48(10):1253–9. doi: 10.1038/ng.3651
8. Brastianos PK, Horowitz PM, Santagata S, Jones RT, McKenna A, Getz G, et al. Genomic Sequencing of Meningiomas Identifies Oncogenic SMO and AKT1 Mutations. *Nat Genet* (2013) 45(3):285–9. doi: 10.1038/ng.2526
9. Abedalthagafi M, Bi WL, Aizer AA, Merrill PH, Brewster R, Agarwalla PK, et al. Oncogenic PI3K Mutations Are as Common as AKT1 and SMO Mutations in Meningioma. *Neuro Oncol* (2016) 18(5):649–55. doi: 10.1093/neuonc/nov316
10. Bi WL, Greenwald NF, Abedalthagafi M, Wala J, Gibson WJ, Agarwalla PK, et al. Genomic Landscape of High-Grade Meningiomas. *NPJ Genom Med* (2017) 2:15. doi: 10.1038/s41525-017-0014-7

11. Sahm F, Schrimpf D, Stichel D, Jones DTW, Hielscher T, Schefzyk S, et al. DNA Methylation-Based Classification and Grading System for Meningioma: A Multicentre, Retrospective Analysis. *Lancet Oncol* (2017) 18(5):682–94. doi: 10.1016/s1470-2045(17)30155-9
12. Patel AJ, Wan YW, Al-Ouran R, Revelli JP, Cardenas MF, Oneissi M, et al. Molecular Profiling Predicts Meningioma Recurrence and Reveals Loss of DREAM Complex Repression in Aggressive Tumors. *Proc Natl Acad Sci USA* (2019) 116(43):21715–26. doi: 10.1073/pnas.1912858116
13. Okano A, Miyawaki S, Hongo H, Dofuku S, Teranishi Y, Mitsui J, et al. Associations of Pathological Diagnosis and Genetic Abnormalities in Meningiomas With the Embryological Origins of the Meninges. *Sci Rep* (2021) 11(1):6987. doi: 10.1038/s41598-021-86298-9
14. Barthelemy E, Loewenstern J, Konuthula N, Pain M, Hall J, Govindaraj S, et al. Primary Management of Atypical Meningioma: Treatment Patterns and Survival Outcomes by Patient Age. *J Cancer Res Clin Oncol* (2018) 144 (5):969–78. doi: 10.1007/s00432-018-2618-4
15. Preusser M, Brastianos PK, Mawrin C. Advances in Meningioma Genetics: Novel Therapeutic Opportunities. *Nat Rev Neurol* (2018) 14(2):106–15. doi: 10.1038/nrneurol.2017.168
16. Harmanci AS, Youngblood MW, Clark VE, Coskun S, Henegariu O, Duran D, et al. Integrated Genomic Analyses of *De Novo* Pathways Underlying Atypical Meningiomas. *Nat Commun* (2017) 8:14433. doi: 10.1038/ncomms14433
17. Youngblood MW, Miyagishima DF, Jin L, Gupte T, Li C, Duran D, et al. Associations of Meningioma Molecular Subgroup and Tumor Recurrence. *Neuro Oncol* (2021) 23(5):783–94. doi: 10.1093/neuonc/noaa226
18. Yesiloz U, Kirches E, Hartmann C, Scholz J, Kropf S, Sahm F, et al. Frequent AKT1E17K Mutations in Skull Base Meningiomas Are Associated With mTOR and ERK1/2 Activation and Reduced Time to Tumor Recurrence. *Neuro Oncol* (2017) 19(8):1088–96. doi: 10.1093/neuonc/nox018
19. von Spreckelsen N, Waldt N, Timmer M, Goertz L, Reinecke D, Laukamp K, et al. Clinical Characteristics and Magnetic Resonance Imaging-Based Prediction of the KLF4(K409Q) Mutation in Meningioma. *World Neurosurg* (2021) 154:e665–70. doi: 10.1016/j.wneu.2021.07.119
20. Gonzalez-Tablas M, Prieto C, Arandia D, Jara-Acevedo M, Otero A, Pascual D, et al. Whole-Exome Sequencing Reveals Recurrent But Heterogeneous Mutational Profiles in Sporadic WHO Grade 1 Meningiomas. *Front Oncol* (2021) 11:740782. doi: 10.3389/fonc.2021.740782
21. Guyot A, Duchesne M, Robert S, Lia AS, Derouault P, Scaon E, et al. Analysis of CDKN2A Gene Alterations in Recurrent and non-Recurrent Meningioma. *J Neurooncol* (2019) 145(3):449–59. doi: 10.1007/s11060-019-03333-6
22. Boetto J, Bielle F, Sanson M, Peyre M, Kalamarides M. SMO Mutation Status Defines a Distinct and Frequent Molecular Subgroup in Olfactory Groove Meningiomas. *Neuro Oncol* (2017) 19(3):345–51. doi: 10.1093/neuonc/now276
23. Hao S, Huang G, Feng J, Li D, Wang K, Wang L, et al. Non-NF2 Mutations Have a Key Effect on Inhibitory Immune Checkpoints and Tumor Pathogenesis in Skull Base Meningiomas. *J Neurooncol* (2019) 144(1):11–20. doi: 10.1007/s11060-019-03198-9
24. Jungwirth G, Warta R, Beynon C, Sahm F, von Deimling A, Unterberg A, et al. Intraventricular Meningiomas Frequently Harbor NF2 Mutations But Lack Common Genetic Alterations in TRAF7, AKT1, SMO, KLF4, PIK3CA, and TERT. *Acta Neuropathol Commun* (2019) 7(1):140. doi: 10.1186/s40478-019-0793-4
25. Maas SLN, Stichel D, Hielscher T, Sievers P, Berghoff AS, Schrimpf D, et al. Integrated Molecular-Morphologic Meningioma Classification: A Multicenter Retrospective Analysis, Retrospectively and Prospectively Validated. *J Clin Oncol* (2021) 39(34):3839–52. doi: 10.1200/JCO.21.00784
26. Nassiri F, Liu J, Patil V, Mamatjan Y, Wang JZ, Hugh-White R, et al. A Clinically Applicable Integrative Molecular Classification of Meningiomas. *Nature* (2021) 597(7874):119–25. doi: 10.1038/s41586-021-03850-3
27. Sievers P, Hielscher T, Schrimpf D, Stichel D, Reuss DE, Berghoff AS, et al. CDKN2A/B Homozygous Deletion Is Associated With Early Recurrence in Meningiomas. *Acta Neuropathol* (2020) 140(3):409–13. doi: 10.1007/s00401-020-02188-w
28. Driver J, Hoffman SE, Tavakol S, Woodward E, Maury EA, Bhave V, et al. A Molecularly Integrated Grade for Meningioma. *Neuro Oncol* (2021) 24 (5):796–808. doi: 10.1093/neuonc/noab213
29. Gupta S, Bi WL, Dunn IF. Medical Management of Meningioma in the Era of Precision Medicine. *Neurosurg Focus* (2018) 44(4):E3. doi: 10.3171/2018.1.FOCUS17754
30. Maggio I, Franceschi E, Di Nunno V, Gatto L, Tosoni A, Angelini D, et al. Discovering the Molecular Landscape of Meningioma: The Struggle to Find New Therapeutic Targets. *Diagn (Basel)* (2021) 11(10):1852. doi: 10.3390/diagnostics11101852

Conflict of Interest: The authors declare that the research was conducted in the absence of any commercial or financial relationships that could be construed as a potential conflict of interest.

Publisher's Note: All claims expressed in this article are solely those of the authors and do not necessarily represent those of their affiliated organizations, or those of the publisher, the editors and the reviewers. Any product that may be evaluated in this article, or claim that may be made by its manufacturer, is not guaranteed or endorsed by the publisher.

Copyright © 2022 Kim, Hwang, Kwon, Lee, Lee, Choe, Han and Kim. This is an open-access article distributed under the terms of the Creative Commons Attribution License (CC BY). The use, distribution or reproduction in other forums is permitted, provided the original author(s) and the copyright owner(s) are credited and that the original publication in this journal is cited, in accordance with accepted academic practice. No use, distribution or reproduction is permitted which does not comply with these terms.

frontiers | Frontiers in Oncology

MINI REVIEW
published: 30 June 2022
doi: 10.3389/fonc.2022.895374

Bone Invasive Meningioma: Recent Advances and Therapeutic Perspectives

Hajime Takase[1,2*] *and Tetsuya Yamamoto*[2]

[1] Center for Novel and Exploratory Clinical Trials (Y-NEXT), Yokohama City University Hospital, Yokohama, Japan,
[2] Department of Neurosurgery, Graduate School of Medicine, Yokohama City University, Yokohama, Japan

Meningioma is the most common primary neoplasm of the central nervous system (CNS). Generally, these tumors are benign and have a good prognosis. However, treatment can be challenging in cases with aggressive variants and poor prognoses. Among various prognostic factors that have been clinically investigated, bone invasion remains controversial owing to a limited number of assessments. Recent study reported that bone invasion was not associated with WHO grades, progression, or recurrence. Whereas, patients with longer-recurrence tended to have a higher incidence of bone invasion. Furthermore, bone invasion may be a primary preoperative predictor of the extent of surgical resection. Increasing such evidence highlights the potential of translational studies to understand bone invasion as a prognostic factor of meningiomas. Therefore, this mini-review summarizes recent advances in pathophysiology and diagnostic modalities and discusses future research directions and therapeutic strategies for meningiomas with bone invasion.

Keywords: meningioma, bone invasion, recurrence, translational study, long-term

OPEN ACCESS

Edited by:
Hailiang Tang,
Fudan University, China

Reviewed by:
Nils Ole Schmidt,
University Medical Center Regensburg, Germany
Shuyu Hao,
Capital Medical University, China

***Correspondence:**
Hajime Takase
htakase@yokohama-cu.ac.jp
orcid.org/0000-0001-5813-1386

Specialty section:
This article was submitted to Neuro-Oncology and Neurosurgical Oncology, a section of the journal Frontiers in Oncology

Received: *13 March 2022*
Accepted: *01 June 2022*
Published: *30 June 2022*

Citation:
Takase H and Yamamoto T (2022) Bone Invasive Meningioma: Recent Advances and Therapeutic Perspectives. Front. Oncol. 12:895374. doi: 10.3389/fonc.2022.895374

INTRODUCTION

Meningiomas

Meningioma is the most common primary neoplasm of the central nervous system (CNS) in adults, originating from arachnoid cap cells covering the CNS. They are classified according to histopathological characteristics and have a broad morphological spectrum, reflected in 15 subtypes. (1–3). The World Health Organization (WHO) has also classified meningiomas into three grades (1–3), similar to other CNS tumors, linked to overall expected clinical-biological behaviors. Most tumors are WHO grade 1, which are slow-growing with benign features and a comparatively good prognosis. WHO grades 2 and 3 (4, 5) have local brain invasiveness and cellular features, including higher mitosis and atypia. In general, symptomatic cases of any WHO grade are surgically treated, and to date, there is no consensus on the effectiveness of pharmacotherapy, including chemotherapy (6). Hence, Simpson's grade, based on the extent of surgical resection, has been considered a good tumor recurrence indicator in addition to WHO grading (7). Simpson grade

Abbreviations: CNS, central nervous system; WHO, World Health Organization; NF2, neurofibromatosis type 2; CT, computer tomography; MRI, magnetic resonance imaging; 5-ALA, 5-aminolevulinic acid; GTR, gross total removal; OR, odds ratio; PET, positron emission tomography; SSR2, somatostatin receptor subtype 2; VEGF, vascular endothelial growth factor; IMRT, intensity modulated radiation therapy; BNCT, boron neutron capture therapy; PDT, photodynamic therapy.

I is defined as complete removal, including resection of the underlying bone and associated dura. However, meningiomas classified as WHO grade 1 and Simpson grade I sometimes recur in long-term follow-up, often requiring additional treatments, such as secondary surgery or salvage radiosurgery, which can be challenging and potentially lead to morbidity (8). Therefore, recent studies have highlighted the importance of long-term recurrence prediction with a different viewpoint than WHO grade and developing diagnostic and therapeutic options for such recurrent cases.

Meningioma *With Bone Invasion*

Meningiomas are categorized inconsistently based on their location (9). Sometimes, meningiomas grow extracerebrally, corresponding with the tumor's origin. Tumors arising from locations other than the subdural compartment have been termed ectopic, extracranial, extraneuraxial, extradural, or intraosseous meningiomas (9, 10).

Primary intraosseous meningioma usually describes tumors that develop mainly from the calvarium and are unequivocally excluded from the subdural component (11). Contrastingly, many unrecognizable meningioma synonyms and subtypes secondarily extend into the adjacent bone, such as secondary intraosseous meningioma, meningioma with bone infiltration, and meningioma with bone invasion. (In this review, they are consistently noted as bone-invasive meningiomas to avoid confusion). In general, bone invasive meningiomas can be preoperatively diagnosed by conventional radiographic modalities, such as magnetic resonance imaging (MRI) and computed tomography (CT). They are histopathologically confirmed after surgery, since the preoperative judgment of bone involvement is sometimes ambiguous (**Figures 1A–D**). Meningioma en plaque, a relatively uncommon and unique form accounting for 2-9% of meningiomas, is often accompanied by hyperostosis in the middle fossa and sphenoid wing, with an incidence rate of 13–49% (12–14). Nevertheless, hyperostosis is seen less in other meningiomas except for lymphoplasmacyte-rich meningioma, a rare histologic subtype (WHO grade 1), which can arise as an en-plaque meningioma, and is characterized by a prominent infiltration of plasma cells and lymphocytes with a variable

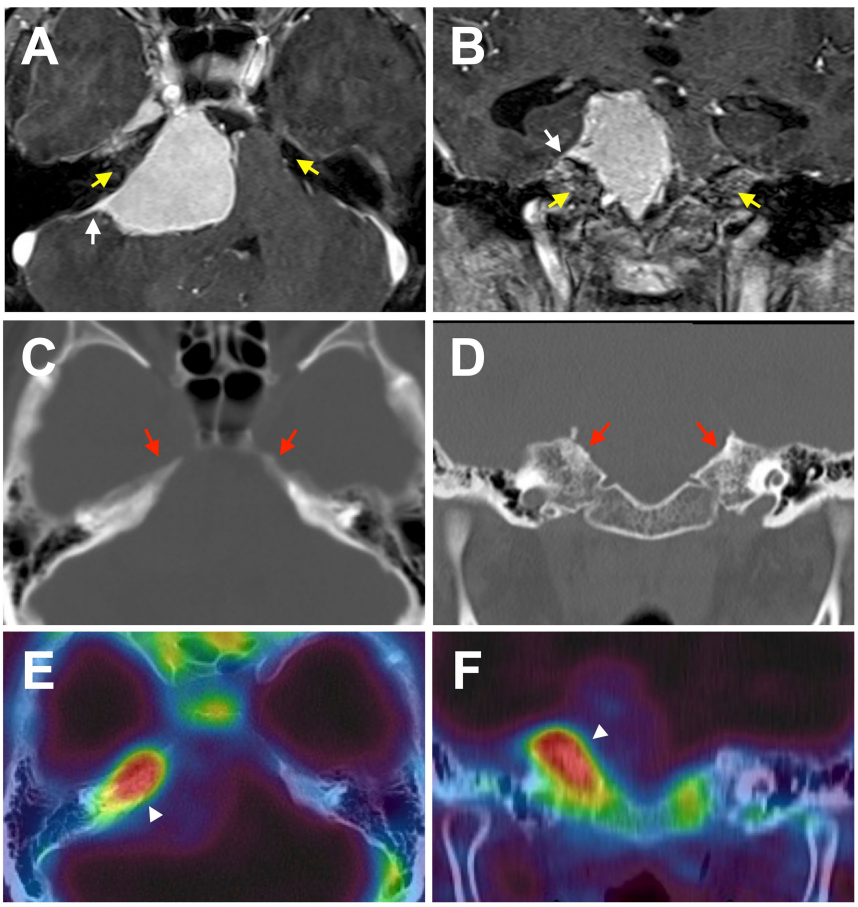

FIGURE 1 | A representative case of meningioma with bone invasion. Axial **(A, C, E)** and coronal **(B, D, F)** images demonstrating a petroclival meningioma. **(A, B)** T1-post contrast MRI shows a characteristic dural tail (white arrows). Enhancement in the adjacent bone is ambiguous, and no obvious laterality is found (yellow arrows). **(C, D)** Non-contrast bone CT does not reveal a hyperostosis with tumor-associated laterality. **(E, F)** However, F^{18} fluoride PET/CT fusion image indicates prominent uptake in the adjacent bone suggesting bone invasion of the tumor (white arrowheads).

proportion of meningothelial elements (15–17). To date, hyperostosis has been thought as due to direct tumor invasion to adjacent bone and reactive hypervascularity of the periosteum leading to benign formation, and thus can often be classified as bone-invasive meningiomas (18–22).

In addition to histopathological aggressiveness and surgical extension, accumulating evidence suggests that bone invasion could predict recurrence and is possibly associated with reduced progression-free and overall survival, even in WHO grade 1 or 2 cases that surgically achieved total removal (Gabeau-Lacet et al.: Simpson I-III in WHO grade 1, Abdelzaher et al.: Simpson grade I-II in WHO grade 2, Lemee et al.: Simpson grade I-III in WHO grade 1-3) (23–25). However, due to the limited assessability, bone invasion as a recurrent predictor remains less understood, and is therefore not reflected in the WHO grading criteria. Taken together, these facts strongly suggest that further integrative study of bone invasive meningioma may provide deeper understanding of bone invasive meningioma and improve the long-term prognosis.

Current Issues

The rarity of bone-invasive meningioma may contribute to the limited number of assessments. Thus, bone-invasive meningiomas has not been well described compared with primary intraosseous meningioma (9, 26–28). Another obstacle is the lack of a standard assessment method for bone-invasive meningiomas, except tissue histopathology. In other words, diagnostic options for meningiomas with bone invasion have been less studied. In addition, the specific mechanism of cellular infiltration and the molecular background characteristics are ambiguous. Overall, these facts result in the underdevelopment of therapeutic alternatives for invasion, except for direct microscopic surgery.

However, clinical evidence of bone-invasive meningioma is increasing, emphasizing the importance of further studies to understand bone invasion as an independent prognostic factor or a preoperative factor related to the extent of surgical resection. Several diagnostic modalities have been developed for meningiomas, including bone invasion. Furthermore, recent molecular biology advances exploring therapeutic targets provide future opportunities to reorganize meningioma issues (3, 29).

Aims

Therefore, this mini-review briefly summarizes recent advances in the clinical knowledge of bone-invasive meningioma as a long-term recurrent predictor and introduces potent diagnostic options and molecular pathophysiology. Finally, we discuss future research directions and therapeutic strategies for meningiomas with bone invasion.

BONE INVASION AS A PREDICTOR OF RECURRENCE

In a surgical series of WHO grade 2 (atypical) meningiomas, as expected, several studies reported a significant association between bone invasion and progression, multiple recurrences, and poor outcomes, even in patients who underwent gross total resection (23, 30–32). In contrast, a surgical series of non-neurofibromatosis type 2 (*NF2*) cases (WHO grade 1; N = 118, grade 2 or 3; N = 26) reported that bone invasion, dural tails (identified by conventional MRI), and reactive hyperostosis (assessed by CT) were not associated with WHO grades, progression, or recurrence (33). Additionally, in a recent large series of WHO grade 1 studies, such as Corniola et al. (N = 1352) and Haddad et al. (N = 239), bone invasion was not associated with progression or recurrence (34, 35). However, patients with post-median recurrence (>24 months after treatment) tended to have a higher incidence of histopathological bone invasion (38.5% vs. 16.9% without recurrence, p = 0.064). Furthermore, Cox regression analysis identified an independent relationship between recurrence and incomplete (subtotal) resection, even in WHO grade 1 tumors with a consistent Simpson's grade (35). Therefore, a long-term clinico-radiological study with histopathological assessment of bone invasion may be preferable to understand how bone invasion affects the recurrence of WHO grade 1 meningioma.

Bone Invasion as a Preoperative Factor to Determine the Extent of Surgical Resection

As previously mentioned, the extent of surgical resection quantified by Simpson grade is the main predictor of recurrence. Microsurgery is "tailor-made" according to the size, surrounding structure, and anatomical location of the tumor, yet complete resection is rarely achieved. Therefore, preoperative factors for determining the extent of surgical resection are also important for predicting the prognosis during the early therapeutic stage (35, 36).

A recent surgical series incorporating retrospectively and prospectively collected data included 1469 meningiomas of all three WHO grades (1, 92.3%; 2, 5.2%; 3, 2.2%) and analyzed predictive factors related to the surgical extent of resection (25). In the largest study among a similar series, bone invasion (definition not addressed) was observed in 18.7% of cases and significantly associated with lower rates of a low Simpson's grade (not defined) and gross total removal (GTR: defined as a Simpson grade I-III resection in this report) [odds ratio: 0.85 (0.73–0.99) and 0.55 (0.73–0.99), respectively]. Based on these results and the classification and regression tree recursive partitioning analysis, the authors demonstrated that the extent of resection could be very low for symptomatic cases, followed by bone invasion as the second main predictor [GTR; 79% (903/1130) of the cases without bone invasion]. Considering the surgical selection bias underlying asymptomatic cases, as the authors addressed, bone invasion would be a primary preoperative predictor of the extent of surgical resection. Furthermore, bone invasion may be an indirect predictor of meningioma recurrence (37–40).

Bone Invasion and Clinicopathological Grading

Prior investigations have identified that aggressive imaging features are associated with clinicopathologically high-grade meningiomas and, therefore, increase the risk of progression or

recurrence (41–45). To date, increasing findings remind us that bone invasion is a unique characteristic, partly resembling a high-grade phenotype, despite not being included in any WHO grading criteria of meningioma (5). As previously described, the incidence of histopathologically confirmed bone invasion in WHO grade 1 tended to be higher in the subgroup of post-median recurrence (>24 months; 38.5%) than in those with early recurrence (<24 months; 16.9%) (35). Nevertheless, another study of 304 cases (grade 1, N = 227; 2, N = 77; 3, N = 5) demonstrated a negative association between histopathological bone invasion and the WHO grade (46). These results suggest that long-term tumor recurrence-related bone invasion may be slower than grade 2 or 3 due to different mechanisms from ordinal histopathological aggressiveness, such as mitosis (**Figure 3**) (4, 20, 47). Since the meningioma characteristics vary tremendously and provide confusing results that are difficult to adopt into clinical practice, molecular biology research of bone-invasive meningioma may help identify therapeutic targets and understand the clinicopathological background, for instance, related to slower recurrence (33).

The findings detailed above highlight two emerging issues: 1) accurately providing a preoperative diagnosis of meningioma with bone invasion, especially for WHO grade 1 and 2) treating these patients without long-term morbidity. Additionally, an ongoing issue is whether meningiomas, including high-grade and/or bone invasive cases, benefit from early irradiation. Biological and diagnostic updates may be helpful in the future to clarify these issues (32, 47, 48).

BIOLOGY AND DIAGNOSIS

Radiological and Histopathological Diagnosis

There is no doubt that a suspected case of WHO grade 1 meningioma identified by MRI should be diagnosed and followed up. In addition, histopathological classification generally helps facilitate a clinico-biological diagnosis, although it is not mandatory in all cases (4). However, in meningiomas with bone invasion, the judgment of bone involvement is sometimes ambiguous as it is difficult to preoperatively diagnose whether the tumor has invaded the adjacent bone using conventional radiographic modalities, such as CT and MRI (**Figures 1A–D**). Nevertheless, progress has been made in several areas of meningioma diagnoses (48). Previously, bone invasion was only postoperatively detected by histopathology in suspected cases of bone resection.

Hyperostosis of the bone adjacent to the meningioma, observable on CT with a bone window, has been well-described, with many reports addressing the possible causes. A primary theory is that cellular/tissue invasion of bone indicates hyperostosis (19, 49). Specifically, histopathological studies have clearly shown invasion of the tumor tissue to adjacent bone in areas of characteristic hyperostosis, possibly associated with strong somatostatin receptor subtype 2A (SSR2A) reactivity (12, 18, 50, 51). Moreover, a photodynamic diagnosis combined with histological study demonstrated the reactive fluorescence signal from the dipole to the inner table at the stump of the cranial window along with dense tumor-cells (52). Then, meningioma tissue invades lamellar bone trabeculae (53) (**Figure 2**). However, some false-negative and -positive hyperostosis cases have been diagnosed using conventional radiography (19, 51, 54). Thus, more accurate diagnostic modalities are required for meningiomas with bone invasion.

The aforementioned facts strongly suggest that the pathogenesis and molecular mechanisms underlying the cellular/tissue invasion of bone are poorly understood. This is potentially due to the high molecular and genetic heterogeneity of meningioma. Further studies for the microenvironment including bony tropism, osteolytic activity, and vascular remodeling between meningioma and the adjacent bone, that is "meningioma-bone niche", may help in deeper understanding

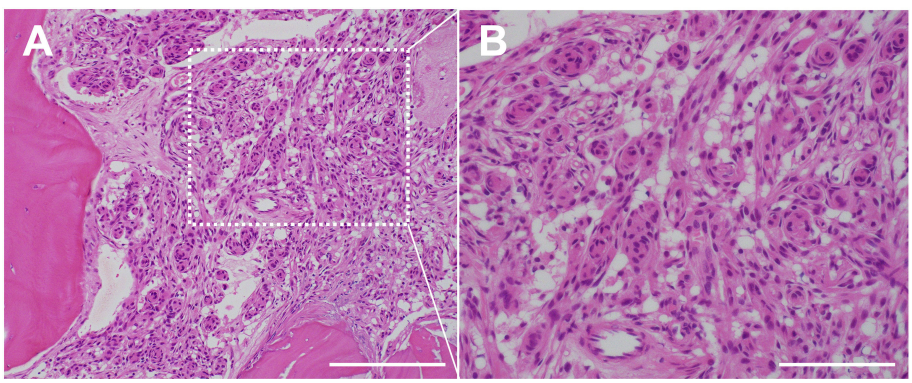

FIGURE 2 | Histopathology of the case of bone invasive meningioma shown in **Figure 1**. **(A)** H&E staining demonstrating a cellular/tissue invasion into bone trabecula. ×200 magnification. Scale bar = 200 μm. **(B)** H&E staining demonstrating a proliferation of tumor cells with round to oval nuclei. Whorl formation of the tumor cells suggests meningothelial meningioma (WHO grade 1). ×400 magnification, Scale bar = 100 μm.

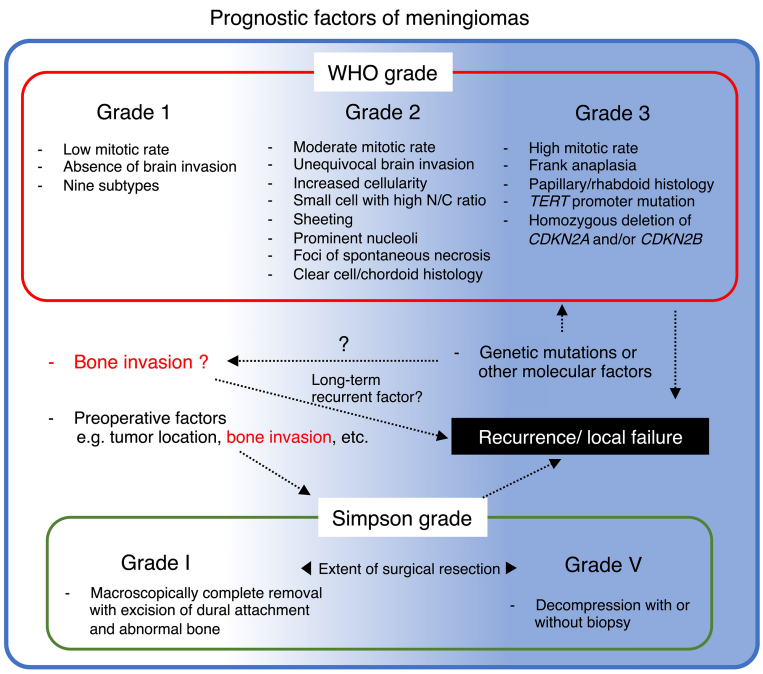

FIGURE 3 | Summary of prognostic factors of meningioma and their potential relationship with bone invasion.

and future development of molecular-based therapies (55) (related to "*protein expression*" section) (**Supplementary Figure 1**).

There is growing evidence that molecular or metabolic imaging using scintigraphy or positron emission tomography (PET) is suitable for meningioma detection. Regarding bone-invasive meningioma, Gay et al. detected SSR2 *via* pre- and postoperative scintigraphy with a radiolabeled somatostatin analog ([^{111}In-DTPA] octreotide) and intraoperative radio detection using a handheld gamma probe in 18 cases of meningioma en plaque. They reported that SSR2 radiodetection might help guide the surgical removal of bone invasive meningioma en plaque, pre- and postoperative management, and follow-up of meningioma with bone invasion that MRI failed to detect (56). Another study reported five cases of meningioma en plaque without previous bone decalcification, showing that all cases histopathologically were strongly positive for SSR2 and associated with intralesional features similar to oncogenic osteomalacia (51). These findings suggest a considerable limitation in the conventional radiographic assessment of meningioma with bone invasion, particularly when postoperative images are difficult to interpret and other biological and clinical implications may be provided, possibly linked to *SSR2A* expression. PET, recently developed using some somatostatin analogs, may also help detect bone invasion in meningioma (57, 58).

Whole-body ^{18}F fluoride PET/CT has primarily been used in the context of possible bone metastases. Interestingly, some authors have incidentally found intense intracranial focal radiotracer accumulation in intracranial meningiomas in patients with a history of cancer (59–61). It has been suggested that ^{18}F fluoride PET/CT may allow for the detection of bone invasion in meningiomas (**Figures 1E, F; Figure 2**) (62, 63). Nevertheless, the accumulation of ^{18}F fluoride theoretically indicates pathological bone diseases that affect osteoblast activity, osteoclast-osteoblast interaction, and bone perfusion. Therefore, ^{18}F fluoride PET can detect various metabolic, autoimmune, and osteogenic bone disorders (64). However, it is necessary to remember that ^{18}F fluoride PET may provide false-positive lesions rather than bone invasion of meningiomas.

Radiomics is a novel imaging technique in the medical field, providing data regarding the biological properties and heterogeneity of the tumor by extracting many high-throughput imaging features (65, 66). Recently, radiomics has presented the possibility of accurately predicting meningioma grades and histological subtypes (67). Furthermore, preoperative imaging has the potential for predicting meningioma bone invasion (68). Zhang et al. evaluated 490 meningioma cases, of which 213 were bone-invasive meningioma primarily defined by surgeons (WHO grade 1; N = 448, 2; N = 38, 3; N = 4; the subtypes were not reported). They reported that radiomics contributed to the amelioration of clinical decision-making and bone invasion meningioma predictions, indicating that future radiomics studies with histopathologically diagnosed cases may be worthwhile to determine the value of radiomics for preoperatively diagnosing bone invasion meningioma (68, 69).

Cytogenesis and Genomics

As previously mentioned, even histologically benign meningiomas may show invasive behavior in the adjacent bone, resulting in repeated recurrences. This phenomenon can

occur even after complete macroscopic resection (7, 70, 71). These are some of the main reasons for accelerating cytogenetics of meningioma, which has been best studied in humans (72) and well-summarized in the literature (73). Briefly, meningiomas typically have a normal karyotype or losses, which are mostly monosomy, but on rare occasions, there are deletions of the tumor suppressor gene *NF2* located on chromosome 22 (74). Additionally, recent studies using next-generation sequencing approach have identified several mutations, such as *TRAF7*, *KLF4*, *AKT1*, *SMO*, and *PIK3CA*, with an interesting finding that mutations of these genes occur to a large degree without concurrent alteration of *NF2*, and that the clinical outcome and recurrence rate are associated with genomic subgroups (75, 76).

Most recently, technological developments have suggested that a higher rate of malignant meningiomas may be induced by increasing hypodiploidy, complex ablations, and even epigenetics (77–80). Furthermore, certain characteristics have been correlated with histological subtypes, especially copy number alterations and mutations, suggesting a greater potential for gene therapy (58, 80). Cytogenetics of lymphoplasmacyte-rich meningioma, a rare type of WHO grade 1 arising as an en plaque meningioma, is worth investigating, to develop therapeutic strategies for bone invasive meningioma.

Even in the era of genomics, epigenomics, and transcriptomics, there are currently no valuable cytogenetic and genetic recurrent predictors for meningioma, including bone-invasive meningiomas. Therefore, approaches combining histology, multi-"omics" patterns including radiomics and genomics, and radiological data may open a window to biology-based diagnostics for meningioma, perhaps leading to stratification of the recurrent risk and aggressive behavior of such tumors.

Protein Expression

Previous studies have revealed the presence of receptors in meningioma tissues (81–87). In particular, SSR2 has been reported in meningioma tissues, thus is being considered for clinical applications based on its molecular characteristics. SSR2 is one of the most studied molecules in bone-invasive meningioma, especially for diagnostic applications. The vascular endothelial growth factor (VEGF) pathway, including VEGF and its receptors, is involved in the dynamic blood vessel structures under normal conditions and cooperates with growth, recurrence, and development of edema of meningioma through their neovascularization effect when overexpressed (88). Although nothing has been reported regarding the VEGF pathway in meningiomas with bone invasion, this angiogenic molecular system is now thought to be a therapeutic target (**Supplementary Figure 1**).

Matrix metalloproteinases (MMPs), a family of calcium-dependent zinc-containing peptidases, are assumed to promote tumor cell growth and invasion (89). To date, the functional role of MMPs in meningioma biology is complex and unclear. Previous studies focused on the role of MMP2 in meningiomas with tumor recurrence and brain invasion, and produced contradictory results (55). MMP2 expression was found to be different depending on histopathological subtypes (90). A study that used high-throughput tissue microarray on bone invasive meningiomas demonstrated that key proteins are differentially expressed, and that the anatomical location of bone invasion is a key determinant of the expression pattern of MMP2, together with osteopontin (OPN) and integrin beta-1 (ITGB1) (55, 91).

Proteomics is a widely accepted screening approach for broad protein profiles that directly analyzes proteins expressed by a cell, tissue, or tumor type. Proteomic approaches for meningioma arose in 2000s, and several methods have been used to demonstrate molecular patterns (92–101). However, few studies have reported on the proteome of benign meningiomas (102, 103). Furthermore, the proteomics of bone-invasion meningioma, first described by Wibom et al., has even fewer reports. Wibom et al. evaluated 42 WHO grade 1 meningiomas (13 fibrous, 29 meningothelial, 16 bone invasive, and 26 noninvasive) by mass spectroscopy, demonstrating that the protein expression pattern distinguishes invasiveness and histological type of meningioma. Furthermore, Mukherjee et al. compared liquid chromatography-mass spectrometry-based protein profiles between WHO grades 1 and 2, including bone invasion, and indicated possible intratumoral heterogeneity, thus requiring close follow-up (104). Nevertheless, proteomics is growing as a characterizing tool for meningiomas, and features of bone-invasion tumors have yet to be identified. In addition to gene-related "omics" studies, proteomic analysis can be useful for the molecular characterization of bone invasion meningiomas.

TREATMENT

Surgery

Longitudinal volumetric studies have determined that meningiomas grow by approximately 1 cm^3 annually. Moreover, there is a significant risk of progression for younger patients (<60 years) and those with larger tumors at the initial diagnosis (>25 mm), tumors without calcification, and tumors at specific locations (e.g., non-skull base) (69, 105). Thus, Oya et al. suggested surgical resection for asymptomatic tumors with a worsening Simpson grade after conservative management if they grow under conservative management (106). In other words, preoperative factors are essential for determining the extent of surgical resection, and bone invasion may be a preoperative factor related to incomplete resection, in addition to tumor location in the skull-base (25, 33, 35). Taken together, in cases of suspected meningioma with bone invasion, maximal resection of the adjacent bone would be preferable (107). Although, meningioma surgery is sometimes challenging due to anatomical circumstances (e.g., venous sinus involvement, arterial or cranial nerve envelopment, and extensive involvement of the base of the skull), especially in skull base cases (108–111). To achieve maximal resection of meningiomas, including the adjacent bone, a multidisciplinary surgical strategy combined with preoperative embolization may help (112). Considering that patients with bone invasion may be

comparatively older and the invasive component of the bone may not be too aggressive, the risk and benefit balance must be assessed to establish a certain case selection and future surgical strategy (113–117).

Intraoperative assistance to detect the suspected bone invasion margin can be key for "complete" resection during meningioma surgery. Growing experience has demonstrated the usefulness of fluorescence guidance using 5-aminolevulinic acid (5-ALA) in meningioma surgery, especially in cases of bone invasion, in addition to intraoperative radio detection of somatostatin analog using a handheld gamma probe (52, 118–126). However, as Scheichel et al. reported, the accumulation result has a positive predictive value of 100% and a negative predictive value of 83% of 5-ALA fluorescence in meningioma bone invasion, demonstrating that it may help to improve the extent of resection. However, further studies are necessary to investigate the rate of false-negative fluorescence and its effect on progression-free survival (PFS) (126).

Recent studies have reported proliferation and invasiveness differences between meningiomas located in the skull base and other areas. Furthermore, the genetic background may differ depending on the location, even in non-*NF2* meningiomas (127–130). Given that skull-base meningioma may be less biologically aggressive than those in other locations, extensive bony resection may be too challenging even after meningioma surgery has considerably improved, especially in skull-base cases. Thus far, it is unclear whether surgical resection plays a central role in meningioma treatment, and radiological follow-up is favorable in cases with suspected bone invasion. Therefore, patients with bone invasion may need additional treatments and future medical therapy in addition to those with WHO grades 2 and 3.

Radiosurgery

Radiosurgery is an alternative for small to medium-sized symptomatic or recurrent meningiomas. Patients with large or post-surgical remaining tumors are also eligible for fractionated radiosurgery (4, 58, 131). To date, therapeutic strategies combining surgery and (fractionated) radiosurgery have been developed. However, details regarding its use based on the WHO grade, tumor size, and the anatomical location remain controversial (111).

Radiosurgery for the bone-invading component of meningiomas has been less studied. However, accumulating evidence highlights that adjuvant radiosurgery improves local control in WHO grade 2 meningiomas irrespective of the initial resection extent compared to observation only. Furthermore, bone invasion might be associated with multiple recurrences. (32, 132). One study evaluated a cohort with mixed WHO grades who underwent irradiation, reporting that PFS did not differ between cases with and without bone invasion. These results suggest that radiation may influence meningioma tissue invading the bone (48). However, the major problem with radiosurgery for bone invading meningioma is target delineation (133). Brastianos et al. suggested that radiation is unnecessary for the dural tail unless they contain suspicious nodular enhancement because they are typically composed of benign and hypervascular tissue. Additionally, WHO grade 1 and radiographically presumed grade 1 meningiomas require a 0–5 mm clinical target volume margin. In contrast, in cases of WHO grade 2 and 3 meningiomas, hyperostosis or direct bone invasion should be included in the gross tumor volume with an additional margin of 3–5 mm (134). Future prospective studies combining radiosurgery with reproducible target planning and image, and histopathology-based therapeutic strategies are needed to set up target delineation for bone-invasive meningiomas.

Recent progress in advanced radiation therapies has resulted in possibilities for the development of future treatments for bone-invasive meningiomas, especially high-grade meningiomas (135–145).

Proton beam therapy and photon radiation therapy are shown to be safe and effective for meningioma treatment (146–149). Intensity-modulated radiation therapy (IMRT) provides some benefits, such as higher dose conformality and improved target coverage, without the contraindications of conventional radiosurgery. It has also demonstrated preferable results for the treatment of meningioma causing visual impairment by minimizing toxicity to the adjacent nervous structure (148). Boron neutron capture therapy (BNCT) is a targeted radiotherapy that enables the selective elimination of malignant cells and the sparing of surrounding normal cells. Although evidence of BNCT for meningioma treatment is not as robust, recent studies have shown relatively good local control and favorable survival along with an acceptable safety profile for recurrent and refractory high-grade meningioma (139, 144). Photodynamic therapy (PDT) adopts a photosensitizer (PS) accumulated into tumor tissue or hypervascular lesion. Irradiation of the PS with a laser at a specific wavelength causes a photochemical reaction and produces singlet oxygen, resulting in cellular injury of the target (141). This mechanism causes an inherent selectivity of the procedure. Since the laser light can only penetrate a few millimeters of tissue, therapeutic potential of PDT is limited for the tumor located in deeper areas (150). Thus, PDT is lacking sufficient clinical evidence for meningioma treatment. However, studies suggest adequate effectiveness in the treatment of high-grade meningioma, in an *in vitro* environment (141, 142). Although the effectiveness of these modalities for bone-invasive meningioma is not well understood, appropriate applications should be studied according to modality-specific advantages and disadvantages (136, 142, 151).

These findings suggest that radiosurgery for bone invasion remains controversial but may show greater potential for prognosis, and further prospective studies are warranted.

Medical Therapies

Compared with surgery and radiosurgery, studies on the clinical application of medical therapies against meningiomas are growing slowly, and some have promising results. However, the European Association of Neuro-Oncology recommended only experimental systemic therapy, with a "C" level class of evidence. Thus, no specific recommendations are provided (58, 73). The National Comprehensive Cancer Network recommends using alpha-interferon, somatostatin receptor agonists, and VEGF inhibitors to treat meningioma (152).

However, their efficacy is limited. Thus far, there is no established evidence for their use, and more studies are required to unravel the mechanistic roles in bone-invasive meningiomas and across the entire meningioma spectrum (58, 78, 80, 153–155).

In vitro cell culture is widely used for oncological investigations, including meningiomas (156). This model provides self-mitogenic agents, autocrine mechanisms, and several molecules for developing novel systemic therapies for meningioma in the future. Studies have demonstrated the effects of signaling suppression on tumor invasion and cell proliferation, highlighting the importance of exploring novel non-toxic drugs for aggressive meningiomas (157–159). However, importantly, cell lines may harbor genomic and transcriptomic alterations, confounding translational research (160). Therefore, primary tumor culture should be performed rather than using transcriptionally different cell lines to understand the molecular mechanisms underlying meningioma invasion and cell proliferation for clinical applications, although there are limitations in availability and logistical concerns (160). Primary culture and specific cell lines have not been established for invasive bone meningiomas. A bone-like culture system formed with minerals structuring pores and a bone-like mechanical environment, similar to those used for other bone tumor research (161), and related assessment methodologies may help specify the molecular characteristics and further provide information on a novel concept of a meningioma-bone niche (**Supplementary Figure 1**).

SUMMARY AND THERAPEUTIC PERSPECTIVES

The abundance of clinical results and advancing research technologies have prompted the exploration of the biological characteristics of bone-invasive meningiomas. Studies have confirmed a significant association between bone invasion and incomplete resection, possibly affecting long-term recurrence and outcomes (**Figure 3**). Moreover, radio detection and fluorescence-guided 5-ALA are confirmed intraoperative assistance tools. If metabolic imaging, such as ^{18}F fluoride PET, is available in addition to a precise combination of CT and MRI, suspected bone invasion can be diagnosed preoperatively. However, postoperative histopathology of adjacent bone remains a crucial part for definitive diagnosis. Advanced preoperative diagnostic modalities, such as radiomics and PET with SSR may play a central role in developing a surgical strategy for suspected cases of bone invasion.

Combined direct surgery and radiosurgery is also becoming more common, and advanced radiations, such as IMRT, BNCT, and PDT, might be good candidates for treating bone-invasive meningioma in the clinic. The specific genomic pattern of bone-invasive meningioma has not been detected. However, proteomics suggests that the protein profile of bone-invasive meningioma is more heterogeneous than that of non-invasive tumors, requiring closer follow-up. Although there is no medical therapy to treat meningiomas, including bone-invasive cases, some medical therapies are promising druggable targets, and their implementation in clinical practice is under consideration. An *in vitro* cell culture model would be a good option to test potential therapeutic targets in bone-invasive meningioma. However, primary culture should be used rather than a transcriptionally different cell line. Bone-like culture systems used for other bone tumor research may help specify the molecular characteristics and mechanisms in meningioma-bone niche, and effects of therapeutic agents for bone-invasive meningiomas.

Translating emerging clinical and basic research knowledge into clinical management remains incipient. Thus, similar to other biomedical research fields, "a valley of death exists between basic and clinical research" (162). The clinicopathological characteristics of bone-invasive meningioma are divergent, and it is challenging to commit to a long-term result when treating these tumors. However, collaborative efforts between basic science and clinics and among clinical experts, such as surgeons, radiosurgeons, radiologists, pathologists, clinician-scientists familiar with basic research, and statisticians, would help cross the valley (163).

AUTHOR CONTRIBUTIONS

Conception and design, drafted and/or critically revised the work, funding acquisition, Final approval of manuscript: HT; Revised the manuscript: HT and TY. All authors contributed to the article and approved the submitted version.

FUNDING

This work was supported in part by Japan Society for the Promotion of Science "KAKENHI" (20K09330) (HT).

ACKNOWLEDGMENTS

We thank Dr. Shoji Yamanaka, Department of Pathology, and Dr. Hiromichi Iwashita, Division of Anatomical and Surgical Pathology, Yokohama City University Hospital, for the histopathological diagnosis. This work is dedicated to the memory of Prof. Nobutaka Kawahara.

SUPPLEMENTARY MATERIAL

The Supplementary Material for this article can be found online at: https://www.frontiersin.org/articles/10.3389/fonc.2022.895374/full#supplementary-material

Supplementary Figure 1 | "Meningioma-bone niche", a microenvironment, in which meningioma shows bone invasion. SSR2A, strong somatostatin receptor subtype 2A; VEGFR, vascular endothelial growth factor receptor; VEGF, vascular endothelial growth factor; MMP2, matrix metalloproteinase; OPN, osteopontin; ITGB1, integrin beta-1.

REFERENCES

1. Louis DN, Ohgaki H, Wiestler OD, Cavenee WK, Burger PC, Jouvet A, et al. The 2007 WHO Classification of Tumours of the Central Nervous System. *Acta Neuropathol* (2007) 114:97–109. doi: 10.1007/s00401-007-0243-4
2. Ostrom QT, Cioffi G, Gittleman H, Patil N, Waite K, Kruchko C, et al. CBTRUS Statistical Report: Primary Brain and Other Central Nervous System Tumors Diagnosed in the United States in 2012-2016. *Neuro Oncol* (2019) 21:v1–v100. doi: 10.1093/neuonc/noz150
3. Louis DN, Perry A, Wesseling P, Brat DJ, Cree IA, Figarella-Branger D, et al. The 2021 WHO Classification of Tumors of the Central Nervous System: A Summary. *Neuro Oncol* (2021) 23:1231–51. doi: 10.1093/neuonc/noab106
4. Goldbrunner R, Minniti G, Preusser M, Jenkinson MD, Sallabanda K, Houdart E, et al. EANO Guidelines for the Diagnosis and Treatment of Meningiomas. *Lancet Oncol* (2016) 17:e383–391. doi: 10.1016/S1470-2045(16)30321-7
5. WHO. *World Health Organization Classification of Tumours of the Central Nervous System*. Lyon: International Agency for Research on Cancer (2021).
6. Chamberlain MC. The Role of Chemotherapy and Targeted Therapy in the Treatment of Intracranial Meningioma. *Curr Opin Oncol* (2012) 24:666–71. doi: 10.1097/CCO.0b013e328356364d
7. Simpson D. The Recurrence of Intracranial Meningiomas After Surgical Treatment. *J Neurol Neurosurg Psychiatry* (1957) 20:22–39. doi: 10.1136/jnnp.20.1.22
8. Zang KD. Meningioma: A Cytogenetic Model of a Complex Benign Human Tumor, Including Data on 394 Karyotyped Cases. *Cytogenet Cell Genet* (2001) 93:207–20. doi: 10.1159/000056986
9. Lang FF, Macdonald OK, Fuller GN, Demonte F. Primary Extradural Meningiomas: A Report on Nine Cases and Review of the Literature From the Era of Computerized Tomography Scanning. *J Neurosurg* (2000) 93:940–50. doi: 10.3171/jns.2000.93.6.0940
10. Shuangshoti S. *Primary Meningiomas Outside the Central Nervous System*. New York: Raven Press (1991).
11. Van Tassel P, Lee YY, Ayala A, Carrasco CH, Klima T. Case Report 680. Intraosseous Meningioma of the Sphenoid Bone. *Skeletal Radiol* (1991) 20:383–6. doi: 10.1007/BF01267669
12. Akutsu H, Sugita K, Sonobe M, Matsumura A. Parasagittal Meningioma En Plaque With Extracranial Extension Presenting Diffuse Massive Hyperostosis of the Skull. *Surg Neurol* (2004) 61:165–9; discussion 169. doi: 10.1016/S0090-3019(03)00521-4
13. Basu K, Majumdar K, Chatterjee U, Ganguli M, Chatterjee S. En Plaque Meningioma With Angioinvasion. *Indian J Pathol Microbiol* (2010) 53:319–21. doi: 10.4103/0377-4929.64306
14. Simas NM, Farias JP. Sphenoid Wing En Plaque Meningiomas: Surgical Results and Recurrence Rates. *Surg Neurol Int* (2013) 4:86. doi: 10.4103/2152-7806.114796
15. Kunimatsu A, Kunimatsu N, Kamiya K, Katsura M, Mori H, Ohtomo K. Variants of Meningiomas: A Review of Imaging Findings and Clinical Features. *Jpn J Radiol* (2016) 34:459–69. doi: 10.1007/s11604-016-0550-6
16. Nambirajan A, Sharma MC, Garg K, Sriram S, Boorgula MT, Suri V. Large Dural-Based Mass With Bony Hyperostosis in a 16-Year-Old Male: IgG4-Related Disease Mimicking Lymphoplasmacyte-Rich Meningioma. *Childs Nerv Syst* (2019) 35:1423–7. doi: 10.1007/s00381-019-04187-z
17. de Almeida GB, Januario G. Lymphoplasmacyte-Rich Meningioma: A Rare Histologic Variant of Benign Meningioma With Atypical Bone Invasion. *Radiol Case Rep* (2022) 17:922–7. doi: 10.1016/j.radcr.2021.12.059
18. Bonnal J, Thibaut A, Brotchi J, Born J. Invading Meningiomas of the Sphenoid Ridge. *J Neurosurg* (1980) 53:587–99. doi: 10.3171/jns.1980.53.5.0587
19. Pieper DR, Al-Mefty O, Hanada Y, Buechner D. Hyperostosis Associated With Meningioma of the Cranial Base: Secondary Changes or Tumor Invasion. *Neurosurgery* (1999) 44:742–6; discussion 746-747. doi: 10.1097/00006123-199904000-00028
20. Bikmaz K, Mrak R, Al-Mefty O. Management of Bone-Invasive, Hyperostotic Sphenoid Wing Meningiomas. *J Neurosurg* (2007) 107:905–12. doi: 10.3171/JNS-07/11/0905
21. Sun SQ, Kim AH, Cai C, Murphy RK, Dewees T, Sylvester P, et al. Management of Atypical Cranial Meningiomas, Part 1: Predictors of Recurrence and the Role of Adjuvant Radiation After Gross Total Resection. *Neurosurgery* (2014) 75:347–54; discussion 354-345; quiz 355. doi: 10.1227/NEU.0000000000000461
22. Watts J, Box G, Galvin A, Brotchie P, Trost N, Sutherland T. Magnetic Resonance Imaging of Meningiomas: A Pictorial Review. *Insights Imaging* (2014) 5:113–22. doi: 10.1007/s13244-013-0302-4
23. Gabeau-Lacet D, Aghi M, Betensky RA, Barker FG, Loeffler JS, Louis DN. Bone Involvement Predicts Poor Outcome in Atypical Meningioma. *J Neurosurg* (2009) 111:464–71. doi: 10.3171/2009.2.JNS08877
24. Abdelzaher E, El-Gendi SM, Yehya A, Gowil AG. Recurrence of Benign Meningiomas: Predictive Value of Proliferative Index, BCL2, P53, Hormonal Receptors and HER2 Expression. *Br J Neurosurg* (2011) 25:707–13. doi: 10.3109/02688697.2010.522743
25. Lemee JM, Corniola MV, Da Broi M, Joswig H, Scheie D, Schaller K, et al. Extent of Resection in Meningioma: Predictive Factors and Clinical Implications. *Sci Rep* (2019) 9:5944. doi: 10.1038/s41598-019-42451-z
26. Elder JB, Atkinson R, Zee CS, Chen TC. Primary Intraosseous Meningioma. *Neurosurg Focus* (2007) 23:E13. doi: 10.3171/FOC-07/10/E13
27. McGuire TP, Palme CE, Perez-Ordonez B, Gilbert RW, Sandor GK. Primary Intraosseous Meningioma of the Calvaria: Analysis of the Literature and Case Report. *Oral Surg Oral Med Oral Pathol Oral Radiol Endod* (2007) 104:e34–41. doi: 10.1016/j.tripleo.2007.03.023
28. Ilica AT, Mossa-Basha M, Zan E, Vikani A, Pillai JJ, Gujar S, et al. Cranial Intraosseous Meningioma: Spectrum of Neuroimaging Findings With Respect to Histopathological Grades in 65 Patients. *Clin Imaging* (2014) 38:599–604. doi: 10.1016/j.clinimag.2014.05.013
29. Ho A, Tang H. Editorial: Meningioma: From Basic Research to Clinical Translational Study. *Front Oncol* (2021) 11:750690. doi: 10.3389/fonc.2021.750690
30. Nowak A, Dziedzic T, Krych P, Czernicki T, Kunert P, Marchel A. Benign Versus Atypical Meningiomas: Risk Factors Predicting Recurrence. *Neurol Neurochir Pol* (2015) 49:1–10. doi: 10.1016/j.pjnns.2014.11.003
31. Shakir SI, Souhami L, Petrecca K, Mansure JJ, Singh K, Panet-Raymond V, et al. Prognostic Factors for Progression in Atypical Meningioma. *J Neurosurg* (2018) 129:1240–8. doi: 10.3171/2017.6.JNS17120
32. Zima L, Baine MJ, Sleightholm R, Wang B, Punsoni M, Aizenberg M, et al. Pathologic Characteristics Associated With Local Recurrence of Atypical Meningiomas Following Surgical Resection. *J Clin Med Res* (2021) 13:143–50. doi: 10.14740/jocmr4444
33. Hwang WL, Marciscano AE, Niemierko A, Kim DW, Stemmer-Rachamimov AO, Curry WT, et al. Imaging and Extent of Surgical Resection Predict Risk of Meningioma Recurrence Better Than WHO Histopathological Grade. *Neuro Oncol* (2016) 18:863–72. doi: 10.1093/neuonc/nov285
34. Corniola MV, Lemee JM, Meling TR. Histological Transformation in Recurrent WHO Grade I Meningiomas. *Sci Rep* (2020) 10:11220. doi: 10.1038/s41598-020-68177-x
35. Haddad AF, Young JS, Kanungo I, Sudhir S, Chen JS, Raleigh DR, et al. WHO Grade I Meningioma Recurrence: Identifying High Risk Patients Using Histopathological Features and the MIB-1 Index. *Front Oncol* (2020) 10:1522. doi: 10.3389/fonc.2020.01522
36. Kawahara N, Suenaga J, Yoshida S, Takase H, Murata H. Surgical Management of Sphenoid Ridge Meningioma. *J Neurol Surg B Skull Base* (2016) 77:A032. doi: 10.1055/s-0036-1579821
37. Gallagher MJ, Jenkinson MD, Brodbelt AR, Mills SJ, Chavredakis E. WHO Grade 1 Meningioma Recurrence: Are Location and Simpson Grade Still Relevant? *Clin Neurol Neurosurg* (2016) 141:117–21. doi: 10.1016/j.clineuro.2016.01.006
38. Gousias K, Schramm J, Simon M. The Simpson Grading Revisited: Aggressive Surgery and its Place in Modern Meningioma Management. *J Neurosurg* (2016) 125:551–60. doi: 10.3171/2015.9.JNS15754
39. Voss KM, Spille DC, Sauerland C, Suero Molina E, Brokinkel C, Paulus W, et al. The Simpson Grading in Meningioma Surgery: Does the Tumor Location Influence the Prognostic Value? *J Neurooncol* (2017) 133:641–51. doi: 10.1007/s11060-017-2481-1
40. Sicking J, Voss KM, Spille DC, Schipmann S, Holling M, Paulus W, et al. The Evolution of Cranial Meningioma Surgery-a Single-Center 25-Year Experience. *Acta Neurochir (Wien)* (2018) 160:1801–12. doi: 10.1007/s00701-018-3617-6

41. Hashiba T, Hashimoto N, Maruno M, Izumoto S, Suzuki T, Kagawa N, et al. Scoring Radiologic Characteristics to Predict Proliferative Potential in Meningiomas. *Brain Tumor Pathol* (2006) 23:49–54. doi: 10.1007/s10014-006-0199-4
42. Hsu CC, Pai CY, Kao HW, Hsueh CJ, Hsu WL, Lo CP. Do Aggressive Imaging Features Correlate With Advanced Histopathological Grade in Meningiomas? *J Clin Neurosci* (2010) 17:584–7. doi: 10.1016/j.jocn.2009.09.018
43. Kawahara Y, Nakada M, Hayashi Y, Kai Y, Hayashi Y, Uchiyama N, et al. Prediction of High-Grade Meningioma by Preoperative MRI Assessment. *J Neurooncol* (2012) 108:147–52. doi: 10.1007/s11060-012-0809-4
44. Lin BJ, Chou KN, Kao HW, Lin C, Tsai WC, Feng SW, et al. Correlation Between Magnetic Resonance Imaging Grading and Pathological Grading in Meningioma. *J Neurosurg* (2014) 121:1201–8. doi: 10.3171/2014.7.JNS132359
45. Liu Y, Chotai S, Chen M, Jin S, Qi ST, Pan J. Preoperative Radiologic Classification of Convexity Meningioma to Predict the Survival and Aggressive Meningioma Behavior. *PLoS One* (2015) 10:e0118908. doi: 10.1371/journal.pone.0118908
46. Saygın I, Çakır E. Retrospective Analysis of Meningioma and Alternative Method of Grading. *Erciyes Med J* (2020) 42:380–5. doi: 10.14744/etd.2020.69851
47. Kim D, Niemierko A, Hwang WL, Stemmer-Rachamimov AO, Curry WT, Barker FG, et al. Histopathological Prognostic Factors of Recurrence Following Definitive Therapy for Atypical and Malignant Meningiomas. *J Neurosurg* (2018) 128:1123–32. doi: 10.3171/2016.11.JNS16913
48. Zwirner K, Paulsen F, Schittenhelm J, Gepfner-Tuma I, Tabatabai G, Behling F, et al. Integrative Assessment of Brain and Bone Invasion in Meningioma Patients. *Radiat Oncol* (2019) 14:132. doi: 10.1186/s13014-019-1341-x
49. Marosi C, Hassler M, Roessler K, Reni M, Sant M, Mazza E, et al. Meningioma. *Crit Rev Oncol Hematol* (2008) 67:153–71. doi: 10.1016/j.critrevonc.2008.01.010
50. Kashimura H, Beppu T, Wada T, Yoshida Y, Suzuki M, Ogawa A. [A Case of Meningioma En Plaque: Review of 73 Cases]. *No Shinkei Geka* (1997) 25:1097–100.
51. Matschke J, Addo J, Bernreuther C, Zustin J. Osseous Changes in Meningioma En Plaque. *Anticancer Res* (2011) 31:591–6.
52. Morofuji Y, Matsuo T, Hayashi Y, Suyama K, Nagata I. Usefulness of Intraoperative Photodynamic Diagnosis Using 5-Aminolevulinic Acid for Meningiomas With Cranial Invasion: Technical Case Report. *Neurosurgery* (2008) 62:102–3; discussion 103-104. doi: 10.1227/01.neu.0000317378.22820.46
53. Abdelzaher E, El Deeb NM, Gowil AG, Yehya A. Biological and Demographic Profile of Meningiomas in a Cohort of Egyptian Patients: Impact on Tumor Recurrence. *Sci World J* (2013) 2013:375139. doi: 10.1155/2013/375139
54. Min JH, Kang SH, Lee JB, Chung YG, Lee HK. Hyperostotic Meningioma With Minimal Tumor Invasion Into the Skull. *Neurol Med Chir (Tokyo)* (2005) 45:480–3. doi: 10.2176/nmc.45.480
55. Salehi F, Jalali S, Alkins R, Lee JI, Lwu S, Burrell K, et al. Proteins Involved in Regulating Bone Invasion in Skull Base Meningiomas. *Acta Neurochir (Wien)* (2013) 155:421–7. doi: 10.1007/s00701-012-1577-9
56. Gay E, Vuillez JP, Palombi O, Brard PY, Bessou P, Passagia JG. Intraoperative and Postoperative Gamma Detection of Somatostatin Receptors in Bone-Invasive En Plaque Meningiomas. *Neurosurgery* (2005) 57:107–113; discussion 107-113. doi: 10.1227/01.NEU.0000163490.15578.FF
57. Galldiks N, Lohmann P, Albert NL, Tonn JC, Langen KJ. Current Status of PET Imaging in Neuro-Oncology. *Neurooncol Adv* (2019) 1:vdz010. doi: 10.1093/noajnl/vdz010
58. Goldbrunner R, Stavrinou P, Jenkinson MD, Sahm F, Mawrin C, Weber DC, et al. EANO Guideline on the Diagnosis and Management of Meningiomas. *Neuro Oncol* (2021) 23(11):1821–34. doi: 10.1093/neuonc/noab150
59. Derlin T, Mester J, Klutmann S. Abnormal F-18 Fluoride Uptake in Intracranial Meningiomas on PET/CT. *Clin Nucl Med* (2010) 35:806–7. doi: 10.1097/RLU.0b013e3181ef0a9e
60. Zacchi SR, Duarte PS, Coura Filho GB, Sapienza MT, Buchpiguel CA. Incidental Finding of Anterior Cranial Fossa Meningioma on 18F-Fluoride PET/CT. *Clin Nucl Med* (2013) 38:913–5. doi: 10.1097/RLU.0b013e3182a77c49
61. Teo TY, Menda Y, Mcneely P, Kahn D, Graham M. Incidental Meningioma Detected on 18F-Fluoride With PET/CT During Initial Staging for Prostate Cancer. *Clin Nucl Med* (2015) 40:596–7. doi: 10.1097/RLU.0000000000000802
62. Tateishi U, Tateishi K, Shizukuishi K, Shishikura A, Murata H, Inoue T, et al. 18f-Fluoride PET/CT Allows Detection of Hyperostosis and Osseous Involvement in Meningioma: Initial Experience. *Clin Nucl Med* (2013) 38:e125–131. doi: 10.1097/RLU.0b013e318279fd79
63. Tateishi U, Tateishi K, Hino-Shishikura A, Torii I, Inoue T, Kawahara N. Multimodal Approach to Detect Osseous Involvement in Meningioma: Additional Value of (18)F-Fluoride PET/CT for Conventional Imaging. *Radiology* (2014) 273:521–8. doi: 10.1148/radiol.14132118
64. Park PSU, Raynor WY, Sun Y, Werner TJ, Rajapakse CS, Alavi A. (18)F-Sodium Fluoride PET as a Diagnostic Modality for Metabolic, Autoimmune, and Osteogenic Bone Disorders: Cellular Mechanisms and Clinical Applications. *Int J Mol Sci* (2021) 22:6504. doi: 10.3390/ijms22126504.
65. Lambin P, Rios-Velazquez E, Leijenaar R, Carvalho S, Van Stiphout RG, Granton P, et al. Radiomics: Extracting More Information From Medical Images Using Advanced Feature Analysis. *Eur J Cancer* (2012) 48:441–6. doi: 10.1016/j.ejca.2011.11.036
66. Aerts HJ, Velazquez ER, Leijenaar RT, Parmar C, Grossmann P, Carvalho S, et al. Decoding Tumour Phenotype by Noninvasive Imaging Using a Quantitative Radiomics Approach. *Nat Commun* (2014) 5:4006. doi: 10.1038/ncomms5006
67. Park YW, Oh J, You SC, Han K, Ahn SS, Choi YS, et al. Radiomics and Machine Learning may Accurately Predict the Grade and Histological Subtype in Meningiomas Using Conventional and Diffusion Tensor Imaging. *Eur Radiol* (2019) 29:4068–76. doi: 10.1007/s00330-018-5830-3
68. Zhang J, Sun J, Han T, Zhao Z, Cao Y, Zhang G, et al. Radiomic Features of Magnetic Resonance Images as Novel Preoperative Predictive Factors of Bone Invasion in Meningiomas. *Eur J Radiol* (2020) 132:109287. doi: 10.1016/j.ejrad.2020.109287
69. Hashimoto N, Rabo CS, Okita Y, Kinoshita M, Kagawa N, Fujimoto Y, et al. Slower Growth of Skull Base Meningiomas Compared With non-Skull Base Meningiomas Based on Volumetric and Biological Studies. *J Neurosurg* (2012) 116:574–80. doi: 10.3171/2011.11.JNS11999
70. Sanson M, Cornu P. Biology of Meningiomas. *Acta Neurochir (Wien)* (2000) 142:493–505. doi: 10.1007/s007010050462
71. Yamasaki F, Yoshioka H, Hama S, Sugiyama K, Arita K, Kurisu K. Recurrence of Meningiomas. *Cancer* (2000) 89:1102–10. doi: 10.1002/1097-0142(20000901)89:5<1102::AID-CNCR20>3.0.CO;2-L
72. Ruttledge MH, Xie YG, Han FY, Peyrard M, Collins VP, Nordenskjold M, et al. Deletions on Chromosome 22 in Sporadic Meningioma. *Genes Chromosomes Cancer* (1994) 10:122–30. doi: 10.1002/gcc.2870100207
73. Ogasawara C, Philbrick BD, Adamson DC. Meningioma: A Review of Epidemiology, Pathology, Diagnosis, Treatment, and Future Directions. *Biomedicines* (2021) 9:319. doi: 10.3390/biomedicines9030319
74. Preusser M, Brastianos PK, Mawrin C. Advances in Meningioma Genetics: Novel Therapeutic Opportunities. *Nat Rev Neurol* (2018) 14:106–15. doi: 10.1038/nrneurol.2017.168
75. Bi WL, Zhang M, Wu WW, Mei Y, Dunn IF. Meningioma Genomics: Diagnostic, Prognostic, and Therapeutic Applications. *Front Surg* (2016) 3:40. doi: 10.3389/fsurg.2016.00040
76. Youngblood MW, Miyagishima DF, Jin L, Gupte T, Li C, Duran D, et al. Associations of Meningioma Molecular Subgroup and Tumor Recurrence. *Neuro Oncol* (2021) 23:783–94. doi: 10.1093/neuonc/noaa226
77. Sahm F, Schrimpf D, Stichel D, Jones DTW, Hielscher T, Schefzyk S, et al. DNA Methylation-Based Classification and Grading System for Meningioma: A Multicentre, Retrospective Analysis. *Lancet Oncol* (2017) 18:682–94. doi: 10.1016/S1470-2045(17)30155-9
78. Sanson M, Kalamarides M. Epigenetics: A New Tool for Meningioma Management? *Lancet Oncol* (2017) 18:569–70. doi: 10.1016/S1470-2045(17)30153-5
79. Hemmer S, Urbschat S, Oertel J, Ketter R. Deletions in the 17q Chromosomal Region and Their Influence on the Clonal Cytogenetic

Evolution of Recurrent Meningiomas. *Mol Cytogenet* (2019) 12:22. doi: 10.1186/s13039-019-0434-4
80. Moussalem C, Massaad E, Minassian GB, Ftouni L, Bsat S, Houshiemy MNE, et al. Meningioma Genomics: A Therapeutic Challenge for Clinicians. *J Integr Neurosci* (2021) 20:463–9. doi: 10.31083/j.jin2002049
81. Blankenstein MA, Berns PM, Blaauw G, Mulder E, Thijssen JH. Search for Estrogen Receptors in Human Meningioma Tissue Sections With a Monoclonal Antibody Against the Human Estrogen Receptor. *Cancer Res* (1986) 46:4268s–70s.
82. Reubi JC, Lang W, Maurer R, Koper JW, Lamberts SW. Distribution and Biochemical Characterization of Somatostatin Receptors in Tumors of the Human Central Nervous System. *Cancer Res* (1987) 47:5758–64.
83. Reubi JC, Horisberger U, Lang W, Koper JW, Braakman R, Lamberts SW. Coincidence of EGF Receptors and Somatostatin Receptors in Meningiomas But Inverse, Differentiation-Dependent Relationship in Glial Tumors. *Am J Pathol* (1989) 134:337–44.
84. Carroll RS, Glowacka D, Dashner K, Black PM. Progesterone Receptor Expression in Meningiomas. *Cancer Res* (1993) 53:1312–6.
85. Carroll RS, Zhang J, Dashner K, Sar M, Wilson EM, Black PM. Androgen Receptor Expression in Meningiomas. *J Neurosurg* (1995) 82:453–60. doi: 10.3171/jns.1995.82.3.0453
86. Wernicke AG, Dicker AP, Whiton M, Ivanidze J, Hyslop T, Hammond EH, et al. Assessment of Epidermal Growth Factor Receptor (EGFR) Expression in Human Meningioma. *Radiat Oncol* (2010) 5:46. doi: 10.1186/1748-717X-5-46
87. Rutkowski R, Reszec J, Hermanowicz A, Chrzanowski R, Lyson T, Mariak Z, et al. Correlation of Leptin Receptor Expression With BMI in Differential Grades of Human Meningiomas. *Oncol Lett* (2016) 11:2515–9. doi: 10.3892/ol.2016.4272
88. Preusser M, Hassler M, Birner P, Rudas M, Acker T, Plate KH, et al. Microvascularization and Expression of VEGF and its Receptors in Recurring Meningiomas: Pathobiological Data in Favor of Anti-Angiogenic Therapy Approaches. *Clin Neuropathol* (2012) 31:352–60. doi: 10.5414/NP300488
89. Duffy MJ, McCarthy K. Matrix Metalloproteinases in Cancer: Prognostic Markers and Targets for Therapy (Review). *Int J Oncol* (1998) 12:1343–8. doi: 10.3892/ijo.12.6.1343
90. Rooprai HK, Van Meter TE, Robinson SD, King A, Rucklidge GJ, Pilkington GJ. Expression of MMP-2 and -9 in Short-Term Cultures of Meningioma: Influence of Histological Subtype. *Int J Mol Med* (2003) 12:977–81. doi: 10.3892/ijmm.12.6.977
91. Ichimura S, Takahara K, Fujii K. Fibrous Meningioma With Skull Invasion. *J Neurosci Rural Pract* (2019) 10:707–10. doi: 10.1055/s-0039-3399600
92. Monleon D, Morales JM, Gonzalez-Darder J, Talamantes F, Cortes O, Gil-Benso R, et al. Benign and Atypical Meningioma Metabolic Signatures by High-Resolution Magic-Angle Spinning Molecular Profiling. *J Proteome Res* (2008) 7:2882–8. doi: 10.1021/pr800110a
93. Saydam O, Senol O, Schaaij-Visser TB, Pham TV, Piersma SR, Stemmer-Rachamimov AO, et al. Comparative Protein Profiling Reveals Minichromosome Maintenance (MCM) Proteins as Novel Potential Tumor Markers for Meningiomas. *J Proteome Res* (2010) 9:485–94. doi: 10.1021/pr900834h
94. Kim JH, Lee SK, Yoo YC, Park NH, Park DB, Yoo JS, et al. Proteome Analysis of Human Cerebrospinal Fluid as a Diagnostic Biomarker in Patients With Meningioma. *Med Sci Monit* (2012) 18:BR450–460. doi: 10.12659/MSM.883538
95. Cui GQ, Jiao AH, Xiu CM, Wang YB, Sun P, Zhang LM, et al. Proteomic Analysis of Meningiomas. *Acta Neurol Belg* (2014) 114:187–94. doi: 10.1007/s13760-013-0253-z
96. Abbritti RV, Polito F, Cucinotta M, Lo Giudice C, Caffo M, Tomasello C, et al. Meningiomas and Proteomics: Focus on New Potential Biomarkers and Molecular Pathways. *Cancer Genomics Proteomics* (2016) 13:369–79.
97. Bassiri K, Ferluga S, Sharma V, Syed N, Adams CL, Lasonder E, et al. Global Proteome and Phospho-Proteome Analysis of Merlin-Deficient Meningioma and Schwannoma Identifies PDLIM2 as a Novel Therapeutic Target. *EBioMedicine* (2017) 16:76–86. doi: 10.1016/j.ebiom.2017.01.020
98. Gupta S, Mukherjee S, Syed P, Pandala NG, Choudhary S, Singh VA, et al. Evaluation of Autoantibody Signatures in Meningioma Patients Using Human Proteome Arrays. *Oncotarget* (2017) 8:58443–56. doi: 10.18632/oncotarget.16997
99. Dunn J, Ferluga S, Sharma V, Futschik M, Hilton DA, Adams CL, et al. Proteomic Analysis Discovers the Differential Expression of Novel Proteins and Phosphoproteins in Meningioma Including NEK9, HK2 and SET and Deregulation of RNA Metabolism. *EBioMedicine* (2019) 40:77–91. doi: 10.1016/j.ebiom.2018.12.048
100. Papaioannou MD, Djuric U, Kao J, Karimi S, Zadeh G, Aldape K, et al. Proteomic Analysis of Meningiomas Reveals Clinically Distinct Molecular Patterns. *Neuro Oncol* (2019) 21:1028–38. doi: 10.1093/neuonc/noz084
101. Bender L, Somme F, Ruhland E, Cicek AE, Bund C, Namer IJ. Metabolomic Profile of Aggressive Meningiomas by Using High-Resolution Magic Angle Spinning Nuclear Magnetic Resonance. *J Proteome Res* (2020) 19:292–9. doi: 10.1021/acs.jproteome.9b00521
102. Wibom C, Moren L, Aarhus M, Knappskog PM, Lund-Johansen M, Antti H, et al. Proteomic Profiles Differ Between Bone Invasive and Noninvasive Benign Meningiomas of Fibrous and Meningothelial Subtype. *J Neurooncol* (2009) 94:321–31. doi: 10.1007/s11060-009-9865-9
103. Barkhoudarian G, Whitelegge JP, Kelly DF, Simonian M. Proteomics Analysis of Brain Meningiomas in Pursuit of Novel Biomarkers of the Aggressive Behavior. *J Proteomics Bioinform* (2016) 9:53–7. doi: 10.4172/jpb.1000389
104. Mukherjee S, Biswas D, Gadre R, Jain P, Syed N, Stylianou J, et al. Comprehending Meningioma Signaling Cascades Using Multipronged Proteomics Approaches & Targeted Validation of Potential Markers. *Front Oncol* (2020) 10:1600. doi: 10.3389/fonc.2020.01600
105. Oya S, Kim SH, Sade B, Lee JH. The Natural History of Intracranial Meningiomas. *J Neurosurg* (2011) 114:1250–6. doi: 10.3171/2010.12.JNS101623
106. Oya S, Fukushima Y, Lee J, Matsui T, Saito N. [Current Evidence for the Management of Intracranial Meningiomas]. *Jpn. J Neurosurg (Tokyo)* (2016) 25:654–9. doi: 10.7887/jcns.25.654
107. Meling TR, Da Broi M, Scheie D, Helseth E, Smoll NR. Meningioma Surgery-Are We Making Progress? *World Neurosurg* (2019) 125:e205–13. doi: 10.1016/j.wneu.2019.01.042
108. Kawahara N, Sasaki T, Nibu K, Sugasawa M, Ichimura K, Nakatsuka T, et al. Dumbbell Type Jugular Foramen Meningioma Extending Both Into the Posterior Cranial Fossa and Into the Parapharyngeal Space: Report of 2 Cases With Vascular Reconstruction. *Acta Neurochir (Wien)* (1998) 140:323–30; discussion 330-321. doi: 10.1007/s007010050105
109. Takase H, Kawasaki T, Tateishi K, Yokoyama TA, Murata H, Kawahara N. Characteristics and Surgical Strategies for Posterior Clinoid Process Meningioma: Two Case Reports and Review of the Literature. *Neurosurg Rev* (2017) 40:163–9. doi: 10.1007/s10143-016-0774-z
110. Sato M, Tateishi K, Murata H, Kin T, Suenaga J, Takase H, et al. Three-Dimensional Multimodality Fusion Imaging as an Educational and Planning Tool for Deep-Seated Meningiomas. *Br J Neurosurg* (2018) 32:509–15. doi: 10.1080/02688697.2018.1485877
111. Huntoon K, Toland AMS, Dahiya S. Meningioma: A Review of Clinicopathological and Molecular Aspects. *Front Oncol* (2020) 10:579599. doi: 10.3389/fonc.2020.579599
112. Manaka H, Sakata K, Tatezuki J, Shinohara T, Shimohigoshi W, Yamamoto T. Safety and Efficacy of Preoperative Embolization in Patients With Meningioma. *J Neurol Surg B Skull Base* (2018) 79:S328–33. doi: 10.1055/s-0038-1667043
113. Rushing EJ, Bouffard JP, Mccall S, Olsen C, Mena H, Sandberg GD, et al. Primary Extracranial Meningiomas: An Analysis of 146 Cases. *Head Neck Pathol* (2009) 3:116–30. doi: 10.1007/s12105-009-0118-1
114. Burkhardt JK, Zinn PO, Graenicher M, Santillan A, Bozinov O, Kasper EM, et al. Predicting Postoperative Hydrocephalus in 227 Patients With Skull Base Meningioma. *Neurosurg Focus* (2011) 30:E9. doi: 10.3171/2011.3.FOCUS117
115. Oya S, Kawai K, Nakatomi H, Saito N. Significance of Simpson Grading System in Modern Meningioma Surgery: Integration of the Grade With MIB-1 Labeling Index as a Key to Predict the Recurrence of WHO Grade I Meningiomas. *J Neurosurg* (2012) 117:121–8. doi: 10.3171/2012.3.JNS111945

116. Shah AH, Patel N, Raper DM, Bregy A, Ashour R, Elhammady MS, et al. The Role of Preoperative Embolization for Intracranial Meningiomas. *J Neurosurg* (2013) 119:364–72. doi: 10.3171/2013.3.JNS121328
117. Przybylowski CJ, Zhao X, Baranoski JF, Borba Moreira L, Gandhi S, Chapple KM, et al. Preoperative Embolization Versus No Embolization for WHO Grade I Intracranial Meningioma: A Retrospective Matched Cohort Study. *J Neurosurg* (2020) 134:693–700. doi: 10.3171/2020.1.JNS19788
118. Kajimoto Y, Kuroiwa T, Miyatake S, Ichioka T, Miyashita M, Tanaka H, et al. Use of 5-Aminolevulinic Acid in Fluorescence-Guided Resection of Meningioma With High Risk of Recurrence. Case Report. *J Neurosurg* (2007) 106:1070–4. doi: 10.3171/jns.2007.106.6.1070
119. Coluccia D, Fandino J, Fujioka M, Cordovi S, Muroi C, Landolt H. Intraoperative 5-Aminolevulinic-Acid-Induced Fluorescence in Meningiomas. *Acta Neurochir (Wien)* (2010) 152:1711–9. doi: 10.1007/s00701-010-0708-4
120. Della Puppa A, Scienza R. 5-Aminolevulinic Acid-Guided Resection of Bone-Invasive Meningiomas. *Neurosurg Focus* (2013) 35:E6. doi: 10.3171/2012.6.FOCUS12236
121. Della Puppa A, Rustemi O, Gioffre G, Troncon I, Lombardi G, Rolma G, et al. Predictive Value of Intraoperative 5-Aminolevulinic Acid-Induced Fluorescence for Detecting Bone Invasion in Meningioma Surgery. *J Neurosurg* (2014) 120:840–5. doi: 10.3171/2013.12.JNS131642
122. Millesi M, Kiesel B, Mischkulnig M, Martinez-Moreno M, Wohrer A, Wolfsberger S, et al. Analysis of the Surgical Benefits of 5-ALA-Induced Fluorescence in Intracranial Meningiomas: Experience in 204 Meningiomas. *J Neurosurg* (2016) 125:1408–19. doi: 10.3171/2015.12.JNS151513
123. Potapov AA, Goryaynov SA, Okhlopkov VA, Shishkina LV, Loschenov VB, Savelieva TA, et al. Laser Biospectroscopy and 5-ALA Fluorescence Navigation as a Helpful Tool in the Meningioma Resection. *Neurosurg Rev* (2016) 39:437–47. doi: 10.1007/s10143-015-0697-0
124. Rustemi O, Della Puppa A. Hyperostosis and Osteolysis in Skull Base Meningiomas: Are Different Nuances of 5-ALA Fluorescence Related to Different Invasion Patterns? *J Neurosurg Sci* (2019) 63:484–5. doi: 10.23736/S0390-5616.17.04244-8
125. Valdes PA, Millesi M, Widhalm G, Roberts DW. 5-Aminolevulinic Acid Induced Protoporphyrin IX (ALA-PpIX) Fluorescence Guidance in Meningioma Surgery. *J Neurooncol* (2019) 141:555–65. doi: 10.1007/s11060-018-03079-7
126. Scheichel F, Popadic B, Kitzwoegerer M, Ungersboeck K, Marhold F. Fluorescence-Guided Resection in Bone and Soft Tissue Infiltrating Meningiomas. *Acta Neurochir (Wien)* (2020) 162:605–11. doi: 10.1007/s00701-019-04179-7
127. Kane AJ, Sughrue ME, Rutkowski MJ, Shangari G, Fang S, Mcdermott MW, et al. Anatomic Location is a Risk Factor for Atypical and Malignant Meningiomas. *Cancer* (2011) 117:1272–8. doi: 10.1002/cncr.25591
128. Brastianos PK, Horowitz PM, Santagata S, Jones RT, Mckenna A, Getz G, et al. Genomic Sequencing of Meningiomas Identifies Oncogenic SMO and AKT1 Mutations. *Nat Genet* (2013) 45:285–9. doi: 10.1038/ng.2526
129. Clark VE, Erson-Omay EZ, Serin A, Yin J, Cotney J, Ozduman K, et al. Genomic Analysis of non-NF2 Meningiomas Reveals Mutations in TRAF7, KLF4, AKT1, and SMO. *Science* (2013) 339:1077–80. doi: 10.1126/science.1233009
130. Williams SR, Juratli TA, Castro BA, Lazaro TT, Gill CM, Nayyar N, et al. Genomic Analysis of Posterior Fossa Meningioma Demonstrates Frequent AKT1 E17K Mutations in Foramen Magnum Meningiomas. *J Neurol Surg B Skull Base* (2019) 80:562–7. doi: 10.1055/s-0038-1676821
131. Kondziolka D, Mathieu D, Lunsford LD, Martin JJ, Madhok R, Niranjan A, et al. Radiosurgery as Definitive Management of Intracranial Meningiomas. *Neurosurgery* (2008) 62:53–8; discussion 58-60. doi: 10.1227/01.NEU.0000311061.72626.0D
132. Lee G, Lamba N, Niemierko A, Kim DW, Chapman PH, Loeffler JS, et al. Adjuvant Radiation Therapy Versus Surveillance After Surgical Resection of Atypical Meningiomas. *Int J Radiat Oncol Biol Phys* (2021) 109:252–66. doi: 10.1016/j.ijrobp.2020.08.015
133. Gehler B, Paulsen F, Oksuz MO, Hauser TK, Eschmann SM, Bares R, et al. [68ga]-DOTATOC-PET/CT for Meningioma IMRT Treatment Planning. *Radiat Oncol* (2009) 4:56. doi: 10.1186/1748-717X-4-56
134. Brastianos PK, Galanis E, Butowski N, Chan JW, Dunn IF, Goldbrunner R, et al. Advances in Multidisciplinary Therapy for Meningiomas. *Neuro Oncol* (2019) 21:i18–31. doi: 10.1093/neuonc/noy136
135. Uy NW, Woo SY, Teh BS, Mai WY, Carpenter LS, Chiu JK, et al. Intensity-Modulated Radiation Therapy (IMRT) for Meningioma. *Int J Radiat Oncol Biol Phys* (2002) 53:1265–70. doi: 10.1016/S0360-3016(02)02823-7
136. Kawabata S, Hiramatsu R, Kuroiwa T, Ono K, Miyatake S. Boron Neutron Capture Therapy for Recurrent High-Grade Meningiomas. *J Neurosurg* (2013) 119:837–44. doi: 10.3171/2013.5.JNS122204
137. Cornelius JF, Slotty PJ, El Khatib M, Giannakis A, Senger B, Steiger HJ. Enhancing the Effect of 5-Aminolevulinic Acid Based Photodynamic Therapy in Human Meningioma Cells. *Photodiagnosis Photodyn Ther* (2014) 11:1–6. doi: 10.1016/j.pdpdt.2014.01.001
138. Kantz S, Sohn M, Troeller A, Reiner M, Weingandt H, Alber M, et al. Impact of MLC Properties and IMRT Technique in Meningioma and Head-and-Neck Treatments. *Radiat Oncol* (2015) 10:184. doi: 10.1186/s13014-015-0447-z
139. Takeuchi K, Kawabata S, Hiramatsu R, Matsushita Y, Tanaka H, Sakurai Y, et al. Boron Neutron Capture Therapy for High-Grade Skull-Base Meningioma. *J Neurol Surg B Skull Base* (2018) 79:S322–7. doi: 10.1055/s-0038-1666837
140. Golub D, Kwan K, Knisely JPS, Schulder M. Possible Abscopal Effect Observed in Frontal Meningioma After Localized IMRT on Posterior Meningioma Resection Cavity Without Adjuvant Immunotherapy. *Front Oncol* (2019) 9:1109. doi: 10.3389/fonc.2019.01109
141. Ichikawa M, Akimoto J, Miki Y, Maeda J, Takahashi T, Fujiwara Y, et al. Photodynamic Therapy With Talaporfin Sodium Induces Dose- and Time-Dependent Apoptotic Cell Death in Malignant Meningioma HKBMM Cells. *Photodiagnosis Photodyn Ther* (2019) 25:29–34. doi: 10.1016/j.pdpdt.2018.10.022
142. Nakahara Y, Ito H, Masuoka J, Abe T. Boron Neutron Capture Therapy and Photodynamic Therapy for High-Grade Meningiomas. *Cancers (Basel)* (2020) 12:1334. doi: 10.3390/cancers12051334
143. Takahashi T, Misawa S, Suzuki S, Saeki N, Shinoda Y, Tsuneoka Y, et al. Possible Mechanism of Heme Oxygenase-1 Expression in Rat Malignant Meningioma KMY-J Cells Subjected to Talaporfin Sodium-Mediated Photodynamic Therapy. *Photodiagnosis Photodyn Ther* (2020) 32:102009. doi: 10.1016/j.pdpdt.2020.102009
144. Takai S, Wanibuchi M, Kawabata S, Takeuchi K, Sakurai Y, Suzuki M, et al. Reactor-Based Boron Neutron Capture Therapy for 44 Cases of Recurrent and Refractory High-Grade Meningiomas With Long-Term Follow-Up. *Neuro Oncol* (2022) 24:90–8. doi: 10.1093/neuonc/noab108
145. Tom MC, Kotecha R. Beating a Benchmark: Boron Neutron Capture Therapy for Recurrent and Refractory Meningiomas. *Neuro Oncol* (2022) 24:99–100. doi: 10.1093/neuonc/noab217
146. Slater JD, Loredo LN, Chung A, Bush DA, Patyal B, Johnson WD, et al. Fractionated Proton Radiotherapy for Benign Cavernous Sinus Meningiomas. *Int J Radiat Oncol Biol Phys* (2012) 83:e633–637. doi: 10.1016/j.ijrobp.2012.01.079
147. Weber DC, Schneider R, Goitein G, Koch T, Ares C, Geismar JH, et al. Spot Scanning-Based Proton Therapy for Intracranial Meningioma: Long-Term Results From the Paul Scherrer Institute. *Int J Radiat Oncol Biol Phys* (2012) 83:865–71. doi: 10.1016/j.ijrobp.2011.08.027
148. Maclean J, Fersht N, Bremner F, Stacey C, Sivabalasingham S, Short S. Meningioma Causing Visual Impairment: Outcomes and Toxicity After Intensity Modulated Radiation Therapy. *Int J Radiat Oncol Biol Phys* (2013) 85:e179–186. doi: 10.1016/j.ijrobp.2012.10.032
149. Harding R, Trnkova P, Weston SJ, Lilley J, Thompson CM, Short SC, et al. Benchmarking of a Treatment Planning System for Spot Scanning Proton Therapy: Comparison and Analysis of Robustness to Setup Errors of Photon IMRT and Proton SFUD Treatment Plans of Base of Skull Meningioma. *Med Phys* (2014) 41:111710. doi: 10.1118/1.4897571
150. Gunaydin G, Gedik ME, Ayan S. Photodynamic Therapy-Current Limitations and Novel Approaches. *Front Chem* (2021) 9:691697. doi: 10.3389/fchem.2021.691697
151. Hefti M, Holenstein F, Albert I, Looser H, Luginbuehl V. Susceptibility to 5-Aminolevulinic Acid Based Photodynamic Therapy in WHO I Meningioma

Cells Corresponds to Ferrochelatase Activity. *Photochem Photobiol* (2011) 87:235–41. doi: 10.1111/j.1751-1097.2010.00821.x
152. Karsy M, Guan J, Cohen A, Colman H, Jensen RL. Medical Management of Meningiomas: Current Status, Failed Treatments, and Promising Horizons. *Neurosurg Clin N Am* (2016) 27:249–60. doi: 10.1016/j.nec.2015.11.002
153. Kawahara N. [Update Knowledge for Brain Tumors(7)Meningioma]. *No Shinkei Geka* (2016) 44:415–30. doi: 10.11477/mf.1436203301
154. Delgado-Lopez PD, Cubo-Delgado E, Gonzalez-Bernal JJ, Martin-Alonso J. A Practical Overview on the Molecular Biology of Meningioma. *Curr Neurol Neurosci Rep* (2020) 20:62. doi: 10.1007/s11910-020-01084-w
155. Shao Z, Liu L, Zheng Y, Tu S, Pan Y, Yan S, et al. Molecular Mechanism and Approach in Progression of Meningioma. *Front Oncol* (2020) 10:538845. doi: 10.3389/fonc.2020.538845
156. Pallini R, Casalbore P, Mercanti D, Maggiano N, Larocca LM. Phenotypic Change of Human Cultured Meningioma Cells. *J Neurooncol* (2000) 49:9–17. doi: 10.1023/A:1006436903976
157. Graillon T, Romano D, Defilles C, Saveanu A, Mohamed A, Figarella-Branger D, et al. Octreotide Therapy in Meningiomas: *In Vitro* Study, Clinical Correlation, and Literature Review. *J Neurosurg* (2017) 127:660–9. doi: 10.3171/2016.8.JNS16995
158. Das A, Martinez Santos JL, Alshareef M, Porto GBF, Infinger LK, Vandergrift WA3rd, et al. *In Vitro* Effect of Dovitinib (TKI258), a Multi-Target Angiokinase Inhibitor on Aggressive Meningioma Cells. *Cancer Invest* (2020) 38:349–55. doi: 10.1080/07357907.2020.1773844
159. Uhlmann EJ, Rabinovsky R, Varma H, El Fatimy R, Kasper EM, Moore JM, et al. Tumor-Derived Cell Culture Model for the Investigation of Meningioma Biology. *J Neuropathol Exp Neurol* (2021) 80:1117–24. doi: 10.1093/jnen/nlab111
160. Batchu S. Caution Using Meningioma Cell Lines as Tumour Models. *Cancer Invest* (2020) 38:535–6. doi: 10.1080/07357907.2020.1821210
161. Eriksson TM, Day RM, Fedele S, Salih VM. The Regulation of Bone Turnover in Ameloblastoma Using an Organotypic *In Vitro* Co-Culture Model. *J Tissue Eng* (2016) 7:2041731416669629. doi: 10.1177/2041731416669629
162. Butler D. Translational Research: Crossing the Valley of Death. *Nature* (2008) 453:840–2. doi: 10.1038/453840a
163. WIN to Avoid the Valley of Death. *Nat Rev Clin Oncol* (2017) 14:453. doi: 10.1038/nrclinonc.2017.113

Conflict of Interest: The authors declare that the research was conducted in the absence of any commercial or financial relationships that could be construed as a potential conflict of interest.

Publisher's Note: All claims expressed in this article are solely those of the authors and do not necessarily represent those of their affiliated organizations, or those of the publisher, the editors and the reviewers. Any product that may be evaluated in this article, or claim that may be made by its manufacturer, is not guaranteed or endorsed by the publisher.

Copyright © 2022 Takase and Yamamoto. This is an open-access article distributed under the terms of the Creative Commons Attribution License (CC BY). The use, distribution or reproduction in other forums is permitted, provided the original author (s) and the copyright owner(s) are credited and that the original publication in this journal is cited, in accordance with accepted academic practice. No use, distribution or reproduction is permitted which does not comply with these terms.

frontiers | Frontiers in Oncology

REVIEW
published: 04 July 2022
doi: 10.3389/fonc.2022.905976

Meningioma Related Epilepsy-Pathophysiology, Pre/postoperative Seizures Predicators and Treatment

Rasha Elbadry Ahmed[1†], Hailiang Tang[2†], Anthony Asemota[1], Lei Huang[1,3], Warren Boling[1‡] and Firas Bannout[4*‡]*

[1] Department of Neurosurgery, Loma Linda University Medical Center, Loma Linda, CA, United States, [2] Department of Neurosurgery, Huasha Hospital, Fudan University, Shanghai, China, [3] Department of Physiology and Pharmacology, Loma Linda University, Loma Linda, CA, United States, [4] Department of Neurology, Loma Linda University Medical Center, Loma Linda, CA, United States

OPEN ACCESS

Edited by:
Christine Marosi,
Medical University of Vienna, Austria

Reviewed by:
Robin Grant,
Edinburgh Royal Infirmary, United Kingdom
Herwig Strik,
Sozialstiftung Bamberg, Germany

***Correspondence:**
Warren Boling
WBoling@llu.edu
Firas Bannnout
FBannout@llu.edu

[†]These authors have contributed equally to this work and share first authorship

[‡]These authors have contributed equally to this work and share last authorship

Specialty section:
This article was submitted to Neuro-Oncology and Neurosurgical Oncology, a section of the journal Frontiers in Oncology

Received: 28 March 2022
Accepted: 06 June 2022
Published: 04 July 2022

Citation:
Elbadry Ahmed R, Tang H, Asemota A, Huang L, Boling W and Bannout F (2022) Meningioma Related Epilepsy-Pathophysiology, Pre/postoperative Seizures Predicators and Treatment. Front. Oncol. 12:905976. doi: 10.3389/fonc.2022.905976

Meningiomas are the most common primary brain tumors accounting for about 30% of all brain tumors. The vast majority of meningiomas are slow-growing and of benign histopathology rendering them curable by surgery alone. Symptomatic lesions depend on the location with signs of mass effect or neurological deficits. Seizures are the presenting symptoms in approximately 30% of cases, which negatively affect quality of life, limit independence, impair cognitive functioning, as well as increase the risk for psychiatric comorbidities including depression. Although surgical resection may offer seizure freedom in 60-90% of meningiomas, seizures persist after surgical resection in approximately 12-19% of patients. Anti-seizure medications (ASMs) are employed in management, however, are limited by adverse neurocognitive side-effects and inefficacy in some patients. The potential predictors of pre- and post-operative seizures in meningioma patients have been identified in the literature. Understanding various factors associated with seizure likelihood in meningioma patients can help guide more effective seizure control and allow for better determination of risk before and after surgery.

Keywords: meningiomas, seizure, epilepsy, risk factor, surgical resection, anti-seizure medications

INTRODUCTION

Meningioma accounts for about 30% of primary brain tumors and approximately 54% of primary benign ones (1–3). The vast majority of meningiomas are slow-growing and of benign histopathology (i.e., World Health organization (WHO) grade I tumors), rendering them curable by surgery alone (4, 5). Symptomatic lesions depend on the location with signs of mass effect or neurological deficits. Seizures are the presenting symptom in approximately 30% of cases, and in some studies, the percentage ranges from 13-60% (6–8). Although surgical resection can offer seizure freedom in 60-90% of meningiomas, seizures may persist after surgical resection in about 12-19% of patients (9, 10). Seizures can negatively affect the quality of life, hindering a patient's independence, cognitive functions, and ability to drive safely (11–13). It puts patients at increased risk for different psychiatric comorbidities, including depression (14). Seizure control using various

anti-seizure medications (ASMs) is usually offered despite adverse side effects on neurocognition and inefficacy in some patients (15).

Many theories have been postulated to explain the pathogenesis of brain tumor-related epilepsy (BTRE) in various brain tumors; however, unanswered questions remain regarding seizure control and management in meningioma patients, for example, the ability of surgical resections to cure seizures, when to start ASMs, duration of treatment as well as structured guidelines for patient selection for ASMs. Understanding and predicting seizures in meningioma can help guide seizure control and allow for better determination of at-risk patients before and after surgery. This review aims to summarize the pathogenesis of seizures in meningioma, pre- and post-operative predictors of seizures, surgical resection resulting in seizure freedom, the benefit of ASMs usage, intraoperative electrocorticography (ECoG) and electroencephalogram (EEG) monitoring in meningioma patients and proper patient selection.

INCIDENCE OF EPILEPSY IN MENINGIOMA

The incidence of pre-operative seizures in meningioma was respectively reported to be 29% of 4709 patients (7) and 14% of 598 patients (16) with supratentorial meningioma. Seizure freedom was achieved in about 69% of patients after surgery with 12% of new seizures onset postoperatively (17). Chozick's study reported 63/158 patients with meningioma had pre-operative seizures and 40 (63.5%) of the 63 patients had complete resolution of seizure after surgery within follow-up years of 7.3± 3.8. In this cohort, 100% of 63 patients were on anti-seizure medications anticonvulsant preoperatively and during the initial stage postoperatively. The authors did not report the exact portion of these 43 patients weaned from anti-seizure medication over time postoperatively. While some neurosurgeons tended to stop using the medication approximately 6 months after surgery if there was no evidence of seizures, the other neurosurgeons continued using the anticonvulsant medications prophylactically. They reported that eighty-five patients (53.8% of 158) were eventually weaned from anticonvulsant and 44.7% were not off anti-seizure medications at the last follow-up visit postoperatively. Seizures recurred in 1 patient during weaning off ASMs process, in 4 patients with subtherapeutic ASMs levels, in 6 patients who were not on ASMs, in 2 patients correlated with alcohol abuse, and 5 patients with tumor recurrence. Eight patients (5.1%) with no history of preoperative epilepsy developed postoperative seizures. Chozick et al. concluded that in their study only the extent of tumor removal was a significant predictor of postoperative seizures. However, a history of preoperative seizures, preoperative language disturbance, postoperative anti-seizure medications status, postoperative hydrocephalus, or parietal region location of tumor were also predictive factors of the occurrence of postoperative seizures (18). Wirsching reported 26.6% of postoperative seizures within median 67 months (95% CI: 63–72) of post-surgery follow-up (19). The incidence of *de-novo* seizures in seizure naïve patients ranges widely from 2.4 to 19.4% (7, 17–23).The wide variation of these studies can be contributed to lacking standardization of retrospectively collected data from patients with different demographics, different features/locations/type of meningiomas, different follow up periods, different age groups analysis between pediatric and adult patients, and different surgical skills and techniques at different institutions. The majority of postoperative seizures were experienced in the first week after surgery, but one-third of patients experienced seizures three months after surgery (17).

PATHOGENESIS OF EPILEPSY IN MENINGIOMA

The pathophysiology of brain tumor related epilepsy is multifactorial and can be divided into morphologic, biochemical and metabolic causes. The morphologic changes in the peritumoral neocortex include the connection of the neurons and the connectivity and localization of the synaptic vesicles, causing higher concentration of voltage-dependent Na+ channel, Ca++ and Glutamate receptors with loss of inhibitory synapses and an increase of the excitatory synapses. Biochemically, there is an increase of Glutamatergic and reduction in GABAergic somatostatin immunoreactive neurons. At the ion level, there is a report of low Mg2+, high extracellular K+, high Fe3+, low neuron-specific K+/Cl− cotransporter-2 (KCC2). Extracellular peritumoral pH is thought to be slightly alkaline. Finally there are enzymatic, amino acid and immunologic changes with upregulation of Glutamatergic receptors for NMDA and AMPA neurotransmitters (24). More recently, the genetic drivers of epileptogenicity in meningiomas have been investigated. NF2 mutation was shown to be predictive marker for preoperative seizures, which was *via* an indirect mediation effect with atypical histology and edema (25). Meningioma originates from arachnoid cap cells and is usually a slow-growing tumor (1). Such slow growth can partially explain the peritumoral changes that lead to epileptogenicity (24, 26). The partial differentiation of cortical brain surface may produce an epileptogenic zone, thus causing denervation hypersensitivity (27). The morphologic changes that develop in the brain tissue adjacent to the lesion, like inefficient neuronal migration, synaptic vesicles, and glial gap-junction coupling alterations, are also thought to contribute to seizure generation (28). Although pediatric meningioma is rare, epilepsy was reported as one of common symptoms (29). Inefficient neuronal migration may serve as an additional peritumoral mechanism of epileptogenesis in this age group of patients.

The percentage of brain edema in patients with meningioma ranges between 30% to 60% (30–32). It is usually vasogenic and related to an increase in pial supply, angiogenesis, and increased expression of vascular endothelial growth factor (VEGF) (33, 34). Chemical changes in the peritumoral milieu and local hypoxia from local tumor compression are thought to be underlying mechanisms that decrease the threshold for seizures (26). Increased levels of glutamate in the peritumoral edema are often described as an instigating factor for the state of hyperexcitability and epilepsy (8, 26). Edema is strongly

correlated with brain invasion (35), and may also be intimately associated with tumor location and more invasive and higher grades of meningioma (31, 32, 36). Notably Hess et al. reported a five-fold increase in edema volume in patients with brain invasion compared to those without, with a reported 20% increase of risk of brain invasion with each 1cm increase in peritumoral edema (35). Chernov, et al. reported a high incidence of peritumoral edema in macroscopically invasive meningiomas (37). Brain invasion and breakdown of the arachnoid layer distort and alter the peritumoral cortex, releasing amino acids and affecting the neurotransmitter pathway (35, 38).

For post-operative seizures onset, intraoperative strong adhesions, the need for microdissection, and possible injury to cortical surface and irritation can contribute to the generation, especially in seizure naïve patients (36). Retraction and manipulation, which are sometimes necessary to achieve total resection in skull base lesions, can also lead to further cortical damage and edema (39). Post-operative complications like infection, hematoma, and hydrocephalus can further increase cerebral edema and increase the risk of seizures (40).

Based on histopathological characteristics, the WHO grading system classifies meningiomas into grade I (benign), grade II (atypical), and grade III (anaplastic) (41). Hess et al. analyzed the brain invasion and risk of seizure retrospectively in a total of 176 patients with meningioma. There were 92 (52%) grade I, 79 (45%) grade II, and 5 (3%) grade III tumors. Grade I meningioma included 16 (17%) transitional, 4 (4%) secretory, 68 (74%) meningothelial, 3 (3%) fibrous, and 1 (1%) angiomatous subtypes. Preoperative seizures were present in 10 (11%) of 92 patients with grade I meningioma, 23 (29%) of 79 patients with grade II meningioma, and absence in patients with anaplastic meningioma. In grade I meningioma, histopathological subtype correlated significantly with the rate of preoperative epilepsy. Overall, the risk of preoperative seizures was significantly higher in patients with a grade II or III tumor than in those with a grade I tumor. Brain invasion was absent in all patients with a grade I meningioma, but it was present in 35 (44%) of those with an atypical and 3 (60%) with an anaplastic meningioma. Brain invasion was independent of tumor volume but strongly correlated with edema volume. Multivariate analyses showed the risk of preoperative seizures was increased distinctly in patients with brain-invasive meningioma over those with noninvasive meningioma (OR 5.26, 95% CI 1.52–18.15; $p = 0.009$). However, postoperative seizure-free rates were similar among patients with invasive and those with noninvasive meningioma. The incidence of postoperative epilepsy was correlated significantly with the increasing preoperative tumor volume (35). In another retrospective study, Gadot et al. reviewed the 384 patients who underwent meningioma resection. The significant association was not found between any histological subtype and worse postoperative seizure outcomes. However, there was an associative tendency between subtypes of higher grades (malignant, rhabdoid) with worse postoperative seizure outcomes. The subtypes of lower grades (fibrous, transitional) trended toward improved postoperative outcomes ($p = 0.081$) (25). There are no data in the medical literature for the incidental small meningioma, which are not part of the epileptogenic network.

PREDICTORS OF EPILEPSY IN MENINGIOMA

In an attempt to better understand and predict seizures in patients with meningioma, several retrospective studies investigated the possible predictors of seizures both pre-operatively and post-operatively. Throughout the literature, peritumoral edema and location have been associated with seizures in meningioma. Peritumoral edema has been extensively studied and considered the strongest predictor of seizure in both pre- and post-operative periods (7, 8, 17, 20, 21, 26, 35). There is a less likelihood of achieving seizure freedom postoperatively in patients with with significant pre-operative edema (21, 42).

Preoperative Predictors

The preoperative predictors of epilepsy/seizures are summarized in **Table 1**.

In a retrospective study by Li et al., peritumoral edema of > 1cm was among the risk factors identified for preoperative seizures in meningioma patients (43). Tumor location in the temporal, parietal, and frontal (adjacent to neocortex) lobes are more likely to be associated with seizures (7, 18, 20, 21). Specifically, Lieu and Howng noted that tumor located in the temporal lobe increased the risk of pre-operative seizures than other lobes. The increased peritumoral edema noticed in convexity and parasagittal meningioma is thought to favor the likelihood of increased seizure frequency in affected individuals. Non-skull base meningiomas are suggested to be more aggressive with a high MIB-index (percentage of immunoreactive tumor cells) which favors brain invasion, edema, and seizure (20, 45). In another study, no consensus was found regarding the most epileptogenic cortical area (46).

Most studies suggest that bigger tumors are naturally associated with a higher risk of seizure preoperatively. Conceivably, larger tumors can cause more irritation and compression on surrounding brain tissue. Similar results reported by Chen et al. showed that tumors larger than 3 cm in size, of higher grade with peritumoral edema more than 1 cm are associated with preoperative seizures (20). In one study, no statistically significant correlation between tumor size and preoperative seizures could be found (43), while mean tumor diameter of 3.5 cm was used at cut-off to demonstrate an association with postoperative in-hospital seizures.

Interestingly meningiomas are more common in females, but males are more likely to present with seizures. Many studies have shown the male gender as a risk factor for developing preoperative seizures (7, 8, 20, 23, 43). There is a possible association of male gender with higher grade meningioma, larger size, and more edema (20). Younger age was a predictor

TABLE 1 | Predictors of preoperative epilepsy/seizures.

Reference	Study type	Summray of findings (bold texts indicating the proposed predictors)
Englot et al., 2016 (6)	A meta-analysis of 39 observational series cases (4709 patients surgically treated menigiomas) published between January 1980 and September 2014	The significantly predictors were **male sex, peritumoral edema and non-skull base location**
Seyedi et al, 2018 (17)	Retrospective cohort study of 295 patients that underwent resection of a supratentorial meningioma between 2007-2015.	Seventy-two (24.4%) of the patients experienced seizures preoperatively. **Peritumoral edema was a significant predictor of preoperative seizure**; headaches and neurological deficits were associated with decreased incidence of preoperative seizures.
Xue et al., 2018 (20)	A retrospective study of 113 consecutive adult (> 18 years old) patients with newly diagnosed meningioma underwent operation between 2006 and 2008 were included and followed up until the end of 2015.	A total of 21/113 (18.6%) patients experienced seizures before surgery. **Tumor diameter >/= 3.5 cm as a risk factor for preoperative seizures**, but presence of headache and skull base tumor location decreased the risk of preoperative seizures
Lieu and Howng, 1999 (22)	A retrospective study of a consecutive series of 222 surgically treated patients with meningiomas,	There were 59 (26.6%) of the patients presented epilepsy as their initial symptom. **Intracranial supratentorial or convexity meningiomas with evidence of severe peritumoral edema** significantly contribute to preoperative epilepsy.
Chen et al., 2017 (23)	Retrospective chart review of 1033 subjects undergoing resection of supratentorial meningioma bewtween1991 and 2014	Preoperative seizures occurred in 234 (22.7%) patients. The predictors of preoperative seizures: **presence of ≥1 cm peritumoral edema, non-skull base tumor location, older patient age.** Presenting symptoms of headache or cranial nerve deficit was associated with decreased odds of preoperative seizures. Non-skull base supratentorial meningiomas with surrounding edema have the highest risk for preoperative seizure.
Kawaguchi et al, 1996 (32)	A retrospective analysis of clinical symptoms and computed tomographic findings in 83 consecutive patients	Twenty sever (33%) patients presenting with epilepsy as the first symptom. **Peritumoral edema** is a significant epileptogenic factor associated with both cerebral convexity and parasagittal meningiomas.
Hess et al., 2018 (35)	Retrospective review of all patients with a histopathologically diagnosed primary meningioma underwent resection between 1991 and 2015.	In grade I meningioma, histopathological subtype correlated significantly with the rate of preoperative epilepsy. Overall, the risk of preoperative seizures in **meningioma grade II or III tumor was** significantly higher than in those with a grade I tumor. Brain invasion was absent in all patients with a grade I meningioma, but it was present in 35 (44%) of those with an atypical and 3 (60%) with an anaplastic meningioma. **Brain invasion is a strong predictor for preoperative,** but not postoperative, seizures. Although associated with increased peritumoral edema, seizures in patients with invasive meningioma might be related to cortical invasion.
Li et al., 2020 (43)	A retrospective study in 778 patients undergoing supratentorial meningiomas surgery between 2011 and 2012	A total of 100 (12.9%) patients experienced preoperative seizures. **Motor cortex involvement and peritumoral edema ≥ 1 cm** were significant risk factors of preoperative seizures. Presenting symptoms of headache, and age ≥ 55 years were associated with decreased incidence of preoperative seizures.
Hamasaki et al., 2012 (44)	A retrospective study restricted to patients with WHO grade I intracranial meningioma in database between 1968 and 2011, of which 44 patients with epilepsy were enrolled in (epilepsy group). The patients with WHO grade I meningioma without epilepsy were recruited consecutively from the database between 2007 and 2011, which resulted in 56 patients in the control group.	Preoperative recurrent epileptic seizures in 12.7% (88) patients. Voxel-wise comparison between 3D MRI scans obtained from patients with meningioma-associated epilepsy and those from control patients using spatial normalization techniques on neuroimaging data The highest incidence of epilepsy was seen with **tumors located on premotor cortex in the frontal lobe. Tumor diameter/volume and patient's age were positive and negative predictors, respectively, for onset of epilepsy.**

The bold texts in Table 1 indicate the the predictors proposed in each study, respectively.

(44), and a lower incidence of preoperative seizures was found in meningioma patients older than 55 years old (43).

Other factor like preoperative Karnofsky score (KPS) were also studied. A KPS <80 was positively associated with preoperative seizures (40). Englot et al. reported a decreased incidence of preoperative seizures in patients presenting with cranial nerve deficits (7). However, there are limitations in symptom frequency studies. Prospective studies are needed to validate these potential predictors.

Postoperative Predictors

The postoperative predictors of epilepsy/seizures are summarized in **Table 2**.

The International League Against Epilepsy (ILAE) defined acute postoperative seizures as seizures happening within seven days of craniotomy (48). The late postoperative seizure is defined as on set of epilepsy beyond the first week of surgery (21, 49). In a retrospective study of 556 patients who underwent meningioma surgery, there were 74 patients with postoperative seizures, in which 43% was late seizures (49). Some studies categorized postoperative seizures into early, late, in-hospital, and post-hospital discharge. Identifying possible predictors of seizures postoperatively can help guide seizure control and minimize complications associated with ASMs long-term usage (13, 17, 20, 43, 47, 50).

Tumor location, size, grade, involvement of motor area and KPS have all been studied as predictors for postoperative seizures (21, 23). In one study, the occurrence of early in-hospital seizures was associated with involvement of motor cortex, post-operative KPS < 70, postoperative complications, and preoperative seizures

TABLE 2 | Predictors of postoperative epilepsy/seizures.

Reference	Study type	Summary of findings (bold texts indicating the proposed predictors)
Englot et al., 2016 (6)	A meta-analysis of 39 observational series cases (4709 patients surgically treated menigiomas) published between January 1980 and September 2014	Seizure freedom was achieved in 69.3% of 703 patients with preoperative epilepsy after surgery. Among patients with **preoperative seizures**, a strong association was observed between persistent postoperative seizures and **peritumoral edema. Tumor progression** after surgery was associated with seizure recurrence. Postoperative *de-novo* seizures were developed in 12.3% of 1085 patients. No difference in the rate of new postoperative seizures was observed with or without perioperative prophylactic anticonvulsants. Postoperative *de-novo* seizures were more common in those with **a history of previous radiation** or with **gross-total resection**. However, the total number of patients with new seizures in each of these categories was low (9–11 patients), limiting the ability to draw conclusions.
Seyedi, et al., 2018 (17)	Retrospective cohort study of 295 patients underwent resection of a supratentorial meningioma between 2007-2015.	Seventy-two (24.4%) of the patients experienced seizures preoperatively, and a complete seizure freedom was achieved in 63.9% of them. A total of 20.3% of the patients experienced seizures after surgery. Two hundred twenty three (75.6%) of the patients did not experience seizures preoperatively, but 15.2% of them developed postoperative *de-novo* seizures. Time to first seizure in patients who developed *de-novo* postoperative seizures was one week (47%), within one month postoperative (21%) and three months after surgery (32%). ASMs had a treatment success rate of 98.2% in preoperative seizures, and 98.0% in postoperative seizures. Postoperative seizures were **increased in left-sided meningiomas, and decreased with convexity/ parasagittal/falx meningiomas as well as with absence of postoperative complications**.
Chozick et al, 1996 (18)	A retrospective access the incidence of postoperative seizures in 158 patients with supratentorial meningiomas diagnosed by computerized tomography (CT) and/or magnetic resonance (MR) imaging	Of 63 patients with preoperative seizures, 40 (63.5%) had complete cessation of seizures after surgery. Overall 88.9% of patients with preoperative seizures achieved complete seizure control postoperatively. The mean follow-up period was 6.4 ± 3.7 years with a minimum follow-up period of 2 years. Eight patients (5.1%) developed postoperative *de-novo* seizures during mean follow-up period of 5.7± 2.8 years. The onset of seizures occurred in conjunction with weaning from anticonvulsant medication in one patient, with subtherapeutic anticonvulsant medication levels in two patients, and with tumor recurrence in three patients; two patients experienced seizures while not receiving anticonvulsant medication. Predictors of postoperative seizures included: **preoperative seizure history, preoperative language disturbance, extent of tumor removal, parietal location of tumor, postoperative anticonvulsant medication status, and postoperative hydrocephalus**. Earlier detection and treatment of supratentorial meningiomas might improve seizure outcome in patients with preoperative epilepsy.
Wirsching et al., 2016 (19)	A retrospective study of 779 patients treated for histologically confirmed intracranial meningioma 2000 and 2013	Epileptic seizures occurred in 244 (31.3%) patients before surgery, of whom 144 (59.0%) became seizure-free after surgery. The follow up period was not reported. Of the 535 patients without preoperative seizures, 104 (19.4%) developed postoperative *de-novo* epilepsy. Predictors of postoperative epilepsy were **preoperative epilepsy, major surgical complications including CNS infections, hydrocephalus, re-craniotomy, and symptomatic intracranial hemorrhage, as well as postoperative epileptiform EEG potentials, younger age, and tumor progression.** Postoperative improvement or recovery from preoperative neurologic deficits is associated with improved seizure control.
Xue et al, 2018 (20)	A retrospective study of 113 consecutive adult (> 18 years old) patients with newly diagnosed meningioma underwent operation between 2006 and 2008.	A total of 21/113 (18.6%) patients experienced preoperative seizure, of whom 8/21 (38.1%) become seizure-free after surgery. The followed up period last until the end of 2015. Thirteen (14%) patients developed postoperative *de-novo* seizures. **Larger tumor size (diameter (>/= 3.5 cm) and preoperative seizures are associated with postoperative seizures.**
Morsy et al, 2019 (21)	A prospective study of 40 patients with intracranial meningioma Group A with preoperative seizures Group B with no preoperative epilepsy.	In Group "A", 8 (40%) patients had good postoperative seizure control, 12 (60%) had poor seizure control. In Group "B" 3 (15%), patients developed postoperative *de-novo* seizures. **Postoperative complication was significantly associated with *de-novo* epilepsy** and poor seizure control.
Lieu and Howng, 1999 (22)	A retrospective study of a consecutive series of 222 surgically treated meningiomas,	A total of 52 patients had postoperative epilepsy. The follow-up periods ranged from 1 to 12 years. Among them, 22 patients (37.3%) had preoperative epilepsy which continued postoperatively. Surgical excision of the intracranial meningiomas stopped the epilepsy in about 62.7% of the patients. A total of 30 (13.5%) patients developed postoperative *de-novo* epilepsy, of which 18 are early onset of postoperative epilepsy (within 1 week) and 12 are late postoperative epilepsy (beyond 1 week). During the follow-up periods, 37 (71.2%) patients were seizure-free after 1 year of anticonvulsant therapy. Patients with **preoperative epilepsy, and tumors with evidence of severe perifocal edema or cerebral edema at the operative site** were significantly more likely to develop postoperative epilepsy.
Chen et al., 2017 (23)	Retrospective chart review of 1033 subjects undergoing resection of supratentorial meningioma between 1991 and 2014. Follow-up occurred through mid-2015.	Preoperative seizures occurred in 234 (22.7%) subjects. Fifty four (5.9%) patients experienced acute postoperative seizures prior to discharge (median duration of postop stay: 4 days, 5.72 ± 6.63), which significantly associated with **weakness as a presenting symptom, nonskull base location, and occurrence of medical/surgical complications.** During at least 1 year of postoperative follow-up, there were 51 (13.7%) of 373 patients had postoperative seizure after discharge. Of whom, 25 (2.4%) patients were *de-novo* postoperative seizures and 26 patients were with preoperative seizures. **The presence of preoperative, the occurrence of postoperative in-hospital seizures and medical/surgical complications were significant predictors of postoperative seizures after discharge.**

(Continued)

TABLE 2 | Continued

Reference	Study type	Summary of findings (bold texts indicating the proposed predictors)
Gadot, 2021 (25)	A retrospective review of 384 patients underwent meningioma resection from 2008 to 2020.	Fifty-nine patients (15.4%) had preoperative seizures, of whom 57 had sufficient postoperative data to determine Engel class outcome. The median follow-up duration for patients with Engel class I outcomes was 14 months (range 3–26 months). Forty-two patients (74%) patients achieved Engel class I seizure freedom, with most achieving complete seizure freedom (Engel class Ia) at longest follow-up. The median follow-up duration was 20 months (range 6–34 months) for Engel class II–IV outcomes Eight (14%) patients experienced poor seizure control (Engel class IV), with the majority of those experiencing worsened seizure burden compared with preoperative baseline (Engel class IVc). ASM status at last follow-up was determined and revealed that 33 (59%) of patients were still taking at least 1 ASM at lengthiest follow-up, whereas 23 (41%) patients were not taking any ASMs. **Postresection ischemia, higher WHO grade, elevated MIB-1 index, and disease recurrence independently predict postoperative seizure.**
Lu et al., 2019 (40)	A meta-analysis, searches of 4 electronic databases from inception to February 2019, resulting 430 reports with 5681 patients with meningioma.	Independent predictors of postoperative seizures identified were: **preoperative seizure history, non-skull base location, postoperative complications, meningioma recurrence**.
Li et al., 2020 (43)	A retrospective study of 778 patients underwent supratentorial meningiomas surgery between 2011 and 2012.	A total of 100 (12.9%) patients experienced preoperative seizures, 41 patients (5.3%) experienced acute postoperative in-hospital seizures, and 91 (13.5%, n = 673) patients experienced postoperative seizures after discharge. The occurrence of any **medical/surgical complication** were significant risk factors for postoperative in-hospital seizures. Postoperative seizures after discharge were associated with **tumor maximal diameter >/= 3.5 cm, preoperative, postoperative in-hospital seizures and tumor recurrence/progression**. **Tumor recurrence/progression was the only predictor of *de-novo* postoperative seizures.** The probability of seizure freedom in the 5-year follow-up was roughly 59% among patients with preoperative seizures, and 87% among patients without preoperative seizures. The use of postoperative prophylactic ASMs did not reduce the incidence of seizures.
Zheng et al., 2013 (47)	A retrospective study of 97 patients with supratentorial meningioma plus preoperative seizures	Sixty-two of 97 patients (63.9%) were seizure free for the entire postoperative follow-up period (29.5 +/- 11.8 months), while 13 patients (13.4%) still had frequent seizures at the end of follow-up. Fourteen of 97 patients (14.4%) experienced early postoperative seizures, and emergence of new postoperative neurological deficits was the only significant risk. Thirty-three patients (34.0%) experienced late postoperative seizures at some time during follow-up, including 12 of 14 patients with early postoperative seizures. **Factors associated with late postoperative seizures included tumor progression and new postoperative neurological deficits.** Decreased cerebral/vascular injury intraoperatively may lead to fewer postoperative neurological deficits and better seizure outcome.

The bold texts in Table 2 indicate the the predictors proposed in each study, respectively.

(43). It was suggested that decreased threshold and the increased cortex sensitivity during the immediate postoperative period are important factors to be considered, and ASMs use may be justifiable in this period. The KPS < 80 was an independent predictor for postoperative seizures, with an almost threefold higher risk of having preoperative seizures (40). This further explains the impact of seizures on quality of life. Skull base lesions were associated with decreased incidence of seizures preoperatively, with an opposite trend and increased incidence in the postoperative period (40). Chen et al., in one study of 1033 patients, reported decreased incidence of seizure in non-skull base lesions (20). Skull base lesions require more brain retraction, further increasing brain edema (7, 51). Scott et al. noted an association of left-sided meningioma with greater risk for developing seizures (52), with higher rates of postoperative seizures reported on the left hemisphere (66.7%) compared to the right (23.3%) (17). In a radiological study analyzing 3D structural magnetic resonance imaging (MRI) of meningioma patients to identify hotspots for seizures, results showed a high likelihood of seizures when the lesion was located on the motor cortex of the frontal lobe (44).

Preoperative seizures were strong predictors of postoperative seizures, especially uncontrolled ones (13, 17, 20, 43). There is a contradiction in the literature regarding neurological deficits as presenting symptoms. In some studies, it was associated with less incidence of preoperative seizures (17, 20), and in others, it was found to be significantly associated with postoperative seizures before discharge (10, 19). On univariate analysis, Chen et al. found that a neurological deficit in the form of new weakness, pneumonia, hematoma, and infarction with edema were significantly associated with in-hospital seizures. In their study, weakness was a predictor for in-hospital but not pre-operative or post-discharge seizures (20). Interestingly, Wirsching et al. found that postoperative improvement and recovery from preoperative neurological deficits were associated with a lower risk of postoperative seizure and improved control (19).

Postoperative complications are independent predictors of postoperative seizures (20). In the immediate postoperative period, the brain is more sensitive with a decreased threshold for seizure (43). Any irritation to the highly sensitive and probably still edematous neocortex can aggravate seizures immediately after surgery. A positive correlation has been established between postoperative complications like hematoma, hydrocephalus, infection, and edema (40). Permanent new postoperative neurological deficits, especially in patients with vascular injury, increased the risk of seizures

postoperatively significantly (47). Wirshing et al. specified major surgical complications like central nervous system infections, hydrocephalus, re-craniotomy, and symptomatic intracranial hemorrhage as risk factors for postoperative seizures (19).

For seizures after discharge, Li et al. identified tumor size > 3.5 cm, preoperative seizures, and tumor progression as strong predictors (43). In the same study, postoperative complications were associated with acute postoperative seizures, but no correlation with postoperative seizures on long-term follow-up. In another study, surgical complications were associated with in-hospital seizures and post-discharge seizures in seizure naïve patients (19, 53). Chen et al. did not find tumor recurrence or subtotal resection to be strong predictors for postoperative seizures (20). Englot et al. found a strong association of cranial nerve deficits with post-discharge seizure on univariate analysis (7).

SURGICAL RESECTION AND EPILEPSY FREEDOM

Improved surgical techniques and earlier diagnosis of meningioma have affected the extent of resection with favorable outcomes. As previously reported, surgery offers seizure freedom in 70% of patients with rates ranging between 19% to 90% (7, 21). In some studies, the overall seizure freedom over a 5-year follow-up was 87% in patients with preoperative seizures and 59% in seizure naïve patients (4, 43). Lu et al. reported a 30-40% postoperative seizures in patients with seizure history preoperatively and 10-15% in seizure naïve patients (40). Komotar et al. showed a significant influence of gross total resection on seizure rates (54). These reports support surgical intervention and cytoreduction in patients with persistent seizures. In contrast, new postoperative seizures were reported to occur more frequently in patients with gross total resection (46). A possible explanation is that greater manipulation, dissection, and retraction of the brain to achieve gross total resection, can cause cortical injury, irritation, edema, and seizures. In one study, Simpson grade I resection was correlated with postoperative seizures (39). Most of these lesions were convexity meningiomas, which strongly correlate with seizures. Therefore, Simpson grading was not clinically relevant in that study. Similar results were reported by Hess et al., with no statistical significance noted between Simpson grade and postoperative seizures (35). Multiple studies showed an association between seizure and tumor recurrence/progression (23, 47). One postulated theory is that there is possible reactivation of previous epileptogenic focus or formation of a new one with tumor recurrence (40, 43). WHO grade I lesions have low recurrence rates, and with gross total resection, this can be a protective factor against postoperative seizures (4, 5).

Most of the data in the literature report seizure freedom after craniotomy and resection, with few studies discussing other treatment modalities like radiosurgery. Kondziolka et al. reported one case of mortality without further details (54). In Zada's study of 116 patients undergoing Gamma knife for meningioma, there were zero seizure rates over 75 months of follow-up (55). Pollack et al. reported a 1.6% rate of new or worsened seizures after radiosurgery (56). Decreased seizure freedom rates have been reported after surgery in patients with intractable seizures preoperatively (40).

MANAGEMENT OF UNCONTROLLED MENINGIOMA RELATED EPILEPSY; MEDICATIONS AND EPILEPSY SURGERY

The American Academy of Neurology does not recommend the prophylactic use of ASMs in newly diagnosed brain tumors. In our institution we do not advocate for obtaining EEG pre-operatively to help in determining placing patient on ASMs. Yet some surgeons advocate for prophylactic use of ASMs in the immediate postoperative period to prevent *de-novo* seizures (57). In one study by Zheng et al., ASMs reduced the risk of early postoperative seizures (8, 58). ASMs can be used in patients with preoperative seizures as a temporizing measure until surgical resection. It is estimated that 40% of patients with well-controlled seizures before surgery could be weaned off ASMs over 27 months postoperatively, and only 22% remained with intractable seizures (8). For better patient selection and ASM use postoperatively, the STAMPE scoring system was an attempt to help guide epilepsy treatment in meningioma patients (19). They suggested a simple scoring system comprised of possible risk factors like sensorimotor deficit, tumor progression, age < 55 years, major surgical complication, preoperative seizures, post-operative EEG, and brain edema. Results were however not statistically significant and needed further validation.

Evaluation for epilepsy surgery for further resection after delineating the epileptogenic zone by intracranial EEG monitoring (grids, strips, or stereotactic electrodes) including intraoperative ECoG has been the gold standard approach in Level 4 epilepsy centers for patients with lesional epilepsies who have failed at least two adequately selected and dosed ASMs. EEG can be helpful for the assessment of seizure recurrence upon weaning or withdrawal of ASMs. Multiple studies suggested routine uses of EEG postoperatively to predict seizure recurrence. In one study of 340 patients, epileptiform discharge predicted postoperative seizures, advocating for routine EEG postoperative use (19). Intraoperative ECoG mapping and resection of secondary seizure focus in the peritumoral cortex can increase rates of seizure freedom postoperatively (23, 27). Postoperative EEG with epileptiform discharges is suggested as predictor for postoperative seizure occurrences (19, 59). However, the American academy of Neurology published a guideline practice in adult patients with epilepsy who achieved seizure freedom (though not specifically for meningioma), ordering EEG to detect interictal epileptiform discharges is not helpful to guide the decision of ASMs continuation. However, higher confidence of this approach exists in pediatric patients. An epileptiform potentials on EEG in pediatric patients increases the risk of seizure recurrence (60).

In our center we assess every patient with meningioma related epilepsy, particularly patients who continue to have uncontrolled postoperative seizures with stereotactic depth electrodes (S-EEG) implantation or by subdural grid/strip electrodes, and in cases where functional mapping is essential to rule out the involvement of eloquent cortex of the epileptogenic zone. S-EEG provides a safer option for patients who are planned to have a second surgery knowing the expected challenges from prior surgery complications like adhesions, infections, bleeding etc. Gross functional mapping can also be performed by S-EEG comparing to detailed functional mapping by grid/strip electrodes. In areas where there is room for safer resection outside eloquent cortices, S-EEG is helpful to encompass the surrounding edges of the lesion and for reaching remote areas of interest as well, like mesial temporal structures to rule out dual pathology.

The following case illustrates our own experience in post-operative seizure management after meningioma resection. A 36-year-old left-handed male who underwent left midfrontal parasagittal superior larger meningioma (6 x 7 cm) resection developed new-onset seizures 8-10 months postoperatively. His 3-month post-surgical MRI showed complete resection of the tumor. Approximately 11 months after the resection he developed his first 'tonic-clonic' seizure. It started with right-sided numbness, weakness and tingling of his back going down his mid-spine. He was subsequently started on Lamotrigine, but continued to experience repeated seizures which started with the same tingling sensations down to his spine, coupled with abnormal butterfly sensations in his abdomen, ultimately culminating in right foot shaking movements, with further spread to his right arm. Due to developing drug resistant epilepsy (DRE) including lamotrigine, lacosamide and levetiracetam, he underwent further epilepsy surgery evaluation, including scalp video EEG and intracranial EEG monitoring with stereotactic S-EEG intracranial monitoring, which resulted in greater delineation of the epileptogenic zone in the left central and paracentral frontal channels behind the posterior and mesial margins of the surgical cavity, likely with earlier onset on the mesial surface of left side of the interhemispheric fissure given early involvement of the right foot (**Figure 1**). Approximately 25 months after his initial surgery, he underwent a second scheduled left sided frontal craniotomy for resection of epileptogenic foci. He was continued on antiseizure medications postoperatively with subsequent self-reported improvement in seizure frequency. Since undergoing his second surgery, there has been notable reduction in seizure frequency from twice per week to twice per year from focal aware type triggered by medication reductions or alcohol consumption.

The case report is used as example to show the complexity of management for meningioma patient underwent craniotomy surgery. A separate IRB-approved project will be performed to analyze retrospectively the success rate of such procedures in our Center.

When it comes to the medical treatment of primary brain tumors (PBTs) in general, there is no robust, randomized studies to support the choice of ASMs. Several factors should be taken into considerations including gender, age, cost, profession, cognition, common medication related side effects, neurological baseline related to tumor/surgery (in order to avoid additive drug adverse events), medications pharmacokinetics, drug-to-drug interactions, efficacy and comorbidities. Other considerations are interaction with chemotherapy treatment and radiation effect on the brain. Some type of tumors (like low grade tumors) are known to be resistant to treatment with ASMs due to several hypothesis like intrinsic severity of the underlying mechanism of epileptogenicity, altered expression of molecules which ASMs work on, or changing of the expression of transporters at the blood-brain barrier limiting drug penetration to the epileptogenic tissue (61). Newer ASMs (oxcarbazepine, topiramate, lamotrigine, levetiracetam, zonisamide, and lacosamide) have provided better tolerability and efficacy due to different aspects including non-

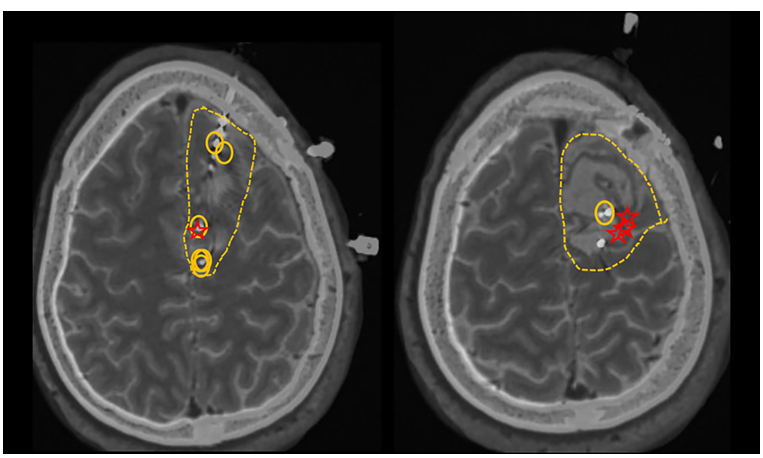

FIGURE 1 | Circles represent active interictal epileptiform discharges (the irritative zones). Stars represent the first involved contacts at the ictal onset. Dashed lines represent the proposed resection zone.

enzyme inducing property, limited drug to drug interaction, pure renal excretion, and lesser side effects. Older generation ASMs like carbamazepine, phenytoin and phenobarbital are falling out of favor due to high protein-bound, medications interaction and hepatic P-450 induction. Adverse events to ASMs are reported to be higher in PBTs than in the general epilepsy population (24% vs 0.5-12%) (57). In PBTs ASMs adverse events directed to the brain function such as executive function, attention span, cognitive function are six fold higher than the adverse events related to the radiation of the brain (62). Overall, the best risk–benefit ratio of which ASM to use is based on the physician's judgment. It is very important to mention that treatment should be started after a single seizure. Based on the American Academy of Neurology (AAN) guideline, there is no need for prophylactic treatment with ASMs in patients with brain tumor, without history of seizures. It is also suggesting that tapering and discontinuing ASMs after the first postoperative week is appropriate if there is no history of seizures (57). In summary, the strategy of drug selection for the management of BTRE should favor drugs with parenteral administration, the ASMs which don't need slow titration, and should avoid enzyme inducing ASMs. If monotherapy fails, consider combination therapy, poor compliance, repeated surgery and tumor recurrence/progression.

There is a wide range of reported efficacy of each individual ASM: oxcarbazepine as a monotherapy: 62.9%; topiramate as a monotherapy: 55.6%; Gabapentin, pregabalin, tiagabine, zonisamide as an adjunctive therapy: 27.4-100%, levetiracetam both in monotherapy and as add-on: 47.4% to 88%; lacosamide as an add-on drug with 42.9% (63). Levetiracetam and valproic acid are the most widely studied medications in tumor related epilepsy. Levetiracetam was studied against Valproic acid and the failure to treat seizures in glioblastoma was 33% vs 50% perhaps due to its tolerability and property of enhancing p53-mediated inhibition of methylguanine-DNA methyltransferase in this patient population (64). The most attractive factors for levetiracetam popularity are its well tolerability, its ease to use without a need for titration, no interaction with other ASMs, not hepatically metabolized by CYP450, and thus the absence of interaction with some chemotherapy drugs used in certain cases of BTRE, and finally good insurance coverage.

In a recent published survey of ASMs prescription preference among the European neuro-oncologists, levetiracetam is considered the first choice for brain tumor patients with the presumed highest efficacy and least adverse effects (65). ASMs are different in the pharmacokinetics, treatment efficacy, and side effects, which were reviewed by Maschio in detail (63).

Management of seizures should extend beyond pharmacological options. Untreated seizures can put patients at a risk of catastrophic outcome such as sudden unexpected death in epilepsy patients. Furthermore, seizures can negatively affect patient lifestyle including work, employment, education and driving. The risk of physical injury or death is not restricted to the driver and passengers, but applies to pedestrians and people in other vehicles. Different American States have different laws to determine which group of patients with epilepsy can drive. Seizures can result in other physical injuries. Patients with intractable epilepsy should be treated in tertiary centers where they can receive medical, social, and behavioral support and more importantly evaluation for epilepsy surgery.

FUTURE INSIGHTS

Despite advancements in understanding the pathophysiologic mechanisms and management of meningioma related epilepsy, important knowledge gaps remain. Pertinent questions include, "who are patients most at risk for seizures?" and "when to start ASMs and for how long?". The risk of persistent postoperative seizures underscores the need for further research on seizure control in meningioma patients. Long-term and arbitrary use of ASMs in meningioma patients emphasize the importance of guidelines for appropriate patient selection. Thus, prospective randomized trials are needed to guide ASMs selection and prescription. STOP 'EM is an ongoing randomized controlled trial, with an end date of Sept 2027 (66). It aims at determining the need for ASMs postoperatively in seizure naïve patients. The study's main goals are determining the efficacy of levetiracetam in seizure prevention over 12 months after surgery, the effect of starting levetiracetam on the ability to resume driving, quality of life, and cost-effectiveness.

CONCLUSION

Understanding and predicting seizures in meningioma can help guide seizures control and allow for better determination of patients at risk before and after surgery. The current medical literature provides limited data for postoperative seizure prediction and optimal management in patients with meningioma related epilepsy. In reference to the cohort of meningioma patients undergoing surgery stratified based on preoperative seizure status to postoperative seizure status, it is logical to identify four different groups: no seizures to no seizures, seizures to no seizures, no seizures to seizures, and seizures to seizures. The future effort on stratifying patients into these four groups including medications alone, surgery/ies alone, medications + surgery/ies will be able to predict surgical outcome and optimally treat patients with the most successful modalities.

AUTHOR CONTRIBUTIONS

RE, HT, LH, WB and FB contributed to conception and design of the review. RE wrote the first draft of the manuscript. AA wrote sections of the manuscript. HT, LH, AA, WB and FB contributed to manuscript revision. All authors approved the submitted version.

ACKNOWLEDGMENTS

This study was supported by the grant (No. 19140900105) from the Shanghai Committee of Science and Technology and Research Fund from Neurosurgery Department, Loma Linda University.

REFERENCES

1. Wiemels J, Wrensch M, Claus EB. Epidemiology and Etiology of Meningioma. *J Neurooncol* (2010) 99(3):307–14. doi: 10.1007/s11060-010-0386-3
2. Porter KR, McCarthy BJ, Freels S, Kim Y, Davis FG. Prevalence Estimates for Primary Brain Tumors in the United States by Age, Gender, Behavior, and Histology. *Neuro Oncol* (2010) 12(6):520–7. doi: 10.1093/neuonc/nop066
3. Ostrom QT, Gittleman H, Fulop J, Liu M, Blanda R, Kromer C, et al. CBTRUS Statistical Report: Primary Brain and Central Nervous System Tumors Diagnosed in the United States in 2008-2012. *Neuro Oncol* (2015) 17 Suppl 4:iv1–iv62. doi: 10.1093/neuonc/nov189
4. Sughrue ME, Kane AJ, Shangari G, Rutkowski MJ, McDermott MW, Berger MS, et al. The Relevance of Simpson Grade I and II Resection in Modern Neurosurgical Treatment of World Health Organization Grade I Meningiomas. *J Neurosurg* (2010) 113(5):1029–35. doi: 10.3171/2010.3.JNS091971
5. Hasseleid BF, Meling TR, Ronning P, Scheie D, Helseth E. Surgery for Convexity Meningioma: Simpson Grade I Resection as the Goal: Clinical Article. *J Neurosurg* (2012) 117(6):999–1006. doi: 10.3171/2012.9.JNS12294
6. Erturk Cetin O, Isler C, Uzan M, Ozkara C. Epilepsy-Related Brain Tumors. *Seizure* (2017) 44:93–7. doi: 10.1016/j.seizure.2016.12.012
7. Englot DJ, Magill ST, Han SJ, Chang EF, Berger MS, McDermott MW. Seizures in Supratentorial Meningioma: A Systematic Review and Meta-Analysis. *J Neurosurg* (2016) 124(6):1552–61. doi: 10.3171/2015.4.JNS142742
8. Chaichana KL, Pendleton C, Zaidi H, Olivi A, Weingart JD, Gallia GL, et al. Seizure Control for Patients Undergoing Meningioma Surgery. *World Neurosurg* (2013) 79(3-4):515–24. doi: 10.1016/j.wneu.2012.02.051
9. Van Breemen MS, Wilms EB, Vecht CJ. Seizure Control in Brain Tumors. *Handb Clin Neurol* (2012) 104:381–9. doi: 10.1016/B978-0-444-52138-5.00026-8
10. Bauer R, Ortler M, Seiz-Rosenhagen M, Maier R, Anton JV, Unterberger I. Treatment of Epileptic Seizures in Brain Tumors: A Critical Review. *Neurosurg Rev* (2014) 37(3):381–8:discussion 8. doi: 10.1007/s10143-014-0538-6
11. Taphoorn MJ, Klein M. Cognitive Deficits in Adult Patients With Brain Tumours. *Lancet Neurol* (2004) 3(3):159–68. doi: 10.1016/S1474-4422(04)00680-5
12. Gilliam F, Kuzniecky R, Faught E, Black L, Carpenter G, Schrodt R. Patient-Validated Content of Epilepsy-Specific Quality-of-Life Measurement. *Epilepsia* (1997) 38(2):233–6. doi: 10.1111/j.1528-1157.1997.tb01102.x
13. Chaichana KL, Parker SL, Olivi A, Quinones-Hinojosa A. Long-Term Seizure Outcomes in Adult Patients Undergoing Primary Resection of Malignant Brain Astrocytomas. Clinical Article. *J Neurosurg* (2009) 111(2):282–92. doi: 10.3171/2009.2.JNS081132
14. Harden CL. The Co-Morbidity of Depression and Epilepsy: Epidemiology, Etiology, and Treatment. *Neurology* (2002) 59(6 Suppl 4):S48–55. doi: 10.1212/WNL.59.6_suppl_4.S48
15. Cramer JA, Mintzer S, Wheless J, Mattson RH. Adverse Effects of Antiepileptic Drugs: A Brief Overview of Important Issues. *Expert Rev Neurother* (2010) 10(6):885–91. doi: 10.1586/ern.10.71
16. Hamasaki T, Yamada K, Kuratsu J. Seizures as a Presenting Symptom in Neurosurgical Patients: A Retrospective Single-Institution Analysis. *Clin Neurol Neurosurg* (2013) 115(11):2336–40. doi: 10.1016/j.clineuro.2013.08.016
17. Seyedi JF, Pedersen CB, Poulsen FR. Risk of Seizures Before and After Neurosurgical Treatment of Intracranial Meningiomas. *Clin Neurol Neurosurg* (2018) 165:60–6. doi: 10.1016/j.clineuro.2018.01.002
18. Chozick BS, Reinert SE, Greenblatt SH. Incidence of Seizures After Surgery for Supratentorial Meningiomas: A Modern Analysis. *J Neurosurg* (1996) 84(3):382–6. doi: 10.3171/jns.1996.84.3.0382
19. Wirsching HG, Morel C, Gmur C, Neidert MC, Baumann CR, Valavanis A, et al. Predicting Outcome of Epilepsy After Meningioma Resection. *Neuro Oncol* (2016) 18(7):1002–10. doi: 10.1093/neuonc/nov303
20. Chen WC, Magill ST, Englot DJ, Baal JD, Wagle S, Rick JW, et al. Factors Associated With Pre- and Postoperative Seizures in 1033 Patients Undergoing Supratentorial Meningioma Resection. *Neurosurgery* (2017) 81(2):297–306. doi: 10.1093/neuros/nyx001
21. Lieu AS, Howng SL. Intracranial Meningiomas and Epilepsy: Incidence, Prognosis and Influencing Factors. *Epilepsy Res* (2000) 38(1):45–52. doi: 10.1016/S0920-1211(99)00066-2
22. Morsy MM, El-Saadany WF, Moussa WM, Sultan AE. Predictive Factors for Seizures Accompanying Intracranial Meningiomas. *Asian J Neurosurg* (2019) 14(2):403–9. doi: 10.4103/ajns.AJNS_152_18
23. Xue H, Sveinsson O, Bartek JJr., Forander P, Skyrman S, Kihlstrom L, et al. Long-Term Control and Predictors of Seizures in Intracranial Meningioma Surgery: A Population-Based Study. *Acta Neurochir (Wien)* (2018) 160(3):589–96. doi: 10.1007/s00701-017-3434-3
24. Schaller B. Brain Tumor and Seizures: Pathophysiology and its Implications for Treatment Revisited (Epilepsia 2003; 44:1223-1232). *Epilepsia* (2006) 47(3):661; discussion. doi: 10.1111/j.1528-1167.2006.00484_1.x
25. Gadot R, Khan AB, Patel R, Goethe E, Shetty A, Hadley CC, et al. Predictors of Postoperative Seizure Outcome in Supratentorial Meningioma. *J Neurosurg* (2021), 1–10. doi: 10.3171/2021.9.JNS211738
26. Shamji MF, Fric-Shamji EC, Benoit BG. Brain Tumors and Epilepsy: Pathophysiology of Peritumoral Changes. *Neurosurg Rev* (2009) 32(3):275–84; discussion 84-6. doi: 10.1007/s10143-009-0191-7
27. Fang S, Zhan Y, Xie YF, Shi Q, Dan W. Predictive Value of Electrocorticography for Postoperative Epilepsy in Patients With Supratentorial Meningioma. *J Clin Neurosci* (2013) 20(1):112–6. doi: 10.1016/j.jocn.2012.02.021
28. van Diessen E, Diederen SJ, Braun KP, Jansen FE, Stam CJ. Functional and Structural Brain Networks in Epilepsy: What Have We Learned? *Epilepsia* (2013) 54(11):1855–65. doi: 10.1111/epi.12350
29. Mehta N, Bhagwati S, Parulekar G. Meningiomas in Children: A Study of 18 Cases. *J Pediatr Neurosci* (2009) 4(2):61–5. doi: 10.4103/1817-1745.57322
30. Simis A, Pires de Aguiar PH, Leite CC, Santana PAJr., Rosemberg S, Teixeira MJ. Peritumoral Brain Edema in Benign Meningiomas: Correlation With Clinical, Radiologic, and Surgical Factors and Possible Role on Recurrence. *Surg Neurol* (2008) 70(5):471–7; discussion 7. doi: 10.1016/j.surneu.2008.03.006
31. Lobato RD, Alday R, Gomez PA, Rivas JJ, Dominguez J, Cabrera A, et al. Brain Oedema in Patients With Intracranial Meningioma. Correlation Between Clinical, Radiological, and Histological Factors and the Presence and Intensity of Oedema. *Acta Neurochir (Wien)* (1996) 138(5):485–93; discussion 93-4. doi: 10.1007/BF01411166
32. Kawaguchi T, Kameyama S, Tanaka R. Peritumoral Edema and Seizure in Patients With Cerebral Convexity and Parasagittal Meningiomas. *Neurol Med Chir (Tokyo)* (1996) 36(8):568–73; discussion 73-4. doi: 10.2176/nmc.36.568
33. Yoshioka H, Hama S, Taniguchi E, Sugiyama K, Arita K, Kurisu K. Peritumoral Brain Edema Associated With Meningioma: Influence of Vascular Endothelial Growth Factor Expression and Vascular Blood Supply. *Cancer* (1999) 85(4):936–44. doi: 10.1002/(sici)1097-0142(19990215)85:4<936::aid-cncr23>3.0.co;2-j
34. Pistolesi S, Fontanini G, Camacci T, De Ieso K, Boldrini L, Lupi G, et al. Meningioma-Associated Brain Oedema: The Role of Angiogenic Factors and Pial Blood Supply. *J Neurooncol* (2002) 60(2):159–64. doi: 10.1023/a:1020624119944
35. Hess K, Spille DC, Adeli A, Sporns PB, Brokinkel C, Grauer O, et al. Brain Invasion and the Risk of Seizures in Patients With Meningioma. *J Neurosurg* (2018) 130(3):789–96. doi: 10.3171/2017.11.JNS172265
36. de Vries J, Wakhloo AK. Cerebral Oedema Associated With WHO-I, WHO-II, and WHO-III-Meningiomas: Correlation of Clinical, Computed Tomographic, Operative and Histological Findings. *Acta Neurochir (Wien)* (1993) 125(1-4):34–40. doi: 10.1007/BF01401825
37. Chernov MF, Kasuya H, Nakaya K, Kato K, Ono Y, Yoshida S, et al. (1)H-MRS of Intracranial Meningiomas: What it can Add to Known Clinical and MRI Predictors of the Histopathological and Biological Characteristics of the Tumor? *Clin Neurol Neurosurg* (2011) 113(3):202–12. doi: 10.1016/j.clineuro.2010.11.008
38. Spille DC, Hess K, Sauerland C, Sanai N, Stummer W, Paulus W, et al. Brain Invasion in Meningiomas: Incidence and Correlations With Clinical Variables and Prognosis. *World Neurosurg* (2016) 93:346–54. doi: 10.1016/j.wneu.2016.06.055
39. Islim AI, McKeever S, Kusu-Orkar TE, Jenkinson MD. The Role of Prophylactic Antiepileptic Drugs for Seizure Prophylaxis in Meningioma Surgery: A Systematic Review. *J Clin Neurosci* (2017) 43:47–53. doi: 10.1016/j.jocn.2017.05.020

40. Lu VM, Wahood W, Akinduro OO, Parney IF, Quinones-Hinojosa A, Chaichana KL. Four Independent Predictors of Postoperative Seizures After Meningioma Surgery: A Meta-Analysis. *World Neurosurg* (2019) 130:537–45 e3. doi: 10.1016/j.wneu.2019.06.063
41. Wilson TA, Huang L, Ramanathan D, Lopez-Gonzalez M, Pillai P, De Los Reyes K, et al. Review of Atypical and Anaplastic Meningiomas: Classification, Molecular Biology, and Management. *Front Oncol* (2020) 10:565582. doi: 10.3389/fonc.2020.565582
42. Tsuji M, Shinomiya S, Inoue R, Sato K. Prospective Study of Postoperative Seizure in Intracranial Meningioma. *Jpn J Psychiatry Neurol* (1993) 47(2):331–4. doi: 10.1111/j.1440-1819.1993.tb02094.x
43. Li X, Wang C, Lin Z, Zhao M, Ren X, Zhang X, et al. Risk Factors and Control of Seizures in 778 Chinese Patients Undergoing Initial Resection of Supratentorial Meningiomas. *Neurosurg Rev* (2020) 43(2):597–608. doi: 10.1007/s10143-019-01085-5
44. Hamasaki T, Yamada K, Yano S, Nakamura H, Makino K, Hide T, et al. Higher Incidence of Epilepsy in Meningiomas Located on the Premotor Cortex: A Voxel-Wise Statistical Analysis. *Acta Neurochir (Wien)* (2012) 154(12):2241–9. doi: 10.1007/s00701-012-1511-1
45. McGovern SL, Aldape KD, Munsell MF, Mahajan A, DeMonte F, Woo SY. A Comparison of World Health Organization Tumor Grades at Recurrence in Patients With non-Skull Base and Skull Base Meningiomas. *J Neurosurg* (2010) 112(5):925–33. doi: 10.3171/2009.9.JNS09617
46. Baumgarten P, Sarlak M, Baumgarten G, Marquardt G, Seifert V, Strzelczyk A, et al. Focused Review on Seizures Caused by Meningiomas. *Epilepsy Behav* (2018) 88:146–51. doi: 10.1016/j.yebeh.2018.09.002
47. Zheng Z, Chen P, Fu W, Zhu J, Zhang H, Shi J, et al. Early and Late Postoperative Seizure Outcome in 97 Patients With Supratentorial Meningioma and Preoperative Seizures: A Retrospective Study. *J Neurooncol* (2013) 114(1):101–9. doi: 10.1007/s11060-013-1156-9
48. Beghi E, Carpio A, Forsgren L, Hesdorffer DC, Malmgren K, Sander JW, et al. Recommendation for a Definition of Acute Symptomatic Seizure. *Epilepsia* (2010) 51(4):671–5. doi: 10.1111/j.1528-1167.2009.02285.x
49. Baumgarten P, Sarlak M, Monden D, Spyrantis A, Bernatz S, Gessler F, et al. Early and Late Postoperative Seizures in Meningioma Patients and Prediction by a Recent Scoring System. *Cancers (Basel)* (2021) 13(3):450. doi: 10.3390/cancers13030450
50. Joiner EF, Youngerman BE, Hudson TS, Yang J, Welch MR, McKhann GM, et al. Effectiveness of Perioperative Antiepileptic Drug Prophylaxis for Early and Late Seizures Following Oncologic Neurosurgery: A Meta-Analysis. *J Neurosurg* (2018) 130(4):1–9. doi: 10.3171/2017.10.JNS172236
51. Raza SM, Gallia GL, Brem H, Weingart JD, Long DM, Olivi A. Perioperative and Long-Term Outcomes From the Management of Parasagittal Meningiomas Invading the Superior Sagittal Sinus. *Neurosurgery* (2010) 67 (4):885–93; discussion 93. doi: 10.1227/NEU.0b013e3181ef2a18
52. Scott DF. Left and Right Cerebral Hemisphere Differences in the Occurrence of Epilepsy. *Br J Med Psychol* (1985) 58(Pt 2):189–92. doi: 10.1111/j.2044-8341.1985.tb02633.x
53. Islim AI, Ali A, Bagchi A, Ahmad MU, Mills SJ, Chavredakis E, et al. Postoperative Seizures in Meningioma Patients: Improving Patient Selection for Antiepileptic Drug Therapy. *J Neurooncol* (2018) 140(1):123–34. doi: 10.1007/s11060-018-2941-2
54. Komotar RJ, Raper DM, Starke RM, Iorgulescu JB, Gutin PH. Prophylactic Antiepileptic Drug Therapy in Patients Undergoing Supratentorial Meningioma Resection: A Systematic Analysis of Efficacy. *J Neurosurg* (2011) 115(3):483–90. doi: 10.3171/2011.4.JNS101585
55. Zada G, Pagnini PG, Yu C, Erickson KT, Hirschbein J, Zelman V, et al. Long-Term Outcomes and Patterns of Tumor Progression After Gamma Knife Radiosurgery for Benign Meningiomas. *Neurosurgery* (2010) 67(2):322–8; discussion 8-9. doi: 10.1227/01.NEU.0000371974.88873.15
56. Pollock BE, Stafford SL, Link MJ, Garces YI, Foote RL. Single-Fraction Radiosurgery for Presumed Intracranial Meningiomas: Efficacy and Complications From a 22-Year Experience. *Int J Radiat Oncol Biol Phys* (2012) 83(5):1414–8. doi: 10.1016/j.ijrobp.2011.10.033
57. Glantz MJ, Cole BF, Forsyth PA, Recht LD, Wen PY, Chamberlain MC, et al. Practice Parameter: Anticonvulsant Prophylaxis in Patients With Newly Diagnosed Brain Tumors. Report of the Quality Standards Subcommittee of the American Academy of Neurology. *Neurology* (2000) 54(10):1886–93. doi: 10.1212/WNL.54.10.1886
58. Zhang B, Zhao G, Yang HF, Wang D, Yu JL, Huang HY. Assessment of Risk Factors for Early Seizures Following Surgery for Meningiomas Using Logistic Regression Analysis. *J Int Med Res* (2011) 39(5):1728–35. doi: 10.1177/147323001103900515
59. Harward SC, Rolston JD, Englot DJ. Seizures in Meningioma. *Handb Clin Neurol* (2020) 170:187–200. doi: 10.1016/B978-0-12-822198-3.00053-7
60. Gloss D, Pargeon K, Pack A, Varma J, French JA, Tolchin B, et al. Antiseizure Medication Withdrawal in Seizure-Free Patients: Practice Advisory Update Summary: Report of the AAN Guideline Subcommittee. *Neurology* (2021) 97 (23):1072–81. doi: 10.1212/WNL.0000000000012944
61. Guerrini R, Rosati A, Giordano F, Genitori L, Barba C. The Medical and Surgical Treatment of Tumoral Seizures: Current and Future Perspectives. *Epilepsia* (2013) 54:84–90. doi: 10.1111/epi.12450
62. Klein M. Neurocognitive Functioning in Adult WHO Grade II Gliomas: Impact of Old and New Treatment Modalities. *Neuro Oncol* (2012) 14:17–24. doi: 10.1093/neuonc/nos161
63. Maschio M, Dinapoli L, Sperati F, Pace A, Fabi A, Vidiri A, et al. Effect of Pregabalin Add-on Treatment on Seizure Control, Quality of Life, and Anxiety in Patients With Brain Tumour-Related Epilepsy: A Pilot Study. *Epileptic Disord* (2012) 14(4):388–97. doi: 10.1684/epd.2012.0542
64. van der Meer PB, Dirven L, Fiocco M, Vos MJ, Kouwenhoven MCM, van den Bent MJ, et al. First-Line Antiepileptic Drug Treatment in Glioma Patients With Epilepsy: Levetiracetam vs Valproic Acid. *Epilepsia* (2021) 62(5):1119–29. doi: 10.1111/epi.16880
65. van der Meer PB, Dirven L, van den Bent MJ, Preusser M, Taphoorn MJB, Rudá R, et al. Prescription Preferences of Antiepileptic Drugs in Brain Tumor Patients: An International Survey Among EANO Members. *Neuro-Oncol Pract* (2021) 9(2):105–13. doi: 10.1093/nop/npab059
66. Jenkinson M, Helmy A, Huckey H, Mills S, Grant R, Hughes D, et al. Surgeons Trial Of Prophylaxis For Epilepsy In Seizure Naïve Patients With Meningioma: A Randomized Controlled Trial (STOP 'Em). *Neuro-Oncol Pract* (2020) 22(Supplement_2):ii195. doi: 10.1093/neuonc/noaa215.815

Conflict of Interest: The authors declare that the research was conducted in the absence of any commercial or financial relationships that could be construed as a potential conflict of interest.

Publisher's Note: All claims expressed in this article are solely those of the authors and do not necessarily represent those of their affiliated organizations, or those of the publisher, the editors and the reviewers. Any product that may be evaluated in this article, or claim that may be made by its manufacturer, is not guaranteed or endorsed by the publisher.

Copyright © 2022 Elbadry Ahmed, Tang, Asemota, Huang, Boling and Bannout. This is an open-access article distributed under the terms of the Creative Commons Attribution License (CC BY). The use, distribution or reproduction in other forums is permitted, provided the original author(s) and the copyright owner(s) are credited and that the original publication in this journal is cited, in accordance with accepted academic practice. No use, distribution or reproduction is permitted which does not comply with these terms.

frontiers | Frontiers in Oncology

TYPE Review
PUBLISHED 22 July 2022
DOI 10.3389/fonc.2022.931371

Check for updates

OPEN ACCESS

EDITED BY
Hailiang Tang,
Fudan University, China

REVIEWED BY
Regina M. Graham,
University of Miami Health System, United States
Mirna Lechpammer,
Foundation Medicine Inc., United States

*CORRESPONDENCE
Jacob S. Young
Jacob.young@ucsf.edu
Nicholas A. Butowski
Nicholas.butowski@ucsf.edu

SPECIALTY SECTION
This article was submitted to Neuro-Oncology and Neurosurgical Oncology, a section of the journal Frontiers in Oncology

RECEIVED 28 April 2022
ACCEPTED 27 June 2022
PUBLISHED 22 July 2022

CITATION
Young JS, Kidwell RL, Zheng A, Haddad AF, Aghi MK, Raleigh DR, Schulte JD and Butowski NA (2022) CDK 4/6 inhibitors for the treatment of meningioma.
Front. Oncol. 12:931371.
doi: 10.3389/fonc.2022.931371

COPYRIGHT
© 2022 Young, Kidwell, Zheng, Haddad, Aghi, Raleigh, Schulte and Butowski. This is an open-access article distributed under the terms of the Creative Commons Attribution License (CC BY). The use, distribution or reproduction in other forums is permitted, provided the original author(s) and the copyright owner(s) are credited and that the original publication in this journal is cited, in accordance with accepted academic practice. No use, distribution or reproduction is permitted which does not comply with these terms.

CDK 4/6 inhibitors for the treatment of meningioma

Jacob S. Young[1*], Reilly L. Kidwell[1], Allison Zheng[1], Alex F. Haddad[1], Manish K. Aghi[1], David R. Raleigh[1,2], Jessica D. Schulte[3,4] and Nicholas A. Butowski[1,5*]

[1]Department of Neurological Surgery, University of California San Francisco, San Francisco, CA, United States, [2]Department of Radiation Oncology, University of California San Francisco, San Francisco, CA, United States, [3]Division of Neuro-Oncology, University of California San Diego, San Diego, CA, United States, [4]Department of Neuroscience, University of California San Diego, San Diego, CA, United States, [5]Division of Neuro-Oncology, University of California San Francisco, San Francisco, CA, United States

Meningiomas are the most common non-metastatic brain tumors, and although the majority are relatively slow-growing and histologically benign, a subset of meningiomas are aggressive and remain challenging to treat. Despite a standard of care that includes surgical resection and radiotherapy, and recent advances in meningioma molecular grouping, there are no systemic medical options for patients with meningiomas that are resistant to standard interventions. Misactivation of the cell cycle at the level of CDK4/6 is common in high-grade or molecularly aggressive meningiomas, and CDK4/6 has emerged as a potential target for systemic meningioma treatments. In this review, we describe the preclinical evidence for CDK4/6 inhibitors as a treatment for high-grade meningiomas and summarize evolving clinical experience with these agents. Further, we highlight upcoming clinical trials for patients meningiomas, and discuss future directions aimed at optimizing the efficacy of these therapies and selecting patients most likely to benefit from their use.

KEYWORDS

CDK inhibitor, meningioma, cell cycle dysregulation, clinical trials, molecular profiling and subtyping

Introduction

Meningiomas are the most common primary intracranial tumor, and although the vast majority of meningiomas are considered Grade 1 tumors by the World Health Organization (WHO) and can be managed effectively, between 20-30% of cases are considered Grade 2 or 3 and prove challenging to treat. Surgery and radiotherapy are the

therapeutic foundation of meningioma management, with no chemotherapeutic agents currently approved for these tumors (1). While there has been significant recent advances in the meningioma prognostication and classification using genomic and DNA methylation classifications, less progress has been made in their therapeutic treatment (2–9). Unfortunately, when these high-grade lesions recur and/or are found in regions along the skull base that make complete resection challenging, they often cause significant morbidity and ultimately prove to be fatal for patients. In this review, we describe the therapeutic rationale and preclinical/clinical evidence for small molecule inhibitors that target key cell cycle regulators, specifically cyclin dependent kinase (CDK) proteins, in the treatment of meningioma.

CDK 4/6 role in tumorigenesis

In non-pathological states, the process of cell division requires cells to progress through a series of highly regulated stages in sequential order, termed the cell cycle, and numerous checkpoints are present to prevent a cell from dividing in the absence of growth factors or in the presence of DNA damage (10). However, dysregulation of these cell division processes and uncontrolled cellular proliferation is a hallmark of cancer (10). CDKs interact with cyclin proteins to regulate this transition from one stage to the next, and, unsurprisingly, increased levels of these CDKs and their regulators, like FOXM1, are commonly observed in cancers such as meningiomas (11–14). CDK4 and 6 are two structurally similar cell cycle regulators that ultimately stimulate a cell forward in cell division to the S phase from G0/G1 (see **Figure 1** for schematic of cyclin-CDK pathway). The downstream targets of CDK4/6 include the classic, canonical tumor suppressor protein, retinoblastoma (Rb), and following phosphorylation of Rb by CDK4/6, the transcription factor E2F is able to initiate DNA synthesis and the S phase of cell division (15). Inhibitors of CDK, termed cyclin-dependent kinase inhibitors (CKIs), regulate CDK activity and decreased expression of these regulatory proteins is frequently observed in many cancers, with p16, which is encoded by the gene *CDKN2A*, being the most well characterized CKI. Furthermore, dysregulation of p16, CDK6, and pRB protein have all been associated with recurrence in atypical meningiomas (16) and homozygous deletions of the *CDKN2A/B* gene has also been associated with early meningioma recurrence (17). Given their position as relatively upstream regulators of these crucial cell cycle pathways, CDK4/6 specific inhibitors have become very attractive cancer therapeutic agents.

Development of CDK inhibitors for treatment of malignancies

Pan-CDK inhibitors were first developed over three decades ago, but their therapeutic potential was thwarted by severe toxicities, and now more specific inhibitors have mostly replaced these early pan-CDK inhibitors (18). There are currently three FDA-approved CDK4/6 specific inhibitors available in the United States: Palbociclib, Ribociclib, and Abemaciclib, each with their own specific pharmacokinetics and toxicities. These agents have been used as monotherapy or in combinatorial approaches with other therapies for the treatment of various cancer types.

Breast cancer was one of the first malignancies where CDK inhibitors were utilized given promising preclinical data demonstrating reliance on CDK signaling during breast cancer tumorigenesis. All three specific inhibitors listed above

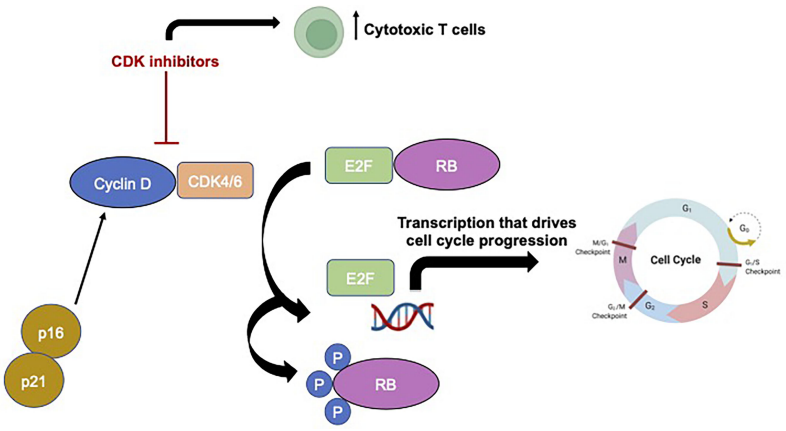

FIGURE 1
Schematic showing basic cyclin-CDK signaling pathway and mechanism of action of CDK inhibitors Made in BioRender.

demonstrated efficacy when used as treatment of estrogen receptor (ER)-positive breast cancer in combination with anti-estrogen therapy, replacing the previous gold standard of anti-estrogen therapy alone for ER-positive breast cancers (19–21). Palbociclib has been shown to be efficacious in other hormone receptor (HR)-positive breast cancer cell lines and is the only agent that can be used for perimenopausal and premenopausal women (22). When combined with an ER antagonist, Palbociclib significantly improved progression free survival, but not overall survival, in HR+ breast cancer (23, 24). Abemaciclib was also found to be safe and have some benefit as a single agent in HR+ breast cancer patients (25). Finally, Ribociclib may have a synergistic effect when used with an ER antagonist, and was found to improve PFS and overall response rate in patients with HR+/HER2- advanced breast cancer (26).

These examples of varying therapeutic efficacy to the different CDK4/6 inhibitors in breast cancer demonstrates the importance of finding biomarkers for tumor sensitivity to these agents. While hormone receptors may prove to be a powerful biomarker for breast cancer responsiveness, other markers are needed for other tumor types. CCND1 amplification and loss of p16 expression may indicate sensitivity to CDK inhibitors in breast cancer, although results are conflicting in the literature (19, 27). Another group of proteins, termed D-cyclin activating features (DCAFs), have also been associated with CDK4/6 inhibitor sensitivity (28). Furthermore, it is equally important to understand how resistance develops to CDK4/6 inhibitors, which seems to be common after prolonged treatment with these agents (29). As CDK4/6 inhibitors are trialed for patients with aggressive meningiomas, it will be important to design clinical trials incorporating window-of-opportunity strategies to obtain tissue for pharmacokinetics, pharmacodynamics, and biomarker analysis from treated patients.

There may be synergistic lethality in targeting CDK4/6 targets in combination with other signaling pathways, particularly those that interact with cell cycle regulation pathways. Other signaling pathways interact with CDK4/6 targets, such as the PI3K-AKT-mTOR and the RAS-RAF-MEK-ERK pathways, may also provide potential therapeutic targets that synergize with CDK4/6 inhibitors. For example, inhibitors of PI3K pathway proteins have been effective in preclinical breast cancer, mesothelioma, and head and neck cancer models when combined with CDK4/6 inhibition (30–32). Mutations in KRAS, NRAS, BRAF genes also lead to activation of the RAS-RAF-MEK-ERK pathway, and treatment with CDK4/6 inhibitors may have a synergistic effect when used with inhibitors of the RAS pathway (33). Like the PI3K pathway, RAS pathway inhibition alters mTOR levels to impact cell proliferation (34–36). Further investigation is needed to determine if inactivation of these overlapping signaling pathways will help prevent resistance to these agents and if there is a role for combinatorial strategies for the treatment of meningioma patients.

Preclinical evidence for CDK inhibitors in meningiomas

As mentioned above, cyclin overexpression has been associated with increased grade and risk of recurrence in meningioma (6, 37–40). Prior to the advent of CDK inhibitors, early preclinical studies utilized targeted small interfering RNA (siRNA) to inhibit CDK. Cheng et al. were one of the first groups to show that targeting cyclin D1 levels decreased cell proliferation, cell viability, and halted tumor cell invasion in malignant meningioma (41). Cyclin D1 knockdown was also shown to decrease antiapoptotic proteins such as survivin and Bcl-2, increasing time in G0/G1 phase and causing cell cycle arrest. siRNA targeting of cyclin D1 also diminished meningioma cell invasion *via* suppression of extracellular matrix metalloproteinases *in vitro*. This work opened the door for investigation of pharmacologic CDK inhibitors as therapeutic agents for meningioma.

Subsequent pre-clinical studies revealed anti-tumor effects for CDK inhibitors in various *in vitro* and *in vivo* meningioma models. The majority of studies utilized Palbociclib, which is the most frequently used CDK4/6 inhibitor in cancer clinical trials (42). Das et al. found Palbociclib induces G1 cell-cycle arrest and tumor cell apoptosis in a radiation-induced malignant meningioma model (43). Using Grade 1 and Grade 3 meningioma cell lines, Palbociclib treatment inhibited the expression of CDK4/6 and downstream E2F transcription factor, resulting in dramatic reduction of pRB and reduced cell proliferation. Treatment with 14 days of Palbociclib (10mg/kg) plus radiation (6 Gy) reduced total tumor volume in an *in vivo* subcutaneous mouse meningioma xenograft model. Work by Horbinski et al. further supported Palbociclib-induced suppression of pRb and cell proliferation *in vitro*, specifically in p16-/Rb+ meningioma cell lines (44). In contrast, p16+/Rb- cell lines were resistant to both radiation and CDK inhibition. This study also demonstrated combination therapy with radiation and Palbociclib significantly delayed tumor growth and prolonged overall survival in mouse xenograft models compared to ether treatment alone. Interestingly, this effect was primarily attributed to decreased cell proliferation, as histological analyses failed to demonstrate any difference in apoptosis or cell death.

Given CDK4/6 inhibitors are thought to be largely cytostatic (45), rather than cytotoxic when used as monotherapy, and there are still toxicities associated with these agents (46, 47), there is significant preclinical interest in combinatorial strategies and/or novel agents that may be cytotoxic. One example, TG02 (SB1317) is an orally available, multi-cyclin-dependent kinase inhibitor of CDK 1,2,5,7 and 9. As specific inhibition of CDK9 has been shown to induce downstream depletion of key oncoproteins including MCL-1 and c-MYC, targeting this CDK protein has also become of interest as a cancer therapy (48, 49). Von Achenbach et al. examined the effects of TG02 in primary patient-derived meningioma cell lines classified as

benign, intermediate, or malignant by DNA methylation profiling and found dose-dependent inhibition of cell proliferation across cultures, without significant induction of apoptosis (50). Importantly, cell lines classified as malignant were overall more sensitive than those considered benign.

As mentioned above, there has significant interest in molecular profiling to improve patient selection and clinical response rates to CDK inhibition in patients with recurrent meningioma. Using DNA methylation profiling of 565 primary meningioma samples, Choudhury et al. identified three DNA methylation groups with distinct clinical outcomes and biological drivers: (A) Merlin-intact, (B) Immune-enriched, and (C) hypermitotic, and the latter group was notably had a loss of the endogenous CDK4/6 negative regulator, *CDKN2A/B* (51). Exposing patient cells from this group to the known CDK4/6 inhibitors Abemaciclib, Palbociclib, and Ribociclib resulted in growth attenuation across cell culture, organoid, and xenograft models. Specifically, *in vivo*, CDK4/6 blockade diminished pRb expression, inhibited cell proliferation, and prolonged overall survival. This study highlights the role DNA methylation profiling may play as a clinical tool to stratify meningioma patients for molecular treatments.

Agents that indirectly alter the CDK pathway are also being explored as potential meningioma therapies. For example, Negroni et al. found upregulation of the zinc finger transcription factor GATA binding protein 4 (GATA-4) in high grade meningioma primary patient samples, which resulted in overexpression of cyclin D (52). Accordingly, administration of NSC140905, a small molecule inhibitor of GATA-4 reduced expression of cyclin D1 and diminished meningioma cell viability *in vitro*. Another group is targeting the eukaryotic initiation factor 4F complex (eIF4F), which regulates the translation of many pro-oncogenic proteins like MYC and cyclins in various cancers (53). Oblinger et al. found elevated levels of eIF4A in primary meningioma samples and showed this protein to be a driver of tumor cell proliferation *via* induction of downstream cyclin-mediated signaling (54). Treatment of cells with silvestrol, an inhibitor of eIF4A, resulted in reduction of cyclins D1 and E1, and G2/M phase arrest. Although these inhibitors are further from clinical trials than the more established CDK inhibitors, these agents pose a novel and promising therapeutic possibility for targeting cyclin-mediated signaling in meningioma.

Meningioma tumor microenvironment on CDK inhibitors

The importance of the brain tumor microenvironment has blossomed in the era of immunotherapy, particularly for highly immunosuppressive tumors like glioblastoma. Given meningiomas ability to invade both brain and bone, early research investigating the meningioma microenvironment focused on specific extracellular matrix components, like matrix metalloproteinase expression (55). However, more recent research has begun to elucidate the importance of immune cells in the microenvironment. For example, new classification schema have emerged based on tumor DNA methylation signatures, with one category of meningiomas considered "immune-enriched" (56). Moreover, in addition to having more immunosuppressive infiltrating immune cells, higher-grade meningiomas appear to express more PD-L1 on tumor cells and tumor-infiltrating CD68+ macrophages (57, 58). Indeed, a large percentage of the meningioma microenvironment consists of CD45+ immune cells (59), with the macrophage population making up the largest percentage of this compartment (60).

Interestingly, the mechanism of action of CDK inhibitors is likely not as simple as once thought. In addition to the direct effect on cycling tumor cells, CDK4 influences the composition of cells in tumor microenvironment and inhibition of this pathway results in changes in the tumor-infiltrating immune cell populations (61). In breast cancer models, CDK inhibition increased antigen presentation and increased the number of cytotoxic T cells in the tumor microenvironment while simultaneously reducing the number of immunosuppressive regulatory T cells (62). Currently, there is very little literature regarding the impact of CDK inhibition on the meningioma tumor microenvironment and even less is known how the meningioma microenvironment contributes to treatment resistance or efficacy.

Clinical trials using CDK inhibitors

To date, one clinical trial investigating CDK inhibitors for meningioma has been one completed and four additional trials are ongoing, for which results have yet to be published (**Table 1**). Many of these trials include multiple central nervous system (CNS) tumors, and the number of meningioma patients enrolled is currently unknown.

PBTC-042 was a phase I open-label dose-escalation trial to assess the maximum tolerated dose (MTD) and pharmacokinetics of daily oral PD-0332991 (Palbociclib isethionate) in Rb1+ recurrent, progressive, or refractory primary CNS tumors in young adults (NCT02255461). Secondary endpoints included evaluation of efficacy, genetic profiling of tumor samples, and further exploration of pharmacokinetic (PK) parameters. The study was terminated upon completion of primary endpoints and identification of the MTD, although detailed results have not yet been presented or published and it is unclear how many, if any, were meningioma patients. Outcomes data on ClinicalTrial.gov indicate a MTD of 75mg/m2 was identified, with hematologic toxicities, including anemia, neutropenia, and leukopenia predominantly being dose-limiting. Other common toxicities

TABLE 1 Ongoing CDK inhibitor trials for meningioma.

Study title	Drug	Phase	Patient population	Sponsor	Status	Trial registration no.
PBTC-042: Palbociclib Isethionate in Treating Younger Patients with Recurrent, Progressive, or Refractory Central Nervous System Tumors	Palbociclib Isethionate	I	Recurrent Rb1+ childhood grade III meningioma; other Rb1+ CNS tumors	Pediatric Brain Tumor Consortium (Collaborator: NCI)	*Terminated* (Primary objective complete; MTD determined)	NCT02255461
SJDAWN: Phase 1 Study Evaluating Molecularly-Driven Doublet Therapies for Children and Young Adults with Recurrent Brain Tumors	Stratum B: Ribociclib + Trametinib	I	Recurrent anaplastic meningioma; other CNS tumors	St. Jude Children's Research Hospital (Collaborator: Novartis)	*Recruiting*	NCT03434262
Ribociclib (LEE011) in Preoperative Glioma and Meningioma Patients	Ribociclib	0/II	Preoperative; Rb+ or non-Rb-mutated recurrent grade II/III meningioma; glioma	Nader Sanai (Collaborators: Novartis, Ivy Brain Tumor Center, Barrow Neurologic Institute)	*Recruiting*	NCT02933736
A071401: Vismodegib, FAK Inhibitor GSK2256098, Capivasertib, and Abemaciclib in Treating Patients with Progressive Meningiomas	Cohort D: Abemaciclib	II	Meningioma with CDK4, CDK6, CDKN2A, CCND1, CCND2, CCND3, or CCNE1 alterations	Alliance for Clinical Trials in Oncology (Collaborators: NCI, GlaxoSmithKline, Genentech, Brain Science Foundation)	*Recruiting*	NCT02523014
MSK 17-261: Abemaciclib (LY2835219) in Patients with Recurrent Primary Brain Tumors	Cohort C: Abemaciclib	II	Recurrent meningioma	Memorial Sloan Kettering Cancer Center (Collaborator: Eli Lilly and Company)	*Recruiting*	NCT03220646

reported in this study included nausea, constipation, diarrhea, fatigue, and transaminitis, although these were not considered serious adverse events. There was also one serious non-hematologic adverse event of dehydration, and these non-hematologic toxicities are one reason these agents have been poorly tolerated by patients and are not more widely used clinically to date. No patients showed objective responses (defined as complete or partial response).

Currently recruiting trials have focused on the CDK4/6 inhibitors Ribociclib (LEE011) and Abemaciclib (LY2835219), the latter of which is distinguished by a shorter half-life and a slightly higher affinity for CDK4 (46). SJDAWN is a Phase 1 dose-escalation clinical trial exploring molecularly driven doublet (or combinatorial) therapies unique to a patient's specific tumor type (NCT03434262). Patients who tolerate the drug combination are eligible for an expansion cohort to assess for early efficacy. Stratum B of this trial includes patients with recurrent or refractory anaplastic meningioma treated with combination Ribociclib and the MEK inhibitor Trametinib. Primary endpoints include determination of MTD and PK analysis and secondary outcomes include response rate and duration of objective response. The trial is currently ongoing, and no interim results have been reported to date.

Another ongoing study is investigating single-agent Ribociclib in the adult population as a phase 0/2 non-randomized open-label trial evaluating preoperative dosing of oral Ribociclib in patients with Rb+ or non-Rb-mutated recurrent WHO Grade 2/3 meningioma or high-grade glioma (NCT02933736). In this trial, patients receive 900mg of Ribociclib daily for 5 days prior to surgical resection and endpoints include evaluation of PK, PD, and tissue analyses for signs of any preliminary clinical response. PD analysis includes assessment of Rb and FOXM1 phosphorylation as markers of halted cellular progression from G1 to S phase (63). Interim results reported a median CSF concentration of ribociclib was 0.25 μM and tumor tissue concentration of unbound ribociclib 1.36 μM, and 4 out of 8 patients had a positive PK and PD tumor response (defined as unbound ribociclib concentration > 5-fold *in vitro* IC50 (0.04 μM) and >20% decrease in pRB levels, respectively) (64). These patients defined as PK/PD responders were subsequently enrolled in an exploratory Phase 2 cohort of continuous Ribociclib therapy (600mg daily for 3 weeks/1 week off). At 1 year on therapy, 2 of 4 patients were assessed to have a partial response (PR) by RANO criteria. Overall progression-free survival (PFS) was >12 months in 3 of 4 patients, and >23 months in the 4th patient. Given continuous Ribociclib in other solid tumors has been shown to have an acceptable safety profile, there is excitement for the final results of this ongoing study (25). Although the reThis study also showcases the importance of performing more Phase 0 and "window-of-opportunity" studies to confirm PK/PD for trials investigating CDK inhibitors for meningioma (65).

The remaining two ongoing studies aim to examine the efficacy of twice daily dosing of oral Abemaciclib. The only trial to enroll meningioma patients alone is A071401, a Phase 2 trial of SMO/AKT/NF2/CDK inhibitors in patients with progressive meningiomas harboring corresponding mutations in the respective signaling pathway (NCT02523014). Patients are considered eligible for Abemaciclib if molecular testing is positive for alterations in CDK4, CDK6, CDKN2A, CCND1, CCND2, CCND3, or CCNE1, with primary endpoints including PFS and response rate by Macdonald criteria. To date, interim results have only been reported for the FAK inhibitor cohorts but have not been

described for the ongoing Abemaciclib group (66). The second investigational study testing this agent is MSK 17-261, a Phase 2 open-label, non-randomized study of Abemaciclib in patients with recurrent primary brain tumors (NCT03220646), including patients with recurrent meningiomas. Dosing is 200mg of Abemaciclib twice a day, which follows the MTD established in the Phase 1 trial which included patients with glioblastoma, breast cancer, non-small cell lung cancer, and other solid tumors (67). Recent interim results suggest promising early efficacy data for the subset of recurrent meningioma patients, although full results have yet to be published (68).

Future directions

As mentioned, one concern with the use of CDK4/6 inhibitors is the development of resistance mechanisms to these therapies through quasi-redundant or alternative signaling pathways, which has been reported in breast cancer and medulloblastoma patients receiving CDK inhibitor monotherapy (12). Daggubati et al. found that in Hedgehog-associated medulloblastoma, decreased ribosomal protein expression in response to CDK inhibitor treatment caused ER stress and activated the unfolded protein response, which ultimately upregulated production of sterol lipids that activate the Smoothened (SMO) to sustain the Hedgehog signaling pathway despite cell cycle attenuation (69). Interestingly, the authors found that combinatorial therapies with CDK inhibitor and a small molecule that inhibited the production of these SMO-activating lipids was able to effectively block cancer cell growth and may help overcome resistance to monotherapy. Additional studies identifying resistance mechanisms to these inhibitors will be critical to translating preclinical successes to durable responses for patients in the clinic. Finally, given the difficulty patients have tolerating these agents, local delivery strategies such as convection enhanced delivery or approaches to improve drug concentration in the tumor such as blood brain barrier disruption *via* focused ultrasound should be explored for these therapies.

Conclusions

Patients with high-grade meningiomas face a difficult prognosis with no good systemic treatments available. Cell cycle regulators are commonly dysregulated in many cancers, including meningiomas, and represent a potential treatment strategy. Preclinical evidence supports the use of CDK4/6 specific inhibitors, Palbociclib, Abemaciclib, and Ribociclib, as potential therapeutic agents for meningioma patients and these agents are actively being explored in ongoing clinical trials. Future work identifying response biomarkers and mechanisms of resistance are needed to better select patients for these agents and improve their efficacy and durability.

Author contributions

JY, RK, and AZ drafted the manuscript. JY, JS, and NB organized and designed topic for review, all authors critically reviewed manuscript. All authors contributed to the article and approved the submitted version.

Funding

JY is supported by the Neurosurgery Research and Education Foundation Research Fellowship, the Glioblastoma Foundation Neil Peart Research Award, the Chan-Zuckerberg Biohub Physician Scientist Fellowship, and the ASCO Conquer Cancer Young Investigator Award in Drug Development. DR is supported by the UCSF Physician Scientist Scholar Program, the UCSF Wolfe Meningioma Program Project, and NIH grant R01 CA262311.

Conflict of interest

The authors declare that the research was conducted in the absence of any commercial or financial relationships that could be construed as a potential conflict of interest.

Publisher's note

All claims expressed in this article are solely those of the authors and do not necessarily represent those of their affiliated organizations, or those of the publisher, the editors and the reviewers. Any product that may be evaluated in this article, or claim that may be made by its manufacturer, is not guaranteed or endorsed by the publisher.

References

1. Brastianos PK, Galanis E, Butowski N, Chan JW, Dunn IF, Goldbrunner R. Advances in multidisciplinary therapy for meningiomas. *Neuro Oncol* (2019) 21 (Suppl 1):I18–31. doi: 10.1093/NEUONC/NOY136

2. Youngblood MW, Duran D, Montejo JD, Li C, Omay SB, Özduman K, et al. Correlations between genomic subgroup and clinical features in a cohort of more than 3000 meningiomas. *J Neurosurg* (2019) 133(5):1345–54. doi: 10.3171/2019.8.JNS191266

3. Youngblood MW, Günel M. Molecular genetics of meningiomas. *Handb Clin Neurol* (2020) 169:101–19. doi: 10.1016/B978-0-12-804280-9.00006-8

4. Youngblood MW, Miyagishima DF, Jin L, Gupte T, Li C, Duran D, et al. Associations of meningioma molecular subgroup and tumor recurrence. *Neuro Oncol* (2021) 23(5):783–94. doi: 10.1093/NEUONC/NOAA226

5. Patel AJ, Wan YW, Al-Ouran R, Revelli JP, Cardenas MF, Oneissi M, et al. Molecular profiling predicts meningioma recurrence and reveals loss of DREAM complex repression in aggressive tumors. *Proc Natl Acad Sci USA* (2019) 116 (43):21715–26. doi: 10.1073/PNAS.1912858116

6. Choudhury A, Magill ST, Eaton CD, Prager BC, Chen WC, Seo K, et al. Meningioma epigenetic grouping reveals biologic drivers and therapeutic vulnerabilities. *medRxiv* (2020) 2020:20237495. doi: 10.1101/2020.11.23.20237495

7. Driver J, Hoffman SE, Tavakol S, Woodward E, Maury EA, Bhave V. A molecularly integrated grade for meningioma. *Neuro Oncol* (2022) 24(5):796–808. doi: 10.1093/NEUONC/NOAB213

8. Sahm F, Schrimpf D, Stichel D, Jones DTW, Hielscher T, Schefzyk S., et al. DNA Methylation-based classification and grading system for meningioma: A multicentre, retrospective analysis. *Lancet Oncol* (2017) 18(5):682–94. doi: 10.1016/S1470-2045(17)30155-9

9. Nassiri F, Liu J, Patil V, Mamatjan Y, Wang JZ, Hugh-White R, et al. A clinically applicable integrative molecular classification of meningiomas. *Nature* (2021) 597(7874):119–25. doi: 10.1038/S41586-021-03850-3

10. Hanahan D. Hallmarks of cancer: new DimensionsHallmarks of cancer: new dimensions. *Cancer Discov* (2022) 12(1):31–46. doi: 10.1158/2159-8290.CD-21-1059

11. Vasudevan HN, Braunstein SE, Phillips JJ, Pekmezci M, Tomlin BA, Wu A, et al. Comprehensive molecular profiling identifies FOXM1 as a key transcription factor for meningioma proliferation. *Cell Rep* (2018) 22(13):3672–83. doi: 10.1016/j.celrep.2018.03.013

12. O'Leary B, Finn RS, Turner NC. Treating cancer with selective CDK4/6 inhibitors. *Nat Rev Clin Oncol* (2016) 13(7):417–30. doi: 10.1038/nrclinonc.2016.26

13. Kim H, Park K-J, Ryu B-K, Park D-H, Kong D-S, Chong K, et al. Forkhead box M1 (FOXM1) transcription factor is a key oncogenic driver of aggressive human meningioma progression. *Neuropathol Appl Neurobiol* (2020) 46(2):125–41. doi: 10.1111/nan.12571

14. Pereira BJA, de Santana Júnior PA, de Almeida AN, Cavalcante SG, de Melo KCM, de Aguiar PHP, et al. Cyclin E1 expression and malignancy in meningiomas. *Clin Neurol Neurosurg* (2020) 190:105647. doi: 10.1016/j.clineuro.2019.105647

15. Kent LN, Leone G. The broken cycle: E2F dysfunction in cancer. *Nat Rev Cancer* (2019) 19(6):326–38. doi: 10.1038/s41568-019-0143-7

16. Kim MS, Kim KH, Lee EH, Lee YM, Lee S-H, Kim HD, et al. Results of immunohistochemical staining for cell cycle regulators predict the recurrence of atypical meningiomas. *J Neurosurg* (2014) 121(5):1189–200. doi: 10.3171/2014.7.JNS132661

17. Sievers P, Hielscher T, Schrimpf D, Stichel D, Reuss DE, Berghoff AS, et al. CDKN2A/B homozygous deletion is associated with early recurrence in meningiomas. *Acta Neuropathol* (2020) 140(3):409–13. doi: 10.1007/s00401-020-02188-w

18. Asghar U, Witkiewicz AK, Turner NC, Knudsen ES. The history and future of targeting cyclin-dependent kinases in cancer therapy. *Nat Rev Drug Discov* (2015) 14(2):130–46. doi: 10.1038/NRD4504

19. Finn RS, Martin M, Rugo HS, Jones S, Im S-A, Gelmon K, et al. Palbociclib and letrozole in advanced breast cancer. *N Engl J Med* (2016) 375(20):1925–36. doi: 10.1056/NEJMOA1607303/SUPPL_FILE/NEJMOA1607303_DISCLOSURES.PDF

20. Hortobagyi GN, Stemmer SM, Burris HA, Yap Y-S, Sonke GS, Paluch-Shimon S, et al. Ribociclib as first-line therapy for HR-positive, advanced breast cancer. *N Engl J Med* (2016) 375(18):1738–48. doi: 10.1056/NEJMOA1609709/SUPPL_FILE/NEJMOA1609709_DISCLOSURES.PDF

21. Goetz MP, Toi M, Campone M, Trédan O, Bourayou N, Sohn J, et al. MONARCH 3: Abemaciclib as initial therapy for advanced breast cancer. *J Clin Oncol* (2017) 35(32):3638–46. doi: 10.1200/JCO.2017.75.6155

22. Finn RS, Dering J, Conklin D, Kalous O, Cohen DJ, Desai AJ, et al. PD 0332991, a selective cyclin d kinase 4/6 inhibitor, preferentially inhibits proliferation of luminal estrogen receptor-positive human breast cancer cell lines *in vitro*. *Breast Cancer Res* (2009) 11(5). doi: 10.1186/BCR2419

23. Turner NC, Ro J, André F, Loi S, Verma S, Iwata H, et al. Palbociclib in Hormone-Receptor–positive advanced breast cancer. *N Engl J Med* (2015) 373(3):209–19. doi: 10.1056/NEJMOA1505270/SUPPL_FILE/NEJMOA1505270_DISCLOSURES.PDF

24. Turner NC, Slamon DJ, Ro J, Bondarenko I, Im S-A, Masuda N, et al. Overall survival with palbociclib and fulvestrant in advanced breast cancer. *N Engl J Med* (2018) 379(20):1926–36. doi: 10.1056/NEJMOA1810527/SUPPL_FILE/NEJMOA1810527_DATA-SHARING.PDF

25. Infante JR, Cassier PA, Gerecitano JF, Witteveen PO, Chugh R, Ribrag V, et al. A phase I study of the cyclin-dependent kinase 4/6 inhibitor ribociclib (LEE011) in patients with advanced solid tumors and lymphomas. *Clin Cancer Res* (2016) 22(23):5696–705. doi: 10.1158/1078-0432.CCR-16-1248

26. Slamon DJ, Neven P, Chia S, Fasching PA, De Laurentiis M, Im SA, et al. Phase III randomized study of ribociclib and fulvestrant in hormone receptor-positive, human epidermal growth factor receptor 2-negative advanced breast cancer: MONALEESA-3. *J Clin Oncol* (2018) 36(24):2465–72. doi: 10.1200/JCO.2018.78.9909

27. Finn RS, Liu Y, Zhu Z, Martin M, Rugo HS, Dieras V, et al. Biomarker analyses of response to cyclin-dependent kinase 4/6 inhibition and endocrine therapy in women with treatment-naïve metastatic breast cancer. *Clin Cancer Res* (2020) 26(1):110–21. doi: 10.1158/1078-0432.CCR-19-0751

28. Gong X, Litchfield LM, Webster Y, Chio LC, Wong SS, Stewart TR, et al. Genomic aberrations that activate d-type cyclins are associated with enhanced sensitivity to the CDK4 and CDK6 inhibitor abemaciclib. *Cancer Cell* (2017) 32(6):761–76.e6. doi: 10.1016/J.CCELL.2017.11.006

29. Garrido-Castro AC, Goel S. CDK4/6 inhibition in breast cancer: Mechanisms of response andTreatment failure. *Curr Breast Cancer Rep* (2017) 9(1):26. doi: 10.1007/S12609-017-0232-0

30. Vora SR, Juric D, Kim N, Mino-Kenudson M, Huynh T, Costa C, et al. CDK 4/6 inhibitors sensitize PIK3CA mutant breast cancer to PI3K inhibitors. *Cancer Cell* (2014) 26(1):136–49. doi: 10.1016/J.CCR.2014.05.020

31. Bonelli MA, Digiacomo G, Fumarola C, Alfieri R, Quaini F, Falco A, et al. Combined inhibition of CDK4/6 and PI3K/AKT/mTOR pathways induces a synergistic anti-tumor effect in malignant pleural mesothelioma cells. *Neoplasia* (2017) 19(8):637–48. doi: 10.1016/J.NEO.2017.05.003

32. Inoki K, Li Y, Zhu T, Wu J, Guan KL. TSC2 is phosphorylated and inhibited by akt and suppresses mTOR signalling. *Nat Cell Biol* (2002) 4(9):648–57. doi: 10.1038/ncb839

33. Chen SH, Gong X, Zhang Y, Van Horn RD, Yin T, Huber L, et al. RAF Inhibitor LY3009120 sensitizes RAS or BRAF mutant cancer to CDK4/6 inhibition by abemaciclib *via* superior inhibition of phospho-RB and suppression of cyclin D1. *Oncogene* (2018) 37(6):821–32. doi: 10.1038/ONC.2017.384

34. Ma L, Chen Z, Erdjument-Bromage H, Tempst P, Pandolfi PP. Phosphorylation and functional inactivation of TSC2 by erk implications for tuberous sclerosis and cancer pathogenesis. *Cell* (2005) 121(2):179–93. doi: 10.1016/J.CELL.2005.02.031

35. Roux PP, Ballif BA, Anjum R, Gygi SP, Blenis J. Tumor-promoting phorbol esters and activated ras inactivate the tuberous sclerosis tumor suppressor complex *via* p90 ribosomal S6 kinase. *Proc Natl Acad Sci USA* (2004) 101(37):13489–94. doi: 10.1073/PNAS.0405659101

36. Lee MS, Helms TL, Feng N, Gay J, Chang QE, Tian F, et al. Efficacy of the combination of MEK and CDK4/6 inhibitors *in vitro* and *in vivo* in KRAS mutant colorectal cancer models. *Oncotarget* (2016) 7(26):39595–608. doi: 10.18632/ONCOTARGET.9153

37. Bi WL, Greenwald NF, Abedalthagafi M, Wala J, Gibson WJ, Agarwalla PK, et al. Genomic landscape of high-grade meningiomas. *NPJ Genom Med* (2017) 2(1). doi: 10.1038/S41525-017-0014-7

38. Boström J, Meyer-Puttlitz B, Wolter M, Blaschke B, Weber RG, Lichter P, et al. Alterations of the tumor suppressor genes CDKN2A (p16(INK4a)), p14 (ARF), CDKN2B (p15(INK4b)), and CDKN2C (p18(INK4c)) in atypical and anaplastic meningiomas. *Am J Pathol* (2001) 159(2):661–9. doi: 10.1016/S0002-9440(10)61737-3

39. Maxwell M, Galanopoulos T, Antoniades HN. Expression of cyclin D1 proto-oncogene mRNA in primary meningiomas may contribute to tumorigenesis. *Int J Oncol* (1996) 9(6):1213–7. doi: 10.3892/IJO.9.6.1213

40. Alama A, Barbieri F, Spaziante R, Bruzzo C, Dadati P, Dorcaratto A, et al. Significance of cyclin D1 expression in meningiomas: A preliminary study. *J Clin Neurosci* (2007) 14(4):355–8. doi: 10.1016/J.JOCN.2006.04.001

41. Cheng G, Zhang L, Lv W, Dong C, Wang Y, Zhang J. Overexpression of cyclin D1 in meningioma is associated with malignancy grade and causes abnormalities in apoptosis, invasion and cell cycle progression. *Med Oncol* (2015) 32(1):1–8. doi: 10.1007/S12032-014-0439-0

42. Finn R, Hurvitz S, Allison M, Applebaum S, Glaspy J, DiCarlo B, et al. Phase I study of PD 0332991, a novel, oral, cyclin-d kinase (CDK) 4/6 inhibitor in combination with letrozole, for first-line treatment of metastatic post-menopausal, estrogen receptor-positive (ER+), human epidermal growth factor receptor 2 (HER2)-negati. *Cancer Res* (2009) 69(Suppl 24):5069–9. doi: 10.1158/0008-5472.SABCS-09-5069

43. Das A, Alshareef M, Martinez Santos JL, Porto GBF, McDonald DG, Infinger LK, et al. Evaluating anti-tumor activity of palbociclib plus radiation in anaplastic and radiation-induced meningiomas: Pre-clinical investigations. *Clin Transl Oncol* (2020) 22(11):2017–25. doi: 10.1007/S12094-020-02341-7

44. Horbinski C, Xi G, Wang Y, Hashizume R, Gopalakrishnan M, Phillips JJ, et al. The effects of palbociclib in combination with radiation in preclinical models of aggressive meningioma. *Neurooncol Adv* (2021) 3(1). doi: 10.1093/NOAJNL/VDAB085

45. McClendon AK, Dean JL, Rivadeneira DB, Yu JE, Reed CA, Gao E, et al. CDK4/6 inhibition antagonizes the cytotoxic response to anthracycline therapy. *Cell Cycle* (2012) 11(14):2747. doi: 10.4161/CC.21127

46. Spring LM, Zangardi ML, Moy B, Bardia A. Clinical management of potential toxicities and drug interactions related to cyclin-dependent kinase 4/6 inhibitors in breast cancer: Practical considerations and recommendations. *Oncologist* (2017) 22(9):1039–48. doi: 10.1634/THEONCOLOGIST.2017-0142

47. Thill M, Schmidt M. Management of adverse events during cyclin-dependent kinase 4/6(CDK4/6) inhibitor-based treatment in breast cancer. *Ther Adv Med Oncol* (2018) 10. doi: 10.1177/1758835918793326

48. Goh KC, Novotny-Diermayr V, Hart S, Ong LC, Loh YK, Cheong A, et al. TG02, a novel oral multi-kinase inhibitor of CDKs, JAK2 and FLT3 with potent anti-leukemic properties. *Leukemia* (2012) 26(2):236–43. doi: 10.1038/LEU.2011.218

49. Juric V, Murphy B. Cyclin-dependent kinase inhibitors in brain cancer: Current state and future directions. *Cancer Drug Resist* (2020) 3(1):48–62. doi: 10.20517/CDR.2019.105

50. von Achenbach C, Le Rhun E, Sahm F, Wang SS, Sievers P, Neidert MC, et al. Sensitivity of human meningioma cells to the cyclin-dependent kinase inhibitor, TG02. *Transl Oncol* (2020) 13(12):100852. doi: 10.1016/j.tranon.2020.100852

51. Choudhury A, Magill S, Eaton CD, Prager BC, Chen WC, Seo K, et al. Meningioma DNA methylation grouping reveals biologic drivers and therapeutic vulnerabilities. *Int J Radiat Oncol* (2021) 111(3):e558–9. doi: 10.1016/J.IJROBP.2021.07.1513

52. Negroni C, Hilton DA, Ercolano E, Adams CL, Kurian KM, Baiz D, et al. GATA-4, a potential novel therapeutic target for high-grade meningioma, regulates miR-497, a potential novel circulating biomarker for high-grade meningioma. *EBioMedicine* (2020) 59. doi: 10.1016/J.EBIOM.2020.102941

53. Kong T, Xue Y, Cencic R, Zhu X, Monast A, Fu Z, et al. eIF4A inhibitors suppress cell-cycle feedback response and acquired resistance to CDK4/6 inhibition in cancer. *Mol Cancer Ther* (2019) 18(11):2158–70. doi: 10.1158/1535-7163.MCT-19-0162

54. Oblinger JL, Burns SS, Huang J, Pan L, Ren Y, Shen R, et al. Overexpression of eIF4F components in meningiomas and suppression of meningioma cell growth by inhibiting translation initiation. *Exp Neurol* (2018) 299(Pt B):299–307. doi: 10.1016/J.EXPNEUROL.2017.06.015

55. Sahab-Negah S, Gorji A. Meningioma tumor microenvironment. *Adv Exp Med Biol* (2020) 1296:33–48. doi: 10.1007/978-3-030-59038-3_3/TABLES/3

56. Choudhury A, Magill ST, Eaton CD, Prager BC, Chen WC, Cady MA, et al. Meningioma DNA methylation groups identify biological drivers and therapeutic vulnerabilities. *Nat Genet* (2022) 54(5). doi: 10.1038/S41588-022-01061-8

57. Han SJ, Reis G, Kohanbash G, Shrivastav S, Magill ST, Molinaro AM, et al. Expression and prognostic impact of immune modulatory molecule PD-L1 in meningioma. *J Neurooncol* (2016) 130(3):543–52. doi: 10.1007/S11060-016-2256-0

58. Du Z, Abedalthagafi M, Aizer AA, Shrivastav S, Magill ST, Molinaro AM, et al. Increased expression of the immune modulatory molecule PD-L1 (CD274) in anaplastic meningioma. *Oncotarget* (2015) 6(7):4704–16. doi: 10.18632/ONCOTARGET.3082

59. Domingues PH, Teodósio C, Ortiz J, Sousa P, Otero Á, Maillo A, et al. Immunophenotypic identification and characterization of tumor cells and infiltrating cell populations in meningiomas. *Am J Pathol* (2012) 181(5):1749–61. doi: 10.1016/J.AJPATH.2012.07.033

60. Garzon-Muvdi T, Bailey DD, Pernik MN, Pan E. Basis for immunotherapy for treatment of meningiomas. *Front Neurol* (2020) 11:945/BIBTEX. doi: 10.3389/FNEUR.2020.00945/BIBTEX

61. Klein ME, Kovatcheva M, Davis LE, Tap WD, Koff A. CDK4/6 inhibitors: The mechanism of action may not be as simple as once thought. *Cancer Cell* (2018) 34(1):9–20. doi: 10.1016/J.CCELL.2018.03.023

62. Goel S, Decristo MJ, Watt AC, Brinjones H, Sceneay J, Li BB, et al. CDK4/6 inhibition triggers anti-tumour immunity. *Nature* (2017) 548(7668):471–5. doi: 10.1038/nature23465

63. Sanai N, Tien A-C, Li J, Bao X, DeRogatis A, Fujita Y, et al. 392O - a phase 0/II clinical trial of a CDK4/6 inhibitor in aggressive meningioma patients. *Ann Oncol* (2019) 30:v144. doi: 10.1093/annonc/mdz243.002

64. Tien A-C, Li J, Bao X, DeRogatis A, Fujita Y, Pennington-Krygier C, et al. Mngi-01. a phase 0 trial of ribociclib in aggressive meningioma patients incorporating a tumor pharmacodynamic- and pharmacokinetic-guided expansion cohort. *Neuro Oncol* (2019) 21(Suppl 6):vi139. doi: 10.1093/NEUONC/NOZ175.583

65. Vogelbaum MA, Krivosheya D, Borghei-Razavi H, Sanai N, Weller M, Wick W, et al. Phase 0 and window of opportunity clinical trial design in neuro-oncology: A RANO review. *Neuro Oncol* (2020) 22(11):1568–79. doi: 10.1093/NEUONC/NOAA149

66. Brastianos PK, Twohy E, Gerstner ER, Kaufmann TJ, Iafrate AJ, Jeyapalan SA, et al. Alliance A071401: Phase II trial of FAK inhibition in meningiomas with somatic NF2 mutations. *J Clin Oncol* (2020) 38(Suppl 15):2502–2. doi: 10.1200/JCO.2020.38.15_SUPPL.2502

67. Patnaik A, Rosen LS, Tolaney SM, Tolcher AW, Goldman JW, Gandhi L, et al. Efficacy and safety of abemaciclib, an inhibitor of CDK4 and CDK6, for patients with breast cancer, non-small cell lung cancer, and other solid tumors. *Cancer Discov* (2016) 6(7):740–53. doi: 10.1158/2159-8290.CD-16-0095

68. Coffee E, Panageas K, Young R, Morrison T, Daher A, Grommes C, et al. Ctni-55. the cdk4/6 inhibitor abemaciclib in patients with recurrent meningioma and other primary cns tumors. *Neuro Oncol* (2021) 23(Supplement_6):vi72–3. doi: 10.1093/NEUONC/NOAB196.280

69. Daggubati V, Hochstelter J, Bommireddy A, Choudhury A, Krup AL, Kaur P, et al. Smoothened-activating lipids drive resistance to CDK4/6 inhibition in hedgehog-associated medulloblastoma cells and preclinical models. *J Clin Invest* (2021) 131(6). doi: 10.1172/JCI141171

frontiers | Frontiers in Oncology

TYPE Review
PUBLISHED 12 August 2022
DOI 10.3389/fonc.2022.962702

Check for updates

OPEN ACCESS

EDITED BY
Hailiang Tang,
Fudan University, China

REVIEWED BY
Jose McFaline Figueroa,
Dana–Farber Cancer Institute, United States
Kristin Huntoon,
University of Texas MD Anderson Cancer Center, United States
Alessia Pellerino,
University Hospital of the City of Health and Science of Turin, Italy

*CORRESPONDENCE
Arnold B. Etame
Arnold.Etame@moffitt.org

SPECIALTY SECTION
This article was submitted to Neuro-Oncology and Neurosurgical Oncology, a section of the journal Frontiers in Oncology

RECEIVED 06 June 2022
ACCEPTED 25 July 2022
PUBLISHED 12 August 2022

CITATION
Lynes J, Flores-Milan G, Rubino S, Arrington J, Macaulay R, Liu JKC, Beer-Furlan A, Tran ND, Vogelbaum MA and Etame AB (2022) Molecular determinants of outcomes in meningiomas.
Front. Oncol. 12:962702.
doi: 10.3389/fonc.2022.962702

COPYRIGHT
© 2022 Lynes, Flores-Milan, Rubino, Arrington, Macaulay, Liu, Beer-Furlan, Tran, Vogelbaum and Etame. This is an open-access article distributed under the terms of the Creative Commons Attribution License (CC BY). The use, distribution or reproduction in other forums is permitted, provided the original author(s) and the copyright owner(s) are credited and that the original publication in this journal is cited, in accordance with accepted academic practice. No use, distribution or reproduction is permitted which does not comply with these terms.

Molecular determinants of outcomes in meningiomas

John Lynes[1,2], Gabriel Flores-Milan[1,2], Sebastian Rubino[1,2], John Arrington[3], Robert Macaulay[4], James K. C. Liu[1,2], Andre Beer-Furlan[1,2], Nam D. Tran[1,2], Michael A. Vogelbaum[1,2] and Arnold B. Etame[1,2]*

[1]Division of Neurosurgery, Moffitt Cancer Center, Tampa, FL, United States, [2]Department of Neuro-Oncology, Moffitt Cancer Center, Tampa, FL, United States, [3]Department of Radiology, Moffitt Cancer Center, Tampa, FL, United States, [4]Department of Pathology, Moffitt Cancer Center, Tampa, FL, United States

Meningiomas are the most common intracranial primary tumor in adults. Surgery is the predominant therapeutic modality for symptomatic meningiomas. Although the majority of meningiomas are benign, there exists a subset of meningiomas that are clinically aggressive. Recent advances in genetics and epigenetics have uncovered molecular alterations that drive tumor meningioma biology with prognostic and therapeutic implications. In this review, we will discuss the advances on molecular determinants of therapeutic response in meningiomas to date and discuss findings of targeted therapies in meningiomas.

KEYWORDS

meningiomas, genetics, epigenetics, outcomes, targeted therapy, molecular classification, brain tumor

Introduction

Meningiomas are the most common primary intracranial benign tumor in adults. They commonly present due to seizures, focal neurologic deficit, or symptoms of elevated intracranial pressure such as headaches or nausea (1). They account for 39% of all tumors and 54.5% of all non-malignant primary intracranial tumors, with a median age of diagnosis of 66 years old. Incidence in the United States from 2014-2018 was 9.49/100,000, with a 2.3 higher incidence in women and more common among non-Caucasian populations (2). Approximately 36,130 patients were diagnosed with meningiomas in 2021 in the United States alone. A large majority of meningiomas are benign with 80% being grade 1, 18.3% grade 2 or atypical, and 1.3% grade 3 or malignant. Prognosis of patients with meningioma correlates with tumor grade. In non-malignant meningiomas, overall 5-year survival of 88.2%, and 10-year survival of 83.7%, while 5-year survival of malignant meningiomas is 67.5% (3). Meningiomas have been historically reported in 4.6% of patients over 80 years old having one meningioma and 8.2% having multiple at

time of autopsy (4). However, a recent review evaluating incidental radiographic discovery of meningiomas found an overall rate of 0.52% in the general population (5). Most meningiomas are asymptomatic at time of presentation (6).

While a majority of meningiomas are sporadic, a subset of cases is associated with familial syndromes. Neurofibromatosis type 2 (NF2) is the most common of these hereditary syndromes, but increased risk of meningioma formation also occurs in multiple endocrine neoplasia (MEN) type 1, von Hippel-Lindau (VHL), Li-Fraumeni syndrome, Gorlin syndrome, Cowden syndrome, nevoid basal cell carcinoma syndrome, BAP1 tumor predisposition syndrome, Rubinstein-Taybi Syndrome, and familial meningiomatosis (7). Through identification of this predisposition and subsequent investigation of the genetic alterations within these syndromes, we hope to contribute to a greater understanding of pathogenesis of the sporadic disease as well.

Radiographic features predictive of grade and outcomes

While meningiomas can have a variable appearance on computerized tomography (CT) and magnetic resonance (MR) imaging, there are characteristic imaging features that allow for a confident and accurate imaging diagnosis. Classically, meningiomas are seen as avidly enhancing and sharply marginated extra-axial masses with a broad based dural attachment and associated smooth dural enhancement (the dural "tail"). There may be adjacent dural involvement with increased enhancement, nodularity, or thickening compared to uninvolved dura. Meningiomas are typically isointense to grey matter on T1 weighted (T1W) and T2 weighted (T2W) MR imaging as well as being isodense to grey matter on non-contrast CT (NCCT) imaging. Meningiomas may have calcifications which are seen best on NCCT and on susceptibility weighted imaging (SWI) MR images. Hyperostosis of the adjacent calvarium is a common imaging finding which is also seen best on NCCT and can be seen with both reactive osseous changes as well as calvarial invasion by meningioma. While these tumors are most often associated with dural structures, they also arise less frequently within the ventricles or optic nerve sheath. As meningiomas grow, they can displace and compress the adjacent brain leading to a CSF cleft seen between meningioma and brain seen best on T2W MR imaging. Meningiomas can invade the underlying brain. Adjacent brain vasogenic edema is also a common imaging finding and can be seen both with and without brain invasion.

Given the variability of radiographic appearance of meningiomas and wide range of pathologies that may involve the dura including inflammatory and infectious etiologies, as well as, hematologic and metastatic malignancies, additional imaging strategies are valuable to assist in accurate diagnosis. More effective imaging technologies are needed to help diagnose various types of meningiomas, as well as, to distinguish meningioma grades. While MR perfusion may help distinguish between meningiomas from some dural-based metastases, there are no MR perfusion findings that are diagnostic for meningiomas which have been shown to have similar hyperperfusion to Merkel cell carcinoma, renal cell carcinoma, and melanoma (8).

Attempting to radiographically determine meningioma grade remains a persistent challenge. Lee EJ et al. reported from 232 patient that only 25.4% showed rapid growth in 5-year interval follow-up (9). In addition, the authors showed that tumor size, absence of calcification, peritumoral edema and hyperintense or isointense signal on T2-weighted MRI were predictors of tumor growth (9). Studies have reported that heterogeneous enhancement, lack of distinct space separating tumor from adjacent brain (10), increased hyperintensity on apparent diffusion coefficient (ADC) (11, 12), and differential activity on O-(2-[18F]fluoroethyl-)-L-tyrosine (F-FET) positron emission tomography have been reported to be associated with higher histologic grade (13). Given the complexity of often subtle differences in radiographic appearance, groups have utilized radiomics and machine learning in an effort to provide better predictive models for meningioma subtyping. However, these studies are limited by the methodology of machine learning, particularly the single or limited-center retrospective patient populations that limit generalizability (14). Gallium-68-DOTATATE PET/CT which targets the somatostatin receptor 2 (SSTR2) has shown utility in meningioma radiographic diagnosis and distinguishing from other pathologies (15). A study found that increased uptake by DOTATE PET/CT is correlated with increased growth rate in grade 1 and 2 meningiomas, though prognosis could not be made grade 3 meningiomas (16). Furthermore, DOTATATE PET/CT allows for a greater delineation between meningioma and other adjacent physiologically contrast enhancing structures, such as pituitary tissue or venous sinuses, as well as post treatment effects (17). The combination of MRI and DOTATATE PET/CT can also aid surgical planning with the goal of maximizing extent of resection as well as improving radiation therapy target planning (18). Beyond diagnosis and grading of meningiomas, the standardization of nomenclature for assessing radiographic response of a known meningioma to treatment has also been described by the Response Assessment in Neuro-Oncology (RANO) working group as complete response (resolution of lesions for at least 8 weeks), partial response (>50% decrease from baseline), minor response (25-50% decrease), progressive disease (>25% growth from baseline), and stable disease (19). These categories allow for more effective reporting and comparison of groups reporting results in effort to determine novel or improved treatment strategies.

Histopathologic features and current classification

While advances in imaging technique and technology may lead to more effective diagnosis in the future, the gold standard

for diagnosis remains tissue analysis. Histologically, meningiomas are typically characterized on H&E staining by whorls of cells with nuclear pseudo-inclusions, pseudo-syncytial growth, and psammoma bodies representing circular calcifications. Additionally, immunohistologic staining positivity for Somatostatin Receptor 2a (SSTR2a) is diagnostic (20). The World Health Organization (WHO) classification scheme for central nervous system tumors categorizes meningiomas into 15 subtypes. Thereafter, the 2016 update added histologic evidence of brain invasion with mitotic count greater than 4, or having 3 of 5 features: necrosis, loss of whirling or fascicular architecture, prominent nucleoli, high cellularity, and cells with high nuclear to cytoplasmic ratio as being diagnostic of atypical, grade 2, meningioma (21). However, reproducibility of grading remained a challenge with one study reporting only 87.2% agreement of meningioma grade between different observers involved in a multicenter trial (22). The 2021 WHO classification clarified several historically used diagnostic criteria. Previously, choroid and clear cell meningioma subtypes were classified as grade 2, while rhabdoid and papillary subtypes were classified as grade 3. However, the authors indicate that though meningiomas with these histologic appearances largely fall within those grades, that appearance alone should not determine the grade, but rather by the grading criteria introduced in 2016. The 2021 update additionally reports commonly altered genes in meningiomas, but largely does not use them as grading criteria with the exception of CDKN2A/B homozygous deletion and TERT promoter mutation as diagnostic for grade 3 meningiomas (23).

The introduction of genetic alterations into meningioma grading reflects a growing body of evidence for the utility of greater understanding of genetic and molecular profiling in meningiomas.

Molecular features in meningiomas

Historically, clinicians have relied only on histological features for classification into three pathological grades. In 2021, the World Health Organization (WHO) Classification of the Central Nervous System (CNS) newly included a series of molecular biomarkers. For the purpose of grading, the classification scheme lists SMARCE1 (clear cell subtype), BAP1 (rhabdoid and papillary subtypes), and KLF4/TRAF7 (secretory subtype) mutations. Separate from grading, TERT promoter mutation, homozygous deletion of CDKN2A/B, and loss of nuclear H3K27me3 expression were included as being indicators of poor prognosis (23).

A genomic study of 300 meningiomas showed mutations in *TRAF7* in approximately 25% of all meningiomas, AKT1 mutations in 10-15% (affecting the PI3K signaling pathway) and KLF4 mutations in 10%. SMO mutations which activate Hedgehog signaling were identified in 5% of non-*NF2* mutant meningiomas and *NF2* and/or chromosome 22 loss were more likely to be atypical meningiomas (24). Furthermore, such mutations were correlated to anatomical tumor location and traditional histological analysis (24, 25). SMARCE1 heterozygous loss of function mutation has been associated with spinal meningiomas and in tumors with clear-cell histology (26). TERT promoter mutation was found to be key in meningiomas undergoing malignant histological progression and predictor for poor survival (27–29).

The impact of molecular profiling of meningioma has been studied and validated to predict clinical courses that affect the post-operative management including imaging surveillance and need for adjuvant radiation (30–33). WHO grades II and III meningiomas have aggressive clinical courses, although poor outcomes may occur in a subset of low-grade lesions. Youngblood et al. found that low grade meningiomas harboring a particularly genomic group (Hedgehog, NF2, PI3K and TRAF7) recurred at rate 21.9 times higher and 17.2 times higher than would be expected given their more benign histopathology (30). Patel et al. analyze 160 meningiomas by classifying in 3 groups base on molecular profile and found increased expression of FOXM1 and MYBL2 causing DREAM complex loss of its repressive activity associated with recurrence (31). This genomic event represented aggressive tumor behavior, and 79% of a sub-group tumors showed a genomic loss of both 1p and 22q (31).

A large cohort retrospective study attempted an integrated scoring system that included histology and molecular risk stratification proving higher accuracy in clinical outcomes, including stratification by DNA methylation (32). Vasudevan et al. found FOXM1 targets accounted for 11% of genes enriched in WHO grade III meningiomas, compared with only 3% of genes in WHO grade I meningiomas, correlating this gene to poor clinical outcomes (33). Furthermore, Magill et al. analyze intratumor heterogeneity suggesting that the loss of chromosome 22q is an early event that tumor evolution, but prove spatially distinct patterns of FOXM1, CDH2, and PTPRZ1 expression providing understanding why meningiomas grow asymmetrically (34).

There is limited data from *in vivo* models to identify key drivers of meningioma cell invasion that may play a role in the mechanism of recurrences, prognostication, and potential targets for therapies of high grade meningiomas. Erson-Omay et al. recently demonstrated that sporadic multiple meningiomas in the same patient can show both genomic and histologic heterogeneity (35). These tumors can have both mono- and multi-clonal origin which can be observed in both NF2-loss and non-NF2 mutant tumors. In addition, those monoclonal multiple meningiomas can acquire inter-tumor heterogeneity due to additional somatic alterations through branched evolution (35). Nigim et al. analyzed the expression of β1 integrin of clinical meningioma specimens and found *in vivo* murine model utilizing two patient-derived high grade

meningioma xenografts, that antibody therapy targeting β1 integrin decreased high grade meningioma cells proliferation and extended overall survival (36). A preclinical study found that 9% of 108 meningiomas demonstrated mutations in the PI3K/AKT/mTOR pathway, suggesting it may play an important role in the growth of meningiomas (37). However, a phase II trial and two retrospective studies failed to show efficacy of bevacizumab and everolimus in patients with recurrent high grade meningiomas (38–40). Appears to be that genetic profiling of meningioma in the next decade will provide prognostication in risk profile stratification for recurrence, risk of malignant progression or transformation and potentially improve efficacy of current target therapies.

Molecular classification schemes for meningiomas

Meningiomas have historically been classified based on histological appearance into 15 histologic subtypes. However, with advances in genetic and epigenetic underpinnings of meningioma pathogenesis several molecular classification schemes have been described with the intent of developing clinically relevant tools.

Classification based on genetic alterations

Approximately 80% of sporadic meningiomas harbor mutations in one of seven genes or pathways, prompting a potential classification scheme on that basis (Table 1). The seven subgroups are 1) Ne*urofibromitosis-2* (NF2) with or without SMARCB1, 2)*TNF Receptor-Associated Factor* 7 (TRAF7) alone, 3)TRAF7 with *Kruppel-Like Factor 4* (KLF4), 4) phosphoinositide 3-kinase (PI3K) pathway including PIK3CA, PIK3R11, and AKT1, 5) Hedgehog (HH) pathway including SMO, SUFU, PRKARIA, 6) RNA Polymerase II Subunit A (PPOL-R2A), and 7) SMARCE1, with over 50% of tumors being within the first subgroup, NF2 mutations (41). There are multiple observed patterns supporting this classification system and its clinical relevance. Meningiomas in different anatomic locations reliably follow these subgroups. For example, HH pathway mutations all localize to the midline anterior skull base, while NF2 plus SMARCB1 mutated tumors involve the falx (42). BAP1 mutant meningiomas localize to cerebral convexities, while SMO mutant meningiomas are located in the anterior skull base, but not midline. Posterior fossa meningiomas harbor mutations in NF-2, POLR2A, or AKT1E17K (43).

Furthermore, the different subgroups may have different epidemiology and clinical behavior. NF2 mutant tumors are often larger, atypical with a more aggressive clinical course, associated with preoperative seizures, and found in a greater proportion of male patients (44) (42). Among the six non-NF2 mutant subtypes, the TRAF7 mutated alone subtype is the most common in 25% of sporadic meningiomas (41) and is associated with a higher grade (42). Conversely, the HH pathway altered tumors are associated with less aggressive clinical behavior (45). By developing genetic classification systems, there may be benefit in the ability to identify patients that have greatest potential benefit from targeted therapies.

TABLE 1 Meningioma classification based on genetic mutations.

Genetic Mutation Subgroup	Clinical features
NF2	Most common, larger, more aggressive course. Highest seizure risk. Male predominance (1). Falcotentorial location (2).
TRAF7	Second most common. associated with higher grade. Higher likelihood of hyperostosis (1) Midline and lateral skull base location (2).
TRAF7 with KLF4	High peritumor edema (1). Midline and lateral skull base location (2).
PI3K Pathway	Low recurrence risk (3) Midline and lateral skull base location (2).
HH pathway	Less aggressive, low grade (1). Localize to midline anterior skull base (2).
PPOL-R2A	Benign, female predominance. Sella, clivus, and posterior fossa location (2).
SMARCE1	High recurrence risk (1), faster growth. Lateral skull base, anterior falcine location (2).

Classification based on epigenetic factors

In addition to genetic mutations and alterations, patterns of epigenetic alterations have also been discovered. An evaluation of the transcriptome of 160 meningiomas including all grades and subsequent clustering analysis identified three molecular subtypes of meningiomas (Table 2). When this analysis was then applied to other databases, the three subtypes predicted progression free survival more accurately than traditional WHO grading, as well as PFS of tumors of different molecular subtypes within each WHO grade (31).

Furthermore, a retrospective DNA methylation analysis was performed on 479 patients to identify six methylation classes, which was then compared to genetic mutations and RNA sequencing findings (46). The investigators reported that while the system of six classes based on DNA methylation did have significant and consistent overlap with particular histologic or genetic subtypes, when they did not match, the clinical behavior was better predicted by methylation class. For example, a tumor graded as atypical but harboring a methylation classification typically seen in benign meningiomas would behave as a grade 1

10.3389/fonc.2022.962702

TABLE 2 Meningioma classification based on transcriptome analysis.

Transcriptome Subtypes	Features
Type A	Low proliferation index. Anterior skull base. 2:1 female to male. No significant chromosomal changes. Only type with TRAF7. High prevalence of KLF4 and AKT1. No NF2 mutations.
Type B	Intermediate proliferation index. 2:1 female to male. Significant prevalence of loss of chr22q. NF2 mutations. Highest prevalence of SMARCB1.
Type C	High proliferation index. Falcine, occipital regions. 56% male. Significantly shorter PFS than Type A or B irrespective of WHO grade. In addition to NF2, numerous chromosomal abnormalities.

tumor as well as the reverse (46). These findings suggest that by having classification systems that can more accurately predict tumor behavior, clinicians can more effectively make treatment decisions such as the use of more aggressive therapies versus observation. These findings were corroborated by a recent study utilizing DNA methylation profiling of over 500 meningiomas to project clinical outcomes based on categorization into three subtypes. The authors found that Merlin-intact (NF2 wild-type) subtype have the best outcome, followed by the immune enriched, and hypermitotic subtypes. The hypermetabolic subtype was associated with CDKN2A/B hypermethylation and NF2 loss, and a majority of these tumors are grade 2 or 3 (47).

Integration of molecular alterations

Due to the complexity of differing classification schemes, Nassiri et al. (48) developed an integrated system with four groups, which they designate molecular groups 1 through 4 (MG1-MG4). The molecular groups were determined by integrating clustering found in DNA methylation and mRNA abundance clusters. Histologic grades were spread between molecular groups with MG1 containing grade 1 and grade 2 meningiomas, while MG2 through MG4 contained all grades. However, grade 2 and 3 tumors were increased in MG3 and MG4. When correlated with clinical behavior of these tumors, MG3 and 4 tumors were found to have lower progression-free survival than MG1 and 2 tumors irrespective of histologic grade. Almost all MG1 tumors contained NF2 mutations, while mutations in TRAF7, AKT1, KLF4, and POLR2A were found only in MG2 tumors. MG3 and MG4 tumors had significantly enriched mutations in epigenetic regulatory genes and tumor suppressor genes compared to MG1 and 2. MG1 tumors were typically diploid, though with chromosome 22q loss corresponding to NF2 loss. MG2 tumors fell into two categories: copy number neutral with point mutations, and lack of point mutations but with corresponding chromosomal polysomies on locations for TRAF7, AKT1, KLF4, or SMO. MG3 and MG4 tumors had high levels of aneuploidy and interchromosomal fusions. Some MG4 tumors additionally demonstrated gain of chromosome 1q and loss of chromosome 10. These alterations and further proteomics to investigate resulting changes to gene products led the group to attribute characteristics to the subgroups. MG1 tumors were immunogenic, MG2 tumors were benign NF2 wild-type, MG3 were hypermetabolic, and MG4 were highly proliferative (48).

Current treatment modalities

Although the overwhelming majority of meningiomas are histologically benign, meningiomas can present as a significant source of physical and psychological morbidity in patients. Even in absence of symptoms that may affect a patient's functional status, health-related quality of life (HRQOL) scores are decreased in patients secondary to awareness of an intracranial tumor and subsequent psychological distress from anxiety and depression (49). Neurocognitive and neurological symptoms resulting in physical limitations from symptomatic meningiomas further impair quality of life. Treatment of the lesion by surgery or radiation therapy as appropriate, conversely, improves HRQOL scores from pre-treatment baseline, though it may not improve to the level of the general population without this disease (49). As such, effective treatment of meningiomas and minimization of deleterious treatment sequelae provides benefit to many patients.

Given the frequency of incidentally discovered meningiomas, it may be reasonable to observe with clinical and radiographic follow-up in patients without symptoms. Though there is no consensus regarding the best protocol for observation, an initial interval of 6 months with subsequent annual surveillance has been proposed (50). Alternatively, patients can be reevaluated in 3 months, then 9 months, and subsequently annually (51). One limitation of observation is lack of pathologic diagnosis confirming meningioma and inability to definitively grade the lesion. Furthermore, meningioma growth can vary widely based on grade. Overall, meningiomas have been reported to grow at an average of 0.24cm per year (51) or 2% per year in a single axis, approximately 5.8% in volume (52). However, in studies where grade was subsequently obtained, grade 2 and grade 3 meningiomas grow significantly more rapidly than their benign counterparts (53). Though atypical and anaplastic may have over double the growth rate of grade 1, they may be comparable to one another (54). Besides grading, meningiomas in different locations may have different growth patterns, with one meta-analysis suggesting that skull base meningiomas grow significantly slower than other locations (55).

If significant growth of a presumed meningioma is discovered or the lesion is symptomatic at time of diagnosis, treatment is warranted if the patient is otherwise a good candidate. Currently, initial treatment modalities are limited to surgery and radiation therapy. Traditionally, the mainstay of treatment for meningiomas is surgical resection, which provides pathologic diagnosis, disease control, and typically ameliorates symptoms such as focal neurologic deficits, sequelae of elevated intracranial pressure, or seizures. The gold standard scale for meningioma resection grading, the Simpson Grade, was first described in 1957 and includes degree of resection not only of the macroscopic tumor, but also of adjacent involved dura, and any involved bone (56). Multiple grading systems have since been proposed as adjuvant treatment modalities have been developed to supplant surgery alone (57). While the Simpson grading system remains debated, more aggressive resection, when able to be safely performed, does confer improved progression-free and overall survival in patients with meningioma. While most dramatic in non-benign meningiomas, it remains significant in grade 1 pathology as well (58). Extent of resection affects progression free and overall survival in atypical meningiomas (59). Patients with atypical meningiomas have 5-year survival of 91.3% and 78.2% with gross total resection and non-gross total resection, respectively. Furthermore, patients with malignant meningioma have 5-year survival of 64.5% and 41.1% with gross total resection and non-gross total resection, respectively (60). However, meningiomas located at the skull base, where the surgical corridor is often limited or where tumor closely involves neurologic or vascular structures, precludes surgical resection of involved dura and bone or even macroscopic tumor.

Non-surgical treatment modalities, both standalone, as well as adjuvant have become increasingly utilized. The least invasive approach aside from observation is radiation alone. A recent meta-analysis found significantly higher progression-free survival in patients that underwent stereotactic radiosurgery *via* gamma knife compared to observation alone with at 5- and 10-year follow up and tumor control of 95% at 5 and 10 years. However, the included studies reported a range of complications of 8.3-39.1%, though most were temporary and either self-limited or addressed with steroids. Loss of tumor control was associated with T2 hyperintensity within the tumor, tumor size, and lack of calcification on imaging (61). However, given the lack of pathologic diagnosis, loss of tumor control may be dependent on tumor grade.

As a result of greater understanding of the risk of recurrence in non-benign meningiomas, radiation as adjuvant treatment after surgery has become increasingly investigated and there are conflicting data reported. A review of retrospective studies suggested the utility of adjuvant stereotactic radiosurgery or external beam radiotherapy in grade 3 and subtotally resected grade 2 meningiomas, which have higher risk of recurrence (62). Subsequently, the phase II trial RTOG 0539 reported 93.8% 3-year progression free survival in intermediate-risk patients with completely resected grade 2 meningiomas and recurrent grade 1 meningiomas that then underwent adjuvant radiation therapy (63) white those considered high risk; grade 3 meningiomas, subtotally resected grade 2 tumors, or recurrent grade 2 tumors; experienced a 3-year PFS of 58.8% after adjuvant therapy (64). A recent meta-analysis of 30 studies found that literature on the subject has been highly variable, with an overall improved progression-free survival without significant change in overall survival in patients that had gross total resection. However, the largest study currently in the literature is a recent single institution study of 170 patients. The authors report that use of adjuvant radiation therapy (89% of patients receiving at least 60Gy) significantly improved progression-free and overall survival in atypical meningiomas in both completely and incompletely resected tumors (65). Due to the heterogeneity of current clinical practice, an ongoing clinical trial is evaluating observation versus radiation therapy in postoperative patients who had gross total resection of an atypical meningioma (NCT03180268 Clinicaltrials.gov). Furthermore, a phase II trial investigating proton-beam radiation treatment in all meningioma grades is underway (NCT04278118) to evaluate the use of this new technology, as well as carbon ion radiotherapy in atypical meningiomas (NCT01166321).

There is no established systemic therapy that has been shown to effectively treat recurrent meningioma or to increase survival. A variety of systemic agents such as chemotherapy, immunotherapy, hormonal therapy, somatostatin analogues, and radionuclide therapy have been or are currently being studied. Nevertheless, there is no strong evidence that any these agents affect the natural history of recurrent meningioma.

Targeted therapies for meningiomas and future directions

Targeted therapies are not currently included in the standard of care for treatment for meningiomas. Chemotherapies including hydroxyurea, temozolomide, irinotecan, and trabectedin have been investigated without clear efficacy. However, use of hormone receptor antagonistic medications, supported by the findings of these receptors in a subset of meningiomas, has been historically attempted with inconsistent results (66), at least in large part because of heterogeneity with how trials studies have been designed, results evaluated, and findings report (67). Tamoxifen, which binds the estrogen receptor, and mifepristone, which binds the progesterone receptor, have been investigated in decades prior. Unfortunately, these primarily small studies showed potential minor response in some patients, with the largest of which showing no efficacy compared to placebo (68).

NEO100, an intranasal administered purified form of perillyl alcohol, has been demonstrated in pre-clinical studies to target multiple pathogenic pathways by affecting the cyclin dependent kinase pathway in the cell cycle, endoplasmic reticulum stress, the JNK-stress response, telomerase function *via* disrupting

TERT and mTOR protein complex formation, the Na/K ATPase, NOTCH, NF-kb, and TGFb, each resulting in anti-proliferative or tumoricidal properties (69). This treatment is now undergoing a phase II study in use of residual, progressive, or recurrent grade 2 and 3 meningiomas (NCT05023018).

However, as genetic and epigenetic alterations and their involved cellular pathways are identified in meningioma pathogenesis, groups are investigating more targeted therapies for these tumors in an effort to provide new clinical treatments. The VEGF pathway has been targeted due to its two-fold elevation in atypical meningiomas and ten-fold elevation in anaplastic tumors. Bevacizumab, which targets circulating VEGF has been reported in retrospective studies to increase progression-free survival (38, 39), while a phase II trial of sunitinib, a RTK inhibitor with antagonistic effect on VEGF receptor functioning demonstrated improved progression free survival in grade 2/3 meningiomas (Kaley 2015). Apatinib, which targets the VEGF receptor directly is being investigated in a phase II clinical trial in grade 2/3 meningiomas (NCT0501705).

The AKT1 mutant pathway has also been targeted in a case report of the use of AZD5363, a AKT inhibitor, in a patient with numerous AKT1 mutant meningiomas resulted in partial response followed by long-term progression free survival (70). Pre-clinical studies of cultured meningioma cell lines from NF2 found targeting of the histone deacetylase (HDAC)resulted in decreased AKT activation and decreased cellular growth, as well as, decreased tumor size in mouse models. Thereafter, AR-42 (REC-2282), a HDAC inhibitor was investigated in two small pilot studies in NF2 patients, which report partial response or stability in four patients and progression in three patients (71). As a result of these findings, a phase II/III trial of REC-2282 in NF2 patients with meningiomas, as well as sporadic meningiomas with NF2 mutations has begun (NCT05130866). AKT is within the mTOR and PI3K pathways, which are being investigated in clinical trials targeting mTOR (NCT03071874) and PI3K (NCT03631953) directly. Also, the trial NCT02523014 incorporates AKT targeting, as well as 3 other arms targeted inhibitors in tumors with mutations in SMO, NF2, and focal adhesion kinase (FAK) (Table 3).

Given the prevalence of somatostatin receptor expression in meningiomas, octreotide and pasireotide, somatostatin receptor antagonists, have been investigated, with some reports of increased progression free survival compared to historical controls, but without evidence of partial or complete responses (72–75). However, new types of drugs may still utilize this target by another mechanism. Multiple studies are investigating the use of somatostatin antagonists with Lu177 radionucleotides that are internalized by the receptor-positive tumors cells and causes DNA damage resulting in cytotoxicity in other SSTR-positive tumors such as neuroendocrine tumors (76). These drugs, Luthera (NCT03971461) and 177Lu-DOTA-JR11 (NCT04997317) have varying levels of affinity for the sstr2 target.

Immune evasion has been a growing field of research and clinical development in a variety of solid tumors. Studies have found predominantly immunosuppressive type macrophages in AKT1 mutated meningiomas, while NF2 gene mutated tumors have high levels of immune active macrophages. Furthermore,

TABLE 3 Current clinical trials investigating medical therapies for meningioma.

Agent	Phase	Pathology	Identifier	Status	Estimated Completion
NEO100	Phase 2	Grade 2, 3	NCT05023018	Not yet recruiting	2025
Apatinib	Phase 1/2	Grade 2, 3	NCT04501705	Recruiting	2025
REC-2282	Phase 2/3	NF2-mut,all grades	NCT05130866	Not yet recruiting	2027
Vistusertib (AZD2014)	Phase 2	Recurrent grade 2,3	NCT03071874	Active, not recruiting	2024
Alpelisib and Trametinib	Phase 1	Grade 1, 2, 3	NCT03631953	Recruiting	2022
Vismodegib, GSK2256098, Capivasertib, Abemaciclib	Phase 2	Grade 1, 2, 3	NCT02523014	Recruiting	2024
177Lu-DOTATATE	Phase 2	Grade 1, 2, 3 (DOTATATE PET pos)	NCT03971461	Recruiting	2023
177Lu-DOTA-JR11, 177Lu-DOTATOC	Phase 1/2	Grade 1, 2, 3 (DOTATATE PET pos)	NCT04997317	Recruiting	2025
Nivolumab, Ipilimumab	Phase 2	Grade 2, 3	NCT02648997	Recruiting	2023
Nivolumab with SRS, Ipilimumab	Phase 1/2	Grade 2, 3	NCT03604978	Recruiting	2022
Pembrolizumab	Phase 2	Grade 1, 2, 3	NCT03279692	Active, not recruiting	2025
Sintilimab	Phase 1/2	Grade 3	NCT04728568	Recruiting	2025
Avelumab, Proton Radiation	Phase 1b	Grade 1, 2, 3	NCT03267836	Active, not recruiting	2025

1.Robert, S.M., et al., The integrated multiomic diagnosis of sporadic meningiomas: a review of its clinical implications. J Neurooncol, 2021.
2.Youngblood, M.W., et al., Correlations between genomic subgroup and clinical features in a cohort of more than 3000 meningiomas. J Neurosurg, 2019: p. 1-10.
3.Proctor, D.T., et al., Towards Molecular Classification of Meningioma: Evolving Treatment and Diagnostic Paradigms. World Neurosurg, 2018. **119**: p. 366-373.

circulating myeloid derived suppressor cells (MDSCs) are elevated in patients with meningiomas suggesting an effect on the systemic immune response and intra-tumoral MDSCs, as well as, immunosuppressive T regulatory cells (Tregs) are greater in high grade meningiomas compared to benign tumors (77). A possible target for therapies is *via* immune checkpoint pathways which are, in normal physiology, a mechanism to prevent autoimmunity by suppressing T-cell activity. TRAF-7 mutated meningiomas demonstrated elevated levels of programmed death ligand-1 (PD-L1), the major ligand for the programmed death checkpoint pathway, while PD-L2 is highly expressed in PI3K/AKT/mTOR pathway mutations and CTLA-4 was frequently expressed in PIK3CA and SMO mutated tumors. Elevated PD-L1 expression has been found in atypical and anaplastic meningiomas compared to benign (78), but a significant correlation between expression and survival has not yet been established (77).

Multiple phase I/II clinical trials are underway investigating immune modulating checkpoint inhibitors. The use of ipilimumab (NCT03604976) targeting CTLA-4, and nivolumab (NCT03604978) targeting PD-1, as well as, both medications together (NCT02648997) in conjunction with stereotactic radiosurgery in recurrent atypical and anaplastic meningiomas is currently being investigated. Other checkpoint inhibitors are also undergoing investigation as sole treatment targeting the programmed death pathway without radiation (NCT03279692), as well as, neoadjuvant treatment alone (NCT04728568) or in addition to neoadjuvant proton radiation (NCT03267836) prior to reresection.

Conclusion

The diagnosis and treatment of meningiomas has remained a clinical challenge greatly affected by evolutions in understanding of natural history, epidemiology, pathogenesis, and treatment modalities. Advances in genetics and epigenetics have permitted further molecular classification of meningiomas as well as identification of molecular determinants of treatment response in meningioma. With the advent and refinement of novel technologies, clinically meaningful developments are emerging that may markedly revolutionize the management for these tumors in the future.

Author contributions

AE contributed to conception of the manuscript. JL and AE contributed to the design of the manuscript. JL, SR, and GF-M contributed to data acquisition/assessment/review, creation of initial manuscript/tables, and critical review and revision of the manuscript. JA, RM, JKCL, AB-F, NT, MV, and AE contributed to critical review and revision of the manuscript. All authors contributed to the article and approved the submitted version.

Conflict of interest

The authors declare that the research was conducted in the absence of any commercial or financial relationships that could be construed as a potential conflict of interest.

Publisher's note

All claims expressed in this article are solely those of the authors and do not necessarily represent those of their affiliated organizations, or those of the publisher, the editors and the reviewers. Any product that may be evaluated in this article, or claim that may be made by its manufacturer, is not guaranteed or endorsed by the publisher.

References

1. Magill ST, Young JS, Chae R, Aghi MK, Theodosopoulos PV, McDermott MW, et al. Relationship between tumor location, size, and WHO grade in meningioma. *Neurosurg Focus* (2018) 44(4):E4. doi: 10.3171/2018.1.FOCUS17752

2. Anzalone CL, Glasgow AE, Van Gompel JJ, Carlson ML. Racial differences in disease presentation and management of intracranial meningioma. *J Neurol Surg B Skull Base* (2019) 80(6):555–61. doi: 10.1055/s-0038-1676788

3. Ostrom QT, Cioffi G, Waite K, Kruchko C, Barnholtz-Sloan JS. CBTRUS statistical report: Primary brain and other central nervous system tumors diagnosed in the united states in 2014-2018. *Neuro Oncol* (2021) 23(12 Suppl 2): iii1–iii105. doi: 10.1093/neuonc/noab200

4. Nakasu S, Hirano A, Shimura T, Llena JF. Incidental meningiomas in autopsy study. *Surg Neurol* (1987) 27(4):319–22. doi: 10.1016/0090-3019(87)90005-X

5. Chamoun R, Krisht KM, Couldwell WT. Incidental meningiomas. *Neurosurg Focus* (2011) 31(6):E19. doi: 10.3171/2011.9.FOCUS11220

6. Naslund O, Skoglund T, Farahmand D, Bontell TO, Jakola AS. Indications and outcome in surgically treated asymptomatic meningiomas: a single-center case-control study. *Acta Neurochir (Wien)* (2020) 162(9):2155–63. doi: 10.1007/s00701-020-04244-6

7. Kerr K, Qualmann K, Esquenazi Y, Hagan J, Kim DH. Familial syndromes involving meningiomas provide mechanistic insight into sporadic disease. *Neurosurgery* (2018) 83(6):1107–18. doi: 10.1093/neuros/nyy121

8. Kremer S, Grand S, Rémy C, Pasquier B, Benabid AL, Bracard S, et al. Contribution of dynamic contrast MR imaging to the differentiation between dural metastasis and meningioma. *Neuroradiology* (2004) 46(8):642–8. doi: 10.1007/s00234-004-1194-2

9. Lee EJ, Kim JH, Park ES, Kim YH, Lee JK, Hong SH, et al. A novel weighted scoring system for estimating the risk of rapid growth in untreated intracranial meningiomas. *J Neurosurg* (2017) 127(5):971–80. doi: 10.3171/2016.9.JNS161669

10. Lin BJ, Chou KN, Kao HW, Lin C, Tsai WC, Feng SW, et al. Correlation between magnetic resonance imaging grading and pathological grading in meningioma. *J Neurosurg* (2014) 121(5):1201–8. doi: 10.3171/2014.7.JNS132359

11. Zhang H, Rödiger LA, Shen T, Miao J, Oudkerk M. Preoperative subtyping of meningiomas by perfusion MR imaging. *Neuroradiology* (2008) 50(10):835–40. doi: 10.1007/s00234-008-0417-3

12. Azizyan A, Eboli P, Drazin D, Mirocha J, Maya MM, Bannykh S. Differentiation of benign angiomatous and microcystic meningiomas with extensive peritumoral edema from high grade meningiomas with aid of diffusion weighted MRI. *BioMed Res Int 2014* (2014) 2014:650939. doi: 10.1155/2014/650939

13. Cornelius JF, Stoffels G, Filß C, Galldiks N, Slotty P, Kamp M, et al. Uptake and tracer kinetics of O-(2-(18)F-fluoroethyl)-L-tyrosine in meningiomas: preliminary results. *Eur J Nucl Med Mol Imaging* (2015) 42(3):459–67. doi: 10.1007/s00259-014-2934-0

14. Ugga L, Perillo T, Cuocolo R, Stanzione A, Romeo V, Green R, et al. Meningioma MRI radiomics and machine learning: systematic review, quality score assessment, and meta-analysis. *Neuroradiology* (2021) 63(8):1293–304. doi: 10.1007/s00234-021-02668-0

15. Rachinger W, Stoecklein VM, Terpolilli NA, Haug AR, Ertl L, Pöschl J, et al. Increased 68Ga-DOTATATE uptake in PET imaging discriminates meningioma and tumor-free tissue. *J Nucl Med* (2015) 56(3):347–53. doi: 10.2967/jnumed.114.149120

16. Sommerauer M, Burkhardt JK, Frontzek K, Rushing E, Buck A, Krayenbuehl N, et al. 68Gallium-DOTATATE PET in meningioma: A reliable predictor of tumor growth rate? *Neuro Oncol* (2016) 18(7):1021–7.

17. Galldiks N, Albert NL, Sommerauer M, Grosu AL, Ganswindt U, Law I, et al. PET imaging in patients with meningioma-report of the RANO/PET group. *Neuro Oncol* (2017) 19(12):1576–87. doi: 10.1093/neuonc/nox112

18. Mahase SS, Roth O'Brien DA, No D, Roytman M, Skafida ME, Lin E, et al. [(68)Ga]-DOTATATE PET/MRI as an adjunct imaging modality for radiation treatment planning of meningiomas. *Neurooncol Adv* (2021) 3(1):vdab012.

19. Huang RY, Bi WL, Weller M, Kaley T, Blakeley J, Dunn I, et al. Proposed response assessment and endpoints for meningioma clinical trials: report from the response assessment in neuro-oncology working group. *Neuro Oncol* (2019) 21(1):26–36. doi: 10.1093/neuonc/noy137

20. Nowosielski M, Galldiks N, Iglseder S, Kickingereder P, von Deimling A, Bendszus M, et al. Diagnostic challenges in meningioma. *Neuro Oncol* (2017) 19(12):1588–98. doi: 10.1093/neuonc/nox101

21. Louis DN, Perry A, Reifenberger G, von Deimling A, Figarella-Branger D, Cavenee WK, et al. The 2016 world health organization classification of tumors of the central nervous system: a summary. *Acta Neuropathol* (2016) 131(6):803–20. doi: 10.1007/s00401-016-1545-1

22. Rogers CL, Perry A, Pugh S, Vogelbaum MA, Brachman D, McMillan W, et al. Pathology concordance levels for meningioma classification and grading in NRG oncology RTOG trial 0539. *Neuro Oncol* (2016) 18(4):565–74. doi: 10.1093/neuonc/nov247

23. Louis DN, Perry A, Wesseling P, Brat DJ, Cree IA, Figarella-Branger D, et al. The 2021 WHO classification of tumors of the central nervous system: a summary. *Neuro Oncol* (2021) 23(8):1231–51. doi: 10.1093/neuonc/noab106

24. Clark VE, Erson-Omay EZ, Serin A, Yin J, Cotney J, Ozduman K, et al. Genomic analysis of non-NF2 meningiomas reveals mutations in TRAF7, KLF4, AKT1, and SMO. *Science* (2013) 339(6123):1077–80. doi: 10.1126/science.1233009

25. Brastianos PK, Horowitz PM, Santagata S, Jones RT, McKenna A, Getz G, et al. Genomic sequencing of meningiomas identifies oncogenic SMO and AKT1 mutations. *Nat Genet* (2013) 45(3):285–9. doi: 10.1038/ng.2526

26. Smith MJ, O'Sullivan J, Bhaskar SS, Hadfield KD, Poke G, Caird J, et al. Loss-of-function mutations in SMARCE1 cause an inherited disorder of multiple spinal meningiomas. *Nat Genet* (2013) 45(3):295–8. doi: 10.1038/ng.2552

27. Maier AD, Stenman A, Svahn F, Mirian C, Bartek J Jr, Juhler M. TERT promoter mutations in primary and secondary WHO grade III meningioma. *Brain Pathol* (2021) 31(1):61–9. doi: 10.1111/bpa.12892

28. Juratli TA, Thiede C, Koerner MVA, Tummala SS, Daubner D, Shankar GM, et al. Intratumoral heterogeneity and TERT promoter mutations in progressive/higher-grade meningiomas. *Oncotarget* (2017) 8(65):109228–37. doi: 10.18632/oncotarget.22650

29. Goutagny S, Nault JC, Mallet M, Henin D, Rossi JZ, Kalamarides M, et al. High incidence of activating TERT promoter mutations in meningiomas undergoing malignant progression. *Brain Pathol* (2014) 24(2):184–9. doi: 10.1111/bpa.12110

30. Youngblood MW, Miyagishima DF, Jin L, Gupte T, Li C, Duran D, et al. Associations of meningioma molecular subgroup and tumor recurrence. *Neuro Oncol* (2021) 23(5):783–94. doi: 10.1093/neuonc/noaa226

31. Patel AJ, Wan YW, Al-Ouran R, Revelli JP, Cardenas MF, Oneissi M, et al. Molecular profiling predicts meningioma recurrence and reveals loss of DREAM complex repression in aggressive tumors. *Proc Natl Acad Sci USA* (2019) 116(43):21715–26. doi: 10.1073/pnas.1912858116

32. Maas SLN, Stichel D, Hielscher T, Sievers P, Berghoff AS, Schrimpf D, et al. Integrated molecular-morphologic meningioma classification: A multicenter retrospective analysis, retrospectively and prospectively validated. *J Clin Oncol* (2021) 39(34):3839–52. doi: 10.1200/JCO.21.00784

33. Vasudevan HN, Braunstein SE, Phillips JJ, Pekmezci M, Tomlin BA, Wu A, et al. Comprehensive molecular profiling identifies FOXM1 as a key transcription factor for meningioma proliferation. *Cell Rep* (2018) 22(13):3672–83. doi: 10.1016/j.celrep.2018.03.013

34. Magill ST, Vasudevan HN, Seo K, Villanueva-Meyer JE, Choudhury A, John Liu S, et al. Multiplatform genomic profiling and magnetic resonance imaging identify mechanisms underlying intratumor heterogeneity in meningioma. *Nat Commun* (2020) 11(1):4803. doi: 10.1038/s41467-020-18582-7

35. Erson-Omay EZ, Vetsa S, Vasandani S, Barak T, Nadar A, Marianayagam NJ, et al. Genomic profiling of sporadic multiple meningiomas. *BMC Med Genomics* (2022) 15(1):112. doi: 10.1186/s12920-022-01258-0

36. Nigim F, Kiyokawa J, Gurtner A, Kawamura Y, Hua L, Kasper EM, et al. A monoclonal antibody against beta1 integrin inhibits proliferation and increases survival in an orthotopic model of high-grade meningioma. *Target Oncol* (2019) 14(4):479–89. doi: 10.1007/s11523-019-00654-4

37. El-Habr EA, Levidou G, Trigka EA, Sakalidou J, Piperi C, Chatziandreou I, et al. Complex interactions between the components of the PI3K/AKT/mTOR pathway, and with components of MAPK, JAK/STAT and notch-1 pathways, indicate their involvement in meningioma development. *Virchows Arch* (2014) 465(4):473–85. doi: 10.1007/s00428-014-1641-3

38. Nayak L, Iwamoto FM, Rudnick JD, Norden AD, Lee EQ, Drappatz J, et al. Atypical and anaplastic meningiomas treated with bevacizumab. *J Neurooncol* (2012) 109(1):187–93. doi: 10.1007/s11060-012-0886-4

39. Lou E, Sumrall AL, Turner S, Peters KB, Desjardins A, Vredenburgh JJ, et al. Bevacizumab therapy for adults with recurrent/progressive meningioma: a retrospective series. *J Neurooncol* (2012) 109(1):63–70. doi: 10.1007/s11060-012-0861-0

40. Shih KC, Chowdhary S, Rosenblatt P, Weir AB3rd, Williams JT, Shepard GC, et al. A phase II trial of bevacizumab and everolimus as treatment for patients with refractory, progressive intracranial meningioma. *J Neurooncol* (2016) 129(2):281–8. doi: 10.1007/s11060-016-2172-3

41. Robert SM, Vetsa S, Nadar A, Vasandani S, Youngblood MW, Gorelick E, et al. The integrated multiomic diagnosis of sporadic meningiomas: a review of its clinical implications. *J Neurooncol* (2021) 156(2):205–14.

42. Youngblood MW, Duran D, Montejo JD, Li C, Omay SB, Özduman K, et al. Correlations between genomic subgroup and clinical features in a cohort of more than 3000 meningiomas. *J Neurosurg* (2019) p:1–10.

43. Pawloski JA, Fadel HA, Huang YW, Lee IY. Genomic biomarkers of meningioma: A focused review. *Int J Mol Sci* (2021) 22(19):10222.

44. Gupte TP, Li C, Jin L, Yalcin K, Youngblood MW, Miyagishima DF, et al. Clinical and genomic factors associated with seizures in meningiomas. *J Neurosurg* (2020) 4:1–10. doi: 10.1093/neuonc/noaa215.588

45. Boetto J, Apra C, Bielle F, Peyre M, Kalamarides M. Selective vulnerability of the primitive meningeal layer to prenatal smo activation for skull base meningothelial meningioma formation. *Oncogene* (2018) 37(36):4955–63. doi: 10.1038/s41388-018-0328-7

46. Sahm F, Schrimpf D, Stichel D, Jones DTW, Hielscher T, Schefzyk S, et al. DNA Methylation-based classification and grading system for meningioma: a multicentre, retrospective analysis. *Lancet Oncol* (2017) 18(5):682–94. doi: 10.1016/S1470-2045(17)30155-9

47. Choudhury A, Magill ST, Eaton CD, Prager BC, Chen WC, Cady MA, et al. Meningioma DNA methylation groups identify biological drivers and therapeutic vulnerabilities. *Nat Genet* (2022) 54(5):649–59. doi: 10.1038/s41588-022-01061-8

48. Nassiri F, Liu J, Patil V, Mamatjan Y, Wang JZ, Hugh-White R, et al. A clinically applicable integrative molecular classification of meningiomas. *Nature* (2021) 597(7874):119–25. doi: 10.1038/s41586-021-03850-3

49. Haider S, Taphoorn MJB, Drummond KJ, Walbert T. Health-related quality of life in meningioma. *Neurooncol Adv* (2021) 3(1):vdab089. doi: 10.1093/noajnl/vdab089

50. Goldbrunner R, Minniti G, Preusser M, Jenkinson MD, Sallabanda K, Houdart E, et al. EANO guidelines for the diagnosis and treatment of meningiomas. *Lancet Oncol* (2016) 17(9):e383–91. doi: 10.1016/S1470-2045(16)30321-7

51. Olivero WC, Lister JR, Elwood PW. The natural history and growth rate of asymptomatic meningiomas: a review of 60 patients. *J Neurosurg* (1995) 83(2):222–4. doi: 10.3171/jns.1995.83.2.0222

52. Zeidman LA, Ankenbrandt WJ, Du H, Paleologos N, Vick NA. Growth rate of non-operated meningiomas. *J Neurol* (2008) 255(6):891–5. doi: 10.1007/s00415-008-0801-2

53. Nakamura M, Roser F, Michel J, Jacobs C, Samii M. Volumetric analysis of the growth rate of incompletely resected intracranial meningiomas. *Zentralbl Neurochir* (2005) 66(1):17–23. doi: 10.1055/s-2004-836225

54. Jaaskelainen J, Haltia M, Laasonen E, Wahlström T, Valtonen S. The growth rate of intracranial meningiomas and its relation to histology. an analysis of 43 patients. *Surg Neurol* (1985) 24(2):165–72.

55. Yao X, Wei T, Zhang H, Li J, Tang A, Ren K. The natural growth rate of skull base meningiomas compared with non-skull base meningiomas. *J Craniofac Surg* (2019) 30(4):1231–3. doi: 10.1097/SCS.0000000000005468

56. Simpson D. The recurrence of intracranial meningiomas after surgical treatment. *J Neurol Neurosurg Psychiatry* (1957) 20(1):22–39. doi: 10.1136/jnnp.20.1.22

57. Schwartz TH, McDermott MW. The Simpson grade: abandon the scale but preserve the message. *J Neurosurg* (2020) p:1–8. doi: 10.3171/2020.6.JNS201904

58. Gousias K, Schramm J, Simon M. The Simpson grading revisited: aggressive surgery and its place in modern meningioma management. *J Neurosurg* (2016) 125 (3):551–60. doi: 10.3171/2015.9.JNS15754

59. Soni P, et al. Extent of resection and survival outcomes in world health organization grade II meningiomas. *J Neurooncol* (2021) 151(2):173–9. doi: 10.1007/s11060-020-03632-3

60. Aizer AA, Bi WL, Kandola MS, Lee EQ, Nayak L, Rinne ML, et al. Extent of resection and overall survival for patients with atypical and malignant meningioma. *Cancer* (2015) 121(24):4376–81. doi: 10.1002/cncr.29639

61. Zhang C, Zhang H. Stereotactic radiosurgery versus observation for treating incidental meningiomas: A systematic review and meta-analysis. *Turk Neurosurg* (2021) 31(2):151–60.

62. Rogers L, Barani I, Chamberlain M, Kaley TJ, McDermott M, Raizer J, et al. Meningiomas: knowledge base, treatment outcomes, and uncertainties. a RANO review. *J Neurosurg* (2015) 122(1):4–23.

63. Rogers L, Zhang P, Vogelbaum MA, Perry A, Ashby LS, Modi JM, et al. Intermediate-risk meningioma: initial outcomes from NRG oncology RTOG 0539. *J Neurosurg* (2018) 129(1):35–47. doi: 10.3171/2016.11.JNS161170

64. Rogers CL, Won M, Vogelbaum MA, Perry A, Ashby LS, Modi JM, et al. High-risk meningioma: Initial outcomes from NRG Oncology/RTOG 0539. *Int J Radiat Oncol Biol Phys* (2020) 106(4):790–9. doi: 10.1016/j.ijrobp.2019.11.028

65. Bray DP, Quillin JW, Press RH, Yang Y, Chen Z, Eaton BR, et al. Adjuvant radiotherapy versus watchful waiting for world health organization grade II atypical meningioma: A single-institution experience. *Neurosurgery* (2021) 88(5): E435–42. doi: 10.1093/neuros/nyaa580

66. Maggio I, Franceschi E, Di Nunno V, Gatto L, Tosoni A, Angelini D, et al. Discovering the molecular landscape of meningioma: The struggle to find new therapeutic targets. *Diagnostics (Basel)* (2021) 11(10):1852. doi: 10.3390/diagnostics11101852

67. Kaley T, Barani I, Chamberlain M, McDermott M, Panageas K, Raizer J, et al. Historical benchmarks for medical therapy trials in surgery- and radiation-refractory meningioma: a RANO review. *Neuro Oncol* (2014) 16(6):829–40. doi: 10.1093/neuonc/not330

68. Chargari C, Védrine L, Bauduceau O, Le Moulec S, Ceccaldi B, Magné N, et al. Reapprasial of the role of endocrine therapy in meningioma management. *Endocr Relat Cancer* (2008) 15(4):931–41. doi: 10.1677/ERC-08-0083

69. Chen TC, da Fonseca CO, Schonthal AH. Intranasal perillyl alcohol for glioma therapy: Molecular mechanisms and clinical development. *Int J Mol Sci* (2018) 19(12):3905. doi: 10.3390/ijms19123905

70. Weller M, Roth P, Sahm F, Burghardt I, Schuknecht B, Rushing EJ, et al. Durable control of metastatic AKT1-mutant WHO grade 1 meningothelial meningioma by the AKT inhibitor, AZD5363. *J Natl Cancer Inst* (2017) 109 (3):1–4. doi: 10.1093/jnci/djw320

71. Welling DB, Collier KA, Burns SS, Oblinger JL, Shu E, Miles-Markley BA, et al. Early phase clinical studies of AR-42, a histone deacetylase inhibitor, for neurofibromatosis type 2-associated vestibular schwannomas and meningiomas. *Laryngoscope Investig Otolaryngol* (2021) 6(5):1008–19. doi: 10.1002/lio2.643

72. Schulz C, Mathieu R, Kunz U, Mauer UM. Treatment of unresectable skull base meningiomas with somatostatin analogs. *Neurosurg Focus* (2011) 30(5):E11. doi: 10.3171/2011.1.FOCUS111

73. Johnson DR, Kimmel DW, Burch PA, Cascino TL, Giannini C, Wu W, et al. Phase II study of subcutaneous octreotide in adults with recurrent or progressive meningioma and meningeal hemangiopericytoma. *Neuro Oncol* (2011) 13(5):530–5. doi: 10.1093/neuonc/nor044

74. Simo M, Argyriou AA, Macià M, Plans G, Majós C, Vidal N, et al. Recurrent high-grade meningioma: a phase II trial with somatostatin analogue therapy. *Cancer Chemother Pharmacol* (2014) 73(5):919–23. doi: 10.1007/s00280-014-2422-z

75. Norden AD, Ligon KL, Hammond SN, Muzikansky A, Reardon DA, Kaley TJ, et al. Phase II study of monthly pasireotide LAR (SOM230C) for recurrent or progressive meningioma. *Neurology* (2015) 84(3):280–6. doi: 10.1212/WNL.0000000000001153

76. Hennrich U, Kopka K. Lutathera((R)): The first FDA- and EMA-approved radiopharmaceutical for peptide receptor radionuclide therapy. *Pharm (Basel)* (2019) 12(3):114.

77. Garzon-Muvdi T, Bailey DD, Pernik MN, Pan E. Basis for immunotherapy for treatment of meningiomas. *Front Neurol* (2020) 11:945. doi: 10.3389/fneur.2020.00945

78. Giles AJ, Hao S, Padget M, Song H, Zhang W, Lynes J, et al. Efficient ADCC killing of meningioma by avelumab and a high-affinity natural killer cell line, haNK. *JCI Insight* (2019) 4(20):e130688.

frontiers | Frontiers in Oncology

TYPE Original Research
PUBLISHED 26 August 2022
DOI 10.3389/fonc.2022.966581

Check for updates

OPEN ACCESS

EDITED BY
Hailiang Tang,
Fudan University, China

REVIEWED BY
Yuki Kuranari,
Keio University Hospital, Japan
Jia-Shu Chen,
Brown University, United States
Carlos Eduardo Da Silva,
Federal University of Health Sciences of Porto Alegre, Brazil

*CORRESPONDENCE
Johannes Wach
Johannes.wach@ukbonn.de

†These authors have contributed equally to this work

SPECIALTY SECTION
This article was submitted to Neuro-Oncology and Neurosurgical Oncology, a section of the journal Frontiers in Oncology

RECEIVED 11 June 2022
ACCEPTED 18 July 2022
PUBLISHED 26 August 2022

CITATION
Wach J, Hamed M, Lampmann T, Güresir Á, Schmeel FC, Becker AJ, Herrlinger U, Vatter H and Güresir E (2022) MAC-spinal meningioma score: a proposal for a quick-to-use scoring sheet of the MIB-1 index in sporadic spinal meningiomas.
Front. Oncol. 12:966581.
doi: 10.3389/fonc.2022.966581

COPYRIGHT
© 2022 Wach, Hamed, Lampmann, Güresir, Schmeel, Becker, Herrlinger, Vatter and Güresir. This is an open-access article distributed under the terms of the Creative Commons Attribution License (CC BY). The use, distribution or reproduction in other forums is permitted, provided the original author(s) and the copyright owner(s) are credited and that the original publication in this journal is cited, in accordance with accepted academic practice. No use, distribution or reproduction is permitted which does not comply with these terms.

MAC-spinal meningioma score: A proposal for a quick-to-use scoring sheet of the MIB-1 index in sporadic spinal meningiomas

Johannes Wach[1*†], Motaz Hamed[1†], Tim Lampmann[1], Ági Güresir[1], Frederic Carsten Schmeel[2], Albert J. Becker[3], Ulrich Herrlinger[4], Hartmut Vatter[1] and Erdem Güresir[1]

[1]Department of Neurosurgery, University Hospital Bonn, Bonn, Germany, [2]Department of Neuroradiology, University Hospital Bonn, Bonn, Germany, [3]Department of Neuropathology, University Hospital Bonn, Bonn, Germany, [4]Department of Neurology, Section of Neuro-Oncology, University Hospital Bonn, Bonn, Germany

Objective: MIB-1 index is an important predictor of meningioma progression. However, MIB-1 index is not available in the preoperative tailored medical decision-making process. A preoperative scoring sheet independently estimating MIB-1 indices in spinal meningioma (SM) patients has not been investigated so far.

Methods: Between 2000 and 2020, 128 patients with clinical data, tumor imaging data, inflammatory laboratory (plasma fibrinogen, serum C-reactive protein) data, and neuropathological reports (MIB-1, mitotic count, CD68 staining) underwent surgery for spinal WHO grade 1 and 2 meningioma.

Results: An optimal MIB-1 index cut-off value (≥5/<5) predicting recurrence was calculated by ROC curve analysis (AUC: 0.83; 95%CI: 0.71-0.96). An increased MIB-1 index (≥5%) was observed in 55 patients (43.0%) and multivariable analysis revealed significant associations with baseline Modified McCormick Scale ≥2, age ≥65, and absence of calcification. A four-point scoring sheet (MAC-Spinal Meningioma) based on **M**odified McCormick, **A**ge, and **C**alcification facilitates prediction of the MIB-1 index (sensitivity 71.1%, specificity 60.0%). Among those patients with a preoperative MAC-Meningioma Score ≥3, the probability of a MIB-1 index ≥5% was 81.3%.

Conclusion: This novel score (MAC-Spinal Meningioma) supports the preoperative estimation of an increased MIB-1 index, which might support preoperative patient-surgeon consultation, surgical decision making and enable a tailored follow-up schedule or an individual watch-and-wait strategy.

KEYWORDS

MIB-1 (Ki-67 labeling) index, score, spinal meningioma, proliferation, clinical implications

Introduction

Spinal meningiomas (SM) account for only 12% of all anatomic types of meningiomas (1–5). Spinal meningiomas are predominantly benign and slowly growing WHO grade 1 tumors. However, higher WHO grades are also reported and the frequency of them ranges between 1.5 and 8.5% (6–10). Gross total microsurgical removal is the treatment of choice for those meningiomas (11, 12). The majority of patients who underwent surgical SM resection improve regarding neurological functioning (10, 13). However, patients ≥ 66 years were found to have significant poorer recovery. The tumor recurrence rate in spinal meningiomas range between 1.3 and 13% (4, 6, 14–20). In addition to the extent of resection, male sex, dural tail sign, younger age, tumor size, foraminal location and en plaque lesions were suggested as predictors of tumor recurrence after spinal meningioma surgery (21, 22)

Increased proliferative activity of tumor cells is an established mechanism of oncogenesis (23, 24). The Molecular Immunology Borstel 1 (MIB-1) index is a widespread immunohistochemical method to detect nuclear structures which are exclusively visible in proliferating cells. The Ki-67 antigen is detectable in the nuclei of cells which are in G1, S, and G2 phases of the cell division cycle. Hence, this method enables a calculation of the growing fraction of a meningioma tissue (25–27). Furthermore, several investigations and meta-analyses revealed that the MIB-1 index is an independent risk factor for tumor progression in meningiomas (28–31). Tailored preoperative evaluation, accurate communication about the aims of surgery, and maximum safe surgery with preservation of neurological functioning are of paramount importance. However, MIB-1 index is not available as a basis for a detailed tailored consultation in the preoperative surgical decision-making and surgeon-patient conversation. In a previous institutional series, we identified that the MIB-1 labeling indices in spinal meningiomas are significantly lower compared to the cranial meningiomas. Hence, sufficient predictors of MIB-1 labeling indices in spinal meningiomas have to be investigated separately from cranial meningiomas (32).

The present study investigates our patient cohort of sporadic spinal WHO grade 1 and 2 meningiomas regarding potential clinical characteristics, laboratory inflammatory markers, and imaging features as predictors of an elevated MIB-1 index.

Methods

Patient population

This investigation reviewed 130 consecutive SM patients who underwent surgery between 2000 and 2020. The aim of the present single-center series is focused on the investigation of SMs located below the craniocervical junction. Patients with craniocervical meningiomas (occipital bone, C1, C2), patients with anterior foramen magnum meningiomas, a recurrent meningioma after radiotherapy, and neurofibromatosis type 2 patients were excluded because of their different clinical symptoms, neuropathology, and treatment strategies (33–36). Patients without neuropathological reports regarding the MIB-1 index were excluded. One-hundred-twenty-eight patients were included in the final study cohort.

Data recording and radiological features

Clinical data such as age, sex, comorbidities, Karnofsky Performance Status, body mass index (BMI), length of stay (in days) and the American society of anesthesiologists physical status classification system (ASA) were recorded in a computerized database (SPSS, version 27 for Windows, IBM Corp., Armonk, NY). Preoperative neurological examination was performed by institutional neurosurgeons and the modified McCormick Scale (MMS) was used to display neurological functioning and ambulatory ability (37). MMS was dichotomized into "good" (I&II) and "poor" (III-V) functioning as previously described (13, 38). Preoperative magnetic resonance imaging (MRI) was conducted within 72 hours prior to surgical treatment. Furthermore, all patients preoperatively underwent CT-scans of the spine segment under investigation. Calcification was confirmed by CT scans representing focal or diffuse hyperdense gross calcifications (39). On MRI, calcification resulted in signal intensity decrease on both T1- and T2-weighted MR images and a more heterogeneous Gd-enhancement compared to the typically encountered MR-imaging characteristics (e.g., homogeneous Gd-enhancement) of meningioma (40) (Figure 1). First postoperative MR imaging was scheduled at 3-months after surgery and further appointments for MRI were scheduled on an annual basis (41). Spinal meningioma recurrence was defined as a visible meningioma progression on follow-up MRI at least one year after surgery (42). T2-weighted images showing high signal intensity changes of the spinal cord were interpreted as myelomalacia (43).

Surgical workflow

Surgery was indicated in case of local back pain combined with absence of competing spinal pathologies, neurological deficits, and compression of the spinal cord. Surgical strategy was dependent on the site of dural attachment of the meningioma, meningioma size, as well as the involved spinal segment of the SM. Hemilaminectomy or laminoplasty was performed in order to preserve functional

FIGURE 1
(A, B) Axial and sagittal CT scans showing a representative case with a gross calcification of a thoracic spinal meningioma. **(C, D)** represent sagittal T1-weighted Gd-enhanced and T2-weighted MR-images. **(C)** shows a heterogeneous ring-enhancing lesion because of the gross calcification.

stability of the spine. Dentate ligament was resected if the SM had a ventral dural attachment. Dural closure and reconstruction was performed with continuous silk sutures and additionally sealed with TachoSil® (Fibrin Sealant Patch) if deemed necessary. Further surgical workflow was as previously described (13).

Histopathology

Neuropathological classification is in line with 2021 WHO criteria (11). Classification and grading of spinal meningiomas did not undergo substantial revision in 2021. Immunohistochemical staining was performed in a similar workflow as described before for paraffin-embedded biopsy tissue specimens (44, 45). The MIB-1 labeling index was determined using the following antibody: anti-Ki67 (Clone Ki-67P, dilution 1:1000, DAKO, Glostrup, Denmark) (24). Visualization was performed with diaminobenzidine, and histopathological investigation was conducted by expert neuropathologists, including A.J.B. The MIB-1 index was analyzed in randomly selected high-power microscopic fields. The amounts of stained and unstained nuclei in the meningioma cells were determined. Further neuropathological examinations were as previously described (24, 46).

Statistical analysis

Data were recorded and analyzed using SPSS for Windows (version 27.0; IBM Corp, Armonk, NY, USA). Receiver-operating characteristic curves (ROC) were created to investigate the diagnostic performance of MIB-1 labeling index in the prediction of a spinal meningioma recurrence. Cut-off point for the MIB-1 labeling index was set based on the ROC analysis. Kaplan-Meier charts of progression-free survival (PFS) stratified by MIB-1 labeling indices as well as extent of resection according to the Simpson grading were also calculated. Statistical results of the log-rank test are reported. Normally distributed data are presented as the mean with the standard deviation (SD). Preoperative demographics, clinical data, imaging characteristics, and inflammatory laboratory markers were compared between patients with a normal and those with an elevated MIB-1 labeling index using Pearson´s $\chi 2$ test (two-sided) for categorical data and independent *t*-test for continuous data. Further ROC curves were constructed for age and MMS. The area under the ROC curve (AUC) were investigated, and cut-off thresholds for the continuous variables (age & MMS) were set using the ROC analyses. Multivariable binary logistic regression analysis was performed to identify predictive variables of an elevated MIB-1 labeling index. A *p*-value threshold of <0.10 in the univariable analysis was set regarding

the inclusion of variables in the multivariable binary logistic regression analysis. Furthermore, sex was also included in the multivariable analysis of factors being associated with an increased MIB-1 labeling index because of the known strong evidence suggesting male sex as a predictor of elevated MIB-1 labeling indices in cranial meningiomas (24, 47, 48). Wald test was used for the analysis of dichotomized variables. A p-value of <0.05 was defined as statistically significant. Significant predictors of the multivariable analysis were included in a 4-point scoring sheet predicting an increased MIB-1 labeling index.

Results

Patient characteristics

One hundred and twenty-eight patients fulfilled the inclusion criteria and were surgically treated for SM at the institutional department. Median age was 68 years (IQR 57-75), and the present investigation included 98 females (76.6%) and 30 males (23.4%; female/male ratio 3.27:1). Median baseline Karnofsky performance scale (KPS was 80 (IQR 70-90). Tumors were predominantly located in the thoracic spine. Tumor classification according to the WHO classification criteria included 119 patients with WHO grade 1 (93.0%) and 9 patients with grade 2 (7.0%). Further characteristics are summarized in Table 1. Regarding histopathological type among WHO grade 1 SMs, psammomatous meningioma (68/119; 57.1%) was the most common subtype. Transitional, meningothelial, fibroblastic, and angiomatous subtypes were observed in 25 (25/119; 21.0%), 18 (18/119; 15.1%), 6 (6/119; 5.0%), and 2 (2/119; 1.7%) WHO grade 1 SMs patients, respectively. Atypical meningioma was observed in all cases among the WHO grade 2 SMs.

TABLE 1 Patient characteristics (n = 128).

Median age (IQR) (in y)	**68 (57-75)**
Sex	
Female	98 (76.6%)
Male	30 (23.4%)
Median preoperative KPS (IQR)	80 (70-90)
Tumor location	
Cervical	32 (25.0%)
Thoracic	94 (73.4%)
Lumbar	2 (1.6%)
Simpson grade	
Simpson grade I&II	123 (96.1%)
Simpson grade ≥ III	5 (3.9%)
WHO grade	
WHO grade 1	119 (93.0%)
WHO grade 2	9 (7.0%)

MIB-1 labeling index in the prediction of recurrent spinal meningioma

The MIB-1 index was available in all patients of the entire cohort. The median MIB-1 labeling index was 4.0 (IQR 3.0-5.0). A ROC curve was created, and the AUC of the MIB-1 labeling index in the diagnostic performance regarding SM recurrence was calculated. The AUC of the MIB-1 labeling index in the prediction of SM recurrence was 0.83 (95% CI: 0.71-0.96, p = 0.03). Sensitivity and specificity of the MIB-1 labeling index for the prediction of a recurrent SM were 100.0% and 60.0%, respectively (Youden´s index: 0.60), with a threshold of ≥5%. Figure 2A displays the ROC curve and summarizes the results of the statistical analysis. Median (range) and mean time of imaging follow-up (n = 88) were 14.0 (3.0-169.0) and 33.70 months, respectively. Analysis of PFS was performed in 88 (69.0%) of the 128 patients. Four recurrent SMs were detected in the group of patients with a MIB-1 labeling index ≥ 5%, whereas no recurrent SM was observed in the group of patients with a MIB-1 labeling index < 5%. Figure 2B displays the Kaplan-Meier curves of the MIB-1 labeling index groups (<5/≥5%). Furthermore, extent of resection according to the Simpson grading system was analyzed with regard to the probability of progression-free survival. Mean time to tumor progression in SM patients who underwent a Simpson grade I or II resection was 159.7 (95% CI: 143.5 – 175.9) months, and in those patients who underwent a Simpson grade ≥III resection it was 48.0 (95% CI: 14.7 – 81.3) months, respectively (log-rank test: p = 0.001). Figure 2C illustrates the Kaplan-Meier chart of progression-free survival stratified by Simpson grade.

Association between the MIB-1 labeling index and clinical, imaging, and laboratory features

Fifty-five patients had a MIB-1 labeling index of ≥ 5%, and 73 patients had a MIB-1 labeling index of <5%. Patients with an elevated MIB-1 labeling index were significantly older compared to patients with a lower MIB-1 labeling index. Patients with a MIB-1 labeling index of ≥ 5% had also a significantly higher MMS at presentation (2.3 +/- 1.2 vs. 1.8 +/- 1.0; p = 0.008). Furthermore, patients with a lower MIB-1 labeling index (<5%) had significantly more often a calcification of the SM compared to patients with an elevated MIB-1 labeling index. Extent of resection was also homogeneously distributed among the SM patients with normal (<5%) MIB-1 labeling index or increased MIB-1 labeling index (≥5%). Among the patients with a normal

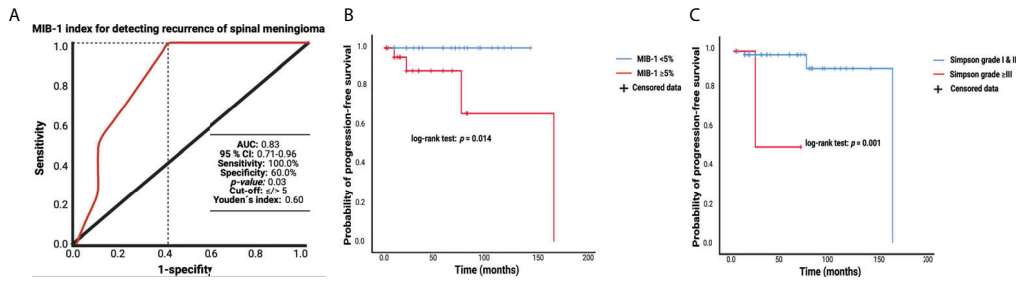

FIGURE 2
(A) Receiver-operating characteristic curve showing the MIB-1 labeling index in the prediction of progression of sporadic spinal meningiomas. The dashed line marks the identified optimum cut-off value. **(B)** Kaplan-Meier analysis of tumor progression probability stratified by "MIB-1 ≥ 5%" (red line) and "MIB-1 < 5" (blue line). Vertical dashes represent censored data (constituting for progression-free at last follow-up) within the PFS curves. The time axis is right-censored at 200 months. **(C)** Kaplan-Meier charts of tumor progression probability stratified by "Simpson grade ≥III" (red line) and "Simpson grade I & II" (blue line). Vertical dashes represent censored data (constituting for progression-free at last follow-up) within the PFS curves. The time axis is right-censored at 200 months.

MIB-1 labeling index (<5%, n = 73), 71 patients (71/73; 97.3%) underwent either a Simpson grade I or II resection, whereas 52 patients (52/55; 94.5%) of those with an increased MIB-1 labeling index (≥5%, n = 55) underwent either a Simpson grade I or II resection (Fisher´s exact test (two-sided): p = 0.65). Further clinical, imaging, and laboratory characteristics are detailed in Table 2.

ROC curves were created, and the AUCs of age and baseline MMS in the prediction of an elevated MIB-1 labeling index (≥5%) were created. The AUCs for age and baseline MMS were 0.61 (95% CI: 0.51-0.72, p = 0.04) and 0.64 (95% CI: 0.54-0.74, p = 0.01). Optimum cut-off values for age and baseline MMS were identified at ≥65/<65 and ≥2/<2. The sensitivity and specificity of age at diagnosis for predicting a MIB-1 labeling index of ≥5% were 70.5% and 50.0%, respectively. Moreover, the sensitivity and specificity of baseline MMS for the prediction of an increased MIB-1 labeling index (≥5%) were 69.3% and 52.1%. Multivariable binary logistic regression analysis with consideration of MMS, calcification, dural tail sign, sex, and age was performed. The multivariable analysis found that MMS ≥ 2, age ≥ 65, and the absence of calcification were significantly associated with a MIB-1 labeling index of ≥ 5%. Figure 3 displays the results of the multivariable binary logistic regression analysis.

Predictive scoring sheet

Hence, we created and investigated a proposal for a predictive scoring system of an increased MIB-1 labeling index in sporadic spinal meningioma. The present proposal was created with the following objectives: (1) to feasibly estimate the MIB-1 labeling index using easily determinable preoperative variables and (2) to quick-to-use in the clinical care for SM patients. These objectives resulted in the following point distribution system for a novel scoring sheet, which we called the "MAC-Spinal Meningioma" score, ranging from 0 to 4 points (Figure 4): Baseline Modified McCormick Scale ≥ 2 (1 point); age ≥ 65 years at diagnosis (1 point); absence of calcification (2 points). In the present study, the mean score in patients with a MIB-1 labeling index of ≥ 5% was 3.2 (SD = 0.78), and it was 2.67 (SD = 0.81) in patients with a MIB-1 labeling index of <5%, respectively (p < 0.001). The AUC for the MAC-Spinal Meningioma score in predicting an increased MIB-1 labeling index (≥5%) was 0.70 (95% CI: 0.60-0.80, p = 0.001). Using a cut-off value of 3 points, the score yields a sensitivity of 71.1%, a specificity of 60.0%, a positive predictive value of 81.3%, and a negative predictive value of 45.8%. Figure 5 shows the ROC curve and the results of the statistical analysis. An additive score of ≥ 3 points implies a probability of 81.3% for finding a MIB-1 labeling index of ≥ 5% in the neuropathological analysis of sporadic spinal meningiomas.

MAC-Spinal Meningioma score and perioperative clinical implications

MAC-Spinal Meningioma score was further investigated regarding perioperative clinical implications. The correlation between length of stay (in days) and MAC-Spinal Meningioma score was analyzed. The mean (+/- SD) length of stay in the study cohort was 13.2 (+/- 12.5) days. Spearman´s correlation analysis revealed a statistically significant (p = 0.047) positive correlation between the length of stay and MAC-Spinal Meningioma score (r = 0.18). Figure 6 displays the correlation analysis. Furthermore, the association between the course of MMS (baseline – 3-months) and MAC-Spinal Meningioma score was investigated. Patients with a high MAC-Spinal Meningioma Score (3-4 points) had a significantly worse mean (+/-SD) baseline MMS at 2.34 +/-

TABLE 2 Baseline clinical, imaging and laboratory characteristics in spinal meningioma patients with a normal and increased MIB-I labeling index (n = 128).

Variable	MIB-I <5 % (n=73)	MIB-I ≥5 % (n=55)	p-value
Age (mean +/- SD))	62.7 +/- 14.0	67.8 +/- 11.0	**0.03**
Sex			0.99
female	56 (76.7%)	42 (76.4%)	
male	17(23.3%)	13 (23.6%)	
KPS (mean +/- SD)	81.6 +/- 11.1	82.0 +/- 11.0	0.86
Modified McCormick Scale (mean +/- SD)	1.8 +/- 1.0	2.3 +/- 1.2	**0.008**
Diabetes			0.62
Present	10 (13.7%)	10 (18.2%)	
Not present	63 (86.3%)	45 (81.8%)	
Smoking			0.99
Present	12 (16.4%)	9 (16.4%)	
Not present	61 (83.6%)	46 (83.6%)	
ASA intake			0.36
Present	8 (11.0%)	10 (18.2%)	
Not present	65 (89.0%)	45 (81.8%)	
Dexamethasone intake			0.93
Present	11 (15.1%)	8 (14.5%)	
Not present	62 (84.9%)	47 (85.5%)	
Location			0.54
Cervical	20 (27.4%)	12 (21.8%)	
Thoracic & lumbar	53 (72.6%)	43 (78.2%)	
Calcification			**0.02**
Present	10 (13.7%)	1 (1.8%)	
Absent	63 (86.3%)	54 (98.2%)	
Cysts			0.51
Present	2 (2.7%)	0 (0.0%)	
Absent	71 (97.3%)	55 (100.0%)	
Dural tail sign			0.07
Present	9 (12.3%)	14 (25.5%)	
Absent	64 (87.7%)	41 (74.5%)	
Dural attachment (one patient was excluded due to selective arachnoid attachment)			0.13
Ventral	19 (26.0%)	19 (35.2%)	
Lateral	27 (37.0%)	24 (44.4%)	
Dorsal	27 (37.0%)	11 (20.4%)	
Involved spinal segments			0.56
≤ 2	67 (91.8%)	48 (87.3%)	
> 2	6 (8.2%)	7 (12.7%)	
Myelomalacia (T2-weighted MR-image)			0.86
Present	39 (53.4%)	28 (50.9%)	
Absent	34 (46.6%)	27 (49.1%)	
Plasma Fibrinogen (mean +/- SD)	3.2 +/- 0.6	3.5 +/- 0.9	0.25
Serum C-reactive protein (mean +/- SD)	4.8 +/- 8.7	5.2 +/- 7.6	0.77
White blood cell count (mean +/- SD)	8.6 +/- 3.9	8.7 +/- 4.3	0.95
Simpson grade			0.65
I & II	71 (97.3%)	52 (94.5%)	
≥ III	2 (2.7%)	3 (5.5%)	

Bold values represent statistically significant results (p<0.05).

1.12, whereas patients with a low MAC-Spinal Meningioma Score (0-2 points) had a mean (+/-SD) baseline MMS at 1.51 +/- 0.92 (p < 0.001). At 3-months after surgery, patients with a high MAC-Spinal Meningioma score improved significantly more regarding ambulatory functioning. Patients with a high MAC-Spinal Meningioma Score (3-4 points) had a mean (+/-SD) MMS of 1.65 +/- 0.87 at 3-months, and patients with a low MAC-Spinal Meningioma Score (0-2 points) had a mean (+/-SD) MMS of 1.30 +/- 0.74, respectively (p = 0.07). Hence, the mean difference of MMS (between baseline and 3-months follow-up) was -0.077 +/- 0.39 in patients with a low MAC-Spinal Meningioma Score (0-2 points), and -0.43 +/-

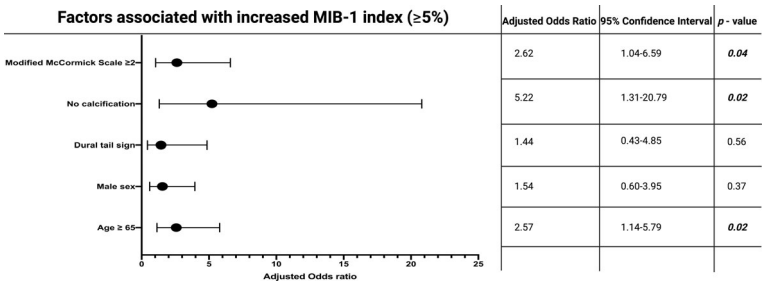

FIGURE 3
Forest plots from multivariable binary logistic regression analysis: Modified McCormick scale ≥ 2 at presentation, age ≥ 65 years at diagnosis, and absence of calcification are independent predictors of increased MIB-1 labeling index. Black circles indicate the adjusted odds ratio of each variable and the lines represent the corresponding 95% confidence interval. *P*-values in bold and italics display statistically significant results.

0.74, respectively (p = 0.007). Figure 7 displays the course of MMS in patients with low- and high-MAC-Spinal Meningioma Score.

Discussion

Established negative predictors of spinal meningioma recurrence are increased MIB-1 labeling indices, arachnoid invasion, and subtotal resection (17, 49, 50). An increased MIB-1 labeling index is inversely correlated with time to tumor progression in SM and has a positive correlation with the grading of meningiomas (14, 31, 51, 52). SM patients predominantly consulate neurosurgeons *via* elective appointments in an outpatient clinic. Hence, it is essential that patients and their relatives are provided with a tailored and extensive consultation. Nevertheless, MIB-1 labeling indices are not available at the preoperative appointments discussing treatment strategies, extent of resection, imaging intervals, and risk-benefit ratios. The present investigation shows a novel scoring sheet to estimate an elevated MIB-1 labeling index. This potential predictive score includes three routinely and easily determinable characteristics to estimate an elevated MIB-1 labeling index. Furthermore, this scoring system might enable a tailored schedule for imaging in patients who prefer a watch-and-wait strategy instead of surgery. For instance, patients with an increased risk profile (e.g., high ASA class) and the absence of a symptomatic spinal meningioma preferring an initial watch-and-wait strategy, might be scheduled for a more stringent follow-up interval in order to not miss a further tumor progression resulting in a neurological deterioration if they have an increased MAC-

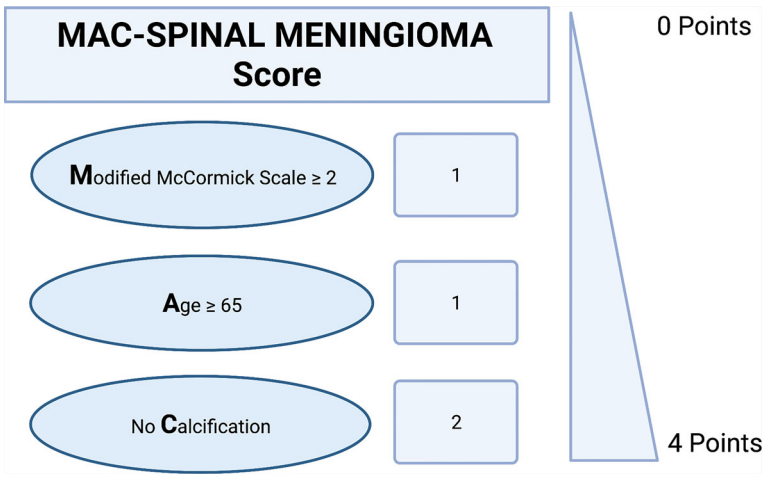

FIGURE 4
A proposal for a novel clinical scoring sheet to preoperatively estimate the risk of an increased MIB-1 labeling index (≥5%). An additive score of ≥ 3 points implies a probability of 81.3% for having an increased proliferative activity.

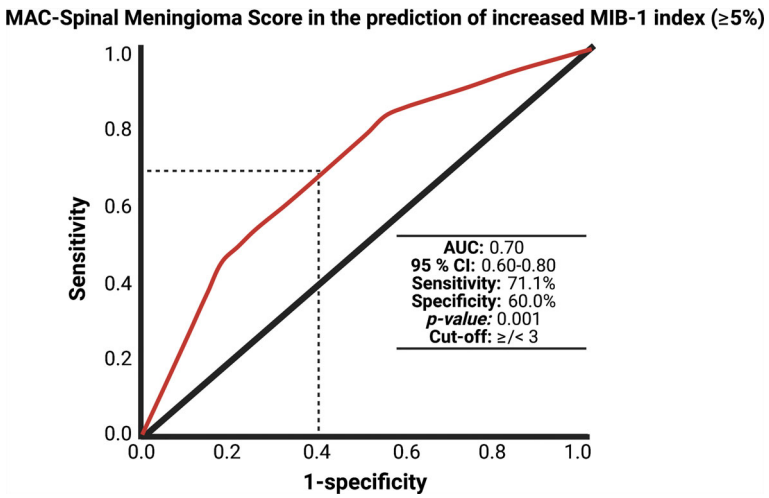

FIGURE 5
Receiver-operating characteristic curve demonstrating the MAC-Spinal Meningioma Score in the prediction of increased MIB-1 labeling index of sporadic spinal meningiomas. The dashed line marks the identified optimum cut-off value of the MAC-Spinal Meningioma score in the prediction of an increased MIB-1 labeling index (≥5%).

Spinal Meningioma score (≥3 points) suggesting a potential increased proliferative activity.

Our results are summarized in the following: (1) a cut-off point of the MIB-1 labeling index set at 5% had the most accurate sensitivity and specificity in the discrimination between stable and progressive SM; (2) Baseline Modified McCormick Scale ≥ 2, age ≥ 65 years at diagnosis, and absence of calcification were significantly associated with an elevated (≥5%) MIB-1 labeling index; (3) the presence of at least one variable among Modified McCormick Scale or age ≥ 65 years at

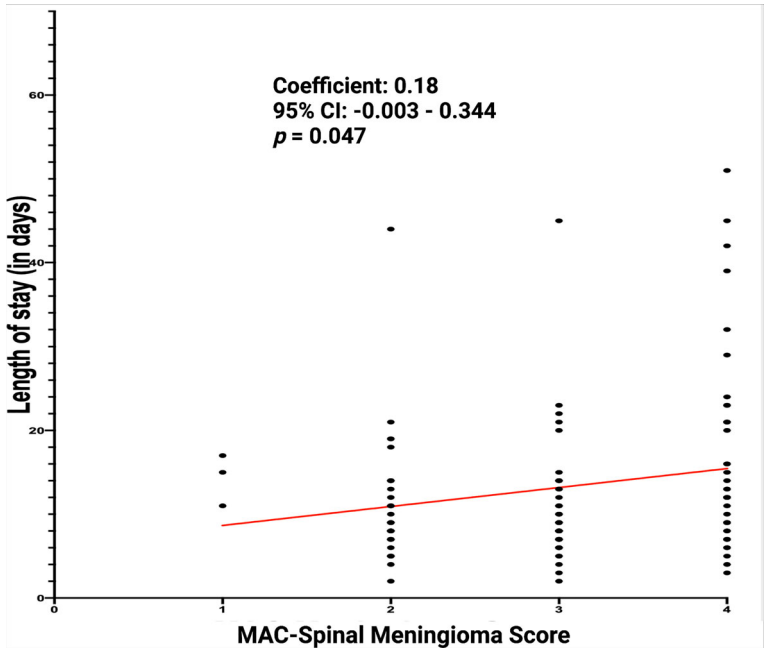

FIGURE 6
Length of stay (in days) in relation to the MAC-Spinal Meningioma Score of 128 primary sporadic spinal meningiomas.

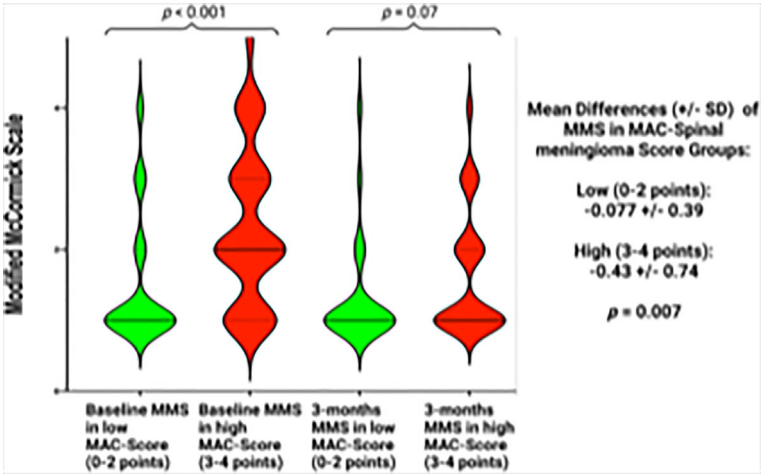

FIGURE 7
Violin plots displaying the Modified McCormick scale at the preoperative examination, and at 3-months after surgery in patients with a low MAC-Spinal Meningioma score (0-2 points, green violin plot) or a high MAC-Spinal Meningioma score (3-4 points, red violin plot). Violin plots show mean and distribution of Modified McCormick scale. The thick horizontal black lines are the median values. *P*-values of the Student´s *t*-test are reported.

diagnosis in combination with the absence of calcification was a strong predictor of an elevated MIB-1 labeling index; (4) high MAC-Spinal Meningioma Score (3-4 points) is strongly associated with a prolonged length of stay; (5) Despite poorer baseline functioning, patients with a high MAC-Spinal Meningioma score (3-4 points) improve significantly more regarding neurological functioning compared to low MAC-Spinal Meningioma Score patients.

ROC curves were constructed in the present study cohort to evaluate the most accurate cut-off point of the MIB-1 labeling in the estimation of SM recurrence. The present investigation revealed a threshold set at ≥5% as the optimal cut-off point. Cut-off points of MIB-1 labeling index are highly debated in the literature and a broad range (2-20%) of optimum thresholds are reported (29). A recent meta-analysis pooling optimum cut-off points of 43 investigations found a cut-off value set a >4% as accurate regarding risk stratification of overall survival and progression-free survival [29]. However, it has to be reminded that the pooling of MIB-1 labeling index regarding the identification of optimum cut-off values might be more appropriate in a setting analyzing spinal and cranial meningiomas separately. Roser et al. (53) revealed that SMs have significantly lower MIB-1 labeling indices compared to intracranial meningiomas. Therefore, the interlaboratory comparison of reported cut-off points is potentially limited by multiple factors. For instance, the extent of resection has to be considered regarding the specimen sampling because a partially resected tumor tissue implies the risk that the "hotspot" area of maximum proliferative potential is not within the specimen (54). Moreover, it has to be considered that the comparison of interlaboratory MIB-1 labeling indices is also limited by different neuropathological methods (e.g., manual or digital) to determine the MIB-1 labeling index (55).

The results of the multivariable analysis demonstrated that increased baseline MMS ≥2, age ≥ 65 years at diagnosis, and absence of calcification in baseline CT imaging are both significant and independent predictors of an elevated MIB-1 labeling index (≥5%) in SM.

Baseline modified McCormick scale displaying the ambulatory mobility of the patients and their functioning at diagnosis was independently associated with an increased MIB-1 labeling index. To date, this finding has not been described in previous clinicopathological investigations of SMs. However, we have also recently showed in a retrospective institutional series of frontal skull base meningiomas that increased MIB-1 labeling indices are strongly associated with the development or aggravation of new cranial nerve deficits after surgery (45). Moreover, a recent retrospective series evaluating 384 patients who underwent surgery for supratentorial meningiomas revealed that increased MIB-1 labeling indices are significantly associated with Engel class outcomes displaying the postoperative seizure burden (56). Hence, MIB-1 labeling indices might be a potential marker for location-specific symptoms of meningiomas. Furthermore, MIB-1 labeling index has been identified in vestibular schwannomas as diagnostic staining marker which is inversely correlated with the degree of baseline symptoms, duration of symptoms at diagnosis, and postoperative facial nerve function (25, 57). We suggest that those primary sporadic SMs having an increased MIB-1 labeling index grew in a shorter time compared to those

with lower MIB-1 labeling indices. Nevertheless, we could not identify differences regarding the tumor size and myelomalacia signs in T2-weighted MR scans among the low or high MIB-1 labeling indices groups. MIB-1 labeling index is known to correlate with the growth rate of primary untreated meningiomas as well as the regrowth of surgically treated meningiomas (58–60).

The present study also showed a simple association between age ≥ 65 years at diagnosis and elevated MIB-1 labeling indices in SM. This relationship was observed in several investigations (61–64). Elderly patients having higher MIB-1 indices were also found by a previous investigation analyzing a prospective database including 1372 cranial meningioma patients (65). Nevertheless, this finding is still controversially debated in the literature. There are also studies which found that proliferation reflected by MIB-1 and progesterone receptor status are not age dependent (66). Furthermore, Maiuri et al. (14) performed a retrospective series of 120 SM patients and dichotomized the study cohort into two groups aged younger or older than 50 years. However, the cut-off set in the mentioned investigation might have been chosen to low because several studies reported mean ages at diagnosis ranging between 60 and 65 years in SM patients (13, 67, 68).

The presence of a calcified spinal meningioma in CT-imaging studies was significantly linked to decreased MIB-1 labeling indices (<5%). Calcification can be observed in up to 25% of meningiomas and was already previously found to be associated with slow growth and lower grade histopathology in cranial meningiomas (69–72). A meta-analysis investigating 777 cranial meningioma patients revealed that tumor calcification is inversely correlated with the meningioma growth rate (69). Moreover, the correlation of CT-imaging signs such as calcification with the immunohistochemical variable MIB-1 labeling index was also investigated in a retrospective series investigating 342 consecutive meningioma patients. Logistic regression analysis of the mentioned study also demonstrated that the absence of calcification is significantly associated with increased MIB-1 labeling indices (47). The implications of calcified or noncalcified meningiomas in terms of a watch and wait approach was also analyzed in a previous series (71). For instance, Rubin et al. (70) followed up both 33 calcified meningioma patients and 27 noncalcified meningioma patients for a mean follow-up time of 65 months. Eighteen of the noncalcified meningiomas showed a tumor growth, whereas only 3 patients of the calcified meningioma group had a meningioma growth. The presence of calcification in SM is more uncommon compared to cranial meningiomas. Gross calcification is described for only 1-5% of SM (73). Previous investigations of calcified SM were predominantly focused on the surgical implications in this rare subgroup of SM regarding functional outcome. Calcified SMs are suggested to be more adherent to spinal nerves and the surrounding layers involving the dura. This condition might be induced by the deposition of calcium in calcified SMs. Several retrospective series debated that the calcification of SMs is strongly associated with poor functional outcomes (4, 74).

The present MAC-Spinal Meningioma score represents a newly created scoring sheet which facilitates the estimation of an increased MIB-1 labeling index in SM. The scoring system might support the preoperative therapy planning and aid physicians in the preoperative consultation with both patients and their relatives because neuropathological characteristics are not available in this setting. Furthermore, SM patients with an elevated MAC-Spinal Meningioma score (≥3) who favor a watch-and-wait policy of their asymptomatic spinal meningiomas should be advised about the need to perform a more stringent schedule of follow-up images. Hence, the MAC-Spinal Meningioma score might facilitate a tailored treatment strategy planning in the preoperative setting. Furthermore, MIB-1 labeling index was demonstrated to be a reliable marker for the time to tumor progression in a prospective trial. This mentioned study analyzed the rates of tumor recurrence and the time to regrowth in WHO grade 1-3 meningiomas. Patients with a MIB-1 index ≥ 5% suffered significantly more often from a tumor progression within the first 24 months after surgery compared to patients with a MIB-1 index ranging between 0 and 4% (75). Moreover, a retrospective series analyzing 239 WHO grade 1 meningiomas showed that the recurrence rates of patients who underwent a gross total resection of a meningioma with a MIB-1 labeling index > 4.5 are similar to patients who had a subtotal resection (60). In a recent institutional intraindividual study of cranial WHO grade 1 and 2 meningiomas we have also confirmed that the MIB-1 labeling indices have a high intraindividual reproducibility which also favors the diagnostic value of the MIB-1 labeling index in terms of tumor progression (76). Therefore, this knowledge might inform the postoperative risk stratification of a meningioma recurrence and facilitate an individualized stringent follow-up strategy. Against this backdrop, it is essential to preoperatively discuss the risk of an increased MIB-1 index and the potential consequences regarding individualized follow-up strategies after surgery. Intraoperative determination of the MIB-1 labeling index to aid the surgical decision making has not been established yet (77, 78). Hence, this scoring system might facilitate the preoperative medical decision-making regarding extent of resection because calcified SMs might be of more benign character, and they are suggested to be associated with poorer functional outcome. Furthermore, the scoring system was also found to be associated with the perioperative course and postoperative course of neurological functioning. A high MAC-Spinal Meningioma score was significantly associated with a prolonged length of stay in the hospital. This strong association might be caused by the fact that patients with a high MAC-Spinal Meningioma score are older and have a

poorer baseline MMS. However, we identified that those patients with a high MAC-Spinal Meningioma score improved significantly more regarding neurological functioning compared to those with a low MAC-Spinal Meningioma score. Hence, both groups had no differences in the MMS at 3-months after surgery. This finding might be caused by the fact that those patients with a high MAC-Spinal Meningioma Score had significantly higher MIB-1 labeling indices which suggests that those spinal meningiomas grew in a shorter time and might have not already resulted in a chronic compression of the spinal cord. Hence, those patients might have a better spinal plasticity. All in all, spinal meningioma patients with a high MAC-Spinal Meningioma score might be educated about a potentially faster growing meningioma with an increased MIB-1 labeling index, and a longer length of stay in the hospital. Nevertheless, those patients with a high MAC-Spinal Meningioma Score have surprisingly a nearly identical ambulatory functioning at 3-months after surgery. Consequently, surgical treatment for patients with a high MAC-Spinal Meningioma Score might be highly recommended due to the following reasons: 1) Prevention of the risk of further tumor progression potentially resulting in further neurological deterioration; 2) despite poorer baseline functioning, excellent chances to recover and achieve a nearly identical neurological functioning as patients with a low MAC-Spinal Meningioma Score at 3-months after surgery.

The present investigation has several limitations. Despite the data were acquired from a highly selective and homogeneous cohort, the retrospective design suffered from the potential limitations of a single institutional series. Additionally, MIB-1 labeling indices have to be interpreted with caution due to potential interobserver variability. Several approaches are possible to determine the MIB-1 labeling index, and digital imaging analysis systems might provide a more objective method because it enables a greater number of microscopic fields for the analysis (79). Furthermore, a multicentric prospective trial including a homogeneous study cohort and detailed data has to provide an external validation of the newly created MAC-Spinal Meningioma scoring proposal for sporadic spinal meningiomas.

Conclusion

MIB-1 labeling index seems to be strongly correlated with an increased risk of tumor progression in sporadic spinal meningioma. The present investigation provides a proposal for a novel scoring sheet ("MAC-Spinal Meningioma"), which might facilitate the preoperative estimation of the MIB-1 labeling index. Moreover, this scoring system might enhance the preoperative surgical decision-making process and guide a tailored treatment strategy in terms of risk-benefit analysis.

Data availability statement

The raw data supporting the conclusions of this article will be made available by the authors, without undue reservation.

Ethics statement

The studies involving human participants were reviewed and approved by Ethics committee of University Hospital Bonn. Written informed consent for participation was not required for this study in accordance with the national legislation and the institutional requirements.

Author contributions

Data acquisition was performed by JW; JW, MH, and EG performed the data interpretation. Writing and creation of figures were performed by JW, MH, and EG. Proof reading was done by AG, TL, FS, AB, UH, HV, and EG. All authors contributed to the article and approved the submitted version.

Acknowledgments

The graphical abstract in this article was created using BioRender.

Conflict of interest

The authors declare that the research was conducted in the absence of any commercial or financial relationships that could be construed as a potential conflict of interest.

Publisher's note

All claims expressed in this article are solely those of the authors and do not necessarily represent those of their affiliated organizations, or those of the publisher, the editors and the reviewers. Any product that may be evaluated in this article, or claim that may be made by its manufacturer, is not guaranteed or endorsed by the publisher.

Supplementary material

The Supplementary Material for this article can be found online at: https://www.frontiersin.org/articles/10.3389/fonc.2022.966581/full#supplementary-material

References

1. Aboul-Enein HA, Khidr WM, Abdeen KM, Madawi AA. Surgical management of ventrally based lower cervical (subaxial) meningiomas through the lateral approach: report on 16 cases. *Clin Neurol Neurosurg* (2015) 139:152–8. doi: 10.1016/j.clineuro.2015.10.008

2. Alafaci C, Grasso G, Granata F, Salpietro FM, Tomasello F. Ossified spinal meningiomas: clinical and surgical features. *Clin Neurol Neurosurg* (2016) 142:93–7. doi: 10.1016/j.clineuro.2016.01.026

3. Davies S, Gregson B, Mitchell P. Spinal meningioma: relationship between degree of cord compression and outcome. *Br J Neurosurg* (2017) 31:209–11. doi: 10.1080/02688697.2016.1206180

4. Roux FX, Nataf F, Pinaudeau M, Borne G, Devaux B, Meder JF. Intraspinal meningiomas: review of 54 cases with discussion of poor prognosis factors and modern therapeutic management. *Surg Neurol* (1996) 46:458–64. doi: 10.1016/s0090-3019(96)00199-1

5. Westwick HJ, Yuh SJ, Shamji MF. Complication avoidance in the resection of spinal meningiomas. *World Neurosurg* (2015) 83:627–34. doi: 10.1016/j.wneu.2014.12.015

6. Solero C, Fornari M, Giombini S, Lasio G, Oliveri G, Cimino C, et al. Spinal meningiomas: Review of 174 operated cases. *Neurosurgery* (1989) 25:153–60. doi: 10.1227/00006123-198908000-00001

7. Pettersson-Segerlind J, Fletcher-Sandersjöö A, Tatter C, Burström G, Persson O, Förander P, et al. Long-term follow-up and predictors of functional outcome after surgery for spinal meningiomas: A population-based cohort study. *Cancers* (2021) 13:3244. doi: 10.3390/cancers13133244

8. Abdulaziz M, Mallory GW, Bydon M, de la Garza Ramos R, Ellis JA, Laack NN, et al. Outcomes following myxopapillary ependymoma resection: The importance of capsule integrity. *Neurosurg Focus* (2015) 39:E8. doi: 10.3171/2015.5.FOCUS15164

9. Jamilson Araújo Pereira B, Nogueira de Almeida A, Silva Paiva W, Henrique Pires de Aguiar P, Jacobsen Teixeira M, Kazue Nagahashi Marie S. Neuro-oncological features of spinal meningiomas: Systematic review. *Neurochirurgie* (2020) 66:41–4. doi: 10.1016/j.neuchi.2019.09.027

10. Krauss WE, Yolcu YU, Alvi MA, Moinuddin FM, Goyal A, Clarke MJ, et al. Clinical characteristics and management differences for grade II and III spinal meningiomas. *J Neuro-Oncol* (2021) 153:313–20. doi: 10.1007/s11060-021-03771-1

11. Louis DN, Perry A, Wesseling P, Brat DJ, Cree IA, Figarella-Branger D, et al. The 2021 WHO classification of tumors of the central nervous system: a summary. *Neuro Oncol* (2021) 23(8):1231–51. doi: 10.1093/neuonc/noab106

12. Alexiou GA, Gogou P, Markoula S, Kyritsis AP. Management of meningiomas. *Clin Neurol Neurosurg* (2010) 112:177–82. doi: 10.1016/j.clineuro.2009.12.011

13. Wach J, Banat M, Schuss P, Güresir E, Vatter H, Scorzin J. Age at diagnosis and baseline myelomalacia sign predict functional outcome after spinal meningioma surgery. *Front Surg* (2021) 8:682930. doi: 10.3389/fsurg.2021.682930

14. Maiuri F, De Caro ML, de Divitiis O, Vergara P, Mariniello G. Spinal meningiomas: age-related features. *Clin Neurol Neursourg* (2011) 25:153–60. doi: 10.1016/j.clineuro.2010.08.017

15. Raco A, Pesce A, Toccaceli G, Domenicucci M, Miscusi M, Delfini R. Factors leading to a poor functional outcome in spinal meningioma surgery: remarks on 173 cases. *Neurosurgery* (2017) 80:602–9. doi: 10.1093/neuros/nyw092

16. Cohen-Gadol AA, Zikel OM, Koch CA, Scheithauer BW, Krauss WE. Spinal meningiomas in patients younger than 50 years of age: a 21-year experience. *J Neurosurg* (2003) 98(3 Suppl.):258–63. doi: 10.3171/spi.2003.98.3.0258

17. Levy WJJr, Bay J, Dohn D. Spinal cord meningioma. *J Neurosurg* (1982) 57:804–12. doi: 10.3171/jns.1982.57.6.0804

18. Mirimanoff RO, Dosoretz DE, Linggood RM, Ojeman RG, Martuza RL. Meningioma analysis of recurrence and progression following neurosurgical resection. *J Neurosurg* (1985) 62:18–24. doi: 10.3171/jns.1985.62.1.0018

19. Sandalcioglu IE, Hunold A, Müller O, Bassiouni H, Stolke D, Asgari S. Spinal meningiomas: critical review of 131 surgically treated patients. *Eur Spine J* (2008) 17:1035–41. doi: 10.1007/s00586-008-0685-y

20. Schick U, Marquardt G, Lorenz R. Recurrence of benign spinal neoplasms. *Neurosurg Rev* (2001) 24:20–5. doi: 10.1007/pl00011961

21. Maiti TK, Bir SC, Patra DP, Kalakoti P, Guthikonda B, Nanda A. Spinal meningiomas: clinicoradiological factors predicting recurrence and functional outcome. *Neurosurg Focus* (2016) 41(2):E6. doi: 10.3171/2016.5.FOCUS16163

22. Park BJ, Dougherty MC, Noeller J, Nourski KV, Gold CJ, Menezes AH, et al. Spinal meningioma in adults: Imaging characteristics, surgical outcomes, and risk factors for recurrence. *World Neurosurg* (2022) S1878–8750(22)00684-2. doi: 10.1016/j.wneu.2022.05.054

23. Van Diest PJ, Brugal G, Baak JP. Proliferation markers in tumours: Interpretation and clinical value. *J Clin Pathol* (1998) 51:716–72. doi: 10.1136/jcp.51.10.716

24. Wach J, Lampmann T, Güresir A, Schuss P, Vatter H, Herrlinger U, et al. FORGE: A novel scoring system to predict the MIB-1 labeling index in intracranial meningiomas. *Cancers (Basel)* (2021) 13(14):3643. doi: 10.3390/cancers13143643

25. Wach J, Brandecker S, Güresir A, Schuss P, Vatter H, Güresir E. The impact of the MIB-1 index on facial nerve outcomes in vestibular schwannoma surgery. *Acta Neurochir* (2020) 162:1205–13. doi: 10.3390/cancers13143643

26. Gerdes J, Schwab U, Lemke H, Stein H. Production of a mouse monoclonal antibody reactive with a human nuclear antigen associated with cell proliferation. *Int J Cancer* (1983) 31:13–20. doi: 10.1002/ijc.2910310104

27. Scholzen T, Gerdes J. The ki-67 protein: From the known and the unknown. *J Cell Physiol* (2000) 182:311–22. doi: 10.1002/(SICI)1097-4652(200003)182:3<311::AID-JCP1>3.0.CO;2-9

28. Vranic A, Popovic M, Cör A, Prestor B, Pizem J. Mitotic count, brain invasion, and location are independent predictors of recurrence-free survival in primary atypical and malignant meningiomas: A study of 86 patients. *Neurosurgery* (2010) 67:1124–32. doi: 10.1227/NEU.0b013e3181eb95b7

29. Oya S, Kawai K, Nakatomi H, Saito N. Significance of Simpson grading system in modern meningioma surgery: Integration of the grade with MIB-1 labeling index as a key to predict the recurrence of WHO grade I meningiomas. *J Neurosurg* (2012) 117:121–8. doi: 10.3171/2012.3.JNS111945

30. Kim MS, Kim KH, Lee EH, Lee YM, Lee SH, Kim HD, et al. Results of immunohistochemical staining for cell cycle regulators predict the recurrence of atypical meningiomas. *J Neurosurg* (2014) 121:1189–200. doi: 10.3171/2014.7.JNS132661

31. Liu N, Song SY, Jiang JB, Wang TJ, Yan CX. The prognostic role of ki-67/MIB-1 in meningioma: A systematic review with meta-analysis. *Medicine* (2020) 99:e18644. doi: 10.1097/MD.0000000000018644

32. Wach J, Lampmann T, Güresir Á, Vatter H, Herrlinger U, Becker A, et al. Proliferative potential, and inflammatory tumor microenvironment in meningioma correlate with neurological function at presentation and anatomical location–from convexity to skull base and spine. *Cancers* (2022) 14:1033. doi: 10.3390/cancers14041033

33. Faraji AH, Tonetti DA, Flickinger JC, Engh JA. Alteration of the ki-67 proliferative index following surgical resection with or without radiation therapy of intracranial meningiomas. *Cureus* (2017) 9:e1873. doi: 10.7759/cureus.1873

34. Antinheimo J, Haapasalo H, Haltia M, Tatagiba M, Thomas S, Brandis A, et al. Proliferation potential and histological features in neurofibromatosis 2-associated and sporadic meningiomas. *J Neurosurg* (1997) 87:610–4. doi: 10.3171/jns.1997.87.4.0610

35. Bassiouni H, Ntoukas V, Asgari S, Sandalcioglu EI, Stolke D, Seifert V. Foramen magnum meningiomas: clinical outcome after microsurgical resection *via* a posterolateral suboccipital retrocondylar approach. *Neurosurgery* (2006) 59:1177–85. doi: 10.1227/01.NEU.0000245629.77968.27

36. Samii M, Klekamp J, Carvalho G. Surgical results for meningiomas of the craniocervical junction. *Neurosurgery* (1996) 39:1086–95. doi: 10.1097/00006123-199612000-00003

37. McCormick PC, Post KD, Stein BM. Intradural extramedullary tumors in adults. *Neurosurg Clin N Am* (1990) 1:591–608. doi: 10.1016/S1042-3680(18)30792-7

38. Wostrack M, Ringel F, Eicker SO, Jägersberg M, Schaller K, Kerschbaumer J, et al. Spinal ependymoma in adults: a multicenter investigation of surgical outcome and progression-free survival. *J Neurosurg Spine* (2018) 28:654–62. doi: 10.3171/2017.9.SPINE17494

39. Zhu Q, Qian M, Xiao J, Wu Z, Wang Y, Zhang J. Myelopathy due to calcified meningiomas of the thoracic spine: minimum 3-year follow-up after surgical treatment. *J Neurosurg Spine* (2013) 18(5):436–42. doi: 10.3171/2013.2.SPINE12609

40. Ono K, Shimizu T, Fujibayashi S, Otsuki B, Murata K, Sakamoto A, et al. Predictive value of heterogeneously enhanced magnetic resonance imaging findings with computed tomography evidence of calcification for severe motor deficits in spinal meningioma. *Neurospine* (2021) 18(1):163–9. doi: 10.14245/ns.2040494.247

41. Nassiri F, Price B, Shebab A, Au K, Cusimano MD, Jenkinson MD, et al. Life after surgical resection of a meningioma: a prospective cross-sectional study evaluating health-related quality of life. *Neuro Oncol* (2019) 21(Suppl. 1):i32–43. doi: 10.1093/neuonc/noy152

42. Kim CH, Chung CK, Lee SH, Jahng TA, Hyun SJ, Kim KJ, et al. Long-term recurrence rates after the removal of spinal meningiomas in relation to Simpson grades. *Eur Spine J* (2016) 25:4025–32. doi: 10.1007/s00586-015-4306-2

43. Ramanauskas WL, Wilner HI, Metes JJ, Lazo A, Kelly JK. MR imaging of compressive myelomalacia. *J Comput Assist Tomogr* (1989) 13:399–404. doi: 10.1097/00004728-198905000-00005

44. Majores M, Schick V, Engels G, Fassunke J, Elger CE, Schramm J, et al. Mutational and immunohistochemical analysis of ezrin-, radixin-, moesin (ERM) molecules in epilepsy-associated glioneuronal lesions. *Acta Neuropathol* (2005) 110:537–46. doi: 10.1007/s00401-005-1088-3

45. Majores M, von Lehe M, Fassunke J, Schramm J, Becker AJ, Simon M. Tumor recurrence and malignant progression of gangliogliomas. *Cancer* (2008) 113:3355–63. doi: 10.1002/cncr.23965

46. Schneider M, Borger V, Güresir A, Becker A, Vatter H, Schuss P, et al. High mib-1-score correlates with new cranial nerve deficits after surgery for frontal skull base meningioma. *Neurosurg Rev* (2021) 44(1):381–7. doi: 10.1007/s10143-019-01222-0

47. Kasuya H, Kubo O, Tanaka M, Amano K, Kato K, Hori T. Clinical and radiological features related to the growth potential of meningioma. *Neurosurg Rev* (2006) 29(4):293–6. doi: 10.1007/s10143-006-0039-3

48. Matsuno A, Fujimaki T, Sasaki T, Nagashima T, Ide T, Asai A, et al. Clinical and histopathological analysis of proliferative potentials of recurrent and non-recurrent meningiomas. *Acta Neuropathol* (1996) 91:504–10. doi: 10.1007/s004010050458

49. Maiuri F, Del Basso De Caro M, de Divitiis O, Guadagno E, Mariniello G. Recurrence of spinal meningiomas: analysis of the risk factors. *Br J Neurosurg* (2020) 34(5):569–74. doi: 10.1080/02688697.2019.1638886

50. Nakamura M, Tsuji O, Fujiyoshi K, Hosogane N, Watanabe K, Tsuji T. Long-term surgical outcomes of spinal meningiomas. *Spine (Phila Pa 1976)* (2012) 37:E617–623. doi: 10.1097/BRS.0b013e31824167f1

51. Tang Y, Dundamadappa SK, Thangasamy S, Flood T, Moser R, Smith T, et al. Correlation of apparent diffusion coefficient with ki-67 proliferation index in grading meningioma. *AJR Am J Roentgenol* (2014) 202:1303–8. doi: 10.2214/AJR.13.11637

52. Pavelin S, Becic K, Forempoher G, Mrklic I, Pogorelic Z, Titlic M, et al. Expression of ki-67 and p53 in meningiomas. *Neoplasma* (2013) 60:480–5. doi: 10.4149/neo_2013_062

53. Roser F, Nakamura M, Bellinzona M, Ritz R, Ostertag H, Tatagiba MS. Proliferation potential of spinal meningiomas. *Eur Spine J* (2006) 15:211–5. doi: 10.1007/s00586-005-0937-z

54. Coons SW, Johnson PC. Regional heterogeneity in the proliferative activity of human gliomas as measured by the ki-67 labeling index. *J Neuropathol Exp Neurol* (1993) 52:609–18. doi: 10.1097/00005072-199311000-00008

55. Pham D, Skaland I, Winther TL, Salvesen Ø, Torp SH. Correlation between digital and manual determinations of ki-67/MIB-1 proliferative indices in human meningiomas. *Int J Surg Pathol* (2020) 28:273–9. doi: 10.1177/1066896919889148

56. Gadot R, Khan AB, Patel R, Goethe E, Shetty A, Hadley CC, et al. Predictors of postoperative seizure outcome in supratentorial meningioma. *J Neurosurg* (2021) 10:1–10. doi: 10.3171/20219.JNS211738

57. Charabi S, Engel P, Jacobsen GK, Tos M, Thomsen J. Growth rate of acoustic neuroma expressed by ki-67 nuclear antigen versus symptom duration. *Ann Otol Rhinol Laryngol* (1993) 102(10):805–9. doi: 10.1177/000348949310201013

58. Hashimoto N, Rabo CS, Okita Y, Kinoshita M, Kagawa N, Fujimoto Y, et al. Slower growth of skull base meninigomas compared with non-skull base meninigomas based on volumetric and biological studies. *J Neurosurg* (2012) 116 (3):574–80. doi: 10.3171/2011.11.JNS11999

59. Fountain DM, Soon WC, Matys T, Guilfoyle MR, Kirollos R, Santarius T. Volumetric growth rates of meningioma and its correlation with histological diagnosis and clinical outcome: a systematic review. *Acta Neurochir (Wien)* (2017) 159(3):435–45. doi: 10.1007/s00701-016-3071-2

60. Haddad AF, Young JS, Kanungo I, Sudhir S, Chen JS, Raleigh DR, et al. WHO grade I meningioma recurrence: Identifying high risk patients using histopathological features and the MIB-1 index. *Front Oncol* (2020) 10:1522. doi: 10.3389/fonc.2020.01522

61. Aguiar PH, Tsanaclis AM, Tella OIJr, Plese JP. Proliferation rate of intracranial meningiomas as defined by the monoclonal antibody MIB-1: correlation with peritumoural oedema and other clinicoradiological and histological characteristics. *Neurosurg Rev* (2003) 26(3):221–8. doi: 10.1007/s10143-003-0261-1

62. Nakaguchi H, Fujimaki T, Matsuno A, Matsuura R, Asai A, Suzuki I, et al. Postoperative residual tumor growth of meningioma can be predicted by MIB-1 immunohistochemistry. *Cancer* (1999) 85(10):2249–54. doi: 10.1002/(SICI)1097-0142(19990515)85:10<2249::AID-CNCR21>3.0.CO;2-5

63. Nakasu S, Nakajima M, Matsumura K, Nakasu Y, Handa J. Meningioma: proliferating potential and clinicoradiological features. *Neurosurgery* (1995) 37 (6):1049–55. doi: 10.1227/00006123-199512000-00003

64. Roser F, Samii M, Ostertag H, Bellinzona M. The ki-67 proliferation antigen in meningiomas. experience in 600 cases. *Acta Neurochir (Wien)* (2004) 146(1):37–44. doi: 10.1007/s00701-003-0173-4

65. Ekşi MŞ, Canbolat Ç, Akbaş A, Özmen BB, Akpınar E, Usseli Mİ, et al. Elderly patients with intracranial meningioma: Surgical considerations in 228 patients with a comprehensive analysis of the literature. *World Neurosurg* (2019) 132:e350–65. doi: 10.106/j.wneu.2019.08.150

66. Roser F, Nakamura M, Ritz R, Bellinzona M, Dietz K, Samii M, et al. Proliferation and progesterone receptor status in benign meningiomas are not age dependent. *Cancer* (2005) 104(3):598–601. doi: 10.1002/cncr.21192

67. Kobayashi K, Ando K, Matsumoto T, Sato K, Kato F, Kanemura T, et al. Clinical features and prognostic factors in spinal meningioma surgery from a multicenter study. *Sci Rep* (2021) 11(1):11630. doi: 10.1038/s41598-021-91225-z

68. Kshettry VR, Ostrom QT, Kruchko C, Al-Mefty O, Barnett GH, Barnholtz-Sloan JS. Descriptive epidemiology of world health organization grades II and III intracranial meninigomas in the united states. *Neur Oncol* (2015) 17(8):1166–73. doi: 10.1093/neuonc/nov069

69. Zeng L, Liang P, Jiao J, Chen J, Lei T. Will an asymptomatic meningioma grow or not grow? a meta-analysis. *J Neurol Surg A Cent Eur Neurosurg* (2015) 76 (5):341–7. doi: 10.1055/s-0034-1543959

70. Rubin G, Herscovici Z, Laviv Y, Jackson S, Rappaport ZH. Outcome of untreated meningiomas. *Isr Med Assoc J* (2011) 13(3):157–60.

71. Niiro M, Yatsushiro K, Nakamura K, Kawahara Y, Kuratsu J. Natural history of elderly patients with asymptomatic meningiomas. *J Neurol Neurosurg Psychiatry* (2000) 68(1):25–8. doi: 10.1136/jnp.68.1.25

72. Kuratsu J, Kochi M, Ushio Y. Incidence and clinical features of asymptomatic meningiomas. *J Neurosurg* (2000) 92(5):766–70. doi: 10.3171/jns.2000.92.5.0766

73. Doita M, Harada T, Nishida K, Marui T, Kurosaka M, Yoshiya S. Recurrent calcified spinal meningioma detected by plain radiograph. *Spine (Phila Pa 1976)* (2001) 26(11):E249–252. doi: 10.1097/00007632-200106010-00005

74. Setzer M, Vatter H, Marquardt G, Seifert V, Vrionis FD. Management of spinal meningiomas: surgical results and a review of the literature. *Neurosurg Focus* (2007) 23(4):E14. doi: 10.3171/FOC-07/10/E14

75. Mirian C, Skyrman S, Bartek JJr, Jensen LR, Kihlström L, Förander P, et al. The ki-67 proliferation index as a marker of time to recurrence in intracranial meningioma. *Neurosurgery* (2020) 87(6):1289–98. doi: 10.1093/neuros/nyaa226

76. Wach J, Lampmann T, Güresir Á, Vatter H, Herrlinger U, Becker A, et al. Inflammatory tumor microenvironment in cranial meningiomas: Clinical implications and intraindividual reproducibility. *Diagnostics* (2022) 12:853. doi: 10.3390/diagnostics12040853

77. Moriya J, Tanino MA, Takenami T, Endoh T, Urushido M, Kato Y, et al. Rapid immunocytochemistry based on alternating current electric field using squash smear preparation of central nervous system tumors. *Brain Tumor Pathol* (2016) 33:13–8. doi: 10.1007/s10014-015-0238-0

78. Terata K, Saito H, Nanjo H, Hiroshima Y, Ito S, Narita K, et al. Novel rapid-immunohistochemistry using an alternating current electric field for intraoperative diagnosis of sentinel lymph nodes in breast cancer. *Sci Rep* (2017) 7:2810. doi: 10.1038/s41598-017-02883-x

79. Kirkegaard LJ, DeRose PB, Yao B, Cohen C. Image cytometric measurement of nuclear proliferation markers (MIB-1, PCNA) in astrocytomas. prognostic significance. *Am J Clin Pathol* (1998) 109:69–74. doi: 10.1093/ajcp/109.1.69

frontiers | Frontiers in Oncology

TYPE Original Research
PUBLISHED 21 September 2022
DOI 10.3389/fonc.2022.967420

Check for updates

OPEN ACCESS

EDITED BY
Hailiang Tang,
Fudan University, China

REVIEWED BY
Mirza Pojskic,
University Hospital of Giessen and Marburg, Germany
Randall Porter,
Barrow Neurological Institute, United States

*CORRESPONDENCE
Martin Andreas Proescholdt
martin.proescholdt@ukr.de

SPECIALTY SECTION
This article was submitted to Neuro-Oncology and Neurosurgical Oncology, a section of the journal Frontiers in Oncology

RECEIVED 12 June 2022
ACCEPTED 29 August 2022
PUBLISHED 21 September 2022

CITATION
Mederer T, Schachinger S, Rosengarth K, Brosig A, Schebesch K-M, Doenitz C, Schmidt N-O and Proescholdt MA (2022) Symptom burden and surgical outcome in non-skull base meningiomas. *Front. Oncol.* 12:967420. doi: 10.3389/fonc.2022.967420

COPYRIGHT
© 2022 Mederer, Schachinger, Rosengarth, Brosig, Schebesch, Doenitz, Schmidt and Proescholdt. This is an open-access article distributed under the terms of the Creative Commons Attribution License (CC BY). The use, distribution or reproduction in other forums is permitted, provided the original author(s) and the copyright owner(s) are credited and that the original publication in this journal is cited, in accordance with accepted academic practice. No use, distribution or reproduction is permitted which does not comply with these terms.

Symptom burden and surgical outcome in non-skull base meningiomas

Tobias Mederer[1,2], Sebastian Schachinger[1,2], Katharina Rosengarth[1,2], Anja Brosig[3], Karl-Michael Schebesch[1,2], Christian Doenitz[1,2], Nils-Ole Schmidt[1,2] and Martin Andreas Proescholdt[1,2]*

[1]Department of Neurosurgery, University Hospital Regensburg, Regensburg, Germany, [2]Wilhelm Sander-NeuroOncology Unit, University Hospital Regensburg, Regensburg, Germany, [3]Department of Otorhinolaryngology, University Hospital Regensburg, Regensburg, Germany

Purpose: Non-skull base meningiomas (NSBM) are a distinct entity and frequently present with focal neurological deficits. This study was designed to analyze functional and oncological outcome following microsurgical tumor resection in patients with NSBM.

Patients and methods: An analysis of 300 patients that underwent NSBM resection between 2003 and 2013 was performed. Assessment measures for functional outcome were Karnofsky Performance Scale (KPS), Medical Research Council - Neurological Performance Scale (MRC-NPS), and improvement rates of focal deficits and seizures. The extent of resection; recurrence-free survival (RFS) and tumor-specific survival (TSS) were also determined.

Results: Impaired KPS and MRC-NPS were present in 73.3% and 45.7%, respectively. Focal neurological deficits were recorded in 123 patients (41.0%), with hemiparesis (21.7%) and aphasia (9.3%) the most prevalent form of impairment. Most meningiomas were localized at the convexity (64.0%), followed by falcine tumors (20.3%). Both KPI and MRC-NPS scores were significantly improved by surgical resection. Postoperative improvement rates of 96.6%, 89.3%, 72.3%, 57.9%, and 27.3% were observed for aphasia, epilepsy, hemiparesis, cranial nerve, and visual field deficits, respectively. Long-term improvement was achieved in 83.2%, 89.3%, 80.0%, 68.4% and 54.6% of patients, respectively. Gross total resection (GTR) over subtotal resection (STR) significantly improved preoperative seizures and visual field deficits and correlated with reduced risk of new postoperative hemiparesis. Poor Simpson grade was the only significant prognostic factor in multivariate analysis for long-term functional deficit, which occurred in 7.3%. Median RFS was 45.9 months (6.0 - 151.5 months), while median TSS was 53.7 months (3.1 – 153.2 months). Both WHO grade (p= 0.001) and Simpson classification (p= 0.014 and p= 0.031) were independent significant prognostic factors for decreased RFS and TSS by multivariate analysis, respectively. Furthermore, tumor

diameter > 50 mm (p= 0.039) significantly correlated with decreased TSS in multivariate analysis.

Conclusion: Surgical resection significantly and stably improves neurological deficits in patients with NSBM.

KEYWORDS

meningioma, neurological deficit, resection, outcome, recurrence

1 Introduction

Meningiomas are the most frequent intracranial neoplasms and arise from arachnoid cap cells in the central nervous system (CNS) (1). According to the World Health Organization (WHO) classification of CNS tumors, meningiomas are divided into three grades with increasing malignancy (2). While roughly 80% of all meningiomas are WHO grade I with a good prognosis, the mortality and recurrence rates increase with WHO grades II and III (3). Based on tumor location, meningiomas are dichotomized into skull base (SBM) and non-skull base meningiomas (NSBM) (4). In addition to localization, several aspects indicate that SBM and NSBM are biologically and clinically distinct entities. Patients with NSBM present at an older age compared to SBM (5), and significantly more male patients are affected (6). Although a gross total resection defined as resection grade I or II according to the Simpson classification (7) is achieved more frequently (8, 9) and consequently, the recurrence rates are lower in NSBM (10), the progression-free interval is shorter (11) and the volumetric growth rate is significantly faster in NSBM (12). This aspect is reflected by the 2-4 times higher risk for WHO grade II or III malignancy grades (11, 13–16) and the significantly higher proliferation index (5, 17) in NSBM even when analyzing WHO grade I tumors only (9). The tendency of NSBM to develop more aggressive lesions may be caused by a different cell of origin in addition to a specific molecular framework of these tumors (18–20). Surgical resection in NSBM patients has three main goals: 1. Acquisition of tissue to establish a histological and molecular diagnosis (21); 2. Maximal removal of neoplastic tissue to achieve optimal tumor control (22); and 3. Decompression of eloquent brain - structures to normalize the neuro-functional status of the affected patients (23). Several studies have addressed the postoperative improvement of neurological symptoms after meningioma resection (24–30). However, no data are available reflecting the role of surgical resection on the functional status in NSBM patients as they reflect a separate entity with regard to localization, symptom burden, and clinical and biological dynamics. Therefore, our study aimed to assess the short and long-term impact of surgery on clinical performance scale rating, focal neurological impairments, and frequency of seizures as well as to evaluate prognostic factors for neurological improvement, tumor recurrence, and tumor-specific survival in NSBM patients.

Abbreviations: EOR, Extent of resection; FLAIR, Fluid-attenuated inversion recovery; GTR, Gross total resection; KPS, Karnofsky performance score; MRC-NPS, Medical Research Council - Neurological Performance Scale; NSBM, Non-skull base meningioma; RFS, Recurrence-free survival; SBM, Skull base meningioma; STR, Subtotal resection; TSS, Tumor-specific survival; vs., Versus.

2 Methods

2.1 Patient population and ethical approval

We conducted a prospective clinical registry for all patients diagnosed with an NSBM between 2003 and 2013 that underwent craniotomy and microsurgical tumor resection at the University Hospital of Regensburg. A total of 300 patients were included in this study. Skull-base meningiomas and patients under the age of 18 were excluded. Informed consent was obtained from all patients. A qualified staff neurosurgeon performed all tumor resections; the intraoperative findings were collected by reviewing the surgery reports. All data was either collected prospectively during follow-up appointments or retrospectively by reviewing outpatient records and/or by contacting the patient's primary care physician. The study was conducted in accordance with the ethical standards of the Helsinki Declaration and approved by the local ethics review board (20-1799-101).

2.2 Functional assessment

Clinical, neurological and oncological outcome was evaluated at three time points: preoperative, postoperative, and last follow-up. Clinical and neurological performance was

classified by the Karnofsky Performance Scale (KPS) and the Medical Research Council - Neurological Performance Scale (MRC-NPS) (31). Tumor recurrence was classified as progression of residual tumor or tumor recurrence after gross total resection (GTR) in follow-up brain imaging according to RANO criteria (32).

2.3 Imaging analysis

Patients received preoperative MRI scans according to a standard screening protocol including in T1-weighted imaging with and without contrast agent, T2-weighted-, FLAIR and diffusion-weighted imaging. Lesions that showed more than 35% peritumoral FLAIR or T2 hyperintensity in relation to the tumor volume were classified as tumors with significant perifocal edema. The largest axial diameter in T1-weighted, contrast-enhanced imaging was measured for tumor size assessment. On the day after surgery, patients underwent a postoperative CT scan. Follow-up imaging included a baseline MRI 3 months after surgery, followed by yearly MRI scans in grade I meningiomas. Higher grade meningiomas were scanned every 6 (grade II) and 3 months (grade III). Extent of resection (EOR) was evaluated by reviewing surgical reports and by an independent neuro-radiologist based on the postoperative baseline MRI scans.

2.4 Histopathological assessment

Histopathological diagnoses were performed by independent neuropathologists according to the WHO grading system for meningiomas. MIB-1 labeling index was determined by neuropathologists as the percent of positively stained tumor cell nuclei in a minimum of four high magnification (400x) visual fields.

2.4 Statistical analysis

Descriptive and comparative statistical analyses were performed with Stata software (version 14.2, Stata Corporation, College Station, TX, USA). Continuous variables are reported as mean, median, and range. Rates and proportions were analyzed using Chi square analysis, group differences were detected by performing two-tailed Mann-Whitney testing, and one-way repeated measure ANOVA. To analyze survival rates, the Kaplan-Meier method was applied, univariate analysis was performed by log-rank test, and multivariate testing was performed by calculating a multivariate logistic regression or a multivariate Cox regression analysis. Violin plots and Sankey plots were created with the online software PlotsOfData (33) and RAWGraphs (34) and modified with Adobe Illustrator CC 2018.

3 Results

3.1 Description of patient characteristics and treatment pattern

A total of 300 consecutive patients with an NSBM surgically treated at the University Hospital of Regensburg between 2003 and 2013 were included in this study. The majority of resections (95.7%) were either performed or supervised by a team of 5 board-certified attending neurosurgeons with a comparable level of experience. The clinical baseline characteristics of the entire study population are summarized in Table 1. The median age was 60.6 years (range: 25.2 - 89.1 years) with a male-to-female ratio of 1:2.3 (91 males and 209 females). The median follow-up time was 87.0 months (range: 3 - 153.4 months). Histopathological diagnosis showed 253 (84.3%) WHO I, 44 (14.7%) WHO II, and 3 (1.0%) anaplastic WHO III meningiomas. Most tumors were localized at the convexity (64.0%), followed by falcine tumors (20.3%), from which the anterior third of the falx was most prevalently affected (68.8%). Parasagittal tumors occurred in 15.7% of all patients. The predominant brain lobe locations were frontal and fronto-parietal with 47.3% and 23.7%, respectively. Gross total resection (GTR) corresponding to Simpson I (51.0%) and Simpson II (28.3%) was achieved in 79.3% of the patients. In 62 patients (20.7%) only subtotal resection (STR) could be achieved (Simpson III: 7.0%, Simpson IV: 13.3% and Simpson V: 3.3%; Figures 1A–D). We found a significantly worse GTR rate in parasagittal tumors (38.3% GTR vs. 86.89% and 86.98% in falcine and convexity, respectively; $p = 0.0001$). A total of 16 patients (5.3%) received radiation treatment. Immediately after resection, seven patients were treated with radiation (2.3%; 6 WHO grade II tumors and 1 WHO grade III tumor). Four patients (1.3%) were radiated following resection of a recurrent tumor, and two patients with recurrent tumors received radiation without another resection. Finally, three patients received radiation after the second recurrence. In incomplete resections, the decision for radiation treatment was made based on clinical, radiological, and histological criteria in the interdisciplinary neurooncological tumor board. In the majority of cases with incomplete resection of a WHO grade I tumor, radiation treatment was started whenever signs of tumor progress were detected.

While 89.7% of the patients initially presented with tumor-related symptoms, 34 of the patients (10.3%) were diagnosed with meningioma because of non-related symptoms that had led to brain imaging. The most frequent presenting symptoms for NSBM consisted of headache (32.3%), generalized or partial seizures (29.7%), and hemiparesis (17.3%). Aphasia or visual field deficits were seen in 9.3% and 3.7% of the patients, respectively. Hemiparesis occurred significantly more frequently in frontoparietal tumors compared to all other

TABLE 1 Clinical characteristics of the entire patient cohort.

Variable	Number (%)
N =	300
Age (years)	60.6
Median	(25.2 – 89.1)
Range	
Sex (f/m)	209 (69.7)/91 (30.3)
Follow up time (months)	87
Median	3 – 153
Range	
WHO grade	253 (84.3)
I	44 (14.7)
II	3 (1.0)
III	
MIB-1 labeling index (%)	5.3
Mean	
Tumor diameter (mm)	
Median	37
Range	4-120
Presurgical KPI	
Median	90
Range	60 - 100
Extent of resection	
GTR (Gross total resection)	238 (79.3)
STR (Subtotal resection)	62 (20.7)
Simpson classification	
I	153 (51.0)
II	85 (28.3)
III	21 (7.0)
IV	40 (13.3)
V	1 (0.3)
Bone infiltration	
Yes	75 (25.0)
No	225 (75.0)
Venous sinus infiltration	
Yes	72 (24.0)
No	228 (76.0)
Localization	
Convexity	192 (64.0)
Falx cerebri	61 (20.3)
Parafalcine	47 (15.7)
Side	
Left	147 (49.0)
Right	136 (45.3)
Bilateral	17 (5.7)
Lobe	
Frontal	142 (47.3)
Fronto-parietal	71 (23.7)
Parietal	31(10.3)
Parieto-occipital	16 (5.3)
Occipital	14 (4.7)
Temporal	14 (4.7)
Fronto-temporal	8 (2.6)
Temporo-parietal	3 (1.0)
Temporo-occipital	1 (0.3)

affected lobes (p = 0.027). Visual field deficits were more prevalent in parasagittal tumors (p = 0.010). Psychoorganic syndrome (memory loss, emotional lability, reduced intellectual capacity) was significantly more frequent in falcine tumors with 13.1% compared to 6.4% in parasagittal and 3.65% in convexity tumors (p = 0.025). Seizures occurred significantly more frequently in convexity tumors (27.08%) vs. 13.11% and 10.64% in falcine and parasagittal tumors, respectively (p = 0.009). WHO grades and histology classes were evenly distributed throughout the lobes and the location of the tumors. Tumors with a higher grade of malignancy (WHO grade II&III) presented significantly more frequently with large perifocal edema compared to WHO grade I tumors (59.9% vs. 38.1%; p = 0.012)). Presurgical median KPI and NPS were significantly worse in WHO grade II&III tumors compared to WHO grade I tumors (p = 0.006 and 0.0156, respectively), also, focal neurological deficits were significantly more frequent in patients with grade II&III compared to grade I tumors (p = 0.001).

3.2 Surgical morbidity and mortality

Perioperative complications were seen in 62 patients (20.7%), while 87.1% of these patients had pre-consisting comorbidities such as arterial hypertension (38.3%), thyroid disease (15.3%), diabetes (13.0%), other neoplasms (10.0%), obesity (9.3%), coronary heart disease (4.0%), smoking (3.6%) and chronic obstructive pulmonary disease (3.3%). In addition, patients showing postoperative complications were significantly older compared to those without complications (p = 0.030). The most frequent complications were CSF leaks (10.6%), wound healing disorders (7.3%), and intracranial hemorrhage (4.3%) (Table 2). The mortality rate was 1.0%, while the three patients that died within 30 days of surgery had either low preoperative Karnofsky Performance Scores (50-60) or higher-grade meningioma (WHO II).

3.3 Functional outcome

The functional outcome of the patients following craniotomy and microsurgical tumor resection was assessed by the Karnofsky Performance Status (KPS) and the Medical Research Council - Neurological Performance Scale (MRC-NPS) preoperatively, postoperatively, and during the long-term follow-up. Both KPS and MRC-NPS scores improved significantly upon surgery (85.80 vs. 89.27, p < 0.0001 and 1.687 vs. 1.477, p = 0.0008 respectively) (Figures 2A, B). During the follow-up the KPS remained stable (89.47, P =

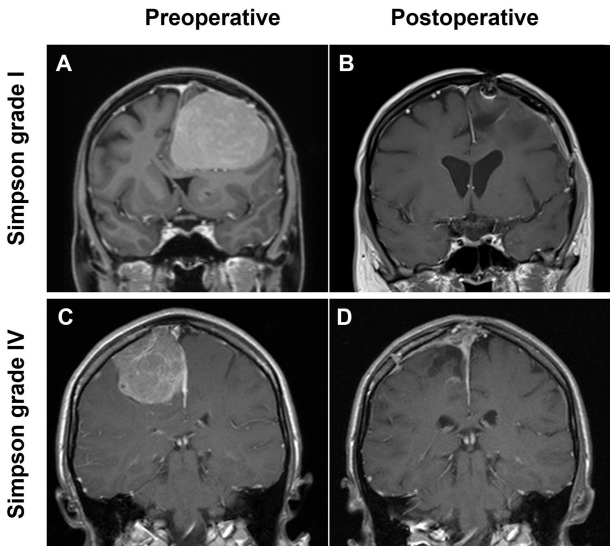

FIGURE 1
Illustration of two cases with large NSBM; T1-weighted, contrast-enhanced MRI scans in coronal orientation are shown. **(A)** Convexity meningioma receiving a grade Simpson I resection **(B)**, **(C)** a parasagittal lesion with a Simpson IV resection **(D)**.

0.359), whereas the neurological outcome - measured by the MRC-NPS - further improved (1.360, p = 0.0036) (Figure 2B). Patients with grade I tumors showed significantly more frequent improvement of both presurgical KPS and MRC-NPS compared to patients with grade II&III tumors (p = 0.004 and p = 0.026, respectively). No significant differences in the KPS or MRC-NPS improvement rates were detected between the separate tumor locations.

3.3.1 Epilepsy

86 of the 89 patients (96.6%) presenting with epilepsy preoperatively were free of seizures following the surgery, and 71 (79.8%) patients remained stable during the follow-up. While for 15 patients that had improved after tumor resection, epilepsy re-occurred, three patients showing no neurological improvement upon surgery were asymptomatic in the follow-up, resulting in a long-term improvement rate of 83.2% (Figure 3A).

TABLE 2 Postoperative complications.

Complication	Number (%)
CSF leakage	32 (10.6)
Wound healing disorder	22 (7.3)
Intracranial hematoma	13 (4.3)
Pulmonary embilism	8 (2.7)
Increased ICP	6 (2.0)
Stroke	4 (1.3)
Pneumonia	3 (1.0)
Cardiac complications	1 (0.3)
Sinus vein thrombosis	1 (0.3)

3.3.2 Aphasia

Aphasia improved both postoperatively and long-term in 25 of the 28 patients (89.3%). One patient experienced worsening of aphasia after being asymptomatic following surgery, while another patient improved during the follow-up (Figure 3B).

3.3.3 Hemiparesis

For hemiparesis, we observed an improvement rate of 72.3% (47/65), while 64.6% (42/65) remained stable in the follow-up. Interestingly, 44.4% (4/9) of patients with initial worsening completely regained motor function in the follow-up, resulting in an overall long-term improvement rate of 80.0% (52/65) (Figure 3C).

3.3.4 Cranial nerve deficits

Cranial nerve deficits were seen in 19 preoperative patients, of which 57.9% (10/19) and 68.4% (13/19) improved after surgery and in the follow-up, respectively. Two patients (10.6%) experienced postoperative worsening of the deficit. (Figure 3D).

3.3.5 Visual field deficits

The lowest improvement rates were observed for visual field deficits. Three of eleven patients (27.3%) improved postoperatively, while a total of six patients (54.6%) improved

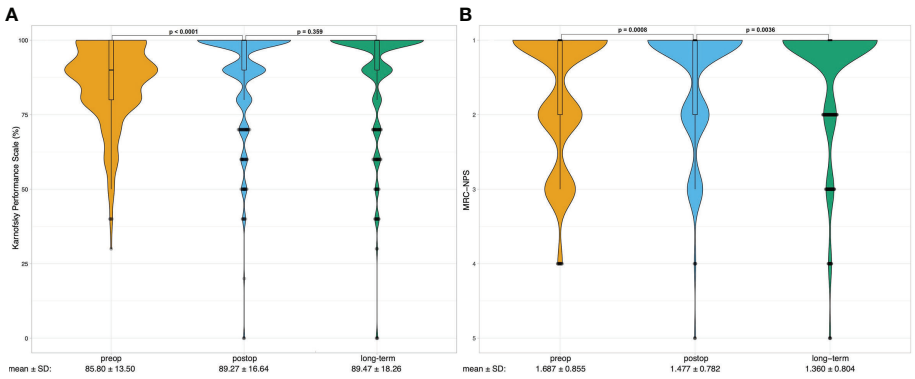

FIGURE 2
Violin plots show the distribution of preoperative (preop, yellow), postoperative (postop, blue) long-term (last follow-up, green) **(A)** Karnofsky Performance Scale (KPS) scores and **(B)** Medical Research Council - Neurological Performance Scale scores of the analyzed patients (n=300). Boxplots are shown within violin plots depicting median with lower and upper quartiles. Whiskers represent 1.5 interquartile range. Outliers are depicted as points. One-way repeated measure ANOVA was calculated to analyze the difference between preop, postop and long-term performance, the p – values are noted on top of the graph. Below the plots mean scores with standard deviations (SD) are shown.

in the follow-up. One patient (9.1%) experienced exacerbated visual field deficit after tumor resection (Figure 3E).

3.3.6 Neurological morbidity

A total of 43 patients (14.3%) experienced a new neurological deficit directly following NSBM surgery. This postoperative neurological morbidity was 9.7%, 4.3%, 2.3%, and 0.7% for newly occurring hemiparesis, epilepsy, aphasia and cranial nerve deficits, respectively. No new postoperative visual field deficit was observed. The deficit remained unchanged in 34.8% (8/23) for hemiparesis, 38.5% (5/13) for epilepsy, and 42.9% (3/7) for aphasia. Thus, 13 patients experienced a new permanent neurological deficit or worsening of a pre-consisting deficit, resulting in an overall neurological morbidity of 4.3% at follow-up. When combining neurological morbidity with reduced clinical performance after tumor resection measured by long-term KPS scores, 22 patients (7.3%) showed long-term neurological or clinical deterioration following surgery for NSBM. Univariate analysis revealed a significant correlation between WHO grading ($p = 0.001$), MIB labeling index ($p = 0.002$), Simpson classification ($p = 0.002$), venous sinus infiltration ($p = 0.003$) and tumor diameter ≤/> 50 mm ($p = 0.042$) with the long-term functional outcome. Age, sex, localization, and bone infiltration did not significantly correlate with permanent neurological or clinical deterioration. Upon multivariate logistic regression analysis, only poor Simpson grade remained a significant independent prognostic factor for decreased functional outcome ($p = 0.012$).

3.3.7 Effect of extent of resection on functional recovery

The extent of resection (EOR) was not associated with the postoperative improvement rates of the presurgical KPS and MRC-NPS scores ($p = 0.122$ and $p = 0.365$, respectively). However, seizures and visual field deficits were more likely to improve postoperatively when GTR of the tumor was achieved ($p = 0.041$ and 0.026, respectively). No significant differences were found between GTR and STR in the improvement of hemiparesis ($p = 0.869$), aphasia ($p = 0.435$), and cranial nerve deficits ($p = 0.570$) (Table 3). There was no significant difference in the incidence of new postoperative deficits between GTR versus STR, except for hemiparesis. A new postoperative hemiparesis was less likely to occur when GTR was achieved ($p = 0.013$) (Table 3).

3.4 Survival outcome

3.4.1 Recurrence-free survival outcome

Within the follow-up, 42 (24 female and 18 male) patients (14.0%) presented with a tumor recurrence. 54.8% (23/42) of the recurred tumors were WHO I, while 40.5% (17/42) and 4.8% (2/42) were WHO II and WHO III. The median RFS was 45.9 months (6.0 - 151.5 months). The Kaplan-Meier plot for the RFS stratified by WHO grades are shown in Figure 4A. The

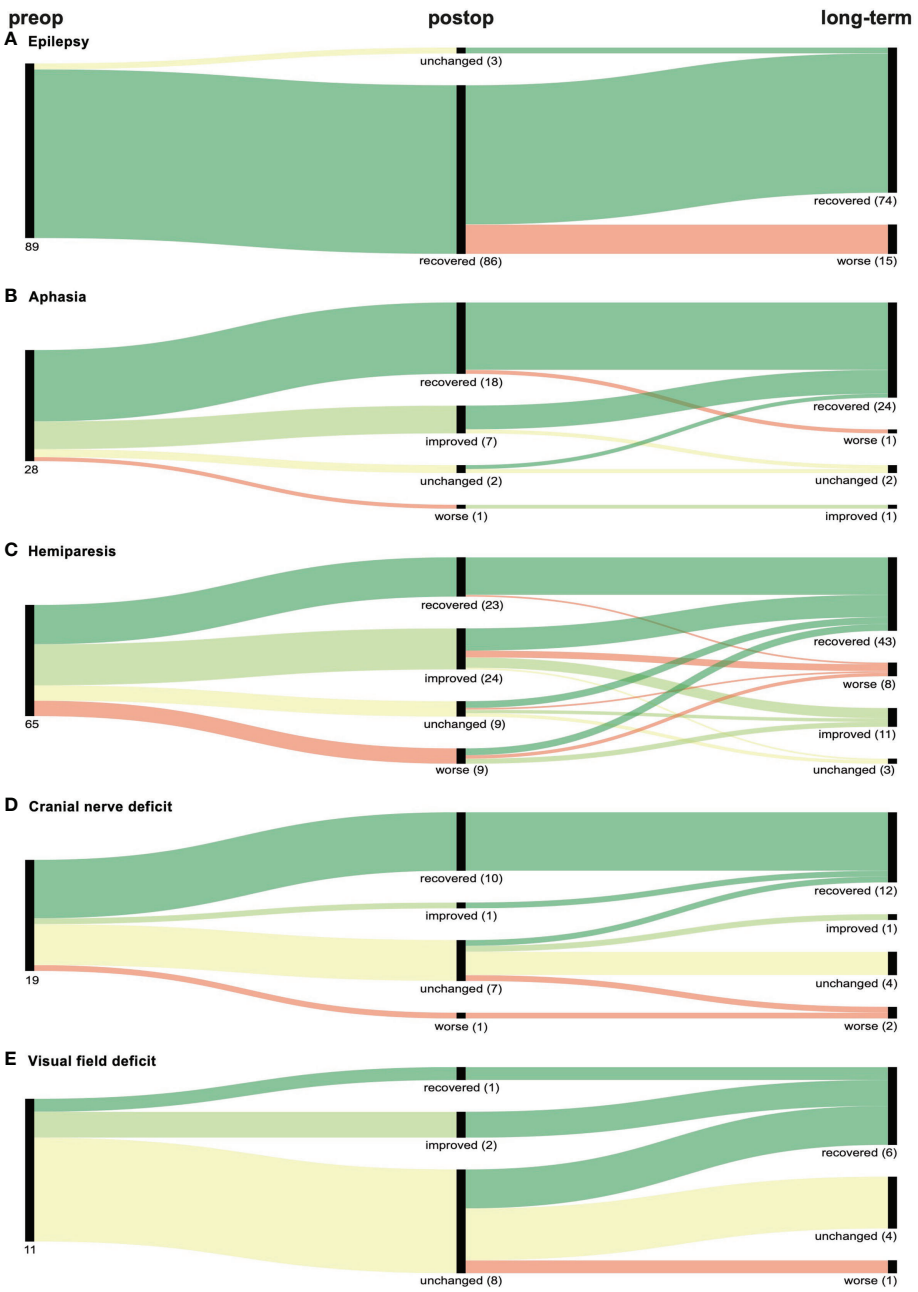

FIGURE 3
Graphical representation (Sankey plots) of the neurological outcome of patients with preoperative (preop) **(A)** epilepsy, **(B)** aphasia, **(C)** hemiparesis, **(D)** cranial nerve deficit or **(E)** visual field deficit within 30 days after surgery (postop) and at last follow-up (long-term). Symptom improvement and recovery is represented in light and dark green respectively while worsening of symptoms is depicted in red. No change in deficits is marked yellow. Numbers in parenthesis indicate number of patients of each branch.

recurrence-rates were 9.1%, 38.6%, and 66.7% for WHO I, II, and III meningiomas, respectively. Univariate analysis (log-rank testing) of tumor characteristics showed a significant correlation of WHO grade ($p = 0.0001$), Simpson classification ($p = 0.0040$), venous sinus infiltration ($p = 0.0010$) and tumor diameter ≤/> 50 mm ($p = 0.0250$) with RFS (Table 4). The MIB labeling index, age, sex, localization, and bone infiltration did not significantly correlate with RFS ($p > 0.05$). Upon multivariate logistic

TABLE 3 Improvement and worsening rates of seizures and focal neurological deficits stratified by gross total resection (GTR) vs. subtotal resection (STR) in NSBM patients.

Deficit	EOR*	Postoperative change			
		Improvement rate (%)	p-value	Worsening rate (%)	p-value
Seizures	GTR	89.3	0.041	9.7	0.522
	STR	69.2		3.3	
Aphasia	GTR	91.3	0.459	2.5	0.759
	STR	80.0		3.2	
Hemiparesis	GTR	74.5	0.529	8.4	0.013
	STR	66.6		19.4	
Cranial nerve deficit	GTR	52.9	0.202	1.3	0.374
	STR	84.4		0.0	
Visual field deficit	GTR	60.0	0.026	0.0	NA**
	STR	0.0		0.0	

*EOR, Extent of resection.
**NA, Not applicable.

regression analysis of the significant variables in the univariate testing, the WHO grade (p = 0.0001), the Simpson classification (p = 0.014) and tumor diameter > 50 mm (p = 0.039) remained significant independent variables for RFS in NSBM (Table 4).

3.4.2 Overall survival (OS) and tumor-specific survival (TSS)

Overall, 49 patients died within the follow-up with a median OS of 51.3 months (0.5 - 153.2 months). For 19 of those patients (38.8%), the cause of death was tumor-related. Therefore, the median TSS was 53.7 months (3.1 – 153.2 months). The TSS Kaplan-Meier plot can be seen in Figure 4B. Eleven, six, and two patients died because of a WHO I, II, or III meningioma, resulting in a mortality of 4.3%, 13.6%, and 66.7% for the median follow-up of 87.0 months, respectively.

There was a significant association of WHO grading (p = 0.0001), Simpson classification (p = 0.0260) and venous sinus infiltration (p = 0.0140) with TSS in univariate log rank testing. All other characteristic (tumor diameter ≤/> 50 mm, age, sex, localization, MIB labeling index, bone infiltration) were not significantly correlated (p > 0.05). Multivariate logistic regression analysis of the three associated variables revealed that only WHO grading (p = 0.001) and Simpson classification (p = 0.031) remained significant independent variables for TSS (Table 5).

4 Discussion

Meningiomas are mostly benign intracranial lesions in which surgical resection leads to durable tumor control (32, 35, 36). A recent study has demonstrated that low-risk meningiomas after GTR, the 10-year progression-free survival rate is 87.6% (37). Even in higher grade meningiomas, treated

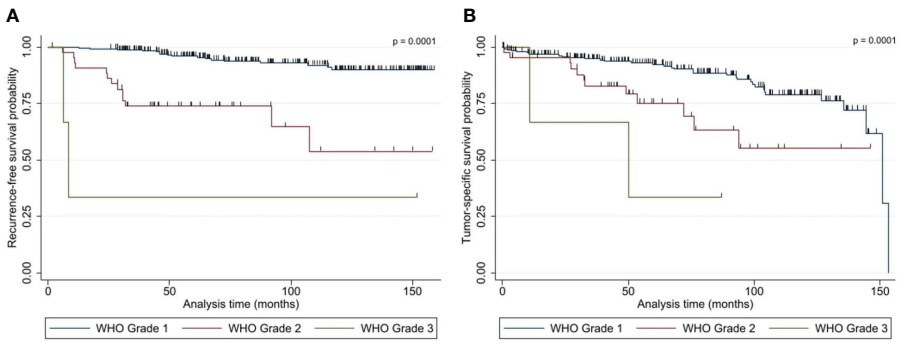

FIGURE 4
Kaplan-Meier plots show the **(A)** recurrence-free survival and **(B)** overall survival of patients with NSBM following tumor resection based on WHO grading (n=300). P-values (log rank test) are shown.

TABLE 4 Univariate (logrank) and multivariate (logistic regression) analysis of factors associated with recurrence–free survival (RFS).

	Univariate analysis	Multivariate logistic regression analysis			
Parameter	**p-value**	**Hazard Ratio**	**95% CI**		**p-value**
WHO grade	0.0001	1.633	0.936	2.330	0.0001
Venous sinus infiltration	0.0010	0.354	-0.549	1.257	0.442
Simpson classification	0.0040	0.457	0.092	0.822	0.014
Tumor diameter > 50 mm	0.0250	0.767	0.038	1.497	0.039

TABLE 5 Univariate (logrank) and multivariate (logistic regression) analysis of factors associated with tumor–specific survival (TSS).

	Univariate analysis	Multivariate logistic regression analysis			
Parameter	**p-value**	**Hazard Ratio**	**95% CI**		**p-value**
WHO grade	0.0001	1.477	0.614	2.341	0.0001
Venous sinus infiltration	0.0140	0.118	-1.105	1.341	0.850
Simpson classification	0.0260	0.535	0.048	10.210	0.031

with surgical resection followed by adjuvant radiation treatment, a 10-year progression-free survival rate of 57.7% can be acomplished (38). In NSBM, recurrence rates range between 2.2% and 15% following gross total resection (39–41). Even after subtotal resection, long-term tumor control can be achieved with adjuvant radiation treatment (42) (38).As meningiomas may be considered to be a potentially curable disease, the actual clinical challenge for both patients and caregivers appears to arise from an entirely different aspect (32). According to a recent study, almost half of NSBM patients present with significant neurological symptoms (43) that stay unresolved over an extended period in 27% of the patients (27). In addition, meningioma patients frequently present with significant neurocognitive impairment (44), which persists in about 40% of the patients following surgical resection (45). Particularly patients with NSMB frequently experience partial and general seizures (26, 46), leading to antiepileptic drug treatment, which additionally causes compromised neurocognitive function (29, 47). These factors cause significantly impaired quality of life, even up to 10 years after initial diagnosis (48). Surgical resection may positively influence focal neurological impairment (24, 43), neurocognitive function (44), seizure frequency (26) and quality of life (30). Given NSBM's specific biology, clinical dynamic, and symptomatology (11, 12, 25, 49), we attempted with our study to assess the functional recovery rates specifically in NSBM patients. Our data revealed that improvement rates of preoperative symptoms vary depending on the type of neurological deficit. Visual field deficits showed with 27.3%, the poorest improvement rate following surgery, which is in accordance with a recent study reporting only 16% recovery rate of visual field deficits in NSBM patients following surgical resection (24). Interestingly, studies summarizing focal neurological improvement rates in stroke patients also demonstrated a significantly worse recovery rate in visual field deficits (50, 51)compared to hemiparesis (52) or aphasia (53, 54). The most probable reason for this observation is founded on the optic system's highly organized retinotopic and cortical functionality (53–55), causing the comparably low functional re–organization rates (55). In addition to location, tumor biology appears to significantly impact the surrounding brain and the resulting functional impairment. We detected a significantly higher frequency of larger edema in tumors with higher malignancy grade, which is in accordance with an earlier study reporting identical findings (56). Correspondingly, patients with higher-grade tumors in our study presented with a significantly higher frequency of focal neurological impairment and a poorer presurgical KPS, which aligns with a recent study reporting 56.1% of patients with atypical meningiomas showing a poor KPS (57). Most importantly, patients harboring higher-grade tumors displayed significantly worse improvement rates than benign lesions, highlighting the importance of tumor biology in this context. In our patient population, GTR is clearly superior compared to STR when analyzing recurrence–free survival. However, regarding neurological symptoms, only patients with seizures or visual field deficits showed a higher benefit from GTR over STR regarding symptom improvement,

which indicates that most patients will benefit from surgical decompression, even if GTR cannot be achieved. Interestingly, GTR, compared to STR, carries a lower risk of developing a new or worsening of a pre–existing hemiparesis. When looking at the long-term functional outcome, poor resection grade was the only prognostic factor for new postoperative and permanent neurological deficit or decreased KPS score, which occurred in 7.3% of our patients.

5 Conclusion

Our study shows that surgical resection leads to long-term improvement of neurological impairment in the majority of patients with NSBM. However, location, tumor biology, and extent of resection are essential co-factors influencing neurological outcome.

Data availability statement

The original contributions presented in the study are included in the article/supplementary material. Further inquiries can be directed to the corresponding author.

Ethics statement

The studies involving human participants were reviewed and approved by Ethics committee of the University Regensburg Medical Center, protocol number 20-1799-101. The patients/participants provided their written informed consent to participate in this study.

Author contributions

Conception and design (MP, TM, AB, and KR); analysis and interpretation of data (MP, TM, SS, AB, K-MS, N-OS, CD, and KR); manuscript draft and/or revision (TM, MP, K-MS, N-OS, and CD). All authors contributed to the article and approved the submitted version.

Acknowledgments

We thank Michael Gerken (Tumor Center Regensburg, Institute of quality assurance and health services research, University of Regensburg, Regensburg, Germany) for his extensive support during clinical data acquisition.

Conflict of interest

The authors declare that the research was conducted in the absence of any commercial or financial relationships that could be construed as a potential conflict of interest.

Publisher's note

All claims expressed in this article are solely those of the authors and do not necessarily represent those of their affiliated organizations, or those of the publisher, the editors and the reviewers. Any product that may be evaluated in this article, or claim that may be made by its manufacturer, is not guaranteed or endorsed by the publisher.

References

1. Dolecek TA, Dressler EV, Thakkar JP, Liu M, Al-Qaisi A, Villano JL. Epidemiology of meningiomas post-public law 107-206: The benign brain tumor cancer registries amendment act. *Cancer* (2015) 121:2400–10. doi: 10.1002/cncr.29379

2. Louis DN, Perry A, Wesseling P, Brat DJ, Cree IA, Figarella-Branger D, et al. The 2021 WHO classification of tumors of the central nervous system: a summary. *Neuro Oncol* (2021) 23:1231–51. doi: 10.1093/neuonc/noab106

3. Holleczek B, Zampella D, Urbschat S, Sahm F, von Deimling A, Oertel J, et al. Incidence, mortality and outcome of meningiomas: A population-based study from Germany. *Cancer Epidemiol* (2019) 62:101562. doi: 10.1016/j.canep.2019.07.001

4. DeMonte F, McDermott MW, Al-Mefty O. *Al-Mefty´s meningiomas. 2nd ed.* New York: Thieme Medical (2011).

5. Mansouri A, Klironomos G, Taslimi S, Kilian A, Gentili F, Khan OH, et al. Surgically resected skull base meningiomas demonstrate a divergent postoperative recurrence pattern compared with non-skull base meningiomas. *J Neurosurg* (2016) 125, 1–10. doi: 10.3171/2015.7.JNS15546

6. Meling TR, Da Broi M, Scheie D, Helseth E. Skull base versus non-skull base meningioma surgery in the elderly. *Neurosurg Rev* (2019) 42:961–72. doi: 10.1007/s10143-018-1005-6

7. Simpson D. The recurrence of intracranial meningiomas after surgical treatment. *J Neurol Neurosurg Psychiatry* (1957) 20:22–39. doi: 10.1136/jnnp.20.1.22

8. Lemee JM, Corniola MV, Da Broi M, Joswig H, Scheie D, Schaller K, et al. Extent of resection in meningioma: Predictive factors and clinical implications. *Sci Rep* (2019) 9:5944. doi: 10.1038/s41598-019-42451-z

9. McGovern SL, Aldape KD, Munsell MF, Mahajan A, DeMonte F, Woo SY. A comparison of world health organization tumor grades at recurrence in patients with non-skull base and skull base meningiomas. *J Neurosurg* (2010) 112:925–33. doi: 10.3171/2009.9.JNS09617

10. Savardekar AR, Patra DP, Bir S, Thakur JD, Mohammed N, Bollam P, et al. Differential tumor progression patterns in skull base versus non-skull base meningiomas: A critical analysis from a long-term follow-up study and review of literature. *World Neurosurg* (2018) 112:e74–83. doi: 10.1016/j.wneu.2017.12.035

11. Meling TR, Da Broi M, Scheie D, Helseth E. Meningiomas: skull base versus non-skull base. *Neurosurg Rev* (2019) 42:163–73. doi: 10.1007/s10143-018-0976-7

12. Hashimoto N, Rabo CS, Okita Y, Kinoshita M, Kagawa N, Fujimoto Y, et al. Slower growth of skull base meningiomas compared with non-skull base meningiomas based on volumetric and biological studies. *J Neurosurg* (2012) 116:574–80. doi: 10.3171/2011.11.JNS11999

13. Kane AJ, Sughrue ME, Rutkowski MJ, Shangari G, Fang S, McDermott MW, et al. Anatomic location is a risk factor for atypical and malignant meningiomas. *Cancer* (2011) 117:1272–8. doi: 10.1002/cncr.25591

14. Kshettry VR, Ostrom QT, Kruchko C, Al-Mefty O, Barnett GH, Barnholtz-Sloan JS. Descriptive epidemiology of world health organization grades II and III intracranial meningiomas in the united states. *Neuro Oncol* (2015) 17:1166–73. doi: 10.1093/neuonc/nov069

15. Modha A, Gutin PH. Diagnosis and treatment of atypical and anaplastic meningiomas: a review. *Neurosurgery* (2005) 57:538–50. discussion 538-550. doi: 10.1227/01.NEU.0000170980.47582.A5

16. Sade B, Chahlavi A, Krishnaney A, Nagel S, Choi E, Lee JH. World health organization grades II and III meningiomas are rare in the cranial base and spine. *Neurosurgery* (2007) 61:1194–8. doi: 10.1227/01.neu.0000306097.38141.65

17. Kasuya H, Kubo O, Tanaka M, Amano K, Kato K, Hori T. Clinical and radiological features related to the growth potential of meningioma. *Neurosurg Rev* (2006) 29:293–6. discussion 296-297. doi: 10.1007/s10143-006-0039-3

18. Figarella-Branger D, Roche PH, Daniel L, Dufour H, Bianco N, Pellissier JF. Cell-adhesion molecules in human meningiomas: correlation with clinical and morphological data. *Neuropathol Appl Neurobiol* (1997) 23:113–22. doi: 10.1111/j.1365-2990.1997.tb01193.x

19. Kepes JJ. Presidential Address: the histopathology of meningiomas. *A Reflection Origins Expected Behavior? J Neuropathol Exp Neurol* (1986) 45:95–107. doi: 10.1097/00005072-198603000-00001

20. Lee JH, Sade B, Choi E, Golubic M, Prayson R. Meningothelioma as the predominant histological subtype of midline skull base and spinal meningioma. *J Neurosurg* (2006) 105:60–4. doi: 10.3171/jns.2006.105.1.60

21. Brastianos PK, Galanis E, Butowski N, Chan JW, Dunn IF, Goldbrunner R, et al. Advances in multidisciplinary therapy for meningiomas. *Neuro Oncol* (2019) 21:i18–31. doi: 10.1093/neuonc/noy136

22. Gousias K, Schramm J, Simon M. The Simpson grading revisited: aggressive surgery and its place in modern meningioma management. *J Neurosurg* (2016) 125, 1–10. doi: 10.3171/2015.9.JNS15754

23. Elzarief AA, Ibrahim MF. Long-term follow-up of motor function deterioration following microsurgical resection of middle third parasagittal and falx meningioma. *Egyptian J Neurol Psychiatry Neurosurg* (2018) 54:9. doi: 10.1186/s41983-018-0013-3

24. Biroli A, Chiocchetta M, Gerosa M, Talacchi A. Surgical treatment of parasagittal and falcine meningiomas of the posterior third. *Acta Neurochir (Wien)* (2012) 154:1987–95. doi: 10.1007/s00701-012-1454-6

25. Chen WC, Magill ST, Englot DJ, Baal JD, Wagle S, Rick JW, et al. Factors associated with pre- and postoperative seizures in 1033 patients undergoing supratentorial meningioma resection. *Neurosurgery* (2017) 81:297–306. doi: 10.1093/neuros/nyx001

26. Englot DJ, Magill ST, Han SJ, Chang EF, Berger MS, McDermott MW. Seizures in supratentorial meningioma: a systematic review and meta-analysis. *J Neurosurg* (2016) 124:1552–61. doi: 10.3171/2015.4.JNS142742

27. van Alkemade H, de Leau M, Dieleman EM, Kardaun JW, van Os R, Vandertop WP, et al. Impaired survival and long-term neurological problems in benign meningioma. *Neuro Oncol* (2012) 14:658–66. doi: 10.1093/neuonc/nos013

28. van Nieuwenhuizen D, Ambachtsheer N, Heimans JJ, Reijneveld JC, Peerdeman SM, Klein M. Neurocognitive functioning and health-related quality of life in patients with radiologically suspected meningiomas. *J Neurooncol* (2013) 113:433–40. doi: 10.1007/s11060-013-1132-4

29. Waagemans ML, van Nieuwenhuizen D, Dijkstra M, Wumkes M, Dirven CM, Leenstra S, et al. Long-term impact of cognitive deficits and epilepsy on quality of life in patients with low-grade meningiomas. *Neurosurgery* (2011) 69:72–8. discussion 78-79. doi: 10.1227/NEU.0b013e318212badb

30. Zamanipoor Najafabadi AH, van der Meer PB, Boele FW, Taphoorn MJB, Klein M, Peerdeman SM, et al. Determinants and predictors for the long-term disease burden of intracranial meningioma patients. *J Neurooncol* (2021) 151:201–10. doi: 10.1007/s11060-020-03650-1

31. Akman F, Cooper RA, Sen M, Tanriver Y, Kentli S. Validation of the medical research council and a newly developed prognostic index in patients with malignant glioma: how useful are prognostic indices in routine clinical practice? *J Neurooncol* (2002) 59:39–47. doi: 10.1023/a:1016353614525

32. Rogers L, Barani I, Chamberlain M, Kaley TJ, McDermott M, Raizer J, et al. Meningiomas: knowledge base, treatment outcomes, and uncertainties. a RANO review. *J Neurosurg* (2015) 122:4–23. doi: 10.3171/2014.7.JNS131644

33. Postma M, Goedhart J. PlotsOfData-a web app for visualizing data together with their summaries. *PloS Biol* (2019) 17:e3000202. doi: 10.1371/journal.pbio.3000202

34. Mauri M, Elli T, Caviglia G, Uboldi G, Azzi. M. In: Proceedings of the Proceedings of the 12th Biannual Conference on Italian SIGCHI Chapter; 2017,. (Cagliari, Italy:ACM), RAWGraphs.

35. Fathi AR, Roelcke U. Meningioma. *Curr Neurol Neurosci Rep* (2013) 13:337. doi: 10.1007/s11910-013-0337-4

36. Marosi C, Hassler M, Roessler K, Reni M, Sant M, Mazza E, et al. Meningioma. *Crit Rev Oncol Hematol* (2008) 67:153–71. doi: 10.1016/j.critrevonc.2008.01.010

37. Rogers CL, Pugh SL, Vogelbaum MA, Perry A, Ashby LS, Modi JM, et al. *Low-risk meningioma: Initial outcomes from NRG Oncology/RTOG 0539. Neuro Oncol (2022)*. (Oxford, UK: Epub 2022/06/04).

38. Kent CL, Mowery YM, Babatunde O, Wright AO, Barak I, McSherry F, et al. Long-term outcomes for patients with atypical or malignant meningiomas treated with or without radiation therapy: A 25-year retrospective analysis of a single-institution experience. *Adv Radiat Oncol* (2022) 7:100878. doi: 10.1016/j.adro.2021.100878

39. Nanda A, Bir SC, Konar S, Maiti TK, Bollam P. World health organization grade I convexity meningiomas: Study on outcomes, complications and recurrence rates. *World Neurosurg* (2016) 89:620–627.e622. doi: 10.1016/j.wneu.2015.11.050

40. Alvernia JE, Dang ND, Sindou MP. Convexity meningiomas: study of recurrence factors with special emphasis on the cleavage plane in a series of 100 consecutive patients. *J Neurosurg* (2011) 115:491–8. doi: 10.3171/2011.4.JNS101922

41. Kamitani H, Masuzawa H, Kanazawa I, Kubo T. Recurrence of convexity meningiomas: tumor cells in the arachnoid membrane. *Surg Neurol* (2001) 56:228–35. doi: 10.1016/S0090-3019(01)00582-1

42. Oya S, Ikawa F, Ichihara N, Wanibuchi M, Akiyama Y, Nakatomi H, et al. Effect of adjuvant radiotherapy after subtotal resection for WHO grade I meningioma: a propensity score matching analysis of the brain tumor registry of Japan. *J Neurooncol* (2021) 153:351–60. doi: 10.1007/s11060-021-03775-x

43. Wu A, Garcia MA, Magill ST, Chen W, Vasudevan HN, Perry A, et al. Presenting symptoms and prognostic factors for symptomatic outcomes following resection of meningioma. *World Neurosurg* (2018) 111:e149–59. doi: 10.1016/j.wneu.2017.12.012

44. Gondar R, Patet G, Schaller K, Meling TR. Meningiomas and cognitive impairment after treatment: A systematic and narrative review. *Cancers* (2021) 13:1–11. doi: 10.3390/cancers13081846

45. Meskal I, Gehring K, van der Linden S, Rutten G-J, Sitskoorn M. Cognitive improvement in meningioma patients after surgery: clinical relevance of computerized testing. *J Neurooncol* (2015) 121:617–25. doi: 10.1007/s11060-014-1679-8

46. Tanti MJ, Marson AG, Chavredakis E, Jenkinson MD. The impact of epilepsy on the quality of life of patients with meningioma: A systematic review. *Br J Neurosurg* (2016) 30:23–8. doi: 10.3109/02688697.2015.1080215

47. Dijkstra M, van Nieuwenhuizen D, Stalpers LJ, Wumkes M, Waagemans M, Vandertop WP, et al. Late neurocognitive sequelae in patients with WHO grade I meningioma. *J Neurol Neurosurg Psychiatry* (2009) 80:910–5. doi: 10.1136/jnnp.2007.138925

48. Nassiri F, Price B, Shehab A, Au K, Cusimano MD, Jenkinson MD, et al. Life after surgical resection of a meningioma: a prospective cross-sectional study evaluating health-related quality of life. *Neuro Oncol* (2019) 21:i32–43. doi: 10.1093/neuonc/noy152

49. Cornelius JF, Slotty PJ, Steiger HJ, Hanggi D, Polivka M, George B. Malignant potential of skull base versus non-skull base meningiomas: clinical series of 1,663 cases. *Acta Neurochir (Wien)* (2013) 155:407–13. doi: 10.1007/s00701-012-1611-y

50. Gray CS, French JM, Bates D, Cartlidge NE, Venables GS, James OF. Recovery of visual fields in acute stroke: homonymous hemianopia associated with adverse prognosis. *Age Ageing* (1989) 18:419–21. doi: 10.1093/ageing/18.6.419

51. Jorge CB, Vanessa CN, Miguel AB, Irene GO, Antonio A. Prognostic factors for long-term recovery of homonymous visual field defects after posterior circulation ischemic stroke. *J Stroke Cerebrovasc Dis Off J Natl Stroke Assoc* (2021) 30:105924. doi: 10.1016/j.jstrokecerebrovasdis.2021.105924

52. Lee KB, Lim SH, Kim KH, Kim KJ, Kim YR, Chang WN, et al. Six-month functional recovery of stroke patients: a multi-time-point study. *Int J Rehabil Res* (2015) 38:173–80. doi: 10.1097/MRR.0000000000000108

53. Laska AC, Hellblom A, Murray V, Kahan T, Von Arbin M. Aphasia in acute stroke and relation to outcome. *J Intern Med* (2001) 249:413–22. doi: 10.1046/j.1365-2796.2001.00812.x

54. Pedersen PM, Vinter K, Olsen TS. Aphasia after stroke: type, severity and prognosis. the Copenhagen aphasia study. *Cerebrovasc Dis* (2004) 17:35–43. doi: 10.1159/000073896

55. Sabel BA, Gao Y, Antal A. Reversibility of visual field defects through induction of brain plasticity: vision restoration, recovery and rehabilitation using alternating current stimulation. *Neural Regeneration Res* (2020) 15:1799–806. doi: 10.4103/1673-5374.280302

56. Osawa T, Tosaka M, Nagaishi M, Yoshimoto Y. Factors affecting peritumoral brain edema in meningioma: special histological subtypes with prominently extensive edema. *J Neurooncol* (2013) 111:49–57. doi: 10.1007/s11060-012-0989-y

57. Cao X, Hao S, Wu Z, Wang L, Jia G, Zhang L, et al. Treatment response and prognosis after recurrence of atypical meningiomas. *World Neurosurg* (2015) 84:1014–9. doi: 10.1016/j.wneu.2015.05.032

frontiers | Frontiers in Oncology

ORIGINAL RESEARCH
published: 28 September 2022
doi: 10.3389/fonc.2022.879528

Application of MRI-Based Radiomics in Preoperative Prediction of *NF2* Alteration in Intracranial Meningiomas

Shuchen Sun[1,2,3], *Leihao Ren*[1,2,3], *Zong Miao*[4], *Lingyang Hua*[1,2,3], *Daijun Wang*[1,2,3], *Jiaojiao Deng*[1,2,3], *Jiawei Chen*[1,2,3], *Ning Liu*[4] *and Ye Gong*[1,2,3,5*]

[1] Department of Neurosurgery, Huashan Hospital, Fudan University, Shanghai, China, [2] Institute of Neurosurgery, Fudan University, Shanghai, China, [3] Shanghai Key Laboratory of Brain Function Restoration and Neural Regeneration, Shanghai, China, [4] Department of Neurosurgery, Changhai Hospital, Naval Medical University (Second Military Medical University), Shanghai, China, [5] Department of Critical Care Medicine, Huashan Hospital, Fudan University, Shanghai, China

Purpose: This study aimed to investigate the feasibility of predicting *NF2* mutation status based on the MR radiomic analysis in patients with intracranial meningioma.

Methods: This retrospective study included 105 patients with meningiomas, including 60 *NF2*-mutant samples and 45 wild-type samples. Radiomic features were extracted from magnetic resonance imaging scans, including T1-weighted, T2-weighted, and contrast T1-weighted images. Student's t-test and LASSO regression were performed to select the radiomic features. All patients were randomly divided into training and validation cohorts in a 7:3 ratio. Five linear models (RF, SVM, LR, KNN, and xgboost) were trained to predict the *NF2* mutational status. Receiver operating characteristic curve and precision-recall analyses were used to evaluate the model performance. Student's t-tests were then used to compare the posterior probabilities of NF2 mut/loss prediction for patients with different NF2 statuses.

Results: Nine features had nonzero coefficients in the LASSO regression model. No significant differences was observed in the clinical features. Nine features showed significant differences in patients with different NF2 statuses. Among all machine learning algorithms, SVM showed the best performance. The area under curve and accuracy of the predictive model were 0.85; the F1-score of the precision-recall curve was 0.80. The model risk was assessed by plotting calibration curves. The p-value for the H-L

OPEN ACCESS

Edited by:
Ian Dunn,
University of Oklahoma Health Sciences Center, United States

Reviewed by:
Guoping Li,
Harvard Medical School, United States
Xiaohua Qian,
Shanghai Jiao Tong University, China

***Correspondence:**
Ye Gong
drgongye@163.com

Specialty section:
This article was submitted to Neuro-Oncology and Neurosurgical Oncology, a section of the journal Frontiers in Oncology

Received: *19 February 2022*
Accepted: *06 June 2022*
Published: *28 September 2022*

Citation:
Sun S, Ren L, Miao Z, Hua L, Wang D, Deng J, Chen J, Liu N and Gong Y (2022) Application of MRI-Based Radiomics in Preoperative Prediction of NF2 Alteration in Intracranial Meningiomas. Front. Oncol. 12:879528. doi: 10.3389/fonc.2022.879528

goodness of fit test was 0.411 ($p > 0.05$), which indicated that the difference between the obtained model and the perfect model was statistically insignificant. The AUC of our model in external validation was 0.83.

Conclusion: A combination of radiomic analysis and machine learning showed potential clinical utility in the prediction of preoperative NF2 status. These findings could aid in developing customized neurosurgery plans and meningioma management strategies before postoperative pathology.

Keywords: meningioma, radiomics, *NF2*, machiene learning, SVM - support vector machine

INTRODUCTION

Meningioma is the most common primary tumor of the central nervous system (CNS), accounting for approximately 26.1-38.3% of all intracranial tumors (1–3). According to the WHO CNS tumor grading criterion, meningiomas are categorized into three grades and 15 histological subtypes based solely on the morphological features of the tumor cells. Despite the widespread use of the WHO classification, it fails to accurately predict the clinical behavior, aggressiveness, and recurrence of particular tumors. With the deeper understanding of the molecular landscape of meningioma, in addition to the histological diagnosis, the newest 2021 CNS tumor diagnostic criterion began to integrate the molecular and genetic profiling to assist in diagnoses and evaluate prognosis.

The *NF2* gene was first implicated in meningiomas after it was found that its inactivation resulted in the genetic tumor predisposition syndrome of neurofibromatosis type 2. *NF2* is a tumor suppressor gene comprised of 17 exons with 2 splicing isoforms that is positioned on chromosome 22q12.2 (4). Alterations in the NF2 gene, which can be caused by mutation, allelic inactivation, splicing alterations, or Chromosome 22 loss, have been implicated in approximately 30-60% of sporadic meningiomas, making it the single most frequent gene alteration in this tumor (5). The frequency of NF2 mutations is simlar in WHO Grade 1, 2 and 3 grades. However, it varies among histological subtypes and locations and are more likely to be observed in atypical and cerebral hemispheres. NF2 gene inactivation is considered to play a significant role in the development of meningiomas (5, 6). Patients with *NF2* mutations were also reported to show worse outcomes (7). Clinical trials targeting NF2 has been under way (NCT02523014). Thus, prediction of the *NF2* status before surgery can aid in the development of personalized treatment strategies for meningioma patients.

Radiomics is a novel practice in the field of machine learning. It could be used to extract and analyze medical imaging data (8). By conversion of sparse magnetic resonance imaging (MRI) into data, an immense amount of imaging information that is otherwise invisible to the naked eye in multiple dimensions could be generated (9). Radiomics is a potential approach for noninvasive high-throughput mining of tumor characteristics and has been applied in several other intracranial tumors, including glioma and schwannoma (10, 11). For meningiomas, algorithms have been developed in previous studies to predict WHO grade, tumor texture, peritumoral edema, and Ki-67 labels through radiomics. These models reported good performance in terms of accuracy and sensitivity (12–14). The status of well-known genetic changes could be accurately predicted by radiomics in several CNS tumors. However, such studies were scarcely mentioned in meningiomas (15, 16).

In this study, we investigated the utility of a radiomics signature based on multiparametric MRI as a preoperative and noninvasive biomarker of NF2 status in meningiomas.

MATERIALS AND METHODS

Patients

A total of 105 meningioma patients underwent surgical resections between 2019 and 2021 at Huashan Neurosurgical Center were enrolled. Histological diagnoses were reviewed according to 2016 WHO meningioma grading criteria by two experienced neuropathologists (Dr. H.C and Dr. HX.C). Clinical information including age, gender, location, treatment status, the extent of resection, surgical outcome, and neurological functions was extracted from the medical records. Patients with recurrent meningioma who underwent another opration to remove the recurrent tumor were considered as recurrent meningioma cases. Patients with multiple meningiomas were also recorded. The clinical data of 105 patients was shown in.

Table 1 30 meningioma patients from First Affiliated Hospital of Nanjing Medical University were enrolled as External verification. The clinical data of 30 patients are shown in **Supplementary Material 1**. The specific research process of this study is shown in **Figure 1**. This study was approved by the Human Subjects Institutional Review Board of Huashan Hospital, Fudan University.

Next Generation Sequencing

Bidirectional sequencing was performed to detect microlesions in the *NF2* gene. DNA was extracted from tumor tissue with TIANamp Genomic DNA Kit (Tiangen Biotech, Beijing, China) as instructed by the manufacturers. The whole coding sequence and the exon-intron boundaries of the gene were amplified by a standard polymerase chain reaction (PCR). Subsequently, the product was used for bidirectional sequencing, as described previously (17). The sequence data were analyzed by Sequencer

TABLE 1 | Clinical data of enrolled patients.

	NF2 mut/loss (60)	NF2 wild (45)	All (105)	P
Age	54.10 ± 9.90	51.93 ± 9.14	53.17± 9.60	0.254
Female/Male	2.33	2.21	2.28	1.00
WHO grade				
WHO grade 1	50 (64.29%)	40 (13.21%)	90	0.47
WHO grade 2	9 (28.57%)	5 (79.25%)	14	
WHO grade 3	1 (4.08%)	0 (7.55%)	1	
Location				
Skull base	20 (33.33%)	25 (55.56%)	45 (42.86%)	0.07
Convexity	14 (23.33%)	7 (15.56%)	21 (20.00%)	
Parasinoidal	26 (43.33%)	13 (28.89%)	39 (37.14%)	
Multiple	3	0	3	0.258
Recurrent	12	4	16	0.170
Ki-67 labeling index(%)	4.10 ± 2.70 (range1-12)	3.67 ± 1.94 (range1-8)	3.91 ± 2.40 (range1-12)	0.341
PR positive	46 (76.67%)	40 (88.89%)	86 (81.9%)	0.130
H3K27me3 positive	51 (85.00%)	39 (86.67%)	91 (86.7%)	0.773

4.9 (Genecode, MI, USA) and compared with the *NF2* sequence (NM_016418) from GenBank. Mutations were described according to the standard nomenclature for DNA sequence changes according to the Human Genome Variation Society (HGVS).

Loss of Heterozygosity Analysis of 22q

Each tumor sample was subjected to PCR analysis. A fraction of the PCR product (0.5 liters) was mixed with 0.1 liters of Genescan 500 size standard (PE Applied Biosystems Foster City, CA, USA) and 0.9 liters of formamide loading buffer. Combinations were eletrophoresed on a 5 percent polyacrylamide gels on an ABI 377 DNA sequencer (PE Applied Biosystems Foster city CA, USA) for 2 hours after being denaturated at 96°C for 5 minutes. Individual gel lanes were visualized using the Genotype 2.0 software. The samples were scored using strict criteria. The two highest peaks within the predicted size range were designated as alleles. A loss of heterozygosity was defined as a ratio of T1:T2/N1:N2 of less than 0.67 or more than 1.50. The majority of normal DNA amplifications yielded two PCR results, showing heterozygozity. The ratio of allelic loss to informative instances was used to calculate the LOH frequency of a locus. The average LOH frequency of the long arm of chromosome 22 was the sum of the LOH frequencies of each location.

Immunohistochemistry

Immunohistochemical staining was performed using monoclonal antibodies against Ki-67 [Signalway (SAB), Shanghai, China; 1:200 dilution]. The cells stained in immunohistochemistry accounting for more than 10% of all cells were considered positive(+), otherwise negative (–). Progesterone receptor (PR) level was also examined to classify the tumors into two categories: PR negative (–) or PR positive (+). H3K27me3 was examined with anti-H3K27me3 (Millipore, 07-449) on ECL Plus films (Carestream).

MRI Image Acquisition

All patients underwent MRI scanning before operation (with or without Gadolinium enhancement). MRI scans were performed by the Trio 3.0-T scanner (Siemens, Erlangen, Germany). The imaging process included axial T1WI (TE, 15 ms; TR, 450 ms; slice thickness, 5 mm), T2WI (TE, 110 ms; TR 5800 ms; slice thickness, 5 mm), and CE scans using 0.1 mM/kg gadopentetate dimeglumine (TE, 15 ms; TR, 450 ms; slice thickness, 5 mm). Tumor location was described according to Al-Mefty's published manuscript, such as parasagittal/falx, skull base, cerebral convexity, etc.

Tumor Segmentation and Feature Extraction

Preprocessing was performed using the 3D-Slicer software (version 4.11). The MRI DICOM files of all patients were imported into 3D-slicer. T1WI, T2Flair, and DWI images were registered to the T1C sequence images; N4 bias field correction was applied to each sequence image to correct non-uniformities in intensity. Two neuroradiologists painted regions of interest (ROIs) on T1c images using the 3D-slicer software. Multiple meningiomas from the same patient were considered as a single case in ROI classification and impact feature extraction. Enhancement of the dural tail sign was included in ROI, while peritumoral edema was excluded. The neuroradiologists were not informed of the clinical and biomarker data. Pyradiomics, an open-source python package (https://github.com/Radiomics/pyradiomics), was used to extract radiomic features.

Feature Selection and Establishment of Prediction Model

Pyradiomics, an open-source python package (https://github.com/Radiomics/pyradiomics), was used to extract radiomic features from the ROIs of each patient's images. After that, we eliminated the time, the checked hospital, machine model and other useless information. 130 radiomics features were retained in each sequence. To avoid degradation in model performance due to overfitting and increase in feature dimension, we evaluated radiomics features in distinguishing between mut/wild type and screened all radiomic features of each sequence to generate a new feature set.

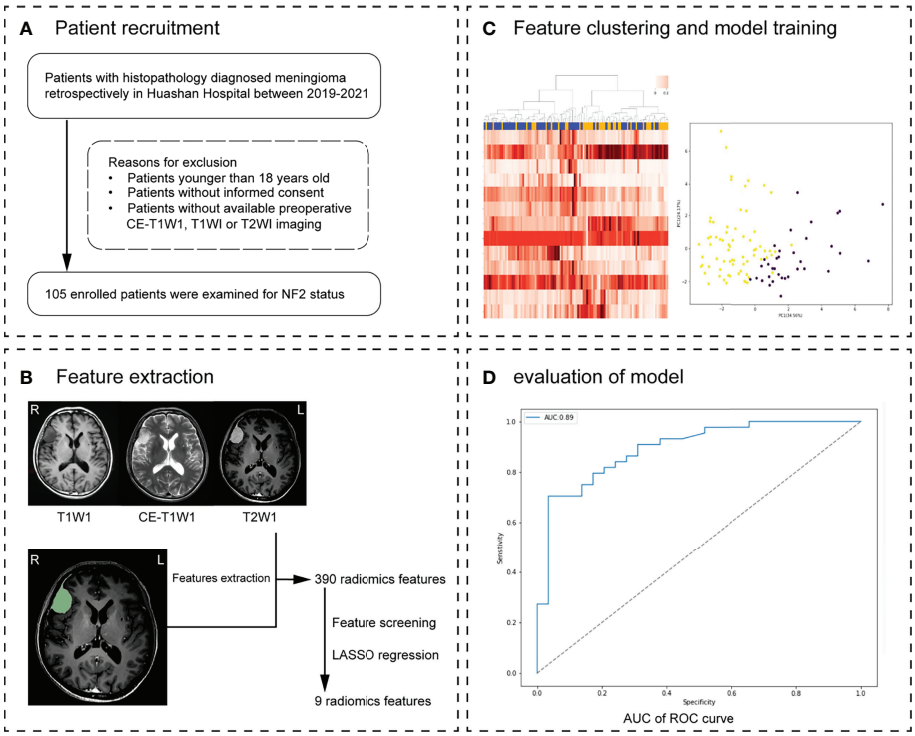

FIGURE 1 | Workflow. **(A)** Patient recruitment strategy. **(B)** 390 features were extracted from region of interest (ROI) on each magnetic resonance imaging (MRI) sequence. **(C)** The inner loop included hyperparameter tuning and features selection in the training datasets. After feature selection, the model with optimal parameters was used for prediction in the test set. This procedure developed 10 different models with specific sets of features and hyperparameters. **(D)** The effectiveness of the model was verified in the validation group. Receiver operating characteristic (ROC) analysis and precision and recall (P-R) analysis were used for model performance evaluation. The MRI scans of 30 meningioma patients from another hospital were used as external validation.

First, three pairs of samples in two groups were tested using t-test analysis. Levene test was used to test the homogeneity of variance. For the data with the homogeneity of variance greater than 0.05, a t-test was used to detect whether the characteristics of the average of the two groups of independent samples showed significant differences ($P < 0.05$). Only characteristics with significant differences were retained.

Second, a further feature screen was performed based on LASSO regression, which added L1 regular expression based on the least square regression. The features screened by t-test were standardized; the optimal parameter lambda was selected after ten-fold cross-validation. Thus, the corresponding coefficients of the model were trained. Features with nonzero coefficients in the LASSO regression model were selected.

Model Training and Evaluation

Machine learning models were developed to predict the outcome of NF2 status based on different algorithm. We used five supervised machine learning algorithms to establish the prediction model. All the cases were randomly divided into training and validation cohorts in the ratio of 7:3. The algorithm was trained based on the training group, and its effectiveness was verified in the validation group. The algorithm with the highest AUC (area under the curve) in the validation cohorts was chosen as the best model. Five prediction models were generated by random forest (RF), k-nearest neighbor (KNN), support vector machine (SVM), logistic regression (LR), and extreme gradient boosting (xgboost) methods. The training and validation cohorts were divided based on the selected feature subset. Predictions were made after iterative optimization. The sensitivity, specificity, accuracy, and F1 score were evaluated. The model performance was analyzed by plotting ROC (receiver operating characteristic), P-R (analysis and precision-recall), and calibration curves. The MRI scans of 30 meningioma patients from First Affiliated Hospital of Nanjing Medical University were used as external validation to verify the accuracy of the best model.

Statistical Analysis

Statistical analysis was performed using SPSS 26.0 (IBM SPSS statistics 26.0 for mac; IBM corp). For continuous variables, the Student t-test was used; for comparison of mean values of continuous variables, ANOVA was used. Categorical variables were compared using the $\chi 2$ test and the Fisher test. Continuous data were expressed as mean ± SD. P-value <0.05 was considered statistically significant.

RESULTS

Clinical Data and Immunohistochemistry

A total of 105 patients (32 males and 73 females) with intracranial meningiomas were recruited in the training and testing cohorts, including 60 patients with NF2 mutation/loss and 45 wild type patients. The mean age of the patients was 53.17 ± 9.60 years (range 31 to 73 years). There are 90 (85.71%) grade 1, 14 grade 2 (13.33%) and 1 grade 3 patients (0.95%), respectively. The most common pathological subtype was fibrous (45, 42.86%). The median Ki-67 labeling index was 3.91 ± 2.40(range 1-12). PR was positive in 86 patients (81.9%). Loss of H3K27me3 expression was observed in 14 patients (13.3%). No diffence was observed of the compared the clinical and immunohistochemical characteristics between *NF2* mutant and wild-type groups. Parasinoidal (26/60) was the most common location in *NF2* mut/loss group, while *NF2* wild tumours were more likely in skull base locations (25/45). Three cases of multiple meningiomas were identified in our cohort. However, only one tumor in each patient was removed, which were all belonged to the *NF2* mutation group. 16 patients (4 with wildtype *NF2* and 12 with *NF2* mutations) were regarded as recurrent meningiomas and no difference was observed between *de novo* and recurrent patients regarding NF2 status (p = 0.170).

NF2 Sequencing Analysis and LOH Analysis

Among all 105 patients, 52 patients (49.52%) had *NF2* mutations; 8 patients (7.62%) showed loss of *NF2* gene due to partial deletion of chromosome 22q. The remaining 45 patients had wild-type *NF2*. Allelic deletion of *NF2* and mutations were classified as NF2 mutation group, amounting to 60 cases. Of all patients with *NF2* mutations, 23 were nonsense mutations; 16 were frameshift mutation; 8 were splice site mutation; 4 were missense mutation. Exon 1 and Exon 6 was detected the highest mutation frequency, accounting for 6 (11.54%) and 7 (13.46%) of all mutants, respectively. However, we did not find any obvious hot spot mutations. The most common copy number deletion occurred in 22q11.21- q13.33. Details of the *NF2* mutation status were shown in **Supplementary Table 1**.

Radiomic Feature Selection and Radiomic Signature Construction

A total of 130 radiomic features were extracted from each sequence. 390 radiomic features were included in the screening process. 147 radiomic features showed statistically significant differences between the *NF2* mut/loss and wild-type groups. Only 9 features had nonzero coefficients in the LASSO regression model. The screening process of Lamda is shown in **Figure 2**. In **Figure 2A**, The red line represents the standard deviation of the mean square error (MSE) of λ. The blue bar indicates the range of the mean square error. The lambda with the lowest standard deviation is the most suitable for classification and the model is the simplest. Therefore, We chose the position with the lowest lambda standard deviation (red line) as the most appropriate λ Value. The details and p-values for these 9 features are shown in **Table 2**. 4 features were from the CE-T1Flair, 3 from T1WI, and 2 from T2WI sequences. 7 features could describe the texture of tumors and 2 described the wavelet of tumors. The 9 radiomics features were selected for the model building. We tried to cluster nine radiomics features through unsupervised hierarchical cluster analysis. PCA (Principal Component Analysis) is used to reduce the dimension and describe the distribution of data (**Figure 3**).

Finally, we decided to incorporate the 9 features into the model. Gray Level Dependence Matrix (GLDM) quantifies gray level dependencies in an image. included descriptors of the three-dimensional size and shape of the ROI. First-order statistics describe the distribution of voxel intensities within the image region defined by the mask through commonly used and basic metrics.

Gray Level Co-occurrence Matrix (GLCM) describes the second-order joint probability function of an image region constrained by the mask.

Model Training and Performance

We randomly divided all patients into training and validation groups in a ratio of 7:3. 73 patients were included in the training group. 9 radiomic features of 73 patients were used to train 5 supervised machine learning algorithms (RF, SVM, LR, KNN,

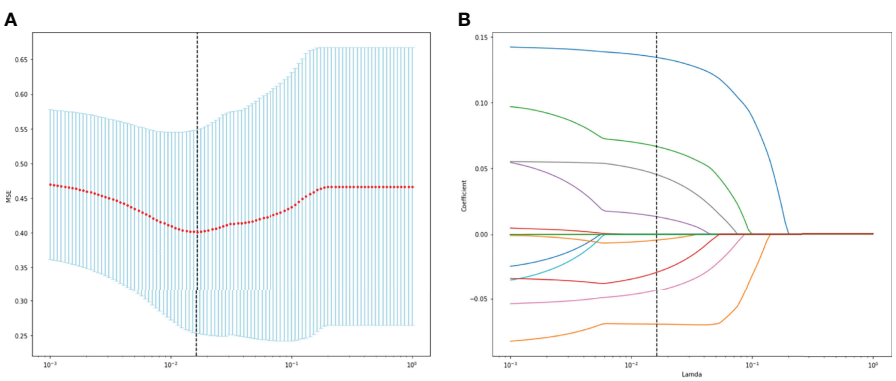

FIGURE 2 | **(A)** The change of MSE corresponding to the LASSO method. **(B)** Lamda value screening of LASSO regression.

TABLE 2 | The details of selected radiomics features.

Name	Sequence	Type	p
glcm_Imc2	T2	Texture	0.027
gldm_DependenceNonUniformity	T2	Texture	0.022
shape_LeastAxisLength	T1	Wavelet	0.037
firstorder_Minimum	T1	Texture	0.025
glcm_ClusterShade	T1	Texture	0.037
firstorder_Skewness	CET1	Wavelet	0.001
glcm_JointAverage	CET1	Texture	0.005
glcm_SumAverage	CET1	Texture	0.005
gldm_LargeDependenceHighGrayLevelEmphasis	CET1	Texture	0.005

and xgboost). The data of a total of 32 patients in the validation cohort was used to evaluate the effectiveness of the algorithms. The AUCs of each algorithm in training and validation cohorts were calculated and compared as shown in **Table 3** and **Figure 4**. SVM (support vector machine) had the highest AUC of 0.89 in the training cohort and 0.85 in the validation cohort. F1 score is the harmonic average of accuracy and recall, while the value was 0.80 in the SVM model. LR (logistic regression) had an AUC of 0.84 in the training cohort and 0.82 in the validation cohort. Most of the algorithms had AUCs above 0.7.

Internal and External Verification

ROC and P-R curve analysis of SVM in training and validation cohorts were shown in **Figure 5**. AUC of SVM were 0.89 and 0.85 in the training cohort and validation cohort respectively. **Figure 6** shows the predicted value and their actual mutation of each validation group sample. Samples with a predicted value greater than 0 were predicted to be NF2 mut-type by the SVM model. The actual mutation of the sample were showen by color, Green represents mut-type and blue represents wild-type. 30 meningioma patients from First Affiliated Hospital of Nanjing Medical University were enrolled as external validation to verify the accuracy of the SVM model. the AUC of SVM model is 0.82 in the external validation cohorts. The calibration curve analysis and Hosmer-Lemeshow test for SVM model demonstrated the observations and predictions in validation cohorts were in good accordance (**Figure 7**).

DISCUSSION

NF2 inactivation was the most common alteration in meningiomas and played an important role in tumor

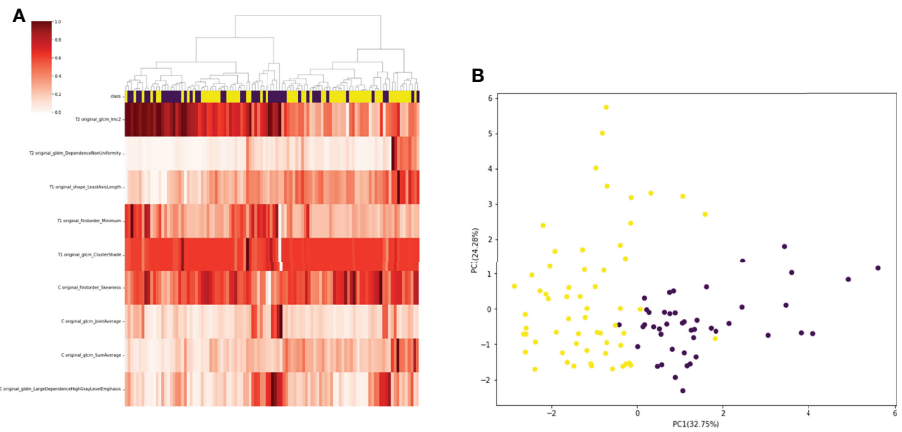

FIGURE 3 | **(A)** 105 patients with meningiomas were divided into two categories by hierarchical cluster analysis. **(B)** PCA (Principal Component Analysis) plot showing the distribution of principal components of the radiomics features. The majority of NF2-mut meningioma and NF2-wild meningioma cases were spatially separated.

TABLE 3 | The performances of five prediction models.

Comparisons	Cohorts	LR	KNN	Xgboost	SVM	RF
AUC	train	0.85	1	1	0.89	1
	test	0.85	0.76	0.82	0.85	0.77
Sensitivity	train	0.775	1	1	0.893	0.806
	test	0.75	0.692	0.74	0.7	0.6
Specificity	train	0.781	1	1	0.737	0.765
	test	0.8	0.789	0.88	0.727	0.765
Accuracy	train	0.779	1	1	0.779	0.779
	test	0.781	0.751	0.78	0.71	0.688
F1-score	train	0.729	1	1	0.685	0.716
	test	0.72	0.692	0.76	0.609	0.643

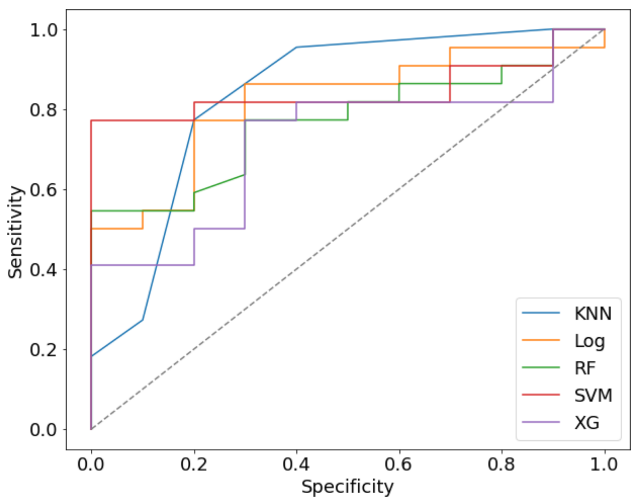

FIGURE 4 | The Receiver operating characteristic (ROC) curve of five prediction models in validation cohort.

progression (5, 18). Given this, the prediction of *NF2* inactivation status before surgery might be meaningful for determining an appropriate personalized treatment strategy. In this study, we built a machine learning model to preoperatively predict the status of *NF2* inactivation by radiomic analysis. We observed that the models based on SVM produced excellent results in the machine-learning experiments. Our radiomics model may aid the early identifcation of meningioma patients with *NF2* mutation.

NF2 is located on the long arm of chromosome 22 (chr22q) and encodes a 69 kDa protein named merlin (moesin-ezrin-radixin-like protein). NF2 is a member of the Band 4.1 FERM gene family (19). Merlin plays important role in several essential pathways, including HIPPO pathway, mTOR/PI3K/AKT pathway, and receptor tyrosine kinases (RTKs) (20, 21). Previous studies showed that more than 60% of sporadic meningioma patients harbored somatic mutation, epigenetic inactivation, or allele loss of *NF2* on chr22q. The proportion is even higher in high-grade meningiomas (22–24). In a study of 88 sporadic meningiomas, 49% exhibited allelic loss of chromosome 22, 24% had *NF2* somatic mutations and 26% had aberrant *NF2* promoter methylation. In 17% of the meningiomas, epigenetic *NF2* inactivation was the only cause of *NF2* deficiency (24). Compared to *NF2*-wt meningioma, *NF2* mutant meningiomas was detected with a higher proliferation index (Ki-67 labels) and often manifested in comparatively larger tumor size (25). In addition, the deletion of *NF2* leads to overexpression of focal adhesion kinase (FAK), resulting in enhanced cell migration and invasion (26). In all, non-invasive preoperative prediction of *NF2* mutation might be of use. The knowledge of NF2 status might

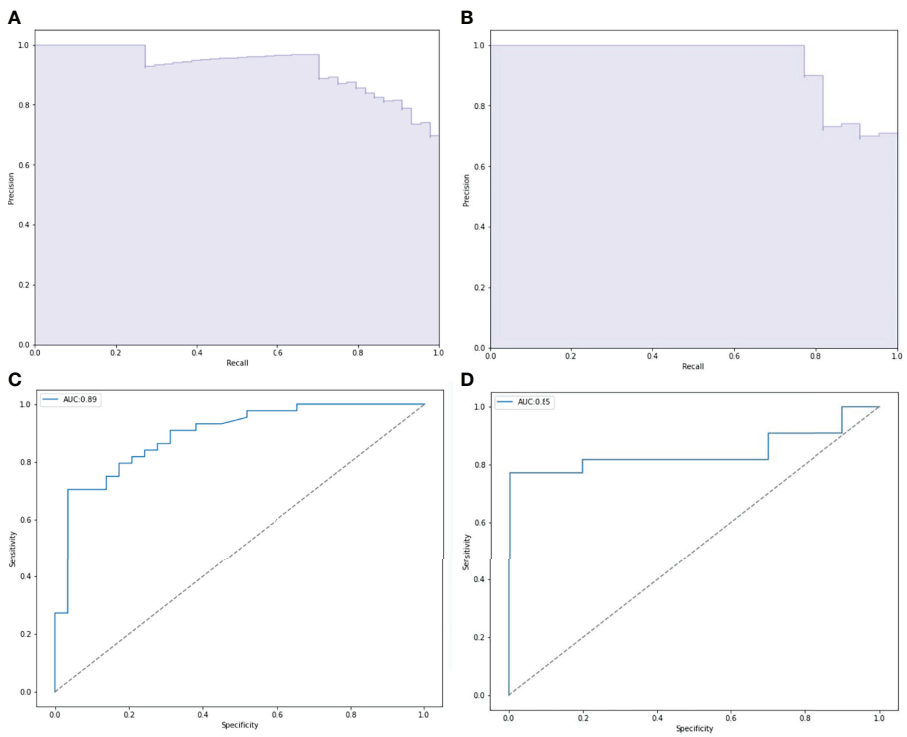

FIGURE 5 | Performance of *NF2* status predictive models based on SVM. **(A, C)** Receiver operating characteristic (ROC) curve and precision-recall (P-R) curve of SVM predictive model in training group. **(B, D)** ROC curve and P-R curve of SVM predictive model in validation group.

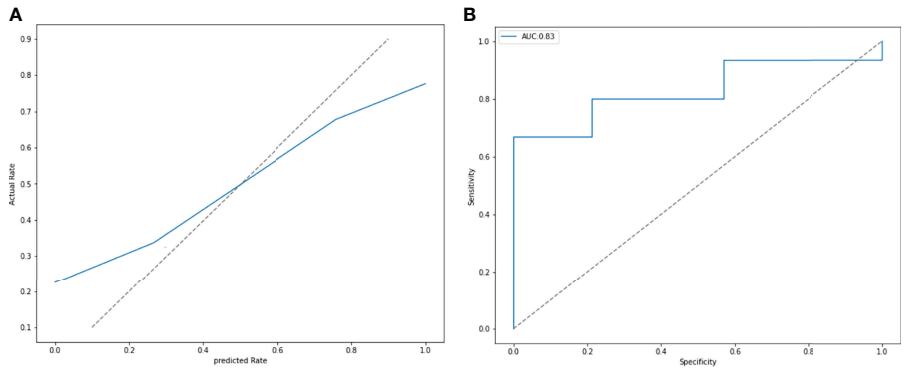

FIGURE 6 | **(A)** The calibration curve analysis and Hosmer-Lemeshow test for SVM model demonstrated the observations and predictions in validation cohorts were in good accordance. (P = 0.411). **(B)** External validation was performed by 30 patients from other hospitals. The SVM model had an AUC of 0.83.

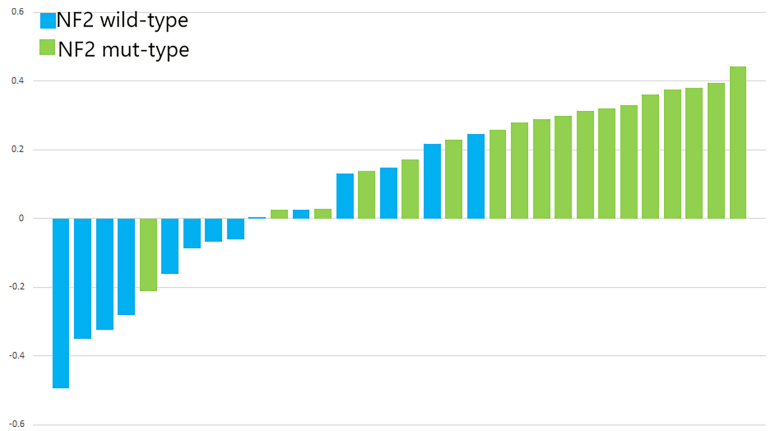

FIGURE 7 | The p-values of SVM for the validation cohorts. The blue bars show the radiomics signature values for the *NF2*-wild meningiomas, and the green bars show the values for the *NF2*-mut meningiomas.

play a role in decision making of appropriate clinical treatment strategies for meningioma patients.

Recently, several studies on radiomics focused on meningiomas and demonstrated encouraging results. Previous studies could distinguish WHO grade I meningiomas out of WHO grade II and III meningiomas by radiomic analysis models. These models were proved to have high accuracy and sensitivity (27, 28). Lei et al. distinguished two subtypes in WHO grade I meningiomas by radiomics with an accuracy higher than 90% (29). Other studies focused on predicting clinical characteristics of meningiomas, such as extent of peritumoral edema and tumor consistency. For example, Bing et al. analyzed peritumoral edema in meningioma patients using an SVM-based machine learning algorithm combined with clinical data (14). Zhai et al. constructed a radiomic-based signature to predict meningioma consistency with AUC of 0.94 in the validation cohort (13). Taken together, previous studies proved the feasibility of radiomic analysis for meningioma imaging. Some studies also predicted the molecular typing of other primary tumors, such as breast cancer and glioma. Monti et al. extracted quantitative radiomic features from DCE-MRI pharmacokinetic data to differentiate ER, PR, and HER2 status in breast cancer (30). In glioma, radiomics had been used to predict IDH mutation and co-deletion of 1p/19q (31, 32). However, up to now, the report of such studies on meningiomas is scarce.

In this study, we first detected the occurrence of *NF2* inactivation in the tumor samples. Mutations or loss of *NF2* gene were also considered as inactivation of *NF2*. By feature extraction and screening, we finally obtained 9 significant radiomic features. In previous studies, screening features of meningiomas ranged between 3 to 22 (27–29). The discrepancy might be attributed to difference in the process of screening and imaging data heterogeneity. Most of the 9 features were extracted from T1WI plain scan and Gadolinium enhanced sequences (33). The AUC of linear model based on SVM was 0.85 and 0.82 in the internal and external validation cohorts

respectively, consistent with findings of other studies which predicted intracranial tumor biomarkers (31, 32). There were many radiomics studies involving HER2 in breast cancers and IDH1 in gliomas (34, 35). Approximately, 70% of HER2 mutations occured between amino acids 755 and 781 (exons 19 and 20) in breast cancers (36). 80% of IDH1 mutations in gliomas occured on R132H (37). *NF2* has 17 exons and harbors no significant hotspot mutations (21). Our cohorts also showed no significant hotspot mutations, in accordance to previous reports. This may affect our prediction results; however, we found AUCs for most of our models were above 0.7 in the validation cohort. The data was not sufficient enough to distinguish the differences between *NF2* mutation types.

In our cohort, multiple meningiomas in a single patient were considered as one tumor in ROI selection and feature extraction. That's because they chose to remove only the symptomatic meningioma. Somatic mutation of *NF2* is related to neurofibromatosis type 2 (38) and is often found in multiple intracranial meningiomas. All our 3 cases of multiple meningiomas belonged to the *NF2* mutation group. Whereas, the difference in number of multiple meningiomas between *NF2* mutant and wild-type groups had no statistical significance. *NF2* plays an important role in progression of meningiomas (39). Additionally, there was no significant difference in number of relapse patients between the two groups, The limitations mentioned above might be attributed to the comparatively small sample size. A study by Clark et al. reported that in meningiomas with *NF2*- mutations, tumor location had a predilection for the posterior and lateral skull base, tentorium, and cerebral falx, while sporadic mutations, such as those in TRAF7 and SMO, tended to be relevant with anterior skull base location (5). This phenomenon was not observed in our cohort. In some previous studies, clinical data were added to radiomic models to optimize the impact (14). No significant clinical features were found in our cohort, so these were not included in the analysis.

Recently, radiomics studies of other diseases selected ROI through automatic segmentation, such as lung cancer, breast cancer and gastric disease (40–42). Jonathan et al. had developed an algorithm based on convolutional neural network to automatically segment vestibular schwannoma and achieved satisfactory results (43). The application of automatic segmentation could benefit our research and clinical practice. Although at present, no research showed that there is a difference in accuracy between automatic segmentation and manual segmentation. Some studies showed that there was no meningioma tumor cell in the gadolinium enhanced meningeal tail sign (44), while some others drew the opposite conclusion (45). We included the meningeal tail sign in ROI analysis because the boundary between the meningeal tail sign and meningioma is difficult to distinguish.

There were limitations in our present study. First, this was a retrospective study with comparatively small sample size which could have limited the accuracy of our model. Probably due to restriction of sample size, many difference in clinical and immunohistochemical features showed no statistical significance. Secend, the result of this study predicts binary variables. All our radiomic algorithms were based on linear models. There might be nonlinear models with a higher fitting degree. Finally, the clinical follow-up of these patients is still underway. Hopefully, the follow-up data might further confirm the significance of preoperative prediction of *NF2* status.

CONCLUSION

This retrospective study demonstrated that multiparametric MRI-based radiomics analysis could be a promising approach for preoperative prediction of *NF2* inactivation in patients with meningioma. It could serve as an effective non-invasive approach to predict *NF2* inactivation and help determine individualized therapeutic regime for patients with meningioma.

DATA AVAILABILITY STATEMENT

The original contributions presented in the study are publicly available. This data can be found here: https://www.ncbi.nlm.nih.gov/sra, PRJNA858222.

ETHICS STATEMENT

Written informed consent was obtained from the individual(s) for the publication of any potentially identifiable images or data included in this article.

AUTHOR CONTRIBUTIONS

SS prepared the first version of the editorial. LR, ZM, LH and YG discuss the editorial content and revised the final editorial text. All authors contributed to the article and approved the submitted version.

ACKNOWLEDGMENTS

This study was supported by grants from the National Natural Science Foundation of China (82072788 to YG, 82203390 to LYH and 82203204 to JJD), the Science and Technology Commission of Shanghai Municipality (22140900200 to YG) and Shanghai Sailing Program (20YF1403900 to LYH).

SUPPLEMENTARY MATERIAL

The Supplementary Material for this article can be found online at: https://www.frontiersin.org/articles/10.3389/fonc.2022.879528/full#supplementary-material

REFERENCES

1. Preusser M, Brastianos P, Mawrin C. Advances in Meningioma Genetics: Novel Therapeutic Opportunities. *Nat Rev Neurol* (2018) 14(2):106–15. doi: 10.1038/nrneurol.2017.168
2. Ostrom Q, Patil N, Cioffi G, Waite K, Kruchko C, Barnholtz-Sloan J. CBTRUS Statistical Report: Primary Brain and Other Central Nervous System Tumors Diagnosed in the United States in 2013-2017. *Neuro-oncology* (2020) 22:iv1–iv96. doi: 10.1093/neuonc/noaa200.
3. Whittle I, Smith C, Navoo P, Collie D. Meningiomas. *Lancet (London England)* (2004) 363(9420):1535–43. doi: 10.1016/s0140-6736(04)16153-9
4. Riemenschneider M, Perry A, Reifenberger G. Histological Classification and Molecular Genetics of Meningiomas. *Lancet Neurol* (2006) 5(12):1045–54. doi: 10.1016/s1474-4422(06)70625-1
5. Clark V, Erson-Omay E, Serin A, Yin J, Cotney J, Ozduman K, et al. Genomic Analysis of non-NF2 Meningiomas Reveals Mutations in TRAF7, KLF4, AKT1, and SMO. *Sci (New York NY)* (2013) 339(6123):1077–80. doi: 10.1126/science.1233009
6. Brastianos P, Horowitz P, Santagata S, Jones R, McKenna A, Getz G, et al. Genomic Sequencing of Meningiomas Identifies Oncogenic SMO and AKT1 Mutations. *Nat Genet* (2013) 45(3):285–9. doi: 10.1038/ng.2526
7. Youngblood M, Miyagishima D, Jin L, Gupte T, Li C, Duran D, et al. Associations of Meningioma Molecular Subgroup and Tumor Recurrence. *Neuro Oncol* (2021) 23(5):783–94. doi: 10.1093/neuonc/noaa226
8. Lambin P, Rios-Velazquez E, Leijenaar R, Carvalho S, van Stiphout R, Granton P, et al. Radiomics: Extracting More Information From Medical Images Using Advanced Feature Analysis. *Eur J Cancer (Oxford Engl 1990)* (2012) 48(4):441–6. doi: 10.1016/j.ejca.2011.11.036
9. Liu Z, Wang S, Dong D, Wei J, Fang C, Zhou X, et al. The Applications of Radiomics in Precision Diagnosis and Treatment of Oncology: Opportunities and Challenges. *Theranostics* (2019) 9(5):1303–22. doi: 10.7150/thno.30309
10. Li Z, Kaiser L, Holzgreve A, Ruf V, Suchorska B, Wenter V, et al. Prediction of TERTp-Mutation Status in IDH-Wildtype High-Grade Gliomas Using Pre-Treatment Dynamic [F]FET PET Radiomics. *Eur J Nucl Med Mol Imaging* (2021) 48(13):4415–25. doi: 10.1007/s00259-021-05526-6
11. Langenhuizen P, Zinger S, Leenstra S, Kunst H, Mulder J, Hanssens P, et al. Radiomics-Based Prediction of Long-Term Treatment Response of Vestibular Schwannomas Following Stereotactic Radiosurgery. *Otology Neurotology* (2020) 41(10):e1321–7. doi: 10.1097/mao.0000000000002886
12. Khanna O, Fathi Kazerooni A, Farrell C, Baldassari M, Alexander T, Karsy M, et al. Machine Learning Using Multiparametric Magnetic Resonance Imaging Radiomic Feature Analysis to Predict Ki-67 in World Health Organization Grade I Meningiomas. *Neurosurgery* (2021) 89(5):928–36. doi: 10.1093/neuros/nyab307.
13. Zhai Y, Song D, Yang F, Wang Y, Jia X, Wei S, et al. Preoperative Prediction of Meningioma Consistency *via* Machine Learning-Based Radiomics. *Front Oncol* (2021) 11:657288. doi: 10.3389/fonc.2021.657288
14. Xiao B, Fan Y, Zhang Z, Tan Z, Yang H, Tu W, et al. Three-Dimensional Radiomics Features From Multi-Parameter MRI Combined With Clinical Characteristics Predict Postoperative Cerebral Edema Exacerbation in Patients With Meningioma. *Front Oncol* (2021) 11:625220. doi: 10.3389/fonc.2021.625220
15. Liu X, Li Y, Li S, Fan X, Sun Z, Yang Z, et al. IDH Mutation-Specific Radiomic Signature in Lower-Grade Gliomas. *Aging* (2019) 11(2):673–96. doi: 10.18632/aging.101769
16. Li Y, Qian Z, Xu K, Wang K, Fan X, Li S, et al. MRI Features Predict P53 Status in Lower-Grade Gliomas *via* a Machine-Learning Approach. *NeuroImage Clin* (2018) 17:306–11. doi: 10.1016/j.nicl.2017.10.030
17. Deng J, Sun S, Chen J, Wang D, Cheng H, Chen H, et al. TERT Alterations Predict Tumor Progression in High-Grade Meningiomas Following Adjuvant Radiotherapy. *Front Oncol* (2021) 11:747592. doi: 10.3389/fonc.2021.747592
18. Birzu C, Peyre M, Sahm F. Molecular Alterations in Meningioma: Prognostic and Therapeutic Perspectives. *Curr Opin Oncol* (2020) 32(6):613–22. doi: 10.1097/cco.0000000000000687
19. Asthagiri A, Parry D, Butman J, Kim H, Tsilou E, Zhuang Z, et al. Neurofibromatosis Type 2. *Lancet (London England)* (2009) 373 (9679):1974–86. doi: 10.1016/s0140-6736(09)60259-2
20. Stamenkovic I, Yu Q. Merlin, a "Magic" Linker Between Extracellular Cues and Intracellular Signaling Pathways That Regulate Cell Motility, Proliferation, and Survival. *Curr Protein Pept Sci* (2010) 11(6):471–84. doi: 10.2174/138920310791824011
21. Petrilli A, Fernández-Valle C. Role of Merlin/NF2 Inactivation in Tumor Biology. *Oncogene* (2016) 35(5):537–48. doi: 10.1038/onc.2015.125
22. Ruttledge M, Sarrazin J, Rangaratnam S, Phelan C, Twist E, Merel P, et al. Evidence for the Complete Inactivation of the NF2 Gene in the Majority of Sporadic Meningiomas. *Nat Genet* (1994) 6(2):180–4. doi: 10.1038/ng0294-180
23. Gutmann D, Giordano M, Fishback A, Guha A. Loss of Merlin Expression in Sporadic Meningiomas, Ependymomas and Schwannomas. *Neurology* (1997) 49(1):267–70. doi: 10.1212/wnl.49.1.267
24. Lomas J, Bello M, Arjona D, Alonso M, Martinez-Glez V, Lopez-Marin I, et al. Genetic and Epigenetic Alteration of the NF2 Gene in Sporadic Meningiomas. *Genes Chromosomes Cancer* (2005) 42(3):314–9. doi: 10.1002/gcc.20141
25. Yuzawa S, Nishihara H, Yamaguchi S, Mohri H, Wang L, Kimura T, et al. Clinical Impact of Targeted Amplicon Sequencing for Meningioma as a Practical Clinical-Sequencing System. *Modern Pathol* (2016) 29(7):708–16. doi: 10.1038/modpathol.2016.81
26. Abedalthagafi M, Bi W, Aizer A, Merrill P, Brewster R, Agarwalla P, et al. Oncogenic PI3K Mutations are as Common as AKT1 and SMO Mutations in Meningioma. *Neuro Oncol* (2016) 18(5):649–55. doi: 10.1093/neuonc/nov316
27. Hamerla G, Meyer H, Schob S, Ginat D, Altman A, Lim T, et al. Comparison of Machine Learning Classifiers for Differentiation of Grade 1 From Higher Gradings in Meningioma: A Multicenter Radiomics Study. *Magnetic Resonance Imaging* (2019) 63:244–9. doi: 10.1016/j.mri.2019.08.011
28. Zhu Y, Man C, Gong L, Dong D, Yu X, Wang S, et al. A Deep Learning Radiomics Model for Preoperative Grading in Meningioma. *Eur J Radiol* (2019) 116:128–34. doi: 10.1016/j.ejrad.2019.04.022
29. Niu L, Zhou X, Duan C, Zhao J, Sui Q, Liu X, et al. Differentiation Researches on the Meningioma Subtypes by Radiomics From Contrast-Enhanced Magnetic Resonance Imaging: A Preliminary Study. *World Neurosurg* (2019) 126:e646–52. doi: 10.1016/j.wneu.2019.02.109
30. Monti S, Aiello M, Incoronato M, Grimaldi A, Moscarino M, Mirabelli P, et al. DCE-MRI Pharmacokinetic-Based Phenotyping of Invasive Ductal Carcinoma: A Radiomic Study for Prediction of Histological Outcomes. *Contrast Media Mol Imaging* (2018) 2018:5076269. doi: 10.1155/2018/5076269
31. Kim M, Jung S, Park J, Jo Y, Park S, Nam S, et al. Diffusion- and Perfusion-Weighted MRI Radiomics Model may Predict Isocitrate Dehydrogenase (IDH) Mutation and Tumor Aggressiveness in Diffuse Lower Grade Glioma. *Eur Radiol* (2020) 30(4):2142–51. doi: 10.1007/s00330-019-06548-3
32. Casale R, Lavrova E, Sanduleanu S, Woodruff H, Lambin P. Development and External Validation of a non-Invasive Molecular Status Predictor of Chromosome 1p/19q Co-Deletion Based on MRI Radiomics Analysis of Low Grade Glioma Patients. *Eur J Radiol* (2021) 139:109678. doi: 10.1016/j.ejrad.2021.109678
33. Elster A, Challa V, Gilbert T, Richardson D, Contento J. Meningiomas: MR and Histopathologic Features. *Radiology* (1989) 170:857–62. doi: 10.1148/radiology.170.3.2916043
34. Pirozzi C, Yan H. The Implications of IDH Mutations for Cancer Development and Therapy. *Nat Rev Clin Oncol* (2021) 18(10):645–61. doi: 10.1038/s41571-021-00521-0
35. Loibl S, Poortmans P, Morrow M, Denkert C, Curigliano G. Breast Cancer. *Lancet (London England)* (2021) 397(10286):1750–69. doi: 10.1016/s0140-6736(20)32381-3
36. Cocco E, Lopez S, Santin AD, Scaltriti M. Prevalence and Role of HER2 Mutations in Cancer. *Pharmacol Ther* (2019) 199:188–96. doi: 10.1016/j.pharmthera.2019.03.010
37. Dang L, Yen K, Attar E. IDH mutations in cancer and progress toward development of targeted therapeutics. *Ann Oncol: Official J Eur Surg Med Oncol.* (2016) 27(4):599–608. doi: 10.1093/annonc/mdw013
38. Evans D. Neurofibromatosis Type 2 (NF2): A Clinical and Molecular Review. *Orphanet J Rare Diseases* (2009) 4:16. doi: 10.1186/1750-1172-4-16
39. Sahm F, Schrimpf D, Stichel D, Jones D, Hielscher T, Schefzyk S, et al. DNA Methylation-Based Classification and Grading System for Meningioma: A

Multicentre, Retrospective Analysis. *Lancet Oncol* (2017) 18(5):682–94. doi: 10.1016/s1470-2045(17)30155-9
40. Liu X, Li K, Yang R, Geng L. Review of Deep Learning Based Automatic Segmentation for Lung Cancer Radiotherapy. *Front Oncol* (2021) 11:717039. doi: 10.3389/fonc.2021.717039
41. Chen X, Men K, Chen B, Tang Y, Zhang T, Wang S, et al. CNN-Based Quality Assurance for Automatic Segmentation of Breast Cancer in Radiotherapy. *Front Oncol* (2020) 10:524. doi: 10.3389/fonc.2020.00524
42. Tan J, Wang L, Chen Y, Xi W, Ji J, Wang L, et al. Predicting Chemotherapeutic Response for Far-Advanced Gastric Cancer by Radiomics With Deep Learning Semi-Automatic Segmentation. *J Cancer* (2020) 11(24):7224–36. doi: 10.7150/jca.46704
43. Shapey J, Kujawa A, Dorent R, Wang G, Dimitriadis A, Grishchuk D, et al. Segmentation of Vestibular Schwannoma From MRI, an Open Annotated Dataset and Baseline Algorithm. *Sci Data* (2021) 8(1):286. doi: 10.1038/s41597-021-01064-w
44. Tokumaru A, O'uchi T, Eguchi T, Kawamoto S, Kokubo T, Suzuki M, et al. Prominent Meningeal Enhancement Adjacent to Meningioma on Gd-DTPA-Enhanced MR Images: Histopathologic Correlation. *Radiology* (1990) 175 (2):431–3. doi: 10.1148/radiology.175.2.2326470
45. Rokni-Yazdi H, Azmoudeh Ardalan F, Asadzandi Z, Sotoudeh H, Shakiba M, Adibi A, et al. Pathologic Significance of the "Dural Tail Sign". *Eur J Radiol* (2009) 70(1):10–6. doi: 10.1016/j.ejrad.2008.01.010

Conflict of Interest: The authors declare that the research was conducted in the absence of any commercial or financial relationships that could be construed as a potential conflict of interest.

Publisher's Note: All claims expressed in this article are solely those of the authors and do not necessarily represent those of their affiliated organizations, or those of the publisher, the editors and the reviewers. Any product that may be evaluated in this article, or claim that may be made by its manufacturer, is not guaranteed or endorsed by the publisher.

Copyright © 2022 Sun, Ren, Miao, Hua, Wang, Deng, Chen, Liu and Gong. This is an open-access article distributed under the terms of the Creative Commons Attribution License (CC BY). The use, distribution or reproduction in other forums is permitted, provided the original author(s) and the copyright owner(s) are credited and that the original publication in this journal is cited, in accordance with accepted academic practice. No use, distribution or reproduction is permitted which does not comply with these terms.

frontiers | Frontiers in Neurology

TYPE Original Research
PUBLISHED 13 October 2022
DOI 10.3389/fneur.2022.893480

Check for updates

OPEN ACCESS

EDITED BY
David D. Eisenstat,
Royal Children's Hospital, Australia

REVIEWED BY
Andrea Carai,
Bambino Gesù Children's Hospital (IRCCS), Italy
Peicong Ge,
Capital Medical University, China

*CORRESPONDENCE
Jianbo Ding
yuanfanghaiyang@163.com

SPECIALTY SECTION
This article was submitted to Neuro-Oncology and Neurosurgical Oncology, a section of the journal Frontiers in Neurology

RECEIVED 10 March 2022
ACCEPTED 20 September 2022
PUBLISHED 13 October 2022

CITATION
Gong X, Ding J, Knisely JPS, Wang E, Pan L, Wang B, Zhang N, Wu H, Dai J, Yu T and Tang X (2022) Dose-staged Gamma Knife radiosurgery for meningiomas: A retrospective study in a single center.
Front. Neurol. 13:893480.
doi: 10.3389/fneur.2022.893480

COPYRIGHT
© 2022 Gong, Ding, Knisely, Wang, Pan, Wang, Zhang, Wu, Dai, Yu and Tang. This is an open-access article distributed under the terms of the Creative Commons Attribution License (CC BY). The use, distribution or reproduction in other forums is permitted, provided the original author(s) and the copyright owner(s) are credited and that the original publication in this journal is cited, in accordance with accepted academic practice. No use, distribution or reproduction is permitted which does not comply with these terms.

Dose-staged Gamma Knife radiosurgery for meningiomas: A retrospective study in a single center

Xiu Gong[1], Jianbo Ding[2,3]*, Jonathan P. S. Knisely[4], Enmin Wang[1], Li Pan[1], Binjiang Wang[1], Nan Zhang[1], Hanfeng Wu[2,3], Jiazhong Dai[1], Tonggang Yu[2,3] and Xuqun Tang[2,3]

[1]Department of Neurosurgery, Huashan Hospital, Shanghai Medical College, Fudan University, Shanghai, China, [2]Department of Neurosurgery, Shanghai Gamma Hospital, Shanghai, China, [3]Department of Neurosurgery, Gamma Knife Center of Huashan Hospital, Shanghai, China, [4]Department of Radiation Oncology, Weill Cornell Medicine and New York-Presbyterian Hospital, New York, NY, United States

Objective: This study aimed to study the efficiency and safety of a dose-staged Gamma Knife radiosurgery strategy for large meningiomas or meningiomas close to important nerve structures.

Methods: This study evaluates the outcome of a prospectively accrued series of 71 consecutive patients with meningiomas treated with staged dose-fractionated Gamma Knife radiosurgery. The average peripheral doses for the first and second fractions were 9.0 ± 0.9 Gy (8–12 Gy) and 8.6 ± 0.7 Gy (range, 7–10 Gy), respectively. The interval between fractions was 6.1 ± 1.9 months (range, 3–12 months). The median follow-up time was 36 months (12–96 months).

Results: During the follow-up period after the second fraction, 97.2% achieved tumor control in our series. A total of 2 patients exhibited local recurrence at 30 and 60 months after the second fraction, respectively. No treatment-related complications or new long-term neurological dysfunctions were reported. MRIs observed slightly or moderately increased peritumoral edema in six patients, but no specific neurological complaints are attributed to this finding.

Conclusion: This study investigates the efficiency and safety of dose-staged Gamma Knife radiosurgery as an alternative option for meningiomas that were large in volume, adjacent to crucial structures, or in patients with contraindications to craniotomy.

KEYWORDS

meningioma, staged radiosurgery, Gamma Knife, dose-staged GKRS, two-stage

Introduction

Meningioma is a common primary intracranial tumor, with 53.7% of all primary non-malignant brain tumors (1). If total resection can be achieved without causing neurological damage, microsurgical resection is the best treatment option. However, when meningiomas are located close to critical structures, morbidity rates are

increased (2). In addition, some patients have contraindications to general anesthesia and craniotomy. Stereotactic radiosurgery is the primary treatment for WHO grade 1 meningioma when the lesion volume is small and the imaging features are typical, with an 85–100% tumor control rate achieved at 5 years of treatment (3, 4). Conventional radiotherapy is mainly used as adjuvant therapy after surgery for WHO grades 2 and 3 meningiomas (3–5). For meningiomas patients who would not tolerate craniotomy, the single-fraction Gamma Knife treatment with a peripheral dose of 12–14 Gy in one session has been proven effective. However, the treatment only works with tumors with an average diameter of <3–3.5 cm to avoid serious radiation-induced toxicity (6, 7). Single-fraction Gamma Knife radiosurgery (GKRS) is limited by the radiation tolerance of critical functional areas, such as the optic nerves or chiasm, which cannot deliver the effective radiation dose to tumors close to these structures (8, 9). The previous studies on superior alternative radiation treatment for patients with surgical contraindications with large meningiomas or meningiomas close to important nerve structures are limited.

Hypofractionated stereotactic radiosurgery, treating a lesion in 2–5 fractions of SRS, can potentially provide the ability to treat large tumors at adequate tumor control and acceptable toxicity (8, 10). However, details on treating large meningiomas with fractionated Gamma Knife radiosurgery are rarely reported. Limited studies have presented early results for the mode of volume-fractionated staged radiosurgery to treat large skull base meningiomas (11–14). This mode divides a large lesion into two parts according to the volume. Each treatment adopts a dose similar to the single-fraction Gamma Knife to treat different tumor parts, with inter-fraction intervals of 3–9 Months. This study developed a dose-staged Gamma Knife radiosurgery strategy (dose-staged GKRS) for patients with surgical contraindications suffering from large meningiomas or meningiomas close to critical nerve structures. The whole target was covered with a lower dose, with an inter-fraction interval of 6 months in every fraction. This study demonstrates the experience obtained in a relatively large series of meningiomas treated with dose-staged GKRS.

Materials and methods

Inclusion criteria and exclusion criteria

Meningiomas patients that meet the following criteria were included in this study: the volume of meningiomas without previous surgery is greater or equal to 10 cc; the volume of residual or recurrent meningiomas after surgery was greater or equal to 10 cc; meningiomas are located near the optic nerve pathway, and the patient has useful vision regardless of the tumor volume or whether or not surgery has been performed.

Patients with WHO grade 2–3 meningiomas or who had progression of their tumor after prior irradiation were excluded.

TABLE 1 Characteristics of the 71 patients in this series.

Sex (*n*, %)	
Male	14 (19.7%)
Female	57 (80.3%)
Age in years (mean ± SD, range)	52.3 ± 11.2 (31–85)
Primary or postoperative treatment (*n*, %)	
Primary	43 (60.6%)
Postoperative	28 (39.4%)
Initial tumor volume (*n*, %)	
<8 cc	29 (40.8%)
8–20 cc	28 (39.4%)
>20 cc	14 (19.7%)
Tumor location (*n*, %)	
Skull base	59 (83.1%)
Parasagittal sinus	9 (12.7%)
Lateral ventricle	1(1.4%)
Pineal region	1(1.4%)
Tentorium	1(1.4%)
Interval in months between radiosurgery stages (mean ± SD, range)	6.1 ± 1.9 (3–12)
Peripheral dose (Gy) for first treatment (mean ± SD, range)	9.0 ± 0.9 (8–13.5)
Peripheral dose (Gy) for second treatment (mean ± SD, range)	8.6 ± 0.7 (7–10)

Patient profile and diagnostic criteria

A total of 71 consecutive patients were included in the retrospective, all with WHO grade 1 meningioma treated with dose-staged GKRS at Shanghai Gamma Hospital (Gamma Knife Center of Huashan Hospital) between June 2013 and March 2020. The characteristics of all patients are listed in Table 1. These patients served as a prospectively accrued consecutive series, consisting of 14 (19.7%) men and 57 (80.3%) women, with an average age of 52.3 ± 11.2 years (range, 31–85). 28 (39.4%) patients had undergone surgical resection, and the meningioma diagnosis was confirmed by histopathology. For 43 (60.6%) patients, radiosurgery was the initial treatment, and the diagnosis of meningioma was based on MRI and CT characteristics. The mean initial tumor volume of all cases in this series was 12.7 ± 9.3 cm^3 (range, 0.6–41.1 cm^3). To analyze the size effect of treated lesions on the volumetric outcome, we divided all cases into three groups (<8 cc for 29 cases, 8–20 cc for 28 cases, >20 cc for 14 cases). Besides, the tumors were located in the skull base (59 cases), parasagittal sinus (9 cases), lateral ventricle (1 case), pineal region (1 case), and tentorium (1 case).

The WHO Classification of Tumors of the Central Nervous System classifies meningiomas into three grades and 15 subtypes. WHO grade 1 meningiomas consist of benign tumors with nine subtypes (15). Before Gamma Knife radiosurgery treatment, the patients were evaluated by a clinical

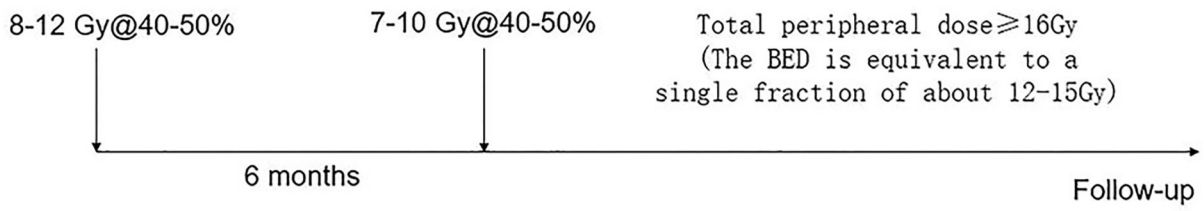

FIGURE 1
The treatment protocol for two-staged radiosurgery for meningiomas in this series is ~6-month interval between fractions.

examination, such as a detailed neurological examination, thin-slice, contrast-enhanced MRI, and high-resolution computed tomography (CT). A multidisciplinary team of neurosurgeons, neuroradiologists, and radiation oncologists evaluated each patient for treatment eligibility. For patients without histopathology, CT and MRI features were evaluated separately by two qualified neuroradiologists following the EANO guidelines by T1WI signal strength, T2WI signal strength, and the degree of peritumoral edema, respectively, and the degree of enhancement of the tumors (5).

Dose-staged Gamma Knife radiosurgery technique

Dose-staged Gamma Knife radiosurgery treatments were conducted under local anesthesia using a Leksell Gamma Knife model Perfexion (before January 2019) and ICON (from February 2019) at Shanghai Gamma Hospital, Gamma Knife Center of Huashan Hospital. Gadolinium-enhanced images of T1-weighted, T2-weighted, and FLAIR sequences were collected from each patient for pretreatment localization using a 1.5-T MR imaging system (Signa Excite, GE, USA). The tumor and adjacent critical structure delineation, dose prescription, and planning were conducted by a neurosurgeon, radiation oncologist, and radiation physicist. Dose planning was performed using MR images mentioned above that were exported to the Leksell GammaPlan software (version 10.0, Elekta Instruments AB, Stockholm, Sweden). The peripheral dose was administered to cover the gross tumor volume with no additional margin. An independent central physician evaluates every experiment plan before treatment is conducted.

Prescription dose and interval

This study used a two-stage treatment mode for all patients. The prescription dose for each fraction depended on the tumor volume and dose tolerance of the near nerves and brain structures. The biological equivalent dose (BED) of normal brain tissue and the tumor was calculated for $\alpha/\beta = 3$ Gy. In theory, the total dose for individual patients was calculated and divided into two-staged treatment. The average peripheral doses for the first and second fractions were 9.0 ± 0.9 Gy (range, 8–12 Gy) and 8.6 ± 0.7 Gy (range, 7–10 Gy), respectively (Table 1). The prescription isodose line for each fraction was between 40 and 50% and did not require to be equal for the two stages. The interval between stages was 6 months. Still, the date of the second stage of treatment was altered for follow-up imaging and side effects after the first stage of treatment (Figure 1).

Follow-up evaluations and toxicity

The first follow-up was carried out for each patient 3–6 months after the first stage of the treatment by interviewing the patients, examinations, and MR imaging to assess changes in patients' clinical symptoms and tumor volumes and determine the second stage administration date. Patients who exhibit satisfactory tumor control would receive regular clinical and MRI follow-up every 6 months after the second stage of treatment during the first year, annually for the next 2 years, and once every 2 years (Figure 1). The tumor volumes at each treatment stage and follow-up were calculated and compared using the patient's MRI data in the Leksell GammaPlan software. The tumor control is evaluated based on the change in tumor volume. Tumor control is considered good when the tumor volume decreases. If the tumor volume increases by more than 20%, an analysis of the causes is required, and salvage treatment is conducted when necessary.

All toxicities were scored according to version 5.0 of the National Cancer Institute Common Terminology Criteria for Adverse Events (16).

Statistical analysis

The SPSS software, version 25.0 (SPSS, Chicago, IL, USA), was used for statistical analysis. Values are presented as mean ±

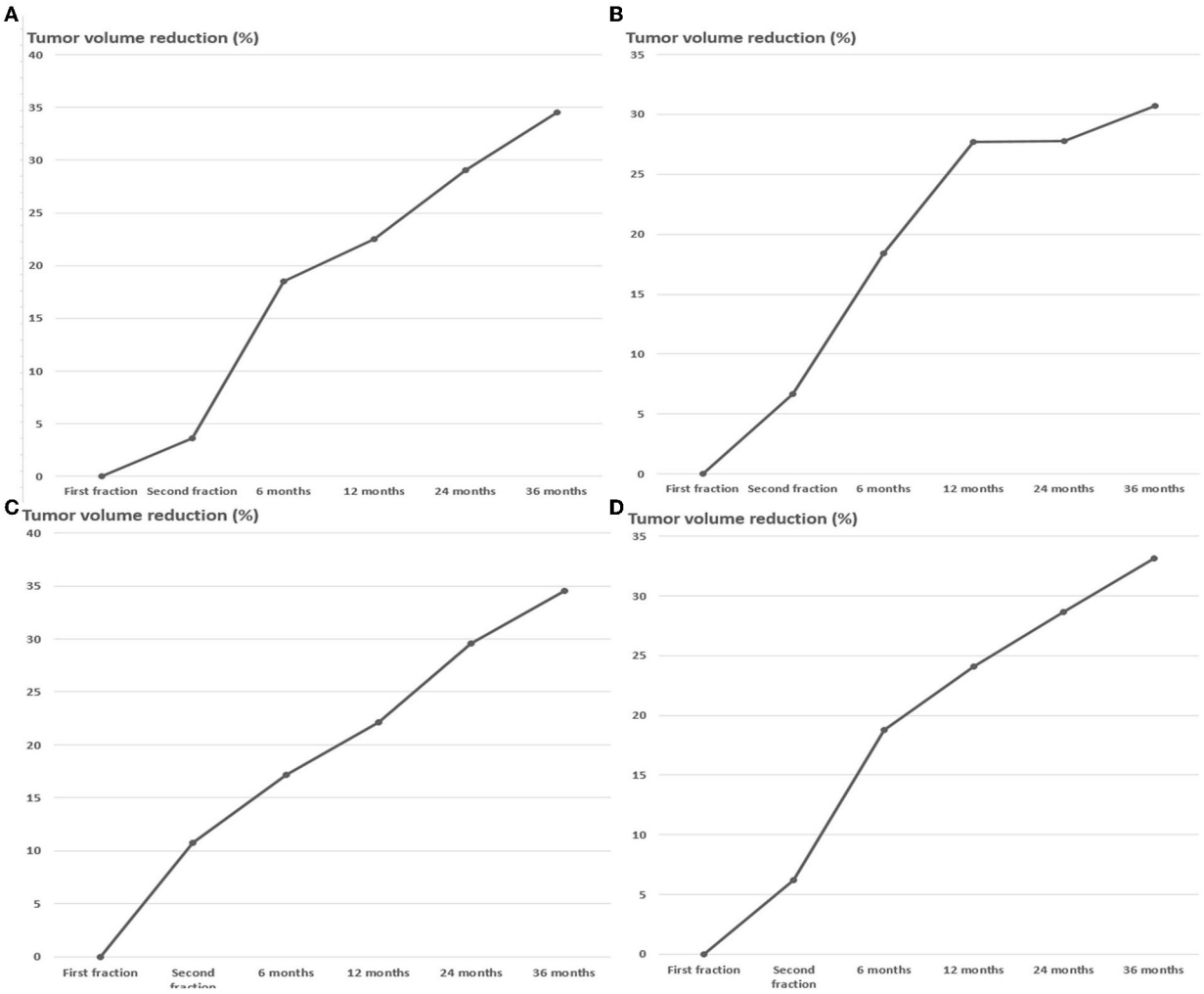

FIGURE 2
Tumor volume trends for meningiomas of different initial volume after dose-staged radiosurgery **(A)** <8 cc group, **(B)** 8–20 cc group, **(C)** >20 cc group, **(D)** Combined group.

standard deviation data with normal distribution or median and interquartile range for data that were abnormally distributed for continuous variables and number (%) for categorical variables. For multi-group comparisons, p values were derived from one-way ANOVA. For all comparisons, $p < 0.05$ was considered statistically significant.

Results

Tumor control

By the end of November 2021, the median follow-up time for this study was 36 months (range, 12–96 months). The average tumor volume between the first and second stages was decreased by 6.2 ± 13.5%. However, the tumor volume of 17 (23.9%) cases increased by 11.1 ± 6.9%. In the other 54 (76.0%) cases, the mean tumor volume decreased by 11.3 ± 8.5%. Most patients were followed-up through November 2021, but some patients missed one or several scheduled follow-up MRI scans. Recurrent cases were excluded from further follow-up. The MRI follow-up data were obtained from 65 (91.5%), 55 (77.5%), 48 (67.6%), and 38 (53.5%) individuals after 6, 12, 24, and 36 months of second-stage treatment, respectively. The follow-up data from 6 months after the second treatment depicted that the volume of all lesions decreased by 18.7 ± 14.5%. The follow-up data at 12, 24, and 36 months demonstrated that the tumor shrank by 24.1 ± 14.5, 28.7 ± 15.0, and 33.1 ± 14.5%, respectively (Figures 2–5). The percentage reduction in the volume of the three subgroups grouped according to the initial volume has no significant difference in each period after treatment (Figure 2, Table 2).

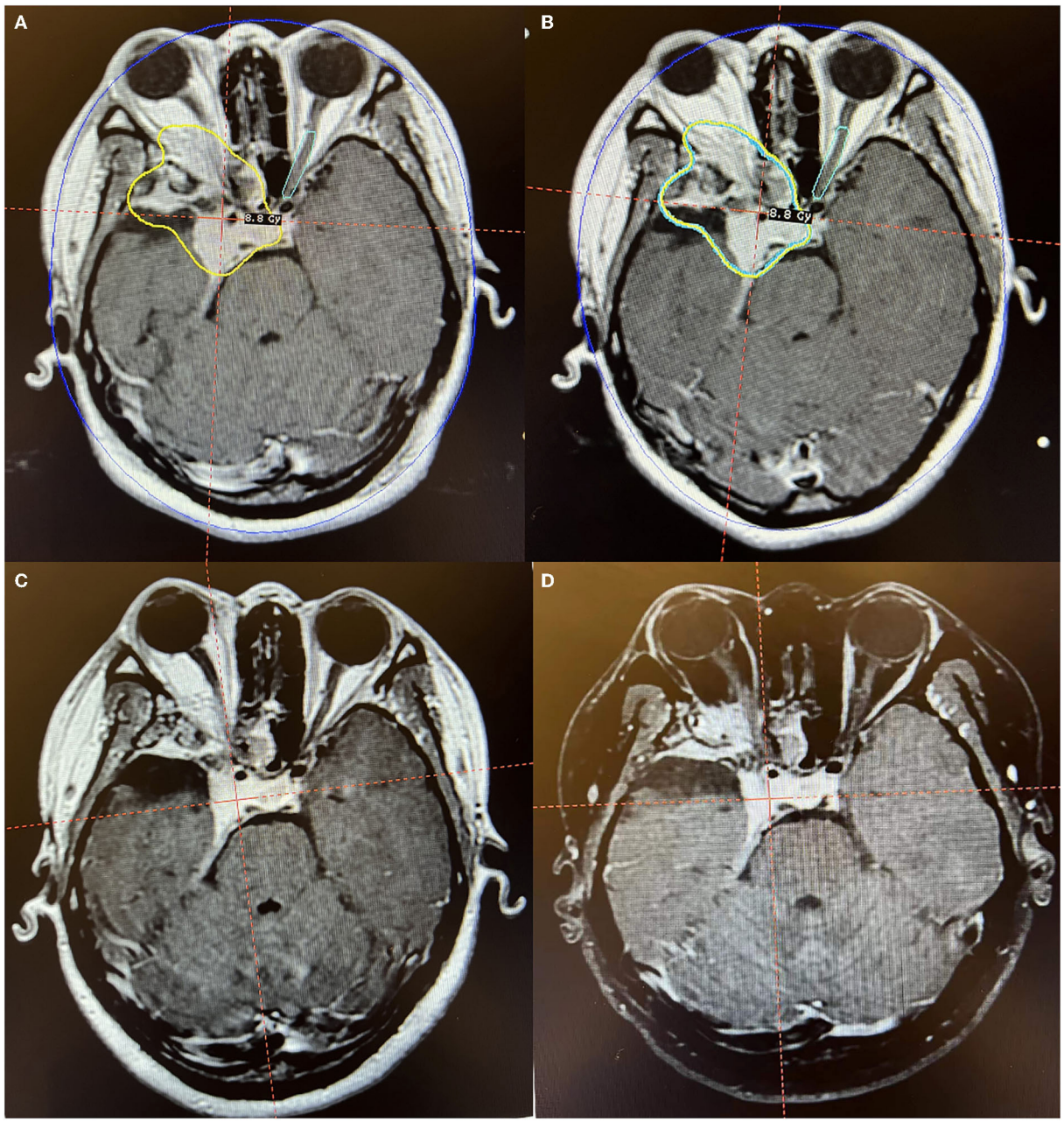

FIGURE 3
Axial MR imaging illustrating a huge postoperative residual orbitocranial meningioma post-operation treated with Gamma Knife radiosurgery. **(A)** The prescription dose planning MRI for the first stage of Gamma Knife radiosurgery showing that the tumor margin was covered by 8.8 Gy (45% isodose surface). **(B)** The prescription dose planning MRI for the second stage of Gamma Knife radiosurgery demonstrated that the tumor decreased by 9.8% and was treated with the same dose as the first stage. **(C)** MRI obtained 12 months after radiosurgery presented a decrease of 27.3% in tumor size. **(D)** MRI obtained 36 months after radiosurgery manifested that the tumor is under stable control. The patient's right eye was blind before radiosurgery. After Gamma Knife treatment, there were no obvious adverse reactions, and the vision of the left eye was unchanged.

After the second stage and in follow-up, the overall tumor control rate was 97.2% (69/71). Local recurrences occurred in 2 cases, with the time of recurrences at 30 and 60 months after the second stage of treatment. Those cases had not undergone previous surgery before Gamma Knife. One case with a sellar region meningioma reported vision loss 60 months after the second stage of radiosurgery. MRI showed the tumor recurred from its original position, and the patient immediately received salvage radiosurgery. After the surgery, the tumor was reduced by 23.3%, and the patient's visuals were restored gradually

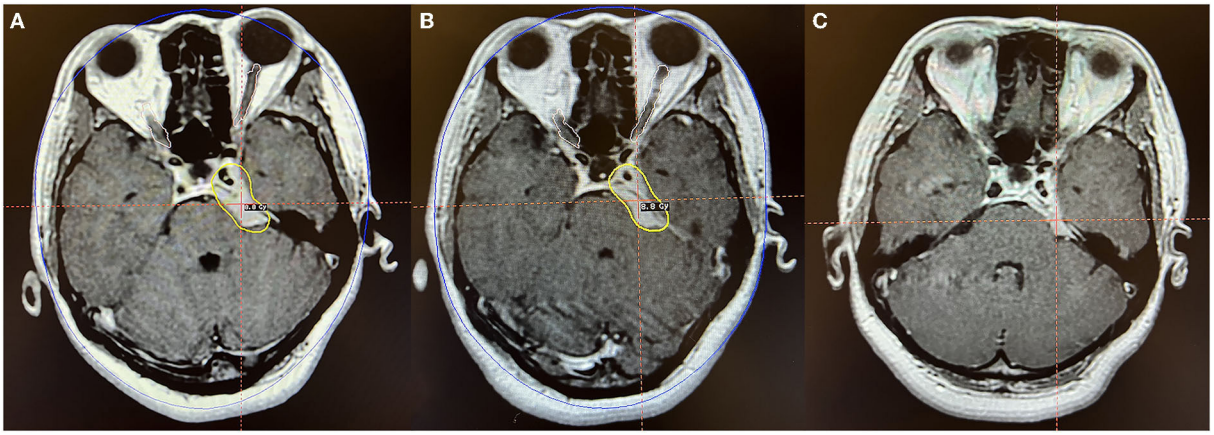

FIGURE 4
Axial MR imaging illustrating a petroclival middle-posterior communicating meningioma treated with Gamma Knife radiosurgery. **(A)** The prescription dose planning MRI for the first stage of Gamma Knife radiosurgery displaying that the tumor margin was covered by 8.8 Gy (45% isodose surface), and the tumor volume was 7.0 cc. **(B)** In the second fraction, the tumor was treated with the same dose as the first stage, and the tumor volume was 6.1 cc. **(C)** MRI obtained 24 months after radiosurgery indicated that the tumor volume is 4.7 cc, decreased by 33.0% compared with the pre-radiosurgery volume. No obvious adverse reactions were observed.

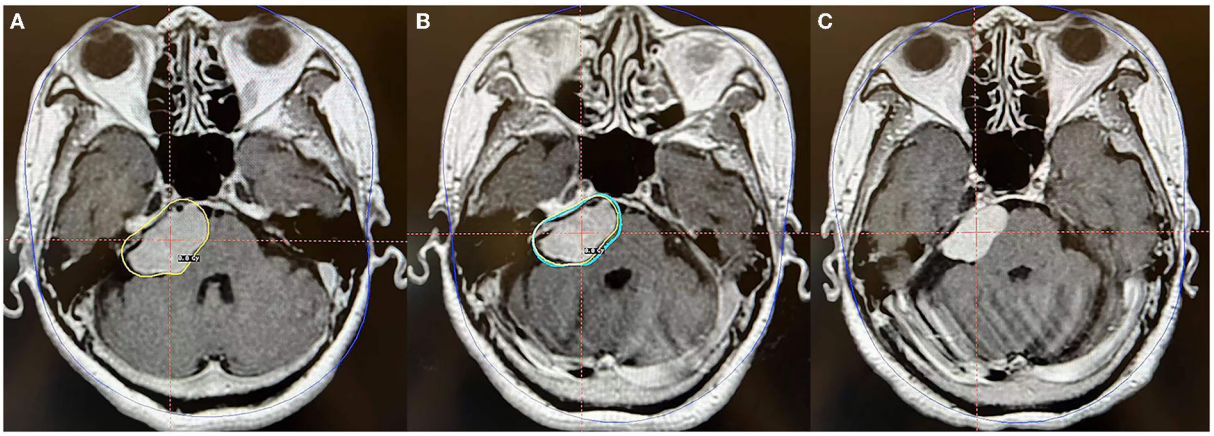

FIGURE 5
Axial MR imaging illustrating a posterior petrosal meningioma treated with Gamma Knife radiosurgery. **(A)** The prescription dose planning MRI for the first stage of Gamma Knife radiosurgery presenting that the tumor margin was covered by 8.8 Gy (45% isodose surface), and the tumor volume was 11.0 cc. **(B)** In the second fraction, the tumor was treated repeatedly with the same precision dose as in the first stage, and the tumor volume was 8.4 cc. **(C)** MRI obtained 24 months after radiosurgery revealed that the tumor volume is 6.1 cc and is decreased by 44.5% compared with that pre-radiosurgery. No obvious adverse reactions were observed.

from 3 months after treatment. Another patient was diagnosed with tumor recurrence on a surveillance MRI 30 months after the second stage of treatment and received further surgery, confirming the diagnosis of WHO grade 1 meningioma.

Clinical response and toxicity

Before radiosurgery, 35 (49.3%) patients had neurological symptoms, and 36 (50.7%) patients were initially asymptomatic. No obvious aggravation was reported in specific symptoms in all patients after the first stage of treatment. However, MRI showed signs of temporary tumor tissue swelling (reduction of central area enhancement and slight expansion of volume) and mild edema of peripheral brain tissue in 13 (18.3%) cases. The second stage was delayed for 1–3 months to reduce the radiation-related risk and improve the tolerance of these patients to radiosurgery. After the second stage, among 35 patients with neurological dysfunction, 11 patients had improvement and remained stable, and the other 24 displayed no aggravation of symptoms. A total of 15 (21.2%) patients reported nonspecific headache or dizziness within 6 months after the second stage

TABLE 2 Mean percentage reduction in volume for meningiomas with different initial volume after dose-staged Gamma Knife (%).

Time period	Total, $n = 71$	<8 cc, $n = 29$	8–12 cc, $n = 28$	>12 cc, $n = 14$	P
Second fraction	5.96	2.97	6.64	10.79	0.263
6 months	16.24	16.78	15.29	17.14	0.928
12 months	23	24.12	22.18	22.12	0.467
24 months	28.19	27.81	27.82	29.61	0.948
36 months	31.16	36.27	33.3	34.52	0.751

TABLE 3 Outcomes of clinical response and toxicity of dose-staged Gamma Knife for meningiomas in different location.

Outcomes	Skull base, $n = 59$, (%)	Parasagittal sinus, $n = 9$, (%)	Lateral ventricle, $n = 1$, (%)	Pineal region, $n = 1$, (%)	Tentorium, $n = 1$, (%)	Total, $n = 71$, (%)
Tumor control	57 (96.6)	9 (100)	1 (100)	1 (100)	1 (100)	69 (97.2)
Progression	2 (3.4)	0	0	0	0	2 (2.8)
GKRS related edema	4 (6.8)	1 (11.1)	1 (100)	0	0	6 (8.5)
Clinical progression	0	0	0	0	0	0
Headache	11 (18.6)	3 (33.3)	1 (100)	0	0	15 (21.1)

of treatment. Still, the headache was mild and had little effect on daily life, and gradually disappeared after 1 month without special treatment. During the follow-up period, limited edema around the lesions was slightly increased in six cases; these tumors were located in the skull base (4 cases), parasagittal sinus (1 case), and lateral ventricle (1 case), respectively (Table 3). Still, the tumor size was stable or shrunk, and these patients reported no specific symptoms.

Discussion

The meningioma treatment is widely dominated by local treatment, such as craniotomy or local radiosurgery. The classic single-fraction Gamma Knife radiosurgery has a therapeutic effect with a low incidence of toxic reactions for "suitable cases" and, in the long-term, can achieve tumor control rates similar to Simpson Grade 1 surgical resection (17, 18). However, "suitable cases" often denote small tumors far from the critical structures (e.g., optic nerve and brainstem). Some meningiomas patients have large lesions in clinical practice, but their physical conditions can poorly tolerate craniotomy. Other patients may present with tumors close to the optic nerve and other critical structures. Despite the small tumor, a conventional prescription dose may risk consequential radiation damage to the brain tissue or critical structures. These circumstances have limited the application of Gamma Knife radiosurgery and make it difficult for single-fraction Gamma Knife radiosurgery (19–22).

About 40 years ago, a staged Gamma Knife strategy was used to treat large AVMs and achieved positive results (23–26). In recent decades, staged Gamma Knife radiosurgery was used to treat brain metastases and meningiomas (11–14, 27–31). Unlike conventional radiotherapy, which requires daily treatments for 5–6 weeks, staged Gamma Knife radiosurgery has a long interval between two sessions. Staged Gamma Knife radiosurgery consists of two stages (11–14, 23–32): volume-staged Gamma Knife radiosurgery in which different fractions of the dose planning curves cover the different subvolumes of the target; and dose-staged Gamma Knife radiosurgery in which every fraction uses a lower dose to cover the whole target.

Few studies have reported the application of staged Gamma Knife radiosurgery for meningioma treatments, which all employed a volume-staged approach. The volume-staged approach divides the target into two or more parts, and the treatment volumes and doses of each stage differ. Iwai et al. reported 7 cases of skull base meningiomas treated with volume-staged Gamma Knife radiosurgery in 2001 (11). The volume of each treatment was 6.8–29.6 cm^3 (mean 18.6 cm^3), with an inter-fraction interval of 6 months and marginal doses of 8–12 Gy for each fraction. Six of seven patients achieved tumor growth control during the follow-up period (mean 39 months). The number of cases increased to 27 in 2019 with a similar treatment strategy. With an average follow-up of 84 months, only 25% of cases reported local tumor control failure, and 4% reported permanent radiation injury (12). In 2009, Haselsberger et al. reported 20 staged Gamma Knife radiosurgery cases for large meningiomas in critical locations (13). The volume treated in each session was 5.4–42.9 cm^3 (median 19.0 cm^3), the treatment interval was between 1 and 12 months (median: 6 months), and the median prescription dose with 45% isodose surface was 12 Gy (range: 10–25 Gy).

TABLE 4 List of studies regarding staged Gamma-Knife radiosurgery for meningioma.

Authors & year	No. of cases	Fractionated mode	Prescribe dose & fractions	Interval (m)	Tumor control	Permanent radiation injury (%)
Iwai et al. (11)	7	volume-staged	8–12 Gy × 2 f	6	86% at 39 m	0
Haselsberger et al. (13)	20	volume-staged	12 Gy × 2 f	6	90% at 7.5 y	0
Su et al. (14)	4	volume-staged	8–15 Gy × 2–3 f	4–6	100% at 100.5 m	0
Iwai et al. (12)	27	volume-staged	8–12 Gy × 2 f	3–9	75% at 84 m	4
Present study	71	dose-staged	9 Gy × 2 f	6	97.2% at 36 m	0

During a median follow-up of 7.5 years, 90% of the patients achieved tumor control (25% tumor regression, 65% stable size). Su et al. reported 4 cases of large skull base meningioma surrounding the optical apparatus (14), for which treatment mode of 2–3 fractions was administered with intervals of 4–6 months. In stage 1, ∼3/4 of the tumor volume far from the optic nerve (13.2 cm^3, range: 3.9–54.7 cm^3) was treated with a marginal dose of 13.5 Gy (range: 12–15 Gy). In stage 2, the upper portion of the tumor located close to the optic nerve was treated (4.3 cm^3; range: 1.5–16.2 cm^3), and the marginal dose was 9 Gy (range: 8–10 Gy). A 34–46% reduction in tumor volume was reported during a median follow-up period of 100.5 months. The efficiency and safety of the treatment are generally satisfactory.

Nevertheless, the number of cases in each series is relatively limited, and the approaches used in each stage vary to a great degree. For volume-staged radiosurgery, at the site of the junction between subvolumes, the center or sub-center of the tumor, the dose delivered to the meningioma is insufficient to control growth durably. Conversely, the dose delivered in 2 fractions to adjoining normal brain tissue may exceed its tolerance level. Experiment and clinical data cannot decide the best approach for fractionated radiosurgery for meningiomas. Detailed research is required to design safe and effective staged Gamma Knife radiosurgery meningioma plans that stabilize the relationship between a single prescription dose and treatment interval.

This study represents the first report of dose-staged Gamma Knife radiosurgery for meningiomas. Dose-staged Gamma Knife radiosurgery more closely fulfills tumor radiobiology's fundamental principles. Unlike volume-staged radiosurgery, the schedule of dose-staged Gamma Knife radiosurgery gives more stable radiation doses to the tumor. The contiguous normal brain tissue has a longer repair period and lowers integral doses of radiation; avoid exposing brain tissue at the sites where adjoining stages of volume-staged radiosurgery complement the high dose of radiation from each fraction. Seventy-one cases were included in our study, and compared with other published articles; this is the largest number of cases reported yet for staged Gamma Knife radiosurgery of meningiomas. It was found that after a median follow-up of 36 months, 97.2% (69/71) of the lesions were reduced or stable after treatment, and only two patients had a local failure. The therapeutic effect is satisfactory compared to previous literature listed in Table 4.

Leksell Gamma Knife model ICON can provide continuously fractionated radiotherapy treatment. A relatively fixed dose is usually implemented in 3–5 consecutive days (10, 33). This study used stage radiosurgery with a long interfraction interval instead of fractionated radiosurgery delivered on interval days. A slow response was observed in benign meningiomas to radiosurgery, where tumor tissue swelling and edema of peripheral brain tissue were reported from 3 to 6 months after radiosurgery (2, 34). Radiation-related adverse reactions after continuously delivered fractionated radiotherapy are unavoidable. Staged radiosurgery can adjust the treatment time and the dose for the second stage based on the treatment results of the first stage and the adverse side effects. After the first stage of treatment, 13 (18.3%) patients showed MRI signs of transient tumor tissue swelling and mild edema of peripheral brain tissue. Reports on the radiosurgery treatment of large meningiomas are limited, and the efficacy and biological mechanism of both continuously delivered fractionated radiotherapy and staged radiosurgery require further investigation.

In addition, 17 (23.9%) lesions had slightly increased by 11.1 ± 6.9% during the second stage of treatment. Although the degree of enlargement in these cases is small, it is considered a transient swelling of tumor tissue after radiosurgery instead of tumor progression. This is due to two aspects: firstly, WHO grade 1 meningioma normally progresses very slowly even without treatment; secondly, contrast-enhanced MRI showed that the enhancement of these tumors had slightly decreased. During the follow-up period of 6–36 months after the two stages of treatment, the lesion volumes gradually reduced to the proportion of the patients with no acute inflammatory changes.

This study suggests that dose-staged Gamma Knife radiosurgery has minimal adverse side effects and is well-tolerated for large meningiomas or those close to important nerve structures. The relatively longer interval of the two stages provided a sufficient "buffer period," ensuring that patients with poor physical conditions could sustain the treatment plan. As a result, the tumor received a sufficient prescription dose,

with only two lesions' recurrence at 30 and 60 months after radiosurgery. The tumor volume of the patients decreased by an average of more than 30% during the follow-up period of 36 months. Although 15 patients reported no headache or dizziness 6 months after the second stage of treatment, these symptoms were usually mild, had little effect on daily life, and gradually relieved after about 1 month without special treatment. After dose-staged Gamma Knife radiosurgery, the MRI detected edema around the tumor was slightly larger than that before Gamma Knife radiosurgery in six cases. Still, the tumor size was stable or reduced, with most patients showing no symptoms. No new neurological dysfunction related to radiosurgery was found in this study. Among the 35 patients with neurological dysfunction, 11 reported relief of symptoms due to reduced tumor volume and reduced normal brain tissue compression. The other 24 patients were stable throughout treatment and in follow-up.

This study has several potential limitations. First, this is a non-prospective controlled study. Further randomized controlled studies need to be conducted to compare other fractionated radiosurgery approaches with dose-staged Gamma Knife radiosurgery for meningiomas. Second, due to the limited follow-up data of more than 3 years, the longer-term efficacy and safety required full monitoring. Furthermore, the treatment response after Gamma Knife radiosurgery in meningiomas could be influenced by many factors, such as prescription dose, location, volume, pathological classification, and surgical history (35). In this study, no difference was found in the percentage reduction in volume for differential initial volume meningiomas. The outcomes of clinical response and toxicity based on tumor location were illustrated in Table 3, however, among 71 cases, 59 cases (83.1%) were skull base meningiomas, and differential treatment response based on location could not be fully clarified. Future studies to analyze the impact of these prognostic factors on dose-staged Gamma Knife radiosurgery in meningiomas are still needed.

Conclusion

This study investigates the efficacy and safety of two-stage dose-fractionated Gamma Knife radiosurgery for meningiomas, providing an innovative and minimally invasive treatment option for meningioma patients with contraindications craniotomy. However, optimizing staged radiosurgery and clarifying the radiobiological details relevant to this approach still needed further investigation.

Data availability statement

The original contributions presented in the study are included in the article/supplementary material, further inquiries can be directed to the corresponding author/s.

Ethics statement

Ethical review and approval was not required for the study on human participants in accordance with the local legislation and institutional requirements. The patients/participants provided their written informed consent to participate in this study. Written informed consent was obtained from the individual(s) for the publication of any potentially identifiable images or data included in this article.

Author contributions

Conception and design: JD, EW, LP, and BW. Drafting the article and statistical analysis: XG and JD. Critically revising the article: JK. Approved the final version of the manuscript on behalf of all authors: XG. Study supervision: EW. Analysis and interpretation of data and reviewed submitted version of manuscript: all authors. All authors contributed to the article and approved the submitted version.

Funding

This study was supported by the National Natural Science Foundation of China grant (No. 81727806) and the Science and Technology Commission of Shanghai Municipality (No. 20194Y0482).

Acknowledgments

We hereby express our gratitude to all authors, reviewers, and independent editors for their valuable participation in this study.

Conflict of interest

The authors declare that the research was conducted in the absence of any commercial or financial relationships that could be construed as a potential conflict of interest.

Publisher's note

All claims expressed in this article are solely those of the authors and do not necessarily represent those of their affiliated organizations, or those of the publisher, the editors and the reviewers. Any product that may be evaluated in this article, or claim that may be made by its manufacturer, is not guaranteed or endorsed by the publisher.

References

1. Ostrom QT, Gittleman H, Fulop J, Liu M, Blanda R, Kromer C, et al. CBTRUS statistical report: primary brain and central nervous system tumors diagnosed in the United States in 2008–2012. *Neuro Oncol.* (2015) 17:iv1–62. doi: 10.1093/neuonc/nov189

2. Santacroce A, Walier M, Régis J, Liščák R, Motti E, Lindquist C, et al. Long-term tumor control of benign intracranial meningiomas after radiosurgery in a series of 4565 patients. *Neurosurgery.* (2012) 70:32–9. doi: 10.1227/NEU.0b013e31822d408a

3. Apra C, Peyre M, Kalamarides M. Current treatment options for meningioma. *Expert Rev Neurother.* (2018) 18:241–9. doi: 10.1080/14737175.2018.1429920

4. Buerki RA, Horbinski CM, Kruser T, Horowitz PM, James CD, Lukas RV. An overview of meningiomas. *Future Oncol.* (2018) 14:2161–77. doi: 10.2217/fon-2018-0006

5. Goldbrunner R, Minniti G, Preusser M, Jenkinson MD, Sallabanda K, Houdart E, et al. EANO guidelines for the diagnosis and treatment of meningiomas. *Lancet Oncol.* (2016) 17:e383–91. doi: 10.1016/S1470-2045(16)30321-7

6. Mansouri A, Guha D, Klironomos G, Larjani S, Zadeh G, Kondziolka D. Stereotactic radiosurgery for intracranial meningiomas: current concepts and future perspectives. *Neurosurgery.* (2015) 76:362–71. doi: 10.1227/NEU.0000000000000633

7. Starke RM, Przybylowski CJ, Sugoto M, Fezeu F, Awad AJ, Dale D, et al. Gamma Knife radiosurgery of large skull base meningiomas. *J Neurosurg.* (2015) 122:363–72. doi: 10.3171/2014.10.JNS14198

8. Kirkpatrick JP, Soltys SG, Lo SS, Beal K, Shrieve DC, Brown PD. The radiosurgery fractionation quandary: single fraction or hypofractionation? *Neuro Oncol.* (2017) 19:ii38–49. doi: 10.1093/neuonc/now301

9. Samanci Y, Ardor GD, Peker S. Gamma Knife radiosurgery for tuberculum sellae meningiomas: a series of 78 consecutive patients. *Neurosurg Rev.* (2022) 45:2315–22. doi: 10.1007/s10143-022-01753-z

10. Inserra F, Barone F, Palmisciano P, Scalia G, DA Ros V, Abdelsalam A, et al. Hypofractionated Gamma Knife radiosurgery: institutional experience on benign and malignant intracranial tumors. *Anticancer Res.* (2022) 42:1851–8. doi: 10.21873/anticanres.15661

11. Iwai Y, Yamanaka K, Nakajima H. Two-staged Gamma Knife radiosurgery for the treatment of large petroclival and cavernous sinus meningiomas. *Surg Neurol.* (2001) 56:308–14. doi: 10.1016/S0090-3019(01)00622-X

12. Iwai Y, Yamanaka K, Shimohonji W, Ishibashi K. Staged Gamma Knife radiosurgery for large skull base meningiomas. *Cureus.* (2019) 11:e6001. doi: 10.7759/cureus.6001

13. Haselsberger K, Maier T, Dominikus K, Holl E, Kurschel S, Ofner-Kopeinig P, et al. Staged gamma knife radiosurgery for large critically located benign meningiomas: evaluation of a series comprising 20 patients. *J Neurol Neurosurg Psychiatry.* (2009) 80:1172–5. doi: 10.1136/jnnp.2008.156745

14. Su CF, Liu DW, Lee CC, Chiu TL. Volume-staged Gamma Knife surgery for the treatment of large skull base meningioma surrounding the optical apparatus: a snowman-shape design. *J Chin Med Assoc.* (2017) 80:697–704. doi: 10.1016/j.jcma.2017.03.011

15. Louis DN, Perry A, Wesseling P, Brat DJ, Cree IA, Figarella-Branger D, et al. The 2021 WHO classification of tumors of the central nervous system: a summary. *Neuro Oncol.* (2021) 23:1231–51. doi: 10.1093/neuonc/noab106

16. US Department of Health and Human Services National Institutes of Health National Cancer Institute. (2017). Common terminology criteria for adverse events (CTCAE) version 5. Available online at: https://ctep.cancer.gov/protocolDevelopment/electronic_applications/ctc.htm#ctc_archive (accessed November 30, 2021).

17. Rogers L, Barani I, Chamberlain M, Kaley TJ, McDermott M, Raizer J, et al. Meningiomas: knowledge base, treatment outcomes, and uncertainties. *A RANO review J Neurosurg.* (2015) 122:4–23. doi: 10.3171/2014.7.JNS131644

18. Dedeciusova M, Komarc M, Faouzi M, Levivier M, Tuleasca C. Tumor control and radiobiological fingerprint after Gamma Knife radiosurgery for posterior fossa meningiomas: a series of 46 consecutive cases. *J Clin Neurosci.* (2022) 100:196–203. doi: 10.1016/j.jocn.2022.04.031

19. Chang JH, Chang JW, Choi JY, Park YG, Chung SS. Complications after gamma knife radiosurgery for benign meningiomas. *J Neurol Neurosurg Psychiatry.* (2003) 74:226–30. doi: 10.1136/jnnp.74.2.226

20. Stafford SL, Pollock BE, Foote RL, Link MJ, Gorman DA, Schomberg PJ, et al. Meningioma radiosurgery: tumor control, outcomes, and complications among 190 consecutive patients. *Neurosurgery.* (2001) 49:1029–37. doi: 10.1227/00006123-200111000-00001

21. Vernimmen FJ, Harris JK, Wilson JA, Melvill R, Smit BJ, Slabbert JP. Stereotactic proton beam therapy of skull base meningiomas. *Int J Radiat Oncol Biol Phys.* (2001) 49:99–105. doi: 10.1016/S0360-3016(00)01457-7

22. Nicolato A, Foroni R, Alessandrini F, Maluta S, Bricolo A, Gerosa M. The role of Gamma Knife radiosurgery in the management of cavernous sinus meningiomas. *Int J Radiat Oncol Biol Phys.* (2002) 53:992–1000. doi: 10.1016/S0360-3016(02)02802-X

23. Pollock BE. Gamma Knife radiosurgery of arteriovenous malformations: long-term outcomes and late effects. *Prog Neurol Surg.* (2019) 34:238–47. doi: 10.1159/000493070

24. El-Shehaby AMN, Reda WA, Abdel Karim KM, Emad Eldin RM, Nabeel AM, Tawadros SR. Volume-staged gamma knife radiosurgery for large brain arteriovenous malformation. *World Neurosurg.* (2019) 132:e604–12. doi: 10.1016/j.wneu.2019.08.065

25. Pollock BE, Kline RW, Stafford SL, Foote RL, Schomberg PJ. The rationale and technique of staged-volume arteriovenous malformation radiosurgery. *Int J Radiat Oncol Biol Phys.* (2000) 48:817–24. doi: 10.1016/S0360-3016(00)00696-9

26. Amponsah K, Ellis TL, Chan MD, Bourland JD, Glazier SS, McMullen KP, et al. Staged gamma knife radiosurgery for large cerebral arteriovenous malformations. *Stereotact Funct Neurosurg.* (2011) 89:365–71. doi: 10.1159/000329363

27. Higuchi Y, Serizawa T, Nagano O, Matsuda S, Ono J, Sato M, et al. Three-staged stereotactic radiotherapy without whole brain irradiation for large metastatic brain tumors. *Int J Radiat Oncol Biol Phys.* (2009) 74:1543–8. doi: 10.1016/j.ijrobp.2008.10.035

28. Yomo S, Hayashi M, Nicholson C. A prospective pilot study of two-session Gamma Knife surgery for large metastatic brain tumors. *J Neurooncol.* (2012) 109:159–65. doi: 10.1007/s11060-012-0882-8

29. Angelov L, Mohammadi AM, Bennett EE, Abbassy M, Elson P, Chao ST, et al. Impact of 2-staged stereotactic radiosurgery for treatment of brain metastases ≥2 cm. *J Neurosurg.* (2018) 129:366–82. doi: 10.3171/2017.3.JNS162532

30. Cho A, Medvedeva K, Kranawetter B, Untersteiner H, Hirschmann D, Lepilina O, et al. How to dose-stage large or high-risk brain metastases: an alternative two-fraction radiosurgical treatment approach. *J Neurosurg.* (2022) 15:1–10. doi: 10.3171/2022.2.JNS212440

31. Dohm A, McTyre ER, Okoukoni C, Henson A, Cramer CK, LeCompte MC, et al. Staged stereotactic radiosurgery for large brain metastases: local control and clinical outcomes of a one-two punch technique. *Neurosurgery.* (2018) 83:114–21. doi: 10.1093/neuros/nyx355

32. Seymour ZA, Sneed PK, Gupta N, Lawton MT, Molinaro AM, Young W, et al. Volume-staged radiosurgery for large arteriovenous malformations: an evolving paradigm. *J Neurosurg.* (2016) 124:163–74. doi: 10.3171/2014.12.JNS141308

33. Park HR, Park KW, Lee JM, Kim JH, Jeong SS, Kim JW, et al. Frameless fractionated Gamma Knife radiosurgery with ICON^{TM} for large metastatic brain tumors. *J Korean Med Sci.* (2019) 34:e57. doi: 10.3346/jkms.2019.34.e57

34. Kollová A, Liscák R, Novotný J Jr, Vladyka V, Simonová G, Janousková L. Gamma Knife surgery for benign meningioma. *J Neurosurg.* (2007) 107:325–36. doi: 10.3171/JNS-07/08/0325

35. Fu J, Zeng J, Huang M, Liang S, He Y, Xie L, et al. Primary vs. postoperative gamma knife radiosurgery for intracranial benign meningiomas: a matched cohort retrospective study. *BMC Cancer.* (2022) 22:206. doi: 10.1186/s12885-022-09321-w

frontiers | Frontiers in Oncology

TYPE Review
PUBLISHED 04 January 2023
DOI 10.3389/fonc.2022.910199

Check for updates

OPEN ACCESS

EDITED BY
Hailiang Tang,
Fudan University, China

REVIEWED BY
Carlos Eduardo Da Silva,
Federal University of Health Sciences of Porto Alegre, Brazil
Zeynep Erson-Omay,
Yale University, United States

*CORRESPONDENCE
Manish K. Aghi
manish.aghi@ucsf.edu

SPECIALTY SECTION
This article was submitted to Neuro-Oncology and Neurosurgical Oncology, a section of the journal Frontiers in Oncology

RECEIVED 01 April 2022
ACCEPTED 17 November 2022
PUBLISHED 04 January 2023

CITATION
Wang EJ, Haddad AF, Young JS, Morshed RA, Wu JPH, Salha DM, Butowski N and Aghi MK (2023) Recent advances in the molecular prognostication of meningiomas. *Front. Oncol.* 12:910199. doi: 10.3389/fonc.2022.910199

COPYRIGHT
© 2023 Wang, Haddad, Young, Morshed, Wu, Salha, Butowski and Aghi. This is an open-access article distributed under the terms of the Creative Commons Attribution License (CC BY). The use, distribution or reproduction in other forums is permitted, provided the original author(s) and the copyright owner(s) are credited and that the original publication in this journal is cited, in accordance with accepted academic practice. No use, distribution or reproduction is permitted which does not comply with these terms.

Recent advances in the molecular prognostication of meningiomas

Elaina J. Wang[1], Alexander F. Haddad[2], Jacob S. Young[2], Ramin A. Morshed[2], Joshua P. H. Wu[1], Diana M. Salha[2], Nicholas Butowski[2] and Manish K. Aghi[2]*

[1]Department of Neurological Surgery, Brown University, Rhode Island Hospital, Providence, RI, United States, [2]Department of Neurological Surgery, University of California, San Francisco, San Francisco, CA, United States

Meningiomas are the most common primary intracranial neoplasm. While traditionally viewed as benign, meningiomas are associated with significant patient morbidity, and certain meningioma subgroups display more aggressive and malignant behavior with higher rates of recurrence. Historically, the risk stratification of meningioma recurrence has been primarily associated with the World Health Organization histopathological grade and surgical extent of resection. However, a growing body of literature has highlighted the value of utilizing molecular characteristics to assess meningioma aggressiveness and recurrence risk. In this review, we discuss preclinical and clinical evidence surrounding the use of molecular classification schemes for meningioma prognostication. We also highlight how molecular data may inform meningioma treatment strategies and future directions.

KEYWORDS

meningioma, cytogenetics, genomics, epigenetics, methylation, atypical, anaplastic

Introduction

Meningiomas account for up to 40% of all primary central nervous system (CNS) tumors, making them the most common primary intracranial tumor (1). While they are thought to be derived from arachnoid cap cells due to cytological similarities (2, 3), the actual cell of origin for meningiomas remains unknown. It is possible they are derived from arachnoid barrier cells, a meningeal cell layer between pia and dura mater separating cerebrospinal fluid from underlying blood vessels, since meningiomas and arachnoid barrier cells have shared expression of prostaglandin D synthase (PGDS) (4, 5). Understanding the origin and natural history of meningiomas is important, since the incidence of meningiomas has been steadily rising, secondary to improvements in imaging resolution and more frequent use of various imaging modalities by providers (6, 7).

The 2021 World Health Organization (WHO) classification system describes 15 meningioma variants categorized into 3 grades based off of histopathological features and molecular biomarkers, with atypical and anaplastic criteria now applied to each of the subtypes (8). Eighty percent of meningiomas fall under the grade 1 category and can be treated with maximally safe resection with the goal of gross total resection (9). However, there remains a 5% 5-year recurrence rate for grade 1 meningiomas that increases to 40% for grade 2 meningiomas (3), and there is no established standard of care (SOC) for grade 2 and 3 meningiomas (10). While meningiomas have been traditionally risk stratified using the World Health Organization (WHO) histopathological grade and extent of surgical resection (8, 11), advances in molecular profiling have highlighted the benefits of utilizing genetic and epigenetic changes to further characterize meningioma aggressiveness and recurrence risk. The inter-observer variability inherent to histopathological diagnoses (12), coupled with advances in genetic and epigenetic technologies that have changed our understanding of meningioma tumor biology, lend support to the need for new molecular classifications for diagnosis and treatment. This review summarizes the use of genetic biomarkers and other forms of molecular data to inform meningioma prognostication and treatment strategies.

Key genetic changes in meningiomas

Germline mutations

Neurofibromatosis 2

Sporadic mutations in the NF2 gene on chromosome 22 are implicated in 40 to 60% of meningioma patients (3), while 50 to 75% of patients with germline mutations develop meningiomas (13) (Table 1). NF2 encodes for the tumor suppressor protein merlin (14), the loss of which is a well-studied driver mutation commonly implicated in high-grade meningiomas (15). NF2 loss-of-function mutations occur through a double-hit mechanism in meningiomas, either through a germline mutation and a second hit with a somatic mutation in syndromic cases, or with a somatic single nucleotide variation or insertion/deletion mutation and an overlapping chromosome 22 deletion event as commonly seen in sporadic cases (15). While 95% of NF2-associated meningiomas remain grade 1 (13), the presence of an NF2 mutation has been associated with increased tumor size and cell proliferation, and it has been suggested that NF2 loss may be the primary and sole initiator of meningioma tumorigenesis in both cranial and spinal meningiomas (16, 17). Two phase II clinical trials (Table 2) are currently underway to test FAK inhibitor GSK2256098 and AZD2014 in patients with NF2-mutated meningiomas and NF2 patients with symptomatic meningiomas respectively (19, 20).

Switch/sucrose non-fermentable

Germline mutations in two SWI/SNF chromatin remodeling complex subunits have also been implicated in meningioma tumorigenesis: SMARCB1 and SMARCE1 (21). Mutations in SMARCB1 have been linked to the development of multiple meningiomas, while SMARCE1 loss of function mutations have been implicated in patients with familial multiple spinal meningiomas with clear cell histology (22, 23).

Suppressor of fused homolog

Germline mutations in known tumor suppressor SUFU on chromosome 10 have long been associated with childhood medulloblastoma, with loss of SUFU leading to disruptions in the sonic hedgehog signaling pathway (24, 25). Germline disruptions in SUFU are also thought to predispose to development of additional cancers such as basal cell carcinoma, gonadal tumors, and meningiomas (26). Mutations in SUFU have been linked to development of isolated familial meningiomas and development of multiple meningiomas (27). In a case series of four related family members with three that had a history of meningiomas, a frameshift mutation in SUFU leading to a premature stop codon was isolated and is posited to be related to development of meningiomas (28).

Somatic mutations

Krueppel like factor 4

KLF4 is a transcriptional regulator known to maintain stemness and found to perform both oncogenic and tumor suppressor functions in a variety of cancers, including but not limited to bladder, esophageal, and gastric cancers (29–32). KLF loss of function has been implicated in colon cancer, while its overexpression has been shown to lead to decreased tumorigenicity of colon cancer cells *in vivo* (33, 34). In meningiomas, it is one of two genes found to be mutated in whole-exome sequencing of sixteen secretory meningiomas (35). KLF4 overexpression in anaplastic meningiomas has been associated with increased expression of tumor suppressor proteins such as p21, p53, and BAX, demonstrating a potential anti-tumor role in higher grade meningiomas (36). Recent *in vitro* data has also suggested that skull-based meningiomas with KLF K409Q mutations have a unique tumor phenotype that may respond to mammalian target of rapamycin (mTOR) inhibition with temsirolimus (37).

TABLE 1 Commonly identified germline and somatic mutations in meningiomas.

Gene	Form of Mutation	Clinical Associations
NF2	Loss of function	Sporadic mutations found in 40-60% of meningioma patients 50-75% of patients with germline mutations develop meningiomas Associated with increased tumor size and cell proliferation
SWI/SNF	Frameshift deletion	ARID1A mutation are independently prognostic of significantly increased hazard of death
KLF4	KLF4 K409 Q missense	The mutation results in upregulation of HIF-1a pathway Meningiomas with this mutation may respond to mTOR inhibition
TRAF7	WD40 domain mutation	TRAF7 mutations are found in nearly one-fourth of all meningiomas Meningiomas harboring TRAF7 mutations tend to be benign, chromosome-stable, and originating from medial skull base
TERT	TERT promoter chr5:1,295,228 (C228T) and chr5:1,295,250 (C250T) regional mutations	TERT promoter mutations are more commonly seen in higher grade meningiomas, particularly WHO grade 3 TERT promoter mutations are associated with significantly shorter time to progression, shorter overall survival, and higher chances of recurrence
AKT1	Gain of function	AKT1 mutations occur with higher frequency among skull base meningiomas and are associated with shorter time to recurrence
SMO/SUFU	Gain of function	Associated with higher recurrence rates among olfactory groove meningiomas Associated with larger tumor volume among anterior skull base meningiomas
PIK3CA	Gain of function	Mutations in PIK3CA are estimated to occur in 7% of non-NF2 mutated meningiomas PIK3CA mutations tend to be mutually exclusive with mutations in AKT1 and SMO
CDKN2A/B	Loss of function mutation	Mutations in CDKN2A/B are associated with shorter time recurrence CDKN2A/B alterations are now included as part of the classification criteria for WHO grade 3 meningiomas
POLR2A	Gain of function mutation	POLR2A-mutant tumors harbor distinct characteristics, including meningothelial histology, and a tendency to originate from tuberculum sellae region POLR2A mutations are found almost exclusively in WHO grade 1 meningiomas

Tumor necrosis factor receptor-associated factor 7

TRAF7 encodes for a ubiquitin E3 ligase and is the second most commonly mutated gene in meningiomas (38). It catalyzes a variety of ubiquitination reactions, including that of tumor suppressor p53, which has been shown to promote tumor progression in hepatocellular cancer while stabilizing p53's anti-tumoral effects in breast cancer (39, 40). TRAF7 and KLF4 mutations often co-occur in secretory meningiomas (35), with 40% of TRAF7-mutated meningiomas harboring a KLF4 mutation as well (41). TRAF7 is also one of four genes including KLF4, AKT1, and SMO, likely to be mutated in non-NF2 mutated meningiomas found at the skull base (38). TRAF7 mutations are also closely associated with hyperostosis and often found in spheno-orbital meningiomas (42).

Telomerase reverse transcriptase

TERT encodes for telomerase reverse transcriptase, a catalytic subunit of telomerase that promotes cell immortalization *via* telomere elongation (43). Mutations in the chr5:1,295,228 (C228T) and chr5:1,295,250 (C250T) regions of the TERT promoter have been associated with uncontrolled proliferation in several cancers (44–46) and recently in meningiomas that demonstrate histological malignant transformation (47). TERT promoter mutations are more commonly seen in higher grade meningiomas, with mutations found in 1.7%, 5.7% and 20% of 2007

TABLE 2 Phase 2 clinical trials targeting genetic mutations in meningiomas.

Clinical Trial	Duration	Phase	Target	Treatment	Outcome Measures	Reference
NCT02523014	2015-2024	2	SMO, FAK, AKT, CDK	Vismodegib, GSK2256098, Capivasertib, Abemaciclib (n=124)	PFS, CR or PR	Brastianos et al. (16)
NCT02831257	2016-2020	2	mTOR	Vistusertib (n=18)	Radiographic response	Plotkin et al. (17)
NCT03071874	2017-2021	2	mTOR	Vistusertib (n=28)	PFS	Plotkin et al. (18)

PFS, Progression-free survival.
CR, Complete response
PR, Partial response.

WHO classification grade 1, 2, and 3 meningiomas respectively (18). Clinically, mutations in the TERT promoter region have been associated with significantly shorter time to progression, shorter overall survival, and higher chances of recurrence (18, 48, 49). TERT promoter mutations are now included in the 2021 WHO classification of grade 3 meningiomas (8).

AKT1

AKT1 encodes for AKT1 kinase, which regulates cell growth and survival through a variety of pathways (50). AKT1 mutations have been shown to lead to PI3K/AKT pathway activation (51). In a study that applied exome sequencing to 300 meningiomas, mutations in AKT1 were found in 13% of tumors (38). Among skull base meningiomas, AKT1 mutations were found at a higher frequency of 30% and was shown to be associated with shorter time to recurrence (52). In the same study, mutations in AKT1 were found to activate mTOR and ERK1/2 signaling pathways (52). AKT inhibitors have been shown to downregulate the expression of osteoglycin (OGN), an oncogene implicated in meningioma growth, *in vitro* and to stabilize meningotheliomatous meningioma growth in the lung of a patient with multiple intra- and extra-cranial tumors (53, 54).

Smoothened

SMO is a G-protein coupled receptor involved in the Hedgehog (Hh) signaling pathway (55). Mutations in SMO have been detected in 3 to 6% of all meningiomas, 28% of olfactory groove meningiomas, and 11% of anterior skull base meningiomas (56–59). Compared to meningiomas with AKT1 mutations, SMO-mutated olfactory groove meningiomas had higher recurrence rates, and when compared to AKT1-mutated or wild type meningiomas, SMO-mutated anterior skull base meningiomas had significantly larger tumor volume (58, 59). Given the targetable nature of SMO mutations, a clinical trial is currently underway to test the SMO inhibitor vismodegib in SMO-mutant meningiomas (19).

PIK3CA

PIK3CA encodes for a catalytic subunit of phosphatidylinositol 3-kinase (PI3K) that has been implicated in several human cancers (60). Mutations in PIK3CA are estimated to occur in 7% of non-NF2 mutated meningiomas and tend to be mutually exclusive with aforementioned mutations in AKT1 and SMO (57). In a study assessing 55 meningioma patient samples, PIK3CA mutations were found in two patients who had atypical and anaplastic meningiomas respectively (61). PI3K alterations have also been seen to co-occur with TRAF7 mutations, with these tumors demonstrating lower levels of chromosomal instability and clinical tendencies to arise in the skull base (57). Targeting PIK3CA has long been an area of therapeutic interest given the role that increased protein expression in the PI3K/AKT pathway plays in more aggressive malignant meningiomas (62). Two phase II clinical trials are currently underway targeting the PI3K/AKT pathway with vistusertib and capivasertib respectively (19, 63).

CDKN2A/B

The cyclin-dependent kinase inhibitor A and B (CDKN2A/B) gene encodes for three tumor suppressor proteins, the loss of which has been demonstrated to contribute to spontaneous development of melanomas in CDKN2A/B knockout mice (64). In addition to NF2 inactivation, loss of CDKN2A/B contributes to meningioma progression and has been associated with shorter time to recurrence in mice (65). Among a series of 17 recurrent and 13 non-recurrent meningiomas, CDKN2A/B alterations were found only in recurrent meningiomas, and a novel SNV (p.Ala148Thr) was identified in 5 recurrent meningiomas, further supporting the association between CDKN2A/B alterations and meningioma recurrence (66). Along with TERT promoter mutations, CDKN2AB alterations are now included in categorizing grade III meningiomas (8).

SUFU

Changes in SUFU lead to dysregulation of the hedgehog (Hh) signaling pathway, the activation of which has been shown to play a critical role in meningioma growth and development, with 72% of Hh signaling pathway genes being differentially expressed in meningiomas compared to normal tissue (67). Across 850 meningiomas that underwent genomic analyses, SUFU mutations were identified in 23 patients and seen to co-occur with PTEN and ARID1A mutations (68).

POL2RA

POLR2A, the catalytic subunit of RNA polymerase II, has been shown to harbor mutations that characterize a distinct subset of meningiomas that lack the aforementioned mutations commonly seen in other meningiomas (69). Meningiomas with mutations in POLR2A were exclusively benign with distinct meningothelial histology and were more likely to arise from the tuberculum sellae (69).

Cytogenetic alterations

There are several copy number variations (CNVs) associated with meningioma pathology (Table 3). The initial loss of chromosome 22q in meningioma tumorigenesis has long been established as an early chromosomal event linked to both NF2 mutated and non-NF2 mutated tumors (3, 70). It is estimated to be found in 60 to 70% of all meningiomas, with significantly increased odds among older patients (71, 72). While the loss of 22q occurs in many patients with established neurofibromatosis

TABLE 3 Commonly identified cytogenetic alterations in meningiomas.

Chromosome	Type of alteration	Implication for prognostication
22q	Deletion	Estimated to be found in 60-70% of all meningiomas Both biallelic loss and macro-mutations in 22q are more commonly detected in fibroelastic than in meningothelial histological subtypes
1p	Deletion	Second most common chromosomal event after loss of 22q Loss of 1p has been linked to higher rates of tumor recurrence and progression
14q	Deletion	Third most common cytogenetic change detected among meningiomas Loss at chromosomal arm 14q has also been correlated with increased risk of tumor recurrence
6q, 10q, 17q, 18q, 20q	Deletion	More commonly found in high-grade meningiomas when compared to low-grade meningiomas

type 2 syndrome, somatic mutations have also been discovered in around 47% of sporadic meningiomas (73, 74).

In the 40% of meningiomas that do not have NF2 inactivation, alternative explanations are sought to explain meningioma tumorigenesis (75). Losses in chromosomal locations 1p and 14q have been identified in higher grade meningiomas (71). Specifically, loss of 1p is the second most common chromosomal event after loss of 22q, and it has been linked to higher rates of tumor recurrence and progression (76). The frequency of mutations in 1p increases roughly from 30% in grade 1 (2000 WHO classification) tumors to 80% and 100% of grade 2 and 3 tumors respectively (76). Losses in 14q are the third most common cytogenetic change detected among meningiomas, with similar frequencies among WHO grade 1 through 3 tumors as 1p losses (76). Similar to 1p losses, a loss at chromosomal arm 14q has also been correlated to increased risk of tumor recurrence (77).

The concurrent loss of 1p and 3p has also been detected in a small subset of meningiomas without detectable losses in chromosome 22. These losses are hypothesized to contribute to meningioma growth, as changes in chromosome 3 have been linked to other cancers such as breast and small cell lung cancer (78, 79). Other chromosomes such as 6 have been found to harbor genes such as *HIST1H1C* and *CTGF*, changes in which are associated with meningioma recurrence (80). Loss of heterozygosity at certain sites of chromosome 10 have also been predictive of recurrence and worse prognosis in meningioma patients (81).

Greater number of chromosomal anomalies within a tumor has also been associated with higher tumor grade. For instance, in Pfisterer et al., the distribution of chromosomal 1, 14, and 22 anomalies was examined among 77 meningioma cases (82). The loss of 1p, 14q, or 22q alone was only found in grade I meningiomas, while 23% of meningiomas with both 1p and 14q deletions were grade II meningiomas, and 80% of meningiomas with losses in all three chromosomes were grade III (82). In the literature, losses of 1p were found in 75% of high-grade versus 23% of low-grade tumors, 14q losses in 67% of high-grade versus 31% of benign tumors, and chromosomal 22 deletions in 47% of grade II versus 19% of grade I tumors (77, 83). Bi et al. examined the genomes of 39 high-grade meningiomas and found that high-grade tumors were more likely to have loss of chromosome 22 and 1p than low-grade meningiomas, with high-grade meningiomas also commonly exhibiting losses of 1p, 6q, 10q, 18q and gains of 17q and 20q (84).

Radiation-induced meningiomas

Meningiomas are one of the most common tumors to arise after radiotherapy, particularly in the pediatric population (85, 86). Radiation-induced meningiomas have a tendency to behave more aggressively than sporadic meningiomas and often arise two decades after radiation treatment (87, 88). Unlike sporadic meningiomas that commonly harbor NF2 mutations, the same mutations are not seen in radiation-induced meningiomas (87). Instead, loss of chromosomal segment 1p was found to play a larger role in development of radiation-induced meningiomas, followed by changes in chromosomal locations 9p, 19q, and 22q (87). Among 16 patients with radiation-induced meningiomas, cytogenetic analyses revealed changes in chromosome 1p in 89% of cases and changes in chromosome 6 in 67% of cases (89). Further work exploring the genetics underlying the aggressive behavior of radiation-induced meningiomas may shed light on how to best distinguish benign from malignant sporadic meningiomas.

Methylation profiling

Epigenetic changes have been found to be useful biomarkers of cancer diagnosis and predictors of recurrence and treatment response. For instance, alterations in hypermethylation of O6-methylguanine DNA methyltransferase (MGMT) in glioblastoma can be useful indicators of chemotherapy response (90). In meningiomas, the absence of trimethylation of H3K27 (H3K27me3) has been shown to be associated with more aggressive growth of tumor, as well as NF2 and SUFU mutations, allowing us to further stratify grade 1 and 2 tumors according to the 2016 WHO classification system (91).

In another study examining 1268 meningiomas, the loss of H3K27me3 was found to be a significant predictor of negative prognosis and recurrence, further underlying the importance of methylation profiling in categorizing meningiomas (92).

Methylation profiling has taken on a similar role in identifying and distinguishing meningiomas. When compared to bulk RNA-sequencing, DNA methylation profiling was found to more accurately identify meningioma metastases to the liver in one case report (93). While both bulk RNA-sequencing and DNA methylation profiling could separate the liver metastasis from the primary intracranial meningioma, DNA methylation could better establish the diagnosis of the liver metastasis as a meningioma while hepatocyte-specific gene expression confounded similar findings using bulk RNA-sequencing (93). However, it is important to note that these findings were in the context of one case report, and the improved accuracy of DNA methylation profiling in this instance cannot be generalized. In another study, application of DNA methylation profiling to more than 3000 meningiomas identified an epigenetically distinct cluster of 31 tumors, the majority of which were histopathologically diagnosed as clear cell meningiomas (94). Several studies that have integrated methylation studies with other techniques to classify meningiomas will be discussed in the upcoming section.

Molecular profiling for meningioma stratification

Advances in computational molecular profiling techniques have allowed for new classifications of meningiomas that account for findings at the DNA level rather than histopathological analysis (95). A variety of techniques including sequencing, methylation profiles, and copy number variation analysis have also been used to generate scores that may better predict prognosis in meningioma patients when compared to standard WHO grading systems.

Genomic sequencing analyses have also been utilized to further classify meningiomas. Patel et al. applied bulk RNA-sequencing and whole-exome sequencing to 160 tumors from 140 meningioma patients to identify 3 classes of meningiomas that were found to predict recurrence more accurately than the standard 2016 WHO grading system (96). Among the three groups (designated type A, B, and C), type C had the highest MIB1 proliferative index, the highest proportion of men, and the shortest recurrence-free survival despite containing primarily WHO grade 1 tumors (96). Type C tumors were also found to have increased expression of FOXM1, leading to loss of the repressive DREAM complex (96). Work by Vasudevan et al. similarly revealed two distinct groups of 280 meningiomas, with aggressive tumors marked by increased expression of FOXM1 (97). FOXM1 has also been implicated as one of three genes upregulated in primary atypical meningiomas, which have also been found to demonstrate NF2 loss, genomic instability, mutations in SMARCB1, and a hypermethylated phenotype (98).

Genomic analyses applied to aggressive meningiomas have also identified 3 distinct groups of meningiomas organized by NF2 status: NF2-mutant, NF2-agnostic, and NF2-wild type (68). NF2-mutant meningiomas were more often associated with men and mutations in CDKN2A/B while NF2-agnostic meningiomas were often associated with TERT and TP53 mutations (68). The third group of NF2-wild type tumors predominantly lacked NF2 mutations and were split further into 3 subgroups: those containing chromatin regulator mutations in BAP1 or PBRM1, skull-based meningiomas with AKT1, PIK3CA, and SMO mutations, and meningiomas with a mix of mutations that shared no discernable pattern (68). Genomic analysis of 300 meningiomas by Clark et al. also revealed benign tumors at the skull base express mutations in TRAF7, KLF4, AKT1, and SMO while higher grade tumors often contained NF2 mutations and were found at the cerebral and cerebellar hemispheres (38).

Genome-wide DNA methylation profiles on 497 meningiomas revealed 6 distinct methylation classes that were found to predict meningioma progression more accurately when compared to 2016 WHO grade 1 tumors and meningioma recurrence more accurately when compared to 2016 WHO grade 2 tumors (99). Similarly, Nassiri et al. applied copy number variation analysis, somatic point mutations, methylation profiles, and messenger RNA abundance to 121 meningioma patient samples to create four molecular groups of meningiomas: immunogenic, benign NF2 wild-type, hypermetabolic, and proliferative (100). The four groups were able to predict patient outcomes more accurately when compared to the existing 2016 WHO classification system and to classification systems based off DNA methylation (100). Methylation analysis by Olar et al. revealed two distinct groups with favorable and unfavorable prognoses respectively (101). Tumors in the unfavorable prognosis group were found to have a higher proportion of copy number aberrations than those in the favorable prognosis group, including losses of 1p and 14q (101).

The integration of histologic findings with genetic profiling including methylation profiling and copy number analysis has further helped improve the precision of meningioma stratification. Using data across 3031 meningiomas, Maas et al. developed an integrated score that predicted risk of meningioma progression more accurately than existing 2016 WHO grading by classifying tumors into low, intermediate, and high-risk groups based off of histology, methylation classes, and CNV analysis (102). While CNV- and methylation-based subtypes independently demonstrated increased prediction accuracy compared to the existing 2016 WHO grading system, the integrated score resulted in further improved accuracy,

emphasizing the value of both histology and molecular risk stratification in meningiomas (102).

Integrated use of DNA methylation, RNA sequencing, and cytogenetic profiling by Patel et al. on 110 grade 1 and II meningiomas according to the 2016 WHO classification system revealed two benign and one malignant tumor group closely resembling the previously established type A, B, and C classifications (103). Methylation analysis further distinguished these groups as tumors with balanced methylation (Meth 1), hypomethylation (Meth 2), and hypermethylation (Meth 3) (103). When comparing these groups to those established by Olar et al., Meth 2 and 3 tumors were conferred a favorable and unfavorable prognosis respectively, corresponding with clinical outcomes (101, 103). Further analysis revealed 75% of tumors classified *via* methylation analysis corresponded to a tumor group established by either transcriptional classification (type A, B, C) or cytogenetic classification (no loss, 22q loss, 1p/22q loss) (103).

In a similar vein, Driver et al. created an integrated scoring system by combining chromosomal losses, CDKN2A losses, and mitotic count to separate meningiomas into three separate groups (104). The subsequent grading system reclassified 32% of meningiomas to a higher or low grade when compared to their original WHO grade and was able to more reliably predict risk of recurrence compared to the existing 2007 and 2016 WHO grading system (104). Key molecular alterations associated with high grade included higher mitotic count, 1p del, 3p del, 4p/q del, 6 p/q del, 10 p/q del, 14q del, 18 p/q del, 19 p/q del, and del CDKN2A/B (104). While both Driver and Maas et al. emphasized 22q, 1p, 6q, and 14q loss as the most frequent deletions encountered, Driver et al. also included 3p, 4p/q, 10p/q, 18p/q, 19p/q alterations and mitotic count instead of methylation families in their scoring system (102, 104).

Most recently, DNA methylation profiling on 565 meningiomas was performed and integrated with single cell, proteomic, and other genetic, transcriptomic, biochemical approaches to categorize meningiomas into three distinct clinical groups: merlin-intact meningiomas, immune-enriched meningiomas, and hypermitotic meningiomas (105). Merlin-intact meningiomas were characterized by gain of function in chromosome 5, loss of function in chromosome 6p, and intact NF2 expression, with the best overall survival among the three groups (105). Immune-enriched meningiomas exhibited gain of function in 6p and loss of function in 22q, and notably, lymphocytes in these tumor microenvironments were prone to exhibiting exhaustion markers, potentially explaining why immune checkpoint blockade has not had the same effect on survival in meningiomas as it has in other cancers (106). Hypermitotic meningiomas had the worst overall survival of all three groups and were distinguished by upregulation of FOXM1 expression, which was found to regulate DNA damage response, potentially increasing hypermitotic meningioma resistance to cytotoxic therapy (105).

Future directions

While the information afforded by integrated scoring systems is an essential first step to guiding meningioma management, many questions remain to be answered particularly regarding adjuvant therapies and post-operative imaging follow-up. For instance, while most studies do not include Simpson grade or gross versus subtotal resection as part of their grading criteria, these are essential factors that guide decisions regarding post-operative management and consideration of radiotherapy. It is important to determine whether there are specific genetic changes that make a tumor amenable to systemic therapies such as upfront radiation versus observation. Since new classification schemes including the recent changes to the WHO grading system may alter how aggressively a tumor is treated, it is also important to determine whether new classification systems are changing outcomes such as recurrence rates.

In addition, with several novel integrated systems of meningioma classification, it will be crucial to compare the accuracy of different systems through further investigation, including cross study group comparisons. Another potential factor limiting the widespread use of novel integrated classification systems is the high cost and limited availability of some of the technologies utilized, including DNA methylation and next generation sequencing. When applying these technologies to categorize meningiomas, it is also important to take note of intratumoral heterogeneity among meningiomas, with spatially distinct areas of the same tumor exhibiting distinct gene expression patterns (107). Moving forward, it is important to determine how the new groupings afforded by integrated scoring systems may change future management of meningiomas.

Conclusions

Meningiomas are the most common primary intracranial neoplasm and among the most genetically well-studied intracranial tumors. While pre-existing classification schemes by the WHO have traditionally been used to predict meningioma prognosis and risk of recurrence, advances in molecular profiling have allowed for development of several new classification schemes utilizing DNA-level rather than histopathological findings. It is critical to continue applying new sequencing and computational technologies to better predict meningioma behavior in the clinical setting.

Author contributions

Conceptualization: MA, NB, RM, JY, AH, EW; Writing - Original draft: EW; Writing - revisions: EW, JW; Visualization: AH, EW, DS; Review & editing: MA, NB, RM, JY, AH, JW;

Supervision: MA, NB. All authors contributed to the article and approved the submitted version.

Conflict of interest

The authors declare that the research was conducted in the absence of any commercial or financial relationships that could be construed as a potential conflict of interest.

Publisher's note

All claims expressed in this article are solely those of the authors and do not necessarily represent those of their affiliated organizations, or those of the publisher, the editors and the reviewers. Any product that may be evaluated in this article, or claim that may be made by its manufacturer, is not guaranteed or endorsed by the publisher.

References

1. Buerki RA, Horbinski CM, Kruser T, Horowitz PM, James CD, Lukas RV. An overview of meningiomas. *Future Oncol* (2018) 14(21):2161–77. doi: 10.2217/fon-2018-0006

2. SHIBUYA M. Pathology and molecular genetics of meningioma: Recent advances. *Neurol Med Chir (Tokyo).* (2015) 55(1):14–27. doi: 10.2176/nmc.ra.2014-0233

3. Riemenschneider MJ, Perry A, Reifenberger G. Histological classification and molecular genetics of meningiomas. *Lancet Neurol* (2006) 5(12):1045–54. doi: 10.1016/S1474-4422(06)70625-1

4. Yamashima T, Sakuda K, Tohma Y, Yamashita J, Oda H, Irikura D, et al. Prostaglandin d synthase (β-trace) in human arachnoid and meningioma cells: Roles as a cell marker or in cerebrospinal fluid absorption, tumorigenesis, and calcification process. *J Neurosci* (1997) 17(7):2376–82. doi: 10.1523/JNEUROSCI.17-07-02376.1997

5. Yasuda K, Cline C, Vogel P, Onciu M, Fatima S, Sorrentino BP, et al. Drug transporters on arachnoid barrier cells contribute to the blood–cerebrospinal fluid barrier. *Drug Metab Dispos* (2013) 41(4):923–31. doi: 10.1124/dmd.112.050344

6. Hoffman S, Propp JM, McCarthy BJ. Temporal trends in incidence of primary brain tumors in the united states, 1985-1999. *Neuro-Oncol.* (2006) 8 (1):27–37. doi: 10.1215/S1522851705000323

7. Campbell BA, Jhamb A, Maguire JA, Toyota B, Ma R. Meningiomas in 2009: Controversies and future challenges. *Am J Clin Oncol* (2009) 32(1):73–85. doi: 10.1097/COC.0b013e31816fc920

8. Louis DN, Perry A, Wesseling P, Brat DJ, Cree IA, Figarella-Branger D, et al. The 2021 WHO classification of tumors of the central nervous system: a summary. *Neuro-Oncol.* (2021) 23(8):1231–51. doi: 10.1093/neuonc/noab106

9. Brastianos PK, Horowitz PM, Santagata S, Jones RT, McKenna A, Getz G, et al. Genomic sequencing of meningiomas identifies oncogenic SMO and AKT1 mutations. *Nat Genet* (2013) 45(3):285–9. doi: 10.1038/ng.2526

10. Wang YC, Chuang CC, Wei KC, Chang CN, Lee ST, Wu CT, et al. Long term surgical outcome and prognostic factors of atypical and malignant meningiomas. *Sci Rep* (2016) 6:35743. doi: 10.1038/srep35743

11. Simpson D. THE RECURRENCE OF INTRACRANIAL MENINGIOMAS AFTER SURGICAL TREATMENT. *J Neurol Neurosurg Psychiatry* (1957) 20 (1):22–39. doi: 10.1136/jnnp.20.1.22

12. van den Bent MJ. Interobserver variation of the histopathological diagnosis in clinical trials on glioma: a clinician's perspective. *Acta Neuropathol (Berl).* (2010) 120(3):297–304. doi: 10.1007/s00401-010-0725-7

13. Goutagny S, Bah AB, Henin D, Parfait B, Grayeli AB, Sterkers O, et al. Long-term follow-up of 287 meningiomas in neurofibromatosis type 2 patients: clinical, radiological, and molecular features. *Neuro-Oncol* (2012) 14(8):1090–6. doi: 10.1093/neuonc/nos129

14. Xu Hm, Gutmann DH. Merlin differentially associates with the microtubule and actin cytoskeleton. *J Neurosci Res* (1998) 51(3):403–15. doi: 10.1002/(SICI)1097-4547(19980201)51:3<403::AID-JNR13>3.0.CO;2-7

15. Lee S, Karas PJ, Hadley CC, Bayley V JC, Khan AB, Jalali A, et al. The role of Merlin/NF2 loss in meningioma biology. *Cancers* (2019) 11(11):1633. doi: 10.3390/cancers11111633

16. Loewenstern J, Rutland J, Gill C, Arib H, Pain M, Umphlett M, et al. Comparative genomic analysis of driver mutations in matched primary and recurrent meningiomas. *Oncotarget.* (2019) 10(37):3506–17. doi: 10.18632/oncotarget.26941

17. Pemov A, Dewan R, Hansen NF, Chandrasekharappa SC, Ray-Chaudhury A, Jones K, et al. Comparative clinical and genomic analysis of neurofibromatosis type 2-associated cranial and spinal meningiomas. *Sci Rep* (2020) 10(1):12563. doi: 10.1038/s41598-020-69074-z

18. Sahm F, Schrimpf D, Olar A, Koelsche C, Reuss D, Bissel J, et al. TERT promoter mutations and risk of recurrence in meningioma. *JNCI J Natl Cancer Inst* (2015) 108(5):djv377. doi: 10.1093/jnci/djv377

19. Alliance for Clinical Trials in Oncology. *Phase II trial of SMO/ AKT/ NF2/ CDK inhibitors in progressive meningiomas with SMO/ AKT/ NF2/CDK pathway mutations* (2021). Available at: https://clinicaltrials.gov/ct2/show/NCT02523014.

20. PhD SRP MD. *A single arm phase 2 study of the dual mTORC1/mTORC2 inhibitor AZD2014 provided on an intermittent schedule for neurofibromatosis 2 patients with progressive or symptomatic meningiomas* (2020). Available at: https://clinicaltrials.gov/ct2/show/NCT02831257.

21. Smith MJ. Germline and somatic mutations in meningiomas. *Cancer Genet* (2015) 208(4):107–14. doi: 10.1016/j.cancergen.2015.02.003

22. Christiaans I, Kenter SB, Brink HC, Os TAMv, Baas F, Munckhof Pvd, et al. Germline SMARCB1 mutation and somatic NF2 mutations in familial multiple meningiomas. *J Med Genet* (2011) 48(2):93–7. doi: 10.1136/jmg.2010.082420

23. Smith MJ, O'Sullivan J, Bhaskar SS, Hadfield KD, Poke G, Caird J, et al. Loss-of-function mutations in SMARCE1 cause an inherited disorder of multiple spinal meningiomas. *Nat Genet* (2013) 45(3):295–8. doi: 10.1038/ng.2552

24. Guerrini-Rousseau L, Dufour C, Varlet P, Masliah-Planchon J, Bourdeaut F, Guillaud-Bataille M, et al. Germline SUFU mutation carriers and medulloblastoma: clinical characteristics, cancer risk, and prognosis. *Neuro-Oncol* (2018) 20(8):1122–32. doi: 10.1093/neuonc/nox228

25. Taylor MD, Liu L, Raffel C, Hui Cc, Mainprize TG, Zhang X, et al. Mutations in SUFU predispose to medulloblastoma. *Nat Genet* (2002) 31 (3):306–10. doi: 10.1038/ng916

26. Guerrini-Rousseau L, Masliah-Planchon J, Waszak SM, Alhopuro P, Benusiglio PR, Bourdeaut F, et al. Cancer risk and tumour spectrum in 172 patients with a germline SUFU pathogenic variation: a collaborative study of the SIOPE host genome working group. *J Med Genet* (2022) 59(11):1123–32. doi: 10.1136/jmedgenet-2021-108385

27. Aavikko M, Li SP, Saarinen S, Alhopuro P, Kaasinen E, Morgunova E, et al. Loss of SUFU function in familial multiple meningioma. *Am J Hum Genet* (2012) 91(3):520–6. doi: 10.1016/j.ajhg.2012.07.015

28. Askaner G, Lei U, Bertelsen B, Venzo A, Wadt K. Novel SUFU frameshift variant leading to meningioma in three generations in a family with gorlin syndrome. *Case Rep Genet* (2019) 2019:e9650184. doi: 10.1155/2019/9650184

29. Ghaleb AM, Yang VW. Krüppel-like factor 4 (KLF4): What we currently know. *Gene.* (2017) 611:27–37. doi: 10.1016/j.gene.2017.02.025

30. Ohnishi S, Ohnami S, Laub F, Aoki K, Suzuki K, Kanai Y, et al. Downregulation and growth inhibitory effect of epithelial-type krüppel-like transcription factor KLF4, but not KLF5, in bladder cancer. *Biochem Biophys Res Commun* (2003) 308(2):251–6. doi: 10.1016/S0006-291X(03)01356-1

31. Wei D, Gong W, Kanai M, Schlunk C, Wang L, Yao JC, et al. Drastic down-regulation of krüppel-like factor 4 expression is critical in human gastric cancer development and progression. *Cancer Res* (2005) 65(7):2746–54. doi: 10.1158/0008-5472.CAN-04-3619

32. Luo A, Kong J, Hu G, Liew CC, Xiong M, Wang X, et al. Discovery of Ca2+-relevant and differentiation-associated genes downregulated in esophageal squamous cell carcinoma using cDNA microarray. *Oncogene.* (2004) 23(6):1291–9. doi: 10.1038/sj.onc.1207218

33. Dang DT, Chen X, Feng J, Torbenson M, Dang LH, Yang VW. Overexpression of krüppel-like factor 4 in the human colon cancer cell line RKO leads to reduced tumorigenecity. *Oncogene* (2003) 22(22):3424–30. doi: 10.1038/sj.onc.1206413

34. Zhao W, Hisamuddin IM, Nandan MO, Babbin BA, Lamb NE, Yang VW. Identification of krüppel-like factor 4 as a potential tumor suppressor gene in colorectal cancer. *Oncogene* (2004) 23(2):395–402. doi: 10.1038/sj.onc.1207067

35. Reuss DE, Piro RM, Jones DTW, Simon M, Ketter R, Kool M, et al. Secretory meningiomas are defined by combined KLF4 K409Q and TRAF7 mutations. *Acta Neuropathol (Berl)* (2013) 125(3):351–8. doi: 10.1007/s00401-013-1093-x

36. Tang H, Zhu H, Wang X, Hua L, Li J, Xie Q, et al. KLF4 is a tumor suppressor in anaplastic meningioma stem-like cells and human meningiomas. *J Mol Cell Biol* (2017) 9(4):315–24. doi: 10.1093/jmcb/mjx023

37. von Spreckelsen N, Waldt N, Poetschke R, Kesseler C, Dohmen H, Jiao HK, et al. KLF4K409Q–mutated meningiomas show enhanced hypoxia signaling and respond to mTORC1 inhibitor treatment. *Acta Neuropathol Commun* (2020) 8 (1):41. doi: 10.1186/s40478-020-00912-x

38. Clark VE, Erson-Omay EZ, Serin A, Yin J, Cotney J, Özduman K, et al. Genomic analysis of non-NF2 meningiomas reveals mutations in TRAF7, KLF4, AKT1, and SMO. *Sci [Internet]* (2013) 7(1):1–8. doi: 10.1126/science.1233009

39. Zhang Q, Zhang X, Dong W. TRAF7 contributes to tumor progression by promoting ubiquitin-proteasome mediated degradation of P53 in hepatocellular carcinoma. *Cell Death Discov* (2021) 7(1):1–8. doi: 10.1038/s41420-021-00749-w

40. Wang L, Wang L, Zhang S, Qu G, Zhang D, Li S, et al. Downregulation of ubiquitin E3 ligase TNF receptor-associated factor 7 leads to stabilization of p53 in breast cancer. *Oncol Rep* (2013) 29(1):283–7. doi: 10.3892/or.2012.2121

41. Najm P, Zhao P, Steklov M, Sewduth RN, Baietti MF, Pandolfi S, et al. Loss-of-Function mutations in TRAF7 and KLF4 cooperatively activate RAS-like GTPase signaling and promote meningioma development. *Cancer Res* (2021) 81 (16):4218–29. doi: 10.1158/0008-5472.CAN-20-3669

42. Jin L, Youngblood MW, Gupte TP, Vetsa S, Nadar A, Barak T, et al. Type of bony involvement predicts genomic subgroup in sphenoid wing meningiomas. *J Neurooncol.* (2021) 154(2):237–46. doi: 10.1007/s11060-021-03819-2

43. Dratwa M, Wysoczańska B, Łacina P, Kubik T, Bogunia-Kubik K. TERT–regulation and roles in cancer formation. *Front Immunol* (2020) 11:2930. doi: 10.3389/fimmu.2020.589929

44. Huang FW, Hodis E, Xu MJ, Kryukov GV, Chin L, Garraway LA. Highly recurrent TERT promoter mutations in human melanoma. *Science.* (2013) 339 (6122):957–9. doi: 10.1126/science.1229259

45. Horn S, Figl A, Rachakonda PS, Fischer C, Sucker A, Gast A, et al. TERT promoter mutations in familial and sporadic melanoma. *Sci [Internet]* (2013) 5 (6):1515–25. doi: 10.1126/science.1230062

46. Killela PJ, Pirozzi CJ, Healy P, Reitman ZJ, Lipp E, Rasheed BA, et al. Mutations in IDH1, IDH2, and in the TERT promoter define clinically distinct subgroups of adult malignant gliomas. *Oncotarget* (2014) 5(6):1515–25. doi: 10.18632/oncotarget.1765

47. Goutagny StéChecktae, Nault J, Mallet M, Henin D, Rossi J, Kalamarides M. High incidence of activating TERT promoter mutations in meningiomas undergoing malignant progression. *Brain Pathol* (2014) 108(5):184–9. doi: 10.1111/bpa.12110

48. Spiegl-Kreinecker S, Lötsch D, Neumayer K, Kastler L, Gojo J, Pirker C, et al. TERT promoter mutations are associated with poor prognosis and cell immortalization in meningioma. *Neuro-Oncol* (2018) 20(12):1584–93. doi: 10.1093/neuonc/noy104

49. Mirian C, Duun-Henriksen AK, Juratli T, Sahm F, Spiegl-Kreinecker S, Peyre M, et al. Poor prognosis associated with TERT gene alterations in meningioma is independent of the WHO classification: an individual patient data meta-analysis. *J Neurol Neurosurg Psychiatry* (2020) 91(4):378–87. doi: 10.1136/jnnp-2019-322257

50. Duggal S, Jailkhani N, Midha MK, Agrawal N, Rao KVS, Kumar A. Defining the Akt1 interactome and its role in regulating the cell cycle. *Sci Rep* (2018) 8 (1):1303. doi: 10.1038/s41598-018-19689-0

51. Carpten JD, Faber AL, Horn C, Donoho GP, Briggs SL, Robbins CM, et al. A transforming mutation in the pleckstrin homology domain of AKT1 in cancer. *Nature.* (2007) 448(7152):439–44. doi: 10.1038/nature05933

52. Yesilöz Ü, Kirches E, Hartmann C, Scholz J, Kropf S, Sahm F, et al. Frequent AKT1E17K mutations in skull base meningiomas are associated with mTOR and ERK1/2 activation and reduced time to tumor recurrence. *Neuro-Oncol.* (2017) 19 (8):1088–96. doi: 10.1093/neuonc/nox018

53. Weller M, Roth P, Sahm F, Burghardt I, Schuknecht B, Rushing EJ, et al. Durable control of metastatic AKT1-mutant WHO grade 1 meningothelial meningioma by the AKT inhibitor, AZD5363. *JNCI J Natl Cancer Inst* (2017) 109(3):djw320. doi: 10.1093/jnci/djw320

54. Mei Y, Du Z, Hu C, Greenwald NF, Abedalthagafi M, Agar NYR, et al. Osteoglycin promotes meningioma development through downregulation of NF2 and activation of mTOR signaling. *Cell Commun Signal* (2017) 15(1):34. doi: 10.1186/s12964-017-0189-7

55. Ruiz-Gómez A, Molnar C, Holguín H, Mayor F, de Celis JF. The cell biology of smo signalling and its relationships with GPCRs. *Biochim Biophys Acta BBA - Biomembr.* (2007) 1768(4):901–12. doi: 10.1016/j.bbamem.2006.09.020

56. Yuzawa S, Nishihara H, Tanaka S. Genetic landscape of meningioma. *Brain Tumor Pathol* (2016) 33(4):237–47. doi: 10.1007/s10014-016-0271-7

57. Abedalthagafi M, Bi WL, Aizer AA, Merrill PH, Brewster R, Agarwalla PK, et al. Oncogenic PI3K mutations are as common as AKT1 and SMO mutations in meningioma. *Neuro-Oncol* (2016) 18(5):649–55. doi: 10.1093/neuonc/nov316

58. Boetto J, Bielle F, Sanson M, Peyre M, Kalamarides M. SMO mutation status defines a distinct and frequent molecular subgroup in olfactory groove meningiomas. *Neuro-Oncol* (2017) 19(3):345–51. doi: 10.1093/neuonc/now276

59. Strickland MR, Gill CM, Nayyar N, D'Andrea MR, Thiede C, Juratli TA, et al. Targeted sequencing of SMO and AKT1 in anterior skull base meningiomas. *J Neurosurg* (2017) 127(2):438–44. doi: 10.3171/2016.8.JNS161076

60. Karakas B, Bachman KE, Park BH. Mutation of the PIK3CA oncogene in human cancers. *Br J Cancer.* (2006) 94(4):455–9. doi: 10.1038/sj.bjc.6602970

61. Bujko M, Kober P, Tysarowski A, Matyja E, Mandat T, Bonicki W, et al. EGFR, PIK3CA, KRAS and BRAF mutations in meningiomas. *Oncol Lett* (2014) 7 (6):2019–22. doi: 10.3892/ol.2014.2042

62. Mawrin C, Sasse T, Kirches E, Kropf S, Schneider T, Grimm C, et al. Different activation of mitogen-activated protein kinase and akt signaling is associated with aggressive phenotype of human meningiomas. *Clin Cancer Res* (2005) 11(11):4074–82. doi: 10.1158/1078-0432.CCR-04-2550

63. PhD SRP MD. *A single arm phase II study of the dual mTORC1/mTORC2 inhibitor vistusertib (AZD2014) provided on an intermittent schedule for sporadic patients with grade II-III meningiomas that recur or progress after surgery and radiation [Internet]* (2021). Available at: https://clinicaltrials.gov/ct2/show/NCT03071874.

64. Krimpenfort P, Snoek M, Lambooij JP, Song JY, van der Weide R, Bhaskaran R, et al. A natural WNT signaling variant potently synergizes with Cdkn2ab loss in skin carcinogenesis. *Nat Commun* (2019) 10(1):1425. doi: 10.1038/s41467-019-09321-8

65. Peyre M, Stemmer-Rachamimov A, Clermont-Taranchon E, Quentin S, El-Taraya N, Walczak C, et al. Meningioma progression in mice triggered by Nf2 and Cdkn2ab inactivation. *Oncogene* (2013) 32(36):4264–72. doi: 10.1038/onc.2012.436

66. Guyot A, Duchesne M, Robert S, Lia AS, Derouault P, Scaon E, et al. Analysis of CDKN2A gene alterations in recurrent and non-recurrent meningioma. *J Neurooncol* (2019) 145(3):449–59. doi: 10.1007/s11060-019-03333-6

67. Laurendeau I, Ferrer M, Garrido D, D'Haene N, Ciavarelli P, Basso A, et al. Gene expression profiling of the hedgehog signaling pathway in human meningiomas. *Mol Med* (2010) 16(7):262–70. doi: 10.2119/molmed.2010.00005

68. Williams EA, Santagata S, Wakimoto H, Shankar GM, Barker FG, Sharaf R, et al. Distinct genomic subclasses of high-grade/progressive meningiomas: NF2-associated, NF2-exclusive, and NF2-agnostic. *Acta Neuropathol Commun* (2020) 8 (1):171. doi: 10.1186/s40478-020-01040-2

69. Clark VE, Harmancı AS, Bai H, Youngblood MW, Lee TI, Baranoski JF, et al. Recurrent somatic mutations in POLR2A define a distinct subset of meningiomas. *Nat Genet* (2016) 48(10):1253–9. doi: 10.1038/ng.3651

70. Choy W, Kim W, Nagasawa D, Stramotas S, Yew A, Gopen Q, et al. The molecular genetics and tumor pathogenesis of meningiomas and the future directions of meningioma treatments. *Neurosurg Focus* (2011) 30(5):E6. doi: 10.3171/2011.2.FOCUS1116

71. Mawrin C, Perry A. Pathological classification and molecular genetics of meningiomas. *J Neurooncol* (2010) 99(3):379–91. doi: 10.1007/s11060-010-0342-2

72. Baser ME, Poussaint TY. Age associated increase in the prevalence of chromosome 22q loss of heterozygosity in histological subsets of benign meningioma. *J Med Genet* (2006) 43(3):285–7. doi: 10.1136/jmg.2005.035162

73. Hansson CM, Buckley PG, Grigelioniene G, Piotrowski A, Hellström AR, Mantripragada K, et al. Comprehensive genetic and epigenetic analysis of sporadic meningioma for macro-mutations on 22q and micro-mutations within the NF2 locus. *BMC Genomics* (2007) 8(1):16. doi: 10.1186/1471-2164-8-16

74. Heinrich B, Hartmann C, Stemmer-Rachamimov AO, Louis DN, MacCollin M. Multiple meningiomas: Investigating the molecular basis of sporadic and familial forms. *Int J Cancer* (2003) 103(4):483–8. doi: 10.1002/ijc.10840

75. Carlson KM, Bruder C, Nordenskjöld M, Dumanski JP. 1p and 3p deletions in meningiomas without detectable aberrations of chromosome 22 identified by comparative genomic hybridization. *Genes Chromosomes Cancer.* (1997) 20(4):419–24. doi: 10.1002/(SICI)1098-2264(199712)20:4<419::AID-GCC15>3.0.CO;2-H

76. Lamszus K. Meningioma pathology, genetics, and biology. *J Neuropathol Exp Neurol* (2004) 63(4):275–86. doi: 10.1093/jnen/63.4.275

77. Cai DX, Banerjee R, Scheithauer BW, Lohse CM, Kleinschmidt-Demasters BK, Perry A. Chromosome 1p and 14q FISH analysis in clinicopathologic subsets of meningioma: Diagnostic and prognostic implications. *J Neuropathol Exp Neurol* (2001) 60(6):628–36. doi: 10.1093/jnen/60.6.628

78. Martinez A, Walker RA, Shaw JA, Dearing SJ, Maher ER, Latif F. Chromosome 3p allele loss in early invasive breast cancer: detailed mapping and association with clinicopathological features. *Mol Pathol* (2001) 54(5):300–6. doi: 10.1136/mp.54.5.300

79. Daly MC, Xiang RH, Buchhagen D, Hensel CH, Garcia DK, Killary AM, et al. A homozygous deletion on chromosome 3 in a small cell lung cancer cell line correlates with a region of tumor suppressor activity. *Oncogene.* (1993) 8(7):1721–9.

80. He S, Pham MH, Pease M, Zada G, Giannotta SL, Wang K, et al. A review of epigenetic and gene expression alterations associated with intracranial meningiomas. *Neurosurg Focus.* (2013) 35(6):E5. doi: 10.3171/2013.10.FOCUS13360

81. Mihaila D, Jankowski M, Gutiérrez JA, Rosenblum ML, Newsham IF, Bögler O, et al. Meningiomas: loss of heterozygosity on chromosome 10 and marker-specific correlations with grade, recurrence, and survival. *Clin Cancer Res Off J Am Assoc Cancer Res* (2003) 9(12):4443–51.

82. Pfisterer WK, Hank NC, Preul MC, Hendricks WP, Pueschel J, Coons SW, et al. Diagnostic and prognostic significance of genetic regional heterogeneity in meningiomas. *Neuro-Oncol.* (2004) 6(4):290–9. doi: 10.1215/S1152851704000158

83. Zattara-Cannoni H, Gambarelli D, Dufour H, Figarella D, Vollot F, Grisoli F, et al. Contribution of cytogenetics and FISH in the diagnosis of meningiomas. a study of 189 tumors. *Ann Genet* (1998) 41(3):164–75.

84. Bi WL, Greenwald NF, Abedalthagafi M, Wala J, Gibson WJ, Agarwalla PK, et al. Genomic landscape of high-grade meningiomas. *NPJ Genomic Med* (2017) 2 (1):1–14. doi: 10.1038/s41525-017-0014-7

85. Neglia JP, Robison LL, Stovall M, Liu Y, Packer RJ, Hammond S, et al. New primary neoplasms of the central nervous system in survivors of childhood cancer: a report from the childhood cancer survivor study. *JNCI J Natl Cancer Inst* (2006) 98(21):1528–37. doi: 10.1093/jnci/djj411

86. Broniscer A, Ke W, Fuller CE, Wu J, Gajjar A, Kun LE. Second neoplasms in pediatric patients with primary central nervous system tumors. *Cancer.* (2004) 100 (10):2246–52. doi: 10.1002/cncr.20253

87. Shoshan Y, Chernova O, Juen SS, Somerville RP, Israel Z, Barnett GH, et al. Radiation-induced meningioma: a distinct molecular genetic pattern? *J Neuropathol Exp Neurol* (2000) 59(7):614–20. doi: 10.1093/jnen/59.7.614

88. Yamanaka R, Hayano A, Kanayama T. Radiation-induced meningiomas: An exhaustive review of the literature. *World Neurosurg* (2017) 97:635–644.e8. doi: 10.1016/j.wneu.2016.09.094

89. Al-Mefty O, Topsakal C, Pravdenkova S, Sawyer JR, Harrison MJ. Radiation-induced meningiomas: clinical, pathological, cytokinetic, and cytogenetic characteristics. *J Neurosurg* (2004) 100(6):1002–13. doi: 10.3171/jns.2004.100.6.1002

90. Heyn H, Esteller M. DNA Methylation profiling in the clinic: applications and challenges. *Nat Rev Genet* (2012) 13(10):679–92. doi: 10.1038/nrg3270

91. Katz LM, Hielscher T, Liechty B, Silverman J, Zagzag D, Sen R, et al. Loss of histone H3K27me3 identifies a subset of meningiomas with increased risk of recurrence. *Acta Neuropathol (Berl).* (2018) 135(6):955–63. doi: 10.1007/s00401-018-1844-9

92. Behling F, Fodi C, Gepfner-Tuma I, Kaltenbach K, Renovanz M, Paulsen F, et al. H3K27me3 loss indicates an increased risk of recurrence in the tübingen meningioma cohort. *Neuro-Oncol* (2021) 23(8):1273–81. doi: 10.1093/neuonc/noaa303

93. Vasudevan HN, Castro MRH, Lee JC, Villanueva-Meyer JE, Bush NAO, McDermott MW, et al. DNA Methylation profiling demonstrates superior diagnostic classification to RNA-sequencing in a case of metastatic meningioma. *Acta Neuropathol Commun* (2020) 8:82. doi: 10.1186/s40478-020-00952-3

94. Sievers P, Sill M, Blume C, Tauziede-Espariat A, Schrimpf D, Stichel D, et al. Clear cell meningiomas are defined by a highly distinct DNA methylation profile and mutations in SMARCE1. *Acta Neuropathol (Berl)* (2021) 141(2):281–90. doi: 10.1007/s00401-020-02247-2

95. Bi WL, Abedalthagafi M, Horowitz P, Agarwalla PK, Mei Y, Aizer AA, et al. Genomic landscape of intracranial meningiomas. *J Neurosurg* (2016) 125(3):525–35. doi: 10.3171/2015.6.JNS15591

96. Patel AJ, Wan YW, Al-Ouran R, Revelli JP, Cardenas MF, Oneissi M, et al. Molecular profiling predicts meningioma recurrence and reveals loss of DREAM complex repression in aggressive tumors. *Proc Natl Acad Sci* (2019) 116(43):21715–26. doi: 10.1073/pnas.1912858116

97. Vasudevan HN, Braunstein SE, Phillips JJ, Pekmezci M, Tomlin BA, Wu A, et al. Comprehensive molecular profiling identifies FOXM1 as a key transcription factor for meningioma proliferation. *Cell Rep* (2018) 22(13):3672–83. doi: 10.1016/j.celrep.2018.03.013

98. Harmancı AS, Youngblood MW, Clark VE, Coşkun S, Henegariu O, Duran D, et al. Integrated genomic analyses of *de novo* pathways underlying atypical meningiomas. *Nat Commun* (2017) 8(1):14433. doi: 10.1038/ncomms14433

99. Sahm F, Schrimpf D, Stichel D, Jones DTW, Hielscher T, Schefzyk S, et al. DNA Methylation-based classification and grading system for meningioma: a multicentre, retrospective analysis. *Lancet Oncol* (2017) 18(5):682–94. doi: 10.1016/S1470-2045(17)30155-9

100. Nassiri F, Liu J, Patil V, Mamatjan Y, Wang JZ, Hugh-White R, et al. A clinically applicable integrative molecular classification of meningiomas. *Nature.* (2021) 597(7874):119–25. doi: 10.1038/s41586-021-03850-3

101. Olar A, Wani KM, Wilson CD, Zadeh G, DeMonte F, Jones DTW, et al. Global epigenetic profiling identifies methylation subgroups associated with recurrence-free survival in meningioma. *Acta Neuropathol (Berl).* (2017) 133 (3):431–44. doi: 10.1007/s00401-017-1678-x

102. Maas SLN, Stichel D, Hielscher T, Sievers P, Berghoff AS, Schrimpf D, et al. Integrated molecular-morphologic meningioma classification: A multicenter retrospective analysis, retrospectively and prospectively validated. *J Clin Oncol* (2021) 39(34):3839–52. doi: 10.1200/JCO.21.00784

103. Bayley JC, Hadley CC, Harmanci AO, Harmanci AS, Klisch TJ, Patel AJ. Multiple approaches converge on three biological subtypes of meningioma and extract new insights from published studies. *Sci Adv* (2022) 8(5):eabm6247. doi: 10.1126/sciadv.abm6247

104. Driver J, Hoffman SE, Tavakol S, Woodward E, Maury EA, Bhave V, et al. A molecularly integrated grade for meningioma. *Neuro-Oncol.* (2021) 11:noab213. doi: 10.14791/btrt.2022.10.F-2747

105. Choudhury A, Magill ST, Eaton CD, Prager BC, Chen WC, Cady MA, et al. Meningioma DNA methylation groups identify biological drivers and therapeutic vulnerabilities. *Nat Genet* (2022) 54(5):649–59. doi: 10.1038/s41588-022-01061-8

106. Bi WL, Nayak L, Meredith DM, Driver J, Du Z, Hoffman S, et al. Activity of PD-1 blockade with nivolumab among patients with recurrent atypical/anaplastic meningioma: phase II trial results. *Neuro-Oncol.* (2022) 24(1):101–13. doi: 10.1093/neuonc/noab118

107. Magill ST, Vasudevan HN, Seo K, Villanueva-Meyer JE, Choudhury A, John Liu S, et al. Multiplatform genomic profiling and magnetic resonance imaging identify mechanisms underlying intratumor heterogeneity in meningioma. *Nat Commun* (2020) 11(1):4803. doi: 10.1038/s41467-020-18582-7

Frontiers in Oncology

Advances knowledge of carcinogenesis and tumor progression for better treatment and management

The third most-cited oncology journal, which highlights research in carcinogenesis and tumor progression, bridging the gap between basic research and applications to imrpove diagnosis, therapeutics and management strategies.

Discover the latest Research Topics

See more →

Frontiers

Avenue du Tribunal-Fédéral 34
1005 Lausanne, Switzerland
frontiersin.org

Contact us

+41 (0)21 510 17 00
frontiersin.org/about/contact